LEABHARLANN CHOLÁISTE NA TRÍONÓIDE, BAILE ÁTHA CLIATH | TRINITY COLLEGE LIBRARY DUBLIN
Ollscoil Átha Cliath | The University of Dublin

Terms and Conditions of Use of Digitised Theses from Trinity College Library Dublin

Copyright statement

All material supplied by Trinity College Library is protected by copyright (under the Copyright and Related Rights Act, 2000 as amended) and other relevant Intellectual Property Rights. By accessing and using a Digitised Thesis from Trinity College Library you acknowledge that all Intellectual Property Rights in any Works supplied are the sole and exclusive property of the copyright and/or other IPR holder. Specific copyright holders may not be explicitly identified. Use of materials from other sources within a thesis should not be construed as a claim over them.

A non-exclusive, non-transferable licence is hereby granted to those using or reproducing, in whole or in part, the material for valid purposes, providing the copyright owners are acknowledged using the normal conventions. Where specific permission to use material is required, this is identified and such permission must be sought from the copyright holder or agency cited.

Liability statement

By using a Digitised Thesis, I accept that Trinity College Dublin bears no legal responsibility for the accuracy, legality or comprehensiveness of materials contained within the thesis, and that Trinity College Dublin accepts no liability for indirect, consequential, or incidental, damages or losses arising from use of the thesis for whatever reason. Information located in a thesis may be subject to specific use constraints, details of which may not be explicitly described. It is the responsibility of potential and actual users to be aware of such constraints and to abide by them. By making use of material from a digitised thesis, you accept these copyright and disclaimer provisions. Where it is brought to the attention of Trinity College Library that there may be a breach of copyright or other restraint, it is the policy to withdraw or take down access to a thesis while the issue is being resolved.

Access Agreement

By using a Digitised Thesis from Trinity College Library you are bound by the following Terms & Conditions. Please read them carefully.

I have read and I understand the following statement: All material supplied via a Digitised Thesis from Trinity College Library is protected by copyright and other intellectual property rights, and duplication or sale of all or part of any of a thesis is not permitted, except that material may be duplicated by you for your research use or for educational purposes in electronic or print form providing the copyright owners are acknowledged using the normal conventions. You must obtain permission for any other use. Electronic or print copies may not be offered, whether for sale or otherwise to anyone. This copy has been supplied on the understanding that it is copyright material and that no quotation from the thesis may be published without proper acknowledgement.



Design, Synthesis and Biochemical Evaluation of Novel Anthracenes, Ethanoanthracenes and Related Compounds to target Burkitt's Lymphoma

A report submitted to the University of Dublin for the degree of Doctor of Philosophy

By

Andrew J. Byrne, B.Sc. (Ind. Chem)

Under the supervision of Prof. Mary J. Meegan, B.Sc., Ph.D. (N.U.I.), M.R.S.C., C. Chem

School of Pharmacy and Pharmaceutical Sciences

Trinity College Dublin

May 2015

DEAN OF GRADUATE STUDIES
20 JAN 2016
TRINITY COLLEGE, DUBLIN

Ph.D.
School of Pharmacy

TRINITY LIBRARY
27 JUL 2016
DUBLIN

Thesis 1164

Declaration

I declare that this thesis has not been submitted as an exercise for a degree at this or any other university and it is entirely my own work. I agree to deposit this thesis in the University's open access institutional repository or allow the library to do so on my behalf, subject to Irish Copyright Legislation and Trinity College Library conditions of use and acknowledgement.

Abstract

Burkitt's lymphoma is an aggressive non-Hodgkin lymphoma occurring with high incidence in developing areas such as equatorial Africa and Papua New Guinea. Within these tropical regions of high incidence (40-50 per 10^6), Burkitt's lymphoma accounts for approximately 50% of childhood cancers and up to 90% of childhood lymphomas diagnosed. The treatment of Burkitt's lymphoma in these regions is insufficient and the development of new, safe and cost effective therapeutics are of current interest. Previous work within the Meegan and Williams groups in Trinity College Dublin identified a potent apoptotic effect induced by the (*E*)-1,3-bis(aryl)-2-nitro-1-propenes and the tetracyclic antidepressant maprotiline in Burkitt's lymphoma cell lines (MUTU-I and DG-75).

The nitrostyrene and related nitrovinyl compounds are a biologically active class of compounds reported to induce anti-cancer effects and stimulate an apoptotic response in a range of cancer cell lines[1-17]. This study reports the synthesis, characterisation and biochemical evaluation of a number of nitrostyrene and related nitrovinyl compounds in the MUTU-I and DG-75 cell lines. A diverse library of compounds related in structure to the previous lead (*E*)-1,3-bis(aryl)-2-nitro-1-propene scaffold and the tetracyclic antidepressant maprotiline were synthesised and initially evaluated for anti-proliferative effect in Burkitt's lymphoma cell lines. These compounds were structurally arranged into four groupings: nitrostyrene derivatives, heterocycles incorporating the nitrovinyl pharmacophore, 9-substituted anthracene compounds and 9,10-dihydro-9,10-ethanoanthracenes.

This thesis identified a number of these compounds which were shown to elicit a potent anti-proliferative and pro-apoptotic effect in the MUTU-I and DG-75 cell lines. A subset of lead compounds were also shown to elicit a potent anti-proliferative and proapoptotic activity towards a range of malignant cell lines (HeLa, MCF-7, HL60, HG3, PGA1, Ramos and Bjab) superior to the cancer therapeutics fludarabine and taxol. The leading nitrostyrene and 9,10-dihydro-9,10-ethanoanthracene based compounds were shown to elicit selective toxicity towards Burkitt's lymphoma over peripheral blood mononuclear cells and subsequently have potential for development as potential drug candidates.

This thesis is dedicated to the memory of

Colm J. Johnson B.Sc. (Ind. Chem.), M.Sc. (Anal. Chem.)

(1987 –2012)

Think where man's glory most begins and ends, and say my glory was I had such friends

W. B. Yeats, 1939

Acknowledgements

I would like to express my deepest gratitude to my supervisor, Prof. Mary J. Meegan for her unwavering patience, support and guidance throughout my research project. Her motivational skills, encyclopaedic knowledge of reactions and spirit of adventure has undoubtedly made my PhD experience all the more rewarding.

Over the course of my biochemistry expedition, I learned from and worked closely with Dr. Sandra A. Bright. Good teachers are not easy to find. Thank you for your sharing your vast experience, wit and friendship throughout my biochemical endeavours.

I would like to thank our collaborators in the School of Biochemistry and Immunology Prof. Dermot Clive Williams and Prof. Daniella Zisterer for the use of their tissue culture facilities. Advice and feedback provided by Prof. Williams has been of great help over the development of this project. Special thanks to Dr. Anthony McElligot (School of Molecular Medicine) for providing the CLL cell lines and *ex vivo* samples. Thank you to Dr. Dermot Walls (School of Biotechnology, Dublin City University) and his postdoctoral fellow Dr. Roya Hakimjavadi for kindly providing the Bjab and RAMOS cell lines. I would also like to thank Asst. Prof. Maria Jose Santos-Martinez (School of Pharmacy) for providing the PBMCs.

Thank you to Dr. John O'Brien and Dr. Manuel Reuthers for their help with NMR spectroscopy (even when I turned up unannounced!) and Brian Talbot for mass spectrometry. I would like to thank Dr. Brendan Twamley, Hans Georg Eckhardt, Prof. Mathias Senge and Dr. Thomas McCabe for their help running the XRD, analysing, resolving and visualising the structures. I would also like to express my gratitude to Barry Moran for his help with flow cytometry.

I am indebted to the hard working technical staff of the School of Pharmacy, in particular Ray, Brian, Rhona, Joe and Irene. The pharmaceutical chemistry technical team offered unrivalled support and for this I am grateful. I would also like to mention Betty (the Oracle), Alison, Marion and Bernadette – your kind smiles, leftover food and prudent advice were greatly appreciated.

I would like to thank all the postgraduate students and postdoctoral fellows of the School of Pharmacy and School of Biochemistry for their support, humour and camaraderie in times of obscurity. Over the years Pat, Shu, Gloria (Gigi), Azizah, Conor ("the crash-out king"), Siddig, Tadhg, Sara, Billy, Yvonne, Niamh, Cormac, James, Kit, Vilmar (Bandito),

Tao, Brian, Adrian, Gary, Feri, Michael, Jason, Mike, Maria, Fran, Shane, Jun, Claire, Keith, Susan, Michelle, Vanessa, Martina, Sweta, Sadhbh, Caoimhe, Stephanny, Manoel, Maria, Vinny, Stefano, Joanne, Christine, Claire, Svenja, Kate, David, Kieran, Peter, Grainne, Cathal, Maire, Nikki, Denise, Mary, Kim, Trev, Mary, Sandra, Jade and Jenny have generously provided me a solid base of extremely knowledgeable friends and peers. A special thanks to my colleague and friend Dr. Gabor Radics for sharing with me some of his vast knowledge of practical chemistry.

I would also like to acknowledge the contributions of my friends Shane, Eugene, Seamus and the hurlers of Faughs and Trinity College GAA clubs – without whom this PhD would have most certainly been finished sooner. Thank you to my girlfriend Olivia, for all her love, support and patience at times when my sanity was questionable. My PhD journey would not been possible without the support of my family; Dad, Mam, James and Margaret have provided unequalled support and motivation. Somehow you all have managed to keep my head out of the clouds and my feet firmly rooted to the ground but equally you've managed to keep me moving forward – thank you!

Abbreviations

^{13}C NMR	Carbon 13 nuclear magnetic resonance
^{1}H NMR	Hydrogen 1 nuclear magnetic resonance
4-MTA	4-Methylthioamphetamine
5-HT	5-hydroxytryptophan
ACN	Acetonitrile
AcOH	Acetic Acid
ADC	Antibody drug conjugates
AM1	Austin Model 1
APCI	Atmospheric pressure chemical ionization
Ara-C	Arabinosylcytosine
ATP	Adenosine triphosphate
ATR	Attenuated Total Reflection
B.C.	Before Christ
BCL-2	B-cell lymphoma 2
BCNU	Carmustine
BH	Baylis-Hillman
BIM	Bcl2-like-protein 11
BL	Burkitt's lymphoma
Ca^{2+}	Calcium
CD20	B-lymphocyte antigen
CHOP	Cyclophosphamide, doxorubicin, vincristine (oncovin) and prednisone
CIDR1α	Cysteine-rich interdomain region 1-alpha
CLL	Chronic lymphocytic leukaemia
COMU	(1-Cyano-2-ethoxy-2-oxoethylidenaminooxy)dimethylamino-morpholino-carbenium hexafluorophosphate
COSY	Correlation spectroscopy
CPMAS	Cross Polarised Magic Angle Spinning
CYDOX-M/IVAC	Cyclophosphamide, doxorubicin, methotrexate/ isofoamide, etoposide and high dose cytarabine
DABCO	1,4-Diazabicyclo[2.2.2]octane
DAT	Dopamine reuptake transporter

DBU	1,8-Diazabicyclo[5.4.0]undec-7-ene
DBU	1,8-Diazabicyclo[5.4.0]undec-7-ene
DCM	Dichloromethane
DDQ	2,3-Dichloro-5,6-Dicyanobenzoquinone
DEPT	Distortionless enhancement by polarization transfer
DMAP	4-Dimethylaminopyridine
DMEM	Dulbecco's Modified Eagle's Medium
DMF	Dimethylformamide
DMSO	Dimethylsulfoxide
DNA	Deoxyribonucleic acid
eBL	Endemic Burkitt's lymphoma
EBNA3A	Epstein-Barr nuclear protein 3A
EBNA3C	Epstein-Barr nuclear protein 3C
EBV	Epstein Barr Virus
EBVNA	Epstein Barr Virus nuclear antigen
EC50	Half maximal effective concentration
EDCi	1-Ethyl-3-(3-dimethylaminopropyl)carbodiimide
EDTA	Ethylenediaminetetraacetic acid
ERK	Extracellular signal-regulated kinases
ESI	Electrospray ionisation
FACS	Fluorescence activated cell sorter
FAD	Flavin adenine dinucleotide
FBS	Foetal bovine serum
FITC	Fluorescein isothiocyanate
FT-IR	Fourier transform infrared spectroscopy
HATU	1-[Bis(dimethylamino)methylene]-1H-1,2,3-triazolo[4,5-b]pyridinium 3-oxid hexafluorophosphate
HBTU	N,N,N′,N′-Tetramethyl-O-(1H-benzotriazol-1-yl)uronium hexafluorophosphate
hDAT	Human dopamine transporter
HEK	Human embryonic kidney
HEPES	4-(2-hydroxyethyl)-1-piperazineethanesulfonic acid
HIV	Human immunodeficiency virus

HMBC	Heteronuclear multiple bond correlation
hNET	Human norepinephrine reuptake transporter
HOBt	Hydroxybenzotriazole
HOMO	Highest occupied molecular orbital
HRMS	High resolution mass spectroscopy
hSERT	Human serotonin reuptake inhibitor
Hyper-CVAD	Cyclophosphamide, vincristine, doxorubicin, and dexamethasone (low, frequent dosing regime)
Hz	Hertz
iBL	Immunodeficiency Burkitt's lymphoma
IC_{50}	Half maximal inhibitory concentration
Ig	Immunoglobulin
IgVH	Immunoglobulin heavy chain genes
IR	Infra-red
LDH	Lactate dehydrogenase
LUMO	Lowest unoccupied molecular orbital
MAB	Monoclonal antibody
MAOI	Monoamine oxidase inhibitor
MDMA	3,4-Methylenedioxymethamphetamine
MDR	Multidrug resistance
MMAE	Monomethyl auristatin E
MOE	Molecular operating environment
MP	Melting point
NAC	N-acetyl cysteine
NADH	Nicotinamide adenine dinucleotide (reduced)
NADPH	Nicotinamide adenine dinucleotide phosphate (reduced)
NARI	Noradrenaline reuptake inhibitor
NHL	Non-Hodgkins Lymphoma
OCD	Obsessive compulsive disorder
PBMC	Peripheral blood mononuclear cells
PCD	Programmed cell death
PI	Propidium iodide
pKa	Acid dissociation constant

pRB	Retinoblastoma protein
PS	Phosphatidylserine
PSA	Polar surface area
PTB1B	Protein tyrosine phosphatase 1B
PTP	Protein tyrosine phosphatase
REDOX	Reduction oxidation
RNA	Ribonucleic acid
RNAase	Ribonuclease A
ROS	Reactive oxygen species
RPMI	Roswell Park Memorial Institute
RT	Room temperature
sBL	Sporadic Burkitt's lymphoma
SERT	Serotonin reuptake transporter
SHP-1	Scr homology phosphatase-1
SN_2	Bimolecular nucleophilic substitution
SSRI	Selective serotonin reuptake inhibitor
Taxol	Paclitaxel
TCA	Tricyclic antidepressant
TEA	Triethylamine
THF	Tetrahydrofuran
TLC	Thin layer chromatography
TMA	Trimethylamine
TMSCl	Trimethylsilyl chloride
$TMSN_3$	Trimethylsilyl azide
WHO	World Health Organisation

Table of Contents

Declaration ..... **I**

Abstract ..... **II**

Acknowledgements ..... **V**

Abbreviations ..... **VI**

Table of figures ..... **XVI**

Table of tables ..... **XXVI**

Chapter 1: Introduction **1**

1.1 General Introduction **2**

1.1.1 Cancer – A Brief Overview **2**

1.1.2 Cancer and the cell cycle **4**

1.1.3 Cell Death **5**

1.1.4 Treatment of cancer **6**

1.2 Burkitt's lymphoma **10**

1.2.1 Introduction to Burkitt's lymphoma **10**

1.2.2 Classification of Burkitt lymphoma **11**

1.2.3 Treatment of Burkitt's lymphoma **14**

1.3 Antidepressants **17**

1.4 Maprotiline **19**

1.5.1 Nitrostyrenes **23**

1.5.2 Biological activity of nitrostyrenes **26**

1.6 Thesis Objectives **31**

Chapter 2: Synthesis, isolation and characterisation of the nitrostyrenes and related structures **33**

2.0 Introduction **34**

2.1 Synthesis of a library of structurally diverse (*E*)-(2-nitrovinyl)benzenes **36**

2.2 Synthesis of 1,3-bis(aryl)-2-nitro-1-propenes and the (2-nitropropane-1,3-diyl)dibenzenes **47**

2.3 Synthesis of the (*E*)-2-nitro-1,3-diphenylprop-2-en-1-ones **54**

2.4 Synthesis of 1-substituted-2-nitroethylbenzenes via the Michael addition **58**

2.5 Synthesis of the ethyl (*E*)-2-hydroxy-3-nitro-4-phenylbut-3-enoates **61**

2.6 Synthesis of (*E*)-2-(2-nitrovinyl)cyclohexa-2,5-diene-1,4-diones **65**

2.7 Synthesis of the 2-alkyl-2-nitro-3-phenyloxiranes **66**

2.8 Synthesis of 5-alkyl-4-phenyl-1*H*-1,2,3-triazoles **68**

2.9 Synthesis of 2-substituted-3-phenylacrylonitriles **72**
2.10 Synthesis of benzylidenehydrazines **76**
2.11 Conclusion **77**
Chapter 3: Synthesis, isolation and characterisation of a range of heterocycles incorporating the active nitrostyrene pharmacophore **78**
3.0 Introduction **79**
3.1 Synthesis of 3-nitro-2-phenyl-2*H*-chromenes and 3-nitro-1,2-dihydroquinolines **80**
3.2 Synthesis of the 3-nitro-2-phenylquinoline and 3-nitroquinolin-2(1*H*)-one **86**
3.3 Synthesis of the 3-nitro-2-phenylchromen-4-ones **88**
3.4 Synthesis of the 2-acetylphenyl benzoates **91**
3.5 Synthesis of the 3-hydroxy-3-phenylprop-2-en-1-ones **94**
3.6 Synthesis of the 2-Phenyl-1-chromen-4-one **98**
3.7 Synthesis of the of 3-nitro-2-phenylchromen-4-ones **102**
3.8 Synthesis of 3-nitro-2,4-diphenyl-2,5-dihydrobenzo[b][1,4]thiazepine **106**
3.9 Synthesis of 3-nitro-2-phenyl-1*H*-indole **107**
3.10 Synthesis of 4-nitro-3,5-diphenylisoxazole **108**
3.11 Conclusion **111**
Chapter 4: Design, synthesis and characterisation of 9-substituted anthracenes **112**
4.0 Introduction **113**
4.1 Synthesis of the substituted anthracene aldehydes **114**
4.2 Synthesis of the (*E*)-9-(2-nitrovinyl)anthracenes **123**
4.3 Synthesis of 4-(anthracen-9-yl)-1*H*-1,2,3-triazoles **131**
4.4 Preparation of anthracen-9-ylmethanimines **133**
4.5 Synthesis of (*E*)-3-(anthracen-9-yl)acrylonitrile derivatives **135**
4.6 Other Knoevenagel condensations of 9-anthraldehyde **138**
4.7 Synthesis of 9-(chloromethyl)anthracene **138**
4.8 Synthesis of the (anthracen-9-yl)methylamines **139**
4.9 Synthesis of the anthracene amides **140**
4.10 Conclusions **143**
Chapter 5: Design, synthesis and characterisation of the 9,10-dihydro-9,10-ethanoanthracene maprotiline analogues **145**
5.0 Introduction **146**
5.1 Synthesis of the maleimide dienophiles **147**
5.2 Synthesis of the (*E*)-11,12-substiuted-9-(2-nitrovinyl)-9,10-dihydro-9,10-ethanoanthracenes **152**
5.3 Preparation of the (*E*)-9-(2-nitrovinyl)-9,10-dihydro-9,10-ethanoanthracenes **171**

5.4 Preparation of the 9 & 10-substituted-9,10-dihydro-9,10-[1,2]benzenoanthracenes **177**

5.5 Synthesis of the (*E*)-3-(12,14-dioxo-9,10-[3,4]furanoanthracen-9(10H)-yl)acrylonitriles and the 9-(iminomethyl)-9,10-dihydro-9,10-[3,4]furanoanthracene-12,14-diones..... **183**

5.6 Conclusion **188**

Chapter 6: Biological evaluation 189

6.0 Introduction **190**

6.1 Materials and Methods **191**

6.1.1 Cell lines **191**

6.1.2 Storage and Growth of Cultured Cells **192**

6.1.3 Seeding of cells **192**

6.1.4 AlamarBlue® anti-proliferative assay **193**

6.1.5 FITC Annexin V / PI FACS analysis **194**

6.1.6 Lactate dehydrogenase (LDH) assay **195**

6.1.7 Inhibitor Studies: Reactive Oxygen Species **196**

6.2 Results of Biochemical Screening **196**

6.2.1 Evaluation of the *in vitro* anti-proliferative activity of the nitrostyrene analogues **196**

6.2.2 *In vitro* anti-proliferative activity screen of the (*E*)-(2-nitrovinyl)benzene library..... **197**

6.2.3 *In vitro* anti-proliferative activity screen of the (*E*)-(2-nitroprop-1-en-1-yl)benzenes **200**

6.2.4 *In vitro* anti-proliferative activity screen of the (*E*)-(2-nitrobut-1-en-1-yl)benzenes... **202**

6.2.5 *In vitro* anti-proliferative activity screen of the (*E*)-1,3-bis(aryl)-2-nitro-1-propenes, 1-aryl-1-nitroethanes and the (2-nitropropane-1,3-diyl)dibenzenes **203**

6.2.6 *In vitro* anti-proliferative activity screen of the (*E*)-2-nitro-1,3-diphenylprop-2-en-1-ones and ethyl (*E*)-2-hydroxy-3-nitro-4-phenylbut-3-enoates **204**

6.2.7 *In vitro* anti-proliferative activity screen of the **205**

6.2.8 *In vitro* anti-proliferative activity screen of the 2-alkyl-2-nitro-3-phenyloxiranes and the 5-alkyl-4-phenyl-1*H*-1,2,3-triazoles **206**

6.2.9 *In vitro* anti-proliferative activity screen of the 2-substituted-3-phenylacrylonitriles . **207**

6.2.10 *In vitro* anti-proliferative activity screen of the benzylidenehydrazines **208**

6.2.11 Summary of preliminary screen findings **208**

6.2.12 *In vitro* anti-proliferative activity (IC_{50s}) of the most potent nitrostyrene derivatives **209**

6.2.13 Investigations into the pro-apoptotic effect of the most potent nitrostyrene derivatives **211**

6.2.14 *In vitro* anti-proliferative activity of the most potent nitrostyrene derivatives in other malignant diseases **212**

6.2.15 *In vitro* and *ex vivo* evaluation of lead compound for the treatment of CLL **213**

6.2.15.1 Cell culture **213**

6.2.15.2 *Ex vivo* patient samples **213**

6.2.15.3 Biochemical results **214**

6.2.16 Effect of compounds 55 and 66 on the viability of PBMCs **217**

6.3.0 Evaluation of the *in vitro* anti-proliferative activity of the nitrostyrene analogues **217**

6.3.1 Preliminary screen for *in vitro* anti-proliferative activity of the 3-nitro-2-phenyl-2*H*-chromenes and 3-nitro-1,2-dihydroquinolines **218**

6.3.2 Preliminary screen for *in vitro* anti-proliferative activity of the 3-nitro-flavones and other heterocycles **219**

6.3.3 Summary of preliminary screen findings **220**

6.3.4 *In vitro* anti-proliferative activity (IC_{50}) and investigation into pro-apoptotic effect of the most potent heterocyclic derivatives. **221**

6.4.0 Evaluation of the *in vitro* anti-proliferative activity of the anthracene based Maprotiline analogues **222**

6.4.1 Preliminary screen for *in vitro* anti-proliferative activity of the (*E*)-9-(2-nitrovinyl)anthracenes **222**

6.4.2 Preliminary screen for *in vitro* anti-proliferative activity of the (anthracen-9-yl)methylamines and the anthracene amides **224**

6.4.3 Preliminary screen for *in vitro* anti-proliferative activity of the anthracen-9-ylmethanimines and the (*E*)-3-(anthracen-9-yl)acrylonitrile derivatives **225**

6.4.4 Preliminary screen for *in vitro* anti-proliferative activity of the 4-(anthracen-9-yl)-1*H*-1,2,3-triazoles and miscellaneous condensation products. **226**

6.4.5 Summary of preliminary screen findings of anthracene based analogues **227**

6.5.0 Evaluation of the *in vitro* anti-proliferative activity of the anthracene based Maprotiline analogues **228**

6.5.1 Preliminary screen for *in vitro* anti-proliferative activity of the 9,10-dihydro-9,10-ethanoanthracenes **228**

6.5.2 Preliminary screen for *in vitro* anti-proliferative activity of the 9-substituted triptycenes **231**

6.5.3 Preliminary screen for anti-proliferative activity of the (*E*)-11,12-substiuted-9-(2-nitrovinyl)-9,10-dihydro-9,10-ethanoanthracenes **232**

6.5.6 Summary of preliminary screen findings of the 9,10-dihydro-9,10-ethanoanthracenes **238**

6.5.7 *In vitro* anti-proliferative activity (IC_{50s}) of the most potent Maprotiline analogues... **239**

6.5.8 Investigations into the pro-apoptotic effect - FITC Annexin V / PI FACS analysis ... **241**

6.5.9 Evaluation of *in vitro* cytotoxity via lactate dehydrogenase (LDH) assay..... **245**

6.5.10 Effect of compounds 289, 287 and 290 on the viability of PBMCs **246**

6.5.11 Investigation into the role of reactive oxygen species in cell death induced by compounds 289, 287 and 290..... **247**

6.5.12 Conclusions **248**

Chapter 7. Conclusion **253**

Chapter 8: Experimental. **262**

Experimental note **263**

8.1 General procedure for preparation of (*E*)-(2-nitrovinyl)benzene (1 – 34, 71 - 74) **264**

8.2 General procedure for synthesis of (*E*)-(2-Nitroprop-1-en-1-yl)benzenes (35 - 59,75 – 78) **276**

8.3 General procedure for preparation of (*E*)-(2-nitrobut-1-en-1-yl)benzenes (60 – 70, 79 - 82) **286**

8.4 General procedure for preparation of nitroethanes (84, 84, 89) **291**

8.5 General procedure for preparation of (*E*)-1,3-bis(aryl)-2-nitro-1-propenes (85 – 88) **292**

8.6 General procedure for preparation of (*E*)-2-nitro-1,3-diphenylprop-2-en-1-ones (90 – 94) **294**

8.7 General procedure for Michael additions of amines and thiols to nitrostyrenes (95 – 100) **296**

8.8 General procedure for preparation of ethyl (*E*)-2-hydroxy-3-nitro-4-phenylbut-3-enoates (101 - 104) **298**

8.9 General procedure for synthesis of (*E*)-2-(2-nitrovinyl)cyclohexa-2,5-diene-1,4-diones (105 – 106) **300**

8.10 General procedure for preparation of 2-alkyl-2-nitro-3-phenyloxiranes (107 – 111) **300**

8.11 General procedure for preparation of 5-alkyl-4-phenyl-1*H*-1,2,3-triazoles (112 – 119) **302**

8.12 General procedure for preparation of alkyl 2-cyano-3-phenylacrylates (120 – 125) **305**

8.13 General procedure for synthesis of 2-benzylidenemalononitriles (126 – 129) **307**

8.14 General procedure for synthesis of benzylidenehydrazines (130 - 134) **309**

8.15 General procedure for preparation of 3-nitro-2-phenyl-2*H*-chromenes (135 - 142) **310**

8.16 General procedure for preparation of 3-nitro-2-phenyl-2*H*-chromenes (143 – 147) **313**

8.17 General procedure for preparation of 3-nitro-2-phenyl-1,2-dihydroquinolines (148, 149) **315**

8.18 General procedure for preparation of *o*-benzoyloxyacetophenones[305] (152 – 160) **317**

8.19 General Procedure for preparation of 3-hydroxy-3-phenylprop-2-en-1-ones [305] (161 - 169) **320**

8.20 General procedure for preparation of Flavones[305] (170 - 178) **324**

8.21 General procedure for preparation of 3-nitroflavones[306] (179 - 188) **327**

8.21 General procedure for the preparation of nitrovinyl anthracene derivatives via Henry Knoevenagel Condensation (7, 41, 210 - 223) **340**

8.22 General procedure for preparation of (anthracen-9-yl)methylamines (241 - 244) **352**

8.23 General procedure for preparation of anthracene amides via the Mukaiyama reaction (245 - 250) **353**

8.24 General procedure for preparation of phenyl and benzyl maleimides (251 - 269) **356**

8.25 General Procedure for the Diels-Alder reactions **362**

8.26 General procedure for preparation of Triptycene derivatives (324 – 327, 329)..... **386**

Chapter 8: References. **400**

References **400**

Appendices **431**

Appendix 1: Biological Screen Data Tables (CD)

Appendix 2: X-ray crystallography reports (CD)

Table of figures

Figure 1: Incidence of cancers worldwide 2012 (excluding melanoma)[25] 3
Figure 2: The Cell Cycle[28] 4
Figure 3: Cancer chemotherapeutic agents: Alkylating agents 7
Figure 4: Cancer chemotherapeutic agents: Antimetabolite agents 7
Figure 5: Cancer chemotherapeutic agents: Antimicrobule agents – Vinca Alkaloids & Taxanes 8
Figure 6: Cancer chemotherapeutic agents: Topoisomerase I & II Inhibitors 8
Figure 7: Cancer chemotherapeutic agents: Hormone targeting agents 9
Figure 8: Brentuximab vedotin[39] 9
Figure 9: The 'lymphoma belt' 10
Figure 10: c-myc translocation from chromosome 8 to Ig locus chromosome 14 13
Figure 11: Components of Magrath's CODOX-M/IVAC regime 14
Figure 12: Therapeutics in development for the treatment of Burkitt's lymphoma 15
Figure 13: Therapeutics in development for the treatment of Burkitt's lymphoma 16
Figure 14: Therapeutics in development for the treatment of Burkitt's lymphoma 16
Figure 15: Tricyclic and tetracyclic antidepressants (TCAs) for treatment of depression 17
Figure 16: Selective serotonin reuptake inhibitors (SSRIs) for treatment of depression 18
Figure 17: Noradrenaline reuptake inhibitors (NARIs) for treatment of depression 18
Figure 18: Monoamine oxidase inhibitors (MAOIs) for treatment of depression 18
Figure 19: Miscellaneous agents for treatment of depression 19
Figure 20: Maprotiline 19
Figure 21: Overall scheme for the synthesis of 3-(anthracen-9-yl)propanoic acid from anthrone 20
Figure 22: Overall synthetic routes (A & B) for the synthesis of maprotiline from 3-(anthracen-9-yl)propanoic acid 20
Figure 23: Lead compounds for the reversal of chloroquine resistance 21
Figure 24: Lead maprotiline analogues (and their EC_{50} values) for treatment of Burkitt's lymphoma from previous study[6] 22
Figure 25: Nitrostyrene scaffold 23
Figure 26: Trans & Cis isomers of the nitrostyrenes 24
Figure 27: Transformations of the nitrostyrenes 24
Figure 28: Transformations of the nitrostyrenes 25
Figure 29: Transformations of the nitrostyrenes 26
Figure 30: Tubulin binding agents (Colchicine, (*E*)-1,2,3-trimethoxy-5-(2-nitrovinyl)benzene, 1,2,3-trimethoxy-5-((*E*)-2-nitrovinyl)-4-((*E*)-styryl) scaffold and (*E*)-2,3,4-trimethoxy-6-(2-nitrovinyl)-1,1'-biphenyl scaffold) 27
Figure 31: (*E*)-1,3-dichloro-5-(3-(2-nitrovinyl)phenoxy)benzene a lead compound for the inhibition of human telomerase 27
Figure 32: Nitrostyrenes found to exhibit PTP inhibition activity 28
Figure 33: Mechanism of reversible inhibition of PTP by nitrostyrenes proposed by Park et al. (2004)[195] 28
Figure 34: Mechanism of reversible inhibition of PTP by nitrostyrenes proposed by Cornell et al. (2014)[186] 28
Figure 35: phospholipase A2 inhibitiors 29

Figure 36: Incorporation structural features of the flavanones, chalcones, nitrostyrenes and stilbenes into the 2-aryl-3-nitro-2H-chromenes[145] 29
Figure 37: Nitrovinyl isatin 30
Figure 38: Example of (arylamidoanilino) nitroethylene compounds designed by Crew et al. (2006) 30
Figure 39: (*E*)-4,4'-(2-nitroprop-1-ene-1,3-diyl)bis(chlorobenzene) 30
Figure 40: MDMA, 4-MTA, N-(1,3-bis(4-(methylthio)phenyl)propan-2-yl)formamide, (*E*)-4,4'-(2-nitroprop-1-ene-1,3-diyl)bis(chlorobenzene) 34
Figure 41: The nitrostyrene scaffold and transformations planned 35
Figure 42: General scheme for Henry-Knoevenagel condensation to synthesise (*E*)-(2-nitrovinyl)benzenes 36
Figure 43: Proposed mechanism of Henry-Knoevenagel condensation for synthesis of (*E*)-(2-nitrovinyl)benzenes 36
Figure 44: Synthesis of (*E*)-(2-nitrovinyl)benzenes, (*E*)-(2-nitroprop-1-en-1-yl)benzenes and (*E*)-(2-nitrobut-1-en-1-yl)benzenes 37
Figure 45: Synthesis of (*E*)-1-(4-chlorophenyl)-2-nitroethene from 4-chlorobenzaldehyde (1) 37
Figure 46: Microwave Study – Optimisation data. 38
Figure 47: Graphical comparison of yield - microwave versus refluxing methods 38
Figure 48: ^{1}H NMR spectrum of (*E*)-4-bromo-1-methoxy-2-(2-nitrovinyl)benzene (9) 40
Figure 49: ^{13}C NMR spectrum of (*E*)-4-bromo-1-methoxy-2-(2-nitrovinyl)benzene (9) 40
Figure 50: ^{1}H NMR spectrum of (*E*)-3-(2-nitrobut-1-en-1-yl)phenol (68) 43
Figure 51: ^{13}C NMR spectrum of (*E*)-3-(2-nitrobut-1-en-1-yl)phenol (68) 44
Figure 52: X-ray crystallography data for (*E*)-3-(2-nitrobut-1-en-1-yl)phenol (68) 44
Figure 53: ^{1}H NMR spectrum of (*E*)-2-methyl-5-(2-nitrobut-1-en-1-yl)thiophene (82) 46
Figure 54: ^{13}C NMR spectrum of (*E*)-2-methyl-5-(2-nitrobut-1-en-1-yl)thiophene (82) 46
Figure 55: Preparation of (*E*)-1,3-bis(aryl)-2-nitro-1-propenes and 1,3-bis(aryl)-2-nitro-1-propanes 48
Figure 56: Scheme for reduction of the (*E*)-(2-nitrovinyl)benzenes 48
Figure 57: Formation of dimeric impurities 48
Figure 58: Synthesis of the (*E*)-1,3-bis(aryl)-2-nitro-1-propenes 49
Figure 59: ^{1}H NMR spectrum of (*E*)-1-chloro-4-(2-nitro-3-phenylprop-1-en-1-yl)benzene (86) 50
Figure 60: ^{13}C NMR spectrum of *(E)*-1-chloro-4-(2-nitro-3-phenylprop-1-en-1-yl)benzene (86) 51
Figure 61: X-ray crystallography data for (*E*)-4,4'-(2-nitroprop-1-ene-1,3-diyl)bis(chlorobenzene) (85) 52
Figure 62: Scheme for synthesis of 4,4'-(2-nitropropane-1,3-diyl)bis(chlorobenzene) 52
Figure 63: ^{1}H NMR NMR spectra of 4,4'-(2-nitropropane-1,3-diyl)bis(chlorobenzene (89). 53
Figure 64: ^{13}C NMR spectrum of 4,4'-(2-nitropropane-1,3-diyl)bis(chlorobenzene) (89) 53
Figure 65: (*E*)-2-nitro-1,3-diphenylprop-2-en-1-one scaffold (green) flexibly allgined to the (*E*)-1,3-bis(aryl)-2-nitro-1-propene scaffold (orange) (MOE 2011.10). 54
Figure 66: Scheme for the synthesis of (*E*)-2-nitro-1,3-diphenylprop-2-en-1-ones 55
Figure 67: ^{1}H NMR spectrum of (*E*)-3-(5-bromo-2-methoxyphenyl)-2-nitro-1-phenylprop-2-en-1-one (94) 56

Figure 68: ^{13}C NMR spectrum of (*E*)-3-(5-bromo-2-methoxyphenyl)-2-nitro-1-phenylprop-2-en-1-one (94) 57
Figure 69: X-ray crystallography data for (*E*)-3-(5-bromo-2-methoxyphenyl)-2-nitro-1-phenylprop-2-en-1-one (94) 57
Figure 70: Scheme for the synthesis of 1-substituted-2-nitroethylbenzenes via the Michael addition 58
Figure 71: Proposed mechanism for the synthesis of 1-substituted-2-nitroethylbenzenes via the Michael addition 58
Figure 72: ^{1}H NMR spectrum of (1-(5-bromo-2-methoxyphenyl)-2-nitroethyl)(ethyl)sulfane (96) 59
Figure 73: ^{13}C NMR spectrum of (1-(5-bromo-2-methoxyphenyl)-2-nitroethyl)(ethyl)sulfane (96) 60
Figure 74: Scheme for the synthesis of Ethyl (*E*)-2-hydroxy-3-nitro-4-phenylbut-3-enoates 61
Figure 75: Amines used to catalyse Baylis-Hillman reaction 61
Figure 76: Proposed mechanism for the synthesis of Ethyl (*E*)-2-hydroxy-3-nitro-4-phenylbut-3-enoates[209] 62
Figure 77: ^{1}H NMR spectrum of Ethyl (*E*)-4-(5-bromo-2-methoxyphenyl)-2-hydroxy-3-nitrobut-3-enoate (101) 63
Figure 78: ^{13}C NMR spectrum of Ethyl (*E*)-4-(5-bromo-2-methoxyphenyl)-2-hydroxy-3-nitrobut-3-enoate 64
Figure 79: General scheme for the synthesis of the (*E*)-2-(2-nitrovinyl)cyclohexa-2,5-diene-1,4-diones 65
Figure 80:Proposed mechanism for the synthesis of the (*E*)-2-(2-nitrovinyl)cyclohexa-2,5-diene-1,4-diones[252] 65
Figure 81: General scheme for the synthesis of 2-alkyl-2-nitro-3-phenyloxirane 66
Figure 82: Mechanism for the synthesis of 2-alkyl-2-nitro-3-phenyloxirane 67
Figure 83: ^{1}H NMR spectrum (101 MHz, CDCl3) of 3-(3-chlorophenyl)-2-ethyl-2-nitrooxirane (110) 68
Figure 84: Scheme for the synthesis of the 5-alkyl-4-phenyl-1H-1,2,3-triazoles 69
Figure 85: Proposed mechanism for the synthesis of the 5-alkyl-4-phenyl-1*H*-1,2,3-triazoles[268] 69
Figure 86: ^{1}H NMR spectrum of 4-(3-chlorophenyl)-5-methyl-1*H*-1,2,3-triazole 70
Figure 87: ^{13}C NMR spectrum of 4-(3-chlorophenyl)-5-methyl-1*H*-1,2,3-triazole 71
Figure 88: Scheme for the synthesis of 2-substituted-3-phenylacrylonitriles 72
Figure 89: Knoevenagel condensation for the synthesis of 2-substituted-3-phenylacrylonitriles[209] 73
Figure 90: ^{1}H NMR spectrum of ethyl 3-(5-bromo-2-methoxyphenyl)-2-cyanoacrylate (124) 74
Figure 91: ^{13}C NMR spectrum of ethyl 3-(5-bromo-2-methoxyphenyl)-2-cyanoacrylate (124) 75
Figure 92: Scheme for the synthesis of benzylidenehydrazines 76
Figure 93: Proposed mechanism for the synthesis of benzylidenehydrazines 76
Figure 94: Fused ring nitrostyrene analogues 79
Figure 95: 3-Nitro-2-phenyl-2*H*-chromene scaffold (green) and 3-nitro-1,2-dihydroquinoline scaffold (purple) flexibly aligned to the (*E*)-1,3-bis(aryl)-2-nitro-1-propene scaffold (orange) (MOE 2011.10) 80

Figure 96: General scheme for synthesis of 3-nitro-2-phenyl-2*H*-chromenes and 3-nitro-1,2-dihydroquinolines 81
Figure 97: Proposed mechanism for synthesis of 3-nitro-2-phenyl-2*H*-chromenes and 3-nitro-1,2-dihydroquinolines 81
Figure 98: Proposed mechanism for the demethylation of 7-methoxy-3-nitro-2-phenyl-2*H*-chromene 82
Figure 99: ^{1}H NMR spectrum of 4-(3-Nitro-2*H*-chromen-2-yl)phenol (137) 84
Figure 100: ^{13}C NMR spectrum of 4-(3-Nitro-2*H*-chromen-2-yl)phenol (137) 85
Figure 101: DEPT 90 NMR spectrum of 4-(3-Nitro-2*H*-chromen-2-yl)phenol (137) 85
Figure 102: Proposed mechanism for the synthesis of 3-nitro-2-phenylquinoline 86
Figure 103: ^{1}H NMR spectrum of 3-nitroquinolin-2(1*H*)-one (151) 87
Figure 104: ^{13}C NMR spectrum of 3-nitroquinolin-2(1*H*)-one (151) 88
Figure 105: (*E*)-(2-Nitrovinyl)benzene pharmacophore (purple), 3-nitro-2-phenylchromen-4-one scaffold with (2-nitrovinyl)benzene pharmacophore (purple) as a substructure, 1,3-bis(aryl)-2-nitro-1-propene scaffold (blue), 3-nitro-2-phenylchromen-4-one scaffold with 1,3-bis(aryl)-2-nitro-1-propene scaffold (blue) as a substructure 88
Figure 106: 3-Nitro-2-phenylchromen-4-one scaffold (purple) flexibly aligned to the (*E*)-1,3-bis(aryl)-2-nitro-1-propene scaffold (blue) (MOE 2011.10) 89
Figure 107: Apigenin and tangeretin 89
Figure 108: General overall reaction scheme for synthesis of 3-nitro-2-phenylchromen-4-ones (including Baker- Venkataraman rearrangement) 90
Figure 109: General scheme for the synthesis of the 2-acetylphenyl benzoates 91
Figure 110: Proposed mechanism for the synthesis of the 2-acetylphenyl benzoates 91
Figure 111: ^{1}H NMR spectrum of 2-acetyl-5-chlorophenyl 4-chlorobenzoate (155) 93
Figure 112: General scheme for the synthesis of the 1,3 diketones 94
Figure 113: Proposed mechanism for the synthesis of the 3-hydroxy-3-phenylprop-2-en-1-ones (Baker-Venkataraman rearrangement)[209, 304, 305] 94
Figure 114: Tautomerism of the 1,3 diketones to the 3-hydroxy-3-phenylprop-2-en-1-ones 95
Figure 115: ^{1}H NMR spectrum of 3-hydroxy-1-(2-hydroxyphenyl)-3-(3,4,5-trimethoxyphenyl)prop-2-en-1-one (166) 96
Figure 116: ^{13}C NMR spectrum of 3-hydroxy-1-(2-hydroxyphenyl)-3-(3,4,5-trimethoxyphenyl)prop-2-en-1-one (166) 97
Figure 117: General scheme for the synthesis of the 2-Phenyl-1-chromen-4-ones 98
Figure 118: Proposed mechanism for the synthesis of the 2-Phenyl-1-chromen-4-ones 98
Figure 119: ^{1}H NMR spectrum of 2-(3,4,5-trimethoxyphenyl)-4H-chromen-4-one (175) 100
Figure 120: NMR spectrum of 2-(3,4,5-trimethoxyphenyl)-4H-chromen-4-one (175) 101
Figure 121: DEPT 90 NMR spectrum of 2-(3,4,5-trimethoxyphenyl)-4H-chromen-4-one (175) 101
Figure 122: General scheme for the synthesis of the 3-nitro-2-phenylchromen-4-ones 102
Figure 123: Proposed mechanism for the synthesis of the 3-nitro-2-phenylchromen-4-ones 102
Figure 124: Isolated nitration side-products 2-(4-methoxy-3-nitrophenyl)-3-nitro-4H-chromen-4-one and 3-nitro-2-(3,4,5-trimethoxy-2-nitrophenyl)-4H-chromen-4-one (Addition nitration position highlighted in blue). 103
Figure 125: ^{1}H NMR spectrum of 7-methoxy-3-nitro-2-phenyl-4*H*-chromen-4-one (188) . 104
Figure 126: ^{13}C NMR spectrum of 7-methoxy-3-nitro-2-phenyl-4*H*-chromen-4-one (188) 105

Figure 127: DEPT 90 NMR spectrum of 7-methoxy-3-nitro-2-phenyl-4*H*-chromen-4-one (188) 105
Figure 128: Scheme for the synthesis of 3-nitro-2,4-diphenyl-2,5-dihydrobenzo[b][1,4]thiazepine 106
Figure 129: Mechanism for the synthesis of 3-nitro-2,4-diphenyl-2,5-dihydrobenzo[b][1,4]thiazepine (189) 106
Figure 130: Synthesis of 3-nitro-2-phenyl-1*H*-indole (190) 107
Figure 131: Proposed mechanism for the synthesis of 3-nitro-2-phenyl-1*H*-indole 107
Figure 132: (*E*)-(2-nitrovinyl)benzene scaffold, 2-nitro-1,3-diphenylprop-1-ene and 4-nitro-3,5-diphenylisoxazole (2-nitro-1,3-diphenylprop-1-ene substructure highlighted in blue) . 108
Figure 133: Overall scheme for the synthesis of Synthesis of 4-nitro-3,5-diphenylisoxazole 108
Figure 134: Scheme for the synthesis of 2,3-dibromo-1,3-diphenylpropan-1-one from chalcone 108
Figure 135: Proposed mechanism for the synthesis of 2,3-dibromo-1,3-diphenylpropan-1-one from chalcone 109
Figure 136: Scheme for the synthesis of 3,5-diphenylisoxazole 109
Figure 137: Proposed mechanism for the synthesis of 3,5-diphenylisoxazole 110
Figure 138: Scheme for the synthesis of 4-nitro-3,5-diphenylisoxazole 110
Figure 139: Proposed mechanism for the synthesis of 4-nitro-3,5-diphenylisoxazole 110
Figure 140: Maprotiline (green) flexibly aligned to the (*E*)-9-(2-nitrovinyl)anthracene (orange) (MOE 2011.10). 113
Figure 141: Overview of anthracene compound library 114
Figure 142: Overall scheme for the synthesis of 10-substituted-9-anthraldehydes (199-203) 114
Figure 143: Proposed mechanisms for formation of Grignard reagents and the Grignard reaction of anthrone 115
Figure 144: Proposed mechanism for the methylation of anthrone 115
Figure 145: Scheme for the synthesis of 9-methylanthracene (195) 116
Figure 146: Proposed mechanism for the synthesis of 9-methylanthracene (195) (Wolff-Kischner mechanism) 116
Figure 147: General scheme for the formylation of 9-substituted anthracene by Vilsmeier Haack reaction 117
Figure 148: Proposed mechanism for the formation of the Vilsmeier Haack reagent[209] 117
Figure 149: Proposed mechanism for the formylation of 9-substituted anthracene by Vilsmeier Haack reaction[209] 118
Figure 150: Overall scheme for synthesis of 10-bromoanthracene-9-carbaldehyde 118
Figure 151: Mechanism for the bromination of anthracene (204) 119
Figure 153: Proposed formylation reaction of organolithium compound 119
Figure 154: Overall synthesis of 4,5-dichloroanthracene-9-carbaldehyde 120
Figure 155: Proposed mechanism for Rieche formylation 120
Figure 156: Overall scheme for synthesis of 2-(anthracen-9-yl)acetaldehyde 121
Figure 157: Proposed mechanism for the synthesis of 9-(2-methoxyvinyl)anthracene[129, 209] 121
Figure 158: Proposed mechanism for the synthesis of 2-(anthracen-9-yl)acetaldehyde[129] ... 122
Figure 159: General schemes for the synthesis of the (*E*)-9-(2-nitrovinyl)anthracene library, (*E*)-9-(3-nitroallyl)anthracenes and (*E*)-9-(2-nitrovinyl)phenanthrene 123

Figure 160: ^{1}H NMR spectrum of (*E*)-9-chloro-10-(2-nitrobut-1-en-1-yl)anthracene (213) 125
Figure 161: ^{13}C NMR spectrum of (*E*)-9-chloro-10-(2-nitrobut-1-en-1-yl)anthracene (213) 126
Figure 162: DEPT 135 NMR spectrum of (*E*)-9-chloro-10-(2-nitrobut-1-en-1-yl)anthracene (213) 126
Figure 163: X-ray crystallography data: Asymmetric unit of (*E*)-9-chloro-10-(2-nitroprop-1-en-1-yl)anthracene (213) 127
Figure 164: ^{1}H NMR spectrum of (*E*)-9-(3-nitroallyl)anthracene (221) 128
Figure 165: ^{13}C NMR spectrum of (*E*)-9-(3-nitroallyl)anthracene (221) 129
Figure 166: DEPT 135 NMR spectrum of (*E*)-9-(3-nitroallyl)anthracene (221) 129
Figure 168: General scheme for the synthesis of 4-(anthracen-9-yl)-1H-1,2,3-triazoles 131
Figure 169: ^{1}H NMR spectrum of 4-(anthracen-9-yl)-4,5-dihydro-1*H*-1,2,3-triazole (227) 132
Figure 170: ^{13}C NMR spectrum of 4-(anthracen-9-yl)-4,5-dihydro-1*H*-1,2,3-triazole (227) 132
Figure 171: General scheme for the synthesis of anthracen-9-ylmethanimine 133
Figure 172: ^{1}H NMR spectrum of (*E*)-((10-chloroanthracen-9-yl)methylene)hydrazine (229) 134
Figure 173: ^{13}C NMR spectrum of (E)-((10-chloroanthracen-9-yl)methylene)hydrazine (229) 135
Figure 174: General scheme for the synthesis of the (*E*)-3-(anthracen-9-yl)acrylonitriles .. 135
Figure 175: Mechanism for the synthesis of the (*E*)-3-(anthracen-9-yl)acrylonitrile 136
Figure 176: ^{1}H NMR spectrum of 2-((10-chloroanthracen-9-yl)methylene)malononitrile (234) 137
Figure 177: ^{13}C NMR spectrum of 2-((10-chloroanthracen-9-yl)methylene)malononitrile (234) 137
Figure 178: Scheme for synthesis of (*E*)-4-(anthracen-9-yl)but-3-en-2-one and 5-(anthracen-9-ylmethylene)-2,2-dimethyl-1,3-dioxane-4,6-dione 138
Figure 179: General scheme for the synthesis of 9-(chloromethyl)anthracene 139
Figure 180: General scheme for the synthesis of 2-(anthracen-9-yl)acetonitrile 139
Figure 181: General scheme for the synthesis of the (anthracen-9-yl)methylamines 139
Figure 182: General scheme for the synthesis of the anthracene amides (245-250) 140
Figure 183: Proposed mechanism for the synthesis of the anthracene amides[209] 140
Figure 185: ^{1}H NMR spectrum of anthracen-9-yl(azepan-1-yl)methanone (247) 142
Figure 186: ^{13}C NMR spectrum of anthracen-9-yl(azepan-1-yl)methanone (247) 143
Figure 187: Overview of proposed maprotiline analogues 146
Figure 188: : Maprotiline (green) flexibly allgined to proposed Diels-Alder adduct (red) (MOE 2011.10). 147
Figure 189: General scheme for the synthesis of the maleimide dienophiles 148
Figure 190: Mechanism for the formation of the amic acid intermediate 148
Figure 191: Mechanism for the formation of maleimide derivatives 148
Figure 192: ^{1}H NMR spectrum of 1-(3,4,5-trimethoxyphenyl)-1*H*-pyrrole-2,5-dione (252) 150
Figure 193: ^{13}C NMR spectrum of 1-(3,4,5-trimethoxyphenyl)-1*H*-pyrrole-2,5-dione (252) 151
Figure 194: DEPT 90 NMR spectrum of 1-(3,4,5-trimethoxyphenyl)-1*H*-pyrrole-2,5-dione (252) 151
Figure 195: General scheme for the Diels-Alder reaction 152

Figure 196: Dienophile library 152
Figure 197: Proposed mechanism for the Diels-Alder reaction of the (*E*)-9-(2-nitrovinyl)anthracenes 153
Figure 198: Endo and Exo configurations 154
Figure 199: ^{1}H NMR spectrum of (*E*)-9-(2-nitrovinyl)-9,10-dihydro-9,10-[3,4]furanoanthracene-12,14-dione (270) 156
Figure 200: H-H COSY NMR spectrum of (*E*)-9-(2-nitrovinyl)-9,10-dihydro-9,10-[3,4]furanoanthracene-12,14-dione (270) 157
Figure 201: ^{13}C NMR spectrum of (*E*)-9-(2-nitrovinyl)-9,10-dihydro-9,10-[3,4]furanoanthracene-12,14-dione (270) 157
Figure 202: DEPT 90 NMR spectrum of (*E*)-9-(2-nitrovinyl)-9,10-dihydro-9,10-[3,4]furanoanthracene-12,14-dione (270) 158
Figure 203: C-H COSY NMR spectrum of (*E*)-9-(2-nitrovinyl)-9,10-dihydro-9,10-[3,4]furanoanthracene-12,14-dione (270) 158
Figure 204: HMBC NMR spectrum of (*E*)-9-(2-nitrovinyl)-9,10-dihydro-9,10-[3,4]furanoanthracene-12,14-dione (270) 159
Figure 205: Scheme for the synthesis of 13,13'-(hexane-1,6-diyl)bis(9-((*E*)-2-nitrovinyl)-9,10-dihydro-9,10-[3,4]epipyrroloanthracene-12,14-dione) 162
Figure 206: ^{1}H NMR spectrum of (*E*)-13-(3,5-dimethoxyphenyl)-9-(2-nitrovinyl)-9,10-dihydro-9,10-[3,4]epipyrroloanthracene-12,14-dione (298) 165
Figure 207: ^{13}C NMR spectrum of (*E*)-13-(3,5-dimethoxyphenyl)-9-(2-nitrovinyl)-9,10-dihydro-9,10-[3,4]epipyrroloanthracene-12,14-dione (298) 166
Figure 208: DEPT 90 NMR spectrum of (*E*)-13-(3,5-dimethoxyphenyl)-9-(2-nitrovinyl)-9,10-dihydro-9,10-[3,4]epipyrroloanthracene-12,14-dione (298) 166
Figure 209: C-H COSY spectrum of (*E*)-13-(3,5-dimethoxyphenyl)-9-(2-nitrovinyl)-9,10-dihydro-9,10-[3,4]epipyrroloanthracene-12,14-dione (298) 167
Figure 210: (*E*)-9-(2-nitrovinyl)-14-phenyl-9,10-dihydro-9,10-[1,2]epitriazoloanthracene-13,15-dione 170
Figure 211: Adducts possible during the reaction of cyanoacrylate and (*E*)-9-(2-nitrovinyl)anthracene 171
Figure 212: Preparation of of dimethyl and diethyl (*E*)-9-(2-nitrovinyl)-9,10-dihydro-9,10-ethanoanthracene-11,12-dicarboxylate 171
Figure 213: Mechanism for the synthesis of dimethyl and diethyl (*E*)-9-(2-nitrovinyl)-9,10-dihydro-9,10-ethanoanthracene-11,12-dicarboxylate from (*E*)-9-(2-nitrovinyl)-9,10-dihydro-9,10-[3,4]furanoanthracene-12,14-dione 172
Figure 214: ^{1}H NMR spectrum of (*E*)-10-(2-nitrovinyl)-9,10-dihydro-9,10-ethanoanthracene-11-carbonitrile (318) 173
Figure 215: H-H COSY spectrum of (*E*)-10-(2-nitrovinyl)-9,10-dihydro-9,10-ethanoanthracene-11-carbonitrile (318) 174
Figure 216: ^{13}C NMR spectrum of (*E*)-10-(2-nitrovinyl)-9,10-dihydro-9,10-ethanoanthracene-11-carbonitrile (318) 174
Figure 217: DEPT 135 spectrum of (*E*)-10-(2-nitrovinyl)-9,10-dihydro-9,10-ethanoanthracene-11-carbonitrile (318) 175
Figure 218: C-H COSY spectrum of (*E*)-10-(2-nitrovinyl)-9,10-dihydro-9,10-ethanoanthracene-11-carbonitrile (318) 175

Figure 219: X-ray crystallography data: Asymmetric unit and packing structure of (*E*)-10-(2-nitrovinyl)-9,10-dihydro-9,10-ethanoanthracene-11-carbonitrile (318) 176
Figure 220: Triptycene 177
Figure 221: Diazotisation of 2-aminobenzoic acid to give benzenediazonium-2-carboxylate. Decomposition of benzenediazonium-2-carboxylate to give benzyne 177
Figure 222: General scheme for the synthesis of (*E*)-9-(2-nitrovinyl)-9,10-dihydro-9,10-[1,2]benzenoanthracenes (324-327) 178
Figure 223: ^{1}H NMR spectrum of (*E*)-9-chloro-10-(2-nitrovinyl)-9,10-dihydro-9,10-[1,2]benzenoanthracene (327) 179
Figure 224: ^{13}C NMR spectrum of (*E*)-9-chloro-10-(2-nitrovinyl)-9,10-dihydro-9,10-[1,2]benzenoanthracene (327) 180
Figure 225: DEPT 90 spectrum of (*E*)-9-chloro-10-(2-nitrovinyl)-9,10-dihydro-9,10-[1,2]benzenoanthracene (327) 180
Figure 226: C-H COSY spectrum of (*E*)-9-chloro-10-(2-nitrovinyl)-9,10-dihydro-9,10-[1,2]benzenoanthracene (327) 181
Figure 227: HMBC spectrum of (*E*)-9-chloro-10-(2-nitrovinyl)-9,10-dihydro-9,10-[1,2]benzenoanthracene (327) 181
Figure 228: X-ray crystallography data: Asymmetric unit and packing structure of (*E*)-9-(2-nitrovinyl)-9,10-dihydro-9,10-[1,2]benzenoanthracene (324) 183
Figure 229: General scheme for the synthesis of the (*E*)-3-(12,14-dioxo-9,10-[3,4]furanoanthracen-9(10*H*)-yl)acrylonitriles and the 9-(iminomethyl)-9,10-dihydro-9,10-[3,4]furanoanthracene-12,14-diones. 183
Figure 230: General scheme for the synthesis of the 9,10-dihydro-9,10-[3,4]furanoanthracene-12,14-diones 184
Figure 231: ^{1}H NMR spectrum of (*E*)-9-(hydrazonomethyl)-9,10-dihydro-9,10-[3,4]epipyrroloanthracene-12,14-dione (348) 186
Figure 232: ^{13}C NMR spectrum of (*E*)-9-(hydrazonomethyl)-9,10-dihydro-9,10-[3,4]epipyrroloanthracene-12,14-dione (348) 187
Figure 233: DEPT 90 NMR spectrum of (*E*)-9-(hydrazonomethyl)-9,10-dihydro-9,10-[3,4]epipyrroloanthracene-12,14-dione (348) 187
Figure 234: Summary graphic of maprotiline analogue library 188
Figure 235: Example of quadrants produced during Annexin V / PI FACS analysis (vehicle - DG-75 cell line) 194
Figure 236: Process for Formazan formation during LDH assay[404] 195
Figure 237: Preliminary anti-proliferative screen for (*E*)-(2-nitrovinyl)benzene (A) 197
Figure 238: Preliminary anti-proliferative screen for (*E*)-(2-nitrovinyl)benzene (B) 197
Figure 239: Preliminary anti-proliferative screen for (*E*)-(2-nitrovinyl)benzene (C) 198
Figure 240: Preliminary anti-proliferative screen for (*E*)-(2-nitrovinyl)benzene (D) 198
Figure 241: Preliminary anti-proliferative screen for (*E*)-(2-nitrovinyl)benzene (E) 199
Figure 242: Preliminary screen for (*E*)-(2-nitroprop-1-en-1-yl)benzenes anti-proliferative activity (A) 200
Figure 243: Preliminary screen for (*E*)-(2-nitroprop-1-en-1-yl)benzenes anti-proliferative activity (B) 200
Figure 244: Preliminary screen for (*E*)-(2-nitroprop-1-en-1-yl)benzenes anti-proliferative activity (C) 201

Figure 245: Preliminary screen for (*E*)-(2-nitroprop-1-en-1-yl)benzenes anti-proliferative activity (D) 201
Figure 246: Preliminary anti-proliferative screen for (*E*)-(2-nitrobut-1-en-1-yl)benzenes (A) 202
Figure 247: Preliminary anti-proliferative screen for (*E*)-(2-nitrobut-1-en-1-yl)benzenes (B) 202
Figure 248: Preliminary screen for anti-proliferative activity of the (*E*)-1,3-bis(aryl)-2-nitro-1-propenes, 1-aryl-1-nitroethanes and the (2-nitropropane-1,3-diyl)dibenzenes 203
Figure 249: Preliminary screen for anti-proliferative activity of the (*E*)-2-nitro-1,3-diphenylprop-2-en-1-ones 204
Figure 250: Preliminary screen for anti-proliferative activity of the ethyl (*E*)-2-hydroxy-3-nitro-4-phenylbut-3-enoates 204
Figure 251: Preliminary screen for anti-proliferative activity of the 1-substituted-2-nitroethylbenzenes 205
Figure 252: Preliminary screen for anti-proliferative activity of the 2-alkyl-2-nitro-3-phenyloxiranes 206
Figure 253: Preliminary screen for anti-proliferative activity of the 5-alkyl-4-phenyl-1H-1,2,3-triazoles 206
Figure 254: Preliminary screen for anti-proliferative activity of the 2-substituted-3-phenylacrylonitriles 207
Figure 255: Preliminary screen for anti-proliferative activity of the 2-substituted-3-phenylacrylonitriles 207
Figure 256: Preliminary screen for anti-proliferative activity of benzylidenehydrazines 208
Figure 257: Optimised nitrostyrene analogue for antiproliferative activity in BL cell lines 209
Figure 258: Annexin V / PI FACS - Apoptosis in MUTU-I and DG-75 cell lines 211
Figure 259: Compounds 55 & 66 in HG3 and PGA1 CLL cell lines - Annexin V / PI FACS analysis (48 h) 214
Figure 260: Compounds 55 & 66 in HG3 and PGA1 CLL cell lines – Inhibitor study Annexin V / PI FACS analysis (48h) 215
Figure 261: Ex vivo CLL patients samples - Annexin V / PI FACS analysis (48 h) 216
Figure 262: In vitro antiproliferative effect of compounds 55 and 66 on PBMCs (24 h), MUTU-I cell line (24 h) and DG-75 cell line (48 h) at 10 μM and 1 μM 217
Figure 263: Preliminary screen for anti-proliferative activity of the 3-nitro-2-phenyl-2*H*-chromenes 218
Figure 264: Preliminary screen for anti-proliferative activity of the 3-nitro-2-phenyl-2*H*-chromenes 218
Figure 265: Preliminary screen for anti-proliferative activity of the 3-nitro-flavones 219
Figure 266: Preliminary screen for anti-proliferative activity of selected heterocycles 219
Figure 267: Annexin V / PI FACS - Apoptosis MUTU-I and DG-75 cell lines 221
Figure 268: Preliminary screen for anti-proliferative activity of the (*E*)-9-(2-nitrovinyl)anthracenes (A) 222
Figure 269: Preliminary screen for anti-proliferative activity of the (E)-9-(2-nitrovinyl)anthracenes (B) 223
Figure 270: Preliminary screen for anti-proliferative activity of anthracene amides 224
Figure 271: Preliminary screen for anti-proliferative activity of (anthracen-9-yl)methylamines 224

Figure 272: Preliminary screen for anti-proliferative activity of anthracen-9-ylmethanimines 225
Figure 273: Preliminary screen for anti-proliferative activity of (*E*)-3-(anthracen-9-yl)acrylonitrile derivatives 225
Figure 274: Preliminary screen for anti-proliferative activity of the 4-(anthracen-9-yl)-1H-1,2,3-triazoles and miscellaneous condensation products. 226
Figure 275: Preliminary screen for anti-proliferative activity of the (*E*)-11,12-substiuted-9-(2-nitrovinyl)-9,10-dihydro-9,10-ethanoanthracenes 228
Figure 276: Preliminary screen for anti-proliferative activity of the 9,10-dihydro-9,10-ethanoanthracenes 229
Figure 277: Preliminary screen for anti-proliferative activity of the 9-substituted 9,10-dihydro-9,10-ethanoanthracenes 230
Figure 278: Preliminary screen for anti-proliferative activity of the 9-substituted 9,10-dihydro-9,10-ethanoanthracenes 230
Figure 279: Preliminary screen for in vitro anti-proliferative activity of the 9-substituted triptycenes 231
Figure 280: Preliminary screen for anti-proliferative activity of the (E)-11,12-substiuted-9-(2-nitrovinyl)-9,10-dihydro-9,10-ethanoanthracenes 232
Figure 281: Preliminary screen for anti-proliferative activity of the (*E*)-11,12-substiuted-9-(2-nitrovinyl)-9,10-dihydro-9,10-ethanoanthracenes 233
Figure 282: Preliminary screen for anti-proliferative activity of the (*E*)-11,12-substiuted-9-(2-nitrovinyl)-9,10-dihydro-9,10-ethanoanthracenes 234
Figure 283: Preliminary screen for anti-proliferative activity of the (*E*)-11,12-substiuted-9-(2-nitrovinyl)-9,10-dihydro-9,10-ethanoanthracenes 235
Figure 284: Preliminary screen for anti-proliferative activity of the 9-((*E*)-2-nitrovinyl)-13-phenyl-9,10-dihydro-9,10-[3,4]epipyrroloanthracene-12,14-diones 236
Figure 285: Preliminary screen for anti-proliferative activity of the (*E*)-11,12-substiuted-9-(2-nitrovinyl)-9,10-dihydro-9,10-ethanoanthracenes 237
Figure 286: Annexin V / PI FACS Maprotiline analogues MUTU-I cell line 241
Figure 287: Annexin V / PI FACS Maprotiline analogues MUTU-I cell line 241
Figure 288: Annexin V / PI FACS Maprotiline analogues MUTU-I cell line 242
Figure 289: Annexin V / PI FACS Maprotiline analogues DG-75 cell line 243
Figure 290: Annexin V / PI FACS Maprotiline analogues DG-75 cell line 243
Figure 291: Annexin V / PI FACS Maprotiline analogues DG-75 cell line 244
Figure 292: LDH assay Maprotiline analogues MUTU-I and DG-75 cell lines 245
Figure 293: *In vitro* antiproliferative effect of compounds 289, 287 and 290 on PBMCs (24 h), MUTU-I cell line (24 h) and DG-75 cell line (48 h) at 1 μM and 0.5 μM 246
Figure 294: Investigation into the role of reactive oxygen species in cell death induced by compounds 289, 287 and 290 247
Figure 295: Summarised SAR for the (*E*)-(2-nitrovinyl)benzenes 248
Figure 296: Summarised SAR for the heterocyclic compounds containing a constrained nitrostyrene pharmacophore 250
Figure 297: Summarised SAR for the 9-substituted anthracene maprotiline analogues 250
Figure 298: Summarised SAR for the 9,10-dihydro-9,10-ethanoanthracene based maprotiline analogues 251
Figure 299: Optimal SAR for the (*E*)-(2-nitrovinyl)benzenes 254

Figure 300: Optimal SAR for the heterocyclic compounds containing a constrained nitrostyrene pharmacophore 256
Figure 301: Optimal SAR for the 9-substituted anthracene maprotiline analogues 257
Figure 302: Optimal SAR for the 9,10-dihydro-9,10-ethanoanthracene based maprotiline analogues 258
Figure 303: Future synthetic modification of the nitrostyrene lead compound (66) 260
Figure 304: Future synthetic modification of the 3-nitro-2-anthracene-2*H*-chromene lead compound 260
Figure 305: Future synthetic targets - TCA analogues 261
Figure 306: Future synthetic objectives for modification of the 9,10-dihydro-9,10-ethanoanthracene lead compound (289) 261

Table of tables

Table 1: *(E)*-(2-nitrovinyl)benzene library. Note: R = H unless otherwise specified. * denotes novel compound.....39
Table 2: *(E)*-(2-nitroprop-1-en-1-yl)benzene library. Note: R = H unless otherwise specified. * denotes novel compound.....41
Table 3: *(E)*-(2-nitrobut-1-en-1-yl)benzene library. Note: R = H unless otherwise specified. * denotes novel compound.....42
Table 4: Heterocyclic *(E)*-(2-nitrovinyl) library. Note: R = H unless otherwise specified. * denotes novel compound.....45
Table 5: *(E)*-1,3-bis(aryl)-2-nitro-1-propene library. Note: R = H unless otherwise specified. * denotes novel compound.....50
Table 6: *(E)*-2-nitro-1,3-diphenylprop-2-en-1-one library. Note: R = H unless otherwise specified. * denotes novel compound.....55
Table 7: 1-subsituted-(2-nitroethyl)benzene library. Note: R = H unless otherwise specified. * denotes novel compound.....59
Table 8: ethyl *(E)*-2-hydroxy-3-nitro-4-phenylbut-3-enoate library. Note: R = H unless otherwise specified. * denotes novel compound.....63
Table 9: 2-alkyl-2-nitro-3-phenyloxirane library. Note: R = H unless otherwise specified. * denotes novel compound.....67
Table 10: 5-alkyl-4-phenyl-1*H*-1,2,3-triazole library. Note: R = H unless otherwise specified. * denotes novel compound.....70
Table 11: alkyl 2-cyano-3-phenylacrylate library. Note: R = H unless otherwise specified. * denotes novel compound.....73
Table 12: 2-benzylidenemalononitrile library. Note: R = H unless otherwise specified. * denotes novel compound.....74
Table 13: benzylidenehydrazines library. Note: R = H unless otherwise specified. * denotes novel compound.....76
Table 14: 3-nitro-2-phenyl-2*H*-chromene and 3-nitro-1,2-dihydroquinoline library. Note: R = H unless otherwise specified. * denotes novel compound.....83
Table 15: 2-acetylphenyl benzoate library. Note: R = H unless otherwise specified. * denotes novel compound.....92
Table 16: 3-hydroxy-3-phenylprop-2-en-1-one library. Note: R = H unless otherwise specified. * denotes novel compound.....96

Table 17: 2-Phenyl-4*H*-chromen-4-one library. Note: R = H unless otherwise specified. * denotes novel compound.....99
Table 18: 3-nitro-2-phenylchromen-4-one library. Note: R = H unless otherwise specified. * denotes novel compound.....103
Table 19: 9-subsituted anthracene library. Note: R = H unless otherwise specified. * denotes novel compound.....117
Table 20: substituted-9-anthraldehyde library. Note: R = H unless otherwise specified. * denotes novel compound.....122
Table 21: Comparison of Henry-Knoevenagel condensation yields for 9-anthraldehyde (Method 1 v Method 2). *cyclohexylamine, acetic acid, 20 min MW, ** Piperidine, DCM, 6 h reflux.....123
Table 22: *(E)*-9-(2-nitrovinyl)anthracene library. Note: R = H unless otherwise specified. * denotes novel compound.....124
Table 23: anthracen-9-ylmethanimine library.....133
Table 24: (anthracen-9-yl)methylamines library.....140
Table 25: anthracene amides library.....141
Table 26: phenylmaleimide library. Note: R = H unless otherwise specified. * denotes novel compound.....149
Table 27: maleimide library.....150
Table 28: *(E)*-9-(2-nitrovinyl)-9,10-dihydro-9,10-[3,4]furanoanthracene-12,14-dione library. * denotes novel compound.....155
Table 29: X-ray crystallography data for the *(E)*-9-(2-nitrovinyl)-9,10-dihydro-9,10-[3,4]furanoanthracene-12,14-diones.....160
Table 30: 9-(2-nitroethyl)-9,10-dihydro-9,10-[3,4]epipyrroloanthracene-12,14-dione library.....161
Table 31: *(E)*-9-(2-nitrovinyl)-13-phenyl-9,10-dihydro-9,10-[3,4]epipyrroloanthracene-12,14-dione library. * denotes novel compound.....163
Table 32: *(E)*-9-(2-nitrovinyl)-13-phenyl-9,10-dihydro-9,10-[3,4]epipyrroloanthracene-12,14-dione library 2. * denotes novel compound.....164
Table 33: X-ray crystallography data for the *(E)*-9-(2-nitrovinyl)-13-phenyl-9,10-dihydro-9,10-[3,4]epipyrroloanthracene-12,14-diones (Part 1)..... 168
Table 34: X-ray crystallography data for the *(E)*-9-(2-nitrovinyl)-13-phenyl-9,10-dihydro-9,10-[3,4]epipyrroloanthracene-12,14-diones (Part 2).....169
Table 35: X-ray crystallography assymetric unit analysis.....170
Table 36: *(E)*-9-(2-nitrovinyl)-9,10-dihydro-9,10-ethanoanthracene library. * denotes novel compound.....172
Table 37: 9 & 10-substituted-9,10-dihydro-9,10-[1,2]benzenoanthracene library. * denotes novel compound.....179
Table 38: substituted 9,10-dihydro-9,10-[3,4]furanoanthracene-12,14-dione library.....184
Table 39: 9-vinyl-9,10-dihydro-9,10-[3,4]furanoanthracene-12,14-dione library. * denotes novel compound.....185
Table 40: IC_{50} value (BL cell lines DG-75 & MUTU-I) and Lipinski properties of leading nitrostyrenes Chapter 1.....210
Table 41: in vitro anti-proliferative activity of compounds 35, 36, 55, 57, 60, 61, 66, 85 in HeLa, MCF-7, HL60, Ramos and Bjab cell lines.....212
Table 42: IC_{50} of fludarabine, 85, 55 and 66 in the CLL cell lines Cll, HG3, I83 and PGA..... 214
Table 43: IC_{50} (BL cell lines DG-75 & MUTU-I) and Lipinski properties of leading heterocycles Chapter 2.....221
Table 44: IC_{50} values for most potent compounds in the MUTU-I cell line (24 h).....239

Table 45: IC_{50} (BL cell lines DG-75 & MUTU-I) & Lipinski properties of leading compounds Chapter 3 & Chapter 4.....240
Table 46: Compound 66: summary physiochemical properties.....255
Table 47: Compound 145: summary physiochemical properties.....256
Table 48: Compound 7: summary physiochemical properties.....257
Table 49: Compound 289: summary physiochemical properties.....259
Table 50: Compound 287: summary physiochemical properties.....259

Chapter 1.

Introduction

1.1 General Introduction

This thesis describes the synthesis and biochemical evaluation of antiproliferative agents specifically designed to target the malignancy Burkitt's lymphoma. Burkitt's lymphoma is a relatively rare disease in the developed world and its diagnosis is strongly associated with HIV. This malignancy has a high incidence in developing areas such as equatorial Africa; within these areas it accounts for over 50% of childhood cancers and up to 90% of childhood lymphomas diagnosed[18]. Treatment of this condition within these high incidence areas is inadequate and consequently the development of new safe, effective and economical therapeutics for Burkitt's lymphoma is of current interest.

1.1.1 Cancer – A Brief Overview

Cancer is defined as a group of diseases characterised by abnormal cell growth, resulting in the formation of malignant tumours. Cancer may spread into nearby tissues and metastasise (form areas of secondary growth). This uncontrolled and up-regulated cell growth is due to mutations in genes that control proliferation, differentiation and the cell cycle. It is because of these mutations that cancer cells no longer are subject to the signals that preside over the growth of normal (non-cancerous) cells[19]. The name 'cancer' originates from the Greek word 'carcinos' meaning 'crab' and was first drawn on by Hippocrates (460-370 B.C.) in the fifth century B.C. to describe the uncontrolled growth and spread of tissue throughout the body, eventually choking off life[20, 21].

Malignant cancers are grouped into several different categories; these categorisations are dependent on the cell type involved. Carcinomas are cancers of the epithelial cells and are the most common form of cancer; carcinomas account for approximately 90% of all cancers. Common carcinomas include urinary, lung, breast and colon cancer. Cancers of the connective tissue, bone, cartilage, fat and muscles are known as sarcomas. Other forms of cancers include leukaemias and lymphomas; these are cancers commonly derived from the white blood cells and the lymphatic system. The term leukaemia however is mainly used to describe the predominant proliferation of cancer cells throughout the bloodstream[20, 21].

In economically developed countries, cancer is the leading cause of death and the second most prevalent in developing countries[22]. Cancer is the second most common cause of death in Ireland (following diseases of the circulatory system), over the three year period 2010-2012, when annual averages of 36,000 new cancer cases were registered in Ireland. This corresponds to a 21% increase on the annual averages registered over the previous three year

period 2007-2009. The incidence rate for cancer in Ireland (2010-2012) was 878 cases per 100,000 persons per year. During this period the cumulative lifetime risk of invasive cancer was higher for males (1 in 3) than for females (1 in 4)[23].

Cancer prevalence in Ireland was quite high in comparison with other European states with females ranked 2nd and males ranked 4th. The incidence of cancer in Ireland over the period 2010-2012 was much higher than the European average, with male incidence 10% higher than average and female incidence 16% higher[24]. The most commonly diagnosed cancers in females were: breast (30.2%), colorectal (11.2%), lung (10.4%) and melanoma (5.3%). Whereas for males the most common cancers were: prostate (31.5%), lung (12.1%), melanoma (3.6%) and lymphoma (4.4%). During the 2010-2012 study period, 8,800 cancer deaths occurred annually within Ireland, with lung cancer identified as the leading cause of cancer death[23].

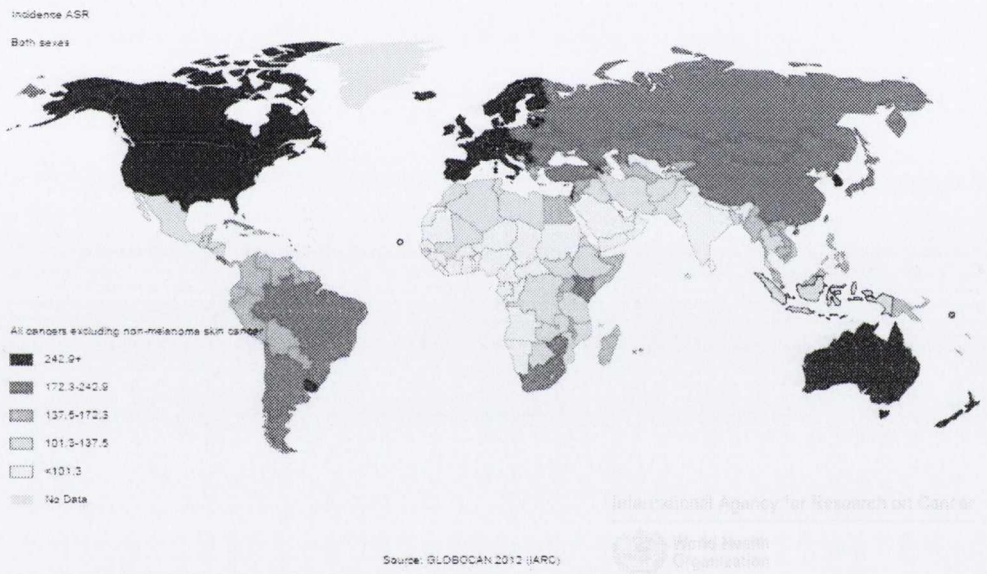

Figure 1: Incidence of cancers worldwide 2012 (excluding melanoma)[25]

The World Health Organisation estimated that in 2012 14.1 million new cases of cancer were diagnosed worldwide and cancer would lead to 8.2 million deaths. Overall lung, breast, colorectal and stomach cancers account for over 40% of all cancer cases diagnosed (Figure 1). Lung cancer was most prevalent in males (16.7% of new cases of cancer diagnosed), while breast cancer was most prominent in females (25.2% of new cases of cancer diagnosed). It is estimated that although only 44% of cancer cases are diagnosed in developing countries, these areas account for over 53% of cancer deaths[26].

1.1.2 Cancer and the cell cycle

Cancers are a complex family of diseases; in order for any given cancer to flourish there are a number of events critical to its development. The deregulation of the cell cycle is one such event, this deregulation leads to a number of consequences favourable for cancer development[27].

The eukaryotic cell cycle is a highly regulated sequence of stages in which a cell duplicates and divides its vast amount of DNA into two daughter cells. This cycle is pivotal to controlled cell growth and loss of its control can lead to genomic instability which is a significant feature in the development of cancers. There are four main stages in the eukaryotic cell cycle; the mitotic phase (M), gap phase one (G_1), the synthesis phase (S) and gap phase two (G_2). The cell cycle initiates in the mitotic phase. This process of cell division is composed of two main events; mitosis (nuclear division and allocation of copied chromosomes) and cytokinesis (complete cellular division).

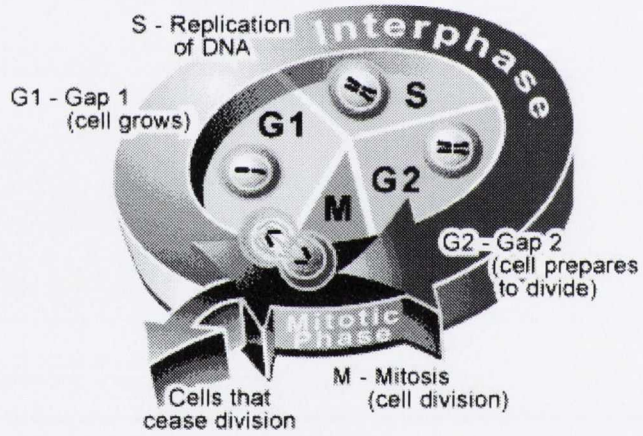

Figure 2: The Cell Cycle[28]

The first gap phase separates the mitotic and synthesis phases; this allows a period of cellular growth to occur. During this period of cellular growth, cells develop a stockpile of the organelles and proteins required for further cell division[20]. Chromosome duplication occurs during the synthesis phase; here nuclear DNA is replicated and synthesised over a period of 10-12 hours – approximately half the overall cell-cycle period. Gap phase two (similar to gap phase one) separates the synthesis and the mitotic phases[20, 21] (Figure 2).

1.1.3 Cell Death

Programmed cell death (PCD) is a vital process in which multicellular organisms maintain homeostasis of their tissues according to precise biochemical mechanisms. Cell death can occur by a number of mechanisms namely apoptosis, autophagy, necrosis, mitotic catastrophe, anoikis, exictotoxicity, Wallerian degeneration and cornification[29]. The three most common types of cell death are apoptosis (type I cell death), autophagy (type II cell death) and necrosis (type III cell death)[20].

Kerr et al. (1972) first used the word 'apoptosis', meaning 'falling leaves', to describe a particular morphological type of cell death - also known as type I cell death. The characteristics of type I cell death are rounding of the cell, retraction of pseudopodes, pyknosis (reduction of cell volume), karyorrhexis (fragmentation of nucleus), plasma membrane blebbing and there is little or no modification of the cytoplasmic organelles. In most cases, diagnosis of apoptosis is often accompanied by evidence of caspase activation or DNA fragmentation[30, 31]. Apoptosis can occur via two different pathways; intrinsic and extrinsic. The intrinsically activated pathway of apoptosis is dependent on cytochrome c release from the mitochondria and the extrinsic pathway is regulated by BCL-2 proteins. BCL-2 proteins control the release of cytochrome c and other pro-apoptotic proteins into the cytosol[20].

Autophagic cell death (type II cell death) also referred to as 'autophagy', is a process of cell decomposition. The word 'autophagy' is of Greek origin meaning 'self-eating'[21]. During autophagic cell death a cell's damaged or long-lived proteins and other essential components are degraded by its own lysomal machinery. Autophagic cell morphology is classified by a lack of chromatin condensation and large autophagic, double membraned vacuolization of the cytoplasm. These double membrane vacuoles encompass the degeneration of cytoplasmic organelles[29]. Necrosis (type III cell death) is a type of cell death with no evidence of autophagy or apoptosis. Necrosis morphology is that of oncosis, defining cell death with cytoplasmic swelling, plasma membrane rupturing, dilation of the cytoplasmic organelles and moderate chromatin condensation[29].

The classification of programmed cell death (PCD) is an area of fundamental importance in the development of potential cancer therapeutics. The aim of such research is to develop a selective therapeutic agent that will induce either apoptosis or autophagy. Cancer cells possess anti-apoptotic alterations which disrupt the signalling pathways within PCD, leading to cell immortalisation. These alterations can include anoxia, the activation of the myc

onocogene, deregulation of the pRB pathway, and an assortment of other DNA damage. BCL2 deregulation and deactivation is a common trait of mutations found in B-cell lymphomas and increased BCL2 expression is found in at least half of all human tumours[20, 32].

1.1.4 Treatment of cancer

The treatment of cancer is achieved through three modalities – surgery, radiotherapy and chemotherapy, either alone or in combination. The removal of the cancerous tissue is one of the oldest treatment avenues. Modern cancer treatment employs surgery for diagnosis, prophylaxis and treatment of neoplastic disease. Radiotherapy exposes cancerous cells to high frequency radio waves, inducing DNA damage and effectively impairing the ability of cancer cells to proliferate. Cancer chemotherapeutic agents are not always selectively toxic to cancer cells and exert a cytotoxic effect to healthy tissue. Chemotherapy drugs selectively affect tumour tissue due to the rapid proliferation of cells during cancer growth; this rapid cell growth makes them more susceptible to these drugs. Cancer chemotherapy is achieved by targeting a number of cellular targets such as tubulin, DNA, hormones, cellular metabolism and other biosynthetic pathways[33-36].

Chemotherapeutic agents can be categorised into seven main groups:

1. Alkylating & metal based agents
2. Antimetabolites
3. Antimicrotubule Agents
4. Topoisomerase inhibitors
5. Anti-hormonal agents
6. Monoclonal antibodies
7. Antibody drug conjugates

DNA alkylating agents are the oldest class of anticancer agents and were developed from the mustard gases used in World War I. Alkylating reagents are highly electrophilic reagents and interact with the bases in DNA. These compounds form strong irreversible covalent bonds and/or crosslink the DNA thus inhibiting transcription and replication of DNA. The alkylating agents as a class are considered non-specific, killing cells at various stages in the cell cycle. Common classes of alkylating agents are the mustards (e.g. melphalan and cyclophosphamide) (Figure 3). The platinum complex compounds also interact with DNA to prevent replication (e.g. Cisplatin and Carboplatin). These drugs are indicated for use with leukaemia, breast cancer, ovarian cancer and non-Hodgkin lymphoma[33-35].

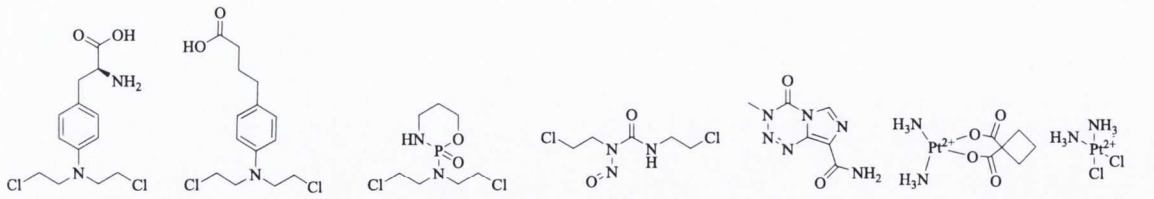

Figure 3: Cancer chemotherapeutic agents: Alkylating agents

Antimetabolites are a class of anticancer agent modelled to mimic natural molecules required for DNA or RNA synthesis (Figure 4). These compounds can lead to the inhibition of DNA and cell function. The first antimetabolite exploited was methotrexate in 1947 as a potent inhibitor of the enzyme dihydrofolate reductase, leading to complete remissions in children with acute lymphoblastic leukaemia. Other examples of the antimetabolite family are 5-fluorouracil, raltitrexed, gemcitabine, Ara-C and pentostatin. The antimetabolites are prescribed for use in the treatment of breast, neck, head, colorectal cancers, non-Hodgkins lymphoma and acute lymphocytic leukaemia[33-35].

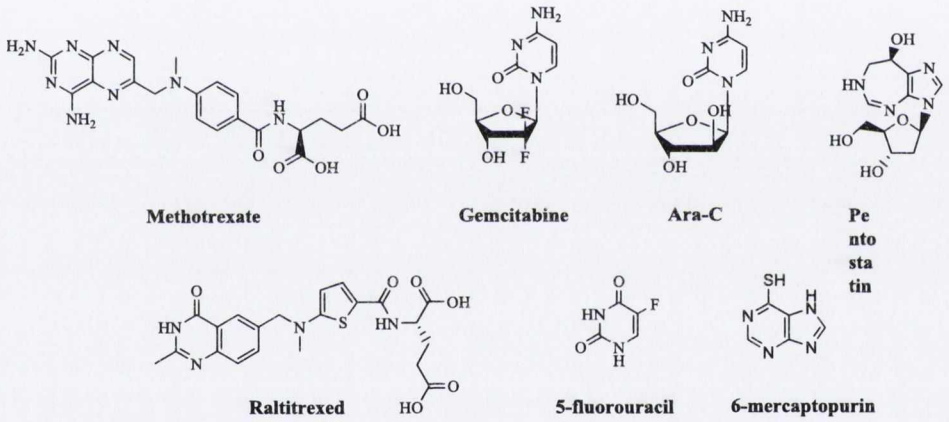

Figure 4: Cancer chemotherapeutic agents: Antimetabolite agents

The antimicrotubule agents are subdivided into two distinct classes; the Vinca alkaloids and the Taxanes. Vinca alkaloids such as vincristine and vinblastine are isolated natural products from the Madagascar periwinkles plant. These alkaloids bind to tubulin, inhibiting mitotic spindle assembly during mitosis thus preventing the migration of chromosomes and destabilising the process. The taxanes paclitaxel and doceltaxel were originally isolated from the Pacific yew tree (*Taxus brevifolia*) and bind to the β-subunit of tubulin and inhibit depolymerisation. This class of drugs are cell-cycle specific, targeting the G2/M phase. These drugs are typically indicated for the treatment of leukaemia, breast, ovary, testicular and lung cancers[33-35] (Figure 5).

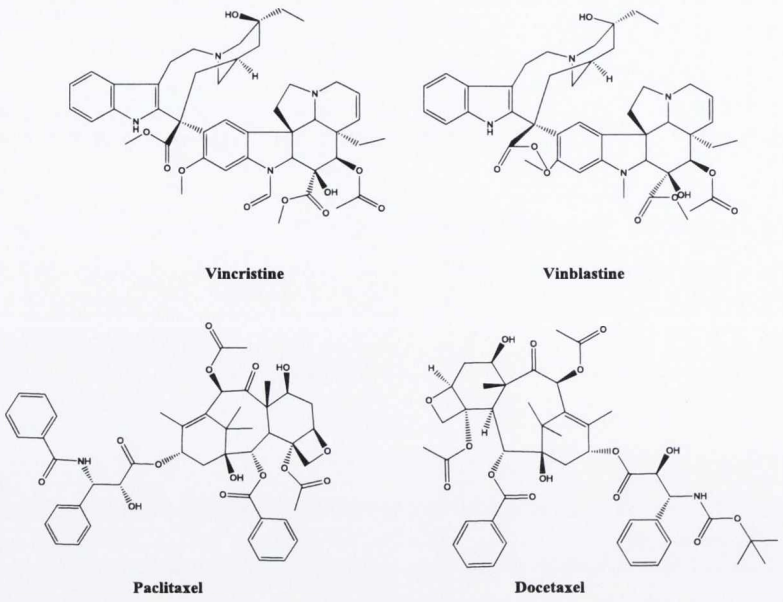

Figure 5: Cancer chemotherapeutic agents: Antimicrobule agents – Vinca Alkaloids & Taxanes

The topoisomerase inhibitors comprise of two families: those inhibiting topoisomerase I and topoisomerase II. The topoisomerases are enzymes critical to maintaining DNA topology during replication and recombination. Examples of topoisomerases I inhibitors are irinotecan and topotecan. Topoisomerase II inhibitors include doxorubicin, etoposide and mitoxantrone. These compounds are employed in the treatment of testicular cancer, sarcomas and paediatric solid tumors[33-35] (Figure 6).

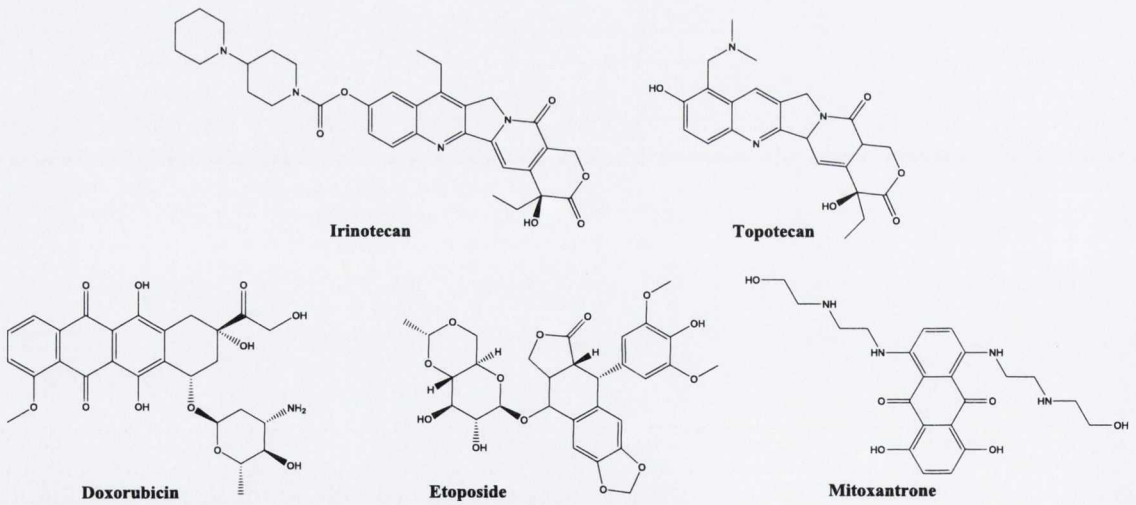

Figure 6: Cancer chemotherapeutic agents: Topoisomerase I & II Inhibitors

Hormone targeting cancer therapeutics take advantage of the dependence of tumours derived from hormone dependent tissues, such as the breast or prostate, for specific hormones. Anti-hormonal agents target and effectively sever the connection between these cancerous tissues and the essential hormones, inhibiting proliferation. Examples of anti-endocrine drugs used to

treat breast cancer are tamoxifen (oestrogen receptor antagonist) and anastrozole (aromatase inhibitor). In prostate cancer anti-androgens such as flutamide and bicalutamide and luteinising hormone releasing hormone analogues such as goserelin and leuprorelin are commonly used[33-35] (Figure 7).

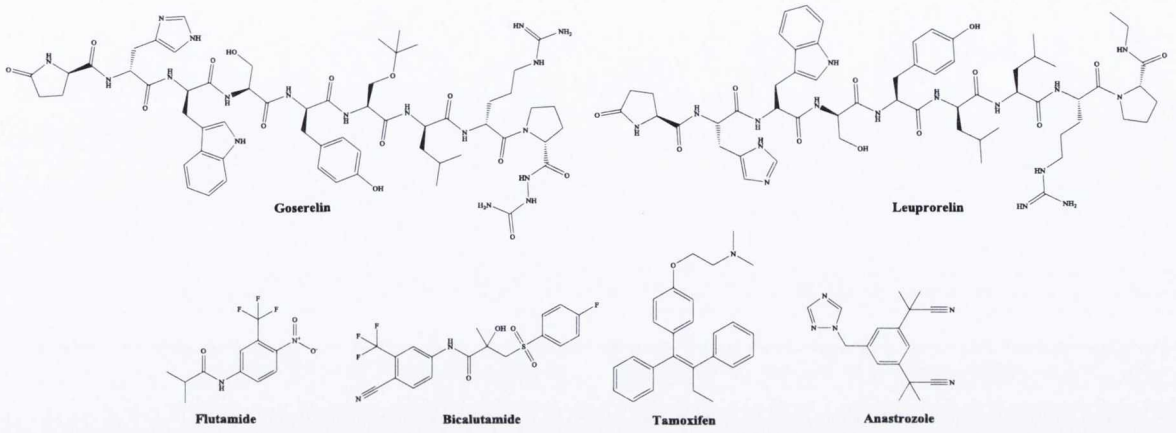

Figure 7: Cancer chemotherapeutic agents: Hormone targeting agents

Monoclonal antibodies (MABs) are genetically engineered immunoglobulins; these antibodies are produced by cloned immune cells of a unique parent cell either of mouse, human or chimeric origin. MABs exert their activity by recognising and reacting with specific molecular targets. Examples of MABs used in the treatment of cancer are gemtuzimab (myeloid leukaemia), alemtuzumab (B cell leukaemia) and rituximab (non-Hodgkin lymphoma)[37]. Antibody drug conjugates (ADCs) are a relatively new class of cancer therapeutics and by design provide a more targeted therapy for cancer. ADCs are composed of an antibody coupled via a stable chemical linker to an anticancer drug. Combining the targeted ability of antibodies with an anticancer drug enhances the potency of the treatment by attacking cancer cells in preference to healthy cells[38]. Brentuximab vedotin is an example of a chimeric ADC indicated for the treatment of Hodgkin lymphoma; this ADC is composed of the antibody linked to monomethyl auristatin E (MMAE)[39] (Figure 8).

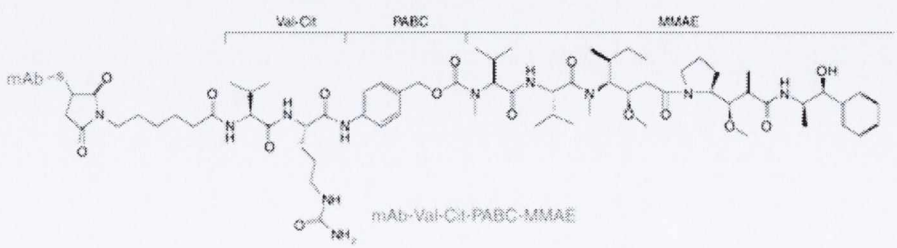

Figure 8: Brentuximab vedotin[39]

1.2 Burkitt's lymphoma

1.2.1 Introduction to Burkitt's lymphoma

Cancers of the lymphatic cells (lymphomas) account for approximately 3.2% of malignant diseases worldwide[25]. Lymphomas are cancers of the immune system and are categorised into two main types defined by the presence (or absence) of abnormal neoplastic cells (known as Reed-Steinberg cells) into Hodgkin lymphoma and non-Hodgkin lymphoma (NHL) respectively[40]. Non-Hodgkin lymphoma accounts for 84% of all lymphomas and is the 10th most common family of cancers with 386,000 new cases worldwide diagnosed in 2012[25]. In NHL, malignant white blood cells proliferate in an uncontrolled manner, impairing the body's ability to combat infections and disease. Burkitt's lymphoma is a high grade NHL, which manifests extra-nodally as fast growing, aggressive tumours typically on the jaws or abdomen composed of small non-cleaved B-cell lymphocytes[41].

Sir Albert Cook, a missionary doctor in Uganda at the start of the 20th century is attributed with the first description and illustration of BL[42] and in the early 20th century the incidence of jaw tumours amongst children in equatorial Africa was noted by several other pathologists[42-44]. BL was first formally described by Denis Parsons Burkitt, a British wartime surgeon while working in the Mulago Hospital in Uganda in 1958[45, 46]. Burkitt noted a distinctive, fast growing jaw malignancy (doubling time 24-48 h) occurring primarily in young children (5-12 years old) in tropical Africa[45]. By surveying the geographical distribution of the incidence of this distinctive malignancy, Burkitt and his co-workers identified a region of high incidence in sub-Saharan Africa (10° – 15° north and 10°– 15° south of the equator) which became known as the 'lymphoma belt' (Figure 9)[47].

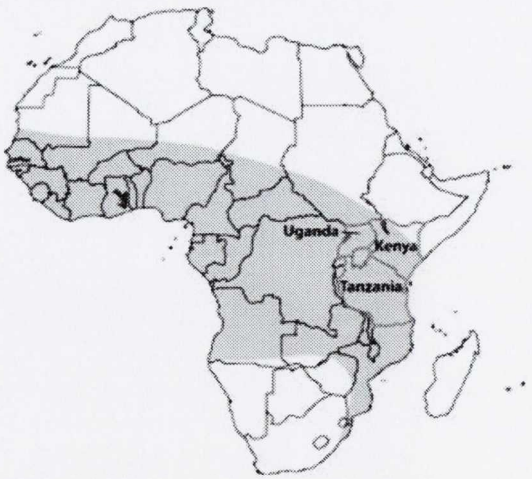

Figure 9: The 'lymphoma belt'

1.2.2 Classification of Burkitt lymphoma

Since this initial epidemiological work carried out by Burkitt, the World Health Organisation (WHO) classified BL as a non-communicable disease and subdivided BL into three distinct clinical presentations[48].

1. Endemic Burkitt's lymphoma (e-BL)
2. Sporadic Burkitt's lymphoma (s-BL)
3. Immunodeficiency related Burkitt's lymphoma (i-BL)

The endemic variant of BL was originally called 'African lymphoma' but was renamed due to perceived specificity of BL to the 'lymphoma belt', however with the recorded occurrence of BL outside the belt this term has become a misnomer. e-BL is mainly found within the tropical regions of equatorial Africa and Papua New Guinea, with an incidence of 40-50 per 1 million children (under the age of 18 years old)[49]. In these high risk regions BL accounts for approximately 50% of childhood cancers and up to 90% of childhood lymphomas diagnosed. Diagnosis peaks at 6 years of age and diagnosis is twice as common in male patients[18]. Due to the nature of healthcare available in these areas statistics are difficult to verify, as large numbers of patients do not reach care in time or diagnosis techniques are inadequate. A retrospective study of spatial distribution of e-BL in Kenya (Rainey et al. 2007) revealed that children in lakeland areas are twice as likely to contract BL than coastal dwellers and up to six times more likely to contract BL than children in arid regions[50].

Soon after Burkitt's 'lymphoma belt' was conceived, it was observed that the area defined overlaid with high correlation over regions of high malaria incidence in Africa, leading to the theory that malaria or some other infectious agent was causative or even contributory in the case of Burkitt's lymphoma[18, 47]. Malaria within these regions is holoendemic with over 75% of malaria related deaths worldwide taking place in the malaria belt[51]. *Plasmodium falciparum* is a parasite carried by mosquitoes, which is known to cause severe cases of malaria has also been strongly associated with e-BL and is present in up to 90% of children (< 5 years of age) in endemic areas[52]. In areas of high malaria infection, individuals experience multiple episodes of malaria during childhood; however only a fraction of these childhood malaria patients continue to develop BL[53]. While exploring the possibilty of malarial impact on BL, Burkitt observed that the incidence of BL in Tanzania changed significantly with the introduction of anti-malarial drug chloroquine over the period 1977-1982. A 2013 study of a cohort of BL patients in Malawi showed a correlation between *Plasmodium falciparum* and e-

BL, this study observed the presence of *Plasmodium falciparum* DNA in BL patient serum[54]. Malarial infection is known to induce B-cell hyperplasia, increasing B-cell antibodies, leading to eventual loss of B-cell memory and culminating in the activation of the B-cell memory compartment via plasmodium membrane protein CIDR1α. The net effect of repeated malarial infection is the immunosuppression of B-cell and T-cell responses; these include responses to viral infection[55, 56].

In 1964, virologists Anthony Epstein, Yvonne Barr and Bert Achong discovered a previously undocumented herpes-like virus in cultures of BL tumours sent to them by Burkitt. This herpes-like virus later became known as the Epstein-Barr virus (EBV) and was found to be present in over 90% of e-BL tumour cultures from the lymphoma belt[57]; however EBV was only present in 25% of patient samples from outside this region[58]. Tumour viruses are known to be at the root of several human cancers, for example the hepatitis B virus - liver cancer and the human papilloma virus – cervical cancer[59]. EBV infection typically occurs in early life and more often produces the symptoms of mononucleosis, however symptom free carriers have been observed. Infection is thought to occur orally through the saliva, infecting immature lymphoid tissues and persistent infection is established. A 2010 report on the global burden of five EBV attributed malignancies, reported 842,674 new cases of EBV-attributed malignancies (143,000 deaths) with 4,396 new cases of EBV+ BL (2,251 deaths)[51]. Although both malarial and EBV infection have a strong relationship with BL incidence, the absence of these factors in most cases outside of the 'lymphoma belt' left many questions unanswered to early BL researchers.

Sporadic Burkitt's lymphoma (s-BL) is essentially BL that occurs outside of the lymphoma / malaria belt and is quite rare with an incidence of 2 per million in North America, Europe and east Asia[60]. In Europe and North America s-BL accounts for 1-2 % of adult lymphomas and 30-40% of childhood non-Hodgkin's lymphomas. The sporadic variant is most common in children aged 3-12 years and manifestation in male patients is 3.5 times more common. As previously mentioned EBV positive s-BL is relatively rare with less than 25% of s-BL testing positive for the EBV. Typical s-BL manifestations include abdominal tumours but spreading of tumours into the bone marrow and / or central nervous system is common at diagnosis[58].

Immunodeficiency related Burkitt's lymphoma (i-BL) prevalence increased significantly since it was first reported by Ziegler et al. (1982) due to the spread of the human

immunodeficiency virus (HIV)[61]. This variant of BL was once 1000 times more common in North America prior to the use of antiviral treatments for HIV[62]. There is also increased risk of contracting i-BL 4 to 5 years after organ transplantation due to induced immunosuppression[63]. Although EBV+ i-BL is possible, only around 40% of America and European patients test positive for EBV. i-BL has been documented worldwide, occurring with an incidence of 22 per 100,000 in North America[64].

Therefore it is not the EBV or malaria that characterises BL, although both contribute through immunosuppression, but another underlying feature of the lymphoma. This characteristic feature first noted in 1975 by Zech et al. and was found in all types of BL, this is the reciprocal chromosomal translocation of the c-myc proto-oncogene from chromosome 8[65]. The translocation and subsequent activation of the deregulated c-myc to an immunoglobin locus (Ig) leads to cell growth with uncontrolled proliferation and genomic instability[66] (Figure 10). In healthy cells (Non-BL cells) the proliferative action of c-myc is counter balanced by the apoptotic p53 and BIM (Bcl2-like-protein 11) pathways.

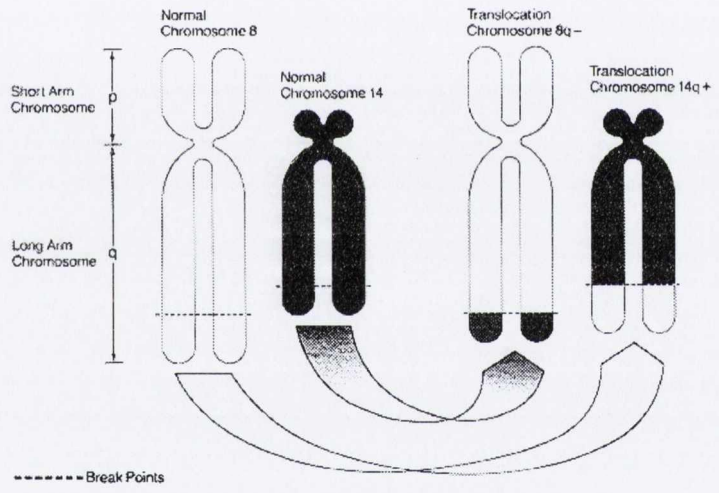

Figure 10: c-myc translocation from chromosome 8 to Ig locus chromosome 14

In EBV positive BL, it is observed that EBNA3A and EBNA3C (EBV nuclear antigens) inhibit the expression of BIM and therefore deregulate this pathway[67]. 30% of EBV positive tumours also possess p53 mutations which could also disrupt its apoptotic pathway[68].

1.2.3 Treatment of Burkitt's lymphoma

The treatment of BL involves high doses of chemotherapeutic agents, typically of the alkylating class. The chemotherapeutic standard for large diffuse B-cell lymphoma is known as CHOP (cyclophosphamide, doxorubicin, vincristine, and prednisone) and remains the leading treatment available for patients with advanced stage NHL[69, 70]. Despite the promising results obtained in B-cell lymphoma using the CHOP treatment, it has proven inadequate in the treatment of BL, with poor 2 to 5 year survival rates of 50-65%[71].

This has led to the development of multiple prospective treatment regimens for the specific treatment of BL, many of which have two year survival rates of 49 – 89%[72]. Magrath et al. (1996) in collaboration with the National Cancer Institute, proposed the CODOX-M/IVAC regimen of cyclophosphamide, vincristine, doxorubicin and methotrexate in tandem with cycling doses of ifosfamide, etoposide, cytarabine and intrathecal methotrexate and cytarabine (Figure 11). This regime gave excellent results with a two year survival rate of 89% in adults[73].

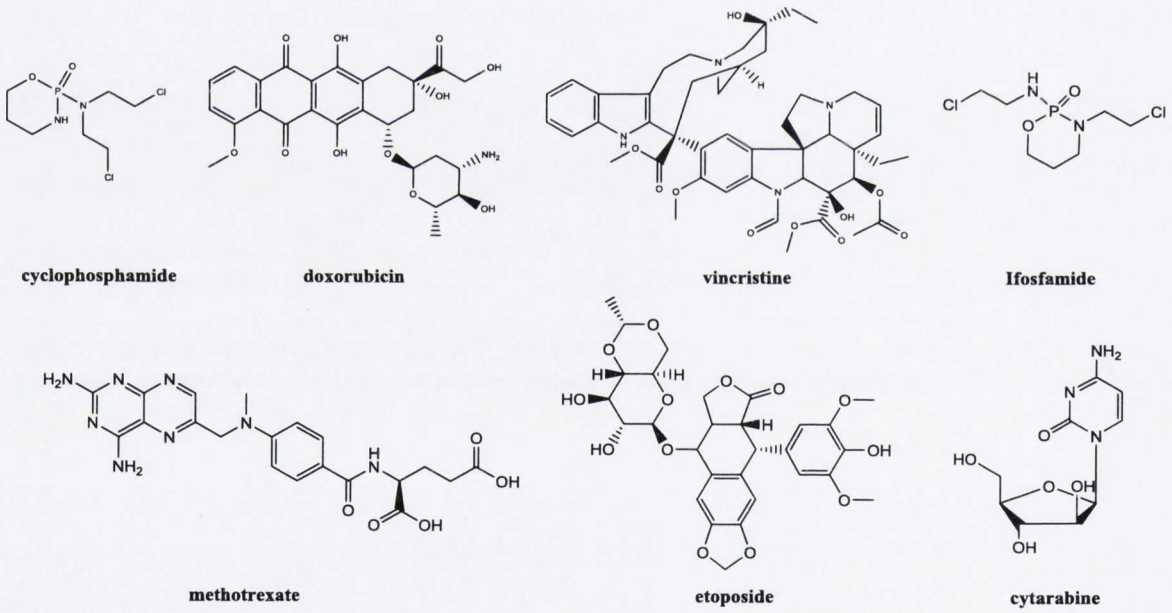

Figure 11: Components of Magrath's CODOX-M/IVAC regime

In more recent times, reduced toxicity versions of the CODOX-M/IVAC regime have been investigated with high 2 year survival rates of ~70%[74, 75] (Figure 11). Rituximab is an immunotherapeutic agent used in the treatment of CD20 positive diffuse B-cell NHL lymphoma, rheumatoid arthritis and other NHLs including stages III-IV follicular lymphoma.

Rituximab has been extensively studied in B-cell lymphoma and has been found to increase the overall survival when used to complement existing chemotherapeutic regimes[76, 77].

The monoclonal antibody rituximab has more recently and is currently being studied for the treatment of BL. Thomas et al. (2006) reported an 89% two year survival rate during implementation of the a dose adjusted Hyper-CVAD regime (cyclophosphamide, vincristine, doxorubicin and dexamethasone) with Rituximab, giving a vast improvement from his original Hyper-CVAD study in 1999[78, 79]. Rituximab has also been studied for the treatment of i-BL as part of a 33 day chemotherapeutic regime (cyclophosphamide, prednisone, rituximab, vincristine, methotrexate, isophosphamide, dexamethasone, teniposide, cytarabine, doxorubicin, vindesine and etoposide). Oriol et al. (2008) found that comparable survival rates could be achieved using the regime, between HIV positive BL patients and HIV negative patients[80]. Upcoming clinical trials involving the treatment of BL, implement dose established chemotherapeutic strategies with the addition of Rituximab[81, 82].

A number of potential therapeutics for BL are under development in academic research groups. Reddy et al. (2008) introduced the (*E*)-styrylbenzylsulfones as a series of potent antiproliferative agents and established activity of the lead structures in a number of cancer cell lines including the BL Raji (IC_{50} 4-9 nM), Daudi (IC_{50} 7-8 nM) and Namalwa (IC_{50} 4-9 nM) cell lines[83]. A series of amidinopiperidine based compounds bearing an N'-acyl-napthalene-2-sulfonohydrazine moiety developed by Gobec et al. (2012) induced a selective apoptotic and antiproliferative effect in the RAMOS and Daudi BL cell lines over PBMCs (peripheral blood mononuclear cells)[84]. Other promising studies include a novel series of 2-benzoxazoylhydrazones, which have been shown to inhibit cell proliferation in cancer cell lines including the BL cell line CA46 (EC_{50} 5-27 nM)[85, 86](Figure 12).

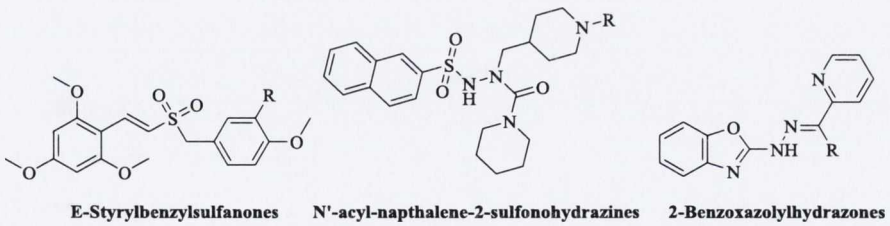

Figure 12: Therapeutics in development for the treatment of Burkitt's lymphoma

Phenothiazines such as chlorpromazine, trifluoroperazine and thioridazine were noted in a paper by Zhelev et al. (2004) to both suppress proliferation and induce apoptosis in BL lines Raji (IC_{50} 6.6-13.9 μmol/L) and Daudi (IC_{50} 10-23.7 μmol/L)[87]. The novel indole based compound NecroX-7 is a nitrogen and oxygen reactive oxygen species scavenger and has

recently been shown to induce G2/M arrest in BL cell lines (RAMOS & Daudi)[88, 89] (Figure 13).

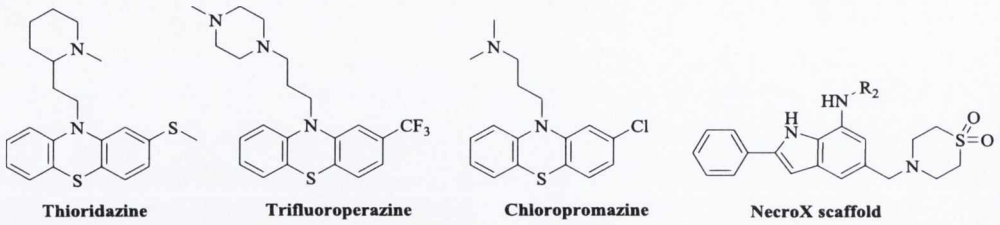

Figure 13: Therapeutics in development for the treatment of Burkitt's lymphoma

Meredith et al. (2005) identified the SERT substrates MDMA, fluoxetine and clomipramine as potent anticancer agents for the treatment of sertogenic B cell malignancies including BL (L3055 & KHM-2B cell lines)[90]. In 2010 Gandy et al. developed a series of non-psychoactive methylenedioxymethamphetamine (MDMA) analogues that exhibited potent activity in BL cell lines. The lead compounds from this study included a naphthalene group at the R-1 position and gave IC_{50} of 6.6-12.6 μM in the SH-SY5Y neuroblastoma cell line[91].

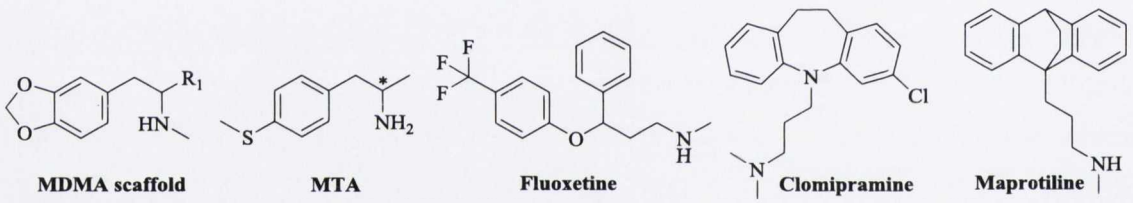

Figure 14: Therapeutics in development for the treatment of Burkitt's lymphoma

Subsequent studies on the antiproliferative activity of amphetamines such as MTA, MDMA and the antidepressants fluoxetine and maprotiline, have shown that these compounds exhibit potential as pro-apoptotic agents for the treatment of BL (MUTU-I, DG75 cell lines)[6, 92-94] (Figure 14).

1.3 Antidepressants

'Antidepressant' is an umbrella term use to collectively describe drugs used for the treatment of mood disorders such as major depression, dysthymic disorder and bipolar disorder. Mood disorders are debilitating and can lead to the development of the following symptoms: sustained melancholia, sleeplessness, restlessness, anxiety and poor concentration. Antidepressant drugs can be sub-categorised by both their mode of action and structural type into the following groups[95, 96]:

1. Tricyclic and tetracyclic antidepressants (TCAs)
2. Selective serotonin reuptake inhibitors (SSRIs)
3. Noradrenaline reuptake inhibitors (NARIs)
4. Monoamine oxidase inhibitors (MAOIs)
5. Miscellaneous agents

Tricyclic and tetracyclic antidepressants (TCAs) were historically the first class of compounds utilised for the treatment of depression, TCAs share many pharmacodynamic and pharmacokinetic properties, as well as inducing many of the same side effects. Examples of some TCAs are presented in Figure 15. Although their mechanism of action is not well understood, it is believed the TCAs induce their antidepressant effects by increasing the concentration of NET, SERT and DAT in the central nervous system by inhibiting their reuptake[93, 97]. More recent research has shown that prolonged use of these TCAs induce hypersensitisation of β-postsynaptic and α-presynaptic receptors.

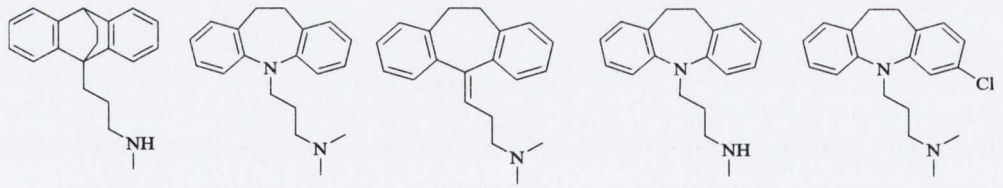

Maprotiline **Imipramine** **Amitriptyline** **Desipramine** **Chlorimpramine**

Figure 15: Tricyclic and tetracyclic antidepressants (TCAs) for treatment of depression

This class of antidepressants are indicated for use with major depressive disorders, anxiety, obsessive compulsive disorder (OCD) and for chronic pain treatment. The TCAs are attributed with a plethora of undesirable side-effects including but not limited to dizziness, insomnia, agitation, drowsiness, headaches, bodyweight increase, photosensitization and constipation[98, 99].

The second class of antipressants, the Selective Serotonin Reuptake Inhibitors (SSRIs) include compounds such as citalopram, fluoxetine, paroxteine and sertraline (Figure 16). These

compounds induce much less undesirable side effects due to their more selective mechanism of action. SSRIs selectively target and inhibit the reuptake of 5-hydroxytryptophan (5-HT), thus increasing the concentration of 5-HT at the synapse.

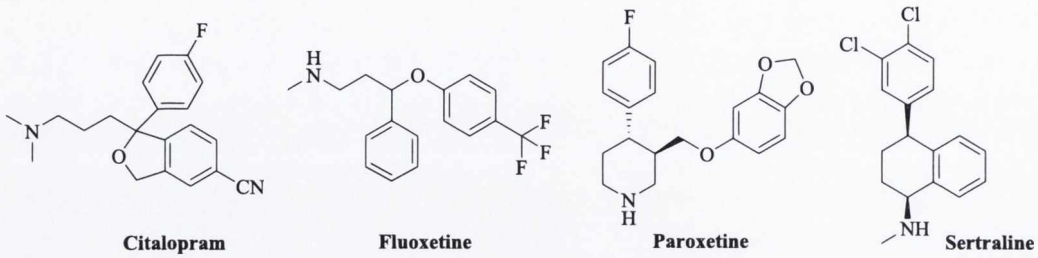

Figure 16: Selective serotonin reuptake inhibitors (SSRIs) for treatment of depression

SSRIs are also indicated for use with major depressive disorder, bipolar disorder, moderate depression, OCD and bulimia nervosa. Adverse effects have also been recorded and amongst these gastrointestinal, restlessness, insomnia, tremors and decreased libido are listed[98, 99].

Nisoxetine and reboxetine are selective noradrenaline reuptake inhibitors (NARIs) prescribed for the treatment of all types of depression and have low affinities to other receptors (Figure 17).

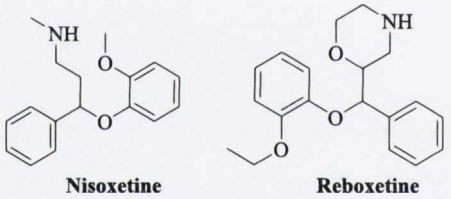

Figure 17: Noradrenaline reuptake inhibitors (NARIs) for treatment of depression

Sedation and motor slowdown are not included in the adverse effects of these compounds, however in older patients dry mouth, constipation, vertigo and insomnia have been noted[98, 99].

Monoamine oxidase inhibitors (MAOIs) tranylcypromine and phenelzine impose their antidepressant effect on the MAO enzyme, the enzyme charged with the degradation of monoamines. This leads to increased monoamine concentration (for example 5-HT) at the synapses (Figure 18).



Figure 18: Monoamine oxidase inhibitors (MAOIs) for treatment of depression

MAOIs are indicated for use in the treatment of atypical depression. MAOIs are more tolerated by the body than TCAs and lead to lesser side effects but infrequently lead to digestive problems (nausea, vomiting), sleep disturbances and anxiety[98, 99].

A range of other miscellaneous agents are also associated with the treatment of depression (Figure 19). Lithium and lithium salts are regularly used for the treatment of depression since the 1930s. Lithium alters cation transport across cell membranes, impairing the ability of SERT and NET reuptake. Divalproex sodium is generally used for the treatment of epilepsy but can also be used for the treatment of depression. The mechanisms of action for viloxazine and bupropion are unclear but they have no effect on MAO and a small influence on SERT and NET reuptake[98, 99].

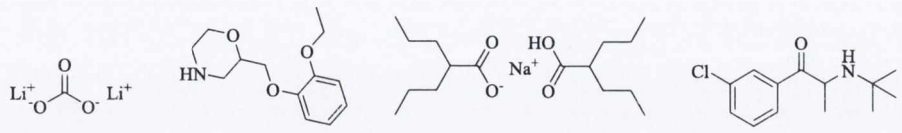

Lithium carbonate **Viloxazine** **Divalproex sodium** **Bupropion**

Figure 19: Miscellaneous agents for treatment of depression

1.4 Maprotiline

The noradrenaline reuptake inhibitor maprotiline contains a tetracyclic core structure bearing a secondary amine side chain at C-9 (Figure 20). Tatsumia et al (1997) elucidated the selectivity factor of maprotiline for the various human monoamine transporters by calculating a ratio of the respective equilibrium dissociation constants, this study demonstrated the potent affinity of maprotiline towards NET when compared to SERT and DAT affinities[100]. The influence of maprotiline is not limited to the aforementioned transporter and effects have been documented on muscarinic, α-adrenergic and β-noradrenergic receptors[101]. Side effects associated with maprotiline use include skin rashes, seizures, headaches and drowsiness[98]. Maprotiline is no longer used as a therapeutic agent for the treatment of depression since the emergence of newer, more effective classes of drugs such as the SSRIs. More recent publications have highlighted some of the further biological activities possessed by this tetracyclic antidepressant[6, 93, 94].

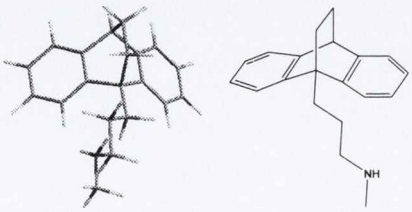

Figure 20: Maprotiline

Maprotiline (IUPAC name 3-(9,10-ethanoanthracen-9(10H)-yl)-N-methylpropan-1-amine) is a TCA that was patented by the Swiss company Ciba-Giegy (now Novartis) in the 1960's[102] and was subsequently launched under the brand name 'Ludomil' for the treatment of depression in 1975[97]. Wilhelm et al. (1969) published both a paper and a patent for the synthesis of maprotiline and these publications outlined two different routes for the synthesis. In both cases the two initial steps of the synthetic route prepare 3-(anthracen-9-yl)propanoic acid from anthrone. These initial steps involve the base catalysed Michael addition of anthrone to acrylonitrile and *in situ* acid hydrolysis to give 3-(10-oxo-9,10-dihydroanthracen-9-yl)propanoic acid. A subsequent dissolving metal reduction (zinc in ammonia) affords the required 3-(anthracen-9-yl)propanoic acid (Figure 21).

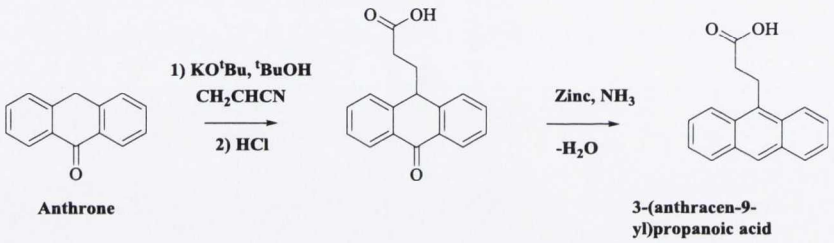

Figure 21: Overall scheme for the synthesis of 3-(anthracen-9-yl)propanoic acid from anthrone

From this 3-(anthracen-9-yl)propanoic acid starting material Wilhelm et al. have outlined two strategies (Route A & Route B), both involving a series of similar functional group transformations. The contrasting feature differentiating the two approaches is the juncture at which the Diels-Alder addition of ethylene is implemented (Figure 22).

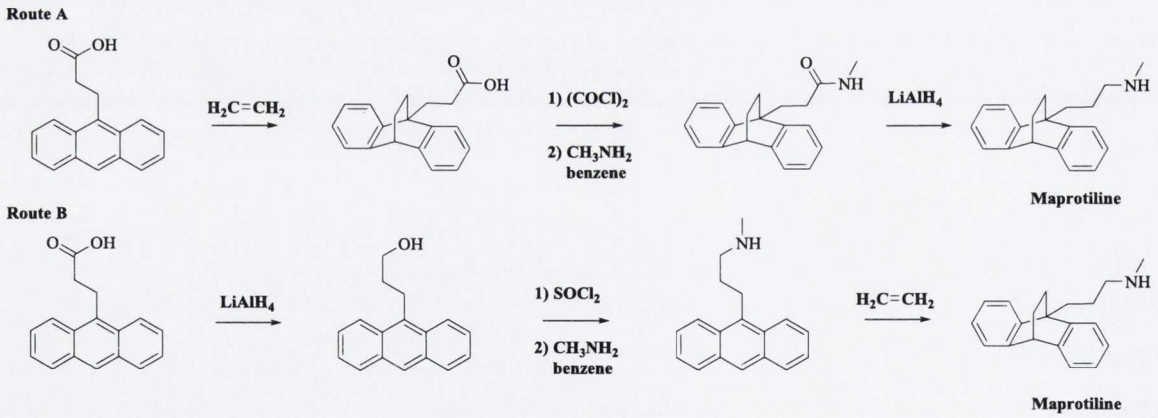

Figure 22: Overall synthetic routes (A & B) for the synthesis of maprotiline from 3-(anthracen-9-yl)propanoic acid

Route A commences with the Diels-Alder addition of ethylene (50 atm, 150 °C) to the diene system provided by 3-(anthracen-9-yl)propanoic acid. The acid Diels-Alder adduct is converted to the corresponding acid chloride using oxalyl chloride and subsequent nucleophilic substitution with methylamine affords the methyl amide. Reduction of this methyl amide with

lithium aluminium hydride leads to the formation of the desired product maprotiline. Route B initiates with the lithium aluminium hydride reduction of 3-(anthracen-9-yl)propanoic acid to the corresponding alcohol. 3-(Anthracen-9-yl)propan-1-ol is then refluxed with thionyl chloride to give 9-(3-chloropropyl)anthracene; the chloride is then subjected to nucleophilic substitution by methylamine yielding 3-(anthracen-9-yl)-N-methylpropan-1-amine. A high pressure Diels-Alder addition of ethylene (50 atm, 150 °C) to a solution of 3-(anthracen-9-yl)-N-methylpropan-1-amine in toluene affords the target compound maprotiline[102, 103]. Production of maprotiline analogues bearing triptycene and 9,10-dihydro-9,10-propanoanthracene rings instead of the typical tetracyclic system have also been documented[104, 105].

Maprotiline and maprotiline analogues have been intensively studied in recent publications outlining other biological properties of this tetracyclic structure such as anti-cancer[6, 93, 94, 106, 107], anti-inflammatory[108] and multi-drug resistance reversal[109-114]. The development of anti-cancer therapeutics that can evade, neutralise or reverse multi-drug resistance is of critical importance. Drug efflux pumps p-glycoprotein and cancer resistant protein are over expressed in many malignant diseases and eliminate the potential therapeutic from the target cell. Maprotiline has been shown to reverse multidrug resistance. Szabo et al. (1999) demonstrated the reversal of multidrug resistance in leukemic tumour cell lines (L121C MDR, L5178 MDR) and leukemic patient samples[109]. The reversal of chloroquine resistance in *Plasmodium falciparum* strains by TCAs was first noted by Bitonti et al. (1988) [110]. More recent work led to the development of a library of dihydroanthracene derivatives based on maprotiline for use as chemosensitizers in *Plasmodium falciparum* strains (Figure 23)[111-114].

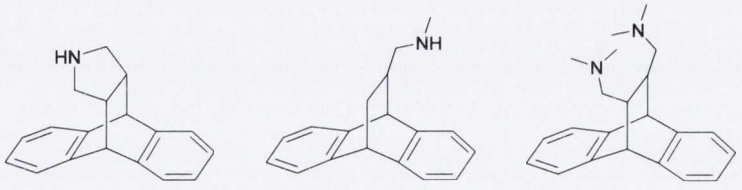

Figure 23: Lead compounds for the reversal of chloroquine resistance

The anti-depressants maprotiline, fluoxetine, desipramine, chlomipramine, amitriptyline and imipramine (Figure 15) have also been shown in recent literature to elicit anti-proliferative and apoptotic effects in a range of cancer cell lines[93, 94, 115-128]. The anti-proliferative effect of maprotiline has been documented in human prostate cancer cell lines and in murine neuroblastoma cells. Hsu et al. (2004) quantified the increase in extracellular and intracellular Ca^{2+} ion concentration in PC3 human prostate cancer cells induced by maprotiline and suggested that this increase in concentration may modulate cancer cell proliferation[106]. In

the Neuro-2-a murine neuroblastoma cells maprotiline induced the activation of caspase-3, an increase in Ca^{2+} ion concentration, ERK phosphorylation and ultimately apoptosis[107].

The antidepressants maprotiline and fluoxetine have furthermore been shown to induce programmed cell death in the chemo-sensitive BL cell line MUTU-I and autophagic cell death type II in the drug resistant BL cell line DG-75 (EC_{50} of 5.9-15.3 μM, treatment time 72 h)[94]. Further work in these BL cell lines by Cloonan et al. (2010) has shown that SERT and NET are not directly involved in the maprotiline mediated cell death pathway[93]. Previous work within our group involved the synthesis and biochemical evaluation of a series of maprotiline analogues for the treatment of BL. Structural modifications of the dihydro-ethanoanthracene structure at the heart of maprotiline, led to the development of a panel of compounds with potent caspase-dependant apoptotic activity in BL cell lines. The leading anthracene and dihydro-ethanoanthracene compounds exhibited promising EC_{50} values ranging from 3-31.5 μM in the MUTU-I when compared to maprotiline which gave an EC_{50} value of 15.8 μM. In the DG-75 chemoresistant cell line the lead compounds gave promising EC_{50} values ranging between 1.5-10.2 μM when compared to maprotiline which gave an EC_{50} value of 37.5 μM (Figure 24). This panel of compounds were also shown to induce apoptosis in a dose dependant manner and to circumvent multi-drug resistance in HL-60 MDR, indicating that these maprotiline analogues are not substrates for the drug efflux pump.

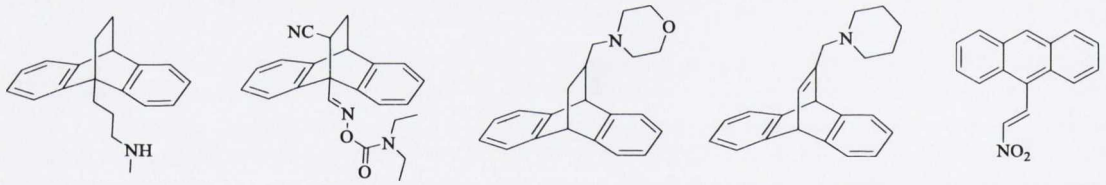

EC_{50} MUTU-I 15.8 μM
EC_{50} DG-75 37.5 μM

EC_{50} MUTU-I 28.4 μM
EC_{50} DG-75 3.1 μM

EC_{50} MUTU-I 23.5 μM
EC_{50} DG-75 8.8 μM

EC_{50} MUTU-I 31.5 μM
EC_{50} DG-75 10.2 μM

EC_{50} MUTU-I 3.0 μM
EC_{50} DG-75 1.5 μM

Figure 24: Lead maprotiline analogues (and their EC_{50} values) for treatment of Burkitt's lymphoma from previous study[6]

Amongst these leading maprotiline analogues was (*E*)-9-(2-nitrovinyl)anthracene eliciting a pro-apoptotic effect and giving EC_{50} values of 1.5 μM in the DG-75 cell line and 3.0 μM in the MUTU-I cell line[6]. Aryl nitrovinyl compounds have been previously shown to exhibit potent antiproliferative effects[1-17]. The inclusion of vinyl and nitrovinyl functionalities in future maprotiline analogues is of significant interest both synthetically and biologically.

1.5.1 Nitrostyrenes

The nitrostyrenes (IUPAC name (2-nitrovinyl)benzenes) are a family of compounds composed of an alkene double bond with a nitro substitution at C-2 and a phenyl ring at position 1 of the alkene. This alkene bond is extremely electron deficient due to the electron withdrawing effect of the nitro group, making the nitrostyrenes excellent Michael acceptors (Figure 25)[129]. Aliphatic nitro compounds provide organic chemists with an intermediate of immense potential. The nitro substituent can easily undergo a number of transformations furnishing the respective amines[130, 131], amides[132], carbonyl compounds[133], hydroxylamines[134], nitrones[135] and nitronates[136]. The nitro group as a substituent is an extremely electron withdrawing group and is unreactive as an electrophilic centre.

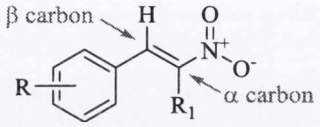

Figure 25: Nitrostyrene scaffold

The earliest syntheses of nitrostyrene derivatives were published in 1884, when Erdmann et al. nitrated and decarboxylated 4-phenylbut-3-enoic acid to give the desired nitrostyrene[137]. Priebs et al. (1884) also published his synthesis of nitrostyrene using N-(1-ethoxycarbonyl-propen-2-yl)urea, benzaldehyde and nitromethane[138]. Since these pioneering publications the synthesis of a diverse range of nitrostyrenes has been achieved via the nitration of styrenes[139-141], the nitro-Hunsdiecker nitrodecarboxylation[142], dehydration of the required 2-nitro-1-phenylethan-1-ols and the Wadsworth-Emmons reaction[143, 144]. The most popular and perhaps most amenable method for the production of these compounds is the base catalysed (typically cyclohexylamine[5], butyl amine[145], ammonium acetate[146] or piperidine[147]) Henry-Knoevenagel condensation of nitroalkanes with aldehydes and ketones[148]. In fact, from review of the Elservier's REAXYS database, selecting a cohort of 1053 published nitrostyrene syntheses, over 60% of authors utilised the Henry-Knoevenagel condensation. The second most popular route to the nitrostyrenes in this analysis was the dehydration of the required 2-nitro-1-phenylethan-1-ol[149] with just under 9% of the total published routes[150]. Negishi et al. (1988) extracted and identified nitrostyrene from commercial smoked chicken[151].

Utilising different nitroalkanes and benzaldehydes during the Henry-Knoevenagel condensation permits the variation of phenyl substitution and substitution at the alpha position, common substitutions include benzyl, methyl and ethyl[6, 152]. Similarly substitution at the beta carbon can be altered by utilising ketones such as acetophenone during this condensation reaction to introduce different alkyl groups[148]. The Henry-Knoevenagel condensation of

heterocyclic aldehydes has also been achieved, introducing moieties such as thiophene[147], furan[153], naphthalene[154] and anthracene[155] instead of a substituted (or unsubstituted) phenyl ring. The Henry-Knoevenagel condensation has been accomplished under a variety of different conditions including but not limited to microwave assisted synthesis[154, 156], ultrasound accelerated synthesis[157], solvent-less (neat reagents)[26], gel entrapped base catalysis[158], ionic liquid promoted[159] and utilising green aqueous conditions[149]. Nitrostyrenes like many alkene systems can exist as either *cis* (*Z*) or *trans* (*E*) isomers, however the *trans* (*E*) conformation predominates as it is sterically favoured. The formation of this *trans* (*E*) adduct can be verified by ^{1}H NMR or X-ray crystallography[160-163] (Figure 26).

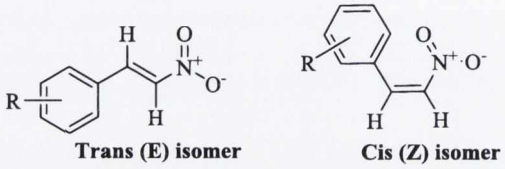

Figure 26: Trans & Cis isomers of the nitrostyrenes

The nitrostyrenes act as an intermediate in the synthesis of a myriad of organic compounds. Reduction reactions of nitrostyrenes with sodium borohydride and lithium aluminium hydride yield the corresponding nitroalkanes[164] and amines[165] respectively. These nitroalkanes can then be utilised in further Henry-Knoevenagel condensations or to synthesise carbonyl compounds using the NEF reaction[133]. A nitro-Mannich reaction of the nitroalkanes formed and imines can lead to the rapid generation of a multi-functional moiety[166, 167]. The amine derivatives can be reacted with aldehydes and acid chlorides to afford corresponding acetamide derivatives[168, 169] (Figure 27).

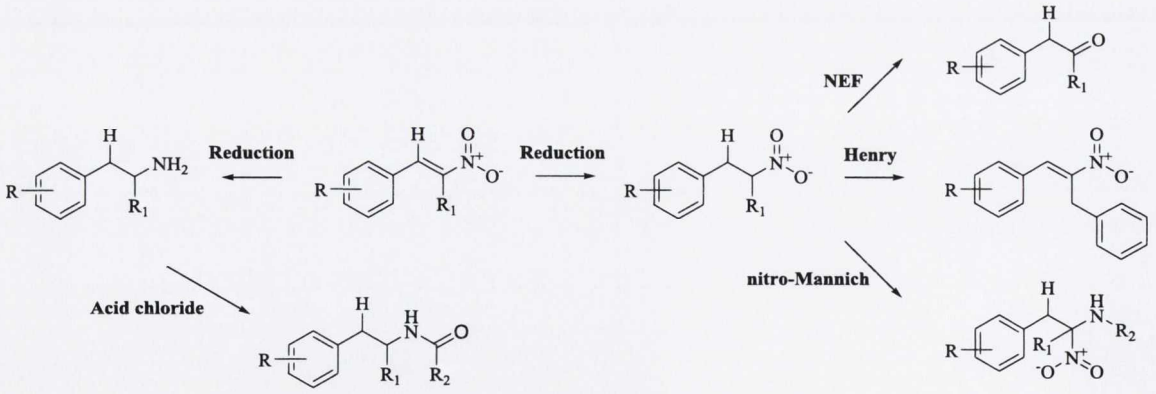

Figure 27: Transformations of the nitrostyrenes

The electron deficient alkene bond is key to many of the transformations available to this class of compounds, and this core scaffold is an excellent substrate for the Michael or conjugate addition. Michael additions of carbon, nitrogen, oxygen and sulfur nucleophiles to a

diverse range of nitrostyrenes are reported[3, 170]. Michael addition facilitates and accelerates the typically slow Morita-Baylis Hillman addition to the nitrostyrenes[171]. This property is then further exploited in the tandem-Baylis-Hillman cyclisation reaction that leads to the formation of 3-nitrochromenes and 3-nitroquinilones[145, 172]. Friedel-Crafts alkylation[173] and esterifications[174] of the Baylis-Hillman adduct of nitrostyrene and formaldehyde have also been achieved (Figure 28). These transformations will be further discussed in Chapters 2 and 3.

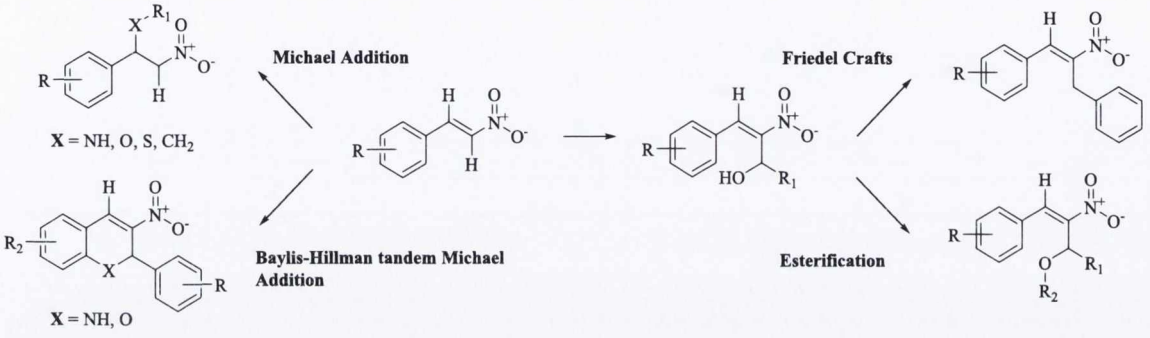

Figure 28: Transformations of the nitrostyrenes

Conjugate addition of azides to nitrostyrenes leads to triazole formation[175, 176]. Epoxides of the nitroalkenes can be formed with relative ease in the presence of peroxides and basic conditions and have been utilised to form 2-nitro-1-phenylethan-1-ones[177]. Nitroalkenes have also be used as dienophiles in the Diels-Alder reaction and Diels-Alder adducts with anthracene and other diene systems have been reported[178]. Other [4+2] cycloadducts of the nitroalkenes have been prepared, by reacting the nitrovinyl compounds with compounds such as cyclopentadiene and N-morpholinocyclohexene[179]. Oxidation of aryl methoxy substituted nitrostyrenes leads to the formation of nitrovinyl benzoquinones, which in turn can be used to generate poly-cyclic molecules of biological interest[180] (Figure 29).

Bromination of the vinyl bond of nitrostyrenes provides brominated nitro compounds susceptible to further modification by nucleophilic substitution[11] and Suzuki coupling[181]. The reaction of the vinyl unit with Grignard reagents has also been achieved, giving Michael-like adducts, oximes, carboxylic acids and acids[182]. The Stetter reaction can also be applied to these nitrostyrenes, reacting the activated nitrovinyl bond with an aldehyde, facilitating the introduction of a carbonyl substituent at the beta carbon[183, 184] (Figure 29).

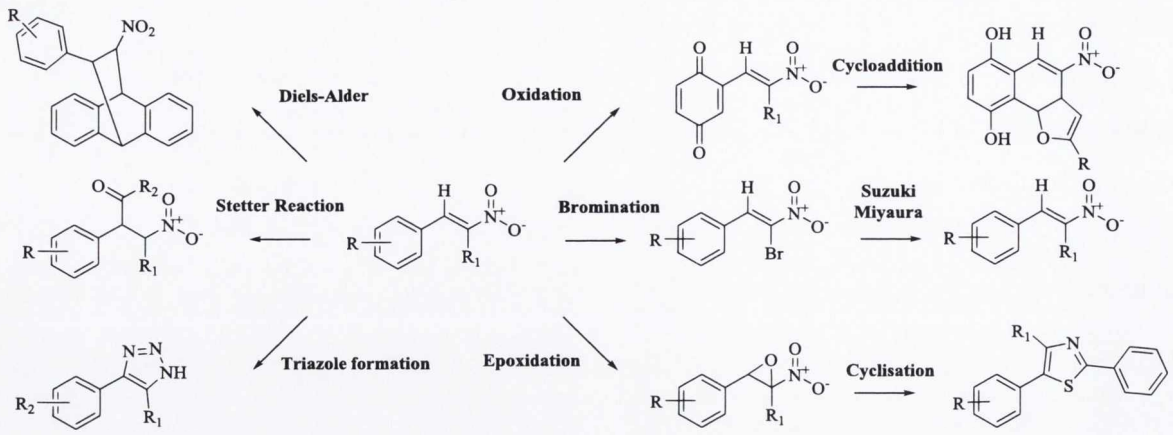

Figure 29: Transformations of the nitrostyrenes

1.5.2 Biological activity of nitrostyrenes

Nitrostyrenes and nitrostyrene derivatives have interested researchers over several decades due to their diverse biological activities, these include antimicrobial (antifungal & antibacterial)[14, 15, 161, 185-190], antiinflammatory[2] and insecticidal[191] properties. These compounds are also known to down-regulate the immune responses by suppressing IL12, IL6 and nitric oxide production[192]. Ramos et al. (1997) also noted a significant mutagenicity associated with these nitroalkene species in *Salmonella typhimurium* strains[11]. Nitrostyrene derivatives have also been reported to induce anti-cancer effects and stimulate an apoptotic response in a range of cancer cell lines[1-17]. For example recent literature details nitrostyrenes with pronounced anticancer activity in Burkitt's lymphoma[5, 6], rat pituitary cancer[3], colon cancer[9], osteosarcoma[1] and Erlich ascetic tumour cell lines[7].

The inhibition of tubulin polymerisation is a mechanism of action for several anti-cancer drugs, these include vinblastine, vincristine, colchicine and paclitaxel. These therapeutic agents bind to tubulin destabilising the microtubules leading to the inhibition of cell mitosis[193]. Pettit et al. (2002) demonstrated the concentration and time dependent fungicidal properties and cancer cell growth inhibition by the (*E*)-1,2,3-trimethoxy-5-(2-nitrovinyl)benzene (A). This compound features a 3,4,5-trimethoxy aryl motif which is characteristic of many tubulin targeting compounds such as combretastatin and as part of the study weak tubulin interactions were recorded[15] (Figure 30).

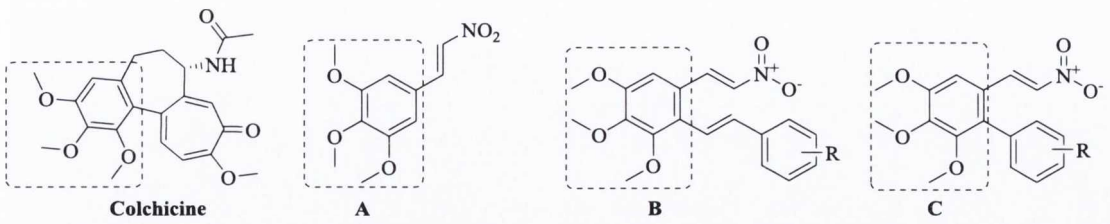

Figure 30: Tubulin binding agents (Colchicine, (*E*)-1,2,3-trimethoxy-5-(2-nitrovinyl)benzene, 1,2,3-trimethoxy-5-((*E*)-2-nitrovinyl)-4-((*E*)-styryl) scaffold and (*E*)-2,3,4-trimethoxy-6-(2-nitrovinyl)-1,1'-biphenyl scaffold)

Following this initial study, Pettit et al. (2009) synthesised a series of related nitrostyrenes designed for the inhibition of tubulin. The lead compounds from this study gave tubulin inhibition IC_{50} of <10 μM and exhibited potent cancer inhibition in breast, pancreas, lung, colon, prostate and renal cancer cell lines[14]. Jain et al. (2011) and Reddy et al. (2011) successfully introduced series of biphenyl nitrostyrenes (C) and resveratrol based (B) nitrovinyl stilbenes respectively as potent tubulin binding anticancer agents. Both studies presented anticancer potential for their compounds in HeLa, MCF-7, A549 and SK-N-SH cell lines[4, 10].

Telomeres protect chromosomal DNA molecules, preventing end-to-end fusion of DNA molecules and ensuring consistent cell function is maintained including programmed cell death. In cancer cells the up-regulation of telomerase activity leads to the shortening of telomeres and eventual deprotection of these DNA molecules leading to the immortalisation and proliferation of cancer cells[40, 194]. Kim et al. (2002) screened a small library of nitrostyrenes for the inhibition of human telomerase, identifying (*E*)-1,3-dichloro-5-(3-(2-nitrovinyl)phenoxy)benzene as a potent telomerase inhibitor (IC50 ~0.4 μM) (Figure 31). This work demonstrated telomerase inhibition at concentrations that were not cytotoxic to normal cells, with no inhibition effect on DNA and RNA polymerases[12, 13].

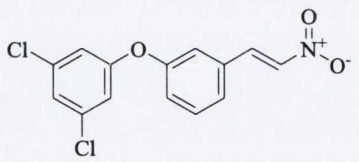

(*E*)-1,3-dichloro-5-(3-(2-nitrovinyl)phenoxy)benzene

Figure 31: (*E*)-1,3-dichloro-5-(3-(2-nitrovinyl)phenoxy)benzene a lead compound for the inhibition of human telomerase

Park et al. (2004) identified a panel of nitrostyrenes as a class of reversible, covalent protein tyrosine phosphatase (PTP) inhibitors[195]. PTPs have been implicated in antibacterial

properties[186] as well as in many aspects of cell growth, differentiation, mitosis and in the immortalisation of cancer cells, thus the study of PTP inhibition is of interest[40].

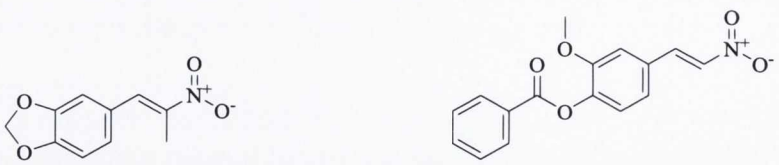

(*E*)-5-(2-nitroprop-1-en-1-yl)benzo[*d*][1,3]dioxole **(*E*)-2-methoxy-4-(2-nitrovinyl)phenyl benzoate**

Figure 32: Nitrostyrenes found to exhibit PTP inhibition activity

Subsequent publications detailed inhibition of human platelet aggregation and inhibited ATP release paired with the aforementioned PTP inhibition[8, 190] (Figure 32). An initial mechanism for this PTP activity was proposed by Park et al. (2004), detailing a nucleophilic addition of thiol and arginine/aspartate residues of PTP to the nitro group within the binding complex, suggesting that the carbon-carbon double bond remained intact and provided an essential planar conformation[195] (Figure 33).

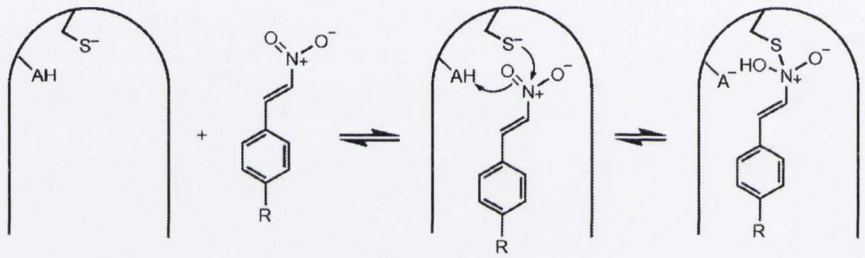

Figure 33: Mechanism of reversible inhibition of PTP by nitrostyrenes proposed by Park et al. (2004)[195]

Cornell et al. (2014) suggested that the nitrovinyl unit played a different role in the mechanism of PTP inhibition, undergoing a Michael type nucleophilic attack by the thiol residues and forming a complex with lysine and amino residues[186] (Figure 34).

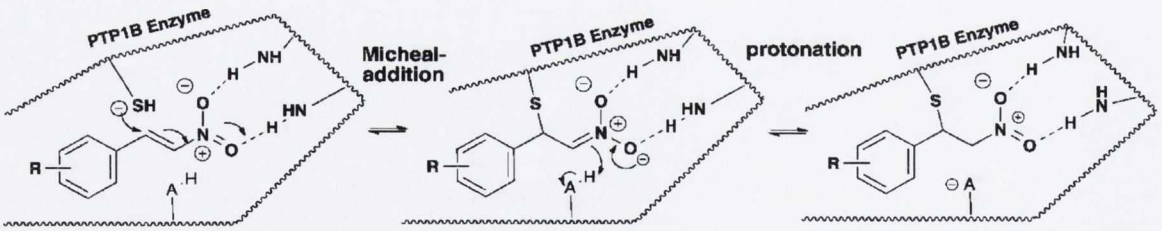

Figure 34: Mechanism of reversible inhibition of PTP by nitrostyrenes proposed by Cornell et al. (2014)[186]

Several nitrostyrene derivatives have been shown to exhibit phospholipase A_2 inhibition. Villar et al. (2008) demonstrated that nitrostyrenes bearing mononitro substitution at the *ortho*, *meta* and *para* positions effectively inhibited phospholipase A_2 derived from snake venom[196] (Figure 35).

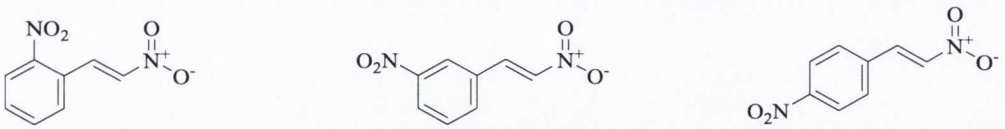

(*E*)-1-nitro-2-(2-nitrovinyl)benzene **(*E*)-1-nitro-3-(2-nitrovinyl)benzene** **(*E*)-1-nitro-4-(2-nitrovinyl)benzene**

Figure 35: phospholipase A2 inhibitiors

Heterocyclic structures containing the nitrostyrene pharmacophore have also been found to possess significant biological activity. Perrella et al. (1994) designed a series of 3-nitrocoumarin, 3-nitrochromone and 3-nitrochromene derivatives intended for the inhibition of phospholipase C (PLC). This series of nitrovinyl compounds performed as intended inhibiting PLC and exhibiting a potent growth inhibitory effect in melanoma cells[172]. A series of 2-aryl-3-nitro-2*H*-chromenes was more recently shown to exhibit a cytotoxic and apoptotic effect in breast cancer cell lines MCF-7, T-47D and MDA-MB-231. These 2-aryl-3-nitro-2*H*-chromenes were designed to incorporate components of anticancer agents from the nitrovinylstilbenes, nitrostyrenes, stilbene, chalcone and flavanone families[145](Figure 36).

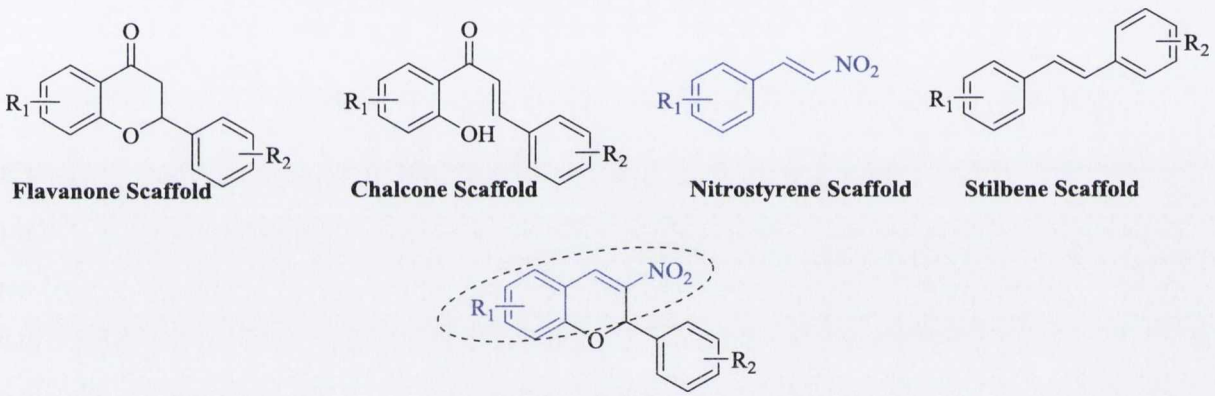

Flavanone Scaffold **Chalcone Scaffold** **Nitrostyrene Scaffold** **Stilbene Scaffold**

2-Aryl-3-nitro-2*H*-chromene Scaffold

Figure 36: Incorporation structural features of the flavanones, chalcones, nitrostyrenes and stilbenes into the 2-aryl-3-nitro-2H-chromenes[145]

Li et al. (2008) reported a series of 3-nitroquinolines as potent inhibitors of epidermoid carcinoma (A431) and breast cancer (MDA-MB-468). These 3-nitroquinolines were designed to mimic known inhibitors (gefitinib & lapatinib) of the epidermal growth factor receptor kinase incorporating a nitro group at C-3 thus forming a nitrovinyl type structure[197]. The Henry-Knoevenagel condensation reaction of isatins with subsequent dehydration allowed Chen et al. (2010) to incorporate a nitrovinyl moiety into isatins. These indolin-2-one nitrovinyl compounds were shown to possess growth inhibition properties in A549 and P388 lung cancer cell lines[198] (Figure 37).

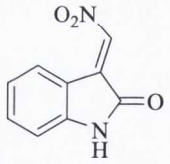

(*E*)-3-(nitromethylene)indolin-2-one

Figure 37: Nitrovinyl isatin

The incorporation of the nitrovinyl unit into a series of protein kinase targeting anticancer drugs has also been achieved and these (arylamidoanilino) nitroethylene compounds have shown activity in leukaemia cell lines. The nitrovinyl system was generated via a two step procedure whereby the conjugate addition of a free amine to (2-nitroethene-1,1-diyl)bis(methylsulfane) takes place in the presence of N,N-diemethylamine[199].

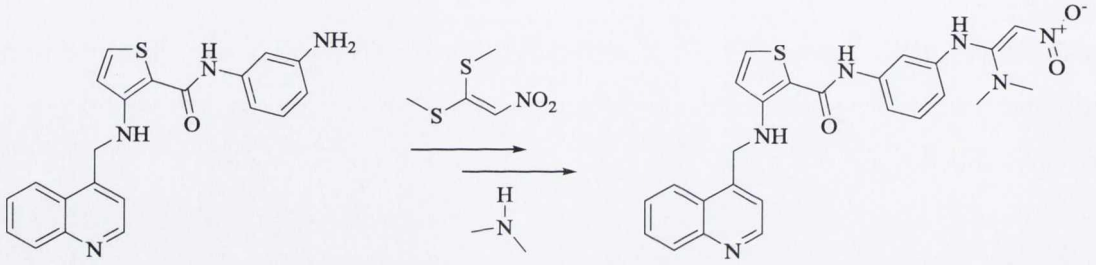

Figure 38: Example of (arylamidoanilino) nitroethylene compounds designed by Crew et al. (2006)

In 2012, McNamara et al. from Trinity College Dublin, reported a series of (*E*)-1,3-bis(aryl)-2-nitro-1-propenes originating from the redesign of illicit amphetamines[92, 200, 201], this series possessed potent antiproliferative activity in BL cell lines MUTU-I (EC_{50} 1-3 μM) and DG-75 (EC_{50} 4-65 μM)[5]. Unlike the related amphetamines, it was concluded that SERT may not be involved in the mechanism of apoptosis for this series of compounds. The lead compound ((*E*)-4,4'-(2-nitroprop-1-ene-1,3-diyl)bis(chlorobenzene)) showed a relatively low SERT inhibitory capacity (IC_{50} 15.7 μM) when compared to the SERT binding activity of MDMA (EC_{50} 425 nM) and 4-MTA (EC_{50} 74 nM). Even so, the 1,3-bis(aryl)-2-nitro-1-propenes, particularly (*E*)-4,4'-(2-nitroprop-1-ene-1,3-diyl)bis(chlorobenzene) (Figure 39), were found to induce the hallmark characteristics of type I programmed cell death (apoptosis). This lead compound gave good EC_{50}s of ~1 μM and ~12 μM in the MUTU-I and DG75 cell lines respectively[5] and hence the development of this lead structure as a potential BL therapeutic is of current interest.

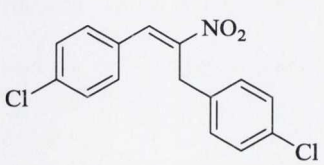

Figure 39: (*E*)-4,4'-(2-nitroprop-1-ene-1,3-diyl)bis(chlorobenzene)

1.6 Thesis Objectives

The main focus of this thesis is the synthesis of compounds that are structurally related to the nitrostyrene (*E*)-1,3-bis(aryl)-2-nitro-1-propene scaffold and the tetracyclic antidepressant maprotiline, with a view to developing these structures as novel antiproliferative agents for use as a potential treatment for the malignancy Burkitt's lymphoma.

The main objectives of Chapter Two include

- Utilisation of the Henry-Knoevenagel condensation reaction to synthesis a comprehensive library of structurally diverse nitrostyrenes structurally related to the (*E*)-1,3-bis(aryl)-2-nitro-1-propenes.
- Further modification of this nitrostyrene library employing a number of transformations including Morita-Baylis Hillman reaction, triazole formation, reduction, oxidation, Michael and epoxidation reactions.
- Preparation of related vinyl compounds including benzylidenehydrazines and the 2-substituted-3-phenylacrylonitriles.

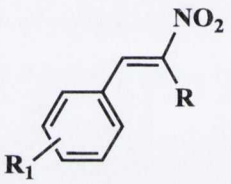

The main objectives of Chapter Three include

- Incorporation of the nitrostyrene and (*E*)-1,3-bis(aryl)-2-nitro-1-propene scaffold into a number of larger heterocyclic structures to give more constrained configurations of the pharmacophore.
- The preparation of a library of 3-nitro-2-phenyl-2*H*-chromenes and 3-nitro-1,2-dihydroquinolines via a Baylis-Hillman tandem Michael reaction.

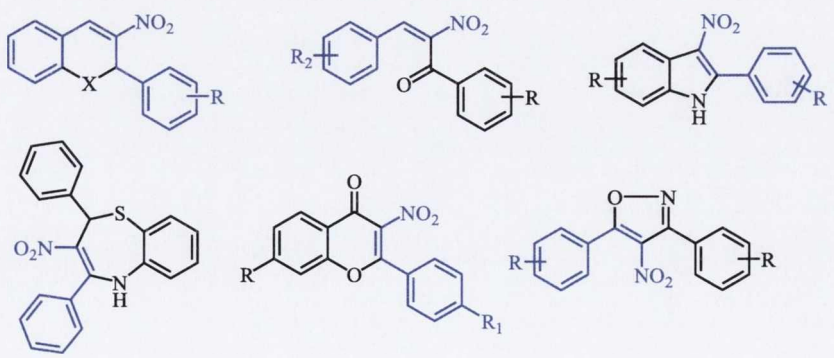

- Synthesis of the 3,5-diphenylisoxazole and flavone scaffolds and subsequent nitration of these heterocycles and the commercially available phenylindole to afford their nitrated adducts.

The main objectives of Chapter Four include

- Design and synthesise of a library of anthracene based compounds structurally related to the TCA maprotiline.
- Utilisation of the Henry-Knoevenagel condensation of formylated anthracenes to synthesise a library of substituted (*E*)-9-(2-nitrovinyl)anthracenes.
- Preparation of related:
  oxime, amine, amide, chloride, cyanovinyl, hydrazone and nitroalkane derivatives.

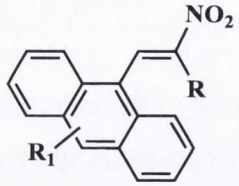

The main objectives of Chapter Five include

- Design and synthesis of maprotiline analogues based on the 9,10-dihydro-9,10-ethanoanthracene scaffold previously shown to exhibit anticancer properties.
- Creation of a diverse dienophile library of commercially available reagents and by synthesising a number of benzylmaleimides and phenylmaleimides.
- Utilisation of the dienophile library and the library of anthracene derivatives synthesised in Chapter 4 to generate a large library of Diels-Alder adducts incorporating the nitrovinyl pharmacophore.

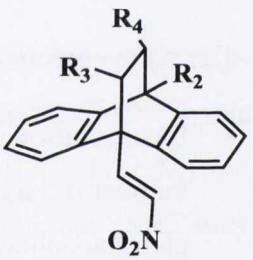

The main objectives of Chapter Six include

- Preliminary biological evaluation of the compound libraries prepared in Chapters 2 – 5 at 10 μM and 1 μM in the DG-75 and MUTU-I BL cell lines leading to the production of IC_{50} curves for the leading compound(s).
- Generation of a structure-activity relationship for potential Burkitt' lymphoma therapeutic(s) based on these preliminary biochemical results.
- Investigation of the mechanism of action e.g. the pro-apoptotic abilities of these compounds using FACS analysis.
- Determination of the selectivity of the antiproliferative effect of these compounds for BL cells using peripheral mononuclear cells (PBMC).

The overall objective of this research is the identification of novel lead compounds with sufficient potency to be useful as potential therapies for Burkitt's lymphoma.

Chapter 2.

Synthesis, isolation and characterisation of the nitrostyrenes and related structures

2.0 Introduction

4-Methylthioamphetamine (4-MTA) and 3,4-methylenedioxymethamphetamine (MDMA) are notorious drugs of abuse and the route specific by-products formed during the synthesis of 4-MTA and MDMA are well documented in literature[200, 202-206]. The redesign of MDMA is of particular interest, as MDMA analogues have been shown to exhibit cytotoxicity in BL cell lines[91, 207]. As part of previous research within our laboratory, a library of a number of route-specific by-products formed during amphetamine synthesis were isolated and characterised. Subsequently a series of over 200 analogues of 4-MTA and MDMA including their route specific by-products were synthesised[200]. This library of compounds was subsequently screened *in vitro* for cytotoxicity in a range of cell lines which overexpressed monoamine transporters, including, human embryonic kidney HEK, hSERT, HEK hNET and HEK hDAT. The compounds were also screened in a neuronal cell line PC-12 and the neuroblastoma cell line SHSY-5Y. A number of leading compounds with antiproliferative effects in BL cell lines (MUTU-I and DG-75) were identified[92].

The most promising of these leading compounds was found to be N-(1,3-bis(4-(methylthio)phenyl)propan-2-yl)formamide (Figure 40); this compound showed significant selective toxicity to cell lines which overexpress SERT (EC_{50} HEK hSERT 50 μM) over those which overexpressed DAT (EC_{50} HEK hDAT 457 μM) or NET (EC_{50} HEK hNET 87 μM)[201]. These findings were consistent and rationalised with literature that highlighted serotonin transporters as targets for the mechanism of cytotoxicity of MDMA[203, 208].

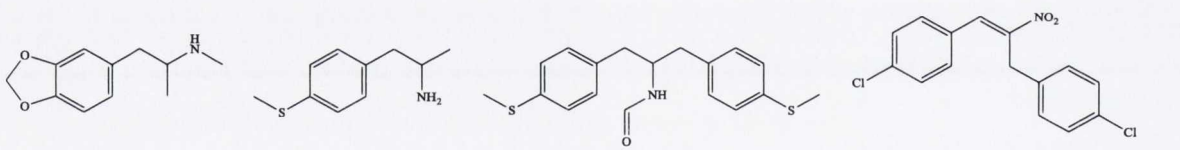

MDMA | **4-MTA** | **N-(1,3-bis(4-(methylthio)phenyl) propan-2-yl)formamide** | **(*E*)-4,4'-(2-nitroprop-1-ene-1,3-diyl) bis(chlorobenzene)**

Figure 40: MDMA, 4-MTA, N-(1,3-bis(4-(methylthio)phenyl)propan-2-yl)formamide, (*E*)-4,4'-(2-nitroprop-1-ene-1,3-diyl)bis(chlorobenzene)

In more recent studies, a series of 1,3-bis(aryl)-2-nitro-1-propenes structurally related to N-formyl-1,3-bis(4-methylthiophenyl)-2-nitro-1-propane were shown to have a more potent antiproliferative activity in BL cell lines MUTU-I and DG-75 than the 1,3-bis(aryl)-2-propanamine derivatives. Having previously evaluated the 1,3-bis(aryl)-2-nitro-1-propenes for SERT specific toxicity[5], more recent work has shown that SERT may not be involved in the mechanism of apoptosis for this series of compounds. The lead compound (*E*)-4,4'-(2-nitroprop-1-ene-1,3-diyl)bis(chlorobenzene) elicited a potent antiproliferative and pro-

apoptotic effect in the DG-75 and MUTU-I BL cell lines (Chapter 1, Section 1.5) and as a result merits further investigation as a potential therapeutic for BL.

(*E*)-4,4'-(2-Nitroprop-1-ene-1,3-diyl)bis(chlorobenzene) contains a classical nitrostyrene pharmacophore and hence derivatives of this structure are amenable to a number of structural transformations (Chapter 1, Section 1.5.1). In the present work a comprehensive library of nitrostyrenes and nitrostyrene derivatives were initially synthesised and characterised. This library not only included nitrostyrenes synthesised from a range of nitroalkanes and aldehydes but also nitroalkanes, Michael adducts, triazoles, epoxides, nitrochalcones and Baylis-Hillman adducts (Figure 41).

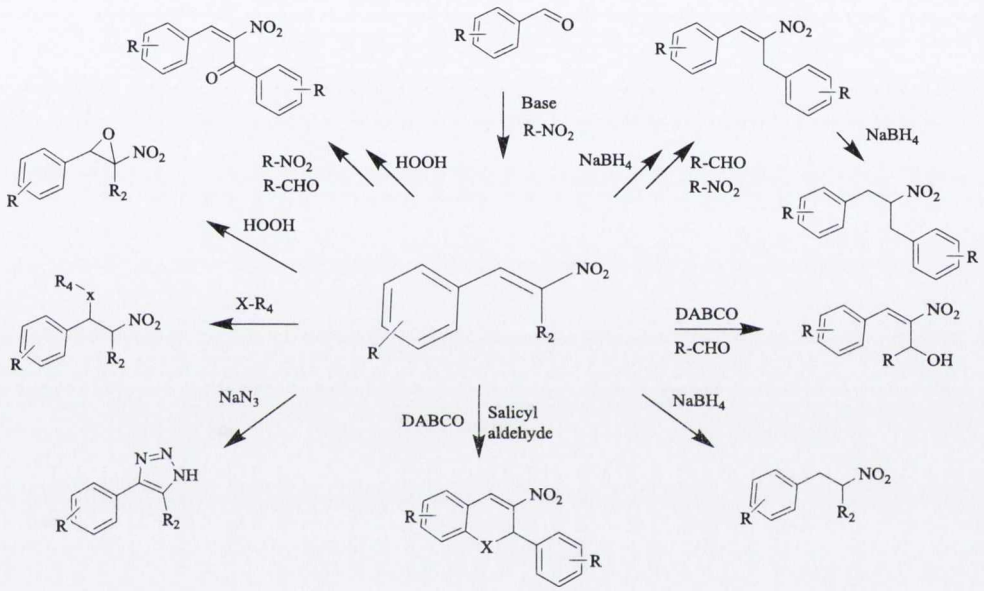

Figure 41: The nitrostyrene scaffold and transformations planned

2.1 Synthesis of a library of structurally diverse (*E*)-(2-nitrovinyl)benzenes

A library of structurally diverse (*E*)-(2-nitrovinyl)benzenes (nitrostyrenes) was generated utilising the Henry-Knoevenagel condensation reaction of an appropriately substituted aryl aldehyde (or heterocyclic aldehyde) and a suitable aliphatic nitro compound; the scheme for the reaction is shown in Figure 42 and the mechanism for the reaction is shown in Figure 43[209].

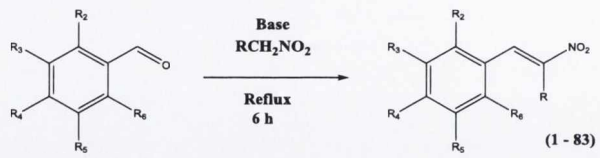

Figure 42: General scheme for Henry-Knoevenagel condensation to synthesise (*E*)-(2-nitrovinyl)benzenes

The Henry or nitroaldol reaction was first noted in 1895 by L. Henry[210]. The Henry reaction is an aldol condensation reaction involving an aliphatic nitro compound bearing α-hydrogens with an aldehyde or ketone, enabling the formation of a new carbon-carbon bond. The mechanism proceeds by deprotonation of α-hydrogen giving a nitronate, followed by nucleophilic addition of the nitronate to the aldehyde / ketone and regeneration of the catalytic base [209, 211]. The Knoevenagel condensation reaction, first documented in 1889, is an amine catalysed condensation reaction between carbonyl compounds and activated methylene compounds. During the Knoevenagel condensation a carbonyl group with acidic α-hydrogens undergoes deprotonation; this carbanion subsequently attacks the iminium ion formed between the aldehyde / ketone and the catalytic amine. This aldol-like reaction is followed by dehydration to give the alkene[209].

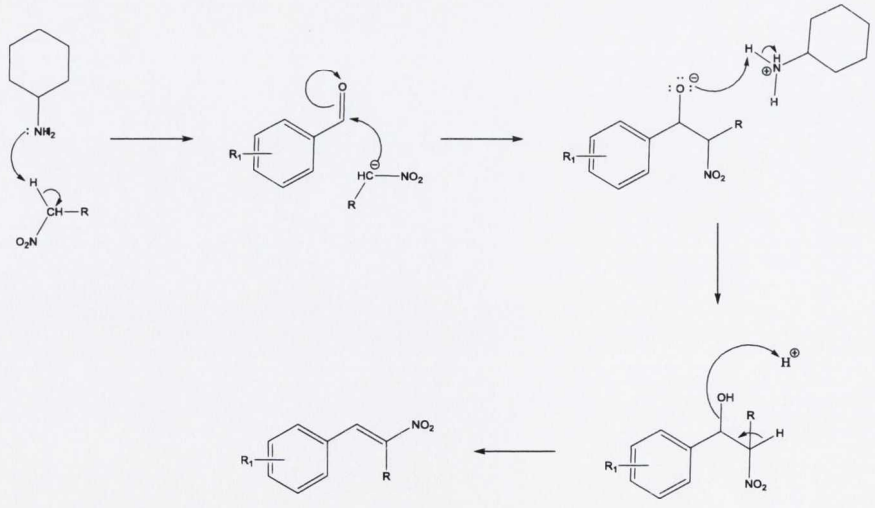

Figure 43: Proposed mechanism of Henry-Knoevenagel condensation for synthesis of (*E*)-(2-nitrovinyl)benzenes

The Henry-Knoevenagel syntheses of nitrostyrenes are well documented and encompass the use of a base such as potassium hydroxide[158], ammonium acetate[212, 213] or a combination of potassium fluoride and dimethyl ammonium chloride / N,N-dimethylamine hydrochloride with azeotropic removal of water facilitated using a Dean-Stark trap[5, 214, 215]. In more recent literature, the microwave and/or ultrasound assisted organic synthesis of nitrostyrenes using ammonium acetate has been reported[8]. Rodriguez et al. (2001) and Wang et al. (2002) also reported the solventless, microwave assisted synthesis of β-nitrostyrenes using a potassium carbonate / aluminium oxide system[216, 217].

In the present work libraries of (*E*)-(2-nitrovinyl)benzenes (**1-34**), (*E*)-(2-nitroprop-1-en-1-yl)benzenes (**35-59**), (*E*)-3/2-(2-nitrovinyl)heterocycles (**71-82**) and (*E*)-(2-nitrobut-1-en-1-yl)benzenes (**60-70**) were synthesised via the microwave assisted organic synthesis Henry-Knoevenagel condensation reaction of nitromethane, nitroethane and nitropropane with the appropriately substituted aryl aldehydes catalysed by cyclohexylamine (Figure 44).

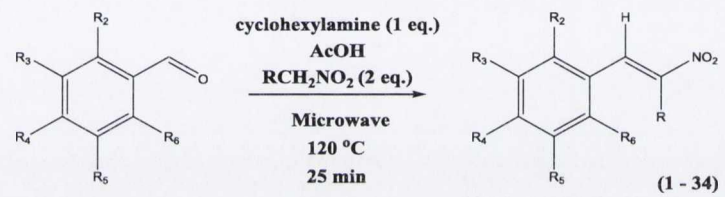

Figure 44: Synthesis of (*E*)-(2-nitrovinyl)benzenes, (*E*)-(2-nitroprop-1-en-1-yl)benzenes and (*E*)-(2-nitrobut-1-en-1-yl)benzenes

Originally the Henry-Knoevenagel condensation reaction used in synthesis of the nitrostyrenes was carried out using methodology which was well established within the group; this involved a 6 hour reflux in acetic acid with cyclohexylamine as base[5, 201]. The reaction has since been optimised using microwave assisted organic synthesis, the findings of which are summarised below. This microwave study was carried out using the synthesis of (*E*)-1-(4-chlorophenyl)-2-nitroethene (**1**) from 4-chlorobenzaldehyde as the model reaction (Figure 45).

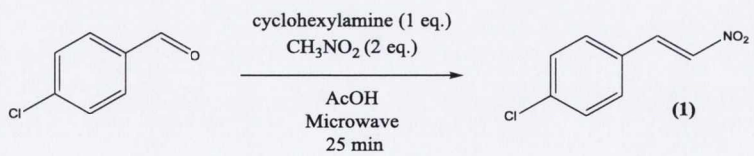

Figure 45: Synthesis of (*E*)-1-(4-chlorophenyl)-2-nitroethene from 4-chlorobenzaldehyde (1)

The optimal reaction conditions for both temperature and reaction time were deduced in a stepwise fashion; by the variation of one reaction variable while holding all other variables constant. From this study it was found that the optimal reaction conditions were reached at 120 °C over 30 minutes (Figure 46), compared to the conventional six hours reflux.

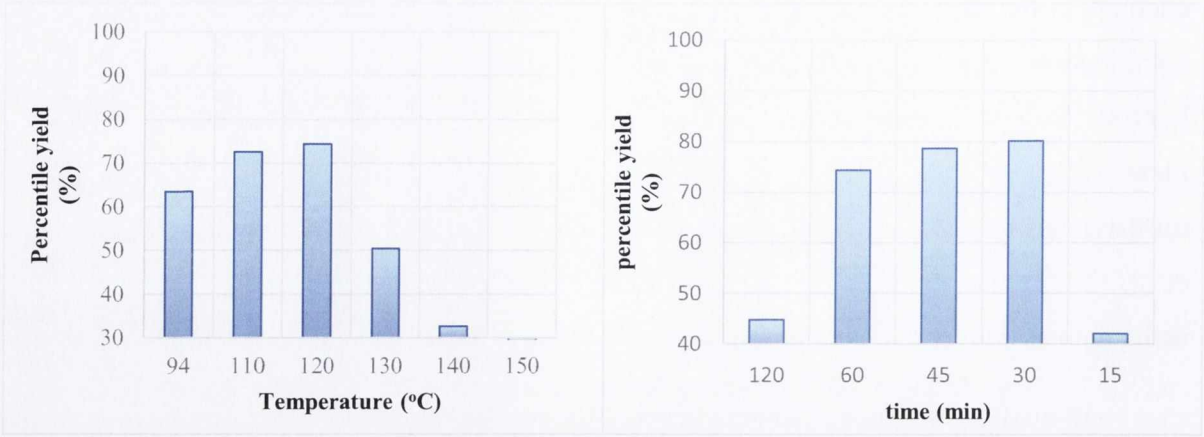

Figure 46: Microwave Study – Optimisation data.

(Please note for temperature variation study t = 20 min. For time variation study T = 120 °C)

In order to verify these findings, the yields from the microwave assisted synthesis of two other nitrostyrene compounds (**6, 21**) were compared to their refluxing alternatives (Figure 47). This new procedure gives comparable yields to the refluxing method previously utilised but with a significant reduction in reaction time.

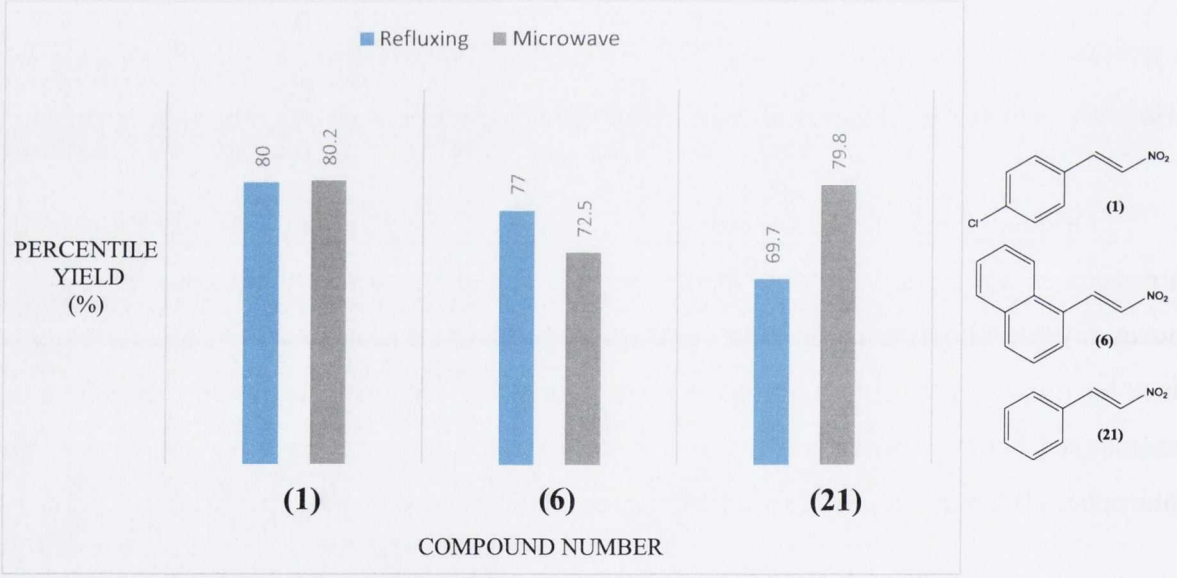

Figure 47: Graphical comparison of yield - microwave versus refluxing methods

Using this procedure a library of structurally diverse nitrostyrenes were synthesised, purified and subsequently characterised (Table 1, Table 2, & Table 4). Aryl substitution patterns achieved included halogen, alkyl, methoxy, hydroxy, benzyloxy and phenoxy with proton, methyl and ethyl vinyl substituents. It was envisaged that these libraries would yield to the establishment of a structure activity relationship for these compounds.

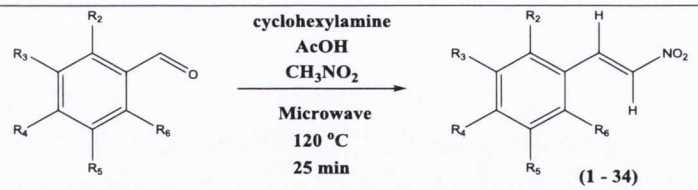

Compound	Substitution pattern	Yield	Compound	Substitution pattern	Yield
1	$R_4 = Cl$	83%	**18**	$R_3 = R_4 = R_5 = OCH_3$	60%
2	$R_4 = OH$	40%	**19**	$R_2 = OCH_2CH_3$	67%
3	$R_3 = R_4 = C_4H_4$	75%	**20**	$R_4 = O(C_6H_5)$	70%
4	$R_4 = F$	78%	**21**	$R_n = H$	80%
5	$R_4 = C_2H_2NO_2$	79%	**22**	$R_3 = R_4 = OCH_2O$	70%
6	$R_2 = R_3 = C_4H_4$	76%	**23**	$R_3 = R_4 = OCH_3$	40%
7	$R_5 = R_6 = C_4H_4$, $R_2 = R_3 = C_4H_4$	99%	**24**	$R_4 = OCH_2(C_6H_5)$	40%
8	$R_3 = OCH_2(C_6H_5)$	82%	**25**	$R_2 = R_4 = Cl$	52%
9	$R_2 = OCH_3$, $R_5 = Br$	86%	**26**	$R_3 = OH$	50%
10	$R_4 = OCH_3$	70%	**27**	$R_2 = OH$	30%
11	$R_4 = OCH_3$, $R_3 = OCH_2(C_6H_5)$	62%	**28**	$R_2 = Cl$	84%
12	$R_2 = R_4 = R_5 = OCH_3$	48%	**29**	$R_4 = Br$	69%
13	$R_2 = OH$, $R_5 = OCH_3$	58%	**30**	$R_4 = OCH_2CH_3$	58%
14	$R_3 = Cl$	73%	**31**	$R_2 = OH$, $R_3 = OCH_3$	29%
15	$R_4 = CH_3$	78%	**32**	$R_3 = Br$, $R_4 = OCH_3$	39%
16	$R_2 = R_4 = OCH_3$	70%	**33**	$R_3 = OH$, $R_4 = OCH_3$	62%
17	$R_2 = R_5 = OCH_3$	80%	**34**	$R_3 = NO_2$	33%

Table 1: (*E*)-(2-nitrovinyl)benzene library. Note: R = H unless otherwise specified. * denotes novel compound

The (*E*)-(2-nitrovinyl)benzenes were synthesised through the Henry-Knoevenagel condensation of nitromethane and the appropriate aldehyde giving yields of 29-99% (Table 1). (*E*)-4-bromo-1-methoxy-2-(2-nitrovinyl)benzene (**9**) was chosen as a representative sample of the (*E*)-(2-nitrovinyl)benzenes and the ^1H NMR and ^{13}C NMR spectra will now be discussed in detail. The ^1H NMR (400 MHz, $CDCl_3$) spectrum of compound **9** (Figure 48) shows a singlet at 3.96 ppm which integrates for one proton. This represents the methoxy group at the 1 position.

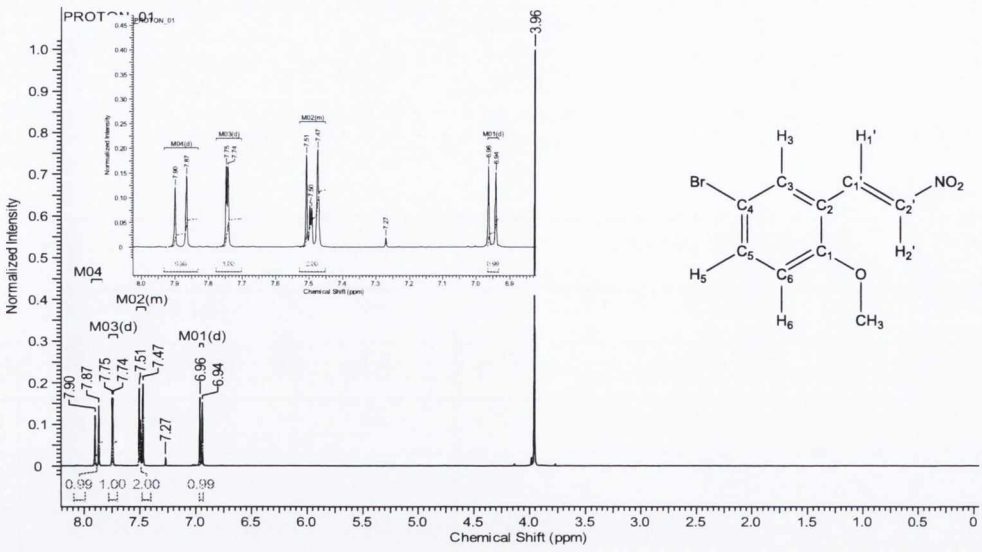

Figure 48: ^{1}H NMR spectrum of (*E*)-4-bromo-1-methoxy-2-(2-nitrovinyl)benzene (9)

A doublet at 6.95 ppm (J = 8.71 Hz) integrating for a single proton corresponds to H_6. The multiplet found at 7.45 - 7.53 ppm integrating for two protons was assigned to H_5 and the nitrovinyl proton $H_{1'}$. The doublet at 7.74 ppm (J = 2.07 Hz) was assigned to H_3, the small coupling constant was attributed to long range coupling. The remaining doublet at 7.88 ppm (J = 13.27 Hz) was assigned to $H_{2'}$ on the nitrovinyl unit. A coupling value of 13.5 Hz indicates *trans* proton coupling (*E*-alkene) for this series[163].

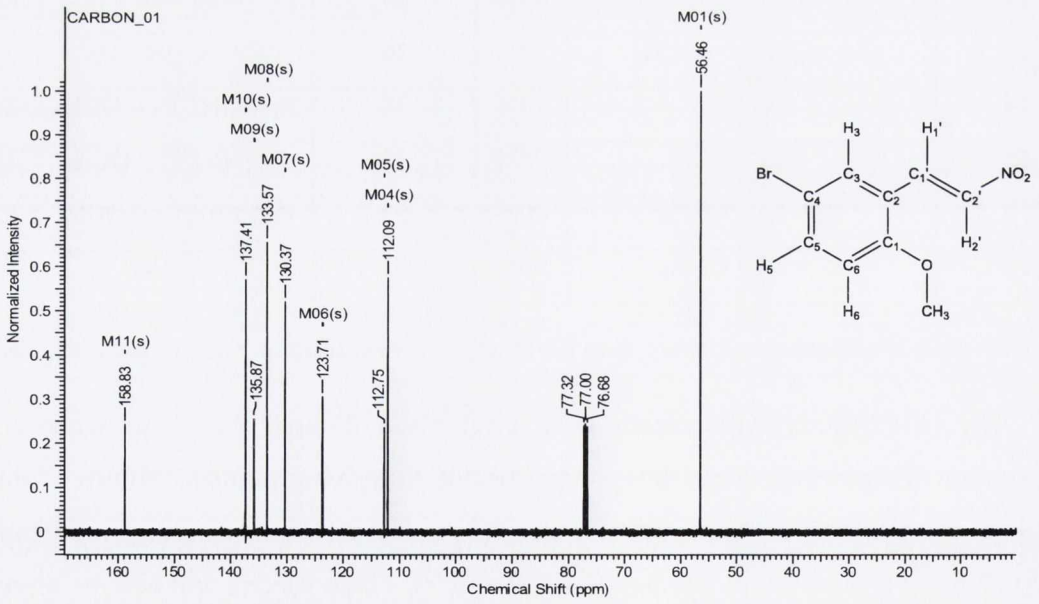

Figure 49: ^{13}C NMR spectrum of (*E*)-4-bromo-1-methoxy-2-(2-nitrovinyl)benzene (9)

The ^{13}C NMR (101 MHz, $CDCl_3$) spectrum of compound **9** (Figure 49) shows CH signals at 112.09 ppm, 130.37 ppm, 133.56 ppm, 135.87 ppm and 137.40 ppm. The resonance at 56.46 ppm was assigned to the methoxy group on C_1. The CH signals at 112.75 ppm, 130.37 ppm and 133.57 ppm corresponded to C_6, C_5 and C_3 respectively, while quaternary resonances at 112.75 ppm and 123.71 ppm were assigned to C_4 and C_2. Two further CH resonances at 135.87 ppm and 137.41 ppm account for $C_{1'}$ and $C_{2'}$. The final downfield quaternary resonance at 158.83 ppm was assigned to the carbon bearing the electronegative methoxy substituent - C_1. FTIR spectroscopy shows bands at 1629 (C=C) and 1486, 1335 (NO_2) cm^{-1}. High resolution mass spectrometry (APCI) was carried out and the required molecular ion was calculated to be $C_9H_9NO_3Br$ $[M^+ + H]$ 257.9766 and found as 257.9760.

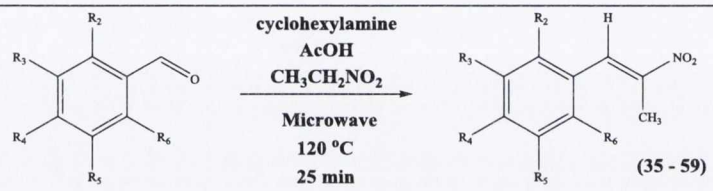

(35 - 59)

Compound	Substitution pattern	Yield	Compound	Substitution pattern	Yield
35	$R_4 = Cl$	64%	**48**	$R_2 = R_5 = OCH_3$	80%
36	$R_4 = OH$	8%	**49**	$R_3 = R_4 = R_5 = OCH_3$	50%
37	$R_3 = R_4 = C_4H_4$	60%	**50**	$R_2 = OCH_2CH_3$	40%
38	$R_4 = F$	50%	**51**	$R_4 = O(C_6H_5)$	72%
39	$R_4 = CHCH(CH_3)NO_2$	60%	**52**	$R_4 = OCH_2(C_6H_5)$	50%
40	$R_2 = R_3 = C_4H_4$	55%	**53**	-	68%
41	$R_2 = R_3 = R_5 = R_6 = C_4H_4$	73%	**54**	$R_5 = Br$, $R_2 = OCH_3$	85%
42	$R_3 = OCH_2(C_6H_5)$	60%	**55**	$R_3 = Cl$	61%
43	$R_3 = OCH_2(C_6H_5)$, $R_4 = OCH_3$	35%	**56**	$R_3 = OH$	37%
44	$R_2 = R_4 = R_5 = OCH_3$	25%	**57**	$R_2 = Cl$	56%
45	$R_4 = CH_3$	40%	**58**	$R_5 = OCH_3$, $R_2 = OH$	18%*
46	$R_4 = Br$	18%	**59**	$R_4 = OCH_2CH_3$	39%
47	$R_2 = R_4 = OCH_3$	35%	-	-	-

Table 2: (*E*)-(2-nitroprop-1-en-1-yl)benzene library. Note: R = H unless otherwise specified. * denotes novel compound

The (*E*)-(2-nitroprop-1-en-1-yl)benzenes (**35-59**) (Table 2) are structurally similar to the (*E*)-(2-nitrovinyl)benzenes (Table 1), however by using nitroethane during the Henry reaction – a methyl sidechain is introduced on C-2 of the vinyl unit. This is evident when examining the ^{1}H NMR and ^{13}C NMR data for the series by the absence of a H_2 proton on the nitrovinyl unit coupled to H_1 – indicative of substitution at the C-2 position. The methyl group is typically represented by a singlet integrating for three protons at ~2.5 ppm. Translating this information to the ^{13}C NMR data – an additional downfield quaternary resonance (C_2) is observed for these nitroethane adducts in place of the CH resonance in the nitromethane adducts discussed earlier. The methyl group can be represented by a resonance in the region 15-20 ppm.

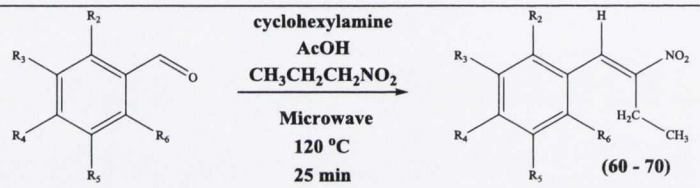

Compound	Substitution pattern	Yield	Compound	Substitution pattern	Yield
60	$R_4 = Cl$	20%	**66**	$R_2 = OCH_3$, $R_5 = Br$	62%*
61	$R_4 = OH$	7%	**67**	$R_2 = Cl$	94%
62	$R_3 = R_4 = C_4H_4$	30%*	**68**	$R_3 = OH$	13%
63	$R_4 = F$	40%	**69**	$R_3 = Cl$	23%
64	$R_4 = CHCH(CH_2CH_3)NO_2$	40%	**70**	$R_2 = OH$, $R_5 = OCH_3$	9%
65	$R_2 = R_3 = C_4H_4$	35%	-	-	-

Table 3: (*E*)-(2-nitrobut-1-en-1-yl)benzene library. Note: R = H unless otherwise specified. * denotes novel compound

Compound **68** was chosen as a representative sample of the (*E*)-(2-nitrobut-1-en-1-yl)benzenes and the ^{1}H NMR and ^{13}C NMR spectra will now be discussed in detail. The ^{1}H NMR (400 MHz, $CDCl_3$) spectrum of compound **68** (Figure 50) shows a triplet at 1.28 ppm (J = 7.26 Hz) which integrates for three protons. This represents the methyl protons group at the $C_{4'}$.

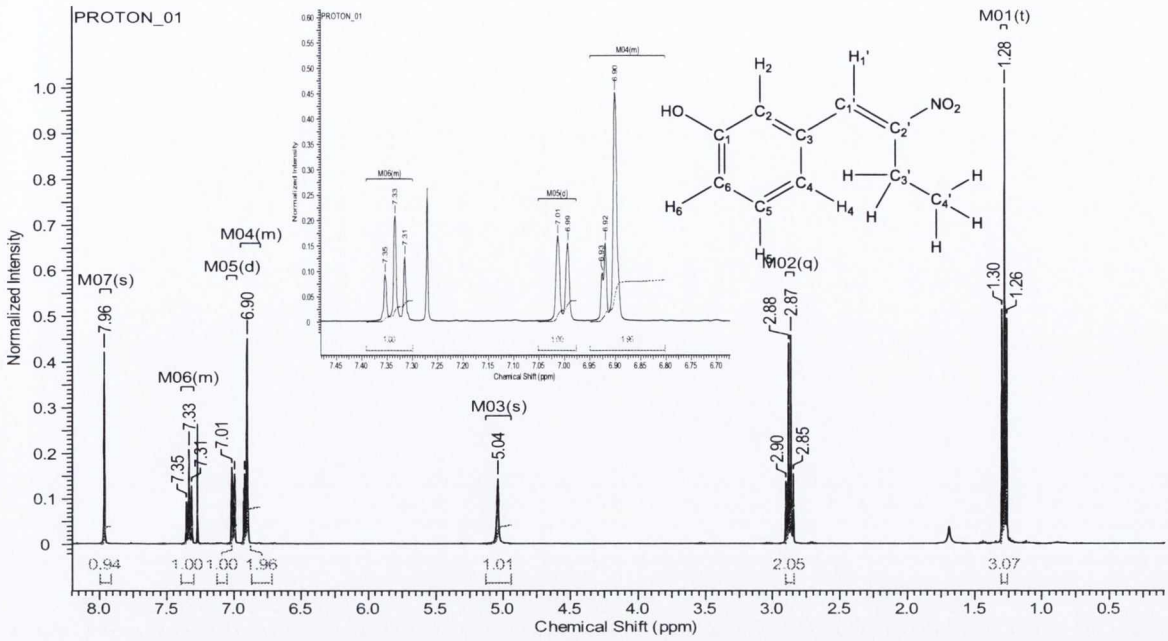

Figure 50: ^{1}H NMR spectrum of (*E*)-3-(2-nitrobut-1-en-1-yl)phenol (68)

The quartet at 2.87 ppm (J = 7.46 Hz) integrates for two protons and was assigned to the two methylene protons on $C_{3'}$. A singlet occurring at 5.04 ppm was found to correspond to the hydroxyl proton at C_1. In the aromatic region; the multiplet occurring at 6.80 - 6.95 ppm integrating for two protons accounted for H_2 and H_6. The doublet (J = 7.88 Hz) at 7.00 ppm integrating for one proton and the multiplet occurring 7.30 - 7.39 ppm were assigned to H_4 and H_5 respectively. The downfield singlet resonance at 7.96 ppm was found to correspond to $H_{1'}$ on the nitrovinyl unit.

The ^{13}C NMR (101 MHz, $CDCl_3$) spectrum of compound **68** (Figure 51) shows resonances at 12.50 ppm and 20.75 ppm (CH_2 DEPT 135) that were assigned to $C_{4'}$ and $C_{3'}$. The CH resonances occurring at 116.20 ppm, 117.03 ppm, 122.21 ppm, 130.24 ppm and 132.73 ppm corresponded to C_6, C_2, C_5 and $C_{1'}$ respectively. The quaternary signal at 133.89 ppm accounted for C_3. The two downfield quaternary signals in the spectrum 153.61 ppm and 155.82 ppm were assigned to $C_{2'}$ and C_1. The most downfield signal was attributed to the electronegative environment provided by the hydroxyl group on C_1.

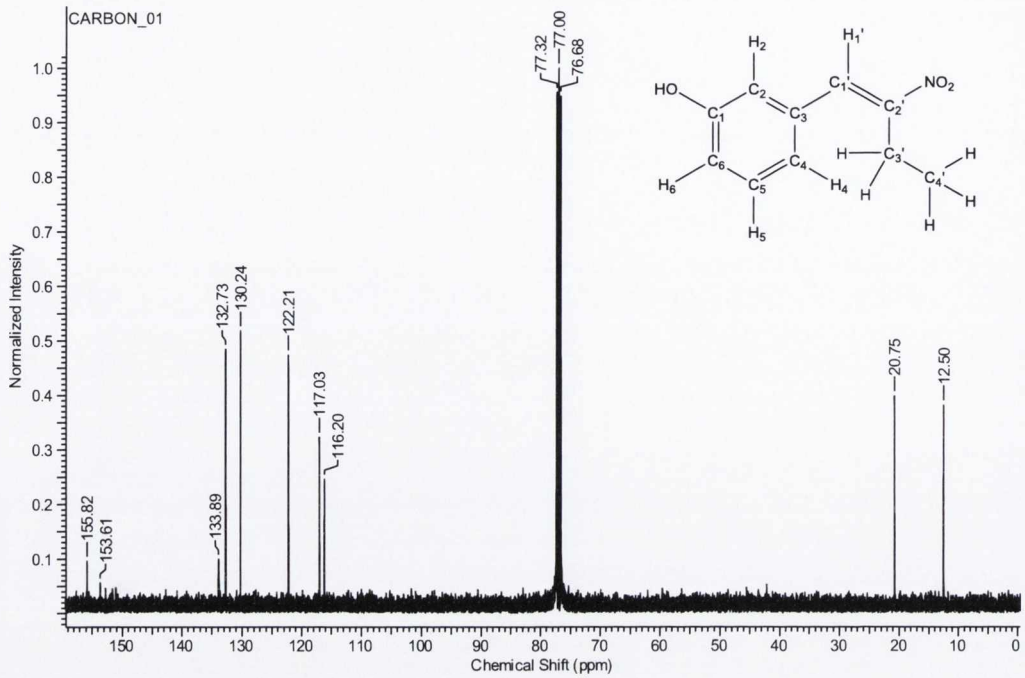

Figure 51: ^{13}C NMR spectrum of (*E*)-3-(2-nitrobut-1-en-1-yl)phenol (68)

FTIR spectroscopy for compound **68** shows absorption bands at 3376 (OH) and 1530, 1330 (NO_2) cm^{-1}. High resolution mass spectrometry (APCI) was carried out and the required molecular ion was calculated to be $C_{10}H_{10}NO_3$ [M-H] 192.0666 and found as 192.0661. X-ray crystallography was carried out on crystals grown from a sample of (*E*)-3-(2-nitrobut-1-en-1-yl)phenol. From the packing diagram it was possible to verify the (*E*) confirmation of the nitrovinyl unit and illustrate the monoclinic nature of the unit cell (Figure 52).

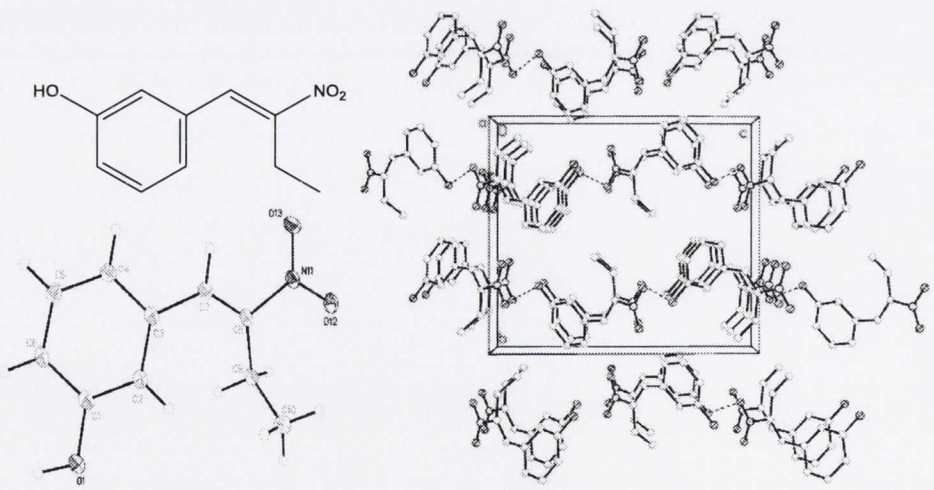

Figure 52: X-ray crystallography data for (*E*)-3-(2-nitrobut-1-en-1-yl)phenol (68)

Heterocyclic (*E*)-(2-nitrovinyl) compounds (**71-82**) were synthesised utilising the Henry-Knoevenagel condensation of the required aldehyde and the desired nitroalkane (Table 4). This library gave yields of 30-89%.

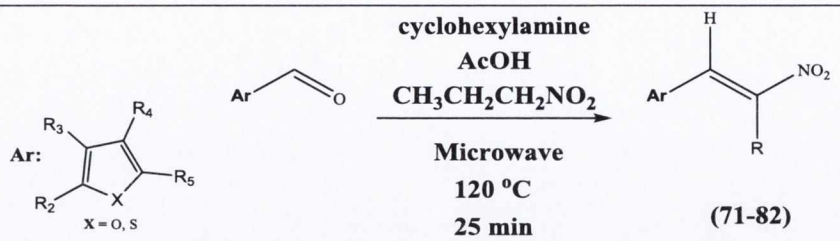

Compound	R	Substitution pattern	Yield	Compound	R	Substitution pattern	Yield
71	H	R_4 = NV, X = O	75%	**77**	CH_3	R_5 = NV, X = S	65%
72	H	R_4 = NV, X = S	74%	**78**	CH_3	$R_2 = CH_3$ R_5 = NV, X = S	55%
73	H	R_5 = NV, X = S	89%	**79**	CH_2CH_3	R_4 = NV, X = O	30%*
74	H	$R_2 = CH_3$ R_5 = NV, X = S	50%	**80**	CH_2CH_3	R_4 = NV, X = S	48%*
75	CH_3	R_4 = NV, X = O	70%	**81**	CH_2CH_3	R_5 = NV, X = S	58%
76	CH_3	R_4 = NV, X = S	62%	**82**	CH_2CH_3	$R_2 = CH_3$ R_5 = NV, X = S	56%*

Table 4: Heterocyclic (*E*)-(2-nitrovinyl) library. Note: R = H unless otherwise specified. * denotes novel compound

Compound **82** was chosen as a representative sample of the heterocyclic (*E*)-(2-nitrovinyl) compounds and the ^{1}H NMR and ^{13}C NMR spectra will now be discussed in detail. The ^{1}H NMR (400 MHz, $CDCl_3$) spectrum of compound **82** (Figure 53) shows a triplet at 1.23 ppm (J = 7.26 Hz) integrating for three protons and was assigned to the three protons on $C_{4'}$.

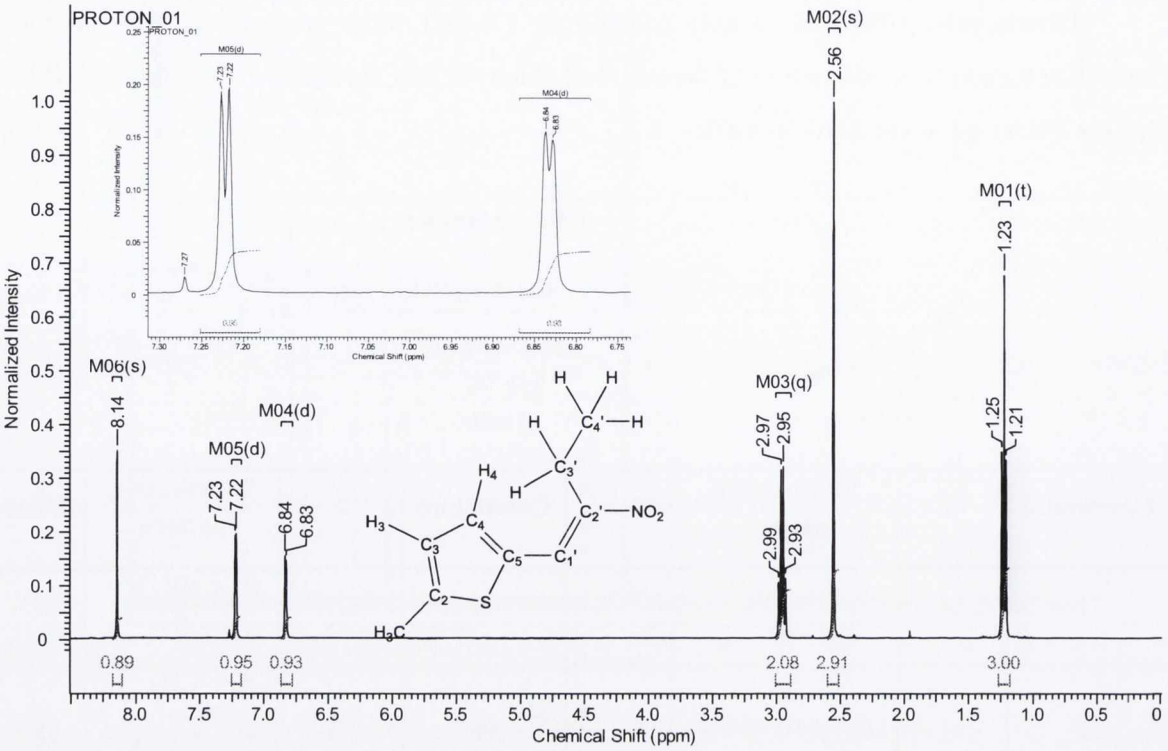

Figure 53: ^{1}H NMR spectrum of (*E*)-2-methyl-5-(2-nitrobut-1-en-1-yl)thiophene (82)

A singlet at 2.56 ppm corresponds to the three methyl protons at C_2 the thiophene ring. The quartet occurring at 2.96 ppm (J = 7.46 Hz) integrating for two protons was assigned to the two protons on $C_{3'}$. Two doublets at 6.83 ppm (J = 3.32 Hz) and 7.22 ppm (J = 3.73 Hz), both integrating for one proton each; were found to correspond H_3 and H_4 respectively. The singlet resonance at 8.19 ppm integrating for one proton denotes the $H_{1'}$ proton on the nitro vinyl group.

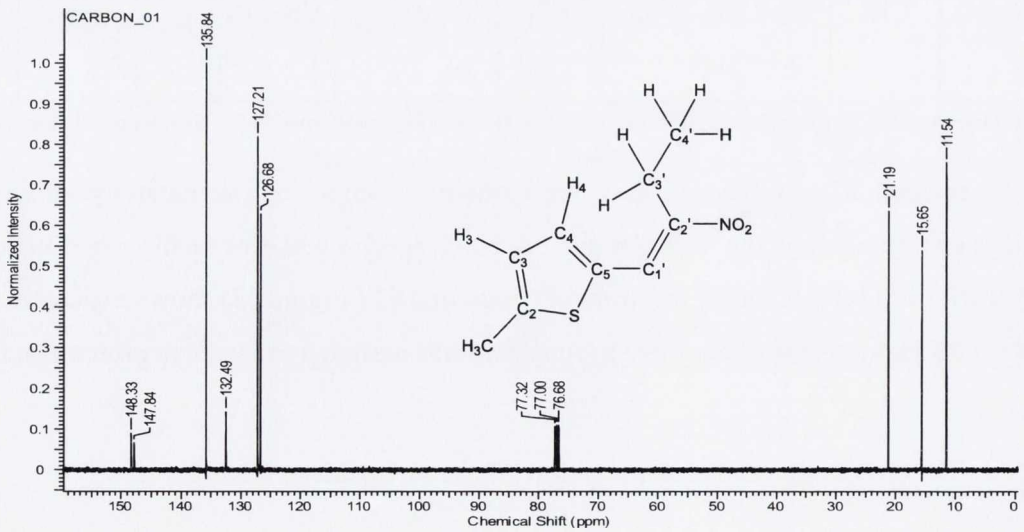

Figure 54: ^{13}C NMR spectrum of (*E*)-2-methyl-5-(2-nitrobut-1-en-1-yl)thiophene (82)

The ^{13}C NMR (101 MHz, $CDCl_3$) spectrum of compound **82** (Figure 54) shows resonances occurring at 11.54 ppm and 15.65 ppm, these were allocated to $C_{4'}$ and the methyl group on C_2. The CH_2 resonance at 21.19 ppm was assigned to $C_{3'}$. The CH resonances at 126.68 ppm, 127.21 ppm and 135.84 ppm were assigned to C_3, C_4 and $C_{1'}$. The quaternary signals occurring at 132.49 ppm, 147.84 ppm and 148.33 ppm account for C_5, C_2 and $C_{2'}$. The resonance for $C_{2'}$ occurring slightly downfield due to the electron withdrawing effects of the nitro group. FTIR spectroscopy shows bands at 2973 (CH), 1635 (C=C) and 1503, 1316 (NO_2) cm^{-1}. High resolution mass spectrometry (APCI) was carried out and the required molecular ion was calculated to be $C_9H_{10}NO_2S$ [M–H] 196.0427 and found as 196.0418.

On analysis of the yields obtained for the nitrostyrene products (Tables 1-3), it was observed that electron withdrawing groups such as the halogens at the *para* position on the aryl ring, seemed to favour the Henry-Knoevenagel reaction, whereas electron donating groups such as the hydroxy group are unfavourable. When using aliphatic nitro compounds with increased chain length (when compared to nitromethane), the yield of nitrostyrene obtained from the Henry reaction was significantly reduced. To rationalise this finding; pKa's of the relevant aliphatic nitro compounds were estimated using the MarvinSketch (version 5.3.02) pKa plugin. The pKa's were calculated to be: nitromethane (8.3), nitroethane (8.7) and nitropropane (9.33); indicating a reduction in acidic strength of the nitroalkane with increased chain length. This reduction in acidic strength can therefore be correlated with the reduced reactivity of these nitroalkanes in the Henry-Knoevenagel condensation reaction.

2.2 Synthesis of 1,3-bis(aryl)-2-nitro-1-propenes and the (2-nitropropane-1,3-diyl)dibenzenes

The synthesis of a panel of structurally varied analogs of (*E*)-4,4'-(2-nitropropane-1,3-diyl)bis(chlorobenzene) was achieved. Previous studies within our laboratory have shown the application of a three step synthetic route for the synthesis of (*E*)-1,3-bis(aryl)-2-nitro-1-propenes[5]. The general synthetic route utilised for the target compounds is illustrated below (Figure 55). The intial step of this synthetic route involved a Henry-Knoevenagel condensation reaction of an appropriately substituted benzaldehyde and a suitable aliphatic nitro compound; the mechanism for this reaction was previously shown in Figure 43.

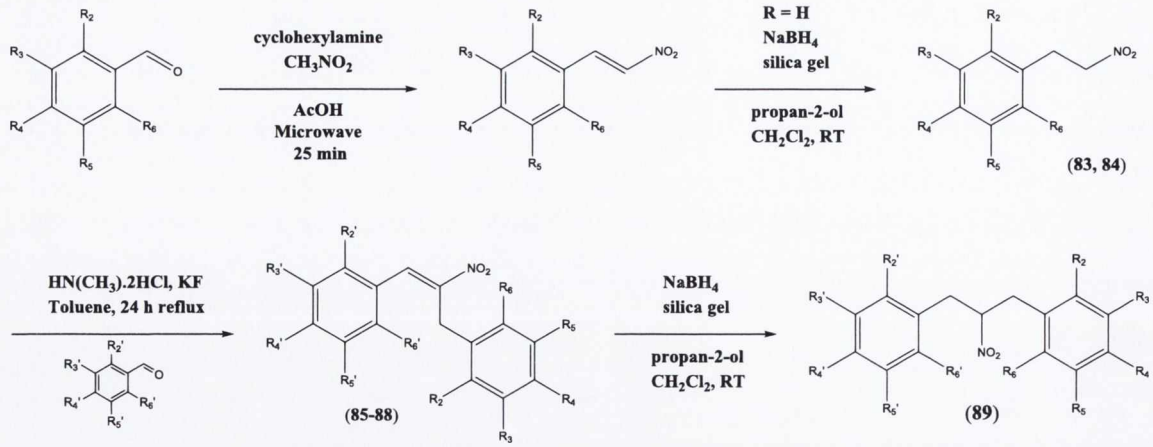

Figure 55: Preparation of (*E*)-1,3-bis(aryl)-2-nitro-1-propenes and 1,3-bis(aryl)-2-nitro-1-propanes

In order to synthesise the 1,3-bis(aryl)-2-nitro-1-propenes via the Henry-Knoevenagel route, the required (*E*)-(2-nitrovinyl)benzenes must first be reduced to nitroalkanes prior to the second Henry-Knoevenagel condensation with the appropriate benzaldehyde.

The nitrostyrenes were selectively reduced to the corresponding 1-aryl-1-nitroethanes using sodium borohydride[5, 201, 218]. Using the sodium borohydride reduction, it was possible to reduce the nitrostyrenes under mild conditions to the subsequent nitroalkanes with a short reaction time and high yields (80-90%) (Figure 56).

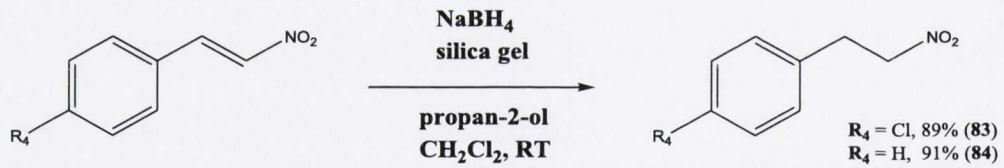

Figure 56: Scheme for reduction of the (*E*)-(2-nitrovinyl)benzenes

The formation of dimeric nitroethane impurities have been reported during this reaction, this formation takes place through a Michael-like addition reaction with the α-carbanion resonance state (Figure 57)[219]. These dimeric nitroethane impurities are not isolated as part of the current work.

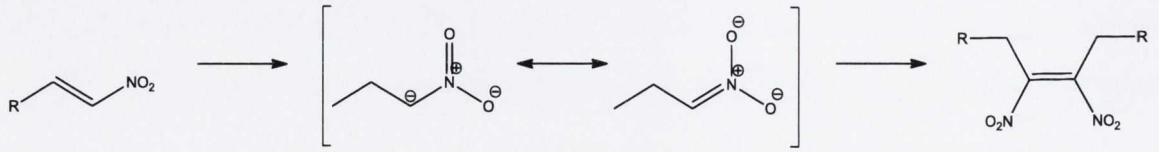

Figure 57: Formation of dimeric impurities

The reduction of nitrostyrenes to the 1-(aryl)-1-nitroethanes has also been noted with the use of bakers' yeast (*Saccharomyces cerevisiae*), this reaction however requires a much longer reaction period (48 hours)[220]. More recently Hu et al. nitrated (2-iodoethyl)benzene using silver nitrate in aqueous conditions, heated to 60 °C for 1.5 hours to give the required 1-(aryl)-1-nitroethane in good yield[221].

The ^{1}H NMR of the (2-nitroethyl)benzenes (**83**, **84**) bears two triplet resonances at ~3.3 ppm and ~4.6 ppm, both integrating for two protons; these were assigned to the pairs of protons on C_1' and C_2' respectively thus accounting for the protons produced during the reduction reaction. A second Henry-Knoevenagel condensation was then utilised to synthesise the required 1,3-bis(aryl)-2-nitro-1-propenes. Here the previously reduced nitroalkanes were condensed with the appropriate benzaldehydes (Figure 58) giving the (*E*)-1,3-bis(aryl)-2-nitro-1-propenes (**85-88**).

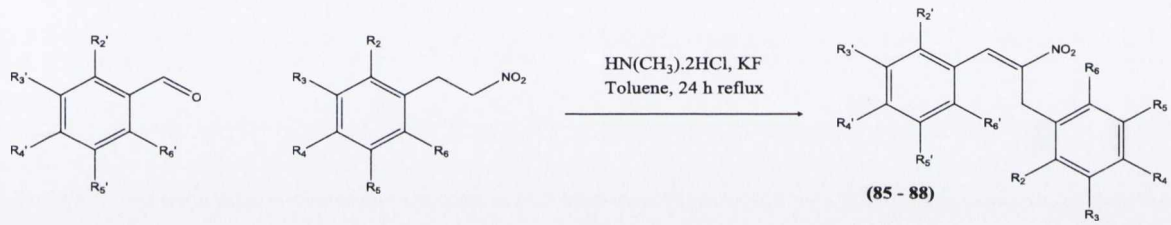

Figure 58: Synthesis of the (*E*)-1,3-bis(aryl)-2-nitro-1-propenes

Potassium fluoride and N,N-dimethylamine generate the correct basic conditions for this reaction to take place. The reaction mixture was refluxed for 24 hours in toluene with a Dean-Stark trap for the azeotropic removal of water from the reaction mixture[5, 214, 215]. The resulting reaction mixture was purified by flash column chromatography over silica gel to give (*E*)-1,3-bis(aryl)-2-nitro-1-propenes (**85-88**) in good yields (20-50%) (Table 5).

The synthesis of (*E*)-1,3-bis(aryl)-2-nitro-1-propenes has also recently been reported via the acid catalysed Friedel-Crafts reaction of Baylis-Hillman 2-nitro-3-phenylprop-2-en-1-ols derived from nitrostyrenes[173]. Franklin *et al.* utilised a potassium carbonate catalysed Horner-Wadsworth-Emmons reaction between diethyl 1-nitro-2-phenylethylphosphonate and benzaldehyde to synthesise 1,3-bis(aryl)-2-nitro-1-propene[222].

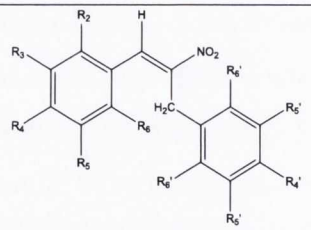

Compound	Substitution pattern	Yield	Compound	Substitution pattern	Yield
85	$R_4' = R_4 = Cl$	50%	**87**	$R_4 = Cl$	25%*
86	$R_{4'} = Cl$	30%*	**88**	-	20%

Table 5: (*E*)-1,3-bis(aryl)-2-nitro-1-propene library. Note: R = H unless otherwise specified. * denotes novel compound

Compound **86** was chosen as a representative sample of the 1,3-bis(aryl)-2-nitro-1-propenes and the ^1H NMR and ^{13}C NMR spectra will now be discussed in detail. The ^1H NMR (400 MHz, $CDCl_3$) spectrum of compound **86** (Figure 59) bears a singlet at 4.25 ppm integrating for two protons which was assigned to the two protons on $C_{3''}$.

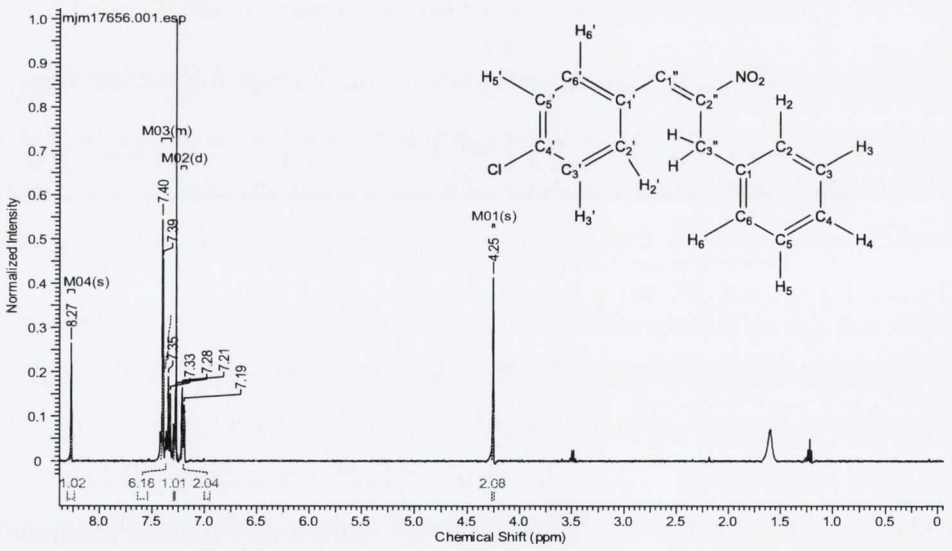

Figure 59: ^1H NMR spectrum of (*E*)-1-chloro-4-(2-nitro-3-phenylprop-1-en-1-yl)benzene (86)

The doublet occurring at 7.20 ppm (J = 7.53 Hz) integrating for two protons was assigned to H_3 and H_5. The multiplet at 7.32 - 7.42 ppm integrating for six aryl protons accounts for the

remaining six aryl protons. The downfield singlet at 8.27 ppm with an integration of 1 proton was assigned to $H_{1''}$ on the nitrovinyl unit.

The ^{13}C NMR spectrum (101 MHz, $CDCl_3$) of compound **86** (Figure 60) shows a signal at 32.87 ppm which was assigned to $C_{3''}$. The CH signals at 127.11 ppm, 127.52 ppm, 129.01 ppm, 129.45 ppm and 130.90 ppm were assigned to C_4, C_3 & C_5, C_2 & C_6, $C_{3'}$ & $C_{5'}$ and $C_{6'}$ & $C_{2'}$ respectively. The quaternary signals at 130.36 ppm, 135.83 ppm and 136.66 ppm accounted for C_1, $C_{1'}$ and $C_{4'}$ respectively. The CH signal at 134.19 ppm corresponds to $C_{1''}$. The downfield resonance at 149.91 ppm was attributed to $C_{2''}$. FTIR spectroscopy shows bands at 1674 (C=C) and 1553, 1368 (NO_2) cm^{-1}. High resolution mass spectrometry (ESI) was carried out and the required molecular ion was calculated to be $C_{15}H_{12}ClNO_2Na$ [M^++Na] 296.0454 and found as 296.0463.

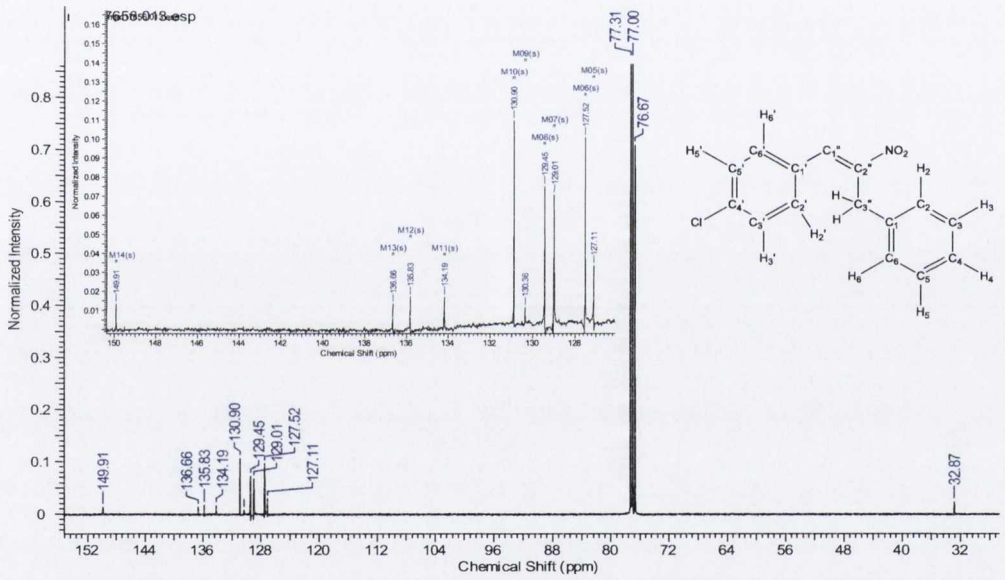

Figure 60: ^{13}C NMR spectrum of *(E)*-1-chloro-4-(2-nitro-3-phenylprop-1-en-1-yl)benzene (86)

X-ray crystallography was carried out on a recrystallized sample of (*E*)-4,4'-(2-nitroprop-1-ene-1,3-diyl)bis(chlorobenzene) (**85**) (Figure 61). The data generated confirmed the conformation of the nitrovinyl unit after the second Henry-Knoevenagel condensation reaction as trans *(E)* and a simple monoclinic packing diagram.

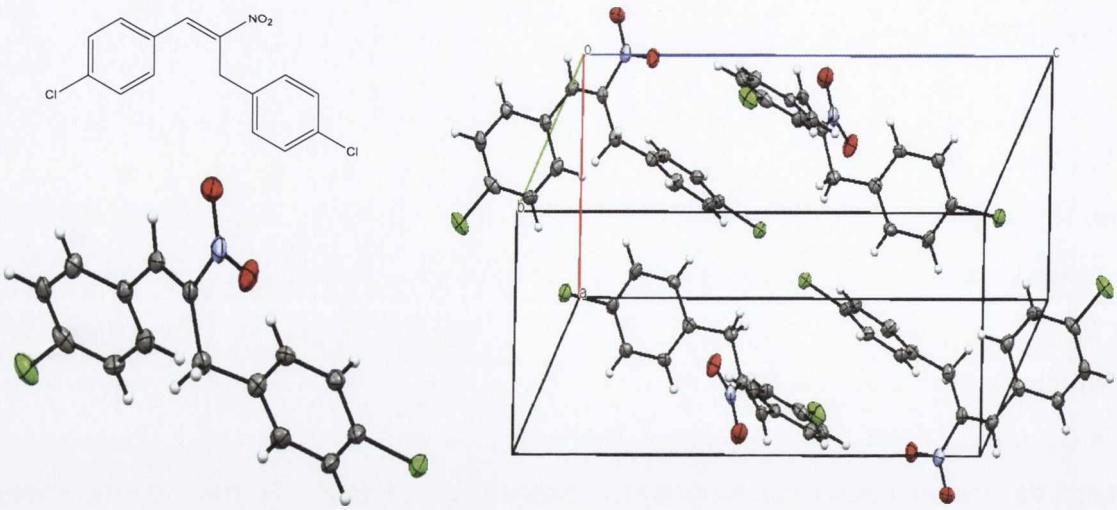

Figure 61: X-ray crystallography data for (*E*)-4,4'-(2-nitroprop-1-ene-1,3-diyl)bis(chlorobenzene) (85)

4,4'-(2-Nitropropane-1,3-diyl)bis(chlorobenzene) (**89**) was synthesised from (*E*)-4,4'-(2-nitroprop-1-ene-1,3-diyl)bis(chlorobenzene) (**85**) using the sodium borohydride procedure described earlier[5].

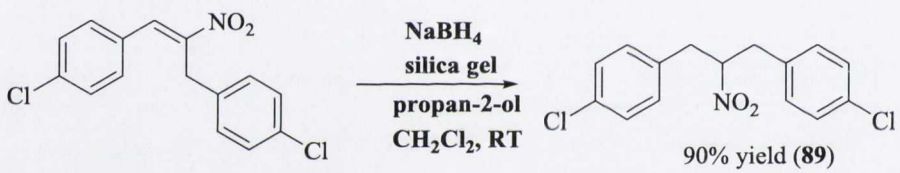

Figure 62: Scheme for synthesis of 4,4'-(2-nitropropane-1,3-diyl)bis(chlorobenzene)

This compound was synthesised in order to determine if the alkene bond was necessary for antiproliferative action induced by (*E*)-4,4'-(2-nitroprop-1-ene-1,3-diyl)bis(chlorobenzene). Nanjo et al achieved a similar reduction of 1,3-bis(aryl)-2-nitro-1-propene to (2-nitropropane-1,3-diyl)dibenzene utilising the reducing conditions produced by formic acid, trimethylamine and N,N-dimethyl-formamide at 114 °C[223]. Using the sodium borohydride procedure gave the reduction from (*E*)-4,4'-(2-nitropropane-1,3-diyl)bis(chlorobenzene) (**85**) to 4,4'-(2-nitropropane-1,3-diyl)bis(chlorobenzene) (**89**) with 90% yield.

The ^{1}H NMR (400 MHz, $CDCl_3$) spectrum of compound **89** bears two double doublets at 3.06 ppm (J = 14.67, 5.87 Hz) and 3.28 ppm (J = 14.67, 8.80 Hz), both integrate for two protons each. These represent the germinal protons on both C_3" and C_1", with one proton under a greater electronegative influence from the nitro group and drawing it further downfield in the spectra. The multiplet at 4.80 - 4.91 ppm integrating for one proton accounts for $C_{2"}$.

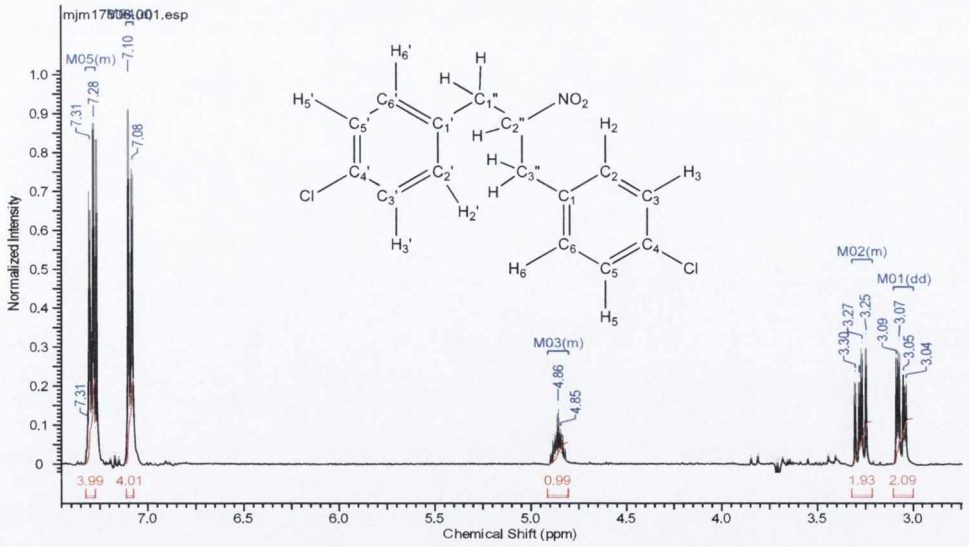

Figure 63: ^{1}H NMR spectrum of 4,4'-(2-nitropropane-1,3-diyl)bis(chlorobenzene (89)

The doublet at 7.09 ppm (J = 8.80 Hz) integrating for four protons and the multiplet occurring at 7.27 - 7.33 ppm integrating for four protons were assigned to the two equivalent groups of protons; group one (H_2, H_6, $H_{2'}$ & $H_{6'}$) and the more downfield group two (H_3, H_5, $H_{3'}$ & $H_{5'}$) respectively.

The ^{13}C NMR spectrum (101 MHz, $CDCl_3$) of compound **89** (Figure 64) shows resonances at 38.90 ppm and 90.58 ppm, these were assigned to $C_{1''}$ & $C_{3''}$ and $C_{2''}$ respectively. The CH shifts at 129.12 ppm, 130.15 ppm were assigned to the two carbon equivalent groups: group one (C_2, C_6, $C_{2'}$ & $C_{6'}$) and group two ($C_{5'}$, $C_{3'}$, C_3 & C_5). The two quaternary signals at 133.47 ppm and 133.61 ppm correspond to $C_{1'}$ & C_1 and C_4 & $C_{4'}$.

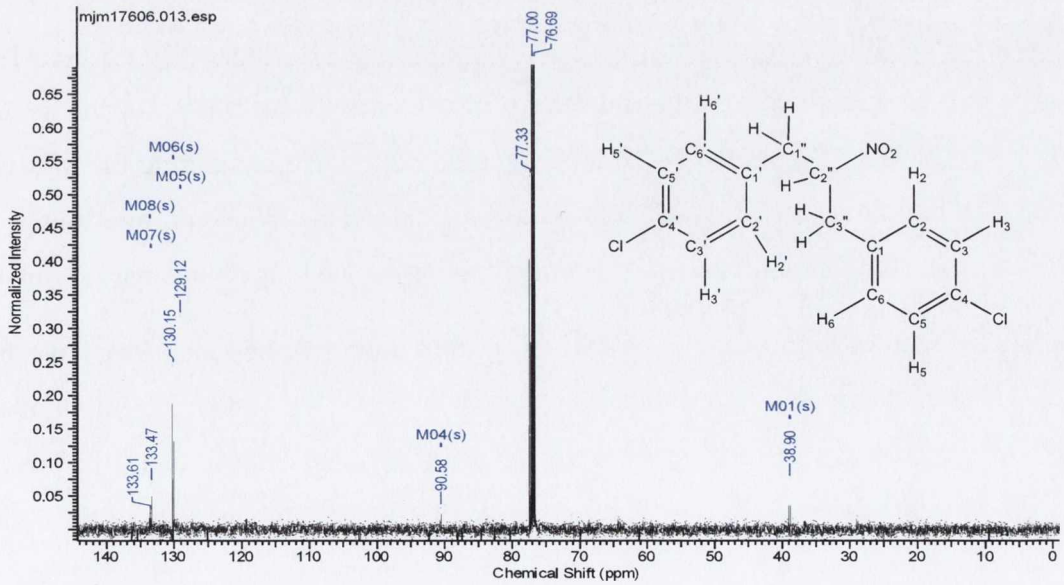

Figure 64: ^{13}C NMR spectrum of 4,4'-(2-nitropropane-1,3-diyl)bis(chlorobenzene) (89)

FTIR spectroscopy shows bands at 1620 (C=C) and 1533, 1326 (NO_2) cm^{-1}. High resolution mass spectrometry (ESI) was carried out and the required molecular ion was calculated to be $C_{15}H_{13}Cl_3NO_2$ [M + Cl] 344.0012 and found as 344.0022.

2.3 Synthesis of the (*E*)-2-nitro-1,3-diphenylprop-2-en-1-ones

A small panel of (*E*)-(2-nitrovinyl)benzenes with phenylprop-2-en-1-one substitution at the 2 position of the nitrovinyl unit was achieved. These (*E*)-2-nitro-1,3-diphenylprop-2-en-1-ones were synthesised using methodology reported by Sagitullina et al. (2002)[152]. These structures were based on the 1,3-bis(aryl)-2-nitro-1-propene scaffold previously shown in our research to have antiproliferative activity in BL cell lines[5] and should offer a slightly altered configuration for the product (Figure 65).

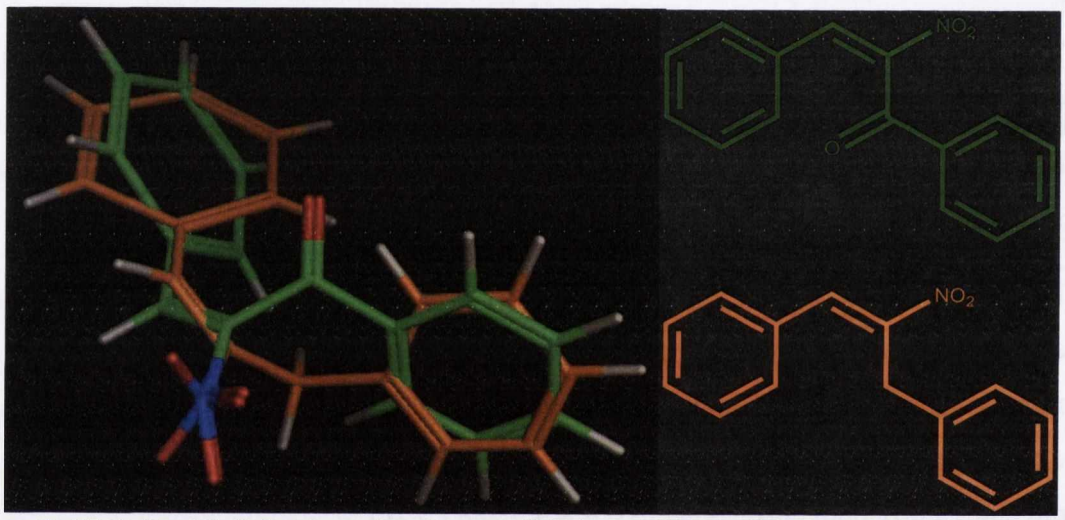

Figure 65: (*E*)-2-nitro-1,3-diphenylprop-2-en-1-one scaffold (green) flexibly allgined to the (*E*)-1,3-bis(aryl)-2-nitro-1-propene scaffold (orange) (MOE 2011.10).

To illustrate this altered conformation; the (*E*)-2-nitro-1,3-diphenylprop-2-en-1-one (chalcone) scaffold was flexibly aligned to the (*E*)-1,3-bis(aryl)-2-nitro-1-propene scaffold using MOE (ver. 2011.10). Altered bond angles can be seen when comparing the nitrovinyl groups and contracting the angle at the carbonyl carbon and the methylene protons on the 1,3-bis(aryl)-2-nitro-1-propene scaffold, also the aromatic rings are no longer coplanar (Figure 65).

Chalcones are a significant class of biologically active compounds that have been previously shown to possess antibacterial[224], anti-cancer[225, 226] and anti-inflammatory activities[227]. Furthermore Dore et al. (1974) has demonstrated that a series of 1,3-bis(aryl)-2-nitro-1-propenes and related chalcones exhibit a cytotoxic effect[16]. The synthesis of the 2-nitro-1,3-diphenylprop-2-en-1-ones utilised the Henry-Knoevenagel condensation of nitroacetophenone with various benzaldehydes catalysed by β-alanine (Figure 66). The

mechanism for this reaction follows the general reaction mechanism for the Henry-Knoevenagel condensation (Figure 43). The reaction was refluxed in a mixture of benzene and glacial acetic acid using a Dean-Stark trap for the azeotropic removal of water. Alternatively this Henry Knoevenagel condensation reaction can be catalysed by 4-methylmorpholine and titanium tetrachloride[228]. 2-Nitro-1,3-diphenylprop-2-en-1-ones can also be synthesised by the selective nitration of chalcones using dinitrogen tetraoxide in tetrachloromethane[16] or nitric dioxide[229].

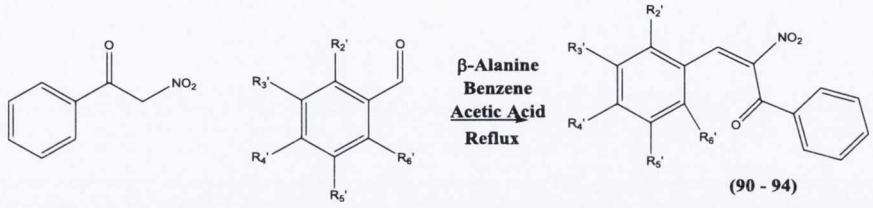

Figure 66: Scheme for the synthesis of (*E*)-2-nitro-1,3-diphenylprop-2-en-1-ones

As shown above (Figure 65) the introduction of the carbonyl at the C_3 position provides a different conformation when compared to the 1,3-bis(aryl)-2-nitro-1-propenes previously studied and provides a reaction centre amenable to a number of further functional group transformations. The carbonyl also introduces an α-β unsaturated ketone system to the 1,3-bis(aryl)-2-nitro-1-propene scaffold and could facilitate the further nucleophilic Michael additions of various carbanions to the β-carbon. One such transformation; the synthesis of a 3-nitro-thiazepine heterocycle (**189**) from compound **90** was achieved and will be discussed later in Chapter 3. The 2-nitro-1,3-diphenylprop-2-en-1-ones (**90-94**) synthesised were purified by flash column chromatography to give good yields (40-78%) and are summarised in Table 6 below.

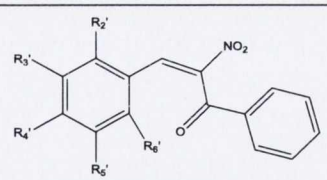

Compound	Substitution pattern	Yield	Compound	Substitution pattern	Yield
90	-	60%	**93**	$R_{2'} = R_{3'} = C_4H_4$	40%*
91	$R_{4'} = Cl$	45%	**94**	$R_{2'} = OCH_3$, $R_{5'} = Br$	78%*
92	$R_4 = OH$	30%*	-	-	-

Table 6: (*E*)-2-nitro-1,3-diphenylprop-2-en-1-one library. Note: R = H unless otherwise specified. * denotes novel compound

The ^{1}H NMR (400 MHz, $CDCl_3$) spectrum of compound **94** (Figure 67) shows a singlet at 3.60 ppm integrating for three protons which were assigned to the three methoxy protons at position C_2 of the nitrostyrene aryl ring.

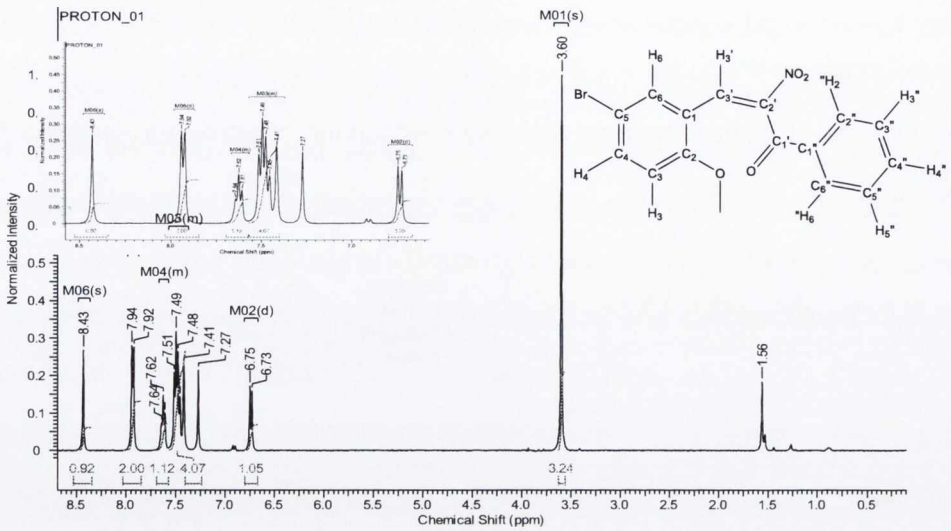

Figure 67: ^{1}H NMR spectrum of (*E*)-3-(5-bromo-2-methoxyphenyl)-2-nitro-1-phenylprop-2-en-1-one (94)

The doublet occurring at 6.74 ppm (J = 8.71 Hz) and the multiplet occurring at 7.57 - 7.67 ppm both integrating for single protons were assigned to H_3 and $H_{4''}$ respectively. The downfield doublet at 7.93 ppm with an integration of two protons accounted for the aryl protons $H_{6''}$ and $H_{2''}$. The large multiplet at 7.37 – 7.57 ppm integrating for four protons was assigned to the remaining aryl protons H_4, H_6, $H_{3''}$ and $H_{5''}$. The remaining downfield singlet occurring at 8.43 ppm with an integration of one proton was assigned to $H_{3'}$ on the nitrovinyl unit.

The ^{13}C NMR spectrum (101 MHz, $CDCl_3$) of compound **94** (Figure 68) shows CH resonances at 112.88 ppm, 131.75 ppm, 134.04 ppm and 134.40 ppm were assigned to C_3, $C_{4''}$, C_6 and C_4. The carbon equivalent CH resonances at 128.95 ppm and 129.03 ppm were assigned to $C_{3''}$ & $C_{5''}$ and $C_{2''}$ & $C_{6''}$. The most downfield CH resonance at 136.18 ppm accounted for $C_{3'}$ on the nitrovinyl unit. The quaternary resonances occurring at 112.88 ppm, 135.34 ppm, 138.26 ppm and 146.11 ppm corresponded to C_3, $C_{1''}$, C_1 and $C_{2'}$. Two downfield quaternary signals at 157.21 ppm and 187.10 ppm were found to correspond to the two remaining quaternary carbons: C_2 and $C_{1'}$. These two signals appeared much further downfield than other quaternary signals due to their proximity to the methoxy and carbonyl respectively.

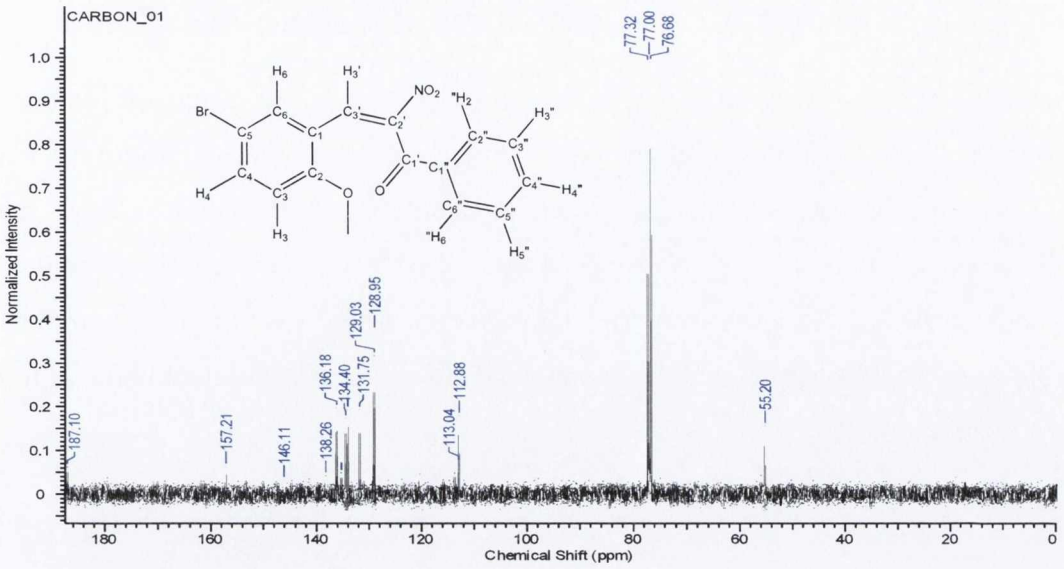

Figure 68: ^{13}C NMR spectrum of (*E*)-3-(5-bromo-2-methoxyphenyl)-2-nitro-1-phenylprop-2-en-1-one (94)

FTIR spectroscopy shows bands at 1675 (C=O), 1592 (C=C) and 1530, 1356 (NO_2) cm^{-1}. High resolution mass spectrometry (APCI) was carried out and the required molecular ion was calculated to be $C_{16}H_{12}BrNO_4$ [M^+] 360.9950 and found as 360.9956.

X-ray crystallography structural determination was carried out on a sample of (*E*)-3-(5-bromo-2-methoxyphenyl)-2-nitro-1-phenylprop-2-en-1-one (**94**), the data generated can be seen in Figure 69. From the asymmetric unit it was possible to verify the orientation of the nitrovinyl unit as (*E*) and the packing diagram calculated was triclinic.

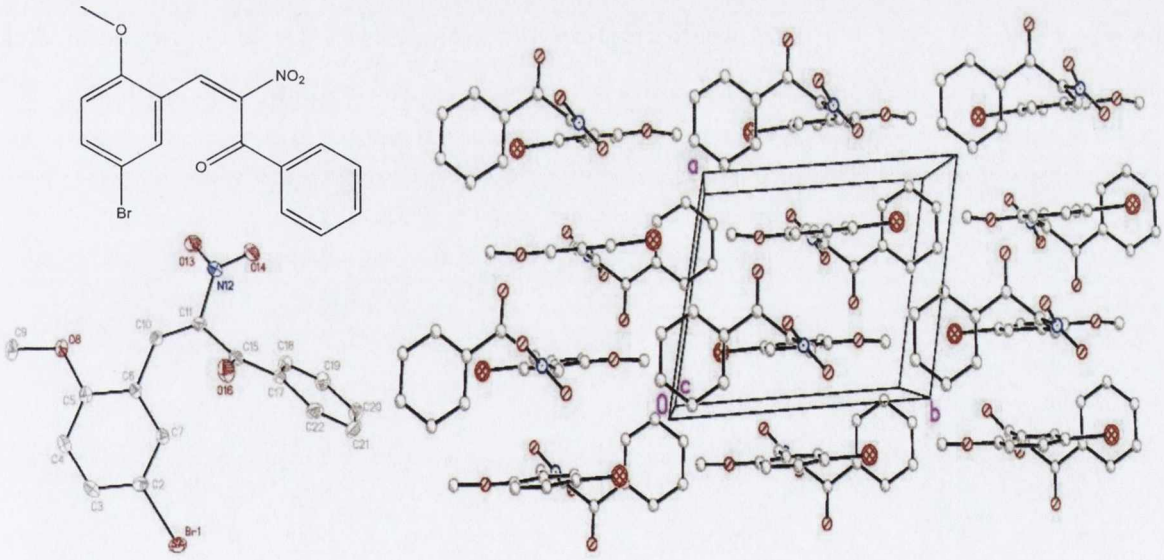

Figure 69: X-ray crystallography data for (*E*)-3-(5-bromo-2-methoxyphenyl)-2-nitro-1-phenylprop-2-en-1-one (94)

2.4 Synthesis of 1-substituted-2-nitroethylbenzenes via the Michael addition

Since its discovery in 1887[230] by Arthur Michael, the conjugate addition of a nucleophile to an α-β-unsaturated system (also known as the Michael addition) has become a staple of organic chemistry. The Michael addition facilitates the base catalysed functionalization of a variety of α-β-unsaturated systems with relatively mild reaction conditions. Utilising the previously generated library of (*E*)-(2-nitrovinyl)benzenes it was possible to elect a number of candidate compounds to undergo Michael addition with selected thiols and aniline (Figure 70).

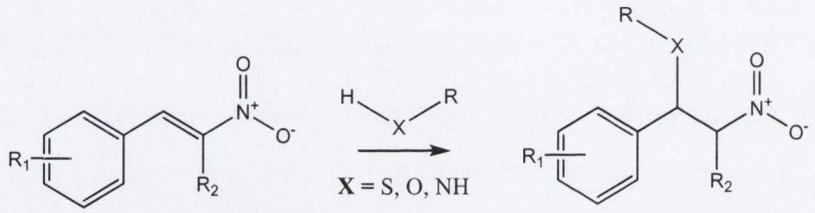

Figure 70: Scheme for the synthesis of 1-substituted-2-nitroethylbenzenes via the Michael addition

Since the first documented Michael addition to (*E*)-(2-nitrovinyl)benzenes in 1905[231] (Heim et al.); the reaction has been recorded with sulfur[170, 232], carbon[233], nitrogen[170, 234, 235] and oxygen[231, 236] nucleophiles successfully undergoing the conjugate addition. The proposed mechanism for the Michael addition is present below in Figure 71; the reaction is initiated by deprotonation and formation of the nucleophile. The nucleophile attacks the nitrovinyl unit at the C_1 or beta position, leading to the formation of the charged nitronate intermediate. Acidic workup allows the reformation of the nitro group through protonation of the nitronate.

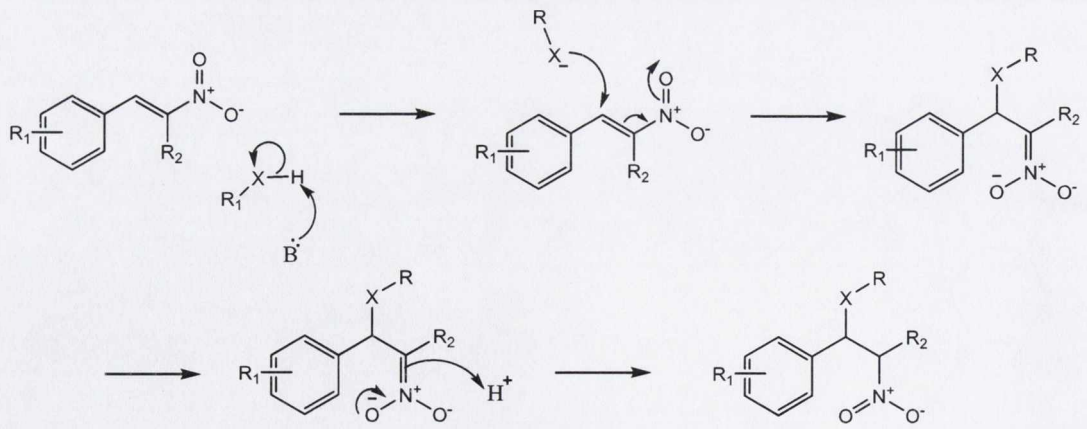

Figure 71: Proposed mechanism for the synthesis of 1-substituted-2-nitroethylbenzenes via the Michael addition

Utilising the procedure outlined by Ziyaei et al. (2007), the synthesis of a number of 1-substituted-2-nitroethylbenzenes (**95-100**) was achieved via the aqueous Michael addition of

thiols and aniline[170]. The reaction afforded quite pure compounds upon workup and removal of organic solvent *in vacuo* with yields of 50-90% (Table 8).

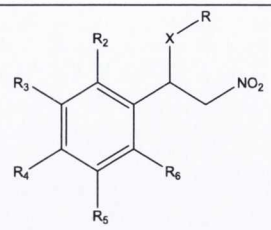

Compound	X	R	Substitution pattern	Yield	Compound	X	R	Substitution pattern	Yield
95	S	CH_2CH_3	-	50%	**98**	NH	C_6H_5	-	85%
96	S	CH_2CH_3	$R_2 = OCH_3$, $R_5 = Br$	90%*	**99**	NH	C_6H_5	$R_4 = Cl$	76%
97	S	C_6H_5	$R_2 = OCH_3$, $R_5 = Br$	70%*	**100**	NH	C_6H_5	$R_4 = Br$	70%*

Table 7: 1-subsituted-(2-nitroethyl)benzene library. Note: R = H unless otherwise specified. * denotes novel compound

The ^1H NMR (400 MHz, $CDCl_3$) spectrum of compound **96** (Figure 72) shows a triplet at 1.24 ppm (J = 7.48 Hz) integrating for three protons, this was assigned to the three alkyl protons on $C_{2''}$. A quartet at 2.55 ppm (J = 7.46 Hz) integrating for two protons was assigned to the two protons on $C_{1''}$.

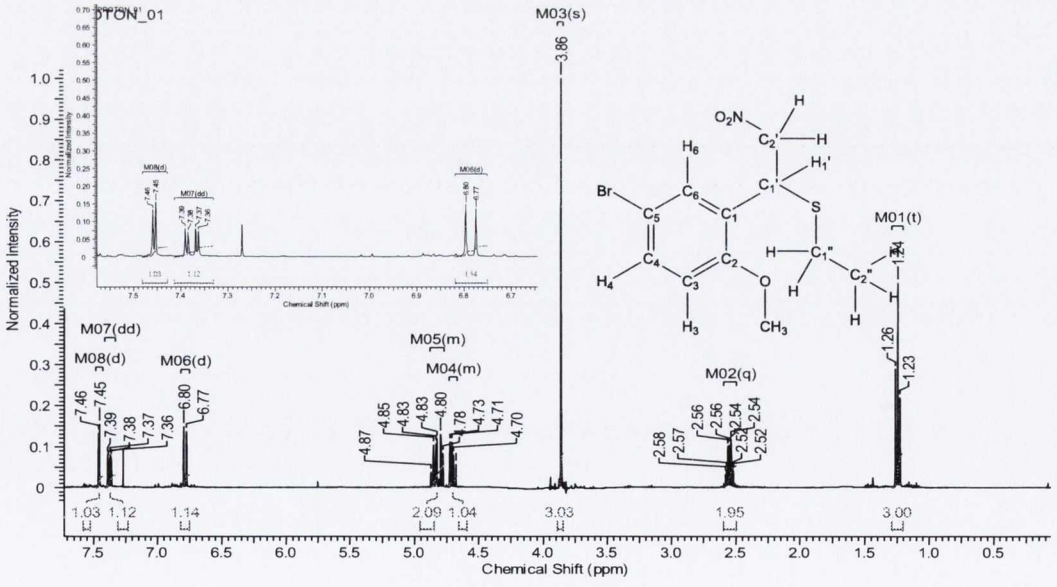

Figure 72: ^1H NMR spectrum of (1-(5-bromo-2-methoxyphenyl)-2-nitroethyl)(ethyl)sulfane (96)

The singlet at 3.86 ppm with an integral value of three protons accounted for the methoxy substituent on the aryl ring at C_2. The multiplets at 4.67 - 4.73 ppm and 4.77 - 4.88 ppm integrating for one and two protons respectively were assigned to $H_{1'}$ and the two protons on $C_{2'}$. The two doublets in the aromatic region of the spectrum occurring at 6.79 ppm (J = 8.71 Hz) and at 7.46 ppm (J = 2.49 Hz) were assigned to H_3 and H_6. The smaller coupling constant was associated with H_6 due to long range coupling with H_4. The remaining downfield double doublet at 7.38 ppm (J =8.71, 2.49 Hz) accounted for the remaining aryl proton H_4.

The ^{13}C NMR spectrum (101 MHz, $CDCl_3$) of compound **96** (Figure 73) shows resonances occurring at 14.45 ppm, 26.55 ppm, 55.94 ppm and 78.34 ppm, these were assigned to $C_{2''}$, $C_{1''}$, the methoxy substituent on C_2 and $C_{2'}$ respectively.

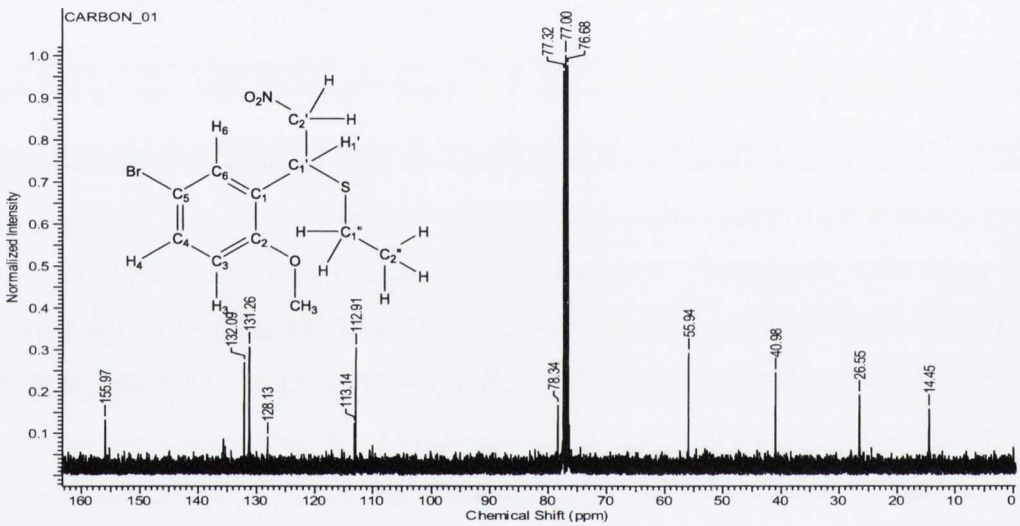

Figure 73: ^{13}C NMR spectrum of (1-(5-bromo-2-methoxyphenyl)-2-nitroethyl)(ethyl)sulfane (96)

The resonance that occurred at 40.98 ppm was assigned to $C_{1'}$.The aromatic CH signals at 112.91 ppm, 131.26 ppm and 132.09 ppm were allocated to C_3, C_4 and C_6. The aromatic quaternary signals at 113.14 ppm and 128.13 ppm accounted for C5 and C1. The downfield signal at 155.97 ppm was found to correspond to C_2, the downfield signal produced was a product of the electron withdrawing environment produced by the methoxy group attached.

2.5 Synthesis of the ethyl (*E*)-2-hydroxy-3-nitro-4-phenylbut-3-enoates

Ethyl (*E*)-2-hydroxy-3-nitro-4-phenylbut-3-enoates (**101-104**) were synthesised using a 4-dimethylaminopyridine (DMAP) catalysed Baylis-Hillman (BH) reaction between the corresponding (*E*)-(2-nitrovinyl)benzene and ethyl glyoxylate (Figure 74). This BH reaction took place in acetonitrile at room temperature with long reaction times of two to seven days[171].

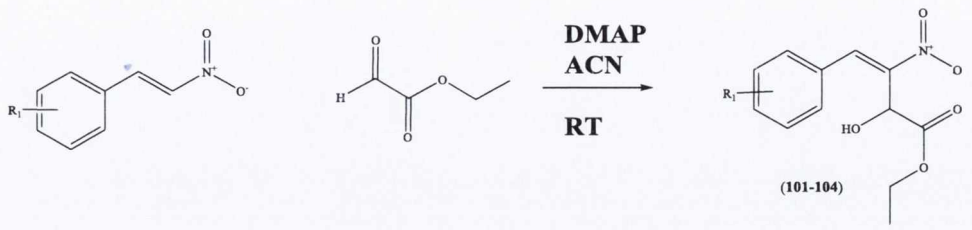

Figure 74: Scheme for the synthesis of Ethyl (*E*)-2-hydroxy-3-nitro-4-phenylbut-3-enoates

The BH reaction was first described by A. B. Baylis and M. E. D. Hillman in a German patent published in 1972[237]. The Baylis-Hillman reaction (also known as the Morita-Baylis-Hillman reaction) is a carbon-carbon bond forming reaction between an activated alkene with a carbon nucleophile[209, 238]. The reaction can be catalysed by the presence of tertiary amines such as DABCO[239,240], DBU[241], DMAP[171], imidazole[173, 242, 243] and TMA[244] (Figure 75). In more recent times the BH reaction has been carried out using microwave assisted organic synthesis[245, 246]. Lewis acids have also been shown to catalyse the BH reaction[247].

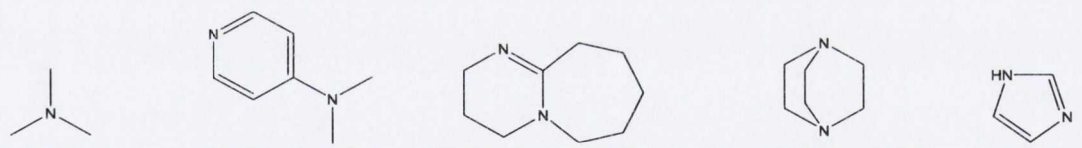

Figure 75: Amines used to catalyse Baylis-Hillman reaction

The BH reaction has been successfully carried out using a range of different electron poor alkene systems such as vinyl ketones, acroleins, acrylonitriles and vinyl sulfones[209]. Rastogi et al first achieved the first BH reaction of (*E*)-(2-nitrovinyl)benzenes, synthesising a library of BH adducts using formaldehyde and imidazole as the catalyst[243].

Deb et al. optimised the reaction conditions necessary to synthesise the a range of alkyl (*E*)-2-hydroxy-3-nitro-4-phenylbut-3-enoates from (*E*)-(2-nitrovinyl)benzene and ethyl glyoxylate. Over the course of this study Deb et al. identified that imidazole (pKa 7.0) and DMAP (pKa 12.0) favoured the reaction. Additional resonance states available to both DMAP and imidazole during the conjugate addition step of the mechanism of formation is also thought

to push this reversible reaction to completion. It was also speculated that DMAP and imidazole would provide less steric hindrance during conjugate addition due to their smaller size[171].

The reaction mechanism (Figure 76) is initiated by a Michael type nucleophilic attack by DMAP on the electron deficient alkene bond, giving a zwitterionic intermediate.

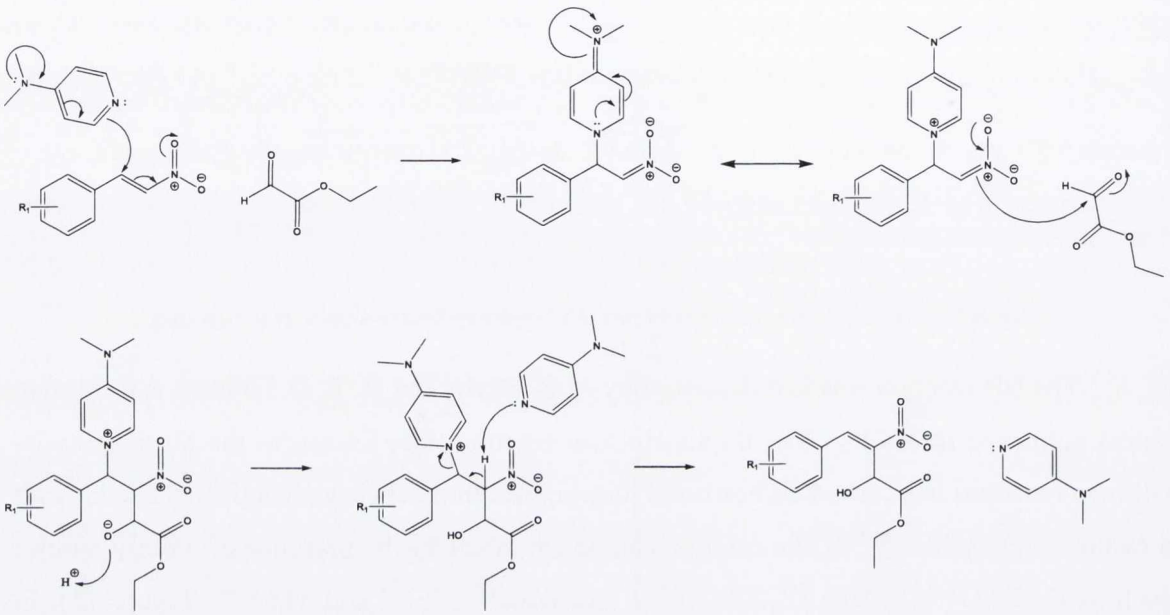

Figure 76: Proposed mechanism for the synthesis of ethyl (*E*)-2-hydroxy-3-nitro-4-phenylbut-3-enoates[209]

As previously mentioned, this conjugate addition is believed to be afforded additional stability through the resonance form accommodated by DMAP and is therefore less likely to undergo a reverse reaction and subsequent elimination of the DMAP nucleophile. The zwitterionic intermediate (produced by the conjugated addition) nucleophilically attacks the aldehyde carbonyl and proceeds to form an aldol intermediate. A second DMAP molecule completes the reaction mechanism through the bimolecular elimination of the original DMAP nucleophile, thus reforming the nitrovinyl double bond.

A panel of ethyl (*E*)-2-hydroxy-3-nitro-4-phenylbut-3-enoate (**101-104**) was successfully synthesised with yields of 12-58% (Table 8). The 3-chlorophenyl product **104** was obtained in surprisingly low yield (12%).

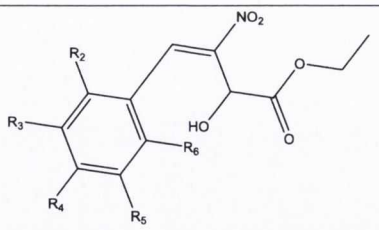

Compound	Substitution pattern	Yield	Compound	Substitution pattern	Yield
101	$R_2 = OCH_3$, $R_5 = Br$	58%*	**103**	$R_4 = OH$	40%*
102	$R_4 = Cl$	45%	**104**	$R_3 = Cl$	12%

Table 8: ethyl (*E*)-2-hydroxy-3-nitro-4-phenylbut-3-enoate library. Note: R = H unless otherwise specified. * denotes novel compound

Compound **101** was chosen as a representative sample of the ethyl (*E*)-2-hydroxy-3-nitro-4-phenylbut-3-enoates and the ^1H NMR and ^{13}C NMR spectra will now be discussed in detail. The ^1H NMR (400 MHz, $CDCl_3$) spectrum of compound **101** (Figure 77) shows a triplet (J = 7.05 Hz) at 1.31 ppm.

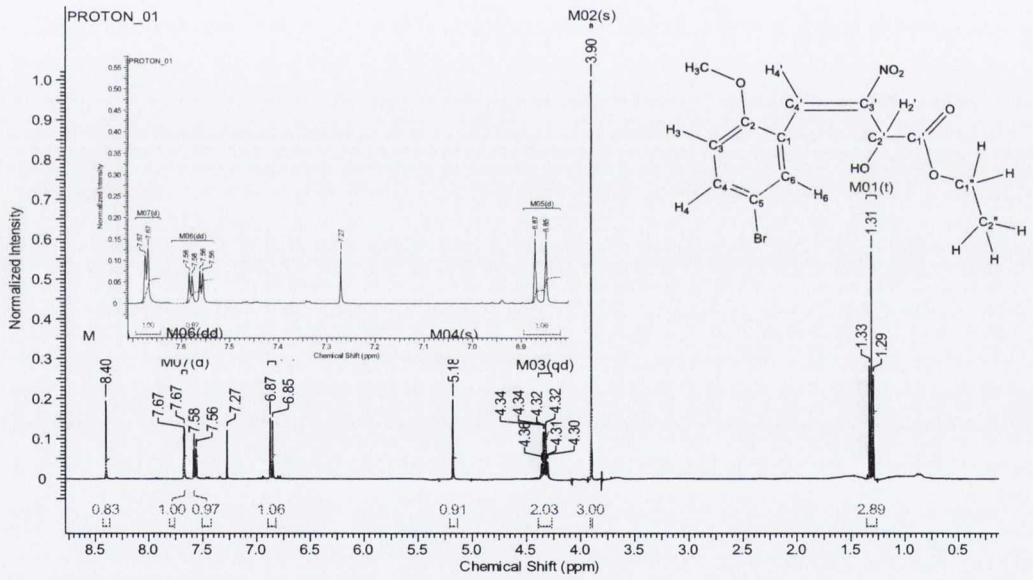

Figure 77: ^1H NMR spectrum of Ethyl (*E*)-4-(5-bromo-2-methoxyphenyl)-2-hydroxy-3-nitrobut-3-enoate (101)

A singlet occurring at 3.90 ppm integrating for three protons was assigned to the methoxy group at position C_2 of the aryl ring. The quartet of doublets (J = 1.87, 7.12 Hz) observed at 4.33 ppm integrated for two protons was allocated to the protons on $C_{1''}$. The singlet at 5.18 ppm bears an integration of one proton and can be attributed to $H_{2'}$, this proton has no neighbouring protons thus accounting for its multiplicity. The doublet 6.86 ppm (J = 9.12 Hz) and the double doublet 7.57 ppm (J = 2.49, 8.71 Hz) both integrating for a single proton each were assigned to H_3 and H_4 respectively. The doublet occurring at 7.67 ppm (J = 2.49 Hz) with

an integral value of 1 proton accounted for H_6. The coupling constant for this doublet at 7.67 ppm was 2.49 Hz indicative of long range (four bond) coupling with the double doublet at 7.57 ppm (H_4). The remaining downfield singlet occurring at 8.40 ppm was attributed to $H_{4'}$ on the nitrovinyl unit.

The ^{13}C NMR spectrum (101 MHz, $CDCl_3$) of compound **101** (Figure 78) shows signals at resonances at 14.02 ppm, 56.00 ppm and 63.08 ppm; these were assigned to $C_{2''}$, the carbon in the methoxy substituent and $C_{1''}$. The CH resonances occurring at 65.92 ppm and 112.61 ppm accounted for $C_{2'}$ and C_3.

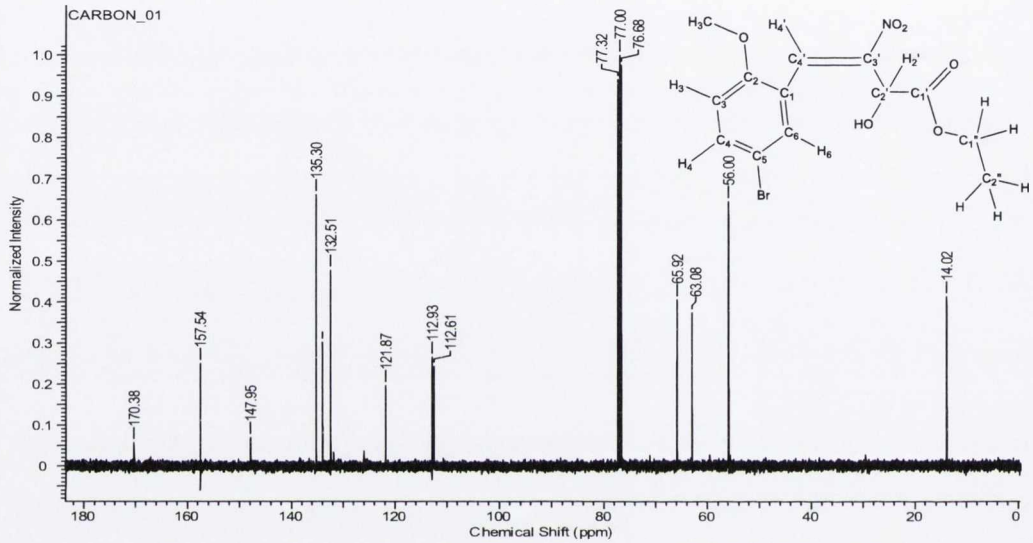

Figure 78: ^{13}C NMR spectrum of Ethyl (*E*)-4-(5-bromo-2-methoxyphenyl)-2-hydroxy-3-nitrobut-3-enoate

Further CH resonances occurring at 132.51 ppm, 134.11 ppm and 135.30 ppm were labelled as C_4, C_6 and $C_{4'}$ in the nitrovinyl unit. Quaternary resonances 112.93 ppm and 121.87 ppm were identified as C_5 and C_1. The remaining downfield quaternary signals 147.95 ppm, 157.54 ppm and 170.38 ppm were attributed to the slightly more electronegative environments produced at $C_{3'}$, C_2 and C_1' respectively. FTIR spectroscopy shows bands at 3326 (O-H), 1730 (C=O) and 1528, 1325 (NO_2) cm^{-1}.

2.6 Synthesis of (*E*)-2-(2-nitrovinyl)cyclohexa-2,5-diene-1,4-diones

(*E*)-2-(2-nitrovinyl)cyclohexa-2,5-diene-1,4-diones were synthesised from the (*E*)-1,4-dimethoxy-2-(2-nitrovinyl)benzenes produced as part of the (*E*)-(2-nitrovinyl)benzene libraries. Benzoquinones as a class of organic compounds are commonly occurring structures in the natural world and are widely used as dyes[248] with noted antimicrobial[249] and antitumor activity[250, 251].The (*E*)-2-(2-nitrovinyl)cyclohexa-2,5-diene-1,4-diones were produced through the redox oxidation of (*E*)-1,4-dimethoxy-2-(2-nitrovinyl)benzenes using ceric ammonium nitrate (CAN) in a mixture of acetonitrile and water over the course of ten minutes[180].

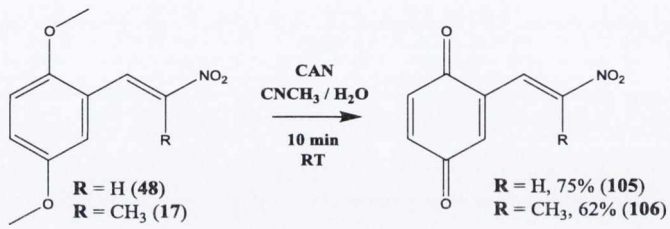

Figure 79: General scheme for the synthesis of the (*E*)-2-(2-nitrovinyl)cyclohexa-2,5-diene-1,4-diones

The first recorded synthesis of a compound of this class was by Jacob et al. (1976) when the preparation of 2-(2-nitroprop-1-en-1-yl)cyclohexa-2,5-diene-1,4-dione was achieved from 1,4-dimethoxy-2-(2-nitroprop-1-en-1-yl)benzene using ceric ammonium nitrate in a mixture of water and acetic acid[252]. Noland et al. (1998) synthesised 2-(2-nitrovinyl)cyclohexa-2,5-diene-1,4-dione as an intermediate for [4+2] cycloaddition with thiophene and furan structures to give angular quinoid heterocycles[180]. The oxidative preparation of benzoquinones has also been noted using barium ferrate (VI)[253], pyridinium chlorochromate[254] and sodium periodate[255]. Jacob et al (1976) carried out a simple radioisotope labelling study and proposed that the cerium ammonium nitrate oxidation mechanism proceeded via aryl oxygen bond cleavage with the net formation of the benzoquinone and methanol (Figure 80).

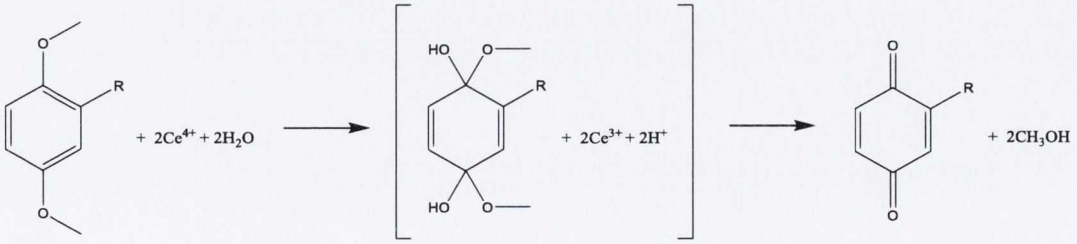

Figure 80:Proposed mechanism for the synthesis of the (*E*)-2-(2-nitrovinyl)cyclohexa-2,5-diene-1,4-diones[252]

Noland et al.'s procedure was chosen as the synthetic route due to the fact that cerium ammonium nitrate was readily available and Noland's oxidation was privy to a shorter reaction

time and more amiable purification by recrystallization. In the present work (*E*)-2-(2-nitrovinyl)cyclohexa-2,5-diene-1,4-diones (**105-106**) were afforded from compounds **48** and **17** in good yields of 62-75%.

2.7 Synthesis of the 2-alkyl-2-nitro-3-phenyloxiranes

Epoxidation of alkenes is a useful reaction in organic chemistry for functionalization of alkenes and a number of candidate (*E*)-(2-nitrovinyl)benzenes were selected for this chemical transformation from the extensive library of (*E*)-(2-nitrovinyl)benzenes previously synthesised. Epoxides are an important class of organic compounds acting as intermediates in synthesis[177, 256] and have been noted to induce apoptosis and cell death in cancer cells[257, 258]. A series of racemic 2-alkyl-2-nitro-3-phenyloxiranes (**107-111**) were synthesised by the base catalysed reaction of the (*E*)-(2-nitrovinyl)benzenes with *tert*-butyl hydroperoxide (Figure 81).

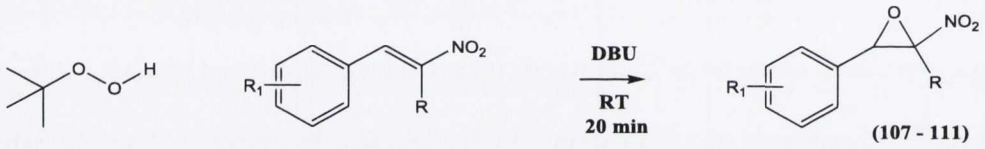

Figure 81: General scheme for the synthesis of 2-alkyl-2-nitro-3-phenyloxirane

The first synthesis of 2-methyl-2-nitro-3-phenyloxiranes was reported in 1969 by Newman et al. Newman achieved the epoxidation with a short reaction time in ice cold methanol using 15% hydrogen peroxide solution and 2N sodium hydroxide[259]. Bortolini et al. (2007) synthesised 2-nitro-3-phenyloxirane using oxonereg (potassium peroxy monosulfate) in ice cold dichloromethane with a longer reaction time of 5 hours[260]. In the process of developing a new method for the preparation of α-nitroacetophenones through the addition of *tert*-butyl hydrogenperoxide and subsequent oxidation; Ashwell et al. (1988) observed under certain reaction conditions the formation of the corresponding 2-methyl-2-nitro-3-phenyloxirane. Ashwell et al. utilised a basic system of *tert*-butyl hydrogenperoxide and *n*-butyl lithium in -78 °C THF and the reaction itself came to completion in 90 minutes[256].

In a more recent work, Weiss et al. (2011) prepared a number of 2-methyl-2-nitro-3-phenyloxiranes as intermediates in the synthesis of 1,3-thiazoles using 1,8-diazabicyclo [5.4.0] undec-7-ene and *tert*-butyl hydrogenperoxide at room temperature with excellent yields over ten minutes[177]. It was this procedure that provided access to the series of 2-alkyl-2-nitro-3-phenyloxiranes (**107-111**) below in the present work.

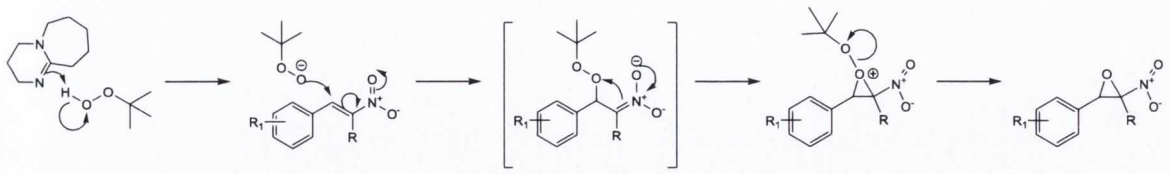

Figure 82: Mechanism for the synthesis of 2-alkyl-2-nitro-3-phenyloxirane

The proposed mechanism for the synthesis of the 2-alkyl-2-nitro-3-phenyloxiranes is presented in Figure 82. 1,8-diazabicyclo [5.4.0] undec-7-ene deprotonates the *tert*-butyl hydrogenperoxide forming a peroxide anion. The nitrovinyl unit acts as a Michael acceptor and undergoes nucleophilic attack by the peroxide species, leading to the formation of a nitronate intermediate. Cyclisation and elimination of the isopropyl leaving group gave the desired alkyl-2-nitro-3-phenyloxirane and isopropanol. Basic conditions favour the formation of the epoxide as it provides an environment suitable for the deprotonation of the *tert*-butyl hydrogenperoxide.

A series of 2-alkyl-2-nitro-3-phenyloxiranes (**107-111**) was synthesised by the base catalysed reaction of the (*E*)-(2-nitrovinyl)benzenes with *tert*-butyl hydrogenperoxide to give excellent yields of 85-92% (Table 9). These compounds include variation of alkyl chain length from methyl to ethyl, benzyl and introduction of aryl halogen substitution with chlorine and bromine.

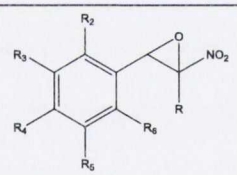

Compound	R	Substitution pattern	Yield	Compound	R	Substitution pattern	Yield
107	CH_3	R_3 = Cl	85%*	**110**	CH_2CH_3	R_3 = Cl	92%*
108	CH_3	R_4 = Cl	89%	**111**	$CH_2(C_6H_4)Cl$	R_4 = Cl	86%*
109	CH_3	R_4 = Br	92%*	-	-	-	-

Table 9: 2-alkyl-2-nitro-3-phenyloxirane library. Note: R = H unless otherwise specified. * denotes novel compound

3-(3-Chlorophenyl)-2-ethyl-2-nitrooxirane (**110**) was chosen as a representative sample of the 2-alkyl-2-nitro-3-phenyloxiranes and the ^{1}H NMR and ^{13}C NMR spectra will now be discussed in detail. The ^{1}H NMR (400 MHz, $CDCl_3$) spectrum of compound **110** (Figure 83) shows a triplet occurring at 1.09 ppm (J = 7.26 Hz) integrating for three protons – this triplet was assigned to the three protons on $C_{4'}$.

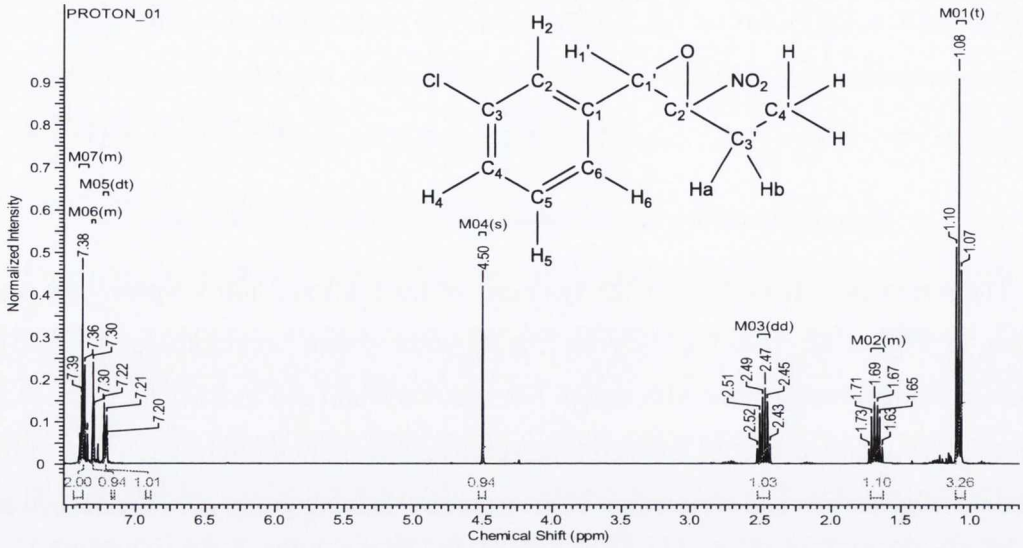

Figure 83: ^{1}H NMR spectrum (101 MHz, CDCl3) of 3-(3-chlorophenyl)-2-ethyl-2-nitrooxirane (110)

The two double doublets occurring at 1.69 ppm (J = 7.67, 15.14 Hz) and 2.48 ppm (J = 7.67, 15.14 Hz) account for geminal protons H_a and H_b on $C_{3'}$. A singlet integrating for a single proton seen at 4.50 ppm was assigned to $H_{1'}$. Analysing the aromatic region of the spectrum it can be seen that an apparent doublet of triplets produced by H_6 occurs at7.22 ppm (J = 1.87, 6.63 Hz). The multiplet at 7.29 - 7.31 ppm integrating for a singlet proton and the multiplet at 7.34 - 7.41 ppm integrating for two protons account for H_5 and H_4 & H_2.

The ^{13}C NMR spectrum (101 MHz, $CDCl_3$) of compound **110** shows resonances occurring at 7.59 ppm, 19.52 ppm and 62.27 ppm, these were assigned to $C_{4'}$, $C_{3'}$ and $C_{1'}$ respectively. The quaternary carbon signals at 92.17 ppm, 133.13 ppm and 134.91 ppm were allocated to $C_{2'}$, C_1 and C_3 respectively. The remaining CH resonances occurring at 124.52 ppm, 126.35 ppm, 129.61 ppm and 130.08 ppm were assigned to the remaining aromatic protons C_6, C_5, C_4 and C_2. FTIR spectroscopy shows bands at 1479, 1462, 1434 (C=C) and 1556, 1351 (NO_2 stretch) cm^{-1}. High resolution mass spectrometry (ESI) was carried out and the required molecular ion was calculated to be $C_{10}H_9ClNO_3$ [M-H] 226.0276 and found as 226.0277.

2.8 Synthesis of 5-alkyl-4-phenyl-1*H*-1,2,3-triazoles

Triazoles and triazole related derivatives are an important class of heterocycle in medicinal chemistry, triazoles have been noted to possess antifungal, antidepressant and anti-inflammatory activity[261]. Triazole derivatives are also of interest as anticancer agents and have

been shown to exhibit antiproliferative activity in endoththelial cells (EAhy 926)[176], leukemia and melanoma cell lines[262].

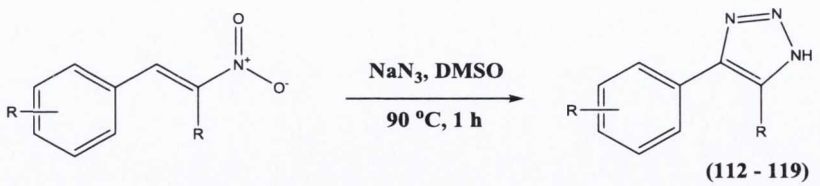

Figure 84: Scheme for the synthesis of the 5-alkyl-4-phenyl-1H-1,2,3-triazoles

Zefirov et al. (1971) first described the synthesis of 1,2,3 triazoles by the reaction of (*E*)-(2-nitrovinyl)benzenes and nitriles with sodium azide in dimethyl sulphoxide at room temperature[263]. Quiclet-Sire et al. (2005) re-examined the 'Zefirov 1,2,3 triazole synthesis' with a view to optimising the yield of the triazole formed[175]. The 1,2,3-triazoles can also be synthesised using the Huisgen cycloaddition (1,3 dipolar cycloaddition) of phenylacetylenes with trimethylsilylazide in the presence of copper (I) iodide in methanol / N,N-dimethyl-formamide with heating over 11-24 hours[264,265,266]. Other vinyl systems can also be used for the production of 1,2,3-triazoles, one such example is the reaction of (*E*)-styryl bromides with sodium azide with the use of palladium catalysis[267].

In the present work 5-alkyl-4-phenyl-1*H*-1,2,3-triazoles (**112-119**) were synthesised (utilising the procedure outlined by Quiclet-Sire et al.) from a number of varied (*E*)-(2-nitrovinyl)benzenes and sodium azide in dimethyl sulphoxide stirred at 90 °C for 90 minutes (Figure 84)[175].

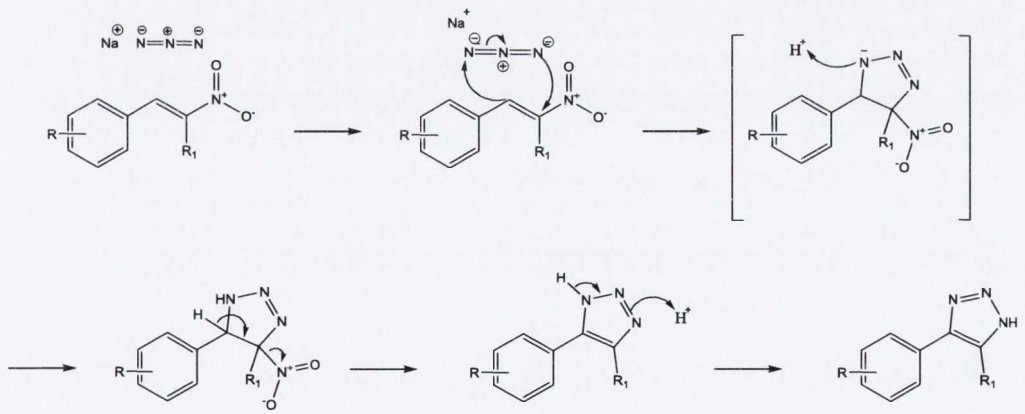

Figure 85: Proposed mechanism for the synthesis of the 5-alkyl-4-phenyl-1*H*-1,2,3-triazoles[268]

The reaction of sodium azide and activated alkenes such as the (*E*)-(2-nitrovinyl)benzenes proceeds via [3+2]-cycloaddition (Figure 85), aromatisation is ultimately achieved through the elimination of the nitro group[268]. A library of 5-alkyl-4-phenyl-1*H*-1,2,3-

triazoles (**112-119**) were successfully synthesised (Table 10); this included the synthesis of a triazole (**119**) from the Baylis-Hillman adduct ethyl (*E*)-4-(3-chlorophenyl)-2-hydroxy-3-nitrobut-3-enoate. The procedure employed afforded a crude product that could be purified easily by column chromatography using a gradient of dichloromethane and methanol. The overall yields achieved during the use of this [3+2]-cycloaddition were good ranging from 55-75% (Table 10).

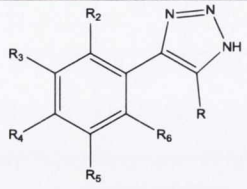

Compound	R	Substitution pattern	Yield	Compound	R	Substitution pattern	Yield
112	CH_3	R_3 = Cl	60%*	**116**	CH_3	R_4 = Cl	62%*
113	CH_3	R_4 = Br	63%*	**117**	CH_2CH_3	R_3 = Cl	68%*
114	CH_3	R_2 = OCH_3, R_5 = Br	60%*	**118**	CH_2CH_3	R_2 = OCH_3, R_5 = Br	75%*
115	CH_3	R_2 = OCH_3, R_5 = OCH_3	55%*	**119**	C(OH)C(O) -OCH_2CH_3	R_3 = Cl	68%*

Table 10: 5-alkyl-4-phenyl-1H-1,2,3-triazole library. Note: R = H unless otherwise specified. * denotes novel compound

The ^{1}H NMR (400 MHz, DMSO-d_6) spectrum of 4-(3-chlorophenyl)-5-methyl-1*H*-1,2,3-triazole (**112**) (Figure 86) shows a singlet integrating for three protons at 2.45 ppm, this singlet was assigned to the three protons of the methyl group on $C_{6'}$.

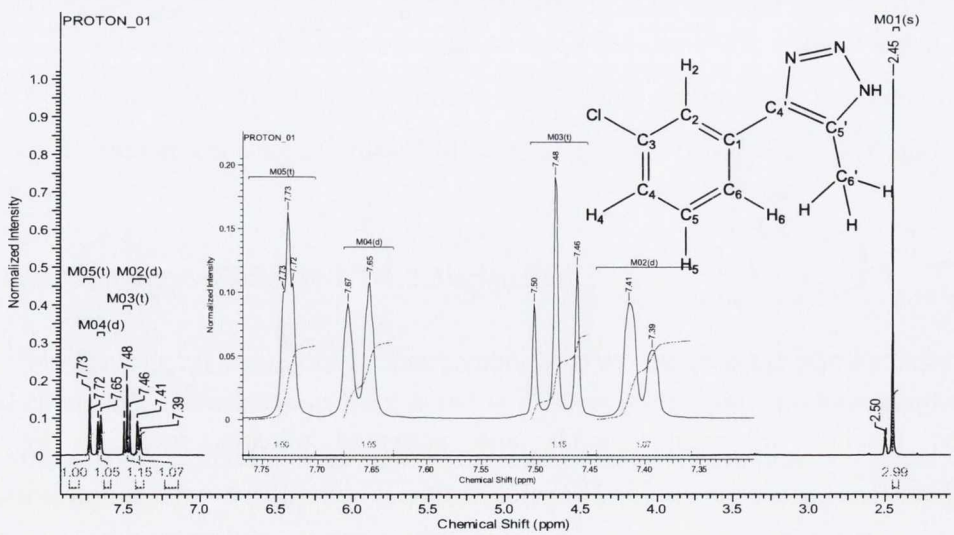

Figure 86: ^{1}H NMR spectrum of 4-(3-chlorophenyl)-5-methyl-1*H*-1,2,3-triazole

The doublet occurring at 7.40 ppm (J = 8.29 Hz) and the apparent triplet at 7.48 ppm (J = 7.88 Hz) both integrated for a single proton each and were assigned to the two aryl protons; H_4 and H_5 respectively. The more downfield doublet 7.66 ppm (J = 7.88 Hz) integrated for one proton and accounted for H_6, this proton appeared further downfield presumably due to proximity to the triazole ring. An apparent triplet signal occurred at 7.73 ppm (J = 1.66 Hz) and its integral was also one proton, this was assigned to H_2.

The ^{13}C NMR spectrum (101 MHz, DMSO-d_6) of compound **112** (Figure 87) shows a resonance occurring at 10.37 ppm accounting for $C_{6'}$, the carbon from the methyl group on the triazole ring. The CH resonances at 125.02 ppm, 125.99 ppm, 127.34 ppm were assigned to C_4, C_5 and C_6 respectively. The CH resonance more downfield at 130.65 ppm accounts for C_2 – its proximity to both the chlorine and triazole ring providing a more electron withdrawing environment than that of the other carbons. A quaternary resonance at 133.53 ppm accounts for C_3. The remaining quaternary carbons were accounted for by signals at 135.31 ppm, 141.30 ppm and 145.21 ppm.

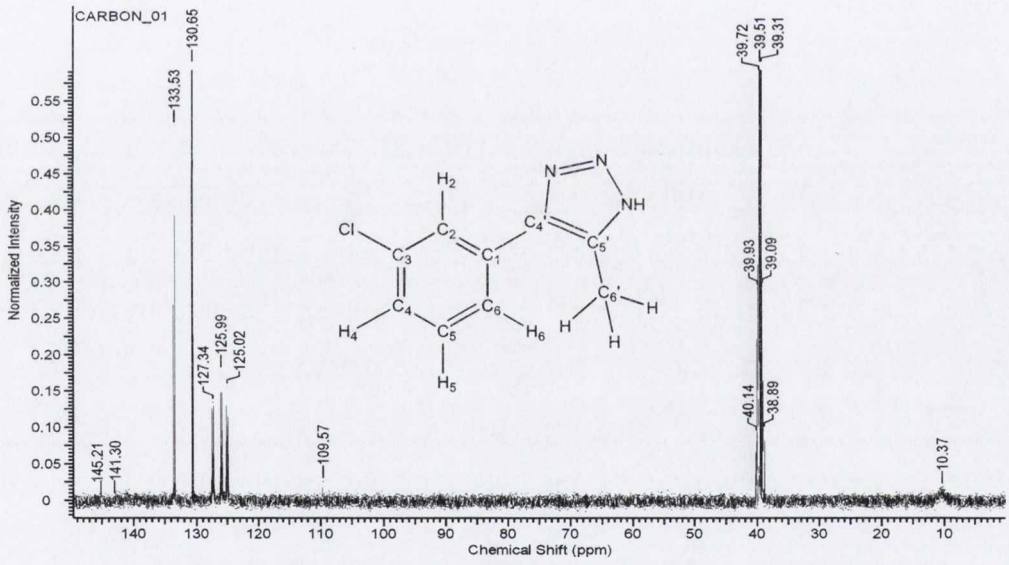

Figure 87: ^{13}C NMR spectrum of 4-(3-chlorophenyl)-5-methyl-1*H*-1,2,3-triazole

FTIR spectrometry shows bands at 1594, 1464 (C=C) and 1231 (C-N) cm^{-1}. High resolution mass spectrometry (ESI) was carried out and the required molecular ion was calculated to be $C_9H_7ClN_3$ [M-H] 192.0334 and found as 192.0335.

X-ray crystallography was carried out on a sample of 4-(5-bromo-2-methoxyphenyl)-5-ethyl-1*H*-1,2,3-triazole (**118**). The results of this study confirmed the formation of the desired product and also established the packing structure as orthorhombic for the unit cell (Figure 88).

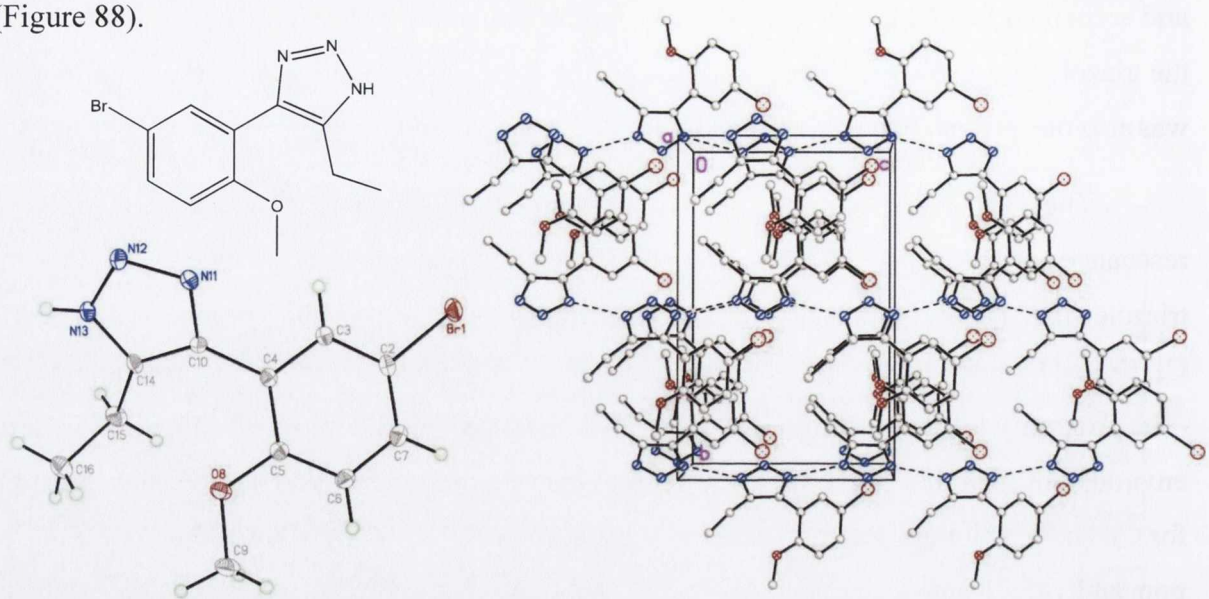

Figure 88: X-ray crystallographic data for 4-(5-bromo-2-methoxyphenyl)-5-ethyl-1*H*-1,2,3-triazole (118)

2.9 Synthesis of 2-substituted-3-phenylacrylonitriles

A series of 2-substituted-3-phenylacrylonitriles were synthesised through the Knoevenagel condensation of the required benzaldehyde and activated cyano methylene compounds. The cyano methylene compounds utilised were methyl 2-cyanoacetate, ethyl 2-cyanoacetate and malonitrile. The general scheme for the base catalysed Knoevenagel condensation can be seen in Figure 88.

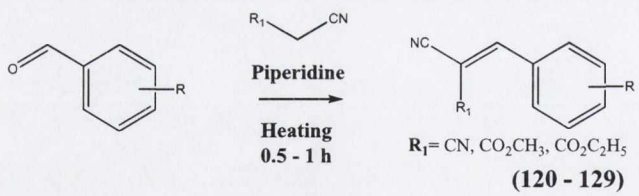

Figure 88: Scheme for the synthesis of 2-substituted-3-phenylacrylonitriles

While the condensation of the required aldehyde with malonitrile was achieved in one hour at reflux, the synthesis of the methyl 2-cyanoacetate and ethyl 2-cyanoacetate adducts was carried out with heating at 80 °C for 30 minutes using microwave assisted synthesis. The preparation of the cyanovinyl adducts was first noted in 1912[269] and since then this Knoevenagel condensation has been carried out using a variety of different catalysts. Examples of catalysts employed include: triethyl amine[270], piperidine[271, 272], ammonium acetate[273] / aluminum oxide[274, 275] and sodium carbonate[276, 277]. The 2-substituted-3-phenylacrylonitriles

are a useful family of compounds acting as intermediates for the synthesis of other, larger heterocyclic structures[277, 278]. Studies on the bioactivity of this class of compounds has yielded some promising results and two series of 2-substituted-3-phenylacrylonitriles have been shown to inhibit cancer cell proliferation[279, 280].

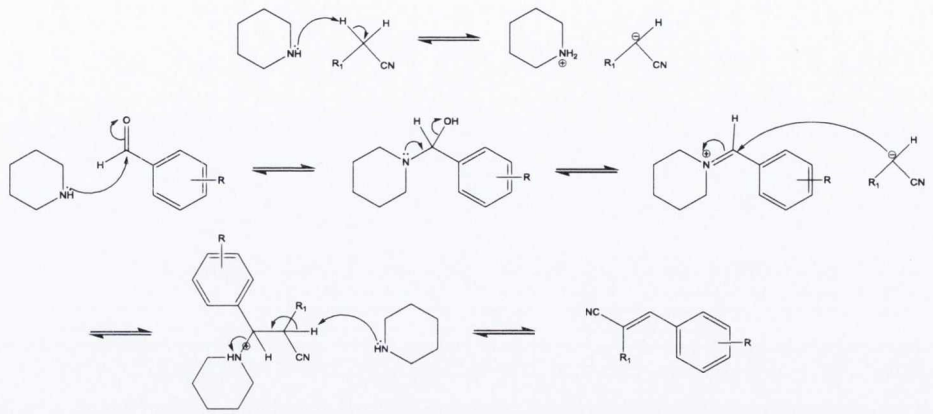

Figure 89: Knoevenagel condensation for the synthesis of 2-substituted-3-phenylacrylonitriles[209]

The mechanism for the Knoevenagel condensation is detailed in Figure 89. Deprotonation of the cyano methylene starting material takes place initially to provide a carbanion. This cyano carbanion nucleophilically attacks the iminium ion formed through the reaction of piperidine and the selected benzaldehyde. Biomolecular elimination then takes place through deprotonation of the addition product, formation of the double bond and subsequent elimination of the piperidine molecule leaving the desired 2-substituted-3-phenylacrylonitrile[209]. A panel of alkyl 2-cyano-3-phenylacrylates (**120-125**) were synthesised using the microwave assisted Knoevenagel condensation giving good yields of 30-70% (Table 12). The 2-benzylidenemalononitriles were synthesised using the reflux method giving excellent yields of 62-90% (Table 11).

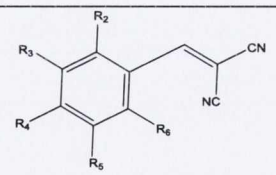

Compound	Substitution pattern	Yield	Compound	Substitution pattern	Yield
126	R_4 = Cl	78%	**128**	R_2 = OCH_3, R_5 = Br	62%
127	R_4 = Br	83%	**129**	R_3 = Cl	90%

Table 11: alkyl 2-cyano-3-phenylacrylate library. Note: R = H unless otherwise specified. * denotes novel compound

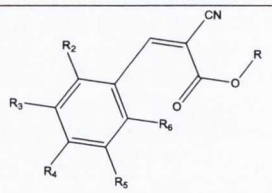

Compound	R	Substitution pattern	Yield	Compound	R	Substitution pattern	Yield
120	CH_3	$R_4 = Cl$	66%	**123**	CH_2CH_3	$R_4 = Cl$	65%
121	CH_3	$R_2 = OCH_3$, $R_5 = Br$	70%	**124**	CH_2CH_3	$R_2 = OCH_3$, $R_5 = Br$	58%
122	CH_3	$R_3 = Cl$	50%	**125**	CH_2CH_3	$R_3 = Cl$	30%

Table 12: 2-benzylidenemalononitrile library. Note: R = H unless otherwise specified.

Ethyl 3-(5-bromo-2-methoxyphenyl)-2-cyanoacrylate (**124**) was chosen as a representative sample of the 2-substituted-3-phenylacrylonitriles and the ^1H NMR and ^{13}C NMR spectra will now be discussed in detail. The ^1H NMR (400 MHz, $CDCl_3$) spectrum of compound 124 (Figure 90) shows a triplet at 1.40 ppm (J = 7.05 Hz) integrating for three protons, this was assigned to the three alkyl protons on $C_{2''}$.

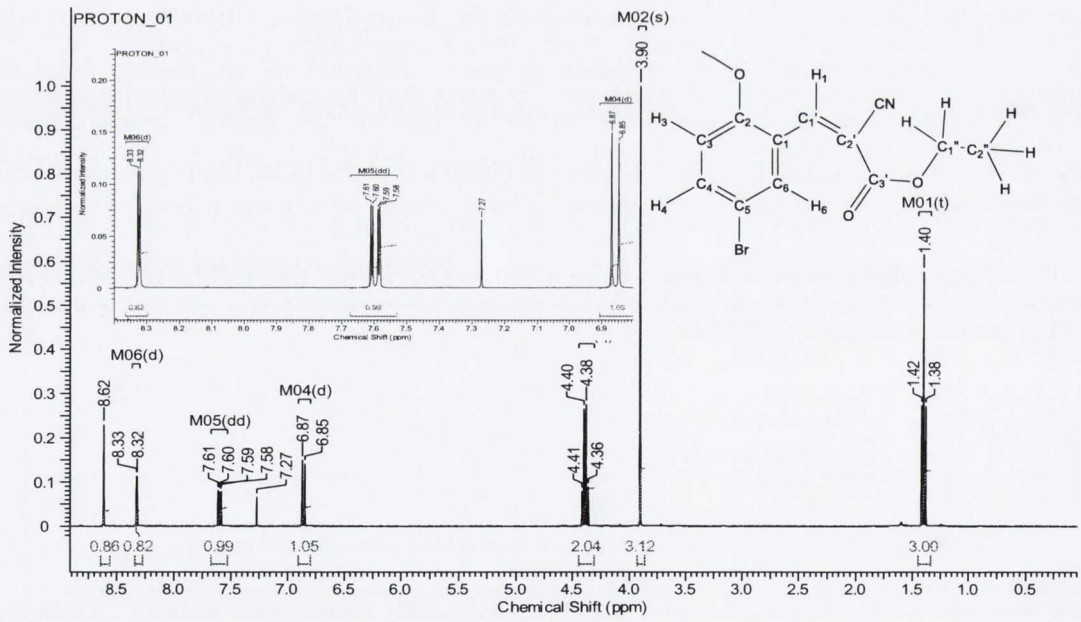

Figure 90: ^1H NMR spectrum of ethyl 3-(5-bromo-2-methoxyphenyl)-2-cyanoacrylate (124)

The singlet at 3.90 ppm also integrated for three protons and was assigned to the three methoxy protons at position C_2 of the aromatic ring. A quartet at 4.39 ppm (J = 7.05 Hz) with an integration of two protons accounted for the two protons on $C_{1''}$. The doublet at 6.86 ppm (J = 8.71 Hz) and the double doublet at 7.60 ppm (J = 8.92, 2.28 Hz) both integrated for a single

proton each – these accounted for H_3 and H_4 respectively. The signal at 7.60 ppm had two coupling constants, the smaller of which was attributed to *meta* coupling with H_6. The doublet at 8.32 ppm (J = 2.49 Hz) integrated for a single proton and accounted for H_6, with *meta* splitting evident by H_4. The remaining downfield singlet at 8.62 ppm integrated for one proton and was assigned to H_1 on the vinyl unit.

The ^{13}C NMR spectrum (101 MHz, $CDCl_3$) of compound **124** (Figure 91) shows resonances at 14.14 ppm, 56.05 ppm, 62.69 ppm and 103.88 ppm, these were assigned to $C_{2''}$, the carbon in the methoxy group on C_2, $C_{1''}$ and $C_{2'}$.

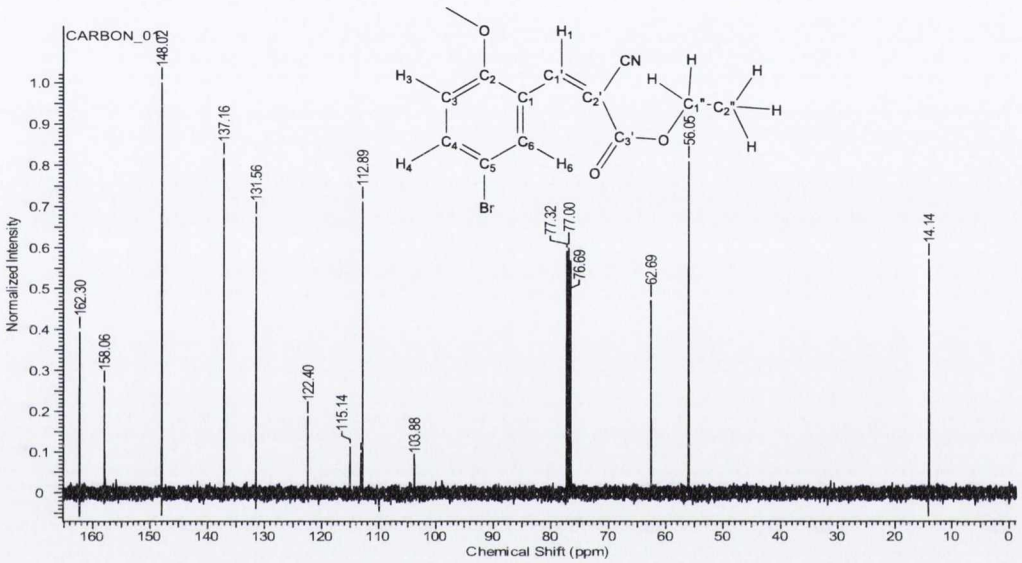

Figure 91: ^{13}C NMR spectrum of ethyl 3-(5-bromo-2-methoxyphenyl)-2-cyanoacrylate (124)

The CH signals occurring at 113.18 ppm, 131.56 ppm, 137.16 ppm and 148.02 ppm accounted for aromatic carbons C_3, C_4, C_6 and the vinyl carbon $C_{1'}$. The quaternary resonances 112.89 ppm, 115.14 ppm and 122.40 ppm were found to correspond to C_5, the carbon in the cyano group and C_1. The downfield quaternary resonances at 158.06 ppm and 162.30 ppm were assigned to C_2 and $C_{3'}$. These two resonances occurred much further downfield due to the presence of the methoxy group at C_2 and the carbonyl at $C_{3'}$.

FTIR spectroscopy shows bands at 2223 (CN), 1719 (C=O), 1609, 1587 (C=C) and 1259 (C-N) cm^{-1}. High resolution mass spectrometry (APCI) was carried out and the required molecular ion was calculated to be $C_{13}H_{12}BrNaNO_3$ [M^++Na] 331.9898 and found as 331.9884.

2.10 Synthesis of benzylidenehydrazines

Hydrazones are characterised by the NNH_2 functional group which can be readily synthesised from aldehydes or ketones. The benzylidenehydrazines (**130-134**) were obtained by refluxing a solution of the required benzaldehyde in ethanol with hydrazine for three hours (Figure 92)[281].

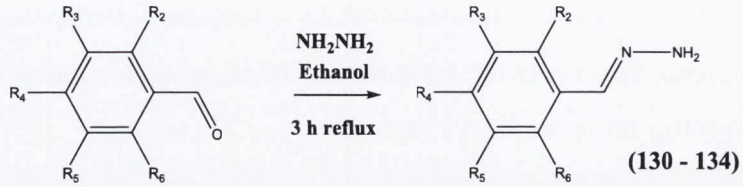

Figure 92: Scheme for the synthesis of benzylidenehydrazines

The mechanism for the synthesis of the benzylidenehydrazines requires nucleophilic attack of hydrazine to the aldehyde carbonyl followed by formation of the hydrazine double bond and subsequent dehydration to give the benzylidenehydrazines. Benzylidenehydrazines have also been synthesised through the reflux of hydrazine with the desired aldo-oximes[282].

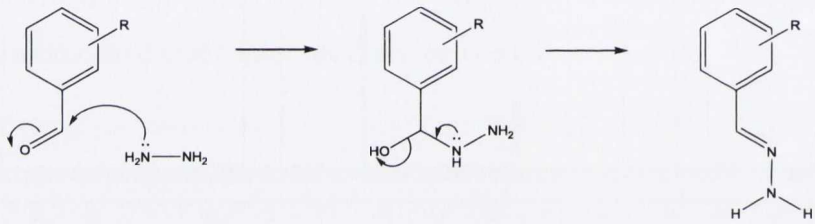

Figure 93: Proposed mechanism for the synthesis of benzylidenehydrazines

A small panel of these simple benzylidenehydrazines (**130-134**) was prepared in order to determine whether these nitrostyrene related compounds possessed any anti antiproliferative activity. The reaction of the required benzaldehyde in ethanol with hydrazine proceeded efficiently affording yields of 12-87% of the corresponding benzylidenehydrazines (Table 13).

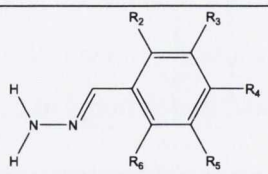

Compound	Substitution pattern	Yield	Compound	Substitution pattern	Yield
130	-	60%	**133**	$R_2 = OCH_3$, $R_5 = Br$	22%*
131	$R_3 = Cl$	72%	**134**	$R_4 = Br$	12%
132	$R_4 = Cl$	87%	-	-	-

Table 13: benzylidenehydrazines library. Note: R = H unless otherwise specified. * denotes novel compound

2.11 Conclusion

The Henry-Knoevenagel condensation reaction was utilised to synthesise a comprehensive library of nitrostyrenes structurally related to the (*E*)-1,3-bis(aryl)-2-nitro-1-propenes. Modifications achieved include increasing chain length at C-2 from unsubstituted to methyl, ethyl, benzyl and benzoyl. Variation of the phenyl ring substitution was also achieved including but not limited to halogen substitution (chlorine, bromine and fluorine), alkyl, nitro, hydroxy phenoxy, methoxy and benzyloxy substitutions. Using heterocyclic aldehydes allowed access to a range of nitrovinyl compounds incorporating furan and thiophene moieties.

Further modifications to the nitrostyrene library were also achieved employing Morita-Baylis Hillman reaction, triazole formation, reduction, oxidation, Michael and epoxidation reactions. These reactions facilitated the formation of a diverse range compounds which may be of interest biologically. A number of other related vinyl compounds e.g. hydrazones & acrylonitriles were synthesised in order to compare any possible activity to the parent nitrostyrene structures. The preliminary biochemical screen for activity and further investigations of the active compounds selected from the 134 compounds prepared in Chapter 2 will be discussed in Chapter 6.

Chapter 3.

Synthesis, isolation and characterisation of a range of heterocycles incorporating the active nitrostyrene pharmacophore

3.0 Introduction

The incorporation of the (2-nitrovinyl)benzene (nitrostyrene) and 1,3-bis(aryl)-2-nitro-1-propene scaffolds into larger heterocyclic structures was also of interest as part of the current work. These heterocyclic structures induce different configurations of the (2-nitrovinyl)benzene (nitrostyrene) and 1,3-bis(aryl)-2-nitro-1-propene scaffolds locking the nitrovinyl unit in either a *cis* (*Z*) or *trans* (*E*) configuration. The heterocyclic structures prepared during the course of this thesis include 3-nitro-2-phenyl-2*H*-chromenes, 3-nitro-1,2-dihydroquinolines, 3-nitroquinolin-2(1*H*)-one, 3-nitro-2-phenylchromen-4-ones, 4-nitro-3,5-diphenylisoxazole, 3-nitrochalcones, 3-nitro-2-phenyl-1*H*-indole and 3-nitro-2,4-diphenyl-2,5-dihydrobenzo[b][1,4]thiazepine (Figure 94). Figure 94 illustrates the concept of this study and this diagram outlines the scaffold of each of the prospective heterocyclic compounds and highlights the nitrostyrene substructure in blue.

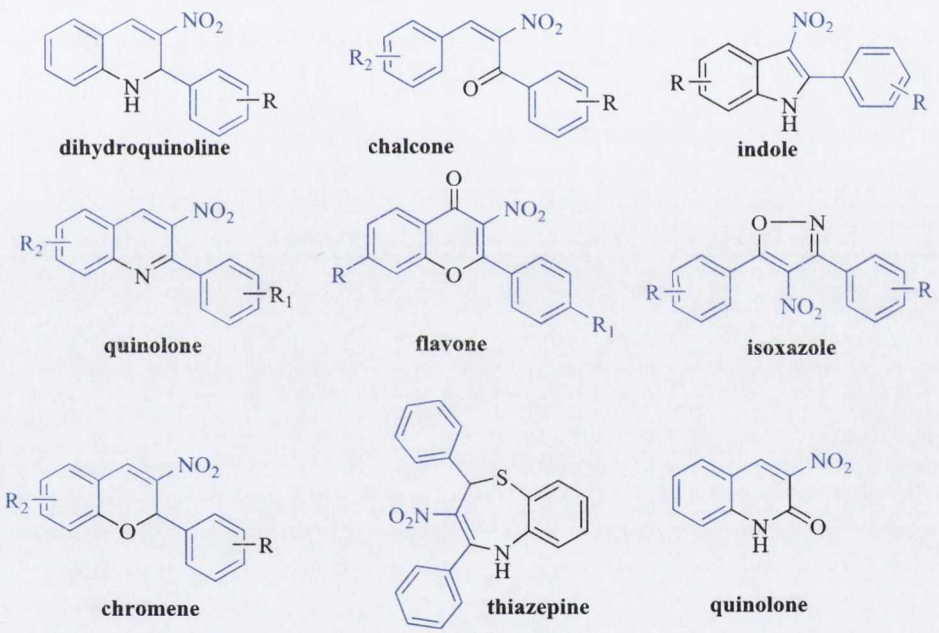

Figure 94: Fused ring nitrostyrene analogues

In the following sections the synthesis and characterisation of these fused ring nitrostyrene analogues will be discussed and initial MOE overlays will illustrate the altered configurations provided by the heterocyclic structures. These altered configurations may well be of interest biologically and the results of a screen in the MUTU-I and DG-75 BL cell lines will be discussed in Chapter 6.

3.1 Synthesis of 3-nitro-2-phenyl-2*H*-chromenes and 3-nitro-1,2-dihydroquinolines

A series of structurally related 3-nitro-2-phenyl-2*H*-chromenes and 3-nitro-1,2-dihydroquinolines were synthesised from the appropriate (*E*)-(2-nitrovinyl)benzenes. This series of chromenes and quinolines were structurally related to the 1,3-bis(aryl)-2-nitro-1-propenes previously shown to have antiproliferative activity in Burkitt's lymphoma cell lines[5]. 3-Nitrochromenes are a significant class of heterocyclic compounds owing to their use as precursors of flavonoids[283] and biological activity[172]. 3-Nitro-2*H*-chromenes have been previously shown to inhibit the proliferation of A549 cancer cells[284]. 3-Nitroquinolines and 3-nitro-2-phenyl-2*H*-chromenes have more recently been shown to exhibit an antiproliferative effect in breast cancer cell lines (MCF-7 & MDA-MB-468)[145,197].

The introduction of the chromene and the dihydroquinoline scaffolds offers an arrangement to the (*E*)-1,3-bis(aryl)-2-nitro-1-propene scaffold which contrains the nitrostyrene in the (*E*) configuration. To illustrate the effect of this constrained configuration, the lowest energy conformation of the 3-nitro-2-phenyl-2*H*-chromene and 3-nitro-1,2-dihydroquinoline scaffolds were flexibly aligned to the 1,3-bis(aryl)-2-nitro-1-propene scaffold (MOE 2011.10) and the aforementioned differences in conformations are highlighted in Figure 95.

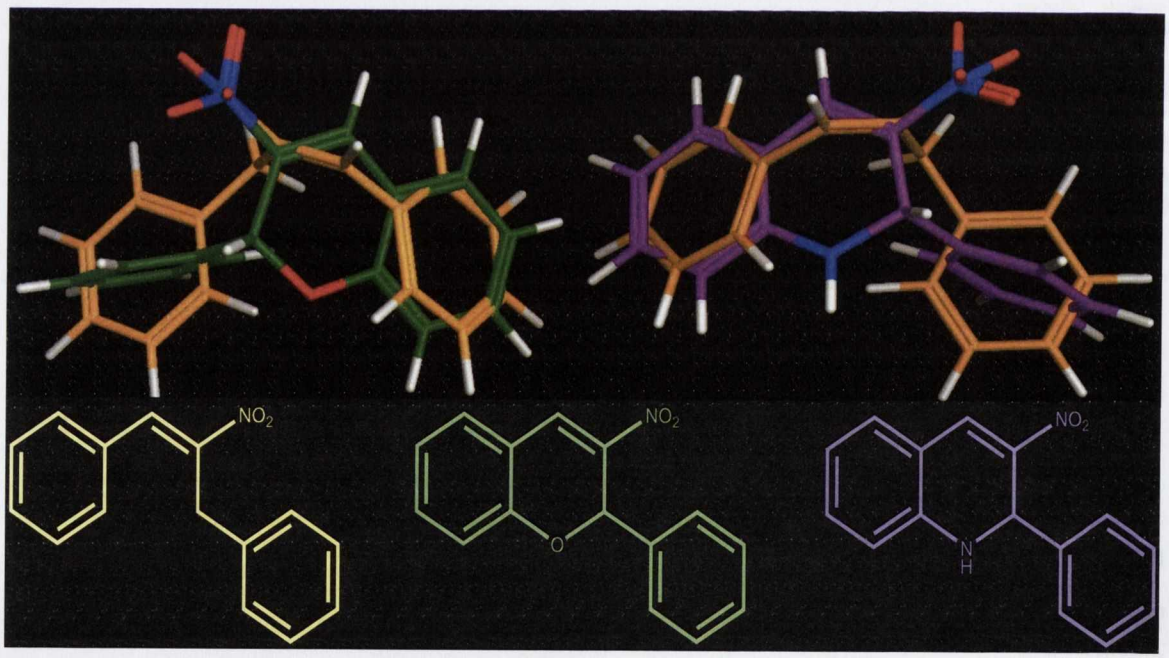

Figure 95: 3-Nitro-2-phenyl-2*H*-chromene scaffold (green) and 3-nitro-1,2-dihydroquinoline scaffold (purple) flexibly aligned to the (*E*)-1,3-bis(aryl)-2-nitro-1-propene scaffold (orange) (MOE 2011.10)

The synthetic strategy chosen involves a one pot reaction by which the Baylis-Hillman reaction of a (*E*)-(2-nitrovinyl)benzenes with appropriately substituted salicylaldehydes or 2-

amino-benzaldehydes, takes place in tandem with the cyclisation and dehydration steps to give the 3-nitro-2-phenyl-2*H*-chromenes[285](**135-147**) and 3-nitro-1,2-dihydroquinolines[286] (**148-149**). The general scheme for this reaction is illustrated in Figure 96.

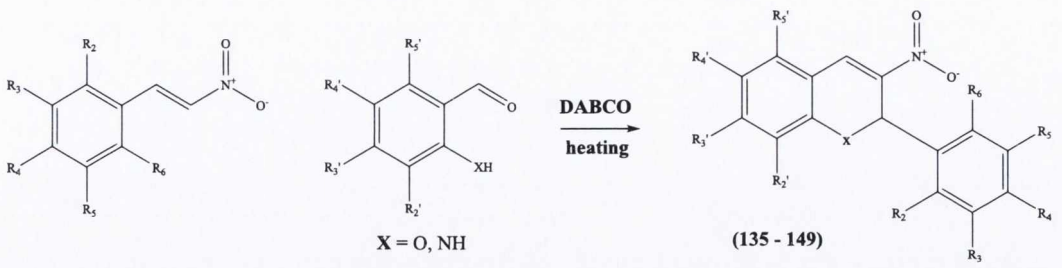

Figure 96: General scheme for synthesis of 3-nitro-2-phenyl-2*H*-chromenes and 3-nitro-1,2-dihydroquinolines

The Baylis-Hillman reaction as previously discussed during the synthesis of the ethyl (*E*)-2-hydroxy-3-nitro-4-phenylbut-3-enoates is a carbon-carbon bond forming reaction between the α-hydrogens of an electron poor alkene with a carbon nucleophile[209, 238]. This tandem Baylis-Hillman-cyclisation, much like the standard Baylis-Hillman reaction can be catalysed by the presence of tertiary amines such as DABCO[285], DBU[287] and TEA[288]. The syntheses of both 3-nitro-2-phenyl-2*H*-chromenes[285, 288] and 3-nitro-1,2-dihydroquinolines[286] has been investigated using various chiral secondary amine organocatalysts, such as L-pipecolonic acid[289, 290]. The neutral alumina catalysed tandem syntheses of both 3-nitro-2-phenyl-2*H*-chromenes and 3-nitro-1,2-dihydroquinolines has also been reported[291]. In more recent times this tandem Baylis-Hillman-cyclisation reaction has been carried out using microwave assisted organic synthesis[246, 292].

The reaction mechanism (Figure 97) is initiated by a Michael type nucleophilic attack by DABCO on the electron deficient alkene bond, giving a zwitterionic intermediate.

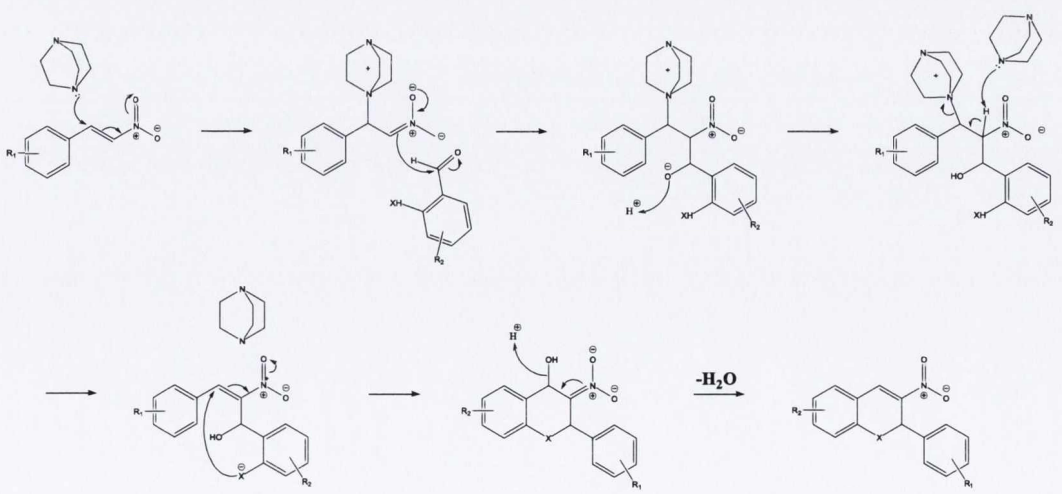

Figure 97: Proposed mechanism for synthesis of 3-nitro-2-phenyl-2*H*-chromenes and 3-nitro-1,2-dihydroquinolines

This zwitterionic intermediate nucleophilically attacks the aldehyde carbonyl and proceeds to form an aldol intermediate. Bimolecular elimination of the initial DABCO conjugate takes place with the reformation of the nitrovinyl bond. The reaction progresses to completion via a Michael type cyclisation and subsequent dehydration to give the 3-nitro-2-phenyl-2*H*-chromenes (**135-147**) when using salicylaldehydes and 3-nitro-1,2-dihydroquinolines (**148**, **149**) when using 2-amino-benzaldehyde[238, 287].

The 3-nitro-1,2-dihydroquinolines and 3-nitro-2-phenyl-2*H*-chromenes are both amenable to various structural modifications. The demethylation of 7-methoxy-3-nitro-2-phenyl-2H-chromene (**145**) was achieved by heating with pyridine hydrochloride neat to give 3-nitro-2-phenyl-2H-chromen-7-ol (**141**) (Figure 98)[293].

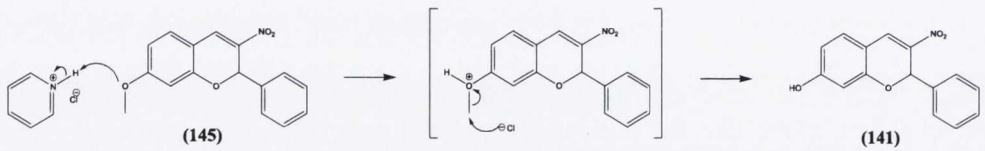

Figure 98: Proposed mechanism for the demethylation of 7-methoxy-3-nitro-2-phenyl-2*H*-chromene

The reduction of the nitrovinyl bond is also conceivably feasible with sodium borohydride[294], however this transformation was not undertaken as part of the current work.

The Baylis-Hillman reaction pathway was chosen for the synthesis of the 3-nitro-2-phenyl-2*H*-chromenes (**135-147**) due to the relatively mild conditions required, adequate to good yields and short reaction time. For the 3-nitro-1,2-dihydroquinolines (**148-149**) additional heating and a longer reaction period was required to drive the reaction. A library of 3-nitro-2-phenyl-2*H*-chromenes (**136-147**) and 3-nitro-1,2-dihydroquinolines (**148-149**) were synthesised from the appropriate (*E*)-(2-nitrovinyl)benzenes with moderate to good yields (Table 14).

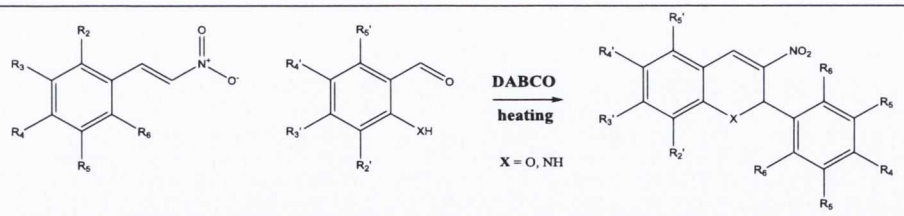

Compound	Substitution pattern	Yield	Compound	Substitution pattern	Yield
135	X = O	40%	**143**	X = O, $R_{2'}$ = OCH_3, R_4 = Cl	50%
136	X = O, R_4 = Cl	35%	**144**	X = O, $R_{2'}$ = OCH_3	45%
137	X = O, R_4 = OH	45%*	**145**	X = O, $R_{3'}$ = OCH_3	60%
138	X = O, R_4 = $OCH_2(C_6H_5)$	60%	**146**	X = O, $R_{4'}$ = Cl	30%
139	X = O, R_3 = R_4 = OCH_2O	39%	**147**	X = O, R_2' = Cl	22%
140	X = O, R_3 = R_4 = OCH_3	60%	**148**	X = NH	23%
141	X = O, $R_{3'}$ = OH	10%*	**149**	X = NH, R_4 = OH	40%*
142	X = O, R_3 = R_4 = C_4H_4	50%	-	-	-

Table 14: 3-nitro-2-phenyl-2*H*-chromene and 3-nitro-1,2-dihydroquinoline library. Note: R = H unless otherwise specified. * denotes novel compound

4-(3-Nitro-2*H*-chromen-2-yl)phenol (**137**) was chosen as a representative sample of the 3-nitro-2-phenyl-2*H*-chromenes and the ^{1}H NMR and ^{13}C NMR spectra will now be discussed in detail. The ^{1}H NMR (400 MHz, DMSO-d_6) spectrum of compound **137** (Figure 99) shows a singlet at 6.52 ppm integrating for a single proton, this singlet was assigned to H_2.

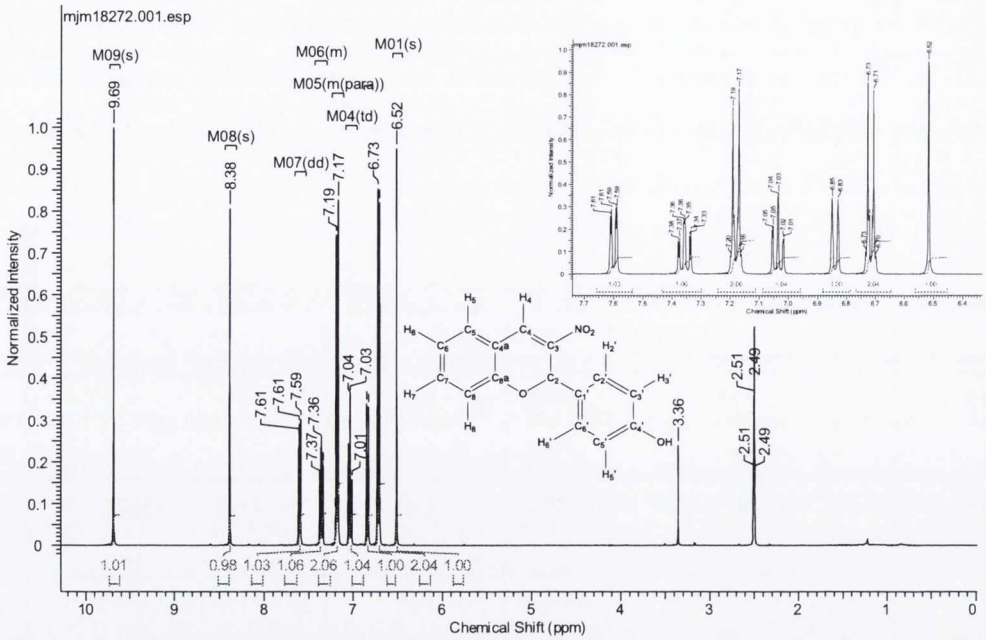

Figure 99: ^{1}H NMR spectrum of 4-(3-Nitro-2*H*-chromen-2-yl)phenol (137)

The multiplets at 6.62 - 6.80 ppm and 7.14 - 7.26 ppm both integrating for two protons were assigned to the *para* substituted phenol ring; $H_{3'}$ & $H_{5'}$ and $H_{2'}$ & $H_{6'}$ respectively. The doublet resonance occurring at 6.84 ppm (J = 8.03 Hz) integrated for a single proton and accounted for H_8. The apparent triplets of doublets at 7.03 ppm (J = 7.53, 1.00 Hz) and the multiplet at 7.26 - 7.43 ppm both integrated for a single proton each; these were allocated to H_6 and H_7. A double doublet occurring at 7.60 ppm (J = 7.53, 1.51 Hz) bearing an integration of one proton was annotated as H_5. The two downfield singlets at 8.38 ppm and 9.69 ppm both integrating for a single proton were found to correspond to H_4 and the hydroxyl proton.

The ^{13}C NMR and DEPT 90 spectra (101 MHz, DMSO-d_6) of compound **137** (Figure 100 and Figure 101) show CH resonances at 73.26 ppm, 116.78 ppm and 122.36 ppm which were assigned to C_2, C_8, and C_6. The CH resonances at 115.53 ppm and 128.64 ppm were found to represent two equivalent carbons each of the *para* substituted phenol ring ($C_{3'}$ & $C_{5'}$ and $C_{2'}$ & $C_{6'}$). Quaternary signals at 118.20 ppm, 127.06 ppm and 140.78 ppm represent C_{4a}, $C_{1'}$ and C_3. C_3 appeared slightly downfield due to the electronegativity of the nitro group attached at this carbon. The CH signals at 129.76 ppm, 131.10 ppm and 134.35 ppm accounted for C_4, C_5 and C_7 in the chromene structure. The downfield quaternary signals 152.84 ppm and 158.47 ppm were attributed to the electronegative environments produced at C_{8a} and $C_{4'}$.

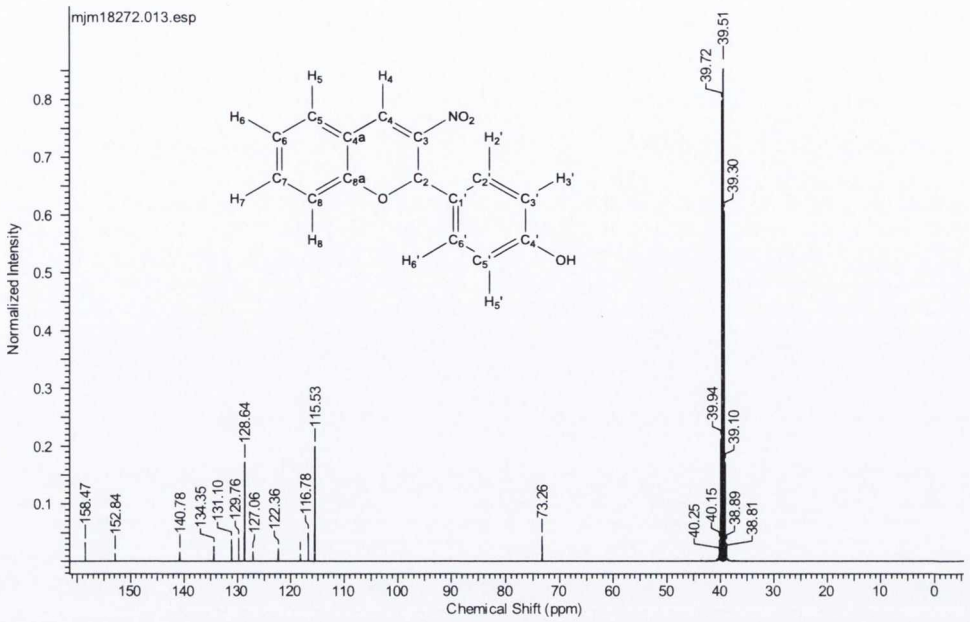

Figure 100: ^{13}C NMR spectrum of 4-(3-Nitro-2*H*-chromen-2-yl)phenol (137)

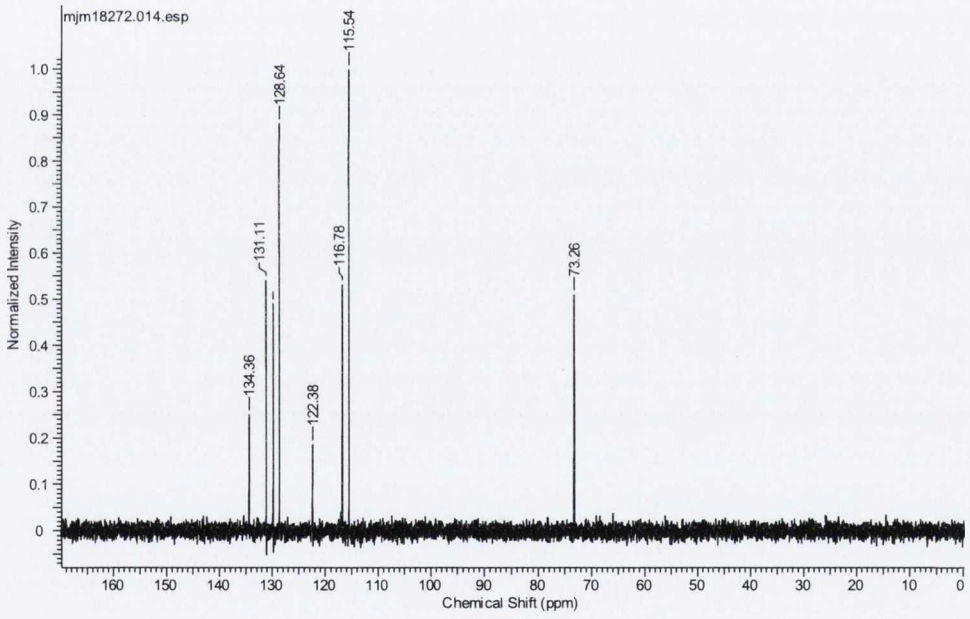

Figure 101: DEPT 90 NMR spectrum of 4-(3-Nitro-2*H*-chromen-2-yl)phenol (137)

FTIR spectroscopy shows absorbances at 3477 (OH), 1648, 1604 (C=C), and 1509, 1319 (NO_2) cm^{-1}. High resolution mass spectrometry (APCI) was carried out and the required molecular ion was calculated to be $C_{15}H_{11}NO_4$ [M^+] 269.0688 and found as 269.0682.

3.2 Synthesis of the 3-nitro-2-phenylquinoline and 3-nitroquinolin-2(1*H*)-one

A procedure for the synthesis of the 3-nitro-2-phenylquinoline (**150**) from 3-nitro-1,2-dihydroquinolone (**148**) using 2,3-dichloro-5,6-dicyano-1,4-benzoquinone (DDQ) and silica gel is available[286]. However the synthesis of 3-nitro-2-phenylquinoline from 2-nitro-1-phenylethan-1-one and 2-amino-benzaldehyde is also possible; this was the method employed due to ease of purification[295]. The condensation mechanism for the synthesis of this quinolone structure is known as the Friedlander synthesis first noted in 1882[209, 296]. The Friedlander synthesis takes place with base catalysis, typically sodium hydroxide. Baumgarten et al. found that refluxing 2-nitro-1-phenylethan-1-one and 2-amino-benzaldehyde without the addition of a base catalyst formed the desired product in good yield. On analysis of the crude reaction product; Baumgarten suggested that traces of ammonia from the 2-amino-benzaldehyde may act as a catalyst to the reaction[295].

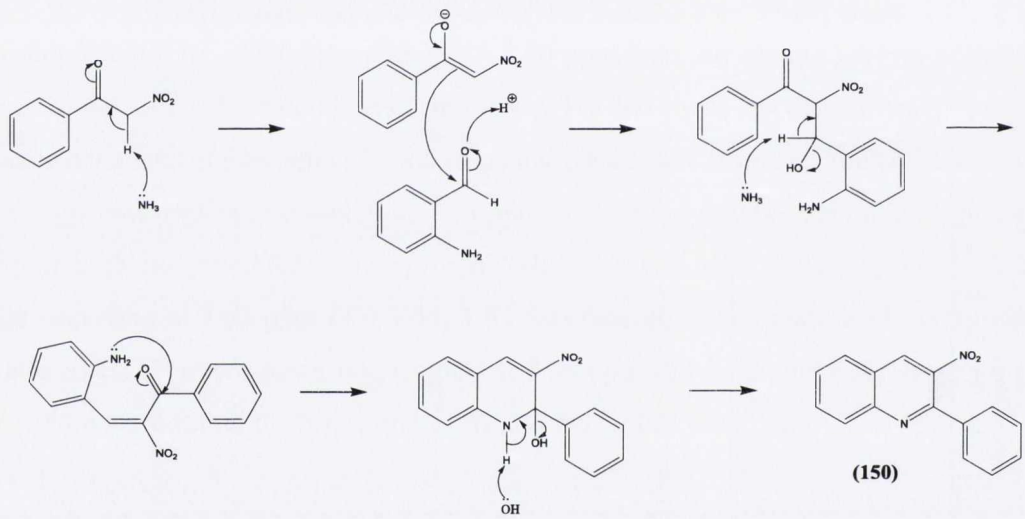

Figure 102: Proposed mechanism for the synthesis of 3-nitro-2-phenylquinoline

The Friedlander synthesis is initiated by the deprotonation of 2-nitro-1-phenylethan-1-one by ammonia forming the activated enolate, followed by an aldol condensation reaction with the 2-amino-benzaldehyde. Cyclisation follows facilitated by the nucleophilic attack of the amine to the carbonyl of the nitro-chalcone intermediate. Deprotonation of the free amine and elimination of water leads to the formation of 3-nitro-2-phenylquinoline (**150**) in 44% yield[295].

3-Nitroquinolin-2(1*H*)-one (**151**) was synthesised from the piperidine catalysed reaction of ethyl 2-nitroacetate and 2-aminobenzaldehyde. It is proposed that the synthesis proceeded *via* the above Friedlander mechanism with elimination of ethanol[297]. This reaction gave a very pure product that was isolated by filtration after cooling (40% yield[297]).

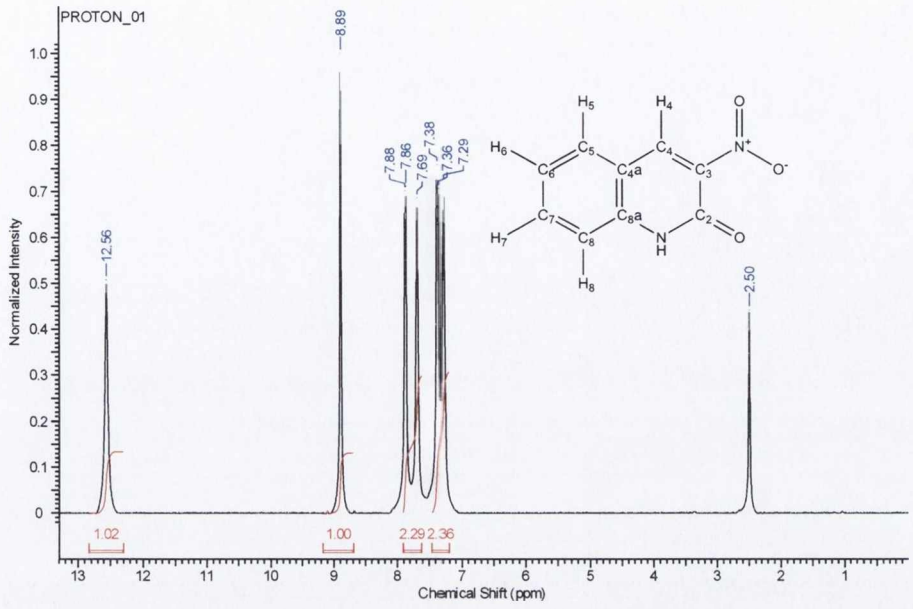

Figure 103: ^{1}H NMR spectrum of 3-nitroquinolin-2(1*H*)-one (151)

The ^{1}H NMR (400 MHz, DMSO-d_6) spectrum of compound **151** (Figure 103) bears a multiplet occurring at a chemical shift of 7.24 - 7.42 ppm integrating for two protons. This multiplet corresponds to H_7 and H_6 – the aryl protons in less electron withdrawing environments. The multiplet at 7.66 - 7.92 ppm also integrating for two protons accounts for H_5 and H_8 – the two aryl protons in closer proximity to electronegative substituents. The singlet occurring at 8.89 ppm with an integral value of one proton was assigned to H_4. The broad singlet occurring downfield at 12.56 ppm, integrating for a single proton; was produced by the NH of the heterocyclic ring.

The ^{13}C NMR spectrum (101 MHz, DMSO-d_6) of compound **151** (Figure 104) shows CH resonances at 115.49 ppm, 123.13 ppm, 130.35 ppm and 134.09 ppm which assigned to the four aryl protons: C_5, C_7, C_6 and C_8. The most downfield CH resonance at 138.00 ppm accounted for C_4. Quaternary carbon signals occurred at 116.31 ppm, 134.10 ppm, 139.98 ppm and 153.85 ppm. The resonances at 116.31 ppm, 134.10 ppm and 139.98 ppm were assigned to C_{4a}, C_3 and C_{8a}. The quaternary resonance further downfield at 153.85 ppm was assigned to the carbonyl at C_2.

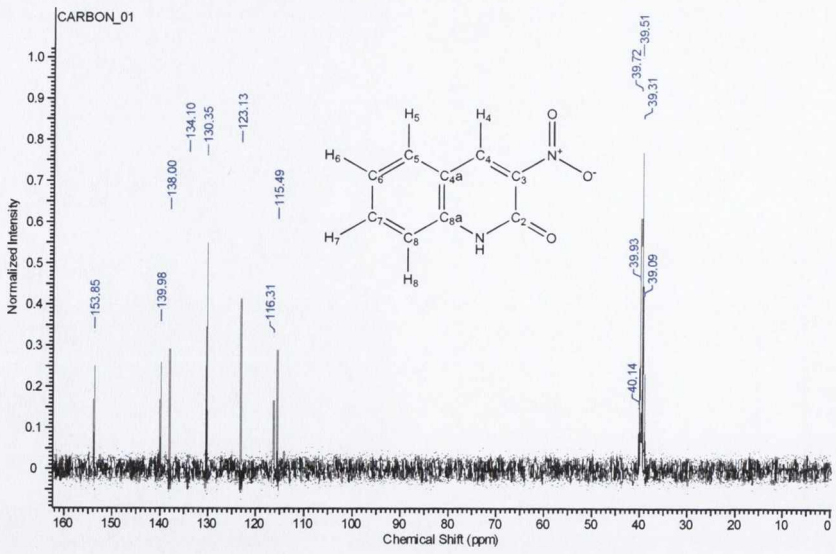

Figure 104: ^{13}C NMR spectrum of 3-nitroquinolin-2(1*H*)-one (151)

FTIR spectroscopy shows bands at 3329 (NH), 1656 (C=C) and 1517, 1332 (NO_2) cm^{-1}. High resolution mass spectrometry (APCI) was carried out and the required molecular ion was calculated to be $C_9H_6N_2O_3Na$ [M^++Na] 213.0276 and found as 213.0267.

3.3 Synthesis of the 3-nitro-2-phenylchromen-4-ones

The objective of this section was to synthesise 3-nitro-2-phenylchromen-4-ones containing different substitution patterns on the chromene and phenyl rings, some of which were novel molecules. These 3-nitro-2-phenylchromen-4-ones compounds contain both the (2-nitrovinyl)benzene pharmacophore and 1,3-bis(aryl)-2-nitro-1-propene scaffold as substructures, orientated differently within its structure and it is this heterocyclic ring system that is of particular interest to us (Figure 105).

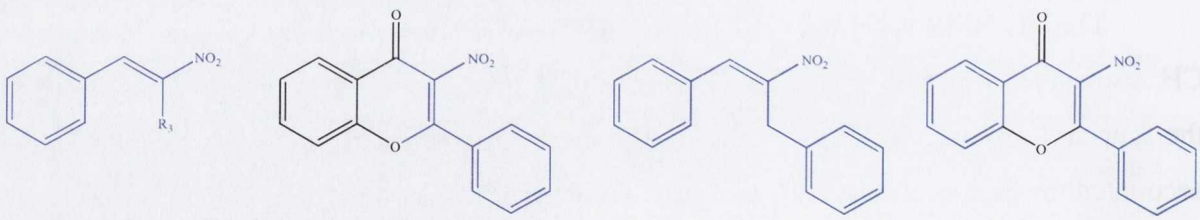

Figure 105: (*E*)-(2-Nitrovinyl)benzene pharmacophore (purple), 3-nitro-2-phenylchromen-4-one scaffold with (2-nitrovinyl)benzene pharmacophore (purple) as a substructure, 1,3-bis(aryl)-2-nitro-1-propene scaffold (blue), 3-nitro-2-phenylchromen-4-one scaffold with 1,3-bis(aryl)-2-nitro-1-propene scaffold (blue) as a substructure

Figure 106 attempts to illustrate the altered configuration of the active pharmacophore through flexible alignment of the 3-nitro-2-phenylchromen-4-one scaffold (pink) and the 1,3-bis(aryl)-2-nitro-1-propene scaffold (green). It is also to be noted that the 1,3-bis(aryl)-2-nitro-1-propene

scaffold is in a much more constrained configuration and assumes a *cis* or (*Z*) like stereochemistry when comparing the nitrovinyl functionality.

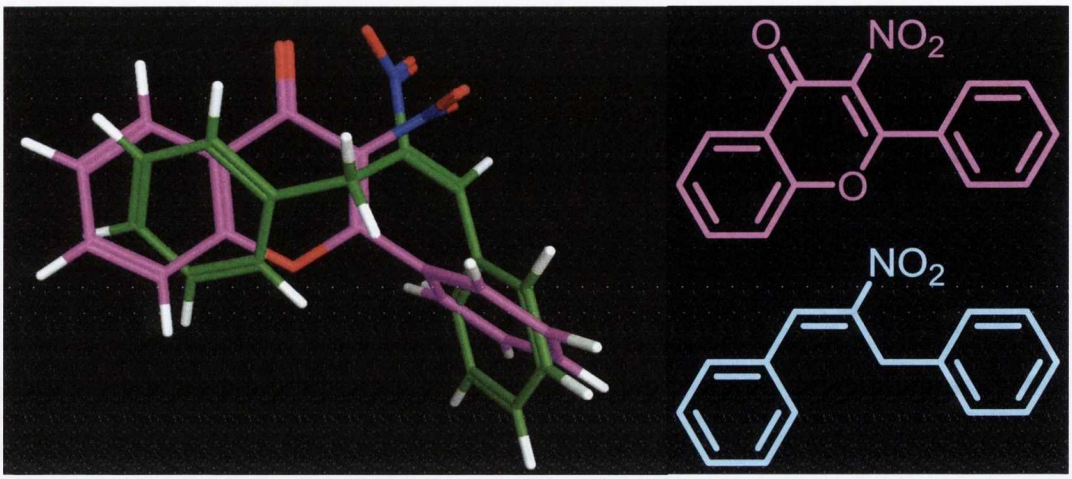

Figure 106: 3-Nitro-2-phenylchromen-4-one scaffold (purple) flexibly aligned to the (*E*)-1,3-bis(aryl)-2-nitro-1-propene scaffold (blue) (MOE 2011.10)

Flavones are a subclass of the flavonoids, these oxygen heterocycles are characterised by the presence of a 2-phenyl-1-chromen-4-one scaffold. The flavones are a well-studied family of naturally occurring organic heterocyclic compounds with noted biological activity. The flavonoids have proven a versatile source of potential therapeutic agents to inhibit the growth of various types of cancer cell *in vivo* and *in vitro*[298]. In one example the citrus flavone tangeretin (5,6,7,8-tetramethoxy-2-(4-methoxyphenyl)-4*H*-chromen-4-one) has been shown to elicit a potent anticancer effect and induce apoptosis in the leukaemia cell line HL-60 (Figure 107). It was also noted over the course of this publication that tangeretin bore no cytotoxic effect against human peripheral blood mononuclear cells (PBMCs)[299]. Apigenin (5,7-dihydroxy-2-(4-hydroxyphenyl)-4H-chromen-4-one) is another naturally occurring flavonoid and was also shown to exhibit an antiproliferative effect in the leukaemia cell line HL-60 by Ruela-de-Sousa et al. (2010)[299].

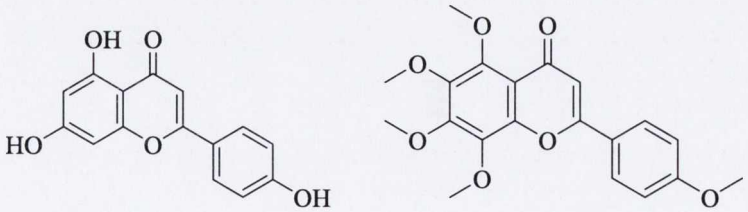

Apigenin **Tangeretin**

Figure 107: Apigenin and tangeretin

Beudot et al. (1998) evaluated a library of forty two 3-nitro-2-phenylchromen-4-one and 3-amino-2-phenylchromen-4-one analogues for mutagenicity and antimutagenicity against

eleven known mutagens. Certain 3-nitro and 3-aminoflavones studied were found to be highly mutagenic but others provided promising antimutagenicity results and could provide interesting scope for future development as cancer chemo-preventive agents[300]. Dauzonne et al (1997) highlighted the *in vitro* cytotoxicity of a series of 3-amino-2-phenylchromen-4-ones derived from the palladium catalysed reduction of the 3-nitro-2-phenylchromen-4-ones. The lead compounds in this study gave good IC_{50} values of 4-22 μM in the leukaemia cell line L1210[301].

There are numerous routes employed for the synthesis of flavones. These include the Kostanecki method, the Robinson method and the Baker-Venkataraman rearrangement. The Allan-Robinson method of flavone and isoflavone synthesis is a one pot synthesis in which the appropriately substituted *o*-hydroxyacetophenone is reacted with both the anhydride and the sodium salt of the desired benzoic acid at 180 °C. The reaction proceeds by enolization of the acetophenone followed by nucleophilic attack on the anhydride and acylation to give the diketone structure intermediate. Deprotonation by benzoic acid, a second enolization and cyclisation by conjugate addition then takes place with the elimination of water to give the required flavone[209, 302]. The Kostanecki method for the synthesis of flavones (also known as the Kostanecki-Robinson method) achieves the synthesis of flavones through the acylation of the desired *o*-hydroxyacetophenone with anhydrides to form a protected *o*-hydroxyacetophenone structure. Enolization of this protected *o*-hydroxyacetophenone structure in the presence of base facilitates cyclisation and dehydration to give the flavone[303].

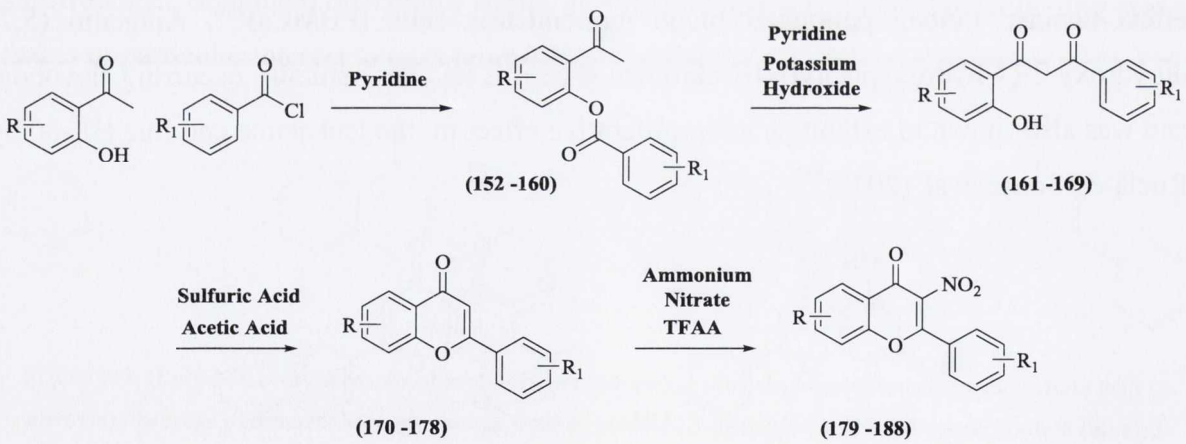

Figure 108: General overall reaction scheme for synthesis of 3-nitro-2-phenylchromen-4-ones (including Baker-Venkataraman rearrangement)

The method employed in this project for the synthesis of the 2-phenyl-1-chromen-4-ones included the Baker-Venkataraman rearrangement (Figure 108). This reaction was discovered both independently and simultaneously by Wilson Baker and Krishnasami Venkataraman in

1933[304]. This particular synthetic route involves the reaction of 2-hydroxyacetophenone with an acid chloride to form the benzoyl ester of the acetophenone. This product is then reacted in the presence of base (potassium hydroxide) and pyridine to give the 1,3-diketone (the Baker-Venkataraman rearrangement). Strong acidic conditions causes the 1,3-diketone to undergo cyclisation, forming the desirable flavone[305]. These flavones are then subsequently nitrated employing the method detailed by Patoilo et al. (2010) in a solution of ammonium nitrate and trifluoroacetic anhydride (TFAA) in dichloromethane / acetonitrile to form 3-nitro-2-phenylchromen-4-ones, our target end product[306].

3.4 Synthesis of the 2-acetylphenyl benzoates

The initial step of the overall synthetic scheme involves the reaction of the appropriately substituted 2-hydroxyacetophenone with the required substituted benzoyl chloride in the presence of pyridine to give the 2-acetylphenyl benzoates (**152-160**) (Figure 109).

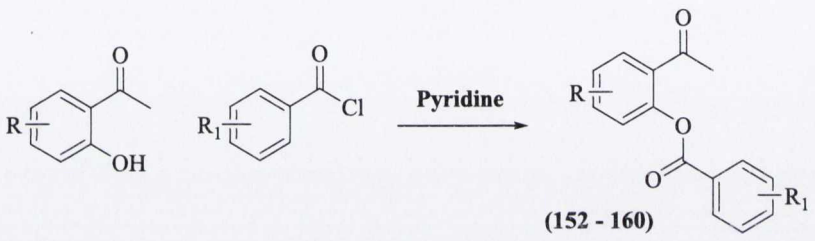

Figure 109: General scheme for the synthesis of the 2-acetylphenyl benzoates

The mechanism for the synthesis of the 2-acetylphenyl benzoates is depicted below (Figure 110). Deprotonation of the hydroxyl group by pyridine leads to nucleophilic attack on the carbonyl group in the acid chloride affording a carbanion tetrahedral intermediate. The carbonyl group is then reformed with the elimination of the chloride ion leading to the formation of the 2-acetylphenyl benzoate structure.

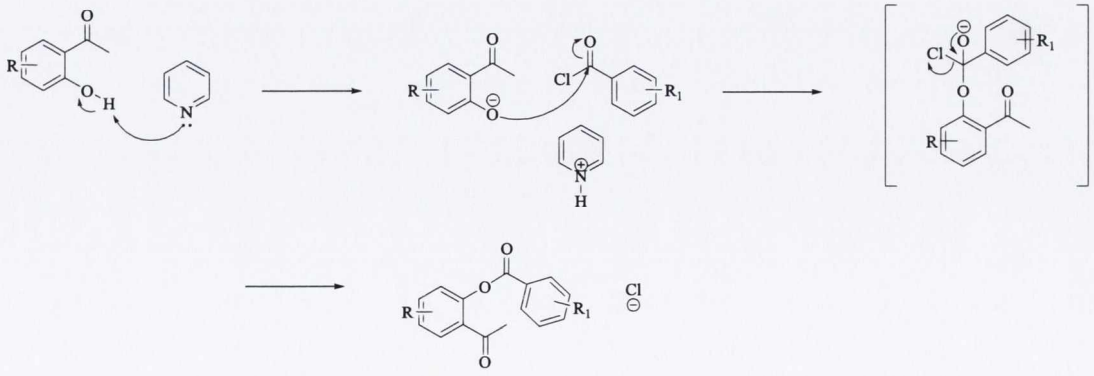

Figure 110: Proposed mechanism for the synthesis of the 2-acetylphenyl benzoates

Other literature methods for the synthesis of the 2-acetylphenyl benzoates are available. One such example describes the reaction of appropriately substituted 2-hydroxyacetophenones and benzaldehydes in the presence of *tert*-butylhydrogenperoxide and copper diacetate in water and dimethyl sulfoxide. This reaction takes place at 80 °C for 6 hours and provides yields of up to 80%[307].

The procedure employed in this project for the synthesis of 2-acetylphenyl benzoates was relatively straightforward, required no heat and had a short reaction time (approx. 30 minutes). However recrystallization in hot methanol was necessary with all compounds to achieve purity. In summary the synthesis of the 2-acetylphenyl benzoates (**152-160**) was achieved with yields ranging from 46-88% (Table 15).

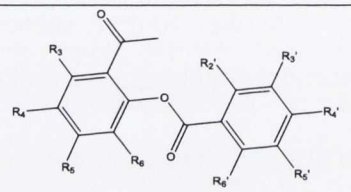

Compound	Substitution pattern	Yield	Compound	Substitution pattern	Yield
152	-	80%	**157**	$R_{3'} = R_{4'} = R_{5'} = OCH_3$	71%
153	$R_{4'} = Cl$	88%	**158**	$R_{3'} = R_{4'} = R_{5'} = R_5 = OCH_3$	85%
154	$R_{4'} = OCH_3$	85%	**159**	$R_5 = OCH_3$	46%
155	$R_5 = R_{4'} = Cl$	76%*	**160**	$R_{4'} = R_5 = OCH_3$	60%
156	$R_{3'} = Cl$	81%	-	-	-

Table 15: 2-acetylphenyl benzoate library. Note: R = H unless otherwise specified. * denotes novel compound

2-Acetyl-5-chlorophenyl 4-chlorobenzoate (**155**) was chosen as a representative sample of the 2-acetylphenyl benzoates and the ^1H NMR and ^{13}C NMR spectra will now be discussed in detail. The ^1H NMR (400 MHz, $CDCl_3$) spectrum of compound **155** (Figure 111) shows a singlet at 2.52 ppm integrating for three protons and this was assigned to the three protons on the acetyl group.

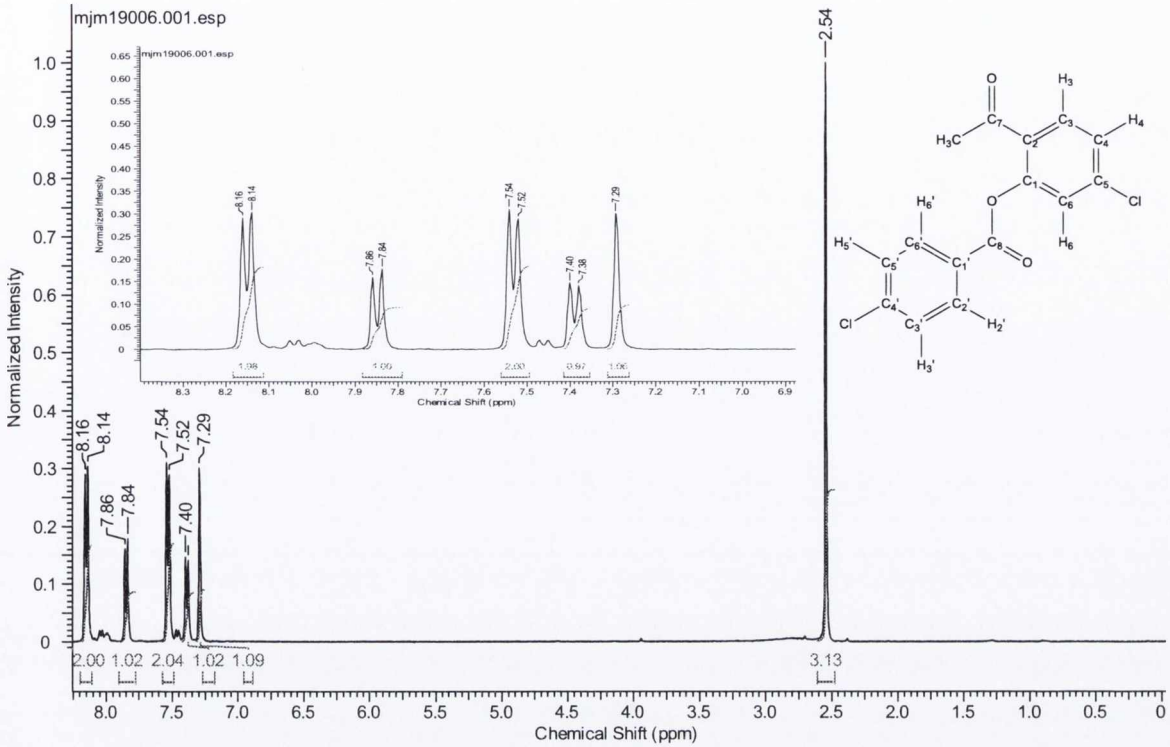

Figure 111: ^{1}H NMR spectrum of 2-acetyl-5-chlorophenyl 4-chlorobenzoate (155)

A singlet occurring at 7.29 ppm and the doublet at 7.37 ppm (J = 8.53 Hz) both integrating for a single proton each were assigned to H_6 and H_4 respectively. The doublets at 7.51 ppm (J = 8.53 Hz) and 8.13 ppm (J = 8.53 Hz) both with integral values for two aromatic protons each were assigned to the 2 sets of equivalent protons on the *para* substituted aromatic ring ($H_{3'}$ & $H_{5'}$ and $H_{2'}$ & $H_{6'}$). The doublet occurring at 7.82 ppm (J = 8.53 Hz) integrated for a single proton; this doublet was more downfield and accounted for H_3 – adjacent to the electron withdrawing acetyl carbonyl.

The ^{13}C NMR spectrum (101 MHz, $CDCl_3$) of compound **155** bears a resonance at 29.47 ppm and assigned to the carbon in the methyl group of the acetyl functionality. The CH resonances at 124.45 ppm, 126.61 ppm and 131.40 ppm were assigned to C_6, C_4 and C_3 respectively. The CH resonances at 129.12 ppm and 131.66 ppm account for the carbon equivalent pairs in the *para* substituted phenyl ring ($C_{3'}$ & $C_{5'}$ and $C_{2'}$ & $C_{6'}$). The more downfield quaternary signals at 149.74 ppm, 164.00 ppm and 196.11 ppm were due to the more electron withdrawing environments of the ester group and the two carbonyls. The resonance at 149.74 ppm was assigned to C_1, while 164.00 ppm and 196.11 were assigned to the carbonyl carbons C_8 and C_7. The carbon signals at 127.25 ppm, 139.07 ppm and 140.58 ppm were assigned to the remaining quaternary carbons.

FTIR spectroscopy shows bands at 1741 (C=O), 1595 (C=C), 1261 (C-O) and 752 (C-Cl) cm^{-1}. High resolution mass spectrometry (ESI) was carried out and the required molecular ion was calculated to be $C_{15}H_{10}Cl_2O_3$ [M+Na] 330.9905 and found as 330.9904.

3.5 Synthesis of the 3-hydroxy-3-phenylprop-2-en-1-ones

After the initial alkylation of the 2-hydroxyacetophenones, the second step of the overall synthetic scheme for nitroflavones utilises the base catalysed, intramolecular Baker-Venkataraman rearrangement of the appropriately substituted 2-acetylphenyl benzoates (**152-160,** Table 15) to the corresponding 1,3-diketones (Figure 112) (**161-169**, Table 16)[304, 305].

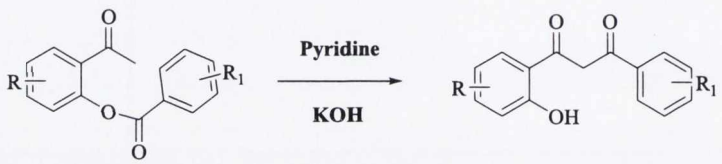

Figure 112: General scheme for the synthesis of the 1,3 diketones

The mechanism involved in the formation of the 1,3 diketones is facilitated by the base-induced transfer of the ester acyl group of the appropriately substituted 2-acetylphenyl benzoate. The reaction is very similar to the Claisen condensation, and results in the formation of an enolate, which then ungoes intramolecular acyl transfer (Figure 113).

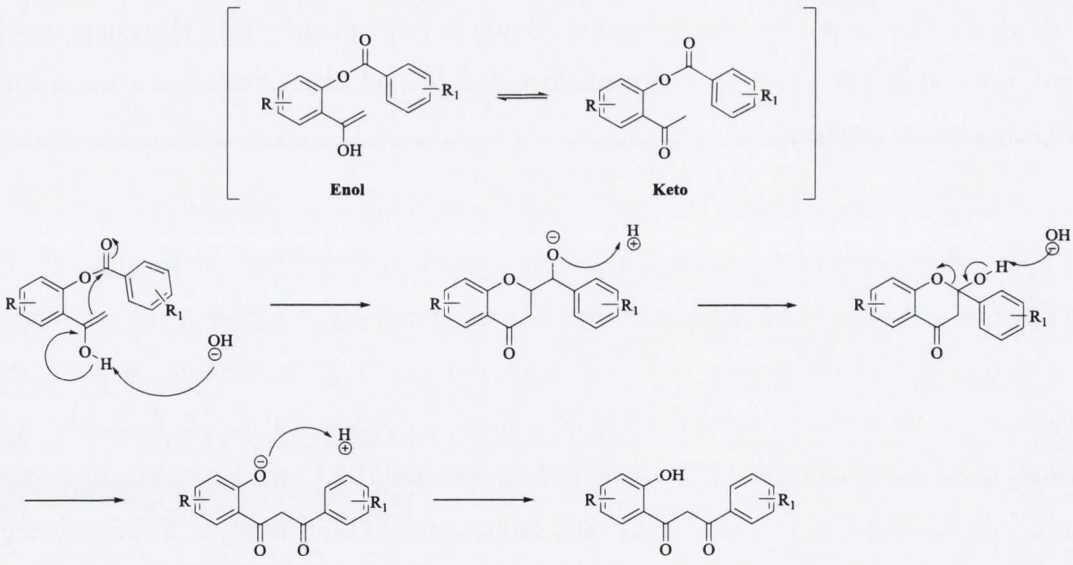

Figure 113: Proposed mechanism for the synthesis of the 3-hydroxy-3-phenylprop-2-en-1-ones (Baker-Venkataraman rearrangement)[209, 304, 305]

Potassium hydroxide dissociates in solution forming the hydroxyl ion which causes deprotonation of the hydroxyl group and the formation of water. Nucleophilic attack of the enol

alkene bond on the ester carbonyl occurs forming a carbanion tetrahedral intermediate. The carbonyl group is reformed leading to total cleavage of the ester bond. Protonation of the nucleophilic oxygen stabilises the molecule resulting in the formation of the 1,3 diketone[209, 304].

Tautomerization is observed with the products of this reaction (Figure 114). In solution aldehydes and ketones undergo structural isomerisation which involves the movement of hydrogen from the alpha carbon onto the ketone oxygen which further results in the formation of a carbon-carbon double bond between the carbon attached to the oxygen and the alpha carbon. This is the enol form of the molecule. This type of structural isomerism is generally known as tautomerization or enolization.

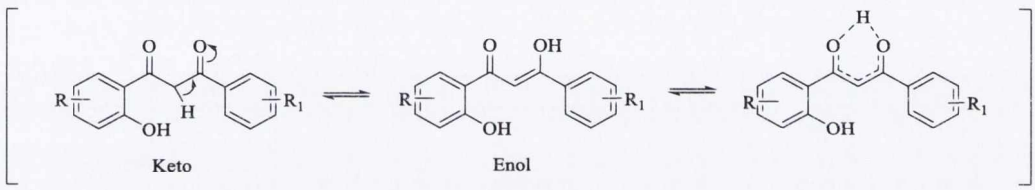

Figure 114: Tautomerism of the 1,3 diketones to the 3-hydroxy-3-phenylprop-2-en-1-ones

The occurrence of keto-enol tautomerization of the 1,3-diketones equates to the observation that almost 100% of the time these molecules exist in the enol form. The ^{1}H NMR spectra of the 1,3–diketones produced in this work do not bear a signal between 4-7 ppm (integral 2 protons) which would be indicative of the CH_2 protons of the keto form. Instead these spectra exhibit a signal (integral 1 proton) resonating at 12-15 ppm which is indicative of the O-H bond resulting from the alkene bond formed by the enol form of the molecule. The alkene proton associated with the enol tautomer resonates in the spectrum at approximately 7 ppm. Alejandro J. Vila et al. published a study of this occurrence in 2000, using a combination of ^{13}C CPMAS (Cross Polarised Magic Angle Spinning) NMR Spectroscopy and AM1 calculations[308].

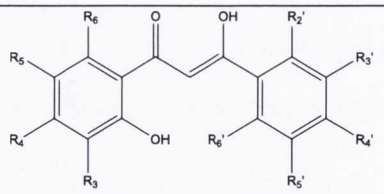

Compound	Substitution pattern	Yield	Compound	Substitution pattern	Yield
161	-	94%	**166**	$R_3' = R_4' = R_5' = OCH_3$	64%
162	$R_4' = Cl$	26%	**167**	$R_3' = R_4' = R_5' = R_4 = OCH_3$	60%
163	$R_4 = R_4' = Cl$	20%*	**168**	$R_4' = R_4 = OCH_3$	80%
164	$R_4' = OCH_3$	48%	**169**	$R_4 = OCH_3$	46%
165	$R_3' = Cl$	14%	-	-	-

Table 16: 3-hydroxy-3-phenylprop-2-en-1-one library. Note: R = H unless otherwise specified. * denotes novel compound

3-Hydroxy-1-(2-hydroxyphenyl)-3-(3,4,5-trimethoxyphenyl)prop-2-en-1-one (**166**) was chosen as a representative sample of the 3-hydroxy-3-phenylprop-2-en-1-ones and the ^1H NMR and ^{13}C NMR spectra will now be discussed in detail. The ^1H NMR (400 MHz, $CDCl_3$) spectrum of compound **166** (Figure 115) shows a multiplet at 3.90 - 3.95 ppm integrating for 9 protons, this was assigned to the nine protons associated with the methoxy substituents.

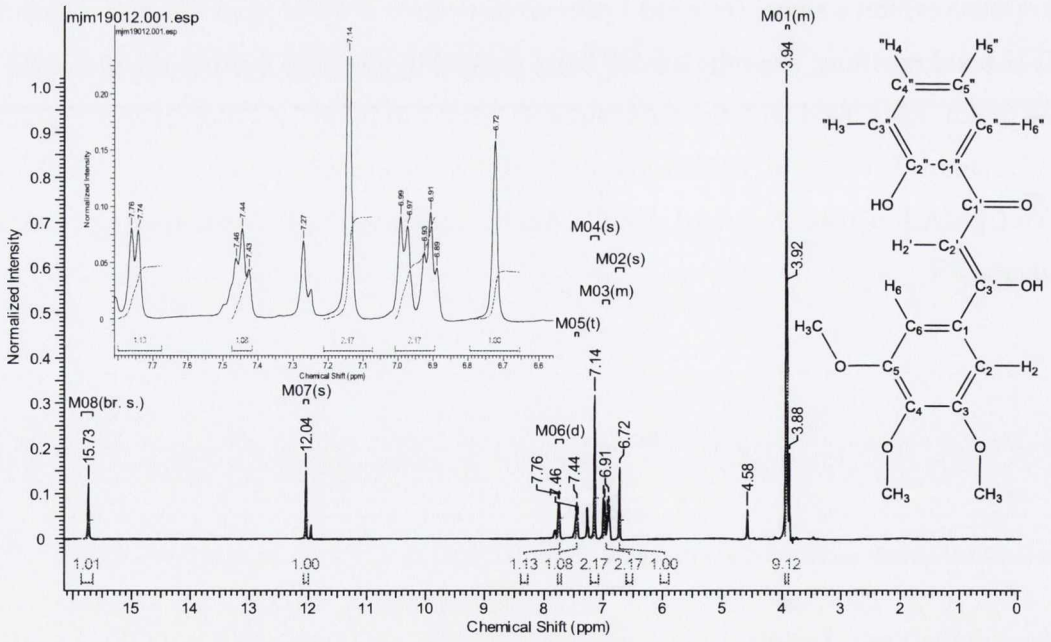

Figure 115: ^1H NMR spectrum of 3-hydroxy-1-(2-hydroxyphenyl)-3-(3,4,5-trimethoxyphenyl)prop-2-en-1-one (166)

The singlet at 6.72 ppm and the multiplet at 6.87 - 6.94 ppm both integrating for a single proton, were assigned to $H_{2'}$ and $H_{5'}$. A multiplet occurring at 6.95 - 7.01 ppm with an integral value of one proton was assigned to the aromatic proton $H_{3'}$. A singlet integrating for two protons was observed at 7.14 ppm, this resonance accounted for the equivalent protons H_6 and H_2. An apparent triplet occurring at 7.44 ppm (J = 7.28 Hz) with an integrating of one proton was assigned to $H_{4'}$. The most downfield signal in the aromatic region at 7.75 ppm (J=8.03 Hz) was a doublet and integrated for a single proton, this signal was designated as $H_{6'}$ due to the electron withdrawing influence of the ketone functionality on the adjacent carbon. The most downfield signals occurring at 12.04 ppm and 15.73 ppm were both broad singlets integrating for single protons. These signals were assigned to the phenol hydroxyl and the enol hydroxyl respectively.

The ^{13}C NMR spectrum (101 MHz, $CDCl_3$) of compound **166** (Figure 116) shows signals at 56.31 ppm and 61.00 ppm. These were assigned to the carbons in the methoxy substituents; the 56.31 ppm signal associated with the carbon equivalent pair of methoxy substituents on C_3 and C_5. The resonance at 61.00 ppm was therefore assigned to the methoxy substituent carbon on C_4.

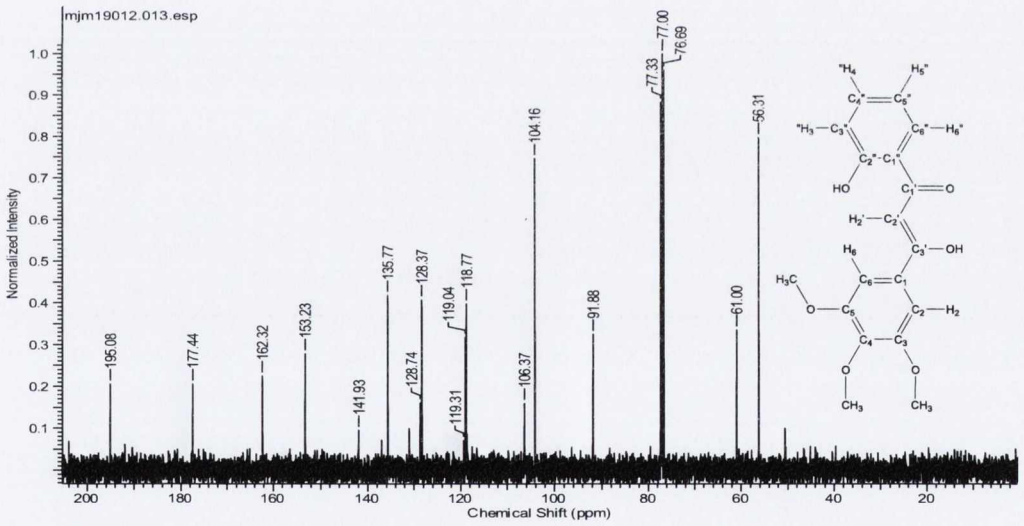

Figure 116: ^{13}C NMR spectrum of 3-hydroxy-1-(2-hydroxyphenyl)-3-(3,4,5-trimethoxyphenyl)prop-2-en-1-one (166)

The CH resonances occurring at 91.88 ppm, 104.16 ppm, 106.37 ppm and 118.77 ppm were assigned to $C_{2'}$, C_6, C_2 and $C_{5'}$ respectively. The remaining CH resonances occurring at 119.04 ppm, 128.37 ppm and 135.77 ppm accounted for aromatic carbons: $C_{3'}$, $C_{4'}$ and $C_{6''}$. Quaternary carbon signals at 119.31 ppm and 128.74 ppm corresponded to $C_{1''}$ and C_1. The carbons bearing methoxy substituent on the aryl ring gave resonances at 141.93 ppm (C_4) and 153.23 ppm (C_5 & C_3). The more downfield resonances at 162.32 ppm, 177.44 ppm and 195.08 ppm accounted

for the more electronegative environments produced at $C_{2''}$, $C_{3'}$ and $C_{1'}$. FTIR spectroscopy shows bands at 1658 (C=O), 1487 (C=C) and 1129 (C-O) cm^{-1}. High resolution mass spectrometry (ESI) was carried out and the required molecular ion was calculated to be $C_{18}H_{18}O_6$ [M-H] 329.1025 and found as 329.1033.

3.6 Synthesis of the 2-Phenyl-1-chromen-4-one

The synthesis of the flavones (**170-178**) occurs by the intramolecular cyclisation of the 3-hydroxy-3-phenylprop-2-en-1-ones (**161-169**) under strongly acidic conditions (Figure 117)[305].

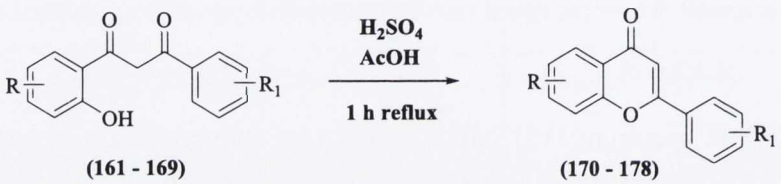

Figure 117: General scheme for the synthesis of the 2-Phenyl-1-chromen-4-ones

The 3-hydroxy-3-phenylprop-2-en-1-one formed due to the tautomerism of the 1,3 diketones is protonated due to the acidic conditions generated by the sulfuric acid and acetic acid. Facilitating an intramolecular nucleophilic addition reaction

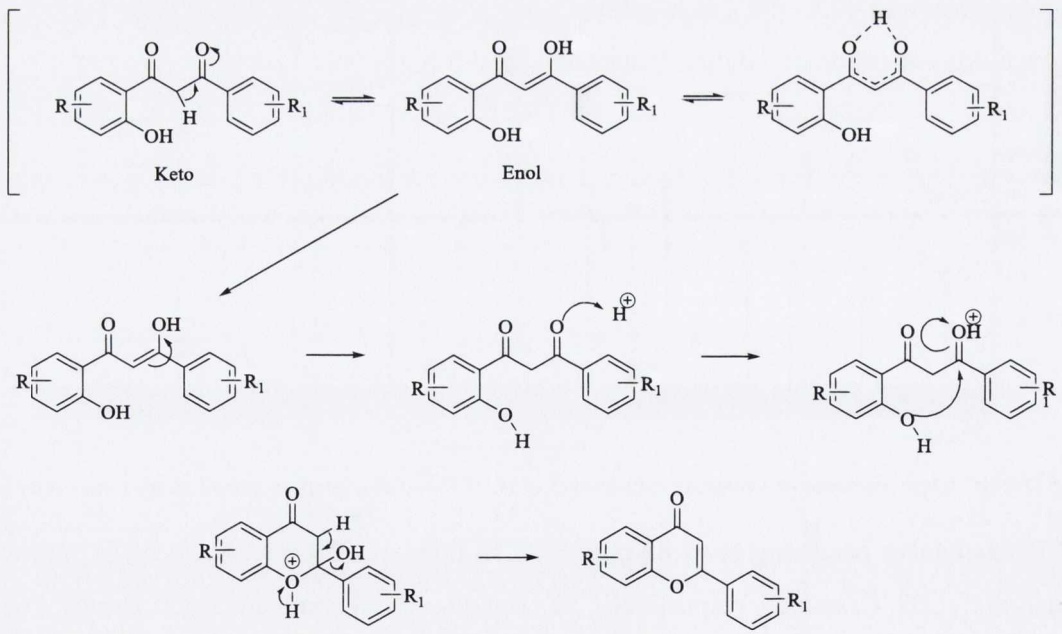

Figure 118: Proposed mechanism for the synthesis of the 2-Phenyl-1-chromen-4-ones

Subsequent deprotonation leads to the migration of electrons and formation of the flavone alkene bond accompanied by the elimination of water (Figure 118).

There is a plethora of procedures for the synthesis of 2-phenyl-1-chromen-4-ones including the Allan-Robinson and Kostanecki-Robinsons synthetic routes. More recently flavones have been synthesised by means of a palladium catalysed ligand free cyclocarbonylation of iodophenols with terminal acetylenes giving flavones with yields 75-96%[309]. In 2011 Yoshida et al. demonstrated the Baylis-Hillman reaction for the synthesis of the 2-phenyl-1-chromen-4-ones. This publication detailed the one pot 4-(N,N-dimethylamino)pyridine catalysed regioselective cyclisation of o-alkynoylphenols at 0-30 °C in 1.5 hours, affording excellent yields[310].

Intramolecular cyclisation of the 2'-hydroxychalones in the presence of ammonium iodide[311] and copper iodide[312] has also been reported. In 2014 the one pot synthesis of 2-phenyl-1-chromen-4-ones catalysed by pyrolidine and iodine at 150 °C over 9 hours was also reported. The reaction sequence that led to this one pot reaction was attributed to an aldol-Michael-dehydrogenative reaction[313].

A library of nine 2-phenyl-1-chromen-4-ones (**170-178**) was synthesised utilising the acid catalysed cyclisation of the 3-hydroxy-3-phenylprop-2-en-1-ones (**161-169**). This provided a crude product that was easily purified by recrystallization, affording yields of 29-95% (Table 17).

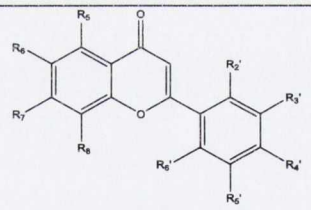

Compound	Substitution pattern	Yield	Compound	Substitution pattern	Yield
170	-	45%	**175**	$R_{3'} = R_{4'} = R_{5'} = OCH_3$	81%
171	$R_{4'} = Cl$	86%	**176**	$R_7 = R_{3'} = R_{4'} = R_{5'} = OCH_3$	29%
172	$R_7 = R_{4'} = Cl$	73%	**177**	$R_7 = R_{4'} = OCH_3$	95%
173	$R_{4'} = OCH_3$	81%	**178**	$R_7 = OCH_3$	49%
174	$R_{3'} = Cl$	70%	-	-	-

Table 17: 2-Phenyl-4*H*-chromen-4-one library. Note: R = H unless otherwise specified.

Compound **175** was chosen as a representative sample of the 2-phenyl-4*H*-chromen-4-ones and the ^{1}H NMR and ^{13}C NMR spectra will now be discussed in detail. The ^{1}H NMR (400 MHz, $CDCl_3$) spectrum of compound **175** (Figure 119) shows a multiplet at 3.85 - 4.01 ppm integrating for 9 protons, this multiplet was assigned to the 9 protons associated with the 3,4,5-trimethoxy substitution.

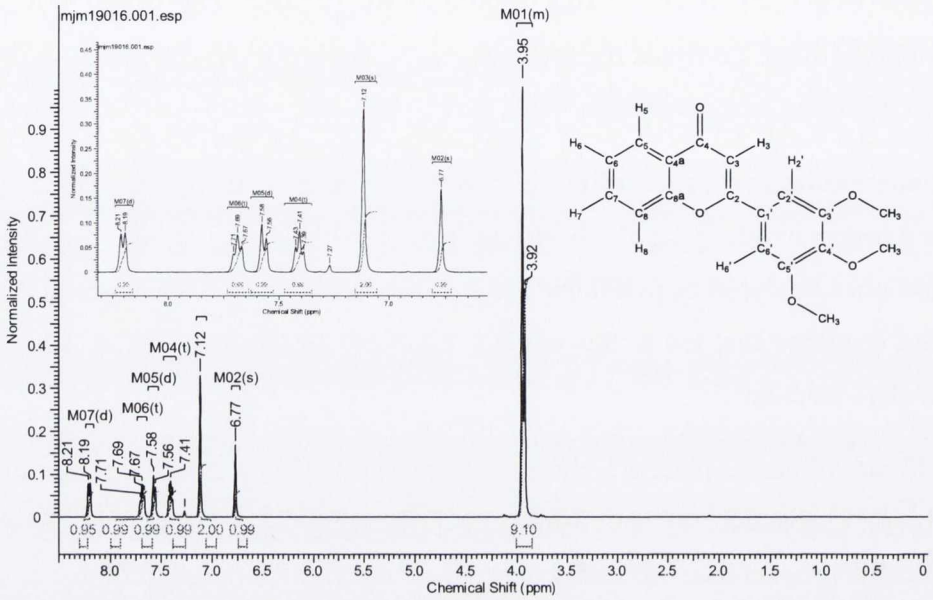

Figure 119: ^{1}H NMR spectrum of 2-(3,4,5-trimethoxyphenyl)-4H-chromen-4-one (175)

The singlets at 6.77 ppm integrating for a single proton and 7.12 ppm integrating for two protons, were assigned to H_3 and the equivalent protons $H_{6'}$ & $H_{2'}$. The apparent triplet occurring at 7.41 ppm (J = 7.28 Hz) and the doublet occurring at 7.57 ppm (J = 8.03 Hz), both integrated for a single proton each and were assigned to H_6 and H_8. Two more downfield aromatic resonances were observed in the spectrum: an apparent triplet occurring at 7.69 ppm (J = 7.53 Hz) and a doublet occurring at 8.20 ppm (J = 7.53 Hz). These resonances both integrated for a single proton each and were assigned to H_7 and H_5 respectively due to the electronegative environments present at these positions due to the ketone carbonyl.

The ^{13}C NMR spectrum (101 MHz, $CDCl_3$) of compound **175** (Figure 120) shows resonances at 56.27 ppm and 61.00 ppm, these were assigned to the carbons in the methoxy substituents, the 56.27 ppm signal associated with the carbon equivalent pair of methoxy substituents on $C_{3'}$ and $C_{5'}$. The resonance at 61.00 ppm was subsequently assigned to the methoxy substituent carbon on C_4. The CH resonances (Figure 121 – DEPT 90 spectrum) occurring at 103.60 ppm, 107.29 ppm and 118.02 ppm accounted for carbon equivalents $C_{6'}$ & $C_{2'}$, C_3 and C_6.

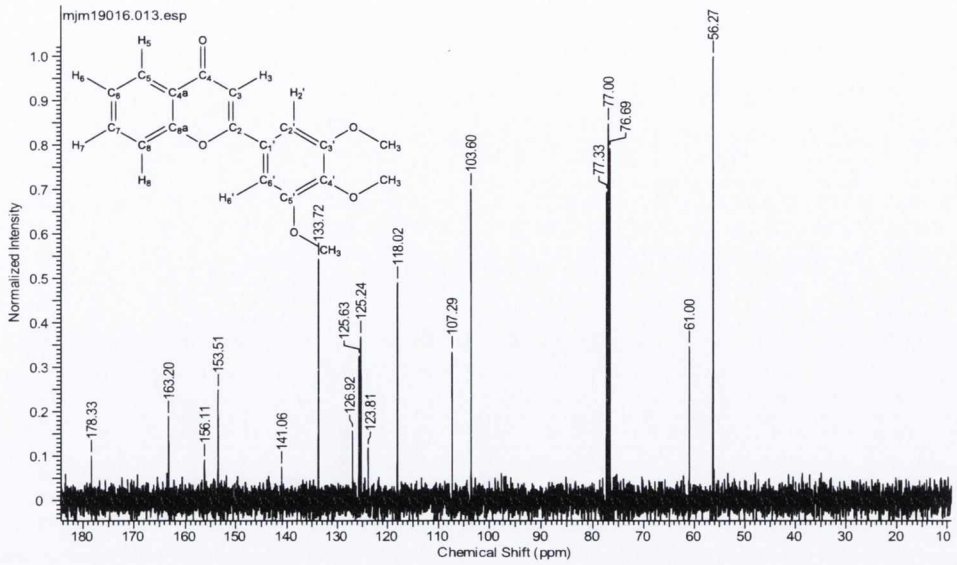

Figure 120: NMR spectrum of 2-(3,4,5-trimethoxyphenyl)-4H-chromen-4-one (175)

The quaternary carbon signals occurring at 123.81 ppm and 126.92 ppm corresponded to $C_{1'}$ and C_{4a}. The remaining CH signals at 125.24 ppm, 125.63 ppm and 133.72 ppm were allocated to C_8, C_7 and C_5 on the chromene ring. The quaternary signals at 141.06 ppm and 153.49 ppm represent $C_{4'}$ and carbon equivalents $C_{5'}$ & $C_{3'}$ – shifted downfield due to their methoxy substituents. The remaining and most downfield quaternary signals occurred at 156.11 ppm, 163.20 ppm and 178.31 ppm these signals denote C_8a, C_2 and C_4 (carbonyl).

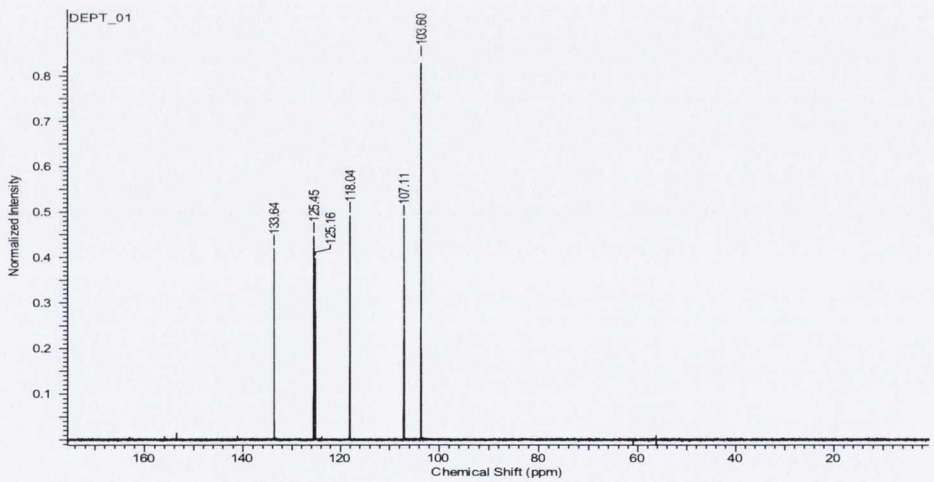

Figure 121: DEPT 90 NMR spectrum of 2-(3,4,5-trimethoxyphenyl)-4H-chromen-4-one (175)

FTIR spectrometry shows bands at 1650 (C=O), 1505 (C=C) and 1127 (C-O) cm^{-1}. High resolution mass spectrometry (ESI) was carried out and the required molecular ion was calculated to be $C_{18}H_{16}O_5$ [M^++Na] 335.0895 and found as 335.0911.

3.7 Synthesis of the of 3-nitro-2-phenylchromen-4-ones

The synthesis of the 3-nitro-2-phenylchromen-4-ones (**179-188**) was achieved by the regioselective nitration of 2-phenyl-1-chromen-4-ones (**170-178**) described by Patoilo et al. (2010). The nitration reaction at C-3 is solvent dependent and proceeds *via* a nitro radical pathway[306] (Figure 122) (Table 18).

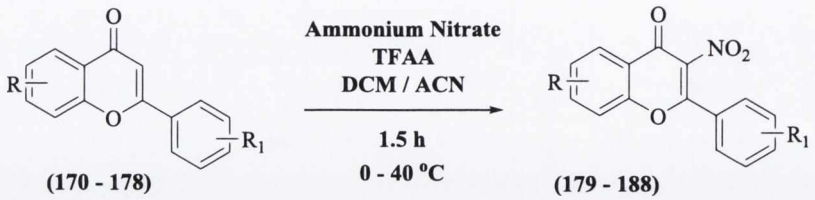

Figure 122: General scheme for the synthesis of the 3-nitro-2-phenylchromen-4-ones

Ammonium nitrate and trifluoroacetic acid react initially to form nitronium trifluoroacetate. This nitronium trifluoroacetate species then decomposes to form a nitro free radical and a trifluoroacetate radical. The nitro free radical then reacts at the flavone's electron rich alkene bond to create 3-nitroflavones, our target product (Figure 123).

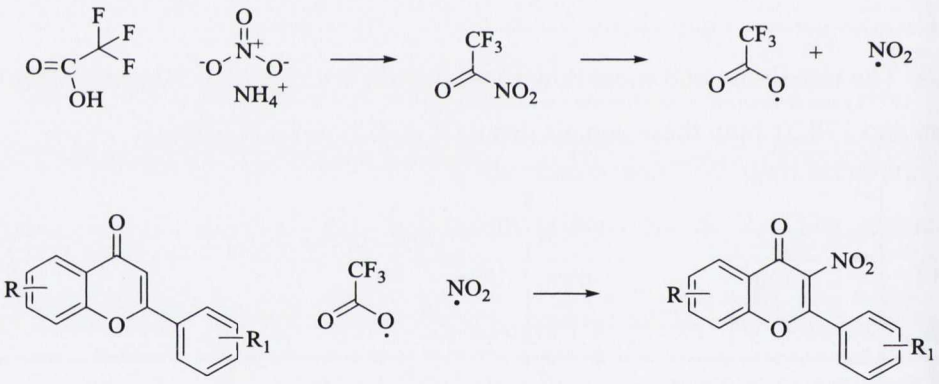

Figure 123: Proposed mechanism for the synthesis of the 3-nitro-2-phenylchromen-4-ones

The 3-nitro-2-phenylchromen-4-ones have been synthesised by means of alternative synthetic routes to the selective nitration of 2-phenyl-1-chromen-4-ones. Iaroshenko et al. (2012) recorded the acid catalysed, one pot synthesis of the 3-nitro-2-phenylchromen-4-one from 2'-hydroxy-2-nitroacetophenone and trimethylorthoformate[314]. Dauzonne et al. (1992) synthesised a library of 3-amino-2-phenylchromen-4-ones via the palladium catalysed reduction of the 3-nitro-2-phenylchromen-4-ones. The group synthesised the 3-nitro-2-phenylchromen-4-ones from a series of 2-aryl-3-chloro-2,3-dihydro-3-nitro-4*H*-1-benzopyran-4-ones employing 1,8-diazobicyclo[5.4.0]undec-7-ene to aid dehydration and elimination of the chloro group[315]. Similarly this reaction has been achieved by dehydration and elimination of bromine from 2-aryl-3-bromo-2,3-dihydro-3-nitro-4*H*-1-benzopyran-4-ones[316].

During the nitration step, high yields of the desired 3-nitro-2-phenylchromen-4-ones (**178-188**) were attained. However nitration side products were also formed in some cases, these side products were isolated and subsequently characterised. The isolated nitration side-products were 2-(4-methoxy-3-nitrophenyl)-3-nitro-4*H*-chromen-4-one (**182**) and 3-nitro-2-(3,4,5-trimethoxy-2-nitrophenyl)-4*H*-chromen-4-one (**185**) (Figure 124). It is proposed that an additional nitration reaction took place during the formation of these two compounds due to the *ortho* activating effect of the methoxy substitutions.

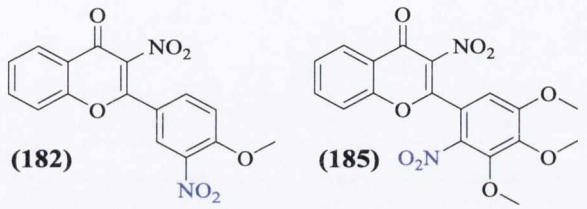

Figure 124: Isolated nitration side-products 2-(4-methoxy-3-nitrophenyl)-3-nitro-4H-chromen-4-one and 3-nitro-2-(3,4,5-trimethoxy-2-nitrophenyl)-4H-chromen-4-one (Addition nitration position highlighted in blue).

The synthesis of ten 3-nitro-2-phenylchromen-4-ones was accomplished, with nine compounds fully isolated and characterised (Table 18). The nitration reaction employed afforded yields of 9-95% of the 3-nitro-2-phenylchromen-4-ones.

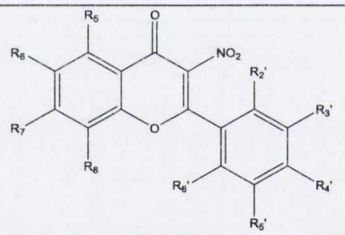

Compound	Substitution pattern	Yield	Compound	Substitution pattern	Yield
179	–	95%	**184**	$R_3' = R_4' = R_5' = OCH_3$	23%
180	$R_4' = Cl$	86%	**185**	$R_2' = NO_2$, $R_3' = R_4' = R_5' = OCH_3$	7%*
181	$R_7 = R_4' = Cl$	33%*	**186**	$R_7 = R_4' = OCH_3$	9%*
182	$R_3' = NO_2$, $R_4' = OCH_3$	30%	**187**	$R_3' = Cl$	21%
183	$R_7 = R_3' = R_4' = R_5' = OCH_3$	trace	**188**	$R_7 = OCH_3$	15%*

Table 18: 3-nitro-2-phenylchromen-4-one library. Note: R = H unless otherwise specified. * denotes novel compound

7-Methoxy-3-nitro-2-phenyl-4*H*-chromen-4-one (**188**) was chosen as a representative sample of the 3-nitro-2-phenylchromen-4-one and the ^{1}H NMR and ^{13}C NMR spectra will now be discussed in detail. The ^{1}H NMR (400 MHz, $CDCl_3$) spectrum of compound **188** (Figure 125) shows a singlet at 3.95 ppm that integrates for three protons – and assigned to the three protons on the methoxy substituent.

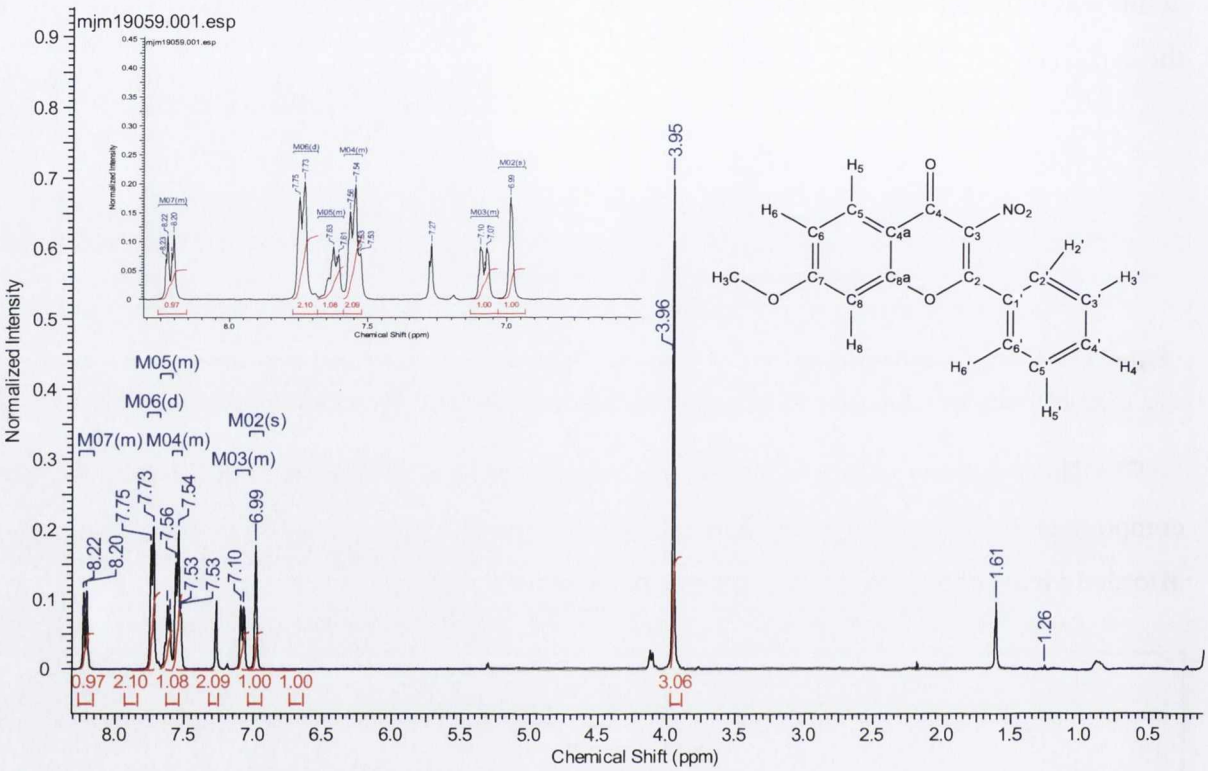

Figure 125: ^{1}H NMR spectrum of 7-methoxy-3-nitro-2-phenyl-4*H*-chromen-4-one (188)

A singlet occurring at 6.99 ppm and a multiplet at 7.03 - 7.13 ppm both integrated for one proton each; these resonances represented H_8 and H_6. The multiplet at 7.52 - 7.59 ppm and the doublet at 7.74 ppm (J = 7.53 Hz) both integrated for two protons each. These resonances corresponded to the equivalent protons on the phenyl substituent at $H_{3'}$ & $H_{5'}$ and $H_{2'}$ & $H_{6'}$. The multiplet occurring at 7.59 - 7.68 ppm and the downfield multiplet occurring at 8.16 - 8.26 ppm both integrating for single protons were assigned to $H_{4'}$ and H_5.

The ^{13}C NMR spectrum (101 MHz, $CDCl_3$) of compound **188** (Figure 126) shows resonances occurring at 56.08 ppm, these corresponded to the carbon in the methoxy substituent on C_7 of the chromene ring. The CH resonances (Figure 127) at 100.67 ppm, 115.77 ppm and 132.72 ppm were assigned to the CH carbon environments in the chromene ring system: C_8, C_6 and C_5. Signals at 127.73 ppm and 129.26 ppm represent the two carbon equivalent environments in the phenyl substituent, $C_{3'}$ & $C_{5'}$ and $C_{2'}$ & $C_{6'}$ respectively.

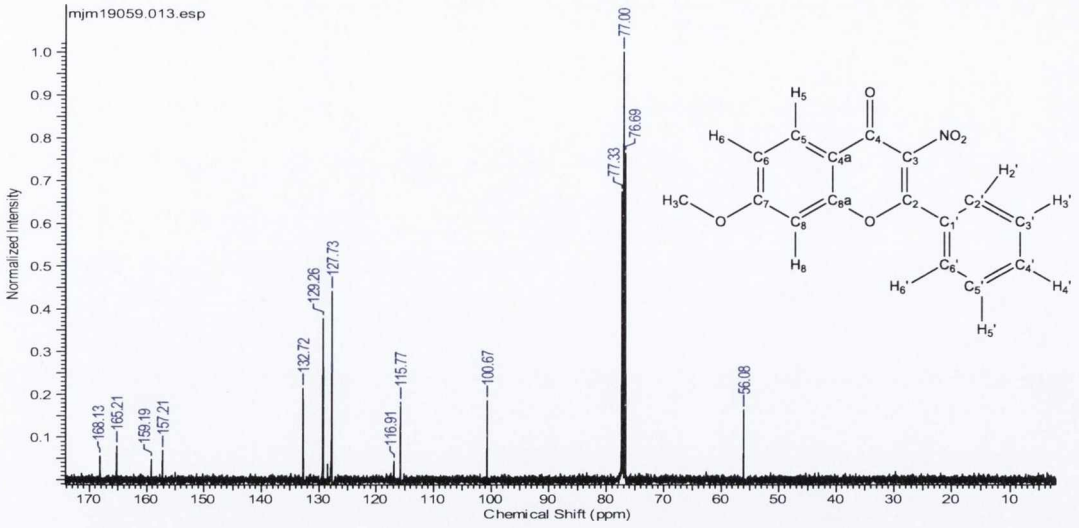

Figure 126: ^{13}C NMR spectrum of 7-methoxy-3-nitro-2-phenyl-4*H*-chromen-4-one (188)

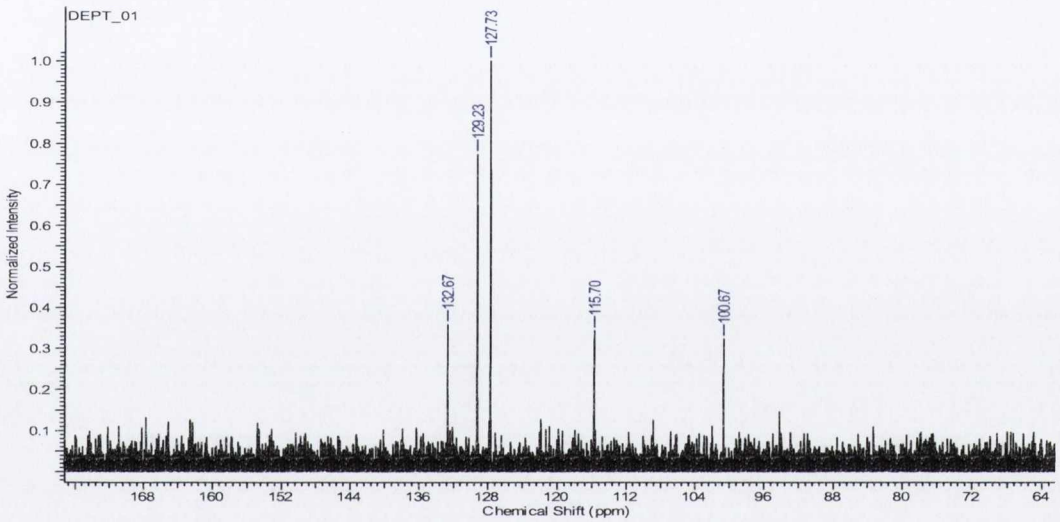

Figure 127: DEPT 90 NMR spectrum of 7-methoxy-3-nitro-2-phenyl-4*H*-chromen-4-one (188)

The quaternary signals occurring at 116.91 ppm, 127.81 ppm and 128.49 ppm accounted for C_3, C_1' and C_{4a}. More electron withdrawing environments induced by the chromene ring and the methoxy substituent are held responsible for 157.21 ppm (C_{8a}) and 159.19 ppm (C_7). The most downfield signals at 165.21 ppm and 168.13 ppm correspond to C_2 and C_4 (carbonyl).

FTIR spectroscopy shows absorbances at 1653 (C=O), 1630 (C=C), 1528 (N-O), 1434 (C=C) and 1253 (C-O) cm^{-1}. High resolution mass spectrometry (ESI) was carried out and the required molecular ion was calculated to be $C_{16}H_{11}NO_5$ $[M^+ + Na]$ 320.0535 and found as 320.0537.

3.8 Synthesis of 3-nitro-2,4-diphenyl-2,5-dihydrobenzo[b][1,4]thiazepine

The acid catalysed synthesis of 3-nitro-2,4-diphenyl-2,5-dihydrobenzo[b][1,4]thiazepine (**189**) from (*E*)-2-nitro-1,3-diphenylprop-2-en-1-one (**90**) and *o*-aminothiophenol was also achieved. It is to be noted that 3-nitro-2,4-diphenyl-2,5-dihydrobenzo[b][1,4]thiazepine also contained the 1,3-bis(aryl)-2-nitro-1-propene scaffold but this time in a constrained conformation, this is highlighted in blue in the reaction scheme below (Figure 128).

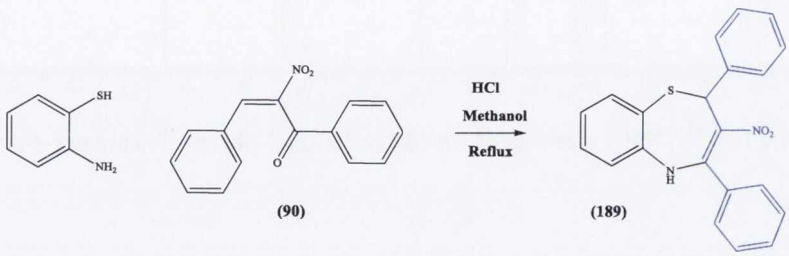

Figure 128: Scheme for the synthesis of 3-nitro-2,4-diphenyl-2,5-dihydrobenzo[b][1,4]thiazepine

The procedure for the synthesis of these heterocyclic structures was first published by Berestovitskaya et al. (2011). It was proposed that the mechanism of formation of the 3-nitro-2,4-diphenyl-2,5-dihydrobenzo[b][1,4]thiazepines initiates with a Michael addition of *o*-aminothiophenol to the nitrovinyl unit followed by the cyclisation through the formation of an imine between the free amine and the carbonyl on (*E*)-2-nitro-1,3-diphenylprop-2-en-1-one. Isomerisation finally leads to the desired product 3-nitro-2,4-diphenyl-2,5-dihydrobenzo[b][1,4]thiazepine (**189**) (Figure 129).

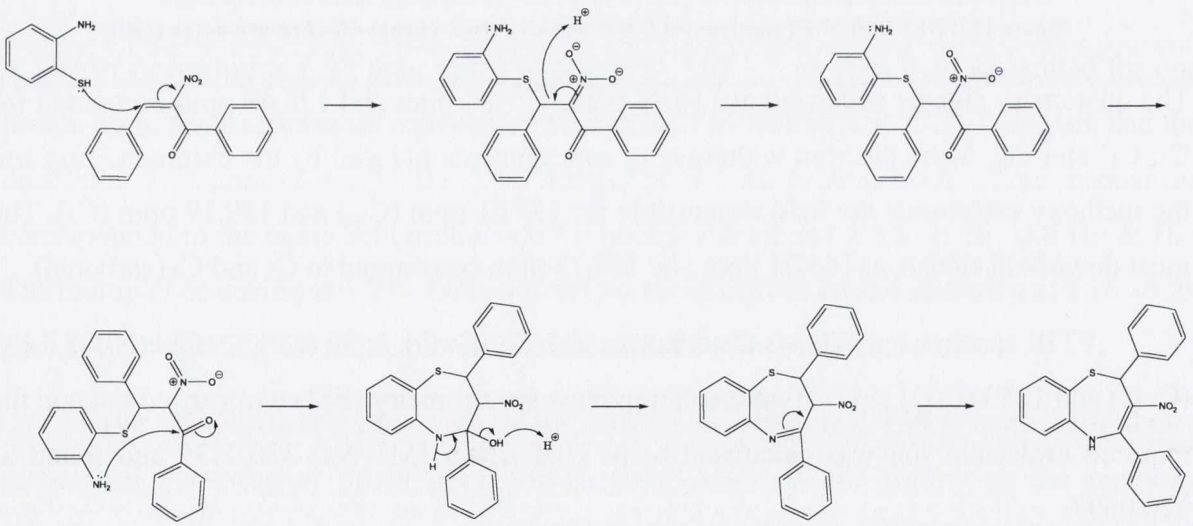

Figure 129: Mechanism for the synthesis of 3-nitro-2,4-diphenyl-2,5-dihydrobenzo[b][1,4]thiazepine (189)

3-Nitro-2,4-diphenyl-2,5-dihydrobenzo[b][1,4]thiazepine (**189**) was synthesised in the present work and purified by column chromatography to give 60% yield as colourless crystals[152].

3.9 Synthesis of 3-nitro-2-phenyl-1*H*-indole

3-Nitro-2-phenyl-1*H*-indole was synthesised in order to assess the effect on antiproliferative activity induced by the inclusion of the (2-nitrovinyl)benzene scaffold as a substructure of a larger heterocyclic compound. Within the 3-nitro-2-phenyl-1*H*-indole structure the (2-nitrovinyl)benzene scaffold is held in a constrained confirmation and no longer possesses nitrovinyl protons (Figure 130). 3-Nitro-2-phenyl-1*H*-indole (**190**) was prepared by the selective 3-nitration of 2-phenylindole. The reaction conditions employed utilised silver nitrate and benzoyl chloride in acetonitrile at 0 °C to produce the required reaction conditions[317] (Figure 130).

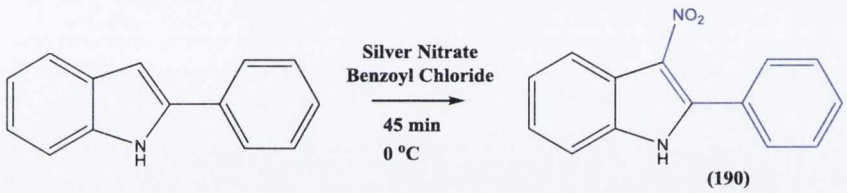

Figure 130: Synthesis of 3-nitro-2-phenyl-1*H*-indole (190)

In the present work the nitration of 2-phenylindole is achieved through the *in situ* formation of benzoyl nitrate from benzoyl chloride and silver nitrate. Benzoyl nitrate decomposes in this one pot nitration to form a nitronium ion and a benzoyloxy carbanion. The benzoyloxy carbanion can in turn decompose to form benzene with the evolution of carbon dioxide[318]. The nitronium ion proceeds to nitrate the 3 position of the 2-phenylindole ring. Alternative methods of synthesising the 3-nitro-2-phenyl-1*H*-indoles have been developed; one recent example is the intramolecular arene alkene coupling of *N*-aryl β-nitroenamines[319]. Recrystallization from benzene afforded 3-nitro-2-phenyl-1H-indole (**190**) with a good yield of 52%.

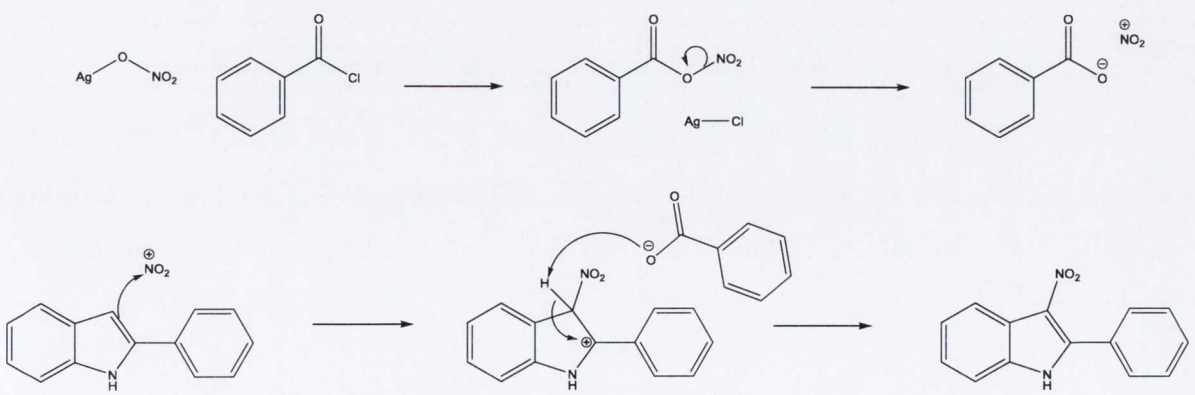

Figure 131: Proposed mechanism for the synthesis of 3-nitro-2-phenyl-1*H*-indole

3.10 Synthesis of 4-nitro-3,5-diphenylisoxazole

4-Nitro-3,5-diphenylisoxazole was synthesised in order to assess the effect on antiproliferative activity induced by the inclusion of the 2-nitro-1,3-diphenylprop-1-ene and the (2-nitrovinyl)benzene scaffolds as substructures of a larger heterocyclic compound (in this case the phenylisoxazole). Within the 4-nitro-3,5-diphenylisoxazole structure both the (2-nitrovinyl)benzene and the 2-nitro-1,3-diphenylprop-1-ene scaffolds are held in a constrained (*Z*) conformations and no longer possess nitrovinyl protons (Figure 132).

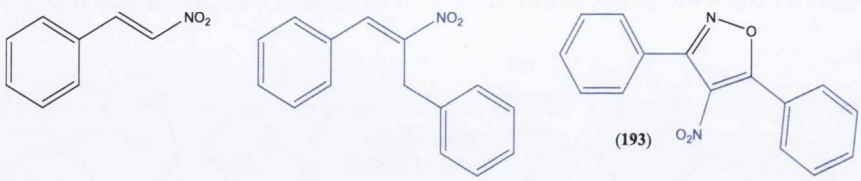

Figure 132: (*E*)-(2-nitrovinyl)benzene scaffold, 2-nitro-1,3-diphenylprop-1-ene and 4-nitro-3,5-diphenylisoxazole (2-nitro-1,3-diphenylprop-1-ene substructure highlighted in blue)

The synthetic route employed for the synthesis of 4-nitro-3,5-diphenylisoxazole was a three step preparation. Chalcone is brominated to give 2,3-dibromo-1,3-diphenylpropan-1-one and when reacted with hydroxylamine undergoes cyclisation to form the 3,5-diphenylisoxazole. This 3,5-diphenylisoxazole is then selectively nitrated to give 4-nitro-3,5-diphenylisoxazole (**193**) (Figure 133).

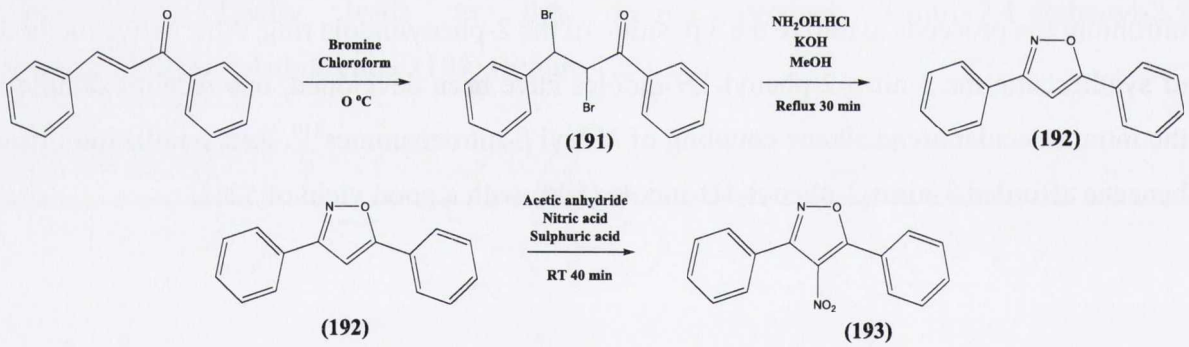

Figure 133: Overall scheme for the synthesis of 4-nitro-3,5-diphenylisoxazole

The first step of the overall synthetic route is the synthesis of 2,3-dibromo-1,3-diphenylpropan-1-one from chalcone (Figure 134). The bromination of alkenes proceeds via a *trans* / *anti*-addition and the bromine adds to different sides of the alkene double bond.

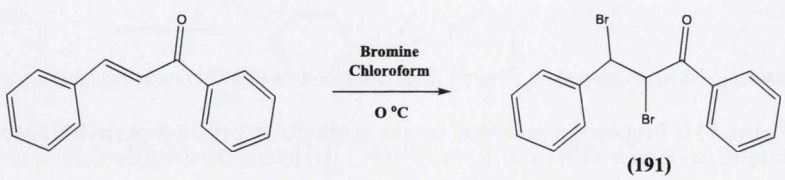

Figure 134: Scheme for the synthesis of 2,3-dibromo-1,3-diphenylpropan-1-one from chalcone

The reaction mechanism initiates with the electrophilic addition of bromine to the alkene with the formation of the bromonium ion. The charged addition intermediate is subsequently nucleophilically attacked by the bromonium ion to give 2,3-dibromo-1,3-diphenylpropan-1-one (**191**). (Figure 135)

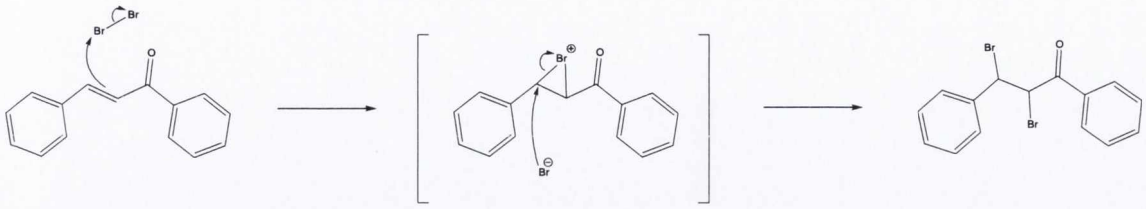

Figure 135: Proposed mechanism for the synthesis of 2,3-dibromo-1,3-diphenylpropan-1-one from chalcone

Bromination of the chalcones has also been achieved using other bromination systems such as oxone / sodium bromide[320], ammonium cerium (IV) bromide / potassium bromide[321] and n-bromosuccinimide / ammonium chloride[322]. 2,3-Dibromo-1,3-diphenylpropan-1-one was successfully synthesised from chalcone according to the method outlined by Baumstark et al. (1980)[323]. The reaction afforded crude product and upon recrystallization from ethanol gave a respectable yield of 45%.

The preparation of the 3,5-diphenylisoxazole ring system was the second step in the overall scheme. 3,5-Diphenylisoxazole (**192**) was synthesised from dibromo-1,3-diphenylpropan-1-one (**191**) in a tandem substitution cyclisation reaction (Figure 136).

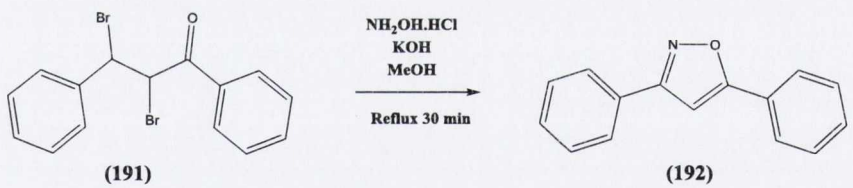

(191) **(192)**

Figure 136: Scheme for the synthesis of 3,5-diphenylisoxazole

The mechanism for this transformation between dibromo-1,3-diphenylpropan-1-one (**191**) and hydroxylamine proceed via elimination of hydrogen bromide and the formation of 2-bromo-1,3-diphenylprop-2-en-1-one. This ketone species reacts in the presence of hydroxyl amine to give the oxime. The hydroxyl of this new imine structure undertakes intramolecular nucleophilic attack on the alkene species. The resulting enamine / imine equilibrium leads to the formation of the final isoxazole double bond by elimination hydrogen bromide (Figure 137).

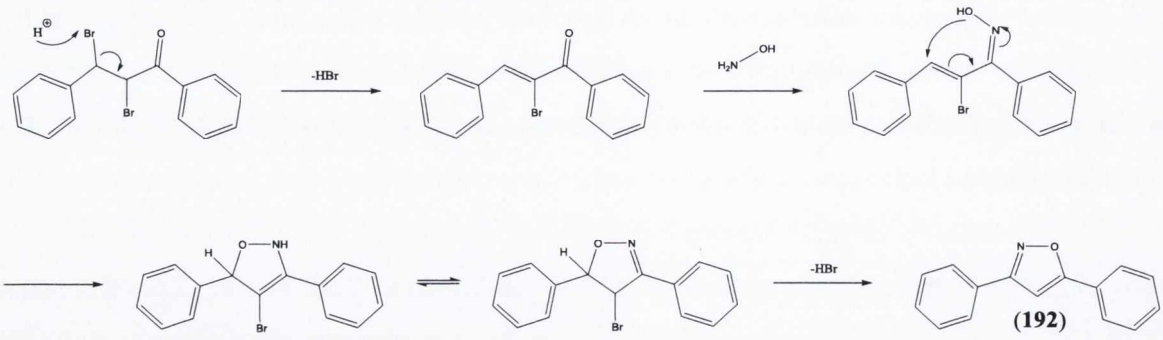

Figure 137: Proposed mechanism for the synthesis of 3,5-diphenylisoxazole

The 3,5-diphenylisoxazoles have been accessed through a number of different synthetic methodologies such as the cyclisation of the 1,3 diketone with hydroxylamine[324] and the reaction of aldoximes with alkynylbenzenes[258]. The 3,5-diphenylisoxazole synthesised in this work followed methodology outlined by Baumstark et al. (1980)[323] and afforded a colourless solid with 52% yield.

The final step of the 4-nitro-3,5-diphenylisoxazole synthesis involved the selective 4-nitration of the 3,5-diphenylisoxazole ring system. The nitrating conditions were achieved with a short reaction time, at room temperature with a mixture of concentrated nitric acid and sulphuric acid in acetic anhydride[325, 326] (Figure 138).

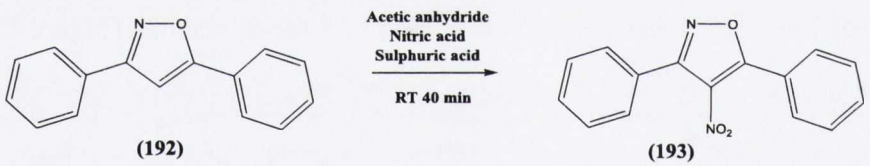

Figure 138: Scheme for the synthesis of 4-nitro-3,5-diphenylisoxazole

Concentrated sulphuric acid and concentrated nitric acid react to form the nitronium ion *in situ*. The nitronium ion undergoes nucleophilic attack from the alkene bond in the 3,5-diphenylisoxazole system, subsequent loss of a proton reforms the double bond giving the 4-nitro-3,5-diphenylisoxazole (**193**) (Figure 139).

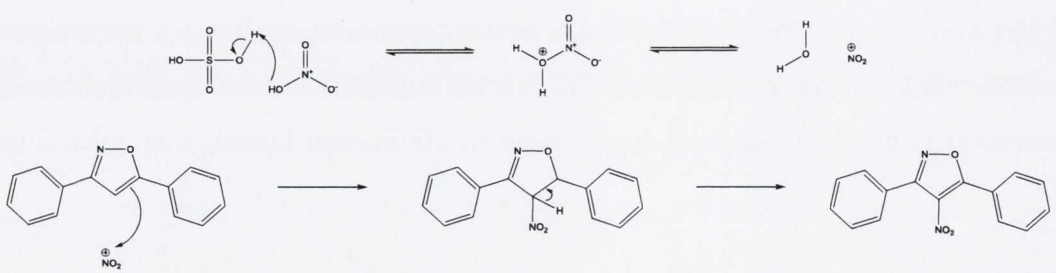

Figure 139: Proposed mechanism for the synthesis of 4-nitro-3,5-diphenylisoxazole

An alternative synthesis of the 4-nitro-3,5-diphenylisoxazoles to the preparation described above is the base catalysed condensation reaction of *alpha*-nitroacetophenone and aldoxime[327]. Cyclisation of secondary acetylenic bromides in the presence of sodium nitrite has also led to the formation of the same synthetic target[328]. In the present work the crude reaction product was purified by column chromatography on silica gel to afford a colourless solid (**193**), 33% yield.

3.11 Conclusion

The incorporation of the nitrostyrene and (*E*)-1,3-bis(aryl)-2-nitro-1-propene scaffold into a number of heterocyclic structures was achieved and the altered configuration induced by these heterocycles has been demonstrated. A library of 3-nitro-2-phenyl-2*H*-chromenes and 3-nitro-1,2-dihydroquinolines was prepared utilising a Baylis-Hillman tandem Michael reaction strategy. A variety of different substitution patterns were achieved including but not limited to methoxy, hydroxy, halogen and benzyloxy. A panel of diversely substituted 3-nitro-2-phenylchromen-4-ones were also prepared *via* nitration of the desired flavone structures. Other fused ring heterocycles nitrated included phenylindole and 3,5-diphenylisoxazole. The biological activity of the compounds synthesised in Chapter 3 in BL cell lines DG-75 and MUTU-I will be discussed in Chapter 6.

Chapter 4.
Design, synthesis and characterisation of 9-substituted anthracenes

4.0 Introduction

Previous work carried out within our laboratory on a series of anthracene based maprotiline analogues identified (*E*)-9-(2-nitrovinyl)anthracene as a potent antiproliferative agent in Burkitt's lymphoma cell lines DG75 and MUTU-I[6]. (*E*)-9-(2-Nitrovinyl)anthracene gave EC_{50} values of 3 μM in the MUTU-I and 1.5 μM in the DG75 cell lines. (*E*)-9-(2-nitrovinyl)anthracene was also noted to induce apoptosis in HL60, DG-75 and MUTU-I cell lines[6]. The lowest energy configuration of (*E*)-9-(2-nitrovinyl)anthracene and maprotiline were flexibly aligned to demonstrate the similarities between the planar anthracene and the bridged structure of maprotiline (Figure 140).

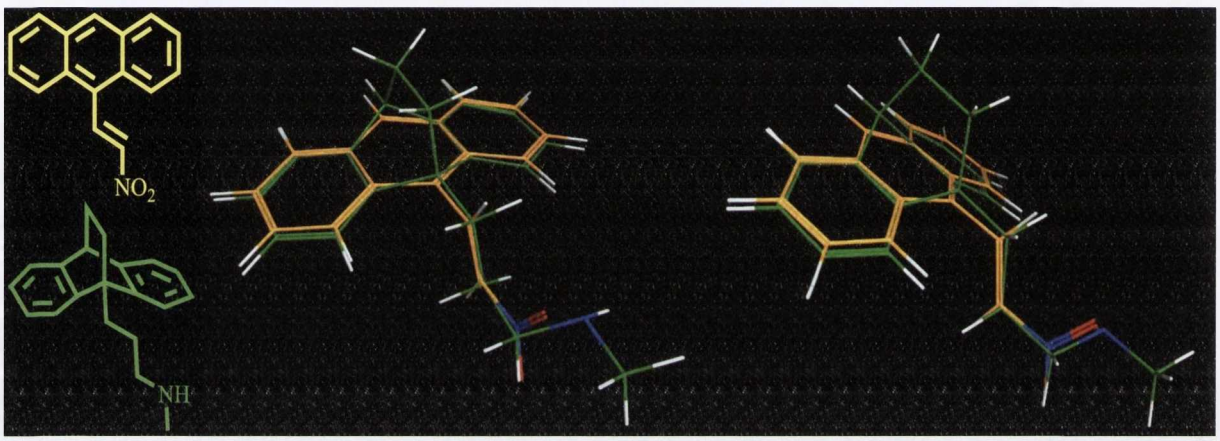

Figure 140: Maprotiline (green) flexibly aligned to the (*E*)-9-(2-nitrovinyl)anthracene (orange) (MOE 2011.10).

Good overlay was observed between the anthracene ring and the two phenyl rings of the tetracyclic structure. The nitrovinyl unit was also shown to correlate well to the secondary amine chain of maprotiline. (*E*)-9-(2-Nitrovinyl)anthracene like many other compounds in this work, contained the (*E*)-(2-nitrovinyl)benzene pharmacophore as a substructure which has been widely shown to be favourable for anticancer activity (Chapter 1, Section 1.5).

The main objective of this section was to synthesise a library of substituted (*E*)-9-(2-nitrovinyl)anthracenes via the Henry-Knoevenagel condensation reaction of the required substituted 9-anthraldehydes. To achieve this objective it was necessary to prepare a number of substituted 9-anthraldehydes from their corresponding anthracenes, anthrones and anthraquinones. 9-Anthraldehydes used throughout the course of this section include chlorine, bromine, methyl, phenyl, methoxy and isopropyl substitutions at C-9 / C-10. The reduction of (*E*)-9-(2-nitrovinyl)anthracene with sodium borohydride was also investigated. The utilisation of the Wittig reaction for the extension of carbon chain between the nitrovinyl unit and the anthracene ring was also of interest. Other double bonded systems would also be introduced at C-9 including oximes, alcohols, cyanovinyl, nitrone and chalcone systems in order to assess

their effect on the activity of the series. The substituted anthracene library is summarised in Figure 141.

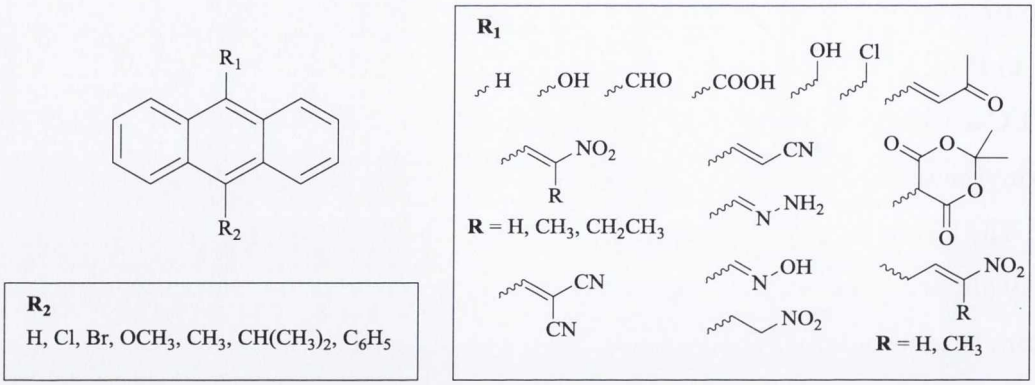

Figure 141: Overview of anthracene compound library

4.1 Synthesis of the substituted anthracene aldehydes

A panel of substituted anthracene aldehydes was synthesised from the corresponding anthracenes, anthrones and anthraquinones (Table 22). The Grignard reaction of alkyl or aryl magnesium bromides and anthrone was exploited to prepare the required substituted anthracenes[329]. These substituted anthracenes were subsequently formylated using the Vilsmeier Haack reagent to give 10-substituted-9-anthraldehydes (Figure 142)

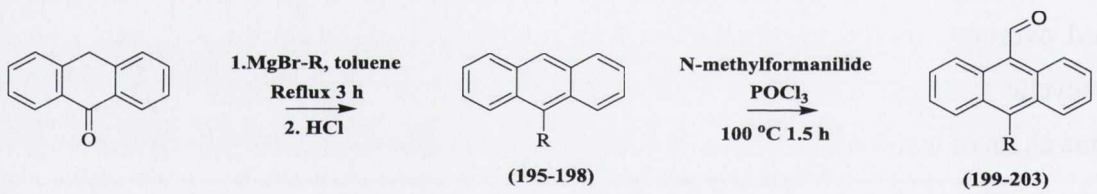

Figure 142: Overall scheme for the synthesis of 10-substituted-9-anthraldehydes (199-203)

Since the first preparation of ethereal solutions of magnesium halides in 1900 by Victor Grignard[330], the Grignard reaction has been developed into a potent synthetic tool for the synthesis of multifunction molecules. The Grignard reagents used the current work were pre-prepared by and purchased from Sigma Aldrich. The preparation of these Grignard reagents is generally a straight forward reaction of the aryl bromide and on contact with magnesium metal via single electron transfer in anhydrous conditions to give the required alkyl or aryl magnesium bromide[209].

The mechanism of the Grignard reaction proceeds *via* an ionic mechanism, where the dipole of the carbonyl and the dipole created across the magnesium bromide facilitates the cleavage of the bond between the alkyl group and magnesium bromide. During the addition

the slightly positive magnesium is nucleophilically attacked by the slightly negative carbonyl double bond, as the slightly negative alkyl group attacks the carbonyl carbon (Figure 143).

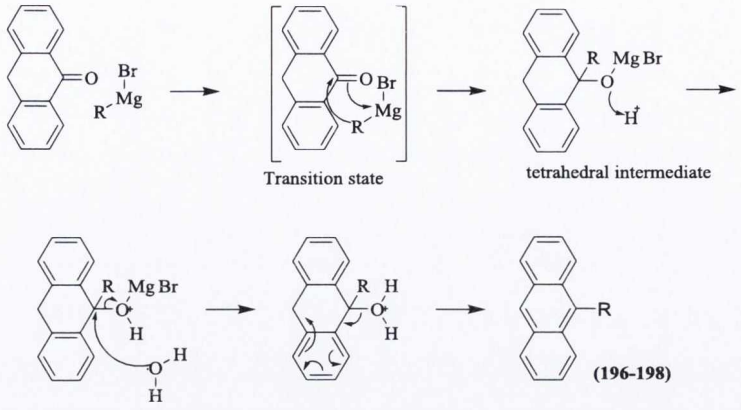

Figure 143: Proposed mechanisms for formation of Grignard reagents and the Grignard reaction of anthrone

Protonation of the tetrahedral addition intermediate and the nucleophilic addition of water leads to the elimination of magnesium hydroxide. Aromaticity is established in the anthracene ring through subsequent protonation of the hydroxyl substituent and elimination of water. This Grignard reaction of alkyl and aryl magnesium bromides with anthrone gave 9-substituted anthracenes (**196-198**) in excellent yields of 76-84% (Table 19).

9-Methoxyanthracene (**194**) was synthesised from anthrone in an acid catalysed one pot methylation reaction with trimethylorthoformate in a solvent mixture of benzene and methanol. The reaction time was quite long and was monitored by thin layer chromatography over a period of three days[331]. The proposed mechanism for the methylation reaction of anthrone is illustrated in Figure 144.

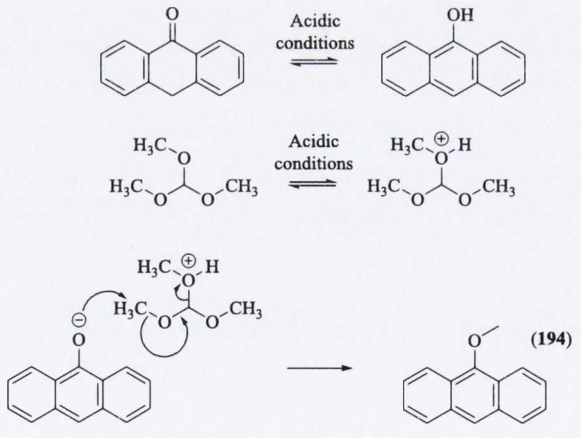

Figure 144: Proposed mechanism for the methylation of anthrone

In acidic conditions anthrone undergoes enolization to anthracen-9-ol. Anthracen-9-ol nucleophilically attacks the protonated form of trimethylorthoformate leading to the cleavage

of the C-O bond in the methoxy group and elimination of methanol from the addition product. The methylation reaction described above afforded 9-methoxy anthracene (**194**) as a pale yellow solid, 76% yield (Table 19).

The Wolff-Kischner reaction was first reported in 1911[332] and entails the reduction of a carbonyl to a methylene group using sodium hydroxide and hydrazine. The 9-methylanthracene analogue (**195**) was synthesised from 9-anthraldehyde using a method described by Huang et al. (1949). This involved the one pot pressure tube reaction of potassium hydroxide and 9-anthraldehyde at 200 °C for 1 hour in diethylene glycol[333] (Figure 145).

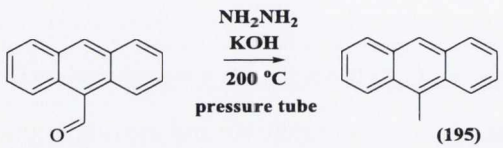

Figure 145: Scheme for the synthesis of 9-methylanthracene (195)

The reaction mechanism for the Wolff-Kischner reaction is displayed below in Figure 146. The reaction initiates with the nucleophilic addition of hydrazine to the aldehyde carbonyl with the elimination of water, forming (anthracen-9-ylmethylene)hydrazine. (Anthracen-9-ylmethylene)hydrazine undergoes base catalysed hydrolysis with the eventual evolution of nitrogen gas.

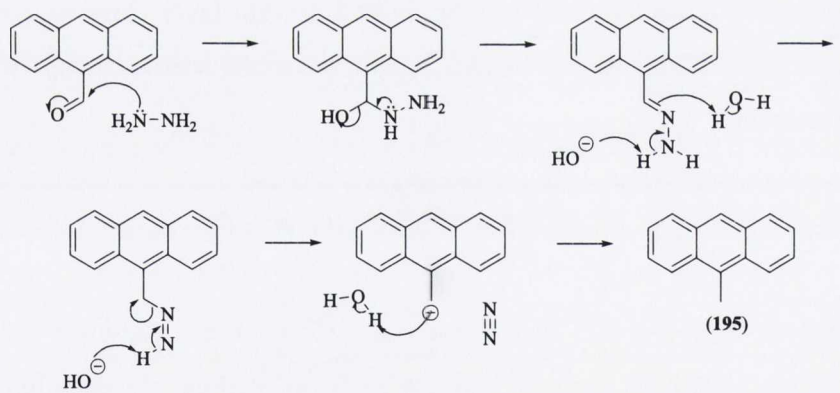

Figure 146: Proposed mechanism for the synthesis of 9-methylanthracene (195) (Wolff-Kischner mechanism)

The first step of this decomposition reaction is deprotonation in the basic conditions is the formation of the nitrogen nitrogen double bond. A second deprotonation subsequently takes place, forming the nitrogen nitrogen triple bond, cleaving the weaker nitrogen carbon bond. Nitrogen gas is then eliminated leaving a carbanion that deprotonates water to form the methyl group. The Wolff-Kischner reaction described above afforded 9-methylanthracene (**195**) as a pale yellow solid with 84% yield (Table 19).

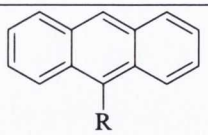

Compound	R	Yield	Compound	R	Yield
194	OCH_3	76%	**197**	$CH(CH_3)$	76%
195	CH_3	84%	**198**	C_6H_5	84%
196	CH_2CH_3	80%	-	-	-

Table 19: 9-subsituted anthracene library. Note: R = H unless otherwise specified.

The Vilsmeier-Haack reaction is a formylation reaction first documented by Anton Vilsmeier and Albrecht Haack in 1927[334]. The Vilsmeier-Haack reaction encompasses the formation of the Vilsmeier-Haack reagent from a substituted amide (typically dimethylformanilide or N-methylformanilide) and phosphorous oxychloride and its subsequent electrophilic reaction with electron rich carbocycles and heterocycles (e.g. anthracene, benzene) to give an aldehyde or ketone[209] (**199-203**) (Figure 147).

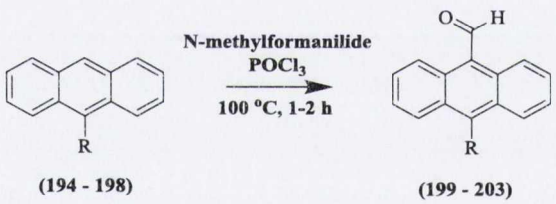

Figure 147: General scheme for the formylation of 9-substituted anthracene by Vilsmeier Haack reaction

As previously mentioned, the first step of this synthesis is to generate the required Vilsmeier-Haack reagent. N-methylformanilide reacts *via* an S_N2 mechanism with phosphorous oxychloride with the formation of an imine and elimination of chloride as a leaving group. The imine then undergoes chlorination and subsequent reformation of the imine bond to eliminate the phosphonoxy group. The two charged ions form a chloroiminium salt that is known as the Vilsmeier-Haack reagent (Figure 148).

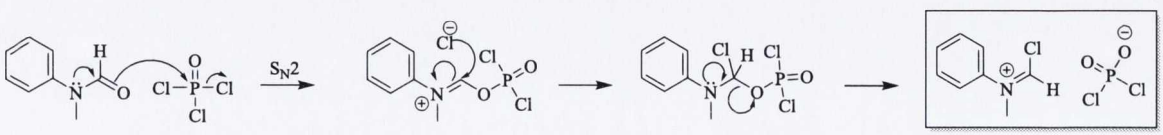

Figure 148: Proposed mechanism for the formation of the Vilsmeier Haack reagent[209]

The Vilsmeier-Haack reagent is a weak electrophile and undergoes nucleophilic attack from the electron rich anthracene ring. The addition product of this nucleophilic attack undergoes aromatisation with the loss of a proton and the imine bond is reformed with the elimination of chlorine as a leaving group. Base catalysed hydrolysis of the imine bond by water takes place and leads to the formation of the carbonyl and elimination of methylaniline as a leaving group (Figure 149).

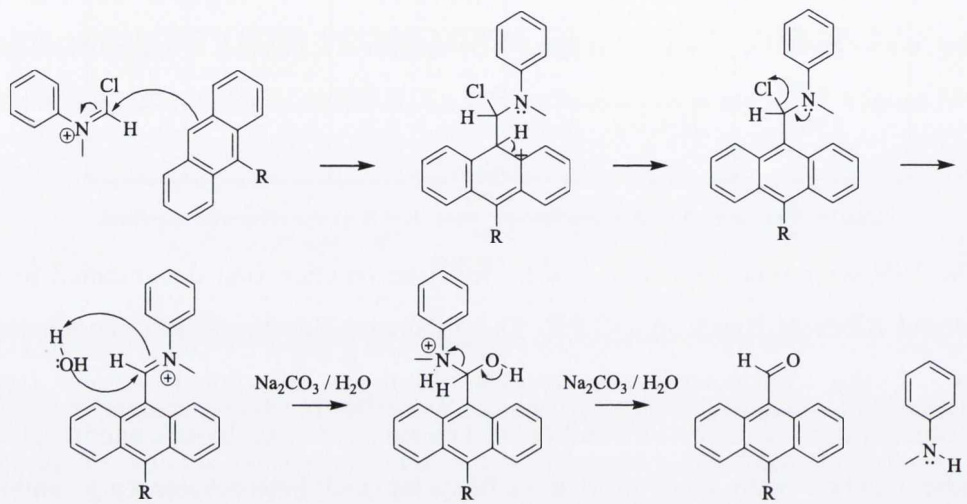

Figure 149: Proposed mechanism for the formylation of 9-substituted anthracene by Vilsmeier Haack reaction[209]

Other formylation systems previously used for the formylation of anthracene derivatives include the substitution of halides using N-methylformanilide / *n*-butyl lithium[335] and nucleophilic attack of the imine intermediate produced by aluminum trichloride / tin (IV) chloride[336]. This Vilsmeier-Haack reaction gave 10-substituted-9-anthraldehydes (**199-203**) in excellent yields of 70-80% (Table 20).

10-Bromoanthracene-9-carbaldehyde (**205**) was prepared via a two-step synthetic route from anthracene. Step one of this route was the 9,10-dibromination of anthracene with bromine in dichloromethane to afford **204**, in a four hour reaction at room temperature[337]. Step two was a lithium-halogen exchange / formylation reaction with *n*-butyllithium and N-methylformanilide in dry THF at -90 °C over 50 minutes[335] (Figure 150).

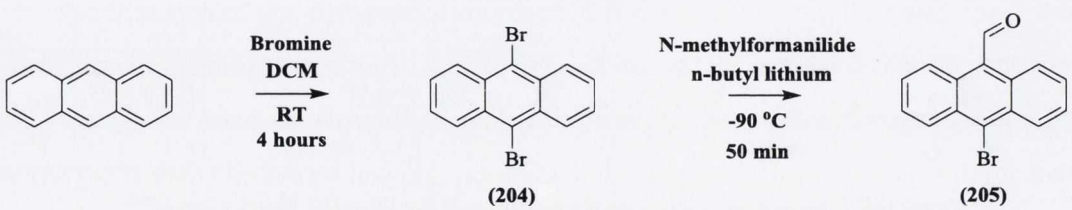

Figure 150: Overall scheme for synthesis of 10-bromoanthracene-9-carbaldehyde

The bromination of anthracene takes place *via* a standard nucleophilic attack on the slightly positive dipole in bromine by the electron rich anthracene. Subsequent re-aromatisation takes place with the loss of a proton. This process is repeated to give the 9,10-dibromoanthracene (**204**) (Figure 151).

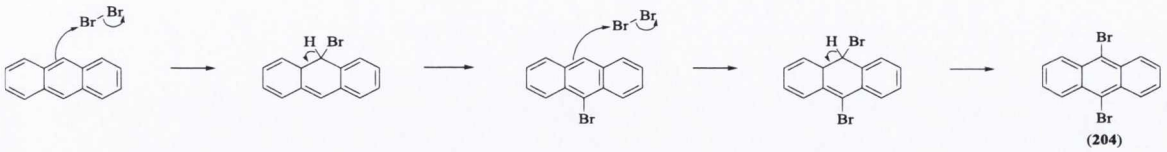

Figure 151: Mechanism for the bromination of anthracene (204)

Lithium-halogen exchange was first noted in 1938 Wittig et al.[338] and it is this property of organolithium compounds that is exploited to achieve selective 9-formylation of anthracene. Georg Wittig proposed that the reaction proceeded via the formation of an 'ate' addition complex[339], although there are also other theories on the mechanism behind the lithium-halogen exchange[340] (Figure 151).

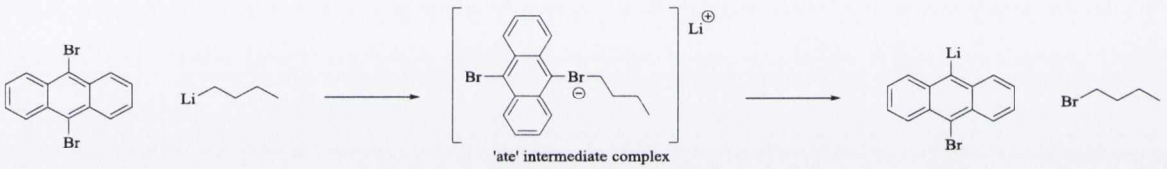

Figure 152: Lithium-halogen exchange via the 'ate' complex

The formylation reaction proceeds after the lithium-halogen exchange reaction, initiated by the nucleophilic attack on the carbonyl of N-methylformanilide. Protonation of the nitrogen of the addition intermediate leads to the reformation of the carbonyl with the elimination of N-methylaniline as a leaving group. This leads to the formation of the desired 9-anthraldehyde (**205**).

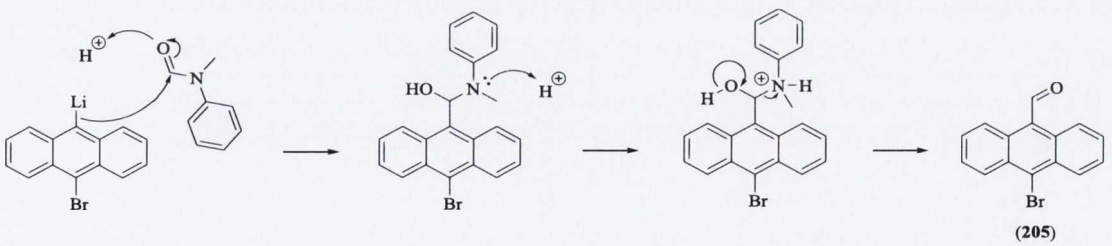

Figure 153: Proposed formylation reaction of organolithium compound

9-Anthraldehyde can also be selectively brominated with N-bromosuccinimide with acetic acid in chloroform[341]. The formylation reaction in the present work afforded a yellow sold yielding 72% 10-bromoanthracene-9-carbaldehyde (**205**) (Table 20).

4,5-Dichloroanthracene-9-carbaldehyde (**207**) was synthesised via a two-step synthetic route. The first step of this route was the reduction of 1,8-dichloroanthracene-9,10-dione to 1,8-dichloroanthracene (**206**) using a zinc dust / ammonia system followed by acidification of the reaction product. Formylation of this 1,8-dichloroanthracene gave the desired 4,5-dichloroanthracene-9-carbaldehyde (Figure 154).

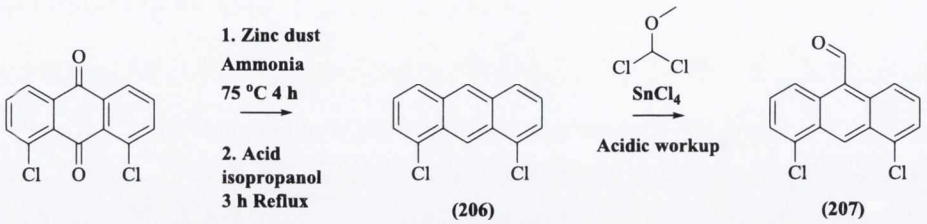

Figure 154: Overall synthesis of 4,5-dichloroanthracene-9-carbaldehyde

The zinc metal reduction of the 1,8-dichloroanthracene-9,10-dione is a two-step reaction in which zinc metal reduction is followed by protonation and aromatisation to form the anthracene ring. Alfred Rieche first documented the Rieche formylation in 1960, achieving formylation with Lewis acid tin (IV) chloride and dichloromethyl methy ether[342]. In more recent literature the Rieche formylation is used for the formylation of phenols[343] and anthracenes[336].

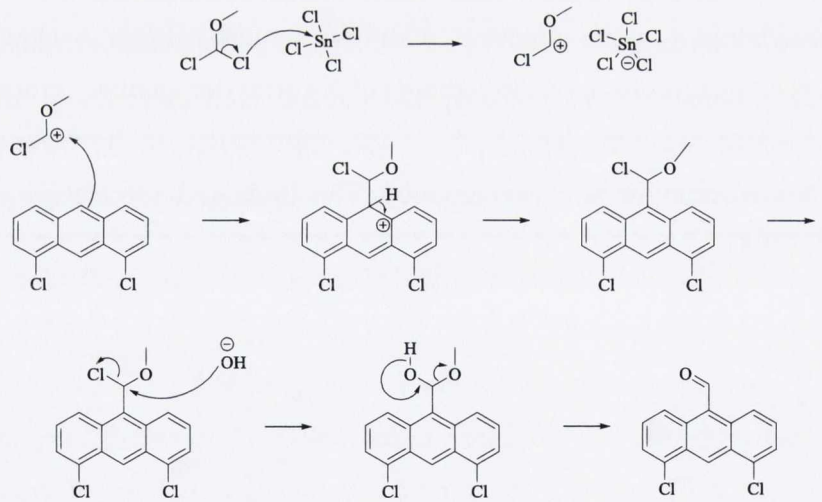

Figure 155: Proposed mechanism for Rieche formylation

The mechanism for the Rieche formylation is believed to follow a Friedel-Crafts type reaction mechanism (Figure 155). The tin (IV) chloride acts as a Lewis acid and reacts with dichloromethyl methyl ether to form a carbocation. This carbocation undergoes nucleophilic attack from the electron rich anthracene ring, leading to the eventual formation of the chloromethoxy intermediate. This intermediate undergoes acid catalysed hydrolysis and

chloride is eliminated as a leaving group. Loss of a proton and elimination of the methoxy group leads to the formation of the 9-anthraldehyde. 4,5-Dichloroanthracene-9-carbaldehyde (**207**) was prepared *via* the method described above affording a yellow solid (30% yield) (Table 20).

2-(Anthracen-9-yl)acetaldehyde (**209**) was synthesised from 9-anthraldehyde. The overall reaction scheme planned involved the Wittig reaction of 9-anthraldehyde, (methoxymethyl)triphenylphosphonium chloride and potassium *tert*-butoxide to form 9-(2-methoxyvinyl)anthracene (**208**) (*E*/*Z* mixture). 2-(Anthracen-9-yl)acetaldehyde (**209**) was synthesised from 9-(2-methoxyvinyl)anthracene (**208**) by cleavage of the enol ether leaving the aldehyde[344].

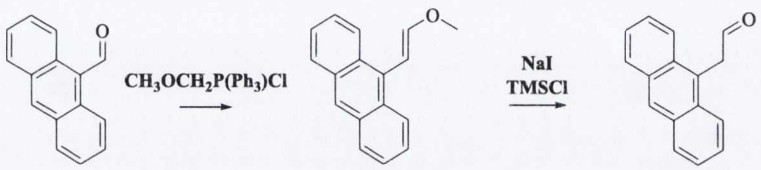

Figure 156: Overall scheme for synthesis of 2-(anthracen-9-yl)acetaldehyde

The mechanism for the Wittig reaction initiates with the deprotonation of the phosphonium salt to form the phosphorous ylide. The ylide and 9-anthraldehyde enter a puckered transition state and undergo [2+2] cycloaddition forming the oxaphosphetane intermediate. This oxaphosphetane intermediate breaks down following the cleavage of the phosphorous oxygen bond with the formation of the vinyl bond (Figure 157)[129, 209].

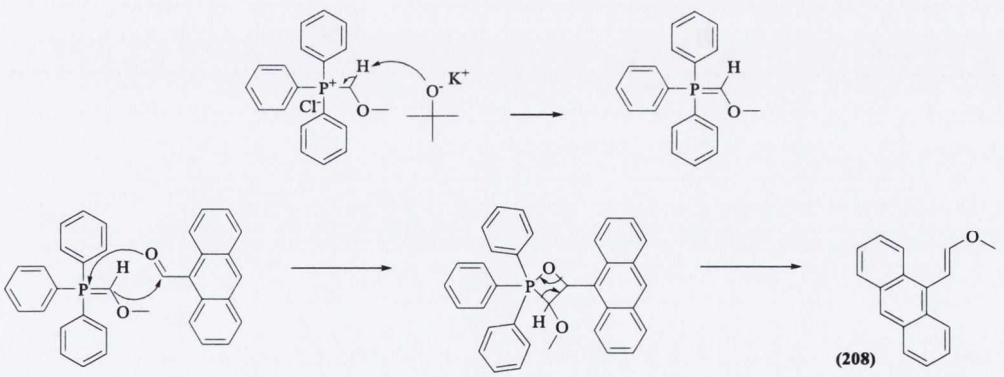

Figure 157: Proposed mechanism for the synthesis of 9-(2-methoxyvinyl)anthracene[129, 209]

Cleavage of the enol ether was achieved using trimethylsilyl chloride and sodium iodide[344]. Trimethylsilyl chloride is a potent electrophile and readily accepts the nucleophilic attack of the methoxy ether. In order to stabilise the resulting charged addition intermediate the

methyl group acts as a leaving group. Enol-keto tautomerization takes place and iodine initiates desilylation with the keto tautomer to give the 2-(anthracen-9-yl)acetaldehyde (**209**) (Figure 158).

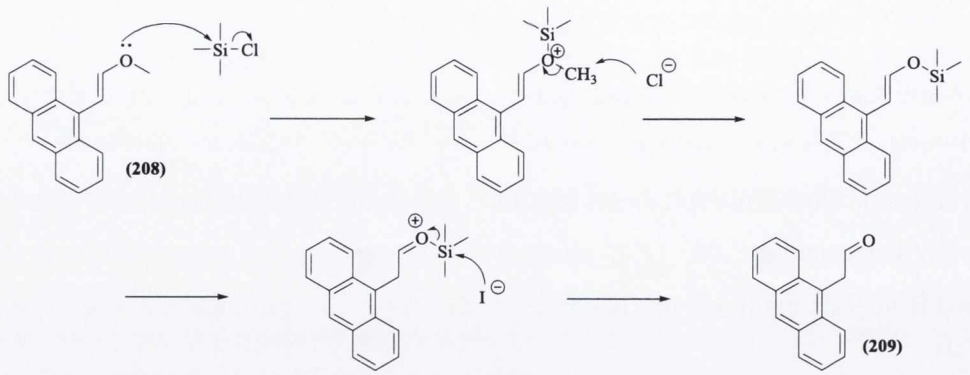

Figure 158: Proposed mechanism for the synthesis of 2-(anthracen-9-yl)acetaldehyde[129]

The above synthetic steps resulted in isolation of 9-(2-methoxyvinyl)anthracene (**208**) (yield 60%) and ultimately yielded 2-(anthracen-9-yl)acetaldehyde (**209**) as a yellow solid (yield 83%) (Table 20).

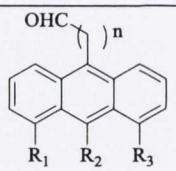

Compound	n	Substitution pattern	Yield	Compound	n	Substitution pattern	Yield
199	0	$R_2 = CH_2CH_3$	80%	**205**	0	$R_2 = Br$	72%
200	0	$R_2 = CH(CH_3)$	60%	**202**	0	$R_2 = OCH_3$	72%
201	0	$R_2 = C_6H_5$	70%*	**203**	0	$R_2 = CH_3$	60%
207	0	$R_1 = R_3 = Cl$,	30%	**209**	1	-	83%

Table 20: substituted-9-anthraldehyde library. Note: R = H unless otherwise specified. * denotes novel compound

4.2 Synthesis of the (*E*)-9-(2-nitrovinyl)anthracenes

A series of diversely substituted (*E*)-9-(2-nitrovinyl)anthracenes were prepared from the substituted-9-anthraldehyde library prepared above and some related aldehydes that were commercially available. A piperidine catalysed Henry-Knoevenagel condensation reaction described by Parker et al. (2008) was utilised to synthesise this extensive library of (*E*)-9-(2-nitrovinyl)anthracenes (**7**, **41**, **210-223**) (Figure 159).

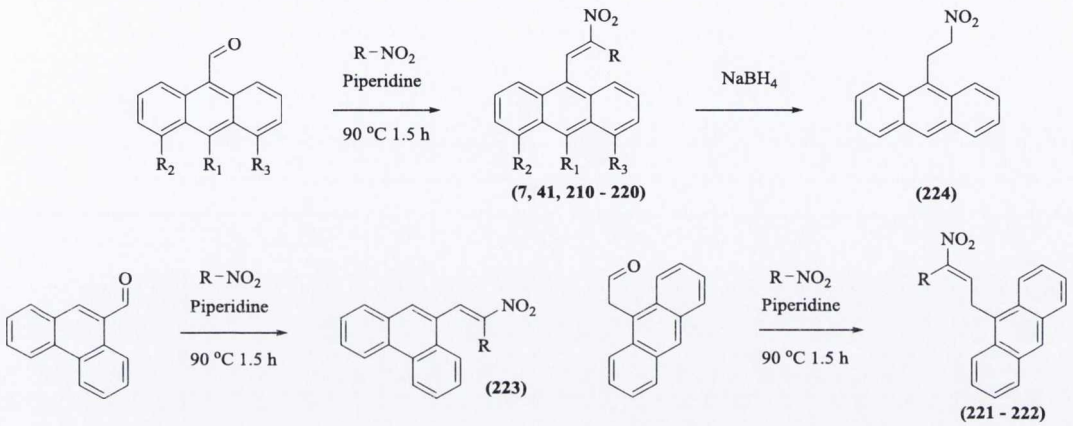

Figure 159: General schemes for the synthesis of the (*E*)-9-(2-nitrovinyl)anthracene library, (*E*)-9-(3-nitroallyl)anthracenes and (*E*)-9-(2-nitrovinyl)phenanthrene

This Parker et al. (2008) (referred to as Method 2) variant of the Henry-Knoevenagel condensation reaction performed much better for the 9-anthraldehydes than the general method used for the (*E*)-(2-nitrovinyl)benzenes (Method 1), increasing the yield of product achieved significantly[345]. Using this method with the 9-anthraldehydes it was possible to achieve the more difficult synthesis of (*E*)-9-(2-nitrobut-1-en-1-yl)anthracene (**210**) from 1-nitropropane with relative ease. The results of this comparison study are displayed below in Table 21.

Compound	Compound name	Yield (Method 1)* Sect. 8.1	Yield (Method 2)** Sect. 8.21
7	(*E*)-9-(2-nitrovinyl)anthracene	25%	99%
41	(*E*)-9-(2-nitroprop-1-en-1-yl)anthracene	10%	73%
210	(*E*)-9-(2-nitrobut-1-en-1-yl)anthracene	Trace	60%

Table 21: Comparison of Henry-Knoevenagel condensation yields for 9-anthraldehyde (Method 1 v Method 2). *cyclohexylamine, acetic acid, 20 min MW, ** Piperidine acetate, excess nitroalkane 1.5 h 90 °C

A series of diversely substituted (*E*)-9-(2-nitrovinyl)anthracenes (**7**, **41**, **210-222**) were prepared affording yields of 10-99% (Table 22). These (*E*)-9-(2-nitrovinyl)anthracenes included a range of C-9 and C-10 substitutions ranging from halogen to alkyl and aryl. The length of the alkyl chain at C-1' was also varied. (*E*)-9-(2-Nitrovinyl)phenanthrene (**223**) was synthesised by the Henry-Knoevenagel condensation of 9-phenanthraldehyde and nitromethane in 15% yield[346]

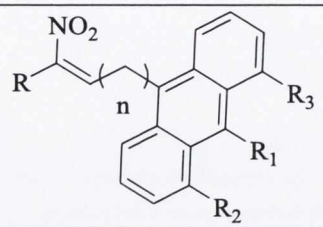

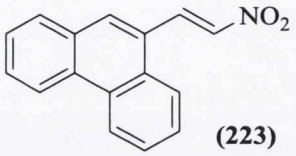

(223)

Compound	n	R	Substitution	Yield
7	0	-	-	99%
41	0	CH_3	-	73%
210	0	CH_2CH_3	-	60%
211	0	-	$R_1 = Cl$	71%*
212	0	CH_3	$R_1 = Cl$	50%*
213	0	CH_2CH_3	$R_1 = Cl$	64%*
214	0	-	$R_1 = OCH_3$	54%
215	0	-	$R_1 = Br$	56%*
216	0	-	$R_1 = CH_3$	30%*
217	0	-	$R_1 = C_6H_5$	60%*
218	0	-	$R_2 = R_3 = Cl$,	10%*
219	0	-	$R_1 = CH_2CH_3$	60%*
220	0	-	$R_1 = CH(CH_3)$	68%*
221	1	-	-	32%*
222	1	CH_3	-	20%*
223	0	-	-	15%

Table 22: (*E*)-9-(2-nitrovinyl)anthracene library. Note: R = H unless otherwise specified. * denotes novel compound

The novel (*E*)-9-chloro-10-(2-nitrobut-1-en-1-yl)anthracene (**213**) was chosen as a representative sample of the (*E*)-9-(2-nitrovinyl)anthracenes and the ^{1}H NMR and ^{13}C NMR spectra will now be discussed in detail. The ^{1}H NMR (400 MHz, $CDCl_3$) spectrum of compound **213** (Figure 160) shows a triplet at 0.90 ppm (J = 7.32 Hz) integrating for three protons, this triplet was assigned to the three methyl protons on $C_{4'}$.

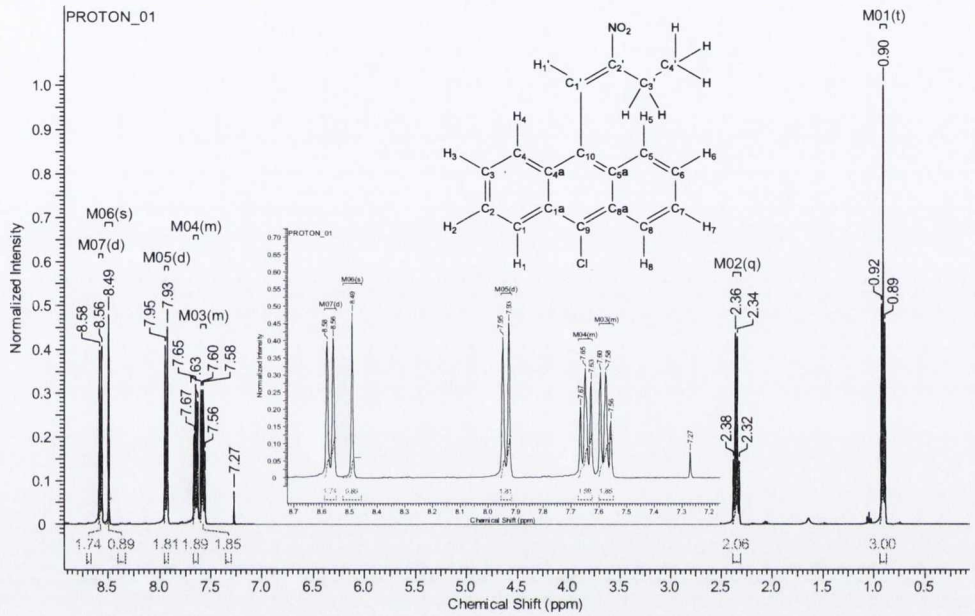

Figure 160: ^{1}H NMR spectrum of (*E*)-9-chloro-10-(2-nitrobut-1-en-1-yl)anthracene (213)

A quartet at 2.35 ppm (J = 7.32 Hz) integrating for two protons accounted for the two protons on $C_{3'}$. The doublets at 7.94 ppm (J = 8.55 Hz) and 8.57 ppm (J = 8.55 Hz) both integrating for two protons each were assigned to the equivalent proton pairs of H_4 & H_6 and H_1 & H_8 respectively. The doublet occurring at 8.57 ppm occurring slightly further downfield due to proximity to the chlorine substituent at C_9. The large multiplet occurring at 7.52 - 7.70 ppm integrating for four protons account for the remaining aryl protons (H_2, H_3, H_6 & H_7). The downfield singlet occurring at 8.49 ppm integrating for a single proton corresponded to $H_{1'}$, the proton on $C_{1'}$ of the nitrovinyl unit.

The ^{13}C NMR spectrum (101 MHz, $CDCl_3$) of compound **213** (Figure 161) shows resonances occurring at 11.54 ppm and 21.35 ppm, these were assigned to the carbons in the ethyl sidechain, $C_{4'}$ and $C_{3'}$ respectively. Carbon equivalent quaternary resonances at 125.42 ppm and 128.39 ppm were assigned to the quaternary carbons within the anthracene ring at C_{4a} & C_{5a} and C_{1a} & C_{8a}.

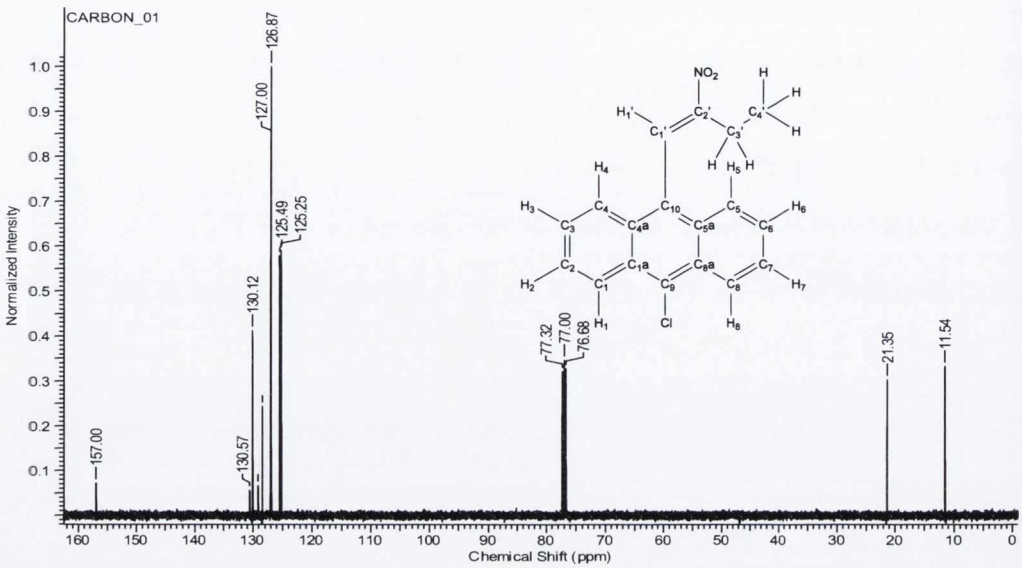

Figure 161: ^{13}C NMR spectrum of (*E*)-9-chloro-10-(2-nitrobut-1-en-1-yl)anthracene (213)

Carbon equivalent CH resonances at 126.87 ppm and 127.00 ppm correspond to C_4 & C_6 and C_1 & C_8. The quaternary signals occurring at 129.11 ppm and 130.57 ppm were assigned to C_{10} and C_9 respectively. The signal at 130.57 ppm occurring further downfield due to the electronegativity of the chlorine substitution. The downfield CH resonance (Figure 162) in the spectrum occurred at 130.12 ppm and was allocated to $C_{1'}$ of the nitrovinyl unit. The most downfield signal in the spectrum was a quaternary signal occurring at 157.00 ppm and was produced by the electronegative environment created at $C_{2'}$ by the nitro group. The remaining aromatic carbons were accounted for by carbon equivalent CH resonances 125.25 ppm and 125.49 ppm.

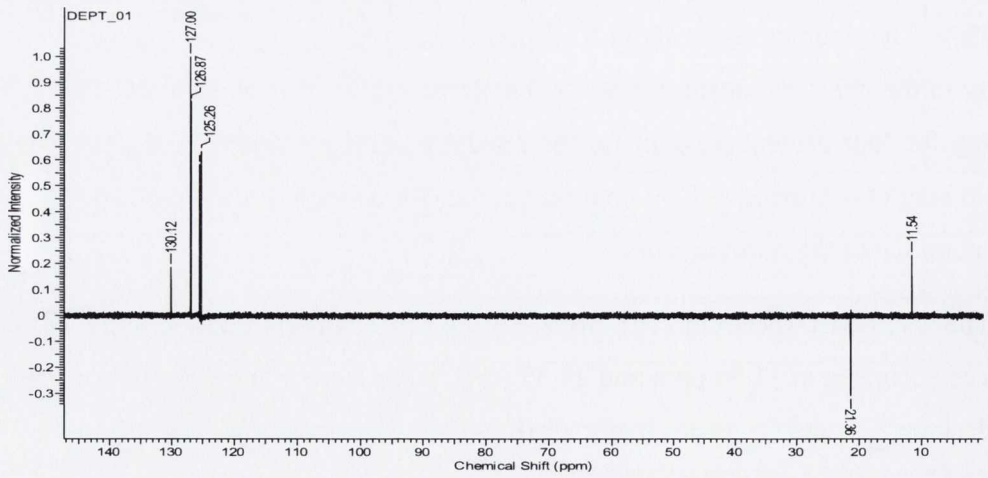

Figure 162: DEPT 135 NMR spectrum of (*E*)-9-chloro-10-(2-nitrobut-1-en-1-yl)anthracene (213)

FTIR spectroscopy shows bands at 1438, 1425 (C=C), 1553, 1328 (NO_2) and 1149 (C-N) cm^{-1}. High resolution mass spectrometry (APCI) was carried out and the required molecular ion was calculated to be $C_{18}H_{15}ClNO_2$ $[M^+ + H]$ 312.0791 and found as 312.0797.

A sample of (*E*)-9-chloro-10-(2-nitroprop-1-en-1-yl)anthracene (**212**) was selected for X-ray structure determination; from the packing structure and asymmetric unit it was possible to verify the (*E*) confirmation of the nitrovinyl unit (Figure 163).

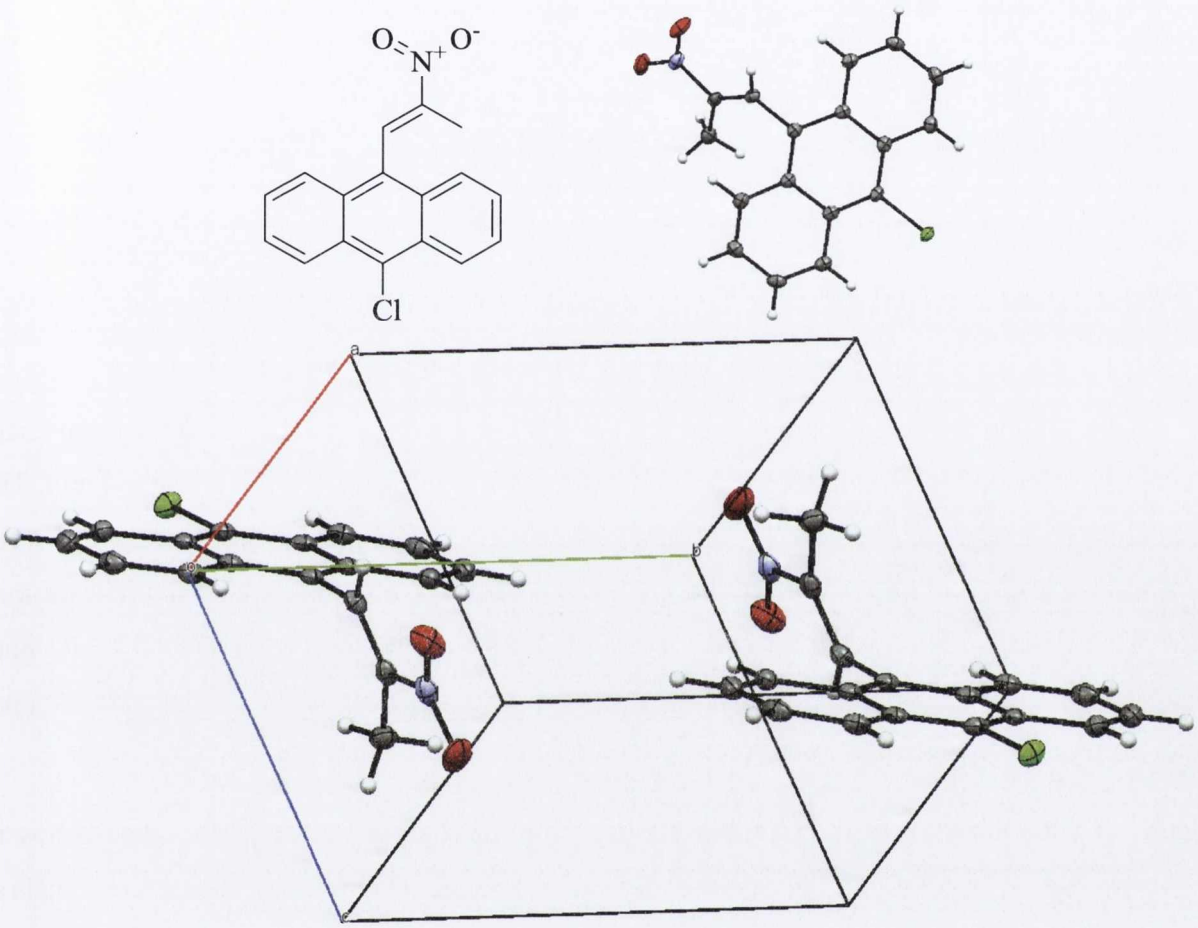

Figure 163: X-ray crystallography data: Asymmetric unit of (*E*)-9-chloro-10-(2-nitroprop-1-en-1-yl)anthracene (212)

(*E*)-9-(3-Nitroallyl)anthracene (**221**) was chosen as a representative sample of the (*E*)-9-(3-nitroallyl)anthracenes and the ^1H NMR and ^{13}C NMR spectra will now be discussed in detail. The ^1H NMR (400 MHz, $CDCl_3$) spectrum of compound **221** (Figure 164) shows a doublet occurring at 4.58 ppm (J = 6.10 Hz) integrating for two protons, this was assigned to the two protons on $C_{1'}$.

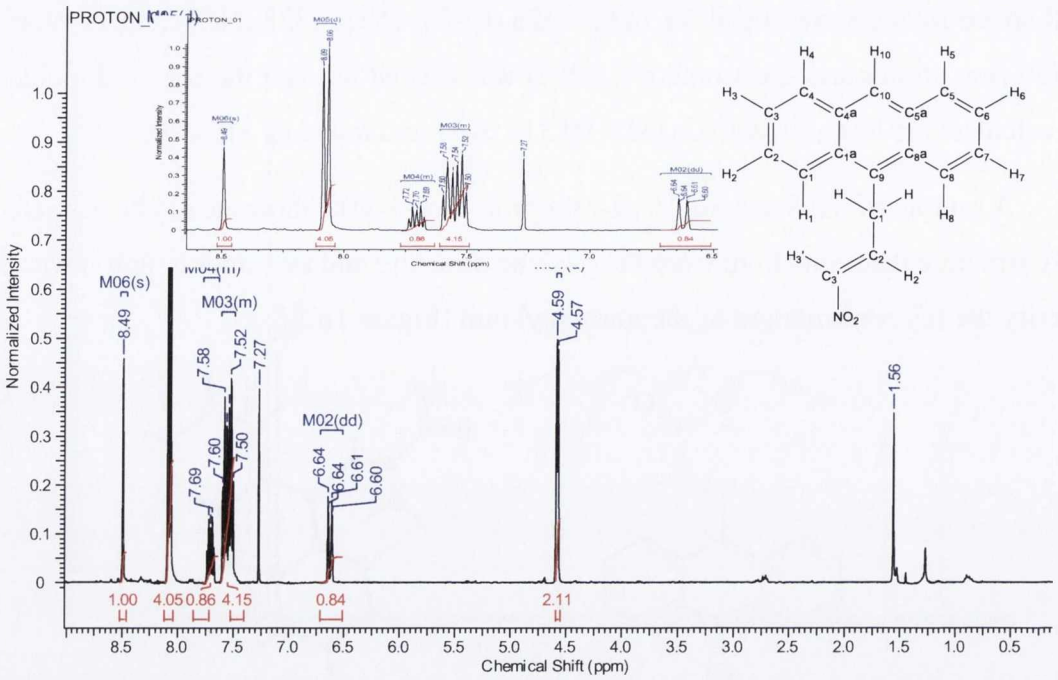

Figure 164: ^{1}H NMR spectrum of (*E*)-9-(3-nitroallyl)anthracene (221)

The double doublet at 6.62 ppm (J = 13.43, 1.83 Hz) was assigned to $H_{3'}$ on the nitrovinyl unit, the large J value in this double doublet indicated *trans* coupling across the nitrovinyl unit. The doublet at 8.07 ppm (J = 8.55 Hz) integrated for four aromatic protons and accounted for H_1, H_8, H_4 and H_5. The large multiplet occurring at 7.49 - 7.61 ppm integrating for four protons was assigned to the remaining aromatic protons. The multiplet occurring at 7.66 - 7.77 ppm integrating for a single proton was allocated to $H_{2'}$. The downfield singlet at 8.49 ppm accounted for H_{10} on the anthracene ring.

The ^{13}C NMR (101 MHz, $CDCl_3$) spectrum of compound **221** is displayed below in Figure 165. A DEPT 135 NMR spectrum of compound **221** (Figure 166) shows CH signals at 123.31 ppm, 125.20 ppm, 126.77 ppm, 127.83 ppm, 129.53 ppm, 140.74 ppm and 141.13 ppm. The inverted resonance at 27.02 ppm denoted a CH_2 carbon signal. A C-H COSY experiment was also completed in order to accurately assign the carbon resonances of the ^{13}C spectrum (Figure 167).

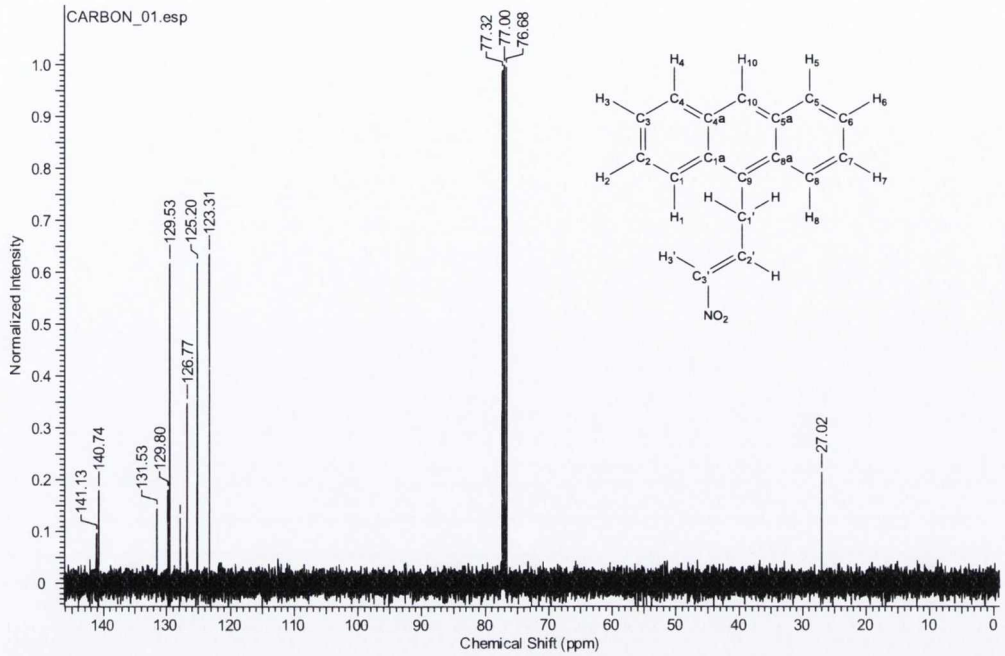

Figure 165: ^{13}C NMR spectrum of (*E*)-9-(3-nitroallyl)anthracene (221)

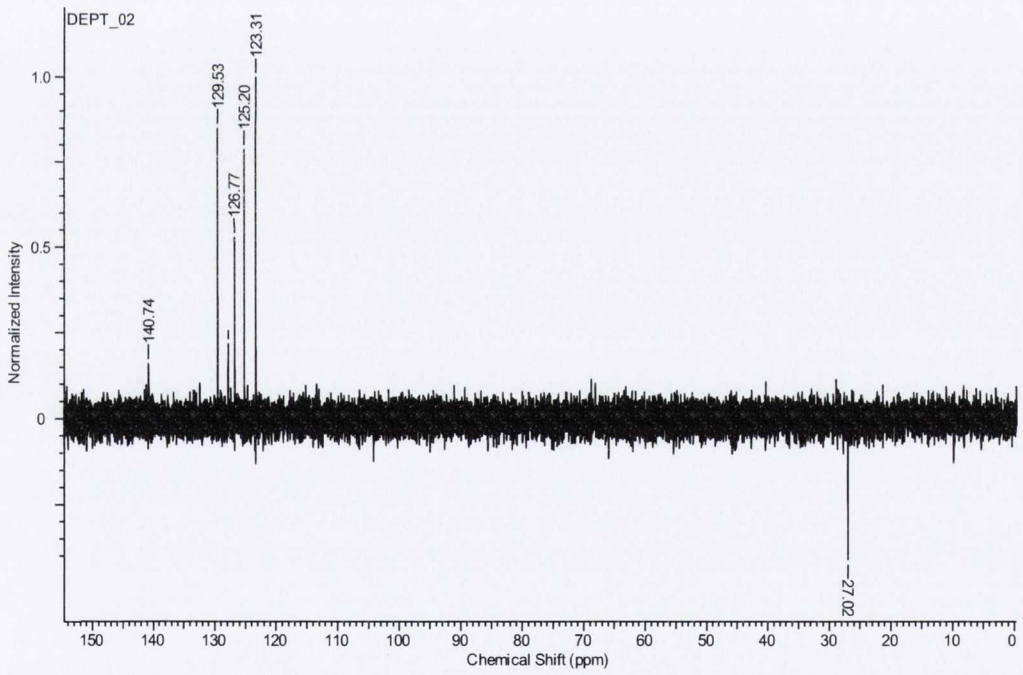

Figure 166: DEPT 135 NMR spectrum of (*E*)-9-(3-nitroallyl)anthracene (221)

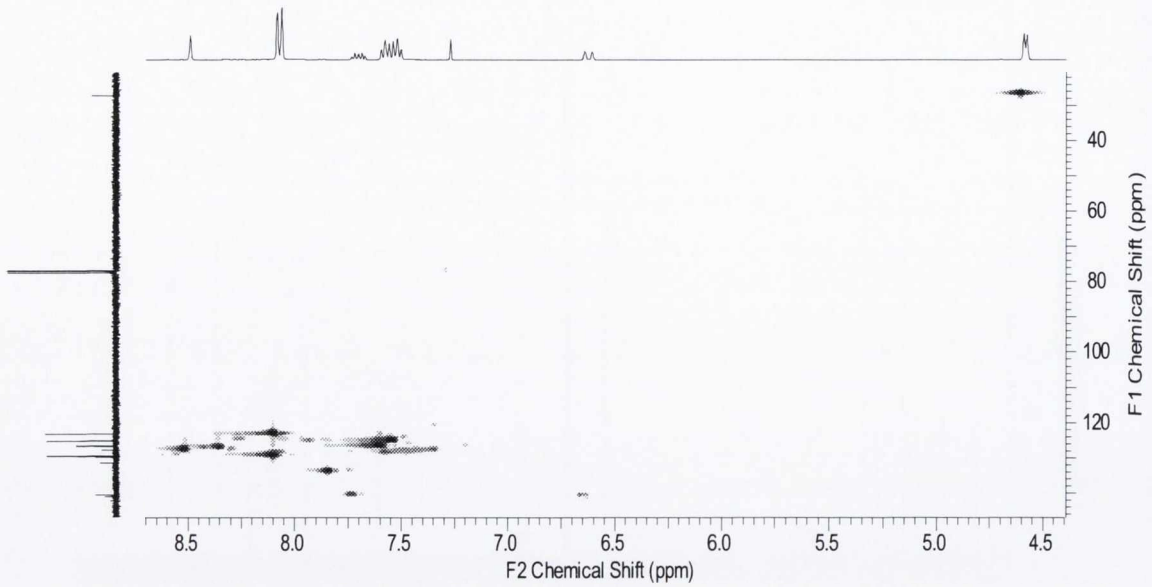

Figure 167: C-H COSY spectrum of (*E*)-9-(3-nitroallyl)anthracene (221)

Combining data obtained (Figure 166-168) it was possible to assign the carbon resonances corresponding to the nitrovinyl unit. The inverted CH_2 resonance at 27.02 ppm was assigned to $C_{1'}$. CH resonances occurring at 140.74 ppm and 141.13 ppm correlated to the multiplet at 7.66 - 7.77 ppm and the double doublet at 6.62 ppm. From the multiplicity produced it was possible to assign the resonances at 140.74 ppm and 141.13 ppm to $C_{2'}$ and $C_{3'}$ on the nitrovinyl unit. Quaternary signals observed at 129.80 ppm and 131.53 ppm were allocated to the two carbon equivalent pairs of C_{4a} & C_{5a} and C_{1a} & C_{8a} within the anthracene system. The proton H_{10} correlated to a carbon 13 resonance at 127.83 ppm. The remaining aromatic CH carbon resonances were accounted for by signals at 123.31 ppm, 125.20 ppm, 126.77 ppm, and 129.53 ppm

FTIR spectroscopy shows bands at 3089, 2928 (C-H), 1667 (C=C), 1551, 1356 (NO_2) and 1514, 1444 (C=C) cm^{-1}. High resolution mass spectrometry (APCI) was carried out and the required molecular ion was calculated to be $C_{17}H_{14}NO_2$ [M^++H] 264.1025 and found as 264.1023.

4.3 Synthesis of 4-(anthracen-9-yl)-1*H*-1,2,3-triazoles

A small selection of anthracene based 4-(anthracen-9-yl)-1*H*-1,2,3-triazoles were also synthesised. These compounds were prepared according to the general procedure and *via* the mechanism previously outlined in Chapter 2. The general scheme for the synthesis of this selection of compounds is outlined below in Figure 168.

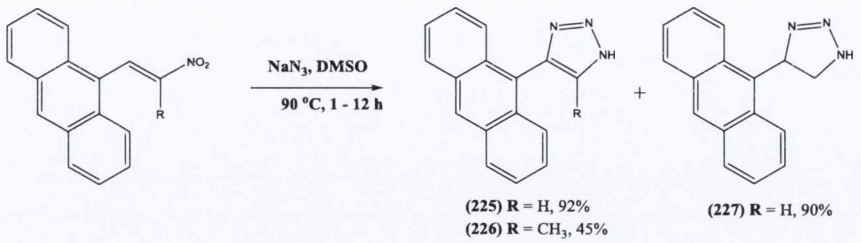

Figure 168: General scheme for the synthesis of 4-(anthracen-9-yl)-1H-1,2,3-triazoles

The synthesis of 4-(anthracen-9-yl)-1*H*-1,2,3-triazoles (**225 -226**) was achieved in good yield by reaction with sodium azide for 1 hour at 90 °C. However during attempts to optimise this reaction another reaction product was isolated. This unexpected product was 4-(anthracen-9-yl)-4,5-dihydro-1*H*-1,2,3-triazole (**227**), a reduced version of the desired end product. It is proposed that increasing the time from 1 to 12 hour allows time for a much slower reduction reaction to take place in the presence of DMSO and sodium azide. Referring to the literature, reductive conditions in hot DMSO and sodium azide solutions have been observed before, it is assumed the sodium metal necessary for triazole reduction is provided by the azide salt[347].

The 4-(anthracen-9-yl)-1*H*-1,2,3-triazoles have been synthesised by an alternative method from 9-ethynly-anthracene, $TMSN_3$ and copper iodide with good yield. Daniele et al. coupled this anthracene-triazole system to various ligands for development as a fluorophore[348]. In the present work the anthracene-triazole compounds (**225-227**) was prepared with yields of 45-95% (Figure 168).

4-(Anthracen-9-yl)-4,5-dihydro-1*H*-1,2,3-triazole (**227**) was chosen as a representative sample of the anthracene-triazoles and the ^1H NMR and ^{13}C NMR spectra will now be discussed in detail. The ^1H NMR (400 MHz, DMSO-d_6) spectrum of compound **227** (Figure 169) shows a doublet at 4.64 ppm (J = 4.88 Hz) with an integration of two protons, this was allocated to the 2 protons on $C_{5'}$.

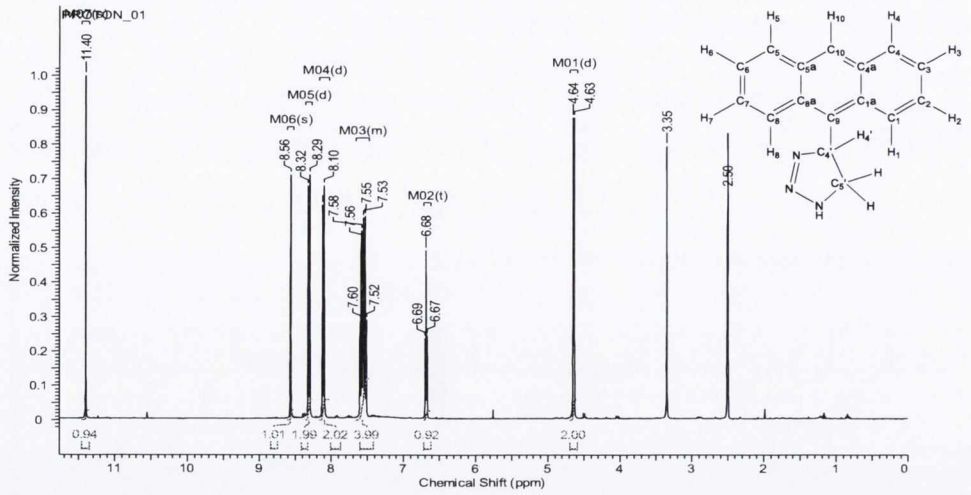

Figure 169: ^{1}H NMR spectrum of 4-(anthracen-9-yl)-4,5-dihydro-1*H*-1,2,3-triazole (227)

The triplet occurring at 6.68 ppm (J = 5.19 Hz) integrated for a single proton and was assigned to the H_4', split by the pair of protons on C_5. The doublets at 8.11 ppm (J = 8.55 Hz) and 8.31 ppm (J = 9.16 Hz) both integrated for two protons each and were assigned to the two pairs of equivalent protons, H_5 & H_4 and H_1 & H_6 respectively. A singlet at 8.56 ppm integrating for a single proton was allocated to H_{10}.The multiplet occurring at 7.45 - 7.70 ppm integrated for four aromatic protons and accounted for the remaining four anthracene protons (H_6, H_7, H_2 & H_3). The downfield singlet 11.40 ppm with an integral value of one proton corresponded to the NH at position 1 of the triazole ring.

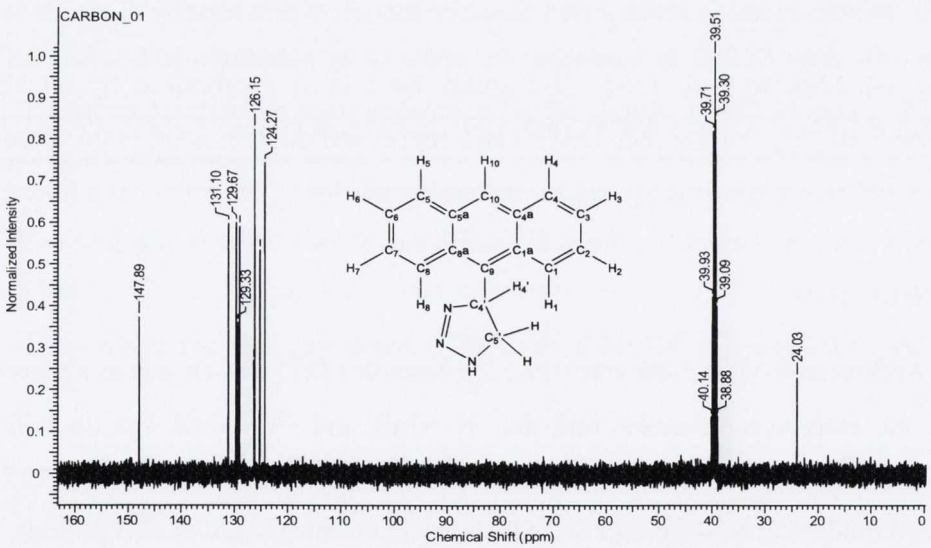

Figure 170: ^{13}C NMR spectrum of 4-(anthracen-9-yl)-4,5-dihydro-1*H*-1,2,3-triazole (227)

The ^{13}C NMR spectrum (101 MHz, DMSO-d_6) of compound **227** (Figure 170), the upfield resonance occurring at 24.03 ppm was assigned to the CH_2 carbon, C_5'. The CH signals at 126.33 ppm and 129.01 ppm were assigned to equivalent carbons C_1 & C_6 and C_{10} on the

anthracene ring The quaternary signals 129.33 ppm and 129.67 ppm account for the carbon equivalent signals within the anthracene ring, C_{5a} & C_{4a} and C_{8a} & C_{1a} respectively. The more downfield quaternary signals were allocated to C_9 and $C_{4'}$. The remaining pairs of equivalent aromatic anthracene CH's were accounted for by signals at 124.27 ppm, 125.19 ppm and 126.15 ppm.

FTIR spectroscopy shows bands at 1614, 1488 (C=C) and 1220 (C-N) cm^{-1}. High resolution mass spectrometry (APCI) was carried out and the required molecular ion was calculated to be $C_{16}H_{13}N_3$ [M^+] 247.1109 and found as 247.1118.

4.4 Preparation of anthracen-9-ylmethanimines

A number of anthracen-9-ylmethanimines (**228-232**) were also prepared to assess the antiproliferative effect of alternative imine systems to replace the nitrostyrene. In this work anthracen-9-ylmethanimines were synthesised from substituted-9-anthraldehydes in a one pot reaction with the required amine in dichloromethane. The reaction mechanism for this preparation was discussed earlier in Chapter 2. The general scheme for the synthesis of anthracen-9-ylmethanimines is displayed below (Figure 171) in yields of 85-90% (Table 23).

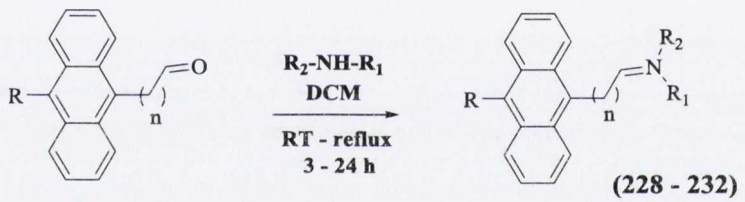

Figure 171: General scheme for the synthesis of anthracen-9-ylmethanimine

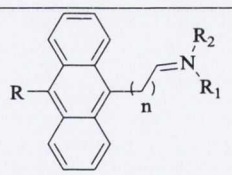

Compound	R	R_1	R_2	n	Yield	Compound	R	R_1	R_2	n	Yield
228	H	NH_2	-	0	90%	**231**	H	O	CH_3	0	89%
229	Cl	NH_2	-	0	85%*	**232**	H	OH	-	1	20%
230	H	OH	-	0	90%	-	-	-	-	-	-

Table 23: anthracen-9-ylmethanimine library

The ^{1}H NMR (400 MHz, DMSO-d_6) spectrum of compound **229** (Figure 172) shows a singlet at 7.30 ppm integrating for two protons, corresponding to the two amine group protons of the hydrazone.

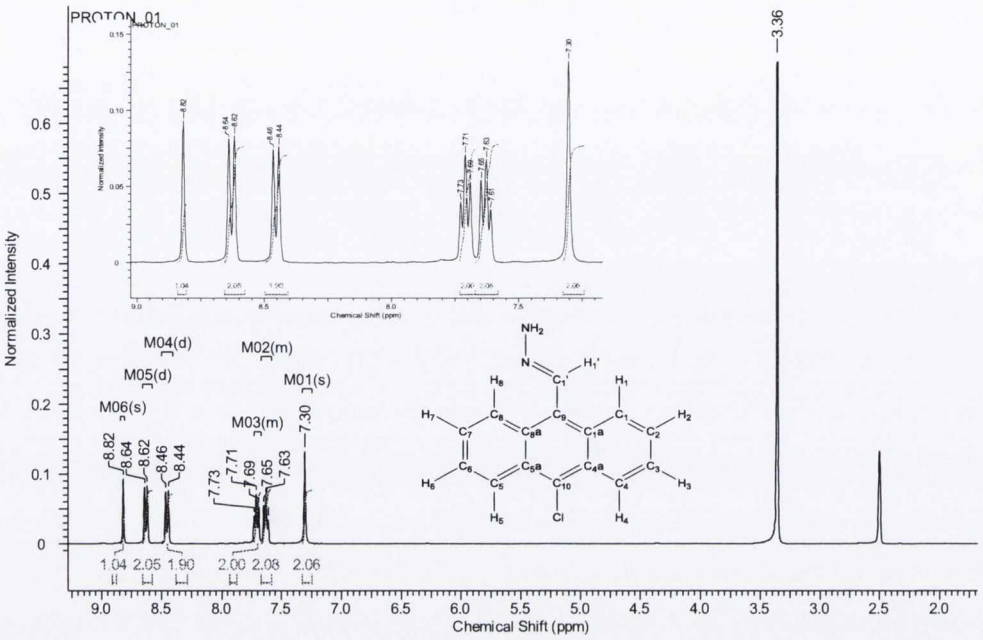

Figure 172: ^{1}H NMR spectrum of (*E*)-((10-chloroanthracen-9-yl)methylene)hydrazine (229)

The doublets at 8.45 ppm (J = 8.55 Hz) and 8.63 ppm (J = 8.55 Hz) both integrated for two protons each and were allocated to H_1 & H_8 and H_4 & H_5. The resonance at 8.63 ppm occurring slightly further downfield was due to proximity to the chlorine atom. The multiplets occurring at 7.58 - 7.67 ppm and 7.67 - 7.73 ppm both integrated for two protons each and were assigned to the remaining aromatic protons (H_2, H_3, H_6 & H_7). The downfield singlet occurring at 8.82 ppm with an integral value of 1 H was assigned to $H_{1'}$ of the imine bond.

The ^{13}C NMR spectrum (101 MHz, DMSO-d_6) of compound **229** (Figure 173) shows CH resonances at 126.27 ppm and 127.39 ppm corresponding to the carbon equivalent signals C_1 & C_8 and C_4 & C_5. Quaternary signals occurring at 127.95 ppm and 128.67 ppm account for the pairs of equivalent quaternary carbons within the anthracene ring (C_{1a} & C_{8a} and C_{5a} & C_{4a}).

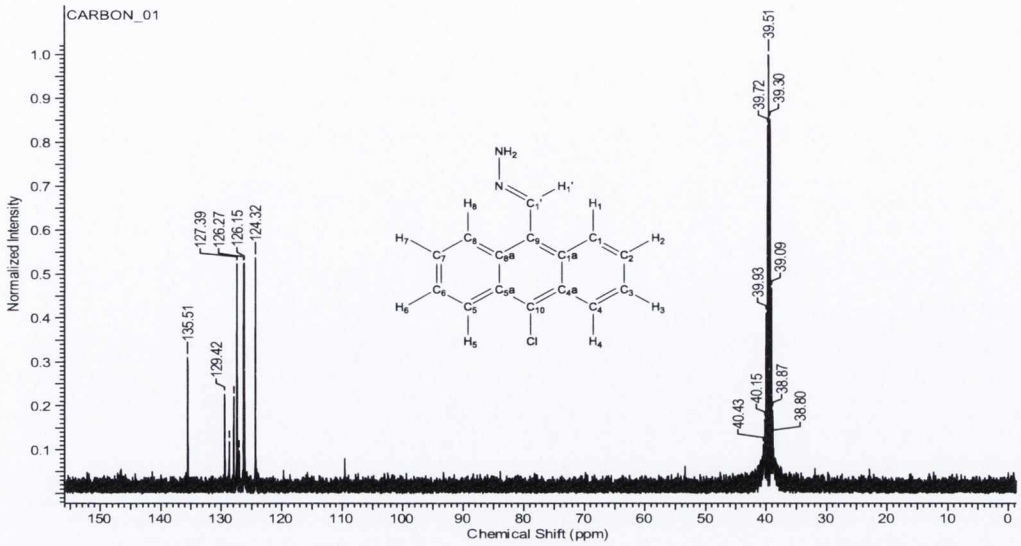

Figure 173: ^{13}C NMR spectrum of (E)-((10-chloroanthracen-9-yl)methylene)hydrazine (229)

The quaternary resonances at 127.04 ppm and 129.42 ppm were allocated to C_9 and C_{10}, with the 129.42 ppm resonance occurring further downfield due to the attached chlorine atom. The remaining equivalent aromatic CHs (C_2, C_3, C_6 & C_7) are accounted for by 124.32 ppm and 126.15 ppm. The downfield CH resonance occurring at 135.51 ppm was assigned to $C_{1'}$ on the imine unit. FTIR spectrometry shows bands at 3351 (N-H), 1621 (C=C) and 1483, 1438 (C=C) cm^{-1}. High resolution mass spectrometry (APCI) was carried out and the required molecular ion was calculated to be $C_{15}H_{12}N_2Cl$ $[M^+ + H]$ 255.0689 and found as 255.0684.

4.5 Synthesis of (*E*)-3-(anthracen-9-yl)acrylonitrile derivatives

(*E*)-3-(Anthracen-9-yl)acrylonitrile derivatives (**233-235**) were synthesised from the 9-anthraldehydes and activated methylenecyano compounds *via* the base catalysed Knoevenagel condensation reaction. The general scheme for this transformation is displayed below (Figure 174).

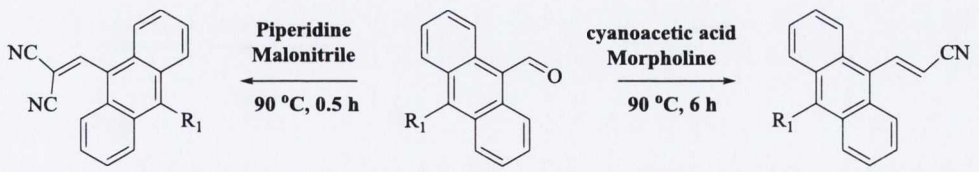

(233) R_1 = H, 95%
(234) R_1 = Cl, 90%

(235) R_1 = H, 40%

Figure 174: General scheme for the synthesis of the (*E*)-3-(anthracen-9-yl)acrylonitriles

Using cyanoacetic acid for the Knoevenagel condensation reaction allowed the formation of the unsubstituted cyanovinyl system. The reaction mechanism is very similar to the one

discussed previously apart from the deprotonation of the acid carbonyl and subsequent elimination as carbon dioxide (Figure 175).

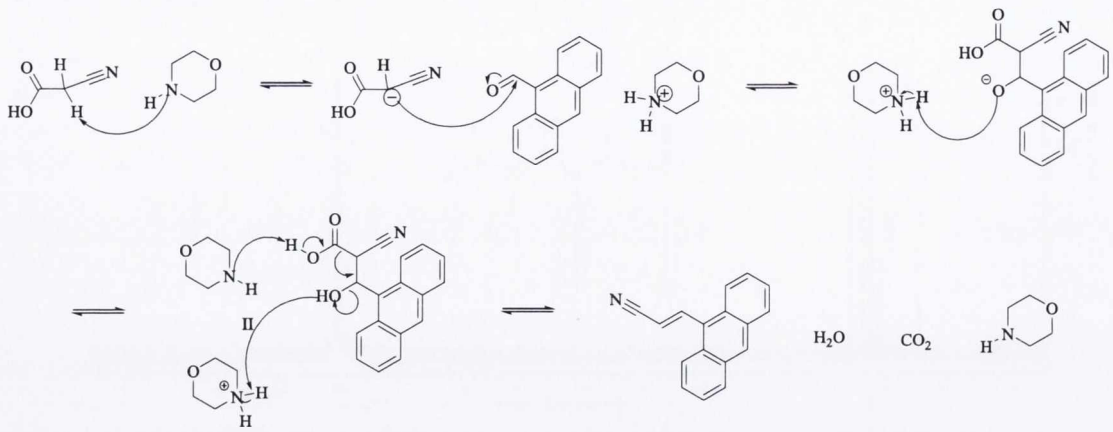

Figure 175: Mechanism for the synthesis of the (*E*)-3-(anthracen-9-yl)acrylonitrile

The synthesis of (*E*)-3-(anthracen-9-yl)acrylonitrile was first noted in 1974 by Hann et al. *via* a base catalysed Knoevenagel condensation using DMF as a solvent[349]. Gopal et al. (1995) synthesised this product from the addition of the stabilised phosphoryl carbanion formed by reacting dimethylphosphonoacetonitrile and sodium hydride in DMF with 9-anthraldehyde[350] The preparation of (anthracen-9-ylmethylene)malononitrile was first documented in 1991 by Katritzky et al. and since it has been synthesised using a number of different bases to catalyse the Knoevenagel condensation reaction[351]. Bases employed include: triethyl amine[352], sodium ethanolate[353] and piperidine[351]. These Knoevenagel condensations were successful with the (anthracen-9-ylmethylene)malononitriles yielding 90-95% and the synthesis of (*E*)-3-(anthracen-9-yl)acrylonitrile was achieved with a 40% yield (Figure 174).

The ^{1}H NMR (400 MHz, $CDCl_3$) spectrum of compound **234** (Figure 176) shows two multiplets at 7.89 - 7.98 ppm and 8.61 - 8.73 ppm both integrating for two protons each, these were assigned to H_6 & H_1 and H_5 & H_4 respectively. The multiplet at 8.61 - 8.73 ppm occurring slightly more downfield due to proximity to the chlorine atom. The multiplet occurring at 7.68 - 7.75 ppm integrated for four protons and this accounted for the remaining aromatic anthracene protons: H_2, H_3, H_6 and H_7. The downfield singlet at 8.91 ppm integrating for a single proton was assigned to $H_{1'}$ on the cyanovinyl unit.

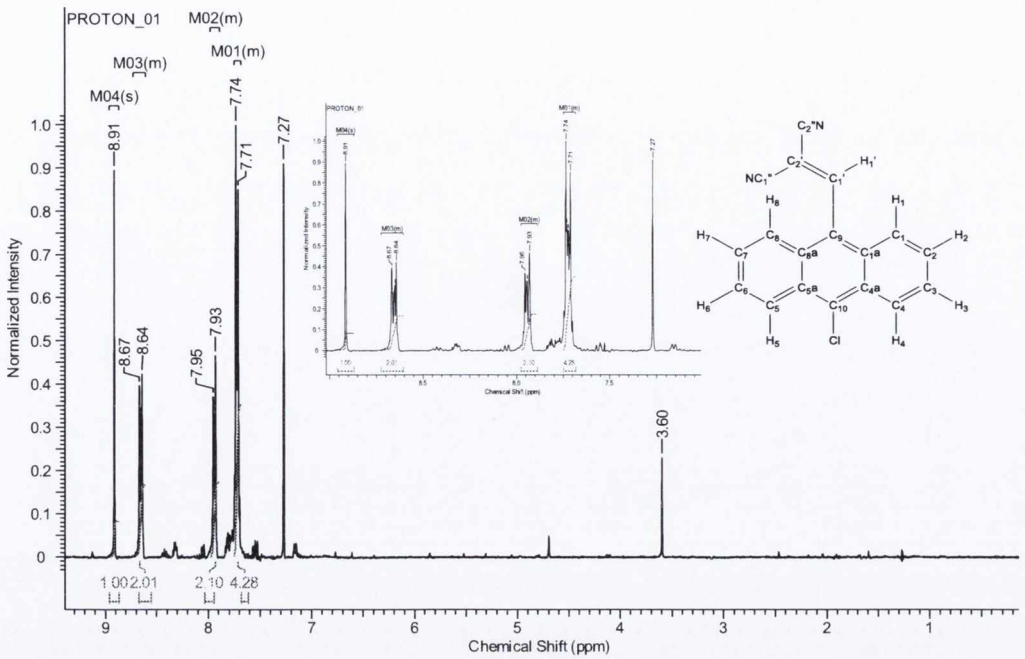

Figure 176: ^{1}H NMR spectrum of 2-((10-chloroanthracen-9-yl)methylene)malononitrile (234)

The ^{13}C NMR spectrum (101 MHz, $CDCl_3$) of compound **234** (Figure 177) shows quaternary resonances occurring at 93.37 ppm, 111.07 ppm and 112.67 ppm; these were assigned to the carbon in the cyanovinyl unit: $C_{2'}$, $C_{1''}$ and $C_{2''}$. The cyano group bearing $C_{2''}$ was *trans* orientated to the anthracene ring allowing a slightly more electronegative influence on this carbon.

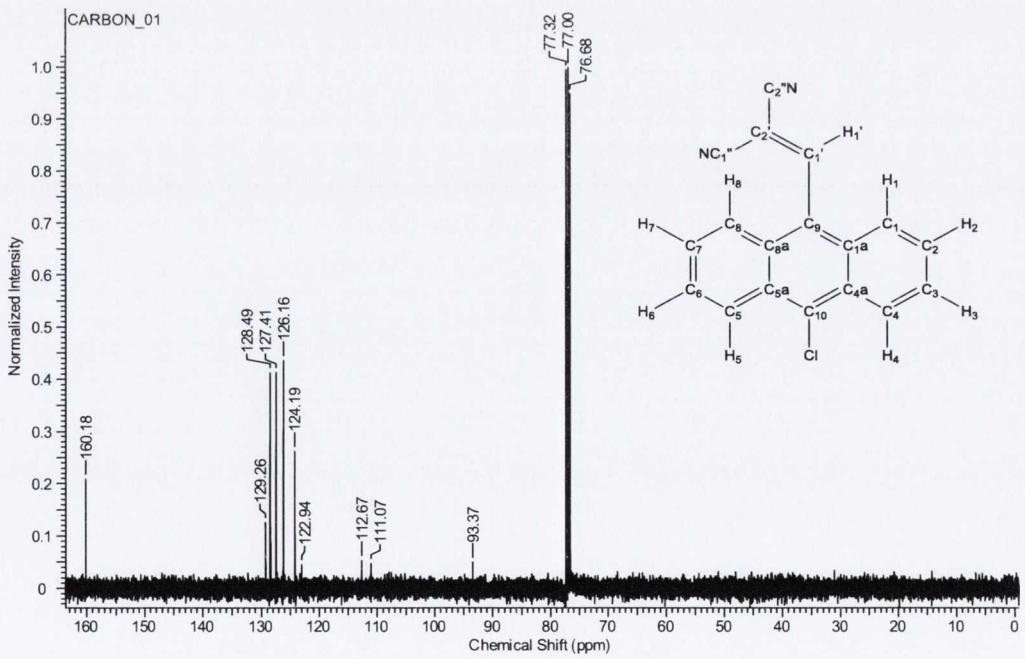

Figure 177: ^{13}C NMR spectrum of 2-((10-chloroanthracen-9-yl)methylene)malononitrile (234)

The quaternary signals at 122.94 ppm and 127.24 ppm accounted for the two pairs of equivalent quaternary carbons within the anthracene ring: C_8a & C_{1a} and C_{5a} & C_{4a}. The CH signals at 127.41 ppm and 128.49 ppm were allocated to the carbon equivalent proton bearing carbons at C_8 & C_1 and C_4 & C_5. The most downfield quaternary carbon resonances in the aromatic region were 128.39 ppm and 129.26 ppm, these signals accounted for C_9 and C_{10}. The signals at 124.19 ppm and 126.16 ppm corresponded to the remaining aromatic carbons: C_7, C_6, C_2 and C_3. The downfield signal at 160.18 ppm was designated as C_1' in the cyanovinyl unit. FTIR spectrometry shows bands at 2228 (CN), 1621 (C=C) and 1574, 1445 (C=C) cm^{-1}. High resolution mass spectrometry (APCI) was carried out and the required molecular ion was calculated to be $C_{18}H_9N_2Cl$ [M^+] 288.0454 and found as 288.0466.

4.6 Other Knoevenagel condensations of 9-anthraldehyde

The Knoevenagel condensations of 9-anthraldehyde and other activated methylene compounds was also achieved. 9-Anthraldehyde and acetone were reacted to give (*E*)-4-(anthracen-9-yl)but-3-en-2-one (**237**)[245], while Meldrum's acid when reacted with 9-anthraldehyde afforded 5-(anthracen-9-ylmethylene)-2,2-dimethyl-1,3-dioxane-4,6-dione (**236**)[354] (Figure 178). These Knoevenagel condensations afforded pure product isolated easily by filtration with 60-70% yield (Figure 178).

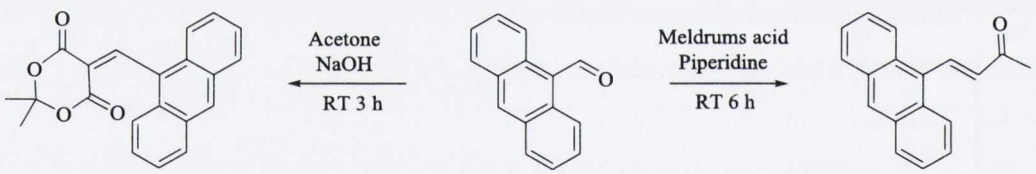

(237) 70% **(236)** 60%

Figure 178: Scheme for synthesis of (*E*)-4-(anthracen-9-yl)but-3-en-2-one and 5-(anthracen-9-ylmethylene)-2,2-dimethyl-1,3-dioxane-4,6-dione

4.7 Synthesis of 9-(chloromethyl)anthracene

In order to synthesise a library of (anthracen-9-yl)methylamines *via* nucleophilic substitution of 9-(chloromethyl)anthracene; 9-(chloromethyl)anthracene was first synthesised by a two step synthetic route. The first step of this route was the sodium borohydride reduction of 9-anthraldehyde to the corresponding anthracen-9-ylmethanol (**238**)[155]. 9-(Chloromethyl)anthracene (**239**) was then obtained through the reaction of the alcohol (**238**) with thionyl chloride in dioxane at reflux (Figure 179).

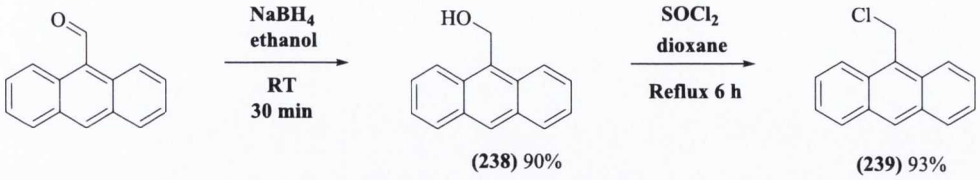

Figure 179: General scheme for the synthesis of 9-(chloromethyl)anthracene

9-(Chloromethyl)anthracene is amenable to nucleophilic substitution and a reaction with potassium cyanide gave 2-(anthracen-9-yl)acetonitrile (**240**)[355] (Figure 180).

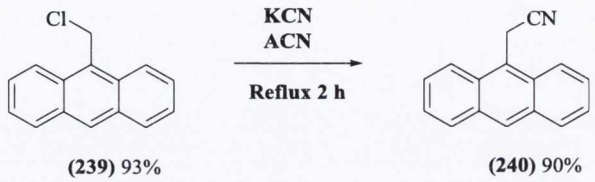

Figure 180: General scheme for the synthesis of 2-(anthracen-9-yl)acetonitrile

The yields for the reduction, chlorination and nucleophilic substitution products are summarised in Figure **179-180**.

4.8 Synthesis of the (anthracen-9-yl)methylamines

A small panel of (anthracen-9-yl)methylamines (**241-244**) were obtained via the nucleophilic substitution reaction of 9-(chloromethyl)anthracene (**239**) and the required amine. This reaction was carried out at room temperature over a long reaction time of 24 hours (Figure 181).

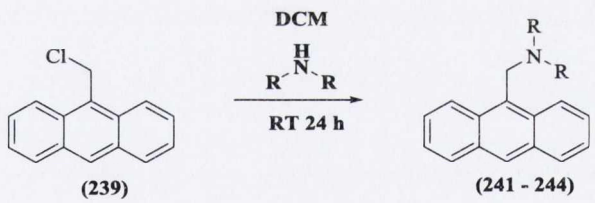

Figure 181: General scheme for the synthesis of the (anthracen-9-yl)methylamines

(Anthracen-9-yl)methylamines can also be synthesised by one pot reductive amination during which the imine formed *in situ* from the reaction of the required amine and the desired aldehyde is reduced to the product amine. Examples of reducing agents used for reductive amination include sodium borohydride[356] and sodium cyano borohydride[357].The nucleophilic substitution of 9-(chloromethyl)anthracene led to the completion of a series of (anthracen-9-yl)methylamines (**241-244**) with yields of 75-90% (Table 24).

	Compound	R	Yield
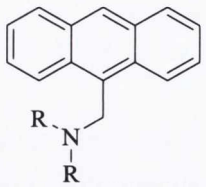	**241**	$(CH_2)_6$	86%
	242	$(CH_2)_4$	75%
	243	$(CH_2)_2O(CH_2)_2$	90%
	244	$(CH_2)_5$	82%

Table 24: (anthracen-9-yl)methylamines library

4.9 Synthesis of the anthracene amides

A series of anthracene amides (**245-250**) were obtained from anthracene-9-carboxylic acid using the Mukaiyama reaction. The Mukaiyama conditions for this series of amides was achieved using triethylamine, 2-chloro-1-methyl-pyridinium iodide (also known as the Mukaiyama reagent) and the required amine (Figure 182).

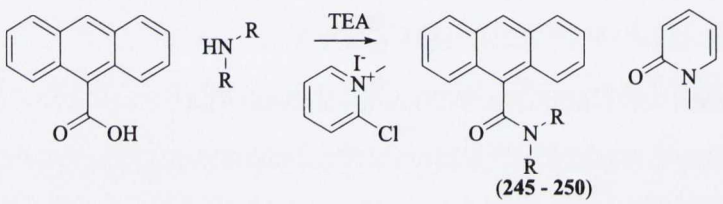

Figure 182: General scheme for the synthesis of the anthracene amides (245-250)

The mechanism for the Mukaiyama reaction is illustrated below in Figure 183. The reaction is initiated by deprotonation of the acid by triethylamine. This increased electron density on the carbonyl triggers a nucleophilic attack on the positively charged 2-chloro-1-methyl-pyridine.

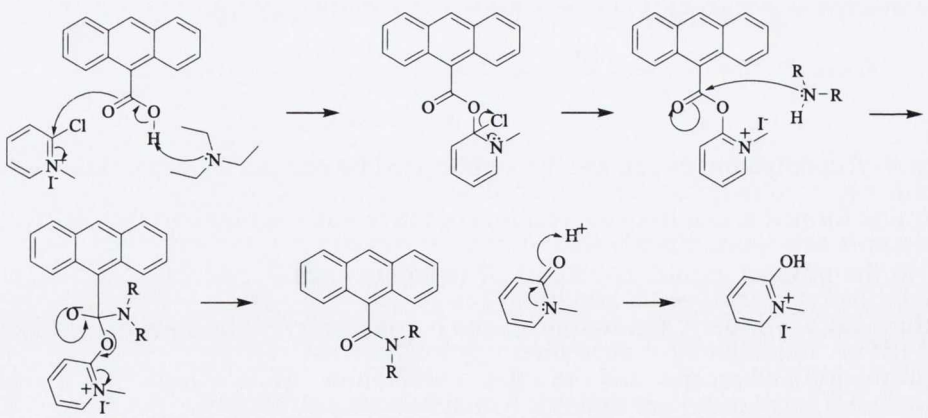

Figure 183: Proposed mechanism for the synthesis of the anthracene amides[209]

Chloride ion is eliminated to form the activated carbonyl intermediate. This activated carbonyl is attacked by the selected amine, reformation of the carbonyl leads to the elimination

of the pyridine group and subsequent formation of 2-hydroxy-1-methylpyridin-1-ium iodide and our desired amide product[209].

Anthracene-9-carboxylic chloride stirred in anhydrous dichloromethane with triethylamine and the desired amine over 2 hours, will also afford the anthracene amides with excellent yields[358]. Amides can be synthetized *via* a plethora of well-studied methodologies such as the Beckmann rearrangement (oximes to amides)[359], the Chapman rearrangement (O-aryliminoethers to amides)[360] and the Schmidt reaction (ketones to amides using ammonia)[361]. Alternative amide coupling reagents can also be utilised such as EDCI / HOBt[6, 362], HATU[363], COMU[364] and HBTU[365] (Figure 184).

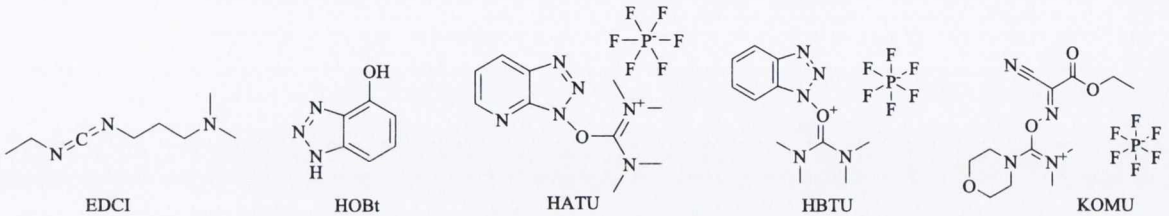

Figure 184: Amide coupling reagents

The Mukaiyama reagent was chosen as the amide coupling reagent for the synthesis of this library due to the excellent yields achieved, its ready availability and relatively straightforward purification of the reaction product. The synthesis afforded the anthracene amides (**245-250**) with yields of 75-90% (Table 25).

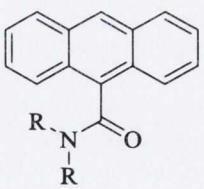

Compound	R	Yield	Compound	R	Yield
245	CH_2CH_3	85%	**248**	$(CH_2)_4$	75%
246	CH_3	80%	**249**	$(CH_2)_2O(CH_2)_2$	88%
247	$(CH_2)_6$	86%*	**250**	$(CH_2)_5$	90%

Table 25: anthracene amides library

Anthracen-9-yl(azepan-1-yl)methanone (**247**) was chosen as a representative sample of the anthracene amides and the ^{1}H NMR and ^{13}C NMR spectra will now be discussed in detail. The ^{1}H NMR (400 MHz, $CDCl_3$) spectrum of compound **247** (Figure 185) shows a triplet occurring at 3.09 ppm (J = 6.10 Hz) and a multiplet occurring at 4.02 ppm both integrating for two protons each, these were assigned to the CH_2 protons on $C_{1'}$ and $C_{6'}$ respectively. Note that although in this 2-dimensional view of anthracen-9-yl(azepan-1-yl)methanone it appears that protons at $C_{1'}$ and $C_{6'}$ should experience similar electronic conditions, in three dimensional space $C_{6'}$, $C_{5'}$ & $C_{4'}$ are closer to the amide carbonyl than $C_{1'}$, $C_{2'}$ & $C_{3'}$. This is due to the alkane nature and the 'boat' like shape homopiperidine assumes.

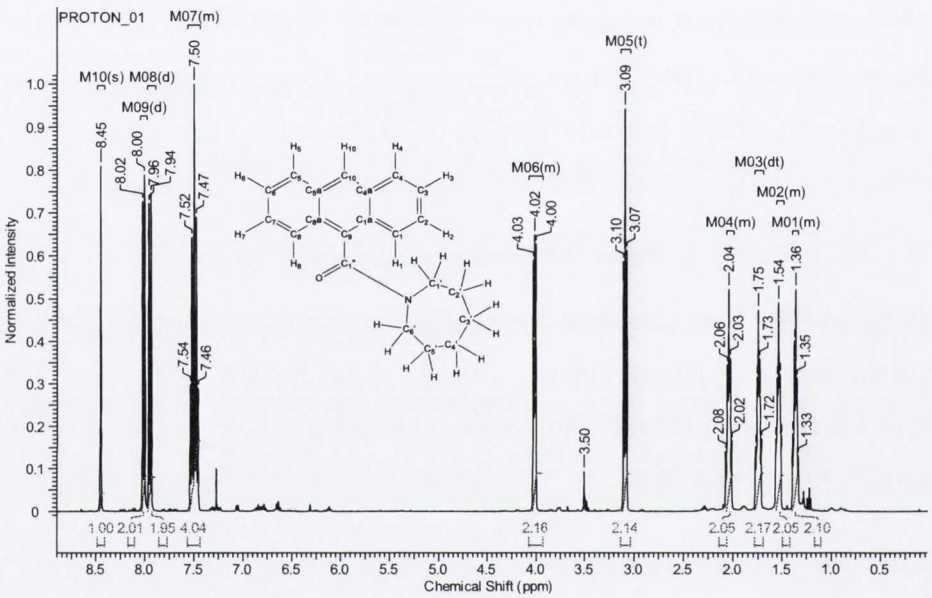

Figure 185: ^{1}H NMR spectrum of anthracen-9-yl(azepan-1-yl)methanone (247)

Multiplets occurring at 1.31 - 1.43 ppm, 1.47 - 1.59 ppm, 1.70 – 1.76 ppm and 1.94 - 2.12 ppm all integrate for two protons, accounting for the remaining protons in the homopiperidine ring. Doublets occurring at 7.95 ppm (J = 8.55 Hz) and 8.01 ppm (J = 7.94 Hz) both integrating for two protons each were assigned to H_4 & H_5 and H_1 & H_8 respectively. The multiplet at 7.43 - 7.57 ppm integrated for four protons and accounted for the remaining aromatic protons. The singlet at 8.45 ppm integrated for a single proton which was allocated to H_{10}.

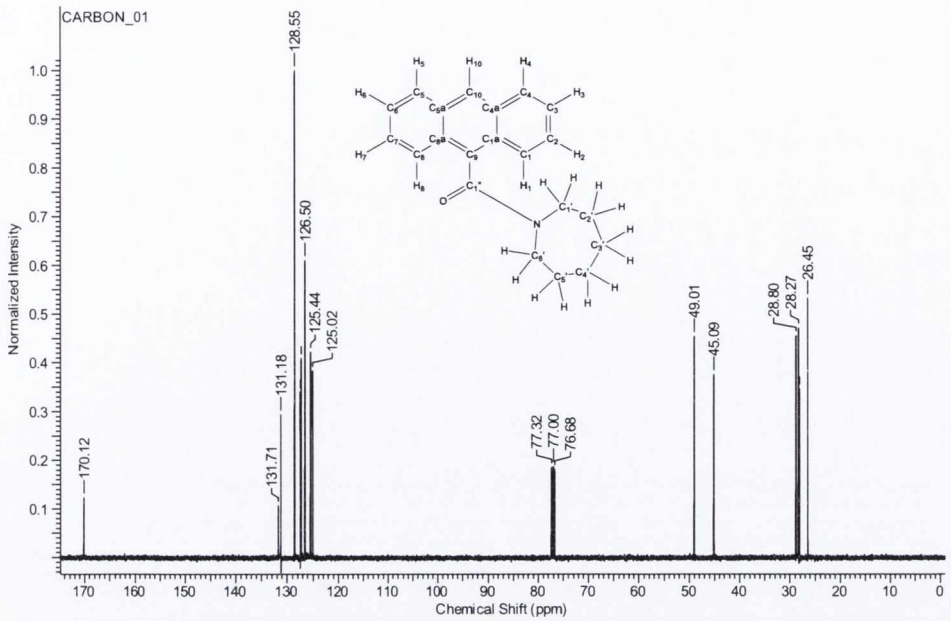

Figure 186: ^{13}C NMR spectrum of anthracen-9-yl(azepan-1-yl)methanone (247)

The ^{13}C NMR spectrum (101 MHz, $CDCl_3$) of compound **247** (Figure 186) shows signals at 45.09 ppm and 49.01 ppm; these were assigned to $C_{1'}$ and $C_{6'}$. The resonance at 49.01 ppm occurring slightly further downfield due to the proximity of $C_{6'}$ to the carbonyl. Resonances occurring at 26.45 ppm, 28.10 ppm, 28.27 ppm and 28.80 ppm accounted for the remaining homopiperidine carbons $C_{2'}$, $C_{3'}$, $C_{4'}$ and $C_{5'}$. CH carbon equivalent resonances at 126.50 ppm, 127.31 ppm and 128.55 ppm were assigned to C_4 & C_5, C_1 & C_8 and C_{10}. The remaining aromatic CH carbons were accounted for by resonances at 125.02 ppm and 125.44 ppm. Quaternary carbon equivalent signals at 127.45 ppm and 131.18 ppm were allocated to C_{5a} & C_{4a} and C_{1a} & C_{8a} respectively. The remaining downfield signals occurring at 131.71 ppm and 170.12 ppm correspond to C_9 and $C_{1''}$ (carbonyl).

FTIR spectroscopy shows bands at 3048, 2929 (C-H), 1615, 1486.60 (C=C) and 1263 (C-N) cm^{-1}. High resolution mass spectrometry (APCI) was carried out and the required molecular ion was calculated to be $C_{21}H_{22}NO$ $[M^+ + H]$ 304.1701 and found as 304.1688.

4.10 Conclusions

A library of 58 anthracene based compounds structurally related to maprotiline were designed and synthesised. A number of substituted anthracenes were synthesised and formylated to give the related anthraldehydes. These anthraldehydes were reacted with the required nitroalkanes in a Henry-Knoevenagel condensation to give a library of 16 substituted (*E*)-9-(2-nitrovinyl)anthracenes (11 novel compounds) related to the previous lead compound

(*E*)-9-(2-nitrovinyl)anthracene. Anthracene substitutions synthesised include methoxy, isopropy, alkyl (methyl, ethyl), phenyl and halogen (chlorine and bromine). The alkyl chain length at C-2 was also altered using different nitroalkanes (nitromethane, nitroethane and nitropropane) from unsubstituted to methyl and ethyl. Insertion of a carbon between the vinyl unit and the anthracene moiety was also achieved using a Wittig reaction.

It was also of interest to vary the nature of the vinyl substitution at C-9 to other related vinyl functionalities including cyanovinyl, oxime, hydrazone and alkyl analogues. A selection of amines and amides were also prepared from the corresponding chloride and acids respectively. The compounds synthesised in Chapter 4 were screened for biological activity in the BL cell lines DG-75 and MUTU-I and the results of this preliminary screen will be discussed in Chapter 6. They were also used as dienes in the Diels-Alder cycloaddition chemistry investigated in Chapter 5.

Chapter 5.

Design, synthesis and characterisation of the 9,10-dihydro-9,10-ethanoanthracene maprotiline analogues

5.0 Introduction

Research carried out in the School of Biochemistry and Immunology, Trinity College Dublin, identified maprotiline as a potent anti-proliferative and pro-apoptotic agent in Burkitt's lymphoma cell lines MUTU-I and DG-75 (EC_{50} 5.9-15.3 μM)[93, 94]. Subsequent work within our laboratory involved the generation of a range of compounds structurally related to maprotiline and a biological screen of this library identified a number of lead compounds with promising EC_{50} values in both the MUTU-I and DG-75 cell lines. From this study the 9,10-dihydro-9,10-ethanoanthracene scaffold was identified as favourable for anti-proliferative activity in these cell lines and the planar compound (*E*)-9-(2-nitrovinyl)anthracene was also shown to elicit a potent pro-apoptotic effect (Chapter 1, Section 1.4 & 1.5)[6].

The main aim of this study is to synthesise a series of maprotiline analogues incorporating both a nitrovinyl functionality and the 9,10-dihydro-9,10-ethanoanthracene scaffold. Synthesis of other 9,10-dihydro-9,10-ethanoanthracene maprotiline analogues with a range of functionalities was also intended including but not limited to hydroxy, aldehyde, imine, acid, cyanovinyl and hydrazone modifications. These 9,10-dihydro-9,10-ethanoanthracene maprotiline analogues would be synthesised *via* Diels-Alder cycloaddition to the required anthracene diene system and hence modification of the ethano bridgehead could be achieved by variation of the dienophile employed. This dienophile library composed of 19 maleimide, phenylmaleimide and benzylmaleimide derivatives that were synthesised as part of the present work and eight commercially available reagents available in house. Figure 187 gives an overview of the structures of the proposed maprotiline analogues. Variation of substitution at C-9 from nitrovinyl to alternative double bonded systems such as cyanovinyl, imine and oxime may be of interest for biological activity, as is the variation of maleimide substituent chain length and phenylmaleimide substitution pattern. Variation of the nitrovinyl unit by reduction and extension of the alkyl chain length at C-2 was also planned.

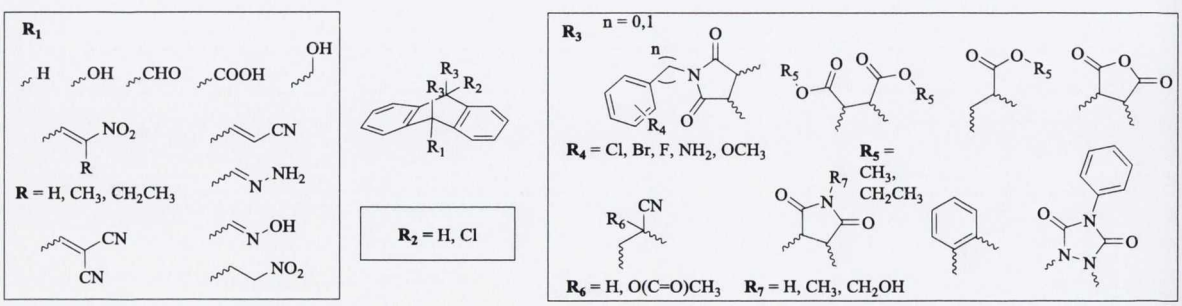

Figure 187: Overview of proposed maprotiline analogues

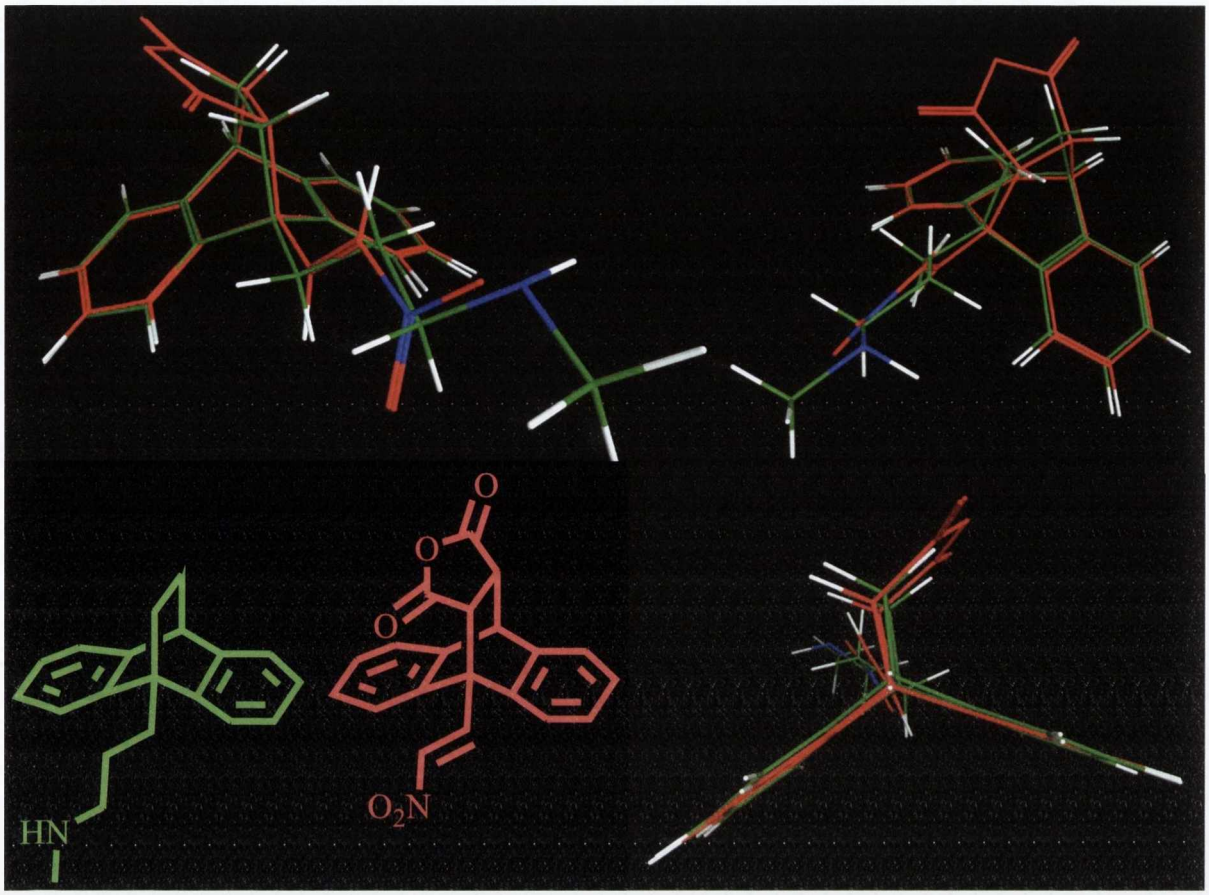

Figure 188: : Maprotiline (green) flexibly allgined to proposed Diels-Alder adduct (red) (MOE 2011.10).

To illustrate proof of concept, preliminary molecular modelling was carried out on a selected Diels-Alder analogue (shown in red) and its lowest energy configuration was flexibly aligned with the lowest energy configuration of maprotiline (green) (MOE 2011) (Figure 188). This study illustrates the high degree of structural similarity between the ethano protons of these bridged structures and that there is significant overlap between the phenyl rings of the tetracyclic structure. The secondary amine sidechain of maprotiline also overlays with the nitrovinyl unit of the chosen Diels-Alder adduct and the sum of these similarities may prove favourable biologically when screened for activity in the DG-75 and MUTU-I BL cell lines.

5.1 Synthesis of the maleimide dienophiles

A library of maleimide based dienophiles was synthesised from maleic anhydride as part of the current work. The synthetic route used to generate the various maleimide derivatives required for Diels-Alder cycloaddition reaction involved generation of corresponding amic acid intermediates from the parent amines in diethyl ether. These amic acid intermediates then underwent intramolecular cyclisation in the presence of sodium acetate and acetic anhydride, resulting in the formation of the related maleimide or phenyl maleimide compounds (**251-269**) (Figure 189).

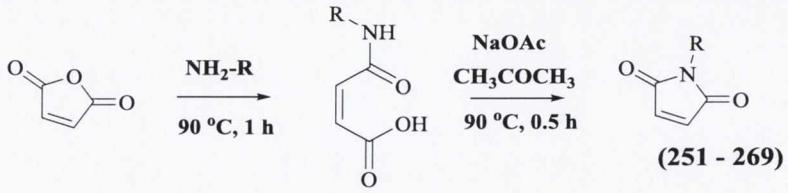

Figure 189: General scheme for the synthesis of the maleimide dienophiles

The mechanism for the synthesis of the maleimide derivatives involves a two-step reaction. The first step comprises of the nucleophilic attack of the desired amine on the slightly positive carbon at the base of the carbonyl group of the maleic anhydride. This results in ring opening of the molecule, facilitated by the protonation of the central ring oxygen atom and the formation of a hydroxyl functional group. The addition product generated is the corresponding amic acid intermediate (Figure 190).

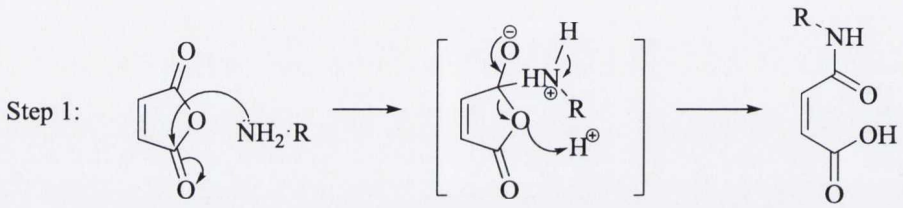

Figure 190: Mechanism for the formation of the amic acid intermediate

The second step of this synthetic route involves complexation of the sodium acetate with the electronegative oxygen of the acid functional group, forming an amic acid salt. This deprotonated acid group attacks the carbonyl groups on acetic anhydride, forming the acetate intermediate. With the formation of this intermediate, sodium acetate is then regenerated.

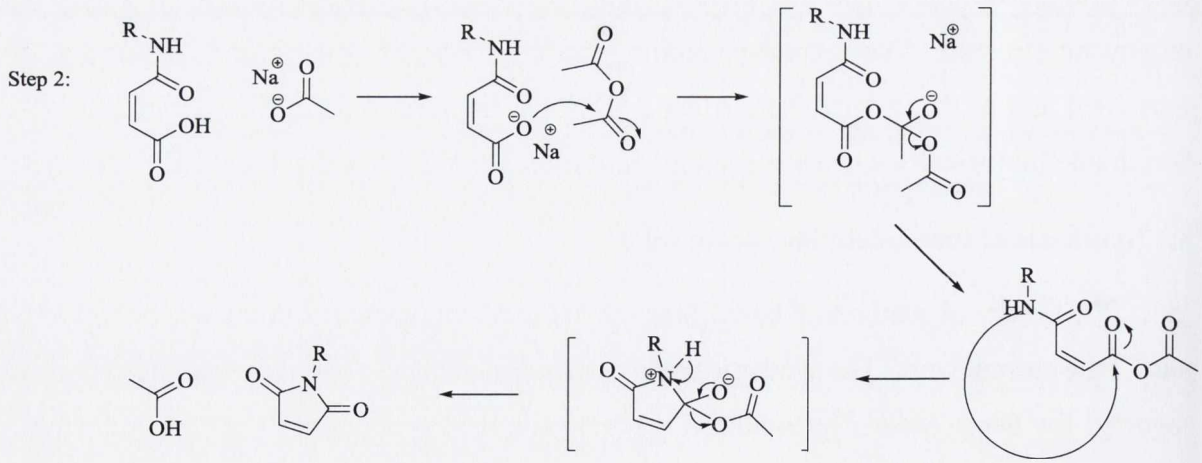

Figure 191: Mechanism for the formation of maleimide derivatives

Following the formation of this acetate derivative, the amide nitrogen attacks the carbonyl closest to the diene double bond (due to a favourable leaving group being present). This causes ring cyclisation / formation, with the cleavage of another acetate group, regenerating the ketone functionality, affording the corresponding maleimide derivative[366].

Phenylmaleimides (1-phenyl-1*H*-pyrrole-2,5-diones) can be accessed from their amic acid precursors using a number of different catalysts such as phosphorous pentoxide[367] and sulphuric acid[368]. Other synthetic routes to the phenyl-maleimides have also been successful, one such route is the reaction of phenylboronic acid 1,3-propylene glycol ester with maleimide in the presence of copper acetate and triethylamine[369]. Maleimides are a biologically active family of compounds with noted antimicrobial[368, 370-372] and antifungal activities[373]. Maleimides are a useful class of dienophile and have also been incorporated into a number of potential metallic anti-cancer agents due to their potent DNA binding properties[374, 375].

A comprehensive library of functionalised phenyl-maleimides and maleimides (**251-269**) was synthesised over the course of this work with yields ranging from 18-70%. This library of compounds is summarised in Table 26 and Table 27.

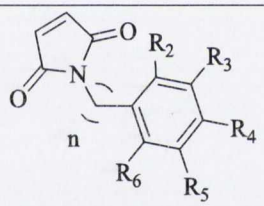

Compound	Substitution pattern	n	Yield	Compound	Substitution pattern	n	Yield
251	-	1	40%	**259**	$R_3 = O(CO)CH_3$	0	43%
252	$R_3 = R_4 = R_5 = OCH_3$	1	20%	**260**	$R_3 = R_4 = OCH_3$	2	15%
253	$R_4 = Cl$	0	55%	**261**	$R_4 = (CO)OCH_3$	0	40%
254	$R_4 = CH_3$	0	40%	**262**	$R_3 = R_5 = OCH_3$	0	69%
255	$R_4 = N(CH_3)$	0	35%	**263**	$R_4 = F$	0	65%
256	$R_4 = (CO)(C_6H_5)$	0	29%	**264**	$R_4 = Br$	0	59%
257	$R_2 = O(CO)CH_3$	0	18%	**265**	$R_3 = R_4 = R_5 = OCH_3$	0	60%*
258	$R_3 = Cl$	0	55%	**266**	$R_4 = NH_2$	0	70%

Table 26: phenylmaleimide library. Note: R = H unless otherwise specified. * denotes novel compound

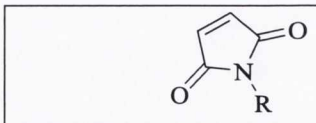

Compound	R	Yield
267	CH_2OH	40%
268	CH_3	60%
269	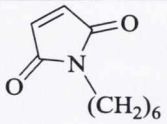	60%

Table 27: maleimide library

1-(3,4,5-Trimethoxyphenyl)-1*H*-pyrrole-2,5-dione (**252**) was chosen as a representative sample of the maleimides and the ^1H NMR and ^{13}C NMR spectra will now be discussed in detail. The ^1H NMR (400 MHz, $CDCl_3$) spectrum of compound **252** (Figure 192) bears three distinct singlets.

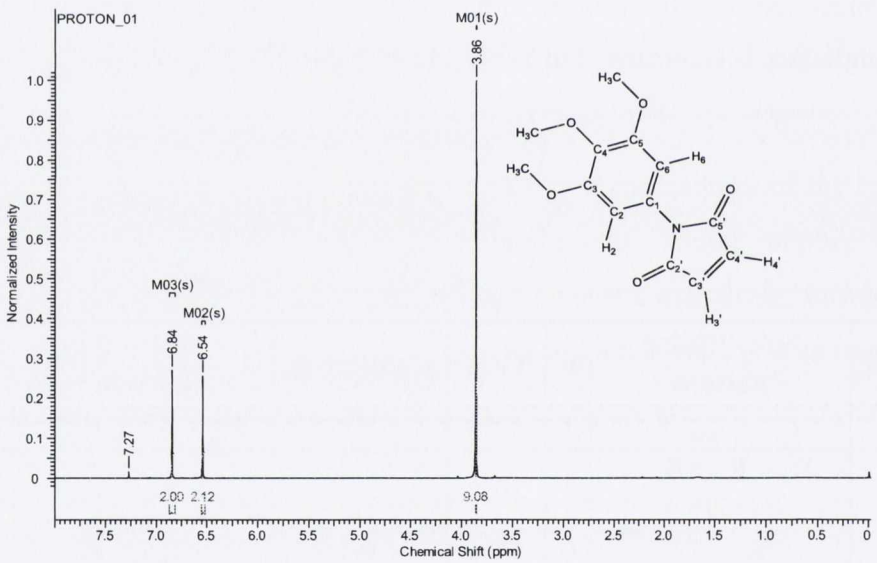

Figure 192: ^1H NMR spectrum of 1-(3,4,5-trimethoxyphenyl)-1*H*-pyrrole-2,5-dione (252)

The singlet occurring at 3.86 ppm integrating for nine protons was assigned to the nine protons of the three methoxy substituents. The singlet seen at 6.54 ppm integrating for two protons accounted for equivalent aromatic protons H_2 and H_6. The remaining and most downfield singlet occurring at 6.84 ppm with an integration of two protons was allocated to the equivalent vinyl protons $H_{4'}$ and $H_{3'}$.

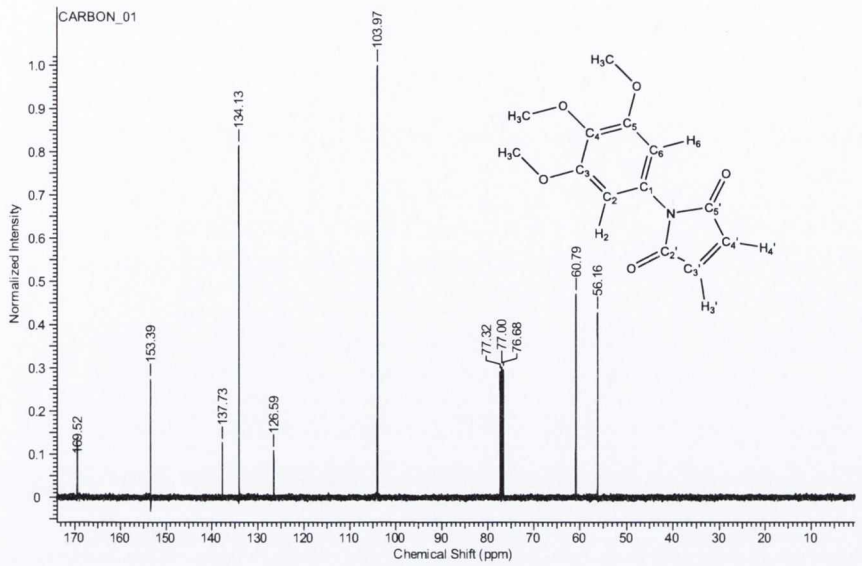

Figure 193: ^{13}C NMR spectrum of 1-(3,4,5-trimethoxyphenyl)-1*H*-pyrrole-2,5-dione (252)

The ^{13}C NMR spectrum (101 MHz, $CDCl_3$) of compound **252** (Figure 193) shows resonances at 56.16 ppm and 60.79 ppm, these were assigned to the carbons within the methoxy substituents.

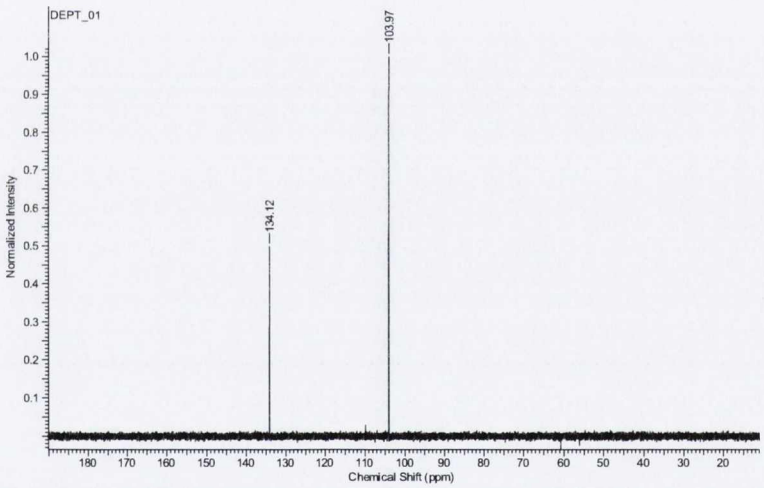

Figure 194: DEPT 90 NMR spectrum of 1-(3,4,5-trimethoxyphenyl)-1*H*-pyrrole-2,5-dione (252)

A DEPT 90 NMR spectrum of compound **252** (Figure 194) shows CH signals at 103.97 ppm and 134.13 ppm. The CH signals at 103.97 ppm and 134.13 ppm were allocated to the pairs of carbon equivalent signals at C_2 & C_6 and the vinyl unit C_3 & C_5. Quaternary signals occurring at 126.59 ppm, 137.73 ppm and 153.39 ppm corresponded to C_1, C_3 & C_5 and C_4 respectively. The downfield quaternary signal occurring at 169.52 ppm was attributed to the pair of equivalent carbons in the carbonyls of the maleimide unit ($C_{2'}$ & $C_{5'}$).

FTIR spectroscopy shows bands at 3085, 2964 (C-H), 1707 (C=O), 1509, 1470 (C=C), 1598 (C=C) and 1127 (CN) cm^{-1}. High resolution mass spectrometry (APCI) was carried out and the required molecular ion was calculated to be $C_{13}H_{14}NO_5$ [M^++H] 264.0872 and found as 264.0867.

5.2 Synthesis of the (*E*)-11,12-substiuted-9-(2-nitrovinyl)-9,10-dihydro-9,10-ethanoanthracenes

An extensive library of (*E*)-11,12-substituted-9-(2-nitrovinyl)-9,10-dihydro-9,10-ethanoanthracenes (**270-352**) was synthesised from the library of (*E*)-9-(2-nitrovinyl)anthracenes (Chapter 4) and the required dienophiles. The Diels-Alder addition was carried out in toluene at 120 °C in the presence of excess dienophile (Figure 195).

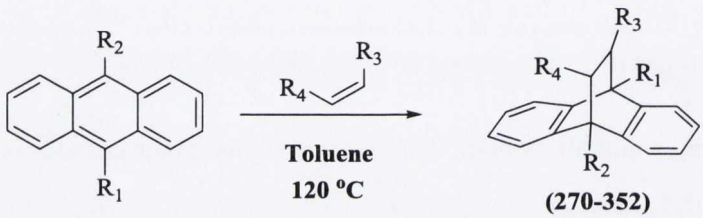

Figure 195: General scheme for the Diels-Alder reaction

A summary of the dienophiles utilised during the Diels-Alder additions of the current work can be seen in Figure 196. The synthesis of the maleimide, benzyl-maleimide and phenyl-maleimide based dienophiles (**251-269**) has been previously discussed and the library of these compounds can be seen in Tables 26 and 27.

The other dienophiles 4-phenyl-3*H*-1,2,4-triazole-3,5(4*H*)-dione, 1-cyanovinyl acetate, methyl acrylate, ethyl acrylate and cyanoacrylate respectively were commercially available in high purity (Figure 196).

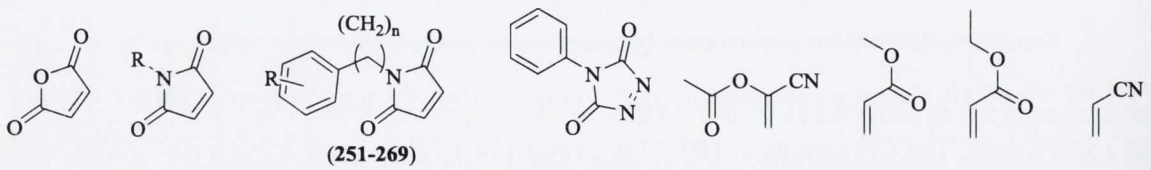

Figure 196: Dienophile library

The Diels-Alder reaction was first documented by Professor Otto Diels and Kurt Alder in 1928 when characterising the addition products formed during the reaction of cyclopentadiene and quinone[376]. The Diels-Alder reaction is a pericyclic [4+2] cycloaddition reaction which takes place between a conjugated diene system and an alkene, in this case known as the dienophile. The alkene systems used to the best effect in the Diels-Alder reaction

bear an electron withdrawing group, increasing the electrophilicity of the already electrophilic alkene system. Maleic anhydride and the maleimides are excellent dienophiles as a result, due to the two electron withdrawing groups attached to the alkene bond. Conversely an electron donating group on the diene system promotes the reaction also, providing additional electron density and a stronger target for the electrophilic dienophile.

As previously mentioned the mechanism of the Diels-Alder reaction is a pericyclic [4+2] cycloaddition implying that the reaction is concerted. Two electrons are provided by the LUMO (lowest unoccupied molecular orbital) of the dienophile and four are provided by the HOMO (highest occupied molecular orbital) of the diene system to form a transition state with six delocalised π electrons. The transition state is stabilised by the delocalised π electrons which offer it aromatic character and this promotes the reaction pathway. The reaction proceeds to the formation of two new σ bonds which are energetically more stable than the delocalised six π electrons (Figure 197).

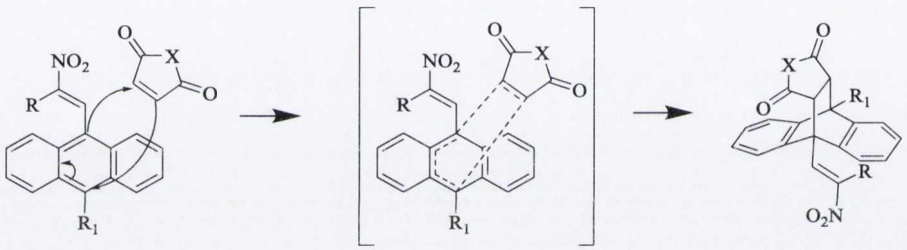

Figure 197: Proposed mechanism for the Diels-Alder reaction of the (*E*)-9-(2-nitrovinyl)anthracenes

The stereochemistry of both the diene and dienophile are maintained during the Diels-Alder cyclisation reaction and this inbuilt stereospecificity ensures the (*E*) configuration of the diene substituent remained intact. There are two configurations available to the transition state formed during the Diels-Alder reaction and these describe the three dimensional orientation of the dienophile to the diene system, these are known as the '*endo*' and '*exo*' configurations. The '*exo*' configuration entails the dienophile substituents facing away from the new π bond with the hydrogens facing this π molecular orbital, the *endo* is therefore the reverse of this. The '*exo*' is presumed to be sterically favourable, however the '*endo*' product with carbonyl dienophiles offers additional stability through secondary orbital interactions between the carbonyl and the

diene (applicable to the majority of products in this work) (Figure 198). Dipolar and Van der Waals forces are also thought to contribute to this additional stability.

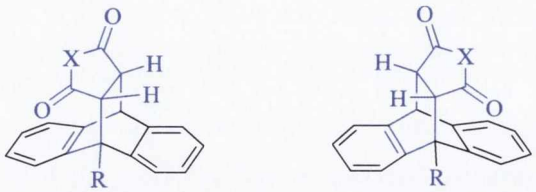

ENDO **EXO**

Figure 198: Endo and Exo configurations

For the greater portion of classical Diels-Alder reactions the *endo* product has been expected when an electron withdrawing group has been part of the dienophile following the rules outlined by Stein and Alder in 1934[129, 377]. The rate of reaction of the dienophile and diene for the cycloaddition can vary depending on the reagents and the rate of reaction can be increased by the addition of a Lewis acid or increased pressure[129, 209]. Diels-Alder additions to (*E*)-9-(2-nitrovinyl)anthracene have been previously achieved using ethylene[103] and benzyne[378] as dienophiles. A photochemical dimerization reaction of (*E*)-9-(2-nitrovinyl)anthracene was also noted by Becker et al. (1986) giving a Diels-Alder type adduct[379]. Wilhelm et al. (1969) attempted the Henry-Knoevenagel condensation of 9,10-ethanoanthracene-9(10*H*)-carbaldehyde but dehydration did not take place and as a result 1-(9,10-ethanoanthracen-9(10*H*)-yl)-2-nitroethan-1-ol was isolated[103].

In the present work, Diels-Alder adducts were also synthesised using the reduced adduct of (*E*)-9-(2-nitrovinyl)anthracene - 9-(2-nitroethyl)anthracene (**224**). 9-(2-Nitroethyl)anthracene was reacted with maleic anhydride, maleimide and phenyl-maleimide with good yields. These 9-(2-nitroethyl)anthracene Diels-Alder adducts (**284-286**) were synthesised to assess the effect(s) of the reduced nitrovinyl unit on anti-proliferative activity. Diels-Alder adducts with a nitroethyl unit have been previously synthesised through reduction of the nitrovinyl Diels-Alder adduct[379].

(*E*)-11,12-substituted-9-(2-nitrovinyl)-9,10-dihydro-9,10-ethanoanthracenes

The libraries of novel (*E*)-11,12-substituted-9-(2-nitrovinyl)-9,10-dihydro-9,10-ethanoanthracenes (**270-352**) are presented in Tables 28, 30, 31 and 32. Variation of alkyl chain length at the C-2 and C-10 substitution was achieved by utilising different nitroalkanes during the Henry-Knoevenagel condensation with substituted 9-anthraldehydes giving access to a number of diverse diene systems (Chapter 4). The (*E*)-9-(2-nitrovinyl)-9,10-dihydro-9,10-[3,4]furanoanthracene-12,14 dione library (**270-283**) encompasses maleic anhydride,

maleimide and simple maleimide Diels-Alder adducts and the (*E*)-9-(2-nitrovinyl)-13-phenyl-9,10-dihydro-9,10-[3,4]epipyrroloanthracene-12,14-dione libraries (**288-316**) include substituted phenyl and benzyl maleimide Diels-Alder adducts. The method of preparation outlined in the current work afforded good yields of 15-97% for the (*E*)-9-(2-nitrovinyl)-9,10-dihydro-9,10-[3,4]furanoanthracene-12,14 diones, 15-88% for the (*E*)-9-(2-nitrovinyl)-13-phenyl-9,10-dihydro-9,10-[3,4]epipyrroloanthracene-12,14-diones (**288-310**) and 30-45% for the 9-(2-nitroethyl)-9,10-dihydro-9,10-[3,4]furanoanthracene-12,14-diones (**284-286**).

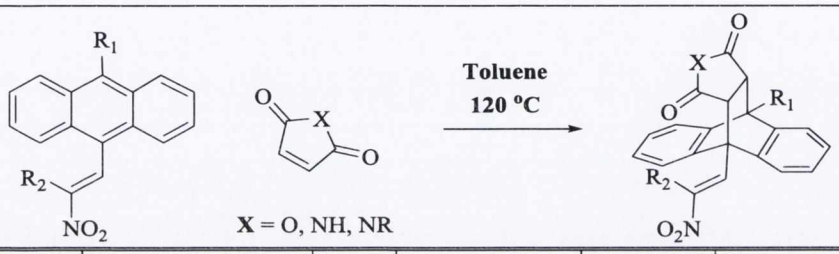

Compound	X	R_1	R_2	Yield	Melting point
270	O	H	H	80%*	244-245 °C
271	O	H	CH_3	72%*	256-258 °C
272	O	H	CH_2CH_3	98%*	230-233 °C
273	O	Cl	H	15%*	275-277 °C
274	O	Cl	CH_3	18%*	270-272 °C
275	O	Cl	CH_2CH_3	55%*	259-263 °C
276	NH	H	H	50%*	176-178 °C
277	NH	H	CH_3	97%*	296-300 °C
278	NH	H	CH_2CH_3	76%*	296-298 °C
279	NH	Cl	H	25%*	>300 °C
280	NH	Cl	CH_3	50%*	295-297 °C
281	NH	Cl	CH_2CH_3	55%*	294-298 °C
282	$N(CH_3)$	H	H	55%*	267-268 °C
283	$N(CH_2)OH$	H	H	80%*	230-232 °C

Table 28: (*E*)-9-(2-nitrovinyl)-9,10-dihydro-9,10-[3,4]furanoanthracene-12,14-dione library. * denotes novel compound

(*E*)-9-(2-nitrovinyl)-9,10-dihydro-9,10-[3,4]furanoanthracene-12,14-dione (**270**) was chosen as a representative sample of the (*E*)-9-(2-nitrovinyl)-9,10-dihydro-9,10-[3,4]furanoanthracene-12,14-diones and the ^{1}H NMR and ^{13}C NMR spectra will now be discussed in detail. The ^{1}H NMR (400 MHz, DMSO-d_6) spectrum of compound **270** (Figure 199) shows a double doublet occurring at 3.82 ppm (J = 9.16, 3.66 Hz) integrating for a single proton, this accounted for H_{11}.

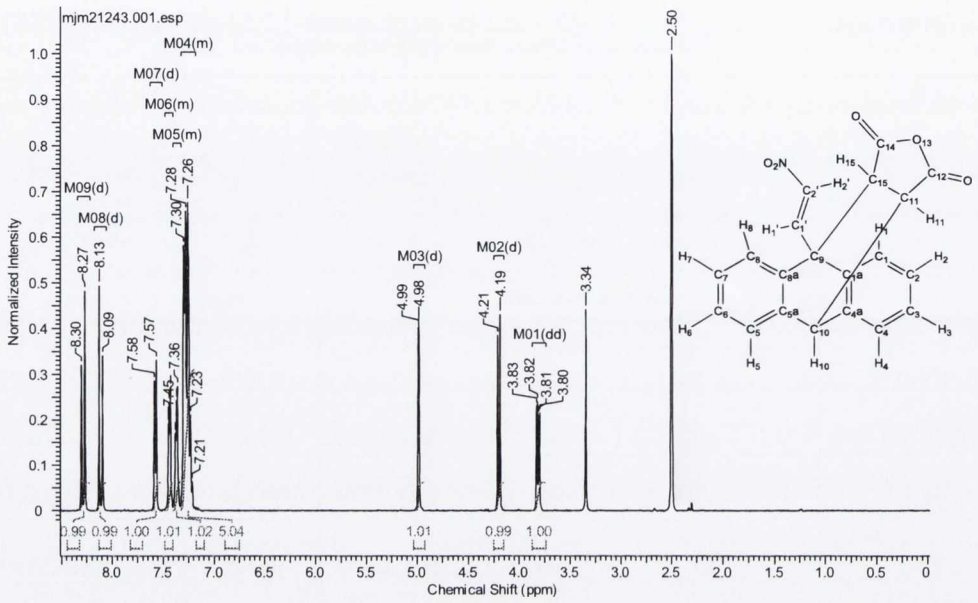

Figure 199: ^{1}H NMR spectrum of (*E*)-9-(2-nitrovinyl)-9,10-dihydro-9,10-[3,4]furanoanthracene-12,14-dione (270)

The doublets at 4.20 ppm (J = 8.55 Hz) and 4.98 ppm (J = 3.05 Hz) both integrating for a single proton each were assigned to H_{15} and H_{10} respectively. The doublet occurring at 7.58 ppm (J = 6.71 Hz) was assigned to H_1, this proton occurred more downfield than the other aromatic protons due to proximity to both the nitrovinyl unit and the carbonyl. The remaining seven aromatic protons were accounted for by multiplets occurring at 7.20 - 7.32 ppm (5 H), 7.32 - 7.40 ppm (1 H) and 7.40 - 7.47 ppm (1 H). The remaining downfield doublets occurring at 8.11 ppm (J = 14.04 Hz) and 8.28 ppm (J = 14.04 Hz) were assigned to $H_{2'}$ and $H_{1'}$ respectively.

A H-H COSY NMR spectrum of compound **270** is displayed below in Figure 200. This H-H COSY experiment was utilised to verify the identity of H_{11} – the central proton in the ethano bridge. It can be seen from examining the H-H COSY that both 4.20 ppm (1H, J = 8.55 Hz) and 4.98 ppm (1H, J = 3.05 Hz) are coupled to the double doublet occurring at 3.82 ppm (1H, J = 9.16, 3.66 Hz). Coupling was also observed between double resonances observed at 8.11 ppm (J = 14.04 Hz) and 8.28 ppm (J = 14.04 Hz).

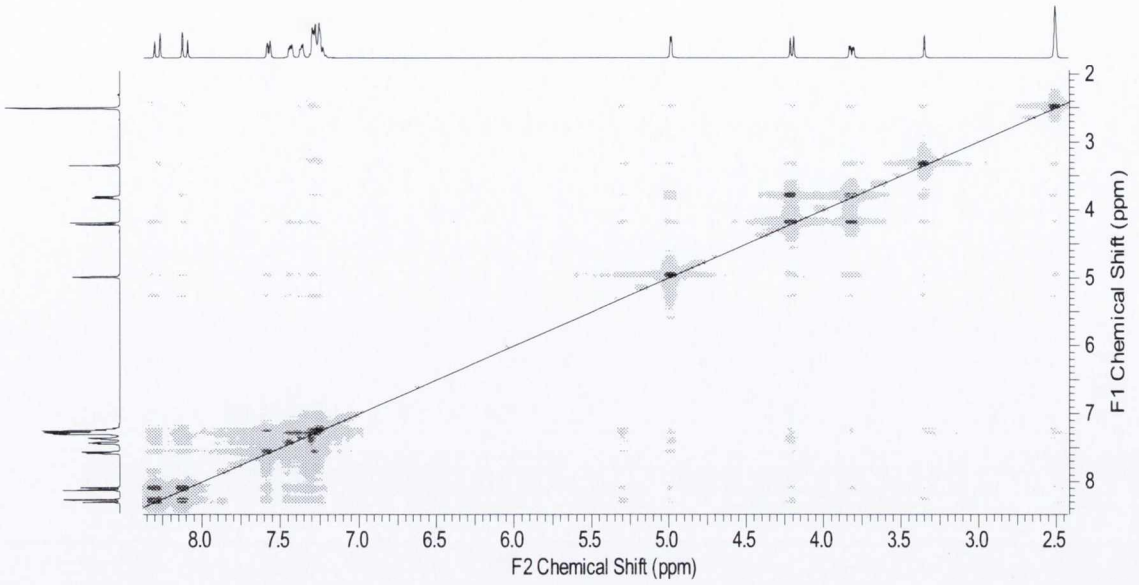

Figure 200: H-H COSY NMR spectrum of (*E*)-9-(2-nitrovinyl)-9,10-dihydro-9,10-[3,4]furanoanthracene-12,14-dione (270)

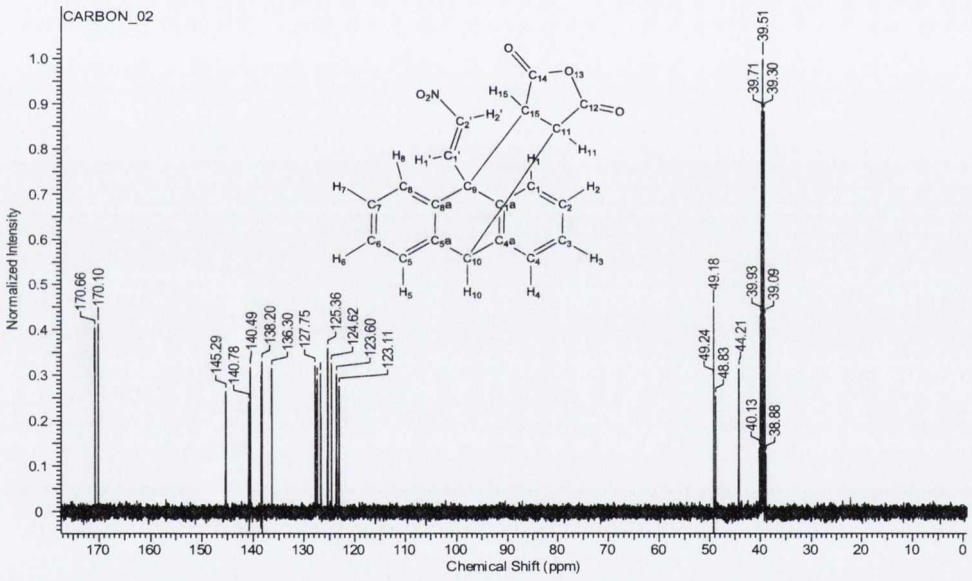

Figure 201: ^{13}C NMR spectrum of (*E*)-9-(2-nitrovinyl)-9,10-dihydro-9,10-[3,4]furanoanthracene-12,14-dione (270)

The ^{13}C NMR spectrum (101 MHz, DMSO-d_6) of compound **270** is displayed in Figure 201. A DEPT 90 NMR spectrum of compound **270** (Figure 202) shows CH signals at 44.21 ppm, 48.83 ppm, 49.24 ppm, 123.11 ppm, 123.60 ppm, 124.62 ppm, 125.36 ppm, 126.66 ppm, 127.32 ppm, 127.39 ppm, 127.75 ppm, 136.30 ppm and 145.29 ppm conversely indicating that signals at 49.18 ppm, 138.20 ppm, 138.40 ppm, 140.49 ppm, 140.78 ppm, 170.10 ppm and 170.66 ppm were corresponding to quaternary carbons.

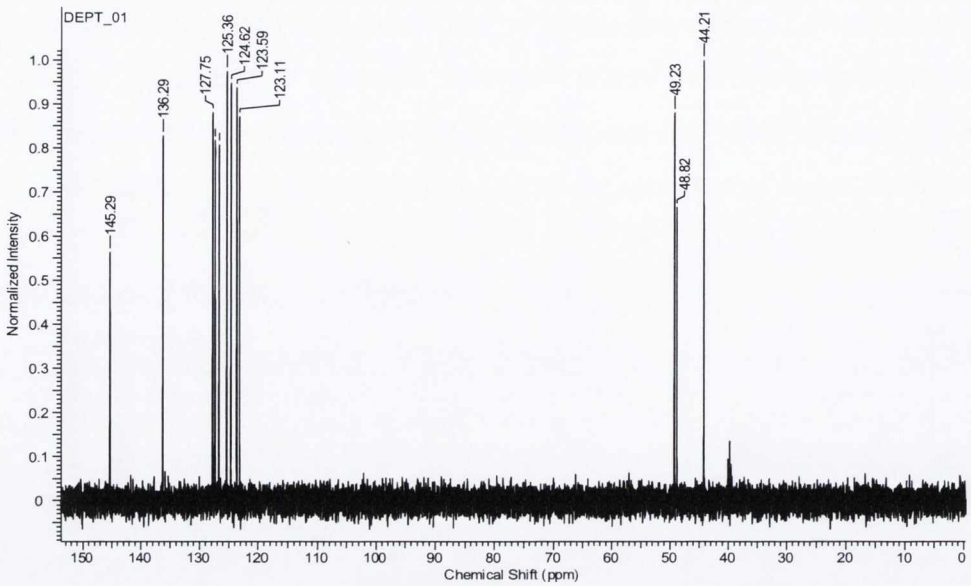

Figure 202: DEPT 90 NMR spectrum of (*E*)-9-(2-nitrovinyl)-9,10-dihydro-9,10-[3,4]furanoanthracene-12,14-dione (270)

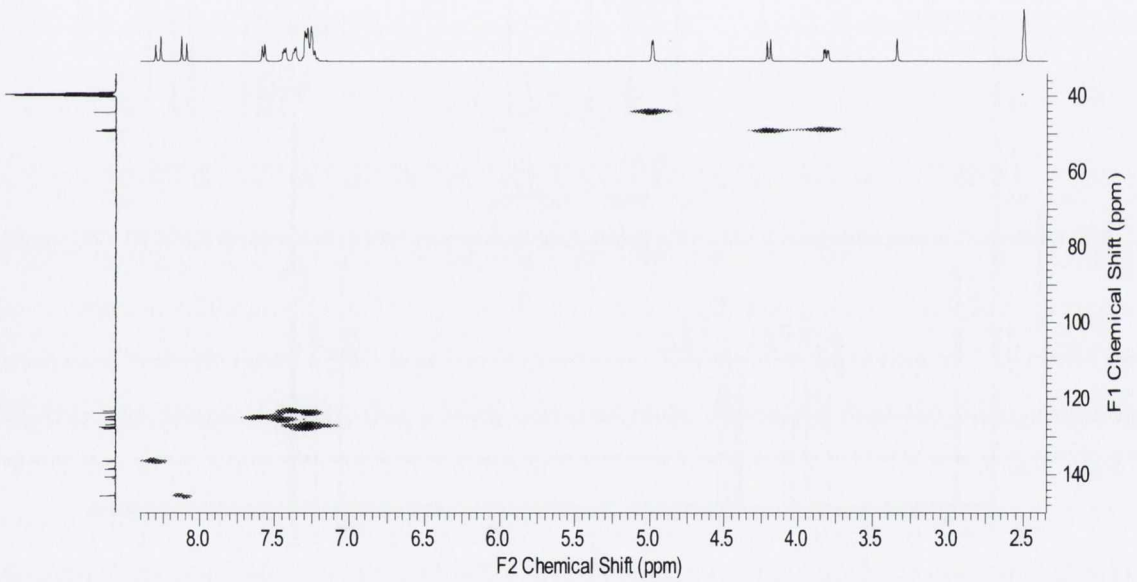

Figure 203: C-H COSY NMR spectrum of (*E*)-9-(2-nitrovinyl)-9,10-dihydro-9,10-[3,4]furanoanthracene-12,14-dione (270)

Utilising the C-H COSY spectrum of compound **270** (Figure 203) and the cumulative data obtained from the DEPT 90 spectra it was possible to assign the carbons of the ethano bridge. CH resonances at 44.21 ppm, 48.83 ppm and 49.24 ppm accounted for C_{10}, C_{11} and C_{15} respectively. The quaternary resonance occurring at 49.18 ppm was therefore assigned to C_9.

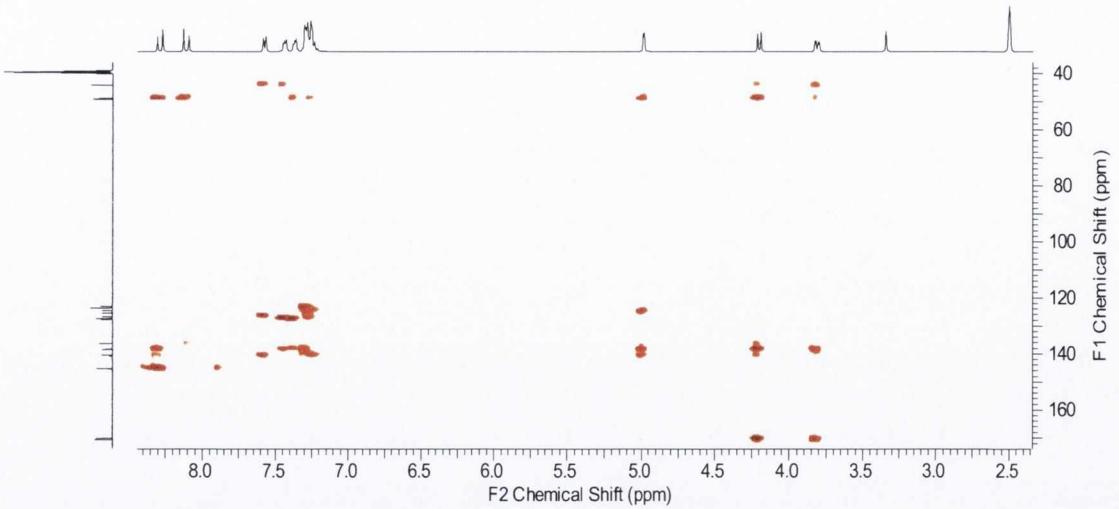

Figure 204: HMBC NMR spectrum of (*E*)-9-(2-nitrovinyl)-9,10-dihydro-9,10-[3,4]furanoanthracene-12,14-dione (270)

In order to assign both the proton and carbon resonances for the nitrovinyl unit it was necessary to run a HMBC experiment (Figure 204), coupling between the doublet representing a single proton in the nitrovinyl unit occurring at 8.28 ppm and three aromatic carbons indicated that this proton signal corresponded to $H_{1'}$. From the C-H COSY this doublet resonance at 8.28 ppm ($H_{1'}$) correlated to the carbon resonance 136.30 ppm. This allowed the assignment of the nitrovinyl carbons $C_{2'}$ and $C_{1'}$ to resonances at 145.29 ppm and 136.30 ppm respectively. Quaternary carbons were observed at 138.20 ppm, 138.40 ppm, 140.49 ppm and 140.78 ppm were allocated to C_{5a}, C_{4a}, C_{8a} and C_{1a}. The more downfield quaternary signals at 170.10 ppm and 170.66 ppm accounted for the carbons in carbonyls at C_{12} and C_{14}. CH resonances at 123.11 ppm, 123.60 ppm, 124.62 ppm, 125.36 ppm, 126.66 ppm, 127.32 ppm, 127.39 ppm and 127.75 ppm account for the remaining eight aromatic carbons

FTIR spectroscopy shows bands at 1860, 1778 (C=O), 1662 (C=C), 1484, 1467 (C=C) and 1525, 1353 (NO_2) cm^{-1}. High resolution mass spectrometry (APCI) was carried out and the required molecular ion was calculated to be $C_{20}H_{12}NO_5$ [M-H] 346.0721 and found as 346.0721.

Single crystal X-ray structure determination was completed on a number of the (*E*)-9-(2-nitrovinyl)-9,10-dihydro-9,10-[3,4]furanoanthracene-12,14-diones (**270**, **276**, **278**, **283**). It was possible to conclude from this data that the packing structure assumed by the products was centrosymmetric and monoclinic. From the asymmetric unit it was possible to confirm both the (*E*) conformation of the nitro vinyl unit and the endo nature of the ethanoanthracene structure (Table 29).

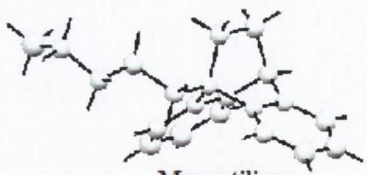

Maprotiline

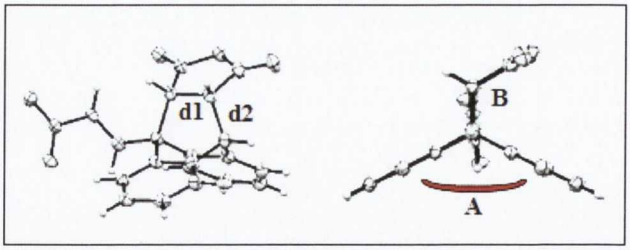

Compound	Structure	Asymmetric Unit	A°	B°	d_1 (Å) C-C	d_2 (Å) C-C
270	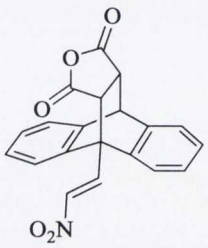	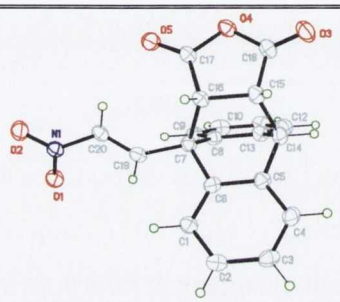	126.08	120.29	1.545	1.56
276	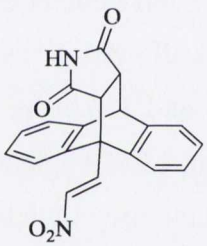	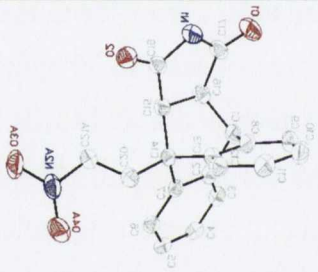	123.17	121.74	1.551	1.549
278	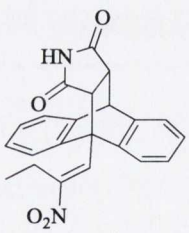	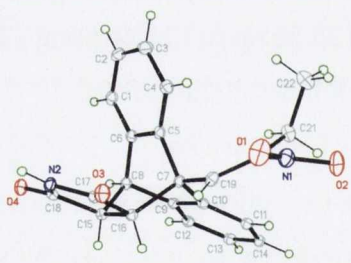	126.11	121.06	1.54	1.557
283	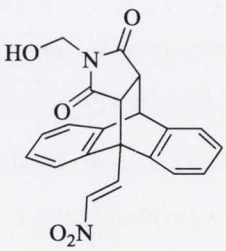	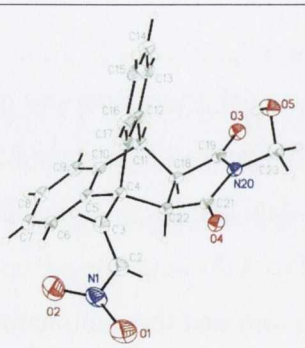	127.92	118.94	1.547	1.567

Table 29: X-ray crystallography data for the (*E*)-9-(2-nitrovinyl)-9,10-dihydro-9,10-[3,4]furanoanthracene-12,14-diones

Table 29 summarises some of the data obtained from crystal structures of compounds for this series. The angle A° was calculated for each compound as the angle between the centroid of phenyl ring 1 and the centroid of phenyl ring 2 – ranging from 123.17-127.92°. This angle is 119.46° in the crystal structure of maprotiline. The angle B° (maleic substituent centroid to centroid of main axis) was also calculated and ranged from 118.94-121.74°. The distance between the carbons in the ethano bridge (d_1) ranged from 1.545-1.551 Å, comparing well to that of maprotiline 1.54 Å. The distance between the carbon at C-10 and the nearest carbon of the ethano bridge (d_2) for the series was 1.549-1.567 Å, in maprotiline this distance is 1.546 Å [380].

9-(2-Nitroethyl)anthracene (**224**) was also reacted with maleic anhydride, maleimide and phenyl-maleimide to give the corresponding Diels-Alder adducts (**284-286**) (Table 30).

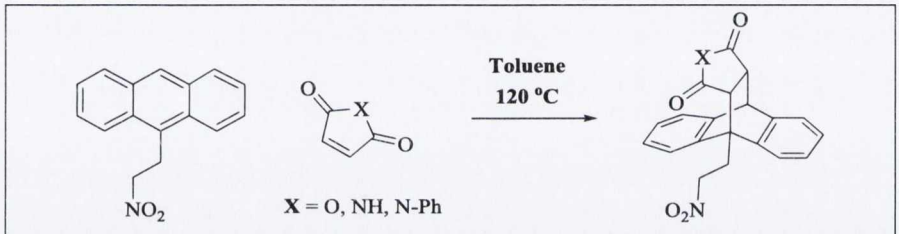

Compound	X	Yield	Melting point
284	O	43%*	242-244 °C
285	NH	45%*	295-297 °C
286	N(C_6H_5)	30%*	248-250 °C

Table 30: 9-(2-nitroethyl)-9,10-dihydro-9,10-[3,4]epipyrroloanthracene-12,14-dione library

The ^{1}H NMR (400 MHz, DMSO-d_6) spectrum of 9-(2-nitroethyl)-9,10-dihydro-9,10-[3,4]furanoanthracene-12,14-dione (**284**) was analogous with the above data for compound **270**. The resonances for the double bond at 8.11 ppm (J = 14.04 Hz, 1 H) and 8.28 ppm (J = 14.04 Hz, 1 H) were replaced by resonances at 3.33-352 ppm (2 H), 5.06ppm (1H, J = 14.65 Hz) and 5.24 ppm (1 H, J = 10.38 Hz). These new resonances accounted for the two new methylene group protons. The ^{13}C NMR (101 MHz, DMSO-d_6) spectrum of 9-(2-nitroethyl)-9,10-dihydro-9,10-[3,4]furanoanthracene-12,14-dione represented these new methylene groups with carbon resonances at 25.60 ppm and 72.81 ppm. High resolution mass spectrometry (APCI) was carried out and the required molecular ion was calculated to be $C_{20}H_{16}NO_5$ [M^++H] 350.1028 and found as 350.1030.

A dimer compound was synthesised from (*E*)-9-(2-nitrovinyl)anthracene and the dimaleimide 1,1'-(hexane-1,6-diyl)bis(1H-pyrrole-2,5-dione). In this reaction the dimaleimide was designed to be the limiting reagent in the presence of two equivalents of (*E*)-9-(2-nitrovinyl)anthracene (**7**) and this reaction afforded 13,13'-(hexane-1,6-diyl)bis(9-((*E*)-2-nitrovinyl)-9,10-dihydro-9,10-[3,4]epipyrroloanthracene-12,14-dione) (**287**) in 10% yield (Figure 205).

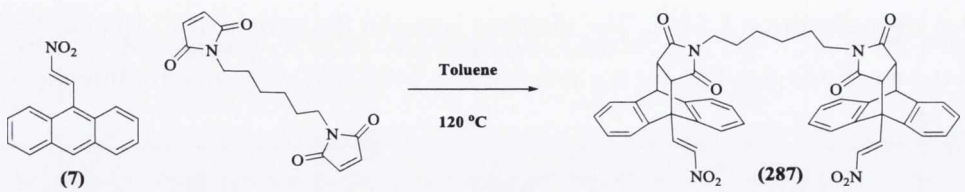

Figure 205: Scheme for the synthesis of 13,13'-(hexane-1,6-diyl)bis(9-((*E*)-2-nitrovinyl)-9,10-dihydro-9,10-[3,4]epipyrroloanthracene-12,14-dione)

The ^{1}H NMR (400 MHz, DMSO-d_6) spectrum of 13,13'-(hexane-1,6-diyl)bis(9-((*E*)-2-nitrovinyl)-9,10-dihydro-9,10-[3,4]epipyrroloanthracene-12,14-dione) (**287**) was analogous with the above data for (*E*)-9-(2-nitrovinyl)-9,10-dihydro-9,10-[3,4]furanoanthracene-12,14-dione (**270**) due to the symmetry within the compound. The spectra presented the ethano bridge protons at 3.36 ppm (double-doublet), 3.76 ppm (double-doublet) and 4.86 - 4.92 ppm (multiplet) as expected, however the integration for this dimer compound was different - with each of these ethano resonances integrating for two protons. Similarly the carbon spectrum presented carbon equivalent resonances for these environments within the dimer with the ethano bridge represented by resonances at 44.45 ppm (C_{10}), 47.24 (C_{11}) and 47.36 ppm (C_{15}). The 12 protons of the hexane bridge were accounted for by three resonances in the proton spectrum at 0.43 ppm (broad singlet, 4 H), 0.47 - 0.57 ppm (m, 4 H) and 2.86 - 2.94 ppm (m, 4 H). This symmetrical environment produced three carbon equivalent environments with CH_2 resonances visible at 25.14 ppm, 26.17 ppm and 37.67 ppm. High resolution mass spectrometry (APCI) was carried out and the required molecular ion was calculated to be $C_{46}H_{39}N_4O_8$ [M+H] 775.2768 and found as 775.2771.

(E)-9-(2-nitrovinyl)-13-phenyl-9,10-dihydro-9,10-[3,4]epipyrroloanthracene-12,14-diones

The (*E*)-9-(2-nitrovinyl)-13-phenyl-9,10-dihydro-9,10-[3,4]epipyrroloanthracene-12,14-diones library (**288-316**) was synthesised from the appropriately substituted (*E*)-9-(2-nitrovinyl)anthracenes *via* Diels-Alder cycloaddition with substituted benzyl and phenyl maleimides with varied substitutions including but not limited to methoxy groups, halogens

(bromine, chlorine & fluorine), alkyl groups, hydroxy and amines. This group of compounds gave yields ranging from 15 to 88% (Table 31 and 32).

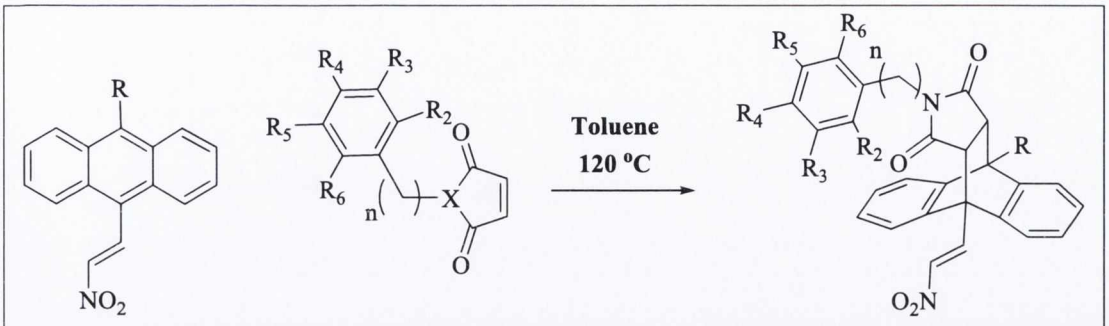

Compound	R	n	Substitution	Yield	Melting point
288	-	0	-	30%*	256-257 °C
289	-	0	$R_4 = Cl$	51%*	238-241 °C
290	-	0	$R_4 = OCH_3$	70%*	240-242 °C
291	Cl	0	-	15%*	263-264 °C
292	-	0	$R_4 = F$	27%*	242-243 °C
293	-	0	$R_3 = R_4 = R_5 = OCH_3$	10%*	270-272 °C
294	-	0	$R_4 = Br$	66%*	267-268 °C
295	-	0	$R_4 = (C=O)OCH_3$	60%*	254-255 °C
296	-	0	$R_4 = (C=O)C_6H_5$	40%*	232-234 °C
297	-	0	$R_4 = N(CH_3)_2$	67%*	280-282 °C
298	-	0	$R_3 = R_5 = OCH_3$	63%*	268-271 °C
299	-	0	$R_3 = Cl$	58%*	258-261 °C
300	-	0	$R_2 = OH$	40%*	203-206 °C
301	-	0	$R_3 = O(C=O)CH_3$	50%*	246-248 °C
302	-	0	$R_4 = NH_2$	45%*	>300 °C

Table 31: (*E*)-9-(2-nitrovinyl)-13-phenyl-9,10-dihydro-9,10-[3,4]epipyrroloanthracene-12,14-dione library. * denotes novel compound. Unless otherwise specified Rn = H.

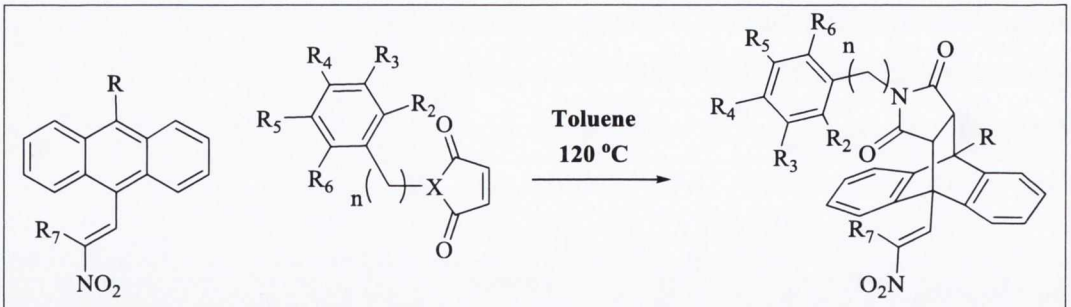

Compound	R	n	R_7	Substitution	Yield	Melting point
303	-	0	CH_3	-	88%*	263-266 °C
304	-	0	CH_2CH_3	-	82%*	259-263 °C
305	-	0	CH_3	$R_4 = Cl$	60%*	298-300 °C
306	-	0	CH_2CH_3	$R_4 = Cl$	44%*	275-279 °C
307	-	0	CH_3	$R_4 = OCH_3$	65%*	276-277 °C
308	-	0	CH_2CH_3	$R_4 = OCH_3$	54%*	254-256 °C
309	Cl	0	CH_3	-	39%*	268-271 °C
310	Cl	0	CH_2CH_3	-	38%*	261-262 °C
311	-	1	H	-	74%*	238-240 °C
312	-	1	CH_3	-	62%*	232-236 °C
313	-	1	CH_2CH_3	-	50%*	188-189 °C
314	-	1	CH_3	$R_3 = R_4 = R_5 = OCH_3$	45%*	227-229 °C
315	-	1	CH_2CH_3	$R_3 = R_4 = R_5 = OCH_3$	54%*	224-228 °C
316	-	2	-	-	77%*	152-156 °C

Table 32: (*E*)-9-(2-nitrovinyl)-13-phenyl-9,10-dihydro-9,10-[3,4]epipyrroloanthracene-12,14-dione library 2. * denotes novel compound. Unless otherwise specified Rn = H.

(*E*)-13-(3,5-dimethoxyphenyl)-9-(2-nitrovinyl)-9,10-dihydro-9,10-[3,4]epipyrroloanthracene-12,14-dione (**298**) was chosen as a representative sample of the (*E*)-9-(2-nitrovinyl)-13-phenyl-9,10-dihydro-9,10-[3,4]epipyrroloanthracene-12,14-diones and the ^1H NMR and ^{13}C NMR spectra will now be discussed in detail. The ^1H NMR (400 MHz,

DMSO-d_6) spectrum of compound **298** (Figure 206) shows a double doublet occurring at 3.53 ppm (J = 8.55, 3.05 Hz) integrating for a single proton, this accounted for H_{11}.

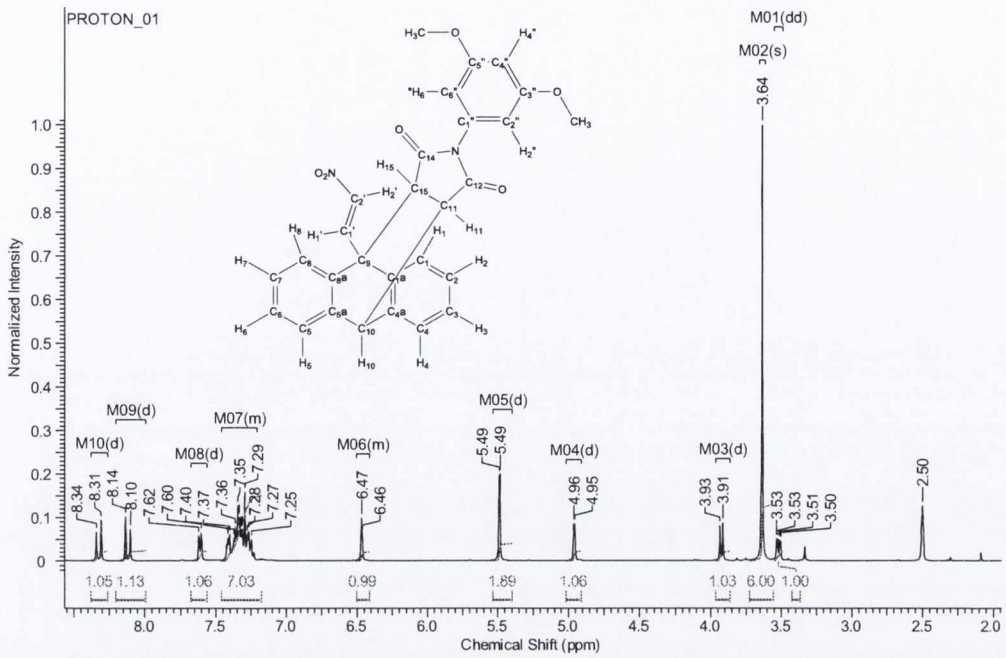

Figure 206: ^{1}H NMR spectrum of (*E*)-13-(3,5-dimethoxyphenyl)-9-(2-nitrovinyl)-9,10-dihydro-9,10-[3,4]epipyrroloanthracene-12,14-dione (298)

The singlet at 3.64 ppm with an integration of six protons was assigned to the six protons on the two equivalent methoxy groups. Doublets occurring at 3.92 ppm (J = 8.55 Hz) and 4.95 ppm (J = 3.05 Hz) both integrating for a single proton each were assigned to H_{15} and H_{10} respectively. A doublet occurring at 5.49 ppm (J = 1.83 Hz) integrated for two protons and was allocated to $H_{2''}$ and $H_{6''}$ whom were coupled long range to H_4. The multiplet at 6.41 - 6.50 ppm integrated for a single proton and was assigned to $H_{4'}$. A doublet observed at 7.61 ppm (J = 6.71 Hz) accounted for H_1 – which occurred more downfield due to the more electronegative environment between the nitrovinyl unit and the carbonyl. A large multiplet occurring at 7.18 - 7.46 ppm integrated for seven protons and accounted for the seven remaining aromatic protons. The remaining doublets occurring at 8.12 ppm (J = 14.04 Hz) and 8.32 ppm (J = 13.43 Hz) both integrated for a single proton each and were assigned to the *trans* coupled protons of the nitrovinyl unit, $H_{2'}$ and $H_{1'}$ respectively.

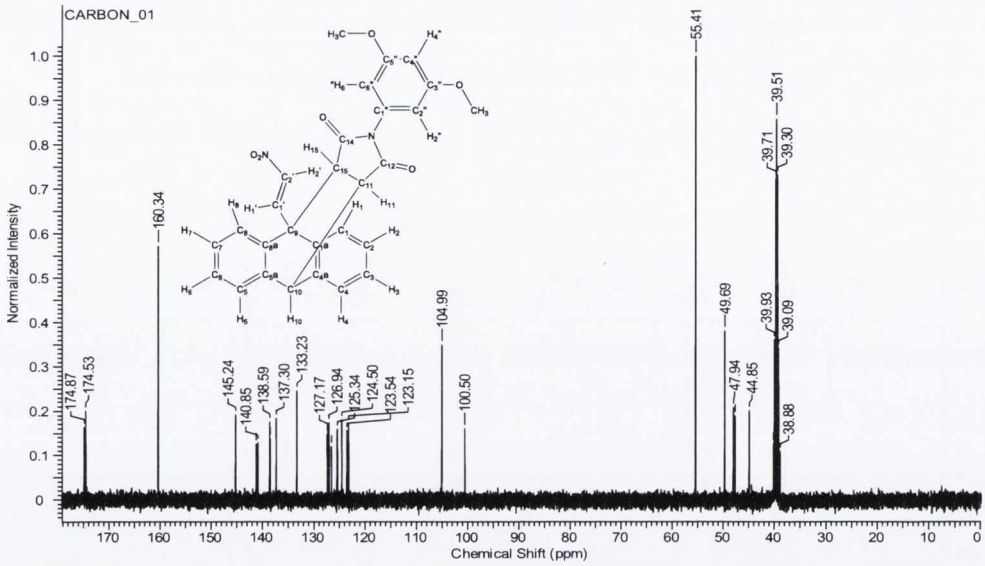

Figure 207: ^{13}C NMR spectrum of (*E*)-13-(3,5-dimethoxyphenyl)-9-(2-nitrovinyl)-9,10-dihydro-9,10-[3,4]epipyrroloanthracene-12,14-dione (298)

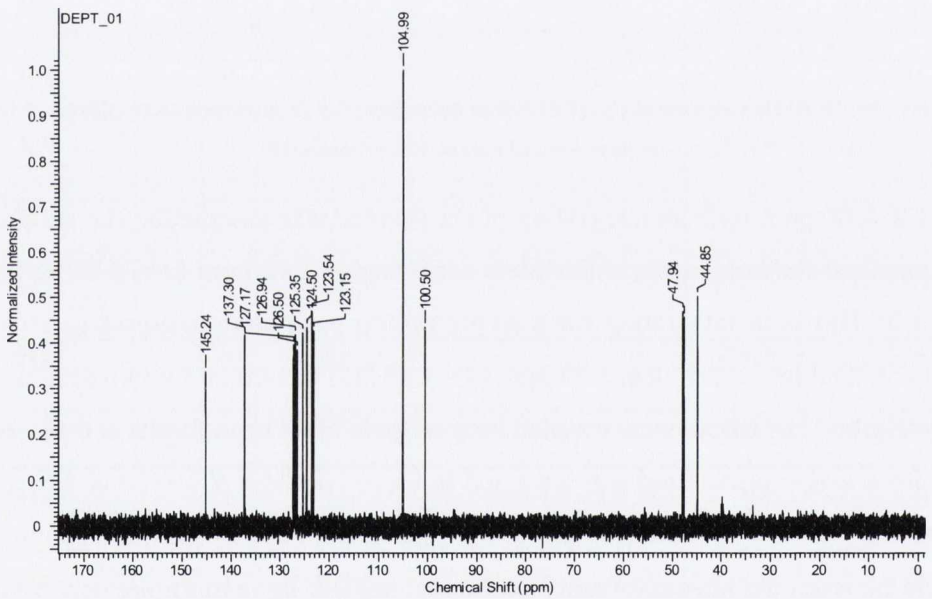

Figure 208: DEPT 90 NMR spectrum of (*E*)-13-(3,5-dimethoxyphenyl)-9-(2-nitrovinyl)-9,10-dihydro-9,10-[3,4]epipyrroloanthracene-12,14-dione (298)

The ^{13}C NMR spectrum (101 MHz, DMSO-d_6) of compound **298** is displayed above in Figure 207. A DEPT 90 NMR spectrum of compound **298** (Figure 208) shows CH signals at 44.85 ppm, 47.65 ppm, 47.94 ppm, 100.50 ppm, 104.99 ppm, 123.15 ppm, 123.54 ppm, 124.50 ppm, 125.34 ppm, 126.50 ppm, 126.94 ppm, 127.17 ppm, 127.29 ppm, 137.30 ppm and 145.24 ppm.

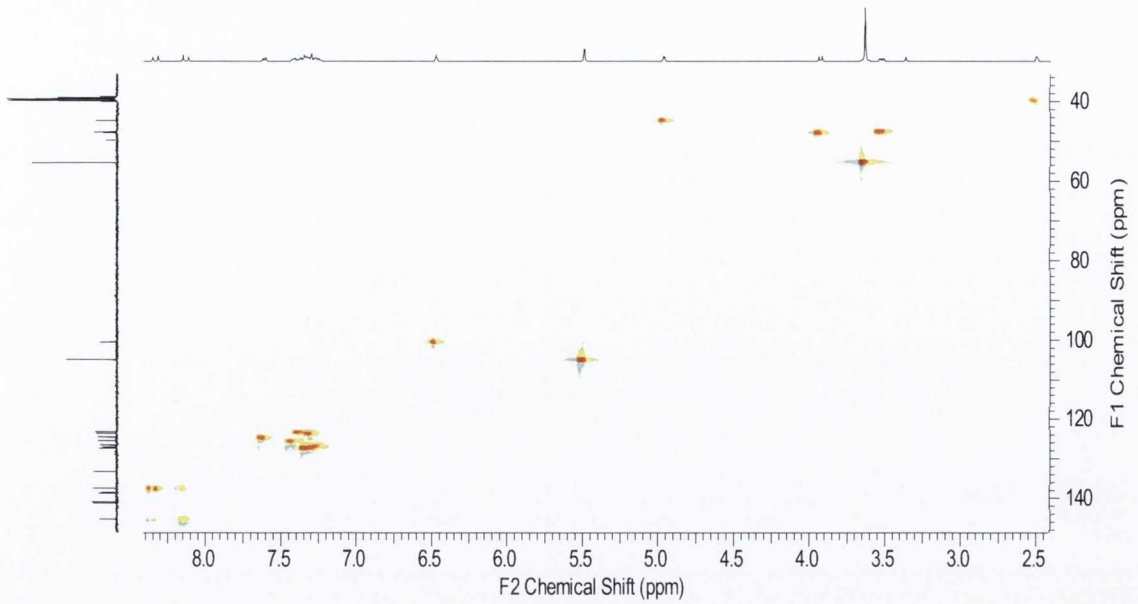

Figure 209: C-H COSY spectrum of (*E*)-13-(3,5-dimethoxyphenyl)-9-(2-nitrovinyl)-9,10-dihydro-9,10-[3,4]epipyrroloanthracene-12,14-dione (298)

Utilising the C-H COSY spectrum of compound 298 (Figure 209) and the cumulative data obtained from the DEPT 90 spectra it was possible to assign the carbons of the ethano bridge. CH resonances occurring at 44.85 ppm, 47.64 ppm and 47.94 ppm were assigned to C_{10}, C_{12} and C_{14}. The quaternary signal at 49.69 ppm was assigned to C_9. The 2 equivalent methoxy substituent carbons on $C_{3''}$ and $C_{5''}$ were represented by a resonance occurring at 55.41 ppm. The CH resonances at 100.50 ppm and 104.99 ppm were allocated to $C_{4''}$ and equivalent carbons $C_{2''}$ & $C_{6''}$ on the phenyl ring adjacent to methoxy substituents. The quaternary signal at 133.23 ppm accounts for $C_{1''}$ in this phenyl ring. The quaternary signals occurring at 138.50 ppm, 138.59 ppm, 140.85 ppm and 141.20 ppm were produced by C_{5a}, C_{4a}, C_{8a} and C_{1a}. The CH resonances occurring at 123.15 ppm, 123.54 ppm, 124.50 ppm, 125.34 ppm, 126.50 ppm, 126.94 ppm, 127.17 ppm and 127.29 ppm account for the remaining aromatic CH carbon environments. Downfield quaternary signals observed at 160.34 ppm, 174.53 ppm and 174.87 ppm were produced in the more electronegative environments at $C_{3''}$ & $C_{5''}$, C_{12} (carbonyl) and C_{14} (carbonyl). The carbons of the nitrovinyl unit $C_{1'}$ and $C_{2'}$ were assigned to 137.30 ppm and 145.24 ppm respectively.

FTIR spectroscopy shows bands at 1714 (C=O), 1601 (C=C), 1531 (NO_2), 1474, 1457 (C=C) and 1159 (C-N) cm^{-1}. High resolution mass spectrometry (APCI) was carried out and

the required molecular ion was calculated to be $C_{28}H_{23}N_2O_6$ [M^++H] 483.1556 and found as 483.1543.

Single crystal X-ray structure determination was completed on a number of the (*E*)-9-(2-nitrovinyl)-13-phenyl-9,10-dihydro-9,10-[3,4]epipyrroloanthracene-12,14-diones (Table 33 & Table 34) It was possible to conclude from this data that the packing structure assumed by the products was centrosymmetric and monoclinic. From the asymmetric unit it was possible to confirm the (*E*) conformation of the nitro vinyl unit.

Compound	Structure	Asymmetric Unit
316	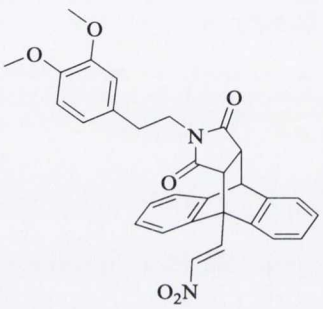	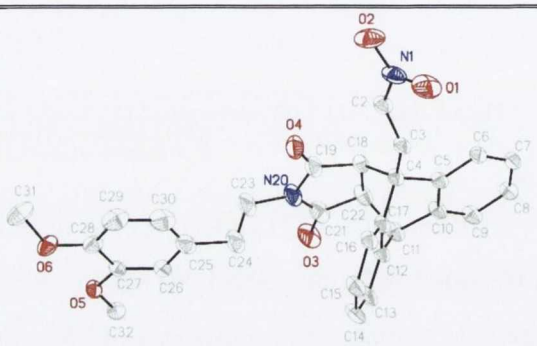
314	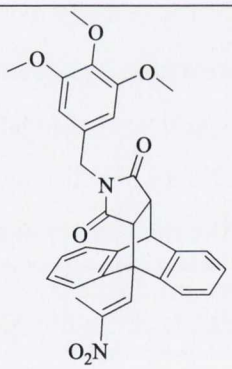	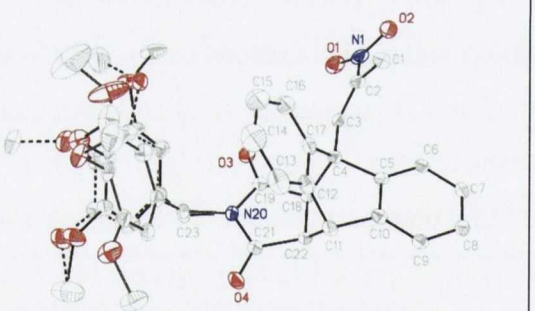

Table 33: X-ray crystallography data for the (*E*)-9-(2-nitrovinyl)-13-phenyl-9,10-dihydro-9,10-[3,4]epipyrroloanthracene-12,14-diones (Part 1)

Compound	Structure	Asymmetric Unit
298	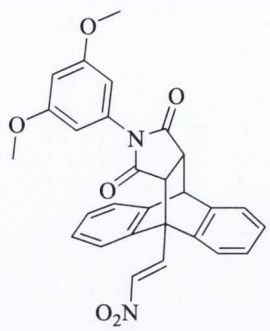	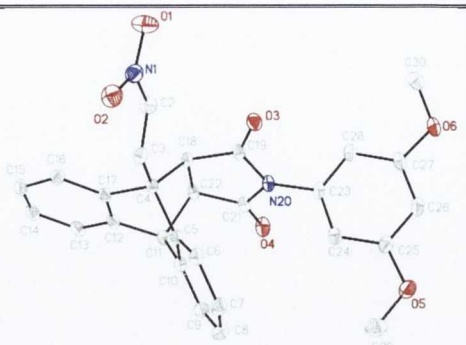
294	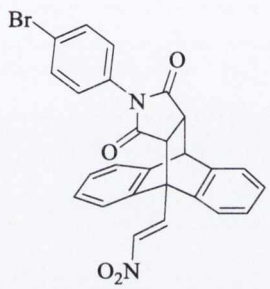	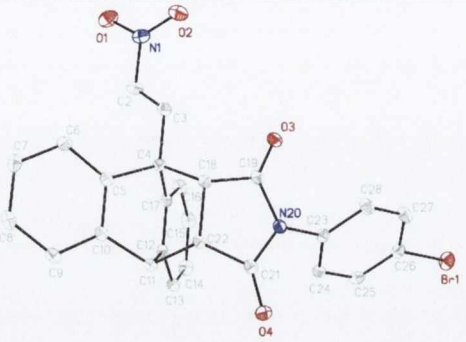
308	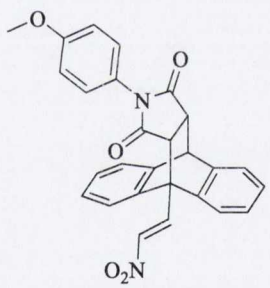	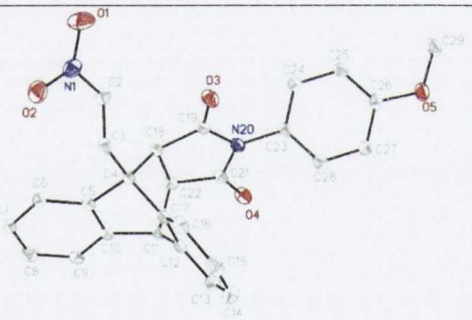
296	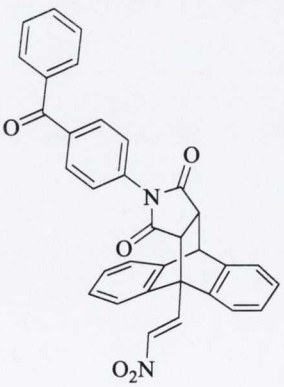	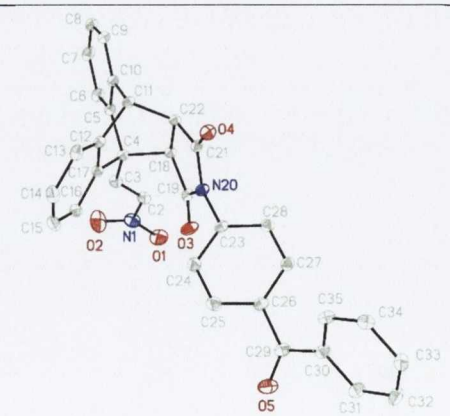

Table 34: X-ray crystallography data for the (*E*)-9-(2-nitrovinyl)-13-phenyl-9,10-dihydro-9,10-[3,4]epipyrroloanthracene-12,14-diones (Part 2)

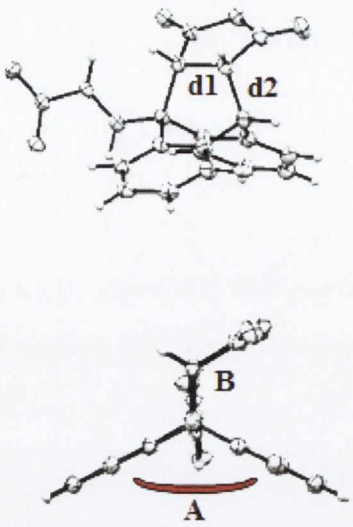

Compound	A°	B°	d_1 (Å) C-C	d_2 (Å) C-C
Maprotiline[380]	119.46	-	1.54	1.546
316	126.73	120.8	1.563	1.573
314	129.35	119.69	1.54	1.557
298	125.99	118.05	1.544	1.563
294	129.16	117.9	1.54	1.582
308	122.05	121.71	1.546	1.555
296	126.82	120.87	1.546	1.563

Table 35: X-ray crystallography assymetric unit analysis

Selected data obtained from crystal structures of compounds for this series of compound **316**, **314**, **298**, **294**, **308** and **296** is summarised in Figure 37. The angle A° was calculated for each compound as the angle between the centroid of phenyl ring 1 and the centroid of phenyl ring 2 – ranging from 122.05-129.16°. This angle is 119.46° in the crystal structure of maprotiline. The angle B° (maleimide substituent centroid to centroid of main axis) was also calculated and ranged from 117.9-121.71°. The distance between the carbons in the ethano bridge (d_1) ranged from 1.542-1.563 Å, comparing well to that of maprotiline 1.54 Å. The distance between the carbon at C-10 and the nearest carbon of the ethano bridge (d_2) for the series was 1.555-1.582 Å, while in maprotiline this distance is 1.546 Å [380].

The Diels-Alder addition of 4-phenyl-3*H*-1,2,4-triazole-3,5(4*H*)-dione to the (*E*)-9-(2-nitrovinyl)anthracenes was also achieved affording (*E*)-9-(2-nitrovinyl)-14-phenyl-9,10-dihydro-9,10-[1,2]epitriazoloanthracene-13,15-dione (**317**) with 68% yield (Figure 210).

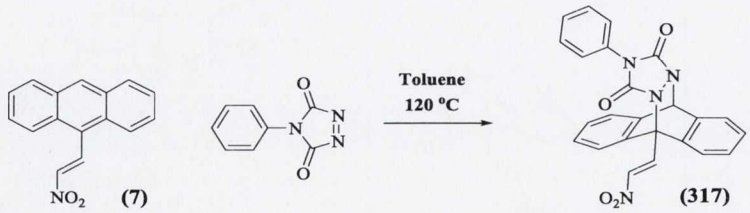

Figure 210: (*E*)-9-(2-nitrovinyl)-14-phenyl-9,10-dihydro-9,10-[1,2]epitriazoloanthracene-13,15-dione

The ^1H and ^{13}C NMR spectra for compound **317** were quite similar to that of the (*E*)-13-(3,5-dimethoxyphenyl)-9-(2-nitrovinyl)-9,10-dihydro-9,10-[3,4]epipyrroloanthracene-12,14-

diones but differed through the absence of signals for the ethano bridge CH resonances in ^{13}C NMR and ethano bridge protons in ^{1}H NMR due this alternative nitrogen-nitrogen bridge.

5.3 Preparation of the (*E*)-9-(2-nitrovinyl)-9,10-dihydro-9,10-ethanoanthracenes

The series of substituted simple (*E*)-9-(2-nitrovinyl)-9,10-dihydro-9,10-ethanoanthracenes (**318-323**) were synthesised using 1-cyanovinyl acetate, methyl acrylate, ethyl acrylate and cyanoacrylate as dienophiles and (*E*)-9-(2-nitrovinyl)anthracene as the diene. During the Diels-Alder addition of the above dienophiles two addition products were possible, an '*ortho*' and a '*meta*' addition product. For example the Diels-Alder addition of cyanoacrylate to diene systems such as 9-anthraldehyde and (*E*)-3-(anthracen-9-yl)acrylonitrile has been previously documented as forming the *ortho* addition adduct only[6, 381].

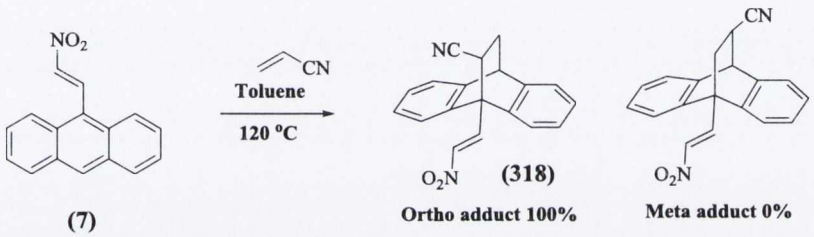

Figure 211: Adducts possible during the reaction of cyanoacrylate and (*E*)-9-(2-nitrovinyl)anthracene.

Alston et al. (1979) accredited this *'ortho'* adduct preference to the stabilising molecular orbital overlap between the nitrile and the carbonyl group[9]. ^{1}H NMR and X-ray crystallography has also, in this work been used to confirm the exclusive formation of the *ortho* adduct (**318**) from the reaction of acrylonitrile and (*E*)-9-(2-nitrovinyl)anthracene (Figure 211).

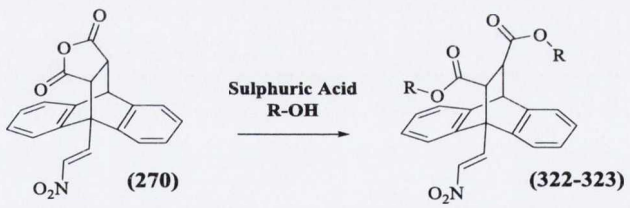

Figure 212: Preparation of of dimethyl and diethyl (*E*)-9-(2-nitrovinyl)-9,10-dihydro-9,10-ethanoanthracene-11,12-dicarboxylate

The synthesis of dimethyl and diethyl (*E*)-9-(2-nitrovinyl)-9,10-dihydro-9,10-ethanoanthracene-11,12-dicarboxylates (**322**, **323**) achieved from (*E*)-9-(2-nitrovinyl)-9,10-dihydro-9,10-[3,4]furanoanthracene-12,14-dione (**270**) using the acid catalysed ring opening conditions previously applied to 9,10-dihydro-9,10-[3,4]furanoanthracene-12,14-dione[382] (Figure 212). The mechanism for this reaction is quite straightforward and initiates with the protonation of a carbonyl in the dione system. Nucleophilic attack of the desired alcohol takes place at the protonated carbonyl resulting in intramolecular deprotonation of the addition

intermediate by the ester oxygen – resulting in protonation of the five membered ring and subsequent decyclisation to the mono ester intermediate (Figure 213). Similarly protonation, nucleophilic attack, deprotonation of the addition intermediate and elimination of water leads to the esterification of the second acid functionality giving the desired ring opened dimethyl and diethyl (*E*)-9-(2-nitrovinyl)-9,10-dihydro-9,10-ethanoanthracene-11,12-dicarboxylates (**322**, **323**).

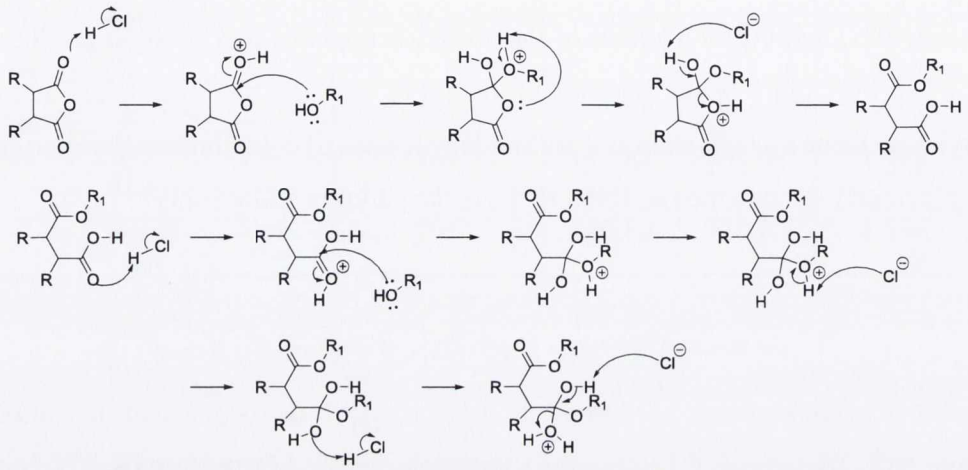

Figure 213: Mechanism for the synthesis of dimethyl and diethyl (*E*)-9-(2-nitrovinyl)-9,10-dihydro-9,10-ethanoanthracene-11,12-dicarboxylate from (*E*)-9-(2-nitrovinyl)-9,10-dihydro-9,10-[3,4]furanoanthracene-12,14-dione

The library of substituted (*E*)-9-(2-nitrovinyl)-9,10-dihydro-9,10-ethanoanthracenes (**318-323**) was prepared from (*E*)-9-(2-nitrovinyl)anthracene and the corresponding dienophiles affording yields of 15-35% or *via* a ring opening reaction affording yields of 15-32%. This library is summarized in Table 36.

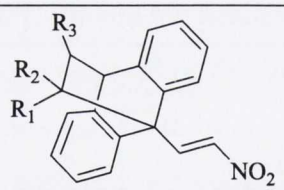

Compound	Substitution	Yield	Melting point
318	R_1 = CN, R_2 = H, R_3 = H	30%*	223-225 °C
319	R_1 = (C=O)OCH_2CH_3, R_2 = H, R_3 = H	18%*	Oil
320	R_1 = (C=O)OCH_3, R_2 = H, R_3 = H	15%*	Oil
321	R_1 = O(C=O)CH_3, R_2 = CN, R_3 = H	35%*	168-170 °C
322	R_1 = R_3 = (C=O)OCH_3, R_2 = H	32%*	141-143 °C
323	R_1 = R_3 = (C=O)OCH_2CH_3, R_2 = H	15%*	151-152 °C

Table 36: (*E*)-9-(2-nitrovinyl)-9,10-dihydro-9,10-ethanoanthracene library. * denotes novel compound

(*E*)-10-(2-Nitrovinyl)-9,10-dihydro-9,10-ethanoanthracene-11-carbonitrile (**318**) was chosen as a representative sample of the simple (*E*)-9-(2-nitrovinyl)-9,10-dihydro-9,10-ethanoanthracenes and the ^{1}H NMR and ^{13}C NMR spectra will now be discussed in detail. The ^{1}H NMR (400 MHz, DMSO-d_6) spectrum of compound **318** (Figure 214) shows a doublet of triplets occurring at 1.96 ppm (J = 12.82, 3.36 Hz) and a doublet of double doublets occurring at 2.30 ppm (J =12.67, 10.53, 2.44 Hz) both integrating for a singlet proton each, these were assigned to H_{12a} and H_{12b} respectively.

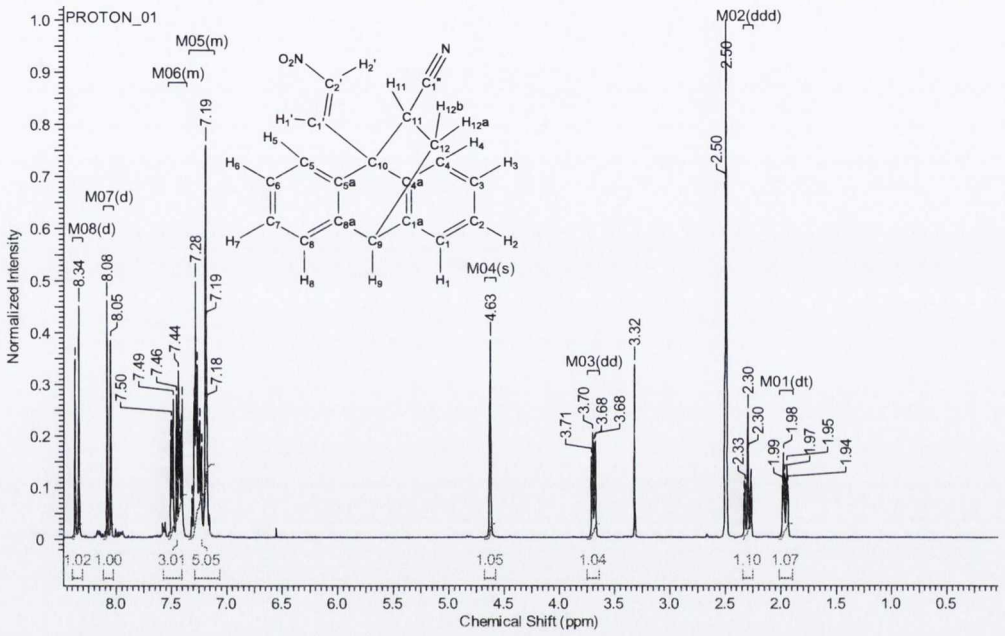

Figure 214: ^{1}H NMR spectrum of (*E*)-10-(2-nitrovinyl)-9,10-dihydro-9,10-ethanoanthracene-11-carbonitrile (318)

A doublet of doublets occurring at 3.69 ppm (J = 10.68, 3.97 Hz) and a singlet at 4.63 ppm account for the remaining bridging protons H_{11} and H_9. Two multiplets at 7.11 - 7.34 ppm (5 H) and 7.36 - 7.53 ppm (3 H) accounted for the eight aromatic protons. The downfield doublets occurring at 8.07 ppm (J = 13.43 Hz) and 8.36 ppm (J = 14.04 Hz) both integrated for single protons and were assigned to the *trans* coupled nitrovinyl protons, $H_{1'}$ and $H_{2'}$.

A H-H COSY NMR spectrum of compound **318** is displayed below in Figure 215. This H-H COSY experiment was utilised to confirm the *ortho* confirmation of the ethano bridge. The inequivalent methylene proton signals (attributed to the CH_2) at 1.96 ppm and 2.30 ppm (1 proton each) were observed to couple to the doublet of doublets occurring at 3.69 ppm. The singlet at 4.63 ppm (integrating for one proton) was also found to couple to these CH_2 signals at 1.96 ppm and 2.30 ppm, implying that these CH_2 protons are between the other two proton environments (i.e. between C_9 and C_{11}) on C_{12} of the ethano bridge. In the case of the *meta* adduct no coupling would be observed between the proton on C_9 and the CH_2 protons on C_{12}.

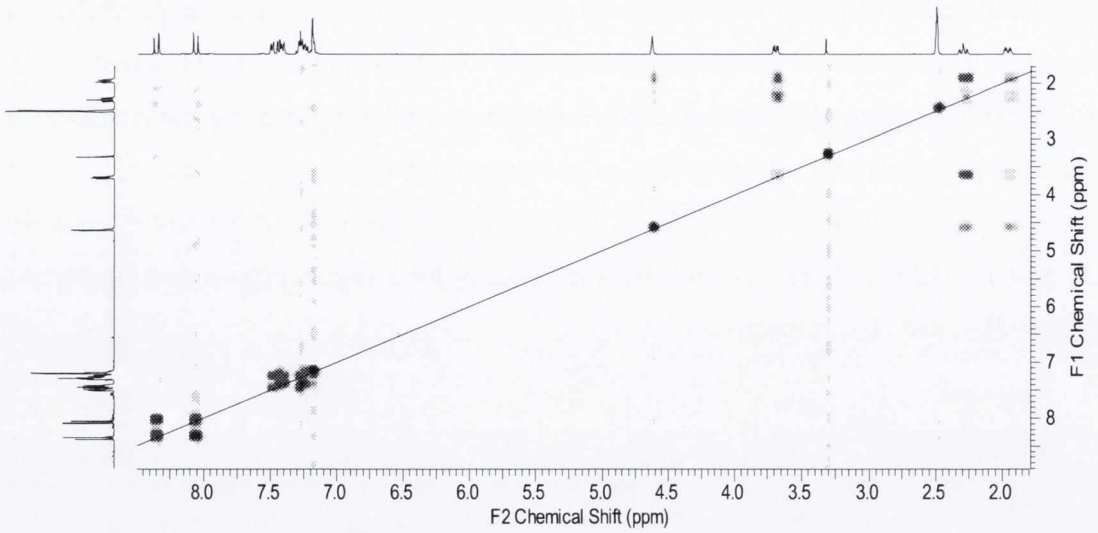

Figure 215: H-H COSY spectrum of (*E*)-10-(2-nitrovinyl)-9,10-dihydro-9,10-ethanoanthracene-11-carbonitrile (318)

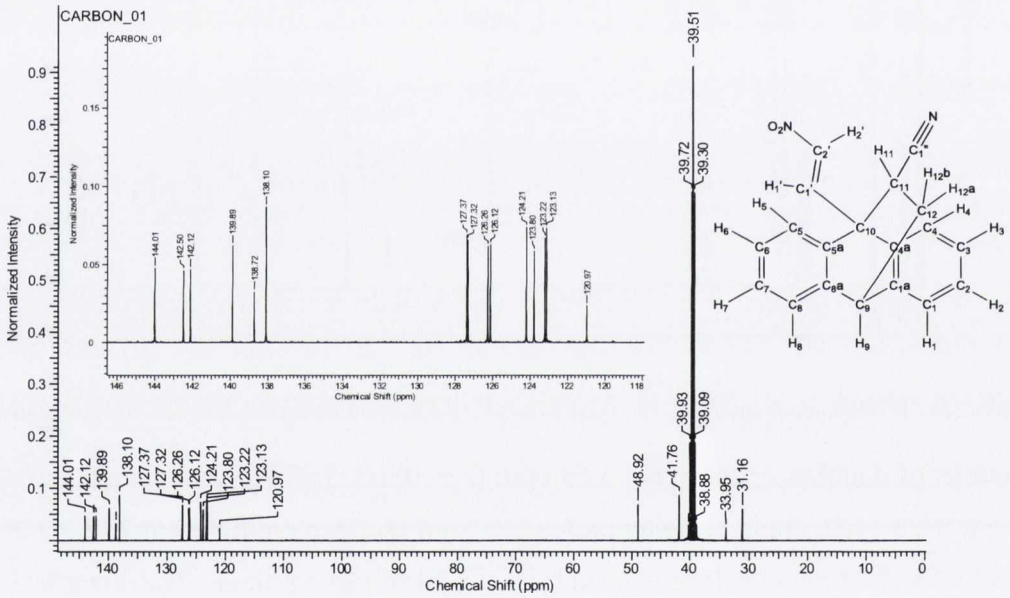

Figure 216: ^{13}C NMR spectrum of (*E*)-10-(2-nitrovinyl)-9,10-dihydro-9,10-ethanoanthracene-11-carbonitrile (318)

The ^{13}C NMR spectrum (101 MHz, DMSO-d_6) of compound **318** is displayed in Figure 216. A DEPT 135 NMR spectrum of compound **318** (Figure 217) shows CH signals at 31.16 ppm, 41.76 ppm, δ 123.13 ppm, 123.21 ppm, 123.80 ppm, 124.21 ppm, 126.12 ppm, 126.26 ppm, 127.32 ppm, 127.36 ppm, 138.09 ppm and 144.01 ppm. A DEPT 135 spectrum shows an inverted signal at 33.94 ppm, corresponding to a CH_2 resonance (Figure 217).

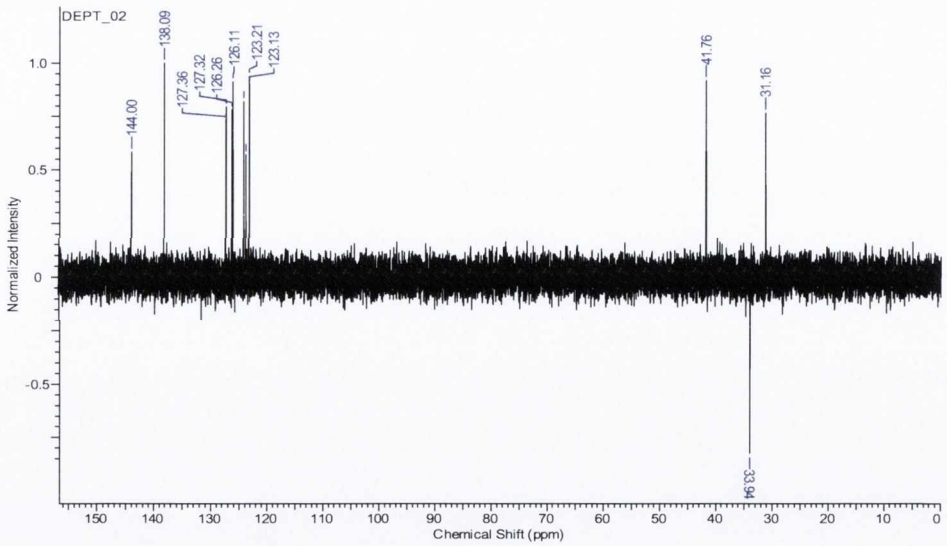

Figure 217: DEPT 135 spectrum of (*E*)-10-(2-nitrovinyl)-9,10-dihydro-9,10-ethanoanthracene-11-carbonitrile (318)

Utilising the C-H COSY spectrum of compound **318** (Figure 218) and the cumulative data obtained from the DEPT 135 spectrum it was possible to assign the carbons of the ethano bridge. CH resonances at 31.16 ppm and 41.76 ppm were assigned to C_{11} and C_9 respectively. The quaternary signal occurring at 48.92 ppm was allocated to C_9, while the CH_2 resonance at 33.94 ppm accounted for C_{12}.

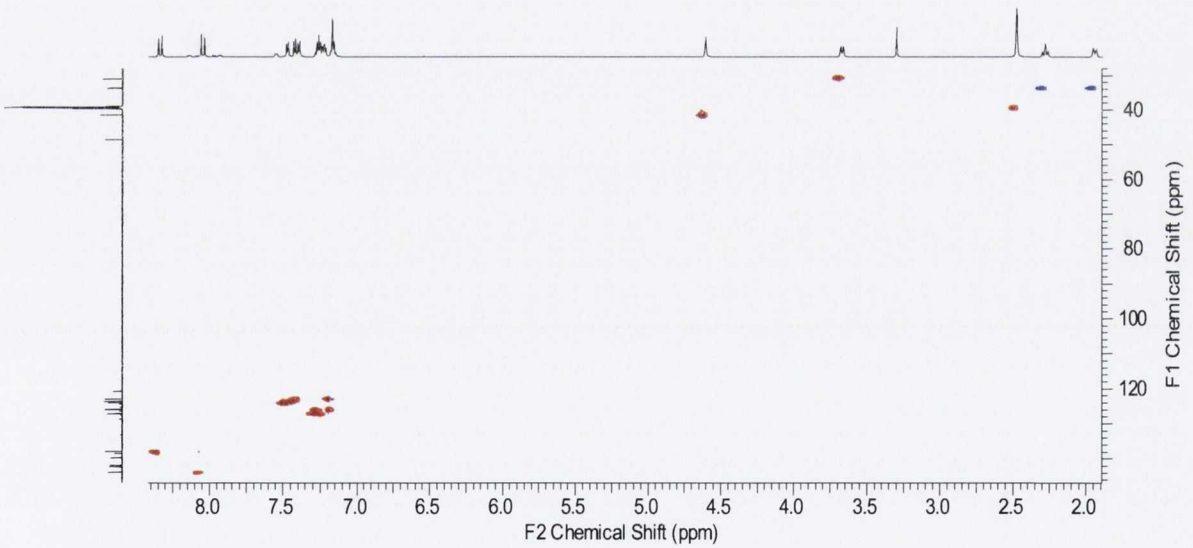

Figure 218: C-H COSY spectrum of (*E*)-10-(2-nitrovinyl)-9,10-dihydro-9,10-ethanoanthracene-11-carbonitrile (318)

The CH resonances at 138.10 ppm and 144.01 ppm correlated to H_1' and H_2' respectively and were therefore assigned to C_1' and C_2'. Quaternary resonance occurring at 120.97 ppm was assigned to the nitrile carbon. The four other quaternary resonances occurring at 138.72 ppm, 139.89 ppm, 142.12 ppm and 142.50 ppm were allocated to C_{8a}, C_{1a}, C_{4a} and C_{5a}. The CH resonances observed at 123.13 ppm, 123.21 ppm, 123.80 ppm, 124.21 ppm,

126.12 ppm, 126.26 ppm, 127.32 ppm, 127.37 ppm were assigned to the remaining eight aromatic carbons. FTIR spectroscopy shows bands at 1658 (C=C), 1485, 1457 (C=C), 1526, 1354 (NO_2) and 1190 (CN) cm^{-1}. High resolution mass spectrometry (APCI) was carried out and the required molecular ion was calculated to be $C_{19}H_{14}N_2O_2$ [M^+] 302.1055 and found as 302.1055.

X-ray crystallographic analysis was determined for the novel Diels-Alder adduct (*E*)-10-(2-nitrovinyl)-9,10-dihydro-9,10-ethanoanthracene-11-carbonitrile (**318**) (Figure 219). It was possible to conclude from this data that the packing structure assumed by the product was centrosymmetric and monoclinic. From the asymmetric unit it was possible to verify the formation of the *ortho* product (discussed earlier) and confirm the (*E*) configuration of the nitro vinyl unit. The angle A° was calculated for this compound as the angle between the centroid of phenyl ring 1 and the centroid of phenyl ring 2 – 126.94°. This angle is 119.46° in the crystal structure of maprotiline. The distance between the carbons in the ethano bridge (d_1) was 1.565 Å, comparing well to that of maprotiline 1.54 Å. The distance between the carbon at C-10 and the nearest carbon of the ethano bridge (d_2) was 1.556 Å, in maprotiline this distance is 1.546 Å.

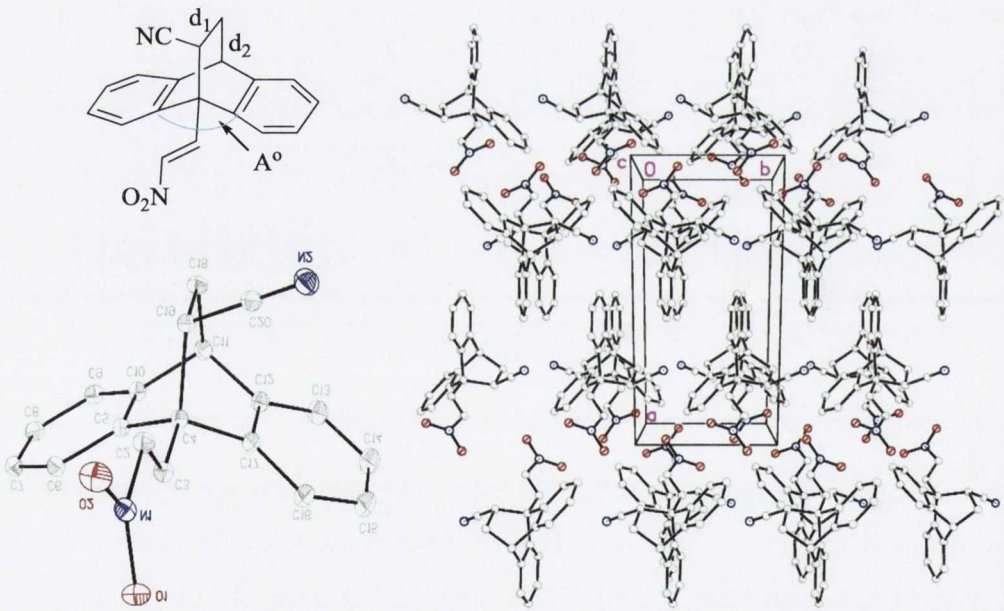

Figure 219: X-ray crystallography data: Asymmetric unit and packing structure of (*E*)-10-(2-nitrovinyl)-9,10-dihydro-9,10-ethanoanthracene-11-carbonitrile (318)

5.4 Preparation of the 9 & 10-substituted-9,10-dihydro-9,10-[1,2]benzenoanthracenes

Triptycenes are a class of compound first introduced by Bartlett et al. in 1942, Bartlett et al. Triptycene was prepared *via* a six step synthetic route from the Diels-Alder adduct of benzoquinone and anthracene[383] (Figure 220). Triptycenes have since been prepared directly from the reaction of anthracene and benzyne; benzyne must be produced *in situ* due to its unstable nature. Benzyne can be produced *in situ* by a number of different methods for example Wittig et al. (1958) produced benzyne through the reaction of halogenated benzenes with magnesium and *n*-butyllithium[384]. Cadogen et al. (1967) similarly used potassium *tert* butoxide and aryl halides to produce benzyne[385].

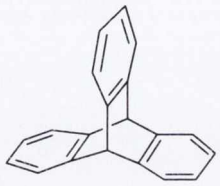

Figure 220: Triptycene

A more popular method is the reaction of anthranilic acid and amyl nitrate to form benzenediazonium-2-carboxylate. Benzenediazonium-2-carboxylate degrades thermally to give benzyne, nitrogen and carbon dioxide[386] (Figure 221). A mixture of the required diene is refluxed in the presence of anthranilic acid and amyl nitrate is added to the reaction mixture *via* syringe pump or portionwise to generate benzyne over a long reaction period[387, 388]. Kornfield et al. (1965) applied this method of benzyne generation to give a series of 9-substituted anthracenes[105].

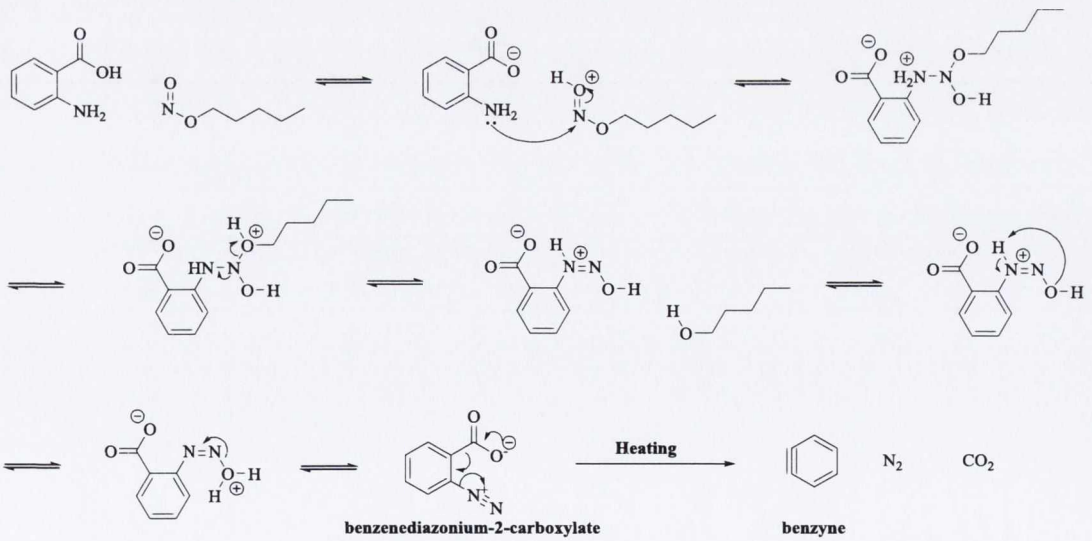

Figure 221: Diazotisation of 2-aminobenzoic acid to give benzenediazonium-2-carboxylate. Decomposition of benzenediazonium-2-carboxylate to give benzyne

Yamamoto et al. (2006) achieved good yields of triptycene based structures by prior preparation of benzenediazonium-2-carboxylate slurry and added this portionwise to a refluxed solution of the diene. The preparation of the benzenediazonium-2-carboxylate slurry had been previously documented by Logullo et al. in 1968[386, 387]. This method produced a much higher yield of triptycene product over a short reaction period of 1 hour – it was this procedure that was selected for the current work. Diphenyl and triphenyl side products have been isolated using *in situ* benzyne generation but these were not isolated during the current work[386].

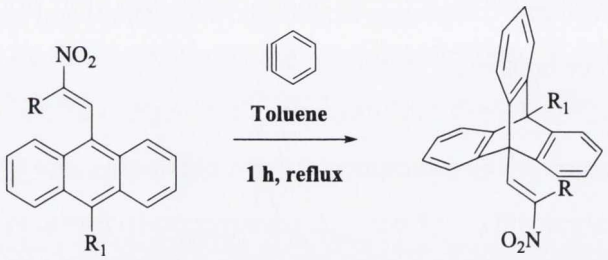

(7, 41, 210,211) **(324 - 327)**

Figure 222: General scheme for the synthesis of (*E*)-9-(2-nitrovinyl)-9,10-dihydro-9,10-[1,2]benzenoanthracenes (324-327)

In the present work a panel of (*E*)-9-(2-nitrovinyl)anthracenes were converted into the corresponding (*E*)-9-(2-nitrovinyl)-9,10-dihydro-9,10-[1,2]benzenoanthracenes (**324-327**) through a Diels-Alder reaction with benzyne generated *in situ* by thermal decomposition of benzenediazonium-2-carboxylate (Figure 222) (Table 37). (*E*)-9-(2-nitrovinyl)-9,10-dihydro-9,10-[1,2]benzenoanthracene (**324**) was previously synthesised by Brunovlenskaya et al. in 1975 via the gradual addition of amyl nitrate described earlier[378]. The addition of benzyne to 9-anthraldehyde was also achieved following the method described above. Sodium borohydride was used to reduce both 9,10-[1,2]benzenoanthracene-9(10H)-carbaldehyde (**329**) and (*E*)-9-(2-nitrovinyl)-9,10-dihydro-9,10-[1,2]benzenoanthracene (**330**) to their alcohol and nitroalkane analogues respectively.

The *in situ* generation and addition of benzyne to the chosen dienes (nitrovinyl anthracenes & 9-anthraldehyde) gave modest yields of 20-32% after purification by column chromatography. The library of novel triptycene analogues synthesised are summarised in Table 37.

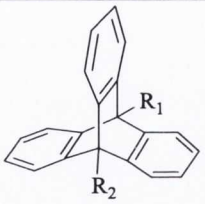

NV = 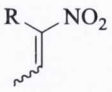

Compound	R_1	R_2	R	Yield	Melting point
324	H	NV	H	20%	258-260 °C
325	H	NV	CH_3	23%*	226-228 °C
326	H	NV	CH_2CH_3	32%*	210-211 °C
327	Cl	NV	H	30%*	259-261 °C
328	H	$CH_2CH_2NO_2$	-	80%*	185-187 °C
329	H	CHO	-	21%	242-244 °C
330	H	CH_2OH	-	85%	240-242 °C

Table 37: 9 & 10-substituted-9,10-dihydro-9,10-[1,2]benzenoanthracene library. * denotes novel compound

(*E*)-9-Chloro-10-(2-nitrovinyl)-9,10-dihydro-9,10-[1,2]benzenoanthracene (**327**) was chosen as a representative sample of the 9 & 10-substituted-9,10-dihydro-9,10-[1,2]benzenoanthracenes and the ^{1}H NMR and ^{13}C NMR spectra will now be discussed in detail.

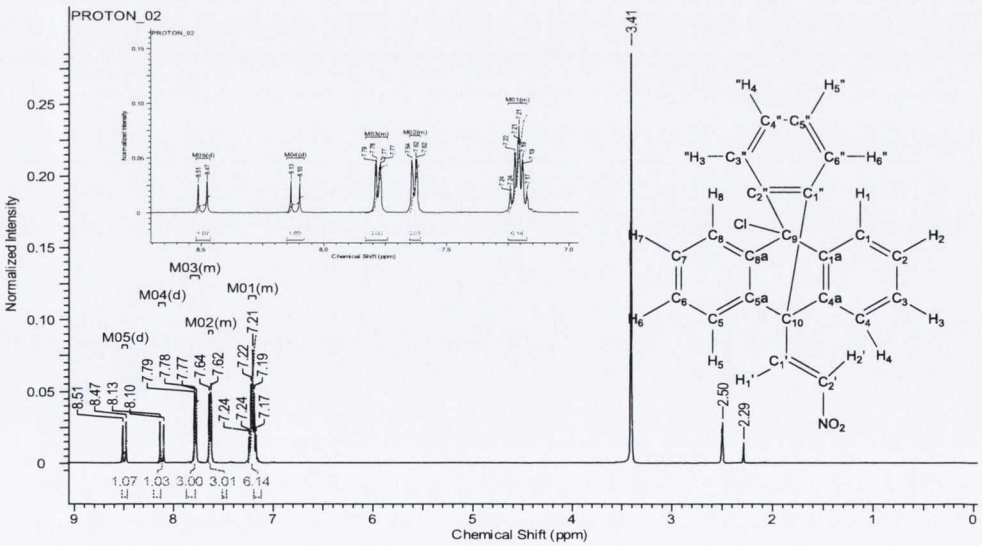

Figure 223: ^{1}H NMR spectrum of (*E*)-9-chloro-10-(2-nitrovinyl)-9,10-dihydro-9,10-[1,2]benzenoanthracene (327)

The ^{1}H NMR (400 MHz, DMSO-d_6) spectrum of compound **327** (Figure 223) shows two multiplets occurring at 7.58 - 7.69 ppm and 7.72 – 7.82 ppm both integrating for three protons each. These signals were assigned to the two groups of three equivalent protons on the compound: H_1, H_8 & $H_{3''}$ and H_4, H_5 & $H_{6''}$ respectively. The remaining six aromatic protons were accounted for by a multiplet occurring at 7.15 - 7.29 ppm integrating for six protons (H_2, H_3, H_6, H_7, $H_{5''}$ & $H_{4''}$). The downfield doublets occurring at 8.12 ppm (J = 14.04 Hz) and 8.50 ppm (J = 14.65 Hz) both integrated for single protons and were assigned to the *trans* coupled nitrovinyl protons, $H_{1'}$ and $H_{2'}$.The ^{13}C NMR spectrum (101 MHz, DMSO-d_6) of compound **327** is displayed in Figure 224.

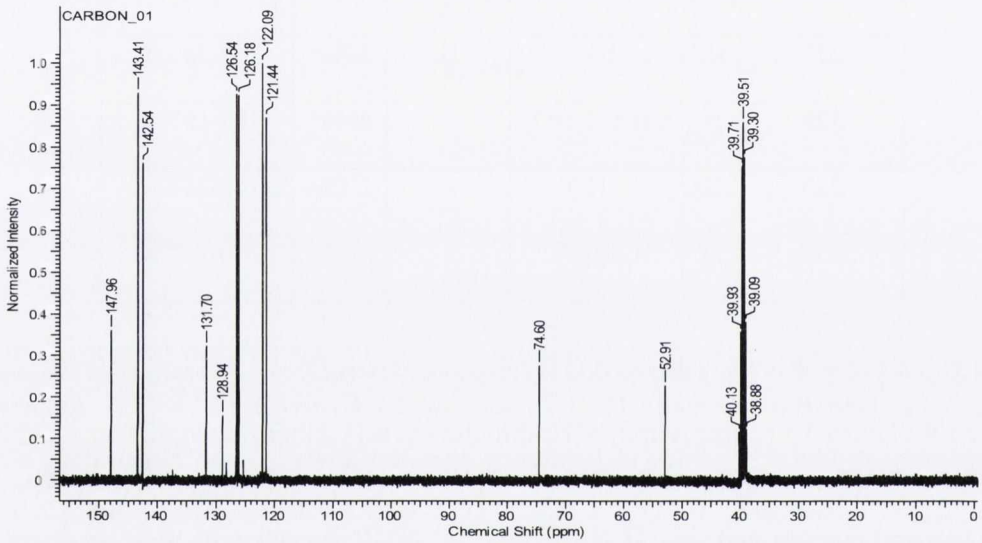

Figure 224: ^{13}C NMR spectrum of (*E*)-9-chloro-10-(2-nitrovinyl)-9,10-dihydro-9,10-[1,2]benzenoanthracene (327)

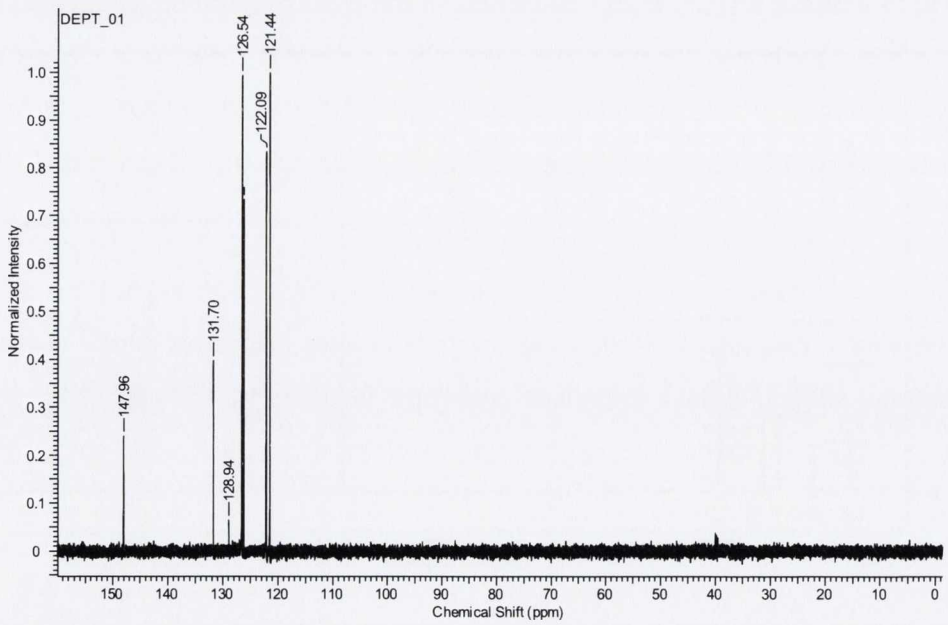

Figure 225: DEPT 90 spectrum of (*E*)-9-chloro-10-(2-nitrovinyl)-9,10-dihydro-9,10-[1,2]benzenoanthracene (327)

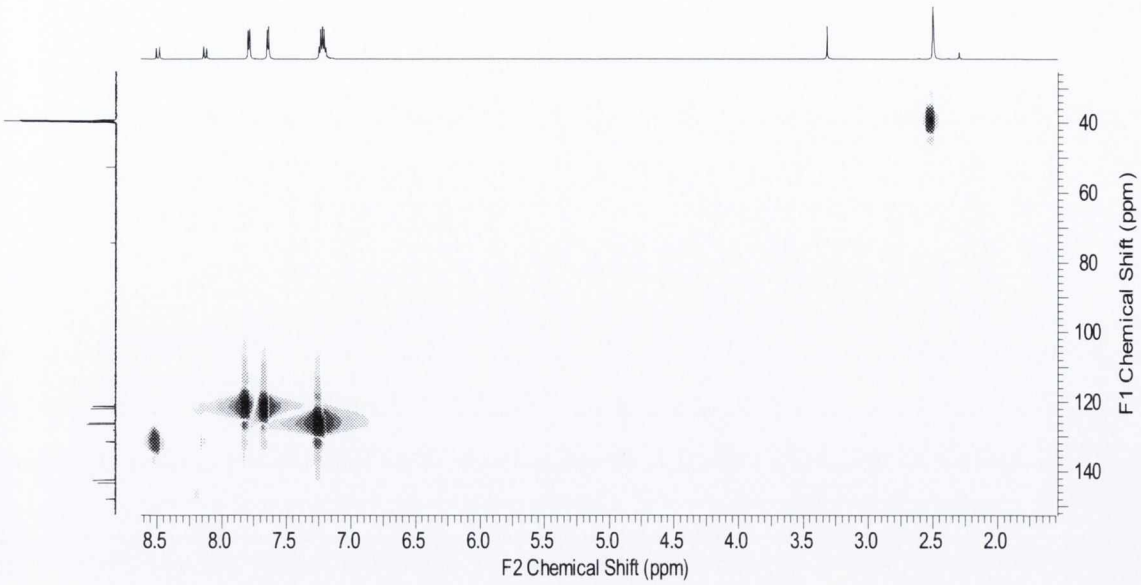

Figure 226: C-H COSY spectrum of (*E*)-9-chloro-10-(2-nitrovinyl)-9,10-dihydro-9,10-[1,2]benzenoanthracene (327)

A DEPT 90 NMR spectrum of compound **327** (Figure 225) shows CH signals at 121.44 ppm, 122.09 ppm, 126.18 ppm, 126.54 ppm, 128.94 ppm, 131.70 ppm and 147.96 ppm. In order to accurately assign the carbon spectrum of compound **327** a C-H COSY (Figure 226) and HMBC (Figure 227) experimental spectra were collected. Quaternary resonances occurring at 52.91 ppm and 74.60 ppm were assigned to C_{10} and C_9 respectively, C_9 appearing further downfield due to the electron withdrawing effect of the attached chlorine atom.

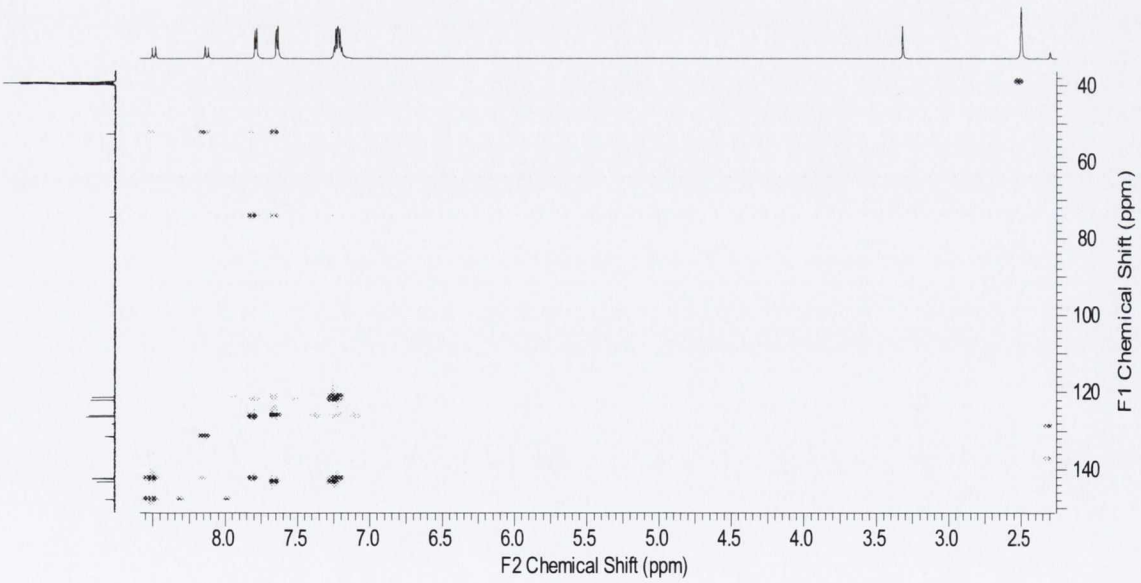

Figure 227: HMBC spectrum of (*E*)-9-chloro-10-(2-nitrovinyl)-9,10-dihydro-9,10-[1,2]benzenoanthracene (327)

CH resonances at 121.44 ppm and 122.09 ppm correlated to proton multiplets occurring at 7.58 - 7.69 ppm and 7.72 – 7.82 ppm, both integrating for three protons each. From the HMBC it

was observed that these multiplets were coupled to the quaternary carbons C_9 and C_{10} indicating proximity to these carbons. Therefore these CH resonances at 121.44 ppm and 122.09 ppm were assigned to carbon equivalent C_5, C_4 & C_6 and $C_{3''}$, C_8 & C_1 respectively. The CH resonances occurring at 126.18 ppm, 126.54 ppm and 128.94 ppm correlated with the large multiplet at 7.15 - 7.29 ppm integrating for six protons and were assigned to the remaining six aromatic CH carbons ($C_{4''}$, $C_{5''}$, C_6, C_7, C_2 & C_3).

Quaternary resonances were observed at 142.54 ppm and 143.41 ppm. The carbons of the nitrovinyl unit were assigned utilising both the CH COSY and HMBC. The proton doublet resonance at 8.50 ppm was observed to couple to two aromatic carbons and the quaternary carbon C_{10}. This doublet was found to correlate to the carbon resonance 131.70 ppm using the C-H COSY experiment. As a result of these findings the resonances occurring at 131.70 ppm and 147.96 ppm were assigned to $C_{1'}$ and $C_{2'}$ respectively.

FTIR spectroscopy shows bands at 1594 (C=C), 1482, 1455 (C=C) and 1526, 1328 (NO_2) cm^{-1}. High resolution mass spectrometry (APCI) was carried out and the required molecular ion was calculated to be $C_{23}H_{17}NO_2$ [M^+] 339.1259 and found as 339.1259.

A sample of (*E*)-9-(2-nitrovinyl)-9,10-dihydro-9,10-[1,2]benzenoanthracene (**324**), was used for the X-ray crystallographic analysis (Figure 228). It was possible to conclude from this data that the packing structure assumed by the product was monoclinic. From the asymmetric unit it was possible to confirm the (*E*) configuration of the nitro vinyl unit. The angles between the centroids of each of the three phenyl rings and the centroid of the central axis were calculated from the asymmetric unit, these were A° (118.5°), B° (121.24°) and C° (120.18°). This angle is 119.46° in the crystal structure of maprotiline. The distance between the carbons in the ethano bridge (d_1) was 1.400 Å, in maprotiline this distance is 1.54 Å. The distance between the carbon at C-10 and the nearest carbon of the ethano bridge (d_2) was 1.518 Å, in maprotiline this distance is 1.546 Å.

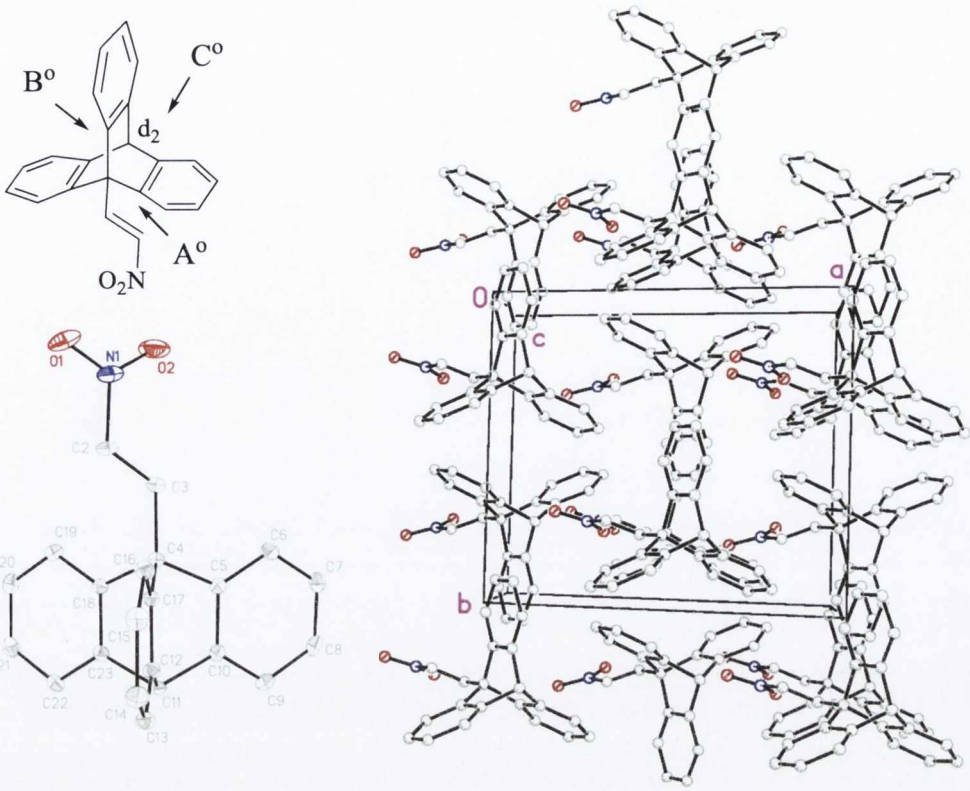

Figure 228: X-ray crystallography data: Asymmetric unit and packing structure of (*E*)-9-(2-nitrovinyl)-9,10-dihydro-9,10-[1,2]benzenoanthracene (324)

5.5 Synthesis of the (*E*)-3-(12,14-dioxo-9,10-[3,4]furanoanthracen-9(10*H*)-yl)acrylonitriles and the 9-(iminomethyl)-9,10-dihydro-9,10-[3,4]furanoanthracene-12,14-diones.

Diels-Alder cycloadditions were also carried out with the anthracenes (**233-235**, **228-230**) using different dienophiles to investigate if changing the nitrovinyl unit for another functionality at C-9 would affect potency of the adducts. The diene systems utilised were anthracene, anthraldehyde, anthrone, (*E*)-3-(anthracen-9-yl)acrylonitrile (**235**), 2-(anthracen-9-ylmethylene)malononitrile (**233**), (*E*)-(anthracen-9-ylmethylene)hydrazine (**228**) and (*E*)-anthracene-9-carbaldehyde oxime (**231**) (Figure 229).

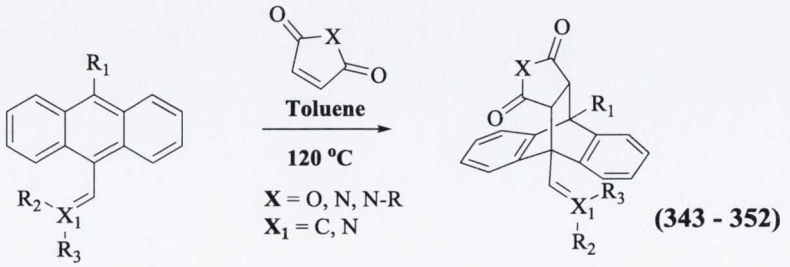

Figure 229: General scheme for the synthesis of the (*E*)-3-(12,14-dioxo-9,10-[3,4]furanoanthracen-9(10*H*)-yl)acrylonitriles and the 9-(iminomethyl)-9,10-dihydro-9,10-[3,4]furanoanthracene-12,14-diones.

Diels-Alder additions to (*E*)-3-(anthracen-9-yl)acrylonitrile (**235**) have been achieved previously by Wilhelm et al. (1969)[103] and McNamara et al (2014)[6]. Herein is reported the first direct Diels-Alder reaction of (*E*)-(anthracen-9-ylmethylene)hydrazine (**228**) and (*E*)-anthracene-9-carbaldehyde oxime (**231**). To synthesise these hydrazine and oxime derivatives in the past, the Diels-Alder adduct of 9-anthraldehyde was reacted to give the desired oxime[6, 379, 389-391] or hydrazine[392, 393]. The current work also achieved the synthesis of a novel panel of Diels-Alder adducts of 2-(anthracen-9-ylmethylene)malononitrile. This library of substituted 9,10-dihydro-9,10-[3,4]furanoanthracene-12,14-diones gave yields of 15-74% (Table 39).

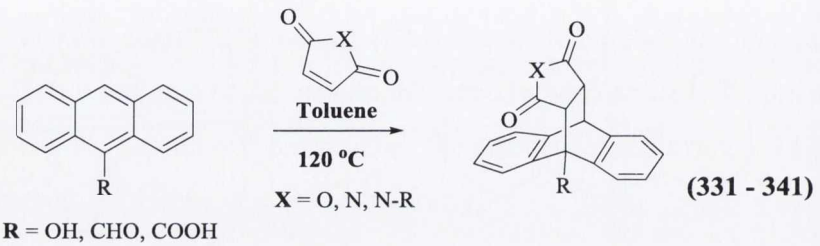

Figure 230: General scheme for the synthesis of the 9,10-dihydro-9,10-[3,4]furanoanthracene-12,14-diones

The preparation of a range of different 9 and 10 substituted Diels-Alder adducts using similar Diels-Alder conditions used for previous libraries, including aldehyde, acid and alcohol functionalities (Figure 230). The library of diversely substituted novel 9 and 10 substituted Diels-Alder adducts is present in Table 38, affording yields of 15-90%.

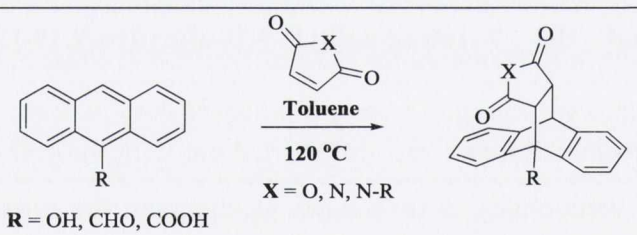

Compound	R	X	Yield	Compound	R	X	Yield
331	H	O	90%	**337**	COOH	O	81%
332	H	NH	85%	**338**	COOH	NH	41%
333	H	$N(C_6H_5)$	90%	**339**	COOH	$N(C_6H_5)$	43%
334	CHO	O	40%	**340**	OH	O	55%
335	CHO	NH	35%	**341**	OH	NH	58%
336	CHO	$N(C_6H_5)$	62%	-	-	-	-

Table 38: substituted 9,10-dihydro-9,10-[3,4]furanoanthracene-12,14-dione library

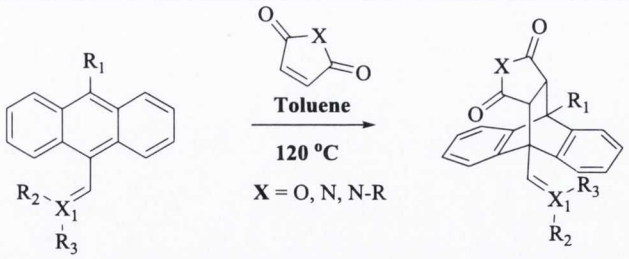

Compound	X	X_1	R_1	R_2	R_3	Yield	Melting point
342	O	C	H	H	CN	74%*	215-219 °C
343	NH	C	H	H	CN	38%*	299-300 °C
344	$N(C_6H_5)$	C	H	H	CN	20%*	274-281 °C
345	O	C	H	CN	CN	15%*	196-198 °C
346	NH	C	H	CN	CN	42%*	281-284 °C
347	$N(C_6H_5)$	C	H	CN	CN	44%*	255-258 °C
348	NH	N	H	-	NH_2	63%*	245-247 °C
349	$N(C_6H_5)$	N	H	-	NH_2	54%*	275-277 °C
350	NH	N	Cl	-	NH_2	34%*	241-244 °C
351	NH	N	H	-	OH	43%*	272-273 °C
352	$N(C_6H_5)$	N	H	-	OH	66%*	238-242 °C

Table 39: 9-vinyl-9,10-dihydro-9,10-[3,4]furanoanthracene-12,14-dione library. * denotes novel compound

The spectral data of (*E*)-3-(12,14-dioxo-9,10-[3,4]furanoanthracen-9(10*H*)-yl)acrylonitrile (**342**) was analogous with the above data for (*E*)-9-(2-nitrovinyl)-9,10-dihydro-9,10-[3,4]furanoanthracene-12,14-diones. In the ^{1}H NMR spectrum of compound **343** is the altered doublet resonance for H_1' on the *trans* vinyl unit at 6.54 ppm due to the decreased electronegativity indicative of replacing the nitro group with the cyano group. In the ^{1}H NMR spectrum of 2-(anthracen-9-ylmethylene)malononitrile derivatives the $H_{2'}$ proton signal is absent as expected. The ^{13}C NMR spectrum reflects the cyano groups' presence with a resonance at approximately 117.60 ppm. The main differences visible in the FTIR absorbance the absence of bands for the nitro group at 1523 & 1348 cm^{-1} and the presence of the nitrile band at 2218 cm^{-1}.

Compound **348** was chosen as a representative sample of the 9-vinyl-9,10-dihydro-9,10-[3,4]furanoanthracene-12,14-diones and the ^{1}H NMR and ^{13}C NMR spectra will now be discussed in detail. The ^{1}H NMR (400 MHz, DMSO-d_6) spectrum of compound **349** (Figure 231) shows a pair of doublets occurring at 3.23 ppm (J = 8.55 Hz) and 3.44 ppm (J = 8.55 Hz) both integrating for a single proton each, these were assigned to H_{11} and H_{15} respectively.

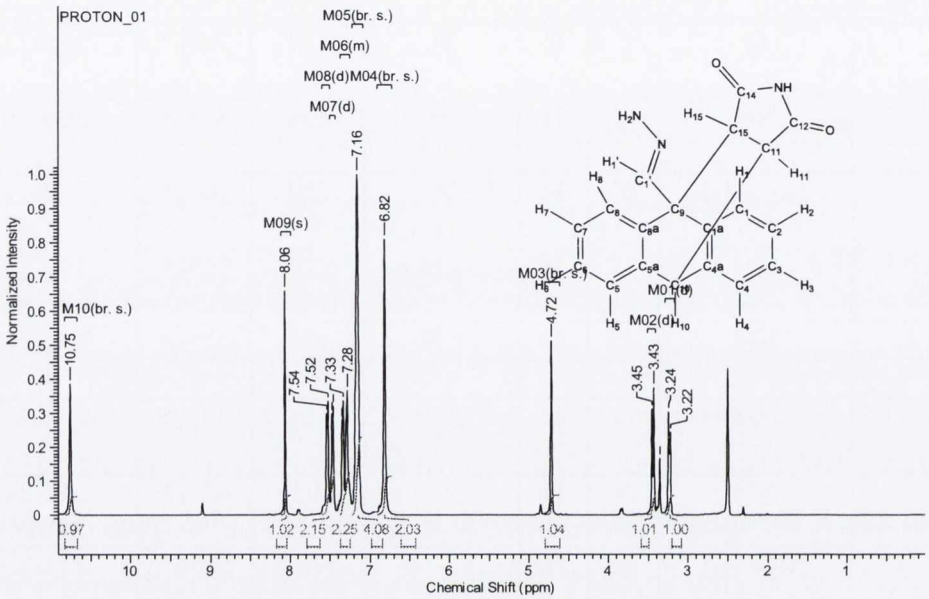

Figure 231: ^{1}H NMR spectrum of (*E*)-9-(hydrazonomethyl)-9,10-dihydro-9,10-[3,4]epipyrroloanthracene-12,14-dione (348)

The singlet occurring at 4.72 ppm integrated for a single proton and accounted for H_{10}. A broad singlet is observed at 6.82 ppm integrating for two protons and was allocated to the NH_2 protons of the hydrazine. A broad singlet occurring at 7.16 ppm integrating for four protons and a doublet occurring at 7.25 - 7.38 ppm integrating for two protons accounted for six of the aromatic protons. The multiplet occurring at 7.39 - 7.55 ppm integrating for two protons was assigned to H_8 and H_1.The sharp singlet at 8.06 ppm integrated for a single proton and was assigned to $H_{1'}$. The most downfield signal was a broad singlet occurring at 10.75 ppm, integrating for one proton and this accounted for the NH in the dione group.

The ^{13}C NMR spectrum (101 MHz, DMSO-d_6) of compound **348** is displayed in Figure 232. CH resonances identified from DEPT 90 NMR spectrum (Figure 233) occurring at 44.71 ppm, 48.56 ppm and 49.81 ppm were assigned to C_{11}, C_{15} and C_{10} respectively. A quaternary signal at 50.19 ppm accounted for C_9. The eight aromatic CH carbons were accounted for by CH resonances at 123.55 ppm, 123.85 ppm, 124.88 ppm, 125.65 ppm, 126.11 ppm, 126.22

ppm and 126.28 ppm. The more downfield CH resonance observed at 137.87 ppm was allocated to $C_{1'}$ on the imine unit. The four quaternary signals recorded at 139.11 ppm, 140.31 ppm, 141.95 ppm and 144.04 ppm were assigned to C_{5a}, C_{4a}, C_{8a} and C_{1a}. The two most downfield quaternary signals occurring at 177.01 ppm and 177.60 ppm accounted for the carbonyl carbons C_{12} and C_{14}.

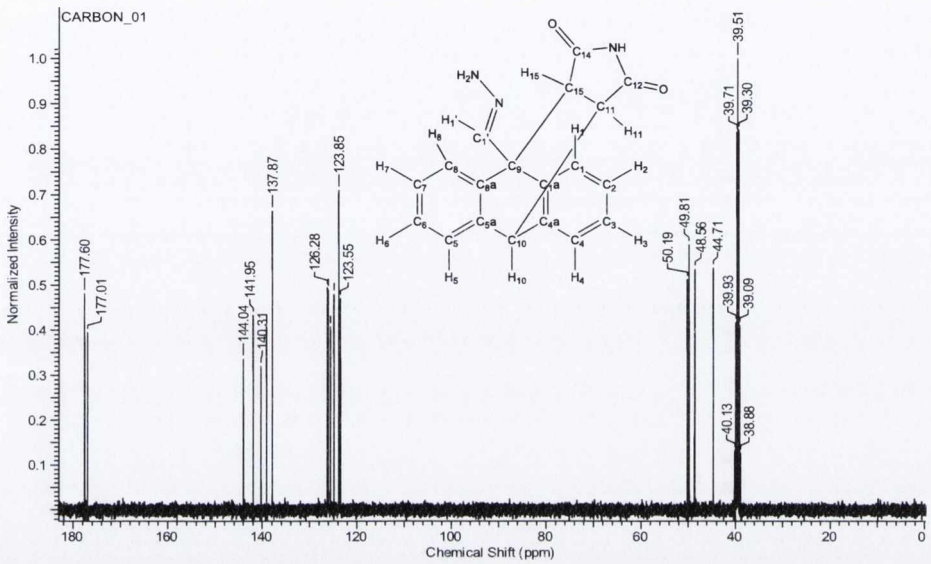

Figure 232: ^{13}C NMR spectrum of (*E*)-9-(hydrazonomethyl)-9,10-dihydro-9,10-[3,4]epipyrroloanthracene-12,14-dione (348)

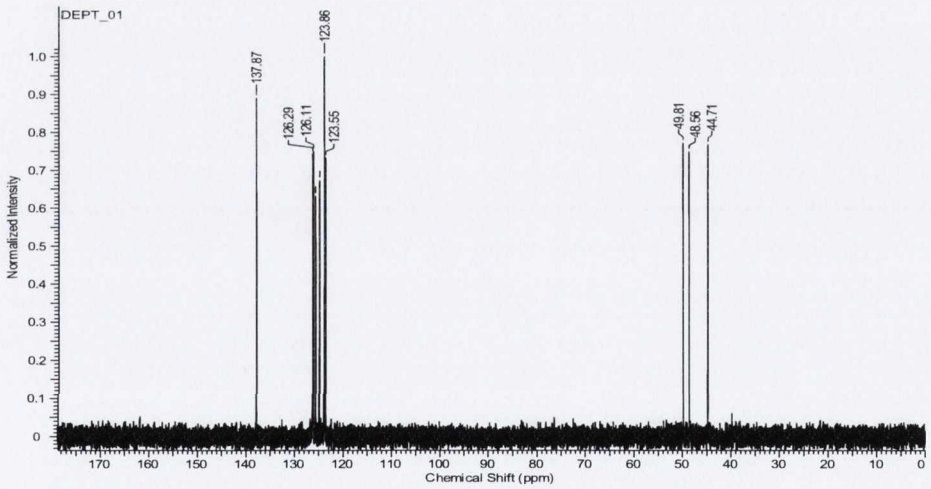

Figure 233: DEPT 90 NMR spectrum of (*E*)-9-(hydrazonomethyl)-9,10-dihydro-9,10-[3,4]epipyrroloanthracene-12,14-dione (348)

FTIR spectroscopy shows bands at 3369 (NH), 1710 (C=O), 1609 (C=C), 1483, 1457 (C=C) and 1213 (C-N) cm^{-1}. High resolution mass spectrometry (APCI) was carried out and the required molecular ion was calculated to be $C_{19}H_{16}N_3O_2$ $[M^+ + H]$ 318.1243 and found as 318.1237.

5.6 Conclusion

A library of dienophiles was compiled using both commercially available reagents and a number of maleimide, benzylmaleimide and phenylmaleimide dienophiles which were synthesised from maleic anhydride. These maleimide dienophiles included halogen, alkyl and methoxy aryl substitutions. Subsequent Diels-Alder reaction of the dienophile library with anthracene derivatives synthesised in Chapter 4 led to the preparation of the libraries of novel Diels-Alder adducts.

The design, synthesis and characterisation of a library of over 80 9,10-dihydro-9,10-ethanoanthracene maprotiline analogues (67 novel compounds) was achieved utilising 27 different dienophiles. The variation of dienophile enabled modification of the ethano bridge of the Diels-Alder adducts including functionalities such as esters, nitriles, phenyl rings, anhydrides and maleimides. The modification of maleimide substitution was also achieved and this led to the preparation of a comprehensive library of substituted maleimide Diels-Alder adducts. Substitution at C-9 and C-10 of the Diels-Alder adducts was altered by changing the diene system and allowed inclusion of functionalities such as cyanovinyl, nitrovinyl, nitro-alkyl, hydrazone, oxime, aldehyde, alcohol and acids. X-ray crystallographic data was also obtained for 12 of these maprotiline analogues and this data was used to compare the designed structures to that of maprotiline. Full X-ray reports can be found in Appendix 1.

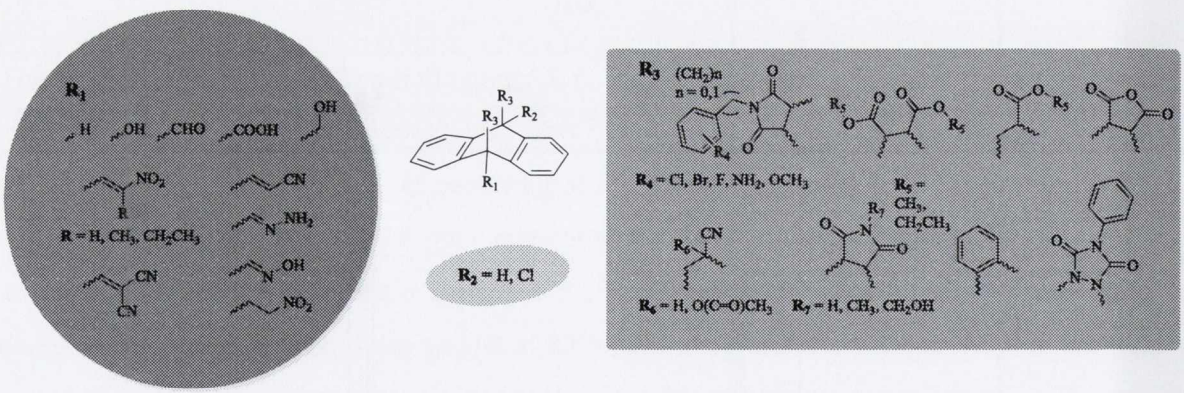

Figure 234: Summary graphic of maprotiline analogue library

The compounds synthesised were then screened for biological activity in the Burkitt's lymphoma MUTU-I and DG-75 cell lines, in order to develop a structure-antiproliferative activity relationship for these maprotiline analogues and to improve potency. The findings of this biological study will be discussed in Chapter 6.

Chapter 6.
Biological evaluation

6.0 Introduction

The anti-proliferative activity of the libraries of compounds synthesised in Chapters 2-5 were evaluated in the malignant BL cell lines DG-75 and MUTU-I. AlamarBlue® dye was used to quantify anti-proliferative activity. AlamarBlue® dye is used to measure cell viability post treatment with a chemotherapeutic agent. Originally, these BL cell lines were chosen for biochemical evaluation of the (*E*)-1,3-bis(aryl)-2-nitro-1-propenes due to SERT over-expression and the assumption that these (*E*)-1,3-bis(aryl)-2-nitro-1-propenes acted like their propamine and MDMA derivatives through SERT binding. More recent work within the group has shown that the anti-proliferative activity of this series of compounds may be SERT independent due to low SERT binding activity when compared to amphetamine analogs[5].

A preliminary *in vitro* screen for anti-proliferative activity was carried out using the alamarBlue® assay in the MUTU-I and DG-75 cell lines, treating at 10 μM and 1 μM. This preliminary alamarBlue® assay identified a number of structural features which appear vital for anti-proliferative activity in DG75 and MUTU-I cell lines. The results of the *in vitro* screen for anti-proliferative activity are presented as bar charts (mean ± SEM) and the data is also presented as tables in the appendices. The more active compounds from the preliminary screen were then selected and full IC_{50} values were then established. To examine the mechanism of cell death (as discussed earlier), the effects of these compounds on the cell death was appraised using Annexin V / propidium iodide (PI) FACS (Fluorescence Activated Cell Sorter) analysis, a lactate dehydrogenase (LDH) cytotoxity assay and a reactive oxygen species (ROS) inhibition assay.

Preliminary *in vitro* anti-proliferative screening of the lead nitrostyrene compounds was also carried out at 10 μM and 1 μM in a range of malignant cell lines including HeLa, MCF-7, HL60 and the BL cell lines Ramos and Bjab. The lead nitrostyrene compounds were taken for biological evaluation in the CLL cell lines CII, HG3, I83 and PGA1. Further work included the evaluation of anti-proliferative and apoptotic activity in the *vivo* CLL patient samples and PBMCs. This work was carried out by Dr. Sandra Bright (Williams Group, School of Biochemistry and Immunology, Trinity College Dublin).

6.1 Materials and Methods

All reagents including foetal bovine serum (FBS and RPMI-1640 cell culture growth medium were purchased from BD Biosciences, Invitrogen or Sigma-Aldrich. Consumables such as 96 well plates, 6 well plates, sterile pipettes, centrifuge vials etc. were purchased from Cruinn. Fluorescence of 96 well plate for alamarBlue® assay was read using BMG-Labtech, fluostar Optima plate reader and Gemini Spectramax plate reader. All data points were analysed using graphpad PRISM (version 5) software (Graphpad software Inc., San Diego, CA). FACS analysis was carried out on CyAn ADP (Beckman Coulter) and processed using FlowJo. The MUTU-I, DG-75, HL60, HeLa and MCF-7 cell lines were kindly supplied by Prof. Clive Williams (School of Biochemistry and Immunology, Trinity College Dublin). The Bjab and Ramos cell lines were generously supplied by Prof. Dermot Walls (School of Biotechnology, Dublin City University).

6.1.1 Cell lines

- **MUTU-I cell line**[5]**:** The MUTU-I (c179) is an isogenic stable group I BL cell line derived from a BL biopsy. MUTU-I is EBV positive, chemosensitive and expresses low levels of Bcl-2.
- **DG-75 cell line**[5]**:** The DG-75 cell line is a B-lymphocyte, this BL line is derived from a metastatic pleural effusion (lung) of a sporadic case of BL and is hence EBV negative.
- **Bjab cell line**[394]**:** The Bjab cell line was derived from an inguinal (lower abdomen) tumor of preterminal stage BL. The Bjab cell line is EBV negative.
- **Ramos cell line**[395]**:** The Ramos cell line is a BL cell line bearing B-lymphocyte characteristics. The Ramos cell line was derived from a 3 year old Caucasian BL patient and is EBV negative.
- **HeLa cell line**[396]**:** The HeLa cell line is the oldest and most commonly used cancer cell line. The adherent line is derived from human cervical cancer and contain the human papilloma virus.
- **MCF-7 cell line**[397]**:** The MCF-7 cell line is an ER positive, adherent cell line derived from a pleural effusion of a 69 year old female with metastatic breast cancer.
- **HL60 cell line**[398]**:** The HL60 cell line is a promyelocytic cell line derived by leukopheresis from a 36 year old Caucasian female with acute promyelocytic leukaemia.

The DG-75, HL60, Bjab and Ramos cell lines were cultured in RPMI-1640 medium containing phenol red and supplemented with 10% (v/v) foetal bovine serum (FBS), L-glutamine (2 mM), penicillin and streptomycin (100 μg/mL). The HeLA and MCF-7 cell lines were cultured in Eagle's Minimum Essential Medium supplemented as described above. The MUTU-I (c179) cell line required the added supplements of alpha-thioglycerol (5 mM in phosphate buffered saline (PBS) with 20 μM bathocuprione disulfonic acid), sodium pyruvate (100 mM) and HEPES (1 mM).

6.1.2 Storage and Growth of Cultured Cells

When not in culture, stocks of cells are stored as a frozen solution in 10% DMSO/30% FBS/60% media. These stocks are initially stored overnight at -80 °C and are subsequently transferred into a vapour phase liquid nitrogen tank at -178 °C. When required for culture, these stocks are removed from the cryogenic storage tank and quickly thawed in a 37 °C water bath. Once thawed, the stock in transferred into ca. 10 mL of media in a centrifuge tube before centrifuging at 160 g for five minutes. The supernatant layer was poured off into waste and the cells were resuspended in 5 mL of the appropriate growth media (preheated to 37 °C) and transferred into a 25 cm^3 cell culture flask. The cells were then incubated at 37 °C under an atmosphere of 5% CO_2/ 95% air until confluent. At 70-80% confluency the cells were transferred into a 75 cm^3 cell culture flask.

At high confluency levels cells need to be split in order to facilitate further cell growth, prevent excessive cell death and to prevent infection and possible mutation. In order to lower confluency levels, a 2 mL aliquot of the cells is transferred into a new cell culture flask containing 20 mL of the required media (prewarmed to 37 °C).

6.1.3 Seeding of cells

In order to prepare for the alamarBlue® and FACS assay, cells must first be counted to determine the number of cells / mL. By doing this, the necessary dilution factors can be calculated to produce stocks with appropriate number of cells / mL for the desired assay. A haemocytometer is a thick glass slide with a gridded central chamber of known area, which is used for counting cells. After placing the coverslip over the gridded area, 20 μL of cells suspended in media is transferred using a micropipette to the loading area at the base of the grid. The 20 μL is then dispensed at the loading area, under the coverslip and covers the gridded area.

The number of cells on the grid is then counted using a microscope and cells within the five core areas of the grid are counted. Not all cells fall directly within the confines of the grid and to account for this cells that fell on the outer border of each grid box are counted on the top and right but not on the bottom and left. This process was repeated for each of the five gridded areas of the haemocytometer on both sides. The number of cells / mL was then calculated using the formula below:

$$(\text{No. of cells} / 2) \times 1/5 \times 10{,}000 = \text{No. of cells} / \text{mL}$$

6.1.4 AlamarBlue® anti-proliferative assay

The anti-proliferative effect of the compounds was evaluated using the alamarBlue® cell viability assay. The active ingredient of the alamarBlue® reagent is resazurin which is a blue, low fluorescence compound. Resazurin is a REDOX indicator and upon entering a viable cell, resazurin is reduced to resorufin – a highly fluorescent, red compound. Resazurin is reduced actively by viable cells, through the acceptance of electrons from electron carriers (NADH, NADPH, FADH) or cytochromes. This colorimetric change takes place over a period of 4-6 hours and is subsequently measured using a fluorescence plate reader at 590 nm. These fluorescence readings are directly proportional to the quantity of viable cells remaining in each of the wells. From this a percentile of viable cells remaining can be calculated, taking media absorbance and vehicle effects into account[399, 400].

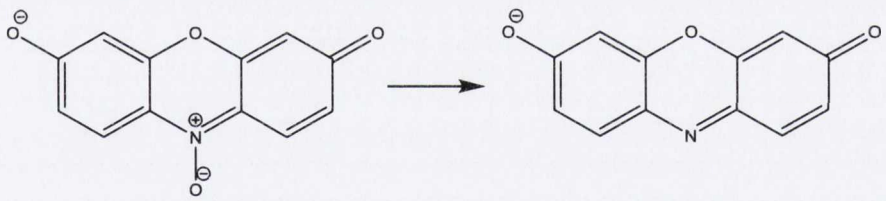

Blue Pink

A 96 well plate was seeded with 1-5x10^4 cells/well (5x10^3 MCF-7 / HeLa) and treated with the desired drug concentration for a predetermined time frame. After treatment and incubation, each well was treated with 20 µL of alamarBlue® (37 °C) and the plate was incubated in the dark at 37 °C for 4-6 hours. Fluorescence of the 96 well plates was then read at 590 nm (excitation 544 nm). The control wells were used to represent cells at 100% viability and by comparing this to the treated wells minus the background fluorescence of the media, the percentile of viable cells remaining was calculated. Taxol (10 µM) was used as an internal standard and resulted in ca. 90% cytotoxicity in each of the cell lines.

6.1.5 FITC Annexin V / PI FACS analysis

FITC (Fluorescein isothiocyanate) Annexin V / PI (Propidium Iodide) FACS (Fluorescence Activated Cell Sorting) analysis was used to characterise the mode of cell death. In healthy cells, phosphatidylserine (PS) is found on the cytoplasmic surface of the cell membrane. In apoptotic cells PS is translocated from this inner cell membrane to the outermost regions of the plasma membrane; here PS is exposed to the external cellular environment. Annexin V is a human cellular protein with proposed anticoagulant activity, Annexin V has a high binding affinity for PS. Once labelled with a fluorophore, Annexin V can be used to identify apoptotic cells by binding to PS in this outer plasma membrane. PI (Propidium Iodide) is a nucleic binding dye that stains dead cells with red fluorescence; PI cannot permeabilise or stain healthy cells. Four populations are produced during the assay Annexin V & PI negative (Q4, healthy cells), Annexin V positive & PI negative (Q3, early apoptosis), Annexin V & PI positive (Q2, late apoptosis) and Annexin V negative & PI positive (Q1, necrosis). These populations can be easily identified and quantified using a flow cytometer[401-403] (Figure 235).

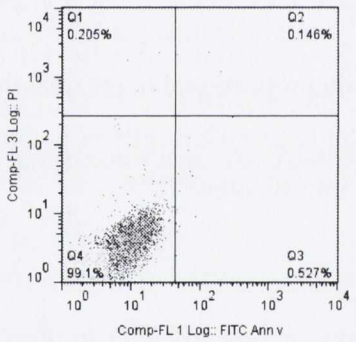

Figure 235: Example of quadrants produced during Annexin V / PI FACS analysis (vehicle - DG-75 cell line)

750,000 cells were treated with the appropriate concentration of compound and incubated for the designated time. Samples were harvested by centrifugation and the pellets were rinsed with 0.5 mL of Ca^{2+} Annexin V binding buffer (0.1 M HEPES, pH 7.4; 1.4 M NaCl; 25 mM $CaCl_2$) each and pelleted again by centrifugation. Supernatants were decanted and the pellets were resuspended in 50 µL FITC Annexin V (diluted 1:33 in Ca^{2+} Annexin V binding buffer), the samples were then placed on ice and incubated for 10 min in the dark. After the incubation period 0.5 mL of Ca^{2+} Annexin V binding buffer was added and samples were pelleted by centrifugation. The supernatant was decanted and the pellet was resuspended in 500 µL of PI solution (0.5 µg/ mL). Samples were analysed within 1 h using CyAn ADP flow cytometer (Beckman Coulter) counting 10,000 cells and analysed using the Flowjo software package. Taxol was used as a positive control for cell death.

6.1.6 Lactate dehydrogenase (LDH) assay

The lactate dehydrogenase (LDH) assay (Sigma Aldrich TOX7) is a simple method to measure membrane integrity as a function of cytoplasmic LDH released into the growth medium. LDH is a cytosolic enzyme present in mammalian cells found in the plasma membrane. The loss of plasma membrane integrity is detectable by the release of LDH into the supernatant growth medium. The assay is initiated by the reduction of NAD^+ to NADH catalysed by LDH. During the second step of the reaction the newly formed NADH catalyses the acidic reduction of a tetrazolium salt to the highly coloured formazan (red). The degree of LDH released is proportional to the degree of colouration by formazan and this can be measured spectroscopically. The LDH assay lysis solution was used to quantify formazan concentration at 100% cell lysis[404, 405] (Figure 236).

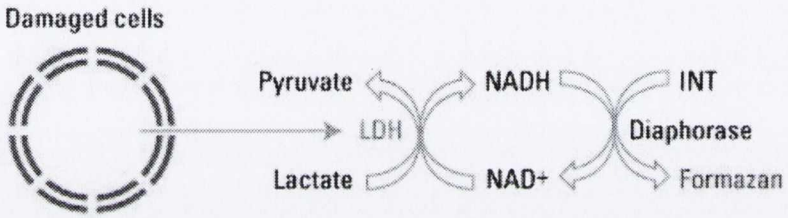

Figure 236: Process for Formazan formation during LDH assay[404]

A 96 well plate was seeded with $2x10^4$ cells/well and treated with the desired drug concentration for a predetermined time frame. After treatment and incubation, 50 µL of cell supernatant was placed in a 96 well plate and 100 µL LDH assay mixture was added to each sample. The plate was covered with tin foil and incubated at RT for 30 min. The reaction was terminated by addition of 15 µL of 1 N HCl to each well. Spectrophotometrically the absorbances of each sample were then obtained at 490 nm and 690 nm. Individual sample values were obtained by subtracting the measurement at 690 nm from the corresponding primary measurement at 490 nm. The lysis solution wells were used to represent cells at 100% lysis and by comparing this to the treated wells minus the background LDH reading of the media; the percentile of LDH released was calculated.

6.1.7 Inhibitor Studies: Reactive Oxygen Species

Reactive oxygen species (ROS) are short lived diffusible entities containing oxygen such as hydroxy, nitroxyl, alkoxy, superoxide or peroxyl radicals. Other ROS species include hydrogen peroxide and organic peroxides. ROS are generated as metabolites of oxygen and are utilised for signalling events for essential cell functions. ROS are often associated with the induction of cell death and apoptosis. In order to ascertain whether ROS have a role in the mechanism of cell death, cells are pre-treated with N-acetyl cysteine (NAC) – a known ROS scavenger and the effect is studied[20, 40]. A 96 well plate was seeded with $2x10^4$ cells/well and were pre-treated with 5 mM NAC for 1 h prior to compound treatment. The wells were treated with the desired drug concentration (10 μM & 1 μM) for a predetermined time frame (24 – 48 h). After treatment and incubation; each well was treated with 20 μL of alamarBlue® (37 °C) and the plate was incubated in the dark at 37°C for 4-6 hours. Fluorescence of the 96 well plates was then read at 590 nm (excitation 544 nm). The control wells were used to represent cells at 100% viability and by comparing this to the treated wells minus the background fluorescence of the media, the percentage of viable cells remaining was calculated. The percentage of viable cells remaining with NAC pre-treatment was compared to the percentage of viable cells remaining without NAC pre-treatment in order to determine the implication of ROS in the mechanism of cell death induced.

6.2 Results of Biochemical Screening

6.2.1 Evaluation of the *in vitro* anti-proliferative activity of the nitrostyrene analogues

A series of over 134 compounds related to nitrostyrenes, anthracenes and ethanoanthracenes were evaluated for anti-proliferative activity at 10 μM and 1 μM in the MUTU-I and DG-75 cell lines. The effect of compounds including a range alternative double bond functionalities such as cyanovinyl, hydrazone and triazoles were also investigated. Chain length and substituents were varied at C-2 of the nitrovinyl unit and the effect of these substitutions were also evaluated. The effect of phenyl ring substitution was investigated and the inclusion of heterocyclic moieties such as furan, epoxides, thiophene, benzoquinone, naphthalene and anthracene were also discussed. These nitrostyrene analogues are discussed in nine main groupings (Sections 6.2.1 – 6.2.10) and categorised within the groups by structural type. The previous lead compound (**85**) was used as a control and demonstrated good activity at 10 μM in the MUTU-I (<5% viable cells remaining) and DG-75 cell lines (<40%).

6.2.2 *In vitro* anti-proliferative activity screen of the (*E*)-(2-nitrovinyl)benzene library

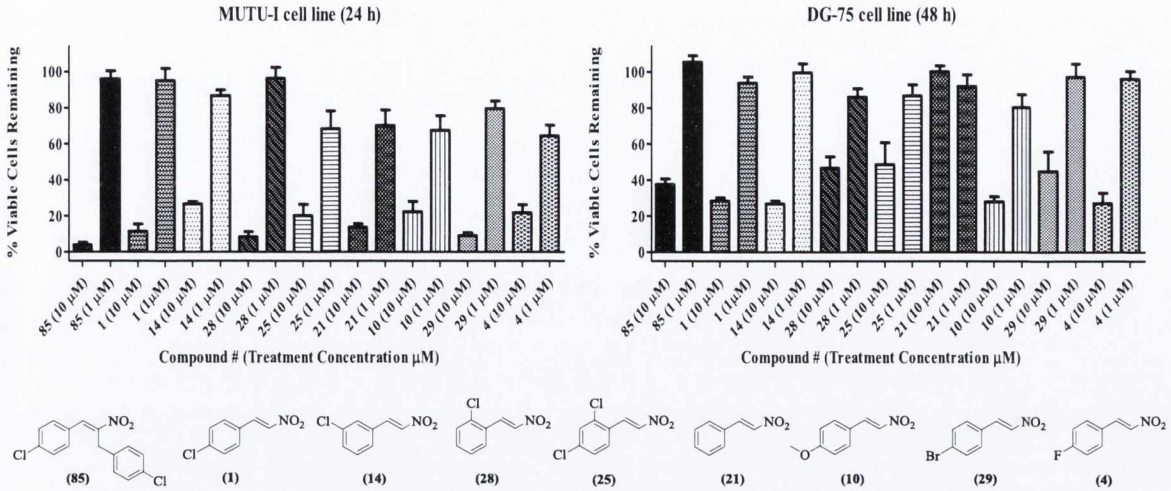

Figure 237: Preliminary anti-proliferative screen for (*E*)-(2-nitrovinyl)benzene (A)

(I) The compound **85** and its simple nitrostyrene analogue (**1**) possessed very similar anti-proliferative effects in the BL lines. The effect of chloro substituent position (*ortho, meta, para*) (Figure 237) on the anticancer activity of the (*E*)-(2-nitrovinyl)benzenes in the MUTU-I cell line was minimal, however in the DG-75 cell line compounds **28** (2-chloro) and **25** (2,4-dichloro) elicited less anti-proliferative activity than compounds **1** and **14**. Comparing the effect of variation of C-4 substituents - it was observed that the decreased electronegativity of bromo (**29**) was detrimental to the anticancer effects induced in the DG-75 cell line. The more electronegative methoxy (**10**), chloro (**1**) and fluoro (**4**) substitutions yielded similar results, while removing the phenyl substitution (**21**) deactivated the pharmacophore in the DG-75 cell line at 10 μM and 1 μM.

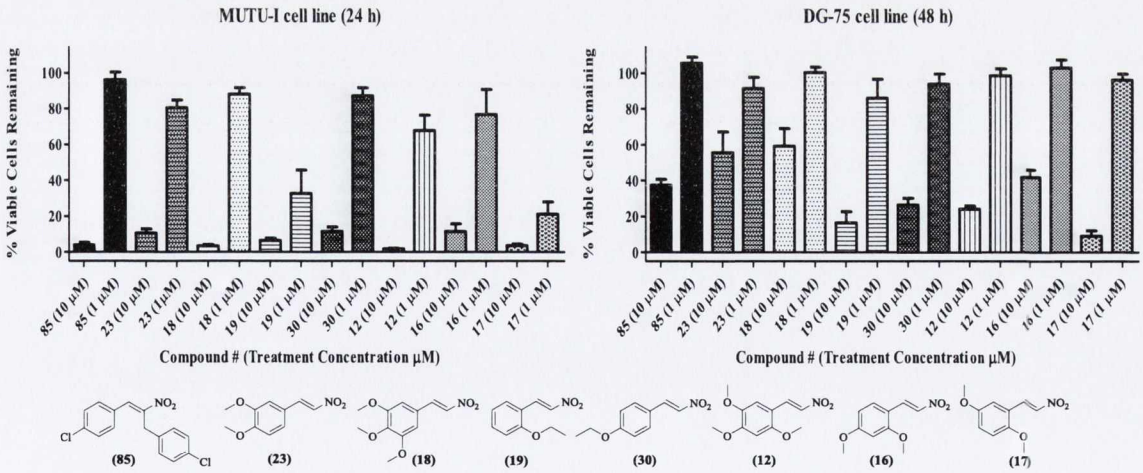

Figure 238: Preliminary anti-proliferative screen for (*E*)-(2-nitrovinyl)benzene (B)

(II) In Figure 238, the anti-proliferative effect of the alkoxy substituted (*E*)-(2-nitrovinyl)benzenes is displayed. It is apparent that although all compounds showed activity in the MUTU-I cell line at 10 μM, only compounds **17** and **19** (with C-2 alkoxy substitution) were

considerably active at 1 μM (~20-30%). In the DG-75 cell line all compounds showed activity at 10 μM but compounds **23** and **18** bearing 3,4-dimethoxy and 3,4,5-trimethoxy substitutions respectively possessed less anti-proliferative activity.

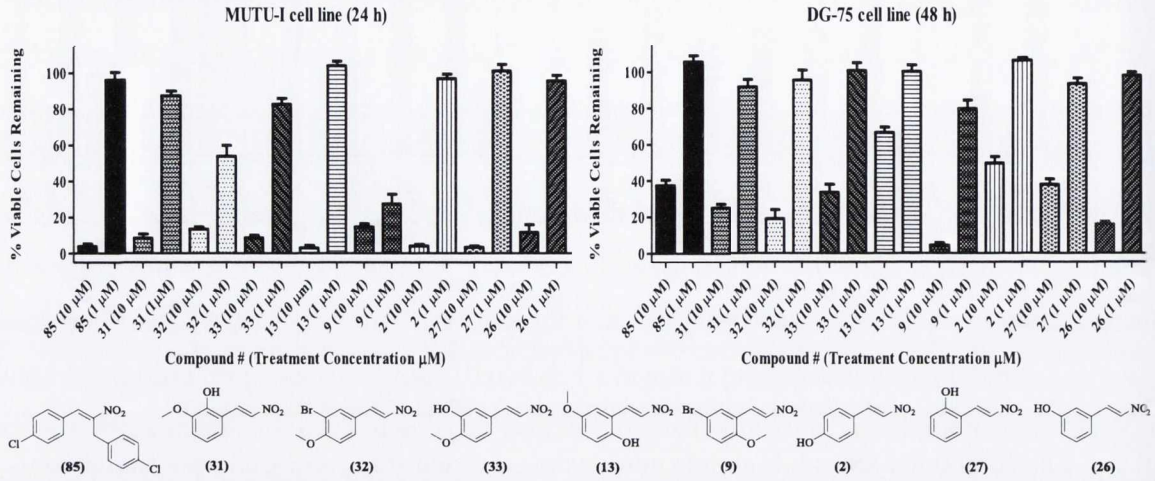

Figure 239: Preliminary anti-proliferative screen for (*E*)-(2-nitrovinyl)benzene (C)

(III) Compounds **9** and **32** (both bearing *meta* bromo & a *para* / *ortho* methoxy substituent) elicited potent anticancer effects at both concentrations in the MUTU-I cell lines. Compound **9** with a C-2 methoxy substituent proved more potent than its C-4 methoxy analogue compound **32**. Compound **9** was the most active in the chemoresistant DG-75 cell line of this cohort also, with below 20% viable cells remaining at 10 μM and reducing the amount of viable cells in the experiments to ~80% at 1 μM. Compound **26** (C-3 hydroxy) was found to be the most active of the hydroxy substituted compounds (**31, 13, 84, 27, 26**) with <15% of viable cells remaining in both lines at 10 μM (Figure 239).

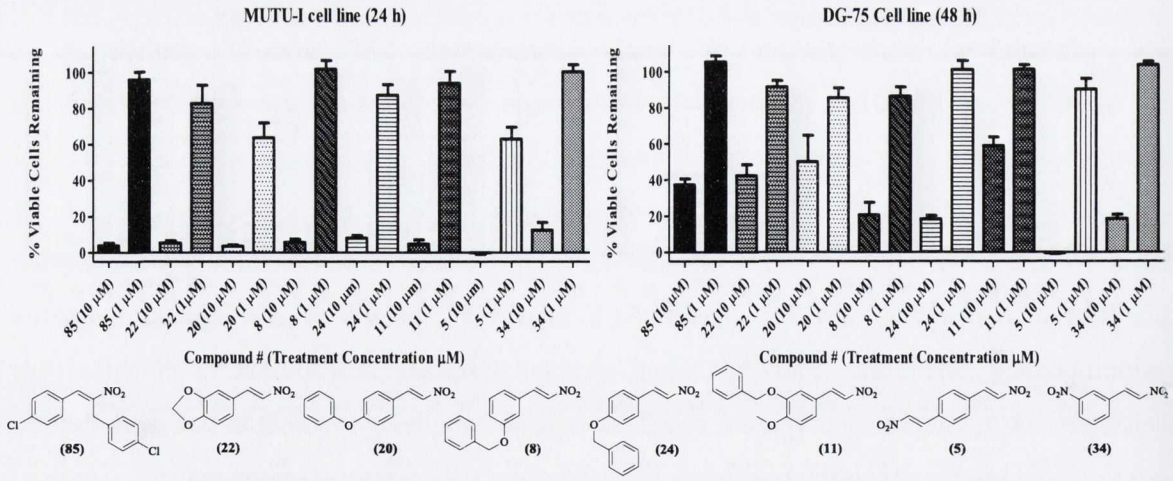

Figure 240: Preliminary anti-proliferative screen for (*E*)-(2-nitrovinyl)benzene (D)

(IV) The alkoxy, phenoxy and benzyloxyl compounds (**22, 20, 8, 24, 11**) were studied in

Figure 240 and compounds **21** and **23** produced promising results in the MUTU-I cell line with activity exhibited at the lower concentration (60–85% viable cells remaining). The 1,4-dinitrovinyl compound (**5**) also produced a promising result in the MUTU-I cell line at both concentrations (<75%). This grouping of compounds produced good activity at the higher concentration in the DG-75 cell line but exhibited low anti-proliferative potential at 1 μM.

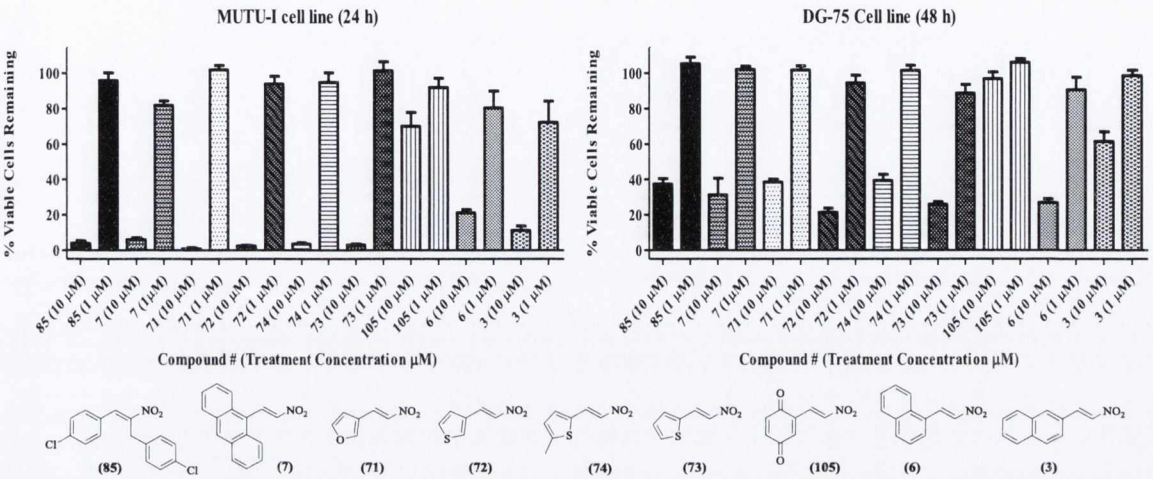

Figure 241: Preliminary anti-proliferative screen for (*E*)-(2-nitrovinyl)benzene (E)

(V) In a study of other cyclic and heterocyclic nitrostyrene adducts, the anthracene based compound **7** elicited activity in both cell lines, with comparable activity to that of the previous lead compound **85**. The C-1 substituted naphthalene compound **6**, was found to be more favourable than its C-2 analogue for activity in the DG-75 cell line. Very small differences in activities were observed when comparing the furan and thiophene based compounds, these compounds (**71, 72, 73, 74**) showed minimal activity at 1 μM in the DG-75 and MUTU-I cell lines. The benzoquinone based compound **105** was observed to possess little anti-proliferative activity at both concentrations in both cell lines (>90% DG-75 cell line) (Figure 241).

6.2.3 *In vitro* anti-proliferative activity screen of the (*E*)-(2-nitroprop-1-en-1-yl)benzenes

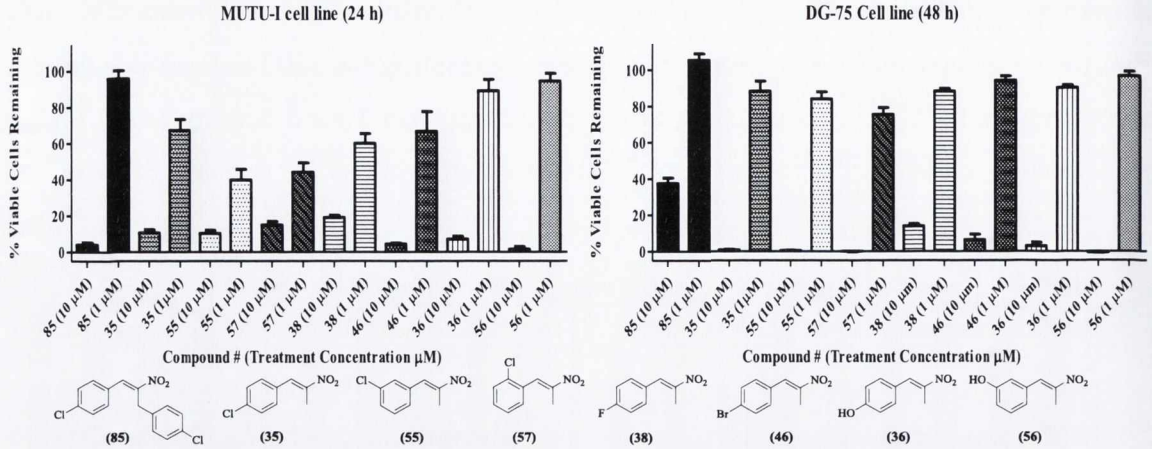

Figure 242: Preliminary screen for (*E*)-(2-nitroprop-1-en-1-yl)benzenes anti-proliferative activity (A)

(I) In this series; introduction of a methyl sidechain to C-4 chloro nitrostyrene (**35**) increased the anti-proliferative effect in both the DG-75 (~85% 1 µM) and MUTU-I (~70% 1 µM) cells when compared to the previous lead **85**. The effect of chloro substituent position was also investigated and it was observed that C-2 (**57**) and C-3 (**55**) chloro substitution was preferred for anticancer activity in both cell lines over the C-4 chloro analogue (**35**). The hydroxy compounds (**36, 56**) were less active than the halogen compounds in the MUTU-I cell line, while the C-3 hydroxy compound (**56**) gave a slightly more potent effect (<2%) than its C-4 hydroxy analogue (<10%) at 10 µM in both cell lines (Figure 242).

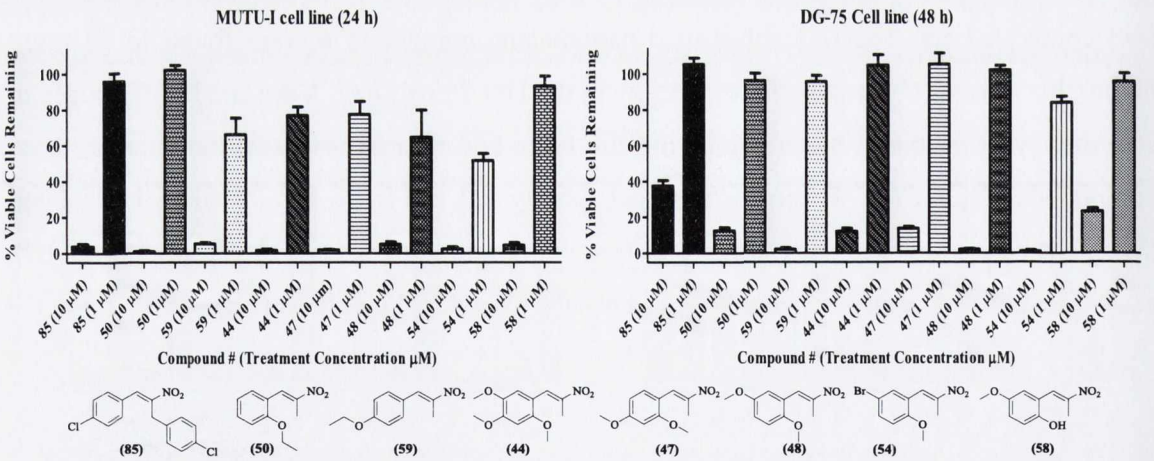

Figure 243: Preliminary screen for (*E*)-(2-nitroprop-1-en-1-yl)benzenes anti-proliferative activity (B)

(II) In a study of C-2 alkoxy substituted (*E*)-(2-nitroprop-1-en-1-yl)benzenes (**50, 44, 47, 48, 54**), compound **54** exhibited the most promising anti-proliferative activity. Compound **54** induced an anti-proliferative effect (1 µM) in both cell lines with only ~55% viable cells remaining in the MUTU-I cell line and ~82% in the DG-75 cell line. Replacing the C-2 methoxy substitution observed in compound **45** with a C-2 hydroxy substituent (**58**) reduced

anti-proliferative activity in the chemoresistant DG-75 cell line at 10 μM by ~20% (Figure 243).

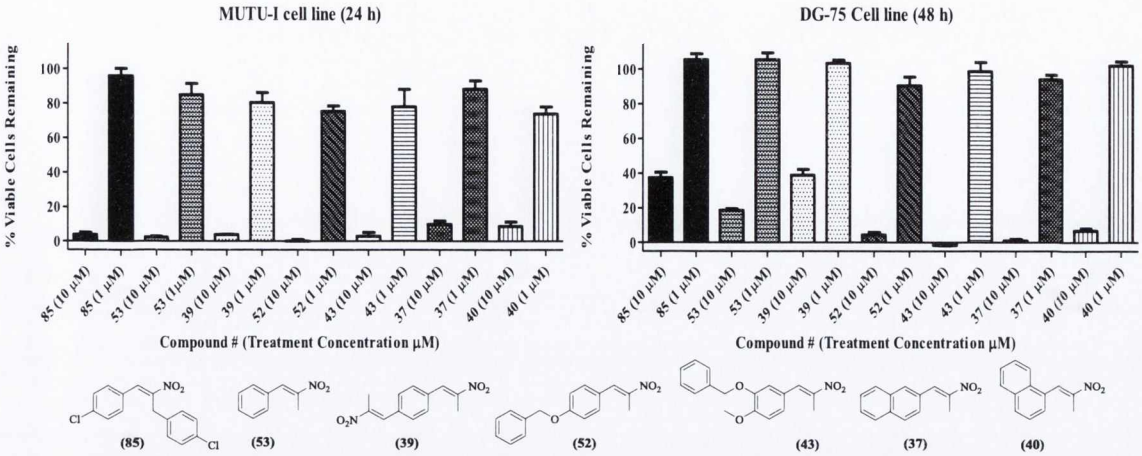

Figure 244: Preliminary screen for (*E*)-(2-nitroprop-1-en-1-yl)benzenes anti-proliferative activity (C)

(III) Compound **53**, the unsubstituted (*E*)-(2-nitroprop-1-en-1-yl)benzene exhibits anti-proliferative activity comparable to the previous lead **85**, however this activity is less than that of the halogenated and alkoxy analogues discussed earlier (Figure 243). The C-2 naphthalene compound **40** was observed to exhibit a more potent effect in both cell lines when compared to its C-3 analogue **37** (Figure 244).

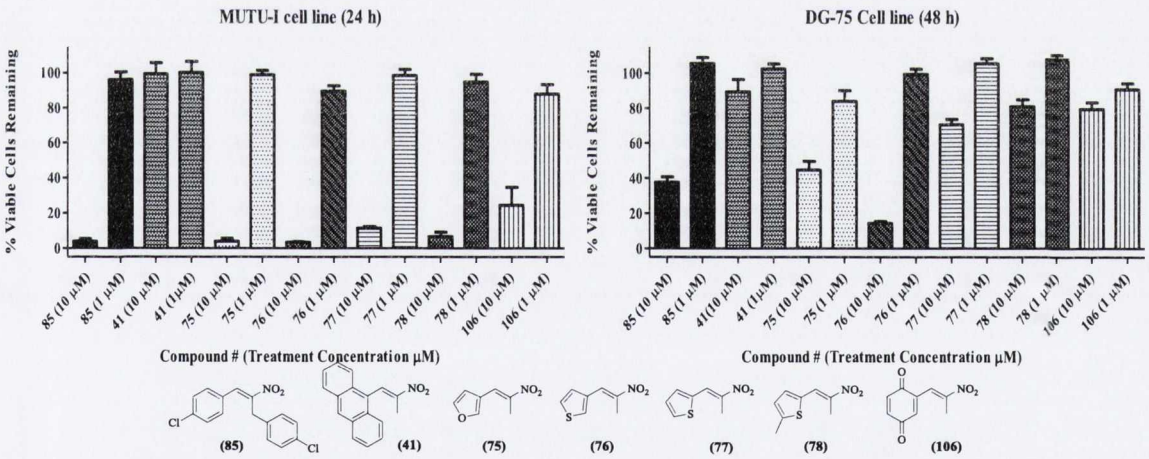

Figure 245: Preliminary screen for (*E*)-(2-nitroprop-1-en-1-yl)benzenes anti-proliferative activity (D)

(IV) The anthracene based compound (**41**) was inactive in both cell lines with >90% viable cells remaining. While the remaining compounds were all active at 10 μM in the MUTU-I cell line (<20% viable cells remaining), compounds **106**, **78** and **77** elicited only a weak anti-proliferative effect at 10 μM in the DG-75 cell line (~70%). The 3-thionyl compound **76** was the most promising of this heterocyclic group giving good activity at 10 μM in both cell lines (<10%) but was inactive at 1 μM in both cell lines (>90%). The C-3 thiophene based heterocycle **76** was shown to be more active in the DG-75 cell line than its C-3 furan analogue

(**75**) however with the nitrovinyl unit at C-2 activity in the DG-75 cell line is diminished to ~80% cell viability (Figure 245).

6.2.4 *In vitro* anti-proliferative activity screen of the (*E*)-(2-nitrobut-1-en-1-yl)benzenes

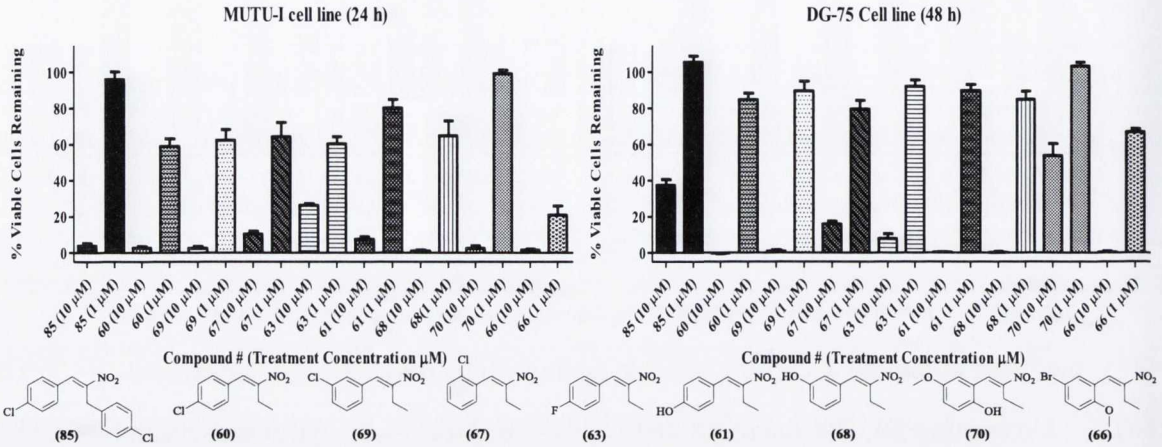

Figure 246: Preliminary anti-proliferative screen for (*E*)-(2-nitrobut-1-en-1-yl)benzenes (A)

(I) Introduction of an ethyl sidechain to C-4 chloro nitrostyrene (**60**) once again increased the anti-proliferative effect in both the DG-75 (~80% 1 µM) and MUTU-I (~59% 1 µM) cell lines when compared to the previous lead **85**. Compound **66** possessed the most potent anti-proliferative activity with good activity at 1 µM in both cell lines (MUTU-I ~20%, DG-75 ~67%). In a study of the position of chloro substituent it was observed that C-3 and C-4 chloro substitutions (**60, 69**) were more favourable for increased anti-proliferative activity in both cell lines over the C-2 chloro analogue (**67**). Increased electronegativity provided by fluoro substitution (**63**) was shown to decrease the anticancer effect in the MUTU-I cell line to ~26% viable cells remaining at 10 µM (Figure 246).

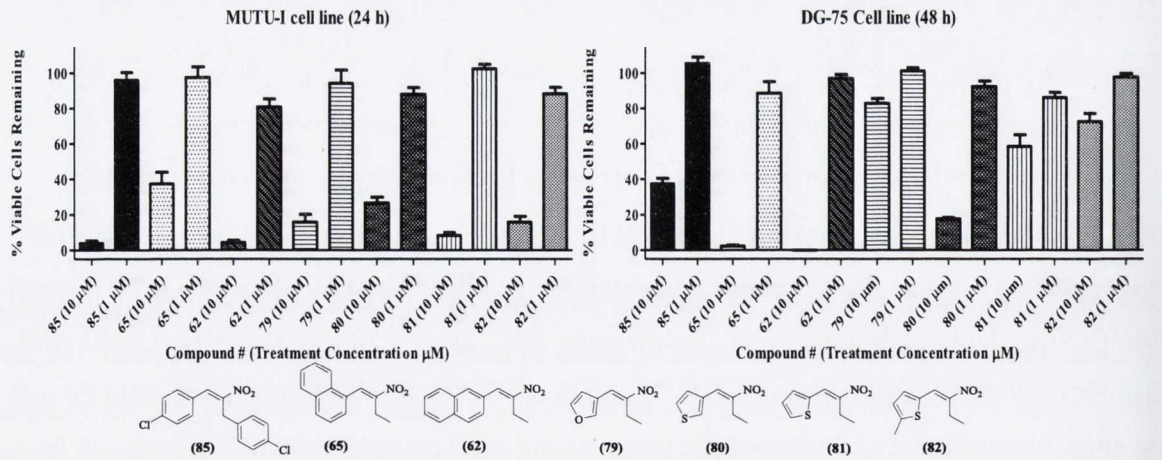

Figure 247: Preliminary anti-proliferative screen for (*E*)-(2-nitrobut-1-en-1-yl)benzenes (B)

By comparing the results obtained by the hydroxy compounds (**68, 70, 61**) it was concluded that C-3 hydroxyl substitution (**68,** 1 μM ~64%) was more favourable for anti-proliferative behaviour in the MUTU-I cell line over its C-4 analogue (**61,** 1 μM ~80%).

(II) The naphthalene based (*E*)-(2-nitrobut-1-en-1-yl)benzenes exhibited good anti-proliferative activity in both cell lines at the higher concentration with ~2-35% viable cells remaining. As previously discussed the C-3 thiophene based analogue (**80**) induced a ~1% response at 10 μM in the DG-75 cell line outperforming its furan based analogue (**79**) and the C-2 thiophene analogues (**81, 82**) >50% viable cells remaining (Figure 247).

6.2.5 *In vitro* anti-proliferative activity screen of the (*E*)-1,3-bis(aryl)-2-nitro-1-propenes, 1-aryl-1-nitroethanes and the (2-nitropropane-1,3-diyl)dibenzenes

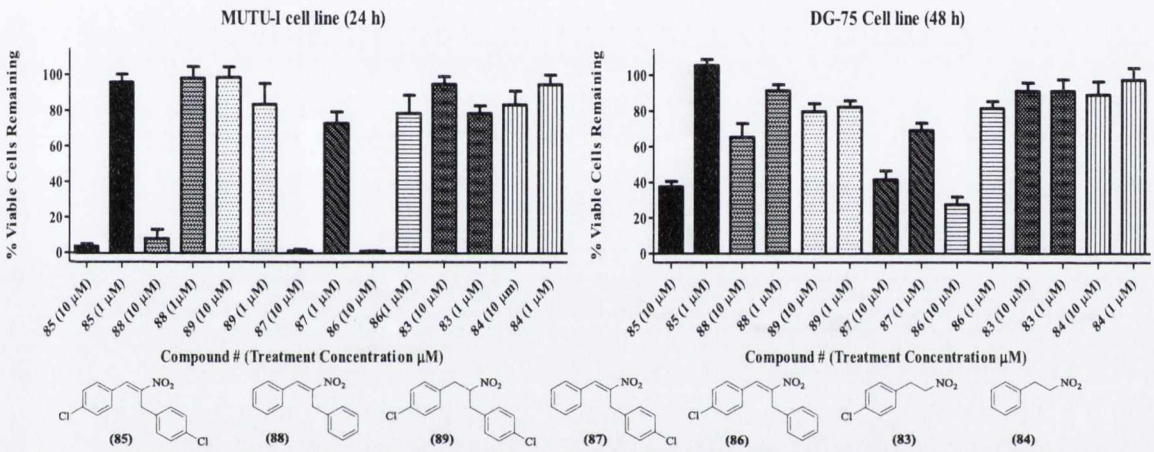

Figure 248: Preliminary screen for anti-proliferative activity of the (*E*)-1,3-bis(aryl)-2-nitro-1-propenes, 1-aryl-1-nitroethanes and the (2-nitropropane-1,3-diyl)dibenzenes

Reducing compounds **1**, **21** and **85** to their respective nitroalkane analogues **83**, **84** and **89** impacted the anti-proliferative potential of the pharmacophore, reducing its effect and allowing >80% of cells to remain viable at both concentrations in both cell lines. An unsubstituted (*E*)-1,3-bis(aryl)-2-nitro-1-propene (**88**) elicited a lesser anti-proliferative effect at both concentrations in the DG-75 cell line (>60%) than the substituted (*E*)-1,3-bis(aryl)-2-nitro-1-propene analogues (**85**, **86**, **87**). Compounds **86** and **87** improved upon activity exhibited by compound **85** and gave comparable activities at the 1 μM in the MUTU-I cell line (~65-83%). Compound **86** (bearing C-4 chloro substitution of the nitrostyrene unit and no substitution of the benzyl sidechain) elicited a more potent effect at 1 μM in the DG-75 cell line (~70%) than compound **87** (~80%) (bearing C-4 chloro substitution of the benzyl sidechain and no substitution of nitrostyrene unit) (Figure 248).

6.2.6 *In vitro* anti-proliferative activity screen of the (*E*)-2-nitro-1,3-diphenylprop-2-en-1-ones and ethyl (*E*)-2-hydroxy-3-nitro-4-phenylbut-3-enoates

The (*E*)-2-nitro-1,3-diphenylprop-2-en-1-ones (**90, 91, 92, 93, 94**) are chalcone based nitrostyrenes bearing structural similarity to the initial lead compound **85** and the (*E*)-1,3-bis(aryl)-2-nitro-1-propenes (**85, 86, 87, 88**).

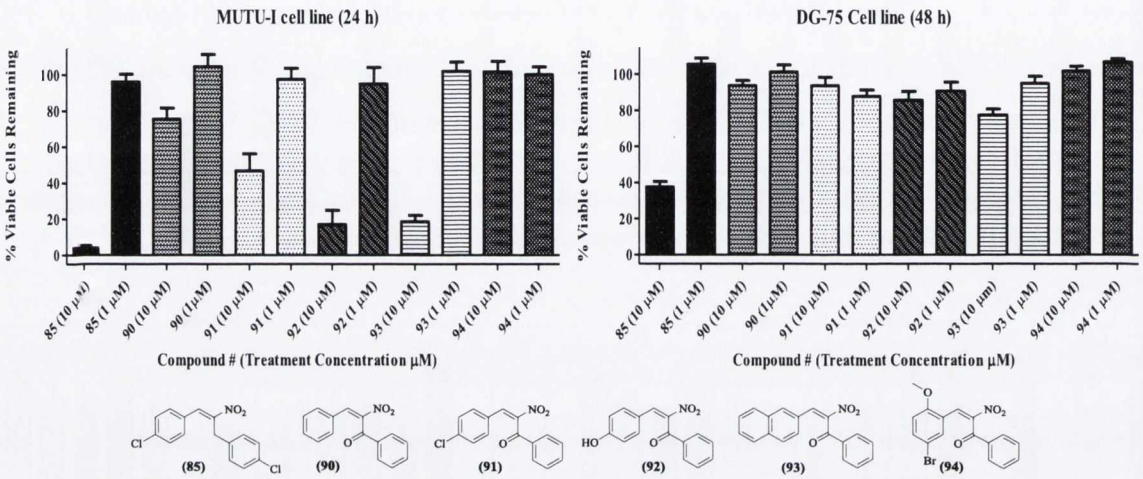

Figure 249: Preliminary screen for anti-proliferative activity of the (*E*)-2-nitro-1,3-diphenylprop-2-en-1-ones

This series of (*E*)-2-nitro-1,3-diphenylprop-2-en-1-ones (**90, 91, 92, 93, 94**) were inactive (>80%) at both the 10 μM and 1 μM concentrations in the DG-75 cell line. In the MUTU-I cell line good anti-proliferative activity was observed at 10 μM by compounds **91**, **92** and **93** with ~15-40% viable cells remaining. The C-4 hydroxy compound **92** was deemed the most potent of this cohort with ~16% viable cells remaining after treatment with 10 μM in the MUTU-I cell line (Figure 249).

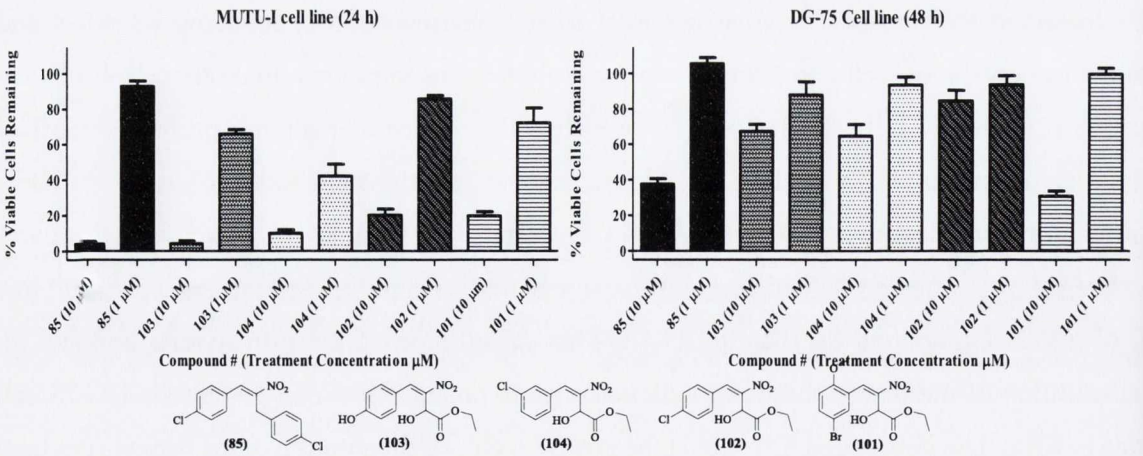

Figure 250: Preliminary screen for anti-proliferative activity of the ethyl (*E*)-2-hydroxy-3-nitro-4-phenylbut-3-enoates

Baylis-Hillman adducts (**101, 102, 103, 104**) were found to possess promising activity in the MUTU-I cell line at both concentrations, the best compound (**104**) gave a response of <10% viable cells at 10 μM and <50% at 1 μM. Anti-proliferative performance was not as prominent in the DG-75 cell line, however the bromomethoxy compound (**101**) equated to a promising ~25% viable cells remaining at the higher concentration. In this cohort of compounds the C-3 chloro substitution possessed a greater anti-proliferative effect (**104**, ~42%) at 1 μM than the C-4 chloro analogue (**102**, ~86%) and C-4 hydroxy analogue (**103**, ~66%) in the MUTU-I cell line (Figure 250).

6.2.7 *In vitro* anti-proliferative activity screen of the 1-substituted-2-nitroethylbenzenes

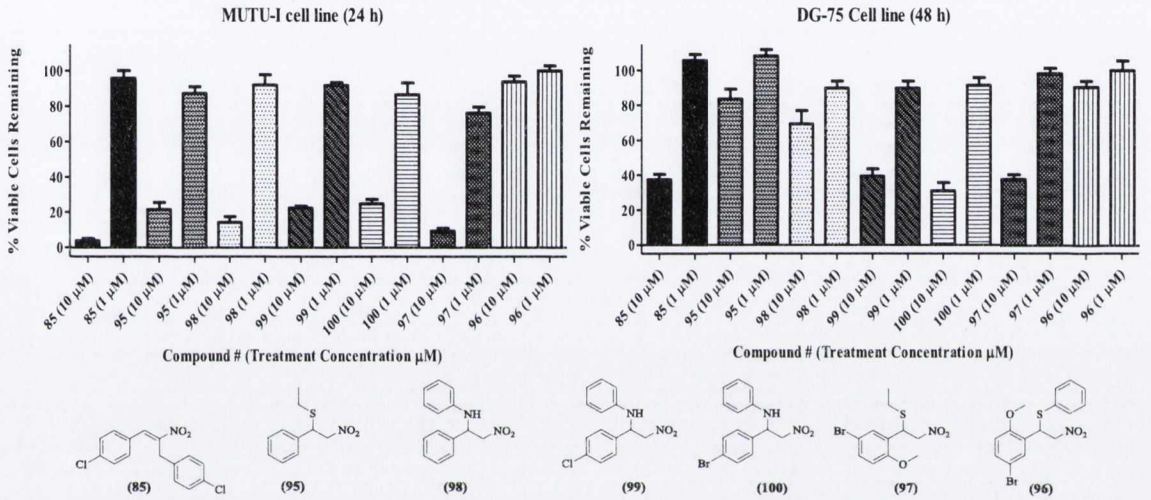

Figure 251: Preliminary screen for anti-proliferative activity of the 1-substituted-2-nitroethylbenzenes

The Michael adducts (**95, 97, 98, 99, 100**) gave good anti-proliferative action at 10 μM in the MUTU-I cell line of ~9-20% viable cells remaining. Compound **96** was found to be inactive (>85%) in both BL cell lines. The activity profile of the nitrogen based Michael adducts (**98, 99, 100**) in the DG-75 cell line was comparable to the lead compound **85**. The C-4 chloro analogue (**99**) was the most potent of these adducts at 1 μM in the MUTU-I cell line with ~73% viable cells remaining (Figure 251). However the observed reduced potency of this series of Michael adducts indicated that the vinyl double bond was favourable for anti-proliferative activity.

6.2.8 *In vitro* anti-proliferative activity screen of the 2-alkyl-2-nitro-3-phenyloxiranes and the 5-alkyl-4-phenyl-1*H*-1,2,3-triazoles

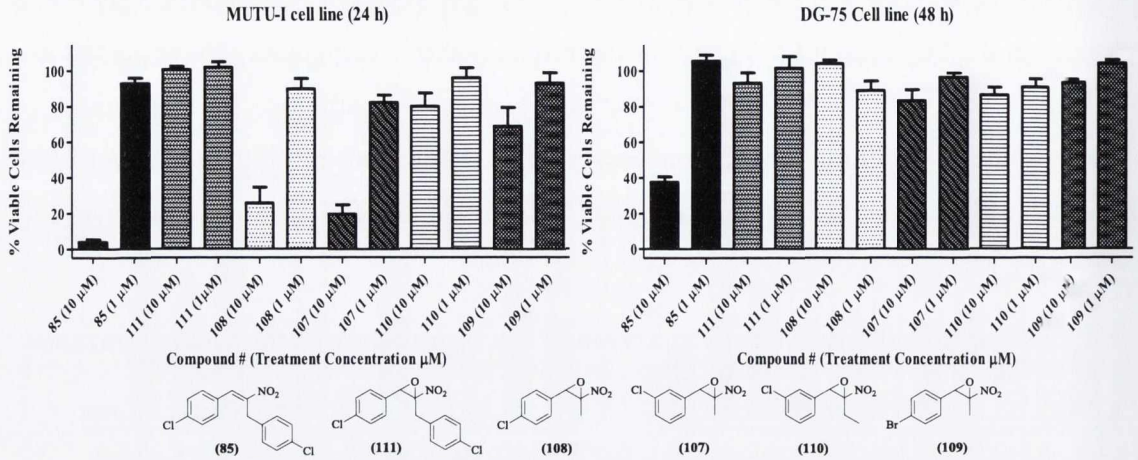

Figure 252: Preliminary screen for anti-proliferative activity of the 2-alkyl-2-nitro-3-phenyloxiranes

The 2-alkyl-2-nitro-3-phenyloxiranes introduced a rigid three member epoxide ring in place of the vinyl functionality of the nitrostyrenes. The epoxides (**107 - 111**) were inactive (>80% viable cells remaining) in the DG-75 cell line at both concentrations. The C-3 and C-4 chloro compounds **108** and **107** were the most active in the MUTU-I cell line at 10 µM (~20-25%) (Figure 253).

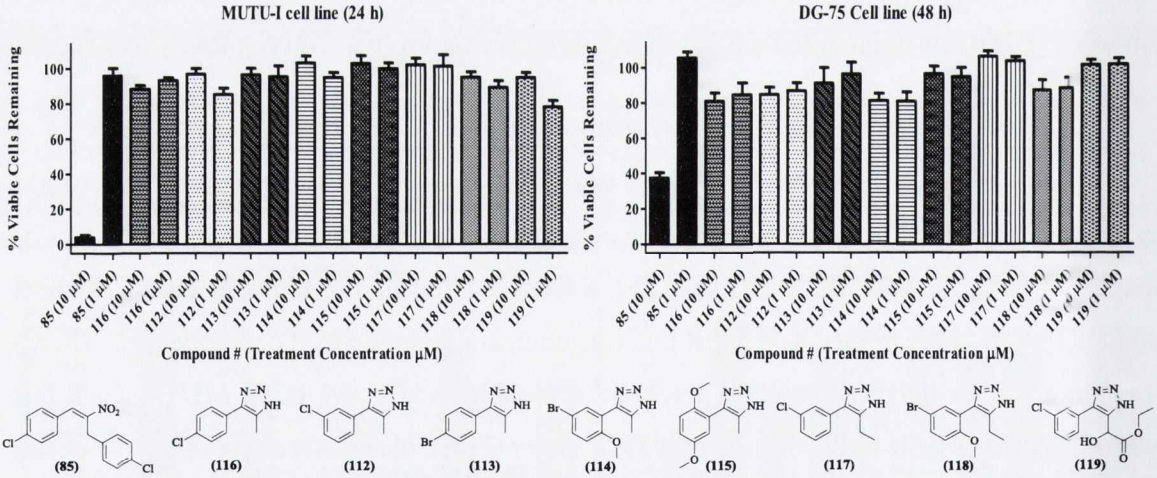

Figure 253: Preliminary screen for anti-proliferative activity of the 5-alkyl-4-phenyl-1H-1,2,3-triazoles

The 5-alkyl-4-phenyl-1*H*-1,2,3-triazoles (**112 - 119**) induced a constrained '(*E*)' configuration on the vinyl system of the nitrostyrenes however at the cost of eliminating the nitro functionality. It was observed that these triazole compounds were inactive (>80% viable cells remaining) in both the MUTU-I and DG-75 cell lines (Figure 253).

6.2.9 *In vitro* anti-proliferative activity screen of the 2-substituted-3-phenylacrylonitriles

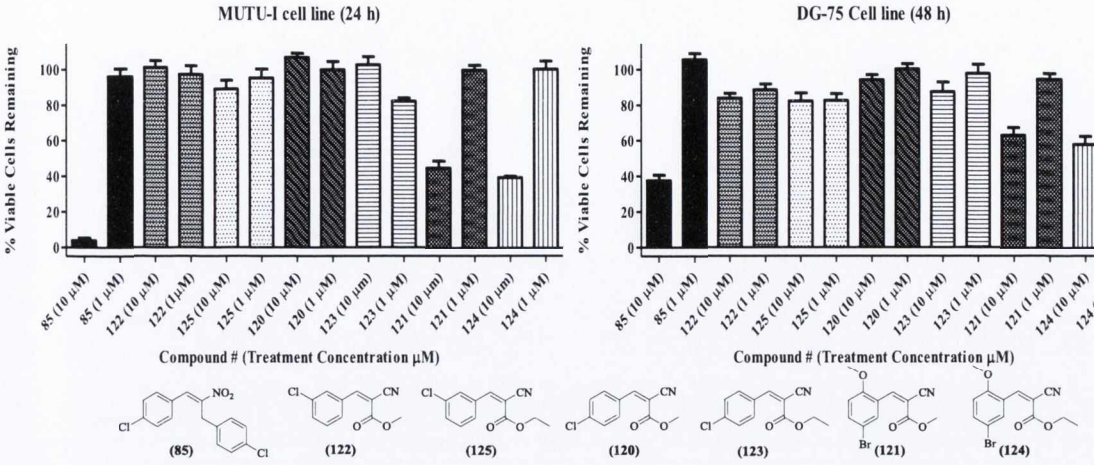

Figure 254: Preliminary screen for anti-proliferative activity of the 2-substituted-3-phenylacrylonitriles

The 2-substituted-3-phenylacrylonitriles (**120, 122, 123, 125**) were found to elicit poor activity at 10 μM and 1 μM in both cell lines. Compounds **121** and **124** bearing C-2 methoxy and C-5 bromo substituents were found to be the more active compounds of this series and gave activity at 10 μM in MUTU-I (~35-40%) and DG-75 (~50-60%) (Figure 254).

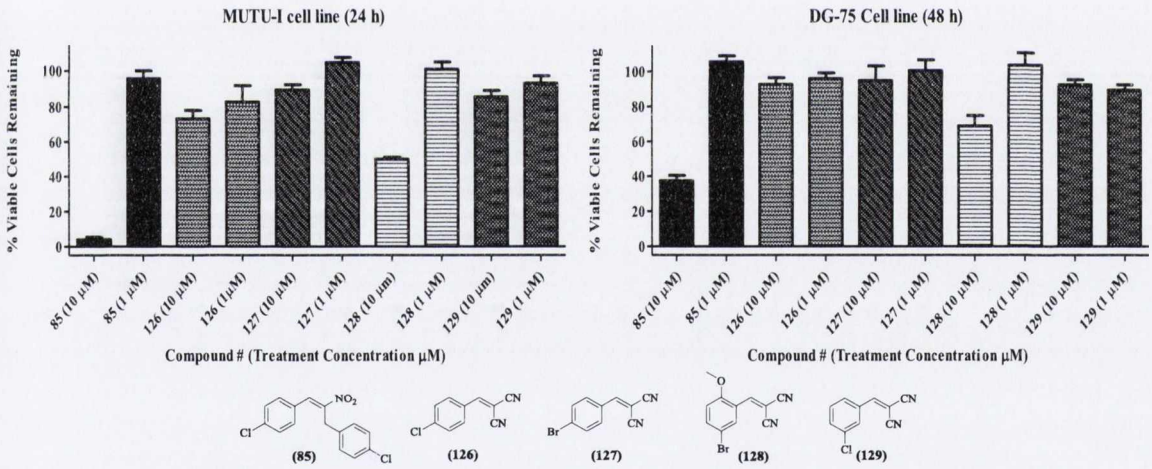

Figure 255: Preliminary screen for anti-proliferative activity of the 2-substituted-3-phenylacrylonitriles

The 2-substituted-3-phenylacrylonitriles (**126, 127, 129**) were also found to possess poor anticancer activity in both cell lines. Similarly compound **128** bearing C-2 methoxy and C-5 bromo substituents was found to be the most active of this family at 10 μM in both the MUTU-I (~64%) and DG-75 (~50%) cell lines (Figure 255).

6.2.10 *In vitro* anti-proliferative activity screen of the benzylidenehydrazines

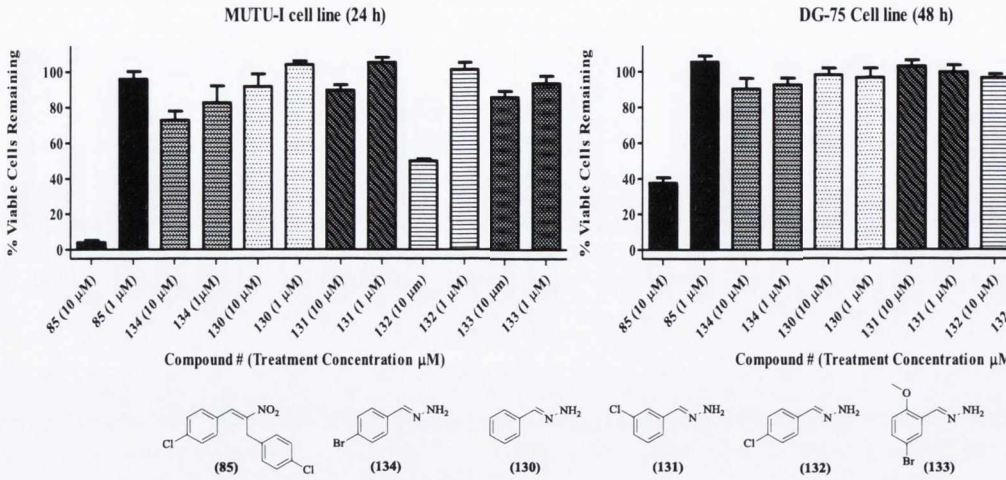

Figure 256: Preliminary screen for anti-proliferative activity of benzylidenehydrazines

The benzylidenehydrazines (**130, 131, 133, 134**) showed poor anti-proliferative properties at 10 µM and 1 µM in both cell lines. Compound **132** provided the largest anti-proliferative effect in this grouping with ~45% viable cells remaining at 10 µM in the MUTU-I cell line but was inactive in the DG-75 cell line (>80%) (Figure 256).

6.2.11 Summary of preliminary screen findings

In summary the *para* chloro (*E*)-(2-nitrovinyl)benzene (**1**) was shown to exhibit comparable anti-proliferative activity to the previous 1,3-bis(aryl)-2-nitro-1-propene lead compound (**85**) (Figure 257). Removing substitution of the phenyl ring was found to reduce the anti-proliferative activity provided by the pharmacophore (**10, 53, 70**). A number of the more potent (*E*)-(2-nitrovinyl)benzenes possessed phenyl C-3 halogen or hydroxy and C-2 alkoxy substitutions and these characteristics were found to be favourable for promoting anti-proliferative activity e.g. compounds (**9**, **14**, **17**, **19**, **26**, **32**) in both cell lines. Increased alkyl chain length at vinyl C-2 of the nitrostyrene pharmacophore to methyl and ethyl leads to increased anti-proliferative effects, this trend continued throughout the preliminary screen with some exceptions particularly in the anthracene, bis-nitrovinyl, furan and C-2 thiophene based nitrovinyl compounds. Some examples for this trend include compounds (**9, 54, 66**), (**1, 35, 60**) and (**2, 36, 61**). The benzoquinone based compounds (**105**, **106**) were found to possess negligible anti-proliferative activity.

Reducing the nitrostyrenes (**1, 10, 85**) to their nitroalkane adducts (**83, 84, 89**) inactivated the pharmacophore (>80% viable cells remaining) at both 10 µM and 1 µM in the BL cell lines. The nitrochalcones (**90, 91, 92, 93, 94**) possessed good activity in the MUTU-I

cell line, however the introduction of the carbonyl did not have a favourable impact on activity in the DG-75 cell line with >80% viable cells remaining at both concentrations. The epoxide, hydrazone and triazole derivatives were also found to elicit a poor anti-proliferative effect (>80% viable cells remaining). The C-2 methoxy and C-5 bromo substituted MBH adducts and the 2-substituted-3-phenylacrylonitrile cohorts were observed to induce the most favourable anti-proliferative effects in both cell lines. The structure activity relationship is depicted in Figure 257.

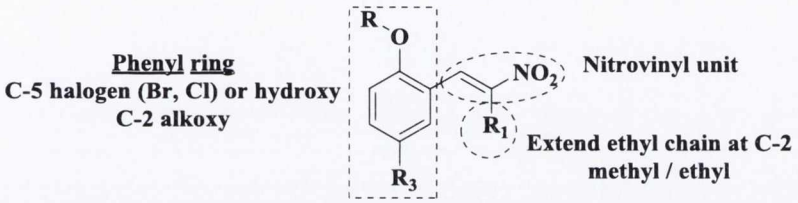

Figure 257: Optimised nitrostyrene analogue for antiproliferative activity in BL cell lines

6.2.12 *In vitro* anti-proliferative activity (IC_{50s}) of the most potent nitrostyrene derivatives

The IC_{50} values of the most promising anti-proliferative nitrostyrene compounds identified during the preliminary biological screen at 10 μM and 1 μM were obtained for both the DG-75 and MUTU-I BL cell lines. Compounds **7**, **9**, **17**, **19** and **26** were selected from the initial (*E*)-(2-nitrovinyl)benzene library, compounds **35**, **36**, **54**, **55**, **57** and **59** were selected from the (*E*)-(2-nitroprop-1-en-1-yl)benzene library. The (*E*)-(2-nitrobut-1-en-1-yl)benzene library provided the active compounds **60**, **61**, **66**, **67** and **69**, while the MBH adduct compound **101** represented the most active ethyl (*E*)-2-hydroxy-3-nitro-4-phenylbut-3-enoate. IC_{50} values were also obtained for the previous lead nitropropene compound (**85**) (2.82-6.03 μM) and the chemotherapeutic agent taxol (0.32-1.32 μM) in the BL cell lines (Table 40). All nitrostyrene compounds gave IC_{50} values <6 μM in the BL cell lines, with many <1 μM. The IC_{50} determination identified compound **66** as the most potent anti-proliferative agent with an IC_{50} of 0.45 μM in the MUTU-I and 1.26 μM in the DG-75.

Lipinski rule of five properties for druggability were calculated for these compounds (Mcule property calculator v1 2015). Lipinski's rules are a series of chemical parameters used to predict the 'drug like' behaviour of a given molecule in a bio-physiological system. In order to be orally available the following criteria must be met:

1. Molecular weight (Mr) of the compound must be < 500 Daltons
2. LogP value (lipophilicity) < 5
3. Number of hydrogen bond acceptors (nON) < 10
4. Number of rotatable bonds (nrotb) < 10

5. Number of hydrogen bond donors (nOHNH) < 5

6. Polar surface area (PSA) < 140 Angstroms^2

These parameters were applied to the library of nitrostyrene derivatives and these compounds were found to satisfy all the Lipinski rule of five criteria (Table 40). On further analysis, no trend between anti-proliferative activity and lipophilicity or PSA was observed.

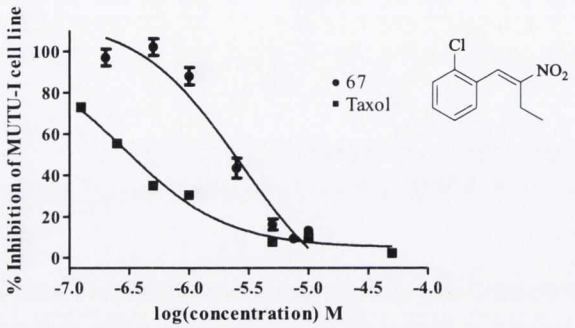

Compound #	IC50 (μM)		Lipinski properties					
	MUTU-I (24 h)	*DG-75 (48 h)*	*Mr*	*logP*	*nrotb*	*nON*	*nOHNH*	*PSA (Å^2)*
Taxol	0.32	1.32	853.9	7.38	15	15	4	221.29
85	2.82	6.03	308.2	5.377	4	3	0	45.82
7	2.57	2.08	249.2	4.763	2	3	0	45.82
9	0.87	4.17	258.0	3.228	3	4	0	55.05
17	0.75	4.16	209.2	2.474	4	5	0	64.28
19	0.72	2.82	193.2	2.856	4	4	0	55.05
26	5.75	8.32	165.2	2.163	2	4	1	46.66
35	1.18	2.75	197.6	3.501	2	3	0	45.82
36	2.14	5.25	179.2	2.553	2	4	1	66.05
54	0.76	1.59	272.1	3.618	3	4	0	55.05
55	0.91	1.99	197.6	3.501	2	3	0	45.82
57	0.76	2.34	197.6	3.501	2	3	0	45.82
59	0.93	3.31	207.2	3.246	4	4	0	55.05
60	1.05	3.09	211.6	3.891	3	3	0	45.82
61	1.55	3.31	193.2	2.943	3	4	1	66.05
66	0.45	1.26	286.1	4.009	4	4	0	55.05
67	2.29	2.24	211.6	3.891	3	3	0	45.82
69	1.12	2.51	211.6	3.891	3	3	0	45.82
101	2.51	3.16	360.2	2.523	7	7	1	101.58

Table 40: IC_{50} value (BL cell lines DG-75 & MUTU-I) and Lipinski properties of leading nitrostyrenes Chapter 1

6.2.13 Investigations into the pro-apoptotic effect of the most potent nitrostyrene derivatives

The design of drugs that induce selective programmed cell death (PCD) (apoptosis) of cancer cells over normal cells is crucial to the development of safer and more effective agents. A compound that induces apoptosis *in vitro* has the potential to become an anticancer agent. In order to quantify the pro-apoptotic effects of the most potent nitrostyrene derivatives Annexin V / PI FACS analysis was carried out on a subset of 6 of the most potent compounds identified from the cell viability study. Annexin V / PI FACS analysis is described in section 7, Chapter 6. The study was carried out at the 10 μM in both the BL cell lines (DG-75 and MUTU-I). The chemotherapeutic agent Taxol (10 μM) was used as a positive control.

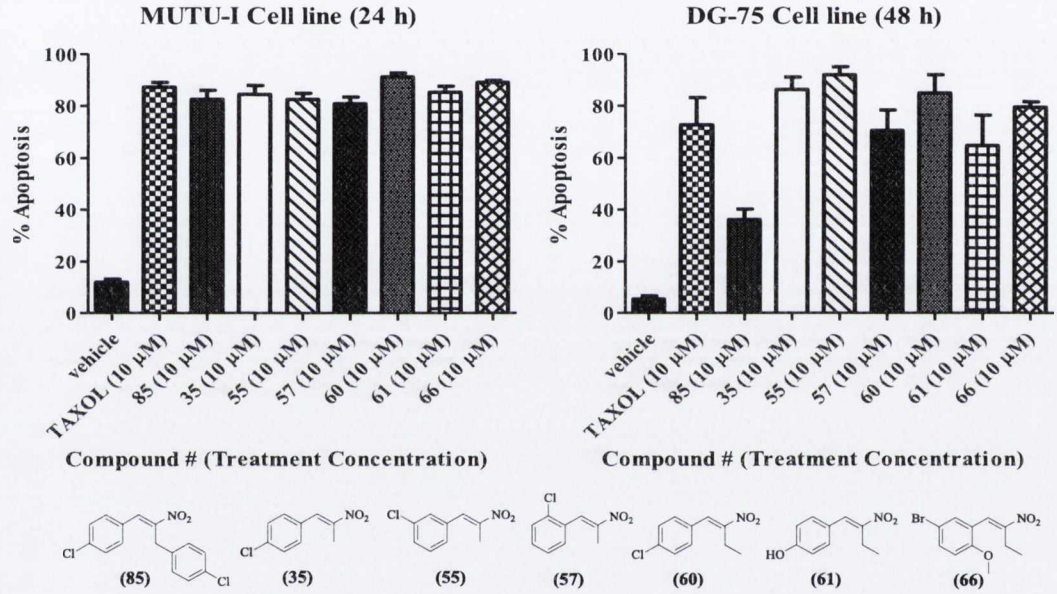

Figure 258: Annexin V / PI FACS - Apoptosis in MUTU-I and DG-75 cell lines

In the MUTU-I cell line all selected compounds elicited >80% apoptosis comparable to the effect induced by Taxol at the same concentration (Figure 258). The previous lead compound (**85**) was found to induce ~40% in the DG-75 cell line and an apoptotic effect was also induced with compounds **55, 57, 69** >85% apoptosis which is double that of compound **85**. The effect of these compounds was also comparable to Taxol at this concentration (MUTU-I >80%, DG-75 >60%).

6.2.14 *In vitro* anti-proliferative activity of the most potent nitrostyrene derivatives in other malignant diseases

The *in vitro* anti-proliferative activity of compounds **35, 55, 57, 60, 61, 66, 85** was further assessed in a number of other malignant cell lines. The cancer cell lines chosen for this study were HeLa (ovarian), MCF-7 (breast), HL60 (leukaemia) and the BL cell lines Ramos and Bjab. This preliminary investigation was carried out 10 μM and 1 μM and the results were quantified as percentage viable cells remaining after treatment (Table 41).

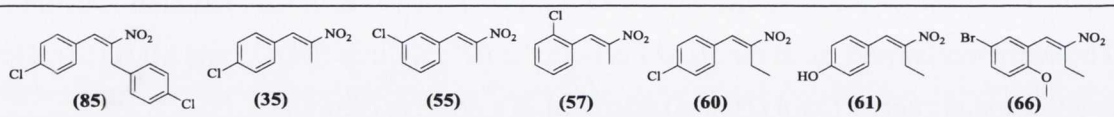

Compound #	% viable cells remaining									
	HeLa 24 h		*MCF-7* 72 h		*Ramos* 24 h		*Bjab* 24 h		*HL60* 24 h	
	10 μM	1 μM	10 μM	1 μM	10 μM	1 μM	10 μM	1 μM	10 μM	1 μM
Taxol	48.4	86.9	75.0	100.8	24.9	69.3	80.2	97.6	69.7	97.6
35	17.7	93.0	37.1	102.7	13.9	62.6	50.8	100.5	6.5	103.8
55	23.2	90.6	29.7	94.3	5.1	27.2	46.2	90.1	6.8	78.2
57	34.2	87.1	41.7	81.4	7.7	53.4	51.9	82.2	16.5	73.4
60	21.8	95.3	20.7	98.1	4.4	66.9	68.9	102.4	9.1	99.8
61	28.4	85.6	23.6	97.2	7.3	87.8	48.4	107.4	15.3	83.5
66	19.7	96.9	11.3	103.6	2.6	47.1	42.2	99.5	3.7	99.1
85	43.6	96.2	77.4	108.6	2.1	80.9	47.8	92.1	36.3	104.4

Table 41: *in vitro* anti-proliferative activity of compounds 35, 36, 55, 57, 60, 61, 66, 85 in HeLa, MCF-7, HL60, Ramos and Bjab cell lines

This selection of compounds elicited good anti-proliferative effects at the 10 μM concentration in all cell lines with comparable activity to the anti-proliferative effects exerted by Taxol. In summary the nitrostyrene compound **66** was found to elicit the most potent anticancer effect over the five lines at 10 μM (2.6-42.2%). The (*E*)-(2-nitrobut-1-en-1-yl)benzenes (**60, 61, 66**) were deemed the most favourable grouping for anti-proliferative activity in this study exerting a more potent effect that Taxol and the previous lead compound **85**. This grouping was particularly potent at 10 μM in the RAMOS (2.6-7.3% viable) and HL60 (3.7-15.3%) cell lines.

6.2.15 *In vitro* and *ex vivo* evaluation of lead compound for the treatment of CLL

Chronic lymphocytic leukaemia (CLL) is a type of B-cell malignancy effecting the blood and bone marrow. CLL is the most common type of leukaemia diagnosed in adults and over 400 new cases are diagnosed in Ireland each year[406, 407]. Compounds **85**, **55** and **66** were selected for further work in the CLL cell lines Cll, HG3, I83 and PGA1. This work was carried out by Dr. Sandra A. Bright in collaboration with the Williams Group, School of Biochemistry and Immunology, Trinity College Dublin.

6.2.15.1 Cell culture

The I83 cell line was isolated in 1994 from the peripheral blood of a 75-year-old Caucasian man with CLL. Epstein-Barr virus-transformed CLL cells PGA1 (mutated immunoglobulin heavy chain genes (IgV_H), good prognosis cell line) and HG3 (unmutated IgV_H, poor prognosis cell line) were grown in RPMI 1640 (Glutamax) medium supplemented with 10% (v/v) foetal bovine serum (FBS) and 50 μg/mL penicillin/streptomycin. Cells were grown in DMEM medium supplemented with 10% (v/v) foetal bovine serum (FBS) and 50 μg/mL penicillin/streptomycin. All cells were grown in a humidified environment maintained at 95% O_2 and 5% CO_2 and passaged at least twice weekly depending on their levels of confluency. Cell lines were seeded at 2 x 10^5 cells/mL prior to treatment.

6.2.15.2 *Ex vivo* patient samples

Fresh peripheral blood (10 mL) was collected with written informed consent from CLL patients (n = 14) in EDTA-anticoagulant tubes. Ethical approval for all work carried out on *ex vivo* CLL patient samples was obtained from the St. James's Hospital and Adelaide and Meath incorporating the National Children's Hospital Ethics Committee. Peripheral blood mononuclear cells (PBMCs) were isolated via lymphoprep ficoll gradient, diluted to a volume of 50 mL with RPMI medium and centrifuged for 10 min at 650 xg. Pelleted cells were resuspended in freezing medium and frozen until required. When required, frozen stocks were resuspended in RPMI 1640 (Glutamax) medium supplemented with 10% (v/v) FBS, 50 μg/ml penicillin/streptomycin and seeded at a density of 1 x 10^6 cells/mL. Cells were then treated for up to 48 h with the compounds or the required vehicles and positive controls (e.g. fludarabine).

6.2.15.3 Biochemical results

Compounds **85**, **55** and **66** exhibited good IC_{50} values in the CLL cell lines (alamarBlue® assay) ranging from 2.17 – 8.69 μM, this compared favourably to Fludarabine (IC_{50} = 20.7 – 49.9 μM) a current frontline treatment for CLL. Compounds **55** and **66** elicited a more potent overall response (IC_{50}: 2.17 - 3.46 μM) than the previous lead compound (**85**) in our study (IC_{50}: 8.05 – 8.69 μM).

Compound	IC_{50} (μM)			
	Cll (48 h)	*HG3 (48 h)*	*I83 (48 h)*	*PGA1 (48 h)*
Fludarabine	49.9	28.1	20.7	32.0
85	8.05	8.69	8.43	6.74
55	3.46	2.54	3.08	2.90
66	3.46	3.08	4.13	2.17

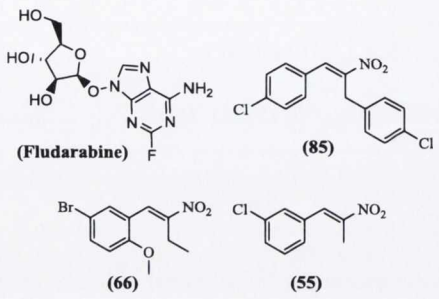

Table 42: IC_{50} of fludarabine, 85, 55 and 66 in the CLL cell lines Cll, HG3, I83 and PGA.

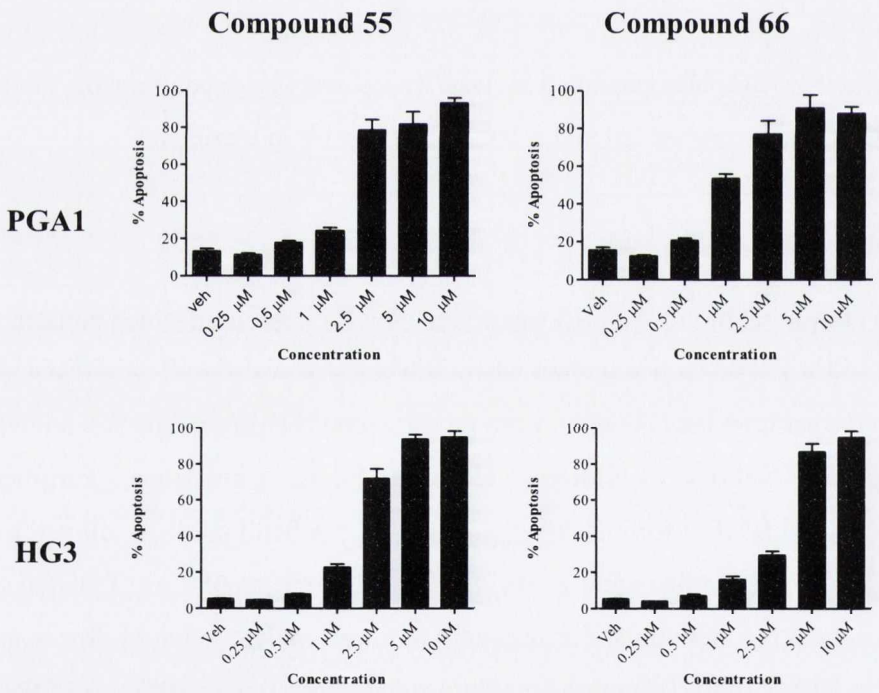

Figure 259: Compounds 55 & 66 in HG3 and PGA1 CLL cell lines - Annexin V / PI FACS analysis (48 h)

Annexin V / PI FACS analysis was carried out using a concentration range of compounds **85**, **55** and **66** in the HG3 and the PGA1 cell lines to determine the mode of cell death. A potent dose dependent apoptotic mechanism of cell death was observed. Compounds **55** and **66** elicited an apoptotic response of over 80% at 10 μM and 5 μM in both CLL cell lines. In the

PGA1 cell line at 1 μM compound **66** exhibited more favourable apoptotic activity (>50%) than compound **55** at the same concentration (<25%). Conversely in the HG3 cell line at 2.5 μM compound **55** exhibited more favourable apoptotic activity (>60%) than compound **66** at the same concentration (<25%) (Figure 259).

Additional annexin V / PI FACS analysis was carried out in the presence of a ROS inhibitor (N-acetyl cysteine) and a caspase inhibitor (Z-vad-fmk) in order to study their effects (if any) on pro-apoptotic effects. In the presence of NAC the apoptosis induced by compounds **55** and **66** decreased from 64-67% to 20-30% at 2.5 μM and from 86-87% to 31-34% at 5 μM in the PGA1 cell line. Similar results were obtained in the HG3 cell line at 2.5 μM (57-91% to 34-36%) and 5 μM (84-86% to 30-50%). In the presence of the caspase inhibitor the apoptosis induced by compounds **55** and **66** decreased from 59-60% to 26-48% at 2.5 μM and from 81-89% to 37-38% at 5 μM in the PGA1 cell line. Similar results were obtained in the HG3 cell line at 2.5 μM (61-83% to 12-30%) and 5 μM (75-83% to 34-49%). These findings indicate that both caspases and ROS may be involved in the mechanism of apoptosis for compounds **55** and **66** (Figure 260).

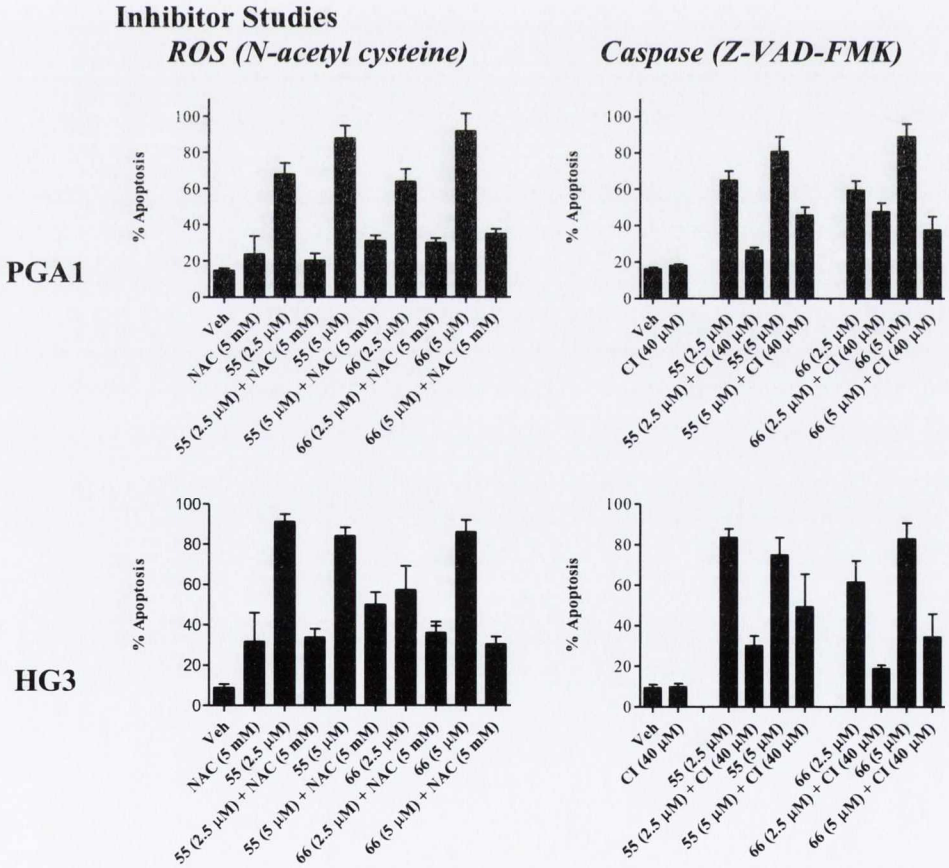

Figure 260: Compounds 55 & 66 in HG3 and PGA1 CLL cell lines – Inhibitor study Annexin V / PI FACS analysis (48h)

Ex vivo CLL patient samples were kindly provided by Dr. Anthony McElligott (School of Molecular Medicine, Trinity College Dublin) and cultured by Dr. Sandra A. Bright (School of Biochemistry and Immunology, Trinity College Dublin). It was observed that compounds **85**, **55** and **66** exhibited potent anti-proliferative and pro-apoptotic activity in a dose dependant manner.

***Ex vivo* patients samples**

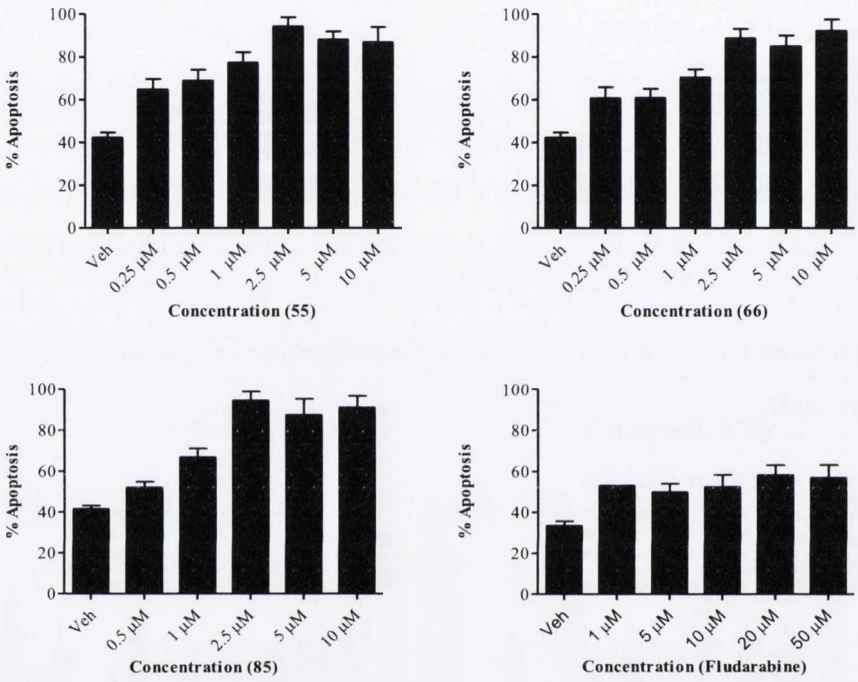

Figure 261: Ex vivo CLL patients samples - Annexin V / PI FACS analysis (48 h)

The activity exhibited by compounds **85**, **55** and **66** was more potent that the frontline treatment Fludarabine. Compounds **55, 66** and **85** were observed to elicit a potent proapoptotic response (>80%) at 10 μM, 5 μM and 2.5 μM (Fludarabine <60%). It is interesting that compounds **55** and **66** elicited an apoptotic response of >60% at 0.25 μM, demonstrating a potent effect at this low concentration.

6.2.16 Effect of compounds 55 and 66 on the viability of PBMCs

Compounds **55** and **66** were evaluated for their toxicity on PBMCs (peripheral blood mononuclear cells) to determine if these potent compounds have a selective toxic effect on malignant BL cell lines over normal lymphatic cells. Compounds were evaluated at 10 μM and 1 μM over a 24 h treatment time (Figure 293). This work was carried out by Dr. Sandra A. Bright in collaboration with the Williams Group, School of Biochemistry and Immunology, Trinity College Dublin.

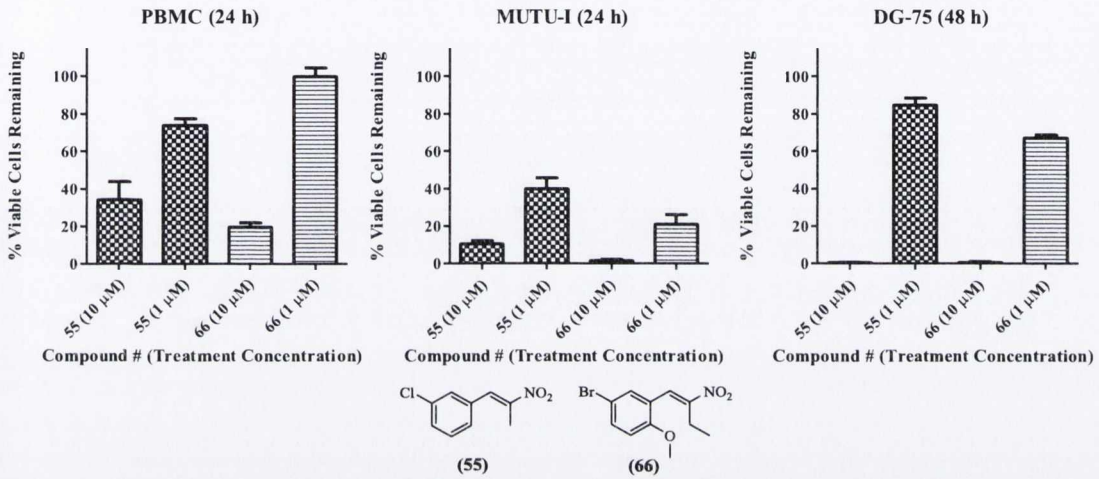

Figure 262: In vitro antiproliferative effect of compounds 55 and 66 on PBMCs (24 h), MUTU-I cell line (24 h) and DG-75 cell line (48 h) at 10 μM and 1 μM

Compound **55** and **66** demonstrated moderate toxicity in the PBMCs at 10 μM (19-34% viable cells) and low toxicity activity at 1 μM (74-99% viable cells) (Figure 262). Compound **55** and **66** exhibit good anti-proliferative effects in both BL cell lines at 10 μM (2-10% viable cells remaining). Anti-proliferative effects are also observed for both compounds at the lower concentration (1 μM) in the MUTU-I cell line (21-40% viable cells) and in the DG-75 cell line (67-85% viable cells). Comparing the results obtained from the BL cell lines and the PBMCs, the results suggest compounds **55** and **66** exert a selectively toxic effect on BL cell lines.

6.3.0 Evaluation of the *in vitro* anti-proliferative activity of the heterocyclic nitrostyrene analogues

A series of over 29 related nitrovinyl heterocycles were evaluated for anti-proliferative activity at 10 μM and 1 μM in the MUTU-I and DG-75 cell lines. These heterocycles induce a constrained configuration on the anti-proliferative nitrostyrene pharmacophore and the effects of these induced configurations was evaluated biologically. These nitrovinyl heterocycles are discussed in two main groupings and categorised within the groups by structural type.

6.3.1 Preliminary screen for *in vitro* anti-proliferative activity of the 3-nitro-2-phenyl-2*H*-chromenes and 3-nitro-1,2-dihydroquinolines

A series of 3-nitro-2-phenyl-2*H*-chromenes were evaluated at 10 μM and 1 μM for anti-proliferative activity in the MUTU-I and DG-75 BL cell lines (Figure 263). Compounds **137**, **139**, **145** were found to possess the most potent anti-proliferative activity in the MUTU-I cell line with good activities at 1 μM (~38-48% cells remaining). These compounds contained hydroxyl and alkoxy substituents on the phenyl ring. Compound **145** (C-7 methoxy chromene ring) exerted the greatest anti-proliferative effect in the DG-75 cell line at 1 μM with 58% viable cells remaining. Compound **141** (the phenol analogue of **145)** was relatively inactive >85% viable cells were remaining with this analogue.

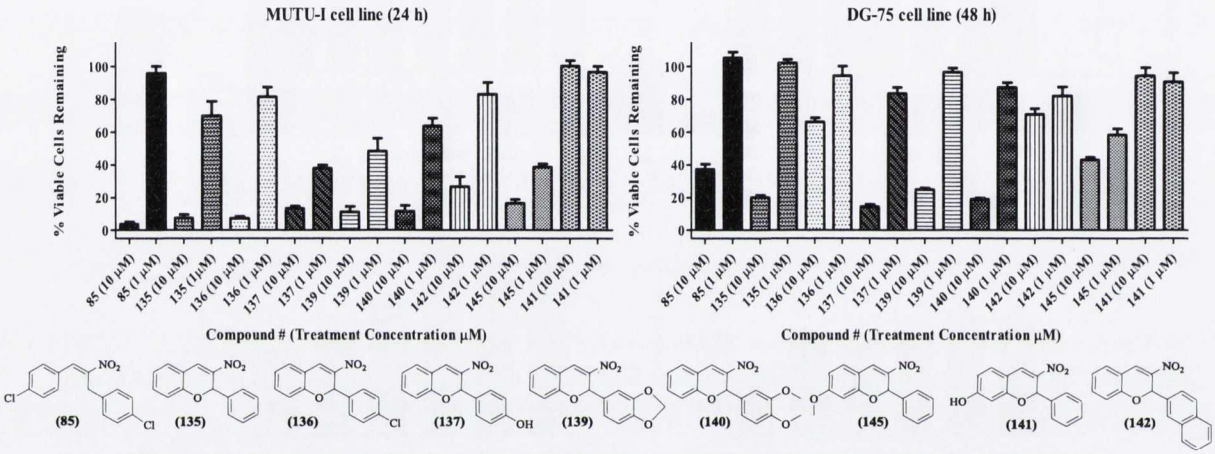

Figure 263: Preliminary screen for anti-proliferative activity of the 3-nitro-2-phenyl-2*H*-chromenes

A number of other chromene ring substitutions (C-6 / C-8 chloro, C-8 methoxy) were also evaluated and found to possess good anti-proliferative effects in both BL lines at 10 μM (<10%) (**146**, **147**, **144**, **143**). The quinoline and quinolone analogues (**149**, **150**, **151**) possessed little anti-proliferative effects at both concentrations (>90% remaining). Compound **148** was the most promising quinoline with activity at 10 μM in both cell lines (~45%) (Figure 264).

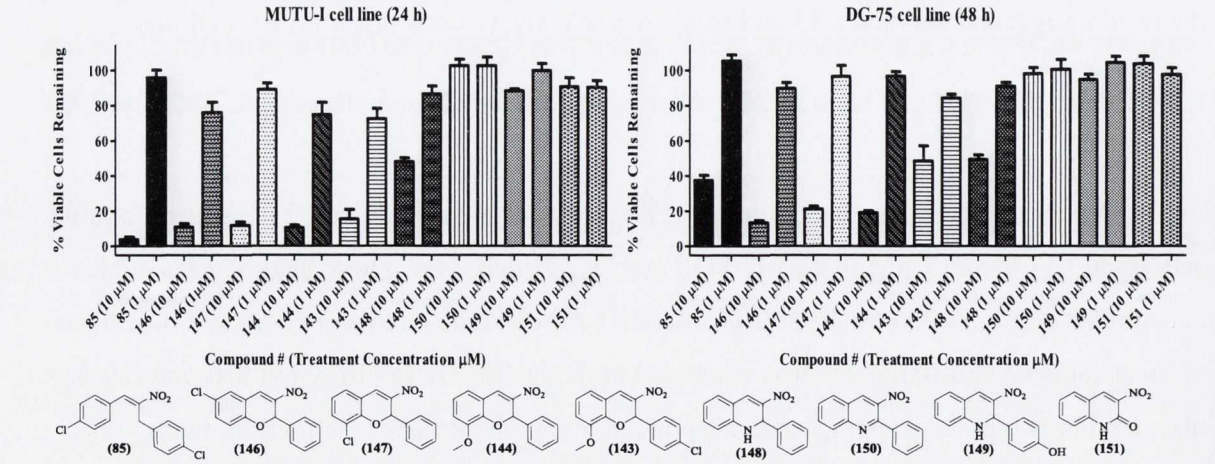

Figure 264: Preliminary screen for anti-proliferative activity of the 3-nitro-2-phenyl-2*H*-chromenes

6.3.2 Preliminary screen for *in vitro* anti-proliferative activity of the 3-nitro-flavones and other heterocycles

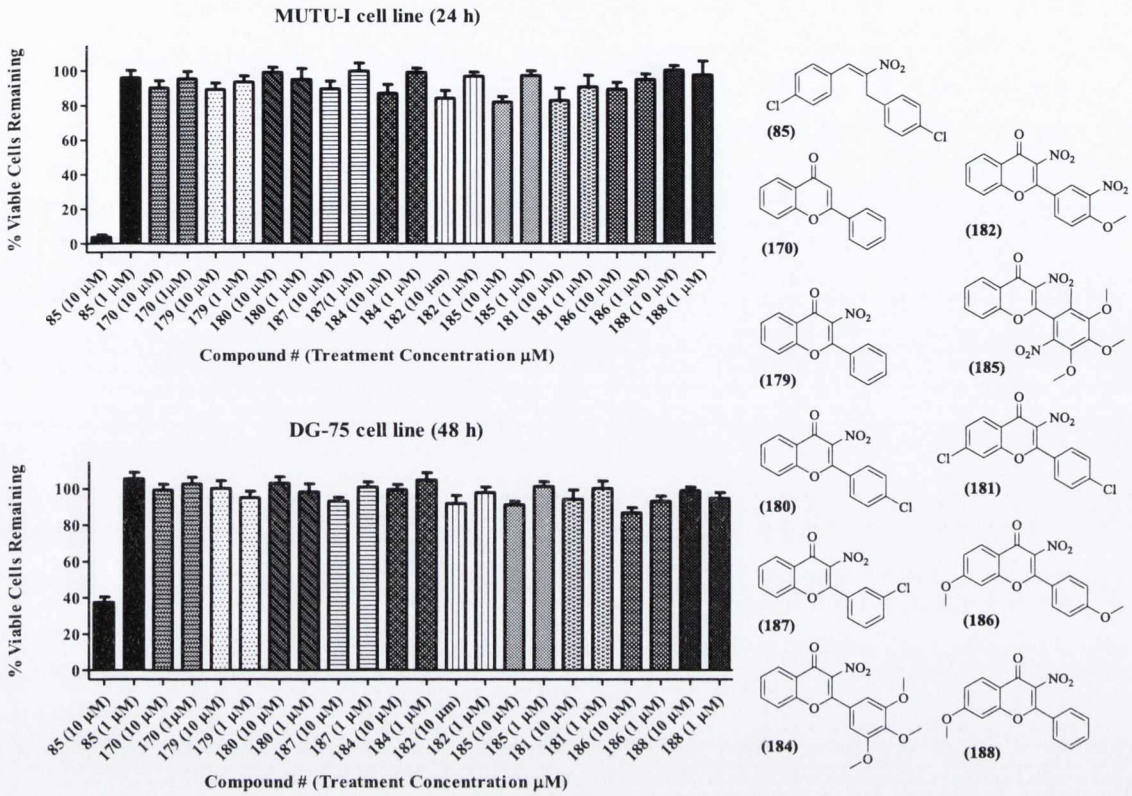

Figure 265: Preliminary screen for anti-proliferative activity of the 3-nitro-flavones

Flavone (**170**) and the 3-nitroflavones (**179** - **188**) were evaluated for anti-proliferative activity in the MUTU-I and DG-75 cell lines at 10 μM and 1 μM. Compound **85** was once again used as the therapeutic standard. It was observed that flavone and the 3-nitroflavones synthesised in the current work were inactive in the BL lines at these concentrations with over 90% of viable cells remaining after the treatment periods (Figure 265).

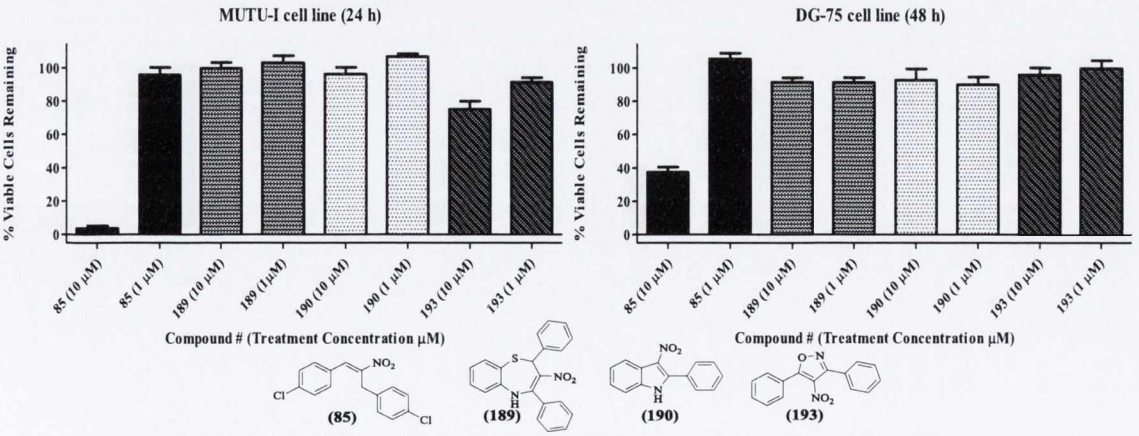

Figure 266: Preliminary screen for anti-proliferative activity of selected heterocycles

Heterocycles **189**, **190** and **193** were also evaluated for anticancer effect and were also found to exhibit poor anticancer properties with ~80% viable cells remaining at both concentrations in both cell lines. The most potent of these compounds was **193**, based on the isoxazole scaffold with 75% viable cells remaining in the MUTU-I cell line (Figure 266).

6.3.3 Summary of preliminary screen findings

The nitro-2-phenyl-2*H*-chromenes **137**, **139**, **140** and **145** were identified as the most potent heterocyclic compounds evaluated containing a constrained nitrostyrene pharmacophore. These compounds were found to exert anti-proliferative effects comparable to the previous lead compound **85**. The *para* hydroxy compound **137** was the most promising of these unsubstituted phenyl-2*H*-chromenes in both the DG-75 and MUTU-I cell lines. The 3,4 alkoxy compounds **139** and **140** were also elicited a good response at 10 μM in both lines (<20%) and potent effects at 1 μM in the MUTU-I cell line (38-60% viable cells remaining). Compound **145** was the most potent substituted phenyl-2*H*-chromene with a C-7 methoxy group on the chromene ring exerting a potent effect in the MUTU-I cell line. This C-7 methoxy compound exerted a more potent effect in the MUTU-I and DG-75 cell line than the C-8 analogues (**144**, **143**). Compound **145** exerted the greatest anti-proliferative effect in the DG-75 cell line at 1 μM with 58% viable cells remaining.

The introduction of a naphthyl group (**142**) and a phenolic group (**141**) were found to be unfavourable for anti-proliferative effects. The 3-nitro-1,2-dihydroquinolines and 3-nitro-1,2-dihydroquinolones (**149**, **150**, **151**) were found to possess little activity at 10 μM and 1 μM in both lines (>90%). The most promising of this class was compound **148** which gave a small effect 10 μM in both cell lines (~45%). Flavone (**170**) and the 3-nitro-flavones (**179** - **188**) were found to elicit poor anticancer effects in the MUTU-I and DG-75 cell lines with over 90% viable cells remaining at both concentrations. Similarly the other heterocycles **189**, **190** and **193** were inactive at both concentrations in the MUTU-I and DG-75 cell lines with over 80-90% viable cells remaining at both concentrations.

Contrasting the heterocyclic structures evaluated, it was concluded that compounds inducing a constrained *trans* (*E*) configuration on (2-nitrovinyl)benzene (nitrostyrene) and 1,3-bis(aryl)-2-nitro-1-propene scaffolds (**135** – **148**) were more potent than compounds inducing a *cis* (*Z*) configuration (**179** – **188**, **189**, **190**, **193**).

6.3.4 *In vitro* anti-proliferative activity (IC_{50}) and investigation into pro-apoptotic effect of the most potent heterocyclic derivatives.

The IC_{50} values of the most promising anti-proliferative heterocyclic compounds identified during the preliminary biological screen were obtained for both the DG-75 and MUTU-I BL cell lines (Table 43). Compounds **137, 145** were selected from the initial 3-nitro-2-phenyl-2*H*-chromene library. Compound **145** was found to have an IC_{50} value of 0.49 μM in the MUTU-I and an IC_{50} value of 2.51 μM in the DG-75 cell line, while compound **137** was slightly less active in both cell lines.

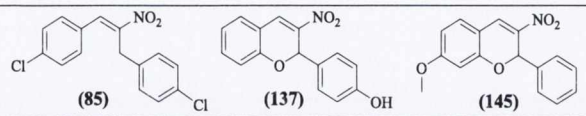

Compound #	IC_{50} (μM)		Lipinski properties					
	MUTU-I 24 h	*DG-75 48 h*	*Mr*	*logP*	*nrotb*	*nON*	*nOHNH*	*PSA (Å²)*
Taxol	0.32	1.32	853.9	7.38	15	15	4	221.29
85	2.82	6.03	308.2	5.377	4	3	0	45.82
137	0.79	2.34	269.3	3.666	2	5	1	75.28
145	0.49	2.51	283.3	3.969	3	5	0	64.28

Table 43: IC_{50} (BL cell lines DG-75 & MUTU-I) and Lipinski properties of leading heterocycles Chapter 2

Lipinski's rule of five properties were calculated for these compounds (Mcule property calculator v1 2015). These parameters were applied to compounds **137, 145** and these compounds were found to satisfy all the Lipinski rule of five criteria. The mode of cell death was identified as apoptotic and compound **145** was found to elicit comparable apoptotic effects to Taxol (>80%) at 10 μM and 1 μM. This effect was superior to that of the previous lead compound **85** at 1 μM (~40%) (Figure 267).

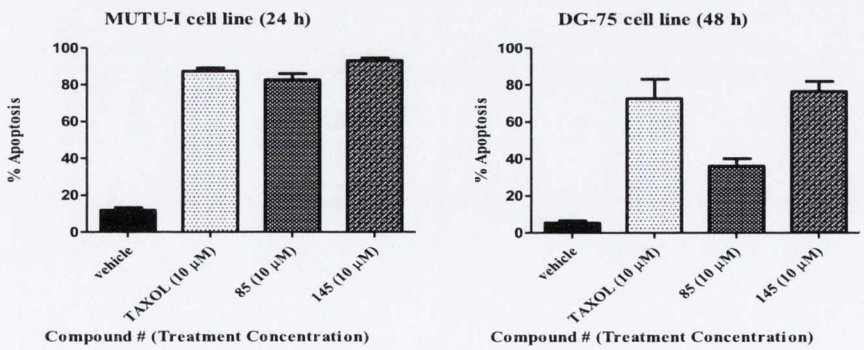

Figure 267: Annexin V / PI FACS - Apoptosis MUTU-I and DG-75 cell lines

6.4.0 Evaluation of the *in vitro* anti-proliferative activity of the anthracene based Maprotiline analogues

A library of 58 anthracene based compounds structurally related to the maprotiline were evaluated for anti-proliferative activity at 10 μM and 1 μM in the MUTU-I and DG-75 cell lines. The anticancer effect of compounds including a range of C-9 functionalities such as hydroxy, aldehyde, imine, acid, cyanovinyl and hydrazone on anticancer effect was quantified. Once the optimum C-9 functionality was identified, the effect of C-10 substitution on anti-proliferative effect was also evaluated. These anthracene based maprotiline analogues are discussed in four main groupings and categorised within the groups by structural type.

6.4.1 Preliminary screen for *in vitro* anti-proliferative activity of the (*E*)-9-(2-nitrovinyl)anthracenes

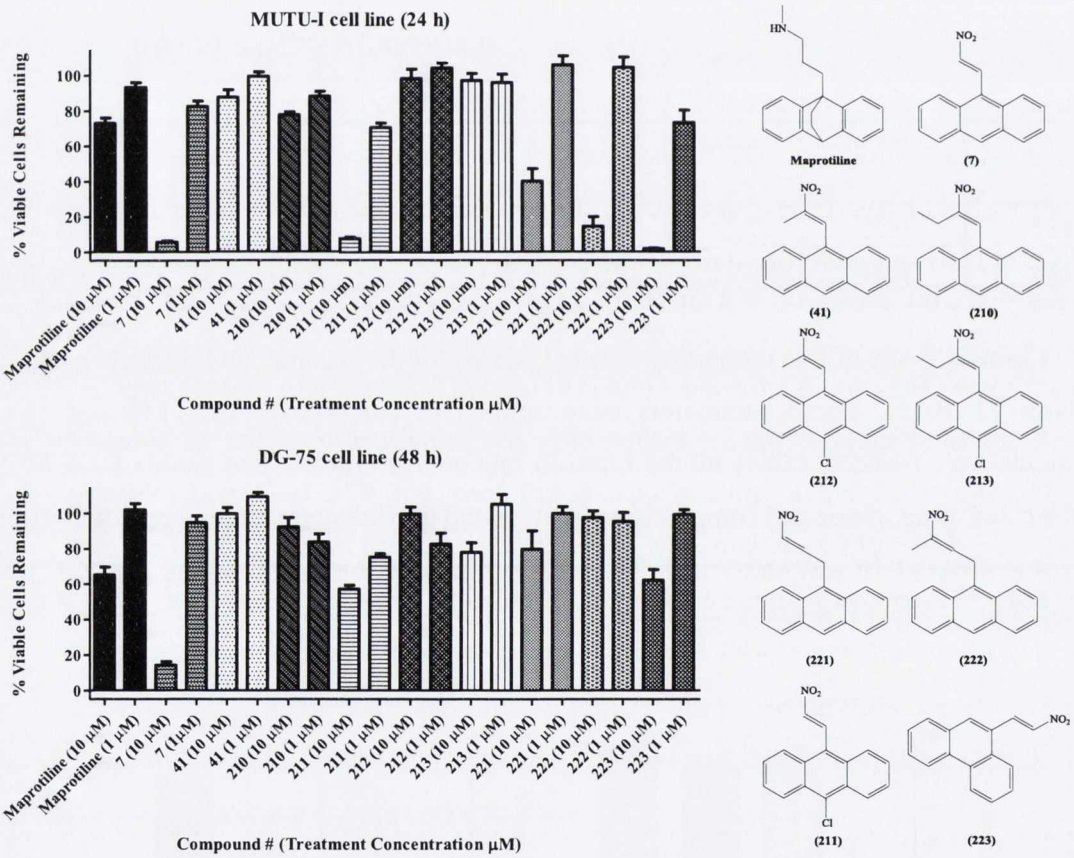

Figure 268: Preliminary screen for anti-proliferative activity of the (*E*)-9-(2-nitrovinyl)anthracenes (A)

(*E*)-9-(2-Nitrovinyl)anthracene (**7**) was found to elicit a more potent anti-proliferative effect (<20% cells remaining) than control maprotiline (>60%) in both cell lines at 10 μM. Extension of the alkyl chain (methyl, ethyl) at C-2 of the nitrovinyl unit deactivated the (*E*)-9-(2-nitrovinyl)anthracene pharmacophore (>80%) and this trend was observed in compounds (**7**, **41**, **210**) and (**211, 212, 213**). Compound **211** introduced C-9 chloro substitution and this

feature appeared favourable for MUTU-I cells at 1 μM when compared to **7** (<20%) but unfavourable for activity in the DG-75 cell line – reducing anti-proliferative effect. Replacing the anthracene moiety (**7**) with a phenanthrene moiety (**223**) reduced anticancer effect in the DG-75 cell line from ~10% to ~60% cell viability. The extended chain nitrovinyl analogues (**221, 222**) were found to induce good activity at 10 μM in the MUTU-I cell line (~15-40%) however these analogues exhibited reduced activity in the DG-75 cell line at 10 μM of ~79-97% when compared to compound **7** (Figure 268).

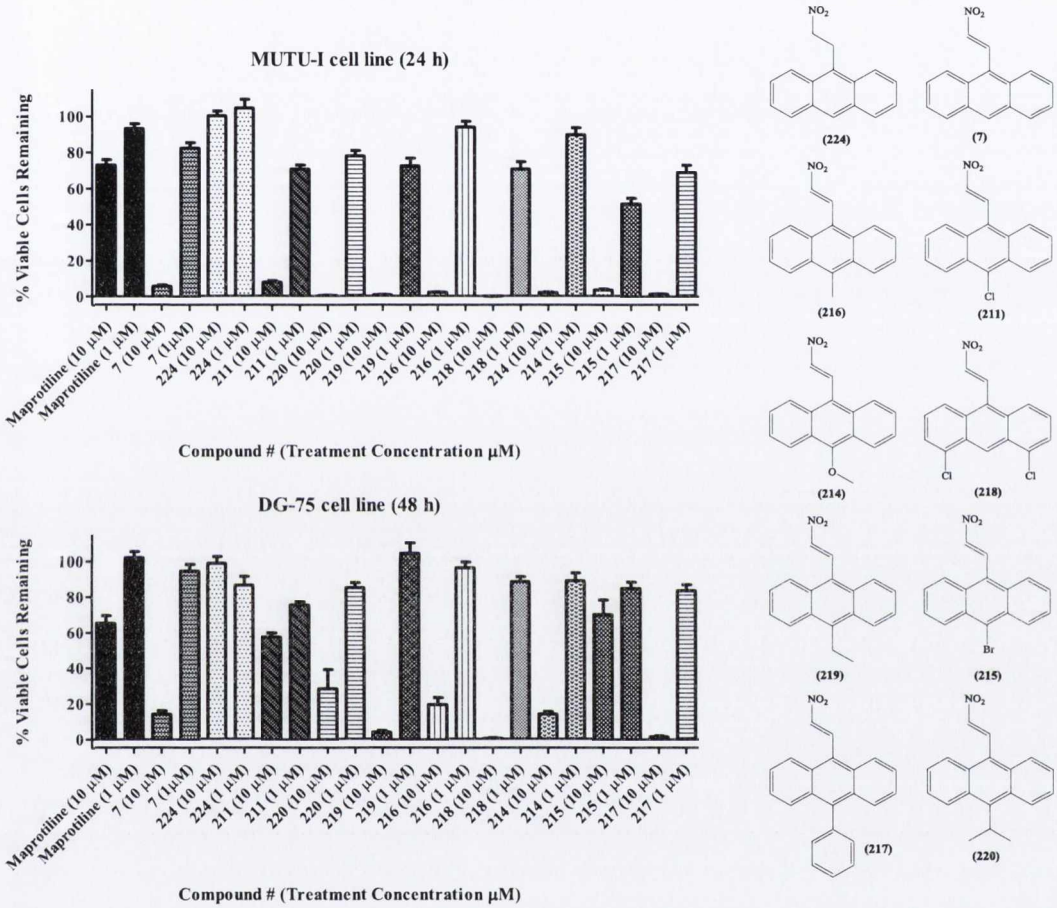

Figure 269: Preliminary screen for anti-proliferative activity of the (E)-9-(2-nitrovinyl)anthracenes (B)

A number of (*E*)-9-(2-nitrovinyl)anthracenes with varied halogen, alkyl, phenyl and methoxy substituents were also synthesised and evaluated for anti-proliferative activity. As stated before the C-9 chloro substitution, this feature appears favourable for MUTU-I cells at 1 μM when compared to **7** but unfavourable for activity in the DG-75 cell line. This appeared also to be the case for the C-9 bromo compound (**215**) with poor activity (> 70%) at 10 μM and 1 μM in the DG-75 cell line (Figure 269).

Reducing the vinyl unit of compound **7** to give compound **224** was detrimental to the anticancer effects with activity lost in both BL cell lines (>85%). The (*E*)-9-(2-

nitrovinyl)anthracenes **217, 218, 219, 220** were found to elicit similar anti-proliferative effects to compound **7** in both the MUTU-I and DG-75 BL cell lines at both concentrations (Figure 269).

6.4.2 Preliminary screen for *in vitro* anti-proliferative activity of the (anthracen-9-yl)methylamines and the anthracene amides

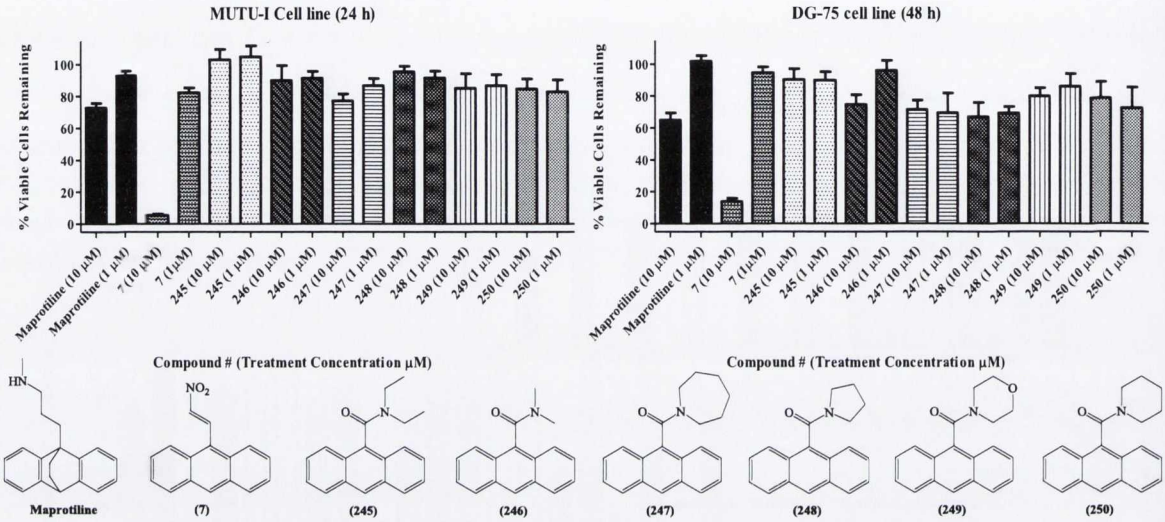

Figure 270: Preliminary screen for anti-proliferative activity of anthracene amides

The anthracene amides (**245-250)** were tested at 10 µM and 1 µM in the MUTU-I and DG-75 cell lines for anti-proliferative activity. These anthracene amides exhibited poor anti-proliferative effects in MUTU-I cell line at 10 µM (> 80%) when compared to compound **7**. Similar effects were recorded in the DG-75 cell line where at 10 µM > 60% cells remained viable (Figure 270) indicating the requirement for the nitrovinyl functionality

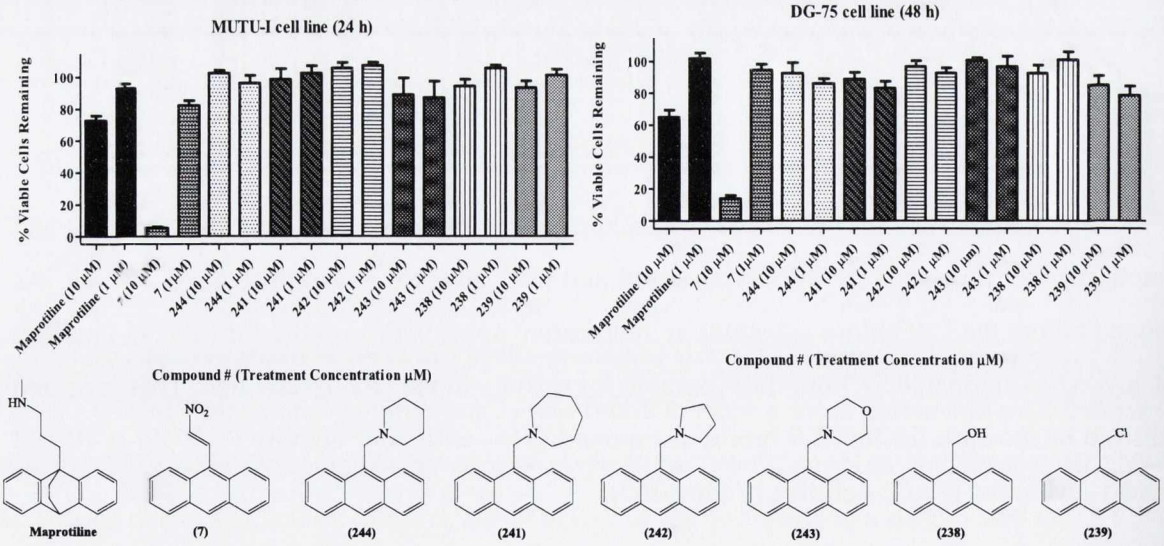

Figure 271: Preliminary screen for anti-proliferative activity of (anthracen-9-yl)methylamines

The (anthracen-9-yl)methylamines (**241-244**) and their precursors (**238-239**) were also shown to exhibit poor anti-proliferative activity in the BL cell lines, with over 80% of cells remaining viable post treatment (Figure 271).

6.4.3 Preliminary screen for *in vitro* anti-proliferative activity of the anthracen-9-ylmethanimines and the (*E*)-3-(anthracen-9-yl)acrylonitrile derivatives

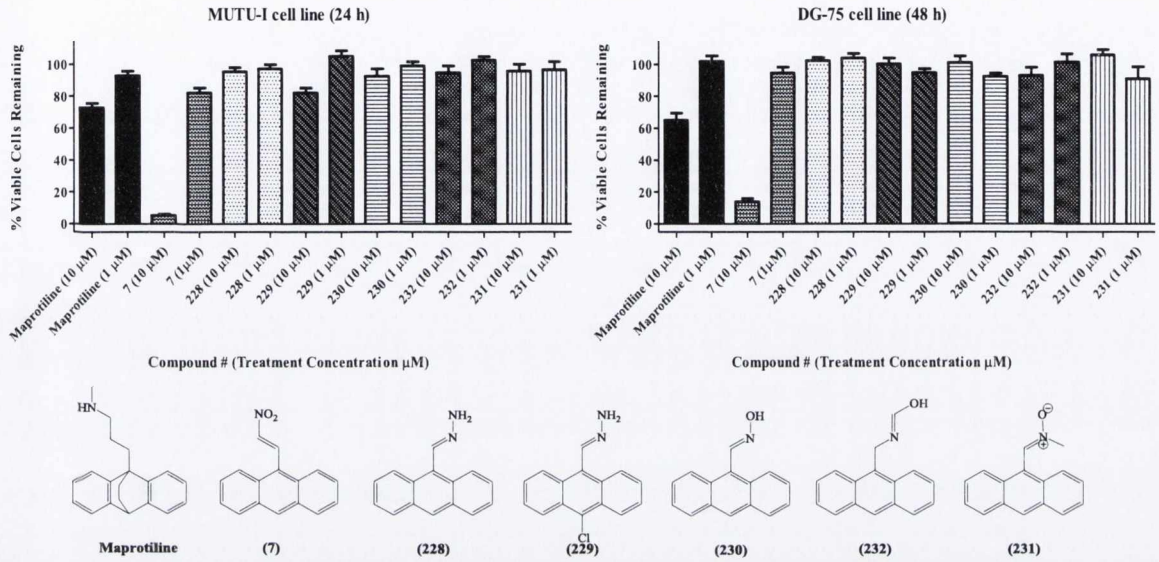

Figure 272: Preliminary screen for anti-proliferative activity of anthracen-9-ylmethanimines

The anthracen-9-ylmethanimines (**228 - 232**) encompassed anthracene based hydrazones, oximes and nitrones. These anthracen-9-ylmethanimines were shown to elicit poor anti-proliferative effects in both BL cells lines at both concentrations (Figure 272) when compared to control compounds maprotiline and compound **7**.

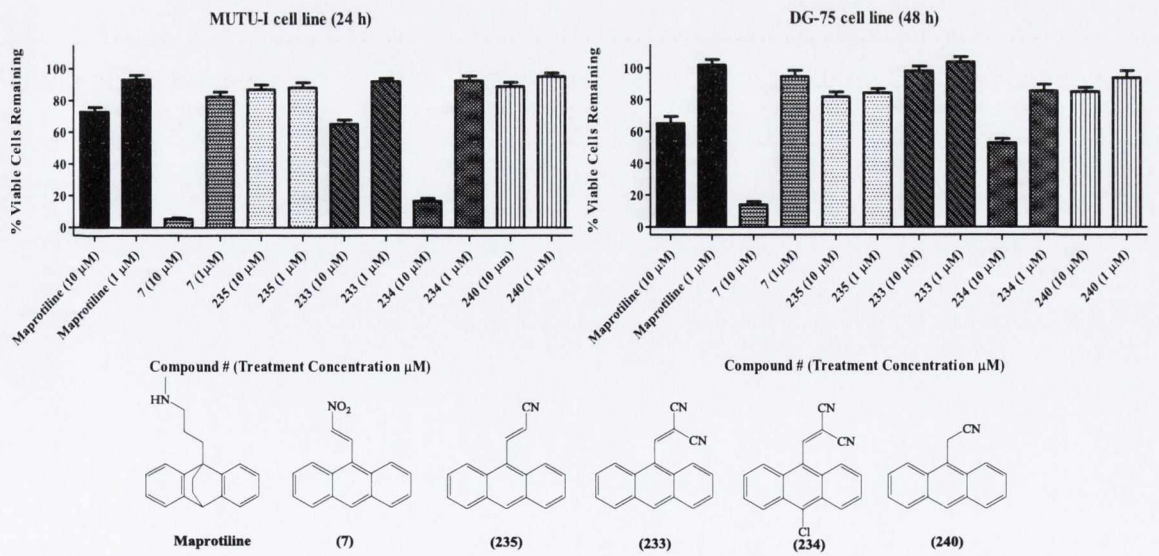

Figure 273: Preliminary screen for anti-proliferative activity of (*E*)-3-(anthracen-9-yl)acrylonitrile derivatives

The (*E*)-3-(anthracen-9-yl)acrylonitriles (**235**, **233**, **234**, **240**) were synthesised in order to evaluate the effects of different substituents at the C-2 carbon of the vinyl unit. The cyano anthracene compounds (**235, 233, 240**) were inactive (> 80%) in both BL cell lines at both concentrations. The C-9 dicyano compound **234** was found to give good activity at 10 μM in the MUTU-I cell line (~20%) and moderate activity at 10 μM in the DG-75 cell line (~55%) (Figure 268). It was concluded that the nitrovinyl unit was required for increased anti-proliferative activity.

6.4.4 Preliminary screen for *in vitro* anti-proliferative activity of the 4-(anthracen-9-yl)-1*H*-1,2,3-triazoles and miscellaneous condensation products.

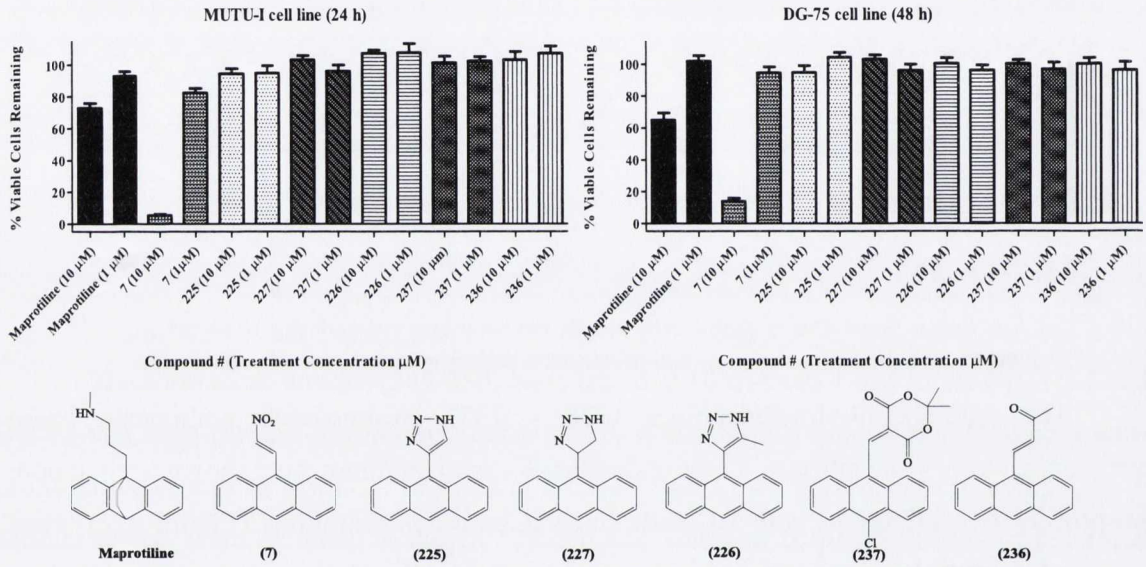

Figure 274: Preliminary screen for anti-proliferative activity of the 4-(anthracen-9-yl)-1H-1,2,3-triazoles and miscellaneous condensation products.

The triazole functionality induced a constrained '(*E*)' conformation on the vinyl system of the (*E*)-9-(2-nitrovinyl)anthracenes, through the elimination of the nitro functionality. The 4-(anthracen-9-yl)-1*H*-1,2,3-triazoles (**225, 226, 227**) were found to possess no anti-proliferative activity in the BL cell lines (> 90%). Compounds **237** and **236** were synthesised in order to assess the impact of alternative vinyl functionalities on anti-proliferative activity. Similarly the condensation products, compounds **237** and **236**, were inactive in both BL cell lines (> 90%) (Figure 274).

6.4.5 Summary of preliminary screen findings of anthracene based analogues

The study of the anti-proliferative action of these diversely substituted (*E*)-9-(2-nitrovinyl)anthracenes allowed a number of observations to be compiled. Maprotiline elicits a moderate effect at 10 μM in both cell lines (>60% cells remaining), compound **7** was found to elicit a more potent effect at 10 μM in both cell lines (<20%). Reducing the nitrovinyl unit of compound **7** to the nitroalkane (**224**) reduced anti-proliferative effect to >80% viable cells remaining. Extension of the nitrovinyl chain to give compounds **221** and **222** was also found to be unfavourable for anticancer effect in both the DG-75 and MUTU-I cell lines (>80%). Extension of alkyl chain length at C-2 of the nitrovinyl unit was also unfavourable, deactivating the pharmacophore in both cell lines (>80%) this trend was observed in (**7**, **41**, **210**) and (**211, 212, 213**). The introduction of a phenanthrene moiety (**223**) was found to decrease anti-proliferative activity at 10 μM in the DG-75 cell line (> 60%). The optimum pharmacophore elucidated from this study was of (*E*)-9-(2-nitrovinyl)anthracene (**7**), which was unsubstituted at C-2 and contained a nitrovinyl functionality directly attached to an anthracene moiety.

The anthracene amides (**245-250**) and anthracene amines (**241-244**) were found to possess minimal anti-proliferative activity in both the MUTU-I and DG-75 cell lines. The anthracene amides were inactive in the MUTU-I and DG-75 cell lines giving >60-80% viable cells remaining, while the amines gave >80% in both cell lines. The anthracen-9-ylmethanimines (**228 - 232**) and 4-(anthracen-9-yl)-1*H*-1,2,3-triazoles (**225-227**) were inactive at 10 μM and 1 μM in both the DG-75 and MUTU-I cell lines (>80%). The cyano anthracene compounds (**235, 233, 240**) exhibited poor anticancer effects at both concentrations in the BL cell lines (> 80%). The C-9 dicyano compound **234** possessed the most promising the activity of the cyano anthracenes at 10 μM in the MUTU-I cell line (~20%) and moderate activity at 10 μM in the DG-75 cell line (~55%). Exchanging the nitrovinyl unit with other vinyl, amine, amide and triazole functionalities was unfavourable for anti-proliferative effectsThe effect of anthracene substitution patterns of the (*E*)-9-(2-nitrovinyl)anthracenes on anti-proliferative activity were also investigated. The C-9 chloro substituted compound **211** and C-9 bromo substituted compound **219** were found to elicit a diminished anti-proliferative effect in the DG-75 cell line at 10 μM (~60%). Although halogen C-9 substitution impacts negatively on anti-proliferative activity, other substitution patterns of the (*E*)-9-(2-nitrovinyl)anthracenes appear to have little effect on anti-proliferative effects and possess similar activity to the previous lead compound **7** and resulted in the identification of a potent series of active compounds.

6.5.0 Evaluation of the *in vitro* anti-proliferative activity of the anthracene based Maprotiline analogues

Based on the 9,10-dihydro-9,10-ethanoanthracene scaffold a series of over 80 maprotiline analogues were evaluated for anti-proliferative activity at 10 μM and 1 μM in the MUTU-I and DG-75 cell lines. The effect of compounds including a range of C-9 functionalities such as hydroxy, aldehyde, imine, acid, cyanovinyl and hydrazone on anticancer effect was quantified. Other modifications such as variation of C-10 substitution, maleimide substituent, phenylmaleimide substitution and ethano bridge modification were also shown to impact on anti-proliferative effect. These maprotiline analogues are discussed in three main groupings (6.5.1, 6.5.2, 6.5.3) and categorised within the groups by structural type.

6.5.1 Preliminary screen for *in vitro* anti-proliferative activity of the 9,10-dihydro-9,10-ethanoanthracenes

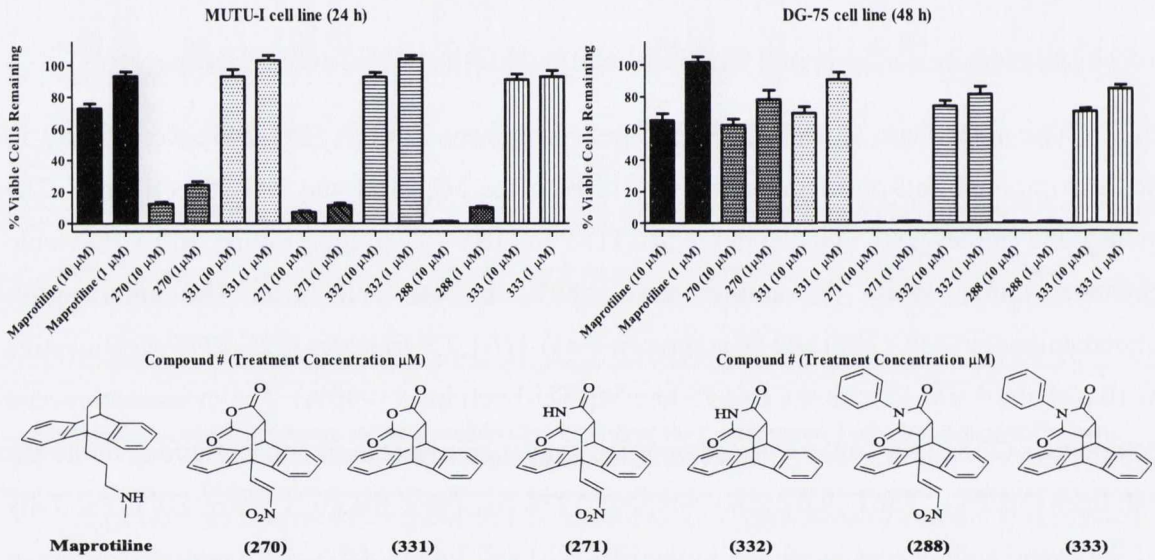

Figure 275: Preliminary screen for anti-proliferative activity of the (*E*)-11,12-substiuted-9-(2-nitrovinyl)-9,10-dihydro-9,10-ethanoanthracenes

(I) Maprotiline was found to induce a modest anti-proliferative effect at 10 μM in the MUTU-I (73% cells remaining) and DG-75 (65%) BL cell lines. No anti-proliferative effect was observed for Maprotiline at 1 μM with > 90% of viable cells remaining (Figure 275). The (*E*)-11,12-substiuted-9-(2-nitrovinyl)-9,10-dihydro-9,10-ethanoanthracenes (**270**, **271**, **288**) were found to elicit a potent anti-proliferative effect at both concentrations in the MUTU-I cell line (~1-12%). In the DG-75 cell line the maleic anhydride derivative (**270**) gave comparable results to maprotiline at both concentrations. The maleimide (**271**) and phenylmaleimide (**288**) derivatives elicited a potent effect at 1 μM in the DG-75 cell line also (0.5-1% cells remaining). The unsubstituted 9,10-dihydro-9,10-ethanoanthracenes (**331**, **332**, **333**) did not contain the

nitrovinyl unit at C-9 and the anti-proliferative activity was greatly reduced at both concentrations in both cell lines (> 60%) (Figure 275) – indicating the C-9 substitution was necessary to enhance anti-proliferative effect.

(II) A cohort of C-9 substituted 9,10-dihydro-9,10-ethanoanthracenes derived from maleic anhydride, maleimide and phenyl maleimide were investigated for anti-proliferative activity, to assess the effect of variation of the C-9 substituent. A series of (*E*)-12,14-dioxo-9,10-[3,4]furanoanthracen-9(10*H*)-yl)acrylonitriles (**342**, **343**, **344**, **345**, **346**, **347**) introduced a cyanovinyl substituent at C-9. The most promising of these cyano compounds, compound **343** elicited comparable activities at 10 μM to Maprotiline in the MUTU-I (79%) and DG-75 (54%) cell lines. The remaining compounds were less active leaving 70-95 % viable cells remaining at both concentrations in both cell lines (Figure 276).

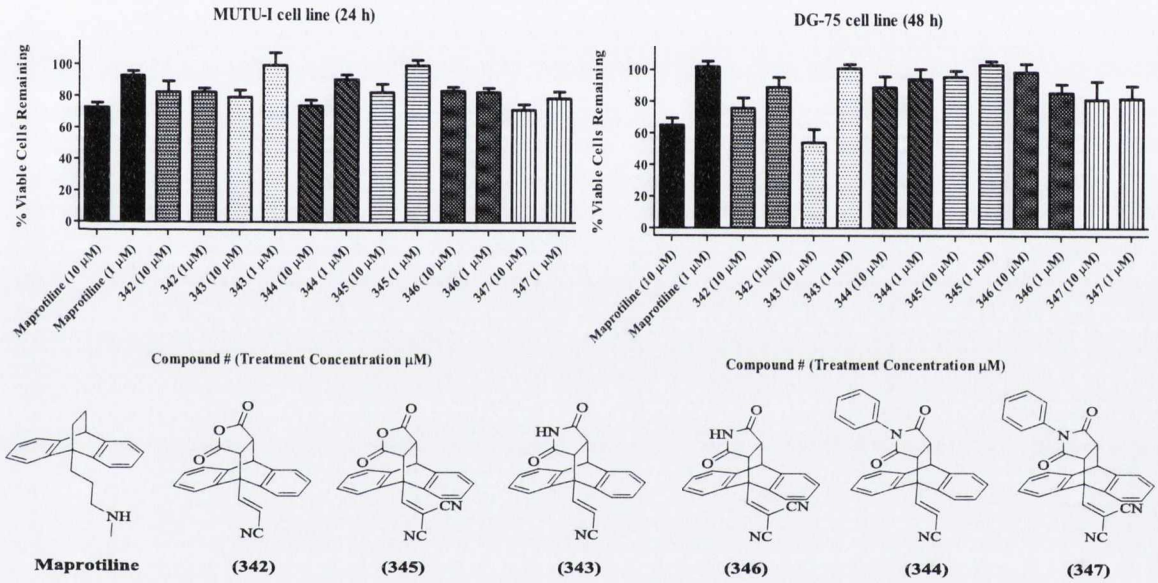

Figure 276: Preliminary screen for anti-proliferative activity of the 9,10-dihydro-9,10-ethanoanthracenes

(III) A second series of C-9 substituted 9,10-dihydro-9,10-ethanoanthracenes encompassed aldehyde (**334**, **335**, **336**), alcohol (**340**, **341**) and acid (**337**, **338**, **339**) functionalities. Although these compounds possess anticancer activity exceeding the activity of Maprotiline at 1 μM in the DG-75 cell line, the anticancer effect in the MUTU-I cell line was minimal with > 80% of viable cells remaining at both concentrations (Figure 277). Comparing the activities of the aldehyde (**334**, **335**, **336**), alcohol (**340**, **341**) and acid (**337**, **338**, **339**) functionalities, it is evident that the aldehyde compounds **334**, **335** possess more anti-proliferative effects in the DG-75 cell line than their alcohol and acid analogues.

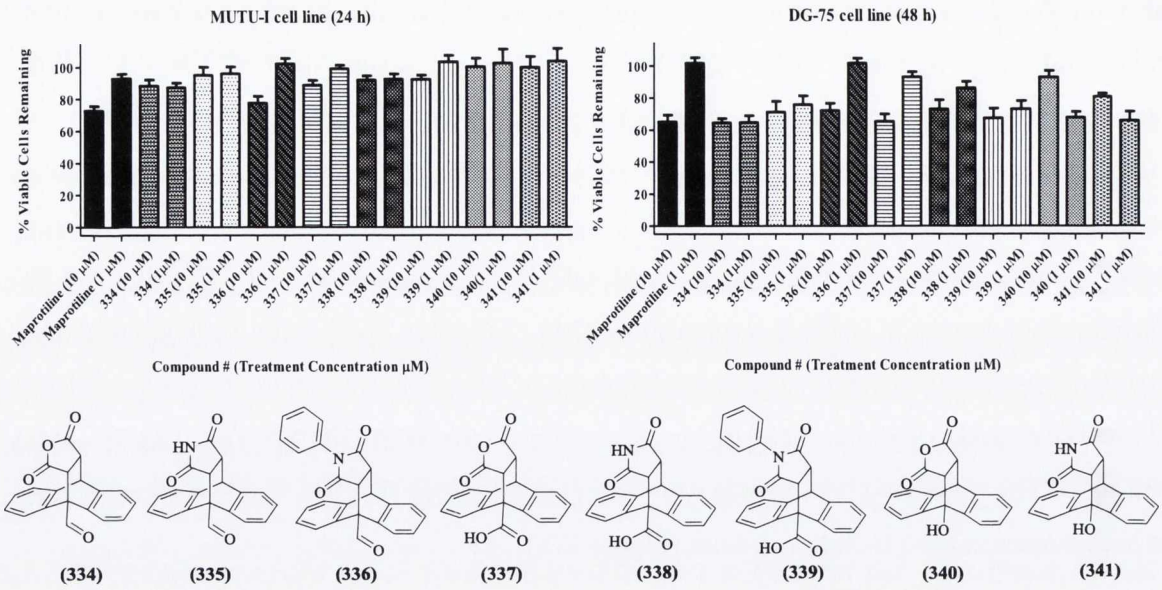

Figure 277: Preliminary screen for anti-proliferative activity of the 9-substituted 9,10-dihydro-9,10-ethanoanthracenes

(IV) Further C-9 substituted 9,10-dihydro-9,10-ethanoanthracenes included variants with nitroalkane (**284**, **285**, **286**), hydrazone (**348**, **349**, **350**) and oxime (**351**, **352**) substitution. This grouping exhibited comparable effects to Maprotiline in the MUTU-I cell line at both concentrations. The most potent analogue was identified as compound **350**, compound **350** elicited a more potent anti-proliferative effect at 10 µM in the DG-75 cell line (19%) than any other compound in this grouping (~58-86%). Similarly to earlier observations the nitroalkane maleic anhydride analogue (**284**) was found to possess less potency than the corresponding maleimide (**285**) and phenyl maleimide (**286**) derivatives (Figure 278).

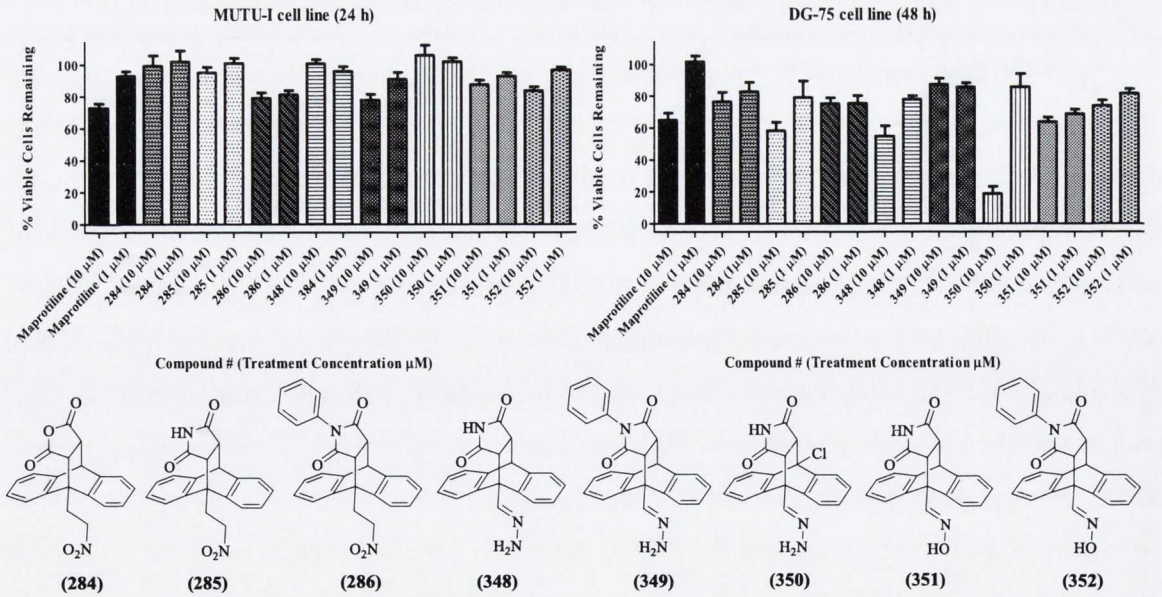

Figure 278: Preliminary screen for anti-proliferative activity of the 9-substituted 9,10-dihydro-9,10-ethanoanthracenes

(V) Reducing the nitrovinyl unit in the (*E*)-11,12-substiuted-9-(2-nitrovinyl)-9,10-dihydro-9,10-ethanoanthracenes (**270**, **271**, **288**) to the corresponding nitroalkanes (**284**, **285**, **286**) diminished the potent anti-proliferative effect observed earlier in the present work. Also introducing alternative double bond units such as cyanovinyl (**342**, **343**, **344**, **345**, **346**, **347**), oxime (**351**, **352**) and hydrazone (**348**, **349**, **350**) were found to reduce the observed anti-proliferative effects (Figure 278).

6.5.2 Preliminary screen for *in vitro* anti-proliferative activity of the 9-substituted triptycenes

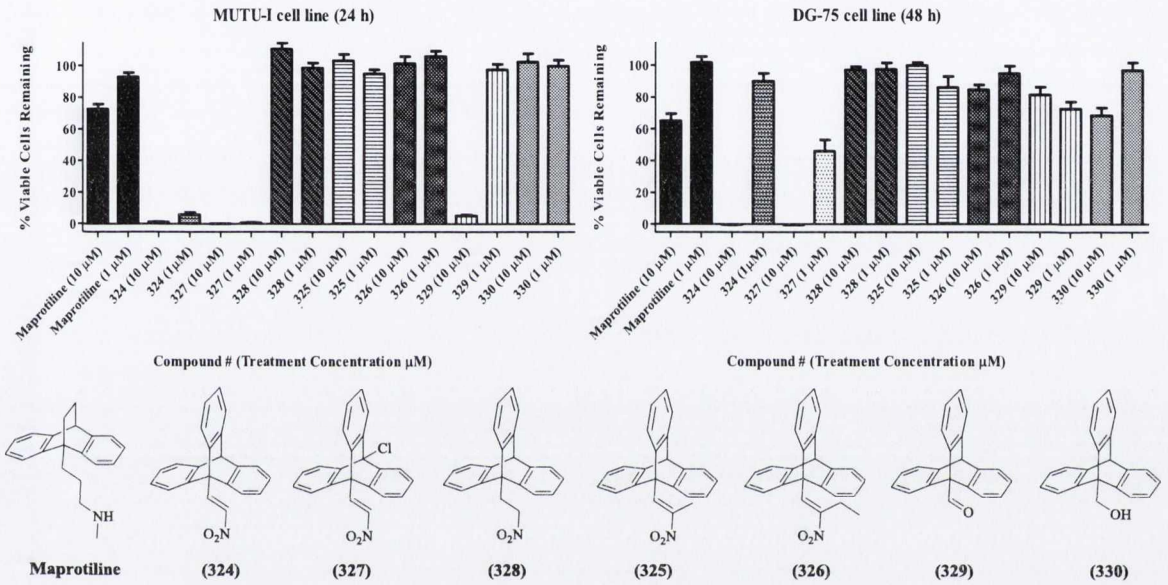

Figure 279: Preliminary screen for in vitro anti-proliferative activity of the 9-substituted triptycenes

A number of triptycene based Diel-Alder adducts were synthesised in order to assess the effect of the triptycene moiety on anti-proliferative effect (Figure 279). The C-9 functionalities such as alcohol (**330**), aldehyde (**329**), nitrovinyl (**324**, **325**, **326**, **327**) and nitroalkane (**328**) were also included to assess their impact on the anticancer properties of the series. The most promising results were obtained by compounds **324** and **327** and these nitrovinyl adducts exhibited potent effects (<5%) at both concentrations in the MUTU-I cell line. A potent effect was also observed at the 10 µM in the DG-75 cell line (<2%). Compound **327** bears a C-10 chloro substitution and elicited a more potent effect (46%) than the unsubstituted compound **324** (90%) at 10 µM in the DG-75 cell line. Reducing the nitrovinyl bond was once again detrimental to anti-proliferative effects in both cell lines at both concentrations (> 90%).

The effect of alkyl chain length was assessed at C-2 of the nitrovinyl unit, chain length was increased from unsubstituted (**324**, **327**) to methyl (**325**) and ethyl (**326**). Compounds **325** and **326** were found to induce poor anticancer effects at 10 μM and 1 μM in both cell lines (> 85%). The aldehyde based triptycene (**329**) exhibited good activity at the higher concentration in the MUTU-I cell line (<5%), however was poorly active in the DG-75 cell line (> 60%) at both concentrations. Reducing the aldehyde (**329**) to the alcohol (**330**) had a negative impact on the favourable anti-proliferative activity shown in the MUTU-I cell line by **329**, however similar activity to that of Maprotiline was observed in the DG-75 cell line (Figure 279).

6.5.3 Preliminary screen for anti-proliferative activity of the (*E*)-11,12-substiuted-9-(2-nitrovinyl)-9,10-dihydro-9,10-ethanoanthracenes

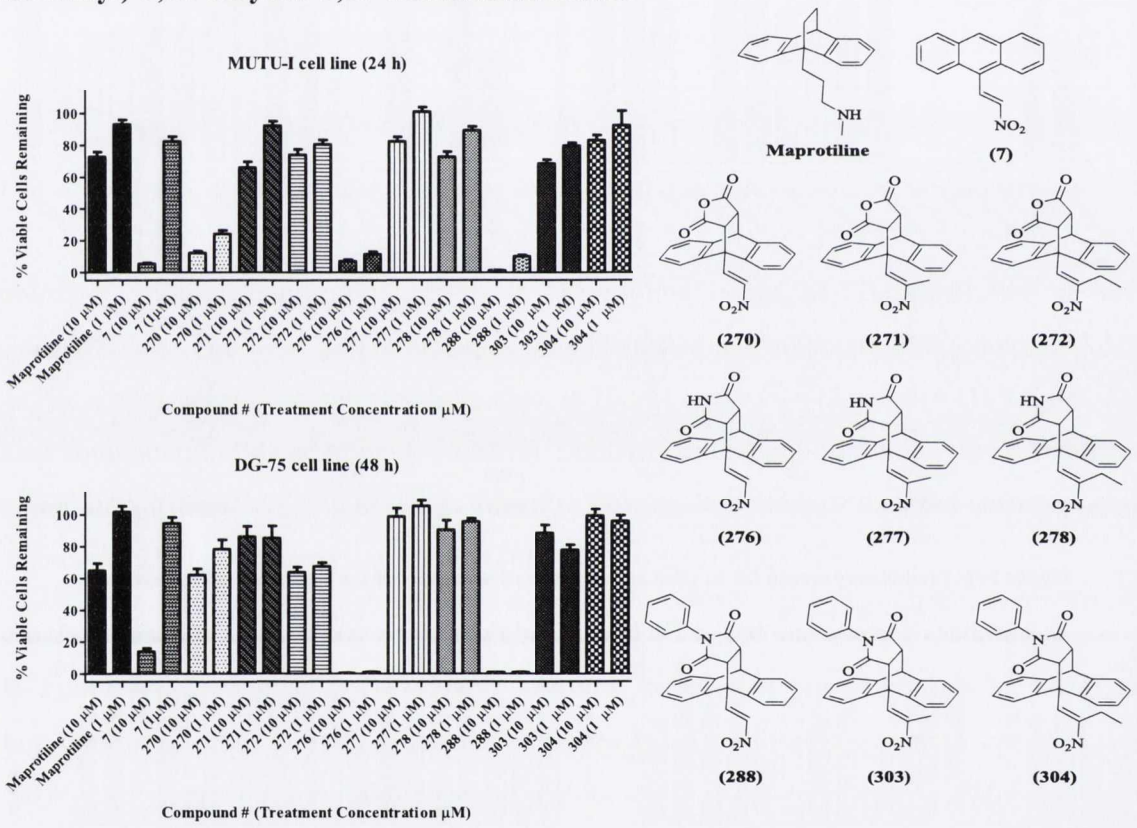

Figure 280: Preliminary screen for anti-proliferative activity of the (E)-11,12-substiuted-9-(2-nitrovinyl)-9,10-dihydro-9,10-ethanoanthracenes

(I) Maleic anhydride based (*E*)-11,12-Substituted-9-(2-nitrovinyl)-9,10-dihydro-9,10-ethanoanthracenes (**270, 271, 272**) were evaluated against their corresponding maleimide (**276**, **277**, **278**) and phenyl maleimide (**288**, **303**, **304**) analogues. These analogues also included compounds (**271**, **277**, **303**, **272**, **278**, **304**) where the effect of alkyl chain length (methyl and ethyl) was assessed at C-2 of the nitrovinyl unit (Figure 278).

Compounds **276** and **288** not only show improved anti-proliferative effects when compared to Maprotiline but also when compared to anthracene compound **7** in both BL cell lines. Compound **7** was found to elicit activity of <20 % in both BL cell lines at 10 μM but possessed minimal effects at the lower concentration. The Diels-Alder adducts of compound **7** (**276**, **288**) improve upon this and endowed excellent activity in both lines at both concentrations (< 5%). Increased chain length at the C-2 position decreased anti-proliferative effect across the series and can be seen in each grouping of adducts (**270**, **271**, **272**), (**276**, **277**, **278**) and (**288**, **303**, **304**). As previously discussed the maleimide (**276**) and phenyl maleimide (**288**) adducts are observed to possess superior anticancer activity in the two BL cell lines than the maleic anhydride adduct (**270**) (Figure 280).

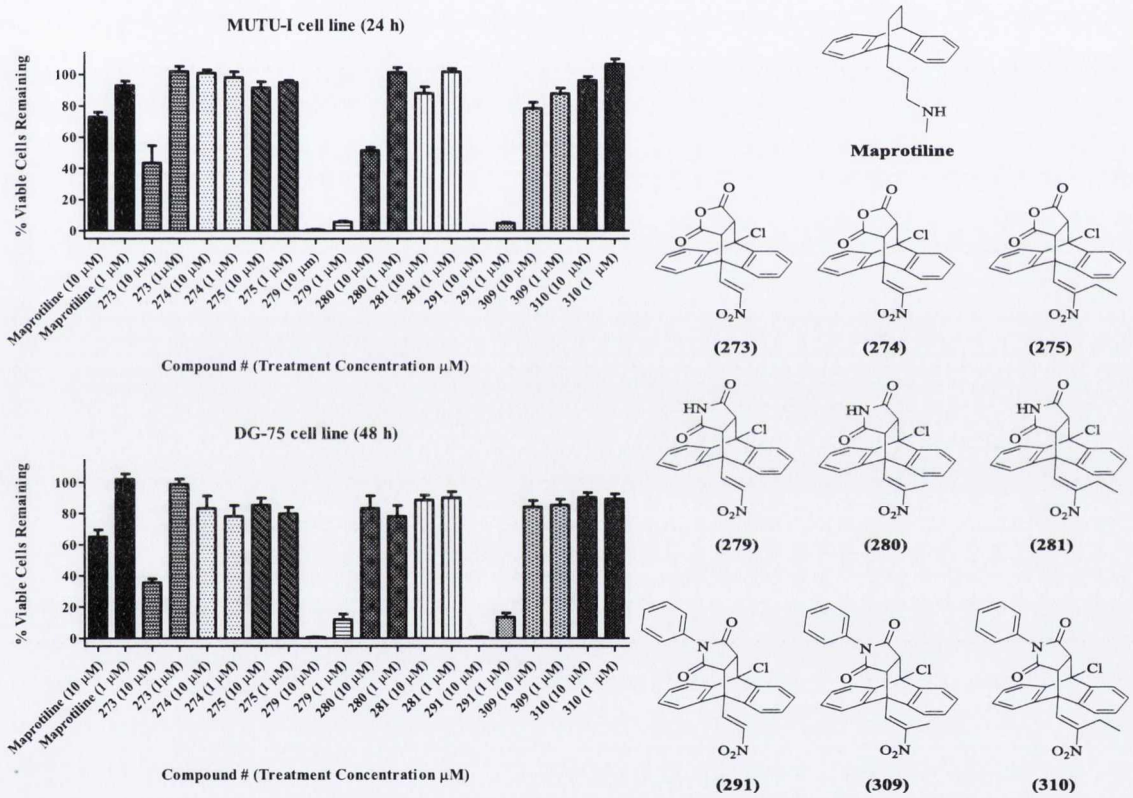

Figure 281: Preliminary screen for anti-proliferative activity of the (*E*)-11,12-substiuted-9-(2-nitrovinyl)-9,10-dihydro-9,10-ethanoanthracenes

(II) Similarly chlorine substituted (*E*)-11,12-Substituted-9-(2-nitrovinyl)-9,10-dihydro-9,10-ethanoanthracenes (**273**, **274**, **275**, **279**, **280**, **281**, **291**, **309**, **310**) were evaluated for their anti-proliferative activity. Compounds **273**, **279**, **291** are Diels-Alder adducts of compound **211** and as with the previous cohort, these compounds elicit enhanced anti-proliferative activity when compared to the parent compound at the 10 μM. These analogues also included compounds (**279**, **280**, **281**, **291**, **309**, **310**) where the effect of alkyl chain length (methyl and

ethyl) was assessed at C-2 of the nitrovinyl unit. Compounds **279** and **291** were found to possess potent anticancer effects at both concentrations in both cell lines with 0.5-15% viable cells remaining. The maleic anhydride based compound **273** gave good anti-proliferative activity at 10 μM in the MUTU-I cell line (44%), however poor activity was observed at 1 μM concentration (> 90%). As a result the C-10 chloro substituted compound **273** was not as effective as its unsubstituted analogue compound (**270**) in the MUTU-I cell line discussed earlier (Figure 281).

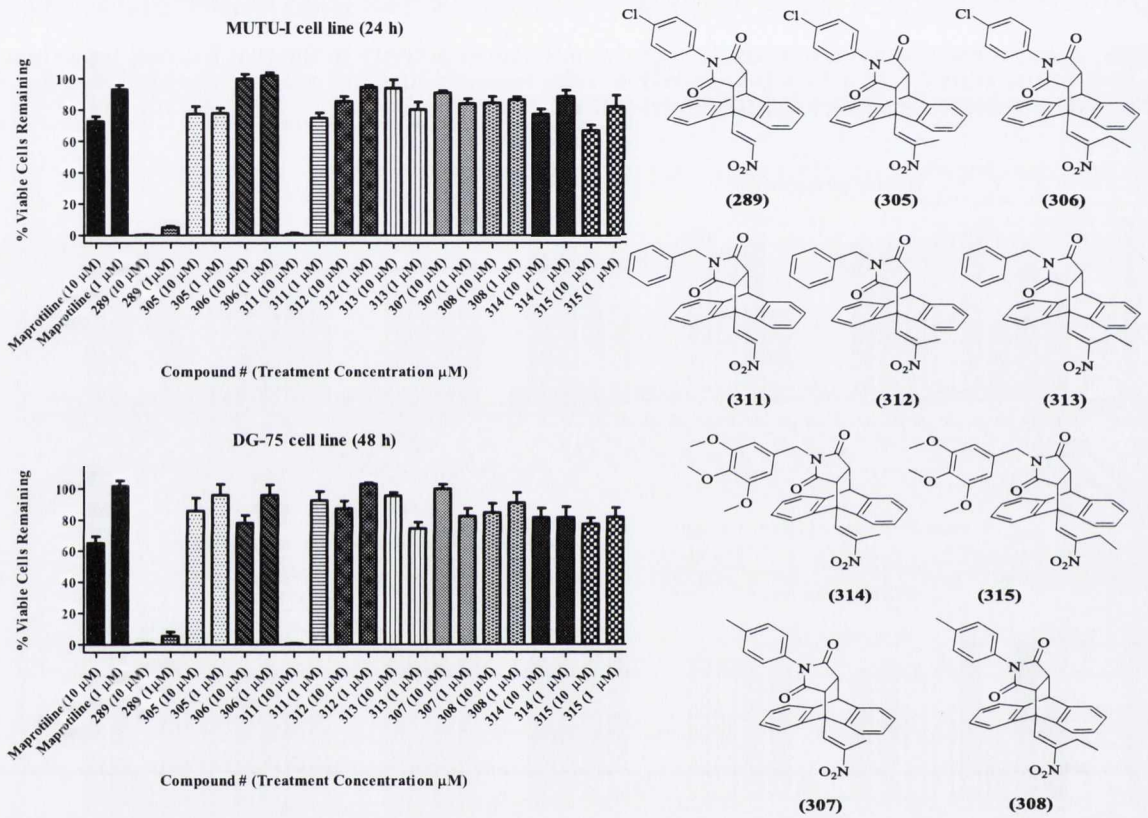

Figure 282: Preliminary screen for anti-proliferative activity of the (*E*)-11,12-substiuted-9-(2-nitrovinyl)-9,10-dihydro-9,10-ethanoanthracenes

(III) When examining the anti-proliferative activity of the N-arylmaleimide compounds **305**, **306**, **312**, **313**, **314**, **315**, **307**, and **308** the deactivating effect of extended alkyl chain length (methyl and ethyl) at C-2 on anticancer activity can once again be observed (70-90% viable cells remaining). Compound **289** is the most potent compound in this grouping eliciting < 2% viable cells remaining in both the DG-75 and MUTU-I cell line at both concentrations. Compounds **311, 312, 313, 314** and **315** were synthesised containing a benzyl substituent on the nitrogen heterocycle, this benzyl substituent was observed to be unfavourable for anti-proliferative activity when comparing the activity of compound **311** to the phenyl substituent in compound **289**. Compound **289** possessed potent anticancer activity at the lower

concentration while the benzyl compound **311** has poor activity at 1 μM in both the MUTU-I (75%) and DG-75 (93%) cell lines (Figure 282).

(IV) The effect of ethano-bridge substitution on anticancer effects was assessed by the use of different dienophiles during the Diels-Alder reaction. Utilising a range of different dienophiles and the ring opening reaction of the anhydride it was possible to introduce nitrile and ester groups on the ethano-bridge. The anthracene compound **7** was found to elicit activity of <20 % cells remaining in both BL cell lines at 10 μM but possessed minimal effects at the lower concentration, once again it was observed that all but two of these simpler Diel-Alder adducts (**317, 322**) possessed enhanced anti-proliferative activity superior to that of the parent anthracene compound (**7**). Compounds **317** and **322** still elicited a potent effect at the 1 μM concentration in both lines (~10%) and a poor effect at the lower concentration. It was noted however that this activity was still comparable to compound **7** and superior to the activity induced by Maprotiline in both cell lines (Figure 283).

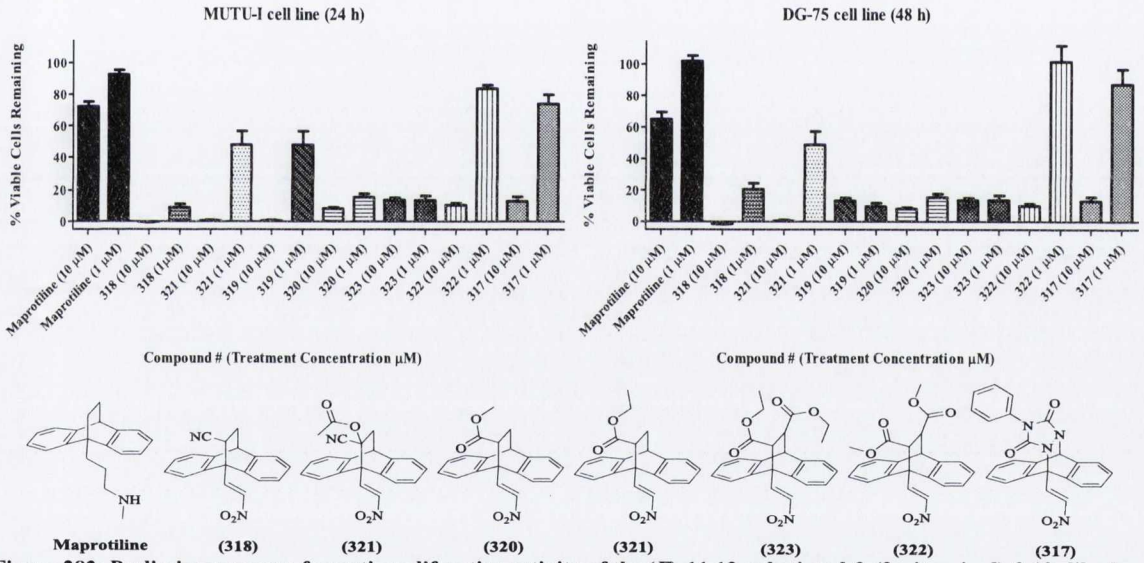

Figure 283: Preliminary screen for anti-proliferative activity of the (*E*)-11,12-substiuted-9-(2-nitrovinyl)-9,10-dihydro-9,10-ethanoanthracenes

Compound **317** was synthesised from an azide dienophile in order to directly compare the nitrogen-nitrogen bridge system in **317** to the carbon-carbon bridge in compound **288**. Compound **288** proved to be more potent at the lower concentration in both BL lines than **317**, indicating that the carbon-carbon bridged system was more favourable for the desired anticancer effect. The most promising compounds from this cohort were compounds **318**, **320** and **323,** and these compounds gave good anti-proliferative effects at both concentration in both cell lines (<10% viable cells remaining). The addition of an acetate group to the nitrile ethano bridged system in **321** reduced the potency observed in compound **318** at 1 μM

concentration in both lines (9% to 49% in the MUTU-I and from 20% to 48% in the DG-75) (Figure 283).

(V) To further explore the structure activity relationship of this series, a panel of 9-((*E*)-2-nitrovinyl)-13-phenyl-9,10-dihydro-9,10-[3,4]epipyrroloanthracene-12,14-diones were synthesised from the corresponding alkyl, benzyl and phenylmaleimides in order to determine the most potent Diels-Alder analogue. Phenyl substitution patterns were also varied by altering the substitution of the dienophiles used during the reaction.

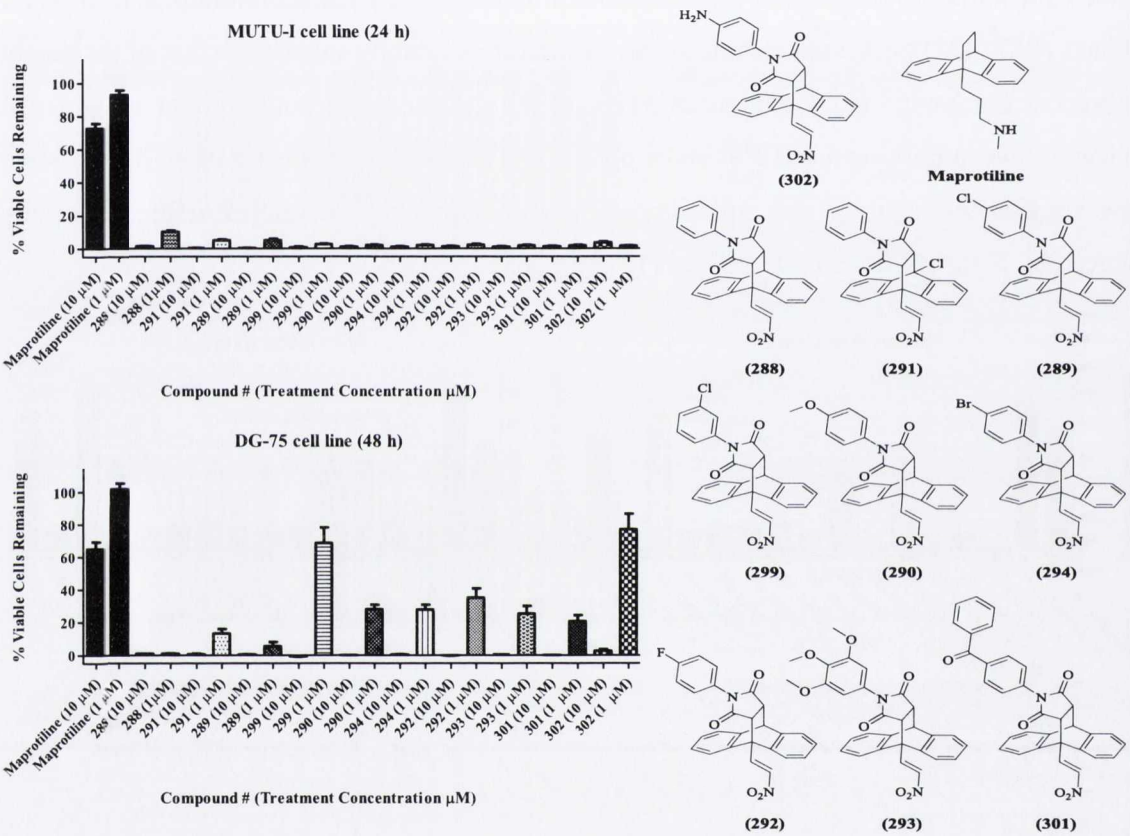

Figure 284: Preliminary screen for anti-proliferative activity of the 9-((*E*)-2-nitrovinyl)-13-phenyl-9,10-dihydro-9,10-[3,4]epipyrroloanthracene-12,14-diones

In the MUTU-I cell line it was observed that all the analogues in the above grouping elicited a very potent anti-proliferative action at both the 10 μM and 1 μM concentrations leaving <5% viable cells. In the DG-75 cell line the most potent activity was produced by compounds **288** and **289**, equating to <6% viable cells remaining at both concentrations. Compound **291** also produced a promising result at 1 μM concentrations leaving <14% viable. Reduced activity was detected when comparing the activities of compounds **289** (*para*-Cl) and **204** (*meta*-Cl). The *para* chloro substitution is more favourable for anti-proliferative activity at 1 μM (<5%) in the DG-75 than its *meta* chloro substituted analogue (> 60%). In a study of

para phenyl substitution of the 9-((*E*)-2-nitrovinyl)-13-phenyl-9,10-dihydro-9,10-[3,4]epipyrroloanthracene-12,14-diones (**288, 302, 289, 290, 204, 180, 187**), the unsubstituted compound **288** and *para* chloro compound **289** were found be more favourable for anticancer activity than the bromo (**294**), fluoro (**292**), amino (**302**), ketone (**301**) and methoxy (**290**) analogues at the 1 μM concentration in the DG-75 cell line (Figure 284).

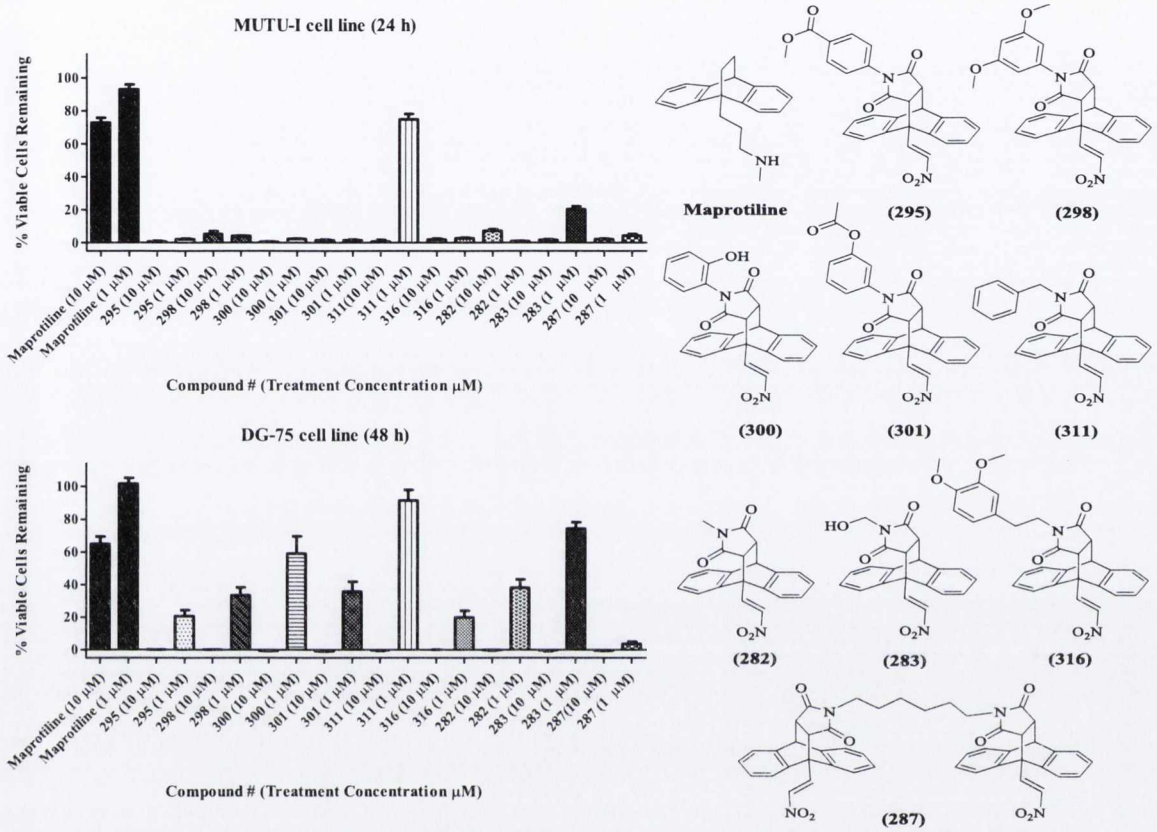

Figure 285: Preliminary screen for anti-proliferative activity of the (*E*)-11,12-substiuted-9-(2-nitrovinyl)-9,10-dihydro-9,10-ethanoanthracenes

(VI) With the exception of two compounds (**311**, **203**) it was observed that all the analogues in the above grouping elicited a very potent anti-proliferative action in the MUTU-I cell line at both 10 μM and 1 μM concentrations leaving <5% viable cells. Similarly these two compounds (**311**, **203**) were the least potent in the DG-75 cell line at 1 μM, however the activity of these compounds was still superior to that exhibited by Maprotiline over the same range. The benzyl substituted compound **311** was found to possess poor activity in both BL lines at the lower concentration leaving > 80% viable cells. Compounds **298** and **316** elicited good activity in the DG-75 cell line, with <5% viable cells remaining in the MUTU-I cell line at 10 μM and <20% at the 1 μM dosing (Figure 285). Surprisingly the dimer compound **287** was found to possess one of the most potent anti-proliferative activities in both BL lines at both concentrations leaving <5% viable cells.

6.5.6 Summary of preliminary screen findings of the 9,10-dihydro-9,10-ethanoanthracenes

Compounds **270**, **271** and **288** introduced a nitrovinyl unit at C-9 and as a result a potent anti-proliferative effect is observed in the MUTU-I cell line at both concentrations (<5%). The C-9 unsubstituted 9,10-dihydro-9,10-ethanoanthracenes analogues **331**, **332** and **333** were shown to elicit reduced anticancer effects at both the 10 μM and 1 μM concentrations in the MUTU-I and DG-75 cell lines. The maleimide and phenylmaleimide adducts compounds **271** and **288** were more potent than the maleic anhydride analogue (**288**) and possessed potent activity in the DG-75 cell line at the 10 μM and 1 μM concentrations (<2%).

The effect of variation of C-9 substitution on anti-proliferative effect was also studied. Compounds including aldehyde (**334**, **335**, **336**), alcohol (**340**, **341**) and acid (**337**, **338**, **339**) functionalities were found to possess reduced anticancer effects at 10 μM and 1 μM in the MUTU-I and DG-75 cell lines (60-80%). A C-9 cyanovinyl substituent was introduced in the (*E*)-12,14-dioxo-9,10-[3,4]furanoanthracen-9(10H)-yl)acrylonitriles (**342**, **343**, **344**, **345**, **346**, **347**) these compounds were found to be less active that the corresponding potent nitrovinyl compounds (**270**, **271**, **288**) with 70-95% viable cells remaining in both BL cell lines. Further variations evaluated included nitroalkane (**284**, **285**, **286**), hydrazone (**348**, **349**, **350**) and oxime (**351**, **352**) C-9 substitution. These compounds however elicited reduced anti-proliferative activity in the MUTU-I cell line (>75%) and moderate DG-75 activity (~58-86%).

Replacement of the 9,10-dihydro-9,10-ethanoanthracene moiety with a triptycene moiety (**324**, **327**) was found to be unfavourable for activity, decreasing activity induced in the DG-75 cell line at 1 μM (~40-85%) and a number of other C-9 functionalities were also found unfavourable such as alcohol (**330**), nitroalkane (**328**) and aldehyde (**329**) (>80% at 10 μM and 1 μM in both cell lines). Increased chain length at the C-2 position of the nitrovinyl unit to methyl and ethyl was also found to be unfavourable for anti-proliferative activity (>80%) and this trend can be seen in (**324**, **325**, **326**), (**270**, **271**, **272**), (**276**, **277**, **278**) and (**288**, **303**, **304**). In this series of ethanoanthracenes a number of key requirements for antiproliferative activity were identified. The nitrovinyl pharmacophore was demonstrated to be critical for antiproliferative effect, epipyrolo bridgeheads were also found to exert a more potent effect than simple ethano and furan based bridgeheads.

6.5.7 *In vitro* anti-proliferative activity (IC_{50s}) of the most potent Maprotiline analogues

In order to identify the most potent anti-proliferative agents in the MUTU-I cell line, IC_{50} values were determined for a number of the most active compounds from the ethanoanthracene series (section 6.5) (Table 44). These IC_{50} values combined with the data provided by the preliminary screen in the DG-75 BL cell line was used to select compounds for IC_{50} determination in the DG-75 cell line. These selected compounds would also be studied using Annexin V/PI for pro apoptotic effects in both the MUTU-I and DG-75 cell lines.

Compound #	IC_{50} (μM) *MUTU-I 24 h*	Compound #	IC_{50} (μM) *MUTU-I 24 h*	Compound #	IC_{50} (μM) *MUTU-I 24 h*
Taxol	0.32	**288**	0.21	**298**	0.26
Maprotiline	> 10	**289**	0.17	**301**	0.23
		290	0.20	**302**	0.3
7	2.57	**291**	0.22	**316**	0.26
		292	0.25	**320**	0.54
279	0.25	**293**	0.24	**323**	0.55
287	0.09	**294**	0.22	**327**	0.28
		295	0.20		
282	0.32	**296**	0.24	**318**	0.38

Table 44: IC_{50} values for most potent compounds in the MUTU-I cell line (24 h)

Compounds **288**, **289**, **290** and **291** were selected from the 9-((*E*)-2-nitrovinyl)-13-phenyl-9,10-dihydro-9,10-[3,4]epipyrroloanthracene-12,14-dione class, compound **318** from the (*E*)-11,12-substiuted-9-(2-nitrovinyl)-9,10-dihydro-9,10-ethanoanthracenes and compounds **287** and **279** as representatives of the 9-((*E*)-2-nitrovinyl)-9,10-dihydro-9,10-[3,4]epipyrroloanthracene-12,14-diones. The calculated Lipinski properties for these compounds and IC_{50} values for the BL cell lines MUTU-I and DG-75 are presented in Table 45.

The IC_{50} values of all the selected compounds were not only more potent than the parental anthracene based compound **7** (MUTU-I; 2.57 μM, DG-75; 2.08 μM) and Maprotiline (MUTU-I > 10 μM, DG-75 > 10 μM) in both BL cell lines but also these compounds exerted a more potent effect than Taxol (MUTU-I; 0.32 μM, DG-75; 1.32 μM). These Maprotiline analogues gave IC_{50} values in the MUTU-I cell line ranging from 0.09 - 0.38 μM and IC_{50} values ranging from 0.24 – 0.78 μM in the DG-75 cell line. Compound **287** was identified as the most potent analogue with an IC_{50} value of 0.09 μM in the MUTU-I cell line and an IC_{50} of 0.24 μM in the DG-75 cell line. Lipinski rule of five properties were calculated for these

compounds (Mcule property calculator v1 2015). These parameters were applied to the above compounds and the compounds **7, 279, 287, 288, 290** and **318** were found to satisfy all the Lipinski rule of five criteria indicating their potential as lead compounds for development.

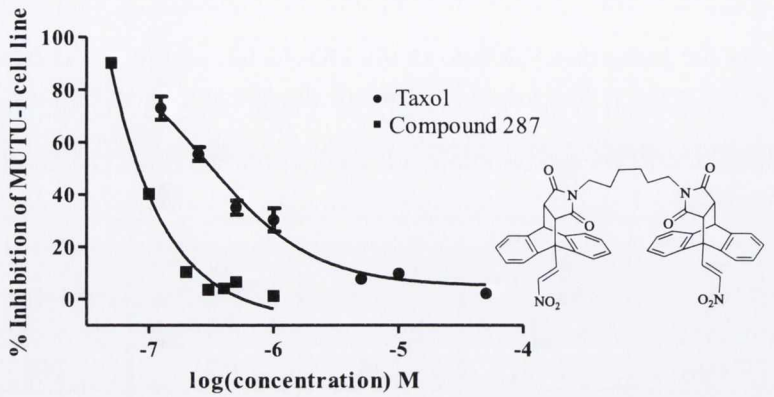

Compound #	IC50 (μM)		Lipinski properties					
	MUTU-I 24 h	*DG-75 48 h*	*Mr*	*logP*	*nrotb*	*nON*	*nOHNH*	*PSA (A^2)*
Taxol	0.32	1.32	853.9	7.38	15	15	4	221.29
Maprotiline	> 10	> 10	277.4	4.602	4	1	1	12.03
7	2.57	2.08	249.3	4.763	2	3	0	45.82
279	0.25	0.78	380.8	3.31	2	6	1	91.99
287	0.09	0.24	774.8	7.143	11	12	0	166.4
288	0.21	0.71	422.4	4.616	3	6	0	83.2
289	0.17	0.45	456.9	5.269	3	6	0	83.2
290	0.20	0.56	452.5	4.625	4	7	0	92.43
291	0.22	0.59	456.9	4.96	3	6	0	83.2
318	0.38	0.69	302.3	4.275	2	4	0	69.61

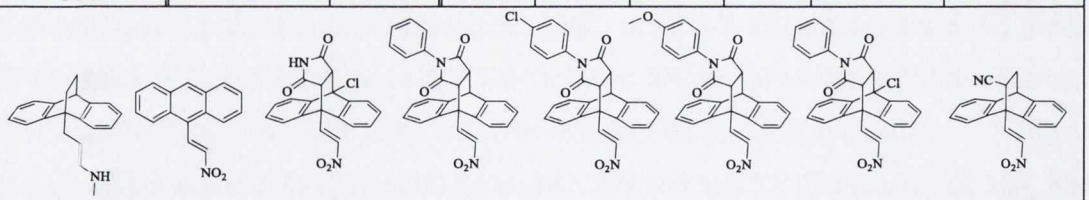

Table 45: IC_{50} (BL cell lines DG-75 & MUTU-I) & Lipinski properties of leading compounds Chapter 3 & Chapter 4

6.5.8 Investigations into the pro-apoptotic effect - FITC Annexin V / PI FACS analysis

(I) In order to determine potential pro-apoptotic effects of the most potent maprotiline analogues, Annexin V / PI FACS analysis was carried out on a subset of compounds identified. Annexin V / PI FACS analysis is described in section 7, Chapter 6. The study was carried out over a concentration range (10 – 0.2 μM) in both the BL cell lines (DG-75 and MUTU-I). Taxol was used as a positive control.

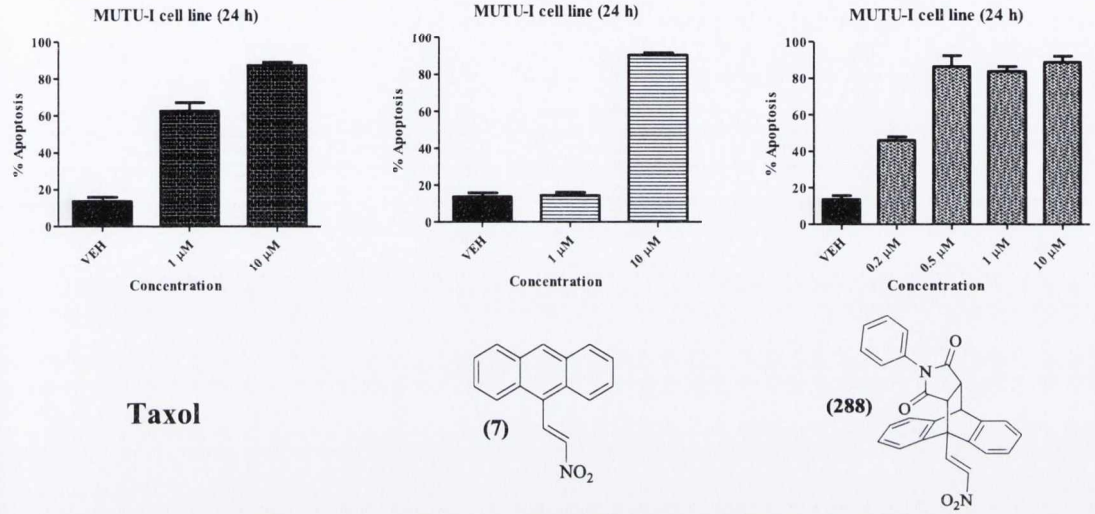

Figure 286: Annexin V / PI FACS Maprotiline analogues MUTU-I cell line

Taxol was found to elicit a pro-apoptotic effect in the MUTU-I at both 10 μM (87%) and 1 μM (63%). Compound **7** was found to possess potent apoptotic activity at 10 μM (90%), however no activity was observed at 1 μM. Compound **288** was much more active than its parent compound **7** and was found to induce over 80% apoptosis at 10 μM, 1 μM and 0.5 μM, at 0.2 μM compound **288** induced 46% apoptosis (Figure 286).

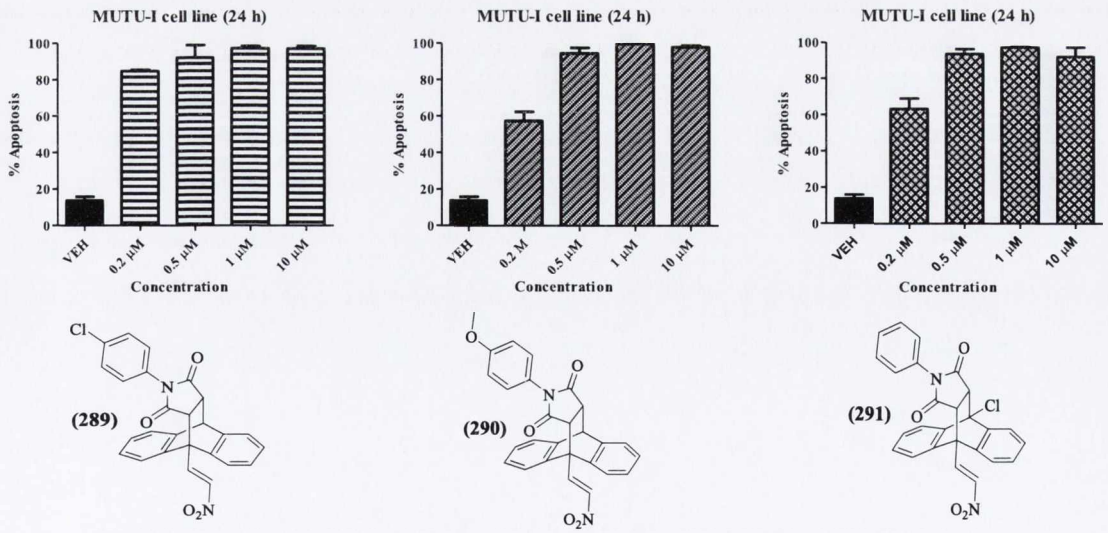

Figure 287: Annexin V / PI FACS Maprotiline analogues MUTU-I cell line

(II) The *para*-chloro phenyl compound **289** induced a more potent effect than the unsubstituted compound **288**. At all concentrations during this experiment in the MUTU-I cell line, compound **289** gave a response of >80% apoptosis. The *para*-methoxy phenyl compound **290** was found to induce over 90% apoptosis at 10 μM, 1 μM and 0.5 μM, at 0.2 μM compound **290** induced 57% apoptosis. Similar activity was observed for C-10 chloro compound **291**; at 0.2 μM 63% apoptosis was recorded (Figure 287).

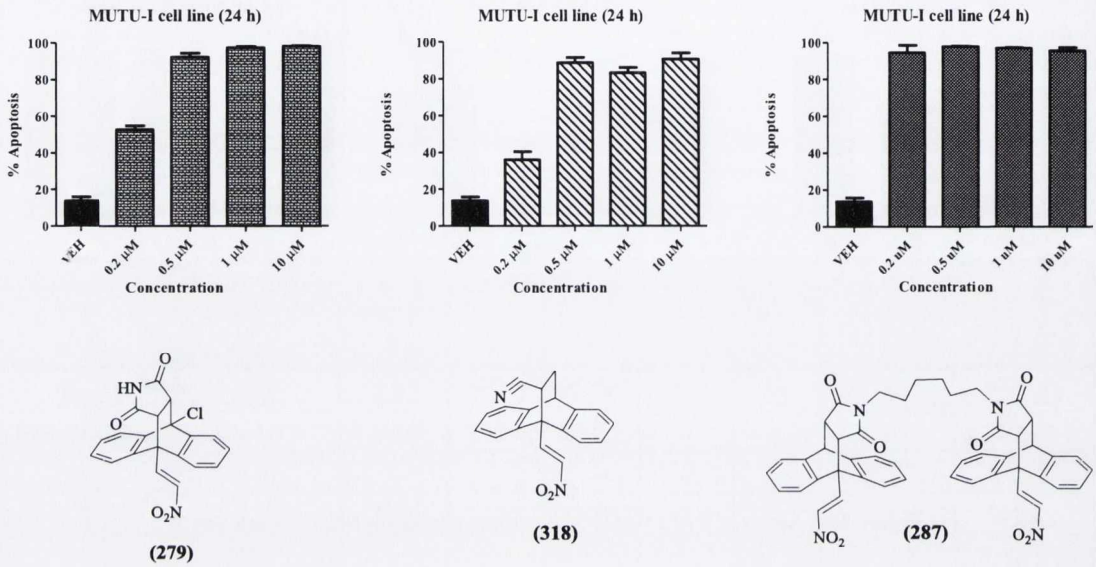

Figure 288: Annexin V / PI FACS Maprotiline analogues MUTU-I cell line

Compounds **279** and **318** were also found to possess potent apoptotic activity at 10 μM, 1 μM and 0.5 μM of over 90% and at 0.2 μM 53% and 36% respectively. The most potent compound was the dimer compound **287**, eliciting over 90% apoptosis at all four concentrations (Figure 288). In summary compounds **287** and **289** not only possessed the most potent IC_{50} values but were found to induce the most favourable pro-apoptotic response in the MUTU-I cell line.

(III) In the chemoresistant DG-75 cell line, Taxol was found to elicit a pro-apoptotic effect at both 10 μM (73%) and 1 μM (21%). Compound **7** elicits similar effects at both 10 μM (82%) and 1 μM (10%). The unsubstituted Diels-Alder adduct compound **288** has a potent apoptotic effect at 10 μM (92%) but is inactive at all other concentrations (<5%) (Figure 289).

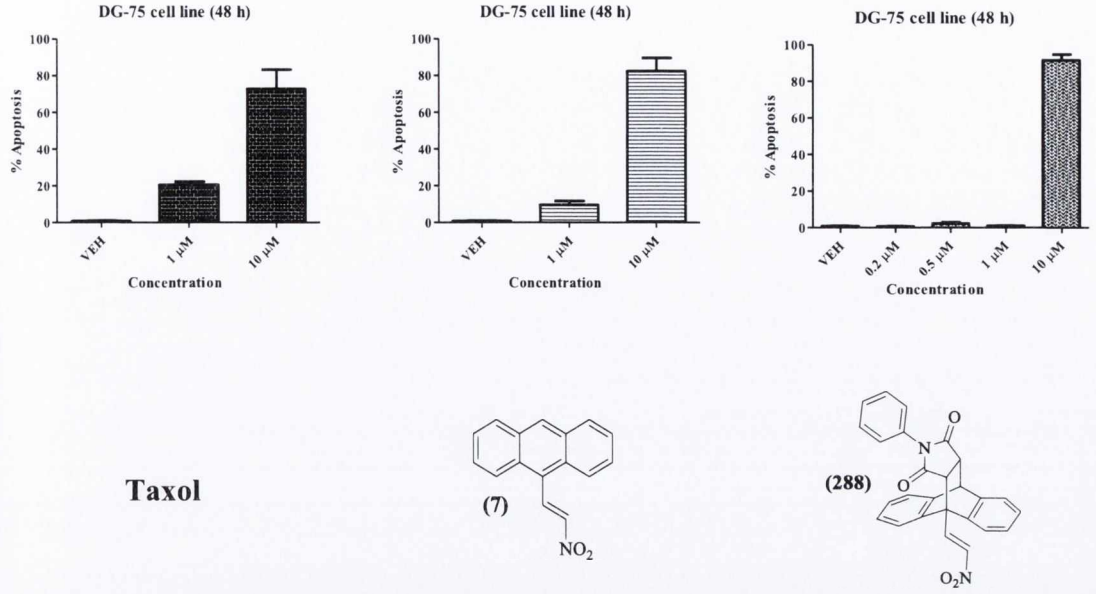

Figure 289: Annexin V / PI FACS Maprotiline analogues DG-75 cell line

(IV) The *para* chlorophenyl maleimide compound **289** and *para*-methoxyphenyl maleimide compound **290** exhibits improved pro-apoptotic activity when compared to the unsubstituted compound **288** in the DG-75 cell line. Compound **289** and **290** induce 61% and 29% apoptosis at 1 μM respectively. The C-10 chloro compound **291** induced 44% apoptosis at 10 μM and a modest 15% at 1 μM (Figure 290).

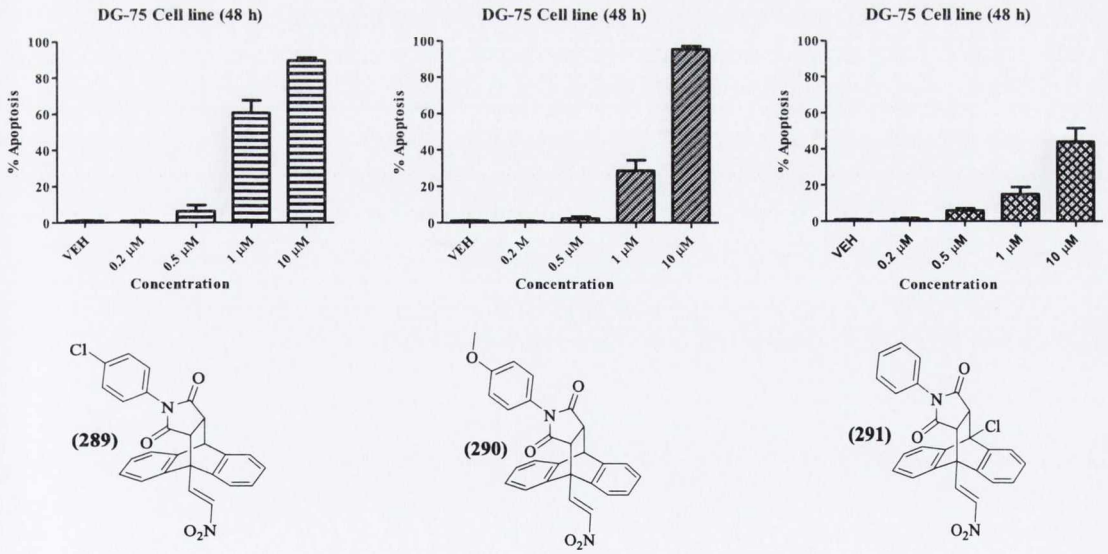

Figure 290: Annexin V / PI FACS Maprotiline analogues DG-75 cell line

The maleimide Diels-Alder adduct compound **279** was shown to induce 90% apoptosis at 10 μM and 11% at 1 μM. Compound **318** also gave good activity at 10 μM of 87%. The leading compound in this experiment was compound **287** and this compound induced dose dependent

apoptosis at all concentrations assayed: 10 μM (95%), 1 μM (46%), 0.5 μM (18%) and 0.2 μM (7%) (Figure 291) in the DG-75 cell line.

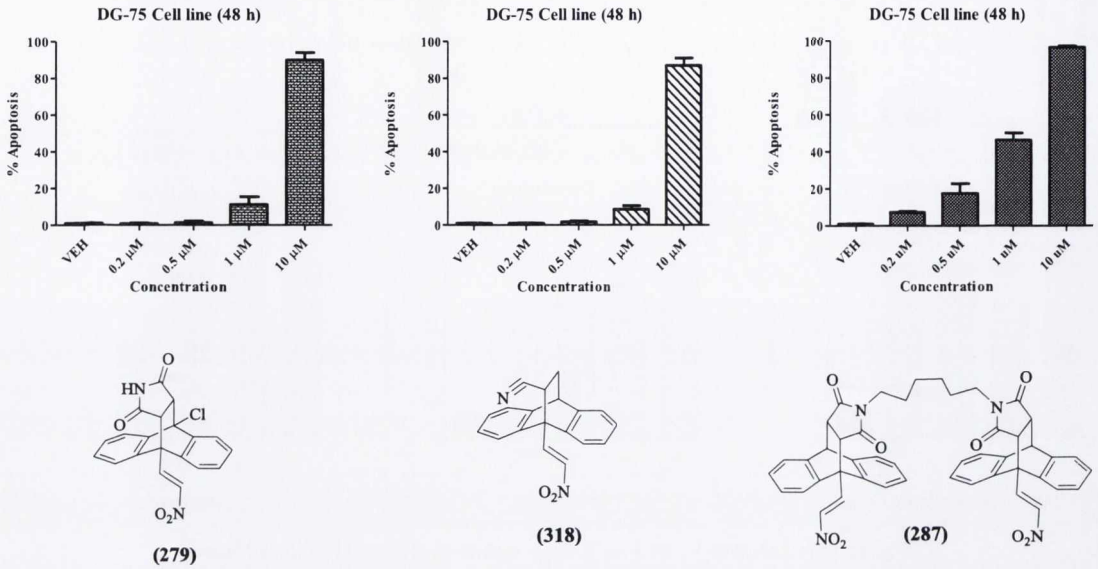

Figure 291: Annexin V / PI FACS Maprotiline analogues DG-75 cell line

Overall compounds **287** and **289** were shown to induce a superior potent pro-apoptotic response in both the MUTU-I and DG-75 BL cell lines than other selected compounds in this grouping and merit further study.

6.5.9 Evaluation of *in vitro* cytotoxity via lactate dehydrogenase (LDH) assay

Compounds **289**, **287** and **290** were found to elicit the most potent anti-proliferative and pro-apoptotic activity. *In vitro* cytotoxicity of these compounds was evaluated using the LDH assay, LDH is released during mechanisms of cell death associated with loss of cell membrane integrity (necrosis). It is important therefore to evaluate potential cytotoxicity of these test compounds. The MUTU-I and DG-75 BL cell lines were treated at 10 μM and 1 μM for the desired treatment period and the results are presented as percentage of total LDH release.

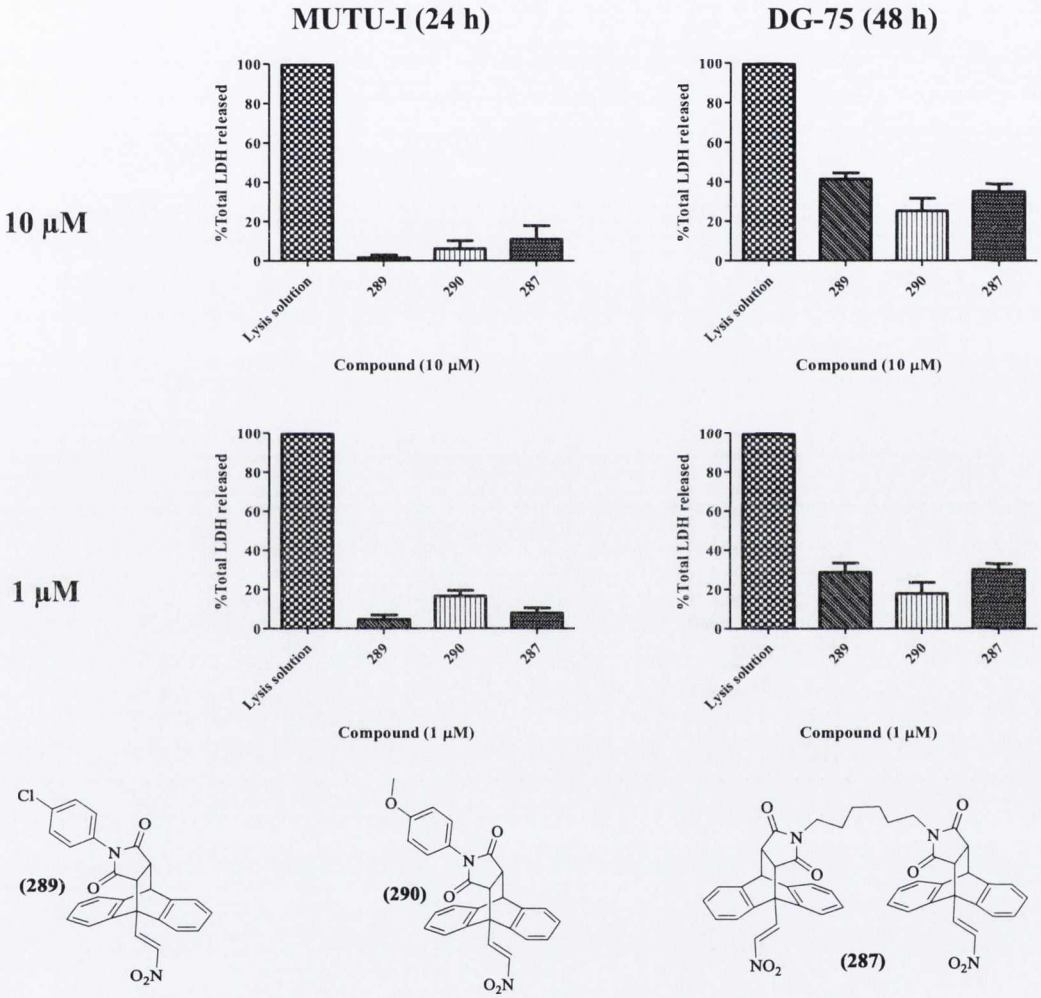

Figure 292: LDH assay Maprotiline analogues MUTU-I and DG-75 cell lines

In the MUTU-I cell line low levels of % LDH released were obtained (2-17%) at 10 μM and 1 μM - indicating low cytotoxity. The lowest % LDH released was obtained by compound **289** - 10 μM (2%) and 1 μM (5%). The compounds were low to moderate cytotoxic in the DG-75 cell line at 10 μM (25-41%) and 1 μM (27-30%). The lowest % LDH released was obtained by compound **290** - 10 μM (25%) and 1 μM (17%).

6.5.10 Effect of compounds 289, 287 and 290 on the viability of PBMCs

The (*E*)-11,12-substiuted-9-(2-nitrovinyl)-9,10-dihydro-9,10-ethanoanthracenes compounds **289**, **287** and **290** were evaluated for their toxicity on PBMCs *(*peripheral blood mononuclear cells*)* to determine if these potent compounds have a selective toxic effect on malignant BL cell lines over normal lymphatic cells. Compounds were evaluated at 1 μM and 0.5 μM over a 24 h treatment time (Figure 293). This work was carried out by Dr. Sandra A. Bright in collaboration with the Williams Group, School of Biochemistry and Immunology, Trinity College Dublin.

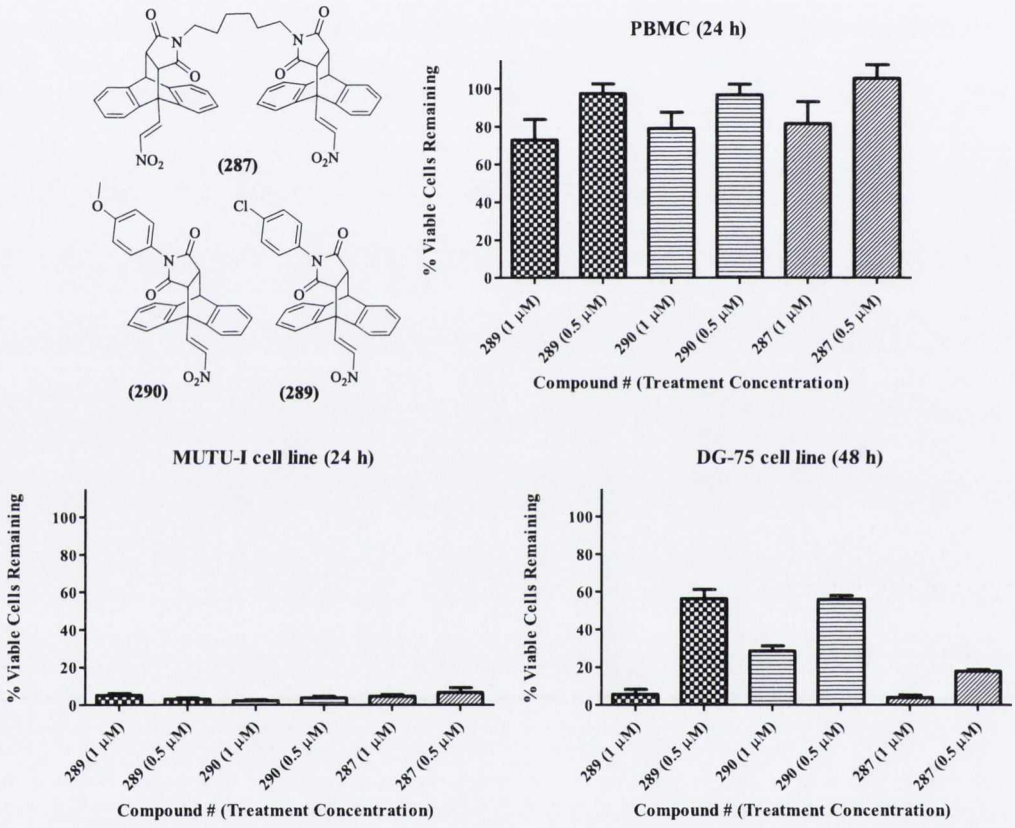

Figure 293: *In vitro* antiproliferative effect of compounds 289, 287 and 290 on PBMCs (24 h), MUTU-I cell line (24 h) and DG-75 cell line (48 h) at 1 μM and 0.5 μM

Compounds **289**, **287** and **290** elicited minimal toxicity in the PBMCs at 0.5 μM (~99% viable cells) and low toxicity activity at 1 μM (72-81% viable cells) (Figure 293). In comparison compounds **289**, **287** and **290** induced a potent anti-proliferative effect in the MUTU-I at 1 μM and 0.5 μM (2-7% viable cells remaining). Compounds **289**, **287** and **290** also induced a potent anti-proliferative effect in the DG-75 at 1 μM (6-28%) and 0.5 μM (18-57%). Comparing the results obtained from the BL cell lines and the PBMCs, the results suggest compounds **289**, **287** and **290** exert a selectively toxic effect on BL cell lines.

6.5.11 Investigation into the role of reactive oxygen species in cell death induced by compounds 289, 287 and 290

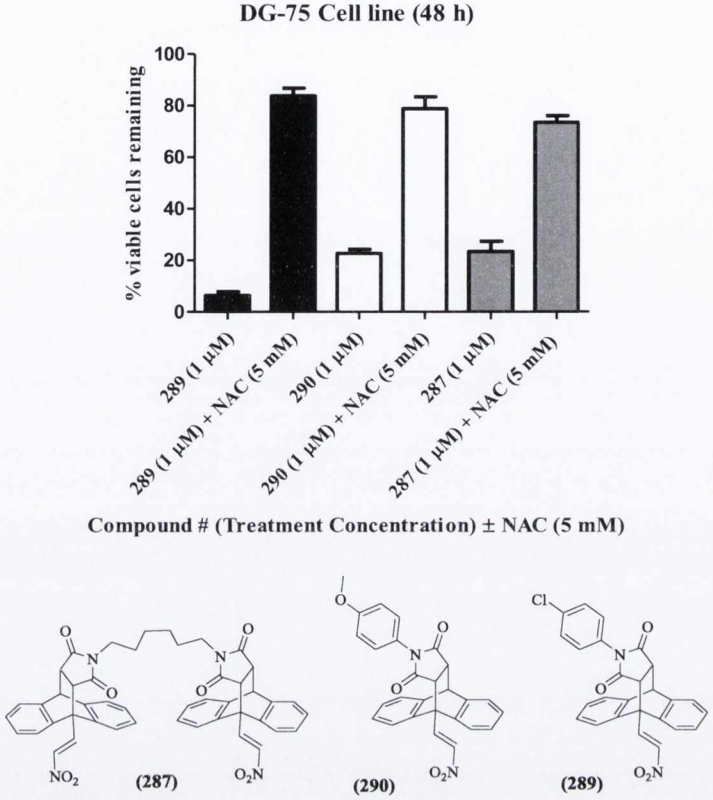

Figure 294: Investigation into the role of reactive oxygen species in cell death induced by compounds 289, 287 and 290

A preliminary experiment to determine if reactive oxygen species play a role in the mechanism of cell death induced by compounds **289**, **287** and **290** was accomplished. Using the DG-75 cell line, cells were pre-treated for 1 h with NAC and subsequently treated with the desired compound and viability was monitored using the alamarBlue® dye. From the results obtained it is evident that in the presence of the reactive oxygen species inhibitor NAC – the anti-proliferative effects of compounds **289**, **287** and **290** at 1 μM was reduced. Overall the anti-proliferative effects previously observed by compounds **289**, **287** and **290** dropped from 6-23% viable cells to 73-83% viable cells in the presence of 5 mM NAC. Thus indicating that ROS may be involved in the mechanism of cell death.

6.5.12 Conclusions

Nitrostyrenes and nitrovinyl containing compounds are known to induce anti-cancer effects and stimulate an apoptotic response in a range of cancer cell lines[1-8, 10-13, 15-17]. In this thesis over 300 compounds were synthesised and evaluated in a preliminary screen for potential anti-proliferative activity in the MUTU-I and DG-75 BL cell lines. A number of structural features favourable for anti-proliferative activity were identified from the study and the preservation of the nitrovinyl unit was recognised as critical for pro-apoptotic and anti-proliferative activity.

A series of 134 nitrostyrene analogues and related structures were first evaluated for potential anti-proliferative activity in the MUTU-I and DG-75 BL cell lines. Structural modifications of the nitrostyrenes evaluated included variations in aryl ring substitution, alkyl chain length at C-2 of the vinyl unit and the inclusion of alternative aryl heterocycles. The preliminary screen identified that the (*E*)-(2-nitrovinyl)benzenes possessing aryl C-3 halogen or hydroxy and C-2 alkoxy substitutions were favourable for promoting an anti-proliferative and pro-apoptotic response in BL cell lines. Reduction of the nitrovinyl unit was detrimental to anticancer activity and a number of alternative vinyl and heterocyclic units were also evaluated for anti-proliferative activity including cyanovinyl, epoxide, chalcone, hydrazone and triazole derivatives. However these latter compounds were found to elicit a poor anti-proliferative effect. This structure activity study is presented in section 6.2.11 and is summarised below in Figure 295.

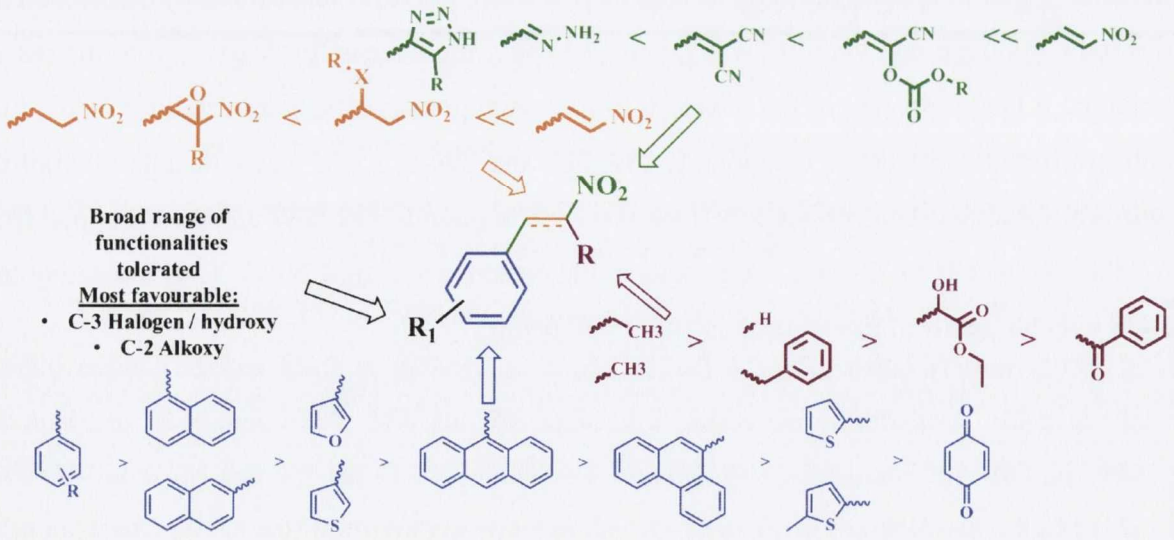

Figure 295: Summarised SAR for the (*E*)-(2-nitrovinyl)benzenes

The study identified a number of compounds with anti-proliferative activity and pro-apoptotic activities in the BL cell lines exceeding that of the previous lead compound **85** ((*E*)-4,4'-(2-nitroprop-1-ene-1,3-diyl)bis(chlorobenzene)). The lead compound identified in this study was compound **66** ((*E*)-4-bromo-1-methoxy-2-(2-nitrobut-1-en-1-yl)benzene). Compound **66** was shown to elicit anti-proliferative activity in the BL cell lines (MUTU-I (IC_{50} = 0.45 μM) and DG-75 (IC_{50} = 1.26 μM)). The compounds also exhibited anticancer properties in a range of other malignant cell lines at 10 μM and 1 μM including HeLa (ovarian), MCF-7 (breast), HL60 (leukaemia), Ramos (BL) and Bjab (BL). Compound **66** was shown to ellicit a pro-apoptotic effect at 10 μM in both the DG-75 and MUTU-I cell lines (≥80%). Compound **66** was also shown to induce potent pro-apoptotic and anti-proliferative effects in CLL cell lines (Cll, HG3, I83 and PGA1) and CLL *ex vivo* samples. This activity was superior to that of the current frontline CLL treatment – Fludarabine. Inhibitor studies carried out in the PGA1 and HG3 cell lines have indicated that caspases and ROS are involved in this apoptotic mechanism of cell death. The present work has demonstrated the selectively toxic effect of compound **66** towards the MUTU-I and DG-75 cell lines over PBMCs.

The nitro-2-phenyl-2*H*-chromenes were selected as the most potent heterocyclic compounds included a constrained nitrostyrene pharmacophore. These compounds were found to exert a potent pro-apoptotic and anti-proliferative effect comparable to the previous lead compound **85.** Comparing the heterocyclic structures evaluated, it was concluded that compounds inducing a constrained *trans* (*E*) configuration on (2-nitrovinyl)benzene (nitrostyrene) and 1,3-bis(aryl)-2-nitro-1-propene scaffolds were more potent anticancer agents than compounds inducing a *cis* (*Z*) configuration (Figure 296). This structure activity study is summarised in section 6.3.3. The lead compound identified in this study was the C-7 methoxy compound **145** (7-methoxy-3-nitro-2-phenyl-2H-chromene), compound **145** was shown to elicit anti-proliferative activity in the BL cell lines (MUTU-I (IC_{50} 0.49 μM) and DG-75 (IC_{50} 2.51 μM)). Compound **145** was shown to elicit a pro-apoptotic effect comparable to Taxol at 10 μM in both the DG-75 and MUTU-I cell lines (≥80%). This improved upon the activity of the previous lead compound **85** in the BL cell lines (MUTU-I (IC_{50} = 2.82 μM) and DG-75 (IC_{50} = 6.03 μM)) indicating that the nitro-2-phenyl-2*H*-chromenes may provide a new potential lead structure for the treatment of BL.

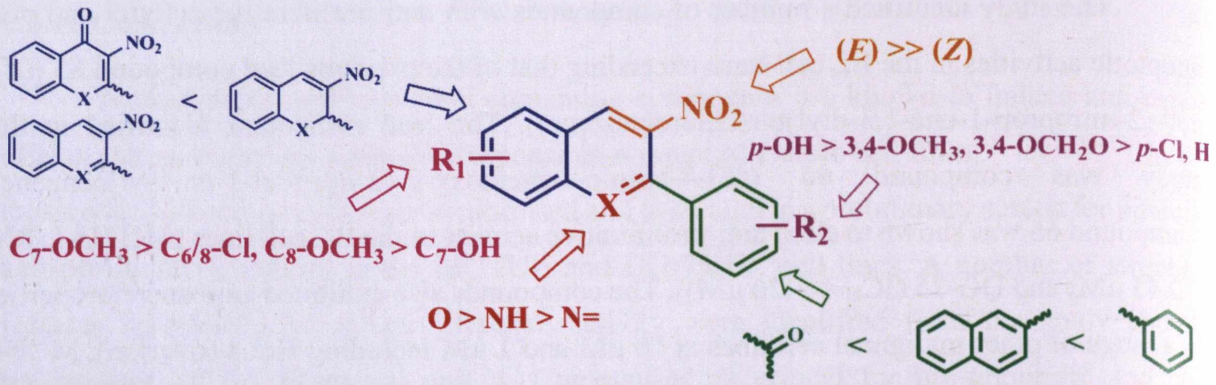

Figure 296: Summarised SAR for the heterocyclic compounds containing a constrained nitrostyrene pharmacophore

As an extension of this work, a series of 52 anthracene based maprotiline analogues was evaluated at 10 μM and 1 μM for anti-proliferative activity in the MUTU-I and DG-75 BL cell lines. A number of anthracenes containing the C-9 and C-10 substituents were evaluated for their anticancer effects; these included cyanovinyl, hydrazone, nitrovinyl, triazole, nitroalkane, nitrone, halogen and hydroxyl. The (*E*)-9-(2-nitrovinyl)anthracene pharmacophore (**7**) was identified as a potent anti-proliferative agent and subsequent study of this pharmacophore yielded a number of conclusions. Reduction of the nitrovinyl unit and extension of chain length at C-9 were unfavourable for antiproliferative action. Extensions of alkyl chain length at C-2 were also unfavourable, in contrast to the series of nitrostyrenes previously examined. The effect of anthracene substitution patterns of the (*E*)-9-(2-nitrovinyl)anthracenes on anti-proliferative activity were also investigated. Halogen substitution at C-10 was found to be unfavourable; however all other C-10 alkyl, phenyl and alkoxy substitutions were found to elicit similar activity to the previous lead compound 7. This structure activity study is summarised in section 6.4.5.

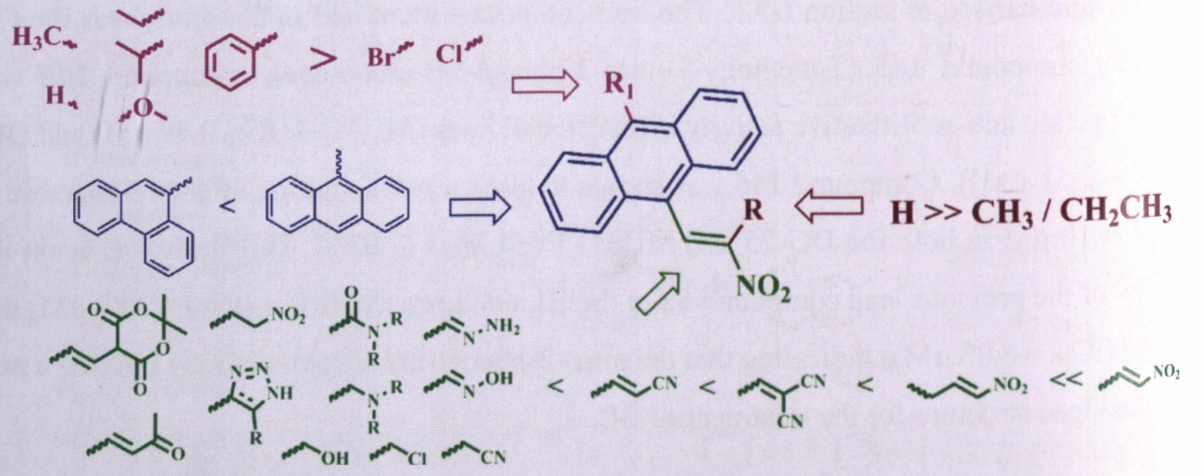

Figure 297: Summarised SAR for the 9-substituted anthracene maprotiline analogues

The lead compound from this study was identified as compound **7**, eliciting a potent anti-proliferative and pro-apoptotic effect in the MUTU-I (IC_{50} = 2.57 μM) and DG-75 cell

lines (IC_{50} = 2.08 μM). This activity compared favourably to that induced by maprotiline in the MUTU-I and DG-75 cell lines (IC_{50} >10 μM). Compound **7** was found to elicit a potent pro-apoptotic effect at 10 μM in both BL cell lines (>90%) that was comparable to Taxol at the same concentration (>90%), however no activity was observed at 1 μM in both BL cell lines. Taxol was found to elicit ~60% apoptosis in the MUTU-I cell line at 1 μM and ~20% in the DG-75 cell line.

A series of 83 9,10-dihydro-9,10-ethanoanthracene based maprotiline analogues were evaluated at 10 μM and 1 μM for potential anti-proliferative activity in the MUTU-I and DG-75 BL cell lines. The effects of the inclusion of a number of C-9 9,10-dihydro-9,10-ethanoanthracene substitutions on anti-proliferative activity were discussed including alcohol, aldehyde, acid, hydrazone, nitrovinyl, nitroalkane and cyanovinyl (Figure 298). The most promising 9,10-dihydro-9,10-ethanoanthracene based maprotiline analogues were identified and these included a nitrovinyl substituent at C-9. The effect of a number of 9,10-dihydro-9,10-ethanoanthracene structural modifications on activity was also investigated; these modifications included but were not limited to ethano bridge modifications, phenyl substitutions, maleimide substitutions and extension of alkyl chain length at C-2 of the nitrovinyl unit.

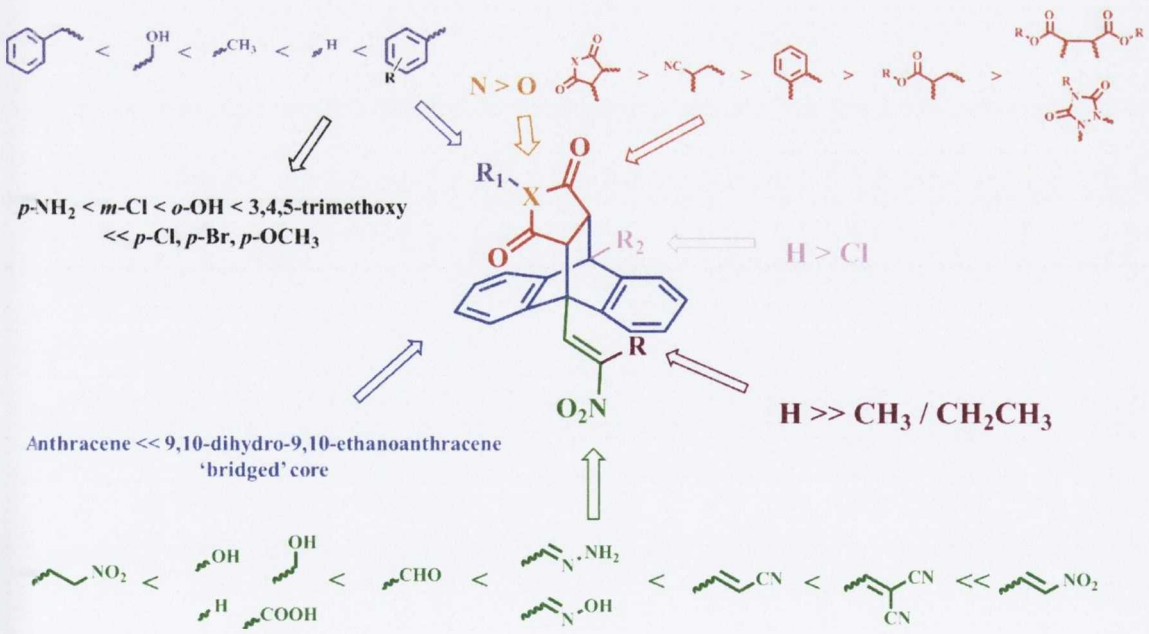

Figure 298: Summarised SAR for the 9,10-dihydro-9,10-ethanoanthracene based maprotiline analogues

The preliminary screen of the 9,10-dihydro-9,10-ethanoanthracenes identified compounds **289** and **287** as the lead compounds of this study. Compound **289** elicited potent anti-proliferative activity in the BL cell lines (MUTU-I (IC_{50} = 0.17 μM) and DG-75 (IC_{50} =

0.45 μM)). The dimer compound **287** was also a potent anticancer agent inducing good activities in both BL lines (MUTU-I (IC_{50} = 0.09 μM) & DG-75 (IC_{50} = 0.24 μM)). These compounds were shown to induce a pro-apoptotic effect of >80% at 0.2 μM in the MUTU-I cell line and 50-60% apoptosis at 1 μM in the DG-75 cell line. An LDH assay was used to demonstrate extremely low cytotoxicity towards the MUTU-I cell line and moderate cytotoxicity in the DG-75 cell line. The present work has also demonstrated the selectively toxic effect of compounds **287** and **289** towards the MUTU-I and DG-75 cell lines over PBMCs at 1 μM and 0.5 μM. In the presence of a ROS inhibitor the anti-proliferative effect of these compounds dramatically decreased indicating that ROS may be involved in the mechanism of cell death. Further study may be required to identify a possible molecular target for these compounds.

Chapter 7. Conclusion

7.0 Conclusion

Burkitt's lymphoma is a rare, aggressive malignancy with high incidence in children in the developing areas such as equatorial Africa. Treatment of this condition in these regions is inadequate and the development of new, safe, effective and economical therapeutics are of current interest. Previous work in our laboratory identified a series of (*E*)-1,3-bis(aryl)-2-nitro-1-propenes related to the amphetamines with potent anticancer activity in BL cell lines[5, 91, 207]. The nitrostyrene and related nitrovinyl compounds are a biologically active class of compounds reported to induce anti-cancer effects and stimulate an apoptotic response in a range of cancer cell lines[1-17]. This study reports the synthesis, characterisation and biochemical evaluation of a number of nitrostyrene and related nitrovinyl compounds in the BL MUTU-I and DG-75 cell lines. A diverse library of compounds related in structure to the previous lead (*E*)-1,3-bis(aryl)-2-nitro-1-propene scaffold and the tetracyclic antidepressant maprotiline were synthesised and initially evaluated for anti-proliferative effect in Burkitt's lymphoma (BL) cell lines. These compounds were structurally arranged into the four groupings: (a) Nitrostyrenes and related structures, (b) Heterocycles containing the nitrovinyl pharmacophore, (c) Anthracene based maprotiline analogues and (d) Ethanoanthracene based maprotiline analogues

(A) Nitrostyrenes: A library of 134 nitrostyrene compounds structurally related to the (*E*)-1,3-bis(aryl)-2-nitro-1-propene scaffold was prepared, isolated and characterised. The Henry-Knoevenagel condensation reaction was utilised to synthesise a comprehensive library of structurally diverse nitrostyrene derivatives. A number of structural modifications of the nitrostyrene scaffold were also achieved including triazole formation, epoxidation, reduction, oxidations, Michael additions and Morita-Baylis-Hillman reactions (Figure 299), to investigate potential SARs for the series.

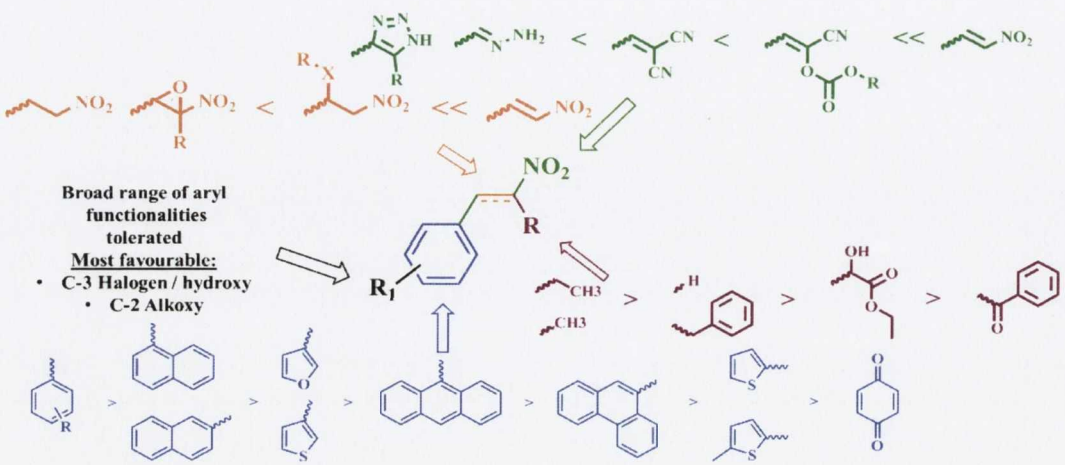

Figure 299: Optimal SAR for the (*E*)-(2-nitrovinyl)benzenes

A number of nitrostyrenes were initially identified as potent anti-proliferative agents in a comprehensive screen in the BL cell lines MUTU-I and DG-75. The optimal structure activity relationship (SAR) was identified for the series and this is summarised in Figure 299. Optimum anti-proliferative activity was achieved with extended chain length at C-2 of the nitrovinyl unit, C-1 phenyl substitution of the vinyl unit with *ortho* alkoxy and *meta* halogen or hydroxy substitutions. The lead compound (**66**) containing 5-bromo-2-methoxy aryl substitution and ethyl C-2 vinyl substitution, not only displayed good anti-proliferative activity in the MUTU-I and DG-75 cell lines, but also exhibited potent effects in CII, PGA1, HG3, HL60, MCF-7, Bjab, Ramos and HeLa cell lines (Table 46).

Compounds were shown to elicit a less toxic effect on PBMCs than to the BL cell lines. Further investigations determined that these nitrostyrenes elicited a pro-apoptotic effect in both the BL lines (MUTU-I and DG-75), *ex vivo* CLL samples and CLL (PGA1 and HG3) cell lines. Additional inhibitor investigations in the PGA1 and HG3 cell lines demonstrated that in the presence of NAC and a caspase inhibitor, the percentage of total apoptosis was greatly reduced and it was concluded that ROS and caspases may be involved in the mechanism of cell death.

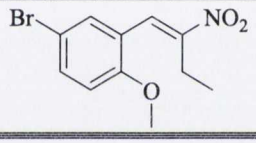

Compound 66: summary physiochemical properties					
Lipinski Properties					
Mr	***logP***	***nrotb***	***nON***	***nOHNH***	***PSA (Å²)***
286.1	4.009	4	4	0	55.05
Malignant cell line IC_{50} (μM)					
MUTU-I (24 h)	***DG- 75 (48 h)***	***CII (48 h)***	***HG3 (48 h)***	***I83 (48 h)***	***PGA1 (48 h)***
0.45	1.26	3.46	3.08	4.13	2.17
Malignant cell line (% viable cells remaining at 10 μM)					
Ramos (24 h)	***Bjab (24 h)***	***HL60 (24 h)***	***MCF-7 (72 h)***	***HeLa (24 h)***	
2.6	42.2	3.7	11.3	19.7	
% Total Apoptosis (10 μM)					
MUTU-I (24 h)	***DG- 75 (48 h)***	***HG3 (48 h)***	***PGA1 (48 h)***	***CLL ex vivo (48 h)***	
89.1	79.6	94.7	88.1	92.3	

Table 46: Compound 66: summary physiochemical properties

(B) Heterocyclic compounds: A series of heterocycles incorporating the (*E*)-1,3-bis(aryl)-2-nitro-1-propene and nitrostyrene pharmacophores were next prepared, isolated and characterised (including 3-nitro-2-phenyl-2*H*-chromenes, 3-nitro-1,2-dihydroquinolines, 3-nitroquinolin-2(1*H*)-one, 3-nitro-2-phenylchromen-4-ones, 4-nitro-3,5-diphenylisoxazole, 3-nitrochalcones, 3-nitro-2-phenyl-1*H*-indole and 3-nitro-2,4-diphenyl-2,5-dihydrobenzo[b][1,4]thiazepine). These heterocycles induced a more constrained configuration on the (*E*)-1,3-bis(aryl)-2-nitro-1-propene scaffold previously shown to exhibit anti-proliferative activity. A Baylis-Hillman tandem Michael reaction was identified for the preparation of the 3-nitro-2-phenyl-2*H*-chromenes and 3-nitro-1,2-dihydroquinolines. Nitration of flavones, isoxazole and phenylindole provided other nitrated adducts (Figure 30)

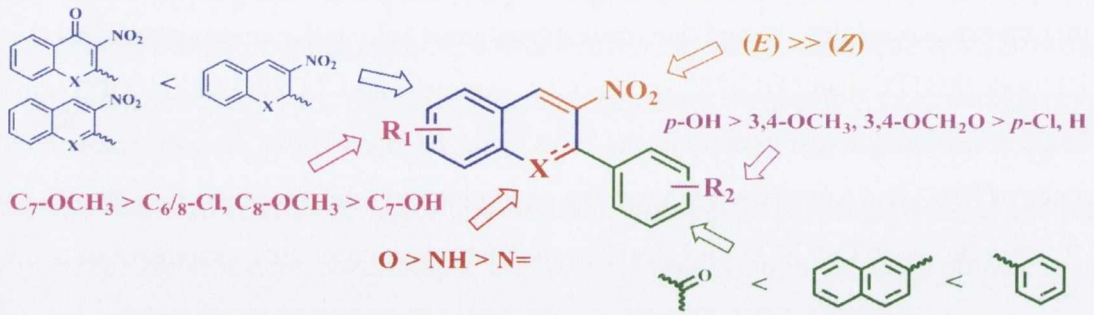

Figure 300: Optimal SAR for the heterocyclic compounds containing a constrained nitrostyrene pharmacophore

The 3-nitro-2-phenyl-2*H*-chromenes were identified as good anti-proliferative agents in the BL cell lines MUTU-I and DG-75. The 3-nitro-2-phenyl-2*H*-chromenes in contrast to other heterocyclic compounds in this study displayed a *trans* (*E*) configuration on the 1,3-bis(aryl)-2-nitro-1-propene pharmacophore and this feature has therefore been identified as favourable for anti-proliferative activity. The lead compound (**145**) not only displayed good anti-proliferative activity in the MUTU-I and DG-75 cell lines but also induced a potent pro-apoptotic response in these cell lines. (Table 47).

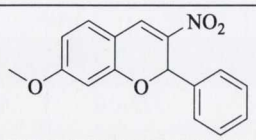

Compound 145: summary physiochemical properties					
Lipinski Properties					
Mr	***logP***	***nrotb***	***nON***	***nOHNH***	***PSA (Å^2)***
283.3	3.969	3	5	0	64.28
Malignant cell line IC_{50} (µM)			**% Total Apoptosis (10 µM)**		
MUTU-I (24 h)	***DG- 75 (48 h)***		***MUTU-I (24 h)***	***DG- 75 (48 h)***	
0.49	2.51		93.2	76.7	

Table 47: Compound 145: summary physiochemical properties

(C) Anthracenes: The antidepressant ethanoanthracene maprotiline and compound **7** ((*E*)-9-(2-nitrovinyl)anthracene) have in our work been previously shown to induce programmed cell death (apoptosis) in the BL cell lines MUTU-I and DG-75[94]. In the present work maprotiline elicited IC_{50} values of >10 μM in both the MUTU-I and DG-75 cell lines. A series of anthracene compounds based on maprotiline were synthesised for evaluation and also as intermediates in the preparation of the 9,10-dihydro-9,10-ethanoanthracene based maprotiline analogues. Preliminary biochemical evaluation was carried out on these anthracenes in order to identify the optimum anti-proliferative diene system for use in the Diels-Alder cycloaddition. The C-9 substitution of these anthracene compounds was varied extensively and functionalities such as alcohol, hydrazone, cyanovinyl, nitroalkane, nitrovinyl, oxime, amine, amide, nitrone and chlorides were installed. The optimal structure-activity relationship (SAR) was identified for the anthracene series and this is summarised in Figure 301. The unsubstituted nitrovinyl unit and the anthracene moieties were identified as key structural features for activity in the BL cell lines, although considerable variation in aryl substitution was achieved without loss of activity.

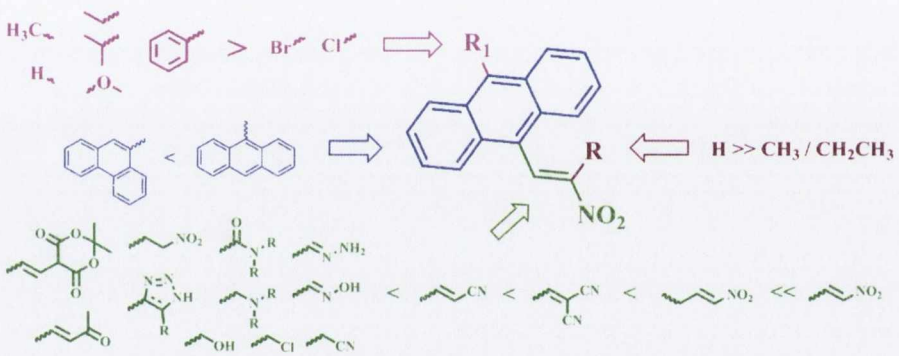

Figure 301: Optimal SAR for the 9-substituted anthracene maprotiline analogues

The study identified a family of (*E*)-9-(2-nitrovinyl)anthracenes exhibiting good anti-proliferative and pro-apoptotic effect in the BL cell lines MUTU-I and DG-75. Compound **7** was selected as one of the most potent representatives of this series for biochemical evaluation (Table 48).

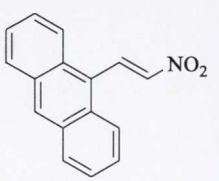

Compound 7: summary physiochemical properties					
Lipinski Properties					
Mr	***logP***	***nrotb***	***nON***	***nOHNH***	***PSA (Å²)***
249.3	4.763	2	3	0	45.82
Malignant cell line IC_{50} (μM)			**% Total Apoptosis (10 μM)**		
MUTU-I (24 h)	***DG- 75 (48 h)***		***MUTU-I (24 h)***	***DG- 75 (48 h)***	
2.57	2.08		90.6	82.4	

Table 48: Compound 7: summary physiochemical properties

(D) Ethanoanthracenes: In order to synthesise the required 9,10-dihydro-9,10-ethanoanthracene based maprotiline analogues a varied panel of dienophiles was assembled and utilised to prepare a library of over 80 examples of 9,10-dihydro-9,10-ethanoanthracenes using the Diels-Alder cycloaddition chemistry. These 9,10-dihydro-9,10-ethanoanthracenes included a number of structural modifications of the ethano bridgehead together with phenyl substitutions. A number of C-9 functionalities were successfully included into the 9,10-dihydro-9,10-ethanoanthracene structure such as hydrazone, alcohol, acid, nitrovinyl, nitroalkane and cyanovinyl (Figure 302). Preliminary MOE overlays were utilised to design the target structures and compare structural similarities with maprotiline. A number of X-ray crystal structures were then obtained and analysis of the asymmetric unit confirmed the structural similarities of maprotiline and 12 of the synthesised 9,10-dihydro-9,10-ethanoanthracenes in the present work.

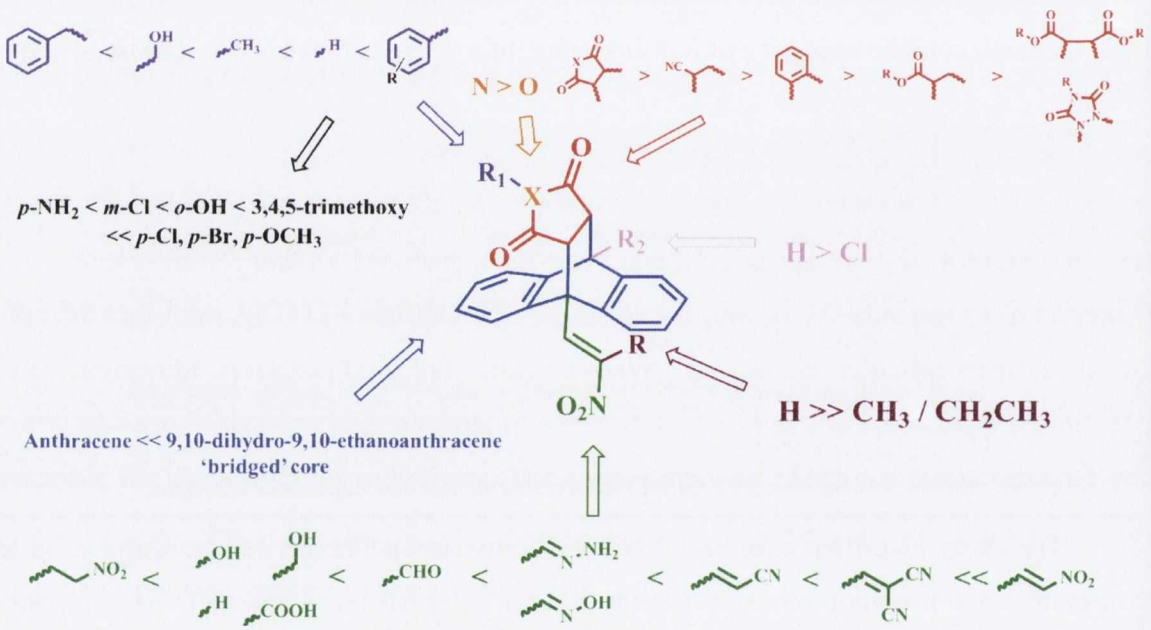

Figure 302: Optimal SAR for the 9,10-dihydro-9,10-ethanoanthracene based maprotiline analogues

The optimal features for structure-activity relationship (SAR) were identified for the anthracene series and are summarised in Figure 302. Preliminary biological evaluation identified compounds **287** and **289** as the leading compounds for anti-proliferative activity in the BL cell lines MUTU-I and DG-75 (Table 49 and Table 50). Further biological investigations demonstrated the potent pro-apoptotic effect induced by these 9,10-dihydro-9,10-ethanoanthracene based compounds in the MUTU-I and DG-75 cell lines. The anti-proliferative effects induced by these compounds was found to be selective to BL cell lines as they had minimal effect on the viability of PBMCs. LDH assays have shown that the compounds are minimally cytotoxic to the MUTU-I cell line and moderately toxic to the DG-

75 cell line. The novel dimeric compound **289** was found to possess favourable characteristics for oral druggability, however logP was slightly >5 (Mcule V1 2015). However compound **287** broke three of the Lipinski criteria for oral druggability with Mr >500, logP >5 (5.269) and nON >10. Additional inhibitor investigations in the DG-75 cell line demonstrated that in the presence of NAC (a ROS inhibitor), the antiproliferative effects of compounds **287** and **289** was greatly reduced and it was concluded that ROS may play a role in the mechanism of cell death.

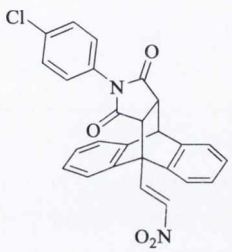

Compound 289: summary physiochemical properties					
Lipinski Properties					
Mr	***logP***	***nrotb***	***nON***	***nOHNH***	***PSA (Å^2)***
456.9	5.269	3	6	0	83.2
Malignant cell line IC_{50} (µM)				**% Total Apoptosis (10 µM)**	
MUTU-I (24 h)		***DG- 75 (48 h)***		***MUTU-I (24 h)***	***DG- 75 (48 h)***
0.17		0.45		97.2	89.6

Table 49: Compound 289: summary physiochemical properties

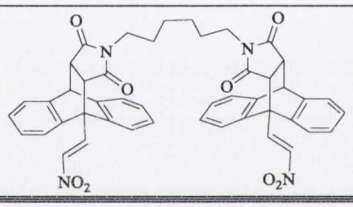

Compound 287: summary physiochemical properties					
Lipinski Properties					
Mr	***logP***	***nrotb***	***nON***	***nOHNH***	***PSA (Å^2)***
774.8	7.143	11	12	0	166.4
Malignant cell line IC_{50} (µM)				**% Total Apoptosis (10 µM)**	
MUTU-I (24 h)		***DG- 75 (48 h)***		***MUTU-I (24 h)***	***DG- 75 (48 h)***
0.09		0.24		95.7	96.5

Table 50: Compound 287: summary physiochemical properties

Previous work within our laboratory has shown that the (*E*)-1,3-bis(aryl)-2-nitro-1-propene based nitrostyrene compounds have a low SERT binding activity[5]. Nitrostyrenes are known to interact with a number of molecular targets such as tubulin[15], telomeres[12, 13] and protein tyrosine phosphates (PTP)[40]. Additional biological studies such as tubulin binding, PTP inhibition and telomerase inhibition are required to evaluate activity at these molecular targets in order to elucidate a possible molecular target for the compounds of the present study and to fully exploit this excellent pharmacophore. Future biochemical studies would also

include a global screen e.g. microarray and / or kinase screen to identify the key molecular targets of these novel compounds. Although specific references to toxicity of the vinyl nitro pharmacophore are not available, future work to identify, synthesise and biologically evaluate bioisosteres[408] (such as carbocycles, carboxylic acids, sulphonate and nitrogen containing heterocycles) for the nitrovinyl unit of the compounds reported in this study is of current interest.

Future synthetic objectives and possible structure activity relationship studies for further optimisations of the lead nitrostyrene compound **66** are outlined in Figure 303.

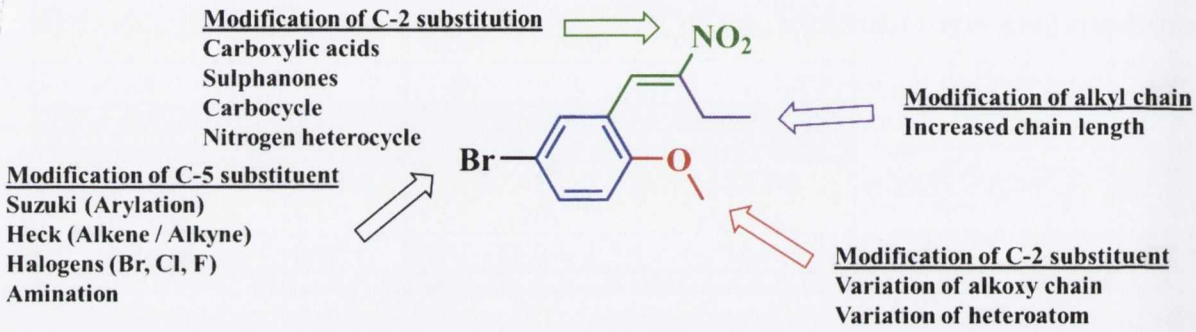

Figure 303: Future synthetic modification of the nitrostyrene lead compound (66)

The incorporation of the favourable 9,10-dihydro-9,10-ethanoanthracene scaffold into a 3-nitro-2-anthracene-2*H*-chromene type structure is also feasible. The proposed synthetic route includes Diels-Alder cycloaddition of a maleimide based dienophile and the anthracene diene structure (Figure 304).

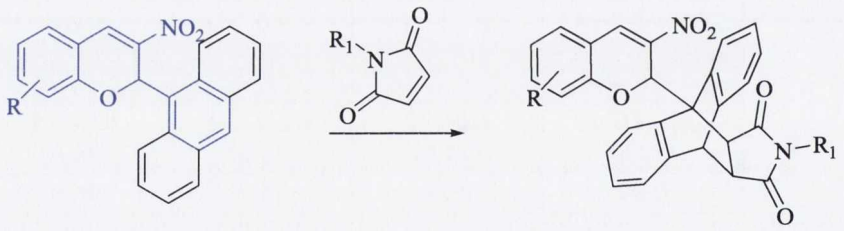

Figure 304: Future synthetic modification of the 3-nitro-2-anthracene-2*H*-chromene lead compound

Based on the potency of the anthracene lead compound **7**, the synthesis of nitrovinyl analogues of other TCAs such as imipramine and amitriptyline is also planned, through Henry-Knoevenagel condensations of the corresponding aldehydes (Figure 305).

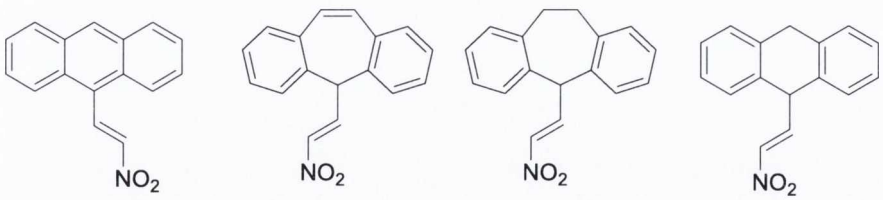

(7)

Figure 305: Future synthetic targets - TCA analogues

In order to exploit the potential of the potent ethanoanthracene compounds discovered in this work, further modification of the ethano bridgehead of the 9,10-dihydro-9,10-ethanoanthracenes is possible through the use of a number of diverse dienophiles in the Diels-Alder cycloadditions such as benzoquinone, nitrostyrene, ethylene, citraconic anhydride and acrylic acid (Figure 306).

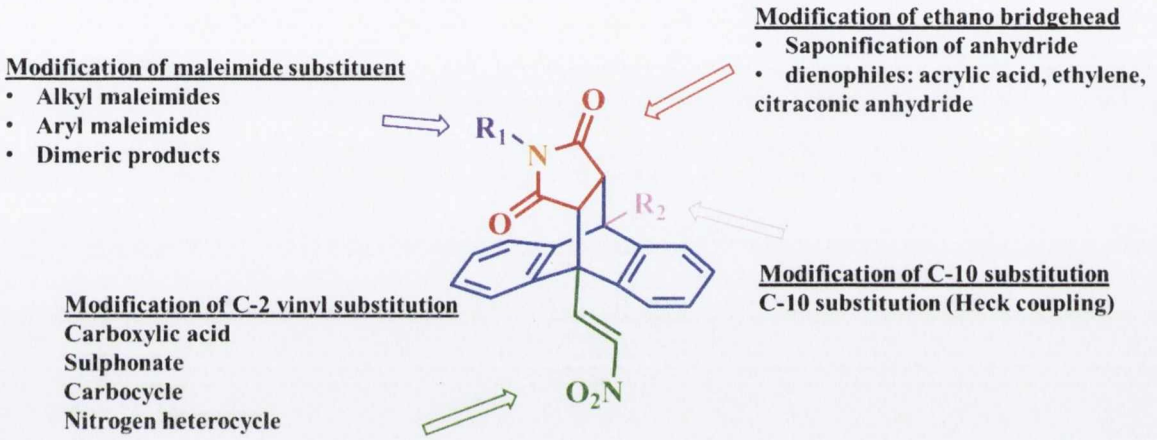

Figure 306: Future synthetic objectives for modification of the 9,10-dihydro-9,10-ethanoanthracene lead compound (289)

In summary a diverse library of nitrostyrenes, heterocyclic derivatives, 9-substituted anthracenes and 9,10-dihydro-9,10-ethanoanthracenes were designed, synthesised and identified as novel anti-proliferative agents in the BL cell lines MUTU-I and DG-75. Selected compounds elicit a potent anti-proliferative and pro-apoptotic effect towards a range of malignant cell lines and have shown superior proapoptotic activity when compared with the control drugs fludarabine and taxol in Burkitt's lymphoma and CLL. The leading nitrostyrene and 9,10-dihydro-9,10-ethanoanthracene based compounds were shown to elicit selective toxicity towards BL over PBMCs and subsequently have potential for preclinical development as potential drug candidates for the treatment of Burkitt's lymphoma and related B-cell malignancies such as CLL.

Chapter 8.
Experimental

Experimental note

Uncorrected melting points were measured on a Gallenkamp apparatus. Infra-red (IR) spectra were recorded on a Perkin Elmer FT-IR Paragon 1000 spectrometer. ^{1}H, ^{13}C and ^{19}F nuclear magnetic resonance spectra (NMR) were recorded at 27 °C on a Brucker DPX 400 spectrometer (400.13 MHz, ^{1}H; 100.61 MHz, ^{13}C; 376.47 MHz, ^{19}F) in either $CDCl_3$ (internal standard tetramethylsilane (TMS)) or CD_3OD or DMSO-d_6. For $CDCl_3$, ^{1}H-NMR spectra were assigned relative to the TMS peak at 0.00 ppm and ^{13}C-NMR spectra were assigned relative to the middle $CDCl_3$ peak at 77.0 ppm. For CD_3OD, ^{1}H and ^{13}C-NMR spectra were assigned relative to the center peaks of the CD_3OD multiplets at 3.30 ppm and 49.00 ppm respectively. Coupling constants are reported in Hertz. For ^{1}H-NMR assignments, chemical shifts are reported: shift value (number of protons, description of absorption, coupling constant(s) where applicable). Electrospray ionisation mass spectrometry (ESI-MS) was performed in the positive ion mode on a liquid chromatography time-of-flight mass spectrometer (Micromass LCT, Waters Ltd., Manchester, UK). The samples were introduced to the ion source by an LC system (Waters Alliance 2795, Waters Corporation, USA) in acetonitrile:water (60:40 %v/v) at 200 μL/min. The capillary voltage of the mass spectrometer was at 3kV. The sample cone (de-clustering) voltage was set at 40V. For exact mass determination, the instrument was externally calibrated for the mass range m/z 100 to m/z 1000. A lock (reference) mass (m/z 556.2771) was used. Mass measurement accuracies of $<\pm 5$ ppm were obtained. R_f values are quoted for thin layer chromatography on silica gel Merck F-254 plates, unless otherwise stated. Flash column chromatography was carried out on Merck Kieselgel 60 (particle size 0.040-0.063mm), Aldrich aluminium oxide (activated, neutral, Brockmann I, 50 mesh) or Aldrich aluminium oxide (activated, acidic, Brockmann I, 50 mesh). Microwave experiments were carried out using the Discover CEM microwave synthesiser on standard power setting if otherwise stated. On standard power setting, the maximum power supplied is 300 watts.

X-ray crystallography data was collected using a Rigaku Saturn 724 and Bruker APEX DUO diffractometer at 90(2) and 100(2)K using Mo Kα and Cu Kα wavelength radiation (λ = 0.71073 and 1.54178 Å) respectively. Data was collected using CrystalClear and APEX2 software. Absorption corrections were performed using REQAB and SADABS respectively. Space group determinations, structure solutions and refinements were performed with Bruker SHELXTL and APEX2 software. All non-hydrogen atoms were refined anisotropically. Hydrogen atoms were assigned to calculated positions using a riding model with appropriately fixed isotropic thermal parameters.

8.1 General procedure for preparation of (*E*)-(2-nitrovinyl)benzene (1 – 34, 71 - 74)

To a solution of the appropriate benzaldehyde (3.6 mmol) in 4 mL glacial acetic acid was added nitromethane (7.2 mmol, 0.5 mL) followed by cyclohexylamine (3.6 mmol, 0.4 mL). The reaction mixture was heated under microwave irradiation at 120 °C for 30 min. After cooling, water (10 mL) was added to the reaction and it was allowed to stand. The precipitated nitroethene was isolated by filtration. The filtrate was further diluted with water (20 mL) and extracted with dichloromethane (3 x 10 mL). The organic phases were combined and washed with saturated aqueous $NaHCO_3$ (3 x 10 mL). The solution was dried over anhydrous Na_2SO_4, filtered and all solvent removed *in vacuo*, to give an oil which was purified by flash column chromatography over silica gel (eluent: dichloromethane / hexanes). The chromatographed and precipitated nitroethene fractions were combined and recrystallised from ethanol.

(*E*)-1-(4-Chlorophenyl)-2-nitroethene (1)

(*E*)-1-(4-Chlorophenyl)-2-nitroethene was prepared from 4-chlorobenzaldehyde (3.6 mmol, 0.5 g) according to general procedure 8.1. The product was purified by flash column chromatography over silica gel (eluent: 4:1 dichloromethane: hexane) and recrystallised from ethanol.
Yellow crystals 547 mg (83%)
Melting Point: 113-115 °C (lit. M.p. 112-112.5 °C[409])
IR$_{\nu max}$ (KBr): 3043 (CH), 1631 (C=C), 1520, 1341 (NO_2), 811 (C-Cl) cm^{-1}
^{1}H NMR (400 MHz, $CDCl_3$) δ 7.46 (d, 2 H, *J* = 8.5 Hz, H2'/H6'), 7.53 (d, 2 H, *J* = 8.5 Hz, H3'/H5'), 7.59 (d, 1 H, *J* = 13.6 Hz, H1), 7.98 (d, 1 H, *J* = 13.6 Hz, H2)
^{13}C NMR ($CDCl_3$) ppm 128.1 (C4'), 129.4, 129.9, 137.0 (C3'/C5'), 137.3 (C1), 137.9 (C2)
HRMS (APCI) calculated for $C_8H_6Cl^{35}NO_2$ [M^+] 183.0087: found 183.0083. Mass accuracy (-2.19 ppm).

(*E*)-4-(2-Nitrovinyl)phenol (2)

(*E*)-4-(2-Nitrovinyl)phenol was prepared from 4-hydroxybenzaldehyde (3.6 mmol, 0.440 g) according to general procedure 8.1. The product was purified by flash column chromatography over silica gel (eluent: dichloromethane) and recrystallised from methanol / H_2O (1:1).
Orange crystals 238 mg (40%)
Melting Point: 165°C (lit. M.p. 167-168 °C[185])
IR$_{\nu max}$ (ATR): 3349 (OH), 3106 (CH), 1599 (C=C), 1515, 1337 (NO_2) cm^{-1}
^{1}H NMR (400 MHz, $CDCl_3$) δ 5.52 (br.s., 1 H, -OH), 6.92 (d, 2 H, *J* = 8.52 Hz, 2x ArH), 7.59 (d, 2 H, *J* = 8.52 Hz, 2 x ArH), 7.54 (d, 1 H, *J* = 13.5 Hz, =CH), 7.99 (d, 1 H, *J* = 13.5 Hz, =CH)
^{13}C NMR ($CDCl_3$) ppm 116.0 (2C), 122.4, 131.0 (2C), 134.7, 138.5 (C2), 158.7 (C4')
HRMS (APCI) calculated for $C_8H_7NO_3$ [M^++H] 165.0426: found 165.0418. Mass accuracy (-4.85 ppm).

(*E*)-2-(2-Nitrovinyl)naphthalene (3)

(*E*)-2-(2-Nitrovinyl)naphthalene was prepared from 2-naphthaldehyde (3.6 mmol, 0.562 g) according to general procedure 8.1. and recrystallised from ethanol.

Yellow crystals 540 mg (75%)
Melting Point: 121-122 °C (lit. M.p. 122 °C[410])
IR$_{Vmax}$ (KBr): 3428 (CH), 1631 (C=C), 1506, 1334 (NO_2) cm^{-1}
^{1}H NMR (400 MHz, $CDCl_3$) δ 7.56-7.66 (m, 3 H, 3 x ArH), 7.72 (d, 1 H, *J* = 13.4 Hz, =CH), 7.86-7.95 (m, 3 H, 3 x ArH), 8.04 (s, 1 H, 1 x ArH), 8.18 (d, 1 H, *J* = 13.4 Hz, =CH)
^{13}C NMR ($CDCl_3$) ppm 122.9 (CH), 126.9 (CH), 127.1, 127.5 (CH), 128.0 (CH), 128.4 (CH), 128.9 (CH), 131.9 (CH), 132.7, 134.5, 136.7 (CH), 138.8 (C2)
HRMS (APCI) calculated for $C_{12}H_{10}NO_2$ [M^++H] 200.0712: found 200.0701. Mass accuracy (4.99 ppm).

(*E*)-1-Fluoro-4-(2-nitrovinyl)benzene (4)

(*E*)-1-Fluoro-4-(2-nitrovinyl)benzene was prepared from 4-fluorobenzaldehyde (3.6 mmol, 0.459 g) according to general procedure 8.1. and recrystallised from ethanol.
Yellow crystals 471 mg (78%)
Melting Point: 99-100 °C (lit. M.p. 100-101 °C[411])
IR$_{vmax}$ (KBr): 3113 (CH), 1637 (C=C), 1513, 1346 (NO_2) cm^{-1}
^{1}H NMR (400 MHz, $CDCl_3$) δ 7.12-7.20 (m, 2 H, 2 x ArH), 7.54-7.62 (m, 3 H, 2 x ArH & 1 x =CH), 7.99 (d, 1 H, *J* = 13.6 Hz, =CH)
^{13}C NMR ppm ($CDCl_3$) ppm 116.2, 116.4, 125.9, 130.8, 136.4, 137.5 (C2), 163.2 (C4'), 165.7 (C4')
HRMS (ESI) calculated for $C_8H_7FNO_2$ [M^++H] 168.0461: found 168.0461. Mass accuracy (0 ppm).

1,4-Bis((*E*)-2-nitrovinyl)benzene (5)

1,4-Bis((*E*)-2-nitrovinyl)benzene was prepared from terephthalaldehyde (3.6 mmol, 0.543 g) according to general procedure 8.1. and recrystallised from ethanol.
Orange crystals 622 mg (79%)
Melting Point: 229-231 °C (lit. M.p. 230-231 °C[412])
IR$_{vmax}$ (KBr): 2940 (CH), 1653 (C=C), 1532, 1326 (NO_2) cm^{-1}
^{1}H NMR (400 MHz, $CDCl_3$) δ 7.62-7.71 (m, 6 H, 4 x ArH & 2 x -CH), 8.02 (d, 2 H, *J* = 13.6 Hz, 2 x =CH)
^{13}C NMR ($CDCl_3$) ppm 129.4 (ArC), 132.9, 136.8, 138.1 (C2)
HRMS (ESI) calculated for $C_{10}H_7N_2O_4$ [M^+-H] 219.0400: found 219.0404. Mass accuracy (1.82 ppm).

(*E*)-1-(2-Nitrovinyl)naphthalene (6)

(*E*)-1-(2-Nitrovinyl)naphthalene was prepared from 1-napthylaldehyde (3.6 mmol) according to general procedure 8.1. and recrystallised from ethanol.
Yellow Crystals 580 mg (76%)
Melting Point: 82-83 °C (lit. M.p. 84 °C[413])
IR$_{vmax}$ (KBr): 3429 (CH), 1629 (C=C), 1512, 1341 (NO_2) cm^{-1}
^{1}H NMR (400 MHz, $CDCl_3$) δ 7.50-7.56 (m, 1 H, ArH), 7.58-7.70 (m, 3 H, 2 x ArH & 1 x =CH), 7.75 (d, 1 H, *J* = 7 Hz, 1 x ArH), 8.02 (d, 1 H, *J* = 7.5 Hz, 1 x ArH), 8.13 (d, 1 H, *J* = 8.5 Hz, 1 x ArH), 8.33 (d, 1 H, *J* = 13.5 Hz, =CH)

^{13}C NMR (101 MHz, $CDCl_3$) ppm 122.5, 125.0, 126.0, 126.4, 126.5, 127.3, 128.6, 131.1, 132.2, 133.3, 135.7, 138.0 (C2)
HRMS (APCI) calculated for $C_{10}H_{14}NO_2S$ [M^++H] 212.0745: found 212.0748. Mass accuracy (1.41 ppm).

(*E*)-9-(2-Nitrovinyl)anthracene (7)

(*E*)-9-(2-Nitrovinyl)anthracene was prepared from 9-anthraldehyde (3.6 mmol, 0.742 g) according to general procedure 8.1. The product was purified by flash column chromatography over silica gel (eluent: Toluene) and recrystallised from ethanol.
Red crystals 225 mg (25%)
Melting Point: 145-147 °C (lit. M.p. 142 °C[191])
IRν_{max} (KBr): 3050, 2948 (C-H), 1617, 1553 (C=C), 1498, 1330 (NO_2), 1250 (C-N) cm^{-1}
^{1}H NMR (400 MHz, $CDCl_3$) δ 7.40 - 7.66 (m, 5 H, 4 x ArH & CH= x 1), 7.80 - 8.05 (m, 2 H, 2 x ArH), 8.05 - 8.25 (m, 2 H, 2 x ArH), 8.45 (br. s., 1 H, H10), 8.90 (d, *J* = 13.43 Hz, 1 H, CH= x 1)
^{13}C NMR (101 MHz, $CDCl_3$) ppm 124.3 (C9) , 125.7 (CH) , 127.5 (CH) , 129.2 (CH) , 129.2, 129.8, 130.4 (CH) , 131.1, 135.6 (CH) , 142.6 (C2')
HRMS (APCI) calculated for $C_{16}H_{12}NO_2$ [M^++H] 250.0868: found 250.0879. Mass accuracy (-4.39 ppm).

(*E*)-1-(Benzyloxy)-3-(2-nitrovinyl)benzene (8)

(*E*)-1-(Benzyloxy)-3-(2-nitrovinyl)benzene was prepared from 3-benzyloxybenzaldehyde (3.6 mmol, 0.763 g) according to general procedure 8.1. The product was purified by flash column chromatography over silica gel (eluent: 3:1 dichloromethane: hexane) and recrystallised from ethanol.
Yellow crystals 756 mg (82%)
Melting Point: 90-92 °C (lit. M.p. 93 °C[414])
IRν_{max} (ATR): 3048, 3032 (C-H), 1633, 1581 (C=C), 1522, 1342 (NO_2), 1165 (C-N) cm^{-1}
^{1}H NMR (400 MHz, $CDCl_3$) δ 5.12 (s, 2 H, CH_2), 7.11 - 7.19 (m, 3 H, 3 x ArH), 7.35 - 7.50 (m, 6 H, 6 x ArH), 7.56 (d, *J* = 13.68 Hz, 1 H, H1'), 7.96 (d, *J* = 13.27 Hz, 1 H, H2')
^{13}C NMR (101 MHz, $CDCl_3$) ppm 70.1 (CH_2), 115.0 (CH), 118.7 (CH), 121.9 (CH), 127.4 (CH), 128.2 (CH), 128.6 (CH), 130.4 (CH), 131.3, 136.2, 137.3 (C1'), 138.9 (C2'), 159.2 (C1)
HRMS (APCI) calculated for $C_{15}H_{14}NO_3$ [M^++H] 256.0974: found 256.0972. Mass accuracy (-0.78 ppm).

(*E*)-4-Bromo-1-methoxy-2-(2-nitrovinyl)benzene (9)

(*E*)-4-Bromo-1-methoxy-2-(2-nitrovinyl)benzene was prepared from 5-bromo-2-methoxybenzaldehyde (3.6 mmol, 0.774 g) according to general procedure 8.1. The product was purified by flash column chromatography over silica gel (eluent: 3:1 dichloromethane: hexane) and recrystallised from ethanol.
Yellow crystals 795 mg (86%)
Melting Point: 121-122 °C (lit. M.p. 121-123 °C[415])
IRν_{max} (KBr): 3143 (CH), 1629 (C=C), 1486, 1335 (NO_2) cm^{-1}
^{1}H NMR (400 MHz, $CDCl_3$) δ 3.96 (s, 3 H, -CH_3), 6.95 (d, 1 H, *J* =8.5 Hz, H6), 7.45-7.53 (m, 2 H, =CH & H5), 7.74 (d, 1 H, *J* = 13.5 Hz, H3), 8.07 (d, 1 H, *J* =13.5 Hz, H2')

^{13}C NMR (101 MHz, $CDCl_3$) ppm 56.5 (CH_3), 112.1 (C6), 112.8 (C4), 123.7 (C2), 130.4 (C5), 133.6 (C3), 135.9 (C1'), 137.4 (C2'), 158.8 (C1)
HRMS (APCI) calculated for $C_9H_9NO_3Br^{79}$ [M^++H] 257.9766: found 257.9760. Mass accuracy (-2.33 ppm).

(*E*)-1-Methoxy-4-(2-nitrovinyl)benzene (10)

(*E*)-1-Methoxy-4-(2-nitrovinyl)benzene was prepared from 4-methoxybenzaldehyde (3.6 mmol, 0.489g) according to general procedure 8.1. The product was purified by flash column chromatography over silica gel (eluent: 3:1 dichloromethane: hexane) and recrystallised from ethanol.
Yellow crystals 453 mg (70%)
Melting Point: 85°C (lit. M.p. 86-87 °C[416])
IR$_{Vmax}$ (ATR): 3108 (CH), 1605 (C=C), 1517, 1343 (NO_2) cm^{-1}
^{1}H NMR (400 MHz, $CDCl_3$) δ 3.90 (s, 3 H, CH_3), 6.98 (d, 2 H, *J* = 9 Hz, 2 x ArH), 7.53 (d, 2 H, *J* = 9 Hz, 2 x ArH), 7.55 (d, 1 H, *J* = 13.5 Hz, =CH), 8.00 (d, 1 H, *J* = 13.5 Hz, =CH)
^{13}C NMR (101 MHz, $CDCl_3$) ppm 55.6 (CH_3), 114.9, 122.6, 131.2, 135.1, 139.1 (C2), 163.0 (C1')
HRMS (ESI) calculated for $C_9H_{10}NO_3$ [M^++H] 180.0661: found 180.0666. Mass accuracy (2.78 ppm).

(*E*)-2-(Benzyloxy)-1-methoxy-4-(2-nitrovinyl)benzene (11)

(*E*)-2-(Benzyloxy)-1-methoxy-4-(2-nitrovinyl)benzene was prepared from 3-benzyloxy-4-methoxybenzaldehyde (3.6 mmol, 0.871 g) according to general procedure 8.1. The product was purified by flash column chromatography over silica gel (eluent: 3:1 dichloromethane: hexane) and recrystallised from ethanol.
Yellow crystals 638 mg (62%)
Melting Point: 124-125 °C (lit. M.p. 125-126 °C[417])
IR$_{Vmax}$ (ATR): 3080, 3036 (C-H), 1622, 1593 (C=C), 1508, 1356 (NO_2), 1138 (C-N) cm^{-1}
^{1}H NMR (400 MHz, $CDCl_3$) δ 3.95 (s, 3 H, OCH_3), 5.18 (s, 2 H, CH_2), 6.94 (d, *J* = 8.29 Hz, 1 H, H5), 7.05 (d, *J* = 2.07 Hz, 1 H, H3), 7.18 (dd, *J* = 8.29, 2.07 Hz, 1 H, 1 x ArH), 7.30 - 7.48 (m, 6 H, 5 x ArH & H1'), 7.91 (d, *J* = 13.27 Hz, 1 H, H2')
^{13}C NMR (101 MHz, $CDCl_3$) ppm 56.1 (OCH_3), 71.1 (CH_2), 111.7 (CH), 113.2 (CH), 122.6, 124.9 (CH), 127.3 (CH), 128.2 (CH), 128.7 (CH), 135.1 (CH), 136.2, 139.2 (C2'), 148.6 (C2 / C1), 153.4 (C1 / C2)
HRMS (APCI) calculated for $C_{16}H_{16}NO_4$ [M^++H] 286.1079: found 286.1075. Mass accuracy (-1.40 ppm).

(*E*)-1,2,4-Trimethoxy-5-(2-nitrovinyl)benzene (12)

(*E*)-1,2,4-Trimethoxy-5-(2-nitrovinyl)benzene was prepared from 2-4-5 trimethoxybenzaldehyde (3.6 mmol, 0.706 g) according to general procedure 8.1. The product was purified by flash column chromatography over silica gel (eluent: 3:1 dichloromethane: hexane) and recrystallised from ethanol.
Orange crystals 414 mg (48%)
Melting Point: 127-128 °C (lit. M.p. 127-128 °C[418])
IR$_{Vmax}$ (KBr): 2942 (CH), 1607 (C=C), 1522, 1335 (NO_2) cm^{-1}

^{1}H NMR (400 MHz, $CDCl_3$) δ 3.90 (s, 3 H, CH_3), 3.97 (s, 3 H, -CH_3), 3.99 (s, 3 H, -CH_3), 6.55 (s, 1 H, ArH), 6.92 (s, 1 H, ArH), 7.80 (d, 1 H, *J* = 13.5 Hz, =CH), 8.17 (d, 1 H, *J* =13.5 Hz, =CH)
^{13}C NMR (101 MHz, $CDCl_3$) ppm 56.2 (OCH_3), 56.2 (OCH_3), 56.5 (OCH_3), 96.3, 110.4, 113.6, 135.4, 135.9 (C2), 143.4, 153.9 (C3'), 155.8 (C2')
HRMS (APCI) calculated for $C_{11}H_{14}NO_5$ [M^++H] 240.0866 found 240.0860. Mass accuracy (-2.50 ppm).

(*E*)-4-Methoxy-2-(2-nitrovinyl)phenol (13)

(*E*)-4-Methoxy-2-(2-nitrovinyl)phenol was prepared from 2-hydroxy-5-methoxybenzaldehyde (1 mmol, 0.15 g) according to general procedure general procedure 8.1. The product was purified by recrystallization from ethanol.
Brown solid 112.5 mg (58%)
Melting Point: 150-152 °C (lit. M.p. 153-153.5 °C[419])
IR$_{\nu max}$ (ATR): 3397 (OH), 3056, 2950 (C-H), 1612, 1584 (C=C), 1554, 1341 (NO_2), 1195 (C-N) cm^{-1}
^{1}H NMR (400 MHz, $CDCl_3$) δ 3.95 (s, 3 H, OCH_3), 6.86 - 7.06 (m, 3 H, 3 x ArH), 7.96 (d, *J* = 13.43 Hz, 1 H, H1'), 8.11 (d, *J* = 13.43 Hz, 1 H, H2')
^{13}C NMR (101 MHz, $CDCl_3$) ppm 56.3 (OCH_3), 113.4 (CH), 116.6, 120.2 (CH), 123.6 (CH), 135.0 (CH), 138.7 (C2'), 146.5 (C4 / C1), 146.8 (C4 / C1)
HRMS (ESI) calculated for $C_9H_8NO_4$ [M^+-H] 194.0459: found 194.0453. Mass accuracy (-3.09 ppm).

(*E*)-1-Chloro-3-(2-nitrovinyl)benzene (14)

(*E*)-1-Chloro-3-(2-nitrovinyl)benzene was prepared from 3-chlorobenzaldehyde (1 mmol, 0.14 g) according to general procedure general procedure 8.1. The product was purified by recrystallization from ethanol.
Yellow crystals 134 mg (73%)
Melting Point: 40-42 °C (lit. M.p. 48 °C[420])
IR$_{\nu max}$ (ATR): 3084, 3052 (C-H), 1635, 1594 (C=C), 1564, 1339 (NO_2), 1196 (C-N) cm^{-1}
^{1}H NMR (400 MHz, $CDCl_3$) δ 7.37 - 7.51 (m, 3 H, 3 x ArH), 7.52 - 7.61 (m, 2 H, H2 & H1'), 7.94 (d, *J* = 13.43 Hz, 1 H, H2')
^{13}C NMR (101 MHz, $CDCl_3$) ppm 127.2 (CH), 128.7 (CH), 130.6 (CH), 131.8, 131.9 (C2), 135.4, 137.4 (C1'), 138.1 (C2')
HRMS (APCI) calculated for $C_8H_7NO_2Cl^{35}$ [M^++H] 184.0165: found 184.0163. Mass accuracy (-1.09 ppm).

(*E*)-1-Methyl-4-(2-nitrovinyl)benzene (15)

(*E*)-1-Methyl-4-(2-nitrovinyl)benzene was prepared from *p*-tolualdehyde (3.6 mmol, 0.432 g) according to general procedure 8.1. The product was purified by flash column chromatography over silica gel (eluent: 3:1 dichloromethane: hexane) and recrystallised from ethanol.
Yellow crystals 460 mg (78%)
Melting Point: 101-103 °C (lit. M.p. 104.5-105 °C[421])
IRν_{max} (KBr): 2932 (CH), 1633 (C=C), 1517, 1339 (NO_2) cm^{-1}

^{1}H NMR (400 MHz, $CDCl_3$) δ 2.44 (s, 3 H, CH_3), 7.26-7.30 (m, 2 H, 2 x ArH), 7.47 (d, 2 H, J = 7 Hz, 2 x ArH), 7.60 (d, 1 H, J = 13.5 Hz, =CH), 8.02 (d, 1 H, J = 13.5 Hz, =CH)
^{13}C NMR (101 MHz, $CDCl_3$) ppm 21.3 (CH_3), 126.8, 128.8, 129.7, 135.8, 138.8 (C2), 142.7 (C1')
HRMS (APCI) calculated for $C_9H_{10}NO_2$ [M^++H] 164.0706: found 164.0703. Mass accuracy (-1.86 ppm).

(*E*)-2,4-Dimethoxy-1-(2-nitrovinyl)benzene (16)

(*E*)-2,4-Dimethoxy-1-(2-nitrovinyl)benzene was prepared from 2,4-dimethoxybenzaldehyde (3.6 mmol, 0.598 g) according to general procedure 8.1. The product was purified by flash column chromatography over silica gel (eluent: 3:1 dichloromethane: hexane) and recrystallised from ethanol.
Yellow crystals 529 mg (70%)
Melting Point: 104-107 °C (lit. M.p. 106-108 °C[422])
IRν_{max} (KBr): 2943 (CH), 1605 (C=C), 1564, 1327 (NO_2) cm^{-1}
^{1}H NMR (400 MHz, $CDCl_3$) δ 3.90 (s, 3 H, -CH_3), 3.96 (s, 3 H, -CH_3), 6.51 (d, 1 H, J = 2.2 Hz, H3'), 6.58 (dd, 1 H, J = 2.3 Hz, 8.5 Hz, ArH), 7.41 (d, 1 H, J = 8.8 Hz, ArH), 7.86 (d, 1 H, J = 13.5 Hz, =CH), 8.12 (d, 1 H, J = 13.5 Hz, =CH)
^{13}C NMR (101 MHz, $CDCl_3$) ppm 55.68 (OCH_3), 98.68 (C3'), 105.90 (C5'), 112.45, 134.44, 135.81, 136.07 (C2), 161.26 (C4' / C2'), 164.40 (C4' / C2')
HRMS (APCI) calculated for $C_{10}H_{12}NO_4$ [M^++H] 210.0766: found 210.0757. Mass accuracy (-4.28 ppm).

(*E*)-1,4-Dimethoxy-2-(2-nitrovinyl)benzene (17)

(*E*)-1,4-Dimethoxy-2-(2-nitrovinyl)benzene was prepared from 2,5 dimethoxybenzaldehyde (3.6 mmol, 0.598 g) according to general procedure 8.1. The product was purified by flash column chromatography over silica gel (eluent: 3:1 dichloromethane: hexane) and recrystallised from ethanol.
Yellow crystals 604 mg (80%)
Melting Point: 119-121 °C (lit. M.p. 121-123 °C[423])
IRν_{max} (KBr): 2966 (CH), 1618 (C=C), 1488, 1352 (NO_2) cm^{-1}
^{1}H NMR (400 MHz, $CDCl_3$) δ 3.83 (s, 3 H, CH_3), 3.93 (s, 3 H, -CH_3), 6.93 (d, 1 H, J = 9 Hz, ArH), 6.99 (d, 1 H, J = 3 Hz, ArH), 7.04 (dd, 1 H, J = 9 Hz, 3 Hz, ArH), 7.89 (d, 1 H, J = 13.5 Hz, =CH), 8.14 (d, 1 H, J = 13.5 Hz, =CH)
^{13}C NMR (101 MHz, $CDCl_3$) ppm 56.0 (OCH_3), 56.0 (OCH_3), 112.4, 116.3, 119.2, 119.5, 135.3, 138.5 (C2), 153.5 (C2' / C5), 153.9 (C2' / C5')
HRMS (APCI) calculated for $C_{10}H_{12}NO_4$ [M^++H] 210.0766: found 210.0756. Mass accuracy (-4.76 ppm).

(*E*)-1,2,3-Trimethoxy-5-(2-nitrovinyl)benzene (18)

(*E*)-1,2,3-Trimethoxy-5-(2-nitrovinyl)benzene was prepared from 3,4,5 trimethoxybenzaldehyde (3.6 mmol, 0.706g) according to general procedure 8.1. Recrystallised from ethanol.
Yellow crystals 518 mg (60%)
Melting Point: 120-122 °C (lit. M.p. 121-123 °C[216])
IRν_{max} (KBr): 2943 (CH), 1627 (C=C), 1510, 1339 (NO_2), 1129 (CO) cm^{-1}

^{1}H NMR (400 MHz, $CDCl_3$) δ 3.94 (s, 9 H, 3 x –OCH_3), 6.79 (s, 2 H, 2 x ArH), 7.57 (d, 1 H, *J* = 11.7 Hz, =CH), 7.96 (d, 1 H, *J* = 11.7 Hz, =CH)
^{13}C NMR (101 MHz, $CDCl_3$) ppm 55.8 (OCH_3), 60.6 (OCH_3), 105.9, 124.8, 135.9, 138.9 (C2), 141.3 (C2'), 153.2 (C1' & C3')
HRMS (ESI) calculated for $C_{11}H_{14}NO_5$ [M+H] 240.0866: found 240.0858. Mass accuracy (-3.66 ppm).

(*E*)-1-Ethoxy-2-(2-nitrovinyl)benzene (19)

(*E*)-1-Ethoxy-2-(2-nitrovinyl)benzene was prepared from 2-ethoxybenzaldehyde (3.6 mmol, 0.540 g) according to general procedure 8.1. The product was purified by flash column chromatography over silica gel (eluent: 3:1 dichloromethane: hexane) and recrystallised from ethanol.
Golden Brown crystals 467 mg (67%)
Melting Point: 34-35 °C (lit. M.p. 37-38 °C[424])
IRν_{max} (KBr): 2982 (CH), 1627 (C=C), 1574, 1338 (NO_2) cm^{-1}
^{1}H NMR (400 MHz, $CDCl_3$) δ 1.59 (t, 3 H, *J* = 7 Hz, -CH_3), 4.20 (q, 3 H, *J* = 7 Hz, -CH_2), 7.01 (m, 2 H, ArH), 7.43-7.50 (m, 2 H, 2 x ArH), 7.94 (d, 1 H, *J* = 13.6 Hz, =CH), 8.17 (d, 1 H, *J* = 13.6 Hz, =CH)
^{13}C NMR (101 MHz, $CDCl_3$) ppm 14.3 (CH_3), 63.9 (-OCH_2), 111.6, 120.5, 132.3, 133.0, 135.3, 137.8 (C2), 158.5 (C1')
HRMS (APCI) calculated for $C_{10}H_{12}NO_3$ [M^++H] 194.0812: found 194.0807. Mass accuracy (-2.42 ppm).

(*E*)-1-(2-Nitrovinyl)-4-phenoxybenzene (20)

(*E*)-1-(2-Nitrovinyl)-4-phenoxybenzene was prepared from 4-phenoxybenzaldehyde (3.6 mmol, 0.712 g) according to general procedure 8.1. The product was purified by flash column chromatography over silica gel (eluent: 3:1 dichloromethane: hexane) and recrystallised from ethanol.
Yellow crystals 609 mg (70%)
Melting Point: 100-102 °C (lit. M.p. 102 °C[425])
IRν_{max} (KBr): 3110 (CH), 1630 (C=C), 1510, 1342 (NO_2) cm^{-1}
^{1}H NMR (400 MHz, $CDCl_3$) δ 7.04 (d, 2 H, *J* = 9 Hz, ArH), 7.10 (d, 2 H, *J* = 7.5 Hz, ArH), 7.22-7.26 (m, 1 H, H4''), 7.40-7.46 (m, 2 H, H3''/H5''), 7.50-7.59 (m, 3 H, 2 x ArH, 1 x =CH), 8.00 (d, 1 H, *J* = 13.6 Hz, =CH)
^{13}C NMR (101 MHz, $CDCl_3$) ppm 117.9, 119.7, 123.9, 124.4, 129.7, 130.7, 135.4, 138.2 (C2), 154.8 (C4" / C4'), 160.9 (C4 / C4')
HRMS (APCI) calculated for $C_{14}H_{12}NO_3$ [M^++H] 242.0812: found 242.0805. Mass accuracy (-2.81 ppm).

(*E*)-(2-Nitrovinyl)benzene (21)

(*E*)-(2-Nitrovinyl)benzene was prepared from benzaldehyde (3.6 mmol, 0.381 g) according to general procedure 8.1. The product was recrystallised from ethanol.
Yellow crystals 432 mg (80%)
Melting Point: 53-54°C (lit. M.p. 55-56 °C[426])

IRν_{max} (KBr): 3110 (CH), 1632 (C=C), 1510, 1347 (NO_2) cm^{-1}
^{1}H NMR (400 MHz, $CDCl_3$) δ 7.47-7.54 (m, 3 H, 3 x ArH), 7.57-7.60 (m, 2 H, 2 x ArH), 7.62 (d, 1 H, *J* = 13.8 Hz, =CH), 8.04 (d, 1 H, *J* = 13.8 Hz, =CH)
^{13}C NMR (101 MHz, $CDCl_3$) ppm 129.2, 129.4, 130.1, 132.2, 137.2 (C1), 139.1 (C2)
HRMS (ESI) calculated for $C_8H_8NO_4$ [M^++H] 150.0550: found 150.0546. Mass accuracy (-2.37 ppm).

(*E*)-5-(2-Nitrovinyl)benzo[d][1,3]dioxole (22)

(*E*)-5-(2-Nitrovinyl)benzo[d][1,3]dioxole was prepared from piperonal (3.6 mmol, 0.540 g) according to general procedure 8.1. The product was purified by flash column chromatography over silica gel (eluent: 3:1 dichloromethane: hexane) and recrystallised from ethanol.
Yellow crystals 488 mg (70%)
Melting Point: 160-161 °C (lit. M.p. 161.5 °C[427])
IRν_{max} (KBr): 2920 (CH), 1626 (C=C), 1490, 1337 (-NO_2) cm^{-1}
^{1}H NMR (400 MHz, $CDCl_3$) δ 6.08 (s, 2 H, -OCH_2O-), 6.87-6.92 (m, 1 H, ArH), 7.03 (s, 1 H, H6'), 7.11 (m, 1 H, ArH), 7.49 (d, 1 H, *J* = 13.6 Hz, ArH, =CH), 7.95 (d, 1 H, *J* = 13.6 Hz, =CH)
^{13}C NMR (101 MHz, $CDCl_3$) ppm 101.6, 106.5, 108.6, 123.7, 126.2, 134.9, 138.7 (C2), 148.3 (C1' / C3'), 150.9 (C1' / C3')
HRMS (APCI) calculated for $C_9H_8NO_4$ [M^++H] 194.0448: found 194.0445. Mass accuracy (-1.26 ppm).

(*E*)-1,2-Dimethoxy-4-(2-nitrovinyl)benzene (23)

(*E*)-1,2-Dimethoxy-4-(2-nitrovinyl)benzene was prepared from 3,4-dimethoxybenzaldehyde (3.6 mmol, 0.598 g) according to general procedure 8.1. The product was purified by flash column chromatography over silica gel (eluent: 3:1 dichloromethane: hexane) and recrystallised from ethanol.
Yellow crystals 501 mg (40%)
Melting Point: 139-141 °C (lit. M.p. 140-141 °C[212])
IRν_{max} (KBr): 2971 (CH), 1627 (C=C), 1581, 1342 (NO_2) cm^{-1}
^{1}H NMR (400 MHz, $CDCl_3$) δ 3.95 (s, 6 H, 2 x OCH_3), 6.93 (d, 1 H, *J* = 8.5 Hz, H3'), 7.02 (d, 1 H, *J* = 2 Hz, 8.5 Hz, ArH), 7.55 (d, 1 H, *J* = 13.6 Hz, =CH), 7.98 (d, 1 H, *J* = 13.6 Hz, =CH)
^{13}C NMR (101 MHz, $CDCl_3$) ppm 55.56 (OCH_3), 55.66 (OCH_3), 109.71 (CH), 110.86 (CH), 122.34 (CH), 124.86, 134.71 (CH), 138.94 (CH), 149.08 (C2' / C1'), 152.35 (C2' / C1')
HRMS (ESI) calculated for $C_{10}H_{11}NO_4Na$ [M^++Na] 232.0586: found 232.0582. Mass accuracy (-1.72 ppm).

(*E*)-1-(Benzyloxy)-4-(2-nitrovinyl)benzene (24)

(*E*)-1-(Benzyloxy)-4-(2-nitrovinyl)benzene was prepared from 4-benzoxybenzaldehyde (3.6 mmol, 0.763 g) according to general procedure 8.1. The product was purified by flash column chromatography over silica gel (eluent: 3:1 dichloromethane: hexane) and recrystallised from ethanol.
Yellow crystals 368 mg (40%)
Melting Point: 120-121 °C (lit. M.p. 121-122 °C[428])
IRν_{max} (ATR): 3107, 3034 (C-H), 1630, 1592 (C=C), 1512, 1342 (NO_2), 1174 (C-N) cm^{-1}

^{1}H NMR (400 MHz, $CDCl_3$) δ 5.14 (s, 2 H, CH_2), 6.96 - 7.09 (m, 2 H, 2 x ArH), 7.30 - 7.47 (m, 5 H, 5 x ArH), 7.47 - 7.59 (m, 3 H, 2 x ArH & H1), 7.98 (d, J = 13.68 Hz, 1 H, H2)
^{13}C NMR (101 MHz, $CDCl_3$) ppm 70.2 (CH_2), 115.7 (CH), 122.7, 127.4 (CH), 128.3 (CH), 128.7 (CH), 131.1 (CH), 135.1 (CH), 135.9, 138.9 (C2), 162.0 (C4)
HRMS (APCI) calculated for $C_{15}H_{14}NO_3$ [M^++H] 256.0974: found 256.0971. Mass accuracy (-1.17 ppm).

(*E*)-2,4-Dichloro-1-(2-nitrovinyl)benzene (25)

(*E*)-2,4-Dichloro-1-(2-nitrovinyl)benzene was prepared from 2,4-dichlorobenzaldehyde (3.6 mmol, 0.630 g) according to general procedure 8.1. The product was purified by flash column chromatography over silica gel (eluent: 3:1 dichloromethane: hexane) and recrystallised from ethanol.
Yellow crystals 406 mg (52%)
Melting Point: 109-110°C (lit. M.p. 110 °C[429])
IRν_{max} (KBr): 3101 (CH), 1631 (C=C), 1585, 1338 (NO_2), 816 (C-Cl) cm^{-1}
^{1}H NMR (400 MHz, $CDCl_3$) δ 7.38 (dd, 1 H, J = 8.5 Hz, 2.3 Hz, ArH), 7.53-7.57 (m, 2 H, 2 x ArH), 7.60 (d, 1 H, J = 13.5 Hz, =CH), 8.38 (d, 1 H, J = 13.5 Hz, =CH)
^{13}C NMR (101 MHz, $CDCl_3$) ppm 127.1, 128.1, 129.3, 130.7, 134.0, 136.7, 138.5 (C1), 139.0 (C2)
HRMS (APCI) calculated for $C_8H_6NO_2Cl_2^{35}$ [M^++H] 217.9770: found 217.9766. Mass accuracy (-2.11 ppm).

(*E*)-3-(2-nitrovinyl)phenol (26)

(*E*)-3-(2-Nitrovinyl)phenol was prepared from 3-hydroxybenzaldehyde (3.6 mmol, 0.440 g) according to procedure 8.1. The product was purified by flash column chromatography over silica gel (eluent: dichloromethane: hexane 3/1).
Orange crystals 298 mg (50%)
Melting Point: 135-136 °C (lit. M.p. 136-137 °C[430])
IRν_{max} (KBr): 3376 (OH), 2919 (CH), 1633C=C), 1505, 1343 (NO_2) cm^{-1}
^{1}H NMR (400 MHz, $CDCl_3$) δ 5.21 (br.s., 1 H , -OH), 6.97-7.05 (m, 1 H, ArH), 7.14-7.17 (m, 1 H, ArH), 7.33-7.40 (m, 1 H, ArH), 7.58 (d, 1 H, J = 13.6 Hz, =CH), 7.98 (d, 1 H, J = 13.6 Hz, =CH)
^{13}C NMR (101 MHz, $CDCl_3$) ppm 110.8, 114.9, 118.9, 121.6, 126.4, 130.2, 131.1, 137.0 (C1), 138.4 (C2), 155.7 (C3')
HRMS (ESI) calculated for $C_8H_8NO_3$ [M^++H] 166.0504: found 166.0498. Mass accuracy (-3.61 ppm).

(*E*)-2-(2-Nitrovinyl)phenol (27)

(*E*)-2-(2-Nitrovinyl)phenol was prepared from 2-hydroxybenzaldehyde (3.6 mmol, 0.439 g) according to general procedure 8.1. The product was purified by flash column chromatography over silica gel (eluent: dichloromethane).
Orange crystals 203 mg (30%)
Melting Point: 130-131 °C (lit. M.p. 133 °C[431])
IRν_{max} (KBr): 3366 (OH), 3040 (CH), 1621 (C=C), 1557, 1333 (NO_2) cm^{-1}

^{1}H NMR (400 MHz, $CDCl_3$) δ 6.09 (br.s., 1 H, -OH), 6.89 (d, 1 H, *J* = 8 Hz, ArH), 7.03 (dd, 1 H, *J* = 7.5 Hz, ArH), 7.33-7.41 (m, 1 H, ArH), 7.45 (dd, 1 H, *J* = 6.52 Hz, 1 Hz, ArH), 7.99 (d, 1 H, *J* = 13.6 Hz, =CH), 8.16 (d, 1 H, *J* = 13.6 Hz, =CH)
^{13}C NMR (101 MHz, $CDCl_3$) ppm 116.0, 117.2, 121.1, 132.2, 132.8, 135.2 (C1), 138.1 (C2), 155.6 (C2')
HRMS (ESI) calculated for $C_8H_7NO_3Na$ [M^++Na] 188.0324: found 188.0318. Mass accuracy (-3.19 ppm).

(*E*)-1-Chloro-2-(2-nitrovinyl)benzene (28)

(*E*)-1-Chloro-2-(2-nitrovinyl)benzenewas prepared from 2-chlorobenzaldehyde (1 mmol, 0.14 g) according to general procedure general procedure 8.1.
Yellow resin 154 mg (84%)
Melting Point: N/A (lit. M.p. 40 °C[420])
IR$_{\nu max}$ (ATR): 3061, 2925 (C-H), 1629, 1588 (C=C), 1522, 1333 (NO_2), 1158 (C-N stretch) cm^{-1}
^{1}H NMR (400 MHz, $CDCl_3$) δ 7.32 - 7.39 (m, 1 H, 1 x ArH), 7.40 - 7.48 (m, 1 H, 1 x ArH), 7.48 - 7.54 (m, 1 H, 1 x ArH), 7.57 - 7.66 (m, 2 H, 1 x ArH & H1'), 8.40 (d, *J* = 14.05 Hz, 1 H, H2')
^{13}C NMR (101 MHz, $CDCl_3$) ppm 127.4 (CH), 128.4, 128.5 (CH), 130.7 (CH), 132.8 (CH), 135.1 (C1'), 136.0, 138.7 (C2')
HRMS (APCI) calculated for $C_8H_7NO_2Cl$ [M^++H] 184.0165: found 184.0163. Mass accuracy (-1.09 ppm).

(*E*)-1-Bromo-4-(2-nitrovinyl)benzene (29)

(*E*)-1-Bromo-4-(2-nitrovinyl)benzene was prepared from 4-bromobenzaldehyde (1 mmol, 0.18 g) according to general procedure general procedure 8.1. The product was purified by recrystallization from ethanol.
Yellow solid 156 mg (69%)
Melting Point: 150-151 °C (lit. M.p. 151-153 °C[432])
IR$_{\nu max}$ (ATR): 3050, 2855 (C-H), 1602, 1574 (C=C), 1550, 1351 (NO_2), 1186 (C-N) cm^{-1}
^{1}H NMR (400 MHz, $CDCl_3$) δ 7.42 (d, *J* = 8.53 Hz, 2H, 2 x ArH), 7.54 - 7.67 (m, 3H, 1 x =CH & 2 x ArH), 7.95 (d, *J* = 13.55 Hz, 1H, HC=)
^{13}C NMR (101 MHz, $CDCl_3$) ppm 126.7, 128.9, 130.4 (CH), 132.7 (CH), 137.4 (C1), 137.8 (C2)
HRMS (ESI) calculated for $C_8H_7Br^{79}NO_4$ [M^++H] 227.9660: found 227.9660. Mass accuracy (0 ppm).

(*E*)-1-Ethoxy-4-(2-nitrovinyl)benzene (30)

(*E*)-1-Ethoxy-4-(2-nitrovinyl)benzene was prepared from 4-ethoxybenzaldehyde (1 mmol, 0.15 g) according to general procedure general procedure 8.1. The product was purified by recrystallization from ethanol.
Tan crystals 112 mg (58%)
Melting Point: 114-116 °C (lit. M.p. 114-115 °C[433])
IR$_{\nu max}$ (ATR): 3010 (C-H), 1632, 1580 (C=C), 1551, 1354 (NO_2), 1180 (C-N) cm^{-1}

^{1}H NMR (400 MHz, $CDCl_3$) δ 1.46 (t, *J* = 6.78 Hz, 3H, CH_3), 4.10 (q, *J* = 7.03 Hz, 2H, CH_2), 6.95 (d, *J* = 9.03 Hz, 2H, 2 x ArH), 7.45 - 7.58 (m, 3H, 1 = =CH, 2 x ArH), 7.99 (d, *J* = 13.55 Hz, 1H, =CH)
^{13}C NMR (101 MHz, $CDCl_3$) ppm 14.6 (CH_3), 63.9 (CH_2), 115.3 (C3' & C5'), 122.3, 131.2 (C2' & C6'), 134.9, 139.2 (C2), 162.4 (C4')
HRMS (ESI) calculated for $C_{10}H_{12}NO_3$ [M^++H] 194.0817: found 194.0820. Mass accuracy (1.55 ppm).

(*E*)-2-Methoxy-6-(2-nitrovinyl)phenol (31)

(*E*)-2-Methoxy-6-(2-nitrovinyl)phenol was prepared from 2-hydroxy-3-methoxybenzaldehyde (1 mmol, 0.15 g) according to general procedure general procedure 8.1. The product was purified by recrystallization from ethanol.
Brown crystals 290 mg (29%)
Melting Point: 125-127 °C (lit. M.p. 128-129 °C[419])
IR$_{\nu max}$ (ATR): 3350 (OH), 3098 (CH), 1580 (C=C), 1545, 1350 (NO_2) cm^{-1}
^{1}H NMR (400 MHz, $CDCl_3$) δ 3.95 (s, 3H, OCH_3), 6.50 (s, 1H, OH), 6.91 - 7.05 (m, 3H, 3 x ArH), 7.97 (d, *J* = 13.55 Hz, 1H, =CH), 8.11 (d, *J* = 13.55 Hz, 1H, =CH)
^{13}C NMR (101 MHz, $CDCl_3$) ppm 56.0 (OCH_3), 113.0, 116.2, 119.9, 123.3, 134.7 (C1), 138.5 (C2), 162.8 (C1')
HRMS (ESI) calculated for $C_9H_{10}NO_4$ [M^++H] 196.0610: found 196.0611. Mass accuracy (0.51 ppm).

(*E*)-2-Bromo-1-methoxy-4-(2-nitrovinyl)benzene (32)

(*E*)-2-Bromo-1-methoxy-4-(2-nitrovinyl)benzene was prepared from 3-bromo-4-methoxybenzaldehyde (1 mmol, 0.22 g) according to general procedure general procedure 8.1. The product was purified by recrystallization from ethanol.
Yellow crystals 391 mg (39%)
Melting Point: 109-111 °C (lit. M.p. 108-109 °C[414])
IR$_{\nu max}$ (ATR): 3088, 3054 (CH), 1598 (C=C), 1555, 1353 (NO_2) cm^{-1}
^{1}H NMR (400 MHz, $CDCl_3$) δ 3.92 - 4.05 (m, 3 H, OCH_3), 6.96 (d, *J* = 8.53 Hz, 1 H, 1 x ArH), 7.44 - 7.61 (m, 2 H, 1 x ArH, 1 x =CH), 7.77 (d, *J* = 2.01 Hz, 1 H, 1 x ArH), 7.91 (d, *J* = 13.55 Hz, 1 H, 1 x =CH)
^{13}C NMR (101 MHz, $CDCl_3$) ppm 56.5 (OCH_3), 112.1, 112.8, 123.7, 130.4, 133.6, 135.9 (C1), 137.5 (C2), 158.9 (C4')
HRMS (ESI) calculated for $C_9H_9Br^{79}NO_3$ [M^++H] 257.9766: found 257.9778. Mass accuracy (4.65 ppm).

(*E*)-2-Methoxy-5-(2-nitrovinyl)phenol (33)

(*E*)-2-Methoxy-5-(2-nitrovinyl)phenol was prepared from 3-hydroxy-4-methoxybenzaldehyde (1 mmol, 0.15 g) according to general procedure general procedure 8.1. The product was purified by recrystallization from ethanol.
Orange crystals 622 mg (62%)
Melting Point: 157-160 °C (lit. M.p. 158-161 °C[161])
IR$_{\nu max}$ (ATR): 3347 (OH), 3091 (CH), 1578 (C=C), 1542, 1349 (NO_2) cm^{-1}

^{1}H NMR (400 MHz, $CDCl_3$) δ 3.99 (s, 3 H, OCH_3), 5.76 (br. s., 1 H, OH), 6.92 (d, *J* = 8.03 Hz, 1 H, 1 x ArH), 7.09 - 7.18 (m, 2 H, 2 x ArH), 7.51 (d, *J* = 13.55 Hz, 1 H, =CH), 7.95 (d, *J* = 13.55 Hz, 1 H, =CH)
^{13}C NMR (101 MHz, $CDCl_3$) ppm 56.1 (OCH_3), 110.8, 113.6, 123.4, 123.8, 135.5 (C1), 139.2 (C2), 150.0 (C4')
HRMS (ESI) calculated for $C_9H_{10}NO_4$ [M^++H] 196.0610: found 196.0611. Mass accuracy (0.51 ppm).

(*E*)-1-Nitro-3-(2-nitrovinyl)benzene (34)

(*E*)-1-Nitro-3-(2-nitrovinyl)benzene was prepared from 3-nitrobenzaldehyde (1 mmol, 0.15 g) according to general procedure general procedure 8.1. The product was purified by recrystallization from ethanol.
Yellow crystals 333 mg (33%)
Melting Point: 120-123 °C (lit. M.p. 123-124 °C[434])
IR$_{\nu max}$ (ATR): 3087 (CH), 1582 (C=C), 1551, 1346 (NO_2) cm^{-1}
^{1}H NMR (400 MHz, $CDCl_3$) δ 7.65 (d, *J* = 13.55 Hz, 1 H, =CH), 7.70 - 7.81 (m, 2 H, 2 x ArH), 8.05 (d, *J* = 13.55 Hz, 1 H, =CH), 8.30 - 8.36 (m, 2 H, 2 x ArH)
^{13}C NMR (101 MHz, $CDCl_3$) ppm 124.6, 126.4, 129.8, 136.0, 136.1, 139.9 (C2), 149.5 (C1')
HRMS (ESI) calculated for $C_8H_7N_2O_4$ [M^++H] 195.0406: found 195.0408. Mass accuracy (1.03 ppm).

(*E*)-3-(2-Nitrovinyl)furan (71)

(*E*)-3-(2-Nitrovinyl)furan was prepared from 3-furaldehyde (3.6 mmol, 0.346 g) according to general procedure 8.1. The product was purified by flash column chromatography over silica gel (eluent: dichloromethane: hexane 3/1).
Golden brown crystals 378 mg (75%)
Melting Point: 100-101 °C (lit. M.p. 101-103 °C[435])
IR ν_{max} (KBr): 3104 (CH), 1638 (C=C), 1520, 1359 (NO_2) cm^{-1}
^{1}H NMR (400 MHz, $CDCl_3$) δ ppm 6.60 (s, 1 H, 1 x ArH), 7.41 (d, 1 H, *J* = 13.5 Hz, =CH), 7.54 (s, 1 H, 1 x ArH), 7.86 (s, 1 H, 1 x ArH), 7.96 (d, 1 H, *J* = 13.5 Hz, =CH)
^{13}C NMR (101 MHz, $CDCl_3$) ppm 106.8, 117.8, 129.1, 136.2, 144.9 (C2 / C5'), 146.9 (C2 / C5')
HRMS (ESI) calculated for $C_6H_6NO_3$ [M^++H] 140.0342: found 140.0338. Mass accuracy (-2.86 ppm).

(*E*)-3-(2-Nitrovinyl)thiophene (72)

(*E*)-3-(2-Nitrovinyl)thiophene was prepared from 3-thiophenealdehyde (3.6 mmol, 0.346 g) according to general procedure 8.1. The product was purified by flash column chromatography over silica gel (eluent: dichloromethane: hexane 3/1).
Golden brown crystals 564 mg (74%)
Melting Point: 96 °C (lit. M.p. 96-97 °C[436])
IRν_{max} (KBr): 3104 (CH), 1628 (C=C), 1528, 1338 (NO_2) cm^{-1}
^{1}H NMR (400 MHz, $CDCl_3$) δ 7.29 (d, 1 H, *J* = 5 Hz, H5'), 7.45 (dd, 1 H, *J* = 5 Hz, 3 Hz, H4'), 7.51 (d, 1 H, *J* = 13.5 Hz, =CH), 7.75 (d, 1 H, *J* = 2 Hz, H2'), 8.04 (d, 1 H, *J* = 13.5 Hz, =CH)

^{13}C NMR ppm ($CDCl_3$) ppm 124.6, 127.7, 131.8, 132.0, 132.1 (C1), 136.3 (C2)
HRMS (APCI) calculated for $C_{10}H_{14}NO_2S$ [M^++H] 212.0745: found 212.0748. Mass accuracy (1.41 ppm).

(*E*)-2-(2-Nitrovinyl)thiophene (73)

(*E*)-2-(2-Nitrovinyl)thiophene was prepared from 2-thiophenecarboxaldehyde (3.6 mmol, 0.404 g) according to general procedure 8.1. The product was purified by flash column chromatography over silica gel (eluent: dichloromethane: hexane 3/1).
Brown crystals 679 mg (89%)
Melting Point: 78-80 °C (lit. M.p. 80 °C[410])
IR ν_{max} (KBr): 3092 (CH), 1622 (C=C), 1524, 1329 (NO_2) cm^{-1}
^{1}H NMR (400 MHz, $CDCl_3$) δ 7.17 (dd, 1 H, *J* = 5 Hz, 1.2 Hz, H4'), 7.47 (d, 1 H, *J* = 5 Hz, H5' / H3'), 7.49 (d, 1 H, *J* = 13.5 Hz, =CH), 7.58 (d, 1 H, *J* = 5 Hz, H3' / H5'), 8.17 (d, 1 H, *J* = 13.5 Hz, =CH)
^{13}C NMR ppm ($CDCl_3$) ppm 128.9, 131.7, 132.1, 133.8, 134.7 (C1), 135.4 (C2)
HRMS (ESI) calculated for $C_6H_6NO_2S$ [M^++H] 156.0119: found 156.0116. Mass accuracy (-1.92 ppm).

(*E*)-2-Methyl-5-(2-nitrovinyl)thiophene (74)

(*E*)-2-Methyl-5-(2-nitrovinyl)thiophene was prepared from 5-methyl-2-thiophenecarboxaldehyde (3.6 mmol, 0.404 g) according to general procedure 8.1. The product was purified by flash column chromatography over silica gel (eluent: dichloromethane: hexane 3/1).
Red crystals 306 mg (50%)
Melting Point: 77-79 °C (lit. M.p. 79-81 °C[437])
IRν_{max} (KBr); 3104 (CH), 1628 (C=C), 1528, 1338 (NO_2) cm^{-1}
^{1}H NMR (400 MHz, $CDCl_3$) δ 2.57 (s, 3 H, -CH_3), 6.83 (m, 1 H, H3'), 7.30 (d, 1 H, *J* = 3.3 Hz, H4'), 7.39 (d, 1 H, *J* = 13.3 Hz, =CH), 8.09 (d, 1 H, *J* = 13.3 Hz, =CH)
^{13}C NMR (101 MHz, $CDCl_3$) ppm 16.0 (CH_3), 127.5, 131.8, 132.6, 134.2, 135.8 (C2), 147.9 (C2')
HRMS (APCI) calculated for $C_7H_8NO_2S$ [M^++H] 170.0276: found 170.0268. Mass accuracy (-4.71 ppm).

8.2 General procedure for synthesis of (*E*)-(2-Nitroprop-1-en-1-yl)benzenes (35 - 59,75 – 78)

To a solution of the appropriate benzaldehyde (3.6 mmol) in 4 mL glacial acetic acid was added nitroethane (7.2 mmol) followed by cyclohexylamine (3.6 mmol, 0.4 mL). The reaction mixture was heated under microwave irradiation at 120 °C for 30 min. After cooling, water (10 mL) was added to the reaction and it was allowed to stand. The precipitated nitroethene was isolated by filtration. The filtrate was further diluted with water (20 mL) and extracted with dichloromethane (3 x 10 mL). The organic phases were combined and washed with saturated aqueous $NaHCO_3$ (3 x 10 mL). The solution was dried over anhydrous Na_2SO_4, filtered and all solvent removed *in vacuo*, to give an oil which was purified by flash column chromatography over silica gel (eluent: dichloromethane / hexanes). The chromatographed and precipitated nitroethene fractions were combined and recrystallised from ethanol.

(*E*)-1-Chloro-4-(2-nitroprop-1-en-1-yl)benzene (35)

(*E*)-1-Chloro-4-(2-nitroprop-1-en-1-yl)benzene was prepared from 4-chlorobenzaldehyde (3.6 mmol, 0.505 g) according to general procedure 8.2. The product was purified by flash column chromatography over silica gel (eluent: 3:1 dichloromethane/hexane) and recrystallised from ethanol.
Yellow crystals 486 mg (64%)
Melting Point: 82-83 °C (lit. M.p. 85 °C[438])
IRν_{max} (KBr): 3053 (CH), 1641 (C=C), 1526, 1353 (NO_2), 831 (C-Cl) cm^{-1}
^{1}H NMR (400 MHz, $CDCl_3$) δ 2.44 (s, 3 H, CH_3), 7.38 (d, 2 H, J = 9 Hz, 2 x ArH), 7.43 (d, 2 H, J = 9 Hz, 2 x ArH), 8.03 (s, 1 H, H1)
^{13}C NMR (101 MHz, $CDCl_3$) ppm 13.6 (C3), 128.8, 130.4, 131.8, 131.8, 135.6 (C1), 147.6 (C2)
HRMS (ESI) calculated for $C_9H_9Cl^{35}NO_2$ [M^++H] 198.0322: found 198.0314. Mass accuracy (-4.04 ppm).

(*E*)-4-(2-Nitroprop-1-en-1-yl)phenol (36)

(*E*)-4-(2-Nitroprop-1-en-1-yl)phenol was prepared from 4-hydroxybenzaldehyde (3.6 mmol, 0.440 g) according to general procedure 8.2. The product was purified by flash column chromatography over silica gel (eluent: dichloromethane / hexane 3/2).
Orange crystals 52 mg (8%)
Melting Point: 124-125 °C (lit. M.p. 125-125.5 °C[185])
IRν_{max} (KBr): 3381 (OH), 2917 (CH), 1602 (C=C), 1521, 1362 (NO_2) cm^{-1}
^{1}H NMR (400 MHz, $CDCl_3$) δ 2.50 (s, 3 H, CH_3), 5.56 (br.s., 1 H, OH), 6.95 (d, 2 H, J = 8.52 Hz, 2 x ArH), 7.40 (d, 2 H, J = 8.52 Hz, 2 x ArH), 8.09 (s, 1 H, H1)
^{13}C NMR (101 MHz, $CDCl_3$) ppm 13.70 (C3), 115.60 (CH), 124.42, 131.90 (CH), 133.31 (C1), 145.29 (C2), 156.95 (C4')
HRMS (ESI) calculated for $C_9H_{10}NO_3$ [M^++H] 180.0661: found 180.0658. Mass accuracy (-1.67 ppm).

(*E*)-2-(2-Nitroprop-1-en-1-yl)naphthalene (37)

(*E*)-2-(2-Nitroprop-1-en-1-yl)naphthalene was prepared from 2-naphthaldehyde (3.6 mmol, 0.562 g) according to general procedure 8.2. and recrystallised from ethanol.
Yellow crystals 460 mg (60%)
Melting Point: 96-97 °C (lit. M.p. 97-98 °C[439])
IRν_{max} (KBr): 3061 (-CH), 1652 (C=C), 1515, 1316 (-NO_2) cm^{-1}
^{1}H NMR (400 MHz, $CDCl_3$) δ 2.57 (s, 3 H, CH_3), 7.50-7.66 (m, 3 H, 3 x ArH), 7.85-7.99 (m, 4 H, 4 x ArH), 8.28 (s, 1 H, =CH)
^{13}C NMR (101 MHz, $CDCl_3$) ppm 13.8 (C3), 126.0, 126.5, 127.2, 127.4, 128.1, 128.2, 129.4, 130.2, 132.6, 133.2, 133.4 (C1), 147.3 (C2)
HRMS (APCI) calculated for $C_{13}H_{11}NO_2$ [M^-] 213.0784: found 213.0779. Mass accuracy (-2.35 ppm).

(*E*)-1-Fluoro-4-(2-nitroprop-1-en-1-yl)benzene (38)

(*E*)-1-Fluoro-4-(2-nitroprop-1-en-1-yl)benzene was prepared from 4-fluorobenzaldehyde (3.6 mmol, 0.459 g) according to general procedure 8.2. and recrystallised from ethanol.
Yellow crystals 324 mg (50%)
Melting Point: 61-62 °C (lit. M.p. 61-63 °C[439])
IRν_{max} (KBr): 3079 (CH), 1653 (C=C), 1518, 1354 (NO_2) cm^{-1}
^{1}H NMR (400 MHz, $CDCl_3$) δ 2.46 (s, 3 H, CH_3), 7.12-7.22 (m, 2 H, 2 x ArH), 7.40-7.50 (m, 2 H, 2 x ArH), 8.07 (s, 1 H, =CH)
^{13}C NMR (101 MHz, $CDCl_3$) ppm 13.5 (C3), 115.6, 115.8, 128.0, 131.6, 132.03 (C1), 147.0 (C2), 161.7 (CF), 164.2 (CF)
HRMS (ESI) calculated for $C_9H_7FNO_2$ [M^+–H] 180.0455: found 180.0459. Mass accuracy (2.22 ppm).

1,4-Bis((*E*)-2-nitroprop-1-en-1-yl)benzene (39)

1,4-Bis((*E*)-2-nitroprop-1-en-1-yl)benzene was prepared from terephthalaldehyde (3.6 mmol, 0.543 g) according to general procedure 8.2. and recrystallised from ethanol.
Orange crystals 585 mg (60%)
Melting Point: 120-121 °C (lit. M.p. 122-123 °C[412])
IRν_{max} (KBr): 2938 (CH), 1651 (C=C), 1519, 1316 (NO_2) cm^{-1}
^{1}H NMR (400 MHz, $CDCl_3$) δ 2.51 (s, 6 H, 2 x –CH_3), 7.54-7.62 (m, 4 H, 4 x ArH), 8.10 (s, 2 H, 2 x =CH)
^{13}C NMR (101 MHz, $CDCl_3$) ppm 13.7 (2 x -CH_3), 129.9, 131.8, 133.4 (C1), 148.3 (C2)
HRMS (ESI) calculated for $C_{12}H_{12}N_2O_4Na$ [M^++Na] 271.0695: found 271.0685. Mass accuracy (-3.69 ppm).

(*E*)-1-(2-nitroprop-1-en-1-yl)naphthalene (40)

(*E*)-1-(2-nitroprop-1-en-1-yl)naphthalene was prepared from 1-naphthaldehyde (3.6 mmol, 0.550g) according to general procedure 8.2. The product was purified by flash column chromatography over silica gel (eluent: dichloromethane / hexane 3/1).
Yellow resin 423 mg (55%)
Melting Point: N/A (lit. M.p. 65-67 °C[426])
IRν_{max} (KBr): 3060 (CH), 1659 (C=C), 1520, 1324 (NO_2) cm^{-1}
^{1}H NMR (400 MHz, $CDCl_3$) δ 2.39 (s, 3 H, -CH_3), 7.46 (d, 1 H, J = 7 Hz, ArH), 7.52-7.58 (m, 1 H, H3'), 7.59-7.66 (m, 2 H, 2 x ArH), 7.90-7.99 (m, 3 H, 3 x ArH), 8.66 (s, 1 H, H1)
^{13}C NMR (101 MHz, $CDCl_3$) ppm 13.8 (C3), 123.7, 124.7, 126.2, 126.7, 126.8, 128.4, 129.3, 129.8, 131.0, 131.5, 133.0 (C1), 148.8 (C2)
HRMS (ESI) calculated for $C_{13}H_{12}NO_2$ [M^++H] 214.0868: found 214.0860. Mass accuracy (-3.74 ppm).

(*E*)-9-(2-Nitroprop-1-en-1-yl)anthracene (41)

(*E*)-9-(2-Nitroprop-1-en-1-yl)anthracene was prepared from 9-anthraldehyde (3.6 mmol, 0.742 g) using according to general procedure 8.2. The product was purified by flash column chromatography over silica gel (eluent: toluene) and recrystallised from ethanol.
Orange crystals 95 mg (10%)
Melting Point: 141-142 °C (lit. M.p. 142-143 °C[440])

IRν_{max} (KBr): 3052, 2825 (C-H), 1510, 1326 (NO_2), 1622.16, 1442.74 (C=C), 1483 (C=C), 385 (CH_3) cm^{-1}
^{1}H NMR (400 MHz, $CDCl_3$) δ 1.98 (s, 1 H, CH_3), 7.42 - 7.63 (m, 4 H, 4 x ArH), 7.86 (d, *J* = 7.93 Hz, 2 H, 2 x ArH), 7.93 - 8.12 (m, 2 H, 2 x ArH), 8.48 (s, 1 H, H10), 8.71 (s, 1 H, H1')
^{13}C NMR (101 MHz, $CDCl_3$) ppm 14.4 (C3'), 124.8 (C9), 125.5 (CH), 126.7, 128.6, 128.8 (CH), 129.0 (CH), 131.0, 131.3 (CH), 151.0 (C2')
HRMS (ESI) calculated for $C_{17}H_{14}NO_2$ [M^++H] 264.1025: found 264.1035. Mass accuracy (3.78 ppm).

(*E*)-1-(Benzyloxy)-3-(2-nitroprop-1-en-1-yl)benzene (42) [441]

(*E*)-1-(Benzyloxy)-3-(2-nitroprop-1-en-1-yl)benzene was prepared from 3-benzyloxybenzaldehyde (3.6 mmol, 0.713 g) according to general procedure 8.2. The product was purified by flash column chromatography over silica gel (eluent: 3:1 dichloromethane / hexane) and recrystallised from ethanol.
Yellow crystals (60%)
Melting Point: 68-71 °C
IRν_{max} (KBr): 3034 (CH), 1657 (C=C), 1513, 1325 (NO_2) cm^{-1}
^{1}H NMR (400 MHz, $CDCl_3$) δ 2.42 (s, 3 H, CH_3), 5.14 (s, 2 H, -CH_2-), 7.01-7.10 (m, 3H, 3 x ArH), 7.36-7.50 (m, 6 H, 6 x ArH), 8.07 (s, 1 H, H1)
^{13}C NMR (101 MHz, $CDCl_3$) ppm 13.6 (C3), 69.7 (CH_2), 115.8, 116.0, 122.2, 126.9, 127.8, 128.29, 129.6, 132.9, 133.3, 136.0 (C1), 147.5 (C2), 158.4 (C3')
HRMS (APCI) calculated for $C_{16}H_{16}NO_3$ [M^++H] 270.1125: found 270.1119. Mass accuracy (-2.07 ppm).

(*E*)-2-(Benzyloxy)-1-methoxy-4-(2-nitroprop-1-en-1-yl)benzene (43)

(*E*)-2-(Benzyloxy)-1-methoxy-4-(2-nitroprop-1-en-1-yl)benzene was prepared from 3-benzyloxy4-methoxybenzaldehyde (3.6 mmol, 0.871 g) according to general procedure 8.2. The product was purified by flash column chromatography over silica gel (eluent: 3:1 dichloromethane / hexane) and recrystallised from ethanol.
Yellow crystals (35%)
Melting Point: 102-103 °C (lit. M.p. 101-103 °C[442])
IRν_{max} (ATR): 3084, 3065 (C-H), 1642, 1594 (C=C), 1517, 1365 (NO_2), 1137 (C-N) cm^{-1}
^{1}H NMR (400 MHz, $CDCl_3$) δ 2.30 (d, *J* = 0.83 Hz, 3 H, CH_3), 3.96 (s, 3 H, OCH_3), 5.21 (s, 2 H, CH_2), 6.93 - 6.99 (m, 2 H, 2 x ArH), 7.08 (dd, *J* = 8.29, 2.07 Hz, 1 H, 1 x ArH), 7.28 - 7.49 (m, 5 H, 5 x ArH), 7.99 (s, 1 H, H1')
^{13}C NMR (101 MHz, $CDCl_3$) ppm 13.9 (CH_3), 56.0 (OCH_3), 71.2 (CH_2), 111.6 (CH), 115.7 (CH), 124.8 (CH), 127.1 (CH), 128.1 (CH), 128.7 (CH), 133.7 (C1'), 136.6, 145.8 (C2'), 147.9 (C1 / C2), 151.4 (C1 / C2)
HRMS (APCI) calculated for $C_{15}H_{14}NO_3$ [M^++H] 300.1236: found 300.1231. Mass accuracy (-1.66 ppm).

(*E*)-1,2,4-Trimethoxy-5-(2-nitroprop-1-en-1-yl)benzene (44)

(*E*)-1,2,4-Trimethoxy-5-(2-nitroprop-1-en-1-yl)benzene was prepared from 2-4-5 trimethoxybenzaldehyde (3.6 mmol, 0.706 g) according to general procedure 8.2. The product

was purified by flash column chromatography over silica gel (eluent: 3:1 dichloromethane / hexane) and recrystallised from ethanol.
Orange crystals 228 mg (25%)
Melting Point: 100-103 °C (lit. M.p. 100-101.5 °C[443])
IRν_{max} (KBr): 2942 (CH), 1606 (C=C), 1508, 1343 (NO_2) cm^{-1}
^{1}H NMR (400 MHz, $CDCl_3$) δ 3.88 (s, 3 H, OCH_3), 3.91 (s, 3 H, OCH_3), 3.98 (s, 3 H, OCH_3), 6.56 (s, 1 H, ArH), 6.90 (s, 1 H, ArH), 8.35 (s, 1 H, H1)
^{13}C NMR (101 MHz, $CDCl_3$) ppm 13.9 (C3), 55.7 (OCH_3), 55.9 (OCH_3), 56.3 (OCH_3), 96.1 (C3'), 112.7, 129.2, 142.4, 145.1 (C2), 151.7 (C4'), 153.6 (C1' & C2')
HRMS (APCI) calculated for $C_{12}H_{15}NO_5$ [M^+] 253.0945: found 253.0941. Mass accuracy (-1.58 ppm).

(*E*)-1-Methyl-4-(2-nitroprop-1-en-1-yl)benzene (45)

(*E*)-1-Methyl-4-(2-nitroprop-1-en-1-yl)benzene was prepared from *p*-tolualdehyde (3.6 mmol, 0.706 g) according to general procedure 8.2. The product was purified by flash column chromatography over silica gel (eluent: 3:1 dichloromethane / hexane) and recrystallised from ethanol.
Yellow crystals 254 mg (40%)
Melting Point: 50-52 °C (lit. M.p. 51.5-52.5 °C[439])
IRν_{max} (KBr): 2984 (CH), 1650 (C=C), 1518, 1358 (NO_2) cm^{-1}
^{1}H NMR (400 MHz, $CDCl_3$) δ 2.43 (s, 3 H, $-CH_3$), 2.49 (s, 3 H, $-CH_3$), 7.28 (d, 2 H, J = 9 Hz, 2 x ArH), 7.37 (d, 2 H, J = 9 Hz, 2 x ArH), 8.10 (s, 1 H, H1)
^{13}C NMR (101 MHz, $CDCl_3$) ppm 13.7 (C3), 21.1 (C1'), 129.1, 129.2, 129.7, 133.3 (C1), 140.1 (C4'), 146.5 (C2)
HRMS (APCI) calculated for $C_{10}H_{11}NO_2$ [M^+] 177.0784: found 177.0781. Mass accuracy (-1.69 ppm)

(*E*)-1-Bromo-4-(2-nitroprop-1-en-1-yl)benzene (46)

(*E*)-1-Bromo-4-(2-nitroprop-1-en-1-yl)benzene was prepared from 4-bromobenzaldehyde (1 mmol, 0.18 g) according to general procedure general procedure 8.2. The product was purified by recrystallization from ethanol.
Yellow solid 18 mg (18%)
Melting Point: 93-96 °C (lit. M.p. 93-95 °C[444])
IRν_{max} (ATR): 3063 (C-H), 1652, 1598 (C=C), 1540, 1351 (NO_2), 1121 (C-N) cm^{-1}
^{1}H NMR (400 MHz, $CDCl_3$) δ 2.44 (d, J = 0.83 Hz, 3 H, CH_3), 7.29 - 7.32 (m, J = 8.29 Hz, 2 H, 2 x ArH), 7.58 - 7.65 (m, J = 8.29 Hz, 2 H, 2 x ArH), 8.02 (s, 1 H, H1)
^{13}C NMR (101 MHz, $CDCl_3$) ppm 13.9 (C3), 124.4, 131.2, 131.3, 131.4, 132.2, 132.2, 148.1 (C2)
HRMS (ESI) calculated for $C_9H_9Br^{79}NO_2$ [M^++H] 241.9817: found 241.9820. Mass accuracy (-1.24 ppm).

(*E*)-2,4-Dimethoxy-1-(2-nitroprop-1-en-1-yl)benzene (47)

(*E*)-2,4-Dimethoxy-1-(2-nitroprop-1-en-1-yl)benzene was prepared from 2,4-dimethoxybenzaldehyde (3.6 mmol, 0.597 g) according to general procedure 8.2. The product

was purified by flash column chromatography over silica gel (eluent: 3:1 dichloromethane / hexane) and recrystallised from ethanol.
Yellow crystals 282 mg (35%)
Melting Point: 75-77 °C (lit. M.p. 77-78 °C[439])
IRν_{max} (KBr): 2984 (CH), 1650 (C=C), 1518, 1358 (NO_2) cm^{-1}
^{1}H NMR (400 MHz, $CDCl_3$) δ 2.43 (s, 3 H, CH_3), 2.49 (s, 6 H, OCH_3), 7.28 (d, 1 H, J = 2 Hz, 1 x ArH), 7.37 (d, 2 H, J = 8 Hz, 2 x ArH), 8.10 (s, 1 H, H1)
^{13}C NMR (101 MHz, $CDCl_3$) ppm 14.3 (C3), 55.5 (OCH_3), 55.6 (OCH_3), 98.4, 104.9, 114.3, 129.6, 131.1 (C1), 145.7 (C2), 159.9 (C2' / C4'), 162.9 (C2' / C4')
HRMS (APCI) calculated for $C_{11}H_{14}NO_4$ [M^++H] 224.0917: found 224.0911. Mass accuracy (-2.65 ppm).

(*E*)-1,4-Dimethoxy-2-(2-nitroprop-1-en-1-yl)benzene (48)

(*E*)-1-4-Dimethoxy-2-(2-nitroprop-1-en-1-yl)benzene was prepared from 2,5-dimethoxybenzaldehyde (3.6 mmol, 0.597 g) according to general procedure 8.2. The product was purified by flash column chromatography over silica gel (eluent: 3:1 dichloromethane / hexane) and recrystallised from ethanol.
Yellow crystals 645 mg (80%)
Melting Point: 73-75 °C (lit. M.p. 74-75 °C[439])
IRν_{max} (KBr): 2946 (CH), 1647 (C=C), 1513, 1353 (NO_2) cm^{-1}
^{1}H NMR (400 MHz, $CDCl_3$) δ 2.42 (s, 3 H, CH_3), 3.82 (s, 3 H, OCH_3), 3.86 (s, 3 H, OCH_3), 6.84-7.00 (m, 3 H, 3 x ArH), 8.26 (s, 1 H, H1)
^{13}C NMR (101 MHz, $CDCl_3$) ppm 13.7 (C3), 55.4 (OCH_3), 55.6 (OCH_3), 111.3, 115.4, 115.6, 121.7, 129.2, 147.3 (C2), 152.0 (C1' / C4'), 152.7 (C1' / C4')
HRMS (APCI) calculated for $C_{11}H_{14}NO_4$ [M^++H] 224.0917: found 224.0911. Mass accuracy (-2.65 ppm).

(*E*)-1,2,3-Trimethoxy-5-(2-nitroprop-1-en-1-yl)benzene (49)

(*E*)-1,2,3-Trimethoxy-5-(2-nitroprop-1-en-1-yl)benzene was prepared from 3,4,5-trimethoxybenzaldehyde (3.6 mmol, 0.705 g) according to general procedure 8.2. The product was purified by flash column chromatography over silica gel (eluent: 3:1 dichloromethane / hexane) and recrystallised from ethanol.
Yellow crystals 455 mg (50%)
Melting Point: 94-96 °C (lit. M.p. 95-96 °C[445])
IRν_{max} (KBr): 2939 (CH), 1645 (C=C), 1581, 1358 (NO_2) cm^{-1}
^{1}H NMR (400 MHz, $CDCl_3$) δ 2.43 (s, 3 H, CH_3), 3.91 (s, 9 H, 3 x OCH_3), 6.68 (s, 2 H, 2 x ArH), 8.06 (s, 1 H, H1)
^{13}C NMR (101 MHz, $CDCl_3$) ppm 13.8 (C3), 55.8 (OCH_3), 60.6 (OCH_3), 107.0, 127.3, 133.4, 139.4 (C2), 146.6 (C2'), 152.9 (C1' & C3')
HRMS (APCI) calculated for $C_{12}H_{15}NO_5$ [M^+] 253.0945: found 253.0942. Mass accuracy (-1.78 ppm).

(*E*)-1-Ethoxy-2-(2-nitroprop-1-en-1-yl)benzene (50)

(*E*)-1-Ethoxy-2-(2-nitroprop-1-en-1-yl)benzene was prepared from 2-ethoxybenzaldehyde (3.6 mmol, 0.540 g) according to general procedure 8.2. The product was purified by flash

column chromatography over silica gel (eluent: 3:1 dichloromethane / hexane) and recrystallised from ethanol.
Yellow crystals 299 mg (40%)
Melting Point: 54-55 °C (lit. M.p. 56 °C[185])
IR ν_{max} (ATR): 3072, 2981 (C-H), 1651, 1596 (C=C), 1545, 1366 (NO_2), 1120 (C-N) cm^{-1}
^{1}H NMR (400 MHz, $CDCl_3$) δ 1.46 (t, *J* = 7.02 Hz, 3 H, CH_3), 2.39 (s, 3 H, CH_3), 4.11 (q, *J* = 6.71 Hz, 2 H, CH_2), 6.94 (d, *J* = 7.94 Hz, 1 H, H6), 7.00 (app.t, *J* = 7.63 Hz, 1 H, H4 / H5), 7.30 (d, *J* = 7.32 Hz, 1 H, H3), 7.35 - 7.43 (m, 1 H, H4 / H5), 8.30 (s, 1 H, H1')
^{13}C NMR (101 MHz, $CDCl_3$) ppm 14.2 (CH_3), 14.7 (CH_3), 64.0 (CH_2), 111.7 (CH), 120.2 (CH), 121.5, 130.0, 130.0 (CH), 131.4 (CH), 147.3 (C2'), 157.5 (C1)
HRMS (APCI) calculated for $C_{11}H_{14}NO_3$ [M^++H] 208.0974: found 208.0970. Mass accuracy (-1.92 ppm).

(*E*)-1-(2-Nitroprop-1-en-1-yl)-4-phenoxybenzene (51)

(*E*)-1-(2-Nitroprop-1-en-1-yl)-4-phenoxybenzene was prepared from 4-phenoxybenzaldehyde (3.6 mmol, 0.712 g) according to general procedure 8.2. The product was purified by flash column chromatography over silica gel (eluent: 3:1 dichloromethane/hexane) and recrystallised from ethanol.
Yellow crystals 663 mg (72%)
Melting Point: 58-60 °C [446])
IRν_{max} (KBr): 3100 (CH), 1620 (C=C), 1520, 1352 (NO_2) cm^{-1}
^{1}H NMR (400 MHz, $CDCl_3$) δ 2.50 (s, 3 H, CH_3), 7.09 (m, 4 H, 4 x ArH), 7.22 (m, 1 H, ArH), 7.43 (m, 4 H, 4 x ArH), 8.11 (s, 1 H, H1)
^{13}C NMR (101 MHz, $CDCl_3$) ppm 14.1 (C3), 118.2, 119.9, 124.5, 126.7, 130.1, 132.0, 133.2 (C1), 146.6 (C2), 155.7 (C4' / C4"), 159.4 (C4' / C4")
HRMS (APCI) calculated for $C_{15}H_{14}NO_3$ [M^++H] 256.0968: found 256.0961. Mass accuracy (-2.81 ppm).

(*E*)-1-(Benzyloxy)-4-(2-nitroprop-1-en-1-yl)benzene (52)

(*E*)-1-(Benzyloxy)-4-(2-nitroprop-1-en-1-yl)benzene was prepared from 4-benzyloxybenzaldehyde (1 mmol, 0.21 g) according to general procedure general procedure 8.2. The product was purified by recrystallization from ethanol.
Yellow crystals 135 mg (50%)
Melting Point: 143-145 °C (lit. M.p. 144-146 °C[447])
IRν_{max} (ATR): 3060, 3037 (C-H), 1598 (C=C), 1514, 1361 (NO_2), 1176 (C-N) cm^{-1}
^{1}H NMR (400 MHz, $CDCl_3$) δ 2.48 (s, 3 H, CH_3), 5.14 (s, 2 H, CH_2), 7.04 - 7.10 (m, 2 H, 2 x ArH), 7.30 - 7.50 (m, 7 H, 7 x ArH), 8.08 (s, 1 H, H1')
^{13}C NMR (101 MHz, $CDCl_3$) ppm 14.1 (CH_3), 70.1 (CH_2), 115.3 (CH), 124.9, 127.4 (CH), 128.2 (CH), 128.7 (CH), 132.1 (CH), 133.5 (C1'), 134.0, 136.2, 145.8 (C2'), 160.2 (C4)
HRMS (APCI) calculated for $C_{16}H_{16}NO_3$ [M^++H] 270.1130: found 270.1123. Mass accuracy (-2.59 ppm).

(*E*)-(2-Nitroprop-1-en-1-yl)benzene (53)

(*E*)-(2-Nitroprop-1-en-1-yl)benzene was prepared from benzaldehyde (1 mmol, 0.11 g) according to general procedure general procedure 8.2. The product was purified by recrystallization from ethanol.

Yellow crystals 112 mg (68%)
Melting Point: 62-64 °C (lit. M.p. 65 °C[448])
IR$_{\nu max}$ (ATR): 3058, 2936 (C-H), 1650, 1598 (Ar C=C), 1574, 1386 (NO_2), 1163 (C-N) cm^{-1}
^{1}H NMR (400 MHz, $CDCl_3$) δ 2.46 (s, 3 H, CH_3), 7.40 - 7.51 (m, 5 H, 5 x ArH), 8.09 (s, 1 H, H1')
^{13}C NMR (101 MHz, $CDCl_3$) ppm 13.9 (CH_3), 128.8, 129.8 (CH), 129.9 (CH), 132.3, 133.4 (C1'), 147.6 (C2')
HRMS (APCI) calculated for $C_9H_{10}NO_2$ [M^++H] 164.0712: found 164.0704. Mass accuracy (-4.88 ppm).

(*E*)-4-Bromo-1-methoxy-2-(2-nitroprop-1-en-1-yl)benzene (54)[439]

(*E*)-4-Bromo-1-methoxy-2-(2-nitroprop-1-en-1-yl)benzene was prepared from 5-bromo-2-methoxybenzaldehyde (1 mmol, 0.21 g) according to general procedure general procedure 8.2. The product was purified by recrystallization from ethanol.
Yellow crystals 230 mg (85%)
Melting Point: 68-70 °C
IR$_{\nu max}$ (ATR): 3072, 2943 (C-H), 1650, 1591 (C=C), 1507, 1354 (NO_2), 1132 (C-N) cm^{-1}
^{1}H NMR (400 MHz, $CDCl_3$) δ 2.37 (s, 3 H, CH_3), 3.87 (s, 3 H, OCH_3), 6.84 (d, J = 9.16 Hz, 1 H, H4), 7.38 (d, J = 2.44 Hz, 1 H, H3), 7.49 (dd, J = 8.55, 2.44 Hz, 1 H, H5), 8.14 (s, 1 H, H1')
^{13}C NMR (101 MHz, $CDCl_3$) ppm 14.0 (CH_3), 55.8 (OCH_3), 112.5 (CH), 123.4, 128.2 (CH), 132.2 (CH), 133.9 (C1'), 148.3 (C2'), 157.1 (C1)
HRMS (APCI) calculated for $C_{10}H_{10}NO_3Br^{79}$ [M^+] 270.9844: found 270.9847. Mass accuracy (1.11 ppm).

(*E*)-1-Chloro-3-(2-nitroprop-1-en-1-yl)benzene (55)

(*E*)-1-Chloro-3-(2-nitroprop-1-en-1-yl)benzene was prepared from 3-chlorobenzaldehyde (1 mmol, 0.14 g) according to general procedure general procedure 8.2. The product was purified by column chromatography (eluent: 1:1 dichloromethane: hexane).
Yellow oil 120 mg (61%)
Melting Point: N/A (lit. M.p. 40 °C[449])
IR$_{\nu max}$ (ATR): 3067, 2926 (Ar C-H), 1660, 1594 (Ar C=C), 1519, 1323 (NO_2), 1168 (C-N) cm^{-1}
^{1}H NMR (400 MHz, $CDCl_3$) δ 2.45 (s, 3 H, CH_3), 7.30 - 7.35 (m, 1 H, 1 x ArH), 7.41 (d, J = 3.73 Hz, 3 H, 3 x ArH), 8.01 (s, 1 H, H1')
^{13}C NMR (101 MHz, $CDCl_3$) ppm 13.9 (CH_3), 124.3 (CH), 129.5 (CH), 129.8 (CH), 130.1 (CH), 131.8 (C1'), 134.1, 134.8, 148.7 (C2')
HRMS (APCI) calculated for $C_9H_8NO_2Cl^{35}$ [M^+] 197.0244: found 197.0242. Mass accuracy (-1.11 ppm).

(*E*)-3-(2-Nitroprop-1-en-1-yl)phenol (56)

(*E*)-3-(2-Nitroprop-1-en-1-yl)phenol was prepared from 3-hydroxybenzaldehyde (1 mmol, 0.12 g) according to general procedure general procedure 8.2. The product was purified by column chromatography (eluent: dichloromethane).
Yellow solid 66 mg (37%)

Melting Point: 95-98 °C (lit. M.p. 96-98 °C[450])
IR$_{Vmax}$ (ATR): 3411 (OH), 3112, 3306 (Ar C-H), 1648, 1630 (Ar C=C), 1506, 1319 (NO_2), 1160 (C-N stretch) cm^{-1}
^{1}H NMR (400 MHz, $CDCl_3$) δ 2.46 (s, 3 H, CH_3), 5.31 (s, 1 H, OH), 6.84 - 6.96 (m, 2 H, H2 & H6), 7.01 (d, J = 7.94 Hz, 1 H, H4), 7.30 - 7.36 (m, 1 H, H5), 8.03 (s, 1 H, H1')
^{13}C NMR (101 MHz, $CDCl_3$) ppm 14.1 (CH_3), 116.5 (C6), 117.1 (C2), 122.6 (C4), 130.2 (C5), 133.3 (C1'), 133.9 (C3), 148.0 (C2'), 155.8 (C1)
HRMS (ESI) calculated for $C_9H_8NO_3$ [M^+-H] 178.0510: found 178.0503. Mass accuracy (-3.93 ppm).

(*E*)-1-Chloro-2-(2-nitroprop-1-en-1-yl)benzene (57)

(*E*)-1-Chloro-2-(2-nitroprop-1-en-1-yl)benzene was prepared from 2-chlorobenzaldehyde (1 mmol, 0.14 g) according to general procedure general procedure 8.2. The product was purified by column chromatography (eluent: 1:1 dichloromethane: hexane).
Yellow oil 110 mg (56%)
Melting Point: N/A (lit. M.p. 40 °C[451])
IR$_{Vmax}$ (ATR): 3068, 2934 (C-H), 1665 (C=C), 1518, 1324 (NO_2), 1055 (C-N) cm^{-1}
^{1}H NMR (400 MHz, $CDCl_3$) δ 2.30 (s, 3 H, CH_3), 7.27 - 7.39 (m, 3 H, 3 x ArH), 7.41 - 7.47 (m, 1 H, H6), 8.06 - 8.20 (m, 1 H, H1')
^{13}C NMR (101 MHz, $CDCl_3$) ppm 13.7 (CH_3), 124.3 (CH), 126.8 (CH), 129.8 (CH), 130.1 (CH), 130.4 (CH), 130.8, 131.0, 134.6, 149.1 (C2')
HRMS (APCI) calculated for $C_9H_9NO_2Cl$ [M^++H] 198.0322: found 198.0321. Mass accuracy (-0.50 ppm).

(*E*)-4-Methoxy-2-(2-nitroprop-1-en-1-yl)phenol (58)

(*E*)-4-Methoxy-2-(2-nitroprop-1-en-1-yl)phenol was prepared from 2-hydroxy-5-methoxybenzaldehyde (1 mmol, 0.15 g) according to general procedure general procedure 8.2. The product was purified by recrystallization from ethanol.
Yellow solid 38 mg (18%)
Melting Point: 110-114 °C
IR$_{Vmax}$ (ATR): 3476 (OH), 3070, 2935 (C-H), 1659, 1585 (C=C), 1510, 1361 (NO_2), 1122 (C-N) cm^{-1}
^{1}H NMR (400 MHz, $CDCl_3$) δ 2.40 (s, 3 H, CH_3), 3.94 (s, 3 H, OCH_3), 6.06 (s, 1 H, H3), 6.92 (s, 2 H, 2 x ArH), 8.28 (s, 1 H, H1')
^{13}C NMR (101 MHz, $CDCl_3$) ppm 14.3 (CH_3), 56.2 (OCH_3), 111.8 (CH), 118.8, 119.7 (CH), 121.6 (CH), 128.8 (C1'), 145.0 (C1), 146.6 (C2'), 147.8 (C4)
HRMS (ESI) calculated for $C_{10}H_{10}NO_4$ [M^++H] 208.0615: found 208.0617. Mass accuracy (0.96 ppm).

(*E*)-1-Ethoxy-4-(2-nitroprop-1-en-1-yl)benzene (59)

(*E*)-1-Ethoxy-4-(2-nitroprop-1-en-1-yl)benzene was prepared from 4-bromobenzaldehyde (1 mmol, 0.15 g) according to general procedure general procedure 8.2. The product was purified by recrystallization from ethanol.
Yellow solid 81 mg (39%)
Melting Point: 73-76 °C (lit. M.p. 74-75 °C[452])

IRν_{max} (ATR): 3060 (C-H), 1660, 1589 (C=C), 1553, 1345 (NO_2), 1202 (C-N) cm^{-1}
^{1}H NMR (400 MHz, $CDCl_3$) δ 1.45 (t, *J* = 7.03 Hz, 3 H), 2.49 (s, 3 H), 4.10 (q, *J* = 7.03 Hz, 2 H), 6.88 - 7.06 (m, *J* = 8.53 Hz, 2 H), 7.36 - 7.50 (m, *J* = 9.03 Hz, 2 H), 8.08 (s, 1 H)
^{13}C NMR (101 MHz, $CDCl_3$) ppm 14.1 (CH_3), 14.7 (CH_3), 63.7 (OCH_2), 114.9, 124.5, 132.1, 133.7, 145.5 (C2), 160.5 (C4')
HRMS (ESI) calculated for $C_{11}H_{14}NO_3$ [M^++H] 208.0974: found 208.0980. Mass accuracy (2.88 ppm).

(*E*)-3-(2-Nitroprop-1-en-1-yl)furan (75)

(*E*)-3-(2-Nitroprop-1-en-1-yl)furan was prepared from 3-furaldehyde (3.6 mmol, 0.346 g) according to general procedure 8.2. The product was purified by flash column chromatography over silica gel (eluent: dichloromethane / hexane 3/1) and recrystallised from ethanol.
Brown crystals 385 mg (70%)
Melting Point: 86-88 °C (lit. M.p. 86-87 °C[453])
IRν_{max} (KBr): 3130 (CH), 1656 (C=C), 1501, 1356 (NO_2) cm^{-1}
^{1}H NMR (400 MHz, $CDCl_3$) δ 2.47 (s, 1 H, -CH_3), 6.70 (s, 1 H, ArH), 7.29 (s, 1 H, ArH), 7.56 (s, 1 H, ArH), 7.96 (s, 1 H, H1)
^{13}C NMR (101 MHz, $CDCl_3$) ppm 13.57 (C3'), 109.38 (C4), 118.58 (C3), 124.06 (C5), 144.21 (C2'), 145.62 (C2)
HRMS (APCI) calculated for $C_7H_7NO_3$ [M^+] 153.0420: found 153.0417. Mass accuracy (-2.51 ppm).

(*E*)-3-(2-Nitroprop-1-en-1-yl)thiophene (76)

(*E*)-3-(2-Nitroprop-1-en-1-yl)thiophene was prepared from 3-thiophenecarboxaldehyde (3.6 mmol, 0.404 g) according to general procedure 8.2. The product was purified by flash column chromatography over silica gel (eluent: dichloromethane / hexane 3/1) and recrystallised from ethanol.
Brown crystals 379 mg (62%)
Melting Point: 71-73 °C (lit. M.p. 72.5-73.5 °C[436])
IRν_{max} (KBr): 3102 (CH), 1646 (C=C), 1502, 1339 (NO_2) cm^{-1}
^{1}H NMR (400 MHz, $CDCl_3$) δ 2.52 (s, 3 H, CH_3), 7.31 (s, 1 H, ArH), 7.47 (s, 1 H, ArH), 7.63 (s, 1 H, ArH), 8.1 (s, 1 H, H1)
^{13}C NMR (101 MHz, $CDCl_3$) ppm 13.8 (C3), 126.6, 127.2, 127.7, 129.6, 133.2 (C1), 145.7 (C2)
HRMS (ESI) calculated for $C_7H_8NO_2S$ [M^++H] 170.0270: found 170.0265. Mass accuracy (-2.94 ppm).

(*E*)-2-(2-Nitroprop-1-en-1-yl)thiophene (77)

(*E*)-2-(2-Nitroprop-1-en-1-yl)thiophene was prepared from 2-thiophenecarboxaldehyde (3.6 mmol, 0.403 g) according to general procedure 8.2. The product was purified by flash column chromatography over silica gel (eluent: dichloromethane / hexane 3/1) and recrystallised from ethanol.
Yellow crystals 395 mg (65%)
Melting Point: 67-68 °C (lit. M.p. 69 °C[410])
IRν_{max} (KBr): 3093 (CH), 1643 (C=C), 1494, 1363 (NO_2) cm^{-1}

^{1}H NMR (400 MHz, $CDCl_3$) δ 2.58 (s, 3 H, CH_3), 7.21 (dd, 1 H, *J* = 3.8 Hz, H4'), 7.45 (d, 1 H, *J* = 5 Hz, H3'/H5'), 7.66 (d, 1 H, *J* = 3.5 Hz, H3'/H5'), 8.33 (s, 1 H, H1)
^{13}C NMR (101 MHz, $CDCl_3$) ppm 14.3 (CH_3), 127.3 (C1'), 128.2 (C4), 131.8 (C3), 134.8 (C5), 135.4 (C2'), 144.4 (C2)
HRMS (ESI) calculated for $C_7H_7NO_2S$ [M^+–H] 169.0197: found 169.0192. Mass accuracy (-2.96 ppm).

(*E*)-2-Methyl-5-(2-nitroprop-1-en-1-yl)thiophene (78)

(*E*)-2-Methyl-5-(2-nitroprop-1-en-1-yl)thiophene was prepared from 5-methyl-2-thiophenecarboxaldehyde (3.6 mmol, 0.454 g) according to general procedure 8.2. The product was purified by flash column chromatography over silica gel (eluent: dichloromethane / hexane 3/1) and recrystallised from ethanol.
Orange crystals (55%)
Melting Point: 116-118 °C (lit. M.p. 117 °C[454])
IRν_{max} (KBr): 3054 (CH), 1639 (C=C), 1494, 1359 (NO_2) cm^{-1}
^{1}H NMR (400 MHz, $CDCl_3$) δ 2.54 (s, 3 H, -CH_3), 2.60 (s, 3 H, -CH_3), 6.88 (dd, 1 H, *J* = 3.5 Hz, 1 Hz, H3'), 7.28 (d, 1 H, *J* = 3.5 Hz, H4'), 8.25 (s, 1 H, H1)
^{13}C NMR (101 MHz, $CDCl_3$) ppm 14.15 (CH_3), 15.82 (CH_3), 126.83, 127.89, 133.21, 135.7 (C1), 142.99 (C2') , 147.93 (C2)
HRMS (ESI) calculated for $C_8H_9NO_2S$ [M^+–H] 182.0265: found 182.0272. Mass accuracy (3.85 ppm).

8.3 General procedure for preparation of (*E*)-(2-nitrobut-1-en-1-yl)benzenes (60 – 70, 79 - 82)

To a solution of the appropriate benzaldehyde (3.6 mmol) in 4 mL glacial acetic acid was added nitropropane (7.2 mmol) followed by cyclohexylamine (3.6 mmol, 0.4 mL). The reaction mixture was heated under microwave irradiation at 120 °C for 30 min. After cooling, water (10 mL) was added to the reaction and it was allowed to stand. The precipitated nitroethene was isolated by filtration. The filtrate was further diluted with water (20 mL) and extracted with dichloromethane (3 x 10 mL). The organic phases were combined and washed with saturated aqueous $NaHCO_3$ (3 x 10 mL). The solution was dried over anhydrous Na_2SO_4, filtered and all solvent removed *in vacuo*, to give an oil which was purified by flash column chromatography over silica gel (eluent: dichloromethane / hexane). The chromatographed and precipitated nitroethene fractions were combined and recrystallised from the appropriate alcohol.

(*E*)-1-Chloro-4-(2-nitrobut-1-en-1-yl)benzene (60)

(*E*)-1-Chloro-4-(2-nitrobut-1-en-1-yl)benzene was prepared from 4-chlorobenzaldehyde (3.6 mmol, 0.500 g) using according to general procedure 8.3. The product was purified by flash column chromatography over silica gel (eluent: 3:1 dichloromethane / hexane) and recrystallised from ethanol.
Yellow crystals 151 mg (20%)
Melting Point: 75-77 °C (lit. M.p. 76-76.5 °C[416])
IRν_{max} (KBr): 2976 (CH), 1651 (C=C), 1520, 1382 (NO_2), 836 (C-Cl) cm^{-1}

^{1}H NMR (400 MHz, $CDCl_3$) δ 1.29 (t, 3 H, *J* = 7.5 Hz, -CH_3), 2.86 (q, 2 H, *J* = 7.5 Hz, -CH_2), 7.37 (d, 2 H, *J* = 8.5 Hz, 2 x ArH), 7.44 (d, 2 H, *J* = 8.5 Hz, 2 x ArH), 7.99 (s, 1 H, H1)
^{13}C NMR (101 MHz, $CDCl_3$) ppm 12.0 (C4), 20.3 (C3), 128.9, 130.3, 130.4, 131.4 (C1), 153.2 (C2)
HRMS (APCI) calculated for $C_{10}H_{10}NO_2Cl^{35}$ [M^++H] 211.0395: found 211.0389. Mass accuracy (-2.45 ppm).

(*E*)-4-(2-Nitrobut-1-en-1-yl)phenol (61)

(*E*)-4-(2-Nitrobut-1-en-1-yl)phenol was prepared from 4-hydroxybenzaldehyde (3.6 mmol, 0.440 g) according to general procedure 8.3. The product was purified by flash column chromatography over silica gel (eluent: dichloromethane / hexane 3/1) and recrystallised from ethanol.
Orange crystals 49 mg (7%)
Melting Point: 75-78 °C (lit. M.p. 78.5-79 °C[455])
IRν_{max} (KBr): 3391 (OH), 2976 (CH), 1644 (C=C), 1519, 1372 (NO_2) cm^{-1}
^{1}H NMR (400 MHz, $CDCl_3$) δ 1.31 (t, 3 H, *J* = 7.5 Hz, CH_3), 2.91 (q, 2 H, *J* = 7.5 Hz, CH_2), 5.74 (br.s., 1 H, OH), 6.96 (d, 2 H, *J* = 8.5 Hz, 2 x ArH), 7.39 (d, 2 H, *J* = 8.5 Hz, 2 x ArH), 8.04 (s, 1 H, H1)
^{13}C NMR (101 MHz, $CDCl_3$) ppm 11.9 (C4), 20.4 (C3), 115.7 (2C), 124.3, 131.6 (2C), 133.0 (C1), 150.8 (C2), 157.2 (C4')
HRMS (ESI) calculated for $C_{10}H_{12}NO_3$ [M^++H] 194.0812: found 194.0807. Mass accuracy (-2.58 ppm).

(*E*)-2-(2-Nitrobut-1-en-1-yl)naphthalene (62)

(*E*)-2-(2-Nitrobut-1-en-1-yl)naphthalene was prepared from 2-naphthaldehyde (3.6 mmol, 0.562 g) according to general procedure 8.3. Purified by flash chromatography over silica gel (eluent: 3/1 dichloromethane / hexane) and recrystallised from ethanol.
Yellow oil 270 mg (30%)
IRν_{max} (KBr): 2982 (CH), 1646 (C=C), 1520, 1330 (NO_2) cm^{-1}
^{1}H NMR (400 MHz, $CDCl_3$) δ 1.37 (t, 3 H, *J* = 7.5 Hz, -CH_3), 2.98 (q, 2 H, *J* = 7 Hz, -CH_2), 7.50-7.64 (m, 3 H, 3 x ArH), 7.85-7.98 (m, 4H, 4 x ArH), 7.92 (s, 1 H, =CH)
^{13}C NMR (101 MHz, $CDCl_3$) ppm 12.2 (C4), 20.4 (C3), 125.6, 126.5, 127.2, 127.3, 128.1, 128.4, 129.3, 129.9, 132.6, 132.9, 133.2, 152.9 (C2)
HRMS (ESI) calculated for $C_{14}H_{13}NO_2Na$ [M^++Na] 250.0844: found 250.0835. Mass accuracy (-3.60 ppm).

(*E*)-1-Fluoro-4-(2-nitrobut-1-en-1-yl)benzene (63)

(*E*)-1-Fluoro-4-(2-nitrobut-1-en-1-yl)benzene was prepared from 4-fluorobenzaldehyde (3.6 mmol, 0.459 g) according to general procedure 8.3. and recrystallised from ethanol.
Yellow crystals 280 mg (40%)
Melting Point: 79-80 °C [456])
IRν_{max} (KBr): 2967 (CH), 1653 (C=C), 1508, 1323 (NO_2) cm^{-1}
^{1}H NMR (400 MHz, $CDCl_3$) δ 1.29 (t, 3 H, *J* = 7.5 Hz, -CH_3), 2.86 (q, 2 H, *J* = 7 Hz, -CH_2), 7.17 (m, 2 H, 2 x ArH), 7.43 (m, 2 H, 2 x ArH), 8.00 (1H, s, =CH)

^{13}C NMR (101 MHz, $CDCl_3$) ppm 12.0 (C4), 20.2 (C3), 115.7, 115.9, 127.9, 131.4, 131.6 (C1), 152.6 (C2), 161.8 (CF), 164.3 (CF)
HRMS (ESI) calculated for $C_{10}H_{10}FNO_2$ [M^+] 195.0690: found 195.0686. Mass accuracy (-2.25 ppm).

1,4-Bis((*E*)-2-nitrobut-1-en-1-yl)benzene (64)

1,4-Bis((*E*)-2-nitrobut-1-en-1-yl)benzene was prepared from terephthalaldehyde (3.6 mmol, 0.543g) using nitropropane (7.2 mmol) according to general procedure 8.3. and recrystallised from ethanol.
Yellow crystals 397 mg (40%)
Melting Point: 133-134 °C (lit. M.p. 134-135 °C[457])
IRν_{max} (KBr): 2975 (CH), 1654 (C=C), 1501, 1324 (NO_2) cm^{-1}
^{1}H NMR (400 MHz, $CDCl_3$) δ 1.33 (t, 6 H, *J* = 7.5 Hz, 2 x -CH_3), 2.90 (q, 4 H, *J* = 7 Hz, 2 x –CH_2), 7.50-7.60 (m, 4 H, 4 x ArH), 8.03 (s, 2 H, 2 x =CH)
^{13}C NMR ppm ($CDCl_3$) 12.1 (2 x CH_3), 20.4 (2 x CH_2), 129.7, 131.4, 133.4 (C1 x 2), 153.8 (C2 x 2)
HRMS (ESI) calculated for $C_{14}H_{16}N_2O_2$ [M^+] 276.1110: found 276.1110. Mass accuracy (0 ppm).

(*E*)-1-(2-Nitrobut-1-en-1-yl)naphthalene (65)[458]

(*E*)-1-(2-Nitrobut-1-en-1-yl)naphthalene was prepared from 1-naphthaldehyde (3.6 mmol, 0.550 g) according to general procedure 8.3. The product was purified by flash column chromatography over silica gel (eluent: dichloromethane / hexane 3/1).
Yellow oil 287 mg (35%)
Melting Point: N/A
IRν_{max} (KBr) 3071 (CH), 1680 (C=C), 1524, 1331 (NO_2) cm^{-1}
^{1}H NMR (400 MHz, $CDCl_3$) δ 1.25 (t, 3 H, *J* = 7.5 Hz, -CH_3), 2.79 (q, 2 H, *J* = 7.5 Hz, -CH_2), 7.46 (d, 1 H, *J* = 7 Hz, ArH), 7.53-7.59 (m, 1 H, H3'), 7.60-7.65 (m, 2 H, 2 x ArH), 7.90-7.98 (m, 3 H, 3 x ArH), 8.58 (s, 1 H, H1)
^{13}C NMR (101 MHz, $CDCl_3$) ppm 12.4 (C4), 20.5 (C3), 123.8, 124.8, 126.0, 126.2, 126.7, 128.3, 129.4, 129.7, 131.0, 131.1, 133.0 (C1), 154.5 (C2)
HRMS (ESI) calculated for $C_{14}H_{14}NO_2$ [M^++H] 228.1025: found 228.1018. Mass accuracy (-3.07 ppm).

(*E*)-4-Bromo-1-methoxy-2-(2-nitrobut-1-en-1-yl)benzene (66)

(*E*)-4-Bromo-1-methoxy-2-(2-nitrobut-1-en-1-yl)benzene was prepared from 5-bromo-2-methoxybenzaldehyde (1 mmol, 0.21 g) according to general procedure general procedure 8.3. The product was purified by flash column chromatography over silica gel (eluent: dichloromethane : hexane 3/1).
Yellow oil 176 mg (62%)
IRν_{max} (ATR): 3075, 3021 (C-H), 1686, 1591 (C=C), 1552, 1333 (NO_2), 1179 (C-N) cm^{-1}
^{1}H NMR (400 MHz, $CDCl_3$) δ 1.16 - 1.20 (m, 3 H, CH_3), 2.69 - 2.76 (m, 2 H, CH_2), 3.81 (s, 3 H, OCH_3), 6.79 (d, *J* = 9.16 Hz, 1 H, H6), 7.29 (d, *J* = 2.44 Hz, 1 H, H3), 7.43 (dd, *J* = 9.16, 2.44 Hz, 1 H, H5), 8.00 (s, 1 H, H1')

^{13}C NMR (101 MHz, $CDCl_3$) ppm 12.3 (CH_3), 20.6 (CH_2), 55.7 (OCH_3), 112.4, 112.4 (CH), 123.3, 127.6 (CH), 131.1, 131.6 (CH), 132.7, 133.8 (CH), 153.7 (C1 / C4), 156.9 (C1 / C4)
HRMS (APCI) calculated for $C_{11}H_{12}Br^{79}NO_3$ [M^+] 285.0001: found 285.0006. Mass accuracy (1.75 ppm).

(*E*)-1-Chloro-2-(2-nitrobut-1-en-1-yl)benzene (67)

(*E*)-1-Chloro-2-(2-nitrobut-1-en-1-yl)benzene was prepared from 2-chlorobenzaldehyde (1 mmol, 0.14 g) according to general procedure general procedure 8.3. The product was purified by flash column chromatography over silica gel (eluent: dichloromethane : hexane 3/1).
Yellow oil 199 mg (94%)
Melting Point: N/A (lit. M.p. 20-21 °C[455])
IR$_{Vmax}$ (ATR): 3066, 2939 (C-H), 1659, 1591 (C=C), 1521, 1330 (NO_2), 1128 (C-N) cm^{-1}
^{1}H NMR (400 MHz, $CDCl_3$) δ 1.12 (t, *J* = 7.32 Hz, 3 H, CH_3), 2.60 - 2.67 (m, 2 H, CH_2), 7.20 - 7.32 (m, 3 H, 3 x ArH), 7.32 - 7.40 (m, 1 H, H6), 7.98 (s, 1 H, H1')
^{13}C NMR (101 MHz, $CDCl_3$) ppm 12.1 (CH_3), 20.3 (CH_2), 126.8 (CH), 129.4 (CH), 129.5 (CH), 129.7 (CH), 130.6 (C1'), 130.8, 134.2, 154.3 (C1)
HRMS (APCI) calculated for $C_{10}H_{11}Cl^{35}NO_2$ [M^++H] 212.0478: found 212.0476. Mass accuracy (-0.94 ppm).

(*E*)-3-(2-Nitrobut-1-en-1-yl)phenol (68) [459]

(*E*)-3-(2-Nitrobut-1-en-1-yl)phenol was prepared from 3-hydroxybenzaldehyde (1 mmol, 0.12 g) according to general procedure general procedure 8.3. The product was purified by column chromatography (eluent: dichloromethane) and recrystallised from ethanol.
Yellow solid 25 mg (13%)
Melting Point: 124-128 °C
IR$_{Vmax}$ (ATR): 3376 (OH), 3065, 2977 (C-H), 1641, 1580 (C=C), 1530, 1330 (NO_2), 1173 (C-N) cm^{-1}
^{1}H NMR (400 MHz, $CDCl_3$) δ 1.26 - 1.30 (t, 3 H, CH_3), 2.87 (q, *J* = 7.32 Hz, 2 H, CH_2), 5.20 (br. s., 1 H, OH), 6.87 - 6.95 (m, 2 H, 2 x ArH), 7.00 (d, *J* = 7.94 Hz, 1 H, H6), 7.29 - 7.40 (m, 1 H, H5), 7.97 (s, 1 H, H1')
^{13}C NMR (101 MHz, $CDCl_3$) ppm 12.5 (CH_3), 20.7 (CH_2), 116.2 (CH), 117.1 (CH), 122.2 (CH), 130.2 (CH), 132.8 (CH), 133.9, 153.6 (C2'), 155.9 (C1)
HRMS (APCI) calculated for $C_{10}H_{10}NO_3$ [M^+-H] 192.0666: found 192.0661. Mass accuracy (-2.60 ppm).

(*E*)-1-Chloro-3-(2-nitrobut-1-en-1-yl)benzene (69) [455]

(*E*)-1-Chloro-3-(2-nitrobut-1-en-1-yl)benzene was prepared from 3-chlorobenzaldehyde (1 mmol, 0.14 g) according to general procedure 8.3. The product was purified by flash column chromatography over silica gel (eluent: dichloromethane : hexane 3:1).
Yellow oil 49 mg (23%)
IR$_{Vmax}$ (ATR): 3066, 2939.63 (C-H), 1657, 1621 (C=C), 1520, 1330 (NO_2), 1168 (C-N) cm^{-1}
^{1}H NMR (400 MHz, $CDCl_3$) δ 1.21 (t, *J* = 7.63 Hz, 3 H, CH_3), 2.75 - 2.84 (m, 2 H, CH_2), 7.21 - 7.28 (m, 1 H, H2), 7.28 - 7.41 (m, 3 H, 3 x ArH), 7.85 (s, 1 H, H1')
^{13}C NMR (101 MHz, $CDCl_3$) ppm 12.2 (CH_3), 20.5 (CH_2), 127.4 (CH), 129.1 (CH), 129.7 (CH), 130.1 (CH), 131.2 (C1'), 134.0, 134.7, 154.1 (C2')

HRMS (APCI) calculated for $C_{10}H_{10}NO_2Cl^{35}$ [M^+] 211.0395: found 211.0399. Mass accuracy (1.89 ppm).

(*E*)-4-Methoxy-2-(2-nitrobut-1-en-1-yl)phenol (70) [215]

(*E*)-4-Methoxy-2-(2-nitrobut-1-en-1-yl)phenol was prepared from 2-hydroxy-5-methoxybenzaldehyde (1 mmol, 0.15 g) according to general procedure general procedure 8.3. The product was purified by column chromatography (eluent 3:1 dichloromethane: hexane).
Yellow resin 20 mg (9%)
IRν_{max} (ATR): 3482 (OH), 3084, 2923 (C-H), 1642, 1586 (C=C), 1540, 1363 (NO_2), 1191 (C-N) cm^{-1}
^{1}H NMR (400 MHz, $CDCl_3$) δ 1.26 (t, J = 7.32 Hz, 3 H, CH_3) 2.84 (q, J = 7.32 Hz, 2 H, CH_2) 3.93 (s, 3 H, OCH_3) 6.05 (s, 1 H, H3) 6.92 (s, 2 H, H5 & H6) 8.23 (s, 1 H, H1')
^{13}C NMR (101 MHz, $CDCl_3$) ppm 12.4 (CH_3), 21.0 (CH_2), 56.1 (OCH_3), 111.8, 118.8 (CH), 119.8 (CH), 121.0 (CH), 128.2 (C1'), 145.0 (C1), 146.6 (C2'), 153.3 (C4)
HRMS (APCI) calculated for $C_{11}H_{12}NO_4$ [M^+-H] 222.0772: found 222.0765. Mass accuracy (-3.15 ppm).

(*E*)-3-(2-Nitrobut-1-en-1-yl)furan (79)

(*E*)-3-(2-Nitrobut-1-en-1-yl)furan was prepared from 3-furaldehyde (3.6 mmol, 0.345 g) according to general procedure 8.3. The product was purified by flash column chromatography over silica gel (eluent: dichloromethane / hexane 3/1).
Yellow resin 205 mg (30%)
IRν_{max} (KBr): 2979 (CH), 1655 (C=C), 1518, 1328 (NO_2) cm^{-1}
^{1}H NMR (400 MHz, $CDCl_3$) δ 1.27 (t, 3 H, J = 7.5 Hz, -CH_3), 2.89 (q, 2 H, J = 7.5 Hz, -CH_2), 6.64 (s, 1 H, ArH), 7.55-7.58 (m, 1 H, ArH), 7.80 (s, 1 H, ArH), 7.91 (s, 1 H, H1)
^{13}C NMR (101 MHz, $CDCl_3$) ppm 12.0 (C4), 21.1 (C3), 109.6, 118.7, 123.7, 144.9, 146.2 (C4'), 151.4 (C2)
HRMS (ESI) calculated for $C_8H_9NO_3Na$ [M^++Na] 190.0480: found 190.0486. Mass accuracy (3.16 ppm).

(*E*)-3-(2-Nitrobut-1-en-1-yl)thiophene (80)

(*E*)-3-(2-Nitrobut-1-en-1-yl)thiophene was prepared from 3-thiophenecarboxaldehyde (3.6 mmol, 0.403 g) according to general procedure 8.3. The product was purified by flash column chromatography over silica gel (eluent: dichloromethane / hexane 3/1) and recrystallised from ethanol.
Yellow crystals 314 mg (48%)
Melting Point: 47-50 °C
IRν_{max} (KBr): 2976 (CH), 1646 (C=C), 1514, 1323 (NO_2) cm^{-1}
^{1}H NMR (400 MHz, $CDCl_3$) δ 1.31 (t, 3 H, J = 7.5 Hz, -CH_3), 2.95 (q, 2 H, J = 7.5 Hz, -CH_2), 7.29 (d, 1 H, J = 4 Hz, H5'), 7.46 (q, 1 H, J = 4 Hz, 1 Hz, H4'), 7.63 (s, 1 H, H2'), 8.05 (s, 1 H, H1)
^{13}C NMR (101 MHz, $CDCl_3$) ppm 11.7 (C4), 20.6 (C3), 126.6, 126.8, 129.5, 133.0 (C1), 151.2 (C2)
HRMS (ESI) calculated for $C_8H_8NO_2S$ [M^+–H] 182.0470: found 182.0461. Mass accuracy (-4.94 ppm).

(*E*)-2-(2-Nitrobut-1-en-1-yl)thiophene (81)

(*E*)-3-(2-Nitrobut-1-en-1-yl)thiophene was prepared from 2-thiophenecarboxaldehyde (3.6 mmol, 0.404 g) according to general procedure 8.3. The product was purified by flash column chromatography over silica gel (eluent: dichloromethane : hexane 3/1).
Yellow Resin 384 mg (58%)
Melting Point: N/A (lit. M.p. 32 °C[436])
IRν_{max} (KBr): 2978 (CH), 1643 (C=C), 1519, 1370 (NO_2) cm^{-1}
^{1}H NMR (400 MHz, $CDCl_3$) δ 1.29 (t, 3 H, *J* = 7.5 Hz, -CH_3), 3.04 (q, 2 H, *J* = 7.5 Hz, -CH_2), 7.20 (dd, 1 H, *J* = 3.8 Hz, H4'), 7.43 (d, 1 H, *J* =3.8 Hz, ArH), 7.65 (dd, 1 H, *J* = 3.8 Hz, ArH), 8.26 (s, 1 H, H1)
^{13}C NMR (101 MHz, $CDCl_3$) ppm 11.6 (C4), 21.4 (C3), 126.7, 128.2, 131.7, 134.7, 134.9 (C1), 149.9 (C2)
HRMS (ESI) calculated for $C_8H_{10}NO_2S$ [M^++H] 184.0427: found 184.0423. Mass accuracy (-2.20 ppm).

(*E*)-2-Methyl-5-(2-nitrobut-1-en-1-yl)thiophene (82)

(*E*)-2-Methyl-5-(2-nitrobut-1-en-1-yl)thiophene was prepared from 5-methyl-2-thiophenecarboxaldehyde (3.6 mmol, 0.454 g) according to general procedure 8.3. The product was purified by flash column chromatography over silica gel (eluent: dichloromethane : hexane 3/1) and recrystallised from ethanol.
Orange crystals 395 mg (56%)
Melting Point: 89-90 °C
IRν_{max} (KBr): 2973 (CH), 1635 (C=C), 1503, 1316 (NO_2) cm^{-1}
^{1}H NMR (400 MHz, $CDCl_3$) δ 1.26 (t, 3 H, *J* = 7.5 Hz, -CH_3), 2.59 (s, 1 H, -CH_3 on C1" thiophene ring), 3.99 (q, 2 H, *J* = 7.5 Hz, -CH_2), 6.85 (s, 1 H, ArH), 7.25 (s, 1 H, ArH), 8.19 (s, 1 H, H1)
^{13}C NMR (101 MHz, $CDCl_3$) ppm 11.2 (C4), 15.4 (C1''), 20.9 (C3), 126.3, 126.9, 132.2, 135.5 (C1), 147.5 (C2 / C2'), 148.0 (C2 / C2')
HRMS (ESI) calculated for $C_9H_{10}NO_2S$ [M^+–H] 196.0427: found 196.0418. Mass accuracy (-4.59 ppm).

8.4 General procedure for preparation of nitroethanes (84, 84, 89)

To a vigorously stirred mixture of the appropriate nitroethene (3.68 mmol), silica gel (9.30 g) and propan-2-ol (100 mL) in dichloromethane (350 mL) at room temperature there was added $NaBH_4$ (15.5 mmol, 0.59 g). The mixture was stirred until the solution turned colourless (~ 20 min). Excess $NaBH_4$ was quenched with the addition of dilute HCl (50 mL). The mixture was filtered and the silica gel was washed with dichloromethane (100 mL). All organic phases were combined and washed with brine (3 x 50 mL) and water (3 x 50 mL). The organic phases were then dried over anhydrous Mg_2SO_4 and the solvent removed *in vacuo,* to give an oil which was then purified by flash chromatography over silica gel to afford the product.

1-(4-Chlorophenyl)-1-nitroethane (83)[460]

1-(4-Chlorophenyl)-1-nitroethane was prepared from (*E*)-1-(4-chlorophenyl)-1-nitroethene (36.8 mmol, 6.76 g) according to general procedure 8.4. No further purification was required.
Brown Oil 6.06 g (89%)
IRν_{max} (KBr): 3023 (CH), 1613 (C=C), 1542, 1350 (NO_2), 815 (C-Cl) cm^{-1}

^{1}H NMR (400 MHz, $CDCl_3$) δ 3.31 (t, 2 H, *J* = 7.3 Hz, CH_2), 4.62 (t, 2 H, *J* = 7.3 Hz, CH_2), 7.17 (d, 2 H, *J* = 8 Hz, H2'/H6'), 7.32 (d, 2 H, *J* = 8.5 Hz, H3'/H5')
^{13}C NMR (101 MHz, $CDCl_3$) ppm 32.7 (C2), 76.0 (C1), 129.1 (C2'/C6'), 130.0 (C3'/C5'), 133.4 (C1'), 134.1 (C4')
HRMS (APCI) calculated for $C_8H_8Cl^{35}NO_2$ [M^+] 185.0244: found 185.0250. Mass accuracy (3.24 ppm).

(2-Nitroethyl)benzene (84)

(2-Nitroethyl)benzene was prepared from (*E*)-(2-nitrovinyl)benzene (36.8 mmol, 5.48 g) according to general procedure 8.4. No further purification was required.
Brown oil 5.09 g (91%[461])
IRν_{max} (KBr): 3050 (CH), 1658 (C=C), 1530, 1371 (NO_2) cm^{-1}
^{1}H NMR (400 MHz, $CDCl_3$) δ 3.35 (t, 2 H, *J* = 7.8 Hz, CH_2), 4.64 (t, 2 H, *J* = 7.8 Hz, CH_2), 7.23 (d, 2 H, *J* = 6.8 Hz, H2'/H6'), 7.31-7.34 (m, 1 H, H4'), 7.35-7.39 (m, 2 H, H3'/H5')
^{13}C NMR (101 MHz, $CDCl_3$) ppm 33.4 (CH_2), 76.3 (CH_2), 127.4, 128.5, 129.0
HRMS (APCI) calculated for $C_8H_{10}NO_2$ [M^+] 152.0706: found 152.0706. Mass accuracy (0 ppm).

4,4'-(2-Nitropropane-1,3-diyl)bis(chlorobenzene) (89)

4,4'-(2-Nitropropane-1,3-diyl)bis(chlorobenzene) was prepared from (*E*)-4,4'-(2-nitroprop-1-ane-1,3-diyl)bis(chlorobenzene) (1 mmol) according to general procedure 8.4. No further purification was necessary.
Colourless oil 309 mg (90%)
IRν_{max} (ATR): 3089, 2981 (CH), 1620 (C=C), 1533, 1326 (NO_2) cm^{-1}
^{1}H NMR (400 MHz, $CDCl_3$) δ 3.06 (dd, 2 H, *J* = 14.67, 5.87 Hz, 2 x Ha), 3.28 (dd, 2 H, *J* = 14.67, 5.87 Hz, 2 x Hb), 4.80-4.91 (m, 1 H, CH), 7.09 (d, 4 H, *J* = 7.8 Hz, 4 x ArH), 7.33 (d, 4 H, *J* = 7.8 Hz, 4 x ArH)
^{13}C NMR (101 MHz, $CDCl_3$) ppm 38.9 (2 x CH_2), 90.6 (CH), 129.12 (CH), 130.15 (CH), 133.5, 133.6
HRMS (ESI) calculated for $C_{15}H_{13}Cl_3{}^{35}NO_2$ [M^++Cl] 344.0012: found 344.0022. Mass accuracy (2.91 ppm).

8.5 General procedure for preparation of (*E*)-1,3-bis(aryl)-2-nitro-1-propenes (85 – 88)

A mixture of the appropriate 1-(aryl)-1-nitroethane (15.0 mmol), dimethylamine hydrochloride (30.0 mmol), potassium fluoride (2.25 mmol) and the appropriate aldehyde (15.0 mmol) in toluene (20 mL) was refluxed using a Dean-Stark trap for 24 h. The reaction was then diluted with toluene (100 mL) and washed with 10% aq. HCl (3 x 30 mL). The organic phase was dried over anhydrous Mg_2SO_4 and solvent removed *in vacuo*. The product was purified by flash chromatography over silica gel (eluent: 10:1 hexane / ethyl acetate).

(*E*)-4,4'-(2-Nitroprop-1-ene-1,3-diyl)bis(chlorobenzene) (85)

(*E*)-4,4'-(2-Nitroprop-1-ene-1,3-diyl)bis(chlorobenzene) was prepared from 4-chlorobenzaldehyde (15.0 mmol) and 1-chloro-4-(2-nitroethyl)benzene (15.0 mmol) according to general procedure 8.5. The product was purified by flash column chromatography over silica gel (eluent: 10:1 hexane / ethyl acetate) and recrystallised from ethanol.

Yellow crystals 2.30 g (50%)
Melting Point: 75-77 °C (lit. M.p. 74-76 °C[5])
IRν_{max} (KBr): 3110 (CH), 1671 (C=C), 1549, 1369 (NO_2) cm^{-1}
^{1}H NMR (400 MHz, $CDCl_3$) δ 4.22 (s, 2 H, CH_2), 7.14 (d, 2 H, *J* = 8 Hz, H3''/H5''), 7.32 (d, 2 H, *J* = 8.5 Hz, H2''/H6''), 7.37 (d, 2 H, *J* = 8.6 Hz, H3'/H5'), 7.43 (d, 2 H, *J* = 8.6 Hz, H2'/H6'), 8.28 (1H, s, H1)
^{13}C NMR (101 MHz, $CDCl_3$) ppm 31.9 (C3'), 128.5, 128.7, 129.1, 129.7, 130.4, 132.6, 133.9, 134.1, 136.4 (C4), 149.0 (C2')
HRMS (ESI) calculated for $C_{15}H_{11}Cl_2{}^{35}NO_2$ [M^+] 307.0161: found 307.0155. Mass accuracy (-1.97 ppm).

(*E*)-1-Chloro-4-(2-nitro-3-phenylprop-1-en-1-yl)benzene (86)

(*E*)-1-Chloro-4-(2-nitro-3-phenylprop-1-en-1-yl)benzene was prepared from 4-chlorobenzaldehyde (15.0 mmol) and (2-nitroethyl)benzene (15.0 mmol) according to general procedure 8.5. The product was purified by flash column chromatography over silica gel (eluent: 10:1 hexane / ethyl acetate).
Yellow Oil 1.33 g (30%)
IRν_{max} (ATR): 3111 (CH), 1674 (C=C), 1553, 1368 (NO_2) cm^{-1}
^{1}H NMR (400 MHz, $CDCl_3$) δ 4.25 (s, 2 H, H3), 7.20 (d, 2 H, *J* = 7.6 Hz, H3), 7.32-7.42 (m, 6 H, 6 x ArH), 8.27 (s, 1 H, H1)
^{13}C NMR (101 MHz, $CDCl_3$) ppm 32.9 (C3'), 127.1, 127.52, 129.0, 130.4, 134.2, 135.8, 136.7 (C4), 149.1 (C2')
HRMS (ESI) calculated for $C_{15}H_{12}Cl^{35}NO_2Na$ [M^++Na] 296.0454: found 296.0463. Mass accuracy (3.04 ppm).

(*E*)-1-Chloro-4-(2-nitro-3-phenylallyl)benzene (87)

(*E*)-1-Chloro-4-(2-nitro-3-phenylallyl)benzene was prepared from benzaldehyde (15.0 mmol) and 1-chloro-4-(2-nitroethyl)benzene (15.0 mmol) according to general procedure 8.5. The product was purified by flash column chromatography over silica gel (eluent: 10:1 hexane / ethyl acetate).
Yellow oil 1.11 g (25%)
IRν_{max} (ATR): 3116 (CH), 1668 (C=C), 1554, 1373 (-NO_2) cm^{-1}
^{1}H NMR (400 MHz, $CDCl_3$) δ 4.25 (s, 2 H, H3), 7.17 (d, 2 H, *J* = 8.5 Hz, 2 x ArH), 7.32 (d, 2 H, *J* = 8.5 Hz, 2 x ArH), 7.43-7.50 (m, 5 H, 5 x ArH), 8.35 (s, 1 H, H1)
^{13}C NMR (101 MHz, $CDCl_3$) ppm 32.5 (C3'), 126.5, 127.2, 128.5, 128.7, 129.2, 130.0, 131.6 (C1'), 135.1 (C4), 148.7 (C2')
HRMS (ESI) calculated for $C_{15}H_{12}Cl^{35}NO_2Na$ [M^++Na] 296.0454: found 296.0463. Mass accuracy (3.04 ppm).

(*E*)-2-Nitro-1,3-diphenylprop-1-ene (88)

(*E*)-2-Nitro-1,3-diphenylprop-1-ene was prepared from benzaldehyde (15.0 mmol) and (2-nitroethyl)benzene (15.0 mmol) according to procedure 5.6. The product was purified by flash column chromatography over silica gel (eluent: 10:1 hexane / ethyl acetate).
Brown Oil 0.786 g (20%[173])
IRν_{max} (ATR): 3116 (CH), 1665 (C=C), 1530, 1353 (NO_2) cm^{-1}

^{1}H NMR (400 MHz, $CDCl_3$) δ 4.30 (s, 2 H, H3), 7.24 (d, 2 H, *J* = 8 Hz, ArH), 7.29-7.32 (m, 1 H, ArH), 7.36 (t, 2 H, *J* = 6.5 Hz, ArH), 7.42-7.52 (m, 5 H, 5 x ArH), 8.34 (s, 1 H, H1)
^{13}C NMR (101 MHz, $CDCl_3$) ppm 32.5 (C3), 126.5, 127.2, 128.5, 129.2, 130.0, 131.6 (C1'), 147.9 (C2')
HRMS (ESI) calculated for $C_{15}H_{13}NO_2Na$ [M^++Na] 262.0844: found 262.0843. Mass accuracy (-0.38 ppm).

8.6 General procedure for preparation of (*E*)-2-nitro-1,3-diphenylprop-2-en-1-ones (90 – 94)

A mixture of nitroacetophenone (4.00 g, 25 mmol), the appropriate benzaldehyde (40 mmol), β-alanine (0.188 g) and glacial acetic acid (4 mL) in benzene (40 mL) was refluxed for 3 h using a Dean-Stark trap. The reaction mixture was washed with water (3 x 5 mL) and the benzene was removed *in vacuo*. The product was purified using flash chromatography over silica gel (eluent: 8:1 hexane / ethyl acetate).

(*E*)-2-Nitro-1,3-diphenylprop-2-en-1-one (90)

(*E*)-2-Nitro-1,3-diphenylprop-2-en-1-one was prepared from benzaldehyde (40.0 mmol) according to general procedure 8.6. The product was purified by flash column chromatography over silica gel (eluent: 8:1 hexane / ethyl acetate) and recrystallised from ethanol.
Yellow crystals 4.14 g (60%)
Melting Point: 90-91 °C (lit. M.p. 92 °C[152])
IR$_{Vmax}$ (KBr): 3061 (CH), 1674 (C=O), 1634 (C=C), 1525, 1318 (NO_2) cm^{-1}
^{1}H NMR (400 MHz, $CDCl_3$) δ 7.34 (d, *J* =7.5 Hz, 2 H, 2 x ArH), 7.43 (d, *J* = 8 Hz, 3 H, 3 x ArH), 7.46-7.58 (m, 2 H, 2 x ArH), 7.60-7.70 (m, 1 H, 1 x ArH), 7.99 (d, 2 H, *J* = 8 Hz, 2 x ArH), 8.37 (s, 1 H, H3)
^{13}C NMR (101 MHz, $CDCl_3$) ppm 128.5, 128.8 (CH), 128.9 (CH), 128.9 (CH), 129.0, 130.7 (CH), 131.9 (CH), 134.5 (CH), 134.6, 137.0 (C3), 144.3 (C2), 187.8 (C=O)
HRMS (ESI) calculated for $C_{15}H_{11}NO_3Na$ [M^++Na] 276.0637: found 276.0650. Mass accuracy (4.71 ppm).

(*E*)-3-(4-Chlorophenyl)-2-nitro-1-phenylprop-2-en-1-one (91)

(*E*)-3-(4-Chlorophenyl)-2-nitro-1-phenylprop-2-en-1-one was prepared from 4-chlorobenzaldehyde (40.0 mmol) according to general procedure 8.6. The product was purified by flash column chromatography over silica gel (eluent: 95:5 hexane / ethyl acetate).
Yellow resin 3.48 g (45%[462])
IR$_{Vmax}$ (KBr): 3062 (CH), 1668 (C=O), 1639 (C=C), 1531, 1324 (NO_2) cm^{-1}
^{1}H NMR (400 MHz, $CDCl_3$) δ 7.33 (d, *J* = 6.5 Hz, 2 H, 2 x ArH), 7.37 (d, *J* = 6.5 Hz, 2 H, 2 x ArH), 7.50-7.60 (m, 2 H, H3'' & H5''), 7.65-7.73 (m, 1 H, H4''), 7.96 (d, *J* = 7 Hz, 2 H, 1 x ArH), 8.31 (s, 1 H, H3)
^{13}C NMR (101 MHz, $CDCl_3$) ppm 126.9, 128.8 (CH), 128.9 (CH), 129.3 (CH), 131.7 (CH), 134.4, 134.8 (CH), 135.5 (C3), 138.2, 144.6 (C2), 187.6 (C=O)
HRMS (ESI) calculated for $C_{15}H_{10}Cl^{35}NO_3Na$ [M^++Na] 310.0247: found 310.0244. Mass accuracy (-0.96 ppm).

(*E*)-3-(4-Hydroxyphenyl)-2-nitro-1-phenylprop-2-en-1-one (92)

(*E*)-3-(4-Hydroxyphenyl)-2-nitro-1-phenylprop-2-en-1-one was prepared from 4-hydroxybenzaldehyde (40.0 mmol) according to general procedure 8.6. The product was purified by flash column chromatography over silica gel (eluent: dichloromethane).
Orange resin 2.01 g (30%)
IR$_{\nu max}$ (KBr): 3390 (OH), 3066 (CH), 1672 (C=O), 1600 (C=C), 1516, 1307 (NO_2) cm^{-1}
^{1}H NMR (400 MHz, $CDCl_3$) δ 6.58 (br.s., 1 H, -OH), 6.77 (d, *J* = 7 Hz, 2 H, 2 x ArH), 7.32 (d, *J* = 7 Hz, 2 H, 2 x ArH), 7.50-7.59 (m, 2 H, H3'' & H5''), 7.64-7.66 (m, 1 H, H4''), 7.99 (d, *J* = 7.5 Hz, 2 H, 2 x ArH), 8.31 (s, 1 H, H3)
^{13}C NMR (101 MHz, $CDCl_3$) ppm 116.2 (CH), 120.7 (C1'), 128.8 (CH), 128.9 (CH), 133.4 (CH), 134.6 (CH), 137.4 (C3), 141.8 (C2), 159.6 (C4'), 188.8 (C=O)
HRMS (ESI) calculated for $C_{15}H_{10}NO_4$ [M^+-H] 268.0615: found 268.0626. Mass accuracy (4.10 ppm).

(*E*)-3-(Naphthalen-1-yl)-2-nitro-1-phenylprop-2-en-1-one (93)

(*E*)-3-(Naphthalen-1-yl)-2-nitro-1-phenylprop-2-en-1-one was prepared from 1-naphthaldehyde (40.0 mmol) according to general procedure 8.6. The product was recrystallised from ethanol.
Yellow crystals 3.26 g (40%)
Melting Point: 136-138 °C
IR$_{\nu max}$ (KBr): 3062 (CH), 1679 (C=O), 1634 (C=C), 1525, 1316 (NO_2) cm^{-1}
^{1}H NMR (400 MHz, $CDCl_3$) δ 7.31 (dd, *J* = 7.5 Hz, 1 H, 1 x ArH), 7.39 (dd, *J* = 8 Hz, 1 H, 1 x ArH), 7.51 (d, *J* = 6.5 Hz, 1 H, 1 x ArH), 7.55 (d, *J* = 7.5 Hz, 1 H, 1 x ArH), 7.61 (dd, *J* = 8 Hz, 1 H, 1 x ArH), 7.70 (m, *J* = 8 Hz, 1 H, 1 x ArH), 7.88 (d, *J* = 8 Hz, 2 H, 1 x ArH), 7.92 (d, *J* = 7.5 Hz, 2 H, 1 x ArH), 8.14 (d, *J* = 8 Hz, 1 H, 1 x ArH), 9.14 (s, 1 H, H3)
^{13}C NMR (101 MHz, $CDCl_3$) ppm 122.9, 124.9, 125.6, 126.5, 127.4, 128.3, 128.6, 128.7, 131.1, 132.0, 133.0, 134.3, 134.5, 134.6 (C3), 145.9 (C2), 187.4 (C=O)
HRMS (ESI) calculated for $C_{19}H_{13}NO_3$ [M^++Na] 326.0793: found 326.0782. Mass accuracy (-3.37 ppm).

(*E*)-3-(5-Bromo-2-methoxyphenyl)-2-nitro-1-phenylprop-2-en-1-one (94)

(*E*)-3-(5-Bromo-2-methoxyphenyl)-2-nitro-1-phenylprop-2-en-1-one was prepared from 5-bromo-2-methoxybenzaldehyde (40.00 mmol) according to general procedure 8.6. The product was purified by flash column chromatography over silica gel (eluent: dichloromethane). The product was recrystallised from ethanol.
Yellow Crystals 7.02 g (78%)
Melting Point: 172-176 °C
IR ν_{max} (KBr): 3066, 2970 (CH), 1675 (C=O), 1592 (C=C), 1530, 1356 (NO_2) cm^{-1}
^{1}H NMR (400 MHz, $CDCl_3$) δ 3.60 (s, 3 H, OCH_3), 6.74 (d, *J*=8.71 Hz, 1 H, H3), 7.37 - 7.57 (m, 4 H, 4 x ArH), 7.57-7.67 (m, *J* = 7.46 Hz, 1 H, H4"), 7.93 (d, *J* = 7.46 Hz, 2 H, H6" & H2"), 8.43 (s, 1 H, H3)
^{13}C NMR (101 MHz, $CDCl_3$) ppm 112.9 (CH), 113.0, 128.9 (CH), 129.0 (CH), 131.8 (CH), 134.0 (CH), 134.4 (CH), 135.3, 136.2 (C3), 138.3, 146.1 (C2), 157.2 (C2"), 187.1 (C=O)

HRMS (APCI) calculated for $C_{16}H_{12}Br^{79}NO_4$ [M^+] 360.9950: found 360.9956. Mass accuracy (1.66 ppm).

8.7 General procedure for Michael additions of amines and thiols to nitrostyrenes (95 – 100)

To a mixture of the required nitrostyrene (1 mmol) in water (4 mL) was added the appropriate thiol / amine (1.1 mmol). The reaction was stirred at room temperature overnight. The aqueous reaction mixture was extracted with dichloromethane. The organic layer was washed with water, brine and dried over anhydrous sodium sulphate. Solvent was removed *in vacuo*. No further purification was required.

Ethyl(2-nitro-1-phenylethyl)sulfane (95)

Ethyl(2-nitro-1-phenylethyl)sulfane was prepared from (*E*)-(2-nitrovinyl)benzene (0.149 g, 1 mmol) and ethanethiol according to general procedure 8.7.
Brown oil 106 mg (50%[170])
IR$_{Vmax}$ (ATR): 3031, 2996 (C-H), 1634 (C=C), 1550, 1374 (NO_2), 1158 (C-N) cm^{-1}
^{1}H NMR (400 MHz, $CDCl_3$) δ 1.23 (t, J = 7.32 Hz, 3 H, CH_3), 2.42 - 2.53 (m, 2 H, CH_2), 4.54 - 4.63 (m, 1 H, CH), 4.76 (d, J = 7.94 Hz, 2 H, CH_2NO_2), 7.28 - 7.41 (m, 5 H, 5 x ArH)
^{13}C NMR (101 MHz, $CDCl_3$) ppm 14.3 (CH_3), 25.6 (CH_2S), 46.2 (C1), 79.3 (C2), 127.6 (CH), 128.4 (CH), 129.0 (CH), 137.4 (C1')
HRMS (APCI) calculated for $C_{10}H_{14}NO_2S$ [M^++H] 212.0745: found 212.0748. Mass accuracy (1.41 ppm).

(1-(5-Bromo-2-methoxyphenyl)-2-nitroethyl)(ethyl)sulfane (96)

(1-(5-Bromo-2-methoxyphenyl)-2-nitroethyl)(ethyl)sulfane was prepared from (*E*)-4-bromo-1-methoxy-2-(2-nitrovinyl)benzene (0.32 g, 1 mmol) and ethanethiol according to general procedure 8.7.
Brown oil 286 mg (90%)
IR$_{Vmax}$ (ATR): 3011, 2966 (C-H), 1639 (C=C), 1550, 1374 (NO_2), 1132 (C-N) cm^{-1}
^{1}H NMR (400 MHz, $CDCl_3$) δ 1.24 (t, J = 7.48 Hz, 3 H, CH_3), 2.55 (q, J = 7.46 Hz, 2 H, CH_2), 3.86 (s, 3 H, OCH_3), 4.65 - 4.85 (m, 3 H, CH & CH_2), 6.79 (d, J = 8.71 Hz, 1 H, H3), 7.38 (d, J = 8.71 Hz, 1 H, H4), 7.46 (d, J = 2.49 Hz, 1 H, H6)
^{13}C NMR (101 MHz, $CDCl_3$) ppm 14.5 (CH_3), 26.6 (CH_2S), 41.0 (C1'), 56.0 (OCH_3), 78.3 (C2'), 112.9 (C3), 113.1 (C5), 128.1 (C1), 131.2 (C4), 132.1 (C6), 156.0 (C2)
HRMS (APCI) calculated for $C_{11}H_{14}NO_3Br^{79}S$ [M^+] 318.9878: found 318.9878. Mass accuracy (0 ppm).

(1-(5-Bromo-2-methoxyphenyl)-2-nitroethyl)(phenyl)sulfane (97)

(1-(5-Bromo-2-methoxyphenyl)-2-nitroethyl)(phenyl)sulfane was prepared from (*E*)-4-bromo-1-methoxy-2-(2-nitrovinyl)benzene (0.32 g, 1 mmol) and thiophenol according to general procedure 8.7.
Brown Oil 256 mg (70%)
IR$_{Vmax}$ (ATR): 3056, 3016 (C-H), 1628 (C=C), 1553, 1364 (NO_2), 1250 (C-N) cm^{-1}

^{1}H NMR (400 MHz, $CDCl_3$) δ 3.83 (s, 3 H, OCH_3), 4.74 (dd, *J* = 13.27, 7.05 Hz, 1 H, Ha), 4.86 (dd, *J*=13.06, 8.50 Hz, 1 H, Hb), 5.17 (dd, *J* = 8.50, 7.26 Hz, 1 H, H4'), 6.76 (d, *J* = 8.71 Hz, 1 H, 1 x ArH), 7.18 (d, *J* = 2.49 Hz, 1 H, H2'), 7.29 - 7.34 (m, 3 H, 3 x ArH), 7.35 - 7.40 (m, 3 H, 3 x ArH), 7.47 - 7.53 (m, 1 H, 1 x ArH)
^{13}C NMR (101 MHz, $CDCl_3$) ppm 44.5 (C1), 55.9 (OCH_3), 77.4 (C2), 112.9 (s), 127.1, 127.5 (CH), 128.7 (CH), 129.0 (CH), 129.2 (CH), 130.9 (CH), 132.2 (CH), 133.7 (CH), 136.9 (C1'), 155.9 (C2')
HRMS (APCI) calculated for $C_{15}H_{14}NO_3Br^{79}S$ [M^+] 366.9878: found 366.9876. Mass accuracy (-0.54 ppm).

N-(2-Nitro-1-phenylethyl)aniline (98)

N-(2-Nitro-1-phenylethyl)aniline was prepared from (*E*)-(2-nitrovinyl)benzene (0.149 g, 1 mmol) and aniline according to general procedure 8.7.
Brown oil 206 mg (85%)
Melting point: N/A (lit. M.p. 86-87.5 °C[463])
IR$_{Vmax}$ (ATR): 3377 (NH), 3055, 3027 (C-H), 1601.52 (C=C), 1544, 1379 (NO_2), 1181 (C-N) cm^{-1}
^{1}H NMR (400 MHz, $CDCl_3$) δ 4.48 (d, *J* = 5.49 Hz, 1 H, NH) 4.68 - 4.75 (m, 2 H, CH_2) 5.23 (d, *J* = 6.10 Hz, 1 H, CH) 6.68 (m, 1 H, 1 x ArH) 6.72 - 6.75 (m, 1 H, 1 x ArH) 6.80 - 6.85 (m, 1 H, 2 x ArH) 7.21 (m, 2 H, 2 x ArH) 7.32 - 7.46 (m, 5 H, 5 x ArH)
^{13}C NMR (101 MHz, $CDCl_3$) ppm 56.6 (CH), 79.9 (C2), 113.9 (CH), 118.9 (CH), 126.4 (CH), 128.6 (CH), 129.3 (CH), 129.3 (CH), 137.7 (C1'), 145.6 (C1")
HRMS (APCI) calculated for $C_{14}H_{15}N_2O_2$ [M^++H] 243.1134: found 243.1128. Mass accuracy (-2.47 ppm).

N-(1-(4-Chlorophenyl)-2-nitroethyl)aniline (99)

N-(1-(4-Chlorophenyl)-2-nitroethyl)aniline was prepared from (*E*)-1-chloro-4-(2-nitrovinyl)benzene (0.183 g, 1 mmol) and aniline according to general procedure 8.7.
Brown oil 210 mg (76%[170])
IR$_{Vmax}$ (ATR): 3400 (NH), 3091, 3053 (Ar C-H), 1601 (Ar C=C), 1548, 1376 (NO_2), 1212 (C-N) cm^{-1}
^{1}H NMR (400 MHz, $CDCl_3$) δ 4.47 (br. s., 1 H, NH) 4.68 (d, *J* = 6.10 Hz, 2 H, CH_2) 5.17 (t, *J* = 6.41 Hz, 1 H, CH) 6.62 (d, *J* = 7.94 Hz, 2 H, 2 x ArH) 6.72 (d, *J* = 7.32 Hz, 1 H, 1 x ArH) 6.81 (t, *J* = 7.32 Hz, 1 H, H4") 7.20 (d, *J* = 6.71 Hz, 2 H, 2 x ArH) 7.33 - 7.38 (m, 3 H, 3 x ArH)
^{13}C NMR (101 MHz, $CDCl_3$) ppm 56.1 (CH), 79.8 (C2), 113.9 (CH), 119.2 (CH), 127.8 (CH), 129.4 (CH), 129.5 (CH), 134.5, 136.2, 145.3 (C1")
HRMS (APCI) calculated for $C_{14}H_{14}N_2O_2Cl^{35}$ [M^++H] 277.0744: found 277.0738. Mass accuracy (-2.16 ppm).

N-(1-(4-Bromophenyl)-2-nitroethyl)aniline (100)

N-(1-(4-Bromophenyl)-2-nitroethyl)aniline was prepared from (*E*)-1-bromo-4-(2-nitrovinyl)benzene 0.23 g (1 mmol) and aniline according to general procedure 8.7.
Brown oil 224 mg (70%)

IR$_{Vmax}$ (ATR): 3400 (NH), 3026 (C-H), 1601 (C=C), 1548, 1335 (NO_2), 1211 (C-N) cm^{-1}
^{1}H NMR (400 MHz, $CDCl_3$) δ 4.43 (br. s., 1 H, NH), 4.57 - 4.70 (m, 2 H, CH_2), 5.12 (br. s., 1 H, CH), 6.53 - 6.62 (m, 2 H, 2 x ArH), 6.69 (d, *J* = 7.94 Hz, 1 H, 1 x ArH), 6.75 - 6.79 (m, 1 H, 1 x ArH), 7.16 - 7.18 (m, 1 H, 1 x ArH), 7.26 (dd, *J* = 8.24, 2.75 Hz, 2 H, 2 x ArH), 7.46 - 7.54 (m, 2 H, 2 x ArH)
^{13}C NMR (101 MHz, $CDCl_3$) ppm 56.1 (CH), 79.8 (C2), 113.9 (CH), 119.2 (CH), 122.6, 128.2 (CH), 129.4 (CH), 132.5 (CH), 137.8, 145.3 (C1")
HRMS (APCI) calculated for $C_{14}H_{14}N_2O_2Br^{79}$ [M^++H] 320.0160: found 320.0163. Mass accuracy (0.94 ppm).

8.8 General procedure for preparation of ethyl (*E*)-2-hydroxy-3-nitro-4-phenylbut-3-enoates (101 - 104)

To a stirred solution of DMAP (50 mg, 40 mol %), the required nitroalkene (1 mmol) in acetonitrile (1 mL) was added ethyl glyoxylate (4 mmol). The reaction was stirred at room temperature and monitored by TLC. After completion the reaction was diluted with water and extracted with ethyl acetate. The organic layer was extracted with water, brine and dried over anhydrous sodium sulphate. The organic phase was concentrated *in vacuo*. The product was purified by column chromatography (eluent 2:1 - hexane : ethyl acetate).

Ethyl (*E*)-4-(5-bromo-2-methoxyphenyl)-2-hydroxy-3-nitrobut-3-enoate (101)

Ethyl (*E*)-4-(5-bromo-2-methoxyphenyl)-2-hydroxy-3-nitrobut-3-enoate was prepared from (*E*)-4-bromo-1-methoxy-2-(2-nitrovinyl)benzene (0.256 g, 1 mmol) according to general procedure 8.8. The product was purified by column chromatography (eluent 2:1 - hexane : ethyl acetate) and recrystallised from ethanol.
Yellow solid 208 mg (58%)
Melting Point: 123-125 °C
IR$_{Vmax}$ (ATR): 3326 (O-H), 3026, 2980 (C-H), 1730 (C=O), 1638, 1591 (C=C), 1528, 1325 (NO_2), 1190 (C-N stretch) cm^{-1}
^{1}H NMR (400 MHz, $CDCl_3$) δ 1.31 (t, *J* = 7.05 Hz, 3 H, CH_3), 3.90 (s, 3 H, OCH_3), 4.33 (dq, *J* = 1.87, 7.12 Hz, 2H, OCH_2), 5.18 (s, 1 H, CH), 6.86 (d, *J* = 9.12 Hz, 1 H, H3), 7.57 (dd, *J* = 8.71, 2.49 Hz, 1 H, H4), 7.67 (d, *J* = 2.49 Hz, 1 H, H6), 8.40 (s, 1 H, H4')
^{13}C NMR (101 MHz, $CDCl_3$) ppm 14.0 (CH_3), 56.0 (OCH_3), 63.1 (OCH_2), 65.9 (C2'), 112.6 (C3), 112.9 (C5), 121.9 (C1), 132.5 (C4), 134.1 (C6), 135.3 (C4'), 148.0 (C3'), 157.5 (C2), 170.4 (C=O)
HRMS (APCI) calculated for $C_{13}H_{14}Br^{79}NO_6$ [M^+] 359.0004: found 359.0005. Mass accuracy (-0.28 ppm).

Ethyl (*E*)-4-(4-chlorophenyl)-2-hydroxy-3-nitrobut-3-enoate (102)

Ethyl (*E*)-4-(4-chlorophenyl)-2-hydroxy-3-nitrobut-3-enoate was prepared from (*E*)-1-chloro-4-(2-nitrovinyl)benzene (0.18 g, 1 mmol) according to general procedure 8.8. The product was purified by column chromatography (3 : 1 – dichloromethane : hexane) and recrystallised from ethanol.
Yellow solid 129 mg (45%)
Melting Point: 100-102 °C (lit. M.p. 102 °C[171])

IR$_{Vmax}$ (ATR): 3328 (O-H), 3095, 3056, 2972 (C-H), 1766 (C=O), 1647, 1589 (C=C), 1539, 1337 (NO_2), 1216 (C-N stretch) cm^{-1}

^{1}H NMR (400 MHz, $CDCl_3$) δ 1.25 (t, *J* =7.05 Hz, 3 H, CH_3), 3.79 (br.s., 1 H, OH), 4.18 - 4.38 (m, 2 H, CH_2), 5.17 (s, 1 H, CH), 7.42 - 7.49 (m, 2 H, 2 x ArH), 7.49 - 7.57 (m, 2 H, 2 x ArH), 8.26 (s, 1 H, H4')

^{13}C NMR (101 MHz, $CDCl_3$) ppm 13.9 (CH_3), 63.0 (OCH_2), 65.7 (CH), 129.2, 129.5 (CH), 131.1 (CH), 137.4, 137.9 (CH), 148.0 (C3'), 170.2 (C=O)

HRMS (APCI) calculated for $C_{12}H_{13}Cl^{35}NO_5$ [M^++H] 286.0482: found 286.0479. Mass accuracy (-1.05 ppm).

Ethyl (*E*)-2-hydroxy-4-(4-hydroxyphenyl)-3-nitrobut-3-enoate (103)

Ethyl (*E*)-2-hydroxy-4-(4-hydroxyphenyl)-3-nitrobut-3-enoate was prepared from (*E*)-4-(2-nitrovinyl)phenol (0.17 g, 1 mmol) according to general procedure 8.8. The product was purified by column chromatography (eluent 5% methanol & 95% dichloromethane) and recrystallised from ethanol.

Yellow solid 106 mg (40%)

Melting Point: 141-144 °C

IR$_{Vmax}$ (ATR): 3327 (O-H), 3054, 2982 (C-H), 1744 (C=O), 1604, 1591 (C=C), 1522, 1330 (NO_2), 1209 (C-N stretch) cm^{-1}

^{1}H NMR (400 MHz, $CDCl_3$) δ 1.19 - 1.30 (m, 3 H, CH_3), 3.70 (br. s., 1 H, OH), 4.21 - 4.38 (m, 2 H, CH_2), 5.25 (s, 1 H, CH), 6.89 - 7.00 (m, 2 H, 2 x ArH), 7.44 - 7.58 (m, 2 H, 2 x ArH), 8.30 (s, 1 H, H4')

^{13}C NMR (101 MHz, $CDCl_3$) ppm 14.0 (CH_3), 63.0 (OCH_2), 66.0 (CH), 116.4 (CH), 129.1, 132.4 (CH), 136.0, 139.5 (CH), 158.5 (C3'), 170.7 (C=O)

HRMS (APCI) calculated for $C_{12}H_{13}NO_6$ [M^+] 267.0743: found 267.0742. Mass accuracy (-0.37 ppm).

Ethyl (*E*)-4-(3-chlorophenyl)-2-hydroxy-3-nitrobut-3-enoate (104) [464]

Ethyl (*E*)-4-(3-chlorophenyl)-2-hydroxy-3-nitrobut-3-enoate was prepared from (*E*)-1-chloro-3-(2-nitrovinyl)benzene (0.18 g, 1 mmol) according to general procedure 8.8. The product was purified by column chromatography (eluent 3:1 – dichloromethane : hexane).

Yellow oil 35 mg (12%)

IR $_{Vmax}$ (ATR): 3475 (O-H), 3058, 2981.18 (C-H), 1742 (C=O), 1645, 1591 (C=C), 1524, 1328 (NO_2), 1211 (C-N stretch) cm^{-1}

^{1}H NMR (400 MHz, $CDCl_3$) δ 1.27 (t, *J* = 7.26 Hz, 3 H, CH_3), 3.96 (br. s., 1 H, OH), 4.19 - 4.40 (m, 2 H, CH_2), 5.18 (s, 1 H, CH), 7.41 - 7.50 (m, 3 H, 3 x ArH), 7.55 (s, 1 H, H2), 8.23 (s, 1 H, H4')

^{13}C NMR (101 MHz, $CDCl_3$) ppm 13.9 (CH_3), 63.1 (OCH_2), 65.7 (CH), 127.7 (CH), 129.5 (CH), 130.4 (CH), 130.9 (CH), 132.5, 135.2, 137.4 (CH), 148.6 (C3'), 170.2 (C=O)

HRMS (APCI) calculated for $C_{12}H_{13}Cl^{35}NO_5$ [M^++H] 286.0482: found 286.0481. Mass accuracy (-0.35 ppm).

8.9 General procedure for synthesis of (*E*)-2-(2-nitrovinyl)cyclohexa-2,5-diene-1,4-diones (105 – 106)

To a rapidly stirred solution of the required (*E*)-1,4-dimethoxy-2-(2-nitrovinyl)benzene (1 mmol) in CH_3CN 5.2 mL was added a solution of ceric ammonium nitrate (1.2 g, 2.19 mmol) in 3:1 water / CH_3CN (2.1 mL). The reaction mixture was stirred for 10 min and was then washed with brine. The brine layer was extracted with CH_3CN and the CH_3CN layer was concentrated until the mixture began to phase separate. The mixture was then extracted with dichloromethane and washed with brine and water. The organic layer was dried over sodium sulphate and solvent removed *in vacuo*. The residual solid was purified by recrystallization (THF / cyclohexane).

(*E*)-2-(2-nitrovinyl)cyclohexa-2,5-diene-1,4-dione (105)

(*E*)-2-(2-nitrovinyl)cyclohexa-2,5-diene-1,4-dione was prepared from (*E*)-1,4-dimethoxy-2-(2-nitrovinyl)benzene 0.21 g (1 mmol) according to general procedure 8.9. The product was purified by recrystallisation from THF / cyclohexane.
Light brown solid 133 mg (75%)
Melting Point: 102–104 °C (lit. M.p. 104-106 °C[180])
IR$_{Vmax}$ (ATR): 3099, 3068 (C-H), 1752 (C=O), 1613, 1560 (C=C), 1560, 1366 (NO_2), 1214 (C-N stretch) cm^{-1}
^{1}H NMR (400 MHz, $CDCl_3$) δ 6.88 - 6.91 (m, 2 H, H5 & H6), 6.99 (d, *J* = 2.07 Hz, 1 H, H3), 7.63 (d, *J* =13.68 Hz, 1 H, H1'), 8.12 (d, *J* = 13.68 Hz, 1 H, H2')
^{13}C NMR (101 MHz, $CDCl_3$) ppm 130.1. 136.4, 136.8 (CH), 137.4 (CH), 137.9 (CH), 144.5 (C2), 184.8 (C=O), 186.0 (C=O)
HRMS (ESI) calculated for $C_8H_4NO_4$ [M^+-H] 178.0146: found 178.0148. Mass accuracy (1.12 ppm).

(*E*)-2-(2-nitroprop-1-en-1-yl)cyclohexa-2,5-diene-1,4-dione (106)

(*E*)-2-(2-nitroprop-1-en-1-yl)cyclohexa-2,5-diene-1,4-dione was prepared from (*E*)-1,4-dimethoxy-2-(2-nitroprop-1-en-1-yl)benzene 0.21 g (1 mmol) according to general procedure 8.9. The product was purified by recrystallisation from THF / cyclohexane.
Light brown solid 119 mg (62%)
Melting Point: 89–92 °C (lit. M.p. 91-92 °C[252])
IR$_{Vmax}$ (ATR): 3068, 3036 (C-H), 1656 (C=O), 1561 (C=C), 1521, 1310 (NO_2), 1128 (C-N stretch) cm^{-1}
^{1}H NMR (400 MHz, $CDCl_3$) δ 2.38 (s, 3 H, CH_3), 6.79 (s, 1 H, H3), 6.86 - 6.90 (m, 2 H, H5 & H6), 7.86 (s, 1 H, H1')
^{13}C NMR (101 MHz, $CDCl_3$) ppm 14.6 (CH_3), 123.7 (CH), 134.8 (CH), 136.7 (CH), 137.0 (CH), 139.7, 152.5 (C2'), 184.7 (C=O), 186.3 (C=O)
HRMS (ESI) calculated for $C_9H_7NO_4$ [M-H] 193.0375: found 193.0379. Mass accuracy (2.07 ppm).

8.10 General procedure for preparation of 2-alkyl-2-nitro-3-phenyloxiranes (107 – 111)

To a stirred solution of the required (*E*)-(2-nitrovinyl)benzene (0.5 mmol), 1 8-diazabicyclo [5.4.0] undec-7-ene 4 uL (0.023 mmol) and hexane (1.5 mL) was added *tert*-butyl

hydrogenperoxide 100 uL (0.023 mmol). The reaction was stirred at room temperature for 10 min. The reaction was quenched with deionised water (10 mL) and extracted into diethyl ether. The organic layer was washed with water, brine and dried over sodium sulphate. Solvent was removed *in vacuo* to afford pure product.

3-(3-Chlorophenyl)-2-methyl-2-nitrooxirane (107)

3-(3-Chlorophenyl)-2-methyl-2-nitrooxirane was prepared from (*E*)-1-chloro-3-(2-nitroprop-1-en-1-yl)benzene (0.20 g, 1 mmol) according to general procedure 8.10.
Yellow oil 180 mg (85%)
IR$_{Vmax}$ (ATR): 3068, 3003 (C-H), 1493, 1454 (C=C), 1557, 1350 (NO_2 stretch) cm^{-1}
^{1}H NMR (400 MHz, $CDCl_3$) δ 1.73 - 1.78 (m, 3 H, CH_3), 4.49 (s, 1 H, CH), 7.14 - 7.21 (m, 1 H, H6'), 7.25 - 7.29 (s, 1 H, H2'), 7.29 - 7.38 (m, 2 H, H4')
^{13}C NMR (101 MHz, $CDCl_3$) ppm 12.4 (CH_3), 61.7 (CH), 88.5 (C2), 124.6 (CH), 126.5 (CH), 129.7 (CH), 130.1 (CH), 133.0, 135.0
HRMS (ESI) calculated for $C_9H_7Cl^{35}NO_3$ [M^+-H] 212.0120: found 212.0118. Mass accuracy (-0.49 ppm).

3-(4-Chlorophenyl)-2-methyl-2-nitrooxirane (108)

3-(4-Chlorophenyl)-2-methyl-2-nitrooxirane was prepared from (*E*)-1-chloro-4-(2-nitroprop-1-en-1-yl)benzene (0.20 g, 1 mmol) according to general procedure 8.10.
Yellow oil 188 mg (89%[465])
IR$_{Vmax}$ (ATR): 3006, 2971 (C-H), 1493, 1456 (C=C), 1560, 1351 (NO_2 stretch) cm^{-1}
^{1}H NMR (400 MHz, $CDCl_3$) δ 1.70 - 1.76 (m, 3 H, CH_3), 4.49 (s, 1 H, CH), 7.22 (m, J = 8.71 Hz, 2 H, 2 x ArH), 7.37 (m, J = 8.71 Hz, 2 H, 2 x ArH)
^{13}C NMR (101 MHz, $CDCl_3$) ppm 12.4 (CH_3), 62.0 (CH), 88.6 (C2), 127.8 (CH), 129.0, 129.1 (CH), 129.4, 135.6
HRMS (ESI) calculated for $C_9H_7Cl^{35}NO_3$ [M^+-H] 212.0120: found 212.0119. Mass accuracy (-0.47 ppm).

3-(4-Bromophenyl)-2-methyl-2-nitrooxirane (109)

3-(4-Bromophenyl)-2-methyl-2-nitrooxirane was prepared from (*E*)-1-bromo-4-(2-nitroprop-1-en-1-yl)benzene (0.24 g, 1 mmol) according to general procedure 8.10.
Yellow oil 234 mg (92%)
IR$_{Vmax}$ (ATR): 3008, 2893 (C-H), 1489, 1410 (C=C), 1553, 1351 (NO_2 stretch) cm^{-1}
^{1}H NMR (400 MHz, $CDCl_3$) δ 1.78 (s, 3 H, CH_3), 4.51 (s, 1 H, CH), 7.20 (m, J = 8.29 Hz, 2 H, 2 x ArH), 7.56 (m, J = 8.29 Hz, 2 H, 2 x ArH)
^{13}C NMR (101 MHz, $CDCl_3$) ppm 12.4 (CH_3), 62.0 (CH), 88.5 (C2), 123.7, 128.0 (CH), 130.0, 132.0 (CH)
HRMS (ESI) calculated for $C_9H_7Br^{79}NO_3$ [M^+-H] 255.9615: found 255.9622. Mass accuracy (2.73 ppm).

3-(3-Chlorophenyl)-2-ethyl-2-nitrooxirane (110)

3-(3-Chlorophenyl)-2-ethyl-2-nitrooxirane was prepared from (*E*)-1-chloro-3-(2-nitrobut-1-en-1-yl)benzene (0.21 g, 1 mmol) according to general procedure 8.10.

Yellow oil 207 mg (92%)
IR$_{Vmax}$ (ATR): 3068, 2945 (C-H), 1479, 1462, 1434 (C=C), 1556, 1351 (NO_2 stretch) cm^{-1}
^{1}H NMR (400 MHz, $CDCl_3$) δ 1.08 (t, *J* = 7.46 Hz, 3 H, CH_3), 1.68 (dq, *J* =14.93, 7.46 Hz, 1 H, CH_a), 2.48 (dq, *J* = 15.24, 7.50 Hz, 1 H, CH_b), 4.50 (s, 1 H, CH), 7.18 - 7.42 (m, 4 H, 4 x ArH)
^{13}C NMR (101 MHz, $CDCl_3$) ppm 7.6 (CH_3), 19.5 (CH_2), 62.3 (CH), 92.2 (C2), 124.5 (CH), 126.4 (CH), 129.6 (CH), 130.1 (CH), 133.1, 134.9
HRMS (ESI) calculated for $C_{10}H_9Cl^{35}NO_3$ [M-H] 226.0276: found 226.0277. Mass accuracy (0.44 ppm).

2-(4-Chlorobenzyl)-3-(4-chlorophenyl)-2-nitrooxirane (111)

2-(4-Chlorobenzyl)-3-(4-chlorophenyl)-2-nitrooxirane was prepared from (*E*)-4,4'-(2-nitroprop-1-ene-1,3-diyl)bis(chlorobenzene) 0.31 g (1 mmol) according to general procedure 8.10.
Colourless oil 276 mg (86%)
IR$_{Vmax}$ (ATR): 3042, 2969 (C-H), 1489, 1423 (C=C), 1553, 1351 (NO_2 stretch) cm^{-1}
^{1}H NMR (400 MHz, $CDCl_3$) δ 2.83 (d, *J* =15.76 Hz, 1 H, CHa), 3.77 (d, *J* =15.34 Hz, 1 H, CHb), 4.54 (s, 1 H, CH), 7.15 (m, *J* = 8.29 Hz, 2 H, 2 x ArH), 7.22 - 7.29 (m, 2 H, 2 x ArH), 7.32 (d, *J* = 8.29 Hz, 2 H, 2 x ArH), 7.40 - 7.46 (m, 2 H, 2 x ArH)
^{13}C NMR (101 MHz, $CDCl_3$) ppm 31.1 (CH_2), 62.3 (CH), 91.2 (C2), 127.7 (CH), 129.0 (CH), 129.2, 129.3 (CH), 130.7, 130.8 (CH), 133.8, 135.9
HRMS (ESI) calculated for $C_{15}H_{10}Cl_2{}^{35}NO_3$ [M^+-H] 322.0043: found 322.0039. Mass accuracy (-1.24 ppm).

8.11 General procedure for preparation of 5-alkyl-4-phenyl-1*H*-1,2,3-triazoles (112 – 119)

To a stirred solution of the required (*E*)-(2-nitrovinyl)benzene (1 mmol) in DMSO (2 mL) was added sodium azide (2 mmol). The reaction was stirred at 90 °C for 90 minutes. After allowing the reaction to cool to room temperature deionised water (10 mL) was added and the aqueous mix was extracted into diethyl ether. The organic layer was washed with water, brine and dried over sodium sulphate. Solvent was removed *in vacuo* to afford crude product. The product was purified by column chromatography over silica gel (gradient dichloromethane – methanol).

4-(3-Chlorophenyl)-5-methyl-1*H*-1,2,3-triazole (112)

4-(3-Chlorophenyl)-5-methyl-1*H*-1,2,3-triazole was prepared from (*E*)-1-chloro-3-(2-nitroprop-1-en-1-yl)benzene (0.197 g, 1 mmol) according to general procedure 8.11. The product was purified by column chromatography (gradient dichloromethane – methanol) and recrystallised from ethanol..
White solid 119 mg (62%)
Melting Point: 166-169 °C
IR$_{Vmax}$ (ATR): 3089, 2981 (C-H), 1594, 1464 (C=C), 1231 (C-N) cm^{-1}
^{1}H NMR (400 MHz, DMSO-*d*$_6$) δ 2.45 (s, 3 H, CH_3), 7.40 (d, *J* = 8.29 Hz, 1 H, H2'), 7.48 (t, *J* = 7.88 Hz, 1 H, H5'), 7.66 (d, *J* = 7.88 Hz, 1 H, H6'), 7.73 (s, 1 H, H2')
^{13}C NMR (101 MHz, DMSO-*d*$_6$) ppm 10.4 (CH_3), 125.0 (CH), 126.0 (CH), 127.3 (CH), 130.7 (CH), 133.5 (C5), 135.3, 141.3, 145.2

HRMS (ESI) calculated for $C_9H_7Cl^{35}N_3$ [M^+-H] 192.0334: found 192.0335. Mass accuracy (0.52 ppm).

4-(4-Bromophenyl)-5-methyl-1*H*-1,2,3-triazole (113)

4-(4-Bromophenyl)-5-methyl-1*H*-1,2,3-triazole was prepared from (*E*)-1-bromo-4-(2-nitroprop-1-en-1-yl)benzene (0.24 g, 1 mmol) according to general procedure 8.11. The product was purified by column chromatography (gradient dichloromethane – methanol) and recrystallised from ethanol..
White solid 148 mg (63%)
Melting Point: 196-199 °C
IR$_{Vmax}$ (ATR): 3120, 3075 (C-H), 1638, 1566 (C=C), 1226 (C-N) cm^{-1}
^{1}H NMR (400 MHz, DMSO-d_6) δ 2.44 (s, 3 H, CH_3), 7.66 (s, 4 H, 4 x ArH)
^{13}C NMR (101 MHz, DMSO-d_6) ppm 11.4 (CH_3), 120.7, 128.4 (CH), 130.9, 131.7 (CH), 139.2, 140.5, 142.4
HRMS (ESI) calculated for $C_9H_7Br^{79}N_3$ [M^+-H] 235.9829: found 235.9828. Mass accuracy (-0.42 ppm).

4-(5-Bromo-2-methoxyphenyl)-5-methyl-1*H*-1,2,3-triazole (114)

4-(5-Bromo-2-methoxyphenyl)-5-methyl-1*H*-1,2,3-triazole was prepared from (*E*)-4-bromo-1-methoxy-2-(2-nitroprop-1-en-1-yl)benzene (0.27 g, 1 mmol) according to general procedure 8.11. The product was purified by column chromatography (gradient dichloromethane – methanol) and recrystallised from ethanol..
White solid 159 mg (60%)
Melting Point: 135-137 °C
IR$_{Vmax}$ (ATR): 3208 (N-H), 2971, 2936 (Ar C-H), 1638, 1530 (C=C), 1221 (C-N) cm^{-1}
^{1}H NMR (400 MHz, DMSO-d_6) δ 2.08 - 2.33 (m, 3 H, CH_3), 3.69 - 3.85 (m, 3 H, OCH_3), 7.09 (d, J = 8.71 Hz, 1 H, H3'), 7.40 - 7.66 (m, 2 H, H6' & H4')
^{13}C NMR (101 MHz, DMSO-d_6) ppm 10.7 (CH_3), 55.6 (OCH_3), 111.7, 113.8 (CH), 132.3 (CH), 132.8 (CH), 138.6, 140.6, 141.5, 156.1
HRMS (ESI) calculated for $C_{10}H_9Br^{79}N_3O$ [M^+-H] 265.9934: found 265.9936. Mass accuracy (0.75 ppm).

4-(2,5-Dimethoxyphenyl)-5-methyl-1*H*-1,2,3-triazole (115)

4-(2,5-Dimethoxyphenyl)-5-methyl-1*H*-1,2,3-triazole was prepared from (*E*)-1,4-dimethoxy-2-(2-nitroprop-1-en-1-yl)benzene (0.22 g, 1 mmol) according to general procedure 8.11. The product was purified by column chromatography (gradient dichloromethane – methanol) and recrystallised from ethanol..
Yellow solid 120 mg (55%)
Melting Point: 76-80 °C
IR$_{Vmax}$ (ATR): 3272 (N-H), 2969, 2936 (C-H), 1615, 1563 (C=C), 1227 (C-N) cm^{-1}
^{1}H NMR (400 MHz, DMSO-d_6) δ 2.20 (s, 3 H, CH_3), 3.73 (d, J = 1.24 Hz, 6 H, 2 x OCH_3), 6.90 - 7.01 (m, 2 H, H3' & H4'), 7.01 - 7.07 (m, 1 H, H6')
^{13}C NMR (101 MHz, DMSO-d_6) ppm 10.2 (CH_3), 55.5 (OCH_3), 55.8 (O CH_3), 112.7 (CH), 114.6 (CH), 116.0 (CH), 120.7, 129.8, 139.8, 141.8, 150.7 (C5'), 153.0 (C2')

HRMS (ESI) calculated for $C_{11}H_{12}N_3O_2$ [M^+-H] 218.0935: found 218.0934. Mass accuracy (-0.45 ppm).

4-(4-Chlorophenyl)-5-methyl-1*H*-1,2,3-triazole (116)

4-(4-Chlorophenyl)-5-methyl-1*H*-1,2,3-triazole was prepared from (*E*)-1-chloro-4-(2-nitroprop-1-en-1-yl)benzene (0.197 g, 1 mmol) according to general procedure 8.11. The product was purified by column chromatography (gradient dichloromethane – methanol) and recrystallised from ethanol.
White solid 119 mg (62%)
Melting Point: 188-190 °C
IR$_{Vmax}$ (ATR): 3199 (N-H), 2980, 2884 (C-H), 1639, 1566 (C=C), 1231 (C-N) cm^{-1}
^{1}H NMR (400 MHz, DMSO-d_6) δ 2.43 (s, 3 H, CH_3), 7.50 (m, J = 8.71 Hz, 2 H, 2 x ArH), 7.72 (m, J = 8.29 Hz, 2 H, 2 x ArH)
^{13}C NMR (101 MHz, DMSO-d_6) ppm 11.0 (CH_3), 128.2 (CH), 128.8 (CH), 130.3, 132.2, 135.2, 141.3, 145.2
HRMS (ESI) calculated for $C_9H_7N_3Cl^{35}$ [M^+-H] 192.0334: found 192.0334. Mass accuracy (0 ppm).

4-(3-Chlorophenyl)-5-ethyl-1*H*-1,2,3-triazole (117)

4-(3-Chlorophenyl)-5-ethyl-1*H*-1,2,3-triazole was prepared from (*E*)-1-chloro-3-(2-nitrobut-1-en-1-yl)benzene (0.21 g, 1 mmol) according to general procedure 8.11. The product was purified by column chromatography (gradient dichloromethane – methanol) and recrystallised from ethanol.
White solid 140 mg (68%)
Melting Point: 115-118 °C
IR$_{Vmax}$ (ATR): 3352 (N-H), 2971, 2932 (C-H), 1605, 1584 (C=C), 1243 (C-N) cm^{-1}
^{1}H NMR (400 MHz, DMSO-d_6) δ 1.22 (t, J = 7.46 Hz, 3 H, CH_3), 2.85 (q, J = 7.33 Hz, 2 H, CH_2), 7.36 - 7.43 (m, 1 H, H4'), 7.48 (t, J = 7.67 Hz, 1 H, H5'), 7.62 (d, J = 7.46 Hz, 1 H, H6'), 7.69 (s, 1 H, H2')
^{13}C NMR (101 MHz, DMSO-d_6) ppm 12.9 (CH_3), 18.5 (CH_2), 109.6, 125.3 (CH), 126.3 (CH), 127.4 (CH), 130.6 (CH), 133.5 (C5), 135.9, 140.1, 141.9, 145.5
HRMS (ESI) calculated for $C_{10}H_9Cl^{35}N_3$ [M^+-H] 206.0490: found 206.0489. Mass accuracy (-0.49 ppm).

4-(5-Bromo-2-methoxyphenyl)-5-ethyl-1*H*-1,2,3-triazole (118)

4-(5-bromo-2-methoxyphenyl)-5-ethyl-1*H*-1,2,3-triazole was prepared from (*E*)-4-bromo-1-methoxy-2-(2-nitrobut-1-en-1-yl)benzene (0.29 g, 1 mmol) according to general procedure 8.11. The product was purified by column chromatography (gradient dichloromethane – methanol) and recrystallised from ethanol.
Yellow crystals 210 mg (75%)
Melting Point: 169-172 °C
IR$_{Vmax}$ (ATR): 2977, 2881 (C-H), 1638, 1585 (C=C), 1249 (C-N) cm^{-1}

^{1}H NMR (400 MHz, DMSO-d_6) δ 1.03 - 1.21 (m, 3 H, CH_3), 2.50 - 2.66 (m, 2 H, CH_2), 3.77 (s, 3 H, OCH_3), 7.07 (d, J = 8.71 Hz, 1 H, 1 x ArH), 7.45 (s, 1 H, H6'), 7.49 - 7.65 (m, 1 H, 1 x ArH)
^{13}C NMR (101 MHz, DMSO-d_6) ppm 13.0 (CH_3), 18.5 (CH_2), 55.6 (OCH_3), 111.7 (s), 113.7 (CH), 122.8, 132.2 (CH), 132.9 (CH), 137.1, 140.0, 146.6, 156.1 (C2')
HRMS (ESI) calculated for $C_{11}H_{11}N_3Br^{79}O$ [M^+-H] 280.0091: found 280.0092. Mass accuracy (0.36 ppm).

Ethyl 2-(4-(3-chlorophenyl)-1*H*-1,2,3-triazol-5-yl)-2-hydroxyacetate (119)

Ethyl 2-(4-(3-chlorophenyl)-1*H*-1,2,3-triazol-5-yl)-2-hydroxyacetate was prepared from ethyl (E)-4-(3-chlorophenyl)-2-hydroxy-3-nitrobut-3-enoate (*E*)-1-chloro-3-(2-nitrovinyl)benzene 0.286 g (1 mmol) according to general procedure 8.11. The product was purified by column chromatography (gradient - dichloromethane: methanol) and recrystallised from ethanol.
Yellow oil 192 mg (68%)
IR$_{Vmax}$ (ATR): 3197 (N-H), 2981, 2931 (Ar C-H), 1734 (C=O), 1604, 1571 (C=C), 1210 (C-N stretch) cm^{-1}
^{1}H NMR (400 MHz, $CDCl_3$) δ 1.13 (t, J = 7.05 Hz, 3 H, CH_3), 4.10 - 4.29 (m, 2 H, CH_2), 5.53 (s, 1 H, CH), 7.31 - 7.42 (m, 2 H, 2 x ArH), 7.58 - 7.70 (m, 1 H, 1 x ArH), 7.77 (s, 1 H, H2)
^{13}C NMR (101 MHz, $CDCl_3$) ppm 13.8 (CH_3), 62.7 (OCH_2), 65.2 (CH), 126.2 (CH), 128.1 (CH), 129.0, 130.1 (CH), 131.0, 134.8, 142.8, 171.8 (C=O)
HRMS (APCI) calculated for $C_{12}H_{13}Cl^{35}N_3O_3$ [M^++H] 282.0645: found 282.0646. Mass accuracy (0.35 ppm).

8.12 General procedure for preparation of alkyl 2-cyano-3-phenylacrylates (120 – 125)

To a solution of the required alkyl 2-cyanoacetate (1 mmol) in ethanol 5 mL was added the appropriate benzaldehyde (1 mmol) and 1 drop of piperidine. The reaction was stirred vigorously and heated to 80 °C for 30 min in a microwave reactor. The solution was allowed to come to room temperature and the precipitate was isolated by filtration. The crude product was recrystallized from ethanol. No further purification was necessary.

Methyl 3-(4-chlorophenyl)-2-cyanoacrylate (120)

Methyl 3-(4-chlorophenyl)-2-cyanoacrylate was prepared from 4-chlorobenzaldehyde (0.14 g, 1 mmol) and methyl 2-cyanoacetate according to general procedure 8.12. and recrystallised from ethanol.
Yellow solid 145 mg (66%)
Melting Point: 120-122 °C (lit. M.p. 122 °C[275])
IR$_{Vmax}$ (ATR): 2987 (C-H), 2222 (CN), 1722 (C=O), 1586, 1548 (Ar C=C), 1260 (CN) cm^{-1}
^{1}H NMR (400 MHz, $CDCl_3$) δ 3.95 (s, 3 H, CH_3), 7.49 (m, J = 8.71 Hz, 2 H, 2 x ArH), 7.94 (m, J = 8.71 Hz, 2 H, 2 x ArH), 8.22 (s, 1 H, H1')
^{13}C NMR (101 MHz, $CDCl_3$) ppm 53.5 (CH_3), 115.2 (CN), 129.0, 129.7 (CH), 129.8 (CH), 132.2 (CH), 139.7, 153.6 (C1'), 162.7 (C=O)
HRMS (APCI) calculated for $C_{11}H_8Cl^{35}NO_2$ [M^+] 221.0244: found 221.0245. Mass accuracy (0.45 ppm).

Methyl 3-(5-bromo-2-methoxyphenyl)-2-cyanoacrylate (121) [466]

Methyl 3-(5-bromo-2-methoxyphenyl)-2-cyanoacrylate was prepared from 5-bromo-2-methoxybenzaldehyde (0.213 g, 1 mmol) and methyl 2-cyanoacetate according to general procedure 8.12. and recrystallised from ethanol.
Yellow solid (70%)
Melting Point: 152-156 °C
IR$_{Vmax}$ (ATR): 3069, 2969 (C-H), 2223 (CN), 1705 (C=O), 1588, 1549 (Ar C=C), 1257 (CN) cm^{-1}
^{1}H NMR (400 MHz, $CDCl_3$) δ 3.94 (s, 3 H, CH_3), 3.91 (s, 3 H, OCH_3), 6.86 (d, J = 9.12 Hz, 1 H, H3), 7.61 (dd, J = 8.92, 2.28 Hz, 1 H, H4), 8.34 (d, J = 2.07 Hz, 1 H, H6), 8.64 (s, 1 H, H1')
^{13}C NMR (101 MHz, $CDCl_3$) ppm 53.4 (CH_3), 56.1 (OCH_3), 103.4, 112.9 (CH), 113.2, 115.1 (CN), 131.6 (CH), 137.3 (CH), 148.3 (CH), 158.1 (C1'), 162.8 (C=O)
HRMS (APCI) calculated for $C_{12}H_{11}Br^{79}NO_3$ [M^++H] 295.9922: found 295.9923. Mass accuracy (0.34 ppm).

Ethyl 3-(3-chlorophenyl)-2-cyanoacrylate (122)

Ethyl 3-(3-chlorophenyl)-2-cyanoacrylate was prepared from 3-chlorobenzaldehyde (0.14 g, 1 mmol) and ethyl 2-cyanoacetate according to general procedure 8.12. and recrystallised from ethanol.
White solid 71 mg (30%)
Melting Point: 100-102 °C (lit. M.p. 101-102 °C[467])
IR$_{Vmax}$ (ATR): 3068 (C-H), 2223 (CN), 1706 (C=O), 1588, 1561 (Ar C=C), 1257 (CN) cm^{-1}
^{1}H NMR (400 MHz, $CDCl_3$) δ 1.41 (t, J = 7.26 Hz, 3 H, CH_3), 4.41 (q, J = 7.05 Hz, 2 H, CH_2), 7.46 (t, J = 7.88 Hz, 1 H, ArH, 1 x ArH), 7.54 (ddd, J = 8.19, 1.97, 1.04 Hz, 1 H, H5), 7.86 - 7.99 (m, 2 H, 2 x ArH), 8.19 (s, 1 H, H1')
^{13}C NMR (101 MHz, $CDCl_3$) ppm 14.1 (CH_3), 63.0 (CH_2), 104.7, 114.9 (CN), 128.6 (CH), 130.5 (CH), 130.8 (CH), 133.0 (CH), 135.3, 153.2 (C1'), 162.0 (C=O)
HRMS (APCI) calculated for $C_{12}H_{10}Cl^{35}NO_2$ [M^+] 235.0400: found 235.0400. Mass accuracy (0 ppm).

Ethyl 3-(4-chlorophenyl)-2-cyanoacrylate (123)

Ethyl 3-(4-chlorophenyl)-2-cyanoacrylate was prepared from 4-chlorobenzaldehyde (0.14 g, 1 mmol) and ethyl 2-cyanoacetate according to general procedure 8.12. and recrystallised from ethanol.
Yellow solid 152 mg (65 %)
Melting Point: 89-92 °C (lit. M.p. 91.5-92.5 °C[468])
IR$_{Vmax}$ (ATR): 3036, 2989 (C-H), 2223 (CN), 1721 (C=O), 1587, 1565 (Ar C=C), 1258 (CN) cm^{-1}
^{1}H NMR (400 MHz, $CDCl_3$) δ 1.40 (t, J = 7.26 Hz, 3 H, CH_3), 4.39 (q, J = 7.33 Hz, 2 H, CH_2), 7.48 (m, J = 8.71 Hz, 2 H, 2 x ArH), 7.94 (m, J = 8 71 Hz, 2 H, 2 x ArH), 8.20 (s, 1 H, H1')
^{13}C NMR (101 MHz, $CDCl_3$) ppm 14.1 (CH_3), 62.8 (CH_2), 103.5, 115.2 (CN), 129.6 (CH), 132.2 (CH), 139.5, 153.3 (C1'), 162.2 (C=O)

HRMS (APCI) calculated for $C_{12}H_{10}Cl^{35}NO_2$ [M^+] 235.0400: found 235.0399. Mass accuracy (-0.43 ppm).

Ethyl 3-(5-bromo-2-methoxyphenyl)-2-cyanoacrylate (124)

Ethyl 3-(5-bromo-2-methoxyphenyl)-2-cyanoacrylate was prepared from 5-bromo-2-methoxybenzaldehyde 0.213 g (1 mmol) and ethyl 2-cyanoacetate according to general procedure 8.12.
Yellow solid 191 mg (58 %)
Melting Point: 101-103 °C (lit. M.p. 103-104 °C[469])
IR$_{Vmax}$ (ATR): 3067, 2900 (C-H), 2223 (CN), 1719 (C=O), 1609, 1587 (Ar C=C), 1259 (CN) cm^{-1}
^{1}H NMR (400 MHz, $CDCl_3$) δ 1.40 (t, J = 7.05 Hz, 3 H, CH_3), 3.90 (s, 3 H, OCH_3), 4.39 (q, J = 7.05 Hz, 2 H, CH_2), 6.86 (d, J = 8.71 Hz, 1 H, H3), 7.60 (dd, J = 8.92, 2.28 Hz, 1 H, H4), 8.32 (d, J = 2.49 Hz, 1 H, H6), 8.62 (s, 1 H, H1')
^{13}C NMR (101 MHz, $CDCl_3$) ppm 14.1 (CH_3CH_2), 56.0 (OCH_3), 62.7 (CH_2), 103.9, 112.9 (CH), 113.2, 115.1 (CN), 122.4, 131.6 (CH), 137.2 (CH), 148.0 (CH), 158.1 (C1'), 162.3 (C=O)
HRMS (APCI) calculated for $C_{13}H_{12}Br^{79}NaNO_3$ [M^++Na] 331.9898: found 331.9884. Mass accuracy (-4.22 ppm).

Methyl 3-(3-chlorophenyl)-2-cyanoacrylate (125)[470]

Methyl 3-(3-chlorophenyl)-2-cyanoacrylate was prepared from 3-chlorobenzaldehyde (0.14 g, 1 mmol) and methyl 2-cyanoacetate according to general procedure 8.12.
White solid 110 mg (50%)
Melting Point: 145-149 °C
IR$_{Vmax}$ (ATR): 3066.69, 2983.21 (C-H), 2223.23 (CN), 1709.24 (C=O), 1588.74, 1562.20 (C=C), 1258.91 (CN) cm^{-1}
^{1}H NMR (400 MHz, $CDCl_3$) δ 3.95 (s, 3 H, CH_3), 7.47 (d, J = 8.29 Hz, 1 H, 1 x ArH), 7.51 - 7.57 (m, 1 H, H5), 7.89 - 7.94 (m, 2 H, 2 x ArH), 8.19 (s, 1 H, H1')
^{13}C NMR (101 MHz, $CDCl_3$) ppm 53.5 (CH_3), 104.1, 114.9 (CN), 128.7 (CH), 130.5 (CH), 130.8 (CH), 132.9, 133.1 (CH), 135.3, 153.4 (C1'), 162.5 (C=O)
HRMS (APCI) calculated for $C_{11}H_8Cl^{35}NO_2$ [M^+] 221.0244: found 221.0244. Mass accuracy (0 ppm).

8.13 General procedure for synthesis of 2-benzylidenemalononitriles (126 – 129)

To a solution of malononitrile (1 mmol) in ethanol (1 mL) was added the appropriate benzaldehyde (1 mmol). To this was added 1 drop of piperidine and the mixture was heated to reflux for one h. The reaction mixture was then allowed to cool to room temperature and the precipitate was isolated by filtration. The solid was recrystallised from ethanol. No further purification was required.

2-(4-Chlorobenzylidene)malononitrile (126)

2-(4-Chlorobenzylidene)malononitrile was prepared from 4-chlorobenzaldehyde (0.14 g, 1 mmol) according to general procedure 8.13.
Yellow solid 147 mg (78%)
Melting Point: 162-165 °C (lit. M.p. 163 °C[471])
IR$_{Vmax}$ (ATR): 3069, 3034 (C-H), 2226 (CN), 1580, 1557 (C=C), 1191 (CN stretch) cm^{-1}
^{1}H NMR (400 MHz, $CDCl_3$) δ 7.53 (m, *J* = 8.29 Hz, 2 H, 2 x ArH), 7.75 (s, 1 H, H1'), 7.86 (m, *J* = 8.71 Hz, 2 H, 2 x ArH)
^{13}C NMR (101 MHz, $CDCl_3$) ppm 83.3 (C2'), 112.3 (CN), 113.4 (CN), 129.2, 130.0 (CH), 131.8 (CH), 141.1, 158.3 (C1')
HRMS (APCI) calculated for $C_{10}H_5Cl^{35}N_2$ [M$^+$] 188.0141: found 188.0140. Mass accuracy (-0.53 ppm).

2-(4-Bromobenzylidene)malononitrile (127)

2-(4-Bromobenzylidene)malononitrile was prepared from 4-bromobenzaldehyde (0.18 g, 1 mmol) according to general procedure 8.13.
Yellow solid 191 mg (83%)
Melting Point: 163-164 °C (lit. M.p. 163 °C[472])
IR$_{Vmax}$ (ATR): 3093, 2971 (C-H), 2226 (CN), 1577, 1555 (C=C), 1152 (CN stretch) cm^{-1}
^{1}H NMR (400 MHz, $CDCl_3$) δ 7.67 - 7.72 (m, 2 H, 2 x ArH), 7.73 (s, 1 H, H1'), 7.76 - 7.80 (m, 2 H, 2 x ArH)
^{13}C NMR (101 MHz, $CDCl_3$) ppm 83.4 (C2'), 112.3 (CN), 113.4 (CN), 129.6, 129.9, 131.8 (CH), 133.0 (CH), 158.4 (C1')
HRMS (APCI) calculated for $C_{10}H_5Br^{79}N_2$ [M$^+$] 231.9636: found 231.9637. Mass accuracy (0.43 ppm).

2-(5-Bromo-2-methoxybenzylidene)malononitrile (128)

2-(5-Bromo-2-methoxybenzylidene)malononitrile was prepared from 2-methoxy-5-bromobenzaldehyde (0.21 g, 1 mmol) according to general procedure 8.13.
Yellow solid 161 mg (62%)
Melting Point: 136-138 °C (lit. M.p. 137-139 °C[473])
IR$_{Vmax}$ (ATR): 3035, 2971 (C-H), 2225 (CN), 1582, 1533 (C=C), 1217 (CN stretch) cm^{-1}
^{1}H NMR (400 MHz, $CDCl_3$) δ 3.93 (s, 3 H, OCH_3), 6.90 (d, *J* = 9.12 Hz, 1 H, H3), 7.59 - 7.75 (m, 1 H, H4), 8.19 (s, 1 H, H1'), 8.24 (d, *J* = 2.49 Hz, 1 H, H6)
^{13}C NMR (101 MHz, $CDCl_3$) ppm 56.3 (OCH_3), 83.2 (C2'), 112.3 (CN), 113.2 (CH), 113.4 (CN), 113.7, 121.7, 131.1 (CH), 138.7 (CH), 152.8 (C1'), 157.8
HRMS (APCI) calculated for $C_{11}H_7Br^{79}N_2O$ [M$^+$] 261.9742: found 261.9747. Mass accuracy (1.91 ppm).

2-(3-Chlorobenzylidene)malononitrile (129)

2-(3-Chlorobenzylidene)malononitrile was prepared from 3-chlorobenzaldehyde (0.14 g, 1 mmol) according to general procedure 8.13.
Yellow solid 169 mg (90 %)
Melting Point: 115-118°C (lit. M.p.116-117 °C[474])

IR$_{\nu max}$ (ATR): 3035, 2971 (C-H), 2226 (CN), 1584, 1560 (C=C), 1214 (CN stretch) cm^{-1}
^{1}H NMR (400 MHz, CDCl$_3$) δ 7.46 - 7.54 (m, 1 H, H5), 7.58 - 7.64 (m, 1 H, H4), 7.74 (s, 1 H, H1'), 7.82 - 7.87 (m, 2 H, H2 & H5)
^{13}C NMR (101 MHz, CDCl$_3$) ppm 84.6 (C2'), 112.0 (CN), 113.2 (CN), 128.3 (CH), 130.4 (CH), 130.8 (CH), 132.3, 134.3 (CH), 135.7, 158.2 (C1')
HRMS (APCI) calculated for $C_{10}H_5Cl^{35}N_2$ [M$^+$] 188.0141: found 188.0140. Mass accuracy (-0.53 ppm).

8.14 General procedure for synthesis of benzylidenehydrazines (130 - 134)

To a solution of hydrazine hydrate (1 mL) in ethanol (1 mL) was added the appropriate benzaldehyde (1 mmol). The reaction mixture was refluxed for three hours and subsequently cooled to room temperature. The precipitate was isolated by filtration and recrystallized with ethanol. No further purification was required.

Benzylidenehydrazine (130)

Benzylidenehydrazine was prepared from benzaldehyde (0.11 g, 1 mmol) according to general procedure 8.14.
Yellow solid 73 mg (60%)
Melting Point: 178-180 °C (lit. M.p. 198 °C[475])
IR$_{\nu max}$ (ATR): 3671 (N-H), 2981, 2888 (C-H), 1624, 1574 (C=C), 1173 (CN stretch) cm^{-1}
^{1}H NMR (400 MHz, CDCl$_3$) δ 7.39 - 7.58 (m, 3 H, 3 x ArH), 7.81 - 7.95 (m, 2 H, H2 & H6), 8.69 (s, 1 H, H1')
^{13}C NMR (101 MHz, CDCl$_3$) ppm 128.5 (CH), 128.8 (CH), 131.2 (CH), 134.1, 162.0 (C1')
HRMS (ESI) calculated for $C_7H_9N_2$ [M$^+$+H] 121.0766: found 121.0765. Mass accuracy (-0.83 ppm).

(3-Chlorobenzylidene)hydrazine (131)

(3-Chlorobenzylidene)hydrazine was prepared from 3-chlorobenzaldehyde (0.14 g, 1 mmol) according to general procedure 8.14.
Yellow solid 111 mg (72%)
Melting Point: 147-149 °C [476])
IR$_{\nu max}$ (ATR): 3338 (N-H), 3076, 2970 (C-H), 1626, 1593 (C=C), 1264 (CN stretch) cm^{-1}
^{1}H NMR (400 MHz, CDCl$_3$) δ 7.35 - 7.50 (m, 2 H, 2 x ArH), 7.64 - 7.74 (m, 1 H, 1 x ArH), 7.89 (t, J =1.87 Hz, 1 H, H1), 8.60 (s, 1 H, H1')
^{13}C NMR (101 MHz, CDCl$_3$) ppm 127.0 (CH), 128.1 (CH), 130.0 (CH), 131.3 (CH), 134.9, 135.7, 161.1 (C1')
HRMS (APCI) calculated for $C_7H_9Cl^{35}N_2$ [M$^+$] 154.0298: found 154.0294. Mass accuracy (-2.60 ppm).

(4-Chlorobenzylidene)hydrazine (132)

(4-Chlorobenzylidene)hydrazine was prepared from 4-chlorobenzaldehyde (0.14 g, 1 mmol) according to general procedure 8.14.
Yellow solid 134 mg (87%)
Melting Point: 182-184 °C (lit. M.p. 275 °C[477])

IR$_{Vmax}$ (ATR): 3660 (N-H), 3048, 2981 (C-H), 1624, 1568 (C=C), 1279 (CN stretch) cm^{-1}
^{1}H NMR (400 MHz, CDCl$_3$) δ 7.36 - 7.60 (m, 2 H, 2 x ArH), 7.69 - 7.98 (m, 2 H, 2 x ArH), 8.62 (s, 1 H, H1')
^{13}C NMR (101 MHz, CDCl$_3$) ppm 129.1 (CH), 129.7 (CH), 137.3, 161.1 (C1')
HRMS (APCI) calculated for $C_7H_9Cl^{35}N_2$ [M$^+$] 154.0298: found 154.0293. Mass accuracy (-3.25 ppm).

(5-Bromo-2-methoxybenzylidene)hydrazine (133)

(5-Bromo-2-methoxybenzylidene)hydrazine was prepared from 5-bromo-2-methoxybenzaldehyde (0.21 g, 1 mmol) according to general procedure 8.14.
Yellow solid 50 mg (22%)
Melting Point: 238-243°C
IR$_{Vmax}$ (ATR): 3662 (N-H), 3004, 2988 (C-H), 1618, 1566 (C=C), 1128 (CN stretch) cm^{-1}
^{1}H NMR (400 MHz, CDCl$_3$) δ 3.89 (s, 3 H, OCH_3), 6.84 (d, J = 9.12 Hz, 1 H, H3), 7.51 (dd, J = 8.71, 2.49 Hz, 1 H, H4), 8.23 (d, J = 2.49 Hz, 1 H, H6), 8.98 (s, 1 H, H1')
^{13}C NMR (101 MHz, CDCl$_3$) ppm 55.9 (OCH_3), 113.0 (CH), 113.4, 129.8 (CH), 134.9 (CH), 156.6 (C1'), 158.1
HRMS (APCI) calculated for $C_8H_9Br^{79}NO_2$ [M$^+$] 227.9894: found 227.9898. Mass accuracy (1.75 ppm).

(4-Bromobenzylidene)hydrazine (134)

(4-Bromobenzylidene)hydrazine was prepared from 4-chlorobenzaldehyde 0.14 g (1 mmol) according to general procedure 8.14.
Yellow solid 154 mg (78%)
Melting Point: 232-235 °C [281])
IR$_{Vmax}$ (ATR): 3661 (N-H), 3047, 2981 (C-H), 1624, 1563 (C=C), 1117 (CN stretch) cm^{-1}
^{1}H NMR (400 MHz, CDCl$_3$) δ 7.60 (m, J = 8.29 Hz, 2 H, 2 x ArH), 7.72 (m, J = 8.29 Hz, 2 H, 2 x ArH), 8.60 (s, 1 H, H1')
^{13}C NMR (101 MHz, CDCl$_3$) ppm 129.9 (CH), 132.1 (CH), 133.7, 140.2, 161.2 (C1')
HRMS (APCI) calculated for $C_7H_9Br^{79}N_2$ [M$^+$+H] 198.9871: found 198.9871. Mass accuracy (0 ppm).

8.15 General procedure for preparation of 3-nitro-2-phenyl-2*H*-chromenes (135 - 142)

To a mixture of salicylaldehyde (6 mmol) and β-nitrostyrene (1 mmol) was added DABCO (1 mmol, 112 mg) at room temperature. The reaction mixture was stirred at 60 °C for 1.5 h. The reaction was extracted with 20 mL DCM and washed with 10 % HCl (2 x 5 mL). The organic extracts were washed with H_2O and brine, then dried over Na_2SO_4, and solvent removed *in vacuo*. The residue was purified by flash column chromatography over silica gel (eluent: hexanes/ethyl acetate (8/1)) to give 3-nitro-2-phenyl-2*H*-chromenes. The product was recrystallised from the appropriate alcohol.

3-Nitro-2-phenyl-2*H*-chromene (135)

3-Nitro-2-phenyl-2*H*-chromene was prepared from (*E*)-(2-nitrovinyl)benzene (1 mmol, 0.149 g) according to general procedure 8.15. and recrystallised from ethanol.
Yellow crystals 110 mg (40%)
Melting Point: 85-87 °C (lit. M.p. 87 °C[288])
IR$_{Vmax}$ (KBr): 3066 (-CH), 1650, 1605 (C=C), 1511, 1327 (NO_2) cm^{-1}
^{1}H NMR (400 MHz, $CDCl_3$) δ 6.61 (s, 1 H, H2), 6.89 (d, *J* = 8 Hz, 1 H, H8), 7.00-7.06 (m, 1 H, H7), 7.41-7.32 (m, 7 H, 7 x ArH), 8.09 (s, 1 H, H4)
^{13}C NMR (101 MHz, $CDCl_3$) ppm 73.8 (C2), 116.8, 117.5, 122.1, 126.6, 128.4, 128.9, 129.0, 130.0, 133.9, 136.31, 140.7 (C3), 153.1 (C8a)
HRMS (ESI) calculated for $C_{15}H_{11}NO_3Na$ [M^++Na] 276.0637: found 276.0628. Mass accuracy (-3.26 ppm).

2-(4-Chlorophenyl)-3-nitro-2*H*-chromene (136)

2-(4-Chlorophenyl)-3-nitro-2*H*-chromene was prepared from (*E*)-1-chloro-4-(2-nitrovinyl)benzene (1 mmol, 0.184 g) according to general procedure 8.15. and recrystallised from ethanol.
Yellow crystals 101 mg (35%)
Melting Point: 135-136 °C (lit M.p. 136 °C[288])
IR$_{Vmax}$ (KBr): 3070 (-CH), 1650, 1605 (C=C), 1514, 1325 (NO_2), 755 (C-Cl) cm^{-1}
^{1}H NMR (400 MHz, $CDCl_3$) δ 6.57 (s, 1 H, H2), 6.89 (d, *J* = 8 Hz, 1 H, H8), 7.05 (dd, *J* = 7.5 Hz, 1 H, H7), 7.40-7.30 (m, 6 H, 6 x ArH), 8.09 (s, 1 H, H4)
^{13}C NMR (101 MHz, $CDCl_3$) ppm 73.0 (C2), 116.8, 117.3, 122.3, 128.0, 128.7, 129.1, 130.1, 134.1, 134.8, 135.0, 140.3 (C3), 152.8 (C8a)
HRMS (ESI) calculated for $C_{15}H_9Cl^{35}NO_3$ [M^+-H] 286.0265: found 286.0260. Mass accuracy (-1.75 ppm).

4-(3-Nitro-2*H*-chromen-2-yl)phenol (137)

4-(3-Nitro-2*H*-chromen-2-yl)phenol was prepared from (*E*)-4-(2-nitrovinyl)phenol (1 mmol, 0.165 g) according to general procedure 8.15. and recrystallised from ethanol.
Yellow crystals 122 mg (45%)
Melting Point: 193-195 °C
IR$_{Vmax}$ (KBr): 3477 (OH), 3071 (CH), 1648, 1604 (C=C), 1509, 1319 (NO_2) cm^{-1}
^{1}H NMR (400 MHz, DMSO-d_6) δ 6.52 (s, 1 H, H2), 6.62 - 6.80 (m, 2 H, H3' & H5'), 6.84 (d, *J* =8.03 Hz, 1 H, H8), 7.03 (td, *J* = 7.53, 1.00 Hz, 1 H, H6), 7.14 - 7.26 (m, 2 H, H2' & H6'), 7.26 - 7.43 (m, 1 H, H7), 7.60 (dd, *J*= 7.53, 1.51 Hz, 1 H, H5), 8.38 (s, 1 H, H4), 9.69 (s, 1 H, OH)
^{13}C NMR (101 MHz, DMSO-d_6) ppm 73.3 (C2), 115.5, 116.8 (C8 C6), 118.2 (C4a), 122.4 (C6), 127.1 (C1'), 128.6, 129.8 (C4), 131.1 (C5), 134.4 (C7), 140.8 (C3), 152.8 (C8a), 158.5 (C4')
HRMS (APCI) calculated for $C_{15}H_{11}NO_4$ [M^+] 269.0688: found 269.0682. Mass accuracy (-2.23 ppm).

2-(4-(Benzyloxy)phenyl)-3-nitro-2*H*-chromene (138)

2-(4-(Benzyloxy)phenyl)-3-nitro-2*H*-chromene was prepared from (*E*)-1-(benzyloxy)-4-(2-nitrovinyl)benzene (1 mmol, 0.255 g) according to general procedure 8.15. and recrystallised from ethanol.
Yellow Crystals 215 mg (60%)
Melting Point: 162-163 °C (lit. M.p. 164 °C[164])
IRν_{max} (KBr): 3068 (CH), 1647, 1606 (C=C), 1509, 1323 (NO_2) cm^{-1}
^{1}H NMR (400 MHz, $CDCl_3$) δ 5.03 (s, 2 H, CH_2), 6.55 (s, 1 H, H2), 6.87 (d, *J* = 8.5 Hz, 1 H, H8), 6.92 (d, *J* = 9 Hz, 2 H, 2 x ArH), 7.01 (t, *J* = 7.5 Hz, 1 H, H7), 7.25-7.41 (m, 9 H, 9 x ArH), 8.07 (s, 1 H, H4)
^{13}C NMR (101 MHz, $CDCl_3$) ppm 69.6 (CH_2), 73.5 (C2), 114.6, 116.9, 117.5, 122.0, 127.0, 127.7, 128.1, 128.2, 128.6, 128.7, 129.9, 138.8, 136.2, 140.8 (C3), 153.1 (C8a), 159.2 (C4')
HRMS (ESI) calculated for $C_{22}H_{16}NO_4$ [M^+-H] 358.1074: found 358.1078. Mass accuracy (1.11 ppm).

2-(Benzo[d][1,3]dioxol-5-yl)-3-nitro-2*H*-chromene (139)

2-(Benzo[d][1,3]dioxol-5-yl)-3-nitro-2*H*-chromene was prepared from (*E*)-5-(2-nitrovinyl)benzo[d][1,3]dioxole (1 mmol, 0.193 g) according to general procedure 8.15. and recrystallised from ethanol.
Orange Crystals 125 mg (39%)
Melting Point: 116-118 °C (lit m.p. 118°C[164])
IRν_{max} (film) 3071, 2962 (CH), 1649, 1606 (C=C), 1509, 1319 (NO_2) cm^{-1}
^{1}H NMR (400 MHz, $CDCl_3$) δ 5.96 (s, 2 H, OCH_2O), 6.50 (s, 1 H, H2), 6.75 (d, *J* = 8.5 Hz, 1 H, H8), 6.87 (d, *J* = 8.5 Hz, 3 H, 3 x ArH), 6.99-7.06 (m, 1 H, H6), 7.30-7.38 (m, 2 H, 2 x ArH), 8.07 (s, 1 H, H4)
^{13}C NMR (101 MHz, $CDCl_3$) ppm 73.6 (C2), 101.0 (OCH_2O), 107.1, 107.9, 116.9, 117.4, 120.7, 122.1, 128.8, 130.1, 133.9, 140.6 (C3), 147.6 (C3' / C2'), 148.2 (C3' / C2'), 152.9 (C8a)
HRMS (ESI) calculated for $C_{16}H_{11}NO_5Na$ [M^++Na] 320.0535: found 320.0545. Mass accuracy (3.12 ppm).

2-(3,4-Dimethoxyphenyl)-3-nitro-2*H*-chromene (140)

2-(3,4-Dimethoxyphenyl)-3-nitro-2H-chromene was prepared from (E)-1,2-dimethoxy-4-(2-nitrovinyl)benzene (1 mmol, 0.209 g) according to general procedure 8.15. and recrystallised from ethanol.
Brown crystals 202 mg (60 %)
Melting Point: 92-93 °C (lit M.p. 90 °C[164])
IRν_{max} (KBr): 3071 (CH), 1648, 1605 (C=C), 1516, 1327 (NO_2) cm^{-1}
^{1}H NMR (400 MHz, $CDCl_3$) δ 3.84 (s, 6 H, 2 x $-CH_3$), 6.54 (s, 1 H, H2), 6.76 (d, *J* = 8 Hz, 1 H, H8), 6.86-6.91 (m, 2 H, 2 x ArH), 6.95 (d, *J* = 2 Hz, 1 H, 2 x ArH), 6.98-7.04 (m, 1 H, H7), 7.34 (d, *J* = 7.5 Hz, 2 H, 2 x ArH), 8.07 (s, 1 H, H4)
^{13}C NMR (101 MHz, $CDCl_3$) ppm 55.4 (2 x OCH_3), 73.7 (C2), 101.0, 110.4, 116.9, 117.6, 118.9, 122.1, 128.7, 128.7, 129.9, 133.8, 140.8 (C3), 148.7 (C3' / C4'), 149.5 (C3' / C4'), 153.0 (C8a)
HRMS (ESI) calculated for $C_{17}H_{15}NO_5Na$ [M^++Na] 336.0848: found 336.0850. Mass accuracy (0.60 ppm).

2-(Naphthalen-2-yl)-3-nitro-2*H*-chromene (142)

2-(Naphthalen-2-yl)-3-nitro-2*H*-chromene was prepared from (*E*)-2-(2-nitrovinyl)naphthalene (1 mmol, 0.199g) according to general procedure 8.15. and recrystallised from ethanol.
Gold Crystals 151 mg (50 %)
Melting Point: 131-133 °C (lit. M.p. 132-133 °C[478])
IR$_{Vmax}$ (KBr): 3061 (CH), 1649, 1605 (C=C), 1512, 1326 (NO_2) cm^{-1}
^{1}H NMR (400 MHz, $CDCl_3$) δ 6.77 (s, 1 H, H2), 6.89 (d, *J* = 8 Hz, 1 H, H8), 7.00-7.05 (m, 1 H, H7), 7.27-7.40 (m, 2 H, 2 x ArH), 7.48-7.50 (m, 2 H, 2 x ArH), 7.50-7.56 (d, *J* = 8.5 Hz, 1 H, 1 x ArH), 7.77-7.86 (m, 4 H, 4 x ArH), 8.17 (s, 1 H, H4)
^{13}C NMR (101 MHz, $CDCl_3$) ppm 73.8 (C2), 116.9, 117.6, 122.2, 124.2, 126.0, 126.1, 126.4, 127.2, 127.9, 128.5, 129.2, 130.0, 132.4, 133.2, 133.5, 133.9, 140.6 (C3), 153.1 (C8a)
HRMS (ESI) calculated for $C_{19}H_{12}NO_3$ [M^+-H] 302.0812: found 302.0814. Mass accuracy (0.65 ppm).

3-Nitro-2-phenyl-2H-chromen-7-ol (141)

To 7-methoxy-3-nitro-2-phenyl-2*H*-chromene (80 mg, 2.83 mmol) was added pyridine hydrochloride (3.2 g, 28.3 mmol). The mixture was heated to 170 °C for 6 h. The reaction was allowed to come to room temperature and 50 mL of water was added and the mixture was extracted with dichloromethane. The organic phases were combined and washed with water, brine and dried over anhydrous sodium sulphate. The solvent was removed *in vacuo*. The crude product was purified by column chromatography on silica gel (dichloromethane) and recrystallised from ethanol.
Orange Crystals 29 mg (10 %)
Melting Point: 153-156 °C
IR$_{Vmax}$ (KBr): 3321 (OH), 3055, 2971 (CH), 1605, 1572 (C=C), 1542, 1323 (NO_2) cm^{-1}
^{1}H NMR (400 MHz, $CDCl_3$) δ 6.35 (d, *J* = 1.66 Hz, 1 H, H8), 6.49 (dd, *J* = 8.29, 2.07 Hz, 1 H, H6), 6.57 (s, 1 H, H2), 7.21 (d, *J* = 8.29 Hz, 1 H, H5), 7.30 - 7.40 (m, 5 H, 5 x ArH), 8.05 (s, 1 H, H4)
^{13}C NMR (101 MHz, $CDCl_3$) ppm 74.5 (C2), 104.3 (CH), 110.0 (CH), 110.6 (CH), 111.4, 127.0 (CH), 128.8 (CH), 129.4 (CH), 129.7 (CH), 132.1 (C4), 136.9, 138.5 (C3), 155.6 (C8a), 161.3 (C7)
HRMS (ESI) calculated for $C_{15}H_{10}NO_4$ [M^+-H] 286.0615: found 286.0607. Mass accuracy (-2.80 ppm).

8.16 General procedure for preparation of 3-nitro-2-phenyl-2*H*-chromenes (143 – 147)

To a mixture of the appropriate methoxysalicylaldehyde or chlorosalicylaldehyde (1.5 mmol) and desired β-nitrostyrene (1 mmol) in acetonitrile 1.5 mL was added DABCO (1 mmol, 112 mg) at room temperature. The reaction mixture was stirred at 60 °C for 1.5 h. The reaction was extracted with 20 mL DCM and washed with 10 % HCl (2 x 5 mL). The organic extracts were washed with H_2O and brine, then dried over Na_2SO_4, and solvent removed in vacuo. The residue was purified by flash column chromatography over silica gel (eluent: hexanes/ethyl

acetate (8/1)) to give 3-nitro-2-phenyl-2*H*-chromenes. The product was recrystallised from the appropriate alcohol.

2-(4-Chlorophenyl)-8-methoxy-3-nitro-2*H*-chromene (143)

2-(4-Chlorophenyl)-8-methoxy-3-nitro-2*H*-chromene was prepared from (*E*)-1-chloro-4-(2-nitrovinyl)benzene (1 mmol, 0.184 g) and 2-hydroxy-3-methoxybenzaldehyde according to general procedure 8.16. and recrystallised from ethanol.
Yellow Crystals 170 mg (50 %)
Melting Point: 160-161 °C (lit. M.p. 161 °C[288])
IR$_{Vmax}$ (KBr): 3069 (CH), 1649, 1603 (C=C), 1512, 1319 (NO_2), 730 (C-Cl) cm^{-1}
^{1}H NMR (400 MHz, $CDCl_3$) δ 3.82 (s, 3 H, CH_3), 6.69 (s, 1 H, H2), 6.82-7.02 (m, 3 H, 3 x ArH), 7.32 (d, *J* = 9 Hz, 2 H, 2 x ArH), 7.36 (d, *J* = 7.5 Hz, 2 H, 2 x ArH), 8.06 (s, 1 H, H4)
^{13}C NMR (101 MHz, $CDCl_3$) ppm 55.8 (CH_3), 73.0 (C2), 116.3, 118.2, 121.7, 122.3, 127.9, 128.6, 129.0, 134.7, 135.0, 140.6 (C8), 142.0 (C3), 148.2 (C8a)
HRMS (ESI) calculated for $C_{16}H_{12}Cl^{35}NO_4Na$ [M^++Na] 340.0353: found 340.0354. Mass accuracy (0.29 ppm).

8-Methoxy-3-nitro-2-phenyl-2*H*-chromene (144)

8-Methoxy-3-nitro-2-phenyl-2*H*-chromene was prepared from (*E*)-(2-nitrovinyl)benzene (1 mmol, 0.149 g) and 2-hydroxy-3-methoxybenzaldehyde according to general procedure 8.16. and recrystallised from ethanol.
Orange Crystals 138 mg (45 %)
Melting Point: 119-121 °C (lit. M.p. 121-122 °C[288])
IR$_{Vmax}$ (KBr): 3066 (CH), 1650, 1605 (C=C), 1512, 1322 (NO_2) cm^{-1}
^{1}H NMR (400 MHz, $CDCl_3$) δ 3.83 (s, 3 H, -OCH_3), 6.70 (s, 1 H, H2), 6.97 (s, 3 H, 3 x ArH), 7.27-7.35 (m, 3 H, 3 x ArH), 7.39-7.44 (m, 2 H, 2 x ArH), 8.06 (s, 1 H, H4)
^{13}C NMR (101 MHz, $CDCl_3$) ppm 55.9 (CH_3), 73.7 (C2), 116.3, 118.3, 121.7, 122.0, 126.5 (2C), 128.3, 128.8 (2C), 129.0, 136.2, 141.0 (C8), 142.3 (C3), 148.2 (C8a)
HRMS (ESI) calculated for $C_{16}H_{13}NO_4Na$ [M^++Na] 306.0742: found 306.0742. Mass accuracy (0 ppm).

7-Methoxy-3-nitro-2-phenyl-2*H*-chromene (145)

7-Methoxy-3-nitro-2-phenyl-2*H*-chromene was prepared from (*E*)-(2-nitrovinyl)benzene (1 mmol, 0.149 g) and 2-hydroxy-4-methoxybenzaldehyde according to general procedure 8.16. and recrystallised from ethanol.
Orange Crystals 184 mg (60%)
Melting Point: 139-141 °C (lit. M.p. 135 °C[479])
IR$_{Vmax}$ (KBr): 3065 (CH), 1642, 1611 (C=C), 1495, 1326 (NO_2) cm^{-1}
^{1}H NMR (400 MHz, $CDCl_3$) δ 3.80 (s, 3 H, -OCH_3), 6.42 (s, 1 H, H2), 6.59 (d, 2 H, 2 x ArH), 7.27 (d, *J* = 8.5 Hz, 1 H, 1 x ArH), 7.32-7.37 (m, 3 H, 3 x ArH), 7.38-7.43 (m, 2 H, 2 x ArH), 8.08 (s, 1 H, H4)
^{13}C NMR (101 MHz, $CDCl_3$) ppm 55.2 (OCH_3), 74.1 (C2), 101.8 (C8), 109.4 (C6), 110.7, 111.9, 126.6 (2C), 128.4, 129.0, 129.4, 131.3, 136.6, 137.9 (C3), 155.2 (C8a), 164.7 (C7)

HRMS (ESI) calculated for $C_{16}H_{13}NO_4Na$ [M^++Na] 306.0742: found 306.0737. Mass accuracy (-0.83 ppm).

6-Chloro-3-nitro-2-phenyl-2*H*-chromene (146)

6-Chloro-3-nitro-2-phenyl-2H-chromene was prepared from (*E*)-(2-nitrovinyl)benzene (1 mmol, 0.149 g) and 2-hydroxy-5-chlorobenzaldehyde according to general procedure 8.16. and recrystallised from ethanol.
Yellow Crystals 87 mg (30%)
Melting Point: 118-121 °C (lit. M.p. 117-118 °C[480])
IR$_{Vmax}$ (KBr): 3083, 3035 (CH), 1654 (C=C), 1517, 1324 (NO_2) cm^{-1}
^{1}H NMR (400 MHz, $CDCl_3$) δ 6.56 (s, 1 H, H2), 6.79 (d, *J* = 8.71 Hz, 1 H, 1 x ArH), 7.23 (dd, *J* = 8.71, 2.49 Hz, 1 H, 1 x ArH), 7.29 (d, *J* = 2.49 Hz, 1 H, 1 x ArH), 7.30 - 7.37 (m, 5 H, 5 x ArH), 7.95 (s, 1 H, H4)
^{13}C NMR (101 MHz, $CDCl_3$) ppm 74.4 (C2), 118.6 (CH), 119.2, 127.0 (CH), 127.1, 127.3, 127.8 (CH), 128.9 (CH), 129.3 (CH), 129.7 (CH), 131.3, 133.7 (C4), 136.2, 142.1 (C3), 151.9 (C8a)
HRMS (APCI) calculated for $C_{15}H_{11}NO_3Cl^{35}$ [M^++H] 288.0427: found 288.0420. Mass accuracy (-2.43 ppm).

8-Chloro-3-nitro-2-phenyl-2*H*-chromene (147)

8-Chloro-3-nitro-2-phenyl-2*H*-chromene was prepared from (*E*)-(2-nitrovinyl)benzene (1 mmol, 0.149 g) and 2-hydroxy-3-chlorobenzaldehyde according to general procedure 8.16. and recrystallised from ethanol.
Yellow Crystals 64 mg (22%)
Melting Point: 117-119 °C (no lit M.p.[481])
IR$_{Vmax}$ (KBr): 3064, 2984 (CH), 1656 (C=C), 1517, 1332 (NO_2) cm^{-1}
^{1}H NMR (400 MHz, $CDCl_3$) δ 6.74 (s, 1 H, H2), 6.95 (t, *J* = 7.88 Hz, 1 H, 1 x ArH), 7.24 (dd, *J* = 7.67, 1.45 Hz, 1 H, 1 x ArH), 7.33 - 7.43 (m, 6 H, 6 x ArH), 8.04 (s, 1 H, H4)
^{13}C NMR (101 MHz, $CDCl_3$) ppm 74.4 (C2), 119.6, 122.6, 122.9 (CH), 126.7 (CH), 128.5 (CH), 128.7 (CH), 128.8 (CH), 129.6 (CH), 134.3 (C4), 136.2, 141.9 (C3), 149.3 (C8a)
HRMS (APCI) calculated for $C_{15}H_{10}NO_3Cl^{35}$ [M^+] 287.0349: found 287.0347. Mass accuracy (-0.70 ppm).

8.17 General procedure for preparation of 3-nitro-2-phenyl-1,2-dihydroquinolines (148, 149)

To a mixture of 2-aminobenzaldehyde (1.2 mmol) and the appropriate (*E*)-(2-nitrovinyl)benzene (1 mmol) in benzene (5 mL) was added DABCO (0.5 mmol, 56 mg) at room temperature. The reaction mixture was refluxed at 100 °C for 10 h. The reaction was cooled and extracted with DCM (20 mL) and washed with 10 % HCL (2 x 5 mL). The organic extracts were washed with H_2O and brine, then dried over Na_2SO_4, and solvent removed *in vacuo*. The residue was purified by flash column chromatography over silica gel (eluent: dichloromethane/hexane (3/1)).

3-Nitro-2-phenyl-1,2-dihydroquinoline (148)

3-Nitro-2-phenyl-1,2-dihydroquinoline was prepared from (*E*)-(2-nitrovinyl)benzene (1 mmol, 0.149 g) and 2-aminobenzaldehyde according to general procedure 8.17.
Recrystallized from ethanol.
Dark purple crystals 59 mg (23%)
Melting Point: 107-109 °C [286]
IR$_{Vmax}$ (KBr): 3361 (NH), 3027, 2981 (CH), 1634 (C=C), 1523, 1315 (NO_2) cm^{-1}
^{1}H NMR (400 MHz, $CDCl_3$) δ 4.72 (br. s., 1 H, NH), 6.00 (d, *J*=1.66 Hz, 1 H, H2), 6.47 (d, *J* = 7.88 Hz, 1 H, 1 x ArH), 6.72 (td, *J* = 7.46, 0.83 Hz, 1 H, 1 x ArH), 7.15 - 7.23 (m, 2 H, 2 x ArH), 7.28 - 7.34 (m, 3 H, 3 x ArH), 7.36 - 7.42 (m, 2 H, 2 x ArH), 7.99 (s, 1 H, C4)
^{13}C NMR (101 MHz, $CDCl_3$) ppm 55.5 (C2), 113.4 (CH), 118.6 (CH), 126.3 (CH), 128.1 (CH), 128.5 (CH), 128.7 (CH), 128.8, 129.0 (CH), 131.3 (CH), 132.7 (CH), 134.1 (CH), 140.1, 142.1 (C3), 144.4 (C8a)
HRMS (APCI) calculated for $C_{15}H_{13}N_2O_2$ [M^+] 253.0977: found 253.0978. Mass accuracy (0.40 ppm).

4-(3-Nitro-1,2-dihydroquinolin-2-yl)phenol (149)

4-(3-Nitro-1,2-dihydroquinolin-2-yl)phenol was prepared from (*E*)-4-(2-nitrovinyl)phenol (1 mmol, 0.149 g) and 2-aminobenzaldehyde according to general procedure 8.17 and recrystallised from ethanol.
Purple Crystals 117 mg (40%)
Melting Point: 207-209 °C
IR$_{Vmax}$ (KBr): 3356 (OH), 2917 (CH), 1603 (C=C), 1492, 1335 (NO_2) cm^{-1}
^{1}H NMR (400 MHz, DMSO-d_6) δ 5.84 (s, 1 H, H2), 6.53-6.58 (m, 2 H, 2 x ArH), 6.69 (d, *J* = 8.6 Hz, 2 H, 2 x ArH), 7.10-7.14 (m, 3 H, 3 x ArH), 7.31 (d, *J* = 7.5 Hz, 1 H, 1 x ArH), 8.15 (s, 1 H, H4), 9.48 (s, 1 H, OH)
^{13}C NMR (101 MHz, DMSO-d_6) ppm 53.5 (C2), 113.3, 114.1, 115.3, 116.8, 127.3, 131.5, 131.9, 133.7, 134.2, 139.5 (C3), 145.7 (C8a), 157.4 (C4')
HRMS (ESI) calculated for $C_{15}H_{12}N_2O_3Na$ [M^++Na] 291.0746: found 291.0736. Mass accuracy (-3.44 ppm).

3-Nitro-2-phenylquinoline (150)

To a solution of 850 mg (7 mmol) of 2-aminobenzaldehyde in 5 mL 95 % ethanol was added 1.1 g (6.6 mmol) nitroacetophenone. The solution was heated to reflux for 3 hours. The solution was allowed to come to room temperature and the resulting yellow precipitate was filtered. The yellow solid was then washed with ethanol and hexane. This yellow solid was then recrystallized from ethanol.
Yellow Crystals 728 mg (44 %)
Melting Point: 150-153 °C (lit. M.p. 155-156 °C[295])
IR$_{Vmax}$ (KBr): 3065, 2981 (CH), 1615 (C=C), 1521, 1334 (NO_2) cm^{-1}

^{1}H NMR (400 MHz, $CDCl_3$) δ 7.47 - 7.55 (m, 3 H, 3 x ArH), 7.63 - 7.73 (m, 3 H, 3 x ArH), 7.86 - 7.94 (m, 1 H, 1 x ArH), 7.97 (d, J = 7.88 Hz, 1 H, 1 x ArH), 8.24 (d, J = 8.29 Hz, 1 H, 1 x ArH), 8.68 (s, 1 H, C4)
^{13}C NMR (101 MHz, $CDCl_3$) ppm 125.5, 128.1 (CH), 128.4, 128.5 (CH), 128.7 (CH), 129.6 (CH), 129.7 (CH), 132.6 (CH), 132.8 (C4), 137.0, 143.9 (C3), 148.3 (C8a), 152.0 (C2)
HRMS (ESI) calculated for $C_{15}H_{11}N_2O_2$ [M^++H] 251.0816: found 251.0821. Mass accuracy (1.99 ppm).

3-Nitroquinolin-2(1*H*)-one (151)

To a solution of ethyl 2-nitroacetate 0.42 mL in toluene 30 mL was added 2-aminobenzaldehyde 460 mg (3.8 mmol). Piperidine 0.38 mL was then added and the reaction mixture was heated to reflux using a Dean Stark trap for removal of water. The reaction was heated at reflux for 2 h. The reaction mixture was allowed to cool to room temperature and the resulting precipitate was filtered and recrystallised from ethanol.
Yellow Crystals 323 mg (40 %)
Melting Point: 258-261 °C ((lit. M.p. 259-260 °C[297])
IR$_{\nu max}$ (KBr): 3329 (NH), 3064, 2984 (CH), 1656 (C=C), 1517, 1332 (NO_2) cm^{-1}
^{1}H NMR (400 MHz, DMSO-d_6) □ 7.24 - 7.42 (m, 2 H, 2 x ArH), 7.66 - 7.92 (m, 2 H, 2 x ArH), 8.89 (br. s., 1 H, H4), 12.56 (br. s., 1 H, NH)
^{13}C NMR (DMSO-d_6) ppm 115.5 (CH), 116.3, 123.1 (CH), 130.4 (CH), 134.1 (C4), 138.0 (C3), 140.0 (C8A), 153.9 (C=O)
HRMS (ESI) calculated for $C_9H_6N_2O_3Na$ [M^++Na] 213.0276: found 213.0267. Mass accuracy (-4.22 ppm).

8.18 General procedure for preparation of *o*-benzoyloxyacetophenones (152 – 160)
The appropriately substituted *o*-hydroxyacetophenone (22 mmol) was added to a round bottomed flask and then the appropriately substituted benzoyl chloride (31 mmol) and pyridine (5 mL) were also added to the flask. The contents were mixed by shaking the flask. The reaction time took 30 min. After the reaction was gone to completion, the reaction mixture was poured onto 100 mL of 1 M hydrochloric acid and 50 g of crushed ice. The product was then filtered off with a Buchner funnel and washed with 20 mL of water and 20 mL of ice cold methanol. The product was then recrystallised from hot methanol and allowed to cool thoroughly.

***o*-Benzoyloxyacetophenone (152)**
o-Benzoyloxyacetophenone was prepared from 2-hydroxyacetophenone (22 mmol, 3 g), benzoyl chloride (31 mmol, 4.32 g) and pyridine (5 mL) according to general procedure 8.18.
Colourless crystalline solid 4.63 g (80%)
Melting Point: 93-97 °C (lit. M.p. 89 °C[482])
IR$_{\nu max}$ (film): 3071 (-CH Ar), 1693 (C=O), 1602 (C=C Ar), 1023 (C-O) cm^{-1}
^{1}H NMR (400 MHz, $CDCl_3$) δ 2.58 (s, 3 H, CH_3), 7.27 (d, 1 H, J = 7.5 Hz, ArH, H3), 7.39-7.43 (m, 1 H, ArH, H5), 7.54-7.69 (m, 4 H, 4 x ArH), 7.90 (d, 1 H, J = 7.5 Hz, ArH, H6), 8.25 (d, 2 H, J = 7 Hz, 2 x ArH, H2' & H6')
^{13}C NMR (101 MHz, $CDCl_3$) ppm 30.1 (CH_3), 124.2, 126.5, 129.0, 129.5, 130.5, 131.5, 133.7, 134.1, 149.7 (C2), 165.5 ($C=O_{ester}$), 197.9 ($C=O_{ketone}$)
HRMS (ESI) calculated for $C_{15}H_{12}O_3$ [M^++Na] 263.0684: found 263.0675. Mass accuracy (-3.42ppm)

2-Acetylphenyl-4-chlorobenzoate (153)

2-Acetylphenyl-4-chlorobenzoate was prepared from 2-hydroxyacetophenone (22 mmol, 3 g), 4-chlorobenzoyl chloride (31 mmol, 5.43 g) and pyridine (5 mL) according to general procedure 8.18.

Colourless crystals 5.75 g (88%)

Melting point: 60-64 °C (lit. M.p. 60-62 °C[483])

IR$_{Vmax}$ (film): 3075 (C-H), 1739 (C=O), 1594 (C=C), 1200 (C-O), 751 (C-Cl) cm^{-1}

^{1}H NMR (400 MHz, $CDCl_3$) δ 2.56 (s, 3 H, CH_3), 7.25 (d, 1 H, *J* = 7.5 Hz, ArH, H3), 7.37-7.43 (m, 1 H, ArH, H5), 7.52 (d, 2 H, *J* = 7 Hz, 2 x ArH, H5'& H3'), 7.58-7.64 (m, 1 H, ArH, H4), 7.89 (d, 1 H, *J* = 8 Hz, ArH, H6), 8.16 (d, 2 H, *J* = 7 Hz, 2 x Ar, H2' & H6')

^{13}C NMR (101 MHz, $CDCl_3$) ppm 29.1 (CH_3), 123.5, 125.9, 127.34, 128.6, 128.9, 130.0, 130.5, 131.2, 131.5, 133.1, 139.9, 148.7 (C2), 164.0 (C=O, $_{ester}$), 197.0 (C=O, $_{ketone}$)

HRMS (ESI) calculated for $C_{15}H_{11}Cl^{35}O_3$ [M^++Na] 297.0294: found 297.0287. Mass accuracy (-2.55 ppm)

4-Methoxybenzoic acid 2-acetylphenyl ester (154)

4-Methoxybenzoic acid 2-acetylphenyl ester was prepared from 2-hydroxyacetophenone (8.3 mmol, 1.1378 g), *p*-anisoyl chloride (11.7 mmol, 2 g) and pyridine (8 mL) according to general procedure 8.18.

Colourless crystals 2.07 g (85%)

Melting point: 118-119 °C (lit. M.p. 113-114 °C[484])

IR$_{Vmax}$ (film): 3003 (CH), 1720 (C=O), 1451 (C=C), 1257 (C-O) cm^{-1}

^{1}H NMR (400 MHz, $CDCl_3$) δ 2.57 (s, 3 H, -CH_3), 3.92 (s, 3 H, OCH_3), 7.02 (d, 2 H, *J* = 7.5 Hz, 2 x ArH, H3'& H5'), 7.25 (d, 1 H, *J* = 8 Hz, ArH, H3), 7.36-7.38(m, 1 H, ArH, H5), 7.59-7.61 (m, 1 H, ArH, H4), 7.87 (d, 1 H, *J* = 8.04 Hz, ArH, H6). 8.19 (d, 2 H, *J* = 7.5 Hz, ArH, H2'&H6')

^{13}C NMR (101 MHz, $CDCl_3$) ppm 29.5 (CH_3), 55.1 (-OCH_3), 113.6, 113.7, 121.1, 123.5, 125.6, 129.7, 131.0, 132.0, 132.4, 132.9, 149.0 (C2), 163.7 (C4'), 164.4 (C_{ester}), 197.6 (C_{ketone})

HRMS (ESI) calculated for $C_{16}H_{14}O_4$ [M^++Na] 293.079: found 293.0789. Mass accuracy (-0.34 ppm)

4-Chlorobenzoic acid 2-acetyl-5-chlorophenyl ester (155)

4-Chlorobenzoic acid 2-acetyl-5-chlorophenyl ester was prepared from 4-chloro-2-hydroxyacetophenone (11.7 mmol, 2 g), 4-chlorobenzoyl chloride (16.4 mmol, 2.866 g) and pyridine (4 mL) according to general procedure 8.18.

Colourless crystals 2.93 g (76%)

Melting point: 93-95 °C

IR$_{Vmax}$ (film): 3095 (CH), 1741 (C=O), 1595 (C=C), 1261 (C-O), 752 (C-Cl) cm^{-1}

^{1}H NMR (400 MHz, $CDCl_3$) δ 2.54 (s, 3 H, CH_3), 7.29 (s, 1 H, ArH, H3), 7.38(d, 1 H, *J* = 8 Hz, ArH, H5), 7.53 (d, 2 H, *J* = 8.5 Hz, 2 x ArH, H3' &H5'), 7.84 (d, 1 H, *J* = 8.5 Hz, ArH, H6), 8.14 (d, 2 H, *J* = 8 Hz, 2 x ArH, H2' & H6')

^{13}C NMR (101 MHz, $CDCl_3$) ppm 29.1 (CH_3), 124.1, 126.2, 126.9, 128.4, 128.7, 128.8, 131.0, 131.3, 138.7 (C4'), 140.2 (C4), 149.4 (C2), 163.6 (C_{ester}), 195.7 (C_{ketone})

HRMS (ESI) calculated for $C_{15}H_{10}Cl_2{}^{35}O_3$ [M^++Na] 330.9905: found 330.9904. Mass accuracy (-0.30 ppm)

3-Chlorobenzoic acid 2-acetylphenyl ester (156)

3-Chlorobenzoic acid 2-acetylphenyl ester was prepared from 2-hydroxyacetophenone (22 mmol, 3 g), 3-chlorobenzoylchloride (30.8 mol, 5.399 g) and pyridine (5 mL) according to general procedure 8.18.
Pink crystals 4.86 g (81%)
Melting point: 60-62 °C (lit. M.p. 60-62 °C[483])
IR$_{Vmax}$ (film): 3004 (CH), 1743 (C=O), 1425 (C=C), 1241 (C-O), 739 (C-Cl) cm^{-1}
^{1}H NMR (400 MHz, CDCl$_3$) δ 2.57 (s, 3 H, CH_3), 7.25 (d, 1 H, *J* = 8 Hz, ArH, H3), 7.41-7.43 (m, 1 H, ArH, H5), 7.47-7.51 (m, 1 H, ArH), 7.59-7.64 (m, 2 H, ArH, H4), 7.90 (d, 1 H, *J* = 8 Hz, ArH, H6), 8.12 (d, 1 H, *J* = 7.5 Hz, ArH, H6'), 8.21 (s, 1 H, ArH, H2')
^{13}C NMR (101 MHz, CDCl$_3$) ppm 29.0 (CH_3), 123.4, 126.0, 128.0, 129.6, 129.9, 130.1, 130.4, 130.6, 133.2, 133.3, 134.4 (C3'), 148.6 (C2), 163.7 (C_{ester}), 196.9 (C_{ketone})
HRMS (ESI) calculated for $C_{15}H_{11}Cl^{35}O_3$ [M^+-H] 273.0318: found 273.0321. Mass accuracy (1.09 ppm)

3,4,5-Trimethoxy-benzoic acid 2-acetylphenyl ester (157)

3,4,5-Trimethoxybenzoic acid 2-acetylphenyl ester was prepared from 2-hydroxyacetophenone (22 mmol, 3 g), 3,4,5-trimethoxybenzyl chloride(30.8 mmol, 7.085 g) and pyridine (5 mL) according to general procedure 8.18.
Colourless crystals 5.51 g (71%)
Melting point: 164-166 °C (lit. M.p. 167 °C[485])
IR$_{Vmax}$ (film): 2942 (CH), 1732 (C=O), 1589 (C=C), 1120 (C-O) cm^{-1}
^{1}H NMR (400 MHz, CDCl$_3$) δ 2.57 (s, 3 H, CH_3), 3.95 (s, 9 H, 3 x OCH_3), 7.25 (d, 1 H, *J* = 8 Hz, ArH, H3), 7.37-7.41 (m, 1 H, ArH. H5), 7.48 (s, 2 H, 2 x ArH, H2'& H6'), 7.59-7.63 (m, 1 H, ArH, H4), 7.88 (d, 1 H, *J*= 7.5 Hz, ArH, H6)
^{13}C NMR (101 MHz, CDCl$_3$) ppm 29.2 (CH_3), 55.8 (2 x OCH3 on C3' & C5'), 60.5 (OCH3 on C4'), 107.0(C2' & C6'), 123.5, 123.7 (C1'), 125.8, 129.9, 130.7 (C1), 133.1, 142.4 (C4'), 148.9 (C2), 152.7 (C3' & C5'), 164.4 (C_{ester}), 197.2 (C_{ketone})
HRMS (ESI) calculated for $C_{18}H_{18}0_6$ [M^++Na] 353.1001: found 353.1007. Mass accuracy (-1.70 ppm)

3,4,5-Trimethoxybenzoic acid 2-acetyl-5-methoxyphenyl ester (158)

3,4,5-Trimethoxybenzoic acid 2-acetyl-5-methoxyphenyl ester was prepared from 4-methoxy-2-hydroxyacetophenone (12 mmol, 2 g), 3,4,5-trimethoxybenzylchloride (16.8 mmol, 3.865 g) and pyridine (11.5 mL) according to general procedure 8.18.
Colourless solid 3.91 g (85%)
Melting point: 160-165 °C [486])
IR$_{Vmax}$ (film): 3091 (CH), 1725 (C=O), 1414 (C=C), 1105 (C-O) cm^{-1}
^{1}H NMR (400 MHz, CDCl$_3$) δ 2.79 (s, 3 H, CH_3), 3.89 (s, 3 H, OCH_3), 3.95 (s, 9 H, 3'4'5'-OCH_3), 6.74 (s, 1 H, ArH, H3), 6.89 (d, 1 H, *J* = 8.5 Hz, ArH, H5), 7.48 (s, 2 H, 2 x ArH, H2' & H6'), 7.90 (d, 1 H, *J* = 8.5 Hz, H6)

^{13}C NMR (101 MHz, $CDCl_3$) ppm 28.9 (CH_3), 55.3 (OCH_3 on C4), 55.8 (2 x OCH_3 on C3' & C5'), 60.5 (OCH3 on C4'), 106.7, 107.0 (C2' & C6'), 108.8, 111.5, 122.9, 123.8, 126.6, 132.1, 142.4, 151.2 (C2), 152.6, 163.3 (C4), 164.3 (C_{ester}), 195.3 (C_{ketone})
HRMS (ESI) calculated for $C_{19}H_{20}O_7$ [M^++Na] 383.1107: found 383.1122. Mass accuracy (3.92 ppm)

Benzoic acid 2-acetyl-5-methoxyphenyl ester (159)

Benzoic acid 2-acetyl-5-methoxyphenyl ester is prepared from 4-methoxy-2-hydroxyacetophenone (12 mmol, 2 g), benzoyl chloride (16.8 mmol, 2.362 g) and pyridine (11.5 mL) according to general procedure 8.18.
Colourless oil 1.62 g (46%)
Melting point: N/A (lit. M.p. 51-52 °C[487])
IR$_{Vmax}$ (film): 3004 (C-H), 2917 (C-H), 1738 (C=O), 1608 (C=C), 1265 (C-O)
^{1}H NMR (400 MHz, $CDCl_3$) δ 2.52 (s, 3 H, CH_3), 3.89 (s, 3 H, OCH3), 6.75 (s, 1 H, ArH, H3), 6.90 (dd, 1 H, ArH, H5), 7.52-7.58 (m, 2 H, 2 x ArH, H3'& H5'), 7.66-7.70 (m, 1 H, ArH, H4'), 7.91 (d, 1 H, J = 9 Hz, ArH, H6), 8.23 (d, 2 H, J = 7.5 Hz, 2 x ArH, H2' & H6')
^{13}C NMR (101 MHz, $CDCl_3$) ppm 29.5 (CH_3), 55.8 (OCH_3 on C4), 109.3, 112.0, 123.5, 128.7, 129.4, 130.3, 132.5, 133.8, 151.7 (C2), 163.8 (C4), 165.2 (C_{ester}), 195.7 (C_{ketone}).
HRMS (ESI) calculated for $C_{16}H_{14}O_4$ [M^++Na] 293.0790: found 293.0800. Mass accuracy (3.41 ppm)

4-Methoxybenzoic acid 2-acetyl-5-methoxyphenyl ester (160)

4-Methoxybenzoic acid 2-acetyl-5-methoxyphenyl ester was prepared from 4-methoxy-2 hydroxyacetophenone (27 mmol, 4.5 g), 4-methoxybenzoyl chloride (38 mmol, 6.45 g) and pyridine (10 mL) according to general procedure 8.18.
Colourless solid 5.23 g (60%)
Melting point: 95-99 (lit. M.p. 94-95 °C[488])
IR$_{Vmax}$ (film): 3006, 2841 (C-H), 1732 (C=O), 1606 (C=C), 1258 (C-O)
^{1}H NMR (400 MHz, $CDCl_3$) δ 2.51 (s, 3 H, CH_3), 3.88 (s, 3 H, OCH_3), 3.92 (s, 3 H, OCH3 on C4'), 6.73 (s, 1 H, ArH, H3), 6.88 (dd, 1 H, ArH, H5), 7.02 (d, 2 H, J = 8.5 Hz, 2 x ArH, H3' & H5'), 7.91 (d, 1 H, J = 9 Hz, ArH, H6), 8.20 (d, 2 H, J = 7 Hz, 2 x ArH, H2' & H6')
^{13}C NMR (101 MHz, $CDCl_3$) ppm 29.7 (CH_3), 55.6 (OCH_3 on C4'), 55.8 (OCH_3 on C4), 109.2, 112.0, 114.0, 121.6, 123.8, 132.3, 151.8 (C2), 163.7, 164.1, 164.8, 195.8 (C_{keto}).
HRMS (ESI) calculated for $C_{17}H_{16}O_5$ [M^++Na] 323.0895: found 323.0896: Mass accuracy (0.31 ppm)

8.19 General Procedure for preparation of 3-hydroxy-3-phenylprop-2-en-1-ones [305] (161 - 169)

The appropriately substituted *o*-benzoyloxyacetophenone (15.8 mmol) was dissolved in dry pyridine (15 mL) in a bolt-necked flask and heated to 50 °C. Potassium hydroxide (KOH), 25 mmol (1.42 g) which was powdered rapidly in a mortar and pestle and preheated at 100 °C in an oven, was then added to the bolt-necked flask. The reaction time was 20 min. The reaction mixture was then cooled to room temperature and acidified by adding 21 mL of 10% acetic acid. The mixture was then filtered with a Buchner funnel and flask. The precipitate was

washed with 20 mL of 10% acetic acid and 20 mL of water. It was then recrystallised with hot methanol.

3-Hydroxy-1-(2-hydroxyphenyl)-3-phenylprop-2-en-1-one (161)

3-Hydroxy-1-(2-hydroxyphenyl)-3-phenylprop-2-en-1-one was prepared from *o*-benzoyloxyacetophenone (15.8 mmol, 3.8 g), KOH (25 mmol, 1.42 g) and pyridine (15 mL) according to general procedure 8.19.
Yellow solid 3.91 g (94%)
Melting point: 115-117 °C (lit. M.p. 116-117 °C[489])
IR$_{Vmax}$ (film): 3379 (OH), 3064 (CH), 1688 (C=O), 1493 (C=C) cm^{-1}
^{1}H NMR (400 MHz, CDCl$_3$) δ 6.87 (s, 1 H, =CH), 6.94-6.98 (m, 1 H, ArH, H5), 7.03 (d, 1 H, J = 8 Hz, ArH, H3), 7.48-7.60 (m, 4 H, 4 x ArH), 7.80 (d, 1 H, J = 7.5 Hz, ArH, H6), 7.96 (d, 2 H, J = 7 Hz, 2 x ArH, H2' & H6'), 12.16 (s, 1 H, OH), 15.58 (s, 1 H, enol OH)
^{13}C NMR (101 MHz, CDCl$_3$) ppm 92.6 (=CH), 119.1, 119.2, 119.4, 127.1, 128.8, 129.1, 132.7, 133.8, 136.1, 162.8 (C2), 177.7 (C_{enol}), 195.9 (C_{keto})
HRMS (ESI) calculated for $C_{15}H_{12}O_3$ [M^++Na] 263.0684: found 263.0676. Mass accuracy (-3.04 ppm)

3-(4-Chlorophenyl)-3-hydroxy-1-(2-hydroxyphenyl)prop-2-en-1-one (162)

3-(4-Chlorophenyl)-3-hydroxy-1-(2-hydroxyphenyl)prop-2-en-1-onewas prepared from 2-acetylphenyl-4-chlorobenzoate (16.4 mmol, 4.5 g), KOH (25.94 mmol, 1.46 g) and pyridine (16 mL) according to general procedure 8.19.
Yellow crystals 1.165 g (26%)
Melting point: 128-133 °C[490]
IR$_{Vmax}$ (film): 3058 (CH), 1615 (C=O), 1486 (C=C), 746 (C-Cl) cm^{-1}
^{1}H NMR (400 MHz, CDCl$_3$) δ 6.82 (s, 1 H, =CH), 6.94-6.97 (m, 1 H, ArH, H5), 7.03 (d, 1 H, J = 8 Hz ArH, H3), 7.46-7.50 (m, 3 H, 3 x ArH, H3'& H5'&H4), 7.89 (d, 2 H, J = 8.5 Hz, ArH, H2'&H6'), 12.06 (s, 1 H, OH), 15.54 (s, 1 H, enol OH)
^{13}C NMR (101 MHz, CDCl$_3$) ppm 91.8 (=CH), 118.3, 118.4, 118.7, 118.9, 127.7, 128.1, 128.7, 128.8. 131.5, 136.0, 138.2, 162.1 (C2), 175.5 (C_{enol}), 195.3 (C_{ketone})
HRMS (ESI) calculated for $C_{15}H_{11}Cl^{35}O_3$ [M^+-H] 273.0318: found 273.0318. Mass accuracy (0 ppm)

1-(4-Chloro-2-hydroxyphenyl)-3-(4-chlorophenyl)-3-hydroxyprop-2-en-1-one (163)

1-(4-Chloro-2-hydroxyphenyl)-3-(4-chlorophenyl)-3-hydroxyprop-2-en-1-one was prepared from 4-chlorobenzoic acid 2-acetyl-5-chlorophenyl ester (8.0 mmol, 2.5 g), KOH (12.8 mmol, 0.720 g) and pyridine (8 mL) according to general procedure 8.19.
Yellow solid 0.489 g (20%)
Melting point: 154-157 °C
IR$_{Vmax}$ (film): 3078 (C-H), 1688 (C=C), 1594 (C=O), 1488 (C=C), 780 (C-Cl)
^{1}H NMR (400 MHz, CDCl$_3$) δ 6.75 (s, 1 H, =CH), 6.92 (dd, 1 H, ArH, H5), 7.29 (s, 1 H, ArH, H3), 7.49 (d, 2 H, J = 8 Hz, 2 x ArH, H3' & H5'), 7.71 (d, 1 H, J = 8 Hz, ArH, H6), 7.89 (d, 2 H, J = 8.5 Hz, 2 x ArH, H2' & H6'), 12.23 (s, 1 H, phenol OH), 15.42 (s, 1 H, enol OH)
^{13}C NMR (101 MHz, CDCl$_3$) ppm 92.2 (=CH), 118.9, 119.8, 128.2, 128.4, 128.9, 129.2, 129.5, 131.7, 131.8, 138.9 (C4'/C4), 141.8 (C4'/C4), 163.2 (C2), 176.4 (C_{enol}), 194.8 (C_{ketone})

HRMS (ESI) calculated for $C_{15}H_{10}Cl_2{}^{35}O_3$ [M^+-H] 306.9929: found 306.9931. Mass accuracy (0.65 ppm)

3-Hydroxy-1-(2-hydroxyphenyl)-3-(4-methoxyphenyl)prop-2-en-1-one (164)

3-Hydroxy-1-(2-hydroxyphenyl)-3-(4-methoxyphenyl)prop-2-en-1-one was prepared from 4-methoxybenzoic acid 2-acetylphenyl ester (5.9 mmol, 1.6 g), KOH (9.3 mmol, 0.5272 g) and pyridine (8 mL) according to general procedure 8.19.
Yellow solid 829 mg (48%)
Melting point: 115-118 °C[491]
IR$_{Vmax}$ (film): 3390 (OH), 2840 (CH), 1678 (C=O), 1601 (C=C), 1334 (C-O) cm^{-1}
^{1}H NMR (400 MHz, $CDCl_3$) δ 3.91 (s, 3 H, OCH_3), 6.79 (s, 1 H, =CH), 6.92-7.04 (m, 4 H, 4 x ArH), 7.46-7.48 (m, 1 H, ArH, H4), 7.78 (d, 1 H, *J* = 7.5 Hz, ArH, H6), 7.94 (d, 2 H, *J* = 7 Hz, 2 x ArH, H2' & H6'), 12.19 (s, 1 H, OH) 15.80 (s, 1 H, enol OH)
^{13}C NMR (101 MHz, $CDCl_3$) ppm 90.6 (=CH), 113.6, 113.7, 118.1, 118.3, 118.6, 118.9, 125.3, 127.9, 128.4, 130.6, 130.8, 135.1, 161.8 (C4), 162.8 (C2), 194.4 (C_{ketone}).
HRMS (ESI) calculated for $C_{16}H_{14}O_4$ [M^++Na] 293.079: found 293.0787. Mass accuracy (-1.02 ppm)

3-(3-Chlorophenyl)-3-hydroxy-1-(2-hydroxyphenyl)prop-2-en-1-one (165)

3-(3-Chlorophenyl)-3-hydroxy-1-(2-hydroxyphenyl)prop-2-en-1-one was prepared from 4-chlorobenzoic acid 2-acetylphenyl ester (10.9 mmol, 3 g), KOH (17.3 mmol, 0.9707 g) and pyridine (15 mL) according to general procedure 8.19.
Yellow solid 416 mg (14%)
Melting point: 115-117 °C (lit. M.p. 116-118 °C[483])
IR$_{Vmax}$ (film): 3070 (C-H), 1614 (C=O), 1564 (C=C), 748 (C-Cl)
^{1}H NMR (400 MHz, $CDCl_3$) δ 6.83 (s, 1 H, =CH), 6.95-6.97 (m, 1 H, ArH), 7.04 (d, 1 H, *J* = 8 Hz, ArH, H3), 7.44-7.54 (m, 3 H, 3 x ArH), 7.80-7.85 (m, 2 H, 2 x ArH, H6 & H6'), 7.93 (s, 1 H, ArH, H2'), 12.04 (s, 1 H, phenol OH), 15.47 (s, 1 H, enol OH)
^{13}C NMR (101 MHz, $CDCl_3$) ppm 92.8 (=CH), 118.9, 119.2, 124.9, 126.9, 128.6, 130.1, 132.2, 135.0, 135.5, 136.2, 162.6 (C2), 185.5 (C_{enol}), 196.0 (C_{ketone})
HRMS (ESI) calculated for $C_{15}H_{11}Cl^{35}O_3$ [M^+-H] 273.0318: found 273.0319. Mass accuracy (0.37 ppm)

3-Hydroxy-1-(2-hydroxyphenyl)-3-(3,4,5-trimethoxyphenyl)prop-2-en-1-one (166)

3-Hydroxy-1-(2-hydroxyphenyl)-3-(3,4,5-trimethoxyphenyl)prop-2-en-1-one was prepared from 3,4,5-trimethoxybenzoic acid 2-acetylphenyl ester (9.0 mmol, 3 g), KOH (14.2 mmol, 0.7967 g) and pyridine (10 mL) according to general procedure 8.19.
Yellow crystals 1.89 g (64%)
Melting point: 139-141 °C (lit. M.p. 135-136 °C[484])
IR$_{Vmax}$ (film): 2964 (C-H), 1608 (C=O), 1487 (C=C), 1129 (C-O) cm^{-1}
^{1}H NMR (400 MHz, $CDCl_3$) δ 3.90 – 3.98 (m, 9 H, 3 x OCH_3), 6.76 (s, 1 H, =CH), 6.92-6.96 (m, 1 H, ArH, H5), 7.02 (d, 1 H, *J* = 8 Hz, ArH, H3), 7.17 (s, 2 H, 2 x ArH, H2'& H6'), 7.46-7.50 (m, 1 H, ArH, H4),7.78 (d, 1 H, *J* = 7.5 Hz, ArH, H6) 12.07 (s, 1 H, OH) 15.77 (s, 1 H, enol OH)

^{13}C NMR (101 MHz, $CDCl_3$) ppm 55.8 / 55.9 (2 x OCH_3 on C3'/C5'), 60.6 (OCH_3 on C4'), 91.5 (=CH), 103.8 (C2' & C6'), 118.4, 118.5, 118.6, 128.0, 128.4, 130.7, 135.4, 141.5. 152.9 (C3'/C5'), 161.9 (C2), 177.0 (C_{enol}) 194.7 (C_{ketone}).
HRMS (ESI) calculated for $C_{18}H_{18}O_6$ [M^+-H] 329.1025: found 329.1033. Mass accuracy (2.43 ppm)

3-Hydroxy-1-(2-hydroxy-4-methoxyphenyl)-3-(3,4,5-trimethoxyphenyl)prop-2-en-1-one (167)

3-Hydroxy-1-(2-hydroxy-4-methoxyphenyl)-3-(3,4,5-trimethoxyphenyl)prop-2-en-1-one was prepared from 3,4,5-trimethoxybenzoic acid 2-acetyl-5-methoxyphenyl ester (8.3 mmol, 3 g), KOH (13.1 mmol, 0.735 g) and pyridine (8 mL) according to general procedure 8.19.
Pale yellow crystals 1.9 g (60%)
Melting point: 116-119 °C (lit. M.p. 119 °C[492])
IR$_{Vmax}$ (film): 3430 (OH), 3091 (C-H), 1726 (C=O), 1674 (C=C), 1414 (C=C), 1122 (C-O) cm^{-1}
^{1}H NMR (400 MHz, $CDCl_3$) δ 3.90 (s, 3 H, OCH_3),3.96 (s, 9 H, 3 x OCH_3 on C3'C4'& C5'), 6.62-6.66 (m, 2 H, =CH & H5), 6.64 (s, 1 H, ArH, H3), 7.16 (s, 2 H, 2 x ArH, H2' & H6'), 7.70 (d, 1 H, J = 8 Hz, ArH, H6), 12.57 (s, 1 H, OH) 15.59 (s, 1 H, enol OH)
^{13}C NMR (101 MHz, $CDCl_3$) ppm 55.2 (OCH_3 on C4), 91.5 (=CH), 100.9, 107.7, 112.0, 127.5, 128.6, 128.7, 129.7, 129.9, 131.8, 137.8, 165.0 (C2), 165.6 (C4), 174.1 (C_{enol}), 194.0 (C_{ketone})
HRMS (ESI) calculated for $C_{19}H_{20}O_7$ [M^++Na] 383.1107: found 383.1101. Mass accuracy (-1.57 ppm)

3-Hydroxy-1-(2-hydroxy-4-methoxyphenyl)-3-(4-methoxyphenyl) prop-2-en-1-one (168)

3-Hydroxy-1-(2-hydroxy-4-methoxyphenyl)-3-(4-methoxyphenyl)prop-2-en-1-one was prepared from 4-methoxybenzoic acid 2-acetyl-5-methoxyphenyl ester (37 mmol, 11 g), KOH (58 mmol, 3.2 g) and pyridine (30 mL) according to general procedure 8.19.
Yellow crystals 9.56 g (80%)
Melting point: 112-115 °C
IR$_{Vmax}$ (film): 2938, 2841 (C-H), 1606 (C=O), 1510 (C=C), 1247 (C-O) cm^{-1}
^{1}H NMR (400 MHz, $CDCl_3$) δ 3.86 (s, 3 H, OCH_3 on C4'), 3.90 (s, 3 H, OCH_3 on C4), 6.48-6.51 (m, 2 H, 2 x ArH, H3 & H5), 6.66 (s, 1 H, =CH), 6.99 (d, 2 H, J = 8.5 Hz, 2 x ArH, H3' & H5'), 7.70 (d, 1 H, J = 8.5 Hz, ArH, H6), 7.91 (d, 2 H, J = 9 Hz, 2 x ArH, H2'& H6') 12.66 (s, 1 H, phenol OH), 15.58 (s, 1 H, enol OH)
^{13}C NMR (101 MHz, $CDCl_3$) ppm 55.1 & 55.6 (2 x OCH_3 on C4/C4'), 90.7 (=CH), 101.3, 107.8, 114.0, 114.1, 128.6, 129.9, 131.3. 162.9 (C2), 165.1 (C4/C4'), 165.7 (C4/C4'), 176.2 (C_{enol}), 193.9 (C_{ketone})
HRMS (ESI) calculated for $C_{17}H_{16}O_5$ [M^++Na] 323.0889: found 323.0895. Mass accuracy (-1.86 ppm).

3-Hydroxy-1-(2-hydroxy-4-methoxyphenyl)-3-phenylprop-2-en-1-one (169)

3-Hydroxy-1-(2-hydroxy-4-methoxyphenyl)-3-phenylprop-2-en-1-one was prepared from benzoic acid 2-acetyl-5-methoxyphenyl ester (4.9 mmol, 1.35 g), KOH (7.7 mmol, 0.432 g) and pyridine (6.74 mL) according to general procedure 8.19.
Brown solid 660 mg (46%)
Melting point: 191-194 °C [493])
IR$_{Vmax}$ (film): 3064 (C-H), 1606 (C=O), 1573 (C=C), 1270 (C-O) cm^{-1}
^{1}H NMR (400 MHz, CDCl$_3$) δ 3.87 (s, 3 H, OCH_3 on C4), 6.48-6.52 (m, 2 H, 2 x ArH, H3 & H5), 6.74 (s, 1 H, =CH), 7.48-7.56 (m, 3 H, 3 x ArH, H3, H4' & H5'), 7.71 (d, 1 H, J = 8 Hz, ArH, H6), 7.94 (d, 2 H, J = 8.5 Hz, 2 x ArH, H2' & H6'), 12.62 (s, 1 H, phenol OH), 15.39 (s, 1 H, enol OH)
^{13}C NMR (101 MHz, CDCl$_3$) ppm 55.7 (OCH_3 on C4), 92.0 (=CH), 101.3, 108.0, 108.3, 112.6, 126.7, 128.8, 128.9, 130.2, 132.1, 133.8, 133.9, 165.3 (C2), 165.9 (C4), 176.0 (C_{enol}), 194.5 (C_{ketone}).
HRMS (ESI) calculated for $C_{16}H_{14}O_4$ [M^++Na] 293.079: found 293.0797. Mass accuracy (2.39 ppm)

8.20 General procedure for preparation of Flavones (170 - 178)

The appropriately substituted 3-hydroxy-3-phenylpropenone (15 mmol) was dissolved in acetic acid (20 mL) in a 500 mL flask. 0.8 mL of sulphuric acid was added to the flask with shaking. The flask was then attached to a reflux condenser and the mixture was heated in a water bath and refluxed at 150 °C for 1 h. The reaction mixture was poured onto 100 mL of crushed ice with stirring and the ice was allowed to melt. The newly formed flavones was then filtered with a Buchner flask and funnel and washed with 200 mL of water. The product was recrystallised with hot methanol.

2-Phenyl-4*H*-chromen-4-one (170)

2-Phenyl-4*H*-chromen-4-one was prepared from 3-hydroxy-1-(2-hydroxyphenyl)-3-phenylpropenone (15 mmol, 3.6 g), conc. acetic acid (20 mL) and conc. sulphuric acid (0.8 mL) according to general procedure 8.20.
Cream crystals 1.51 g (45%)
Melting point: 104-106 °C (lit. M.p. 99-100 °C[493])
IR$_{Vmax}$ (film): 3072 (C-H), 1648 (C=O), 1606 (C=C), 1466 (C=C), 1378 (C-O) cm^{-1}
^{1}H NMR (400 MHz, CDCl$_3$) δ 6.85 (s, 1 H, =CH), 7.42-7.47 (m, 1 H, ArH), 7.53-7.57 (m, 3 H, ArH), 7.59-7.61 (m, 1 H, ArH, H8), 7.70-7.74 (m, 1 H, ArH, H7), 7.94 (d, 2 H, J = 8 Hz, 2 x ArH, H2' & H6'), 8.25 (d, 1 H, J = 8 Hz, 1 x ArH, H5)
^{13}C NMR (101 MHz, CDCl$_3$) ppm 107.6 (C3), 118.1 (C7), 124.0, 125.3, 125.7, 126.3, 129.1, 131.6, 131.8, 133.8, 152.3 ($C8_a$), 163.4 (C2), 178.5 (C4)
HRMS (ESI) calculated for $C_{15}H_{10}O_2$ [M^++H] 223.0759: found 223.0754. Mass accuracy (-2.24 ppm)

2-(4-Chlorophenyl)chromen-4-one (171)

2-(4-Chlorophenyl)chromen-4-one was prepared from 3-(4-chlorophenyl)-3-hydroxy-1-(2-hydroxyphenyl)propenone (3.6 mmol, 1 g), conc. acetic acid (5 mL) and conc. sulphuric acid (0.20 mL) according to general procedure 8.20.
Colourless crystals 0.795 g (86%)

Melting point: 193-196 °C (lit. M.p. 188-189 °C[494])
IR$_{Vmax}$ (KBr): 3064 (CH), 1638 (C=O), 1468 (C=C), 1092 (C-O) cm^{-1}
^{1}H NMR (400 MHz, CDCl$_3$) δ 6.81 (s, 1 H, =CH), 7.41-7.47 (m, 1 H, ArH, H6), 7.51 (d, 2 H, *J*=7Hz, 2 x ArH, H5' & H3'), 7.57 (d, 1 H, *J* = 8 Hz, ArH, H8), 7.69-7.75 (m, 1 H, ArH, H7), 7.87 (d, 2 H, *J* = 7 Hz, 2 x ArH, H2' & H6'), 8.23 (d, 1 H, *J* = 8 Hz, ArH, H5)
^{13}C NMR (101 MHz, CDCl$_3$) ppm 107.2 (C3), 117.6 (C7), 123.4, 124.9, 125.3, 127.1 (C3' & C5'), 129.0 (C2' & C6'), 129.8, 133.5, 137.5, 155.7 (C8a), 161.8 (C2), 177.8 (C4)
HRMS (ESI) calculated for $C_{15}H_9Cl^{35}O_2$ [M$^+$+H] 257.0369: found 257.0376. Mass accuracy (2.72 ppm)

7-Chloro-2-(4-chlorophenyl)chromen-4-one (172)

7-Chloro-2-(4-chlorophenyl)chromen-4-one was prepared from 1-(4-chloro-2-hydroxyphenyl)-3-(4-chlorophenyl)-3-hydroxypropenone (2.01 mmol, 0.620 g), conc. acetic acid (3 mL) and conc. sulphuric acid (0.11 mL) according to general procedure 8.20.
Colourless solid 425 mg (73%)
Melting point: 222-224 °C[495]
IR$_{Vmax}$ (film): 3069 (C-H), 1638 (C=O), 1617 (C=C), 1430 (C=C), 1095 (C-O), 815(C-Cl) cm^{-1}
^{1}H NMR (400 MHz, CDCl$_3$) δ 6.82 (s, 1 H, =CH, H3), 7.42-7.54 (m, 2 H, 2 x ArH, H3' & H5'), 7.55-7.64 (m, 2 H, 2 x ArH, H6 & H8), 7.86 (d, 2 H, *J* = 8 Hz, ArH, H2' & H6'), 8.19 (d, 1 H, *J* = 8 Hz, ArH, H5)
^{13}C NMR (101 MHz, CDCl$_3$) ppm 107.8 (=CH), 118.1 (C7), 122.4, 126.3, 127.1, 127.5, 129.5, 138.2, 139.9, 156.2 (C8$_a$), 162.4 (C2), 177.4 (C$_{ketone}$)
HRMS (ESI) calculated for $C_{15}H_8Cl_2^{35}O_2$ [M$^+$+H] 290.998: found 290.9991. Mass accuracy (3.78 ppm)

2-(4-Methoxyphenyl)chromen-4-one (173)

2-(4-Methoxyphenyl)chromen-4-one was prepared from 3-hydroxy-1-(2-hydroxy-phenyl)-3-(4-methoxyphenyl)propenone (2.2 mmol, 0.6 g), conc. acetic acid (5 mL) and conc. sulphuric acid (0.1 mL) according to general procedure 8.20.
Colourless crystals 490 mg (81%)
Melting point: 162-165 °C (lit. M.p. 158.5 °C[496])
IR$_{Vmax}$ (KBr): 3013 (CH), 1648 (C=O), 1608 (C=C Ar), 1267 (C-O) cm^{-1}
^{1}H NMR (400 MHz, CDCl$_3$) δ 3.89 (s, 3 H, OCH$_3$) 6.77 (s, 1 H, =CH), 7.02 (d, 2 H, *J* = 7.5 Hz, 2 x ArH, H5' & H3'), 7.38-7.44 (m, 1 H, ArH, H6), 7.55 (d, 1 H, *J* = 8 Hz, ArH, H8), 7.66-7.71 (m, 1 H, ArH, H7), 7.88 (d, 2 H, *J* = 8.5 Hz, 2 x ArH, H2' & H6'), 8.23 (d, 1 H, *J* = 7.5 Hz, ArH, H5)
^{13}C NMR (101 MHz, CDCl$_3$) ppm 55.1 (CH$_3$), 105.6 (=CH, C3), 114.0, 117.5 (C7), 123.4, 123.5, 124.6, 125.2, 127.5, 133.2, 155.7 (C8$_a$), 161.9 (C4'), 163.0 (C2), 177.9 (C$_{ketone}$).
HRMS (ESI) calculated for $C_{16}H_{12}O_3$ [M$^+$+Na] 275.0684: found 275.0688. Mass accuracy (1.45 ppm)

2-(3-Chlorophenyl)chromen-4-one (174)

2-(3-Chlorophenyl)-chromen-4-one was prepared from 3-(3-chlorophenyl)-3-hydroxy-1-(2-hydroxyphenyl)propenone (1.39 mmol, 0.380 mg), conc. acetic acid (5 mL) and conc. sulphuric acid (0.1 mL) according to general procedure 8.20.
Colourless solid 271 mg (70%)
Melting point: 185-187 °C (lit. M.p. 188-189 °C[494])
IR$_{Vmax}$ (film): 3067 (C-H), 1643 (C=O), 1466 (C=C), 1372 (C-O), 765 (C-Cl) cm^{-1}
^{1}H NMR (400 MHz, $CDCl_3$) δ 6.82 (s, 1 H, =CH), 7.41-7.54 (m, 3 H, 3 x ArH), 7.59 (d, 1H, J = 8.5 Hz, ArH, H8), 7.72 (dd, 1 H, ArH, H7), 7.80 (d, 1 H, J = 8 Hz, ArH, H6'), 7.94 (s, 1 H, ArH, H2'), 8.24 (d, 1 H, J = 8 Hz, 1 x ArH, H5)
^{13}C NMR (101 MHz, $CDCl_3$) ppm 108.2 (C3), 118.1 (C7), 123.9, 124.4, 125.5, 125.8, 126.4, 130.4, 131.5, 133.6, 134.0, 135.3 (C3), 156.2 ($C8_a$), 161.8 (C2), 178.3 (C4)
HRMS (ESI) calculated for $C_{15}H_9Cl^{35}O_2$ [M^++Na] 279.0189: found 279.0188. Mass accuracy (-0.36 ppm)

2-(3,4,5-Trimethoxyphenyl)chromen-4-one (175)

2-(3,4,5-Trimethoxyphenyl)chromen-4-one was prepared from 3-hydroxy-1-(2-hydroxyphenyl)-3-(3,4,5-trimethoxyphenyl)propenone (5.1 mmol, 1.7 g), conc. acetic acid (6.8 mL) and conc. sulphuric acid (0.27 mL) according to general procedure 8.20.
Colourless crystals 1.38 g (81%)
Melting point: 181-184 °C (lit. M.p. 174-175 °C[497])
IR$_{Vmax}$ (film): 3059 (C-H), 1650 (C=O), 1505 (C=C), 1127 (C-O) cm^{-1}
^{1}H NMR (400 MHz, $CDCl_3$) δ 3.94 (s, 3 H, 1 x 4 -OCH_3), 3.96 (s, 6 H, 2 x 3,5 -OCH_3) 6.78 (s, 1 H, =CH), 7.13 (s, 2 H, 2 x ArH, H2' & H6'), 7.41-7.45 (m, 1 H, ArH, H6), 7.58 (d, 1 H, J = 8 Hz, ArH, H8), 7.67-7.71 (m, 1 H, ArH, H7), 8.21 (d, 1 H, J = 7.5 Hz, ArH, H5)
^{13}C NMR (101 MHz, $CDCl_3$) ppm 55.9 (2 x OCH_3 on C3' & C5'), 60.6 (OCH_3 on C4'), 103.2 (C2' & C6'), 106.9 (C3), 117.6 (C7), 123.4, 124.9, 125.2, 126.5, 133.3, 140.7, 153.1 (C3' & C5'), 155.7 ($C8_a$), 162.8 (C2), 177.9 (C_{ketone})
HRMS (ESI) calculated for $C_{18}H_{16}O_5$ [M^++Na] 335.0895: found 335.0911. Mass accuracy (4.77 ppm)

7-Methoxy-2-(3,4,5-trimethoxyphenyl)chromen-4-one (176)

7-Methoxy-2-(3,4,5-trimethoxyphenyl)chromen-4-one was prepared from 3-hydroxy-1-(2-hydroxy-4-methoxyphenyl)-3-(3,4,5-trimethoxyphenyl)propenone (4.4 mmol, 1.6 g), conc. acetic acid (6 mL) and conc. sulphuric acid(0.3 mL) according to general procedure 8.20.
Cream crystals 465 mg (29%)
Melting point: 191-194 ° C (Lit. M.p. 191-192 °C[498])
IR$_{Vmax}$ (KBr): 3094 (C-H), 3000 (C-H), 1698 (C=O), 1627 (C=C), 1229 (-C-O) cm^{-1}
^{1}H NMR (400 MHz, $CDCl_3$) δ 3.93-3.99 (m, 12 H, 4 x OCH_3), 6.87 (s, 1 H, =CH), 7.00 (d, 1 H, J = 8.5 Hz, ArH, H6), 7.15 (s, 1 H, ArH, H8), 7.39 (s, 2 H, 2 x ArH, H2' & H6'), 8.16 (d, 1 H, J = 8.5 Hz, ArH, H5)
^{13}C NMR (101 MHz, $CDCl_3$) ppm 55.5 (OCH_3 on C7), 55.8 / 55.9 (2 x OCH_3 on C3' & C5'), 60.5 (OCH_3 on C4'), 100.0, 103.2 (=CH, C3), 106.7 / 106.8 (C2'/C6'), 114.2, 117.0, 124.0, 126.5, 126.4, 152.5, 153.1, 157.6 ($C8_a$), 162.8 (C2), 163.9 (C7), 177.5 (C_{ketone}).

HRMS (ESI) calculated for $C_{19}H_{18}O_6$ [M^++Na] 365.1001: found 365.0988. Mass accuracy (-3.56 ppm)

7-Methoxy-2-(4-methoxyphenyl)chromen-4-one (177)

7-Methoxy-2-(4-methoxyphenyl)chromen-4-one was prepared from 3-hydroxy-1-(2-hydroxy-4-methoxyphenyl)-3-(4-methoxyphenyl)propenone (6 mmol, 2 g), conc. acetic acid (13.63 mL) and conc. sulphuric acid (0.27 mL) according to general procedure 8.20.
Cream solid 1.74 g (95%)
Melting point: 153-155 °C (lit. M.p. 149-150 °C[499])
IR$_{\nu max}$ (film): 3005 (C-H), 1655 (C=O), 1626 (C=C), 1513 (C=C), 1266 (C-O) cm^{-1}
^{1}H NMR (400 MHz, $CDCl_3$) δ 3.87 (s, 3 H, OCH_3 on C7), 3.92 (s, 3 H, OCH_3 on C4'), 7.65 (s, 1 H, =CH), 6.90-6.95 (m, 2 H, 2 x ArH), 6.98 (d, 2 H, J = 9 Hz, 2 x ArH, H3' & H5'), 7.82 (d, 2 H, J = 9 Hz, 2 x ArH, H2' & H6'), 8.10 (d, 1 H, J = 8.5 Hz, H5)
^{13}C NMR (101 MHz, $CDCl_3$) ppm 55.5 / 55.8 (2 x OCH_3), 100.4, 105.4 (=CH), 114.2, 114.4, 117.7, 124.1, 126.9, 127.8, 157.8 ($C8_a$), 162.2 (C4'), 163.0 (C2), 164.0 (C7), 177.8 (C_{ketone})
HRMS (ESI) calculated for $C_{17}H_{14}O_4$ [M^++Na] 305.079: found 305.0782. Mass accuracy (-2.62 ppm)

7-Methoxy-2-phenylchromen-4-one (178)

7-Methoxy-2-phenylchromen-4-one was prepared from 3-hydroxy-1-(2-hydroxy-4-methoxyphenyl)-3-phenylpropenone (2 mmol, 0.53 g), conc. acetic acid (4.54 mL) and conc. sulphuric acid (0.09 mL) according to general procedure 8.20.
Brown crystals 270 mg (49%)
Melting point: 107-110 °C (lit. M.p. 109-110 °C[500])
IR$_{\nu max}$ (film): 3067 (C-H,Ar), 1641 (C=O), 1607 (C=C,Ar), 1283 (C-O) cm^{-1}
^{1}H NMR (400 MHz, $CDCl_3$) δ 3.96 (s, 3 H, OCH_3), 6.80 (s, 1 H, =CH), 6.98-7.02 (m, 2 H, 2 x ArH, H3' & H5'), 7.52-7.56 (m, 3 H, 3 x ArH), 7.92 (d, 2 H, J = 7.5 Hz, 2 x ArH, H2' & H6'), 8.15 (d, 1 H, J = 8.5 Hz, ArH, H5)
^{13}C NMR (101 MHz, $CDCl_3$) ppm 55.9 (OCH_3 on C7), 100.4 (=CH), 107.5, 114.5, 117.8, 126.2, 127.1, 129.0, 131.5, 131.8, 158.1 ($C8_a$), 163.1 (C2), 164.3 (C7), 178.0 (C_{ketone})
HRMS (ESI) calculated for $C_{16}H_{12}O_3$ [M^++Na] 275.0684: found 275.0674. Mass accuracy (-3.64 ppm)

8.21 General procedure for preparation of 3-nitroflavones (179 - 188)

The appropriate substituted flavone (1.58 mmol) was weighed out and placed into a 100 mL round bottomed flask (predried in an oven at 100 °C). 5 mmol (400 mg) of ammonium nitrate was then added. A rubber septum was fitted and a nitrogen balloon attached. 1.58 mmol (25 mL) of dry dichloromethane was added followed by 1.58 mmol (25 mL) of dry acetonitrile (HPLC grade). 8.49 mmol (1.2 mL) of trifluoroacetic acid was then added with cooling in an ice bath. Once addition was complete, the reaction mixture was heated to 40 °C and allowed to react for 1.5 hours. After reaction was completed the mixture was neutralised with 100 mL of water. It was then extracted with 2 x 20mL dichloromethane in a separating funnel. An appropriate amount of sodium sulphate was added and then mixture was filtered. The solvent was removed *in vacuo*. The 3-nitroflavone obtained was then recrystallised from hot methanol.

3-Nitro-2-phenylchromen-4-one (179)

3-Nitro-2-phenylchromen-4-one was prepared from 2-phenyl-4*H*-chromen-4-one (1.58 mmol, 0.350 g), ammonium nitrate (5.0 mmol, 0.4 g), trifluoroacetic acid (8.49 mmol, 1.2 mL), dry dichloromethane (25 mL) and dry acetonitrile (25 mL) according to general procedure 8.21.
Yellow crystals 435 mg (95%)
Melting point: 143-146 °C (lit. M.p. 141-142 °C[501])
IR$_{\nu max}$ (KBr): 3423 (CH), 1659 (C=O), 1622 (C=C), 1532 (N-O), 761 (C-Cl) cm^{-1}
^{1}H NMR (400 MHz, $CDCl_3$) δ 7.51-7.59 (m, 3 H, 3 x ArH, H8, H3' & H5'), 7.61-7.67 (m, 2 H, 2 x ArH, H4' & H6'), 7.76 (d, 2 H, *J* = 7 Hz, 2 x ArH, H2' & H6'), 7.80-7.85 (m, 1 H, ArH, H7), 8.32 (d, 1 H, *J* = 8 Hz, ArH, H5)
^{13}C NMR (101 MHz, $CDCl_3$) ppm 118.0 (C7), 122.9, 126.0, 126.1, 127.3, 127.9, 128.9, 132.5, 134.8, 154.9 (C8a), 159.3 (C2), 168.4 (C4)
HRMS (ESI) calculated for $C_{15}H_9NO_4$ [M^++Na] 290.0429: found 290.0420. Mass accuracy (-3.10 ppm)

2-(4-Chlorophenyl)-3-nitrochromen-4-one (180)

2-(4-Chlorophenyl)-3-nitrochromen-4-one was prepared from 2-(4-chlorophenyl)chromen-4-one (1.58 mmol 0.405 g), ammonium nitrate (5.0 mmol, 0.4 g), trifluoroacetic acid (8.49 mmol, 1.2 mL), dry dichloromethane (25 mL) and dry acetonitrile (25 mL) according to general procedure 8.21.
Yellow crystals 440 mg (86%)
Melting point: 158-160 °C [315])
IR$_{\nu max}$ (KBr): 3428 (CH), 1659 (C=O), 1622 (C=C), 1531 (N-O), 1372 (-C-O) cm^{-1}
^{1}H NMR (400 MHz, $CDCl_3$) δ 7.52-7.58 (m, 3 H, 3 x ArH, H3',H5', H6), 7.62 (d, 1 H, *J* = 8.5 Hz, ArH, H8), 7.71 (d, 2 H, *J* = 8 Hz, 2 x ArH, H2'& H6'), 7.81-7.86 (m, 1 H, ArH, H7), 8.32 (d, 1 H, *J* = 7.5 Hz, ArH, H5).
^{13}C NMR (101 MHz, $CDCl_3$) ppm 117.9 (C7), 122.9, 126.1, 126.2, 126.3, 127.2, 128.7 (C3' & C5'), 129.2 (C2' & C6'), 129.3, 134.9, 139.0 (C3), 154.8 (C8a), 158.0 (C2), 168.2 (C4)
HRMS (ESI) calculated for $C_{15}H_8Cl^{35}NO_4$ [M^++Na] 324.004: found 324.0034. Mass accuracy (-1.85 ppm).

7-Chloro-2-(4-chlorophenyl)-3-nitrochromen-4-one (181)

7-Chloro-2-(4-chlorophenyl)-3-nitrochromen-4-one was prepared from 7-chloro-2-(4-chlorophenyl)chromen-4-one (0.9 mmol, 0.3 g), ammonium nitrate (3 mmol, 0.24 g), trifluoroacetic acid (4.8 mmol, 0.7 mL), dry dichloromethane (10 mL) and dry acetonitrile (10 mL) according to general procedure 8.21.
Colourless crystals 109 mg (33%)
Melting point: 197-199 °C
IR$_{\nu max}$ (KBr): 3068 (C-H), 1660 (C=O), 1613 (C=C), 1599 (N-O), 1426 (C=C), 794 (C-Cl) cm^{-1}
^{1}H NMR (400 MHz, $CDCl_3$) δ 7.51-7.58 (m, 3 H, 3 x ArH, H3' H5' & H6), 7.66-7.71 (m, 3 H, 3 x ArH, H2', H6' & H8), 8.27 (d, 1 H, *J* = 8 Hz, ArH, H5)
^{13}C NMR (101 MHz, $CDCl_3$) ppm 118.1 (C7), 121.4, 125.9, 127.1, 127.4, 128.7 (C3' & C5'), 129.4 (C2' & C6'), 139.4, 141.2 (C3), 154.9 (C8a), 158.9 (C2), 167.5 (C4)

HRMS (ESI) calculated for $C_{15}H_7Cl_2{}^{35}NO_4$ [M^++Cl] 369.9441: found 369.9428. Mass accuracy (-3.51 ppm)

2-(3-Nitro-4-methoxyphenyl)-3-nitrochromen-4-one (182)

2-(3-Nitro-4-methoxyphenyl)-3-nitrochromen-4-one was prepared from 2-(4-methoxyphenyl)chromen-4-one (1.1 mmol, 0.3 g), ammonium nitrate (3.5 mmol, 0.28 g), trifluoroacetic acid (5.9 mmol, 0.83 mL), dry dichloromethane (10 mL) and dry acetonitrile (10 mL) according to general procedure 8.21.
Yellow crystals 105 mg (30%)
Melting point: 221-223 °C (lit. M.p. 221-223 °C[315])
IR$_{Vmax}$ (KBr): 3094 (C-H), 1655 (C=O), 1616 (C=C), 1528 (N-O), 1465 (C=C), 1293 (C-O) cm^{-1}
^{1}H NMR (400 MHz, DMSO -d$_6$) δ 3.39 (s, 3 H, OCH_3), 7.64-7.68 (m, 2 H, 2 x ArH, H6 & H8), 7.90 (d, 1 H, J = 8 Hz, ArH, H5'), 7.97-8.00 (m, 2 H, 2 x ArH, H6' & H7), 8.19 (d, 1 H, J = 8 Hz, ArH, H5), 8.41 (s, 1 H, ArH, H2')
^{13}C NMR (101 MHz, DMSO -d$_6$) ppm 57.9 (CH_3), 116.0, 119.6, 120.6, 123.2, 125.7, 125.9, 127.4, 134.4, 136.4, 138.0, 139.7 (C3), 155.4 ($C8_a$), 155.6, 158.7 (C2), 168.9 (C_{ketone})
HRMS (ESI) calculated for $C_{15}H_{11}NO_5$ [M^++Na] 320.0535: found 320.0530. Mass accuracy (-1.56 ppm)

7-Methoxy-3-nitro-2-(3,4,5-trimethoxyphenyl)chromen-4-one (183)

7-Methoxy-3-nitro-2-(3,4,5-trimethoxyphenyl)chromen-4-one was prepared from 7-methoxy-2-(3,4,5-trimethoxyphenyl)chromen-4-one (0.9 mmol, 0.350 g),), ammonium nitrate (2.8 mmol, 0.224 g), trifluoroacetic acid (4.8 mmol, 0.677 mL), dry dichloromethane (14.24 mL) and dry acetonitrile (14.24 mL) according to general procedure 8.21.
HRMS (ESI) calculated for $C_{19}H_{17}NO_8$ [M^++Na] 410.0852: found 410.0843. Mass accuracy (-2.19 ppm)

3-Nitro-2-(3,4,5-trimethoxyphenyl)chromen-4-one (184)

3-Nitro-2-(3,4,5-trimethoxyphenyl)chromen-4-one was prepared from 2-(3,4,5-trimethoxyphenyl)chromen-4-one (1.2 mmol, 0.4 g), ammonium nitrate (3.8 mmol, 0.304 g), trifluoroacetic acid (6 mmol, 0.9 mL), dry dichloromethane (18.98 mL) and dry acetonitrile (18.98 mL) according to general procedure 8.21.
Colourless solid 104 mg (23%)
Melting point: 178-181 °C (lit. M.p. 177-178 °C[315])
IR$_{Vmax}$ (KBr): 3083 (C-H), 1673 (C=O), 1655 (C=C), 1504 (C=C), 1520 (N-O), 1244 (C-O) cm^{-1}
^{1}H NMR (400 MHz, CDCl$_3$) δ 3.91 (s, 6 H, 2 x OCH_3 on C3' & C5') 3.95 (s, 3 H, OCH_3 on C4'), 6.96 (s, 2 H, 2 x ArH, H2' & H6'), 7.50-7.56 (m, 1 H, ArH, H6), 7.63 (d, 1 H, J = 8 Hz, ArH, H8), 7.78-7.84 (m, 1 H, ArH, H7), 8.29 (d, 1 H, J = 8 Hz, ArH, H5)
^{13}C NMR (101 MHz, CDCl$_3$) ppm 55.9 (C3' & C5'), 60.6 (OCH_3 on C4'), 104.8 (2 x CH, C2' & C6'), 118.0 (CH, C7), 122.7, 122.9, 125.9 (CH), 126.0(CH), 134.7 (CH), 137.6, 141.5 (C3, C_q), 153.2 (C3' & C5',C_q), 154.8 (C8a, C_q), 158.8 (C2, C_q), 168.3 (C4, C_q)
HRMS (ESI) calculated for $C_{18}H_{15}NO_7$ [M^++Na] 380.0746: found 380.0741. Mass accuracy (-1.32 ppm)

3-Nitro-2-(3,4,5-trimethoxy-2-nitrophenyl)chromen-4-one (185)

Obtained as a by product of the above synthesis of 3-nitro-2-(3,4,5-trimethoxyphenyl)chromen-4-one.
Yellow resin 36 mg (7%)
IR$_{Vmax}$ (film): 2947 (C-H), 1671 (C=O), 1532 (N-O), 1464 (C=C), 1375 (C-O) cm^{-1}
^{1}H NMR (400 MHz, $CDCl_3$) δ 3.95 (s, 3 H, OCH_3), 4.02 (s, 3 H, OCH_3), 4.10 (s, 3 H, OCH_3) 6.92 (s, 1 H, ArH, H6'), 7.49 (d, 1 H, J = 8.5 Hz, ArH, H8), 7.53-7.56 (m, 1 H, ArH, H6), 7.78-7.84 (m, 1 H, ArH, H7), 8.31(d, 1 H, J = 7.5 Hz, ArH, H5)
^{13}C NMR (101 MHz, $CDCl_3$) ppm 55.9 (2 x OCH_3 on C3' & C5'), 60.6 (OCH_3 on C4'), 106.9, 117.5, 117.9 (C7), 123.1, 126.1, 126.4, 135.1, 145.6 (C3), 147.9, 154.8 ($C8_a$), 155.3, 156.7 (C2), 167.9 (C_{ketone})
HRMS (ESI) calculated for $C_{18}H_{14}N_2NaO_9$ [M^++Na] 425.0597: found 425.0583. Mass accuracy 3.29 ppm)

7-Methoxy-2-(4-methoxyphenyl)-3-nitrochromen-4-one (186)

7-Methoxy-2-(4-methoxyphenyl)-3-nitrochromen-4-one was prepared from 7-methoxy-2-(4-methoxyphenyl)chromen-4-one (1.77 mmol, 0.5 g), ammonium nitrate (5.9 mmol, 0.447 g), trifluoroacetic acid (9.6 mmol, 1.34 mL), dry dichloromethane (25 mL) and dry acetonitrile (25 mL) according to general procedure 8.21.
Yellow resin 56 mg (9%)
IR$_{Vmax}$ (KBr): 2933 (C-H), 1643 (C=C), 1623 (C=0), 1603 (C=C), 1529 (N-O), 1269 (C-O) cm^{-1}
^{1}H NMR (400 MHz, $CDCl_3$) δ 3.90 (s, 3 H, OCH_3 on C4') 3.96 (s, 3 H, OCH_3 on C7), 6.98 (s, 1 H, ArH, H8), 7.02-7.08 (m, 3 H, 3 x ArH, H3',H5', H4), 7.70 (d, 2 H, J = 8 Hz, 2 x ArH, H2' & H6'), 8.19 (d, 1 H, J = 8.5 Hz, ArH, H5)
^{13}C NMR ppm ($CDCl_3$) ppm 55.1 (OCH_3 on C4'), 55.6 (OCH_3 on C7), 100.2, 114.34 (C3' & C5'), 115.1, 116.3, 119.9, 127.3, 129.2 (C2' & C6'), 156.6 ($C8_a$), 158.4 (C7), 162.7 (C4'), 164.6 (C2), 167.8 (C_{ketone})
HRMS (ESI) calculated for $C_{17}H_{13}NO_6$ [M^++Na] 350.0641: found 350.0632. Mass accuracy (-2.57 ppm)

2-(3-Chlorophenyl)-3-nitrochromen-4-one (187)

2-(3-Chlorophenyl)-3-nitrochromen-4-one was prepared from 2-(4-chlorophenyl)chromen-4-one (0.779 mmol, 0.2 g), ammonium nitrate (2.4 mmol 0.389 g), trifluoroacetic acid (4.2 mmol, 0.59 mL), dry dichloromethane (11 mL) and dry acetonitrile (11 mL) according to general procedure 8.21.
Colourless solid 54 mg (21%)
Melting point: 159-162 °C (lit. M.p. 157-158 °C[315])
IR$_{Vmax}$ (KBr): 3096 (C-H), 1658 (C=O), 1617 (C=C), 1520 (N-O), 1466 (C=C), 768 (C-Cl) cm^{-1}
^{1}H NMR (400 MHz, $CDCl_3$) δ 7.47-7.66 (m, 5 H, 5 x ArH), 7.77 (s, 1 H, ArH, H2'), 7.82-7.88 (m, 1 H, ArH, H7), 8.23 (d, 1 H, J = 7.5 Hz, ArH, H5)

^{13}C NMR (101 MHz, $CDCl_3$) ppm 118.0 (C7), 122.9, 125.5, 126.1, 126.3, 127.4, 129.6, 130.2, 132.5, 135.0, 135.1, 137.8 (C3), 154.9 (C_{8a}), 157.7 (C2), 168.2 (C_{ketone})
HRMS (ESI) calculated for $C_{15}H_8Cl^{35}NO_4$ [M^++Na] 324.0040: found 324.0024. Mass accuracy (-4.94 ppm).

7-Methoxy-3-nitro-2-phenylchromen-4-one (188)

7-Methoxy-3-nitro-2-phenylchromen-4-one was prepared from 7-methoxy-2-phenylchromen-4-one (0.7 mmol 0.2 g), ammonium nitrate (2.2 mmol, 0.176 g), trifluoroacetic acid (3.78 mmol, 0.533 mL), dry dichloromethane (9.88 mL) and dry acetonitrile (9.88 mL) according to general procedure 8.21.
Yellow resin 106 mg (15%)
IR$_{Vmax}$ (KBr): 2961 (C-H), 1653 (C=O), 1630 (C=C), 1528 (N-O), 1434 (C=C), 1253 (C-O) cm^{-1}
^{1}H NMR (400 MHz, $CDCl_3$) δ 3.97 (s, 3 H, OCH_3) 7.00 (s, 1 H, ArH, H8), 7.09 (d, 1 H, J = 7.5 Hz, ArH, H6), 7.55-7.59 (m, 2 H, 2 x ArH, H3'&H5'), 7.61-7.65 (m, 1 H, ArH, H4'), 7.75 (d, 2 H, J = 8 Hz, 2 x ArH, H2' & H6'), 8.23 (d, 1H, J = 8 Hz, ArH, H5)
^{13}C NMR (101 MHz, $CDCl_3$) ppm 55.6 (CH_3), 100.2, 115.3, 116.5, 127.3, 127.4 (C3' & C5'), 128.0, 128.8, 129.0 (C2' & C6'), 132.2, 137.6 (C3), 156.8 (C_{8a}), 158.7 (C7), 164.8 (C2), 167.7 (C_{ketone})
HRMS (ESI) calculated for $C_{16}H_{11}NO_5$ [M^++Na] 320.0535: found 320.0537. Mass accuracy 0.62 ppm).

3-Nitro-2,4-diphenyl-2,5-dihydrobenzo[b][1,4]thiazepine (189)

To a solution of 2-nitro-1,3-diphenylprop-2-en-1-one (250 mg, 0.98 mmol) in methanol (10 mL) was added o-aminothiophenol (0.125 g, 1 mmol) and concentrated hydrochloric acid 10 drops. The reaction was heated to reflux for 3 hours. Organic solvent was removed *in vacuo*. Crude product was purified by column chromatography on silica gel (eluent 8:1 hexane: ethyl acetate).
Colourless crystals 212 mg (60%)
Melting Point: 159-162 °C (lit. M.p. 161-163 °C[502])
IR$_{Vmax}$ (KBr): 3328 (NH), 3056, 2981 (CH), 1791 (C=O), 1625 (C=C), 1524, 1355 (NO_2), 1234 (CN) cm^{-1}
^{1}H NMR (400 MHz, $CDCl_3$) δ 6.31 (s, 1 H, CH), 6.47 (br. s., 1 H, NH), 6.81 - 6.96 (m, 2 H), 6.97 - 7.21 (m, 7 H), 7.47 - 7.62 (m, 5 H)
^{13}C NMR (101 MHz, $CDCl_3$) ppm 51.2 (C4), 122.1 (CH), 125.2, 125.3 (CH), 126.9 (CH), 127.2 (CH), 128.0 (CH), 129.0 (CH), 129.3 (CH), 129.8 (CH), 135.3 (CH), 139.6, 139.8, 143.3 (C2), 151.4 (C-NH)
HRMS (APCI) calculated for $C_{21}H_{17}N_2O_2S$ [M^++H] 361.1011: found 361.1009. Mass accuracy (2.22 ppm).

3-Nitro-2-phenyl-1H-indole (190)

To a mixture of indole (1 g, 8.55 mmol) and silver nitrate (1.55 g, 9.1 mmol) in acetonitrile 8 mL was added benzoyl chloride 1.25 g (9.1 mmol) dropwise at 0 °C. The reaction mixture was stirred at 0 °C for 45 min. The reaction mixture was diluted with water (200 mL) and the

precipitate was filtered off. This precipitate was recrystallized from benzene to give pure product.
Yellow-green solid 1.01 g (52%)
Melting Point: 230–233 °C (lit. M.p. 237-238 °C[317])
IR$_{Vmax}$ (ATR): 3246 (NH), 3055, 2981 (C-H), 1605 (C=C), 1543, 1356 (NO_2), 1243 (C-N) cm^{-1}
^{1}H NMR (400 MHz, $CDCl_3$) δ 7.36 - 7.47 (m, 3 H, 3 x ArH) 7.52 - 7.56 (m, 3 H, 3 x ArH) 7.69 - 7.75 (m, 2 H, 2 x ArH) 8.36 - 8.42 (m, 1 H, H7) 8.59 (br. s., 1 H, NH)
^{13}C NMR (101 MHz, $CDCl_3$) ppm 111.4 (CH), 121.5, 124.2 (CH), 125.0 (C2), 128.7 (CH), 129.5 (CH), 130.4 (C7A)
HRMS (APCI) calculated for $C_{14}H_{11}N_2O_2$ [M^++H] 239.0821: found 239.0816. Mass accuracy (-2.09 ppm).

2,3-Dibromo-1,3-diphenylpropan-1-one (191)

To a solution of bromine (1.997 g, 12.5 mmol) in chloroform (10 mL) was added (2 g, 9.6 mmol) chalcone at 0 °C. The reaction mixture was allowed to heat to room temperature and the reaction was monitored by TLC. After the desired completion level was attained, solvent was removed *in vacuo*. The crude product was purified by column chromatography (eluent: dichloromethane). Product was then recrystallised from ethanol.
Colourless crystals (45%)
Melting Point: 153-156 °C (lit. M.p. 158-158 °C[503])
IR$_{Vmax}$ (KBr): 3058, 3028 (CH), 1682 (C=O), 1594 (C=C) cm^{-1}
^{1}H NMR (400 MHz, $CDCl_3$) δ 5.68 (d, *J* = 11.61 Hz, 1 H, H3), 5.87 (d, *J* = 11.20 Hz, 1 H, H2), 7.39 - 7.49 (m, 3 H, 3 x ArH), 7.52 - 7.61 (m, 4 H, 4 x ArH), 7.65 - 7.72 (m, 1 H, 1 x ArH), 8.11 - 8.17 (m, 2 H, 2 x ArH)
^{13}C NMR (101 MHz, $CDCl_3$) ppm 46.8 (C3), 49.8 (C2), 128.3 (CH), 128.8 (CH), 128.9 (CH), 129.0 (CH), 129.3 (CH), 134.1 (CH), 134.4 (C1"), 138.2 (C1'), 191.1 (C=O)
HRMS (APCI) calculated for $C_{15}H_{13}OBr_2^{79}$ [M^++H] 366.9333: found 366.9328. Mass accuracy (-1.36 ppm).

3,5-Diphenylisoxazole (192)

To a solution of 2,3-dibromo-1,3-diphenylpropan-1-one (1.45 g, 3.96 mmol) in (35 mL) methanol was added hydroxylamine hydrochloride 0.69 g (in 1.25 mL water). The reaction mixture was heated to reflux and KOH (1.7 g in 3 mL water) was added and the solution was refluxed for 30 min. The reaction mixture was allowed to cool to room temperature and the precipitate was filtered. This precipitate was recrystallized from methanol to give pure product.
Colourless crystals 457 mg (52%)
Melting Point: 135-138 °C (lit. M.p. 141 °C[504])
IR$_{Vmax}$ (KBr): 3056, 2981 (CH), 1681, 1579 (C=C), 1127 (CN) cm^{-1}
^{1}H NMR (400 MHz, $CDCl_3$) δ 6.85 (s, 1 H, =CH), 7.45 - 7.54 (m, 6 H, 6 x ArH), 7.84 - 7.93 (m, 4 H, 4 x ArH)
^{13}C NMR (101 MHz, $CDCl_3$) ppm 97.5 (C4), 125.8 (CH), 126.8 (CH), 128.9 (CH), 129.0 (CH), 130.0 (CH, 130.2 (CH), 163.0 (C3), 170.4 (C5)
HRMS (APCI) calculated for $C_{15}H_{12}ON$ [M^++H] 222.0919: found 222.0915. Mass accuracy (-1.80 ppm).

4-Nitro-3,5-diphenylisoxazole (193)

To a solution of 3,5-diphenylisoxazole (500 mg, 2.26 mmol) in acetic anhydride (4 mL) was added concentrated nitric acid 0.1 mL and concentrated sulphuric acid (10 drops). The reaction was stirred at room temperature for 40 min. The water (200 mL) was added to the reaction vessel and was extracted into dichloromethane. The organic phase was washed with water, brine and dried over anhydrous sodium sulphate. Solvent was removed *in vacuo*. The crude product was purified by column chromatography (eluent: 4:1 hexane: ethyl acetate).
Colourless crystals 199 mg (33%)
Melting Point: 172-176 °C (lit. M.p. 174-176 °C[325])
IR$_{Vmax}$ (KBr): 3054, 2971 (CH), 1614, 1590 (C=C), 1534, 1389 (NO_2), 1127 (CN) cm^{-1}
^{1}H NMR (400 MHz, $CDCl_3$) δ 7.42 - 7.72 (m, 6 H, 6 x ArH), 7.83 - 7.97 (m, 2 H, H2' & H6' / H2' & H6'), 8.02 - 8.17 (m, 2 H, H2' & H6' / H2' & H6')
^{13}C NMR (101 MHz, $CDCl_3$) ppm 104.6 (C4), 126.5, 126.5 (CH), 126.7, 127.0 (CH), 127.4, 127.8, 128.2 (CH), 128.6 (CH), 128.6 (CH), 128.7 (CH), 128.8 (CH), 128.9 (CH), 130.1 (CH), 130.2 (CH), 130.6 (CH), 130.6 (CH), 160.7 (C3), 165.8 (C5)
HRMS (APCI) calculated for $C_{15}H_{11}O_3N_2$ [M^++H] 267.0770: found 267.0763. Mass accuracy (-2.62 ppm).

9-Methoxyanthracene (194)

To a stirred solution of anthrone (1.94 g, 10 mmol) in methanol (30 mL) and benzene (30 mL), was added trimethyl orthoformate (1.06 g) and concentrated sulfuric acid (10 drops). The reaction mixture was heated to reflux for 3 days. The reaction was cooled and poured onto 100 mL saturated sodium hydrogen carbonate solution and extracted with ether. The organic extracts were washed with water, brine and dried over Na_2SO_4. Solvent was removed *in vacuo* and the solid was recrystallized from ethanol.
Pale yellow solid 1.59 g (76%)
Melting Point: 90-94 °C (lit. M.p. 94 °C[505])
IR$_{Vmax}$ (ATR): 3051, 2969 (C-H), 1620 (C=C), 1571, 1462 (C=C) cm^{-1}
^{1}H NMR (400 MHz, $CDCl_3$) δ 4.18 (s, 3 H, OCH_3), 7.50 (dqd, J = 8.05, 6.27, 6.27, 6.27, 1.83 Hz, 4 H, 4 x ArH), 7.97 - 8.06 (m, 2 H, 2 x ArH), 8.25 (s, 1 H, H10), 8.29 - 8.38 (m, 2 H, 2 x ArH)
^{13}C NMR (101 MHz, $CDCl_3$) ppm 63.1 (CH_3), 122.2 (CH), 122.2 (CH), 124.4, 125.1 (CH), 125.4 (CH), 128.4 (CH), 132.4, 152.2 (C9)
HRMS (APCI) calculated for $C_{15}H_{13}O$ [M^++H] 209.0966: found 209.0958. Mass accuracy (-3.82 ppm).

9-Methylanthracene (195)

To a mixture of 9-anthraldehyde (2 g, 9.7 mmol), hydrazine hydrate (3.33 g, 85 %) and diethylene glycol (20 mL) was added potassium hydroxide (3.33 g). The reaction mixture was heated to 200 °C for 1 h in a pressure tube. The reaction mix was allowed to cool to room temperature, diluted with water and extracted with dichloromethane. Solvent was removed *in vacuo* and residual solid was recrystallized from aqueous ethanol.
Pale yellow solid 1.57 g (84%)
Melting Point: 82-84 °C (lit. M.p. 79-80 °C[506])
IR$_{Vmax}$ (ATR): 3088, 2981 (C-H), 1659 (C=C), 1555, 1478 (C=C) cm^{-1}

^{1}H NMR (400 MHz, $CDCl_3$) δ 3.15 (s, 3 H, CH_3), 7.47 - 7.62 (m, 4 H, 4 x ArH), 8.03 - 8.11 (m, 2 H, 2 x ArH), 8.32 - 8.37 (m, 2 H, 2 x ArH), 8.39 (s, 1 H, H10)
^{13}C NMR (101 MHz, $CDCl_3$) ppm 13.9 (CH_3), 124.6 (CH), 124.7 (CH), 125.2 (CH), 125.2 (CH), 129.0 (CH), 130.1, 130.1, 131.4
HRMS (APCI) calculated for $C_{15}H_{13}$ [M^++H] 193.1012: found 193.1006. Mass accuracy (-3.11 ppm).

9-Ethylanthracene (196)

To a hot solution of anthrone (2 g, 10.3 mmol) in anhydrous toluene (20 mL) was added portion-wise a solution of 3.0 M ethyl magnesium bromide (3.8 mL) in THF (11.33 mmol). The reaction was heated to reflux under nitrogen for 2 h until the mixture turned green. The mixture was allowed to cool to room temperature and poured over a slurry of 20 % HCl and crushed ice (50 mL). Once the ice had melted; the aqueous layer was extracted into toluene and the solvent was removed *in vacuo*. The crude product was washed with hot water and recrystallized from ethanol.
Yellow solid 1.71 g (80%)
Melting Point: 55-58 °C (lit. M.p. 59 °C[507])
IR$_{\nu max}$ (ATR): 3025, 2977 (C-H), 1621 (C=C), 1494, 1443 (C=C) cm^{-1}
^{1}H NMR (400 MHz, $CDCl_3$) δ 1.47 - 1.52 (m, 3 H, CH_3), 3.68 (q, J = 7.32 Hz, 2 H, CH_2), 7.44 - 7.61 (m, 4 H, 4 x ArH), 8.04 (d, J = 8.55 Hz, 2 H, 2 x ArH), 8.26 - 8.41 (m, 3 H, 2 x ArH & H10)
^{13}C NMR (101 MHz, $CDCl_3$) ppm 15.5 (CH_3), 21.1 (CH_2), 123.5 (CH), 124.3 (CH), 124.8 (CH), 125.3 (CH), 125.4 (CH), 125.5 (CH), 126.2 (CH), 128.1 (CH), 129.2, 129.2 (CH), 131.7, 136.6
HRMS (APCI) calculated for $C_{16}H_{15}$ [M^++H] 207.1174: found 207.1168. Mass accuracy (-2.90 ppm).

9-Isopropylanthracene (197)

To a hot solution of anthrone (2 g, 10.3 mmol) in anhydrous toluene 20 mL was added portion-wise 8.3 mL of 3.0 M of isopropyl magnesium bromide (11.33 mmol) in diethyl ether. The reaction was heated to reflux under nitrogen for 2 h until the mixture turned green. The mixture was allowed to cool to room temperature and poured over a slurry of 20 % HCl and crushed ice. Once the ice had melted the aqueous layer was extracted into toluene and the solvent was removed *in vacuo*. The crude product was washed with hot water and recrystallized from ethanol.
Yellow solid 1.72 g (76%)
Melting Point: 61-65 °C (lit. M.p. 76 °C[508])
IR$_{\nu max}$ (ATR): 3069, 2988 (C-H), 1591 (C=C), 1485, 1442 (C=C) cm^{-1}
^{1}H NMR (400 MHz, $CDCl_3$) δ 1.78 (d, J = 7.05 Hz, 6 H, 2 x CH_3), 4.60 (s, 1 H, CH), 7.41 - 7.53 (m, 5 H, 5 x ArH), 8.02 (dd, J = 8.50, 1.45 Hz, 3 H, 3 x ArH), 8.35 (s, 1 H, H10)
^{13}C NMR (101 MHz, $CDCl_3$) ppm 22.9 (CH_3), 28.3 (CH), 110.0 (CH), 124.5 (CH), 125.3 (CH), 126.2 (CH), 126.3 (CH), 127.2 (CH), 128.1 (CH), 129.5 (CH), 131.6, 134.1 (CH)
HRMS (APCI) calculated for $C_{17}H_{16}$ [M^+] 220.1252: found 220.1248. Mass accuracy (-1.82 ppm).

9-Phenylanthracene (198)

To a solution of anthrone (4 g, 20.6 mmol) in anhydrous toluene (20 mL) under nitrogen, was added portion-wise of 3.0 M phenyl magnesium bromide (24.72 mmol, 8.3 mL) in diethyl ether. The reaction mixture was refluxed under nitrogen for 3 h until the reaction mix turned green. The mixture was allowed to cool to room temperature and poured over a slurry of 20 % HCl and crushed ice (50 mL). The organic layer was separated and solvent was removed *in vacuo*. Product was purified by column chromatography (eluent dichloromethane: hexane (1:4)).

Yellow solid 4.41 g (84%)

Melting Point: 150-153 °C (lit. M.p. 153-154 °C[509])

IR$_{\nu max}$ (ATR): 3029, 2998 (C-H), 1667 (C=C), 1511, 1486 (C=C) cm^{-1}

^{1}H NMR (400 MHz, CDCl$_3$) δ 7.40 - 7.47 (m, 2 H, 2 x ArH), 7.50 - 7.57 (m, 4 H, 4 x ArH), 7.60 - 7.70 (m, 3 H, 3 x ArH), 7.79 (d, *J* = 8.71 Hz, 2 H, 2 x ArH), 8.12 (d, *J* = 8.29 Hz, 2 H, 2 x ArH), 8.57 (s, 1 H, H10)

^{13}C NMR (101 MHz, CDCl$_3$) ppm 125.0 (CH), 125.3 (CH), 126.5 (CH), 126.8 (CH), 127.4 (CH), 128.3 (CH), 128.3 (CH), 130.2, 131.2 (CH), 131.3, 136.9, 138.7 (C9)

HRMS (APCI) calculated for $C_{20}H_{15}$ [M$^+$+H] 255.1168: found 255.1158. Mass accuracy (-3.92 ppm).

10-Ethylanthracene-9-carbaldehyde (199)

To a cooled, stirred solution of 9-ethylanthracene (1.65 g, 8 mmol) in phosphorus oxychloride (2.30 g, 15 mmol) was added N-methylformanilide (2.03 g, 15 mmol). The flask was heated to 100 °C for 1.5 h. The solution was then allowed to cool to room temperature and quenched by adding a solution of sodium acetate 8.3 g in water 15 mL. The reaction mixture was then extracted with dichloromethane, washed with water and brine and subsequently dried over sodium sulphate. The solvent was evaporated *in vacuo*. The product was purified by column chromatography (dichloromethane: hexane (1:4)).

Yellow solid 1.51 g (80%)

Melting Point: 95-98 °C (lit. M.p. 96-96.5 °C[510])

IR$_{\nu max}$ (ATR): 3023, 2978 (C-H), 1603 (C=C), 1523, 1448 (C=C) cm^{-1}

^{1}H NMR (400 MHz, CDCl$_3$) δ 1.48 (t, *J* = 7.63 Hz, 3 H, CH_3), 3.67 (q, *J* = 7.83 Hz, 2 H, CH_2), 7.48 - 7.72 (m, 4 H, 4 x ArH), 8.35 (d, *J* = 8.61 Hz, 2 H, 2 x ArH), 8.96 (d, *J* = 9.00 Hz, 2 H, 2 x ArH), 11.46 (s, 1 H, CHO)

^{13}C NMR (101 MHz, CDCl$_3$) ppm 15.5 (CH_3), 22.1 (CH_2), 121.6 (CH), 123.5 (CH), 124.2 (CH), 125.0 (CH), 125.6 (CH), 125.7 (CH), 127.3 (CH), 128.3 (CH), 128.6, 129.0 (CH), 129.2 (CH), 131.8, 135.2 (CH), 146.0, 193.4 (CHO)

HRMS (APCI) calculated for $C_{17}H_{15}O$ [M$^+$+H] 235.1123: found 235.1121. Mass accuracy (-0.85 ppm).

10-Isopropylanthracene-9-carbaldehyde (200)

To a cooled, stirred solution of 9-isopropylanthracene (1.76 g, 8 mmol) in phosphorus oxychloride (2.30 g, 15 mmol) was added N-methylformanilide (2.03 g, 15 mmol). The flask

was heated to 100 °C for 1.5 h. The solution was then allowed to cool to room temperature and quenched by adding a solution of sodium acetate 8.3 g in water 15 mL. The reaction mixture was then extracted with dichloromethane, washed with water and brine and subsequently dried over sodium sulphate. The solvent was evaporated *in vacuo*. The product was purified by column chromatography (dichloromethane: hexane (1:4)).
Dark brown resin 1.19 g (60%)
IR$_{Vmax}$ (ATR): 3077, 2950 (C-H), 1622 (C=C), 1520, 1445 (C=C) cm^{-1}
^{1}H NMR (400 MHz, CDCl$_3$) δ 1.77 (d, *J* = 7.32 Hz, 6 H, 2 x CH$_3$), 4.52 - 4.62 (m, 1 H, CH), 7.50 - 7.55 (m, 2 H, 2 x ArH), 7.58 - 7.65 (m, 2 H, 2 x ArH), 8.53 (d, *J* = 9.16 Hz, 2 H, 2 x ArH), 8.93 (d, *J* = 9.16 Hz, 2 H, 2 x ArH), 11.46 (s, 1 H, CHO)
^{13}C NMR (101 MHz, CDCl$_3$) ppm 21.3 (CH$_3$), 22.1 (CH), 121.6 (CH), 123.5 (CH), 124.2 (CH), 125.0 (CH), 125.6 (CH), 125.7 (CH), 127.3 (CH), 128.3 (CH), 128.7, 129.1 (CH), 129.2 (CH), 131.8, 135.2 (CH), 146.1, 195.4 (CHO)
HRMS (APCI) calculated for $C_{18}H_{17}O$ [M$^+$+H] 249.1279: found 249.1276. Mass accuracy (-1.20 ppm).

10-Phenylanthracene-9-carbaldehyde (201)

To a cooled, stirred solution of 9-phenylanthracene (2 g, 8 mmol) in phosphorus oxychloride (2.30 g, 15 mmol) was added N-methylformanilide (2.03 g, 15 mmol). The flask was heated to 100 °C for 1.5 h. The solution was then allowed to cool to room temperature and quenched by adding a solution of sodium acetate 8.3 g in water 15 mL. The reaction mixture was then extracted with dichloromethane, washed with water and brine and subsequently dried over sodium sulphate. The solvent was evaporated *in vacuo*. The product was purified by column chromatography (dichloromethane: hexane (1:4)).
Yellow solid 1.58 g (70%)
Melting Point: 162-163 °C (lit M.p. 165-166 °C[511])
IR$_{Vmax}$ (ATR): 2981, 2884 (C-H), 1732 (C=O), 1665 (C=C), 1554, 1479 (C=C) cm^{-1}
^{1}H NMR (400 MHz, CDCl$_3$) δ 7.32 - 7.48 (m, 4 H, 4 x ArH), 7.54 - 7.68 (m, 5 H, 5 x ArH), 7.72 (d, *J* = 8.71 Hz, 2 H, 2 x ArH), 9.01 (d, *J* = 9.12 Hz, 2 H, 2 x ArH), 11.55 (s, 1 H, CHO)
^{13}C NMR (101 MHz, CDCl$_3$) ppm 123.3 (CH), 124.9, 125.4 (CH), 127.9 (CH), 127.9 (CH), 128.4 (CH), 128.5 (CH), 129.7, 130.5 (CH), 131.5, 138.1, 145.3, 193.1 (CHO)
HRMS (APCI) calculated for $C_{21}H_{15}O$ [M$^+$+H] 283.1117: found 283.1112. Mass accuracy (-1.77 ppm).

10-Methoxyanthracene-9-carbaldehyde (202)

To a cooled, stirred solution of 9-methoxyanthracene (2 g, 8.5 mmol) in phosphorus oxychloride (2.30 g, 15 mmol) was added N-methylformanilide (2.03 g, 15 mmol). The flask was heated to 100 °C for 1.5 h. The solution was then allowed to cool to room temperature and quenched by adding a solution of sodium acetate 8.3 g in water 15 mL. The reaction mixture was then extracted with dichloromethane, washed with water and brine and subsequently dried over sodium sulphate. The solvent was evaporated *in vacuo*. The product was recrystallized from ethanol.
Bright yellow solid 1.45 g (72%)
Melting Point: 160-162 °C (lit. M.p. 165 °C[506])

IR$_{Vmax}$ (ATR): 3029, 2997 (C-H), 1730 (C=O), 1625 (C=C), 1555, 1436 (C=C) cm^{-1}
^{1}H NMR (400 MHz, CDCl$_3$) δ 4.21 (s, 3 H, OCH$_3$), 7.54 - 7.63 (m, 2 H, 2 x ArH), 7.65 - 7.75 (m, 2 H, 2 x ArH), 8.42 (d, *J* = 8.55 Hz, 2 H, 2 x ArH), 9.08 (d, *J* = 9.16 Hz, 2 H, 2 x ArH), 11.48 (s, 1 H, CHO)
^{13}C NMR (101 MHz, CDCl$_3$) ppm 63.9 (CH$_3$), 121.2 (CH), 123.1 (CH), 123.9 (CH), 124.2, 125.6 (CH), 127.0 (CH), 127.2 (CH), 128.4, 129.3 (CH), 133.8, 134.1 (CH), 159.2 (C10), 191.9 (CHO)
HRMS (APCI) calculated for $C_{16}H_{13}O_2$ [M$^+$+H] 237.0916: found 237.0907. Mass accuracy (-3.80 ppm).

10-Methylanthracene-9-carbaldehyde (203)

To a cooled, stirred solution of 9-methylanthracene (2 g, 8.5 mmol) in phosphorus oxychloride (2.30 g, 15 mmol) was added N-methylformanilide (2.03 g, 15 mmol). The flask was heated to 100 °C for 1.5 h. The solution was then allowed to cool to room temperature and quenched by adding a solution of sodium acetate 8.3 g in water 15 mL. The reaction mixture was then extracted with dichloromethane, washed with water and brine and subsequently dried over sodium sulphate. The solvent was evaporated *in vacuo*. The product was recrystallized from ethanol.
Bright orange solid 1.12 g (60%)
Melting Point: 171-174 °C (lit. M.p. 171.9-172.6 °C[512])
IR$_{Vmax}$ (KBr): 3076, 2981 (C-H), 1681 (C=O), 1561 (C=C), 1542, 1449 (C=C) cm^{-1}
^{1}H NMR (400 MHz, CDCl$_3$) δ 3.18 (s, 3 H, CH$_3$), 7.51 - 7.77 (m, 4 H, 4 x ArH), 8.39 (d, *J* = 9.16 Hz, 2 H, 2 x ArH), 8.99 (d, *J* = 8.55 Hz, 2 H, 2 x ArH), 11.50 (s, 1 H, CHO)
^{13}C NMR (101 MHz, CDCl$_3$) ppm 15.4 (CH$_3$), 123.9, 124.1 (CH), 125.4 (CH), 125.6 (CH), 128.4 (CH), 129.7, 131.6, 139.9, 193.4 (CHO)
HRMS (APCI) calculated for $C_{16}H_{13}O$ [M$^+$+H] 221.0961: found 221.0953. Mass accuracy (-3.62 ppm).

9,10-Dibromoanthracene (204)

To a solution of anthracene (5 g, 28 mmol) in dichloromethane (100 mL) was added dropwise Bromine (2.9 mL) in dichloromethane (50 mL). The reaction mixture was allowed to stir at room temperature for 4 h. Solvent was removed *in vacuo* and residual solid was recrystallized from dichloromethane.
Yellow solid 8.41 g (90%)
Melting Point: 210-215 °C (lit. M.p. 221 °C[513])
IR$_{Vmax}$ (ATR): 3077, 2981, (C-H), 1621 (C=C), 1506, 1435 (C=C) cm^{-1}
^{1}H NMR (400 MHz, CDCl$_3$) δ 7.57 - 7.71 (m, 4 H, 4 x ArH), 8.48 - 8.67 (m, 4 H, 4 x ArH)
^{13}C NMR (101 MHz, CDCl$_3$) ppm 123.5, 127.5 (CH), 128.3 (CH), 131.1
HRMS (APCI) calculated for $C_{14}H_9Br_2^{79}$ [M$^+$+H] 334.9071: found 334.9084. Mass accuracy (3.88 ppm).

10-Bromoanthracene-9-carbaldehyde (205)

To a suspension of 9,10-dibromoanthracene (2 g, 5.95 mmol) in dry THF (20 mL) under nitrogen, at -90 °C was added *n*-butyl lithium (2.9 mL, 7.2 mmol, 2.5 M in hexane) dropwise. The solution was stirred at -90 °C for 50 min before the addition of N-methylformanilide (1.46 mL, 11.9 mmol). The reaction mixture was allowed to heat to room temperature and was stirred overnight. The reaction was quenched with the addition of deionised water (50 mL) and extracted into dichloromethane. Organic layers were combined, washed with water and brine and dried over sodium sulphate. Solvent was removed *in vacuo*. Residue was purified by column chromatography (dichloromethane: hexane (1:2)).
Yellow solid (72%)
Melting Point: 210-213°C (lit. M.p. 218 °C[335])
IR$_{Vmax}$ (ATR): 3086, 2970 (C-H), 1731 (C=O), 1666 (C=C), 1544, 1439 (C=C) cm^{-1}
^{1}H NMR (400 MHz, $CDCl_3$) δ 7.59 - 7.74 (m, 4 H, 4 x ArH), 8.61 - 8.68 (m, 2 H, 2 x ArH), 8.79 - 8.90 (m, 2 H, 2 x ArH), 11.47 (s, 1 H, CHO)
^{13}C NMR (101 MHz, $CDCl_3$) ppm 123.8, 125.6 (CH), 127.3 (CH), 128.8 (CH), 128.9 (CH), 130.2, 131.8, 131.8, 193.2 (CHO)
HRMS (APCI) calculated for $C_{15}H_{10}Br^{79}O$ [M^++H] 284.9915: found 284.9906. Mass accuracy (-3.16 ppm).

1,8-Dichloroanthracene (206)

A slurry of 1,8-dichloroanthracene-9,10-dione (5 g, 18.1 mmol) in NH_3 (60 mL aqueous 28 %) and deionised water (45 mL) was cooled in an ice bath. Zinc dust (25 g, 0.38 mol) was added portion-wise with stirring over 15 min. The resulting red coloured slurry was heated slowly to 75 °C and stirred at this temperature for 4 h. The reaction mixture was allowed to cool to room temperature and was filtered to remove excess zinc solids. The filtrate was extracted with dichloromethane and the organic extracts were concentrated *in vacuo* to give a white residue. This residual white solid was suspended in a mixture of 12 M HCl (20 mL) and isopropanol (220 mL). The resulting suspension was refluxed for 3 hours resulting in a pale yellow solution. The reaction mixture was allowed to stand overnight at room temperature and the precipitated solid was collected by filtration. Further concentration of the mother liquor led to the formation of a second crop of crystals when allowed to stand for a second night.
Yellow crystals 2.53 g (57%)
Melting Point: 152-155 °C (lit. M.p. 156-157 °C[514])
IR$_{Vmax}$ (ATR): 3028, 2981 (C-H), 1618 (C=C), 1508, 1382 (C=C) cm^{-1}
^{1}H NMR (400 MHz, $CDCl_3$) δ 7.36 - 7.42 (m, 2 H, 2 x ArH), 7.59 - 7.64 (m, 2 H, 2 x ArH), 7.90 (d, J = 8.71 Hz, 2 H, 2 x ArH), 8.40 (s, 1 H, H10), 9.21 (s, 1 H, H9)
^{13}C NMR (101 MHz, $CDCl_3$) ppm 120.9 (CH), 125.6 (CH), 125.9 (CH), 127.2 (CH), 127.5 (CH), 129.4, 132.4, 132.5
HRMS (APCI) calculated for $C_{14}H_9Cl_2^{35}$ [M^+] 246.0003: found 245.9999. Mass accuracy (-1.63 ppm).

4,5-Dichloroanthracene-9-carbaldehyde (207)

To a solution of 1,8-dichloroanthracene (5 g, 20.3 mmol) and $AlCl_3$ (5 g in of dichloromethane (145 mL) was added of n,n-dichloromethyl methyl ether (2.7 g in dichloromethane 2 mL). After 1 h the reaction was poured onto ice cold dilute HCl and extracted into dichloromethane. Organic extracts were combined, washed with water and brine and dried over sodium sulphate.

Solvent was removed *in vacuo*. Purification was carried out using column chromatography (toluene).
Yellow solid 1.67 g (30%)
Melting Point: 220-222 °C (lit. M.p. 224-226 °C[336])
IR$_{Vmax}$ (ATR): 3094, 2981 (C-H), 1734 (C=O), 1618 (C=C), 1510, 1479 (Ar C=C) cm^{-1}
^{1}H NMR (400 MHz, $CDCl_3$) δ 7.54 - 7.64 (m, 2 H, 2 x ArH), 7.64 - 7.73 (m, 2 H, 2 x ArH), 8.77 (d, *J* = 8.29 Hz, 2 H, 2 x ArH), 9.58 (br. s., 1 H, H10), 11.41 (br. s., 1 H, CHO)
^{13}C NMR (101 MHz, $CDCl_3$) ppm 122.3 (CH), 126.1 (CH), 128.1 (CH), 128.5 (CH), 128.6 (CH), 130.4, 132.2, 133.2, 192.5 (CHO)
HRMS (APCI) calculated for $C_{15}H_9Cl_2{}^{35}O$ [M$^+$+H] 275.0030: found 275.0030. Mass accuracy (0 ppm).

9-(2-Methoxyvinyl)anthracene (208)

To a suspension of (methoxymethyl)triphenylphosphonium chloride (4.46 g, 13 mmol) in THF 25 mL under nitrogen at 0 °C was added potassium *tert*-butoxide (13 mL, 1 M solution in THF) dropwise. The resultant mixture was stirred for 1 hour. After 1 h a solution of anthraldehyde (10 mmol) in THF 20 mL was added. The reaction was stirred at 0 °C for 5 minutes and then allowed to heat to room temperature, after which the reaction was allowed to stir for two further hours. The reaction was then filtered through a short column of silica and eluted with diethyl ether. Solvent was removed *in vacuo*. Product was purified by column chromatography (hexane: dichloromethane (3:2)) to afford a mixture of *E* / *Z* methyl enol ethers.
Orange resin 1.83 g (60%)
IR$_{Vmax}$ (ATR): 2981, 2924 (C-H), 1622 (C=C), 1524, 1445 (C=C) cm^{-1}
^{1}H NMR (400 MHz, $CDCl_3$) δ 3.66 (s, 3 H, Z CH_3), 3.96 (s, 3 H, E CH_3), 6.04 (d, *J* = 6.71 Hz, 1 H, Z =CH), 6.46 (d, *J* = 13.43 Hz, 1 H, E =CH), 6.61 (d, *J* = 7.32 Hz, 1 H, Z =CH), 6.81 (d, *J* = 12.82 Hz, 1 H, E =CH), 7.46 - 7.58 (m, 6 H), 7.99 - 8.09 (m, 3 H), 8.36 - 8.49 (m, 3 H)
^{13}C NMR (101 MHz, $CDCl_3$) ppm 56.5 (CH_3), 59.9 (CH_3), 98.9, 101.3, 124.9, 125.0, 125.1, 125.7, 126.1, 126.2, 126.7, 128.4, 128.5, 128.6, 128.7, 129.4, 129.6, 130.1, 130.5, 131.4, 131.5, 133.6, 133.8, 148.5, 152.8
HRMS (APCI) calculated for $C_{17}H_{15}O$ [M$^+$+H] 235.1123: found 235.1115. Mass accuracy (-3.40 ppm).

2-(Anthracen-9-yl)acetaldehyde (209)

To a solution of (1.8 g, 7.6 mmol) of the enol ether mixture and NaI (13 mmol) in dry acetonitrile (76 mL) under nitrogen was added TMSCI (13 mmol) dropwise. The reaction was stirred vigorously for 10 min and poured over of 0.5 M aqueous sodium thiosulfate 100 mL and extracted into diethyl ether. The combined organic layers were washed with water, brine and subsequently dried over sodium sulphate. The solvent was removed *in vacuo*. Product was purified by column chromatography (hexane: dichloromethane (3:2)).
Yellow solid 1.39 g (83%)
Melting Point: 140-144 °C (lit. M.p. 144-145 °C[391])
IR$_{Vmax}$ (ATR): 3032, 2881 (C-H), 1621 (C=C), 1522, 1423 (C=C) cm^{-1}
^{1}H NMR (400 MHz, $CDCl_3$) δ ppm 4.67 (d, *J* = 1.83 Hz, 2 H, CH_2), 7.46 - 7.62 (m, 4 H, 4 x ArH), 8.07 (d, *J* = 8.55 Hz, 2 H, 2 x ArH), 8.18 (d, *J* = 9.16 Hz, 2 H, 2 x ArH), 8.48 (s, 1 H, H10), 9.76 - 9.82 (m, 1 H, CHO)

^{13}C NMR (101 MHz, $CDCl_3$) δ ppm 43.0 (CH_2), 123.3, 123.7 (CH), 125.1 (CH), 126.5 (CH), 127.7 (CH), 129.3 (CH), 131.4, 198.8 (CHO)
HRMS (APCI) calculated for $C_{16}H_{13}O$ [M^++H] 221.0966: found 221.0960. Mass accuracy (-2.71 ppm).

8.21 General procedure for the preparation of nitrovinyl anthracene derivatives via Henry Knoevenagel Condensation (7, 41, 210 - 223)

To a solution of 9-anthraldehyde (2 g, 9.7 mmol) in the appropriate nitroalkane (15 mL) was added piperidinium acetate (1.5 g, 10.3 mmol). (Piperidinium acetate was prepared from piperidine 6.6 mL and acetic acid 3 mL). The solution was heated at 90 °C for 1.5 h under nitrogen gas. After one hour the reaction was cooled to room temperature and poured onto 100 mL of ice cold H_2O. The resultant mixture was extracted into DCM, washed with brine and the organic layers were combined, dried over Na_2SO_4 and solvent removed *in vacuo*. The product was recrystallised from an appropriate solvent.

(*E*)-9-(2-nitrovinyl)anthracene (7)

(*E*)-9-(2-Nitrovinyl)anthracene was prepared from 9-anthraldehyde (9.7 mmol, 2 g) and nitromethane (15 mL) according to general procedure 3.1. The product was recrystallized from methanol and diethyl ether.
Red Crystals 2.41 g (99%)
Melting Point: 145-147 °C (lit. M.p. 142 °C[191])
IR$_{Vmax}$ (KBr): 3050, 2948 (C-H), 1617, 1553 (C=C), 1498, 1330 (NO_2), 1250 (C-N) cm^{-1}
^{1}H NMR (400 MHz, $CDCl_3$) δ 7.40 - 7.66 (m, 5 H, 4 x ArH & CH= x 1), 7.80 - 8.05 (m, 2 H, 2 x ArH), 8.05 - 8.25 (m, 2 H, 2 x ArH), 8.45 (br. s., 1 H, H10), 8.90 (d, *J* = 13.43 Hz, 1 H, CH= x 1)
^{13}C NMR (101 MHz, $CDCl_3$) ppm 124.3 (C9) , 125.7 (CH) , 127.5 (CH) , 129.2 (CH) , 129.2, 129.8, 130.4 (CH) , 131.1, 135.6 (CH) , 142.6 (C2')
HRMS (APCI) calculated for $C_{16}H_{12}NO_2$ [M^++H] 250.0868: found 250.0879. Mass accuracy (-4.39 ppm).

(*E*)-9-(2-Nitroprop-1-en-1-yl)anthracene (41)

(*E*)-9-(2-Nitroprop-1-en-1-yl)anthracene was prepared from 9-anthraldehyde (9.7 mmol, 2 g) and nitroethane (15 mL) according to general procedure 3.1. The product was recrystallized from ethanol and diethyl ether.
Orange Crystals 1.87 g (73%)
Melting Point: 141-142 °C (lit. M.p. 142-143 °C[515])
IR$_{Vmax}$ (KBr): 3052, 2825 (C-H), 1510, 1326 (NO_2), 1622.16, 1442.74 (C=C), 1483 (C=C), 385 (CH_3) cm^{-1}
^{1}H NMR (400 MHz, $CDCl_3$) δ 1.98 (s, 1 H, CH_3), 7.42 - 7.63 (m, 4 H, 4 x ArH), 7.86 (d, *J* = 7.93 Hz, 2 H, 2 x ArH), 7.93 - 8.12 (m, 2 H, 2 x ArH), 8.48 (s, 1 H, H10), 8.71 (s, 1 H, H1')
^{13}C NMR (101 MHz, $CDCl_3$) ppm 14.4 (C3'), 124.8 (C9), 125.5 (CH), 126.7, 128.6, 128.8 (CH), 129.0 (CH), 131.0, 131.3 (CH), 151.0 (C2')
HRMS (ESI) calculated for $C_{17}H_{14}NO_2$ [M^++H] 264.1025: found 264.1035. Mass accuracy (3.78 ppm).

(*E*)-9-(2-Nitrobut-1-en-1-yl)anthracene (210)

(*E*)-9-(2-Nitrobut-1-en-1-yl)anthracene was prepared from 9-anthraldehyde (9.7 mmol, 2 g) and nitropropane (15 mL) according to general procedure 8.21. The product was recrystallized from ethanol and diethyl ether.
Gold Crystals 1.62 g (60%)
Melting Point: 159-160 °C [516]
IR$_{\nu max}$ (KBr): 2982, 2937 C-H), 1622, 1427 (C=C), 1520, 1341 (NO_2), 1444 (CH_2), 1376 (CH_3) cm^{-1}
^{1}H NMR (400 MHz, $CDCl_3$) δ 0.90 (t, *J* = 7.32 Hz, 3 H, CH_3), 2.37 (q, *J* = 7.32 Hz, 2 H, CH2), 7.48 - 7.54 (m, 4 H,4 x ArH), 7.88 - 7.93 (m, 2 H, H4 & H5), 8.01 - 8.05 (m, 2 H, H8 & H1), 8.48 (s, 1 H, H10), 8.54 (s, 1 H, H1')
^{13}C NMR (101 MHz, $CDCl_3$) ppm 11.6 (C3'), 21.4 (C2'), 124.9 (C9), 125.6 (CH), 125.7, 126.6 (CH), 128.3 (CH), 128.8, 128.9 (CH), 130.7 (CH), 131.1, 156.7 (C2')
HRMS (APCI) calculated for $C_{18}H_{16}NO_2$ [M^++H] 278.1181: found 278.1189. Mass accuracy (2.87 ppm).

(*E*)-9-Chloro-10-(2-nitrovinyl)anthracene (211)

(*E*)-9-Chloro-10-(2-nitrovinyl)anthracene was prepared from 10-chloroanthracene-9-carbaldehyde (5 mmol, 1.2 g) and nitromethane (15 mL) according to general procedure 8.21. The product was recrystallized from methanol and diethyl ether.
Orange Crystals 1.01 g (71%)
Melting Point: 232-234 °C
IR$_{\nu max}$ (ATR): 3066, 2973 (C-H), 1623 (C=C), 1439 (C=C), 1538, 1326 (NO_2), 1110 (C-N) cm^{-1}
^{1}H NMR (400 MHz, $CDCl_3$) δ 7.52 (d, *J* = 14.04 Hz, 1 H, =CH), 7.60 - 7.77 (m, 4 H, 4 x ArH), 8.20 (d, *J* = 8.55 Hz, 2 H, 2 x ArH), 8.62 (d, *J* = 8.55 Hz, 2 H, 2 x ArH), 8.96 (d, *J* = 14.04 Hz, 1 H, =CH)
^{13}C NMR (101 MHz, $CDCl_3$) ppm 124.8, 125.8, 127.1, 127.6, 128.5, 130.1, 135.4 (C1), 143.3 (C2),
HRMS (APCI) calculated for $C_{16}H_{11}Cl^{35}NO_2$ [M+H] 284.0478: found 284.0492. Mass accuracy (4.93 ppm).

(*E*)-9-Chloro-10-(2-nitroprop-1-en-1-yl)anthracene (212)

(*E*)-9-Chloro-10-(2-nitroprop-1-en-1-yl)anthracene was prepared from 10-chloroanthracene-9-carbaldehyde (5 mmol, 1.2 g) and nitroethane (15 mL) according to general procedure 8.21. The product was recrystallized from methanol and diethyl ether.
Orange Crystals 722 mg (50%)
Melting Point: 158-160 °C
IR$_{\nu max}$ (ATR): 3023, 2977 (C-H), 1622 (C=C), 1480, 1438 (C=C), 1512, 1327 (NO_2), 1171 (C-N) cm^{-1}
^{1}H NMR (400 MHz, $CDCl_3$) δ 1.99 (s, 3 H, CH_3), 7.53 - 7.77 (m, 4 H, 4 x ArH), 7.92 (d, *J* = 8.55 Hz, 2 H, 2 x ArH), 8.60 (d, *J* = 9.16 Hz, 2 H, 2 x ArH), 8.70 (s, 1 H, H1')
^{13}C NMR (101 MHz, $CDCl_3$) ppm 14.4 (C3'), 125.2, 125.6, 127.0, 127.0, 128.4, 129.2, 130.8, 131.0 (C1'), 151.5 (C2')

HRMS (APCI) calculated for $C_{17}H_{13}Cl^{35}NO_2$ [M^++H] 298.0635: found 298.0637. Mass accuracy (0.67 ppm).

(*E*)-9-Chloro-10-(2-nitrobut-1-en-1-yl)anthracene (213)

(*E*)-9-Chloro-10-(2-nitrobut-1-en-1-yl)anthracene was prepared from 10-chloroanthracene-9-carbaldehyde (5 mmol, 1.2 g) and nitropropane (15 mL) according to general procedure 8.21. The product was recrystallized from methanol and diethyl ether.
Orange Crystals 998 mg (64%)
Melting Point: 157-159 °C
IR*Vmax* (ATR): 3086, 2850 (C-H), 1621 (C=C), 1438, 1425 (C=C), 1553, 1328 (NO_2), 1149 (C-N) cm^{-1}
^{1}H NMR (400 MHz, $CDCl_3$) δ 0.90 (t, *J* = 7.32 Hz, 3 H, CH_3), 2.35 (q, *J* = 7.32 Hz, 2 H, CH_2), 7.52 - 7.70 (m, 4 H, 4 x ArH), 7.94 (d, *J* = 8.55 Hz, 2 H, H4 & H6), 8.49 (s, 1 H, H1'), 8.57 (d, *J* = 8.55 Hz, 2 H, H1 & H8)
^{13}C NMR (101 MHz, $CDCl_3$) ppm 11.5 (C4'), 21.4 (C3') 125.3 (CH), 125.2 (CH), 125.4 (CH), 125.5, 126.9 (CH), 128.4, 129.1, 130.1 (C1'), 130.6, 157.0 (C2')
HRMS (APCI) calculated for $C_{18}H_{15}Cl^{35}NO_2$ [M^++H] 312.0791: found 312.0797. Mass accuracy (1.92 ppm).

(*E*)-9-Methoxy-10-(2-nitrovinyl)anthracene (214)

(*E*)-9-Methoxy-10-(2-nitrovinyl)anthracene was prepared from 10-methoxyanthracene-9-carbaldehyde (2 mmol, 0.5 g) and nitromethane (6 mL) according to general procedure 8.21. The product was purified by column chromatography (dichloromethane: hexane (1:1)). The product was recrystallized from methanol and diethyl ether.
Orange solid 302 mg (54%)
Melting Point: 151-153 °C[517]
IR*Vmax* (KBr): 3048, 2971 (C-H), 1610, 1468 (C=C), 1559, 1352 (NO_2), 1234 (C-N) cm^{-1}
^{1}H NMR (400 MHz, $CDCl_3$) δ 4.19 (s, 3 H, OCH_3), 7.53 - 7.66 (m, 5 H, 4 x ArH & H1'), 8.24 (d, *J* = 9.16 Hz, 2 H, 2 x ArH), 8.40 (d, *J* = 7.94 Hz, 2 H, 2 x ArH), 9.02 (d, *J* = 13.43 Hz, 1 H, H2')
^{13}C NMR (101 MHz, $CDCl_3$) ppm 63.7 (OCH_3), 123.1 (CH), 124.3, 124.7 (CH), 125.6 (CH), 127.7 (CH), 131.1, 135.5 (CH), 142.3 (CH), 155.4 (C2')
HRMS (APCI) calculated for $C_{17}H_{14}NO_3$ [M^++H] 280.0974: found 280.0965. Mass accuracy (-3.21 ppm).

(*E*)-9-Bromo-10-(2-nitrovinyl)anthracene (215)

(*E*)-9-Bromo-10-(2-nitrovinyl)anthracene was prepared from 10-bromoanthracene-9-carbaldehyde (1.7 mmol, 0.5 g) and nitromethane (5.1 mL) according to general procedure 8.21. The product was purified by column chromatography (dichloromethane: hexane (1:2)).
Orange solid 311 mg (56%)
Melting Point: 227-230 °C
IR*Vmax* (ATR): 3101, 3048 (C-H), 1626, 1508, (C=C), 1543, 1347 (NO_2), 1251 (C-N) cm^{-1}

^{1}H NMR (400 MHz, DMSO-d_6) δ 7.71 (br. s., 2 H, 2 x ArH), 7.80 (br. s., 2 H, 2 x ArH), 7.92 (d, *J* = 13.27 Hz, 1 H, H1'), 8.31 (d, *J* = 7.46 Hz, 2 H, 2 x ArH), 8.54 (d, *J* = 7.46 Hz, 2 H, 2 x ArH), 8.94 (d, *J* = 13.68 Hz, 1 H, H2')
^{13}C NMR (101 MHz, DMSO-d_6) ppm 109.5, 126.0 (CH), 127.4 (CH), 127.5 (CH), 128.2 (CH), 129.4 (CH), 129.6 (CH), 135.1, 137.6, 144.5, 148.3 (C2')
HRMS (APCI) calculated for $C_{16}H_{11}Br^{79}NO_2$ [M^++H] 327.9973: found 327.9966. Mass accuracy (-2.13 ppm).

(*E*)-9-Methyl-10-(2-nitrovinyl)anthracene (216)

(*E*)-9-Methyl-10-(2-nitrovinyl)anthracene was prepared from 10-methylanthracene-9-carbaldehyde (2.2 mmol, 0.5 g) and nitromethane (6.6 mL) according to general procedure 8.21. The product was purified by column chromatography (dichloromethane: hexane (1:2)). The product was recrystallized from methanol and diethyl ether.
Bright orange solid 175 mg (30%)
Melting Point: 140-142 °C
IR$_{Vmax}$ (ATR): 3100, 2981 (C-H), 1624 (C=C), 1549, 1332 (NO_2), 1504, 1461 (C=C) cm^{-1}
^{1}H NMR (400 MHz, $CDCl_3$) δ 3.08 (s, 3 H, CH_3), 7.45 (d, *J* = 13.43 Hz, 1 H, H1'), 7.51 - 7.61 (m, 4 H, 4 x ArH), 8.08 - 8.17 (m, 2 H, 2 x ArH), 8.23 - 8.34 (m, 2 H, 2 x ArH), 8.88 (d, *J* = 14.04 Hz, 1 H, H2')
^{13}C NMR (101 MHz, $CDCl_3$) ppm 14.6 (CH_3), 121.7, 124.9 (CH), 125.4 (CH), 125.5 (CH), 126.8 (CH), 129.4, 129.6, 134.6, 136.2 (CH), 142.5 (C2')
HRMS (APCI) calculated for $C_{17}H_{14}NO_2$ [M^++H] 264.1019: found 264.1006. Mass accuracy (-4.92 ppm).

(*E*)-9-(2-Nitrovinyl)-10-phenylanthracene (217)

(*E*)-9-(2-Nitrovinyl)-10-phenylanthracene was prepared from 10-phenylanthracene-9-carbaldehyde (1.7 mmol, 0.5 g) and nitromethane (5.1 mL) according to general procedure 8.21. The product was purified by column chromatography (dichloromethane: hexane (1:1)). The product was recrystallized from methanol and diethyl ether.
Orange solid 332 mg (60%)
Melting Point: 119-121 °C
IR v_{max} (ATR): 3094, 2981 (C-H), 1630 (C=C), 1510, 1437 (C=C), 1542, 1331 (NO_2) cm^{-1}
^{1}H NMR (400 MHz, $CDCl_3$) δ 7.43 (t, *J* = 7.02 Hz, 4 H, 4 x ArH), 7.55 - 7.66 (m, 6 H, 5 x ArH & H1'), 7.73 (d, *J* = 8.55 Hz, 2 H, 2 x ArH), 8.25 (d, *J* = 9.16 Hz, 2 H, 2 x ArH), 9.08 (d, *J* = 14.04 Hz, 1 H, H2')
^{13}C NMR (101 MHz, $CDCl_3$) ppm 123.3, 124.4 (CH), 125.5 (CH), 127.1 (CH), 127.9 (CH), 128.5 (CH), 129.6, 129.9, 130.9 (CH), 136.1 (CH), 138.1, 140.9, 142.9 (C2')
HRMS (APCI) calculated for $C_{22}H_{16}NO_2$ [M^++H] 326.1181: found 326.1177. Mass accuracy (-1.23 ppm).

(*E*)-1,8-Dichloro-10-(2-nitrovinyl)anthracene (218)

(*E*)-1,8-Dichloro-10-(2-nitrovinyl)anthracene was prepared from 4,5-dichloroanthracene-9-carbaldehyde (1.8 mmol, 0.5 g) and nitromethane (5.1 mL) according to general procedure 8.21. The product was purified by column chromatography dichloromethane: hexane (1:1).
Yellow solid 58 mg (10%)

Melting Point: 206-209 °C
IR$_{Vmax}$ (ATR): 2981, 2889 (C-H), 1631 (C=C), 1510, 1437 (C=C), 1543, 1361 (NO_2) cm^{-1}
^{1}H NMR (400 MHz, $CDCl_3$) δ 7.40 - 7.63 (m, 3 H, 2 x ArH & H1'), 7.71 (d, *J* = 7.32 Hz, 2 H, 2 x ArH), 8.08 (d, *J* = 8.55 Hz, 2 H, 2 x ArH), 8.91 (d, *J* = 14.04 Hz, 1 H, H2'), 9.47 (s, 1 H, H9)
^{13}C NMR (101 MHz, $CDCl_3$) ppm 123.6 (CH), 124.3 (CH), 126.3, 126.5, 127.5 (CH), 129.0, 130.7, 133.5, 135.3 (CH), 143.6 (C2')
HRMS (APCI) calculated for $C_{16}H_9Cl_2{}^{35}NO_2$ [M^+] 317.0010: found 317.0009. Mass accuracy (-0.32 ppm).

(*E*)-9-Ethyl-10-(2-nitrovinyl)anthracene (219)

(*E*)-9-Ethyl-10-(2-nitrovinyl)anthracene was prepared from 10-ethylanthracene-9-carbaldehyde (4.4 mmol, 1.1 g) and nitromethane (12 mL) according to general procedure 8.21. The product was recrystallized from methanol and diethyl ether.
Orange solid 733 mg (60%)
Melting Point: 130-134 °C
IR$_{Vmax}$ (ATR): 3087, 2976 (C-H), 1629 (C=C), 1554, 1338 (NO_2), 1539, 1442 (C=C) cm^{-1}
^{1}H NMR (400 MHz, $CDCl_3$) δ 1.49 (t, *J* = 7.63 Hz, 3 H, CH_3), 3.68 (q, *J* = 7.32 Hz, 2 H, CH_2), 7.46 - 7.66 (m, 5 H, 4 x ArH & H1'), 8.14 - 8.25 (m, 2 H, 2 x ArH), 8.30 - 8.42 (m, 2 H, 2 x ArH), 8.98 (d, *J* = 13.43 Hz, 1 H, H2')
^{13}C NMR (101 MHz, $CDCl_3$) ppm 15.5 (CH_3), 21.6 (CH_2), 122.0, 124.3 (CH), 125.1 (CH), 125.2 (CH), 125.7 (CH), 125.7 (CH), 126.8 (CH), 127.5 (CH), 128.8, 129.2 (CH), 129.8, 136.4 (CH), 140.9, 142.6 (C2')
HRMS (APCI) calculated for $C_{18}H_{16}NO_2$ [M^++H] 278.1181: found 278.1178. Mass accuracy (-1.08 ppm).

(*E*)-9-Isopropyl-10-(2-nitrovinyl)anthracene (220)

(*E*)-9-Isopropyl-10-(2-nitrovinyl)anthracene was prepared from 10-isopropylanthracene-9-carbaldehyde (4.4 mmol, 1.1 g) and nitromethane (12 mL) according to general procedure 8.21. The product was recrystallized from methanol and diethyl ether.
Dark red resin 873 mg (68%)
IR$_{Vmax}$ (ATR): 3087, 2962 (C-H), 1628 (C=C), 1552, 1333 (NO_2), 1514, 1443 (C=C) cm^{-1}
^{1}H NMR (400 MHz, $CDCl_3$) δ 1.80 (m, 6 H, 2 x CH_3), 4.52 - 4.71 (m, 1 H, CH), 7.43 - 7.62 (m, 5 H, 4 x ArH & H1'), 8.12 - 8.24 (m, 2 H, 2 x ArH), 8.47 - 8.63 (m, 2 H, 2 x ArH), 8.99 (dd, *J* = 13.43, 1 H, H2')
^{13}C NMR (101 MHz, $CDCl_3$) ppm 22.9 (CH_3), 28.8 (CH), 122.5, 124.3 (CH), 125.1, 125.4 (CH), 125.6 (CH), 125.8 (CH), 126.4 (CH), 127.5 (CH), 129.0, 129.0, 129.2 (CH), 129.9, 130.0, 136.5 (CH), 142.8 (C2'), 144.7
HRMS (APCI) calculated for $C_{19}H_{18}NO_2$ [M^++H] 292.1338: found 292.1334. Mass accuracy (-1.37 ppm).

9-(3-Nitroallyl)anthracene (221)

9-(3-Nitroallyl)anthracene was prepared from 2-(anthracen-9-yl)acetaldehyde (6.7 mmol, 1.5 g) and nitroethane (15 mL) according to general procedure 8.21. The product was purified by column chromatography (eluent 3:1 dichloromethane: hexane)

Dark orange oil 566 mg (32%)
IR$_{\nu max}$ (ATR): 3089, 2928 (C-H), 1667 (C=C), 1551, 1356 (NO_2), 1514, 1444 (C=C) cm^{-1}
^{1}H NMR (400 MHz, $CDCl_3$) δ 4.58 (d, *J* = 6.10 Hz, 2 H, CH_2), 6.62 (dd, *J* = 13.43, 1.83 Hz, 1 H, H3'), 7.49 - 7.61 (m, 4 H, 4 x ArH), 7.66 - 7.77 (m, 1 H, H2'), 8.07 (d, *J* = 8.55 Hz, 4 H, 4 x ArH), 8.49 (s, 1 H, H10)
^{13}C NMR (101 MHz, $CDCl_3$) ppm 27.0 (CH_2), 123.3 (CH), 125.2 (CH), 126.8 (CH), 127.8 (CH), 129.5 (CH), 129.8, 131.5, 140.7 (C2'), 141.1
HRMS (APCI) calculated for $C_{17}H_{14}NO_2$ [M^++H] 264.1025: found 264.1023. Mass accuracy (-0.75 ppm).

9-(3-Nitrobut-2-en-1-yl)anthracene (222)

9-(3-Nitrobut-2-en-1-yl)anthracene was prepared from 2-(anthracen-9-yl)acetaldehyde (6.7 mmol, 1.5 g) and nitroethane (15 mL) according to general procedure 8.21. The product was purified by column chromatography (eluent 3:1 dichloromethane: hexane)
Brown oil 372 mg (20%)
IR$_{\nu max}$ (ATR): 3088, 2951 (C-H), 1667 (C=C), 1545, 1360 (NO_2), 1513, 1473 (C=C) cm^{-1}
^{1}H NMR (400 MHz, $CDCl_3$) δ 2.54 (s, 3 H, CH_3), 4.53 (d, *J* = 6.71 Hz, 2 H, CH_2), 7.49 - 7.60 (m, 5 H, 4 x ArH & H2'), 8.05 - 8.13 (m, 4 H, 4 x ArH), 8.47 (s, 1 H, H10)
^{13}C NMR (101 MHz, $CDCl_3$) ppm 13.1 (CH_3), 26.7 (CH_2), 123.4 (CH), 125.1 (CH), 126.5 (CH), 127.5 (CH), 128.5, 129.6 (CH), 129.8, 131.6, 134.9 (C2')
HRMS (APCI) calculated for $C_{18}H_{16}NO_2$ [M^++H] 278.1181: found 278.1177. Mass accuracy (-1.44 ppm).

(*E*)-9-(2-Nitrovinyl)phenanthrene (223)

(*E*)-9-(2-Nitrovinyl)phenanthrene was prepared from phenanthrene-9-carbaldehyde (7.3 mmol, 1.5 g) and nitromethane (18 mL) according to general procedure 8.21. The product was purified by column chromatography (toluene) and recrystallized from ethanol.
Orange solid 273 mg (15%)
Melting Point: 170-173 °C (lit. M.p. 173 °C[346])
IR$_{\nu max}$ (ATR): 2981, 2885 (C-H), 1633 (C=C), 1534, 1338 (NO_2), 1442 (C=C) cm^{-1}
^{1}H NMR (400 MHz, $CDCl_3$) δ 7.65 - 7.78 (m, 5 H, 4 x ArH & H1'), 7.91 (d, J = 7.94 Hz, 1 H, 1 x ArH), 7.95 (s, 1 H, H10), 8.11 (d, J = 8.55 Hz, 1 H, 1 x ArH), 8.68 (d, J = 8.55 Hz, 1 H, 1 x ArH), 8.74 (d, J = 7.93 Hz, 1 H, 1 x ArH), 8.79 (d, J = 13.43 Hz, 1 H, H2')
^{13}C NMR (101 MHz, $CDCl_3$) ppm 122.7 (CH), 122.8, 123.4 (CH), 123.9 (CH), 126.1, 127.4 (CH), 127.5 (CH), 127.5 (CH), 128.4 (CH), 128.7 (CH), 129.5, 129.5 (CH), 130.6, 131.7, 136.8 (CH), 138.8 (C2')
HRMS (APCI) calculated for $C_{16}H_{12}NO_2$ [M^++H] 250.0868: found 250.0861. Mass accuracy (-2.80 ppm).

9-(2-Nitroethyl)anthracene (224)

To a solution of (*E*)-9-(2-nitrovinyl)anthracene (100mg, 0.4 mmol) in dichloromethane (10 mL) and isopropanol 2 mL was added sodium borohydride (60 mg, 1.6 mmol). The reaction mixture was stirred at room temperature for 24 h and neutralised using 1 M HCl. The solution

was extracted with dichloromethane, dried with sodium sulphate and solvent removed *in vacuo*. The product was recrystallized from methanol and diethyl ether.
Orange Crystals 85mg (85%)
Melting Point: 147-149 °C
IR$_{Vmax}$ (ATR): 3053, 2974 (C-H), 1622, 1493 (C=C), 1546, 1377 (NO_2), 1137 (C-N) cm^{-1}
^{1}H NMR (400 MHz, $CDCl_3$) δ 4.35 - 4.44 (m, 2 H, CH_2), 4.70 - 4.78 (m, 2 H, CH_2), 7.48 - 7.56 (m, 2 H, 2 x ArH), 7.57 - 7.65 (m, 2 H, 2 x ArH), 8.06 (d, *J* = 8.55 Hz, 2 H, 2 x ArH), 8.25 (d, *J* = 9.16 Hz, 2 H, 2 x ArH), 8.46 (s, 1 H, C10)
^{13}C NMR (101 MHz, $CDCl_3$) ppm 26.1 (C2'), 74.7 (C1'), 122.9 (CH), 125.2 (CH), 126.2, 126.9 (CH), 127.8, 129.6 (CH), 129.9, 131.5
HRMS (APCI) calculated for $C_{16}H_{12}NO_2$ [M^+-H] 250.0874: found 250.0874. Mass accuracy (0 ppm).

4-(Anthracen-9-yl)-1*H*-1,2,3-triazole (225)

To a stirred solution of (*E*)-9-(2-nitrovinyl)anthracene (1 mmol, 0.25 g) in DMSO (2 mL) was added sodium azide (2 mmol). The reaction was stirred at 90 °C for 90 min. After allowing the reaction to cool to room temperature, deionised water 10 mL was added and aqueous mix was extracted into diethyl ether. The organic layer was washed with water, brine and dried over sodium sulphate. Solvent was removed *in vacuo* to afford crude product. The product was purified by column chromatography (gradient dichloromethane – methanol) and recrystallized from ethanol.
Yellow solid 226 mg (92%)
Melting Point: 241-245 °C (lit. M.p. 243-244 °C[348])
IR$_{Vmax}$ (KBr): 3035, 2881 (C-H), 1624. (C=C), 1554, 1441 (C=C), 1149 (C-N) cm^{-1}
^{1}H NMR (400 MHz, DMSO-d_6) δ 7.43 - 7.59 (m, 4 H, 4 x ArH), 7.68 (d, *J* = 9.16 Hz, 2 H, 2 x ArH), 8.16 (d, *J* = 8.55 Hz, 2 H, 2 x ArH), 8.23 (s, 1 H, H10), 8.74 (s, 1 H, =CH)
^{13}C NMR (101 MHz, DMSO-d_6) ppm 125.5 (CH), 125.6 (CH), 126.4 (CH), 128.0 (CH), 128.5 (CH), 130.6, 130.8
HRMS (APCI) calculated for $C_{16}H_{12}N_3$ [M^++H] 246.1031: found 246.1033. Mass accuracy (0.81 ppm).

4-(Anthracen-9-yl)-5-methyl-1*H*-1,2,3-triazole (226)

To a stirred solution of (*E*)-9-(2-nitroprop-1-en-1-yl)anthracene (1 mmol, 0.25 g) in DMSO (2 mL) was added sodium azide (2 mmol). The reaction was stirred at 90 °C for 90 minutes. After allowing the reaction to cool to room temperature, deionised water (10 mL) was added and aqueous mix was extracted into diethyl ether. The organic layer was washed with water, brine and dried over sodium sulphate. Solvent was removed *in vacuo* to afford crude product. The product was purified by column chromatography (gradient dichloromethane – methanol) and recrystallized from ethanol.
Yellow solid 117 mg (45%)
Melting Point: 231-232 °C
IR$_{Vmax}$ (ATR): 3082, 3026 (C-H), 1623, 1587 (C=C), 1249 (C-N) cm^{-1}
^{1}H NMR (400 MHz, DMSO-d_6) □ 2.01 (s, 3 H, CH_3), 7.40 - 7.63 (m, 6 H, 6 x ArH), 8.17 (d, *J* = 8.29 Hz, 2 H, 2 x ArH), 8.76 (s, 1 H, H10)

^{13}C NMR (101 MHz, DMSO-*d*$_6$) ppm 9.3 (CH_3), 125.5 (CH), 126.4 (CH), 128.6 (CH), 130.5, 130.8
HRMS (APCI) calculated for $C_{17}H_{14}N_3$ [M^++H] 260.1188: found 260.1181. Mass accuracy (-2.69 ppm).

4-(Anthracen-9-yl)-4,5-dihydro-1*H*-1,2,3-triazole (227)

To a stirred solution of (*E*)-9-(2-nitrovinyl)anthracene (1 mmol, 0.25 g) in DMSO (2 mL) was added sodium azide (2 mmol). The reaction was stirred at 90 °C for 12 h. After allowing the reaction to cool to room temperature deionised water (10 mL) was added and aqueous mix was extracted into diethyl ether. The organic layer was washed with water, brine and dried over sodium sulphate. Solvent was removed *in vacuo* to afford crude product. The product was purified by column chromatography (gradient dichloromethane – methanol) and recrystallized from ethanol.
Yellow crystals 222 mg (90%)
Melting Point: 266-268 °C
IR$_{Vmax}$ (ATR): 3054, 2920 (C-H), 1614, 1488 (C=C), 1220 (C-N) cm^{-1}
^{1}H NMR (400 MHz, DMSO-*d*$_6$) δ 4.64 (d, *J* = 4.88 Hz, 2 H, CH_2), 6.68 (t, *J* = 5.19 Hz, 1 H, CH), 7.45 - 7.70 (m, 4 H, 4 x ArH), 8.11 (d, *J* = 8.55 Hz, 2 H, 2 x ArH), 8.31 (d, *J* = 9.16 Hz, 2 H, 2 x ArH), 8.56 (s, 1 H, H10), 11.40 (s, 1 H, NH)
^{13}C NMR (101 MHz, DMSO-*d*$_6$) ppm 24.0 (CH_2), 124.3 (CH), 125.2 (CH), 126.2 (CH), 126.3 (CH), 129.0 (CH), 129.3, 129.7, 131.1, 147.9 (CH)
HRMS (APCI) calculated for $C_{16}H_{13}N_3$ [M^+] 247.1109: found 247.1118. Mass accuracy (3.64 ppm).

(*E*)-(Anthracen-9-ylmethylene)hydrazine (228)

To a solution of 9-anthraldehyde (1 g, 4.85 mmol) in DCM (20 ml) and ethanol (10 mL), was added dropwise hydrazine (1 g, 20 mmol). The solution was then stirred at RT for 24 h. The solvent was removed *in vacuo*. The residual solid was recrystallized from a mixture of dichloromethane and hexane. Product was isolated by filtration.
Orange solid 0.965 g (90%)
Melting Point: 122-124 °C (lit. M.p. 125-126 °C[518])
IR$_{Vmax}$ (ATR): 3363 (N-H), 3044, 2982 (C-H), 1622 (C=C), 1484, 1440 (C=C) cm^{-1}
^{1}H NMR (400 MHz, DMSO-*d*$_6$) δ 7.18 (s, 2 H, NH_2), 7.52 (br. s., 4 H, 4 x ArH), 8.07 (d, *J* = 7.32 Hz, 2 H, 2 x ArH), 8.52 (s, 1 H, C10), 8.62 (d, *J* = 8.55 Hz, 2 H, 2 x ArH), 8.89 (s, 1 H, C1')
^{13}C NMR (101 MHz, DMSO-*d*$_6$) ppm 125.3 (CH), 125.4 (CH), 125.9 (CH), 126.8 (CH), 127.8, 128.6 (CH), 129.0, 131.1, 136.5 (C1')
HRMS (APCI) calculated for $C_{15}H_{13}N_2$ [M^++H] 221.1079: found 221.1080. Mass accuracy (0.45 ppm).

(*E*)-((10-Chloroanthracen-9-yl)methylene)hydrazine (229)

To a solution of 10-chloro-9-anthraldehyde (1.16 g, 4.85 mmol) in DCM (20 mL) and ethanol 10 mL, was added dropwise hydrazine (1 g, 20 mmol). The solution was then stirred at RT for

24 h. The solvent was removed *in vacuo*. The residual solid was recrystallized from a mixture of dichloromethane and hexane. Product was isolated by filtration.
Orange solid 1.05 g (85%)
Melting Point: 205-207 °C
IR$_{Vmax}$ (KBr): 3351 (N-H), 3038, 2904 (C-H), 1621 (C=C), 1483, 1438 (C=C) cm^{-1}
^{1}H NMR (400 MHz, DMSO-d_6) δ 7.30 (s, 2 H, NH_2), 7.58 - 7.67 (m, 2 H, 2 x ArH), 7.67 - 7.76 (m, 2 H, 2 x ArH), 8.45 (d, *J* = 8.55 Hz, 2 H, 2 x ArH), 8.63 (d, *J* = 8.55 Hz, 2 H, 2 x ArH), 8.82 (s, 1 H, C1')
^{13}C NMR (101 MHz, DMSO-d_6) ppm 109.6 (C10), 124.3 (CH), 126.2 (CH), 126.3 (CH), 127.0, 127.4 (CH), 127.9, 128.7, 129.4, 135.5 (C1')
HRMS (APCI) calculated for $C_{15}H_{12}N_2Cl^{35}$ [M^++H] 255.0689: found 255.0684. Mass accuracy (-1.96 ppm).

(*E*)-Anthracene-9-carbaldehyde oxime (230)

9-Anthraldehyde (1 g) was dissolved in ethanol (20 mL) and heated to 75 °C. To this was added hydroxylamine hydrochloride 0.4 g in water 3.33 mL (neutralised with sodium carbonate). The mixture was heated for ten minutes and diluted with water until cloudy. The reaction mixture was then iced and the precipitate was filtered to give pure product.
White solid 0.99 g (90%)
Melting Point: 157-160 °C (lit. M.p. 159-162 °C[519])
IR$_{Vmax}$ (ATR): 3420 (O-H), 3084, 3012, 2980 (C-H), 1634, 1622, 1482 (C=C) cm^{-1}
^{1}H NMR (400 MHz, DMSO-d_6) δ 7.45 - 7.65 (m, 4 H, 4 x ArH), 8.03 - 8.19 (m, 2 H, 2 x ArH), 8.41 - 8.54 (m, 2 H, 2 x ArH), 8.62 (s, 1 H, H10), 9.23 (s, 1 H, OH)
^{13}C NMR (101 MHz, DMSO-d_6) ppm 124.8, 125.1 (CH), 125.2 (CH), 125.4 (CH), 126.1 (CH), 126.7 (CH), 128.4 (CH), 128.6, 128.7 (CH), 129.5, 130.9, 146.4 (CH), 146.5 (CH)
HRMS (APCI) calculated for $C_{15}H_{12}NO$ [M^++H] 222.0919: found 222.0914. Mass accuracy (-2.25 ppm).

(*E*)-1-(Anthracen-9-yl)-N-methylmethanimine oxide (231)

To an ice cold solution of sodium acetate (7.5 mmol) in dichloromethane (30 mL), was added N-methylhydroxylamine (7.5 mmol). A solution of 9-anthaldehyde (1 g, 5 mmol) in dichloromethane was added dropwise. The reaction mixture was stirred at 0 °C for 2 h and allowed to heat to RT overnight. The organic layer was washed successively with brine, water and dried over sodium sulphate. The solvent was removed *in vacuo* and the residual solid was recrystallized from ethanol and diethyl ether.
Colourless Crystals 1.05 g (89%)
Melting Point: 90-93 °C (lit. M.p. 92-94 °C[520])
IR$_{Vmax}$ (ATR): 2981, 2895 (C-H), 1622, 1484, 1438 (C=C), 1146 (C-N) cm^{-1}
^{1}H NMR (400 MHz, $CDCl_3$) δ 4.15 (s, 3 H, CH_3), 7.44 - 7.59 (m, 4 H, 4 x ArH), 7.87 (d, *J* = 8.55 Hz, 2 H, 2 x ArH), 8.01 (d, *J* = 7.93 Hz, 2 H, 2 x ArH), 8.25 (s, 1 H, C10), 8.51 (s, 1 H, C1')
^{13}C NMR (101 MHz, $CDCl_3$) ppm 53.7 (CH_3), 122.3, 124.3 (CH), 125.0 (CH), 125.4 (CH), 125.8 (CH), 126.7 (CH), 127.6 (CH), 129.0 (CH), 129.1 (CH), 129.5, 130.0 (CH), 131.2, 134.1 (C1')

HRMS (APCI) calculated for $C_{16}H_{14}NO$ [M^++H] 236.1066: found 236.1070. Mass accuracy (-1.78 ppm).

(*E*)-2-(Anthracen-9-yl)acetaldehyde oxime (232)

9-Anthraldehyde (1 g) was dissolved in ethanol (20 mL) and heated to 75 °C. To this was added hydroxylamine hydrochloride 0.4 g in water 3.33 mL (neutralised with sodium carbonate). The mixture was heated for ten minutes and diluted with water until cloudy. The reaction mixture was then iced and the precipitate was filtered to give pure product.
Yellow Crystals 236 mg (20%)
Melting Point: 178-180 °C (lit. M.p. 177-180 °C[521])
IR$_{Vmax}$ (ATR): 3025, 2852 (C-H), 1621, 1488 (C=C) cm^{-1}
^{1}H NMR (400 MHz, DMSO-d_6) δ 4.63 (d, *J* = 5.49 Hz, 2 H, CH_2), 6.68 (t, *J* = 5.19 Hz, 1 H, CH), 7.51 - 7.61 (m, 4 H, 4 x ArH), 8.12 (d, *J* = 7.94 Hz, 2 H, 2 x ArH), 8.31 (d, *J* = 8.55 Hz, 2 H, 2 x ArH), 8.57 (s, 1 H, H10), 11.39 (s, 1 H, =N-OH)
^{13}C NMR (101 MHz, DMSO-d_6) ppm 24.0 (CH_2), 124.3 (CH), 125.2 (CH), 126.2 (CH), 126.3 (CH), 129.0 (CH), 129.3, 129.7, 131.1, 147.9 (N=CH)
HRMS (APCI) calculated for $C_{16}H_{14}NO$ [M^++H] 236.1075: found 236.1069. Mass accuracy (-2.54 ppm).

2-(Anthracen-9-ylmethylene)malononitrile (233)

To a solution of 9-anthraldehyde (0.393 g, 1.91 mmol) and malononitrile (0.372 g, 6.11 mmol) in ACN (50 mL), was added 1 drop of piperidine. The solution was then heated at 90 °C for 0.5 h. The solution was then concentrated *in vacuo*, the residual solid dissolved in DCM and washed with HCl, water and brine. The organic phases were combined and dried over Na_2SO_4, solvent removed *in vacuo* and recrystallized from ethanol.
Orange crystals 459 mg (95%)
Melting Point: 256-257 °C (lit. M.p. 206 °C[522])
IR$_{Vmax}$ (KBr): 2965, 2932 (C-H), 2228 (CN), 1621 (C=C), 1574, 1445 (Ar C=C) cm^{-1}
^{1}H NMR (400 MHz, $CDCl_3$) δ 7.55 (t, *J* = 7.63 Hz, 3 H, 3 xArH), 7.65 (t, *J* = 7.63 Hz, 2 H, 2 x ArH), 7.89 (d, *J* = 8.54 Hz, 2 H, H4 & H5), 8.05 (d, *J* = 7.93 Hz, 2 H, H8 & H1), 8.59 (s, 1 H, H10), 8.88 (s, 1 H, H1')
^{13}C NMR (101 MHz, $CDCl_3$) ppm 92.2, 108.9, 111.5 (CN), 113.0 (CN), 123.4 (C9), 123.8, 126.1, 128.3, 129.1, 129.5, 130.8, 132.5, 160.8 (C2')
HRMS (ESI) calculated for $C_{18}H_9N_2$ [M^+-H] 253.0771: found 253.0764. Mass accuracy (-2.77 ppm).

2-((10-Chloroanthracen-9-yl)methylene)malononitrile (234)

To a solution of 10-chloro-9-anthraldehyde (0.458 g, 1.91 mmol) and malonitrile (0.372 g. 6.11 mmol) in ACN 50 mL, was added 1 drop of piperidine. The solution was then heated at 90 °C for 0.5 h. The solution was then concentrated *in vacuo*, the residual solid dissolved in DCM and washed with HCl, water and brine. The organic phases were combined and dried over Na_2SO_4 and solvent removed *in vacuo*.
Orange crystals 495 mg (90%)
Melting Point: 196-198 °C

IR$_{\nu max}$ (ATR):, 3088, 2965 (C-H), 2228 (CN), 1621 (C=C), 1574, 1445 (C=C) cm^{-1}
^{1}H NMR (400 MHz, CDCl$_3$) δ 7.68 - 7.76 (m, 4 H, 4 x ArH), 7.91 - 7.97 (m, 2 H, 2 x ArH), 8.61 - 8.71 (m, 2 H, 2 x ArH), 8.91 (s, 1 H, C1')
^{13}C NMR (101 MHz, CDCl$_3$) ppm 93.4 (C2'), 111.1 (CN), 112.7 (CN), 122.9, 124.2 (CH), 126.2 (CH), 127.2, 127.4 (CH), 128.4, 128.5 (CH), 129.3, 160.2 (C1')
HRMS (APCI) calculated for $C_{18}H_9N_2Cl^{35}$ [M$^+$] 288.0454: found 288.0466. Mass accuracy (4.16 ppm).

(*E*)-3-(Anthracen-9-yl)acrylonitrile (235)

To a solution of 9-anthraldehyde (1 g, 4.85 mmol) and cyanoacetic acid (0.52 g, 6.11 mmol) in DMF (6 mL), was added morpholine (0.7 mL). The solution was then heated at 90 °C for 6 h. The solution was then cooled to -10 °C overnight. The resultant crystals were filtered and washed with diethyl ether.
Orange crystals 446 mg (40%)
Melting Point: 205-207 °C (lit. M.p. 209.5-210.5 °C[349])
IR$_{\nu max}$ (KBr): 3051 (C-H), 2218 (CN), 1623, 1442.02 (C=C) cm^{-1}
^{1}H NMR (400 MHz, CDCl$_3$) δ 5.84 (d, *J* = 17.09 Hz, 1 H =CH), 7.43 - 7.54 (m, 4 H, 4 x ArH), 7.97 (d, *J* = 7.93 Hz, 2 H, H4 & H5), 8.06 (d, *J* = 8.54 Hz, 2 H, H1 & H8), 8.27 (d, *J* = 17.09 Hz, 1 H, =CH), 8.41 (s, 1 H, H10)
^{13}C NMR (101 MHz, CDCl$_3$) ppm 105.4 (C2'), 117.4 (CN), 124.3 (C9), 125.4 (CH), 126.9 (CH), 127.6, 128.9 (CH), 129.0 (CH), 129.2, 131.0, 148.4 (C1')
HRMS (APCI) calculated for $C_{17}H_{12}N$ [M$^+$+H] 230.0966: found 230.097. Mass accuracy (1.74 ppm)

(*E*)-4-(Anthracen-9-yl)but-3-en-2-one (236)

To a stirred solution of 9-anthraldehyde (1 g, 4.5 mmol) in acetone (50 mL) was added aqueous 10 % NaOH 0.5 mL. The solution was stirred for 3 h and concentrated *in vacuo*. Pure product was isolated by filtration and recrystallized from ethanol.
Orange solid 666 mg (60%)
Melting Point: 99-100 °C (lit. M.p. 100-102 °C[245])
IR ν_{max} (ATR): 3046, 2971 (C-H), 1661 (C=O), 1622 (C=C), 1442, 1441 (C=C) cm^{-1}
^{1}H NMR (400 MHz, *CDCl$_3$*) δ ppm 2.56 (s, 3 H, CH$_3$), 6.71 (d, *J* = 16.48 Hz, 1 H, H3'), 7.51 (m, 4 H, 4 x ArH), 8.01 (d, *J* = 7.32 Hz, 2 H, 2 x ArH), 8.20 (d, *J* = 7.32 Hz, 2 H, 2 x ArH), 8.39 - 8.53 (m, 2 H, 1 x H10 & H4')
^{13}C NMR (101 MHz, *CDCl$_3$*) δ ppm 27.9 (CH$_3$), 125.0 (CH), 125.3 (CH), 126.3 (CH), 128.4 (CH), 128.9 (CH), 129.1, 129.3, 131.2, 135.8 (CH), 140.4 (CH), 197.8 (C=O)
HRMS (APCI) calculated for $C_{18}H_{15}O$ [M$^+$+H] 247.1123: found 247.1116. Mass accuracy (-2.83 ppm).

5-(Anthracen-9-ylmethylene)-2,2-dimethyl-1,3-dioxane-4,6-dione (237)

A solution of 9-anthraldehyde (0.5 g, 2.4 mmol) and Meldrums acid (0.35 g, 2.5 mmol) in pyridine (2 mL) was stirred at room temperature for six hours. Solvent was removed from the resulting mixture *in vacuo*. The crude product was recrystallized from ethanol.
Orange solid 558 mg (70%)

Melting Point: 187-188 °C (lit. M.p. 193-194 °C[354])
IR$_{\nu max}$ (ATR): 3029, 2970 (C-H), 1730 (C=O), 1625 (C=C), 1555, 1444 (C=C) cm^{-1}
^{1}H NMR (400 MHz, CDCl$_3$) δ 1.90 (s, 6 H, 2 x CH$_3$), 7.45 - 7.57 (m, 4 H, 4 x ArH), 7.83 (d, *J* = 9.16 Hz, 2 H, 2 x ArH), 7.98 - 8.07 (m, 2 H, 2 x ArH), 8.53 (s, 1 H, H10), 9.45 (s, 1 H, =CH)
^{13}C NMR (101 MHz, DMSO-*d*$_6$) ppm 28.1 (CH$_3$), 104.9, 120.9, 124.4 (CH), 125.5 (CH), 126.7, 127.0 (CH), 128.5, 129.3 (CH), 130.2 (CH), 130.8, 157.6 (CH), 157.8 (C=O), 161.8 (C=O)
HRMS (APCI) calculated for $C_{21}H_{16}O_4$ [M$^+$+H] 332.1049: found 332.1051. Mass accuracy (0.60 ppm).

Anthracen-9-ylmethanol (238)

To a suspension of 9-anthraldehyde (206 mg, 1 mmol) in ethanol (3 mL) was added sodium borohydride (152 mg, 4 mmol). After stirring for 30 min at room temperature the reaction mixture was quenched with water (10 mL). The reaction mixture was then extracted with diethyl ether. The organic phase was washed with water, brine and dried over anhydrous sodium sulphate. Solvent was removed *in vacuo*. No further purification was necessary.
Pale yellow crystals 187 mg (90%)
Melting Point: 155-158 °C (lit. M.p. 158 °C[523])
IR$_{\nu max}$ (ATR): 3372 (O-H), 3045, 2970 (C-H), 1621, 1435 (C=C) cm^{-1}
^{1}H NMR (400 MHz, CDCl$_3$) δ 1.75 (br. s., 1 H, OH), 5.66 (s, 2 H, CH$_2$), 7.42 - 7.64 (m, 4 H, 4 x ArH), 8.04 (d, *J* = 7.93 Hz, 2 H, 2 x ArH), 8.33 - 8.54 (m, 3 H, 3 x ArH)
^{13}C NMR (101 MHz, CDCl$_3$) ppm 57.4 (CH$_2$), 123.9 (CH), 125.1 (CH), 126.4 (CH), 128.4 (CH), 129.1 (CH), 130.2, 131.0, 131.5
HRMS (APCI) calculated for $C_{15}H_{11}O$ [M$^+$-H] 207.0815: found 207.0805. Mass accuracy (-4.83 ppm).

9-(Chloromethyl)anthracene (239)

To a solution of anthracen-9-ylmethanol (1.2 g, 5.77 mmol) in dry dioxane (10 mL) was added thionyl chloride (0.6 mL). The reaction mixture was then refluxed for 6 h. The reaction was allowed to come to room temperature and the reaction mixture was concentrated *in vacuo*. The remaining solids were washed with hexane, filtered and dried.
Yellow crystals 1.21 g (93%)
Melting Point: 138-140 °C (lit. M.p. 141-142.5 °C[524])
IR$_{\nu max}$ (ATR): 2970, 2884 (C-H), 1623, 1505 (C=C) cm^{-1}
^{1}H NMR (400 MHz, CDCl$_3$) δ 5.63 (s, 2 H, CH$_2$), 7.46 - 7.58 (m, 2 H, 2 x ArH), 7.59 - 7.68 (m, 2 H, 2 x ArH), 8.05 (d, *J* = 7.93 Hz, 2 H, 2 x ArH), 8.34 (d, *J* = 8.55 Hz, 2 H, 2 x ArH), 8.50 (s, 1 H, H10)
^{13}C NMR (101 MHz, CDCl$_3$) ppm 38.9 (CH$_2$), 123.4 (CH), 125.2 (CH), 126.9 (CH), 127.6, 129.2 (CH), 129.3 (CH), 129.9, 131.4
HRMS (APCI) calculated for $C_{15}H_{10}Cl^{35}$ [M$^+$+H] 225.0477: found 225.0466. Mass accuracy (-4.89 ppm).

2-(Anthracen-9-yl)acetonitrile (240)

To a solution of 9-(chloromethyl)anthracene (1.5 g, 6.6 mmol) in acetonitrile (160 mL) was added potassium cyanide (6.6 mmol). The reaction mixture was refluxed for 2 h, cooled and then filtered. The solvent was removed *in vacuo* and the residue was dissolved in dichloromethane. The organic layer was washed with water, brine and dried over magnesium sulphate. Solvent was removed *in vacuo* to give pure product.
Yellow solid 1.29 g (90%)
Melting Point: 161-162 °C (lit. M.p. 159-163 °C[524])
IR$_{Vmax}$ (ATR): 3087, 2981 (C-H), 2240 (CN), 1658 (C=C), 1511, 1472 (C=C) cm^{-1}
^{1}H NMR (400 MHz, CDCl$_3$) δ 4.54 (s, 2 H, CH_2), 7.45 - 7.54 (m, 2 H, 2 x ArH), 7.57 - 7.65 (m, 2 H, 2 x ArH), 8.02 (d, *J* = 7.93 Hz, 2 H, 2 x ArH), 8.13 (d, *J* = 9.16 Hz, 2 H, 2 x ArH), 8.47 (s, 1 H, H10)
^{13}C NMR (101 MHz, CDCl$_3$) ppm 16.1 (CH_2), 117.7 (CN), 120.7, 122.9 (CH), 125.2 (CH), 127.2 (CH), 128.8 (CH), 129.4 (CH), 129.7, 131.3
HRMS (APCI) calculated for $C_{16}H_{12}N$ [M^++H] 218.0970: found 218.0964. Mass accuracy (-2.75 ppm).

8.22 General procedure for preparation of (anthracen-9-yl)methylamines (241 - 244)

To a solution of 9-chloromethylanthracene (225 mg, 1 mmol) in dry dichloromethane (5 mL) was added the required amine (2 mmol). The reaction mixture was stirred at room temperature for 24 h. The reaction mixture was then poured onto water and extracted into dichloromethane. The organic layer was washed with water, brine and dried over anhydrous sodium sulphate. Solvent was removed *in vacuo* and product was recrystallized from dichloromethane : hexane (1:3).

1-(Anthracen-9-ylmethyl)azepane (241)

1-(Anthracen-9-ylmethyl)azepane was prepared from 9-(chloromethyl)anthracene (0.23 g, 1 mmol) and homopiperidine according to general procedure 8.22.

Yellow crystals 249 mg (86%)

Melting Point: 100-101 °C (lit. M.p. 102-104 °C[525])
IR$_{Vmax}$ (ATR): 3048, 2930 (C-H), 1598, 1518 (C=C), 1195 (C-N) cm^{-1}
^{1}H NMR (400 MHz, CDCl$_3$) δ 1.63 (s, 8 H, 4 x CH_2), 2.80 (br. s., 4 H, 2 x NCH_2), 4.56 (s, 2 H, NCH_2-ANT), 7.41 - 7.61 (m, 4 H, 4 x ArH), 8.03 (d, *J* = 8.55 Hz, 2 H, 2 x ArH), 8.43 (s, 1 H, H10), 8.59 (d, *J* = 8.55 Hz, 2 H, 2 x ArH)
^{13}C NMR (101 MHz, CDCl$_3$) ppm 27.2 (CH_2), 28.3 (CH_2), 53.9 (CH_2), 54.9 (CH_2), 124.7 (CH), 125.3 (CH), 125.4 (CH), 127.1 (CH), 128.8 (CH), 131.3, 131.3, 131.4
HRMS (APCI) calculated for $C_{21}H_{24}N$ [M^++H] 290.1909: found 290.1899. Mass accuracy (-3.44 ppm).

1-(Anthracen-9-ylmethyl)pyrrolidine (242)

1-(Anthracen-9-ylmethyl)pyrrolidine was prepared from 9-(chloromethyl)anthracene (0.23 g, 1 mmol) and pyyrolidine according to general procedure 8.22.

Yellow crystals 196 mg (75%)
Melting Point: 109-110 °C (lit. M.p. 108-110 °C[525])
IR$_{Vmax}$ (ATR): 3083, 2919 (C-H), 1572, 1490.91 (C=C), 1232 (C-N) cm^{-1}

^{1}H NMR (400 MHz, $CDCl_3$) δ 1.77 (dt, *J* = 6.56, 3.13 Hz, 4 H, 2 x CH_2N), 2.63 - 2.75 (m, 4 H, 2 x CH_2), 4.61 (s, 2 H, NCH_2), 7.38 - 7.57 (m, 4 H, 4 x ArH), 8.02 (d, *J* = 8.55 Hz, 2 H, 2 x ArH), 8.42 (s, 1 H, H10), 8.56 (d, *J* = 9.16 Hz, 2 H, 2 x ArH)
^{13}C NMR (101 MHz, $CDCl_3$) ppm 23.6 (C3" & C4"), 51.4 (C1'), 54.3 (C2" & C5"), 124.8 (CH), 125.0 (CH), 125.4 (CH), 127.1 (CH), 128.9 (CH), 130.9, 131.2, 131.4
HRMS (APCI) calculated for $C_{19}H_{20}N$ [M^++H] 262.1596: found 262.1590. Mass accuracy (-2.29 ppm).

Anthracen-9-yl(morpholino)methanone (243)

Anthracen-9-yl(morpholino)methanone was prepared from 9-(chloromethyl)anthracene (0.23 g, 1 mmol) and morpholine according to general procedure 8.22.

Yellow crystals 250 mg (90%)
Melting Point: 118-122 °C (lit. M.p. 122-124 °C[525])
IR$_{Vmax}$ (ATR): 2924, 2854 (C-H), 1622, 1422 (C=C), 1110 (C-N) cm^{-1}
^{1}H NMR (400 MHz, $CDCl_3$) δ 2.57 - 2.71 (m, 4 H, 2 x CH_2), 3.58 - 3.75 (m, 4 H, 2 x CH_2), 4.47 (s, 2 H, C1'H_2), 7.44 - 7.60 (m, 4 H, 4 x ArH), 8.02 (d, *J* = 7.93 Hz, 2 H, 2 x ArH), 8.44 (s, 1 H, H10), 8.50 (d, *J* = 9.16 Hz, 2 H, 2 x ArH)
^{13}C NMR (101 MHz, $CDCl_3$) ppm 53.6 (CH_2), 54.6 (CH_2), 67.1 (CH_2), 124.8 (CH), 125.0 (CH), 125.6 (CH), 127.2 (CH), 127.6 (CH), 129.0 (CH), 131.3, 131.4, 134.1 (CH)
HRMS (APCI) calculated for $C_{19}H_{20}NO$ [M^++H] 278.1545: found 278.1539. Mass accuracy (-2.15 ppm).

1-(Anthracen-9-ylmethyl)pyrrolidine (244)

1-(Anthracen-9-ylmethyl)pyrrolidine was prepared from 9-(chloromethyl)anthracene (0.23 g, 1 mmol) and pyyrolidine according to general procedure 8.22.
Yellow crystals 226 mg (82%)
Melting Point: 117-118 °C (lit. M.p. 119-121 °C[525])
IR$_{Vmax}$ (ATR): 3049, 2849 (C-H), 1599, 1449 (C=C), 1118 (C-N) cm^{-1}
^{1}H NMR (400 MHz, $CDCl_3$) δ 1.39 - 1.58 (m, 6 H, 3 x CH_2), 2.57 (br. s., 4 H, 2 x NCH_2), 4.38 (s, 2 H, NCH_2), 7.38 - 7.58 (m, 4 H, 4 x ArH), 7.99 (d, *J* = 7.94 Hz, 2 H, 2 x ArH), 8.40 (s, 1 H, H10), 8.53 (d, *J* = 8.55 Hz, 2 H, 2 x ArH)
^{13}C NMR (101 MHz, $CDCl_3$) ppm 24.6 (C4"), 26.2 (C3" & C5"), 54.8 (C2" & C6"), 55.1 (C1'), 124.7 (CH), 125.3 (CH), 127.1 (CH), 128.8 (CH), 130.6, 131.4, 131.4
HRMS (APCI) calculated for $C_{20}H_{22}N$ [M^++H] 276.1752: found 276.1745. Mass accuracy (-2.53 ppm).

8.23 General procedure for preparation of anthracene amides via the Mukaiyama reaction (245 - 250)

To a suspension of anthracene-9-carboxylic acid (0.22 g, 1 mmol) in anhydrous dichloromethane (10 mL) was added chloro-1-methylpyridinium iodide (0.76 g, 3 mmol). The solution turned yellow and was stirred for a further five min. To this was added the required amine (1 mmol) followed by the addition of trimethylamine (0.7 mL, 5 mmol). The reaction mixture was stirred at room temperature for 1 h and was then diluted with 10% hydrochloric acid (10 mL) followed by extraction with dichloromethane (10 mL). The organic layer was

washed with 10% sodium hydroxide solution, water and brine. Solvent was removed *in vacuo* and the residue was purified by column chromatography (eluent: dichloromethane) and recrystallized from ethanol.

N,N-Diethylanthracene-9-carboxamide (245)

N,N-Diethylanthracene-9-carboxamide was prepared from 9-anthracenecarboxylic acid (0.2 g, 1 mmol) and diethylamine according to general procedure 8.23.
Brown solid 236 mg (85%)
Melting Point: 188-190 °C (lit. M.p. 189-192 °C[129])
IR$_{\nu max}$ (ATR): 3049, 2970, 2931 (C-H), 1623, 1486 (C=C), 1257 (C-N) cm^{-1}
^{1}H NMR (400 MHz, $CDCl_3$) δ 0.85 (t, *J* = 7.02 Hz, 3 H, CH_3), 1.52 (t, *J* = 7.02 Hz, 3 H, CH_3), 2.88 - 3.11 (m, 2 H, CH_2), 3.77 - 4.01 (m, 2 H, CH_2), 7.36 - 7.61 (m, 4 H, 4 x ArH), 7.93 (d, *J* = 8.55 Hz, 2 H, 2 x ArH), 8.01 (d, *J* = 7.94 Hz, 2 H, 2 x ArH), 8.45 (s, 1 H, H10)
^{13}C NMR (101 MHz, $CDCl_3$) ppm 13.1 (CH_3), 14.1 (CH_3), 39.1 (CH_2), 43.1 (CH_2), 124.9 (CH), 125.4 (CH), 126.5 (CH), 127.3 (CH), 127.5, 128.5 (CH), 131.2 (s), 131.5 (s), 169.6 (C=O)
HRMS (APCI) calculated for $C_{19}H_{20}NO$ [M^++H] 278.1539: found 278.1528. Mass accuracy (-3.95 ppm).

N,N-Dimethylanthracene-9-carboxamide (246)

N,N-Dimethylanthracene-9-carboxamide was prepared from 9-anthracenecarboxylic acid (0.2 g, 1 mmol) and dimethylamine according to general procedure 8.23.
Brown solid 200 mg (80%)
Melting Point: 150-152 °C (lit. M.p. 151.3-153.5 °C[358])
IR$_{\nu max}$ (ATR): 3058, 2853 (C-H), 1629, 1560 (C=C), 1262 (C-N) cm^{-1}
^{1}H NMR (400 MHz, $CDCl_3$) δ 2.71 (s, 3 H, CH_3), 3.43 (s, 3 H, CH_3), 7.44 - 7.57 (m, 4 H, 4 x ArH), 7.88 (d, *J* = 8.55 Hz, 2 H, 2 x ArH), 8.03 (d, *J* = 7.93 Hz, 2 H, 2 x ArH), 8.47 (s, 1 H, H10)
^{13}C NMR (101 MHz, $CDCl_3$) ppm 34.7 (CH_3), 38.1 (CH_3), 124.9 (CH), 125.5 (CH), 126.7 (CH), 127.5, 127.5 (CH), 128.6 (CH), 131.1, 170.4 (C1')
HRMS (APCI) calculated for $C_{17}H_{16}NO$ [M^++H] 250.1232: found 250.1223. Mass accuracy (-3.60 ppm).

Anthracen-9-yl(azepan-1-yl)methanone (247)

Anthracen-9-yl(azepan-1-yl)methanone was prepared from 9-anthracenecarboxylic acid (0.2 g, 1 mmol) and homopiperidine according to general procedure 8.23.
Brown solid 261 mg (86%)
Melting Point: 134-137 °C
IR$_{\nu max}$ (ATR): 3048, 2929 (C-H), 1615, 1486.60 (C=C), 1263 (C-N) cm^{-1}
^{1}H NMR (400 MHz, $CDCl_3$) δ 1.31 - 1.43 (m, 2 H, CH_2), 1.47 - 1.59 (m, 2 H, CH_2), 1.75 (dt, *J* = 11.75, 6.03 Hz, 2 H, CH_2), 1.94 - 2.12 (m, 2 H, CH_2), 3.09 (t, *J* = 6.10 Hz, 2 H, CH_2), 3.95 - 4.06 (m, 2 H, CH_2), 7.42 - 7.57 (m, 4 H, 4 x ArH), 7.90 - 8.06 (m, 4 H, 4 x ArH), 8.45 (s, 1 H, H10)

^{13}C NMR (101 MHz, $CDCl_3$) ppm 26.5 (C5" / C4"), 28.1 (C5" / C4"), 28.3 (C3" / C6"), 28.8 (C3" / C6"), 45.1 (C7" / C2"), 49.0 (C7" / C2"), 125.0 (CH), 125.4 (CH), 126.5 (CH), 127.3 (CH), 127.5, 128.6 (CH), 131.2, 131.7, 170.1 (C1')
HRMS (APCI) calculated for $C_{21}H_{22}NO$ [M^++H] 304.1701: found 304.1688. Mass accuracy (-4.27 ppm).

Anthracen-9-yl(pyrrolidin-1-yl)methanone (248)

Anthracen-9-yl(pyrrolidin-1-yl)methanone was prepared from 9-anthracenecarboxylic acid (0.2 g, 1 mmol) and pyrrolidine according to general procedure 8.23.
Yellow crystals 207 mg (75%)
Melting Point: 149-151 °C (lit. M.p. 150-152 °C[358])
IR$_{Vmax}$ (ATR): 3048, 2969 (C-H), 1616, 1578 (C=C), 1224 (C-N) cm^{-1}
^{1}H NMR (400 MHz, $CDCl_3$) δ 1.80 (quin, J = 6.87 Hz, 2 H, CH_2), 2.05 (quin, J = 6.87 Hz, 2 H, CH_2), 2.93 (t, J = 7.02 Hz, 2 H, CH_2), 3.98 (t, J = 7.02 Hz, 2 H, CH_2), 7.43 - 7.55 (m, 4 H, 4 x ArH), 7.93 (d, J = 8.55 Hz, 2 H, 2 x ArH), 7.98 - 8.06 (m, 2 H, 2 x ArH), 8.46 (s, 1 H, H10)
^{13}C NMR (101 MHz, $CDCl_3$) ppm 24.7 (C3" / C4"), 25.9 (C3" / C4"), 45.6 (C5" / C2"), 47.6 (C5" / C2"), 124.8 (CH), 125.4 (CH), 126.7 (CH), 127.2, 127.5 (CH), 128.6 (CH), 131.23, 132.3, 168.7 (C1')
HRMS (APCI) calculated for $C_{19}H_{18}NO$ [M^++H] 276.1388: found 276.1380. Mass accuracy (-2.90 ppm).

Anthracen-9-yl(morpholino)methanone (249)

Anthracen-9-yl(morpholino)methanone was prepared from 9-anthracenecarboxylic acid (0.2 g, 1 mmol) and morpholine according to general procedure 8.23.
Yellow crystals 256 mg (88%)
Melting Point: 160-163 °C (lit. M.p. 161.5-163.5 °C[358])
IR$_{Vmax}$ (ATR): 3084, 2970 (C-H), 1610, 1487 (C=C), 1234 (C-N) cm^{-1}
^{1}H NMR (400 MHz, $CDCl_3$) δ 3.01 - 3.09 (m, 2 H, CH_2), 3.41 - 3.48 (m, 2 H, CH_2), 3.88 - 4.00 (m, 2 H, CH_2), 4.09 - 4.19 (m, 2 H, CH_2), 7.43 - 7.59 (m, 4 H, 4 x ArH), 7.94 (d, J = 8.55 Hz, 2 H, 2 x ArH), 8.03 (d, J = 8.55 Hz, 2 H, 2 x ArH), 8.48 (s, 1 H, H10)
^{13}C NMR (101 MHz, $CDCl_3$) ppm 42.0 (CH_2), 47.0 (CH_2), 67.0 (CH_2), 67.1 (CH_2), 124.6 (CH), 125.6 (CH), 126.9 (CH), 127.6, 127.9 (CH), 128.7 (CH), 129.9, 131.1, 168.8 (C1')
HRMS (APCI) calculated for $C_{19}H_{18}NO$ [M^++H] 292.1338: found 292.1328. Mass accuracy (-3.42 ppm).

Anthracen-9-yl(piperidin-1-yl)methanone (250)

Anthracen-9-yl(piperidin-1-yl)methanone was prepared from 9-anthracenecarboxylic acid (0.2 g, 1 mmol) and piperidine according to general procedure 8.23.
Yellow crystals 261 mg (90%)
Melting Point: 181-183 °C (lit. M.p. 183.2-185 °C[358])
IR$_{Vmax}$ (ATR): 3051, 2992 (C-H), 1753 (C=O), 1655, 1458 (C=C), 1222 (C-N) cm^{-1}
^{1}H NMR (400 MHz, $CDCl_3$) δ 1.27 - 1.40 (m, 2 H, CH_2), 1.61 - 1.75 (m, 2 H, CH_2), 1.85 (dt, J = 11.29, 5.95 Hz, 2 H, CH_2), 2.96 - 3.11 (m, 2 H, CH_2), 3.99 - 4.15 (m, 2 H, CH_2), 7.38 -

7.57 (m, 4 H, 4 x ArH), 7.95 (d, *J* = 7.93 Hz, 2 H, 2 x ArH), 7.98 - 8.13 (m, 2 H, 2 x ArH), 8.46 (s, 1 H, H10)
^{13}C NMR (101 MHz, $CDCl_3$) ppm 24.5 (C4"), 26.0 (C3" / C5"), 26.7 (C3" / C5"), 42.5 (C2" / C6"), 47.9 (C2" / C6"), 125.0 (CH), 125.5 (CH), 126.5 (CH), 127.3 (CH), 127.5, 128.6 (CH), 131.2, 131.2, 168.5 (C1')
HRMS (APCI) calculated for $C_{20}H_{20}NO$ [M^++H] 290.1536: found 290.1545. Mass accuracy (3.1 ppm).

8.24 General procedure for preparation of phenyl and benzyl maleimides (251 - 269)
To a solution of maleic anhydride (20 mmol) dissolved in diethyl ether (25 mL) was added the appropriate benzyl or aryl amine (20 mmol) dissolved in diethyl ether (10 mL). The reaction was stirred under reflux at RT for 1 h. The precipitated solid was isolated by filtration and washed with diethyl ether. This solid was immediately used in the next step and placed in a conical flask containing sodium acetate (0.7 g) and acetic anhydride (10 mL). This mixture was heated to 90 °C for 0.5 h, after which the mixture was poured over ice water (100 mL). The precipitated solid was isolated by filtration and recrystallised from ethanol.

1-Benzyl-1*H*-pyrrole-2,5-dione (251)

1-Benzyl-1*H*-pyrrole-2,5-dione was prepared from maleic anhydride (20 mmol) and benzyl amine (20 mmol) according to general procedure 8.24.
Tan Crystals 1.51 g (40%)
Melting Point: 69-72 °C (lit. M.p. 68-69 °C[526])
IR$_{Vmax}$ (KBr): 3039, 2947 (C-H), 1700 (C=O), 1631 (C=C), 1530, 1496 (C=C), 1456 (CH_2), 1137 (C-N) cm^{-1}
^{1}H NMR (400 MHz, $CDCl_3$) δ 4.64 (s, 2 H, CH_2), 6.66 (s, 2 H, HC=CH), 7.11 - 7.41 (m, 5 H, 5 x ArH)
^{13}C NMR (101 MHz, $CDCl_3$) ppm 41.3 (CH_2), 127.7 (CH), 128.1, 128.1, 128.2 (CH) , 128.6 (CH), 128.8, 130.9, 134.1 (HC=CH), 136.1, 170.3 (O=C)
HRMS (APCI) calculated for $C_{11}H_{10}NO_2$ [M^++H] 188.0712: found 188.0705. Mass accuracy (-3.72 ppm).

1-(3,4,5-Trimethoxybenzyl)-1*H*-pyrrole-2,5-dione (252)

1-(3,4,5-Trimethoxybenzyl)-1*H*-pyrrole-2,5-dione was prepared from maleic anhydride (20 mmol) and 3,4,5-trimethoxybenzyl amine (20 mmol) according to general procedure 8.24.
Brown Crystals 1.11 g (20%)
Melting Point: 135-138 °C (lit. M.p. 128-130 °C[527])
IR$_{Vmax}$ (KBr): 3017, 2990 (C-H), 1709 (C=O), 1592 (C=C), 1508, 1429 (C=C), 1464 (CH_2), 1358 (CH_3), 1122 (C-N) cm^{-1}
^{1}H NMR (400 MHz, $CDCl_3$) δ 3.75 - 3.85 (m, 9 H, 3 x OCH_3), 4.56 (s, 2 H, CH_2), 6.57 (s, 2 H, HC=CH), 6.69 (s, 2 H, 2 x ArH)
^{13}C NMR (101 MHz, $CDCl_3$) ppm 41.6 (CH_2), 56.0 (m-OCH_3 x 2), 60.7 (p-OCH_3), 76.7, 77.3, 105.6 (CH), 131.8, 134.1 (HC=CH), 137.5, 153.2, 170.3 (C=O)
HRMS (APCI) calculated for $C_{14}H_{16}NO_5$ [M^++H] 278.1028: found 278.1025. Mass accuracy (-1.07ppm).

1-(4-Chlorophenyl)-1*H*-pyrrole-2,5-dione (253)

1-(4-Chlorophenyl)-1*H*-pyrrole-2,5-dione was prepared from maleic anhydride (20 mmol) and 4-chloroaniline (20 mmol) according to general procedure 8.24.
Yellow Crystals 2.29 g (55%)
Melting Point: 118-124 °C (109-110 °C[528])
IR$_{Vmax}$ (KBr): 3116, 3084 (Ar C-H), 1583 (C=C), 1497, 1452 (C=C), 1712 (C=O), 1149 (C-N) cm^{-1}
^{1}H NMR (400 MHz, $CDCl_3$) δ 6.83 (s, 2 H, HC=CH) 7.29 (d, *J* = 8.54 Hz, 2 H, 2 x ArH) 7.41 (d, *J* = 8.54 Hz, 2 H, 2 x ArH)
^{13}C NMR (101 MHz, $CDCl_3$) ppm 127.0 (CH), 129.2 (CH), 129.7 (s), 133.5 (s), 134.2 (HC=CH), 169.1 (O=C)
HRMS (APCI) calculated for $C_{10}H_7Cl^{35}NO_2$ [M^++H] 208.0165: found 208.0165. Mass accuracy (0 ppm).

1-(4-Methylphenyl)-1*H*-pyrrole-2,5-dione (254)

1-(4-Methylphenyl)-1*H*-pyrrole-2,5-dione was prepared from maleic anhydride (20 mmol) and 4-methylaniline (20 mmol) according to general procedure 4.1
Yellow Crystals (40%)
Melting Point: 145-155 °C (lit. M.p. 148 °C[528])
IR$_{Vmax}$ (KBr): 3075, 2924 (C-H), 1707 (C=O), 1517, 1449 (C=C), 1585.38 (C=C), 1314 (CH_3), 1152 (CN) cm^{-1}
^{1}H NMR (400 MHz, $CDCl_3$) δ 2.37 (s, 3 H, CH_3), 6.81 (s, 2 H, HC=CH), 7.16 - 7.32 (m, 4 H, 4 x ArH)
^{13}C NMR (101 MHz, $CDCl_3$) ppm 21.1 (CH_3), 126.0 (CH), 128.5, 129.8 (CH), 134.1 (HC=CH), 138.0, 169.7 (O=C)
HRMS (APCI) calculated for $C_{11}H_{10}NO_2$ [M^++H] 188.0712: found 188.0713. Mass accuracy (0.53 ppm).

1-(4-(Dimethylamino)phenyl)-1*H*-pyrrole-2,5-dione (255)

1-(4-(Dimethylamino)phenyl)-1*H*-pyrrole-2,5-dione was prepared from maleic anhydride (20 mmol) and N,N-dimethylbenzene-1,4-diamine (20 mmol) according to general procedure 8.24.
Red Crystals 1.52 g (35%)
Melting Point: 159-162 °C (lit. M.p. 153-154 °C[529])
IR ν_{max} (KBr): 3066, 2984 (C-H), 1693 (C=O), 1520, 1447.01 (C=C), 1568 (C=C), 1153 (CN) cm^{-1}
^{1}H NMR (400 MHz, $CDCl_3$) δ 2.98 (s, 6 H, 2 x CH_3), 6.77 (d, *J* = 9.16 Hz, 2 H, 2 x ArH), 6.80 (s, 2 H, 2 x =CH), 7.14 (d, *J* = 8.55 Hz, 2 H, 2 x ArH)
^{13}C NMR (101 MHz, $CDCl_3$) ppm 40.4 (2 x CH_3), 112.4 (CH), 119.4, 127.2 (CH), 134.0 (CH), 150.1, 170.2 (C=O)
HRMS (APCI) calculated for $C_{12}H_{13}N_2O_2$ [M^++H] 217.0977: found 217.0975. Mass accuracy (-0.92 ppm).

1-(4-Benzoylphenyl)-1*H*-pyrrole-2,5-dione (256)

1-(4-Benzoylphenyl)-1*H*-pyrrole-2,5-dione was prepared from maleic anhydride (20 mmol) and (4-aminophenyl)(phenyl)methanone (20 mmol) according to general procedure 8.24.
Yellow solid 1.61 g (29%)
Melting Point: 149-159 °C (lit. M.p. 162-164 °C[530])
IR$_{Vmax}$ (KBr): 3093, 2988 (C-H), 1711 (C=O), 1592, 1510 (C=C), 1148 (CN) cm^{-1}
^{1}H NMR (400 MHz, DMSO-*d*$_6$) δ 7.23 (s, 2 H, 2 x =CH), 7.55 - 7.59 (m, 4 H, 4 x ArH), 7.67 (d, *J* = 7.32 Hz, 1 H, 1 x ArH), 7.76 (d, *J* = 7.32 Hz, 2 H, 2 x ArH), 7.85 (d, *J* = 8.55 Hz, 2 H, 2 x ArH)
^{13}C NMR (101 MHz, DMSO-*d*$_6$) ppm 126.1 (CH), 128.6 (CH), 129.7 (CH), 129.7 (CH), 130.3 (CH), 132.8 (CH), 134.9 (CH), 135.3, 135.7, 136.8, 169.6 (2 x NC=O), 195.0 (C=O)
HRMS (APCI) calculated for $C_{17}H_{12}NO_3$ [M$^+$+H] 278.0817: found 278.0817. Mass accuracy (0 ppm).

2-(2,5-Dioxo-2,5-dihydro-1*H*-pyrrol-1-yl)phenyl acetate (257)

2-(2,5-Dioxo-2,5-dihydro-1*H*-pyrrol-1-yl)phenyl acetate was prepared from maleic anhydride (20 mmol) and 2-aminophenol (20 mmol) according to general procedure 8.24.
Colourless solid 0.84 g (18%)
Melting Point: 70-75 °C [531]
IR$_{Vmax}$ (KBr): 3098, 2988 (C-H), 1707 (C=O), 1504, 1456 (C=C), 1586.53 (C=C), 1156 (CN) cm^{-1}
^{1}H NMR (400 MHz, $CDCl_3$) δ 2.15 (s, 3 H, CH_3), 6.82 (s, 2 H, 2 x =CH), 7.19 - 7.34 (m, 3 H, 3 x ArH), 7.35 - 7.47 (m, 1 H, 1 x H3)
^{13}C NMR (101 MHz, $CDCl_3$) ppm 20.7 (CH_3), 123.0, 123.8 (CH), 126.2 (CH), 129.2 (CH), 129.7 (CH), 134.4 (CH), 146.1, 167.9 (C=O), 168.6 (2 x NC=O)
HRMS (APCI) calculated for $C_{12}H_{10}NO_4$ [M$^+$+H] 232.0610: found 232.0616. Mass accuracy (2.59 ppm).

1-(3-Chlorophenyl)-1*H*-pyrrole-2,5-dione (258)

1-(3-Chlorophenyl)-1*H*-pyrrole-2,5-dione was prepared from maleic anhydride (20 mmol) and 3-chloroaniline (20 mmol) according to general procedure 8.24.
Colourless solid 2.28 g (55%)
Melting Point: 96-102 °C (lit. M.p. 87-89.5 °C[532])
IR$_{Vmax}$ (KBr): 3107, 3083 (C-H), 1712 (C=O), 1577, 1542 (C=C), 1591 (C=C), 1143 (CN) cm^{-1}
^{1}H NMR (400 MHz, $CDCl_3$) δ 6.80 (s, 2 H, 2 x =CH), 7.21 - 7.26 (m, 1 H, H2), 7.27 - 7.38 (m, 3 H, 3 x ArH)
^{13}C NMR (101 MHz, $CDCl_3$) ppm 123.8 (CH), 125.9 (CH), 127.8 (CH), 129.9 (CH), 132.3, 134.1 (CH), 134.4, 168.8 (C=O)
HRMS (APCI) calculated for $C_{10}H_6Cl^{35}NO_4$ [M$^+$-e$^-$] 207.0087: found 207.0097. Mass accuracy (4.83 ppm).

3-(2,5-Dioxo-2,5-dihydro-1H-pyrrol-1-yl)phenyl acetate (259)

3-(2,5-Dioxo-2,5-dihydro-1H-pyrrol-1-yl)phenyl acetate was prepared from maleic anhydride (20 mmol) and 3-aminophenol (20 mmol) according to general procedure 8.24.

Yellow oil 1.99 g (43%[531])
IR$_{\nu max}$ (KBr): 3103, 2988, (C-H), 1709 (C=O), 1489, 1449 (C=C), 1595 (C=C), 1369 (CH_3), 1191 (CN) cm^{-1}
^{1}H NMR (400 MHz, $CDCl_3$) δ 2.27 (s, 3 H, CH_3), 6.81 (s, 2 H, 2 x =CH), 7.06 - 7.13 (m, 1 H, 1 x ArH), 7.17 (t, *J* = 2.14 Hz, 1 H, 1 x ArH), 7.23 - 7.29 (m, 1 H, 1 x ArH), 7.37 - 7.48 (m, 1 H, 1 x ArH)
^{13}C NMR (101 MHz, $CDCl_3$) ppm 21.0 (CH_3), 119.0 (CH), 120.9 (CH), 122.8 (CH), 129.6 (CH), 132.1, 134.2 (CH), 150.8, 169.0 (C=O), 169.1 (2 x N=O)
HRMS (APCI) calculated for $C_{12}H_{10}NO_4$ [M^++H] 232.0610: found 232.0617. Mass accuracy (3.02 ppm).

1-(3,4-Dimethoxyphenethyl)-1*H*-pyrrole-2,5-dione (260)

1-(3,4-Dimethoxyphenethyl)-1*H*-pyrrole-2,5-dione was prepared from maleic anhydride (20 mmol) and 2-(3,4-dimethoxyphenyl)ethan-1-amine (20 mmol) according to general procedure 8.24.
Yellow solid 0.79 g (15%)
Melting Point: 138-144 °C (lit. M.p. 122-124 °C[533])
IR$_{\nu max}$ (KBr): 3093, 2988 (C-H), 1698 (C=O), 1608, 1514.87 (C=C), 1592 (C=C), 1261 (CH_3), 1140 (CN) cm^{-1}
^{1}H NMR (400 MHz, DMSO-d_6) δ 2.74 (t, *J* = 7.32 Hz, 2 H, CH_2), 3.62 (t, *J* = 7.32 Hz, 2 H, CH_2), 3.71 (s, 3 H, OCH_3), 3.70 (s, 3 H, OCH_3), 6.64 (dd, *J* = 8.24, 1.53 Hz, 1 H, 1 x ArH), 6.74 (d, *J* = 1.83 Hz, 1 H, H2"), 6.82 (d, *J* = 7.94 Hz, 1 H, 1 x ArH), 6.97 (s, 2 H, 2 x =CH)
^{13}C NMR (101 MHz, DMSO-d_6) ppm 33.2 (CH_2), 38.6 (CH_2), 55.4 (OCH_3), 55.4 (OCH_3), 111.7 (CH), 112.3 (CH), 120.5 (CH), 1305, 134.4 (CH), 147.4, 148.6, 170.8 (C=O)
HRMS (APCI) calculated for $C_{14}H_{16}NO_4$ [M^++H] 262.1079: found 262.1074. Mass accuracy (-1.91 ppm).

Methyl 4-(2,5-dioxo-2,5-dihydro-1*H*-pyrrol-1-yl)benzoate (261)

Methyl 4-(2,5-dioxo-2,5-dihydro-1*H*-pyrrol-1-yl)benzoate was prepared from maleic anhydride (20 mmol) and methyl 4-aminobenzoate (20 mmol) according to general procedure 8.24.
Colourless solid 1.85 g (40%)
Melting Point: 161-168 °C (lit. M.p. 161-163 °C[534])
IR$_{\nu max}$ (KBr): 3108, 2958 (C-H), 1705 (C=O), 1601, 1510 (C=C), 1585.52 (C=C), 1140 (CN) cm^{-1}
^{1}H NMR (400 MHz, $CDCl_3$) δ 3.91 (s, 3 H, OCH_3), 6.86 (s, 2 H, 2 x =CH), 7.48 (m, *J* = 8.55 Hz, 2 H, 2 x ArH), 8.11 (m, *J* = 8.55 Hz, 2 H, 2 x ArH)
^{13}C NMR (101 MHz, $CDCl_3$) ppm 52.2 (OCH_3), 125.1 (CH), 129.0, 130.3 (CH), 134.3 (CH), 135.3, 166.1 (C=O), 168.9 (2 x NC=O)
HRMS (APCI) calculated for $C_{12}H_{10}NO_4$ [M^++H] 232.0610: found 232.0610. Mass accuracy (0 ppm).

1-(3,5-Dimethoxyphenyl)-1*H*-pyrrole-2,5-dione (262)

1-(3,5-Dimethoxyphenyl)-1*H*-pyrrole-2,5-dione was prepared from maleic anhydride (20 mmol) and 3,5-dimethoxyaniline (20 mmol) according to general procedure 8.24.

Yellow solid 3.21 g (69%)
Melting Point: 161-168 °C (lit. M.p. 121.8 °C[535])
IR$_{Vmax}$ (KBr): 3027, 2970 (C-H), 1717 (C=O), 1602, 1453 (C=C), 1475 (C=C), 1146 (CN) cm^{-1}
^{1}H NMR (400 MHz, $CDCl_3$) δ 3.79 (s, 6 H, 2 x OCH_3), 6.44 - 6.51 (m, 3 H, 3 x ArH), 6.83 (s, 2 H, 2 x =CH)
^{13}C NMR (101 MHz, $CDCl_3$) ppm 55.4 (OCH_3), 100.3 (CH), 104.6 (CH), 132.6, 134.1 (CH), 160.9, 169.3 (C=O)
HRMS (APCI) calculated for $C_{12}H_{11}NO_4$ [M^+] 233.0688: found 233.0692. Mass accuracy (1.72 ppm).

1-(4-Fluorophenyl)-1*H*-pyrrole-2,5-dione (263)

1-(4-Fluorophenyl)-1*H*-pyrrole-2,5-dione was prepared from maleic anhydride (20 mmol) and 4-fluoroaniline (20 mmol) according to general procedure 8.24.
Yellow crystals 2.48 g (65%)
Melting Point: 160-162 °C (lit. M.p. 136-138 °C[536])
IR$_{Vmax}$ (KBr): 3073, 2988 (C-H), 1708 (C=O), 1601, 1584 (Ar C=C), 1514 (C=C), 1148 (CN) cm^{-1}
^{1}H NMR (400 MHz, $CDCl_3$) δ 6.85 (s, 2 H, =CH), 7.16 (t, *J* = 8.55 Hz, 2 H, 2 x ArH), 7.33 (dd, *J* = 9.16, 4.88 Hz, 2 H, 2 x ArH)
^{13}C NMR (101 MHz, $CDCl_3$) ppm 116.0 (CH), 116.2 (CH), 127.8 (CH), 127.9, 134.2 (CH), 160.5, 163.0, 169.3 (C=O)
HRMS (APCI) calculated for $C_{10}H_6FNO_2$ [M^+] 191.0383: found 191.0384. Mass accuracy (0.52 ppm).

1-(4-Bromophenyl)-1*H*-pyrrole-2,5-dione (264)

1-(4-Bromophenyl)-1*H*-pyrrole-2,5-dione was prepared from maleic anhydride (20 mmol) and 4-bromoaniline (20 mmol) according to general procedure 4.1
Yellow crystals (59%)
Melting Point: 120-125 °C (lit. M.p. 122-123 °C[524])
IR$_{Vmax}$ (KBr): 3089, 2988 (C-H), 1719 (C=O), 1592, 1444 (C=C), 1488 (C=C), 1146 (CN) cm^{-1}
^{1}H NMR (400 MHz, $CDCl_3$) δ 6.84 (s, 2 H, 2 x =CH), 7.22 - 7.28 (m, 2 H, 2 x ArH), 7.55 - 7.60 (m, 2 H, 2 x ArH)
^{13}C NMR (101 MHz, $CDCl_3$) ppm 121.5, 127.3 (CH), 130.2, 132.2 (CH), 134.2 (CH), 169.0 (C=O)
HRMS (APCI) calculated for $C_{10}H_6Br^{79}NO_2$ [M^+] 250.9582: found 250.9585. Mass accuracy (1.19 ppm).

1-(3,4,5-Trimethoxyphenyl)-1*H*-pyrrole-2,5-dione (265)

1-(3,4,5-Trimethoxyphenyl)-1*H*-pyrrole-2,5-dione was prepared from maleic anhydride (20 mmol) and 3,4,5 trimethoxyaniline (20 mmol) according to general procedure 8.24.
Yellow crystals 3.17 g (60%)
Melting Point: 120-128 °C

IR$_{\nu max}$ (KBr): 3085, 2964 (C-H), 1707 (C=O), 1509, 1470 (C=C), 1598 (C=C), 1127 (CN) cm^{-1}
^{1}H NMR (400 MHz, $CDCl_3$) δ 3.86 (s, 9 H, 3 x OCH_3), 6.54 (s, 2 H, 2 x ArH), 6.84 (s, 2 H, 2 x =CH)
^{13}C NMR (101 MHz, $CDCl_3$) ppm 56.2 (OCH_3), 60.8 (OCH_3), 104.0 (CH), 126.6, 134.1 (CH), 137.7, 153.4, 169.5 (C=O)
HRMS (APCI) calculated for $C_{13}H_{14}NO_5$ [M^++H] 264.0872: found 264.0867. Mass accuracy (-1.89 ppm).

1-(4-Aminophenyl)-1*H*-pyrrole-2,5-dione (266)

1-(4-Aminophenyl)-1*H*-pyrrole-2,5-dione was prepared from maleic anhydride (20 mmol) and benzene-1,4-diamine (20 mmol) according to general procedure 8.24.
Yellow solid 2.65 g (70%)
Melting Point: 120-128 °C (lit. M.p. 153 °C[537])
IR$_{\nu max}$ (ATR): 3355 (N-H), 2970, 2938 (C-H), 1692 (C=O), 1585, 1469 (C=C), 1129 (CN) cm^{-1}
^{1}H NMR (400 MHz, $CDCl_3$) δ 5.75 (s, 2 H. 2 x =CH), 7.21 (s, 2 H, 2 x ArH), 7.46 (s, 2 H, 2 x ArH)
^{13}C NMR (101 MHz, DMSO-d_6) ppm 127.2 (CH), 130.8, 134.7 (CH), 152.3 169.8 (C=O)

HRMS (APCI) calculated for $C_{10}H_9N_2O_2$ [M^++H] 189.0659: found 189.0653. Mass accuracy (-2.82 ppm).

1-(Hydroxymethyl)-1*H*-pyrrole-2,5-dione (267)

1-(Hydroxymethyl)-1*H*-pyrrole-2,5-dione was prepared from maleimide and formaldehyde. A solution of 36% formaldehyde (aqueous) (5 mL) and maleimide (2 g) was refluxed at 100 °C for one h. After the reaction time had elapsed the volume of solvent in the flask was reduced to approximately 50% of the total volume and was cooled on ice. A crop of colourless crystals formed and were isolated by filtration. The crystals were purified by recrystallisation from 2-propanol.
Colourless solid 2.15 g (84%)
Melting Point: 101-104 °C (lit. M.p. 103.5-104.5 °C[538])
IR$_{\nu max}$ (KBr): 3570 (O-H), 1703 (C=O), 1506 (C=C), 1150 (CN) cm^{-1}
^{1}H NMR (400 MHz, $CDCl_3$) δ 3.13 (t, J = 7.94 Hz, 1 H, OH), 5.09 (d, J = 7.94 Hz, 2 H, CH_2), 6.78 (s, 2 H, 2 x =CH)
^{13}C NMR (101 MHz, $CDCl_3$) ppm 61.1 (CH_2), 134.6 (CH), 170.1 (C=O))
HRMS (APCI) calculated for $C_5H_6NO_3$ [M^++H] 128.0348: found 128.0348. Mass accuracy (0 ppm).

1-Methyl-1*H*-pyrrole-2,5-dione (268)

1-Methyl-1*H*-pyrrole-2,5-dione was prepared from maleic anhydride (20 mmol) and methylamine (20 mmol) according to general procedure 8.24.
Yellow crystals 1.34 g (60%)
Melting Point: 60-68 °C (lit. M.p. 67 °C[539])

IR$_{\nu max}$ (ATR): 3173, 3095 (C-H), 1696 (C=O), 1600, 1437 (C=C), 1222 (CN) cm^{-1}
^{1}H NMR (400 MHz, DMSO-d_6) δ 2.86 (s, 3 H, CH_3), 6.99 (s, 2 H, 2 x =CH)
^{13}C NMR (101 MHz, DMSO-d_6) ppm 20.3, 23.3, 24.5, 35.2 (CH_3), 67.9, 134.6 (HC=CH), 169.7, 171.1, 174.1, 174.1
HRMS (APCI) calculated for $C_5H_6NO_2$ [M^++H] 112.0399: found 112.0395. Mass accuracy (-3.57 ppm).

1,1'-(Hexane-1,6-diyl)bis(1H-pyrrole-2,5-dione) (269)

1,1'-(Hexane-1,6-diyl)bis(1H-pyrrole-2,5-dione) was prepared from maleic anhydride (20 mmol) and (20 mmol) according to general procedure 8.24.
Yellow crystals (60%)
Melting Point: 130-136 °C (lit. M.p. 136-141 °C[540])
IR$_{\nu max}$ (ATR): 3103, 2939 (C-H), 1688 (C=O), 1587, 1453 (C=C), 1227 (CN) cm^{-1}
^{1}H NMR (400 MHz, $CDCl_3$) δ 1.09 - 1.34 (m, 4 H, 2 x CH_2), 1.34 - 1.56 (m, 4 H, 2 x CH_2), 3.39 (t, J = 7.26 Hz, 4 H, 2 x CH_2), 6.60 (s, 3 H, 2 x =CH)
^{13}C NMR (101 MHz, $CDCl_3$) ppm 25.9 (CH_2), 28.1 (CH_2), 37.4 (CH_2), 133.9 (=CH), 169.7 (C=O), 170.7 (C=O)
HRMS (APCI) calculated for $C_{14}H_{17}N_2O_4$ [M^++H] 277.1188: found 277.1183. Mass accuracy (-1.80 ppm).

8.25 General Procedure for the Diels-Alder reactions
To a solution of the appropriate anthracene derivative (1 mmol) in toluene (2 mL) was added the required dienophile (1.3 mmol). The mixture was heated, with stirring at 90 °C for 48 h. The reaction was then cooled to RT and the resulting solid was isolated by filtration. The solid product was sequentially washed with toluene (2 mL) and diethyl ether (2 mL) and recrystallized from toluene.

(*E*)-9-(2-Nitrovinyl)-9,10-dihydro-9,10-[3,4]furanoanthracene-12,14-dione (270)

(*E*)-9-(2-Nitrovinyl)-9,10-dihydro-9,10-[3,4]furanoanthracene-12,14-dione was prepared from (*E*)-9-(2-nitrovinyl)anthracene (0.25 g, 1 mmol) and maleic anhydride (0.13 g, 1.3 mmol) according to general procedure 8.25.
Colourless solid 276 mg (80%)
Melting Point: 244-245 °C
IR$_{\nu max}$ (KBr): 3030, 2966 (C-H), 1860, 1778 (C=O), 1662 (C=C), 1484, 1467 (C=C), 1525, 1353 (NO_2) cm^{-1}
^{1}H NMR (400 MHz, DMSO-d_6) δ 3.81 (dd, J = 8.85, 3.36 Hz, 1 H, H11), 4.20 (d, J = 9.16 Hz, 1 H, H15), 4.98 (d, J = 3.66 Hz, 1 H, H10), 7.19 - 7.32 (m, 5 H, 5 x ArH), 7.32 - 7.40 (m, 1 H, ArH), 7.40 - 7.48 (m, 1 H,ArH), 7.57 (d, J = 6.71 Hz, 1 H, 1 x ArH), 8.10 (d, J = 14.04 Hz, 1 H, H1'), 8.28 (d, J = 13.43 Hz, 1 H, H2')
^{13}C NMR (101 MHz, DMSO-d_6) ppm 44.2 (C10), 48.8 (C11), 49.2 (C9), 49.2 (C15), 123.1 (CH), 123.6 (CH), 124.6 (CH), 125.4 (CH), 126.7 (CH), 127.3 (CH), 127.4 (CH), 127.7 (CH), 136.3 (C2'), 138.2 (Cq), 138.4 (Cq), 140.5 (Cq), 140.8 (Cq), 145.3 (C1'), 170.1 (Cq, C=O, C12), 170.7 (Cq, C=O, C14)
HRMS (APCI) calculated for $C_{20}H_{12}NO_5$ [M^+-H] 346.0721: found 346.0721. Mass accuracy (0 ppm).

(*E*)-9-(2-Nitroprop-1-en-1-yl)-9,10-dihydro-9,10-[3,4]furanoanthracene-12,14-dione (271)

(*E*)-9-(2-Nitroprop-1-en-1-yl)-9,10-dihydro-9,10-[3,4]furanoanthracene-12,14-dione was prepared from (*E*)-9-(2-nitroprop-1-en-1-yl)anthracene (0.26 g, 1 mmol) and maleic anhydride (0.13 g, 1.3 mmol) according to general procedure 8.25.
Colourless solid 259 mg (72%)
Melting Point: 256-258 °C
IR*νmax* (KBr): 3009, 2960 (C-H), 1831, 1771 (C=O), 1641, 1521 (C=C), 1529, 1390 (NO_2), 1333 (CH_3) cm^{-1}
^{1}H NMR (400 MHz, DMSO-*d*$_6$) δ 1.81 (br. s., 3 H, -CH_3), 3.65 (dd, *J* = 8.85, 2.75 Hz, 1 H, H11), 3.88 (d, *J* = 8.54 Hz, 1 H, H15), 4.95 (d, *J* = 2.44 Hz, 1 H, H10), 7.11 - 7.34 (m, 6 H, 6 x ArH), 7.41 (d, *J* = 6.71 Hz, 1 H, ArH), 7.56 (d, *J* = 7.32 Hz, 1 H, ArH), 8.16 (s, 1 H. H1')
^{13}C NMR (101 MHz, DMSO-*d*$_6$) ppm 17.2 (C3'), 44.4 (C10), 48.5 (C11), 49.8 (C9), 51.8 (C15), 123.8 (CH), 124.0 (CH), 124.9 (CH), 125.4 (CH), 126.6 (CH), 127.2 (CH), 127.3 (CH), 127.8 (CH), 138.0 (C1'), 138.2 (Cq), 140.3 (Cq), 153.0 (C2'), 170.6 (C12), 170.7 (C14)
HRMS (APCI) calculated for $C_{21}H_{14}NO_5$ [M^+-H] 360.877: found 360.0865. Mass accuracy (-3.3 ppm).

(*E*)-9-(2-Nitrobut-1-en-1-yl)-9,10-dihydro-9,10-[3,4]furanoanthracene-12,14-dione (272)

(*E*)-9-(2-Nitrobut-1-en-1-yl)-9,10-dihydro-9,10-[3,4]furanoanthracene-12,14-dionewas prepared from (*E*)-9-(2-nitrobut-1-en-1-yl)anthracene (0.27 g, 1 mmol) and maleic anhydride (0.13 g, 1.3 mmol) according to general procedure 8.25.
Colourless solid 336 mg (98%)
Melting Point: 230-233 °C
IR*νmax* (KBr): 2981, 2943 (C-H), 1837, 1775 (C=O), 1528, 1340 (NO_2), 1479 (C=C), 1458 (CH_2), 1386 (CH_3) cm^{-1}
^{1}H NMR (400 MHz, DMSO-*d*$_6$) δ 0.92 - 1.04 (m, 3 H, -CH3) 2.19 (br. s., 2 H, CH2) 3.69 (d, *J* = 6.71 Hz, 1 H, H11) 3.93 (d, *J* = 8.55 Hz, 1 H, H15) 5.01 (d, *J* = 3.66 Hz, 1 H, H10) 7.19 - 7.35 (m, 6 H, 6 x ArH) 7.39 - 7.50 (m, 1 H, ArH) 7.52 - 7.66 (m, 1 H, ArH) 8.08 (s, 1 H, C1')
^{13}C NMR (101 MHz, DMSO-*d*$_6$) ppm 9.5 (C4'), 23.4 (C3'), 44.6 (C10), 48.5 (C11), 49.9 (C9), 51.2 (C15), 123.3 (CH), 124.6 (CH), 125.4 (CH), 126.1 (CH), 126.5 (CH), 127.2 (CH), 127.3 (CH), 135.2 (C1'), 139.3 (Cq), 156.9 (C2'), 177.1 (C12), 177.3 (C14)
HRMS (APCI) calculated for $C_{22}H_{16}NO_5$ [M^+-H] 374.1034: found 374.1044. Mass accuracy (2.7 ppm).

(*E*)-9-Chloro-10-(2-nitrovinyl)-9,10-dihydro-9,10-[3,4]furanoanthracene-12,14-dione (273)

(*E*)-9-Chloro-10-(2-nitrovinyl)-9,10-dihydro-9,10-[3,4]furanoanthracene-12,14-dione was prepared from (*E*)-9-chloro-10-(2-nitrovinyl)anthracene (0.28 g, 1 mmol) and maleic anhydride (0.13 g, 1.3 mmol) according to general procedure 8.25.
Colourless solid 58 mg (15%)
Melting Point: 275-277 °C
IR*νmax* (ATR): 3049, 2957 (C-H), 1706 (C=O), 1599 (C=C), 1456, 1420 (C=C), 1530, 1350 (NO_2) cm^{-1}

^{1}H NMR (400 MHz, DMSO-d_6) δ 3.96 (d, *J* = 9.16 Hz, 1 H, H11), 4.44 (d, *J* = 9.16 Hz, 1 H, H15), 7.33 - 7.51 (m, 6 H, 6 x ArH), 7.71 (d, *J* = 7.32 Hz, 1 H, 1 x ArH), 7.83 (d, *J* = 7.94 Hz, 1 H, 1 x ArH), 8.12 (d, *J* = 14.04 Hz, 1 H, H1'), 8.28 (d, *J* = 14.04 Hz, 1 H, H2')
^{13}C NMR (101 MHz, DMSO-d_6) ppm 48.3 (C10), 50.8 (C11), 55.0 (C15), 69.4 (C9), 122.5 (CH), 123.0 (CH), 123.4 (CH), 123.7 (CH), 127.8 (CH), 128.0 (CH), 128.3 (CH), 128.7 (CH), 135.1 (C2'), 136.7, 136.9, 139.4, 145.8 (C1'), 166.7 (C12), 168.8 (C14)
HRMS (APCI) calculated for $C_{20}H_{13}Cl^{35}NO_5$ [M^++H] 382.0482: found 382.0478. Mass accuracy (-1.05 ppm).

(*E*)-9-Chloro-10-(2-nitroprop-1-en-1-yl)-9,10-dihydro-9,10-[3,4]furanoanthracene-12,14-dione (274)

(*E*)-9-Chloro-10-(2-nitroprop-1-en-1-yl)-9,10-dihydro-9,10-[3,4]furanoanthracene-12,14-dione was prepared from (*E*)-9-chloro-10-(2-nitroprop-1-en-1-yl)anthracene (0.298 g, 1 mmol) and maleic anhydride (0.13 g, 1.3 mmol) according to general procedure 8.25.
Colourless solid 72 mg (18%)
Melting Point: 270-272 °C
IR$_{Vmax}$ (ATR): 3012, 2977 (C-H), 1781 (C=O), 1656 (C=C), 1474, 1459 (C=C), 1516, 1334 (NO_2) cm^{-1}
^{1}H NMR (400 MHz, DMSO-d_6) δ 1.82 (br. s., 3 H, CH_3), 3.81 (d, *J* = 9.16 Hz, 1 H, H15), 4.18 (d, *J* = 8.55 Hz, 1 H, H11), 7.33 - 7.49 (m, 6 H, 6 x ArH), 7.74 (d, *J* = 7.32 Hz, 1 H, 1 x ArH), 7.86 (d, *J* = 7.94 Hz, 1 H, 1 x ArH), 8.20 (s, 1 H, H1')
^{13}C NMR (101 MHz, DMSO-d_6) ppm 17.4 (C3'), 49.0 (C10), 53.1 (C11), 54.9 (C15), 69.7 (C9), 122.9 (CH), 123.1 (CH), 124.0 (CH), 127.8 (CH), 127.9 (CH), 128.3 (CH), 128.5 (CH), 136.7, 136.9, 139.0, 153.4 (C2'), 166.8 (C12 & C14)
HRMS (APCI) calculated for $C_{21}H_{14}NCl^{35}O_5$ [M^+] 395.0561: found 395.0553. Mass accuracy (-2.03 ppm).

(*E*)-9-Chloro-10-(2-nitrobut-1-en-1-yl)-9,10-dihydro-9,10-[3,4]furanoanthracene-12,14-dione (275)

(*E*)-9-Chloro-10-(2-nitrobut-1-en-1-yl)-9,10-dihydro-9,10-[3,4]furanoanthracene-12,14-dione was prepared from (*E*)-9-chloro-10-(2-nitrobut-1-en-1-yl)anthracene (0.312 g, 1 mmol) and maleic anhydride (0.13 g, 1.3 mmol) according to general procedure 8.25.
Colourless solid 224 mg (55%)
Melting Point: 259-263 °C
IR$_{Vmax}$ (KBr): 3065, 2951 (C-H), 1711 (C=O), 1610 (C=C), 1454 (C=C), 1530, 1346 (NO_2) cm^{-1}
^{1}H NMR (400 MHz, DMSO-d_6) δ 0.99 (br. s., 3 H, CH_3) 2.02 - 2.23 (m, 2 H, CH_2) 3.80 (br. s., 1 H, H15) 4.18 (d, *J* = 8.55 Hz, 1 H, H11) 7.29 - 7.50 (m, 6 H, 6 x ArH) 7.75 (d, *J* = 7.32 Hz, 1 H, 1 x ArH) 7.87 (d, *J* = 7.32 Hz, 1 H, 1 x ArH) 8.06 (br. s., 1 H, H1')
^{13}C NMR (101 MHz, DMSO-d_6) ppm 55.0 (C10), 56.4 (C15 & C11), 69.7 (C9), 115.6 (CH), 122.9 (CH), 123.1 (CH), 123.8 (CH), 127.9 (CH), 128.0 (CH), 128.5 (C1'), 137.1, 149.7 (C2'), 157.7 (C15 & C11)
HRMS (APCI) calculated for $C_{22}H_{16}Cl^{35}NO_5$ [M^+] 409.0717: found 409.0717. Mass accuracy (0 ppm).

(*E*)-9-(2-Nitrovinyl)-9,10-dihydro-9,10-[3,4]epipyrroloanthracene-12,14-dione (276)

(*E*)-9-(2-Nitrovinyl)-9,10-dihydro-9,10-[3,4]epipyrroloanthracene-12,14-dione was prepared from (*E*)-9-(2-nitrovinyl)anthracene (0.25 g, 1 mmol) and maleimide (0.13 g, 1.3 mmol) according to general procedure 8.25.
Colourless solid 172 mg (50%)
Melting Point: 176-178 °C
IR$_{\nu max}$ (KBr): 3551 (N-H), 3058, 2963 (Ar C-H), 1722 (C=O), 1527, 1354 (NO_2), 1167 (N-C) cm^{-1}
^{1}H NMR (400 MHz, DMSO-d_6) δ 3.28 (br. s., 1 H, H11), 3.70 (d, *J* = 8.54 Hz, 1 H, H15), 4.79 (br. s., 1 H, H10), 6.99 - 7.36 (m, 7 H, 7 x ArH), 7.51 (d, *J* = 6.71 Hz, 1 H, ArH), 8.04 (d, *J* = 14.04 Hz, 1 H, H1'), 8.24 (d, *J* = 13.43 Hz, 1 H, H2'), 10.89 (br. s., 1 H, NH)
^{13}C NMR (101 MHz, DMSO-d_6) ppm 44.3 (C10), 48.6 (C11) 48.7 (C15), 49.2 (C9), 122.9 (CH), 123.3 (CH), 124.3 (CH), 125.3 (CH), 126.3 (CH), 126.8 (CH), 127.0 (CH), 127.2 (CH), 137.5 (C2'), 138.5 (Cq), 138.7 (Cq), 141.4 (Cq), 141.7 (Cq), 145.1 (C1'), 176.9 (C12), 177.1 (C14)
HRMS (APCI) calculated for $C_{20}H_{13}N_2O_4$ [M^+-H] 345.0881: found 345.0896. Mass accuracy (-4.34 ppm).

(*E*)-9-(2-Nitroprop-1-en-1-yl)-9,10-dihydro-9,10-[3,4]epipyrroloanthracene-12,14-dione (277)

(*E*)-9-(2-Nitroprop-1-en-1-yl)-9,10-dihydro-9,10-[3,4]epipyrroloanthracene-12,14-dione was prepared from (*E*)-9-(2-nitroprop-1-en-1-yl)anthracene (0.26 g, 1 mmol) and maleimide (0.13 g, 1.3 mmol) according to general procedure 8.25.
Colourless solid 348 mg (97%)
Melting Point: 296-300 °C
IR$_{\nu max}$ (KBr): 3368 (N-H), 3090, 3008 (C-H), 1520, 1350 (NO_2), 1771 (C=O), 1346 (CH_3) cm^{-1}
^{1}H NMR (400 MHz, DMSO-d_6) δ 1.80 (br. s., 3 H, CH3), 3.17 (dd, *J* = 8.54, 3.05 Hz, 1 H, H11), 3.35 (d, *J* = 7.93 Hz, 1 H, H15), 4.79 (d, *J* = 3.66 Hz, 1 H, H10), 7.13 - 7.27 (m, 6 H, 6 x ArH), 7.33 (d, *J* = 6.71 Hz, 1 H, ArH), 7.52 (d, *J* = 7.32 Hz, 1 H, ArH), 8.28 (s, 1 H, H1'), 10.83 (s, 1 H, NH)
^{13}C NMR (101 MHz, DMSO-d_6) ppm 17.2 (C3'), 44.5 (C10), 48.3 (C11), 49.8 (C9), 51.1 (C15), 123.4 (CH), 124.6 (CH), 125.3 (CH), 126.2 (CH), 126.6 (CH), 127.0 (CH), 127.2 (CH), 131.9 (C1'), 138.4 (Cq), 139.0 (Cq), 141.2 (Cq), 152.4 (C2'), 177.1 (C12), 177.4 (C14)
HRMS (APCI) calculated for $C_{21}H_{16}N_2O_4$ [M^+-H] 359.1037: found 359.1024. Mass accuracy (-3.60 ppm).

(*E*)-9-(2-Nitrobut-1-en-1-yl)-9,10-dihydro-9,10-[3,4]epipyrroloanthracene-12,14-dione (278)

(*E*)-9-(2-Nitrobut-1-en-1-yl)-9,10-dihydro-9,10-[3,4]epipyrroloanthracene-12,14-dione was prepared from (*E*)-9-(2-nitrobut-1-en-1-yl)anthracene (0.27 g, 1 mmol) and maleimide (0.13 g, 1.3 mmol) according to general procedure 8.25.

Colourless solid 283 mg (76%)
Melting Point: 296-298 °C
IR$_{Vmax}$ (KBr): 3182 (N-H), 3015, 2988 (C-H), 1707 (C=O), 1523, 1348 (NO_2), 1457 (CH_2) cm^{-1}
^{1}H NMR (400 MHz, DMSO-d_6) δ 3.00 (br. s., 3 H, CH3), 2.12 (br. s., 2 H, CH2), 3.17 (br. s., 1 H, H11), 3.35 (br. s., 1 H, H15), 4.81 (d, *J* = 2.44 Hz, 1 H, H10), 7.09 - 7.27 (m, 6 H, 6 x ArH), 7.28 - 7.40 (m, 1 H, ArH), 7.53 (d, *J* = 6.10 Hz, 1 H, ArH), 8.13 (s, 1 H, H1'), 10.84 (s, 1 H)
^{13}C NMR (101 MHz, DMSO-d_6) ppm 9.5 (C4'), 23.4 (C3'), 44.6 (C10), 48.5 (C11), 49.8 (C9), 51.2 (C15), 123.3 (CH), 124.6 (CH), 125.4 (CH), 126.1 (CH), 126.5 (CH), 127.2 (CH), 127.3 (CH), 135.2, 139.2 (C1'), 156.9 (C2'), 177.1 (C12), 177.3 (C14)
HRMS (APCI) calculated for $C_{22}H_{17}N_2O_4$ [M^+-H] 373.1194: found 373.1176. Mass accuracy (4.82 ppm).

(*E*)-9-Chloro-10-(2-nitrovinyl)-9,10-dihydro-9,10-[3,4]epipyrroloanthracene-12,14-dione (279)

(*E*)-9-Chloro-10-(2-nitrovinyl)-9,10-dihydro-9,10-[3,4]epipyrroloanthracene-12,14-dione was prepared from (*E*)-9-chloro-10-(2-nitrovinyl)anthracene (0.28 g, 1 mmol) and maleimide (0.13 g, 1.3 mmol) according to general procedure 8.25.
Colourless solid 95 mg (25 %)
Melting Point: >300 °C
IR$_{Vmax}$ (ATR): 3050, 2963 (C-H), 1707 (C=O), 1599 (C=C), 1457, 1419 (C=C), 1518, 1349 (NO_2) cm^{-1}
^{1}H NMR (400 MHz, DMSO-d_6) δ 3.51 (d, *J* = 8.55 Hz, 1 H, H11), 3.95 (d, *J* = 8.55 Hz, 1 H, H15), 7.25 - 7.49 (m, 6 H, 6 x ArH), 7.67 (d, *J* = 7.32 Hz, 1 H, 1 x ArH), 7.80 (d, *J* = 7.32 Hz, 1 H, 1 x ArH), 8.08 (d, *J* = 14.04 Hz, 1 H, H1'), 8.27 (d, *J* = 14.04 Hz, 1 H, H2'), 11.09 (br. s., 1 H, NH)
^{13}C NMR (101 MHz, DMSO-d_6) ppm 48.3 (C10), 50.4 (C11), 54.1 (C15), 70.2 (C9), 122.3 (CH), 123.0 (CH), 123.1 (CH), 123.3 (CH), 127.4 (CH), 127.6 (CH), 127.7, 128.1 (CH), 136.3 (C2'), 137.1, 137.3, 140.1, 140.4, 145.6 (C1'), 173.4 (C12), 175.5 (C14)
HRMS (APCI) calculated for $C_{20}H_{12}Cl^{35}N_2O_4$ [M^+-H] 379.0491: found 379.0478. Mass accuracy (-3.43 ppm).

(*E*)-9-Chloro-10-(2-nitroprop-1-en-1-yl)-9,10-dihydro-9,10-[3,4]epipyrroloanthracene-12,14-dione (280)

(*E*)-9-Chloro-10-(2-nitroprop-1-en-1-yl)-9,10-dihydro-9,10-[3,4]epipyrroloanthracene-12,14-dione was prepared from (E)-9-chloro-10-(2-nitroprop-1-en-1-yl)anthracene (0.298 g, 1 mmol) and maleimide (0.13 g, 1.3 mmol) according to general procedure 8.25.
Colourless solid 197 mg (50%)
Melting Point: 295-297 °C
IR$_{Vmax}$ (ATR): 3368 (N-H), 3067, 2942 (C-H), 1711 (C=O), 1610 (C=C), 1455 (C=C), 1521, 1344 (NO_2) cm^{-1}

^{1}H NMR (400 MHz, DMSO-d_6) δ 1.81 (br. s., 3 H, CH_3), 3.38 (d, J = 8.55 Hz, 1 H, H15), 3.60 (d, J = 7.94 Hz, 1 H, H11), 7.28 - 7.47 (m, 6 H, 6 x ArH), 7.70 (d, J = 7.94 Hz, 1 H, 1 x ArH), 7.84 (d, J = 7.94 Hz, 1 H, 1 x ArH), 8.32 (s, 1 H, H1'), 11.04 (s, 1 H, NH)
^{13}C NMR (101 MHz, DMSO-d_6) ppm 17.4 (C3'), 49.0 (C10), 52.6 (C11), 53.9 (C15), 70.4 (C9), 122.7 (CH), 123.0 (CH), 123.5 (CH), 124.1, 127.5 (CH), 127.6 (CH), 127.7 (CH), 127.9 (CH), 130.8, 135.1, 137.1, 137.6, 140.1, 152.8 (C2'), 173.5 (C12), 175.9 (C14)
HRMS (APCI) calculated for $C_{21}H_{16}Cl^{35}N_2O_4$ [M^++H] 395.0799: found 395.0787. Mass accuracy (-3.03 ppm).

(*E*)-9-Chloro-10-(2-nitrobut-1-en-1-yl)-9,10-dihydro-9,10-[3,4]epipyrroloanthracene-12,14-dione (281)

(*E*)-9-Chloro-10-(2-nitrobut-1-en-1-yl)-9,10-dihydro-9,10-[3,4]epipyrroloanthracene-12,14-dione was prepared from (*E*)-9-chloro-10-(2-nitrobut-1-en-1-yl)anthracene (0.312 g, 1 mmol) and maleimide (0.13 g, 1.3 mmol) according to general procedure 8.25.
Colourless solid 224 mg (55%)
Melting Point: 294-298 °C
IR$_{Vmax}$ (ATR): 3369 (N-H), 3022, 2942 (C-H), 1710 (C=O), 1608 (C=C), 1455, 1426 (C=C), 1519, 1342 (NO_2) cm^{-1}
^{1}H NMR (400 MHz, DMSO-d_6) δ 0.98 (br. s., 3 H, CH_3), 2.11 (br. s., 2 H, CH_2), 3.36 (d, J = 7.32 Hz, 1 H, H15), 3.48 - 3.76 (m, 1 H, H11), 7.26 (m, 1 H, 1 x ArH), 7.30 - 7.51 (m, 5 H, 5 x ArH), 7.71 (d, J = 7.32 Hz, 1 H, 1 x ArH), 7.85 (d, J = 7.94 Hz, 1 H, 1 x ArH), 8.16 (s, 1 H, H1'), 11.04 (br. s., 1 H, NH)
^{13}C NMR (101 MHz, DMSO-d_6) ppm 9.4 (C4'), 23.5 (C3'), 49.2 (C10), 52.6 (C11), 54.0 (C15), 70.4 (C9), 122.7 (CH), 123.1 (CH), 123.4 (CH), 127.5 (CH), 127.6 (CH), 127.8 (CH), 130.5, 137.8, 157.2 (C2'), 173.5 (C12), 175.9 (C14)
HRMS (APCI) calculated for $C_{22}H_{18}Cl^{35}N_2O_4$ [M^+-H] 409.0955: found 409.0974. Mass accuracy (4.64 ppm).

(*E*)-13-Methyl-9-(2-nitrovinyl)-9,10-dihydro-9,10-[3,4]epipyrroloanthracene-12,14-dione (282)

(*E*)-13-Methyl-9-(2-nitrovinyl)-9,10-dihydro-9,10-[3,4]epipyrroloanthracene-12,14-dione was prepared from (*E*)-9-(2-nitrovinyl)anthracene (0.25 g, 1 mmol) and 1-methyl-1*H*-pyrrole-2,5-dione (0.144 g, 1.3 mmol) according to general procedure 8.25.
Yellow solid 198 mg (55%)
Melting Point: 267-268 °C
IR$_{Vmax}$ (ATR): 3070, 2951 (C-H), 1713 (C=O), 1594 (C=C), 1481, 1450 (C=C), 1531, 1349 (NO_2) cm^{-1}
^{1}H NMR (400 MHz, DMSO-d_6) δ 2.35 (s, 3 H, CH_3), 3.38 (dd, J = 8.24, 2.75 Hz, 1 H, H11), 3.78 (d, J = 8.55 Hz, 1 H, H15), 4.87 (d, J = 2.44 Hz, 1 H, H10), 7.15 - 7.36 (m, 7 H, 7 x ArH), 7.56 (d, J = 6.71 Hz, 1 H, 1 x ArH), 8.11 (d, J = 13.43 Hz, 1 H, H1'), 8.29 (d, J = 13.43 Hz, 1 H, H2')
^{13}C NMR (101 MHz, DMSO-d_6) ppm 24.0 (CH_3), 44.4 (C10), 47.5 (C11), 47.6 (C15), 49.3 (C9), 122.8 (CH), 123.4 (CH), 124.4 (CH), 125.1 (CH), 126.4 (CH), 126.8 (CH), 127.1 (CH), 127.2 (CH), 137.4 (CH), 138.2, 138.4, 141.1, 141.5, 145.1 (C1'), 175.4 (C12), 175.8 (C14)

HRMS (APCI) calculated for $C_{21}H_{17}N_2O_4$ [M^++H] 361.1188: found 361.1180. Mass accuracy (-2.21 ppm).

(*E*)-13-(Hydroxymethyl)-9-(2-nitrovinyl)-9,10-dihydro-9,10-[3,4]epipyrroloanthracene-12,14-dione (283)

(*E*)-13-(Hydroxymethyl)-9-(2-nitrovinyl)-9,10-dihydro-9,10-[3,4]epipyrroloanthracene-12,14-dione was prepared from (E)-9-(2-nitrovinyl)anthracene 0.25 g (1 mmol) and 1-(hydroxymethyl)-1*H*-pyrrole-2,5-dione 0.165 g (1.3 mmol) according to general procedure 8.25.
Colourless solid 301 mg (80%)
Melting Point: 230-232 °C
IR$_{Vmax}$ (KBr): 3463 (OH), 2964, 2899 (C-H), 1778 (C=O), 1698 (C=C), 1523 (NO), 1482, 1456 (C=C), 1198 (C-N stretch) cm^{-1}
^{1}H NMR (400 MHz, DMSO-d_6) δ 3.43 (dd, *J* = 8.55, 3.05 Hz, 1 H, H11), 3.85 (d, *J* = 8.55 Hz, 1 H, H15), 4.19 - 4.31 (m, 2 H, CH_2), 4.88 (d, *J* = 3.05 Hz, 1 H, H10), 6.12 (t, *J* = 7.02 Hz, 1 H, OH), 7.14 - 7.35 (m, 7 H, 7 x ArH), 7.57 (d, *J* = 7.32 Hz, 1 H, 1 x ArH), 8.13 (d, *J* = 14.04 Hz, 1 H, H1'), 8.30 (d, *J* = 14.04 Hz, 1 H, H2')
^{13}C NMR (101 MHz, DMSO-d_6) ppm 44.4 (C10), 47.4 (C11), 47.4 (C15), 49.3 (C9), 60.2 (CH_2), 122.8 (CH), 123.3 (CH), 124.4 (CH), 125.2 (CH), 126.4 (CH), 126.8 (CH), 127.1 (CH), 127.2 (CH), 137.4 (C2'), 138.2, 138.4, 141.3, 141.7, 145.1 (C1'), 174.9 (C12), 175.3 (C14)
HRMS (APCI) calculated for $C_{21}H_{17}N_2O_5$ [M^++H] 377.1137: found 377.1138. Mass accuracy (0.26 ppm).

9-(2-Nitroethyl)-9,10-dihydro-9,10-[3,4]furanoanthracene-12,14-dione (284)

9-(2-Nitroethyl)-9,10-dihydro-9,10-[3,4]furanoanthracene-12,14-dione was prepared from 9-(2-nitroethyl)anthracene (0.25 g, 1 mmol) and maleic anhydride (0.13 g, 1.3 mmol) according to general procedure 8.25.
Colourless solid 150 mg (43%)
Melting Point: 242-244 °C
IR$_{Vmax}$ (ATR): 3065, 2974 (C-H), 1773 (C=O), 1581 (C=C), 1469, 1457 (C=C), 1546, 1338 (NO_2) cm^{-1}
^{1}H NMR (400 MHz, DMSO-d_6) δ 3.33 - 3.52 (m, 2 H, CH_2), 3.60 (d, *J* = 9.16 Hz, 1 H, H11), 3.78 (d, *J* = 9.16 Hz, 1 H, H15), 4.88 (br. s., 1 H, H10), 5.06 (t, *J* = 14.65 Hz, 1 H, H1'a), 5.24 (t, *J* = 10.38 Hz, 1 H, H1'b), 7.25 (quin, *J* = 7.02 Hz, 4 H, 4 x ArH), 7.33 - 7.43 (m, 2 H, 2 x ArH), 7.53 (d, *J* = 6.71 Hz, 1 H, 1 x ArH), 7.49 (d, *J* = 7.32 Hz, 1 H, 1 x ArH)
^{13}C NMR (101 MHz, DMSO-d_6) ppm 25.6 (C1'), 44.4 (C10), 46.3 (C11), 48.4 (C9), 49.0 (C15), 72.8 (C2'), 122.6 (CH), 122.9 (CH), 125.3 (CH), 125.5 (CH), 127.1 (CH), 127.1, 127.7 (CH), 127.7, 139.7, 140.7, 141.3, 142.4, 170.9 (C12), 171.5 (C14)
HRMS (APCI) calculated for $C_{20}H_{16}NO_5$ [M^++H] 350.1028: found 350.1030. Mass accuracy (0.57 ppm).

9-(2-Nitroethyl)-9,10-dihydro-9,10-[3,4]epipyrroloanthracene-12,14-dione (285)

9-(2-Nitroethyl)-9,10-dihydro-9,10-[3,4]epipyrroloanthracene-12,14-dione was prepared from 9-(2-nitroethyl)anthracene (0.25 g, 1 mmol) and maleimide (0.13 g, 1.3 mmol) according to general procedure 8.25.
Colourless solid 157 mg (45%)
Melting Point: 295-297 °C
IR$_{\nu max}$ (ATR): 3049, 2936 (C-H), 1702 (C=O), 1599 (C=C), 1456, 1419 (C=C), 1548, 1349 (NO_2) cm^{-1}
^{1}H NMR (400 MHz, DMSO-d_6) δ 3.16 (d, J = 8.55 Hz, 1 H, H2'a), 3.23 - 3.31 (m, 2 H, H2'b & H11), 3.44 - 3.62 (m, 1 H, H15), 4.72 (br. s., 1 H, C10), 5.15 (d, J = 7.32 Hz, 2 H, CH_2), 7.11 - 7.37 (m, 6 H, 6 x ArH), 7.48 (t, J = 8.55 Hz, 2 H, 2 x ArH), 10.89 (br. s., 1 H, NH)
^{13}C NMR (101 MHz, DMSO-d_6) ppm 25.5 (C1'), 44.1 (C10), 45.6 (C11), 46.9 (C15), 48.3 (C9), 72.7 (C2'), 121.9, 122.1 (CH), 124.5 (CH), 124.9 (CH), 126.3 (CH), 126.3 (CH), 126.6 (CH), 126.7 (CH), 139.6, 140.8, 142.0, 142.8, 177.3 (C12), 177.6 (C14)
HRMS (APCI) calculated for $C_{20}H_{17}N_2O_5$ [M^++H] 349.1188: found 349.1181. Mass accuracy (-2.00 ppm).

9-(2-Nitroethyl)-13-phenyl-9,10-dihydro-9,10-[3,4]epipyrroloanthracene-12,14-dione (286)

9-(2-Nitroethyl)-13-phenyl-9,10-dihydro-9,10-[3,4]epipyrroloanthracene-12,14-dione was prepared from 9-(2-nitroethyl)anthracene (0.25 g, 1 mmol) and phenylmaleimide (0.224 g, 1.3 mmol) according to general procedure 8.25.
Colourless solid 127 mg (30%)
Melting Point: 248-250 °C
IR$_{\nu max}$ (ATR): 2964, 2939 (C-H), 1710 (C=O), 1595 (C=C), 1491, 1456 (C=C), 1541, 1388 (NO_2) cm^{-1}
^{1}H NMR (400 MHz, DMSO-d_6) δ 3.37 (d, J = 8.55 Hz, 2 H, H2'a), 3.49 - 3.60 (m, 2 H, H2'b & H15), 4.87 (br. s., 1 H, C10), 5.10 - 5.31 (m, 2 H, CH_2), 6.44 (d, J = 5.49 Hz, 2 H, 2 x ArH), 7.20 - 7.42 (m, 9 H, 9 x ArH), 7.57 (d, J = 7.32 Hz, 1 H, 1 x ArH), 7.54 (d, J = 7.32 Hz, 1 H, 1 x ArH)
^{13}C NMR (101 MHz, DMSO-d_6) ppm 25.5 (C1'), 44.6 (C10), 46.2 (C11), 46.2 (C9), 47.4 (C15), 72.7 (C2'), 122.0 (CH), 122.3 (CH), 124.7 (CH), 125.0 (CH), 126.5 (CH), 126.5 (CH), 126.7 (CH), 126.8 (CH), 128.5 (CH), 128.9 (CH), 131.6, 139.4, 140.5, 141.6, 142.4, 175.0 (C12), 175.5 (C14)
HRMS (APCI) calculated for $C_{26}H_{21}NO_4$ [M^++H] 425.1501: found 425.1512. Mass accuracy (2.58 ppm).

13,13'-(Hexane-1,6-diyl)bis(9-((*E*)-2-nitrovinyl)-9,10-dihydro-9,10[3,4]epipyrroloanthracene -12,14-dione) (287)

13,13'-(Hexane-1,6-diyl)bis(9-((*E*)-2-nitrovinyl)-9,10-dihydro-9,10[3,4]epipyrroloanthracene -12,14-dione) was prepared from (*E*)-9-(2-nitrovinyl)anthracene (0.25 g, 1 mmol) and the required maleimide (0.5 mmol) according to general procedure 8.25.
Colourless solid 39 mg (10%)
Melting Point: 186-188 °C
IR$_{\nu max}$ (KBr): 3050, 2961 (Ar C-H), 1699 (C=O), 1533, 1358 (NO_2), 1203 (N-C) cm^{-1}

^{1}H NMR (400 MHz, DMSO-d_6) δ 0.43 (br. s., 4 H, 2 x CH_2), 0.47 - 0.57 (m, 4 H, 2 x CH_2), 2.86 - 2.94 (m, 4 H, 2 x NCH_2), 3.36 (dd, *J* = 8.44, 3.30 Hz, 2 H, 2 x H11), 3.76 (dd, *J* = 8.44, 1.83 Hz, 2 H, 2 x H15), 4.86 - 4.92 (m, 2 H, 2 x H10), 7.18 - 7.31 (m, 12 H, 12 x ArH), 7.31 - 7.38 (m, 2 H, 2 x ArH), 7.54 - 7.59 (m, 2 H, 2 x ArH), 8.12 (d, *J* = 13.94 Hz, 2 H, 2 x H1'), 8.27 - 8.34 (m, 2 H, 2 x H2')
^{13}C NMR (101 MHz, DMSO-d_6) ppm 25.14 (CH_2), 26.17 (CH_2), 37.67 (NCH_2), 44.45 (C10 & C10'), 47.24 (C11 & C11'), 47.36 (C15 & C15'), 49.35 (C9 & C9'), 122.87 (CH), 123.32 (CH), 124.35 (CH), 125.19 (CH), 126.39 (CH), 126.79 (CH), 127.07 (CH), 137.33 (C2'), 138.44, 138.54, 141.29, 141.61, 145.15 (C1'), 175.35 (C11), 175.73 (C15)
HRMS (APCI) calculated for $C_{46}H_{39}N_4O_8$ [M^++H] 775.2768: found 775.2771. Mass accuracy (0.39 ppm).

(*E*)-9-(2-Nitrovinyl)-13-phenyl-9,10-dihydro-9,10-[3,4]epipyrroloanthracene-12,14-dione (288)

(*E*)-9-(2-Nitrovinyl)-13-phenyl-9,10-dihydro-9,10-[3,4]epipyrroloanthracene-12,14-dione was prepared from (*E*)-9-(2-nitrovinyl)anthracene (0.25 g, 1 mmol) and phenylmaleimide (0.23 g, 1.3 mmol) according to general procedure 8.25.
Colourless solid 126 mg (30%)
Melting Point: 256-257 °C
IR$_{Vmax}$ (KBr): 3035, 2961 (C-H), 1709 (C=O), 1529, 1349 (NO_2), 1596, 1457 (C=C), 1201 (C-N) cm^{-1}
^{1}H NMR (400 MHz, DMSO-d_6) δ 3.51 (m, *J* = 8.24, 2.75 Hz, 1 H, H11), 3.91 (d, *J* = 8.54 Hz, 1 H, H15), 4.86 - 4.98 (m, 1 H, H10), 6.28 - 6.46 (m, 2 H, H6''&H2''), 7.14 - 7.34 (m, 10 H, 10 x ArH), 7.58 (d, *J* = 6.71 Hz, 1 H, ArH), 8.08 (d, *J* = 14.04 Hz, 1 H, H1'), 8.28 (d, *J* = 14.04 Hz, 1 H, H2')
^{13}C NMR (101 MHz, DMSO-d_6) ppm 44.8 (C10), 47.6 (C11), 47.9 (C15), 49.6 (C9), 123.1 (CH), 123.5 (CH), 124.5 (CH), 125.3 (CH), 126.5 (CH), 126.97 (CH), 127.16 (CH), 127.31 (CH), 128.6 (CH), 128.8 (CH), 131.5 (CH), 137.3 (C2'), 138.5 (Cq), 140.9 (Cq), 141.3 (Cq), 145.2 (C1'), 174.7 (C12), 175.1 (C14)
HRMS (APCI) calculated for $C_{26}H_{19}N_2O_4$ [M^++H] 423.1345: found 423.1364. Mass accuracy (4.49 ppm).

(*E*)-13-(4-Chlorophenyl)-9-(2-nitrovinyl)-9,10-dihydro-9,10-[3,4]epipyrroloanthracene-12,14-dione (289)

(*E*)-13-(4-Chlorophenyl)-9-(2-nitrovinyl)-9,10-dihydro-9,10-[3,4]epipyrroloanthracene-12,14-dione was prepared from (*E*)-9-(2-nitrovinyl)anthracene (0.25 g, 1 mmol) and 1-(4-chlorophenyl)-1*H*-pyrrole-2,5-dione (0.27 g, 1.3 mmol) according to general procedure 8.25.
Colourless solid 233 mg (51%)
Melting Point: 238-241 °C
IR$_{Vmax}$ (KBr): 3035, 2946 (C-H), 1714 (C=O), 1659 (C=C), 1537, 1493 (C=C), 1191 (C-N) cm^{-1}
^{1}H NMR (400 MHz, DMSO-d_6) δ 3.55 (dd, *J* = 8.54, 3.05 Hz, 1 H, H11), 3.95 (d, *J* = 7.93 Hz, 1 H, H15), 4.97 (d, *J* = 3.05 Hz, 1 H, H10), 6.48 (d, *J* = 8.54 Hz, 2 H, H6"& H2"), 7.21 - 7.47 (m, 10 H, 10 x ArH), 7.61 (d, *J* = 6.71 Hz, 1 H, ArH), 8.12 (d, *J* = 14.04 Hz, 1 H, H1'), 8.32 (d, *J* = 14.04 Hz, 1 H, H2')

^{13}C NMR (101 MHz, DMSO-d_6) ppm 44.8 (C10), 47.7 (C11), 48.0 (C15), 49.6 (C9), 123.0 (CH), 123.5 (CH), 124.5 (Cq), 125.3 (CH), 126.5 (CH), 127.0 (CH), 127.2 (Cq), 127.3 (CH), 128.1 (CH), 129.0 (CH), 130.3 (Cq), 133.1 (Cq), 137.2 (C2'), 138.4 (Cq), 138.5 (Cq), 140.9 (Cq), 141.2 (Cq), 145.2 (C1'), 174.5 (C12), 174.9 (C14)
HRMS (APCI) calculated for $C_{26}H_{18}Cl^{35}N_2O_4$ [M^++H] 457.0955: found 457.0968. Mass accuracy (2.84 ppm).

(*E*)-13-(4-Methoxyphenyl)-9-(2-nitrovinyl)-9,10-dihydro-9,10-[3,4]epipyrroloanthracene-12,14-dione (290)

(*E*)-13-(4-Methoxyphenyl)-9-(2-nitrovinyl)-9,10-dihydro-9,10-[3,4]epipyrroloanthracene-12,14-dione was prepared from (*E*)-9-(2-nitrobut-1-en-1-yl)anthracene (0.26 g, 1 mmol) and 1-(4-methoxyphenyl)-1*H*-pyrrole-2,5-dione (0.243 g, 1.3 mmol) according to general procedure 8.25.
Tan solid 317 mg (70%)
Melting Point: 240-242°C
IR$_{\nu max}$ (KBr): 2988, 2938 (C-H), 1717 (C=O), 1515, 1349. (NO_2), 1657, 1607 (C=C), 1250 (C-N) cm^{-1}
^{1}H NMR (400 MHz, DMSO-d_6) δ 3.51 (d, J = 6.71 Hz, 1 H, H11), 3.71 (br. s., 3 H, CH_3), 3.91 (d, J = 7.93 Hz, 1 H, H15), 4.95 (br. s., 1 H, H10), 6.32 (d, J = 7.32 Hz, 2 H, H3" & H5"), 6.87 (d, J = 7.93 Hz, 2 H, H6" & H2"), 7.23 - 7.46 (m, 7 H, 7 x ArH), 7.61 (d, J = 6.10 Hz, 1 H, 1 x ArH), 8.11 (d, J = 13.43 Hz, 1 H, H2'), 8.31 (d, J = 14.04 Hz, 1 H, H1')
^{13}C NMR (101 MHz, DMSO-d_6) ppm 44.8 (C10), 47.5 (C11), 47.8 (C15), 49.6 (C9), 55.3 (OCH_3), 114.1, 123.1, 123.5, 124.0, 124.5, 125.3, 126.5, 126.9, 127.2, 127.3, 127.6, 137.3 (C2'), 138.5, 138.6, 141.0, 141.3, 145.2 (C1'), 159.0 (C4"), 174.9 (C12), 175.3 (C14)
HRMS (APCI) calculated for $C_{27}H_{21}N_2O_5$ [M^++H] 453.1450: found 453.1448. Mass accuracy (-0.44 ppm).

(*E*)-9-Chloro-10-(2-nitrovinyl)-13-phenyl-9,10-dihydro-9,10-[3,4]epipyrroloanthracene-12,14-dione (291)

(*E*)-9-Chloro-10-(2-nitrovinyl)-13-phenyl-9,10-dihydro-9,10-[3,4]epipyrroloanthracene-12,14-dione was prepared from (*E*)-9-chloro-10-(2-nitrovinyl)anthracene (0.28 g, 1 mmol) and phenylmaleimide (0.22 g, 1.3 mmol) according to general procedure 8.25.
Colourless solid 69 mg (15%)
Melting Point: 263-264 °C
IR$_{\nu max}$ (KBr): 3125, 3068 (C-H), 1705 (C=O), 1596 (C=C), 1494, 1453 (C=C), 1528, 1347 (NO_2) cm^{-1}
^{1}H NMR (400 MHz, DMSO-d_6) δ 3.71 (d, J = 8.55 Hz, 1 H, H11), 4.16 (d, J = 8.55 Hz, 1 H, H15), 6.38 - 6.49 (m, 2 H, 2 x ArH), 7.34 (br. s., 3 H, 3 x ArH), 7.37 - 7.52 (m, 6 H, 6 x ArH), 7.73 (d, J = 7.32 Hz, 1 H, 1 x ArH), 7.88 (d, J = 7.32 Hz, 1 H, 1 x ArH), 8.13 (d, J = 14.04 Hz, 1 H, H1'), 8.33 (d, J = 14.04 Hz, 1 H, H2')
^{13}C NMR (101 MHz, DMSO-d_6) ppm 48.8 (C10), 49.7 (C11), 53.3 (C15), 70.4 (C9), 122.6 (CH), 123.0 (CH), 123.3 (CH), 123.6 (CH), 126.4 (CH), 127.6 (CH), 127.8 (CH), 127.9 (CH), 128.3 (CH), 128.7 (CH), 128.9 (CH), 129.0, 131.4, 136.2 (CH), 136.9 (C2'), 137.2, 139.7, 139.9, 145.7 (C1'), 171.4 (C12), 173.4 (C14)

HRMS (APCI) calculated for $C_{20}H_{18}Cl^{35}N_2O_4$ [M^++H] 457.0955: found 457.0946. Mass accuracy (-1.97 ppm).

(*E*)-13-(4-Fluorophenyl)-9-(2-nitrovinyl)-9,10-dihydro-9,10-[3,4]epipyrroloanthracene-12,14-dione (292)

(*E*)-13-(4-Fluorophenyl)-9-(2-nitrovinyl)-9,10-dihydro-9,10-[3,4]epipyrroloanthracene-12,14-dione was prepared from (*E*)-9-(2-nitrovinyl)anthracene (0.25 g, 1 mmol) and 1-(4-fluorophenyl)-1*H*-pyrrole-2,5-dione (0.248 g, 1.3 mmol) according to general procedure 8.25.
Colourless solid 120 mg (27%)
Melting Point: 242-243 °C
IR$_{Vmax}$ (KBr): 3099, 2892 (C-H), 1711 (C=O), 1688 (C=C), 1505, 1456 (C=C), 1156 (C-N) cm^{-1}
^{1}H NMR (400 MHz, DMSO-d_6) δ 3.55 (dd, *J* = 7.94, 3.05 Hz, 1 H, H11), 3.95 (d, *J* = 8.55 Hz, 1 H, H15), 4.97 (d, *J* = 3.05 Hz, 1 H, H10), 6.47 (dd, *J* = 8.55, 4.88 Hz, 2 H, 2 x ArH), 7.14 - 7.44 (m, 9 H, 9 x ArH), 7.61 (d, *J* = 7.32 Hz, 1 H, 1 x ArH), 8.12 (d, *J* = 14.04 Hz, 1 H, H1'), 8.33 (d, *J* = 14.04 Hz, 1 H, H2')
^{13}C NMR (101 MHz, DMSO-d_6) ppm 45.2 (C10), 48.1 (C11), 48.4 (C15), 50.1 (C9), 116.0, 115.8, 123.5 (CH), 124.0 (CH), 125.0 (CH), 125.7 (CH), 127.0 (CH), 127.4 (CH), 127.6 (CH), 127.8 (CH), 128.9 (CH), 129.1 (CH), 135.1 (CH), 137.7 (C2'), 138.9, 139.0, 141.3, 141.7, 145.7 (C1'), 162.7, 160.3, 175.1 (C12), 175.5 (C14)
HRMS (APCI) calculated for $C_{26}H_{18}FN_2O_4$ [M^++H] 441.1251: found 441.1240. Mass accuracy (-2.49 ppm).

(*E*)-9-(2-Nitrovinyl)-13-(3,4,5-trimethoxyphenyl)-9,10-dihydro-9,10-[3,4]epipyrroloanthracene-12,14-dione (293)

(*E*)-9-(2-Nitrovinyl)-13-(3,4,5-trimethoxyphenyl)-9,10-dihydro-9,10-[3,4]epipyrroloanthracene-12,14-dione was prepared from (*E*)-9-(2-nitrovinyl)anthracene (0.25 g, 1 mmol) and 1-(3,4,5-trimethoxyphenyl)-1*H*-pyrrole-2,5-dione (0.341 g, 1.3 mmol) according to general procedure 8.25.
Yellow solid 52 mg (10%)
Melting Point: 270-272 °C
IR$_{Vmax}$ (ATR): 3049, 2964 (C-H), 1707 (C=O), 1660 (C=C), 1457, 1420 (C=C), 1518, 1349 (NO_2), 1196 (C-N) cm^{-1}
^{1}H NMR (400 MHz, $CDCl_3$) δ 3.43 - 3.56 (m, 2 H, H11 & H15), 3.71 (s, 6 H, 2 x OCH_3), 3.78 (s, 3 H, p-OCH_3), 4.90 - 5.03 (m, 1 H, H10), 5.58 (s, 2 H, H6" & H2"), 7.27 - 7.37 (m, 6 H, 6 x ArH), 7.43 - 7.55 (m, 2 H, 2 x ArH), 7.91 (d, *J* = 14.04 Hz, 1 H, H1'), 8.30 (d, *J* = 14.04 Hz, 1 H, H2')
^{13}C NMR (101 MHz, $CDCl_3$) ppm 45.8 (C10), 48.0 (C11), 48.2 (C15), 50.4 (C9), 56.1 (C3" & C5"), 60.7 (C4"), 103.9 (C6" & C2"), 123.3 (CH), 123.4 (CH), 124.6 (CH), 125.9 (CH), 126.4 (CH), 127.2 (CH), 127.4 (CH), 127.7 (CH), 127.9 (CH), 136.7 (C2'), 138.2, 138.5, 140.4, 140.8 (C1'), 144.7, 153.5, 174.3 (C12), 174.9 (C14)
HRMS (APCI) calculated for $C_{29}H_{25}N_2O_7$ [M^++H] 513.1662: found 513.1643. Mass accuracy (-3.70 ppm).

(*E*)-13-(4-Bromophenyl)-9-(2-nitrovinyl)-9,10-dihydro-9,10-[3,4]epipyrroloanthracene-12,14-dione (294)

(*E*)-13-(4-Bromophenyl)-9-(2-nitrovinyl)-9,10-dihydro-9,10-[3,4]epipyrroloanthracene-12,14-dione was prepared from (E)-9-(2-nitrovinyl)anthracene (0.25 g, 1 mmol) and 1-(4-bromophenyl)-1*H*-pyrrole-2,5-dione (0.325 g, 1.3 mmol) according to general procedure 8.25.
Tan solid 330 mg (66%)
Melting Point: 267-268 °C
IR$_{\nu max}$ (KBr): 3059, 2965 (C-H), 1701 (C=O), 1524, 1351 (NO_2), 1537, 1493 (C=C), 1174 (C-N) cm^{-1}
^{1}H NMR (400 MHz, DMSO-d_6) δ 3.55 (dd, *J* = 8.55, 3.05 Hz, 1 H, H11), 3.95 (d, *J* = 8.55 Hz, 1 H, H15), 4.97 (d, *J* = 3.05 Hz, 1 H, H10), 6.42 (d, *J* = 8.55 Hz, 2 H, 2 x ArH), 7.20 - 7.45 (m, 7 H, 7 x ArH), 7.51 - 7.65 (m, 3 H, 3 x ArH), 8.12 (d, *J* = 14.04 Hz, 1 H, H1'), 8.32 (d, *J* = 13.43 Hz, 1 H, H2')
^{13}C NMR (101 MHz, DMSO-d_6) ppm 44.8 (C10), 47.7 (C11), 48.0 (C15), 49.7 (C9), 121.6, 123.0 (CH), 123.5 (CH), 124.5 (CH), 125.3 (CH), 126.5 (CH), 127.0 (CH), 127.2 (CH), 127.3 (CH), 128.4 (CH), 130.7, 131.9 (CH), 137.2 (C2'), 138.4, 138.5, 140.8, 141.2, 145.2 (C1'), 174.5 (C12), 174.8 (C14)
HRMS (APCI) calculated for $C_{26}H_{18}Br^{79}N_2O_4$ [M^++H] 501.0450: found 501.0468. Mass accuracy (3.59 ppm).

Methyl (*E*)-4-(9-(2-nitrovinyl)-12,14-dioxo-9,10-dihydro-9,10-[3,4]epipyrroloanthracen-13-yl)benzoate (295)

Methyl (*E*)-4-(9-(2-nitrovinyl)-12,14-dioxo-9,10-dihydro-9,10-[3,4]epipyrroloanthracen-13-yl)benzoate was prepared from (*E*)-9-(2-nitrovinyl)anthracene (0.25 g, 1 mmol) and methyl 4-(2,5-dioxo-2,5-dihydro-1*H*-pyrrol-1-yl)benzoate (0.3 g, 1.3 mmol) according to general procedure 8.25.
Colourless solid 288 mg (60%)
Melting Point: 254-255 °C
IR$_{\nu max}$ (KBr): 2989, 2901 (C-H), 1705 (C=O), 1524 (NO), 1459, 1433 (C=C), 1115 (C-N) cm^{-1}
^{1}H NMR (400 MHz, DMSO-d_6) δ 3.58 (dd, *J* = 8.24, 3.36 Hz, 1 H, H11), 3.83 (s, 3 H, OCH_3), 3.97 (d, *J* = 8.55 Hz, 1 H, H15), 4.98 (d, *J* = 3.05 Hz, 1 H, H10), 6.66 (m, *J* = 8.55 Hz, 2 H, H6" & H2"), 7.24 - 7.34 (m, 5 H, 5 x ArH), 7.39 (td, *J* = 8.24, 4.88 Hz, 2 H, 2 x ArH), 7.62 (d, *J* = 6.71 Hz, 1 H, 1 x ArH), 7.92 (m, *J* = 8.55 Hz, 2 H, H3" & H5"), 8.13 (d, *J* = 14.04 Hz, 1 H, H1'), 8.33 (d, *J* = 14.04 Hz, 1 H, H2')
^{13}C NMR (101 MHz, DMSO-d_6) ppm 44.8 (C10), 47.7 (C11), 48.1 (C15), 49.7 (C9), 52.3 (OCH_3), 123.1 (CH), 123.5 (CH), 124.5 (CH), 125.3 (CH), 126.5 (CH), 126.6 (CH), 127.0 (CH), 127.2 (CH), 127.4 (CH), 129.5, 129.7 (CH), 135.5, 137.2 (C2'), 138.4, 138.5, 140.8, 141.2, 145.3 (C1'), 165.3 (Ester C=O), 174.4 (C12), 174.8 (C14)
HRMS (APCI) calculated for $C_{28}H_{21}N_2O_6$ [M^++H] 481.1400: found 481.1384. Mass accuracy (-3.25 ppm).

(*E*)-13-(4-Benzoylphenyl)-9-(2-nitrovinyl)-9,10-dihydro-9,10-[3,4]epipyrroloanthracene-12,14-dione (296)

(*E*)-13-(4-Benzoylphenyl)-9-(2-nitrovinyl)-9,10-dihydro-9,10-[3,4]epipyrroloanthracene-12,14-dione was prepared from (E)-9-(2-nitrovinyl)anthracene (0.25 g, 1 mmol) and 1-(4-benzoylphenyl)-1*H*-pyrrole-2,5-dione (0.36 g, 1.3 mmol) according to general procedure 8.25.
Yellow solid 210 mg (40%)
Melting Point: 232-234 °C
IR$_{Vmax}$ (ATR): 3071, 2966 (C-H), 1708 (C=O), 1660 (C=C), 1458, 1448 (C=C), 1529, 1353 (NO_2), 1195 (C-N) cm^{-1}
^{1}H NMR (400 MHz, DMSO-*d*$_6$) δ 3.60 (dd, *J* = 8.55, 3.05 Hz, 1 H, H11), 3.99 (d, *J* = 8.55 Hz, 1 H, H15), 5.00 (d, *J* = 3.05 Hz, 1 H, H10), 6.69 (d, *J* = 8.55 Hz, 2 H, H6" & H2"), 7.22 - 7.35 (m, 5 H, 5 x ArH), 7.35 - 7.46 (m, 2 H, 2 x ArH), 7.50 - 7.60 (m, 2 H, 2 x ArH), 7.60 - 7.74 (m, 6 H, 6 x ArH), 8.14 (d, *J* = 14.04 Hz, 1 H, H1'), 8.34 (d, *J* = 14.04 Hz, 1 H, H2')
^{13}C NMR (101 MHz, DMSO-*d*$_6$) ppm 44.8 (C10), 47.8 (C11), 48.1 (C15), 49.7 (C9), 123.1 (CH), 123.6 (CH), 124.5 (CH), 125.3 (CH), 126.4 (CH), 126.5 (CH), 127.1 (CH), 127.2 (CH), 127.4 (CH), 128.2, 128.6 (CH), 129.6 (CH), 130.2 (CH), 132.9 (CH), 134.9, 136.5, 136.9, 137.2 (C2'), 138.4, 138.5, 140.9, 141.2, 145.3 (C1'), 174.5 (C12), 174.8 (C14), 194.8 (C=O)
HRMS (APCI) calculated for $C_{33}H_{23}N_2O_5$ [M^++H] 527.1607: found 527.1599. Mass accuracy (-1.52 ppm).

(*E*)-13-(4-(Dimethylamino)phenyl)-9-(2-nitrovinyl)-9,10-dihydro-9,10-[3,4]epipyrroloanthracene-12,14-dione (297)

(*E*)-13-(4-(Dimethylamino)phenyl)-9-(2-nitrovinyl)-9,10-dihydro-9,10-[3,4]epipyrroloanthracene-12,14-dione was prepared from (*E*)-9-(2-nitrovinyl)anthracene (0.25 g, 1 mmol) and 1-(4-(dimethylamino)phenyl)-1*H*-pyrrole-2,5-dione (0.28 g, 1.3 mmol) according to general procedure 8.25.
Yellow solid 312 mg (67%)
Melting Point: 280-282 °C
IR$_{Vmax}$ (KBr): 3133, 2968 (C-H), 1711 (C=O), 1610 (C=C), 1520, 1459 (C=C), 1200 (C-N) cm^{-1}
^{1}H NMR (400 MHz, DMSO-*d*$_6$) δ 2.84 (s, 6 H, 2 x CH_3), 3.49 (dd, *J* = 8.55, 3.05 Hz, 1 H, H11), 3.88 (d, *J* = 8.55 Hz, 1 H, H15), 4.94 (d, *J* = 3.05 Hz, 1 H, H10), 6.20 (m, *J* = 9.16 Hz, 2 H. H3" & H5"), 6.58 (m, *J* = 9.16 Hz, 2 H, H2" & H6"), 7.20 - 7.43 (m, 7 H, 7 x ArH), 7.60 (d, *J* = 7.32 Hz, 1 H, 1 x ArH), 8.12 (d, *J* = 14.04 Hz, 1 H, H1'), 8.32 (d, *J* = 14.04 Hz, 1 H, H2')
^{13}C NMR (101 MHz, DMSO-*d*$_6$) ppm 40.0 (2 x NCH_3), 44.8 (C10), 47.4 (C11), 47.7 (C15), 49.7 (C9), 111.8 (CH), 119.8 (CH), 123.0 (CH), 123.5 (CH), 124.4 (CH), 125.3 (CH), 126.5 (CH), 126.9 (CH), 126.9 (CH), 127.1 (CH), 127.2 (CH), 137.4 (CH), 138.5, 138.6, 141.0, 141.3, 145.2 (C1'), 150.1 (C4"), 175.1 (C12), 175.5 (C14)
HRMS (APCI) calculated for $C_{28}H_{24}N_3O_4$ [M^++H] 466.1777: found 466.1793. Mass accuracy (3.43 ppm).

(*E*)-13-(3,5-Dimethoxyphenyl)-9-(2-nitrovinyl)-9,10-dihydro-9,10-[3,4]epipyrroloanthracene-12,14-dione (298)

(*E*)-13-(3,5-Dimethoxyphenyl)-9-(2-nitrovinyl)-9,10-dihydro-9,10-[3,4]epipyrroloanthracene-12,14-dione was prepared from (*E*)-9-(2-nitrovinyl)anthracene

(0.25 g, 1 mmol) and 1-(3,5-dimethoxyphenyl)-1*H*-pyrrole-2,5-dione (0.3 g, 1.3 mmol) according to general procedure 8.25.
Colourless solid 304 mg (63%)
Melting Point: 268-271 °C
IR$_{\nu max}$ (KBr): 2966, 2960 (C-H), 1714 (C=O), 1601 (C=C), 1531 (NO), 1474, 1457 (C=C), 1159 (C-N) cm^{-1}
^{1}H NMR (400 MHz, DMSO-d_6) **δ** 3.52 (dd, *J* = 8.55, 3.05 Hz, 1 H, H11), 3.64 (s, 6 H, 2 x OCH_3), 3.92 (d, *J* = 8.55 Hz, 1 H, H15), 4.96 (d, *J* = 3.05 Hz, 1 H, H10), 5.49 (d, *J* = 1.83 Hz, 2 H, H1" & H6"), 6.42 - 6.49 (m, 1 H, H4"), 7.19 - 7.45 (m, 7 H, 7 x ArH), 7.61 (d, *J* = 6.71 Hz, 1 H, 1 x ArH), 8.12 (d, *J* = 14.04 Hz, 1 H, H1'), 8.32 (d, *J* = 13.43 Hz, 1 H, H2')
^{13}C NMR (101 MHz, DMSO-d_6) ppm 44.9 (C10), 47.6 (C11), 47.9 (C15), 49.7 (C9), 55.4 (OCH_3), 100.5 (C2" & C6"), 105.0 (C4"), 123.2 (CH), 123.5 (CH), 124.5 (CH), 125.3 (CH), 126.5 (CH), 126.9 (CH), 127.2 (CH), 127.3 (CH), 133.2, 137.3 (CH), 138.5, 138.6, 140.9, 141.2, 145.2 (C1'), 160.3 (C3" & C5"), 174.5 (C12), 174.9 (C14)
HRMS (APCI) calculated for $C_{28}H_{23}N_2O_6$ [M^++H] 483.1556: found 483.1543. Mass accuracy (-2.69 ppm).

(*E*)-13-(3-Chlorophenyl)-9-(2-nitrovinyl)-9,10-dihydro-9,10-[3,4]epipyrroloanthracene-12,14-dione (299)

(*E*)-13-(3-Chlorophenyl)-9-(2-nitrovinyl)-9,10-dihydro-9,10-[3,4]epipyrroloanthracene-12,14-dione was prepared from (*E*)-9-(2-nitrovinyl)anthracene (0.25 g, 1 mmol) and 1-(3-chlorophenyl)-1*H*-pyrrole-2,5-dione (0.27 g, 1.3 mmol) according to general procedure 8.25.
Tan solid 265 mg (58%)
Melting Point: 258-261 °C
IR$_{\nu max}$ (ATR): 3069, 2966 (C-H), 1713 (C=O), 1594 (C=C), 1481, 1434 (C=C), 1537, 1351 (NO_2) cm^{-1}
^{1}H NMR (400 MHz, DMSO-d_6) **δ** 3.57 (dd, *J* = 8.29, 3.32 Hz, 1 H, H11), 3.97 (d, *J* = 8.29 Hz, 1 H, H15), 4.98 (d, *J* = 3.32 Hz, 1 H, H10), 6.41 - 6.52 (m, 2 H, 2 x ArH), 7.23 - 7.42 (m, 9 H, 9 x ArH), 7.56 - 7.65 (m, 1 H, 1 x ArH), 8.13 (d, *J* = 13.68 Hz, 1 H, H1'), 8.34 (d, *J* = 13.68 Hz, 1 H, H2')
^{13}C NMR (101 MHz, DMSO-d_6) ppm 44.8 (C10), 47.7 (C11), 48.1 (C15), 49.7 (C9), 123.1 (CH), 123.6 (CH), 124.5 (CH), 125.3 (CH), 126.4 (CH), 126.4 (CH), 126.5 (CH), 127.0 (CH), 127.2 (CH), 127.3 (CH), 128.7 (CH), 130.6 (CH), 132.8, 132.9, 134.7 (CH), 138.5, 138.5, 140.8, 141.2, 145.3 (C1"), 174.5 (C12), 174.8 (C14)
HRMS (APCI) calculated for $C_{26}H_{18}Cl^{35}N_2O_4$ [M^++H] 457.0955: found 457.0951. Mass accuracy (-0.87 ppm).

(*E*)-13-(2-Hydroxyphenyl)-9-(2-nitrovinyl)-9,10-dihydro-9,10-[3,4]epipyrroloanthracene-12,14-dione (300)

(*E*)-13-(2-Hydroxyphenyl)-9-(2-nitrovinyl)-9,10-dihydro-9,10-[3,4]epipyrroloanthracene-12,14-dione was prepared from (*E*)-9-(2-nitrovinyl)anthracene (0.25 g, 1 mmol) and 1-(2-hydroxyphenyl)-1*H*-pyrrole-2,5-dione (0.245 g, 1.3 mmol) according to general procedure 8.25.
Colourless solid 175 mg (40%)
Melting Point: 203-206 °C

IR$_{Vmax}$ (KBr): 3030, 2969 (C-H), 1710 (C=O), 1663 (C=C), 1527 (NO), 1495, 1456 (C=C), 1192 (C-N) cm^{-1}

^{1}H NMR (400 MHz, DMSO-d_6) δ 3.55 (dd, J = 8.55, 3.05 Hz, 1 H, H11), 3.96 (d, J = 8.55 Hz, 1 H, H15), 4.97 (d, J = 3.05 Hz, 1 H, H10), 6.41 - 6.50 (m, 2 H, 2 x ArH), 7.23 - 7.41 (m, 9 H, 9 x ArH), 7.61 (d, J = 7.32 Hz, 1 H, 1 x ArH), 8.12 (d, J = 14.04 Hz, 1 H, H1'), 8.32 (d, J = 14.04 Hz, 1 H, H2')

^{13}C NMR (101 MHz, DMSO-d_6) ppm 44.8 (C10), 47.7 (C11), 48.1 (C15), 49.7 (C9), 123.1 (CH), 123.6 (CH), 124.5 (CH), 125.3 (CH), 126.4 (CH), 126.5 (CH), 127.0 (CH), 127.2 (CH), 127.3 (CH), 128.2 (CH), 128.7 (CH), 130.6 (CH), 132.8, 132.9, 137.2, 138.5, 138.5, 140.8, 141.2, 145.3 (C1'), 174.5 (C12), 174.8 (C14)

HRMS (APCI) calculated for $C_{26}H_{19}N_2O_5$ [M$^+$+H] 439.1294: found 439.1306. Mass accuracy (2.73 ppm).

(*E*)-3-(9-(2-Nitrovinyl)-12,14-dioxo-9,10-dihydro-9,10-[3,4]epipyrroloanthracen-13-yl)phenyl acetate

(*E*)-3-(9-(2-Nitrovinyl)-12,14-dioxo-9,10-dihydro-9,10-[3,4]epipyrroloanthracen-13-yl)phenyl acetate was prepared from (*E*)-9-(2-nitrovinyl)anthracene (0.25 g, 1 mmol) and 3-(2,5-dioxo-2,5-dihydro-1*H*-pyrrol-1-yl)phenyl acetate (0.3 g, 1.3 mmol) according to general procedure 8.25.

Colourless solid 240 mg (50%)

Melting Point: 246-248 °C

IR$_{Vmax}$ (ATR): 3085, 3065 (C-H), 1715 (C=O), 1606 (C=C), 1484, 1482 (C=C), 1538, 1338 (NO_2) cm^{-1}

^{1}H NMR (400 MHz, DMSO-d_6) δ 2.25 (s, 3 H, CH_3), 3.55 (dd, J = 8.24, 3.36 Hz, 1 H, H11), 3.95 (d, J = 8.55 Hz, 1 H, H15), 4.97 (d, J = 3.05 Hz, 1 H, H10), 6.25 - 6.36 (m, 2 H, C4" & C2"), 7.08 - 7.15 (m, 1 H, 1 x ArH), 7.21 - 7.43 (m, 8 H, 8 x ArH), 7.62 (d, J = 7.32 Hz, 1 H, 1 x ArH), 8.12 (d, J = 13.43 Hz, 1 H, H1'), 8.33 (d, J = 14.04 Hz, 1 H, H2')

^{13}C NMR (101 MHz, DMSO-d_6) ppm 20.7 (CH_3), 44.8 (C10), 47.7 (C11), 48.0 (C15), 49.7 (C9), 120.0 (CH), 122.2 (CH), 123.1 (CH), 123.5 (CH), 123.7 (CH), 124.5 (CH), 125.3 (CH), 126.5 (CH), 127.0 (CH), 127.2 (CH), 127.3 (CH), 128.2, 128.9, 129.6 (CH), 132.2, 137.2 (CH), 138.4, 138.5, 140.9, 141.2, 145.3 (C1'), 150.3 (C3"), 168.8 (Acetate C=O), 174.5 (C12), 174.8 (C14)

HRMS (APCI) calculated for $C_{28}H_{21}N_2O_6$ [M$^+$+H] 481.1388: found 481.1394. Mass accuracy (-1.23 ppm).

(*E*)-13-(4-Aminophenyl)-9-(2-nitrovinyl)-9,10-dihydro-9,10-[3,4]epipyrroloanthracene-12,14-dione (302)

(*E*)-13-(4-Aminophenyl)-9-(2-nitrovinyl)-9,10-dihydro-9,10-[3,4]epipyrroloanthracene-12,14-dione was prepared from (*E*)-9-(2-nitrovinyl)anthracene 0.25 g (1 mmol) and 1-(4-aminophenyl)-1*H*-pyrrole-2,5-dione 0.244 g (1.3 mmol) according to general procedure 8.25.

Brown solid 197 mg (45%)

Melting Point: >300 °C

IR$_{Vmax}$ (ATR): 3070, 2953 (C-H), 1712 (C=O), 1595 (C=C), 1482, 1457 (C=C), 1518, 1349 (NO_2) cm^{-1}

^{1}H NMR (400 MHz, DMSO-d_6) **δ** 3.53 (dd, *J* = 7.94, 3.05 Hz, 1 H, H11), 3.93 (d, *J* = 8.55 Hz, 1 H, H15), 4.90 - 5.00 (m, 1 H, H10), 6.42 (s, 2 H, NH_2), 7.12 - 7.42 (m, 11 H, 11 x ArH), 7.60 (d, *J* = 7.32 Hz, 1 H, 1 x ArH), 8.10 (d, *J* = 14.04 Hz, 1 H, H1'), 8.30 (d, *J* = 13.43 Hz, 1 H, H2')
^{13}C NMR (101 MHz, DMSO-d_6) ppm 43.6 (C10), 44.7 (C11), 47.9 (C15), 49.7 (C9), 123.0 (CH), 123.5 (CH), 124.5 (CH), 125.2 (CH), 125.3 (CH), 126.5 (CH), 126.8 (CH), 127.2 (CH), 127.4 (CH), 128.2 (CH), 128.9 (CH), 131.3, 134.8 (C1'), 137.2, 138.4, 138.4, 140.8, 141.2, 145.2 (C1'), 174.5 (C12), 174.9 (C14)
HRMS (APCI) calculated for $C_{26}H_{20}N_3O_4$ [M+H] 438.1454: found 438.1461. Mass accuracy (1.60 ppm).

(*E*)-9-(2-Nitroprop-1-en-1-yl)-13-phenyl-9,10-dihydro-9,10-[3,4]epipyrroloanthracene-12,14-dione (303)

(*E*)-9-(2-Nitroprop-1-en-1-yl)-13-phenyl-9,10-dihydro-9,10-[3,4]epipyrroloanthracene-12,14-dione was prepared from (*E*)-9-(2-nitroprop-1-en-1-yl)anthracene (0.26 g, 1 mmol) and phenylmaleimide (0.22 g, 1.3 mmol) according to general procedure 8.25.
Colourless solid 384 mg (88%)
Melting Point: 263-266 °C
IR$_{Vmax}$ (KBr): 3045, 2934 (C-H), 1700 (C=O), 1598, 1460 (C=C), 1519 (C=C), 1523, 1390 (NO_2), 1328 (CH_3) cm^{-1}
^{1}H NMR (400 MHz, DMSO-d_6) **δ** 1.86 (br. s., 3 H, CH3), 3.38 - 3.51 (m, 1 H, H11), 3.61 (d, *J* = 7.32 Hz, 1 H, H15), 4.97 (d, *J* = 3.66 Hz, 1 H, H10), 6.33 - 6.51 (m, 2 H, H6" & H2"), 7.19 - 7.41 (m, 10 H, 10 x ArH), 7.63 (d, *J* = 7.32 Hz, 1 H, ArH), 8.37 (s, 1 H, H1')
^{13}C NMR (101 MHz, DMSO-d_6) ppm 17.2 (C3'), 44.9 (C11), 47.4 (C15), 50.2 (C9), 50.3 (C10), 123.7 (CH), 123.9 (CH), 124.8 (CH), 125.3 (CH), 125.4 (CH), 126.4 (CH), 126.8 (CH), 127.2 (CH), 127.4 (CH), 128.2 (CH), 128.5 (CH), 128.8 (CH), 131.5 (C1"), 131.8, 138.3 (C1'), 138.6, 140.7, 152.5 (C2'), 175.1 (C14 & C12)
HRMS (APCI) calculated for $C_{27}H_{21}N_2O_4$ [M^++H] 437.1501: found 437.1513. Mass accuracy (-2.74 ppm).

(*E*)-9-(2-Nitrobut-1-en-1-yl)-13-phenyl-9,10-dihydro-9,10-[3,4]epipyrroloanthracene-12,14-dione (304)

(*E*)-9-(2-Nitrobut-1-en-1-yl)-13-phenyl-9,10-dihydro-9,10-[3,4]epipyrroloanthracene-12,14-dione was prepared from (*E*)-9-(2-nitrobut-1-en-1-yl)anthracene (0.27 g, 1 mmol) and phenylmaleimide (0.22 g, 1.3 mmol) according to general procedure 8.25.
Colourless solid 368 mg (82%)
Melting Point: 259-263 °C
IR$_{Vmax}$ (KBr): 2968, 2939 (C-H), 1707 (C=O), 1597 (C=C), 1500, 1456 (C=C), 1519, 1390 (NO_2), 1464 (CH_2), 1340 (CH_3) cm^{-1}
^{1}H NMR (400 MHz, $CDCl_3$) **δ** 1.03 (br. s., 3 H, CH_3), 2.28 (br. s., 2 H, CH_2), 3.34 (br. s., 2 H, H15 & H11), 4.95 (s, 1 H, H10), 6.47 (dd, *J* = 6.41, 2.75 Hz, 2 H, H6" & H2"), 7.19 - 7.45 (m, 11 H, 11 x ArH), 8.20 (s, 1 H, H1')
^{13}C NMR (101 MHz, $CDCl_3$) ppm 9.8 (C4'), 23.9 (C3'), 46.0 (C10), 47.8 (C11), 49.7 (C9), 50.3 (C15), 123.5 (CH), 124.8 (CH), 125.8 (CH), 126.0, 126.2 (CH), 126.7 (CH), 127.1 (CH),

127.8 (CH), 127.9, 128.0 (CH), 128.8 (CH), 129.0 (C1'), 129.1, 129.9, 130.9, 134.2, 137.8, 139.0 (C2'), 174.9 (C12 & C14)
HRMS (APCI) calculated for $C_{28}H_{21}N_2O_4$ [M^+-H] 449.1507: found 449.1490. Mass accuracy (-3.8 ppm).

(*E*)-13-(4-Chlorophenyl)-9-(2-nitroprop-1-en-1-yl)-9,10-dihydro-9,10-[3,4]epipyrroloanthracene-12,14-dione (305)

(*E*)-13-(4-Chlorophenyl)-9-(2-nitroprop-1-en-1-yl)-9,10-dihydro-9,10-[3,4]epipyrroloanthracene-12,14-dione was prepared from (*E*)-9-(2-nitroprop-1-en-1-yl)anthracene (0.26 g, 1 mmol) and 1-(4-chlorophenyl)-1*H*-pyrrole-2,5-dione (0.27 g, 1.3 mmol) according to general procedure 8.25.
Colourless solid 282 mg (60%)
Melting Point: 298-300 °C
IR$_{Vmax}$ (KBr): 3003, 2967 (C-H), 1700 (C=O), 1524, 1390 (NO_2), 1494 (C=C), 1460 (CH_3), 1198 (C-N), 778.31 (Cl-C) cm^{-1}
^{1}H NMR (400 MHz, $CDCl_3$) δ 1.96 (br. s., 3 H, CH_3), 3.35 (br. s., 2 H, H11 & H15), 4.94 (br. s., 1 H, H10), 6.44 (d, *J* = 7.32 Hz, 2 H, H6" & H2"), 7.14 - 7.34 (m, 11 H, 11 x ArH), 8.45 (br. s., 1 H, H1')
^{13}C NMR (101 MHz, $CDCl_3$) ppm 18.2 (C3'), 46.0 (C10), 47.7 (C11), 48.6 (C15), 50.6 (C9), 123.4, 124.9, 125.9, 126.9, 127.3, 127.4, 127.9, 128.0, 129.3, 137.2 (C2'), 174.7 (C14 & C12)
HRMS (APCI) calculated for $C_{27}H_{20}Cl^{35}N_2O_4$ [M^++H] 471.1112: found 471.1099. Mass accuracy (-2.75 ppm).

(*E*)-13-(4-Chlorophenyl)-9-(2-nitrobut-1-en-1-yl)-9,10-dihydro-9,10-[3,4]epipyrroloanthracene-12,14-dione (306)

(*E*)-13-(4-Chlorophenyl)-9-(2-nitrobut-1-en-1-yl)-9,10-dihydro-9,10-[3,4]epipyrroloanthracene-12,14-dione was prepared from (*E*)-9-(2-nitrobut-1-en-1-yl)anthracene (0.26 g, 1 mmol) and 1-(4-chlorophenyl)-1*H*-pyrrole-2,5-dione (0.27 g, 1.3 mmol) according to general procedure 8.25.
Colourless solid 212 mg (44%)
Melting Point: 275-279 °C
IR$_{Vmax}$ (KBr): 3005, 2941 (C-H), 1702 (C=O), 1598 (C=C), 1458, 1429 (C=C), 1520, 1383.10 (NO_2), 1341 (CH_2), 1310 (CH_3), 762 (Cl-C) cm^{-1}
^{1}H NMR (400 MHz, DMSO-d_6) δ 0.99 (br. s., 3 H, CH3), 2.17 (br. s., 2 H, CH2), 3.42 (br. s., 1 H, H11), 3.62 (d, *J* = 6.10 Hz, 1 H, H15), 4.98 (d, *J* = 3.05 Hz, 1 H, H10), 6.47 (d, *J* = 9.16 Hz, 2 H, H6" & H2"), 7.17 - 7.48 (m, 10 H, 10 x ArH), 7.64 (d, *J* = 6.71 Hz, 1 H, ArH), 8.19 (s, 1 H, H1')
^{13}C NMR (101 MHz, DMSO-d_6) ppm 8.4 (C3'), 23.4 (C4'), 39.8 (C10), 45.0 (C11), 47.5 (C15), 50.4 (C9), 123.6 (CH), 124.9 (CH), 125.4 (CH), 126.4 (CH), 126.8 (CH), 127.4 (CH), 128.1 (CH), 129.0 (CH), 130.2 (Cq), 133.1 (Cq), 138.8 (Cq), 142.6 (Cq), 157.0 (C2'), 174.8 (C14 & C12)
HRMS (APCI) calculated for $C_{28}H_{20}Cl^{35}N_2O_4$ [M^+-H] 483.1117: found 483.1101. Mass accuracy (-3.3 ppm).

(*E*)-13-(4-Methylphenyl)-9-(2-nitroprop-1-en-1-yl)-9,10-dihydro-9,10-[3,4]epipyrroloanthracene-12,14-dione (307)

(*E*)-13-(4-Methylphenyl)-9-(2-nitroprop-1-en-1-yl)-9,10-dihydro-9,10-[3,4]epipyrroloanthracene-12,14-dione was prepared from (*E*)-9-(2-nitrobut-1-en-1-yl)anthracene (0.26 g, 1 mmol) and 1-(4-methylphenyl)-1*H*-pyrrole-2,5-dione (0.243 g, 1.3 mmol) according to general procedure 8.25.
Colourless solid 293 mg (65%)
Melting Point: 276-277 °C
IR$_{\nu max}$ (KBr): 3071, 3010 (C-H), 1700 (C=O), 1518, 1391 (NO_2), 1198 (C-N) cm^{-1}
^{1}H NMR (400 MHz, DMSO-d_6) δ 1.85 (br. s., 3 H, CH_3), 2.25 (s, 3 H, CH_3), 3.41 (dd, *J* = 8.24, 2.75 Hz, 1 H, H11), 3.59 (d, *J* = 7.32 Hz, 1 H, H15), 4.96 (d, *J* = 3.05 Hz, 1 H, H10), 6.30 (d, *J* = 8.54 Hz, 2 H, H5" & H3"), 7.12 (d, *J* = 7.93 Hz, 2 H, H6" & H2"), 7.20 - 7.43 (m, 7 H, 7 x ArH), 7.63 (d, *J* = 6.71 Hz, 1 H,1 x ArH), 8.35 (s, 1 H, H1')
^{13}C NMR (101 MHz, DMSO-d_6) ppm 21.0 (C3'), 45.4 (C10), 47.8 (C11), 49.9 (C15), 51.0 (C9), 55.0 (OCH_3), 124.1, 125.2, 125.8, 126.6, 126.8, 127.2, 127.6, 127.7, 129.3, 129.7, 138.5, 139.1, 159.7 (C2'), 175.6 (C12 & C14),
HRMS (APCI) calculated for $C_{28}H_{23}N_2O_4$ [M+H] 451.1658: found 451.1666. Mass accuracy (1.77 ppm).

(*E*)-13-(4-Methylphenyl)-9-(2-nitrobut-1-en-1-yl)-9,10-dihydro-9,10-[3,4]epipyrroloanthracene-12,14-dione (308)

(*E*)-13-(4-Methylphenyl)-9-(2-nitrobut-1-en-1-yl)-9,10-dihydro-9,10-[3,4]epipyrroloanthracene-12,14-dione was prepared from (*E*)-9-(2-nitrobut-1-en-1-yl)anthracene (0.26 g, 1 mmol) and 1-(4-methyoxyphenyl)-1*H*-pyrrole-2,5-dione (0.243 g, 1.3 mmol) according to general procedure 8.25.
Colourless solid 251 mg (54%)
Melting Point: 254-256 °C
IR$_{\nu max}$ (KBr): 3006, 2962 (C-H), 1700 (C=O), 1523, 1387 (NO_2), 1192 (C-N) cm^{-1}
^{1}H NMR (400 MHz, DMSO-d_6) δ 0.99 (br. s., 3 H, CH_2-$\underline{CH_3}$), 2.17 (br. s., 2 H, CH_2), 2.25 (s, 3 H, CH_3), 3.40 (br. s., 1 H, H11), 3.58 (br. s., 1 H, H15), 4.97 (d, *J* = 3.05 Hz, 1 H, H10), 6.30 (d, *J* = 7.93 Hz, 2 H, H5" & H3"), 7.11 (d, *J* = 8.54 Hz, 2 H, H6" & H2"), 7.21 - 7.47 (m, 7 H, 7 x ArH), 7.63 (d, *J* = 6.71 Hz, 1 H, 1 x ArH), 8.20 (s, 1 H, H1')
^{13}C NMR (101 MHz, DMSO-d_6) ppm 9.5 (C3'), 20.6 (OCH_3), 23.4 (C4) 45.0 (C11), 47.4 (C15), 50.3 (C9), 109.5, 123.6, 124.8, 125.4, 126.1, 126.3, 126.7, 127.3, 127.5, 128.8, 129.2, 138.1, 138.9, 156.9 (C2'), 175.1 (C12 & C14)
HRMS (APCI) calculated for $C_{29}H_{25}N_2O_5$ [M^++H] 465.1814: found 465.1831. Mass accuracy (3.65 ppm).

(*E*)-9-Chloro-10-(2-nitroprop-1-en-1-yl)-13-phenyl-9,10-dihydro-9,10-[3,4]epipyrroloanthracene-12,14-dione (309)

(*E*)-9-Chloro-10-(2-nitroprop-1-en-1-yl)-13-phenyl-9,10-dihydro-9,10-[3,4]epipyrroloanthracene-12,14-dione was prepared from (*E*)-9-chloro-10-(2-nitroprop-1-en-1-yl)anthracene (0.298 g, 1 mmol) and phenylmaleimide (0.224 g, 1.3 mmol) according to general procedure 8.25.

Colourless solid 183 mg (39%)
Melting Point: 268-271 °C
IR$_{Vmax}$ (ATR): 3072, 2981 (C-H), 1713 (C=O), 1625 (C=C), 1499, 1455 (C=C), 1520, 1332 (NO_2) cm^{-1}
^{1}H NMR (400 MHz, $CDCl_3$) δ 1.94 (br. s., 3 H, CH_3), 3.46 (br. s., 2 H, H11 & H15), 6.49 (dd, *J* = 6.10, 3.66 Hz, 2 H, 2 x ArH), 7.14 - 7.29 (m, 5 H, 5 x ArH), 7.29 - 7.45 (m, 4 H, 4 x ArH), 7.89 (d, *J* = 7.93 Hz, 1 H, 1 x ArH), 8.01 (d, *J* = 7.32 Hz, 1 H, 1 x ArH), 8.49 (s, 1 H, H1')
^{13}C NMR (101 MHz, $CDCl_3$) ppm 17.8 (C3'), 52.0 (C10), 53.4 (C15 & C11), 70.1 (C9), 122.8 (CH), 124.0 (CH), 124.2 (CH), 126.1 (CH), 127.9 (CH), 128.1 (CH), 128.2 (CH), 128.4 (CH), 128.9 (CH), 129.0 (CH), 130.8, 136.9, 137.3, 140.8 (C2'), 171.2 (C12 & C14)
HRMS (APCI) calculated for $C_{27}H_{20}Cl^{35}N_2O_4$ [M^++H] 471.1112: found 471.1101. Mass accuracy (-2.33 ppm).

(*E*)-9-Chloro-10-(2-nitrobut-1-en-1-yl)-13-phenyl-9,10-dihydro-9,10-[3,4]epipyrroloanthracene-12,14-dione (310)

(*E*)-9-Chloro-10-(2-nitrobut-1-en-1-yl)-13-phenyl-9,10-dihydro-9,10-[3,4]epipyrroloanthracene-12,14-dione was prepared from (*E*)-9-chloro-10-(2-nitrobut-1-en-1-yl)anthracene (0.312 g, 1 mmol) and phenyl maleimide (0.224 g, 1.3 mmol) according to general procedure 8.25.
Colourless solid 184 mg (38%)
Melting Point: 261-262 °C
IR$_{Vmax}$ (ATR): 3075, 2981, 2942 (C-H), 1712 (C=O), 1623 (C=C), 1498, 1455 (C=C), 1520, 1348 (NO_2) cm^{-1}
^{1}H NMR (400 MHz, $CDCl_3$) δ 0.94 - 1.10 (m, 3 H, CH_3), 2.26 (dd, *J* = 19.23, 7.02 Hz, 2 H, CH_2), 3.44 (br. s., 2 H, H11 & H15), 6.50 (dd, *J* = 5.80, 3.36 Hz, 2 H, 2 x ArH), 7.20 - 7.50 (m, 9 H, 9 x ArH), 7.90 (d, *J* = 7.94 Hz, 1 H, 1 x ArH), 8.02 (d, *J* = 7.93 Hz, 1 H, 1 x ArH), 8.21 (s, 1 H, H1')
^{13}C NMR (101 MHz, $CDCl_3$) ppm 10.0 (C4'), 24.4 (C3'), 52.2 (C10), 53.5 (C15 & C11), 70.1 (C9), 123.0 (CH), 123.9 (CH), 124.1 (CH), 126.1 (CH), 127.7 (CH), 128.1, 128.2 (CH), 128.4, 128.9 (CH), 129.0 (C1'), 130.7, 137.5 (C2'), 171.1 (C12 & C14)
HRMS (APCI) calculated for $C_{28}H_{22}Cl^{35}N_2O_4$ [M^+-H] 485.1268: found 485.1248. Mass accuracy (-4.12 ppm).

(*E*)-13-Benzyl-9-(2-nitrovinyl)-9,10-dihydro-9,10-[3,4]epipyrroloanthracene-12,14-dione (311)

(*E*)-13-Benzyl-9-(2-nitrovinyl)-9,10-dihydro-9,10-[3,4]epipyrroloanthracene-12,14-dione was prepared from (*E*)-9-(2-nitrovinyl)anthracene (0.25 g, 1 mmol) and 1-benzyl-1*H*-pyrrole-2,5-dione (0.24 g, 1.3 mmol) according to general procedure 8.25.
Colourless solid 323 mg (74%)
Melting Point: 232-236 °C
IR$_{Vmax}$ (KBr): 3033 2933 (C-H), 1702 (C=O), 1657 (C=C), 1496, 1464 (C=C), 1533, 1390 (NO_2), 1464 (CH_2), 1189 (C-N) cm^{-1}
^{1}H NMR (400 MHz, DMSO-*d*$_6$) δ 3.47 (d, *J* = 5.49 Hz, 1 H, H11), 3.86 (d, *J* = 7.93 Hz, 1 H, H15), 4.22 (br. s., 2 H, CH2), 4.90 (br. s., 1 H, H10), 6.31 (d, *J* = 6.71 Hz, 2 H, H2" & H6"),

7.01 - 7.39 (m, 10 H, 10 x ArH), 7.57 (d, *J* = 6.10 Hz, 1 H, 1 x ArH), 8.12 (d, *J* = 14.04 Hz, 1 H, H2'), 8.28 (d, *J* = 14.04 Hz, 1 H, H1')
^{13}C NMR (101 MHz, DMSO-*d*$_6$) ppm 41.3 (C10), 43.6 (C11), 44.2 (C15), 47.5 (C16), 49.2 (C9), 109.5, 122.9, 123.3, 124.3, 125.3, 126.1, 126.4, 126.8, 127.0, 127.4, 128.2, 134.9, 137.2 (C1'), 138.5, 138.6, 141.4, 141.8, 145.2 (C2'), 175.3 (C12), 175.6 (C14)
HRMS (APCI) calculated for $C_{27}H_{21}N_2O_4$ [M^++H] 437.1501: found 437.1505. Mass accuracy (0.91 ppm).

(*E*)-13-Benzyl-9-(2-nitroprop-1-en-1-yl)-9,10-dihydro-9,10-[3,4]epipyrroloanthracene-12,14-dione (312)

(*E*)-13-Benzyl-9-(2-nitroprop-1-en-1-yl)-9,10-dihydro-9,10-[3,4]epipyrroloanthracene-12,14-dione was prepared from (*E*)-9-(2-nitroprop-1-en-1-yl)anthracene (0.26 g, 1 mmol) and 1-benzyl-1*H*-pyrrole-2,5-dione (0.24 g, 1.3 mmol) according to general procedure 8.25.
Colourless solid 279 mg (62%)
Melting Point: 232-236 °C
IR$_{\nu max}$ (KBr): 3007, 2960 (C-H), 1692 (C=O), 1586 (C=C), 1631, 1431 (Ar C=C), 1520, 1399 (NO_2), 1457 (CH_2), 1362 (CH_3), 1175 (C-N) cm^{-1}
^{1}H NMR (400 MHz, DMSO-*d*$_6$) δ 1.80 (br. s., 3 H, CH3), 3.49 (d, *J* = 7.32 Hz, 1 H11), 4.13 (s, 2 H, CH2), 4.37 (d, *J* = 5.49 Hz, 1 H15), 4.88 (d, *J* = 3.05 Hz, 1 H, H10), 6.30 (d, *J* = 6.71 Hz, 2 H, H6' & H2'), 6.97 - 7.37 (m, 10 H, 10 x ArH), 7.55 (d, *J* = 6.71 Hz, 1 H, ArH), 8.33 (s, 1 H, H1')
^{13}C NMR (101 MHz, DMSO-*d*$_6$) ppm 17.3 (C3'), 41.3 (C10), 42.6 (C11), 44.4 (C15), 47.2 (C16), 50.0 (C9), 123.5, 124.7, 125.3, 126.2, 126.3, 126.8, 126.8, 127.1, 127.2, 127.4, 127.6, 128.2, 128.4, 131.5, 132.4, 135.0, 137.9, 138.3, 139.1, 141.2, 152.6 (C2'), 165.2, 165.8, 175.7 (C12), 175.8 (C14)
HRMS (APCI) calculated for $C_{28}H_{23}N_2O_4$ [M^++H] 451.1658: found 451.1671. Mass accuracy (2.88 ppm).

(*E*)-13-Benzyl-9-(2-nitrobut-1-en-1-yl)-9,10-dihydro-9,10-[3,4]epipyrroloanthracene-12,14-dione (313)

(*E*)-13-Benzyl-9-(2-nitrobut-1-en-1-yl)-9,10-dihydro-9,10-[3,4]epipyrroloanthracene-12,14-dione was prepared from (*E*)-9-(2-nitrobut-1-en-1-yl)anthracene (0.26 g, 1 mmol) and 1-benzyl-1*H*-pyrrole-2,5-dione (0.24 g, 1.3 mmol) according to general procedure 8.25.
Colourless solid 232 mg (50%)
Melting Point: 188-199 °C
IR$_{\nu max}$ (KBr): 3002, 2943 (C-H), 1695 (C=O), 1496, 1456 (C=C), 1518, 1339 (NO_2), 1400 (CH_2), 1362 (CH_3), 1175 (C-N) cm^{-1}
^{1}H NMR (400 MHz, DMSO-*d*$_6$) δ 0.98 (br. s., 3 H, CH3), 2.15 (br. s., 2 H, CH_2), 3.52 (br. s., 1 H, H11), 4.20 (d, *J* = 2.44 Hz, 2 H, CH_2 benzyl), 4.41 (d, *J* = 6.10 Hz, 1 H, H15), 4.93 (d, *J* = 3.05 Hz, 1 H, H10), 6.35 (s, 2 H, H2" & H6"), 7.07 - 7.32 (m, 10 H, 10 x ArH), 7.59 (d, *J* = 6.10 Hz, 1 H, ArH), 8.21 (s, 1 H, H1')
^{13}C NMR (101 MHz, DMSO-*d*$_6$) ppm 9.9 (C4'), 23.9 (C3') 41.3 (C10), 42.7 (C11), 44.4 (C15), 47.3 (C16), 49.9 (C9), 123.4, 124.7, 125.4, 126.2, 126.3, 126.8, 126.8, 127.2, 127.2,

127.6, 127.6, 128.2, 128.4, 131.5, 132.45 , 135.0, 139.4, 157.1 (C2'), 165.2, 165.7, 175.6 (C12 & C14)
HRMS (APCI) calculated for $C_{29}H_{27}N_2O_4$ [M^++H] 465.1814: found 465.1795. Mass accuracy (-4.1ppm).

(*E*)-9-(2-Nitroprop-1-en-1-yl)-13-(3,4,5-trimethoxybenzyl)-9,10-dihydro-9,10-[3,4]epipyrroloanthracene-12,14-dione (314)

(*E*)-9-(2-Nitroprop-1-en-1-yl)-13-(3,4,5-trimethoxybenzyl)-9,10-dihydro-9,10-[3,4]epipyrroloanthracene-12,14-dione was prepared from (*E*)-9-(2-nitroprop-1-en-1-yl)anthracene (0.26 g, 1 mmol) and 1-(3,4,5-trimethoxybenzyl)-1*H*-pyrrole-2,5-dione (0.36 g, 1.3 mmol) according to general procedure 8.25.
Yellow crystals 243 mg (45%)
Melting Point: 227-229 °C
IR$_{Vmax}$ (KBr): 2961, 2997 (C-H), 1697 (C=O), 1592 (C=C), 1462, 1426 (C=C), 1522, 1330 (NO_2), 1241, 1103 (C-O), 1126 (C-N) cm^{-1}
^{1}H NMR (400 MHz, DMSO-*d*$_6$) δ 3.21 - 3.29 (m, 1 H, H11), 3.45 (br. s., 1 H, H15), 3.60 (s, 3 H, p-OCH3), 3.66 (s, 6 H, 2 x OCH_3), 3.95 (s, 2 H, CH_2), 4.82 (d, *J* = 3.05 Hz, 1 H, H10), 6.18 (s, 2 H, H2" & H6"), 6.78 - 7.05 (m, 3 H, 3 x ArH), 7.10 - 7.32 (m, 4 H, 4 x ArH), 7.53 (d, *J* = 6.71 Hz, 1 H, ArH), 8.30 (s, 1 H, H1')
^{13}C NMR (101 MHz, DMSO-*d*$_6$) ppm 17.6 (C3'), 41.5 (C10), 44.6 (C11), 47.0 (C15), 50.2 (C9), 55.9 (2 x OCH_3), 59.8 (*p*-OCH_3), 106.1, 123.6, 124.6, 124.9, 126.3, 126.8, 127.1, 130.9, 138.9, 141.0, 152.4 (C2'), 175.6 (C12), 175.7 (C14)
HRMS (APCI) calculated for $C_{31}H_{29}N_2O_7$ [M^++H] 541.1975: found 541.1953. Mass accuracy (-4.1 ppm).

(*E*)-9-(2-Nitrobut-1-en-1-yl)-13-(3,4,5-trimethoxybenzyl)-9,10-dihydro-9,10-[3,4]epipyrroloanthracene-12,14-dione (315)

(*E*)-9-(2-Nitrobut-1-en-1-yl)-13-(3,4,5-trimethoxybenzyl)-9,10-dihydro-9,10-[3,4]epipyrroloanthracene-12,14-dione was prepared from (*E*)-9-(2-nitrobut-1-en-1-yl)anthracene (0.26 g, 1 mmol) and 1-(3,4,5-trimethoxybenzyl)-1*H*-pyrrole-2,5-dione (0.36 g, 1.3 mmol) according to general procedure 8.25.
Tan solid 299 mg (54%)
Melting Point: 224-229 °C
IR$_{Vmax}$ (KBr): 2940, 2836 (C-H), 1700 (C=O), 1593 (C=C), 1508, 1426 (C=C), 1521, 1340 (NO_2), 1460 (CH_2), 1401 (CH_3), 1127 (C-N) cm^{-1}
^{1}H NMR (400 MHz, DMSO-*d*$_6$) δ 0.93 (br. s., 3 H, CH_3), 2.09 (br. s., 2 H, CH_2), 3.23 - 3.27 (m, 1 H, H11), 3.47 (d, *J* = 7.32 Hz, 1 H, H15), 3.60 (s, 3 H, p-OCH_3), 3.67 (s, 6 H, 2 x OCH_3), 3.94 (s, 2 H, CH_2 benzyl), 4.84 (d, *J* = 3.05 Hz, 1 H, H10), 6.18 (s, 2 H, H2" & H6"), 6.93 (d, *J* = 6.10 Hz, 3 H, 3 x ArH), 7.12 - 7.30 (m, 4 H, 4 x ArH), 7.54 (d, *J* = 6.71 Hz, 1 H, ArH), 8.14 (s, 1 H, H1')
^{13}C NMR (101 MHz, DMSO-*d*$_6$) ppm 9.5 (C4'), 23.4 (C3'), 41.5 (C10), 44.6 (C11), 47.1 (C15), 50.0 (C9), 55.9 (OCH_3 x 2), 59.8 (*p*-OCH_3), 106.1 (CH), 123.4, 124.7, 124.9, 126.2, 127.0, 127.3, 130.9, 137.1, 139.1, 152.5 (C2'), 156.9 (C4"), 175.6 (C12 & C14)
HRMS (APCI) calculated for $C_{32}H_{30}N_2O_7$ [M^++H] 555.2131: found 555.2122. Mass accuracy (-1.62 ppm).

(*E*)-13-(3,4-Dimethoxyphenethyl)-9-(2-nitrovinyl)-9,10-dihydro-9,10-[3,4]epipyrroloanthracene-12,14-dione (316)

(*E*)-13-(3,4-Dimethoxyphenethyl)-9-(2-nitrovinyl)-9,10-dihydro-9,10-[3,4]epipyrroloanthracene-12,14-dionewas prepared from (*E*)-9-(2-nitrovinyl)anthracene (0.25 g, 1 mmol) and 1-(3,4-dimethoxyphenethyl)-1*H*-pyrrole-2,5-dione (0.34 g, 1.3 mmol) according to general procedure 8.25.
Colourless solid 393 mg (77%)
Melting Point: 152-156 °C
IR$_{Vmax}$ (KBr): 2941, 2837 (C-H), 1771 (C=O), 1698 (C=C), 1528 (NO), 1494, 1450 (C=C), 1155 (C-N) cm^{-1}
^{1}H NMR (400 MHz, DMSO-d_6) **δ** 1.62 - 1.81 (m, 2 H, CH_2), 3.00 - 3.19 (m, 2 H, CH_2), 3.40 (dd, *J* = 8.55, 3.05 Hz, 1 H, H11), 3.71 (s, 3 H, OCH_3), 3.69 (s, 3 H, OCH_3), 3.81 (d, *J* = 7.94 Hz, 1 H, H15), 4.91 (d, *J* = 3.05 Hz, 1 H, H10), 6.50 (d, *J* = 7.94 Hz, 1 H, H6"), 6.59 (s, 1 H, H2"), 6.80 (d, *J* = 8.55 Hz, 1 H, H5"), 7.21 - 7.39 (m, 7 H, 7 x ArH), 7.58 (d, *J* = 7.32 Hz, 1 H, 1 x ArH), 8.14 (d, *J* = 14.04 Hz, 1 H, H1'), 8.32 (d, *J* = 14.04 Hz, 1 H, H2')
^{13}C NMR (101 MHz, DMSO-d_6) ppm 21.0 (CH_2), 32.1 (CH_2-N), 44.6 (C10), 47.3 (C11), 47.5 (C15), 49.5 (C9), 55.4 (OCH_3), 55.5 (OCH_3), 111.9 (CH), 111.9 (CH), 120.1 (CH), 123.0 (CH), 123.4 (CH), 124.4 (CH), 125.3 (CH), 126.5 (CH), 126.8 (CH), 127.1 (CH), 127.2 (CH), 128.2 (CH), 128.9 (CH), 129.9, 137.4 (C2'), 138.3, 138.5, 141.1, 141.4, 145.2 (C1'), 147.5 (C3"), 148.7 (C4"), 175.2 (C12), 175.5 (C14)
HRMS (APCI) calculated for $C_{30}H_{27}N_2O_6$ [M^++H] 511.1869: found 511.1881. Mass accuracy (2.35 ppm).

(*E*)-9-(2-Nitrovinyl)-14-phenyl-9,10-dihydro-9,10-[1,2]epitriazoloanthracene-13,15-dione (317)

(*E*)-9-(2-Nitrovinyl)-14-phenyl-9,10-dihydro-9,10-[1,2]epitriazoloanthracene-13,15-dione acetate was prepared from (*E*)-9-(2-nitrovinyl)anthracene (0.25 g, 1 mmol) and 4-phenyl-3*H*-1,2,4-triazole-3,5(4*H*)-dione (1.3 mmol) according to general procedure 8.25.
Brown solid 289 mg (68%)
Melting Point: 168-169 °C
IR$_{Vmax}$ (ATR): 3048, 2998 (C-H), 1730 (C=O), 1625 (C=C), 1555, 1486 (C=C) cm^{-1}
^{1}H NMR (400 MHz, $CDCl_3$) **δ** 6.39 (s, 1 H, H10), 7.10 (d, *J* = 7.93 Hz, 2 H, 2 x ArH), 7.34 - 7.45 (m, 9 H, 9 x ArH), 7.58 (d, *J* = 6.71 Hz, 2 H, 2 x ArH), 7.70 (d, *J* = 14.04 Hz, 1 H, H1'), 8.46 (d, *J* = 14.04 Hz, 1 H, H2')
^{13}C NMR (101 MHz, DMSO-d_6) ppm 60.0 (C10), 67.1 (C9), 123.1 (CH), 124.5 (CH), 125.9 (CH), 128.3 (CH), 128.8 (CH), 129.0 (CH), 129.1 (CH), 130.4, 131.8 (C1'), 135.6, 136.3, 145.4 (C2'), 155.8 (C12 / C14), 156.4 (C12 /C14)
HRMS (APCI) calculated for $C_{24}H_{17}N_4O_4$ [M^++H] 425.1250: found 425.1251. Mass accuracy (0.23 ppm).

(*E*)-10-(2-Nitrovinyl)-9,10-dihydro-9,10-ethanoanthracene-11-carbonitrile (318)

(*E*)-10-(2-Nitrovinyl)-9,10-dihydro-9,10-ethanoanthracene-11-carbonitrile was prepared from (*E*)-9-(2-nitrovinyl)anthracene (0.25 g, 1 mmol) and acrylonitrile (3 mmol) according to general procedure 8.25.
Orange crystals 91 mg (30%)
Melting Point: 223-225 °C
IR*Vmax* (ATR): 3113, 3072, 2952 (C-H), 1658 (C=C), 1485, 1457 (C=C), 1526, 1354 (NO_2), 1190 (CN) cm^{-1}
^{1}H NMR (400 MHz, DMSO-*d*$_6$) δ 1.93 (dt, *J* = 12.82, 3.36 Hz, 1 H, H12a), 2.27 (ddd, *J* = 12.67, 10.53, 2.44 Hz, 1 H, H12b), 3.66 (dd, *J* = 10.68, 3.97 Hz, 1 H, H11), 4.60 (s, 1 H, C9), 7.11 - 7.31 (m, 5 H, 5 x ArH), 7.34 - 7.49 (m, 3 H, 3 x ArH), 8.04 (d, *J* = 13.43 Hz, 1 H, H1'), 8.33 (d, *J* = 14.04 Hz, 1 H, H2')
^{13}C NMR (101 MHz, DMSO-*d*$_6$) ppm 31.2 (C11), 34.0 (C12), 41.7 (C9), 48.9 (C10), 121.0, 123.1 (CH), 123.2 (CH), 123.8 (CH), 124.2 (CH), 126.1 (CH), 126.3 (CH), 127.3 (CH), 127.4 (CH), 138.1 (C1'), 138.7, 139.9, 142.1, 142.5, 144.0 (C2')
HRMS (APCI) calculated for $C_{19}H_{14}N_2O_2$ [M^+] 302.1055: found 302.1055. Mass accuracy (0 ppm).

Ethyl (*E*)-10-(2-nitrovinyl)-9,10-dihydro-9,10-ethanoanthracene-11-carboxylate (319)

Ethyl (*E*)-10-(2-nitrovinyl)-9,10-dihydro-9,10-ethanoanthracene-11-carboxylate was prepared from (*E*)-9-(2-nitrovinyl)anthracene (0.25 g, 1 mmol) and ethyl acrylate (1.3 mmol) according to general procedure 8.25. Purification by column chromatography (hexane: ethyl acetate 9:1).
Yellow oil 63 mg (18%)
IR*Vmax* (ATR): 3123, 2981 (C-H), 1731 (C=O), 1626 (C=C), 1486, 1443 (C=C), 1510, 1361 (NO_2), 1120 (CN) cm^{-1}
^{1}H NMR (400 MHz, $CDCl_3$) δ 1.12 (t, *J* = 7.32 Hz, 3 H, CH_3), 1.99 (d, *J* = 12.21 Hz, 1 H, H12a), 2.31 (t, *J* = 11.60 Hz, 1 H, H11), 3.01 (dd, *J* = 10.68, 4.58 Hz, 1 H, H12b), 4.00 (dd, *J* = 16.18, 7.63 Hz, 2 H, OCH_2), 4.43 (br. s., 1 H, H9), 7.11 - 7.26 (m, 5 H), 7.28 - 7.42 (m, 3 H), 7.49 (d, *J* = 14.04 Hz, 1 H, H1'), 8.35 (d, *J* = 14.04 Hz, 1 H, H2')
^{13}C NMR (101 MHz, $CDCl_3$) ppm 14.0 (C2", CH_3), 34.2 (C11), 43.7 (C9), 46.3 (C12), 49.3 (C10), 60.9 (C1", OCH_2), 122.2 (CH), 123.6 (CH), 123.6 (CH), 123.9 (CH), 126.0 (CH), 126.0 (CH), 126.8 (CH), 127.1 (CH), 139.0, 140.2 (C1'), 142.0, 142.5 (C2'), 142.8, 142.9, 172.7 (C=O)
HRMS (APCI) calculated for $C_{21}H_{20}NO_4$ [M^++H] 350.1392: found 350.1389. Mass accuracy (0.86 ppm).

Methyl (*E*)-10-(2-nitrovinyl)-9,10-dihydro-9,10-ethanoanthracene-11-carboxylate (320)

Methyl (*E*)-10-(2-nitrovinyl)-9,10-dihydro-9,10-ethanoanthracene-11-carboxylate was prepared from (*E*)-9-(2-nitrovinyl)anthracene (0.25 g, 1 mmol) and methyl acrylate (1.3 mmol) according to general procedure 8.25. Purification by column chromatography (hexane: ethyl acetate 9:1).
Gold oil 50 mg (15%)
IR*Vmax* (ATR): 3086, 2990 (C-H), 1730 (C=O), 1625 (C=C), 1466, 1444 (C=C), 1555, 1361 (NO_2), 1120 (CN) cm^{-1}

^{1}H NMR (400 MHz, $CDCl_3$) δ 1.97 (d, *J* = 12.21 Hz, 1 H, H12a), 2.33 (t, *J* = 11.29 Hz, 1 H, H11), 3.03 (dd, *J* = 10.07, 4.58 Hz, 1 H, H12b), 3.56 (s, 3 H, OCH_3), 4.43 (br. s., 1 H, H9), 7.05 - 7.30 (m, 6 H, 6 x ArH), 7.30 - 7.48 (m, 4 H, 4 x ArH & H1'), 8.34 (d, *J* = 14.65 Hz, 1 H, H2')
^{13}C NMR (101 MHz, $CDCl_3$) ppm 34.26 (C11), 43.68 (C9), 46.06 (C12), 49.24 (C10), 52.01 (OCH_3), 122.19 (CH), 123.58 (CH), 123.73 (CH), 123.92 (CH), 126.05 (CH), 126.81 (CH), 127.13 (CH), 139.01, 140.29 (CH), 141.98, 142.41 (C2'), 142.76, 142.86, 173.20 (C=O)
HRMS (APCI) calculated for $C_{20}H_{18}NO_4$ [M^++H] 336.1236: found 336.1233. Mass accuracy (-0.89 ppm).

(*E*)-11-Cyano-10-(2-nitrovinyl)-9,10-dihydro-9,10-ethanoanthracen-11-yl acetate (321)

(*E*)-11-Cyano-10-(2-nitrovinyl)-9,10-dihydro-9,10-ethanoanthracen-11-yl acetate was prepared from (*E*)-9-(2-nitrovinyl)anthracene (0.25 g, 1 mmol) and 1-cyanovinyl acetate (1.3 mmol) according to general procedure 8.25.
Purification by column chromatography (hexane: ethyl acetate 9:1)
Yellow solid 127 mg (35%)
Melting Point: 168-170 °C
IR$_{\nu max}$ (ATR): 3062, 2956 (C-H), 1753 (C=O), 1650 (C=C), 1484, 1422 (C=C), 1534, 1351 (NO_2), 1193 (CN) cm^{-1}
^{1}H NMR (400 MHz, $CDCl_3$) δ 2.08 (dd, *J* = 14.65, 2.44 Hz, 1 H, H12a), 2.94 (dd, *J* = 14.65, 3.05 Hz, 1 H, H12b), 4.40 (t, *J* = 2.75 Hz, 1 H, C9), 7.22 - 7.30 (m, 5 H, 5 x ArH), 7.33 - 7.41 (m, 3 H, 3 x ArH), 7.60 (d, *J* = 14.65 Hz, 1 H, H1'), 8.11 (d, *J* = 14.04 Hz, 1 H, H2')
^{13}C NMR (101 MHz, $CDCl_3$) ppm 20.7 (CH_3), 42.8 (C10), 45.2 (C12), 55.1 (C9), 74.8 (C11), 117.1 (CN), 123.8 (CH), 124.2 (CH), 124.8 (CH), 124.9 (CH), 126.8 (CH), 127.2 (CH), 128.1 (CH), 128.6 (CH), 134.9 (C1'), 135.9, 136.0, 141.8, 142.0, 144.5 (C2'), 168.5 (C=O)
HRMS (APCI) calculated for $C_{21}H_{17}N_2O_4$ [M^++H] 361.1188: found 361.1191. Mass accuracy (0.83 ppm).

Dimethyl (*E*)-9-(2-nitrovinyl)-9,10-dihydro-9,10-ethanoanthracene-11,12-dicarboxylate (322)

Dimethyl (*E*)-9-(2-nitrovinyl)-9,10-dihydro-9,10-ethanoanthracene-11,12-dicarboxylate was prepared from (*E*)-9-(2-nitrovinyl)-9,10-dihydro-9,10-[3,4]furanoanthracene-12,14-dione. (*E*)-9-(2-nitrovinyl)-9,10-dihydro-9,10-[3,4]furanoanthracene-12,14-dione (150 mg, 0.5 mmol) was refluxed in methanol (10 mL) and concentrated hydrochloric acid (2 drops) for 6 h. The reaction was cooled to room temperature and solvent was removed *in vacuo*, residue was taken up in dichloromethane, washed with 10% NaOH solution, water, brine and dried over anhydrous sodium sulphate. Solvent was removed *in vacuo*. Purification by column chromatography (hexane: ethyl acetate 9:1) and recrystallized from ethanol.
White solid 126 mg (32%)
Melting Point: 141-143 °C
IR$_{\nu max}$ (ATR): 3031, 2948 (C-H), 1746 (C=O), 1662 (C=C), 1467, 1422 (C=C), 1539, 1353 (NO_2), 1211 (CN) cm^{-1}
^{1}H NMR (400 MHz, $CDCl_3$) δ 3.30 (d, *J* = 10.99 Hz, 1 H, H11), 3.43 (d, *J* = 10.99 Hz, 1 H, H12), 3.46 - 3.50 (m, 3 H, OCH_3), 3.54 (s, 3 H, OCH_3), 4.71 (s, 1 H, H10), 7.05 - 7.31 (m, 6

H, 6 x ArH), 7.36 (d, *J* = 7.32 Hz, 1 H, 1 x ArH), 7.41 - 7.54 (m, 2 H, 1 x ArH & H1'), 8.24 (d, *J* = 14.04 Hz, 1 H, H2')

^{13}C NMR (101 MHz, $CDCl_3$) ppm 45.7 (C10), 49.2 (C11), 49.6 (C12), 49.7 (C9), 51.9 (OCH_3), 52.0 (OCH_3), 122.6 (CH), 123.3 (CH), 123.9 (CH), 126.0 (CH), 126.3 (CH), 126.5 (CH), 126.8 (CH), 127.4 (CH), 139.2 (C1'), 139.2, 139.6, 141.7, 142.3, 142.7 (C2'), 170.6 (C=O), 170.9 (C=O)

HRMS (APCI) calculated for $C_{22}H_{20}NO_6$ [M^++H] 394.1291: found 394.1285. Mass accuracy (-1.52 ppm).

Diethyl (*E*)-9-(2-nitrovinyl)-9,10-dihydro-9,10-ethanoanthracene-11,12-dicarboxylate (323)

Dimethyl (*E*)-9-(2-nitrovinyl)-9,10-dihydro-9,10-ethanoanthracene-11,12-dicarboxylate was prepared from (*E*)-9-(2-nitrovinyl)-9,10-dihydro-9,10-[3,4]furanoanthracene-12,14-dione. (*E*)-9-(2-nitrovinyl)-9,10-dihydro-9,10-[3,4]furanoanthracene-12,14-dione (150 mg, 0.5 mmol) was refluxed in ethanol (10 mL) and concentrated hydrochloric acid (2 drops) for 6 h. The reaction was cool to room temperature and solvent was removed *in vacuo*, residue was taken up in dichloromethane, washed with 10% NaOH solution, water, brine and dried over anhydrous sodium sulphate. The solvent was removed *in vacuo*. Purification was achieved by column chromatography (hexane: ethyl acetate 9:1) and recrystallized from ethanol.

White solid 64 mg (15%)

Melting Point: 151-152 °C

IR$_{Vmax}$ (ATR): 2980, 2928 (C-H), 1745 (C=O), 1655 (C=C), 1467, 1442 (C=C), 1522, 1347 (NO_2), 1175 (CN) cm^{-1}

^{1}H NMR (400 MHz, $CDCl_3$) δ 1.04 (t, *J* = 7.32 Hz, 3 H, CH_3), 1.14 (t, *J* = 7.02 Hz, 3 H, CH_3), 3.26 (d, *J* = 10.99 Hz, 1 H, H12), 3.43 (d, *J* = 10.99 Hz, 1 H, H11), 3.79 - 4.09 (m, 4 H, 2 x OCH_2), 4.71 (s, 1 H, H10), 7.04 - 7.30 (m, 6 H, 6 x ArH), 7.35 (d, *J* = 6.71 Hz, 1 H, 1 x ArH), 7.46 (d, *J* = 6.71 Hz, 1 H, 1 x ArH), 7.58 (d, *J* = 14.65 Hz, 1 H, H1'), 8.24 (d, *J* = 14.04 Hz, 1 H, H2')

^{13}C NMR (101 MHz, $CDCl_3$) ppm 13.7 (CH_3), 13.9 (CH_3), 45.6 (C10), 49.2 (C11), 49.8 (C12), 49.8 (C9), 60.9 (OCH_2), 61.0 (OCH_2), 122.6 (CH), 123.2 (CH), 123.8 (CH), 126.1 (CH), 126.2 (CH), 126.5 (CH), 126.7 (CH), 127.3 (CH), 129.8 , 139.1 (C1'), 139.5, 139.8, 141.7, 142.6, 142.9 (C2'), 169.9 (C=O), 170.6 (C=O)

HRMS (APCI) calculated for $C_{24}H_{24}NO_6$ [M^++H] 422.1604: found 422.1596. Mass accuracy (-1.90 ppm).

8.26 General procedure for preparation of Triptycene derivatives (324 – 327, 329)

Preparation of benzenediazonium-2-carboxylate

Anthranilic acid (5.4 g, 0.04 mmol) and trichloroacetic acid 0.06 g in tetrahydrofuran (60 mL) was placed in a 250 mL conical flask. The reaction mixture was stirred and cooled on an ice water bath. Isoamyl nitrite (10 mL) was added portionwise over 1 min. The mixture is allowed to warm to RT over 1.5 h. The mixture was then cooled again over ice and filtered using a plastic Buchner funnel. Subsequently the tan solid was washed with ice cold tetrahydrofuran until the washings were colourless. The yield of air dried benzenediazonium-2-carboxylate was

78 – 80 %. The benzenediazonium-2-carboxylate was washed with toluene and the tan solid was then stored in solution with toluene (60 mL).

Preparation of Triptycene derivatives

To a boiling solution of the appropriate anthracene derivative (4 mmol) in toluene (60 mL) was slowly added a slurry of benzenediazonium-2-carboxylate (prepared from 5.4 g (0.04 mmol) of anthranilic acid) in toluene over the course of 1 h. The mixture was heated to reflux for 1 h. After evaporation of the solvent, the residual oil was subjected to column chromatography (dichloromethane: hexane 1:1) to afford the product which was recrystallised from dichloromethane – hexane gave pure product which was isolated by filtration.

(*E*)-9-(2-Nitrovinyl)-9,10-dihydro-9,10-[1,2]benzenoanthracene (324)

(*E*)-9-(2Nitrovinyl)-9,10-dihydro-9,10-[1,2]benzenoanthracene was prepared from (*E*)-9-(2-nitrovinyl)anthracene (1 g, 4 mmol) and benzenediazonium-2-carboxylate (prepared from anthranilic acid (5.4 g, 0.04 mmol)) according to general procedure 8.26.
Colourless solid 260 mg (20%)
Melting Point: 258-260 °C (lit. M.p. 262-265 °C[378])
IR$_{\nu max}$ (ATR): 3111, 3069 (C-H), 1651 (C=C), 1457 (C=C), 1526, 1347 (NO_2) cm^{-1}
^{1}H NMR (400 MHz, $CDCl_3$) δ 5.53 (s, 1 H, C10), 7.05 - 7.16 (m, 6 H, 6 x ArH), 7.44 (d, J = 6.71 Hz, 3 H, 3 x ArH), 7.51 (d, J = 6.71 Hz, 3 H, 3 x ArH), 7.75 (d, J = 14.04 Hz, 1 H, H1'), 8.66 (d, J = 14.04 Hz, 1 H, H2')
^{13}C NMR (101 MHz, $CDCl_3$) ppm 54.1 (C10), 121.4 (CH), 124.2 (CH), 125.2 (CH), 126.0 (CH), 134.6 (C1'), 143.8, 145.2, 146.1 (C2')
HRMS (APCI) calculated for $C_{22}H_{16}NO_2$ [M^++H] 326.1181: found 326.1190. Mass accuracy (2.76 ppm).

(*E*)-9-(2-Nitroprop-1-en-1-yl)-9,10-dihydro-9,10-[1,2]benzenoanthracene (325)

(*E*)-9-(2-Nitroprop-1-en-1-yl)-9,10-dihydro-9,10-[1,2]benzenoanthracene was prepared from (*E*)-9-(2-nitroprop-1-en-1-yl)anthracene (1.05 g, 4 mmol) and benzenediazonium-2-carboxylate (prepared from anthranilic acid (5.4 g, 0.04 mmol)) according to general procedure 8.26.
Yellow solid 311 mg (23%)
Melting Point: 226-228 °C
IR$_{\nu max}$ (ATR): 3071, 3016, (C-H), 1594 (C=C), 1482, 1455 (C=C), 1526, 1328 (NO_2) cm^{-1}
^{1}H NMR (400 MHz, DMSO-d_6) δ 1.97 (s, 3 H, CH_3), 5.75 (s, 1 H, C10), 6.97 - 7.14 (m, 6 H, 6 x ArH), 7.42 (d, J = 6.71 Hz, 3 H, 3 x ArH), 7.50 - 7.58 (m, 3 H, 3 x ArH), 8.51 (s, 1 H, H1')
^{13}C NMR (101 MHz, DMSO-d_6) ppm 18.0 (C3'), 52.6 (C10), 54.0 (C9), 122.2 (CH), 124.3 (CH), 124.9 (CH), 125.7 (C1'), 126.8, 145.4, 154.3 (C2')
HRMS (APCI) calculated for $C_{23}H_{17}NO_2$ [M^+] 339.1259: found 339.1259. Mass accuracy (0 ppm).

(*E*)-9-(2-Nitrobut-1-en-1-yl)-9,10-dihydro-9,10-[1,2]benzenoanthracene

(*E*)-9-(2-Nitrobut-1-en-1-yl)-9,10-dihydro-9,10-[1,2]benzenoanthracene was prepared from (*E*)-9-(2-nitrobut-1-en-1-yl)anthracene (1.1 g, 4 mmol) and benzenediazonium-2-carboxylate (prepared from anthranilic acid (5.4 g, 0.04 mmol)) according to general procedure 8.26.
Colourless solid 453 mg (32%)
Melting Point: 210-211 °C
IR$_{Vmax}$ (ATR): 3071, 2952 (C-H), 1713 (C=O), 1594 (C=C), 1481, 1459 (C=C), 1527, 1349 (NO_2) cm^{-1}
^{1}H NMR (400 MHz, DMSO-*d*$_6$) δ 1.00 (t, *J* = 7.32 Hz, 3 H, CH_3), 2.25 (q, *J* = 7.12 Hz, 2 H, CH_2), 5.72 (s, 1 H, C10), 6.99 - 7.10 (m, 6 H, 6 x ArH), 7.30 - 7.40 (m, 3 H, 3 x ArH), 7.46 - 7.53 (m, 3 H, 3 x ArH), 8.28 (s, 1 H, H1')
^{13}C NMR (101 MHz, DMSO-*d*$_6$) ppm 9.4 (C4'), 24.1 (C3'), 49.7 (C9), 52.5 (C10), 122.0 (CH), 124.3 (CH), 124.8 (CH), 125.8 (CH), 126.1 (C1'), 142.8, 145.2, 158.9 (C2')
HRMS (APCI) calculated for $C_{24}H_{20}NO_2$ [M^++H] 354.1494: found 354.1490. Mass accuracy (-1.13 ppm).

(*E*)-9-Chloro-10-(2-nitrovinyl)-9,10-dihydro-9,10-[1,2]benzenoanthracene (327)

(*E*)-9-Chloro-10-(2-nitrovinyl)-9,10-dihydro-9,10-[1,2]benzenoanthracene was prepared from (*E*)-9-chloro-10-(2-nitrovinyl)anthracene (1.13 g, 4 mmol) and benzenediazonium-2-carboxylate (prepared from anthranilic acid (5.4 g, 0.04 mmol)) according to general procedure 8.26.
Colourless solid 430 mg (30%)
Melting Point: 259-261 °C
IR$_{Vmax}$ (ATR): 3070, 2953 (C-H), 1713 (C=O), 1648 (C=C), 1481, 1481 (C=C), 1540, 1350 (NO_2) cm^{-1}
^{1}H NMR (400 MHz, DMSO-*d*$_6$) δ 7.15 - 7.29 (m, 6 H, 6 x ArH), 7.58 - 7.69 (m, 3 H, 3 x ArH), 7.72 - 7.82 (m, 3 H, 3 x ArH), 8.12 (d, *J* = 14.04 Hz, 1 H, H1'), 8.50 (d, *J* = 14.65 Hz, 1 H, H2')
^{13}C NMR (101 MHz, DMSO-*d*$_6$) ppm 52.9 (C10), 74.6 (C9), 121.4 (CH), 122.1 (CH), 126.2 (CH), 126.5 (CH), 128.9, 131.7 (C1'), 142.5, 143.4, 148.0 (C2')
HRMS (APCI) calculated for $C_{22}H_{14}NO_2Cl^{35}$ [M^+] 359.0713: found 359.0712. Mass accuracy (-0.28 ppm).

9-(2-Nitroethyl)-9,10-dihydro-9,10-[1,2]benzenoanthracene (328)

To a solution of (*E*)-9-(2-nitrovinyl)-9,10-dihydro-9,10-[1,2]benzenoanthracene (100mg, 0.3 mmol) in dichloromethane (10 mL) and isopropanol (2 mL) was added sodium borohydride (60 mg, 1.6 mmol). The reaction mixture was stirred at room temperature for 24 hours and neutralised using 1 M HCl. The solution was extracted with dichloromethane, dried with sodium sulphate and solvent removed *in vacuo*
Colourless solid 79 mg (80%)
Melting Point: 185-187 °C
IR$_{Vmax}$ (ATR): 3069, 2951 (C-H), 1594 (C=C), 1482, 1450 (C=C), 1523, 1349 (NO_2) cm^{-1}
^{1}H NMR (400 MHz, CDCl$_3$) δ 3.75 - 3.84 (m, 2 H, CH_2), 5.25 - 5.36 (m, 2 H, CH_2), 5.44 (s, 1 H, H10), 7.02 - 7.13 (m, 6 H, 6 x ArH), 7.35 (d, *J* = 7.32 Hz, 3 H, 3 x ArH), 7.46 (d, *J* = 6.71 Hz, 3 H, 3 x ArH)

^{13}C NMR (101 MHz, $CDCl_3$) ppm 25.7 (C1'), 52.3 (C9), 54.3 (C10), 72.8 (C2'), 121.2, 124.0, 125.2, 125.5, 146.5
HRMS (APCI) calculated for $C_{22}H_{17}NO_2$ [M^+] 327.1259: found 327.1255. Mass accuracy (-1.22 ppm).

9,10-[1,2]Benzenoanthracene-9(10*H*)-carbaldehyde (329)

9,10-[1,2]Benzenoanthracene-9(10*H*)-carbaldehyde was prepared from 9-anthraldehyde (1.1 g, 5 mmol) and benzenediazonium-2-carboxylate (prepared from anthranilic acid (5.4 g, 0.04 mmol)) according to general procedure 8.26.
Colourless solid 296 mg (21%)
Melting Point: 242-244 °C (lit. M.p. 243-257 °C[541])
IR$_{\nu max}$ (ATR): 3020, 2833 (C-H), 1728 (C=O), 1579 (C=C), 1451 (C=C) cm^{-1}
^{1}H NMR (400 MHz, $CDCl_3$) δ 5.42 (s, 1 H, C10), 7.00 - 7.13 (m, 6 H, 6 x ArH), 7.37 - 7.52 (m, 3 H, 3 x ArH), 7.60 - 7.69 (m, 3 H, 3 x ArH), 11.24 (s, 1 H, CHO)
^{13}C NMR (101 MHz, $CDCl_3$) ppm 54.2 (C10), 60.8 (C9), 122.4 (CH), 124.0 (CH), 125.2 (CH), 125.8 (CH), 142.6, 145.8, 201.0 (CHO)
HRMS (APCI) calculated for $C_2H_{14}O$ [M^+] 282.1045: found 282.1040. Mass accuracy (-1.77 ppm).

9,10-[1,2]Benzenoanthracen-9(10*H*)-ylmethanol (330)

To a solution of 9,10-[1,2]benzenoanthracene-9(10*H*)-carbaldehyde (100mg, 0.35 mmol) in dichloromethane (10 mL) and isopropanol (2 mL) was added sodium borohydride (60 mg, 1.6 mmol). The reaction mixture was stirred at room temperature for 24 h and neutralised using 1 M HCl. The solution was extracted with dichloromethane, dried with sodium sulphate and solvent removed *in vacuo*
Colourless solid 91 mg (85%)
Melting Point: 240-242 °C (lit. M.p. 242-243 °C[542])
IR$_{\nu max}$ (ATR): 3369 (O-H), 3051, 2981 (C-H), 1712 (C=O), 1609 (C=C), 1455 (C=C) cm^{-1}
^{1}H NMR (400 MHz, $CDCl_3$) δ 2.21 (br. s., 1 H, OH), 5.26 (br. s., 2 H, CH_2), 5.42 (s, 1 H, C10), 6.98 - 7.10 (m, 6 H, 6 x ArH), 7.42 (d, J = 6.71 Hz, 4 H, 4 x ArH), 7.50 (br. s., 2 H, 2 x ArH)
^{13}C NMR (101 MHz, $CDCl_3$) ppm 54.3 (C10), 54.4 (C9), 61.1 (CH_2), 122.0 (CH), 123.6 (CH), 125.1 (CH), 125.2 (CH), 144.4, 146.8
HRMS (ESI) calculated for $C_{21}H_{16}ONa$ [M^++Na] 307.1099: found 307.1097. Mass accuracy (-0.65 ppm).

9,10-Dihydro-9,10-[3,4]furanoanthracene-12,14-dione (331)

9,10-Dihydro-9,10-[3,4]furanoanthracene-12,14-dione was prepared from anthracene (0.18 g, 1 mmol) and maleic anhydride (0.13 g, 1.3 mmol) according to general procedure 8.25.
Colourless solid 249 mg (90%)
Melting Point: 264-266 °C (lit. M.p. 267-268 °C[543])
IR$_{\nu max}$ (ATR): 3065 (C-H), 1711 (C=O), 1610 (C=C), 1497, 1455 (C=C) cm^{-1}
^{1}H NMR (400 MHz, DMSO-d_6) δ 3.66 (s, 2 H, H9 & H10), 4.88 (s, 2 H, H11 & H15), 7.08 - 7.27 (m, 4 H, 4 x ArH), 7.29 - 7.40 (m, 2 H, 2 x ArH), 7.40 - 7.55 (m, 2 H, 2 x ArH)

^{13}C NMR (101 MHz, DMSO-d_6) ppm 44.3 (C9 & C10), 47.9 (C11 & C15), 124.4 (CH), 124.8 (CH), 126.5 (CH), 127.0 (CH), 139.1, 141.1, 171.5 (C12 & C14)
HRMS (APCI) calculated for $C_{18}H_{13}O_3$ [M^++H] 277.0865: found 277.0858. Mass accuracy (-2.52 ppm).

9,10-Dihydro-9,10-[3,4]epipyrroloanthracene-12,14-dione (332)

9,10-Dihydro-9,10-[3,4]epipyrroloanthracene-12,14-dione was prepared from anthracene (0.18 g, 1 mmol) and maleimide (0.13 g, 1.3 mmol) according to general procedure 8.25.
Colourless solid 234 mg (85%)
Melting Point: 299-300 °C (lit. M.p. 300-301 °C[544])
IR$_{Vmax}$ (ATR): 3347 (O-H), 3065, 2935 (C-H), 1712 (C=O), 1456, 1439 (C=C) cm^{-1}
^{1}H NMR (400 MHz, DMSO-d_6) δ 3.20 (s, 2 H, H9 & H10), 4.73 (s, 2 H, H11 & H15), 7.08 - 7.21 (m, 4 H, 4 x ArH), 7.21 - 7.32 (m, 2 H, 2 x ArH), 7.37 - 7.51 (m, 2 H, 2 x ArH), 10.77 (br. s., 1 H, NH)
^{13}C NMR (101 MHz, DMSO-d_6) ppm 44.4 (C9 & C10), 47.6 (C11 & C15), 124.1 (CH), 124.7 (CH), 126.1 (CH), 126.4 (CH), 139.5, 142.0, 178.0 (C12 & C14)
HRMS (APCI) calculated for $C_{18}H_{14}NO_2$ [M^++H] 276.1025: found 276.1012. Mass accuracy (-4.71 ppm).

9,10-Dihydro-9,10-[3,4]epipyrroloanthracene-12,14-dione (333)

9,10-Dihydro-9,10-[3,4]epipyrroloanthracene-12,14-dione was prepared from anthracene (0.18 g, 1 mmol) and phenylmaleimide (0.224 g, 1.3 mmol) according to general procedure 8.25.
Colourless solid 316 mg (90%)
Melting Point: 227-229 °C (lit. M.p. 228-230 °C[545])
IR$_{Vmax}$ (ATR): 3059, 3001 (C-H), 1710 (C=O), 1596 (C=C), 1497, 1445 (C=C) cm^{-1}
^{1}H NMR (400 MHz, DMSO-d_6) δ 3.41 (s, 2 H, H9 & H10), 4.86 (s, 2 H, H11 & H15), 6.32 - 6.49 (m, 2 H, 2 x ArH), 7.11 - 7.26 (m, 5 H, 5 x ArH), 7.26 - 7.37 (m, 4 H, 4 x ArH), 7.51 (dd, J = 5.19, 3.36 Hz, 2 H, 2 x ArH)
^{13}C NMR (101 MHz, DMSO-d_6) ppm 44.8 (C9 & C10), 46.6 (C11 & C15), 124.3, 124.8, 125.3, 126.3, 126.5, 126.6, 128.2, 128.4, 128.8, 128.9, 131.8, 139.3, 141.6, 175.9 (C12 & C14)
HRMS (APCI) calculated for $C_{24}H_{18}NO_2$ [M^++H] 352.1338: found 352.1341. Mass accuracy (0.85 ppm).

12,14-Dioxo-9,10-[3,4]furanoanthracene-9(10*H*)-carbaldehyde (334)

To a solution of 9-anthraldehyde (1.03 g, 5 mmol) in xylene (10 mL) was added maleic anhydride (0.5 g, 5 mmol). The reaction mixture was heated to reflux for 1 h. The reaction was cooled to room temperature, filtered and the precipitate was washed with toluene and hexane. The solid was allow to dry at room temperature and was recrystallized from toluene.
Colourless solid 610 mg (40%)
Melting Point: 235-237 (lit. M.p. 238-239 °C[524])
IR$_{Vmax}$ (ATR): 2980, 2883 (C-H), 1745 (C=O), 1654 (C=C), 1517, 1466 (C=C) cm^{-1}
^{1}H NMR (400 MHz, DMSO-d_6) δ 3.80 (dd, J = 9.16, 3.05 Hz, 1 H, H10), 4.32 (d, J = 9.16 Hz, 1 H, H11), 4.95 (d, J = 3.66 Hz, 1 H, H15), 7.10 - 7.34 (m, 5 H, 5 x ArH), 7.38 - 7.48 (m,

1 H, 1 x ArH), 7.58 (dd, *J* = 7.32, 1.22 Hz, 1 H, 1 x ArH), 7.65 - 7.76 (m, 1 H, 1 x ArH), 10.84 (s, 1 H, CHO)

^{13}C NMR (101 MHz, DMSO-*d*$_6$) ppm 44.6 (C10), 48.4 (C11), 48.7 (C15), 57.0 (C9), 122.8 (CH), 123.4 (CH), 125.1 (CH), 125.5 (CH), 126.5 (CH), 127.2 (CH), 127.4 (CH), 127.6 (CH), 136.9, 138.8, 138.8, 141.0, 170.9 (C=O x 2), 201.6 (C=O)

HRMS (APCI) calculated for $C_{19}H_{13}O_4$ [M^++H] 305.0814: found 305.0812. Mass accuracy (-0.66 ppm).

12,14-Dioxo-9,10-[3,4]epipyrroloanthracene-9(10*H*)-carbaldehyde (335)

To a solution of 9-anthraldehyde (1.03 g, 5 mmol) in xylene (10 mL) was added maleimide (0.5 g, 5 mmol). The reaction mixture was heated to reflux for 1 h. The reaction was cooled to room temperature, filtered and the precipitate was washed with toluene and hexane. The solid was allow to dry at room temperature and was recrystallized from toluene.

Colourless solid 532 mg (35%)

Melting Point: 280-283 °C (lit. M.p. 286-287 °C[544])

IR$_{\nu max}$ (ATR): 3674 (N-H), 2980, 2892 (C-H), 1732 (C=O), 1583 (C=C), 1468, 1440 (C=C) cm^{-1}

^{1}H NMR (400 MHz, DMSO-*d*$_6$) δ 3.37 (d, *J* = 3.66 Hz, 1 H, H10), 3.91 (d, *J* = 8.55 Hz, 1 H, H11), 4.79 (d, *J* = 3.66 Hz, 1 H, H15), 7.06 - 7.30 (m, 5 H, 5 x ArH), 7.30 - 7.40 (m, 1 H, 1 x ArH), 7.55 (d, *J* = 7.32 Hz, 1 H, 1 x ArH), 7.62 - 7.83 (m, 1 H, 1 x ArH), 10.78 (s, 1 H, NH), 10.97 (br. s., 1 H, CHO)

^{13}C NMR (101 MHz, DMSO-*d*$_6$) ppm 45.0 (C10), 48.2 (C11), 49.5 (C15), 55.4 (C9), 122.8 (CH), 124.2 (CH), 124.8 (CH), 125.2 (CH), 126.3 (CH), 126.3 (CH), 126.6 (CH), 126.9 (CH), 135.3 (CH), 137.5, 138.9, 140.7, 141.8, 171.1 (C=O), 172.8 (C=O), 177.1 (CHO)

HRMS (APCI) calculated for $C_{19}H_{14}NO_3$ [M^++H] 304.0974: found 304.0971. Mass accuracy (-0.99 ppm).

12,14-Dioxo-13-phenyl-9,10-[3,4]epipyrroloanthracene-9(10*H*)-carbaldehyde (336)

To a solution of 9-anthraldehyde (1.03 g, 5 mmol) in xylene (10 mL) was added phenylmaleimide (0.865 g, 5 mmol). The reaction mixture was heated to reflux for 1 h. The reaction was cooled to room temperature, filtered and the precipitate was washed with toluene and hexane. The solid was allow to dry at room temperature and was recrystallized from toluene.

Colourless solid 1.18 g (62%)

Melting Point: 225-226 °C[546]

IR ν_{max} (ATR): 2970, 2884 (C-H), 1724 (C=O), 1596 (C=C), 1481, 1457 (C=C) cm^{-1}

^{1}H NMR (400 MHz, DMSO-*d*$_6$) δ 3.57 (dd, *J* = 8.55, 3.66 Hz, 1 H, H10), 4.12 (d, *J* = 8.55 Hz, 1 H, H11), 4.93 (d, *J* = 3.05 Hz, 1 H, H15), 6.35 - 6.48 (m, 2 H, 2 x ArH), 7.13 - 7.43 (m, 9 H, 9 x ArH), 7.62 (d, *J* = 6.71 Hz, 1 H, 1 x ArH), 7.69 - 7.79 (m, 1 H, 1 x ArH), 10.83 (s, 1 H, CHO)

^{13}C NMR (101 MHz, DMSO-*d*$_6$) ppm 45.1 (C10), 47.1 (C11), 47.8 (C15), 57.2 (C9), 122.8 (CH), 123.5 (CH), 125.0 (CH), 125.3 (CH), 126.4 (CH), 126.4 (CH), 126.7 (CH), 127.1 (CH), 127.2 (cH), 128.6 (CH), 128.9 (CH), 131.5 (CH), 137.0, 139.1, 139.2, 141.5, 175.4 (C=O), 175.5 (C=O), 202.0 (CHO)

HRMS (APCI) calculated for $C_{25}H_{18}NO_3$ [M^++H] 380.1287: found 380.1282. Mass accuracy (-1.32 ppm).

12,14-Dioxo-9,10-[3,4]furanoanthracene-9(10*H*)-carboxylic acid (337)

To a solution of anthracene-9-carboxylic acid (1.1 g, 5 mmol) in xylene (10 mL) was added maleic anhydride (0.5 g, 5 mmol). The reaction mixture was heated to reflux for 1 h. The reaction was cooled to room temperature, filtered and the precipitate was washed with toluene and hexane. The solid was allow to dry at room temperature and was recrystallized from toluene.
Colourless solid 1.30 g (81%)
Melting Point: 265-267 °C (lit. M.p. 268 °C[547]
IR$_{Vmax}$ (ATR): 2980, 2884 (C-H), 1746 (C=O), 1656 (C=C), 1583, 1469 (C=C) cm^{-1}
^{1}H NMR (400 MHz, DMSO-d_6) δ 3.70 (dd, *J* = 9.16, 3.05 Hz, 1 H, H10), 4.16 (d, *J* = 9.77 Hz, 1 H, H11), 4.91 (d, *J* = 3.05 Hz, 1 H, H15), 7.15 - 7.32 (m, 5 H, 5 x ArH), 7.34 - 7.40 (m, 1 H, 1 x ArH), 7.52 - 7.59 (m, 1 H, 1 x ArH), 7.88 - 7.98 (m, 1 H, 1 x ArH), 14.14 (br. s., 1 H, COOH)
^{13}C NMR (101 MHz, DMSO-d_6) ppm 44.8 (C10), 48.4 (C11), 50.1 (C15), 55.8 (C9), 122.8 (CH), 124.6 (CH), 125.0 (CH), 125.0 (CH), 126.8 (CH), 127.0 (CH), 127.3 (CH), 137.2, 138.4, 139.7, 140.7, 170.3 (C=O), 170.3 (C=O), 171.1 (C=O)
HRMS (APCI) calculated for $C_{19}H_{13}O_5$ [M^++H] 321.0763: found 321.0760. Mass accuracy (-0.93 ppm).

12,14-Dioxo-9,10-[3,4]epipyrroloanthracene-9(10*H*)-carboxylic acid (338)

To a solution of anthracene-9-carboxylic acid (1.1 g, 5 mmol) in xylene (10 mL) was added maleimide (0.5 g, 5 mmol). The reaction mixture was heated to reflux for 1 h. The reaction was cooled to room temperature, filtered and the precipitate was washed with toluene and hexane. The solid was allow to dry at room temperature and was recrystallized from toluene.
Colourless solid 656 mg (41%)
Melting Point: 298-299 °C [548]
IR$_{Vmax}$ (ATR): 3327 (N-H), 2970, 2931 (C-H), 1719 (C=O), 1583 (C=C), 1482, 1459 (C=C) cm^{-1}
^{1}H NMR (400 MHz, DMSO-d_6) δ 3.23 (dd, *J* = 8.55, 3.05 Hz, 1 H, H10), 3.78 (d, *J* = 8.55 Hz, 1 H, H11), 4.71 (d, *J* = 3.05 Hz, 1 H, H15), 7.04 - 7.30 (m, 6 H, 6 x ArH), 7.31 - 7.60 (m, 1 H, 1 x ArH), 7.87 - 8.06 (m, 1 H, 1 x ArH), 10.78 (s, 1 H, NH), 13.69 (br. s., 1 H, COOH)
^{13}C NMR (101 MHz, DMSO-d_6) ppm 45.0 (C10), 48.2 (C11), 49.5 (C5), 55.4 (C9), 122.8 (CH), 124.2 (CH), 124.8 (CH), 125.2 (CH), 126.3 (CH), 126.3 (CH), 126.6 (CH), 126.9 (CH), 135.3 (CH), 137.5, 139.0, 140.7, 141.7, 171.1 (C=O), 172.7 (C=O), 177.1 (COOH)
HRMS (APCI) calculated for $C_{19}H_{14}NO_4$ [M^++H] 320.0923: found 320.0921. Mass accuracy (-0.62 ppm).

12,14-dioxo-13-phenyl-9,10-[3,4]epipyrroloanthracene-9(10H)-carboxylic acid

To a solution of anthracene-9-carboxylic acid 1.1 g (5 mmol) in 10 mL of xylene was added phenyl maleimide 0.865 g (5 mmol). The reaction mixture was heated to reflux for 1 hour. The reaction was cooled to room temperature, filtered and the precipitate was washed with toluene

and hexane. The solid was allow to dry at room temperature and was recrystallized from toluene.
Colourless solid (43%)
Melting Point: 290-292 °C [548]
IR ν_{max} (ATR): 3292 (O-H), 2980, 2891 (C-H), 1743 (C=O), 1583 (C=C), 1483, 1465 (C=C) cm^{-1}
^{1}H NMR (400 MHz, DMSO-d_6) δ ppm 3.48 (dd, *J* = 8.55, 3.05 Hz, 1 H, H10), 4.00 (d, *J* = 8.55 Hz, 1 H, H11), 4.89 (d, *J* = 3.05 Hz, 1 H, H15), 6.44 (dd, *J* = 7.63, 1.53 Hz, 2 H, 2 x ArH), 7.16 - 7.41 (m, 9 H, 9 x ArH), 7.58 (dd, *J* = 5.49, 3.05 Hz, 1 H, 1 x ArH), 7.95 - 8.06 (m, 1 H, 1 x ArH), 13.89 (br. s., 1 H, COOH)
^{13}C NMR (101 MHz, DMSO-d_6) δ ppm 45.4 (C10), 47.2 (C11), 48.7 (C15), 55.9 (C9), 122.9 (CH), 124.4 (CH), 124.8 (CH), 125.3 (CH), 126.5 (CH), 126.5 (CH), 126.6 (CH), 126.8 (CH), 127.1 (CH), 128.5 (CH), 128.8 (CH), 131.7, 137.4, 138.9, 140.2, 141.3, 171.0 (C=O), 175.0 (C=O), 175.5 (C=O)
HRMS (APCI) calculated for $C_{25}H_{18}NO_4$ [M+H] 396.1236: found 396.1230. Mass accuracy (-1.51 ppm).

12,14-Dioxo-13-phenyl-9,10-[3,4]epipyrroloanthracene-9(10H)-carboxylic acid (339)

To a solution of anthracene-9-carboxylic acid (1.1 g, 5 mmol) in xylene (10 mL) was added phenyl maleimide (0.865 g, 5 mmol). The reaction mixture was heated to reflux for 1 h. The reaction was cooled to room temperature, filtered and the precipitate was washed with toluene and hexane. The solid was allow to dry at room temperature and was recrystallized from toluene.
Colourless solid 851 mg (43%)
Melting Point: 290-292 °C[548]
IR$_{Vmax}$ (ATR): 3292 (O-H), 2980, 2891 (C-H), 1743 (C=O), 1583 (C=C), 1483, 1465 (C=C) cm^{-1}
^{1}H NMR (400 MHz, DMSO-d_6) δ 3.48 (dd, *J* = 8.55, 3.05 Hz, 1 H, H10), 4.00 (d, *J* = 8.55 Hz, 1 H, H11), 4.89 (d, *J* = 3.05 Hz, 1 H, H15), 6.44 (dd, *J* = 7.63, 1.53 Hz, 2 H, 2 x ArH), 7.16 - 7.41 (m, 9 H, 9 x ArH), 7.58 (dd, *J* = 5.49, 3.05 Hz, 1 H, 1 x ArH), 7.95 - 8.06 (m, 1 H, 1 x ArH), 13.89 (br. s., 1 H, COOH)
^{13}C NMR (101 MHz, DMSO-d_6) ppm 45.4 (C10), 47.2 (C11), 48.7 (C15), 55.9 (C9), 122.9 (CH), 124.4 (CH), 124.8 (CH), 125.3 (CH), 126.5 (CH), 126.5 (CH), 126.6 (CH), 126.8 (CH), 127.1 (CH), 128.5 (CH), 128.8 (CH), 131.7, 137.4, 138.9, 140.2, 141.3, 171.0 (C=O), 175.0 (C=O), 175.5 (C=O)
HRMS (APCI) calculated for $C_{25}H_{18}NO_4$ [M^++H] 396.1236: found 396.1230. Mass accuracy (-1.51 ppm).

9-Hydroxy-9,10-dihydro-9,10-[3,4]furanoanthracene-12,14-dione (340)

To a solution of anthrone (0.97 g, 5 mmol) in xylene (10 mL) was added maleic anhydride (0.5 g, 5 mmol). The reaction mixture was heated to reflux for 1 h. The reaction was cooled to room temperature, filtered and the precipitate was washed with toluene and hexane. The solid was allow to dry at room temperature and was recrystallized from toluene.
Colourless solid 805 mg (55%)

Melting Point: 215-218 °C (lit. M.p. 218-219 °C[549])
IR$_{\nu max}$ (ATR): 3481 (O-H), 2970, 2883 (C-H), 1767 (C=O), 1660 (C=C), 1479, 1458 (C=C) cm^{-1}
^{1}H NMR (400 MHz, DMSO-d_6) δ 3.50 (d, *J* = 9.16 Hz, 1 H, H11), 3.74 (dd, *J* = 9.16, 3.66 Hz, 1 H, H10), 4.82 (d, *J* = 3.05 Hz, 1 H, H15), 7.14 - 7.29 (m, 4 H, 4 x ArH), 7.33 (d, *J* = 6.71 Hz, 1 H, 1 x ArH), 7.46 (d, *J* = 7.32 Hz, 1 H, 1 x ArH), 7.55 (t, *J* = 6.41 Hz, 2 H, 2 x ArH)
^{13}C NMR (101 MHz, DMSO-d_6) ppm 43.3 (C11), 49.2 (C10), 52.2 (C15), 76.1 (C9), 120.9 (CH), 121.2 (CH), 123.9 (CH), 124.4 (CH), 126.3 (CH), 126.5 (CH), 126.9 (CH), 126.9 (CH), 137.2, 139.5, 140.9, 144.2, 168.8 (C=O), 171.4 (C=O)
HRMS (APCI) calculated for $C_{18}H_{13}O_4$ [M^++H] 293.0814: found 293.0814. Mass accuracy (0 ppm).

9-Hydroxy-9,10-dihydro-9,10-[3,4]epipyrroloanthracene-12,14-dione (341)

To a solution of anthrone (0.97 g, 5 mmol) in xylene (10 mL) was added maleimide (0.5 g, 5 mmol). The reaction mixture was heated to reflux for 1 h. The reaction was cooled to room temperature, filtered and the precipitate was washed with toluene and hexane. The solid was allow to dry at room temperature and was recrystallized from toluene.
Colourless solid 846 mg (58%)
Melting Point: 253-255 °C
IR$_{\nu max}$ (ATR): 3474 (O-H), 3125, 2981 (C-H), 1752 (C=O), 1665 (C=C), 1571, 1478 (C=C) cm^{-1}
^{1}H NMR (400 MHz, DMSO-d_6) δ 3.12 (d, *J* = 8.55 Hz, 1 H, H11), 3.32 (dd, *J* = 8.24, 2.75 Hz, 1 H, H10), 4.60 - 4.79 (m, 1 H, H15), 6.64 (s, 1 H, 1 x ArH), 7.13 - 7.29 (m, 4 H, 4 x ArH), 7.44 (d, *J* = 7.32 Hz, 1 H, 1 x ArH), 7.56 (t, *J* = 6.71 Hz, 2 H, 2 x ArH), 10.76 (br. s., 1 H, NH)
^{13}C NMR (101 MHz, DMSO-d_6) ppm 43.5 (C11), 49.0 (C10), 51.5 (C15), 76.6 (C9), 120.7 (CH), 121.2 (CH), 123.5 (CH), 124.3 (CH), 126.0 (CH), 126.2 (CH), 126.3 (CH), 126.4 (CH), 137.6, 140.2, 141.5, 145.1, 176.5 (C=O), 177.7 (C=O)
HRMS (APCI) calculated for $C_{18}H_{14}NO_3$ [M^++H] 292.0974: found 292.0974. Mass accuracy (0 ppm).

(*E*)-3-(12,14-Dioxo-9,10-[3,4]furanoanthracen-9(10*H*)-yl)acrylonitrile (342)

(*E*)-3-(12,14-Dioxo-9,10-[3,4]furanoanthracen-9(10*H*)-yl)acrylonitrile was prepared from (*E*)-3-(anthracen-9-yl)acrylonitrile (0.23 g, 1 mmol) and maleic anhydride (0.13 g, 1.3 mmol) according to general procedure 8.25.
Colourless solid 241 mg (74%)
Melting Point: 215-219 °C
IR$_{\nu max}$ (KBr): 3054, 2965 (C-H), 2218 (CN), 1863, 1700 (C=O), 1626 (C=C), 1458, 1436, 1403 (C=C), 1235 (C-O) cm^{-1}
^{1}H NMR (400 MHz, DMSO-d_6) δ 3.77 (dd, *J* = 8.85, 3.36 Hz, 1 H, H11), 4.06 (d, *J* = 8.55 Hz, 1 H, H15), 4.94 (d, *J* = 3.05 Hz, 1 H, H10), 6.54 (d, *J* = 17.09 Hz, 1 H, H2'), 7.15 - 7.32 (m, 5 H, 5 x ArH), 7.33 - 7.47 (m, 2 H, 2 x ArH), 7.55 (d, *J* = 6.10 Hz, 1 H, 1 x ArH), 7.95 (d, *J* = 17.09 Hz, 1 H, H1')

^{13}C NMR (101 MHz, DMSO-d_6) ppm 44.3 (C10), 48.8 (C11), 49.6 (C9), 51.6 (C15), 106.6 (CH), 117.6 (CN), 123.1 (CH), 123.5 (CH), 124.6 (CH), 125.3 (CH), 126.6 (CH), 127.2 (CH), 127.3 (CH), 127.6 (CH), 138.3, 138.6, 140.6, 141.0, 149.2 (C2'), 169.9 (C12), 170.8 (C14)
HRMS (APCI) calculated for $C_{21}H_{12}NO_3$ [M^+-H] 326.0823: found 326.0817. Mass accuracy (-1.84ppm).

(*E*)-3-(12,14-Dioxo-9,10-[3,4]epipyrroloanthracen-9(10*H*)-yl)acrylonitrile (343)

(*E*)-3-(12,14-Dioxo-9,10-[3,4]epipyrroloanthracen-9(10*H*)-yl)acrylonitrile was prepared from (*E*)-3-(anthracen-9-yl)acrylonitrile (0.23 g, 1 mmol) and maleimide anhydride (0.13 g, 1.3 mmol) according to general procedure 8.25.
Colourless solid 123 mg (38%)
Melting Point: 289-300 °C
IR$_{Vmax}$ (KBr): 3238 (N-H), 3064, 2970 (C-H), 2222 (CN), 1717 (C=O), 1636 (C=C), 1482, 1457.43 (C=C), 1341 (C-N) cm^{-1}
^{1}H NMR (400 MHz, DMSO-d_6) δ 3.26 - 3.38 (m, 1 H, H11), 3.63 (d, *J* = 8.54 Hz, 1 H, H15), 4.78 (d, *J* = 3.05 Hz, 1 H, H10), 6.51 (d, *J* = 17.09 Hz, 1 H, H1'), 6.88 (s, 1 H, H10), 7.17 - 7.27 (m, 3 H, 3 x ArH), 7.27 - 7.40 (m, 2 H, 2 x ArH), 7.52 (d, *J* = 5.49 Hz, 1 H, ArH), 7.91 (d, *J* = 17.09 Hz, 1 H, H2'), 10.88 (s, 1 H, NH)
^{13}C NMR (101 MHz, DMSO-d_6) ppm 44.4 (C10), 48.3 (C11), 48.7 (C15), 48.8 (C9), 106.1, 117.9 (CN), 122.9 (CH), 123.2 (CH), 124.2 (CH), 125.2 (CH), 126.2 (CH), 126.6 (CH), 126.8 (CH), 127.0 (CH), 135.2 (CH), 138.7, 139.0, 141.6, 141.9, 150.3 (C2'), 172.7 (C14* / C12*), 176.8 (C12), 177.1 (C14)
HRMS (APCI) calculated for $C_{21}H_{13}N_2O_2$ [M^+-H] 325.0983: found 325.0975. Mass accuracy (-2.46 ppm).

(*E*)-3-(12,14-Dioxo-13-phenyl-9,10-[3,4]epipyrroloanthracen-9(10*H*)-yl)acrylonitrile (344)

(*E*)-3-(12,14-Dioxo-13-phenyl-9,10-[3,4]epipyrroloanthracen-9(10*H*)-yl)acrylonitrile was prepared from (*E*)-3-(anthracen-9-yl)acrylonitrile (0.23 g, 1 mmol) and phenylmaleimide (0.22 g, 1.3 mmol) according to general procedure 8.25.
Colourless solid 81 mg (20%)
Melting Point: 274-281 °C
IR$_{Vmax}$ (KBr): 3024, 2940 (C-H), 2221 (CN), 1714 (C=O), 1638, 1500 (C=C), 1595 (C=C), 1383 (CN) cm^{-1}
^{1}H NMR (400 MHz, DMSO-d_6) δ 3.51 (dd, *J* = 8.54, 3.05 Hz, 1 H, H11), 3.82 (d, *J* = 8.54 Hz, 1 H, H15), 4.92 (d, *J* = 3.05 Hz, 1 H, H10), 6.38 - 6.45 (m, 2 H, H6" & H2"), 6.55 (d, *J* = 17.09 Hz, 1 H, H1'), 7.23 - 7.44 (m, 10 H, 10 x ArH), 7.59 (d, *J* = 5.49 Hz, 1 H, ArH), 7.95 (d, *J* = 17.09 Hz, 1 H, H2')
^{13}C NMR (101 MHz, DMSO-d_6) ppm 45.1 (C10), 47.6 (C11), 47.6 (C15), 52.3 (C9), 106.6 (CN), 123.3 (CH), 123.6 (CH), 124.6 (CH), 125.4 (CH), 126.6 (CH), 126.7 (CH), 127.0 (CH), 127.2 (CH), 127.3 (CH), 128.7 (CH), 129.1 (C1'), 131.8, 138.8, 139.0, 141.3, 141.7, 150.3 (C2'), 174.8 (C12), 175.4 (C14)
HRMS (APCI) calculated for $C_{27}H_{17}N_2O_2$ [M^+-H] 401.1296: found 401.1285. Mass accuracy (-2.74 ppm).

2-((12,14-Dioxo-9,10-[3,4]furanoanthracen-9(10*H*)-yl)methylene)malononitrile (345)

2-((12,14-Dioxo-9,10-[3,4]furanoanthracen-9(10*H*)-yl)methylene)malononitrile was prepared from 2-(anthracen-9-ylmethylene)malononitrile (0.35 g, 1 mmol) and maleic anhydride (0.13 g, 1.3 mmol) according to general procedure 8.25.
Colourless solid 53 mg (15%)
Melting Point: 196-198 °C
IR$_{Vmax}$ (KBr): 2941, 2970 (C-H), 2231 (CN), 1864, 1776 (C=O), 1623 (C=C), 1551, 1457.45, (C=C), 1078 (C-O) cm^{-1}
^{1}H NMR (400 MHz, DMSO-d_6) δ 3.74 (br. s., 1 H, H11), 4.12 (br. s., 1 H, H15), 5.00 (d, J = 3.05 Hz, 1 H, H10), 7.20 - 7.38 (m, 4 H, 4 x ArH), 7.44 (t, J = 6.41 Hz, 2 H, 2 x ArH), 7.52 - 7.65 (m, 2 H, 2 x ArH), 8.80 (br. s., 1 H, H1')
^{13}C NMR (101 MHz, DMSO-d_6) ppm 44.3 (C10), 48.5 (C11), 50.2 (C15), 51.1 (C9), 113.1 (CN), 123.5 (CH), 125.3 (CH), 125.6 (CH), 126.6 (CH), 127.1 (CH), 127.7 (CH), 128.1 (CH), 163.6 (C1'), 170.4 (C14 & C12)
HRMS (APCI) calculated for $C_{22}H_{11}N_2O_3$ [M$^+$-H] 351.0775: found 351.0788. Mass accuracy (3.70 ppm).

2-((12,14-Dioxo-9,10-[3,4]epipyrroloanthracen-9(10*H*)-yl)methylene)malononitrile (346)

2-((12,14-Dioxo-9,10-[3,4]epipyrroloanthracen-9(10*H*)-yl)methylene)malononitrile was prepared from 2-(anthracen-9-ylmethylene)malononitrile (0.35 g, 1 mmol) and maleimide (0.13 g, 1.3 mmol) according to general procedure 8.25.
Colourless solid 147 mg (42%)
Melting Point: 281-284 °C
IR$_{Vmax}$ (KBr): 3338 (N-H), 3063, 3010 (C-H), 2239 (CN), 1719 (C=O), 1467, 1457 (C=C), 1336 (C-N) cm^{-1}
^{1}H NMR (400 MHz, DMSO-d_6) δ 3.20 - 3.32 (m, 1 H, H11), 3.67 (br. s., 1 H H15), 4.83 (d, J = 2.44 Hz, 1 H, H10), 7.17 - 7.43 (m, 6 H, 6 x ArH), 7.43 - 7.69 (m, 2 H, 2 x ArH), 8.84 (br. s., 1 H, H1'), 10.95 (s, 1 H, NH)
^{13}C NMR (101 MHz, DMSO-d_6) ppm 44.4 (C10), 48.1 (C11), 50.4 (C15), 52.3 (C9), 111.8 (CN), 113.3 (CN), 123.2 (CH), 123.4 (CH), 125.0 (CH), 125.5 (CH), 126.2 (CH), 126.5 (CH), 127.4 (CH), 127.5 (CH), 138.1, 140.9, 165.3 (C1'), 177.1 (C14 & C12)
HRMS (APCI) calculated for $C_{22}H_{12}N_3O_2$ [M$^+$-H] 350.0935: found 350.0925. Mass accuracy (-2.86 ppm).

2-((12,14-Dioxo-13-phenyl-9,10-[3,4]epipyrroloanthracen-9(10*H*)-yl)methylene)malononitrile (347)

2-((12,14-Dioxo-13-phenyl-9,10-[3,4]epipyrroloanthracen-9(10*H*)-yl)methylene)malononitrile was prepared from 2-(anthracen-9-ylmethylene)malononitrile (0.35 g, 1 mmol) and phenylmaleimide (0.22 g, 1.3 mmol) according to general procedure 8.25.
Colourless solid 188 mg (44%)
Melting Point: 255-258 °C
IR$_{Vmax}$ (KBr): 3039, 2970 (C-H), 2240 (CN), 1712 (C=O), 1597 (C=C), 1470, 1457 (C=C), 1387 (C-N) cm^{-1}

^{1}H NMR (400 MHz, DMSO-d_6) δ 3.48 (br. s., 1 H, H11), 3.84 (br. s., 1 H, H15), 4.95 (br. s., 1 H, H10), 6.32 - 6.54 (m, 2 H, H2" & H6"), 7.20 - 7.70 (m, 11 H, 11 x ArH), 8.87 (br. s., 1 H, H1')
^{13}C NMR (101 MHz, DMSO-d_6) ppm 44.9 (C10), 47.2 (C11), 49.6 (C15), 52.6 (C9), 113.2 (CN), 123.4 (CH), 125.2 (CH) , 125.3 (CH) , 125.6 (CH) , 126.4 (CH), 126.7 (CH), 127.5 (CH), 127.6 (CH), 128.2, 128.6 (CH), 128.8 (CH), 131.4, 165.0 (C1'), 175.0 (C14 & C12)
HRMS (APCI) calculated for $C_{28}H_{18}N_3O_2$ [M^++H] 428.1399: found 428.1382. Mass accuracy (-3.97 ppm).

(*E*)-9-(Hydrazonomethyl)-9,10-dihydro-9,10-[3,4]epipyrroloanthracene-12,14-dione (348)

(*E*)-9-(Hydrazonomethyl)-9,10-dihydro-9,10-[3,4]epipyrroloanthracene-12,14-dione was prepared from (*E*)-(anthracen-9-ylmethylene)hydrazine (0.25 g, 1 mmol) and maleimide (0.13 g, 1.3 mmol) according to general procedure 8.25.
Colourless solid 200 mg (63%)
Melting Point: 245-247 °C
IR$_{Vmax}$ (ATR): 3369 (NH), 3062, 2972 (C-H), 1710 (C=O), 1609 (C=C), 1483, 1457 (C=C), 1213 (C-N) cm^{-1}
^{1}H NMR (400 MHz, DMSO-d_6) δ 3.23 (d, *J* = 8.55 Hz, 1 H, H11), 3.44 (d, *J* = 8.55 Hz, 1 H, H15), 4.72 (br. s., 1 H, H10), 6.82 (br. s., 2 H, NH_2), 7.16 (br. s., 4 H, 4 x ArH), 7.25 - 7.38 (m, 2 H, 2 x ArH), 7.46 (d, *J* = 5.49 Hz, 1 H, 1 x ArH), 7.53 (d, *J* = 6.10 Hz, 1 H, 1 x ArH), 8.06 (s, 1 H, H1'), 10.75 (br. s., 1 H, NH)
^{13}C NMR (101 MHz, DMSO-d_6) ppm 44.7 (C10), 48.6 (C11), 49.8 (C15), 50.2 (C9), 123.6 (CH), 123.9 (CH), 124.9 (CH), 125.7 (CH), 126.1 (CH), 126.2 (CH), 126.3 (CH), 137.9 (C1'), 139.1, 140.3, 142.0, 144.0, 177.0 (C12), 177.6 (C14)
HRMS (APCI) calculated for $C_{19}H_{16}N_3O_2$ [M^++H] 318.1243: found 318.1237. Mass accuracy (-1.88 ppm).

(*E*)-9-(Hydrazonomethyl)-13-phenyl-9,10-dihydro-9,10-[3,4]epipyrroloanthracene-12,14-dione (349)

(*E*)-9-(Hydrazonomethyl)-13-phenyl-9,10-dihydro-9,10-[3,4]epipyrroloanthracene-12,14-dione was prepared from (*E*)-(anthracen-9-ylmethylene)hydrazine (0.25 g, 1 mmol) and phenylmaleimide (0.224 g, 1.3 mmol) according to general procedure 8.25.
Colourless solid 171 mg (54%)
Melting Point: 275-277 °C
IR$_{Vmax}$ (ATR): 3630 (NH), 3072, 2981 (C-H), 1711 (C=O), 1628 (C=C), 1498, 1455 (C=C), 1203 (C-N) cm^{-1}
^{1}H NMR (400 MHz, DMSO-d_6) δ 3.44 (d, *J* = 7.94 Hz, 1 H, H11), 3.64 (d, *J* = 7.94 Hz, 1 H, H15), 4.85 (br. s., 1 H, H10), 6.42 (d, *J* = 5.49 Hz, 2 H, 2 x ArH), 6.84 (s, 2 H, NH_2), 7.15 - 7.40 (m, 10 H, 10 x ArH), 7.58 (d, *J* = 6.71 Hz, 1 H, 1 x ArH), 7.53 (d, *J* = 6.10 Hz, 1 H, 1 x ArH), 8.09 (s, 1 H, H1')
^{13}C NMR (101 MHz, DMSO-d_6) ppm 45.1 (C10), 47.6 (C11), 48.9 (C15), 50.6 (C9), 123.7 (CH), 124.0 (CH), 124.1 (CH), 124.9 (CH), 125.9 (CH), 126.3 (CH), 126.4 (CH), 126.4 (CH),

126.5 (CH), 128.4 (CH), 128.8 (CH), 131.8, 137.5 (C1'), 139.0, 140.1, 141.5, 143.7, 174.7 (C12), 175.5 (C14)
HRMS (APCI) calculated for $C_{19}H_{16}N_3O_2$ [M^++H] 318.1243: found 318.1237. Mass accuracy (-1.88 ppm).

(*E*)-9-Chloro-10-(hydrazonomethyl)-9,10-dihydro-9,10-[3,4]epipyrroloanthracene-12,14-dione (350)

(*E*)-9-Chloro-10-(hydrazonomethyl)-9,10-dihydro-9,10-[3,4]epipyrroloanthracene-12,14-dione was prepared from (*E*)-((10-chloroanthracen-9-yl)methylene)hydrazine (0.25 g, 1 mmol) and maleimide (0.13 g, 1.3 mmol) according to general procedure 8.25.
Colourless solid 119 mg (34%)
Melting Point: 241-244 °C
IR$_{Vmax}$ (ATR): 3635 (NH), 3066, 2980 (C-H), 1713 (C=O), 1597 (C=C), 1498, 1455 (C=C), 1185 (C-N) cm^{-1}
^{1}H NMR (400 MHz, DMSO-d_6) δ 3.41 (d, *J* = 8.55 Hz, 1 H, H11), 3.63 (d, *J* = 8.55 Hz, 1 H, H15), 6.90 (br. s., 2 H, NH_2), 7.24 - 7.36 (m, 4 H, 4 x ArH), 7.40 (d, *J* = 7.32 Hz, 1 H, 1 x ArH), 7.62 (br. s., 2 H, 2 x ArH), 7.74 (d, *J* = 7.32 Hz, 1 H, 1 x ArH), 8.03 (s, 1 H, H1'), 10.91 (br. s., 1 H, NH)
^{13}C NMR (101 MHz, DMSO-d_6) ppm 49.2 (C10), 51.5 (C11), 54.1 (C15), 70.7 (C9), 122.0 (CH), 122.6 (CH), 123.6 (CH), 126.7 (CH), 126.8 (CH), 127.0 (CH), 127.4 (CH), 136.7 (C1'), 137.9, 138.7, 141.0, 142.6, 173.9 (C12), 175.6 (C14)
HRMS (APCI) calculated for $C_{19}H_{15}Cl^{35}N_3O_2$ [M^++H] 352.0853: found 352.0848. Mass accuracy (-1.42 ppm).

(*E*)-12,14-Dioxo-9,10-[3,4]epipyrroloanthracene-9(10*H*)-carbaldehyde oxime (351)

(*E*)-12,14-Dioxo-9,10-[3,4]epipyrroloanthracene-9(10*H*)-carbaldehyde oxime was prepared from (*E*)-anthracene-9-carbaldehyde oxime (0.22 g, 1 mmol) and maleimide (0.13 g, 1.3 mmol) according to general procedure 8.25.
Colourless solid 137 mg (43 %)
Melting Point: 272-273 °C
IR$_{Vmax}$ (ATR): 3043, 2939 (C-H), 1710 (C=O), 1595 (C=C), 1491, 1456 (C=C), 1192 (C-N) cm^{-1}
^{1}H NMR (400 MHz, DMSO-d_6) δ 3.28 (dd, *J* = 8.55, 3.05 Hz, 1 H, H11), 3.54 (d, *J* = 8.55 Hz, 1 H, H15), 4.77 (d, *J* = 3.05 Hz, 1 H, H10), 7.06 - 7.26 (m, 4 H, 4 x ArH), 7.33 (d, *J* = 4.88 Hz, 2 H, 2 X ArH), 7.45 - 7.62 (m, 2 H, 2 x ArH), 8.44 (s, 1 H, H1'), 10.83 (s, 1 H, NH), 11.49 (s, 1 H, =N-OH)
^{13}C NMR (101 MHz, DMSO-d_6) ppm 44.7 (C10), 48.4 (C11), 49.4 (C9), 49.9 (C15), 123.6 (CH), 124.1 (CH), 125.1 (CH), 125.9 (CH), 126.3 (CH), 126.6 (CH), 126.6 (CH), 139.0, 139.3, 141.8, 142.9, 147.5 (C1'), 177.0 (C12), 177.5 (C14)
HRMS (APCI) calculated for $C_{19}H_{15}N_2O_3$ [M^++H] 319.1083: found 319.1077. Mass accuracy (-1.88 ppm).

(*E*)-12,14-Dioxo-13-phenyl-9,10-[3,4]epipyrroloanthracene-9(10*H*)-carbaldehyde oxime (352)

(*E*)-12,14-dioxo-13-phenyl-9,10-[3,4]epipyrroloanthracene-9(10*H*)-carbaldehyde oxime was prepared from (*E*)-anthracene-9-carbaldehyde oxime (0.22 g, 1 mmol) and phenylmaleimide (0.22 g, 1.3 mmol) according to general procedure 8.25.

Colourless solid 260 mg (66%)

Melting Point: 238-242 °C

IR$_{\nu max}$ (ATR): 3380 (OH), 3053, 2972 (C-H), 1760 (C=O), 1598 (C=C), 1483, 1457 (C=C), 1210 (C-N) cm^{-1}

^{1}H NMR (400 MHz, DMSO-d_6) δ 3.48 (dd, *J* = 8.55, 3.05 Hz, 1 H, H11), 3.75 (d, *J* = 8.55 Hz, 1 H, H15), 4.90 (d, *J* = 3.05 Hz, 1 H, H10), 6.34 - 6.51 (m, 2 H, 2 x ArH), 7.14 - 7.43 (m, 9 H, 9 x ArH), 7.50 - 7.65 (m, 2 H, 2 x ArH), 8.49 (s, 1 H, H1'), 11.51 (s, 1 H, =N-OH)

^{13}C NMR (101 MHz, DMSO-d_6) ppm 45.0 (C10), 47.3 (C11), 49.0 (C9), 49.9 (C15), 123.7 (CH), 124.3 (CH), 125.1 (CH), 126.1 (CH), 126.5 (CH), 126.5 (CH), 126.7 (CH), 126.8 (CH), 128.5 (CH), 128.8 (CH), 131.7, 138.8, 139.0, 141.3, 142.5, 147.3 (C1'), 174.7 (C12), 175.4 (C14)

HRMS (APCI) calculated for $C_{25}H_{19}N_2O_3$ [M^++H] 395.1396: found 395.1390. Mass accuracy (-1.51 ppm).

Chapter 8.
References

1. Messerschmitt, P. J.; Rettew, A. N.; Schroeder, N. O.; Brookover, R. E.; Jakatdar, A. P.; Getty, P. J.; Greenfield, E. M. Osteosarcoma Phenotype Is Inhibited by 3,4-Methylenedioxy-β-nitrostyrene. *Sarcoma* **2012**, 2012, 11.
2. He, Y.; Varadarajan, S.; Munoz-Planillo, R.; Burberry, A.; Nakamura, Y.; Nunez, G. 3,4-methylenedioxy-beta-nitrostyrene inhibits NLRP3 inflammasome activation by blocking assembly of the inflammasome. *J Biol Chem*, **2014**; Vol. 289, pp 1142-50.
3. Kaap, S.; Quentin, I.; Tamiru, D.; Shaheen, M.; Eger, K.; Steinfelder, H. J. Structure activity analysis of the pro-apoptotic, antitumor effect of nitrostyrene adducts and related compounds. *Biochem Pharmacol* **2003**, 65, 603-10.
4. Reddy, M. A.; Jain, N.; Yada, D.; Kishore, C.; Vangala, J. R.; R, P. S.; Addlagatta, A.; Kalivendi, S. V.; Sreedhar, B. Design and synthesis of resveratrol-based nitrovinylstilbenes as antimitotic agents. *J Med Chem* **2011**, 54, 6751-60.
5. McNamara, Y. M.; Cloonan, S. M.; Knox, A. J. S.; Keating, J. J.; Butler, S. G.; Peters, G. H.; Meegan, M. J.; Williams, D. C. Synthesis and serotonin transporter activity of 1,3-bis(aryl)-2-nitro-1-propenes as a new class of anticancer agents. *Bioorg. Med. Chem.* **2011**, 19, 1328-1348.
6. McNamara, Y. M.; Bright, S. A.; Byrne, A. J.; Cloonan, S. M.; McCabe, T.; Williams, D. C.; Meegan, M. J. Synthesis and antiproliferative action of a novel series of maprotiline analogues. *European Journal of Medicinal Chemistry* **2014**, 71, 333-353.
7. Calgarotto, A. K.; da Silva Pereira, G. J.; Bechara, A.; Paredes-Gamero, E. J.; Barbosa, C. M.; Hirata, H.; de Souza Queiroz, M. L.; Smaili, S. S.; Bincoletto, C. Autophagy inhibited Ehrlich ascitic tumor cells apoptosis induced by the nitrostyrene derivative compounds: relationship with cytosolic calcium mobilization. *Eur J Pharmacol* **2012**, 678, 6-14.
8. Hsieh, P. W.; Chang, Y. T.; Chuang, W. Y.; Shih, H. C.; Chiang, S. Z.; Wu, C. C. The synthesis and biologic evaluation of anti-platelet and cytotoxic beta-nitrostyrenes. *Bioorg Med Chem* **2010**, 18, 7621-7.
9. Werner, J. M.; Eger, K.; Jurgen Steinfelder, H. Comparison of the rapid pro-apoptotic effect of trans-beta-nitrostyrenes with delayed apoptosis induced by the standard agent 5-fluorouracil in colon cancer cells. *Apoptosis* **2007**, 12, 235-46.
10. Jain, N.; Yada, D.; Shaik, T. B.; Vasantha, G.; Reddy, P. S.; Kalivendi, S. V.; Sreedhar, B. Synthesis and antitumor evaluation of nitrovinyl biphenyls: anticancer agents based on allocolchicines. *ChemMedChem* **2011**, 6, 859-68.
11. Ramos, A.; Vizoso, A.; Edreira, A.; Betancourt, J.; decalo, M. Activity of a nitroalkene derivative, 1-(5-bromofur-2-il)-2-bromo-2-nitroethene, in the Salmonella/microsome assay and the mouse bone marrow micronucleus test. *Mutation Research/Genetic Toxicology and Environmental Mutagenesis* **1997**, 390, 233-238.
12. Kim, J. H.; Kim, J. H.; Lee, G. E.; Lee, J. E.; Chung, I. K. Potent Inhibition of Human Telomerase by Nitrostyrene Derivatives. *Molecular Pharmacology* 2003, 63, 1117-1124.
13. Chung, I. K.; Kim, J. H.; Kim, S. W.; Lee, E. J.; Lee, G. E.; Lee, J. E.; Lee, J. G. (2004) Beta-nitrostyrene compound and telomerase inhibitor having an anticancer activity: patent WO2004046081 A1
14. Pettit, R. K.; Pettit, G. R.; Hamel, E.; Hogan, F.; Moser, B. R.; Wolf, S.; Pon, S.; Chapuis, J. C.; Schmidt, J. M. E-Combretastatin and E-resveratrol structural modifications: antimicrobial and cancer cell growth inhibitory beta-E-nitrostyrenes. *Bioorg Med Chem* **2009**, 17, 6606-12.
15. Pettit, R. K.; Hamel, E.; Verdier-Pinard, P.; Roberson, R. W.; Hazen, K. C.; Pettit, G. R.; Crews, L. C. Antifungal and cancer cell growth inhibitory activities of 1-(3',4',5'-trimethoxyphenyl)-2-nitro-ethylene. *Mycoses*, **2002**; Vol. 45, pp 65-74.

16. Dore, J. C.; Viel, C. Antitumor chemotherapy. XII. Correlation between ethylenimine addition and cytotoxic properties on tumor cells of compounds with activated ethylene double bonds. *Eur. J. Med. Chem. - Chim. Ther.* **1974**, 9, 666-72.
17. Doré, J. C.; Viel, C. Research in antitumoral chemotherapy. X. Cytotoxic and antitumoral activity of beta-nitrostyrenes and of composed nitrovinyl derivatives. *Il Farmaco; edizione scientifica* **1975**, 30, 81-109.
18. Burkitt, D. P. Epidemiology of Burkitt's lymphoma. *Proceedings of the Royal Society of Medicine* **1971**, 64, 909-910.
19. Smith, C.; Marks, A. D.; Lieberman, M. *Mark's Basic Medical Biochemistry: A Clinical Approach*. 2 ed.; Lippincott Williams & Wilkins: China, **2004**; 319-342.
20. Alberts, B.; Wilson, J. H.; Hunt, T. *Molecular biology of the cell*. 5th ed.; Garland Science: New York, N.Y. ; Abingdon, **2008**; 1601
21. Becker, W. M. *The world of the cell*. Pearson International ed.; Pearson/Benjamin Cummings: San Francisco, Calif. ; London, **2009**, 791.
22. World Health Organisation. *The Global Burden of Disease: 2004 Update*; Geneva, 2008.
23. National Cancer Registry, Cancer in Ireland 1994-2012: Annual report of the National Cancer Registry. NCR, Cork, Ireland, **2014**.
24. Ferlay, J.; Steliarova-Foucher, E.; Lortet-Tieulent, J.; Rosso, S.; Coebergh, J. W. W.; Comber, H.; Forman, D.; Bray, F. Cancer incidence and mortality patterns in Europe: Estimates for 40 countries in 2012. *European Journal of Cancer* **2013**, 49, 1374-1403.
25. Worldwide data | World Cancer Research Fund International. http://www.wcrf.org/int/cancer-facts-figures/worldwide-data [05/01/2015]
26. World Health Organisation, World Cancer Factsheet, Cancer Research UK, **2012**.
27. Evan, G. I.; Vousden, K. H. Proliferation, cell cycle and apoptosis in cancer. *Nature* 2001, 411, 342-348.
28. cellcycle.gif (GIF Image, 343 × 241 pixels). http://www.scq.ubc.ca/wp-content/cellcycle.gif [06/02/2014]
29. Kroemer, G.; El-Deiry, W. S.; Golstein, P.; Peter, M. E.; Vaux, D.; Vandenabeele, P.; Zhivotovsky, B.; Blagosklonny, M. V.; Malorni, W.; Knight, R. A.; Piacentini, M.; Nagata, S.; Melino, G. Classification of cell death: recommendations of the Nomenclature Committee on Cell Death. *Cell Death Differ* **2009**, 12, 1463-1467.
30. Kerr, J. F.; Wyllie, A. H.; Currie, A. R. Apoptosis: a basic biological phenomenon with wide-ranging implications in tissue kinetics. *Br J Cancer* 1972, 26, 239-57.
31. Herrmann, M.; Kalden, J. R. *Apoptosis and autoimmunity*. Wiley-VCH: Weinheim ; Great Britain, **2003**; 381
32. Pecorino, L. *Molecular biology of cancer : mechanisms, targets, and therapeutics*. Oxford University Press: Oxford, **2005**; 243
33. Avendaño, C.; Menéndez, J. C. Chapter 1 - Introduction. In *Medicinal Chemistry of Anticancer Drugs*, Avendaño, C.; Menéndez, J. C., Eds. Elsevier: Amsterdam, 2008; pp 1-8.
34. Cunningham, S; The Royal Marsden Hospital Handbook of Cancer Chemotherapy. *Nursing Standard* **2006**, 20, 26-26.
35. Thurston, D. E., *Chemistry and pharmacology of anticancer drugs*. CRC press Florida: **2006**.
36. Neidle, S. *Cancer drug design and discovery*. Academic Press London: 2011.
37. Rang, H. P.; Dale, M. M.; Ritter, J. M.; Flower, R. J.; Henderson, G. *Rang & Dale's Pharmacology*. Elsevier Health Sciences UK: **2011**.
38. Antibody-Drug Conjugates: Guided Missiles Deployed Against Cancerous Cells. http://www.onclive.com/publications/oncology-live/2012/june-2012/Antibody-Drug-Conjugates-Guided-Missiles-Deployed-Against-Cancerous-Cells [12/02/2015]

39. Senter, P. D.; Sievers, E. L. The discovery and development of brentuximab vedotin for use in relapsed Hodgkin lymphoma and systemic anaplastic large cell lymphoma. *Nat Biotech* **2012**, 30, 631-637.
40. Weinberg, R. A. *The biology of cancer*. Garland Science: New York ; London, **2007**
41. Kearns, D. B.; Smith, R. J. H.; Pitcock, J. K. Burkitt's lymphoma. *International Journal of Pediatric Otorhinolaryngology* **1986**, 12, 73-84.
42. Davies, J. N. P.; Elmes, S.; Hutt, M.; Mtimavalye, L.; Owor, R.; Sharper, L. Reticuloendothelial tumours. *East African Medical Journal* **1948**, 117.
43. Davies, J. N.; Elmes, S.; Hutt, M. S.; Mtimavalye, L. A.; Owor, R.; Shaper, L. cancer in an african community, 1897--1956. an analysis of the records of mengo hospital, kampala, uganda. *Br Med J* **1964**, 1, 336-41.
44. Smith, E. C.; Elmes, B. G. T. Malignant diseases in natives of nigeria. In *Annals of tropical medicine and parasitology*, **1934**; Vol. 28, pp 461-512.
45. Burkitt, D. A sarcoma involving the jaws in African children. *Br J Surg* **1958**, 46, 218-223
46. Kellock, B. *The fibre man : the life-story of Dr. Denis Burkitt*. Lion: Tring, **1985**; p 208p.
47. Burkitt, D. P. Determining the climatic limitations of a childrens cancer common in Africa. Br Med J: **1962**; Vol. 2, pp 1019-1023.
48. Histopathological definition of Burkitt's tumour. *Bulletin of the World Health Organisation* **1969**, 40, 601-607.
49. Orem, J.; Mbidde, E. K.; Lambert, B.; de Sanjose, S.; Weiderpass, E. Burkitt's lymphoma in Africa, a review of the epidemiology and etiology. *Afr Health Sci* **2007**, 7, 166-75.
50. Rainey, J. J.; Mwanda, W. O.; Wairiumu, P.; Moormann, A. M.; Wilson, M. L.; Rochford, R. Spatial distribution of Burkitt's lymphoma in Kenya and association with malaria risk. *Trop Med Int Health* **2007**, 12, 936-43.
51. Khan, G.; Hashim, M. J. Global burden of deaths from Epstein-Barr virus attributable malignancies 1990-2010. *Infect Agent Cancer* **2014**, 9, 38.
52. Bloland, P. B.; Boriga, D. A.; Ruebush, T. K.; McCormick, J. B.; Roberts, J. M.; Oloo, A. J.; Hawley, W.; Lal, A.; Nahlen, B.; Campbell, C. C. Longitudinal cohort study of the epidemiology of malaria infections in an area of intense malaria transmission II. Descriptive epidemiology of malaria infection and disease among children. *The American Journal of Tropical Medicine and Hygiene* **1999**, 60, 641-648.
53. Chene, A.; Donati, D.; Orem, J.; Björkman, A.; Mbidde, E. R.; Kironde, F.; Wahlgren, M.; Bejarano, M. T. Endemic Burkitt's lymphoma as a polymicrobial disease: New insights on the interaction between Plasmodium falciparum and Epstein–Barr virus. *Seminars in Cancer Biology* **2009**, 19, 411-420.
54. Johnston, W. T.; Mutalima, N.; Sun, D.; Emmanuel, B.; Bhatia, K.; Aka, P.; Wu, X.; Borgstein, E.; Liomba, G. N.; Kamiza, S.; Mkandawire, N.; Batumba, M.; Carpenter, L. M.; Jaffe, H.; Molyneux, E. M.; Goedert, J. J.; Soppet, D.; Newton, R.; Mbulaiteye, S. M. Relationship between Plasmodium falciparum malaria prevalence, genetic diversity and endemic Burkitt lymphoma in Malawi. *Sci Rep* **2014**, 4, 3741.
55. Ho, M.; Webster, H. K.; Looareesuwan, S.; Supanaranond, W.; Phillips, R. E.; Chanthavanich, P.; Warrell, D. A. Antigen-Specific Immunosuppression in Human Malaria Due to Plasmodium falciparum. *Journal of Infectious Diseases* **1986**, 153, 763-771.
56. Ho, M.; Webster, H.; Green, B.; Looareesuwan, S.; Kongchareon, S.; White, N. Defective production of and response to IL-2 in acute human falciparum malaria. *The Journal of Immunology* **1988**, 141, 2755-2759.

57. Epstein, M. A.; Achong, B. G.; Barr, Y. M. Virus Particles in cultured lymphoblasts from Burkitt's lymphoma. Lancet., **1964**; pp 702-703.
58. Dong, H. Y. *Aggressive B-cell lymphoma and Burkitt lymphoma*. Humana Press: New York, **2010**; p 303-322.
59. Zur Hausen, H. *Infections causing human cancer*. Wiley-VCH ; John Wiley [distributor]: Weinheim Chichester, **2006**; 517
60. Cardy, A.; Sharp, L.; Little, J. Burkitt's lymphoma: a review of the epidemiology. *Kuwait Med J* **2001**, 33, 293-306.
61. Ziegler, J. L.; Drew, W. L.; Miner, R. C.; Mintz, L.; Rosenbaum, E.; Gershow, J.; Lennette, E. T.; Greenspan, J.; Shillitoe, E.; Beckstead, J.; Casavant, C.; Yamamoto, K. Outbreak of Burkitt's-like lymphoma in homosexual men. *Lancet* 1982, 2, 631-3.
62. Knowles, D. M. Etiology and pathogenesis of AIDS-related non-Hodgkin's lymphoma. *Hematol Oncol Clin North Am* **2003**, 17, 785-820.
63. Ferry, J. A. Burkitt's lymphoma: clinicopathologic features and differential diagnosis. *Oncologist* **2006**, 11, 375-83.
64. Guech-Ongey, M.; Simard, E. P.; Anderson, W. F.; Engels, E. A.; Bhatia, K.; Devesa, S. S.; Mbulaiteye, S. M. AIDS-related Burkitt lymphoma in the United States: what do age and CD4 lymphocyte patterns tell us about etiology and/or biology? *Blood* **2010**, 116, 5600-4.
65. Zech, L.; Haglund, U.; Nilsson, K.; Klein, G. Characteristic chromosomal abnormalities in biopsies and lymphoid-cell lines from patients with burkitt and non-burkitt lymphomas. *International Journal of Cancer* **1976**, 17, 47-56.
66. Wade, M.; Wahl, G.; Eisenman, R. N. c-Myc, Genome Instability, and Tumorigenesis: The Devil Is in the Details, The Myc/Max/Mad Transcription Factor Network. In Springer Berlin Heidelberg: **2006**; Vol. 302, pp 169-203.

67. Anderton, E.; Yee, J.; Smith, P.; Crook, T.; White, R. E.; Allday, M. J. Two Epstein-Barr virus (EBV) oncoproteins cooperate to repress expression of the proapoptotic tumour-suppressor Bim: clues to the pathogenesis of Burkitt's lymphoma. *Oncogene* **2008**, 27, 421-433.
68. Lindström, M. S.; Wiman, K. G. Role of genetic and epigenetic changes in Burkitt lymphoma. *Seminars in Cancer Biology* **2002**, 12, 381-387.
69. Fisher, R. I.; Gaynor, E. R.; Dahlberg, S.; Oken, M. M.; Grogan, T. M.; Mize, E. M.; Glick, J. H.; Coltman, C. A., Jr.; Miller, T. P. Comparison of a standard regimen (CHOP) with three intensive chemotherapy regimens for advanced non-Hodgkin's lymphoma. *N Engl J Med* **1993**, 328, 1002-6.
70. Wilson, W. H.; Dunleavy, K.; Pittaluga, S.; Hegde, U.; Grant, N.; Steinberg, S. M.; Raffeld, M.; Gutierrez, M.; Chabner, B. A.; Staudt, L.; Jaffe, E. S.; Janik, J. E. Phase II study of dose-adjusted EPOCH and rituximab in untreated diffuse large B-cell lymphoma with analysis of germinal center and post-germinal center biomarkers. *J Clin Oncol* **2008**, 26, 2717-24.
71. Diviné, M.; Casassus, P.; Koscielny, S.; Bosq, J.; Sebban, C.; Le Maignan, C.; Stamattoulas, A.; Dupriez, B.; Raphaël, M.; Pico, J. L.; Ribrag, V. Burkitt lymphoma in adults: a prospective study of 72 patients treated with an adapted pediatric LMB protocol. *Annals of Oncology* **2005**, 16, 1928-1935.
72. Perkins, A. S.; Friedberg, J. W. Burkitt lymphoma in adults. *Hematology Am Soc Hematol Educ Program* **2008**, 341-8.
73. Magrath, I. T.; Haddy, T. B.; Adde, M. A. Treatment of patients with high grade non-Hodgkin's lymphomas and central nervous system involvement: is radiation an essential component of therapy? *Leuk Lymphoma* **1996**, 21, 99-105.

74. Mead, G. M.; Sydes, M. R.; Walewski, J.; Grigg, A.; Hatton, C. S.; Pescosta, N.; Guarnaccia, C.; Lewis, M. S.; McKendrick, J.; Stenning, S. P.; Wright, D.; collaborators, U. L. An international evaluation of CODOX-M and CODOX-M alternating with IVAC in adult Burkitt's lymphoma: results of United Kingdom Lymphoma Group LY06 study. *Ann Oncol* **2002**, 13, 1264-74.
75. Lacasce, A.; Howard, O.; Lib, S.; Fisher, D.; Weng, A.; Neuberg, D.; Shipp, M. Modified magrath regimens for adults with Burkitt and Burkitt-like lymphomas: preserved efficacy with decreased toxicity. *Leuk Lymphoma* **2004**, 45, 761-7.
76. Marcus, R.; Imrie, K.; Belch, A.; Cunningham, D.; Flores, E.; Catalano, J.; Solal-Celigny, P.; Offner, F.; Walewski, J.; Raposo, J.; Jack, A.; Smith, P. CVP chemotherapy plus rituximab compared with CVP as first-line treatment for advanced follicular lymphoma. *Blood* **2005**, 105, 1417-23.
77. Coiffier, B.; Altman, A.; Pui, C. H.; Younes, A.; Cairo, M. S. Guidelines for the management of pediatric and adult tumor lysis syndrome: an evidence-based review. *J Clin Oncol* **2008**, 26, 2767-78.
78. Thomas, D. A.; Cortes, J.; O'Brien, S.; Pierce, S.; Faderl, S.; Albitar, M.; Hagemeister, F. B.; Cabanillas, F. F.; Murphy, S.; Keating, M. J.; Kantarjian, H. Hyper-CVAD program in Burkitt's-type adult acute lymphoblastic leukemia. *J Clin Oncol* **1999**, 17, 2461-70.
79. Thomas, D. A.; Faderl, S.; O'Brien, S.; Bueso-Ramos, C.; Cortes, J.; Garcia-Manero, G.; Giles, F. J.; Verstovsek, S.; Wierda, W. G.; Pierce, S. A.; Shan, J.; Brandt, M.; Hagemeister, F. B.; Keating, M. J.; Cabanillas, F.; Kantarjian, H. Chemoimmunotherapy with hyper-CVAD plus rituximab for the treatment of adult Burkitt and Burkitt-type lymphoma or acute lymphoblastic leukemia. *Cancer* **2006**, 106, 1569-80.
80. Oriol, A.; Ribera, J. M.; Bergua, J.; Gimenez Mesa, E.; Grande, C.; Esteve, J.; Brunet, S.; Moreno, M. J.; Escoda, L.; Hernandez-Rivas, J. M.; Hoelzer, D. High-dose chemotherapy and immunotherapy in adult Burkitt lymphoma: comparison of results in human immunodeficiency virus-infected and noninfected patients. *Cancer* **2008**, 113, 117-25.
81. Phase II Study of Dose-Adjusted EPOCH-Rituximab in Adults With Untreated Burkitt Lymphoma and c-MYC+ Diffuse Large B-Cell Lymphoma - Full Text View - ClinicalTrials.gov. http://clinicaltrials.gov/ct2/show/NCT01092182?term=burkitt+lymphoma&rank=1 [19/03/2015]
82. Chemotherapy Plus Rituximab Combination for Adult Lymphoblastic Leukemia (B-ALL) and Burkitt's Non-Hodgkin Lymphoma - Full Text View - ClinicalTrials.gov. http://clinicaltrials.gov/ct2/show/NCT01290120?term=burkitt+lymphoma&rank=2 [19/03/2015]
83. Reddy, M. V.; Mallireddigari, M. R.; Cosenza, S. C.; Pallela, V. R.; Iqbal, N. M.; Robell, K. A.; Kang, A. D.; Reddy, E. P. Design, synthesis, and biological evaluation of (E)-styrylbenzylsulfones as novel anticancer agents. *J Med Chem* **2008**, 51, 86-100.
84. Gobec, M.; Obreza, A.; Prijatelj, M.; Brus, B.; Gobec, S.; Mlinaric-Rascan, I. Selective cytotoxicity of amidinopiperidine based compounds towards Burkitt's lymphoma cells involves proteasome inhibition. *PLoS One*, United States, **2012**; Vol. 7, 41961.
85. Easmon, J.; Puerstinger, G.; Roth, T.; Fiebig, H. H.; Jenny, M.; Jaeger, W.; Heinisch, G.; Hofmann, J. 2-benzoxazolyl and 2-benzimidazolyl hydrazones derived from 2-acetylpyridine: a novel class of antitumor agents. *Int J Cancer*, 2001 Wiley-Liss, Inc.: United States, **2001**; Vol. 94, pp 89-96.
86. Easmon, J.; Purstinger, G.; Thies, K. S.; Heinisch, G.; Hofmann, J. Synthesis, structure-activity relationships, and antitumor studies of 2-benzoxazolyl hydrazones derived from alpha-(N)-acyl heteroaromatics. *J Med Chem* **2006**, 49, 6343-50.

87. Zhelev, Z.; Ohba, H.; Bakalova, R.; Hadjimitova, V.; Ishikawa, M.; Shinohara, Y.; Baba, Y. Phenothiazines suppress proliferation and induce apoptosis in cultured leukemic cells without any influence on the viability of normal lymphocytes. Phenothiazines and leukemia. *Cancer Chemother Pharmacol* **2004**, 53, 267-75.
88. Park, J.; Park, E.; Ahn, B. H.; Kim, H. J.; Park, J. H.; Koo, S. Y.; Kwak, H. S.; Park, H. S.; Kim, D. W.; Song, M.; Yim, H. J.; Seo, D. O.; Kim, S. H. NecroX-7 prevents oxidative stress-induced cardiomyopathy by inhibition of NADPH oxidase activity in rats. *Toxicol Appl Pharmacol*, 2012 Elsevier Inc: United States, **2012**; Vol. 263, pp 1-6.
89. Kim, E.-J.; Lee, E. S.; Im, K.-I.; Kim, S. H.; Lim, J.-Y.; Kim, N.; Cho, S.-G. Abstract 2720: In vitro evaluation of a novel chemotherapeutic agent, NecroX-7, in human Burkitt lymphoma cells. *Cancer Research* **2014**, 74, 2720-2720.
90. Meredith, E. J.; Holder, M. J.; Chamba, A.; Challa, A.; Drake-Lee, A.; Bunce, C. M.; Drayson, M. T.; Pilkington, G.; Blakely, R. D.; Dyer, M. J.; Barnes, N. M.; Gordon, J. The serotonin transporter (SLC6A4) is present in B-cell clones of diverse malignant origin: probing a potential anti-tumor target for psychotropics. *FASEB J*, **2005**; Vol. 19, pp 1187-9.
91. Gandy, M.N.; McIldowie, Lewis, K.; Wasik, A. M.; Salmonczyk, D.; Wagg, K.; Millar, Z.A.; Tindiglia, Huot, P.; Johnston, T.; Thiele, S.; Nguyen, B.; Barnes, N.M.; Brotchie, J.M.; Iverson, M.M.; Nash, J.; Gordon, J.; Piggott, M.J. Redesigning the designer drug ecstasy: non-psychoactive MDMA analogues exhibiting Burkitt's lymphoma cytotoxicity. *MedChemComm* **2010,** 1, 287-293
92. Cloonan, S. M.; Keating, J. J.; Butler, S. G.; Knox, A. J. S.; Jørgensen, A. M.; Peters, G. H.; Rai, D.; Corrigan, D.; Lloyd, D. G.; Williams, D. C.; Meegan, M. J. Synthesis and serotonin transporter activity of sulphur-substituted α-alkyl phenethylamines as a new class of anticancer agents. *European Journal of Medicinal Chemistry* **2009**, 44, 4862-4888.
93. Cloonan, S. M.; Drozgowska, A.; Fayne, D.; Williams, D. C. The antidepressants maprotiline and fluoxetine have potent selective antiproliferative effects against Burkitt lymphoma independently of the norepinephrine and serotonin transporters. *Leuk Lymphoma* **2010**, 51, 523-39.
94. Cloonan, S. M.; Williams, D. C. The antidepressants maprotiline and fluoxetine induce Type II autophagic cell death in drug-resistant Burkitt's lymphoma. *Int J Cancer* **2011**, 128, 1712-23.
95. Leonard, B. E., Principles of Neuropsychopharmacology., Sinauer Associates Inc., Mass. U.S.A., 1997. *Human Psychopharmacology: Clinical and Experimental* **1998**, 13, 70-70
96. Romero, L.; Montero, A.; Fernández, B.; Vela, J. M. Introductory and Basic Aspects. In *Antidepressants, Antipsychotics, Anxiolytics*, Wiley-VCH Verlag GmbH: 2008; pp 2-50.
97. Holenz, J.; Díaz, J. L.; Buschmann, H. Chemistry. In *Antidepressants, Antipsychotics, Anxiolytics*, Wiley-VCH Verlag GmbH: **2007**; pp 173-296.
98. Pérez-Egea, R.; Pérez, V.; Puigdemont, D.; Álvarez, E. Clinics. In *Antidepressants, Antipsychotics, Anxiolytics*, Wiley-VCH Verlag GmbH: **2008**; pp 51-110.
99. Fuller, M. A.; Sajatovic, M. *Drug Information Handbook for Psychiatry: Including Psychotropic, Nonpsychotropic and Herbal Agents*. Lexi-Comp Incorporated: 2009.
100. Tatsumia, M.; Groshana, K.; Blakely, R. D.; Richelson, E. Pharmacological profile of antidepressants and related compounds at human monoamine transporters. **1997,** 340, 249–258.
101. Gareri, P.; Falconi, U.; De Fazio, P.; Sarro, G. D. Conventional and new antidepressant drugs in the elderly. Prog Neurobiol, **2000,** 61, 353–396.
102. Wilhelm, M.; Schmidt, P.; Eichenberger, K. Verfahren zur Herstellung eines neuen Amins Ger Patent DE19914114221 1969.

103. Wilhelm, M.; Schmidt, P. Synthese und Eigenschaften von 1-Aminoalkyl-dibenzo[b, e]bicyclo[2.2.2]octadienen. *Helvetica Chimica Acta* 1969, 52, 1385-1395.
104. Sunagawa, M.; Sato, H.; Katsube, J. Dibenzotetracyclic Derivatives. III. Synthesis of 9-γ-Methylaminopropyl-9, 10-dihydro-9, 10-propanoanthracene. *chemical & pharmaceutical bulletin* 1980, 28, 1644-1647.
105. Kornfeld, E. C.; Barney, P.; Blankley, J.; Faul, W. Triptycene Derivatives as Medicinal Agents. *Journal of Medicinal Chemistry* **1965,** 8, 342-347.
106. Hsu, S. S.; Chen, W. C.; Lo, Y. K.; Cheng, J. S.; Yeh, J. H.; Cheng, H. H.; Chen, J. S.; Chang, H. T.; Jiann, B. P.; Huang, J. K.; Jan, C. R. Effect of the antidepressant maprotiline on Ca2+ movement and proliferation in human prostate cancer cells. *Clin Exp Pharmacol Physiol* **2004,** 31, 444-9.
107. Jan, C. R.; Su, J. A.; Teng, C. C.; Sheu, M. L.; Lin, P. Y.; Chi, M. C.; Chang, C. H.; Liao, W. C.; Kuo, C. C.; Chou, C. T. Mechanism of maprotiline-induced apoptosis: role of [Ca2+](i), ERK, JNK and caspase-3 signaling pathways. *Toxicology* **2013,** 304, 1-12.
108. Gurgel, J. A.; Lima-Junior, R. C.; Rabelo, C. O.; Pessoa, B. B.; Brito, G. A.; Ribeiro, R. A. Amitriptyline, clomipramine, and maprotiline attenuate the inflammatory response by inhibiting neutrophil migration and mast cell degranulation. *Rev Bras Psiquiatr* **2013,** 35, 387-92.
109. Szabó, D.; Szabó, G., Jr.; Ocsovszki, I.; Aszalos, A.; Molnár, J. Anti-psychotic drugs reverse multidrug resistance of tumor cell lines and human AML cells ex-vivo. *Cancer Letters **1999*** 139, 115-119.
110. Bitonti, A. J.; Sjoerdsma, A.; McCann, P. P.; Kyle, D. E.; Oduola, A. M.; Rossan, R. N.; Milhous, W. K.; Davidson, D. E., Jr. Reversal of chloroquine resistance in malaria parasite Plasmodium falciparum by desipramine. *Science* **1988,** 242, 1301-3.
111. Alibert, S.; Santelli-Rouvier, C.; Pradines, B.; Houdoin, C.; Parzy, D.; Karolak-Wojciechowska, J.; Barbe, J. Synthesis and effects on chloroquine susceptibility in Plasmodium falciparum of a series of new dihydroanthracene derivatives. *J Med Chem* **2002,** 45, 3195-209.
112. Pradines, B.; Alibert, S.; Houdoin, C.; Santelli-Rouvier, C.; Mosnier, J.; Fusai, T.; Rogier, C.; Barbe, J.; Parzy, D. In vitro increase in chloroquine accumulation induced by dihydroethano- and ethenoanthracene derivatives in Plasmodium falciparum-parasitized erythrocytes. *Antimicrob Agents Chemother* **2002,** 46, 2061-8.
113. Pradines, B.; Alibert-Franco, S.; Houdoin, C.; Mosnier, J.; Santelli-Rouvier, C.; Papa, V.; Rogier, C.; Fusai, T.; Barbe, J.; Parzy, D. In vitro reversal of chloroquine resistance in Plasmodium falciparum with dihydroethanoanthracene derivatives. *Am J Trop Med Hyg* **2002,** 66, 661-6.
114. Millet, J.; Torrentino-Madamet, M.; Alibert, S.; Rogier, C.; Santelli-Rouvier, C.; Mosnier, J.; Baret, E.; Barbe, J.; Parzy, D.; Pradines, B. Dihydroethanoanthracene derivatives as in vitro malarial chloroquine resistance reversal agents. *Antimicrob Agents Chemother* **2004,** 48, 2753-6.
115. Arimochi, H.; Morita, K. Characterization of cytotoxic actions of tricyclic antidepressants on human HT29 colon carcinoma cells. *Eur J Pharmacol* **2006,** 541, 17-23.
116. Mao, X.; Hou, T.; Cao, B.; Wang, W.; Li, Z.; Chen, S.; Fei, M.; Hurren, R.; Gronda, M.; Wu, D.; Trudel, S.; Schimmer, A. D. The tricyclic antidepressant amitriptyline inhibits D-cyclin transactivation and induces myeloma cell apoptosis by inhibiting histone deacetylases: in vitro and in silico evidence. *Mol Pharmacol* **2011,** 79, 672-80.
117. Jeon, S.-H.; Kim, S. H.; Kim, Y.; Kim, Y. S.; Lim, Y.; Lee, Y. H.; Shin, S. Y. The tricyclic antidepressant imipramine induces autophagic cell death in U-87MG glioma cells. *Biochemical and Biophysical Research Communications* **2011,** 413, 311-317.

118. Walker, A. J.; Grainge M Fau - Bates, T. E.; Bates Te Fau - Card, T. R.; Card, T. R. Survival of glioma and colorectal cancer patients using tricyclic antidepressants post-diagnosis, cancer causes and control **2012**, 12, 1959
119. Walker, A. J.; Card, T.; Bates, T. E.; Muir, K. Tricyclic antidepressants and the incidence of certain cancers: a study using the GPRD. *Br J Cancer* **2011,** 104, 193-197.
120. Daley, E.; Wilkie, D.; Loesch, A.; Hargreaves, I. P.; Kendall, D. A.; Pilkington, G. J.; Bates, T. E. Chlorimipramine: A novel anticancer agent with a mitochondrial target. *Biochemical and Biophysical Research Communications* **2005,** 328, 623-632.
121. Parker, K. A.; Glaysher, S.; Hurren, J.; Knight, L. A.; McCormick, D.; Suovouri, A.; Amberger-Murphy, V.; Pilkington, G. J.; Cree, I. A. The effect of tricyclic antidepressants on cutaneous melanoma cell lines and primary cell cultures. *Anticancer Drugs* **2012,** 23, 65-9.
122. Higgins, S. C.; Pilkington, G. J. The in vitro effects of tricyclic drugs and dexamethasone on cellular respiration of malignant glioma. *Anticancer Res* **2010,** 30, 391-7.
123. Lieb, J. Defeating cancer with antidepressants. *Ecancermedicalscience* **2008,** 2, 88.
124. Kinjo, T.; Kowalczyk, P.; Kowalczyk, M.; Walaszek, Z.; Slaga, T. J.; Hanausek, M. Effects of desipramine on the cell cycle and apoptosis in Ca3/7 mouse skin squamous carcinoma cells. *Int J Mol Med* **2010,** 25, 861-7.
125. Xia, Z.; Karlsson, H.; DePierre, J. W.; NÄSsberger, L. Tricyclic antidepressants induce apoptosis in human T lymphocytes. *International Journal of Immunopharmacology* **1998,** 19, 645-654.
126. Karlsson, H.; Gu, Y.; DePierre, J.; Nassberger, L. Induction of apoptosis in proliferating lymphocytes by tricyclic antidepressants. *Apoptosis*, **1998**; Vol. 3, pp 255-60.
127. Xia, Z.; DePierre, J. W.; Nassberger, L. Modulation of apoptosis induced by tricyclic antidepressants in human peripheral lymphocytes. *J Biochem Mol Toxicol*, **1998**; Vol. 12, pp 115-23.
128. Xia, Z.; Bergstrand, A.; DePierre, J. W.; Nassberger, L. The antidepressants imipramine, clomipramine, and citalopram induce apoptosis in human acute myeloid leukemia HL-60 cells via caspase-3 activation. *J Biochem Mol Toxicol*, **1999**; Vol. 13, pp 338-47.
129. Clayden, J.; Frampton, C. S.; McCarthy, C.; Westlund, N. Perilithiation and the synthesis of 8-substituted-1-naphthamides. *Tetrahedron* **1999,** 55, 14161-14184.
130. Hemantha, H. P.; Sureshbabu, V. V. Poly(vinyl)chloride supported palladium nanoparticles: catalyst for rapid hydrogenation reactions. *Organic & Biomolecular Chemistry* **2011,** 9, 2597-2601.
131. Kelly, S. M.; Lipshutz, B. H. Chemoselective Reductions of Nitroaromatics in Water at Room Temperature. *Organic letters* **2014,** 16, 98-101.
132. Li, M.; Hu, L.; Cao, X.; Hong, H.; Lu, J.; Gu, H. Direct Hydrogenation of Nitroaromatics and One-Pot Amidation with Carboxylic Acids over Platinum Nanowires. *Chemistry – A European Journal* **2011,** 17, 2763-2768.
133. Noland, W. E. The NEF Reaction. *Chemical Reviews* **1955,** 55, 137-155.
134. Feuer, H.; Bartlett, R. S.; Vincent, B. F.; Anderson, R. S. Diborane Reduction of Nitro Salts. A New Synthesis of N-Monosubstituted Hydroxylamines. *The Journal of Organic Chemistry* **1965,** 30, 2880-2882.
135. Cisneros, L.; Serna, P.; Corma, A. Selective Reductive Coupling of Nitro Compounds with Aldehydes to Nitrones in H2 Using Carbon-Supported and -Decorated Platinum Nanoparticles. *Angewandte Chemie International Edition* **2014,** 53, 9306-9310.
136. Soengas, R. G.; Acurcio, R.; Silva, A. M. S. Preparation of indium nitronates and their Henry reactions. *Organic & Biomolecular Chemistry* **2014,** 12, 8593-8597.
137. Erdmann. *Chemische Berichte* **1884,** 17, 412.
138. Priebs. *Justus Liebigs Annalen der Chemie* **1884,** 225, 321.

139. Maity, S.; Manna, S.; Rana, S.; Naveen, T.; Mallick, A.; Maiti, D. Efficient and Stereoselective Nitration of Mono- and Disubstituted Olefins with $AgNO_2$ and TEMPO. *Journal of the American Chemical Society* **2013,** 135, 3355-3358.
140. Begari, E.; Singh, C.; Nookaraju, U.; Kumar, P. Clay-Supported Copper Nitrate (Claycop): A Mild Reagent for the Selective Nitration of Aromatic Olefins. *Synlett* **2014,** 25, 1997-2000.
141. Naveen, T.; Maity, S.; Sharma, U.; Maiti, D. A Predictably Selective Nitration of Olefin with Fe(NO3)3 and TEMPO. *The Journal of Organic Chemistry* **2013,** 78, 5949-5954.
142. Das, J. P.; Sinha, P.; Roy, S. A nitro-hunsdiecker reaction: from unsaturated carboxylic acids to nitrostyrenes and nitroarenes. *Org Lett*, **2002**; Vol. 4, pp 3055-8.
143. Wadsworth, W. S. Synthetic Applications of Phosphoryl-Stabilized Anions. *Organic Reactions*, John Wiley & Sons, Inc. London: **2004**.
144. Black, P. J.; Cami-Kobeci, G.; Edwards, M. G.; Slatford, P. A.; Whittlesey, M. K.; Williams, J. M. J. Borrowing hydrogen: iridium-catalysed reactions for the formation of C-C bonds from alcohols. *Organic & Biomolecular Chemistry* **2006,** 4, 116-125.
145. Rahmani-Nezhad, S.; Safavi, M.; Pordeli, M.; Ardestani, S. K.; Khosravani, L.; Pourshojaei, Y.; Mahdavi, M.; Emami, S.; Foroumadi, A.; Shafiee, A. Synthesis, *in vitro* cytotoxicity and apoptosis inducing study of 2-aryl-3-nitro-2H-chromene derivatives as potent anti-breast cancer agents. *Eur J Med Chem* **2014,** 86, 562-9.
146. Qian, W.; Lu, W.; Sun, H.; Li, Z.; Zhu, L.; Zhao, R.; Zhang, L.; Zhou, S.; Zhou, Y.; Jiang, H.; Zhen, X.; Liu, H. Design, synthesis, and pharmacological evaluation of novel tetrahydroprotoberberine derivatives: Selective inhibitors of dopamine D1 receptor. *Bioorganic & Medicinal Chemistry* **2012,** 20, 4862-4871.
147. Jalal, S.; Sarkar, S.; Bera, K.; Maiti, S.; Jana, U. Synthesis of Nitroalkenes Involving a Cooperative Catalytic Action of Iron(III) and Piperidine: A One-Pot Synthetic Strategy to 3-Alkylindoles, 2H-Chromenes and N-Arylpyrrole. *European Journal of Organic Chemistry* **2013,** 2013, 4823-4828.
148. Xu, C.; Du, J.; Ma, L.; Li, G.; Tao, M.; Zhang, W. Tertiary amine functionalized polyacrylonitrile fiber catalyst for the synthesis of tetrahydrothiophenes. *Tetrahedron* **2013,** 69, 4749-4757.
149. Chandrasekhar, S.; Shrinidhi, A. Useful Extensions of the Henry Reaction: Expeditious Routes to Nitroalkanes and Nitroalkenes in Aqueous Media. *Synthetic Communications* **2014,** 44, 3008-3018.
150. Reaxys. (2014) https://www.reaxys.com/reaxys/secured/search.do [20/01/2015]
151. Negishi, T.; Nakano, M.; Yanai, K.; Kim, C. H.; Fukushima, M. Isolation and identification of beta-nitrostyrene from smoked chicken. *Environ Pollut*, **1988**; Vol. 50, 279-83.
152. Sagitullina, G. P.; Glizdinskaya, L. V.; Sitnikov, G. V.; Sagitullin, R. S. Nitropyridines. Part 1. Hantzsch Synthesis of Nitropyridines and Their Quaternary Salts. *ChemInform* **2003,** 34.
153. Shengule, S. R.; Ryder, G.; Willis, A. C.; Pyne, S. G. Highly diastereoselective N-acyliminium ion cyclization reactions of a tethered furan. *Tetrahedron* **2012,** 68, 10280-10285.
154. Varma, R. S.; Dahiya, R.; Kumar, S. Microwave-assisted Henry reaction: Solventless synthesis of conjugated nitroalkenes. *Tetrahedron Letters* **1997,** 38, 5131-5134.
155. Mase, N.; Takabe, K.; Tanaka, F. Fluorogenic probes for chemical transformations: 9-anthracene derivatives for monitoring reaction progress by an increase in fluorescence. *Tetrahedron Letters* **2013,** 54, 4306-4308.
156. Weber, M.; Frey, W.; Peters, R. Asymmetric Palladium(II)-Catalyzed Cascade Reaction Giving Quaternary Amino Succinimides by 1,4-Addition and a Nef-Type Reaction. *Angewandte Chemie International Edition* **2013,** 52, 13223-13227.

157. McNulty, J.; Steere, J. A.; Wolf, S. The ultrasound promoted Knoevenagel condensation of aromatic aldehydes. *Tetrahedron Letters* **1998,** 39, 8013-8016.
158. Bandgar, B. P., Uppalla, L.S. Gel Entrapped Base Catalysed (GEBC) Henry Reaction: Synthesis of Conjugated Nitroalkenes. Synthetic Communications: **2000**; Vol. 30, pp 2071-2075.
159. Alizadeh, A.; Khodaei, M. M.; Eshghi, A. Ambiphilic Dual Activation Role of a Task-Specific Ionic Liquid: 2-Hydroxyethylammonium Formate as a Recyclable Promoter and Medium for the Green Synthesis of β-Nitrostyrenes. *J. Org. Chem.* **2010,** 75, 8295-8298.
160. Bailey, K.; Legault, D. Analysis of the 13C NMR spectra of mono- and dimethoxy-β-methyl-β-nitrostyrenes: Spectral assignments and conformational effects. *Organic Magnetic Resonance* **1981,** 16, 47-51.
161. Milhazes, N.; Calheiros, R.; Marques, M. P. M.; Garrido, J.; Cordeiro, M. N. D. S.; Rodrigues, C.; Quinteira, S.; Novais, C.; Peixe, L.; Borges, F. β-Nitrostyrene derivatives as potential antibacterial agents: A structure–property–activity relationship study. *Bioorganic & Medicinal Chemistry* **2006,** 14, 4078-4088.
162. Calheiros, R.; Milhazes, N.; Borges, F.; Marques, M. P. M. β-Nitrostyrene derivatives—a conformational study by combined Raman spectroscopy and ab initio MO calculations. *Journal of Molecular Structure* **2004,** 692, 91-106.
163. Concellón, J. M.; Bernad, P. L.; Rodríguez-Solla, H.; Concellón, C. A Convenient Samarium-Promoted Synthesis of Aliphatic (E)-Nitroalkenes under Mild Conditions†. *The Journal of Organic Chemistry* **2007,** 72, 5421-5423.
164. Arora, P. K.; Bhaduri, A. P. Sodium borohydride reduction of 3-nitro-2-substituted-phenyl-2H-[1]benzopyrans. *Indian J. Chem., Sect. B* **1981,** 20B, 951-4.
165. Silveira, C. C.; Bernardi, C. R.; Braga, A. L.; Kaufman, T. S. Pictet-Spengler condensation of N-sulfonyl-β-phenethylamines with α-chloro-α-phenylselenoesters. New synthesis of 1,2,3,4-tetrahydroisoquinoline-1-carboxylates. *Tetrahedron Letters* **1999,** 40, 4969-4972.
166. Anderson, J. C.; Blake, A. J.; Koovits, P. J.; Stepney, G. J. Diastereoselective Reductive Nitro-Mannich Reactions. *The Journal of Organic Chemistry* **2012,** 77, 4711-4724.
167. Huang, W.; Peng, C.; Guo, L.; Hu, R.; Han, B. Enantio- and Diastereoselective Nitro-Mannich Reactions with in situ Generated N-Boc-imines Catalyzed by a Bifunctional Thiourea-Guanidine Catalyst. *Synlett* **2011,** 2011, 2981-2984.
168. Prasad, V.; Kale, R. R.; Mishra, B. B.; Kumar, D.; Tiwari, V. K. Diacetoxyiodobenzene Mediated One-Pot Synthesis of Diverse Carboxamides from Aldehydes. *Organic Letters* **2012,** 14, 2936-2939.
169. Moore, J. D.; Herpel, R. H.; Lichtsinn, J. R.; Flynn, D. L.; Hanson, P. R. ROMP-Generated Oligomeric Sulfonyl Chlorides as Versatile Soluble Scavenging Agents. *Organic Letters* **2003,** 5, 105-107.
170. Ziyaei-Halimehjani, A.; Saidi, M. R. Synthesis of aza-Henry products and enamines in water by Michael addition of amines or thiols to activated unsaturated compounds. *Tetrahedron Lett.* **2008,** 49, 1244-1248.
171. Deb, I.; Shanbhag, P.; Mobin, S. M.; Namboothiri, I. N. N. Morita–Baylis–Hillman Reactions Between Conjugated Nitroalkenes or Nitrodienes and Carbonyl Compounds. *European Journal of Organic Chemistry* **2009,** 2009, 4091-4101.
172. Perrella, F. W.; Chen, S.-F.; Behrens, D. L.; Kaltenbach, R. F., III; Seitz, S. P. Phospholipase C Inhibitors: A New Class of Agents. *Journal of Medicinal Chemistry* **1994,** 37, 2232-2237.
173. Bakthadoss, M.; Sivakumar, N. First Friedel-Crafts reaction of the Baylis-Hillman adducts derived from nitroolefins: application towards synthesis of pyrrolidines and spiropyrrolidines. *Synlett* **2011**, 1296-1302.

174. An, J.; Lu, L.-Q.; Yang, Q.-Q.; Wang, T.; Xiao, W.-J. Enantioselective Construction of Oxa- and Aza-Angular Triquinanes through Tandem [4 + 1]/[3 + 2] Cycloaddition of Sulfur Ylides and Nitroolefins. *Organic Letters* **2013,** 15, 542-545.
175. Quiclet-Sire, B.; Zard, S. Z. The Synthesis of 1,2,3-Triazoles from Nitroalkenes - Revisited. *Synthesis* **2005,** 2005, 3319-3326.
176. Mur Blanch, N.; Chabot, G. G.; Quentin, L.; Scherman, D.; Bourg, S.; Dauzonne, D. In vitro and in vivo biological evaluation of new 4,5-disubstituted 1,2,3-triazoles as cis-constrained analogs of combretastatin A4. *European Journal of Medicinal Chemistry* **2012,** 54, 22-32.
177. Weiss, K. M.; Wei S Fau - Tsogoeva, S. B.; Tsogoeva, S. B. Novel one-pot process for the synthesis of 1,3-thiazoles via organocatalysed epoxidation of nitro-olefins, org. biomol. Chem, **2011**,9, 3457
178. Noland, W. E.; Freeman, H. I.; Baker, M. S. The Diels-Alder Reaction of Anthracene with Nitroölefins. A New Route to 11-Nitro- and 11-Amino-9,10-dihydro-9,10-ethanoanthracenes1. *Journal of the American Chemical Society* **1956,** 78, 188-192.
179. Denmark, S. E.; Thorarensen, A. Tandem [4+2]/[3+2] Cycloadditions of Nitroalkenes. *Chem Rev*, 1996; Vol. 96, pp 137-166.
180. Noland, W. E.; Kedrowski, B. L. Synthesis of angular quinoid heterocycles from 2-(2-nitrovinyl)-1,4-benzoquinone. *J. Org. Chem.* **1999,** 64, 596-603.
181. Ganesh, M.; Namboothiri, I. N. N. Stereospecific approach to α,β-disubstituted nitroalkenes via coupling of α-bromonitroalkenes with boronic acids and terminal acetylenes. *Tetrahedron* **2007,** 63, 11973-11983.
182. Yao, C.-F.; Chen, W.-C.; Lin, Y.-M. Reactions of β-nitrostyrenes with Gragnard reagents. *Tetrahedron Letters* **1996,** 37, 6339-6342.
183. Durini, M.; Sahr, F. A.; Kuhn, M.; Civera, M.; Gennari, C.; Piarulli, U. Bifunctional 2,5-Diketopiperazines as Efficient Organocatalysts for the Enantioselective Conjugate Addition of Aldehydes to Nitroolefins. *European Journal of Organic Chemistry* **2011,** 2011, 5599-5607.
184. Stetter, H. Catalyzed Addition of Aldehydes to Activated Double Bonds—A New Synthetic Approach. *Angewandte Chemie International Edition in English* **1976,** 15, 639-647.
185. Schales, O.; Graefe, H. A. Arylnitroalkenes: A New Group of Antibacterial Agents1. *Journal of the American Chemical Society* **1952,** 74, 4486-4490.
186. Cornell, H.; Nguyen, T.; Nicoletti, G.; Jackson, N.; Hügel, H. Comparisons of Halogenated β-Nitrostyrenes as Antimicrobial Agents. *Applied Sciences* **2014,** 4, 380-389.
187. Denisenko, P. P.; Sapronov, N. S.; Tarasenko, A. A. (2012) Nitro-styrene derivatives having antimicrobial activity. Patent: EP2471531 A2
188. McGowan, J. C.; Brian, P. W.; Hemming, H. G. The Fungistatic Activity of Ethylenic and Acetylenic Compounds. *Annals of Applied Biology* **1948,** 35, 25-36.
189. Nicoletti, G.; Cornell, H. J.; Hugel, H. M.; White, K. S.; Nguyen, T.; Zalizniak, L.; Nugegoda, D. Synthesis and Antimicrobial Activity of Nitroalkenyl Arenes. *Anti-Infective Agents* **2013,** 11, 179-191.
190. White, K. S.; Nicoletti, G.; Borland, R. Nitropropenyl benzodioxole, an anti-infective agent with action as a protein tyrosine phosphatase inhibitor. *Open Med Chem J*, 2014; Vol. 8, pp 1-16.
191. Koremura, M.; Oku, H.; Shono, T.; Nakanishi, T. Relation between chemical structure and antimicrobial and insecticidal activities in organonitro compounds. VIII. Synthesis of heterocyclic nitroalkene derivatives and their activities. *Takamine Kenkyusho Nenpo* **1961,** 13, 216-21.

192. Carter, K. C.; Finnon, Y. S.; Daeid, N. N.; Robson, D. C.; Waddell, R. the effect of nitrostyrene on cell proliferation and macrophage immune responses. *Immunopharmacology and Immunotoxicology* **2002,** 24, 187-197.
193. Jordan, A.; Hadfield, J. A.; Lawrence, N. J.; McGown, A. T. Tubulin as a target for anticancer drugs: Agents which interact with the mitotic spindle. *Medicinal Research Reviews* **1998,** 18, 259-296.
194. Borah, S.; Xi, L.; Zaug, A. J.; Powell, N. M.; Dancik, G. M.; Cohen, S. B.; Costello, J. C.; Theodorescu, D.; Cech, T. R. TERT promoter mutations and telomerase reactivation in urothelial cancer. *Science* **2015,** 347, 1006-1010.
195. Park, J.; Pei, D. trans-β-Nitrostyrene Derivatives as Slow-Binding Inhibitors of Protein Tyrosine Phosphatases. *Biochemistry* **2004,** 43, 15014-15021.
196. Villar, J. A.; Lima, F. T.; Veber, C. L.; Oliveira, A. R.; Calgarotto, A. K.; Marangoni, S.; da Silva, S. L. Synthesis and evaluation of nitrostyrene derivative compounds, new snake venom phospholipase A2 inhibitors. *Toxicon*, 2008; Vol. 51, pp 1467-78.
197. Li, H.-h.; Huang, H.; Zhang, X..; Luo, X..; Lin, L.; Jiang, H..; Ding, J.; Chen, K.; Liu, H. Discovering novel 3-nitroquinolines as a new class of anticancer agents. *Acta Pharmacol Sin* **2008,** 29, 1529-1538.
198. Chen, G.; Hao, X.-J.; Sun, Q.-Y.; Ding, J. Rapid synthesis and bioactivities of 3-(nitromethylene)indolin-2-one analogues. *Chemical Papers* **2010,** 64, 673-677.
199. Crew, A.; Li, A. H.; Panicker, B. (2005) (arylamidoanilino) nitroethylene compounds. Patent: US7618965 B2
200. Keating, J. J. Studies in the synthesis and impurity profiling of methlenedioxy and alkylthioamphetamines, PhD Thesis. Trinity College Dublin, Dublin, 2001.
201. Cloonan, S. M.; Keating, J. J.; Corrigan, D.; O'Brien, J. E.; Kavanagh, P. V.; Williams, D. C.; Meegan, M. J. Synthesis and *in vitro* toxicity of 4-MTA, its characteristic clandestine synthesis byproducts and related sulfur substituted α-alkylthioamphetamines. *Bioorganic & Medicinal Chemistry* **2010,** 18, 4009-4031.
202. Renton, R. J.; Cowie, J. S.; Oon, M. C. A study of the precursors, intermediates and reaction by-products in the synthesis of 3,4-methylenedioxymethylamphetamine and its application to forensic drug analysis. *Forensic Sci Int* **1993,** 60, 189-202.
203. Rudnick, G.; Wall, S. C. The molecular mechanism of "ecstasy" [3,4-methylenedioxy-methamphetamine (MDMA)]: serotonin transporters are targets for MDMA-induced serotonin release. *Proceedings of the National Academy of Sciences* **1992,** 89, 1817-1821.
204. Huizer, H.; Theeuwen, A. B. E.; Verweij, A. M. A.; Sinnema, A.; Van Der Toorn, J. M. Impurities in Illicit Amphetamine. *Journal of the Forensic Science Society* **1981,** 21, 225-232.
205. Kirkbride, K. P.; Ward, A. D.; Jenkins, N. F.; Klass, G.; Coumbaros, J. C. Synthesis of 4-methyl-5-arylpyrimidines and 4-arylpyrimidines: route specific markers for the Leuckardt preparation of amphetamine, 4-methoxyamphetamine, and 4-methylthioamphetamine. *Forensic Sci Int* **2001,** 115, 53-67.
206. Bohn, M.; Bohn, G.; Blaschke, G. Synthesis markers in illegally manufactured 3,4-methylenedioxyamphetamine and 3,4-methylenedioxymethamphetamine. *Int J Legal Med* **1993,** 106, 19-23.
207. Wasik, A. M.; Gandy, M. N.; McIldowie, M.; Holder, M. J.; Chamba, A.; Challa, A.; Lewis, K. D.; Young, S. P.; Scheel-Toellner, D.; Dyer, M. J.; Barnes, N. M.; Piggott, M. J.; Gordon, J. Enhancing the anti-lymphoma potential of 3,4-methylenedioxymethamphetamine ('ecstasy') through iterative chemical redesign: mechanisms and pathways to cell death. *Invest New Drugs* **2011**.
208. Simantov, R.; Tauber, M. The abused drug MDMA (Ecstasy) induces programmed death of human serotonergic cells. *The FASEB Journal* **1997,** 11, 141-146.

209. Li, J. J. *Name Reactions, A Collection of Detailed Reaction Mechanisms*. 2 ed.; Springer-Verlag: Heidelberg, 2003.
210. Henry, L. Compt. Rend.: 1895; Vol. 120, p 1265.
211. Smith, B. S.; J., M. *March's Advanced Organic Chemistry*. 6 ed.; John Wiley & Sons: New Jersey, 2007.
212. Raiford, L. C.; Fox, D. E. condensation of vanillin substitution products with nitromethane. *The Journal of Organic Chemistry* **1944,** 09, 170-174.
213. Martínez-Bescos, P.; Cagide-Fagín, F.; Roa, L. F.; Ortiz-Lara, J. C.; Kierus, K.; Ozores-Viturro, L.; Fernández-González, M.; Alonso, R. Synthesis, Structure, and E−Z Isomerization of β-(Hetero)aryl-α-nitro-α,β-enals. *The Journal of Organic Chemistry* **2008,** 73, 3745-3753.
214. Dauzonne, D.; Royer, R. A Verstatile Synthesis of 1-Aryl-2-nitro-3-(3,4,5-trimethoxyphenyl)-propenes are Precursors of Novel Mescaline Derivatives. Chem. Pharm. Bull: **1986**; Vol. 34, 1628-1633.
215. Kodukulla, R. P. K.; Trivedi, G. K.; Vora, J. D.; Mathur, H. H. Synthesis, Chemical Transformation and Antimicrobial Activity of a Novel Class of Nitroolefins: 1,3-Diaryl-2-nitroprop-1-enes. *Synthetic Communications* **1994,** 24, 819-832.
216. Rodríguez, J. M.; Dolors Pujol, M. Straightforward synthesis of nitroolefins by microwave- or ultrasound-assisted Henry reaction. *Tetrahedron Letters* **2011,** 52, 2629-2632.
217. Wang, C.; Wang, S. The rapid synthesis of B-nitrostyrenes under microwave irradiation without solvent. Synthetic Communications: **2002**; Vol. 32, pp 3481-3486.
218. Bhattacharjya, A.; Mukhopadhyay, R.; Pakrashi, S. C. Sodium Borohydride Reduction of Nitrostyrenes by Reverse Addition: A Simple and Efficient Method for the Large-Scale Preparation of Phenylnitroethanes. *Synthesis* **1985,** 1985, 886,887.
219. Sinhababu, A. K.; Borchardt, R. T. Silica gel-assisted reduction of nitrostyrenes to 2-aryl-1-nitroalkanes with sodium borohydride. *Tetrahedron Letters* **1983,** 24, 227-230.
220. Ohta, H.; Kobayashi, N.; Ozaki, K. Asymmetric reduction of nitro olefins by fermenting bakers' yeast. *The Journal of Organic Chemistry* **1989,** 54, 1802-1804.
221. Hu, H.; Huang, Y.; Guo, Y. Henry reaction of fluorinated nitro compounds. *Journal of Fluorine Chemistry* **2012,** 133, 108-114.
222. Franklin, A. S. A modified Horner-Wadsworth-Emmons reaction for the synthesis of nitroalkenes. *Synlett* **2000**, 1154-1156.
223. Nanjo, K.; Sekiya, M. Formic Acid Reduction. XXVII. Selective Reduction of Carbon-Carbon Double Bonds conjugated with Nitro and Sulfonyl Groups. *chemical & pharmaceutical bulletin* **1979,** 27, 198-203.
224. Božić, D. D.; Milenković, M.; Ivković, B.; Ćirković, I. Antibacterial activity of three newly-synthesized chalcones & synergism with antibiotics against clinical isolates of methicillin-resistant Staphylococcus aureus. *Indian Journal of Medical Research. Jul2014* **2014,** 140, 130.
225. Nakhjavani, M.; Zarghi, A.; Shirazi, F. H. Cytotoxicity of selected novel chalcone derivatives on human breast, lung and hepatic carcinoma cell lines. *Iran. J. Pharm. Res.* **2014,** 13, 953-958.
226. Kupcewicz, B.; Jarzęcki, A. A.; Małecka, M.; Krajewska, U.; Rozalski, M. Cytotoxic activity of substituted chalcones in terms of molecular electronic properties. *Bioorganic & Medicinal Chemistry Letters* **2014,** 24, 4260-4265.
227. Bharat, K. B.; Kaladhar, S. V. G. K. D.; Vasudeva, R. A.; Divakar, N. L. S.; Subhash, Y.; Amita, C. M. P. Evaluation of anti-inflammatory activity of some novel diarylsulfonylurea-chalcone hybrids in carrageenan-induced paw edema in rats. *Int. J. Pharm. (Hyderabad, India)* **2014,** 4, 313-316.

228. Mélot, J. M.; Texier-Boullet, F.; Foucaud, A. Alumina supported potassium fluoride promoted reaction of nitroalkanes with electrophilic alkenes : synthesis of 4,5-dihydro furans and isoxazoline n-oxides. *Tetrahedron* **1988,** 44, 2215-2224.
229. Li, R.; Liu, Z.; Zhou, Y.; Wu, L. Highly Stereoselective Nitration of Chalcone Derivatives with Nitric Oxide. *Synlett* **2006,** 2006, 1367-1368.
230. Michael, A. Ueber die Addition von Natriumacetessig- und Natriummalonsäureäthern zu den Aethern ungesättigter Säuren. *Journal für Praktische Chemie* **1887,** 35, 349-356.
231. Meisenheimer, J.; Heim, F. Ueber das Verhalten des Phenyl-nitro-äthylens gegen Alkali. *Berichte der deutschen chemischen Gesellschaft* **1905,** 38, 466-473.
232. Kotrusz, P.; Toma, S. L-Proline Catalyzed Michael Additions of Thiophenols to α,β-Unsaturated Compounds, Particularly α-Enones, in the Ionic Liquid [bmim]PF6. *Molecules* **2006,** 11, 197-205.
233. Menguy, L.; Couty, F. Azetidine-derived bifunctional organocatalysts for Michael reactions. *Tetrahedron: Asymmetry* **2010,** 21, 2385-2389.
234. Choudhary, G.; Peddinti, R. K. An expeditious, highly efficient, catalyst-free and solvent-free synthesis of nitroamines and nitrosulfides by Michael addition. *Green Chemistry* **2011,** 13, 276-282.
235. Tamaddon, F.; Tayefi, M.; Hosseini, E.; Zare, E. Dolomite (CaMg(CO3)2) as a recyclable natural catalyst in Henry, Knoevenagel, and Michael reactions. *Journal of Molecular Catalysis A: Chemical* **2013,** 366, 36-42.
236. Katerinopoulos, H. E.; Tagmatarchis, N.; Zaponakis, G.; Kefalakis, N.; Kordatos, K.; Spyrakis, M.; Thermos, K. β-Alkoxy-substituted phenethylamines: a family of compounds potentially active at the dopamine and α-adrenergic receptors. *European Journal of Medicinal Chemistry* **1995,** 30, 949-954.
237. Baylis, A. B.; Hillman, M. E. D. Ger. Pat. 155: 1972; Vol. 2, p 113.
238. Basavaiah, D.; Rao, A. J.; Satyanarayana, T. Recent Advances in the Baylis−Hillman Reaction and Applications - Chemical Reviews (ACS Publications). *Chem. Rev.* **2003**, 811-891.
239. Park, K.-S.; Kim, J.; Choo, H.; Chong, Y. Octanol-Accelerated Baylis-Hillman Reaction. *Synlett* **2007,** 2007, 0395-0398.
240. Yu, C.; Hu, L. Successful Baylis−Hillman Reaction of Acrylamide with Aromatic Aldehydes. *The Journal of Organic Chemistry* **2001,** 67, 219-223.
241. K. Aggarwal, V.; Mereu, A. Superior amine catalysts for the Baylis-Hillman reaction: the use of DBU and its implications. *Chemical Communications* **1999**, 2311-2312.
242. Bakthadoss, M.; Sivakumar, N.; Devaraj, A. ChemInform Abstract: First Synthesis of Bromo and Chloro Derivatives of Baylis—Hillman Adducts Derived from Nitroolefins: Application Towards the Synthesis of a Dendrimer Core. *ChemInform* **2012,** 42.
243. Rastogi, N.; Namboothiri, I. N. N.; Cojocaru, M. α-Hydroxymethylation of conjugated nitroalkenes via the Morita–Baylis–Hillman reaction. *Tetrahedron Letters* **2004,** 45, 4745-4748.
244. Cai, J.; Zhou, Z.; Zhao, G.; Tang, C. Dramatic Rate Acceleration of the Baylis−Hillman Reaction in Homogeneous Medium in the Presence of Water. *Organic Letters* **2002,** 4, 4723-4725.
245. Kumar, N. N. B.; Chakravarty, M.; Kumar, N. S.; Sajna, K. V.; Swamy, K. C. K. Allenylphosphonates with a 1,3,2-dioxaphosphorinane ring: synthesis, structures, stability and utility. *J. Chem. Sci. (Bangalore, India)* **2009,** 121, 23-36.
246. Sousa, S. C. O.; Junior, C. G. L.; Silva, F. P. L.; Andrade, N. G.; Barbosa, T. P.; Vasconcellos, M. L. A. A. Microwave-promoted morita-baylis-hillman reactions: efficient synthesis of new monoacylglycerols (MAGs) as potential anti-parasitic compounds. *Journal of the Brazilian Chemical Society* **2012,** 22, 1634-1643.

247. Pei, W.; Wei, H.-X.; Li, G. Lewis acid-promoted Baylis-Hillman-type reaction of [small alpha],[small beta]-unsaturated ethyl thioester with aldehydes without the use of a Lewis base. *Chemical Communications* **2002**, 1856-1857.
248. Griffiths, J. Benzoquinone and Naphthoquinone Dyes. In *Ullmann's Encyclopedia of Industrial Chemistry*, Wiley-VCH Verlag GmbH & Co. KGaA: 2000.
249. Kim, M. H.; Jo Sh Fau - Ha, K.-S.; Ha Ks Fau - Song, J.-H.; Song Jh Fau - Jang, H.-D.; Jang Hd Fau - Kwon, Y.-I.; Kwon, Y. I. Antimicrobial activities of 1,4-benzoquinones and wheat germ extract., J Microbiol Biotechnol, **2010,** 8, 20, 1204
250. Witty, T. R.; Remers, W. A. Synthesis and antitumor and antibacterial activity of benzoquinones related to the mitomycins. *Journal of Medicinal Chemistry* **1973,** 16, 1280-1284.
251. Lusthof, K. J.; Richter W Fau - de Mol, N. J.; de Mol Nj Fau - Janssen, L. H.; Janssen Lh Fau - Verboom, W.; Verboom W Fau - Reinhoudt, D. N.; Reinhoudt, D. N. Reductive activation of potential antitumor bis(aziridinyl)benzoquinones by xanthine oxidase: competition between oxygen reduction and quinone reduction, Arch Biochem Biophys, **1990** 1, 137
252. Jacob, P.; Callery, P. S.; Shulgin, A. T.; Castagnoli, N. A convenient synthesis of quinones from hydroquinone dimethyl ethers. Oxidative demethylation with ceric ammonium nitrate. *The Journal of Organic Chemistry* **1976,** 41, 3627-3629.
253. Firouzabadi, H.; Mohajer, D.; Entezari-Moghadam, M. *Bulletin of the Chemical Society of Japan* **1988,** 61, 2185-2189.
254. Willis, J. P.; Gogins, K. A. Z.; Miller, L. L. Pyridinium chlorochromate releases quinones from hydroquinone silyl ethers. *The Journal of Organic Chemistry* **1981,** 46, 3215-3218.
255. Gupta, D. N.; Hodge, P.; Davies, J. E. Oxidation reactions using sodium metaperiodate supported on silica gel. *Journal of the Chemical Society, Perkin Transactions 1* **1981**, 2970-2973.
256. Ashwell, M.; Jackson, R. F. W. Phenylsulphonyl oxirane: a versatile reagent for organic synthesis. *Journal of the Chemical Society, Chemical Communications* **1988**, 645-647.
257. Eilon, G. F.; Gu J Fau - Slater, L. M.; Slater Lm Fau - Hara, K.; Hara K Fau - Jacobs, J. W.; Jacobs, J. W. Tumor apoptosis induced by epoxide-containing piperazines, a new class of anti-cancer agents, Cancer Chemother Pharmacol. **2000**, 3, 45
258. Han, H.; Zhao Y Fau - Cuthbertson, T.; Cuthbertson T Fau - Hartman, R. F.; Hartman Rf Fau - Rose, S. D.; Rose, S. D. Cell cycle arrest and apoptosis induction by an anticancer chalcone epoxide, **2010**, 8, 429
259. Newman, H.; Angier, R. B. The preparation and chemistry of α-nitroepoxides. *Tetrahedron* **1970,** 26, 825-836.
260. Bortolini, O.; Nino, A. D.; Fogagnolo, M.; Fantin, G.; Mariuolo, L.; Tocci, A. Oxidative Cleavage of Nitroalkenes with Hydrogen Peroxide in Environmentally Acceptable Solvents. *Chemistry Letters* **2007,** 36, 472-473.
261. Wamhoff, H. *1,2,3-Triazoles and their Benzo Derivatives Comprehensive Heterocyclic Chemistry*. Pergamon Press: Oxford, 1984; Vol. 5.
262. Pokhodylo, N.; Shyyka, O.; Matiychuk, V. Synthesis and anticancer activity evaluation of new 1,2,3-triazole-4-carboxamide derivatives. *Medicinal Chemistry Research* **2014,** 23, 2426-2438.
263. Zefirov, N. S.; Chapovskaya, N. K.; Kolesnikov, V. V. Synthesis of 1,2,3-triazoles by reaction of azide ion with αβ-unsaturated nitro-compounds and nitriles. *Journal of the Chemical Society D: Chemical Communications* **1971**, 1001-1002.

264. Jin, T.; Kamijo, S.; Yamamoto, Y. Copper-Catalyzed Synthesis of N-Unsubstituted 1,2,3-Triazoles from Nonactivated Terminal Alkynes. *European Journal of Organic Chemistry* **2004**, 3789-3791.
265. Oh, S.; Shin, W.-S.; Ham, J.; Lee, S. Acid-catalyzed synthesis of 10-substituted triazolyl artemisinins and their growth inhibitory activity against various cancer cells. *Bioorganic & Medicinal Chemistry Letters* **2010,** 20, 4112-4115.
266. Lee, S.-J. Synthesis of 10β-Substituted Triazolyl Artemisinins and Their Growth Inhibitory Activity against Various Cancer Cells. *Bulletin of the Korean Chemical Society* **2011,** 32, 737-740.
267. Barluenga, J.; Valdés, C.; Beltrán, G.; Escribano, M.; Aznar, F. Developments in Pd Catalysis: Synthesis of 1H-1,2,3-Triazoles from Sodium Azide and Alkenyl Bromides. *Angewandte Chemie International Edition* **2006,** 45, 6893-6896.
268. Dehaen, W.; Bakulev, V. A.; Belskaya, N.; Subbotina, J.; Lesogorova, S. Synthesis of 2H-1,2,3-Triazoles. In *Chemistry of 1,2,3-triazoles*, Springer International Publishing: **2015**; Vol. 40, pp 51-116.
269. Posner, T. Unsaturated Compounds. IX. Addition of Hydroxylamine to Unsaturated Acids and Esters of the Cinnamic Acid Series and Analogous Compounds. *Justus Liebigs Ann. Chem.* **1912,** 389, 1-120.
270. Takaya, H.; Murahashi, S.-i. Activation of C-H bonds α to nitriles for combinatorial chemistry: ruthenium-catalyzed aldol and Michael reactions of polymer-supported nitriles. *Synlett* **2001**, 991-994.
271. Vink, M. K. S. *From Nitriles to Nitrogen Heterocycles: Chemoenzymatic Approaches Toward Diversely Substituted Enantiopure Building Blocks*. Universiteit van Amsterdam: **2003**.
272. Ania, D. B. *Parallel Synthesis of Potential Drugs Based on the 2-arylethyl Amine Moiety*. Thesis Radboud Universiteit Nijmegen **2009**.
273. Chen, Z.; Li, Y.; Zhou, J.; Wang, D.; Ge, M. K3PO4-catalyzed regiospecific bromoamidation of β,β-dicyanostyrene derivatives with N-bromoacetamide (NBA). *Chem. Res. Chin. Univ.* **2014,** 30, 266-271.
274. Balalaie, S.; Nemati, N. Ammonium Acetate-Basic Alumina Catalyzed Knoevenagel Condensation Under Microwave Irradiation Under Solvent-Free Condition. *Synthetic Communications* **2000,** 30, 869-875.
275. Balalaie, S.; Bararjanian, M.; Hekmat, S.; Salehi, P. Novel, efficient, and green procedure for the Knoevenagel condensation catalyzed by diammonium hydrogen phosphate in water. *Synth. Commun.* **2006,** 36, 3703-3711.
276. Linares, C. F.; Goldwasser, M. R.; Machado, F. J.; Rivera, A.; Rodríguez-Fuentes, G.; Barrault, J. Advantages of base exchanged natural clinoptilolite as a catalyst for the Knoevenagel reaction. *Microporous and Mesoporous Materials* **2000,** 41, 69-77.
277. Javanshir, S.; Safari, M.; Dekamin, M. G. A facile and green three-component synthesis of 2-amino-3-cyano-7-hydroxy-4H-chromenes on grinding. *Sci. Iran., Trans. C* **2014,** 21, 742-747.
278. Moirangthem, N.; Laitonjam, W. S. A facile synthesis of 7-amino-1,3-diaryl-5-phenyl-2-thioxo-pyrano[2,3-d]pyrimidin-4(5H)-ones. *Am. Chem. Sci. J.* **2011,** 1, 58-70.
279. Issum Research Development Company (**2006**), 2-Sulfonyl-3-phenylacrylonitrile compounds and compositions for inhibiting cell proliferative disorders. IL112921A Patent 118
280. Yaish, P.; Gazit, A.; Gilon, C.; Levitzki, A. Blocking of EGF-dependent cell proliferation by EGF receptor kinase inhibitors. *Science* **1988,** 242, 933-5.
281. Shastin, A. V.; Korotchenko, V. N.; Nenajdenko, V. G.; Balenkova, E. S. A Novel Synthetic Approach to Dichlorostyrenes. *Tetrahedron* **2000,** 56, 6557-6563.

282. Pasha, M. A.; Nanjundaswamy, H. M. A Novel Transformation of Oximes into Hydrazones by Hydrazine Hydrate. *Synthetic Communications* **2004,** 34, 3827-3831.
283. Sharma, S. K.; Mudhoo, A. *Green Chemistry for Environmental Sustainability*. CRC Press Florida: 2010.
284. Xiao, G. Q.; Liang, B. X.; Chen, S. H.; Ou, T. M.; Bu, X. Z.; Yan, M. 3-Nitro-2H-chromenes as a new class of inhibitors against thioredoxin reductase and proliferation of cancer cells. *Arch Pharm (Weinheim)* **2012,** 345, 767-70.
285. Yan, M.-C.; Jang, Y.-J.; Yao, C.-F. An easy and efficient method for the synthesis of 2,2-dialkyl-3-nitrochromene. *Tetrahedron Letters* **2001,** 42, 2717-2721.
286. Yan, M.-C.; Tu, Z.; Lin, C.; Ko, S.; Hsu, J.; Yao, C.-F. An investigation of the reaction of 2-aminobenzaldehyde derivatives with conjugated nitro-olefins: an easy and efficient synthesis of 3-nitro-1,2-dihydroquinolines and 3-nitroquinolines. *J. Org. Chem.* **2004,** 69, 1565-1570.
287. Dai, L. Z.; Shi, Y. L.; Zhao, G. L.; Shi, M. A Facile Synthetic Route to 2 H-Chromenes: Reconsideration of the Mechanism of the DBU-Catalyzed Reaction between Salicylic Aldehydes and Ethyl 2-Methylbuta-2,3-dienoate. *Chemistry - A European Journal* **2012,** 13, 3701-3706.
288. Rene, L.; Royer, R. Synthesis of 3-chromenes with electron-attracting substituents as pharmacological benzofuran analogs. *Eur. J. Med. Chem. - Chim. Ther.* **1975,** 10, 72-8.
289. Das, B. C.; Mohapatra, S.; Campbell, P. D.; Nayak, S.; Mahalingam, S. M.; Evans, T. Synthesis of function-oriented 2-phenyl-2H-chromene derivatives using l-pipecolinic acid and substituted guanidine organocatalysts. *Tetrahedron Letters* **2010,** 51, 2567-2570.
290. Xu, D.-Q.; Wang, Y.-F.; Luo, S.-P.; Zhang, S.; Zhong, A.-G.; Chen, H.; Xu, Z.-Y. A Novel Enantioselective Catalytic Tandem Oxa-Michael–Henry Reaction: One-Pot Organocatalytic Asymmetric Synthesis of 3-Nitro-2H-chromenes. *Advanced Synthesis & Catalysis* **2008,** 350, 2610-2616.
291. Ballini, R.; Bosica, G.; Fiorini, D.; Palmieri, A. Neutral alumina catalysed synthesis of 3-nitro-1,2-dihydroquinolines and 3-nitrochromenes, under solvent-free conditions, via tandem process. *Green Chemistry* **2005,** 7, 825-827.
292. Koussini, R.; Al-Shihri, A. S. Microwave-Assisted Synthesis of 3-Nitro-2H-Chromenes Under Solventless Phase-Transfer Catalytic Conditions. *Jordan Journal of Chemistry* **2008,** 3, 103-107.
293. P. Kulkarni, P.; J. Kadam, A.; B. Mane, R.; V. Desai, U.; P. Wadgaonkar, P. Demethylation of Methyl Aryl Ethers using Pyridine Hydrochloride in Solvent-free Conditions under Microwave Irradiation. *Journal of Chemical Research, Synopses* **1999**, 394-395.
294. Varma, R. S.; Gai, Y.-Z.; Kabalka, G. W. Reduction of α,β-unsaturated nitroalkenes with borane and borohydrides. A convenient route to 3-nitro-, 3-hydroxylamino-, and 3-amino-2h-1-benzopyran derivatives. *Journal of Heterocyclic Chemistry* **1987,** 24, 767-772.
295. Baumgarten, H. E.; Saylor, J. L. Synthesis of 3-amino- and 3-nitro-2-arylquinolines. *J. Am. Chem. Soc.* **1957,** 79, 1502-5.
296. Friedlaender, P. Ueber o-Amidobenzaldehyd. *Berichte der deutschen chemischen Gesellschaft* **1882,** 15, 2572-2575.
297. Kaneko, C. Polarization of aromatic heterocyclic compounds. CXXXII. 2-Hydroxyquinoline 1-oxide. *Chem. Pharm. Bull.* **1959,** 7, 273-7.
298. Chahar, M. K.; Sharma, N.; Dobhal, M. P.; Joshi, Y. C. Flavonoids: A versatile source of anticancer drugs. *Pharmacognosy Reviews* **2011,** 5, 1-12.
299. Ruela-de-Sousa, R. R.; Fuhler, G. M.; Blom, N.; Ferreira, C. V.; Aoyama, H.; Peppelenbosch, M. P. Cytotoxicity of apigenin on leukemia cell lines: implications for prevention and therapy. *Cell Death & Disease* **2010,** 1, e19.

300. Beudot, C.; De Meo Mp Fau - Dauzonne, D.; Dauzonne D Fau - Elias, R.; Elias R Fau - Laget, M.; Laget M Fau - Guiraud, H.; Guiraud H Fau - Balansard, G.; Balansard G Fau - Dumenil, G.; Dumenil, G. Evaluation of the mutagenicity and antimutagenicity of forty-two 3-substituted flavones in the Ames test, *Mutat. Res.*, **1998**, 141
301. Dauzonne, D.; Folleas, B.; Martinez, L.; Chabot, G. G. Synthesis and in vitro cytotoxicity of a series of 3-aminoflavones. *Eur. J. Med. Chem.* **1997,** 32, 71-82.
302. Allan, J.; Robinson, R. CCXC.—An accessible derivative of chromonol. *J. Chem. Soc., Trans.* **1924,** 125, 2192-2195.
303. V. Kostanecki, S.; Różycki, A. Ueber eine Bildungsweise von Chromonderivaten. *Berichte der deutschen chemischen Gesellschaft* **1901,** 34, 102-109.
304. Baker, W. Molecular rearrangement of some o-acyloxyacetophenones and the mechanism of the production of 3-acylchromones. *Journal of the Chemical Society (Resumed)* **1933**, 1381-1389.
305. Furniss, B. S.; Hannaford, A. J.; Smith, P. W. G.; Tatchell, A. R. *Vogel's Textbook of Practical Organic Chemistry*. 5th ed.; Harlow: Longman: New York, 1989.
306. Patoilo, D. T.; Silva, A. M. S.; Cavaleiro, J. A. S. Regioselective 3-Nitrationof Flavones: A New Synthesis of 3-Nitro- and 3-Aminoflavones. *Synlett* **2010,** 2010, 1381-1385.
307. Kumar, G. S.; Maheswari, C. U.; Kumar, R. A.; Kantam, M. L.; Reddy, K. R. Copper-Catalyzed Oxidative C-O Coupling by Direct C-H Bond Activation of Formamides: Synthesis of Enol Carbamates and 2-Carbonyl-Substituted Phenol Carbamates. *Angewandte Chemie International Edition* **2011,** 50, 11748-11751.
308. Vila, A. J.; Lagier, C. M.; Olivieri, A. C. Proton transfer in solid 1-phenylbutane-1,3-dione and related 1,3-diones as studied by carbon-13 CPMAS NMR spectroscopy and AM1 calculations. *The Journal of Physical Chemistry* **1991,** 95, 5069-5073.
309. Yang, Q.; Alper, H. Synthesis of Chromones via Palladium-Catalyzed Ligand-Free Cyclocarbonylation of o-Iodophenols with Terminal Acetylenes in Phosphonium Salt Ionic Liquids. *The Journal of Organic Chemistry* **2010,** 75, 948-950.
310. Yoshida, M.; Fujino, Y.; Saito, K.; Doi, T. Regioselective synthesis of flavone derivatives via DMAP-catalyzed cyclization of o-alkynoylphenols. *Tetrahedron* **2011,** 67, 9993-9997.
311. Kulkarni, P. S.; Kondhare, D. D.; Varala, R.; Zubaidha, P. K. Cyclization of 2′-hydroxychalcones to flavones using ammonium iodide as an iodine source: An eco-friendly approach. *Journal of the Serbian Chemical Society* **2013,** 78, 909-916.
312. Du, Z.; Ng, H.; Zhang, K.; Zeng, H.; Wang, J. Ionic liquid mediated Cu-catalyzed cascade oxa-Michael-oxidation: efficient synthesis of flavones under mild reaction conditions. *Organic & Biomolecular Chemistry* **2011,** 9, 6930-6933.
313. Naik, M. M.; Tilve, S. G.; Kamat, V. P. Pyrrolidine and iodine catalyzed domino aldol-Michael-dehydrogenative synthesis of flavones. *Tetrahedron Letters* **2014,** 55, 3340-3343.
314. Iaroshenko, V. O.; Mkrtchyan, S.; Gevorgyan, A.; Vilches-Herrera, M.; Sevenard, D. V.; Villinger, A.; Ghochikyan, T. V.; Saghiyan, A.; Sosnovskikh, V. Y.; Langer, P. Synthesis of heteroannulated 3-nitro- and 3-aminopyridines by cyclocondensation of electron-rich aminoheterocycles with 3-nitrochromone. *Tetrahedron* **2012,** 68, 2532-2543.
315. Dauzonne, D.; Grandjean, C. Synthesis of 2-aryl-3-nitro-4H-1-benzopyran-4-ones. *Synthesis* **1992**, 677-80.
316. Paparao, C.; Rao, K. V.; Sundaramurthy, V. A One-Step Synthesis of 3-Nitroflavanones and their Conversion to 3-Nitroflavones. *Synthesis* **1981,** 1981, 236-237.
317. Gonzalez, A.; Galvez, C. Phase-transfer catalyzed nitration and nitrosation of 2-arylindoles with 2-cyano-2-propyl nitrate. *Synthesis* **1983**, 212-14.
318. Barlow, L. R. The free radical decomposition of benzoyl nitrate and its pressure dependence. *Tetrahedron* **1968,** 24, 4913-4915.

319. Nguyen, H. H.; Kurth, M. J. Microwave-assisted Synthesis of 3-Nitroindoles from N-Aryl Enamines via Intramolecular Arene-Alkene Coupling. *Organic letters* **2013,** 15, 362-365.
320. Wang, G.-W.; Gao, J. Solvent-free bromination reactions with sodium bromide and oxone promoted by mechanical milling. *Green Chemistry* **2012,** 14, 1125-1131.
321. Nair, V.; Panicker, S. B.; Augustine, A.; George, T. G.; Thomas, S.; Vairamani, M. An efficient bromination of alkenes using cerium(IV) ammonium nitrate (CAN) and potassium bromide. *Tetrahedron* **2001,** 57, 7417-7422.
322. Stodulski, M.; Goetzinger, A.; Kohlhepp, S. V.; Gulder, T. Halocarbocyclization versus dihalogenation: substituent directed iodine(iii) catalyzed halogenations. *Chemical Communications* **2014,** 50, 3435-3438.
323. Baumstark, A. L.; Chrisope, D. R.; Keel, R. A.; Boykin, D. W. A carbon-13 Nmr assignment study of 3,5-diarylisoxazoles. *Journal of Heterocyclic Chemistry* **1980,** 17, 1719-1721.
324. Stephens, C. E.; Arafa, R. K. 3,5-Diarylisoxazoles: Individualized Three-Step Synthesis and Isomer Determination Using 13C NMR or Mass Spectroscopy. *Journal of Chemical Education* **2006,** 83, 1336.
325. Dal Piaz, V.; Pinzauti, S.; Lacrimini, P. 4-Nitro-1,2-oxazoles from hydroximic acid chlorides. *Synthesis* **1975**, 664-5.
326. Sokolov, S. D.; Egorova, T. N.; Yudintseva, I. M. Research in the isoxazole series. *Chemistry of Heterocyclic Compounds* **1974,** 10, 516-520.
327. Kawai, H.; Tachi, K.; Tokunaga, E.; Shiro, M.; Shibata, N. Trifluoromethylation of Aromatic Isoxazoles: Regio- and Diastereoselective Route to 5-Trifluoromethyl-2-isoxazolines. *Angewandte Chemie International Edition* **2011,** 50, 7803-7806.
328. Duranti, E.; Balsamini, C.; Spadoni, G.; Staccioli, L. Reaction of secondary acetylenic bromides with sodium nitrite: synthesis of 3,5-alkyl(aryl)-4-nitroisoxazoles. *The Journal of Organic Chemistry* **1988,** 53, 2870-2872.
329. Ikeda, T.; Lee, B.; Tazuke, S.; Takenaka, A. Time-resolved observation of excitation hopping between two anthryl moieties attached to both ends of alkanes: simulation based on conformational analysis. *Journal of the American Chemical Society* **1990,** 112, 4650-4656.
330. Grignard, V. Sur quelques nouvelles combinaisons organometaliques du magnesium et leur application a des sytheses d'alcools et d'hydrocabures. *Académie des sciences*, 1900; Vol. 130, pp 1322-25.
331. Pirkle, W. H.; Finn, J. M. Useful routes to 9-anthryl ethers and sulfides. *The Journal of Organic Chemistry* **1983,** 48, 2779-2780.
332. Wolff, L. Chemischen Institut der Universität Jena: Methode zum Ersatz des Sauerstoffatoms der Ketone und Aldehyde durch Wasserstoff. [Erste Abhandlung.]. *Justus Liebigs Annalen der Chemie* **1912,** 394, 86-108.
333. Huang, M. Reduction of Steroid Ketones and other Carbonyl Compounds by Modified Wolff--Kishner Method. *Journal of the American Chemical Society* **1949,** 71, 3301-3303.
334. Vilsmeier, A.; Haack, A. Über die Einwirkung von Halogenphosphor auf Alkyl-formanilide. Eine neue Methode zur Darstellung sekundärer und tertiärer p-Alkylamino-benzaldehyde. *Berichte der deutschen chemischen Gesellschaft (A and B Series)* **1927,** 60, 119-122.
335. Kuhn, R.; Fischer, H. Cumulenes. XIII. Amalgam-hydrogenation of cumulenes and prototropic rearrangements. *Chem. Ber.* **1961,** 94, 3060-71.
336. Stogryn, E. L. Synthesis and antimalarial activity of anthracene amino alcohols. *J. Med. Chem.* **1974,** 17, 563-5.
337. Stern, D.; Finkelmeier, N.; Stalke, D. Assessment of the LiX salt-effect in anthracenyl lithiums. *Chemical Communications* **2011,** 47, 2113-2115.

338. Wittig, G.; Pockels, U.; Dröge, H. Über die Austauschbarkeit von aromatisch gebundenem Wasserstoff gegen Lithium mittels Phenyl-lithiums. *Berichte der deutschen chemischen Gesellschaft (A and B Series)* **1938,** 71, 1903-1912.
339. Wittig, G. The role of ate complexes as reaction-determining intermediates. *Quarterly Reviews, Chemical Society* **1966,** 20, 191-210.
340. Bailey, W. F.; Patricia, J. J. The mechanism of the lithium - halogen Interchange reaction : a review of the literature. *Journal of Organometallic Chemistry* **1988,** 352, 1-46.
341. Ooyama, Y.; Uenaka, K.; Matsugasako, A.; Harima, Y.; Ohshita, J. Molecular design and synthesis of fluorescence PET (photo-induced electron transfer) sensors for detection of water in organic solvents. *RSC Advances* **2013,** 3, 23255-23263.
342. Rieche, A.; Gross, H.; Höft, E. Über α-Halogenäther, IV. Synthesen aromatischer Aldehyde mit Dichlormethyl-alkyläthern. *Chemische Berichte* **1960,** 93, 88-94.
343. García, O.; Nicolás, E.; Albericio, F. o-Formylation of electron-rich phenols with dichloromethyl methyl ether and TiCl4. *Tetrahedron Letters* **2003,** 44, 4961-4963.
344. Jiang, H.; Rodríguez-Escrich, C.; Johansen, T. K.; Davis, R. L.; Jørgensen, K. A. Organocatalytic Activation of Polycyclic Aromatic Compounds for Asymmetric Diels–Alder Reactions. *Angewandte Chemie International Edition* **2012,** 51, 10271-10274.
345. Parker, M. A.; Kurrasch, D. M.; Nichols, D. E. The Role of Lipophilicity in Determining Binding Affinity and Functional Activity for 5-HT(2A) Receptor Ligands. *Bioorganic & medicinal chemistry* **2008,** 16, 4661-4669.
346. Reichert, B.; Wegner, E. β-Nitrodicarboxylic esters and their conversion into oxidopyrrolidines. *Ber. Dtsch. Chem. Ges. B* **1938,** 71B, 1254-9.
347. Smith, P. A. *Azides and Nitrenes: Reactivity and Utility*. Academic Press Inc.: Orlando, Florida, 1984.
348. Daniele, M. A.; Bandera, Y. P.; Foulger, S. H. Manipulation of Forster energy transfer of coupled fluorophores through biotransformation by Pseudomonas resinovorans CA10. *Photochem. Photobiol.* **2012,** 88, 129-134.
349. Hann, R. A. Use of dimethylformamide as a solvent for the knoevenagel reaction. *Journal of the Chemical Society, Perkin Transactions 1* **1974**, 1379-1380.
350. Gopal, V. R.; Reddy, A. M.; Rao, V. J. Wavelength Dependent Trans to Cis and Quantum Chain Isomerizations of Anthrylethylene Derivatives. *The Journal of Organic Chemistry* **1995,** 60, 7966-7973.
351. Katritzky, A. R.; Zhu, D. W.; Schanze, K. S. Intramolecular charge transfer properties of dicyanovinyl-substituted aromatics. *The Journal of Physical Chemistry* **1991,** 95, 5737-5742.
352. Elassar, A.-Z. A. Synthesis, characterisation and bioactivity of polysubstituted 1-(4-(1H-pyrrol-1-yl)phenyl)-1H-pyrrole derivatives. *Journal of Chemical Research* **2012,** 36, 328-332.
353. Noroozi Pesyan, N.; Rezaee, M. Solvent-free, one-pot synthesis of pentasubstituted cyclopropanes in the presence of BrCN and EtONa by milling. *Monatshefte für Chemie - Chemical Monthly* **2014,** 145, 1165-1171.
354. Andrews, S. P.; Ladlow, M. Convenient Preparation and Use of a New Analytical Construct for the Analysis and Development of Solid-Phase Chemistries. *J. Org. Chem.* **2003,** 68, 5525-5533.
355. Wawzonek, S.; Hallum, J. V. Abnormal Beckmann rearrangement of 9,10-dihydro-9,10-(11-oxoethano)anthracene oxime. *J. Org. Chem.* **1959,** 24, 364-6.
356. Tajbakhsh, M.; Hosseinzadeh, R.; Alinezhad, H.; Ghahari, S.; Heydari, A.; Khaksar, S. Catalyst-Free One-Pot Reductive Alkylation of Primary and Secondary Amines and N,N-Dimethylation of Amino Acids Using Sodium Borohydride in 2,2,2-Trifluoroethanol. *Synthesis* **2011,** 2011, 490-496.

357. Dangerfield, E. M.; Plunkett, C. H.; Win-Mason, A. L.; Stocker, B. L.; Timmer, M. S. M. Protecting-Group-Free Synthesis of Amines: Synthesis of Primary Amines from Aldehydes via Reductive Amination. *The Journal of Organic Chemistry* **2010,** 75, 5470-5477.
358. Karthikeyan, J.; Yoshikai, N. Rhodium(III)-Catalyzed Directed peri-C-H Alkenylation of Anthracene Derivatives. *Org. Lett.* **2014,** 16, 4224-4227.
359. Beckmann, E. Zur Kenntniss der Isonitrosoverbindungen. *Berichte der deutschen chemischen Gesellschaft* **1886,** 19, 988-993.
360. Chapman, A. W. CCLXIX.-Imino-aryl ethers. Part III. The molecular rearrangement of N-phenylbenziminophenyl ether. *Journal of the Chemical Society, Transactions* **1925,** 127, 1992-1998.
361. Schmidt, K. F. Über den Imin-Rest. *Berichte der deutschen chemischen Gesellschaft (A and B Series)* **1924,** 57, 704-706.
362. Glossop, P. A.; Lane, C. A. L. (2012) Novel compounds active as muscarinic receptor antagonists. Patent: WO2010007561 A1
363. Dakin, L.; Dowling, J. E.; Lamb, M.; Read, J.; Su, Q.; Zheng, X. (2010) Chemical compounds 251. Patent:WO2010001169 A3.
364. Carpino, L. A.; Imazumi, H.; El-Faham, A.; Ferrer, F. J.; Zhang, C.; Lee, Y.; Foxman, B. M.; Henklein, P.; Hanay, C.; Mügge, C.; Wenschuh, H.; Klose, J.; Beyermann, M.; Bienert, M. The Uronium/Guanidinium Peptide Coupling Reagents: Finally the True Uronium Salts. *Angewandte Chemie International Edition* **2002,** 41, 441-445.
365. Markworth, C. J.; Marron, B. E.; Swain, N. A. (2010) Benzamide derivatives. Patent WO2010035166 A1
366. Cava, M. P., Deana, A.A., Muth, K. N-phenylmaleimide. In Organic syntheses: Organic syntheses, 1961; Vol. 41.
367. Marrian, D. H. The reactions of substituted maleimides with thiols. *Journal of the Chemical Society (Resumed)* **1949**, 1515-1516.
368. Patil, N. S.; Deshmukh, G. B.; Patil, S. V.; Bholay, A. D.; Gaikwad, N. D. Synthesis and biological evaluation of novel N-aryl maleimide derivatives clubbed with α-hydroxyphosphonates. *European Journal of Medicinal Chemistry* **2014,** 83, 490-497.
369. Chernick, E. T.; Ahrens, M. J.; Scheidt, K. A.; Wasielewski, M. R. Copper-Promoted N-Arylations of Cyclic Imides within Six-Membered Rings: A Facile Route to Arylene-Based Organic Materials. *The Journal of Organic Chemistry* **2005,** 70, 1486-1489.
370. Watanabe, S.; Igarashi, Y.; Yagami, K. Antimicrobial activity of some N-(arylalkyl)maleimides. *Pesticide Science* **1992,** 34, 99-104.
371. Marrian, D. H.; Friedmann, E.; Ward, J. L. The antibacterial effects of substances structurally resembling maleimide. *Biochemical Journal* **1953,** 54, 65-68.
372. Igarashi, Y.; Watanabe, S. Antimicrobial activities of 2-arylthio-N-alkylmaleimides. *Journal of Industrial Microbiology* **1992,** 9, 91-96.
373. Sortino, M.; Garibotto, F.; Cechinel Filho, V.; Gupta, M.; Enriz, R.; Zacchino, S. Antifungal, cytotoxic and SAR studies of a series of N-alkyl, N-aryl and N-alkylphenyl-1,4-pyrrolediones and related compounds. *Bioorganic & Medicinal Chemistry* **2011,** 19, 2823-2834.
374. Warnecke, A.; Fichtner I Fau - Garmann, D.; Garmann D Fau - Jaehde, U.; Jaehde U Fau - Kratz, F.; Kratz, F. Synthesis and biological activity of water-soluble maleimide derivatives of the anticancer drug carboplatin designed as albumin-binding prodrugs. *Bioconjug Chem* **2004,** 6, 1349-1359
375. Moon, S.; Hanif, M.; Kubanik, M.; Holtkamp, H.; Söhnel, T.; Jamieson, S. M. F.; Hartinger, C. G. Organoruthenium and Osmium Anticancer Complexes Bearing a Maleimide Functional Group: Reactivity to Cysteine, Stability, and Cytotoxicity. *ChemPlusChem* **2015,** 80, 231-236.

376. Diels, O.; Alder, K. Synthesen in der hydroaromatischen Reihe. *Justus Liebigs Annalen der Chemie* **1928,** 460, 98-122.
377. Alder, K., Stein, G., Von udendenbrock, F., Eckhardt, W. V., Frercks, W., Schneider, S. steric course of addition and substitution reactions, I: Stereochemistry of the Diene synthesis. *Justus Liebigs Ann. Chem* **1934,** 514, 1-33.
378. Brunovlenskaya, I. I.; Sengal, N.; Skvarchenko, V. R. Deamination of certain amines with amino group at the substituent in the head of a triptycene molecule bridge. *Dokl. Akad. Nauk SSSR* **1975,** 225, 1323
379. Becker, H. D.; Soerensen, H.; Sandros, K. Photochemical isomerization and dimerization of 1-(9-anthryl)-2-nitroethylene. *The Journal of Organic Chemistry* **1986,** 51, 3223-3226.
380. Research Council of Lithuania (2010), Crystallography open database [online] available: http://www.crystallography.net/cod/2003498.html [accessed 25/05/2015].
381. Alston, P. V.; Ottenbrite, R. M.; Newby, J. Regioselectivity in the Diels-Alder reaction of 9-substituted anthracenes. *The Journal of Organic Chemistry* **1979,** 44, 4939-4943.
382. Russell, G. A.; Whittle, P. R.; Keske, R. G.; Holland, G.; Aubuchon, C. Application of electron spin resonance spectroscopy to problems of structure and conformation. XXIV. Aliphatic semidiones. XIX. Polycyclic derivatives of cyclobutanesemidione. *Journal of the American Chemical Society* **1972,** 94, 1693-1698.
383. Bartlett, P. D.; Ryan, M. J.; Cohen, S. G. Triptycenel (9,10-o-Benzenoanthracene). *Journal of the American Chemical Society* **1942,** 64, 2649-2653.
384. Wittig, G.; Benz, E. Über lithium-natrium-organische Komplexe, III. Über Anionisierungsreaktionen mit Diphenyl-lithium-natrium. *Chemische Berichte* **1958,** 91, 873-882.
385. Cadogan, J. I. G.; Hall, J. K. A.; Sharp, J. T. The formation of arynes by reaction of potassium t-butoxide with aryl halides. *Journal of the Chemical Society C: Organic* **1967**, 1860-1862.
386. Logullo, F. M., Seitz, A.H., Friedman, L. benzenediazonium-2-carboxylate and biphenylene. *Organic Syntheses* **1968,** 48.
387. Friedman, L.; Logullo, F. M. Benzynes via Aprotic Diazotization of Anthranilic Acids: A Convenient Synthesis of Triptycene and Derivatives. *Journal of the American Chemical Society* **1963,** 85, 1549-1549.
388. Hemetsberger, H.; Neustern, F.-U. Photochemical deuterium effect on the rearrangement of triptycene. *Tetrahedron* **1982,** 38, 1175-1182.
389. Yamamoto, G.; Koseki, A.; Sugita, J.; Mochida, H.; Minoura, M. Deamination of 1-Alkyl-9-aminomethyltriptycenes. Participation of a Neighboring 1-Alkyl Substituent. *Bulletin of the Chemical Society of Japan* **2006,** 79, 1585-1600.
390. Yamamoto, G.; Mochida, H. Deamination of 1-Alkyl-9-aminomethyltriptycenes: Participation of the α-C-H Bond of the 1-Alkyl Group. *Chemistry Letters* **2000,** 29, 454-455.
391. Becker, H. D.; Hansen, L.; Andersson, K. Synthesis and photochemical isomerization of 1,2-di-9-anthrylethanol and 1,2-di-9-anthrylethanone. *J. Org. Chem.* **1986,** 51, 2956-61.
392. Ishii, A.; Kawai, T.; Noji, M.; Nakayama, J. Synthesis and reactions of a monosubstituted dithiirane 1-oxide, 3-(9-triptycyl)dithiirane 1-oxide. *Tetrahedron* **2005,** 61, 6693-6699.
393. Tomioka, H.; Nakajima, J.; Mizuno, H.; Iiba, E.; Hirai, K. *Canadian Journal of Chemistry* **1999,** 77, 1066-1076.
394. Menezes, J.; Leibold, W.; Klein, G.; Clements, G. Establishment and characterization of an Epstein-Barr virus (EBC)-negative lymphoblastoid B cell line (BJA-B) from an exceptional, EBV-genome-negative African Burkitt's lymphoma. *Biomedicine* **1975,** 22, 276-84.

395. ATCC (2014), Ramos (RA 1) ATCC ® CRL-1596™ Homo sapiens Burkitt's lympho. [online] available: http://www.lgcstandards-atcc.org/Products/All/CRL-1596.aspx [accessed 20/02/2015]
396. Gey, G.; Coffman, W. D.; Kubicek, M. T. Tissue culture studies of the proliferative capacity of cervical carcinoma and normal epithelium, 1952, *amer assoc cancer research*: pp 264-265.
397. Levenson, A. S.; Jordan, V. C. MCF-7: the first hormone-responsive breast cancer cell line. *Cancer Res* **1997,** 57, 3071-8.
398. Birnie, G. D. The HL60 cell line: a model system for studying human myeloid cell differentiation. *The British Journal of Cancer. Supplement* **1988,** 9, 41-45.
399. Hamid, R.; Rotshteyn, Y.; Rabadi, L.; Parikh, R.; Bullock, P. Comparison of alamar blue and MTT assays for high through-put screening. *Toxicol In Vitro* **2004,** 18, 703-10.
400. Invitrogen (2014); AlamarBlue - Rapid and Accurate Cell Health Indicator. [online] http://www.invitrogen.com/site/us/en/home/brands/Molecular-Probes/Key-Molecular-Probes-Products/alamarBlue-Rapid-and-Accurate-Cell-Health-Indicator.html#how [03/02/12].
401. Vermes, I.; Haanen, C.; Steffens-Nakken, H.; Reutelingsperger, C. A novel assay for apoptosis. Flow cytometric detection of phosphatidylserine expression on early apoptotic cells using fluorescein labelled Annexin V. In *J Immunol Methods*, Netherlands, 1995; Vol. 184, pp 39-51.
402. Zhang, G.; Gurtu, V.; Kain, S. R.; Yan, G. Early detection of apoptosis using a fluorescent conjugate of annexin V. *Biotechniques* **1997,** 23, 525-31.
403. Invitrogen (2014); FITC Annexin V/Dead Cell Apoptosis Kit with FITC annexin V and PI, for Flow Cytometry [online] http://tools.lifetechnologies.com/content/sfs/manuals/mp13242.pdf [20/01/2015]
404. Lifetechnologies (2014); Pierce LDH Cytotoxicity Assay Kit - Life Technologies. [online] https://www.lifetechnologies.com/order/catalog/product/88953 [24/02/2015]
405. Chan, F. K.; Moriwaki, K.; De Rosa, M. J. Detection of necrosis by release of lactate dehydrogenase activity. *Methods Mol Biol* **2013,** 979, 65-70.
406. NCRI (2014); CancerTrends No.6-Leukaemia.pdf. http://www.ncri.ie/sites/ncri/files/pubs/CancerTrendsNo.6-Leukaemia.pdf [01/03/2015]
407. Irish Cancer Society (2015); About chronic lymphocytic leukaemia (CLL) | Irish Cancer Society. [online] http://www.cancer.ie/cancer-information/chronic-lymphocytic-leukaemia/about#sthash.MXbfMTTu.wvJh9zUS.dpbs [26/03/2015]
408. Meanwell, N. A. Synopsis of some recent tactical application of bioisosteres in drug design. *J Med Chem* **2011,** 54, 2529-91.
409. Kamlet, M. J. The Michael Reaction in Non-alkaline Media. I. The Synthesis of 5-(2-Nitro-1-arylethyl)-barbituric Acids. *Journal of the American Chemical Society* **1955,** 77, 4896-4898.
410. Bourguignan, J.; Le Nard, G.; Queguimer, G. Synthese d'aryl nitronorbornenes par cycloaddition de Diels- Alder entre les aryl-nitroethylenes et le cyclopentadiene. Justification de la stereochimie et de la reactivite relative observees par la methode CNDOIII. Obtention d'aryl aminonorbornenes, *Canadian Journal of Chemistry* **1985,** 63, 2354-2361.
411. Taft, R. W.; Price, E.; Fox, I. R.; Lewis, I. C.; Andersen, K. K.; Davis, G. T. Fluorine Nuclear Magnetic Resonance Shielding in *p*-Substituted Fluorobenzenes. The Influence of Structure and Solvent on Resonance Effects. *Journal of the American Chemical Society* **1963,** 85, 3146-3156.
412. Perekalin, V. V.; Lerner, O. M. *Zhurnal Obschchei Khimii* **1958,** 28, 1815-1819.
413. Alizadeh, A.; Khodaei, M. M.; Eshghi, A. Ambiphilic Dual Activation Role of a Task-Specific Ionic Liquid: 2-Hydroxyethylammonium Formate as a Recyclable Promoter and

Medium for the Green Synthesis of β-Nitrostyrenes. *The Journal of Organic Chemistry* **2010,** 75, 8295-8298.
414. Kondo, H.; Ishiwata, S. Studien Zur Synthese der Aporphin-Alkaloide (I. Mitteil.). *Berichte der deutschen chemischen Gesellschaft (A and B Series)* **1931,** 64, 1533-1540.
415. Rangisetty, J. B.; Dukat, M.; Dowd, C. S.; Herrick-Davis, K.; DuPre, A.; Gadepalli, S.; Teitler, M.; Kelley, C. R.; Sharif, N. A.; Glennon, R. A. 1-[2-Methoxy-5-(3-phenylpropyl)]-2-aminopropane Unexpectedly Shows 5-HT2A Serotonin Receptor Affinity and Antagonist Character. *Journal of Medicinal Chemistry* **2001,** 44, 3283-3291.
416. Pianka, M. Studies in fungitoxicity. III.—fungitoxicity of certain β-nitrostyrenes and related compounds. *Journal of the Science of Food and Agriculture* **1963,** 14, 48-55.
417. McDonald, E.; Martin, R. T. Synthesis of unsymmetrical dibenzylketones: new procedures for the preparation and reduction of nitrostyrenes. *Tetrahedron Letters* **1977,** 18, 1317-1320.
418. Jansen, M. P. J. M. β-2: 4: 5-Trimethoxyphenylethylamine, an isomer of mescaline. *Recueil des Travaux Chimiques des Pays-Bas* **1931,** 50, 291-312.
419. Dauzonne, D.; Royer, R. A convenient synthesis of 2-(2-nitroethyl)phenols. *Synthesis* **1984**, 1054-7.
420. Campbell, N.; Anderson, W.; Gilmore, J. Structure of aromatic compounds. II. *J. Chem. Soc.* **1940**, 446-51.
421. Ohwada, T.; Ohta, T.; Shudo, K. Protonation of nitro groups. Diprotonation of .beta.-nitrostyrenes in trifluoromethanesulfonic acid. *Journal of the American Chemical Society* **1986,** 108, 3029-3032.
422. Buechi, G.; Mak, C.-P. Nitro olefination of indoles and some substituted benzenes with 1-dimethylamino-2-nitroethylene. *The Journal of Organic Chemistry* **1977,** 42, 1784-1786.
423. Anderson, W. K.; Dabrah, T. T.; Houston, D. M. Synthesis of erbstatin, a naturally occurring inhibitor of tyrosine-specific protein kinase. *The Journal of Organic Chemistry* **1987,** 52, 2945-2947.
424. Gairaud, C. B.; Lappin, G. R. the synthesis of ω-nitrostyrenes. *The Journal of Organic Chemistry* **1953,** 18, 1-3.
425. Slotta, K. H.; Soremba, K. H. Synthesen thyroxinähnlicher Substanzen aus Diphenyläther. *Berichte der deutschen chemischen Gesellschaft (A and B Series)* **1936,** 69, 566-572.
426. Kinstle, T. H.; Stam, J. G. Vacuum pyrolysis of nitrostyrenes. *The Journal of Organic Chemistry* **1970,** 35, 1771-1774.
427. Lange, N. A.; Hambourger, W. E. condensation of aromatic aldehydes with nitromethane in the presence of alcoholic sodium hydroxide. *Journal of the American Chemical Society* **1931,** 53, 3865-3867.
428. Parham, W. E.; Serres, C.; O'Connor, P. R. Reaction of Diazo Compounds with Nitroölefins. V. The Orientation of Addition of Disubstituted Diazo Compounds to Nitroölefins1. *Journal of the American Chemical Society* **1958,** 80, 588-590.
429. Butler, G.; Carter, M. New Compound. Some New Substituted β-Nitrostyrenes. *Journal of the American Chemical Society* **1950,** 72, 2303-2303.
430. Stewart, R.; Walker, L. G. the polar effect of the β-nitrovinyl group. *Canadian Journal of Chemistry* **1957,** 35, 1561-1569.
431. Fuganti, C.; Sacchetti, A. Biocatalytic enantioselective approach to 3-aryl-2-nitropropanols: Synthesis of enantioenriched (R)-5-methoxy-3-aminochroman, a key precursor to the antidepressant drug Robalzotan. *Journal of Molecular Catalysis B: Enzymatic* **2010,** 66, 276-284.

432. Ohe, T.; Uemura, S. Palladium(II)-catalyzed michael-type hydroarylation of nitroalkenes using aryltins and sodium tetraarylborates. *Bull. Chem. Soc. Jpn.* **2003,** 76, 1423-1431.
433. Noyce, W. K.; Coleman, C. H.; Barr, J. T. Vinology in sweetening agents. I. A vinylog of dulcin. *J. Am. Chem. Soc.* **1951,** 73, 1295-6.
434. Rokhum, L; Bez, G., One-pot solid synthesis of (*E*)-nitroalkenes. *Tetrahedron letters* **2013,** 54, 5500
435. Arnoldi, A.; Bregante, G.; Caldirola, P.; Merlini, L.; Tamburini, B. A New synthesis of 4,5,6,7-tetrahydrofuro[2,3-c]pyridines and furo[2,3-c]pyrrolidines. *Journal of Heterocyclic Chemistry* **1990,** 27, 1169-1171.
436. Campaigne, E.; McCarthy, W. C. 3-Substituted Thiophenes. VIII.1 3-Thienylalkylamines2. *Journal of the American Chemical Society* **1954,** 76, 4466-4468.
437. King, W. J.; Nord, F. F. studies in the thiophene series. iii. condensations of thiophenealdehydes. *The Journal of Organic Chemistry* **1949,** 14, 405-410.
438. Neher, M. B.; Goldberg, E. W.; Fairchild, R. W. Chloronitrostyrenes in the Diels-Alder Reaction1. *The Journal of Organic Chemistry* **1961,** 26, 5220-5221.
439. Silver, R. F.; Kerr, K. A.; Frandsen, P. D.; Kelley, S. J.; Holmes, H. L. Synthesis and chemical reactions of some conjugated heteroenoid compounds. *Canadian Journal of Chemistry* **1967,** 45, 1001-1006.
440. Becker, H. D.; Skelton, B. W.; Soerensen, H.; White, A. H. Photochemical cis-trans isomerization of 2-substituted 9-(2-nitroethenyl)anthracenes. X-ray structure analyses of (E)- and (Z)-9-(2-nitro-2-phenylethenyl)anthracene. *Aust. J. Chem.* **1989,** 42, 593-601.
441. Giulio Matassa, V.; Puig Duran, C.; Prat Quinones, M.; Sole Fue, L.; Llera Soldevila, O. Preparation of 4-(2-amino-1-hydroxyethyl)phenol derivatives as agonists of the β2 adrenergic receptor. *PCT Int. Appl.* **2009**, 83.
442. Glennon, R. A.; Liebowitz, S. M.; Leming-Doot, D.; Rosecrans, J. A. Demethyl analogs of psychoactive methoxyphenalkylamines: synthesis and serotonin receptor affinities. *J. Med. Chem.* **1980,** 23, 990-4.
443. Ho, B.-T.; McIsaac, W. M.; An, R.; Tansey, L. W.; Walker, K. E.; Englert, L. F.; Noel, M. B. Analogs of .alpha.-methylphenethylamine (amphetamine). I. Synthesis and pharmacological activity of some methoxy and/or methyl analogs. *Journal of Medicinal Chemistry* **1970,** 13, 26-30.
444. Agafonov, N. E.; Sedishev, I. P.; Dudin, A. V.; Kutin, A. A.; Stashina, G. A.; Zhulin, V. M. Henry condensation under high pressure. 2. Influence of the aromatic aldehyde and pressure on the ω-nitrostyrene yield and by-products. *Izv. Akad. Nauk SSSR, Ser. Khim.* **1991**, 426-33.
445. Pepper, J. M.; Saha, M. the synthesis of aroyl methyl ketones as lignin model substances. *Canadian Journal of Chemistry* **1964,** 42, 113-120.
446. Yeates, C. L.; Batchelor, J. F.; Capon, E. C.; Cheesman, N. J.; Fry, M.; Hudson, A. T.; Pudney, M.; Trimming, H.; Woolven, J.; Bueno, J. M.; Chicharro, J.; Fernández, E.; Fiandor, J. M.; Gargallo-Viola, D.; Gómez de las Heras, F.; Herreros, E.; León, M. L. Synthesis and Structure–Activity Relationships of 4-Pyridones as Potential Antimalarials. *Journal of Medicinal Chemistry* **2008,** 51, 2845-2852.
447. Dijk, J. V. Individual racemates of N-(p-hydroxyphenylisopropyl)arterenol. **1966**, Patent US3250803.
448. Hass, H. B.; Susie, A. G.; Heider, R. L. Nitroalkene derivatives. *J. Org. Chem.* **1950,** 15, 8-14.
449. Foucaud, A.; Razorilalana-Rabearivony, C.; Loukakou, E.; Person, H. The [1 + 4] cycloaddition of isocyanides with 1-aryl-2-nitro-1-propenes. Methyl 2-nitro-3-arylpropenoates

and methyl 2-nitro-2,4-pentadienoates. Synthesis of 1-hydroxyindoles and 1-hydroxypyrroles. *J. Org. Chem.* **1983,** 48, 3639-44.
450. Sarabhai Research Centre, Novel nitrostyrene derivatives, process for their preparation and compositions containing same. Brit.Patent GB1449540A **1976**,
451. Gilsdorf, R. T.; Nord, F. F. Reverse addition of lithium aluminium hydride to nitro olefins. *J. Am. Chem. Soc.* **1952,** 74, 1837-43.
452. Yang, J.; Dong, J.; Lü, X.; Zhang, Q.; Ding, W.; Shi, X. Ethylenediamine: A Highly Effective Catalyst for One-Pot Synthesis of Aryl Nitroalkenes via Henry Reaction and Dehydration. *Chinese Journal of Chemistry* **2012,** 30, 2827-2833.
453. Fernandez Mateos, A.; De la Fuente Blanco, J. A. Stereoselective addition of enol silanes to nitro olefins. A simple synthesis of compounds related to the insect antifeedants azadiradione and gedunin. *The Journal of Organic Chemistry* **1990,** 55, 1349-1354.
454. Dulenko, L. V.; Dorofeenko, G. N.; Baranov, S. N.; Katts, I. G.; Dulenko, V. I. Thienopyrylium salts. *Chemistry of Heterocyclic Compounds* **1971,** 7, 294-299.
455. Koremura, M. Relations between chemical structures and antimicrobial and insecticidal activities in organo nitro compounds. VI. Synthesis of β-alkyl-β-nitrostyrene derivatives and their antimicrobial and insecticidal activities. *Nippon Nogei Kagaku Kaishi* **1962,** 36, 552-6.
456. Boehringer, C. H.,1-Phenyl-2-aminoethanes. FR1528540 **1968**,
457. Cavier, E. A. *Annales Pharmaceutiques Francaises* 36, 607-613.
458. Severin, T.; Scheel, D.; Adhikary, P. Rearrangements with nitroenamines. VII. Rearrangement of nitroenamines with organo metallic compounds. *Chem. Ber.* **1969,** 102, 2966-71.
459. Swastik Household and Industrial Products Private Ltd, Hydroxynitrostyrene derivatives. *Fr. Demande* FR2384496A1 **1978**, 22
460. Seebach, D.; Henning, R.; Gonnermann, J. Zweifache Deprotonierung von 2-Aryl-1-nitroethanen Umpolung der Nitroolefin-Reaktivität. *Chemische Berichte* **1979,** 112, 234-248.
461. Dupas, G.; Bourguignon, J.; Ruffin, C.; Queguiner, G. Reduction with polymer -bound nadh models. *Tetrahedron Letters* **1982,** 23, 5141-5144.
462. Ciller, J. A.; Seoane, C.; Soto, J. L. Synthesis of heterocyclic compounds XLIX. An unexpected synthesis of isoxazolamines. *Journal of Heterocyclic Chemistry* **1985,** 22, 1663-1665.
463. Leonard, N. J.; Leubner, G. W.; Burk, E. H., Jr. Reactions of nitroparaffins with imines and pseudo bases. *J. Org. Chem.* **1950,** 15, 979-83.
464. Kuan, H.-H.; Reddy, R. J.; Chen, K. An efficient Morita-Baylis-Hillman reaction for the synthesis of multifunctional 2-hydroxy-3-nitrobut-3-enoate derivatives. *Tetrahedron* **2010,** 66, 9875-9879.
465. Bowman, W. R.; Brown, D. S.; Chaffin, J. D. E.; Symons, M. C. R.; Jackson, S. W.; Willcocks, N. A. Oxidative addition of hydroxide anions to nitroalkenes via the radical anions of α-nitrooxiranes. *Tetrahedron Lett.* **1991,** 32, 2285-8.
466. Karver, C. E.; Molina, E. S.; Economos, E. T.; Fuentes, J. C.; Kaitson, S. M.; Kogan, S.; Levi, G.; Marcus, J. K.; Mei, S.; Reinsalu, S. C.; Rico, K.; Zuzek, M. M.; Kharas, G. B. Novel copolymers of styrene. 12. Halogen ring-substituted methyl 2-cyano-3-phenyl-2-propenoates. *J. Macromol. Sci., Part A: Pure Appl. Chem.* **2014,** 51, 101-105.
467. Yukhnovski, I. N. Influence of weakened polar effect of substituents of the infrared spectral frequency of nitrile group in cinnamonitriles and derivatives. *C. R. Acad. Bulg. Sci.* **1966,** 19, 743-6.
468. Ertel, W.; Friedrich, K. Activated ethylenes, V. Reactions of aromatic compounds with derivatives of chloromethylenemalonic acid. A new synthesis of aromatic aldehydes. *Chem. Ber.* **1977,** 110, 86-95.

469. Barnes, R. A.; Kraft, E. R.; Gordon, L. A synthesis for 4-bromo-7-methoxyhydrindene. *J. Am. Chem. Soc.* **1949,** 71, 3523-8.
470. Buschauer, A.; Friese-Kimmel, A.; Baumann, G.; Schunack, W. Synthesis and histamine H2 agonistic activity of arpromidine analogs: replacement of the pheniramine-like moiety by non-heterocyclic groups. *Eur. J. Med. Chem.* **1992,** 27, 321-30.
471. Patai, S.; Israeli, Y. The kinetics and mechanisms of carbonyl-methylene condensations. VI. The reaction of malonitrile with aromatic aldehydes in water. *J. Chem. Soc.* **1960**, 2020-4.
472. Zabicky, J. The kinetics and mechanism of carbonyl-methylene condensation reactions. XI. Stereochemistry of the products. *J. Chem. Soc.* **1961**, 683-7.
473. Weinberger, M. A.; Heggie, R. M.; Holmes, H. L. Solvent effects in the nuclear magnetic resonance spectra of benzalmalononitriles. *Can. J. Chem.* **1965,** 43, 2585-93.
474. Sturz, H. G.; Noller, C. R. Some substituted benzylidenemalononitriles. *J. Am. Chem. Soc.* **1949,** 71, 2949.
475. Instituto de biologia y sueroterapia (1955), Antitubercular compounds. Patent ES225317
476. Maaskant, L. Chloro- and bromo-nitrophenylhydrazines and methylhydrazines and their derivatives. *Recl. Trav. Chim. Pays-Bas Belg.* **1937,** 56, 211-32.
477. Kunze, W. Hydrazine compounds. Cassella Farbwerke Mainkur Akt.-Ges, DE947971 **1956**.
478. Varma, R. S.; Kadkhodayan, M.; Kabalka, G. W. The synthesis of 2-naphthyl-3-nitro-2H-1-benzopyrans. *Synthesis* **1986**, 486-8.
479. Karthikeyan, T.; Sankararaman, S. New pyrrolidine-triazole-based C 2 symmetric organocatalysts and their utility in the asymmetric Michael reaction of β-nitrostyrenes and the synthesis of nitrochromenes. *Tetrahedron: Asymmetry* **2008,** 19, 2741-2745.
480. Varma, R. S.; Kabalka, G. W. A convenient one-pot synthesis of 3-nitro-2H-chromenes by ultrasonic agitation on basic alumina. *Heterocycles* **1985,** 23, 139-41.
481. Ono, N.; Banshou, N.; Ito, S.; Murashima, T.; Ogawa, T. A new synthesis of 4-phosphorylchromenes from 3-nitrochromenes. *J. Heterocycl. Chem.* **1997,** 34, 1243-1246.
482. Renson, M.; d'Harcour, J. C. Structure of benzoylsalicyloyl chloride and preparation of benzo-1,3-dioxan-4-ones by the action of organocadmium derivatives. *Bull. Soc. Chim. Belg.* **1962,** 71, 245-59.
483. Bapna, M.; Nema, R. K. Synthesis of some novel non-nucleoside reverse transcriptase inhibitor. *Asian J. Chem.* **2009,** 21, 1244-1248.
484. Baker, W.; Glockling, F. Unambiguous synthesis of 3-aroylflavones and their reaction with benzylamine. *J. Chem. Soc.* **1950**, 2759-64.
485. Reichel, L.; Henning, H. G. Chemistry and biochemistry of plant products. XV. Conditions of formation of flavones and flavone glucosides. *Justus Liebigs Ann. Chem.* **1959,** 621, 72-9.
486. Liu, X.; Dong, B.; Wang, Z.; Lv, X.; Xu, W. Microwave-assisted method for synthesis of polyhydroxy flavonoid. *Zhuanli Shenqing* **2012**, 7.
487. Schmid, H.; Banholzer, K. The intramolecular nature of the Baker-Venkataraman rearrangement. *Helv. Chim. Acta* **1954,** 37, 1706-16.
488. Dunne, A. T. M.; Gowan, J. E.; Keane, J.; O'Kelly, B. M.; O'Sullivan, D.; Roche, M. M.; Ryan, P. M.; Wheeler, T. S. Thermal cyclization of o-aroyloxyacetoarones. A new synthesis of flavones. *J. Chem. Soc.* **1950**, 1252-9.
489. Sechi, M.; Sannia, L.; Carta, F.; Palomba, M.; Dallocchio, R.; Dessi, A.; Derudas, M.; Zawahir, Z.; Neamati, N. Design of novel bioisosteres of β-diketo acid inhibitors of HIV-1 integrase. *Antiviral Chem. Chemother.* **2005,** 16, 41-61.

490. Ahmed, R.; Malik, M. A.; Zia-Ul-Haq, M. Synthesis and spectroscopic studies of some phenolic β-diketones. *J. Chem. Soc. Pak.* **1990,** 12, 352-4.
491. Vaz, P. A. A. M.; Pinto, D. C. G. A.; Rocha, D. H. A.; Silva, A. M. S.; Cavaleiro, J. A. S. New syntheses of 3-aroylflavone derivatives; Knoevenagel condensation and oxidation versus one-pot synthesis. *Synlett* **2012,** 23, 2353-2356.
492. Banerji, A.; Goomer, N. C. A new synthesis of flavones. *Synthesis* **1980**, 874-5.
493. Nishinaga, A.; Ando, H.; Maruyama, K.; Mashino, T. A new metal complex promoted system for highly selective synthesis of 4H-chromen-4-ones (chromones). *Synthesis* **1992**, 839-41.
494. Baker, W.; Harborne, J. B.; Ollis, W. D. Reaction of primary amines with o-hydroxydibenzoylmethane and the preparation of derivatives of flavone imine. *J. Chem. Soc.* **1952**, 1294-302.
495. Lakshmi, M. V.; Rao, N. V. S. Improved method of synthesis of amino- and chloroflavones. *Indian J. Chem.* **1972,** 10, 34-7.
496. Hattori, L. S. Acaciin, a new flavone glucoside from the leaves of Robinia pseudacacia. *Acta Phytochim.* **1925,** 2, 99-112.
497. Hattori, S. Spectrography of flavone. V. Relation between light absorption and hydroxyl substitution in flavone derivatives. *Acta Phytochim.* **1932,** 6, 131-54.
498. Vialard-Goudou, A.; Blanchecotte, N. Formation of flavones by thermal condensation of monosubstituted monophenols and ethyl 3,4,5-trimethoxybenzoylacetate. *Compt. Rend.* **1965,** 8, 6930-2.
499. Anand, N.; Venkataraman, K. Synthetic experiments in the chromone group. XXII. Nitroflavones as intermediates for the synthesis of hydroxy- and hydroxymethoxyflavones. *Proc. - Indian Acad. Sci., Sect. A* **1947,** 26A, 279-87.
500. Hill, D. W.; Melhuish, R. R. Structure of flavylium salts. *J. Chem. Soc.* **1935**, 1161-6.
501. Michalska, M. Synthesis of 3-nitroflavone. *Chem. Ind. (London, U. K.)* **1966**, 628-9.
502. Berestovitskaya, V.; Baichurin, R.; Aboskalova, N.; Lysenko, K.; Anan'ev, I. Geminal acylnitrostyrenes in the reaction with ortho-aminothiophenol. *Russian Journal of General Chemistry.* **2011,** 81, 1163.
503. Bauer, K. H.; Werner, F. Condensation of α-halogen ketones with aldehydes. *Ber. Dtsch. Chem. Ges. B* **1922,** 55B, 2494-500.
504. Asahina, Y.; Mayeda, S. 1,3-Diketone oximes. *Yakugaku Zasshi* **1933,** 53, 548-57 (in German 87-92).
505. Meyer, K. H.; Schlosser, H. Anthracene. VII. Alkylation of anthranol. *Justus Liebigs Ann. Chem.* **1920,** 420, 126-33.
506. Krollpfeiffer, F.; Branscheid, F.; Thorn, F.; Schneider, K. Transformation products of anthranols and hydroxythionaphthene. *Ann.* **1928,** 462, 46-72.
507. Krollpfeiffer, F. Spectrochemical investigation of the polynuclear aromatic compounds in solution. *Justus Liebigs Ann. Chem.* **1923,** 430, 161-229.
508. Barnett, E. d.; Matthews, M. A. Alkylanthracene and "trans-annular" tautomerism. *Ber. Dtsch. Chem. Ges. B* **1926,** 59B, 1429-38.
509. Schlenk, W.; Bergmann, E.; Benedikt, B.; Blum, O.; Bresiewicz, C.; Rodloff, I.; Appenrodt, J.; Ehninger, K.; Ender, H.; Israel, R.; Knorr, A.; Kohler, T.; Michael, A.; Muller, E.; Rubens, E.; Schmidt-Nickels, W.; Stoffers, W.; Wiegandt, A.; Willstadt, H. Alkali organic compounds. II. New knowledge in the field of the stereochemistry of carbon. *Justus Liebigs Ann. Chem.* **1928,** 463, 98-227.
510. Martin, V.H. *Bulletin des Societes Chimiques Belges*, **1952** , vol. 61, p. 504,511
511. Norman, R. O. C.; Waters, W. A. Action of the phenyl radical on anthracene and meso-substituted anthracenes. *J. Chem. Soc.* **1958**, 167-70.

512. Fieser, L. F.; Jones, J. E. N-Methylformanilide synthesis of aldehydes. *J. Am. Chem. Soc.* **1942,** 64, 1666-9.
513. Grandmougin, E. Intermediate products of the synthesis of alizarin. *Compt. rend.* **1921,** 173, 1176-8.
514. House, H. O.; Ghali, N. I.; Haack, J. L.; VanDerveer, D. Reactions of the 1,8-diphenylanthracene system. *J. Org. Chem.* **1980,** 45, 1807-17.
515. Becker, H. D.; Skelton, B. W.; Sorensen, H.; White, A. H. Photochemical <I>cis-trans</I> Isomerization of 2-Substituted 9-(2-Nitroethenyl)anthracenes. X-Ray Structure Analyses of (E)- and (Z)-9-(2-Nitro-2-phenylethenyl)anthracene. *Australian Journal of Chemistry* **1989,** 42, 593-601.
516. Nakajima, S.; Osuka, A. Synthesis of a tetrakis(9-anthryl) substituted porphyrin and intramolecular charge-transfer emission in its dication. *Tetrahedron Lett.* **1995,** 36, 8457-60.
517. Misra, R.; Sharma, R.; Bhattacharyya, S. P. Exploring NLO response of 9,10-donor-acceptor substituted bichromophoric anthracene derivatives. *J. Comput. Methods Sci. Eng.* **2010,** 10, 149-164.
518. Lock, G.; Stach, K. Catalytic decomposition of hydrazones. I. Aromatic aldehyde hydrazones. *Ber. Dtsch. Chem. Ges. B* **1943,** 76B, 1252-6.
519. Zhang, X. M.; Bordwell, F. G.; Bares, J. E.; Cheng, J. P.; Petrie, B. C. Homolytic bond dissociation energies of the acidic carbon-hydrogen bonds in .alpha.-substituted and 10-substituted 9-methylanthracenes and their related radical anions. *The Journal of Organic Chemistry* **1993,** 58, 3051-3059.
520. Rescifina, A.; Chiacchio, M. A.; Corsaro, A.; De Clercq, E.; Iannazzo, D.; Mastino, A.; Piperno, A.; Romeo, G.; Romeo, R.; Valveri, V. Synthesis and Biological Activity of Isoxazolidinyl Polycyclic Aromatic Hydrocarbons: Potential DNA Intercalators. *J. Med. Chem.* **2006,** 49, 709-715.
521. Kabalka, G. W.; Goudgaon, N. M. A facile aldoxime preparation via the reduction of α,β-unsaturated nitroalkenes using tin(II) chloride. *Synth. Commun.* **1988,** 18, 693-7.
522. Jiang, L.; Fu, Y.; Li, H.; Hu, W. Single-Crystalline, Size, and Orientation Controllable Nanowires and Ultralong Microwires of Organic Semiconductor with Strong Photoswitching Property. *Journal of the American Chemical Society* **2008,** 130, 3937-3941.
523. Metayer, M. Hydrogenation of 9-anthraldehyde. *Bull. Soc. Chim. Fr.* **1954**, 614-15.
524. Hunter, W.T., Buck, J.S. (1956); New chemical compounds and their preparation, US Pat. 2734920A
525. Mallia, R.R., Prathapan, S.; Studies on the solvent dependence in the reaction of a few (anthracen-9-yl)methylamines and sulfanes with reactive acetylenes, unpublished thesis (PhD), Cochin University of Science and Technology
526. Tawney, P. O.; Snyder, R. H.; Conger, R. P.; Leibbrand, K. A.; Stiteler, C. H.; Williams, A. R. Maleimide and derivatives. II. Maleimide and N-methylolmaleimide. *J. Org. Chem.* **1961,** 26, 15-21.
527. Kharitonov, Y. V.; Shul'ts, E. E.; Shakirov, M. M.; Tolstikov, G. A. Synthetic Transformations of Higher Terpenoids: VIII. [4+2]-Cycloaddition Reactions of Lambertianic Acid. *Russ. J. Org. Chem.* **2003,** 39, 57-74.
528. Kretov, A. E.; Kul'chitskaya, N. E. N-Arylmaleimides, their preparation, and properties. *Zh. Obshch. Khim.* **1956,** 26, 221-5.
529. Roderick, W. R.; Bhatia, P. L. Action of trifluoroacetic anhydride on N-substituted amic acids. *J. Org. Chem.* **1963,** 28, 2018-24.
530. Wang, H.; Wei, J.; Jiang, X.; Yin, J. Novel polymerizable N-aromatic maleimides as free radical initiators for photopolymerization. *Polym. Int.* **2006,** 55, 930-937.
531. Caulfield, M. J.; Solomon, D. H. Studies on polyimides: 2. Formation of high molecular weight poly(N-(hydroxyphenyl) maleimides). *Polymer* **1998,** 40, 1251-1260.

532. United States Rubber Co. (1961); Vulcanizing agents for unsaturated and polyurethan elastomers. Patent GB880947
533. Manteca, I.; Etxarri, B.; Ardeo, A.; Arrasate, S.; Osante, I.; Sotomayor, N.; Lete, E. Functionalized organolithium compounds: generation via reductive lithiation and nucleophilic addition to N-phenethylimides. Access to functionalized dihydropyrrolo[2,1-a]isoquinolinones. *Tetrahedron* **1998,** 54, 12361-12378.
534. Kolyamshin, O. A.; Danilov, V. A.; Kol'tsov, N. I. 4-(3-Dialkylamino-2,5-dioxopyrrolidin-1-yl)benzoic acid esters. *Russ. J. Org. Chem.* **2007,** 43, 393-396.
535. Abblard, J.; Baudoin, M. Imides substituted on the nitrogen atom. *Ger. Offen.* **1978**, 43 pp.
536. Pal, B.; Pradhan, P. K.; Jaisankar, P.; Giri, V. S. First triphenylphosphine-promoted reduction of maleimides to succinimides. *Synthesis* **2003**, 1549-1552.
537. Trujillo-Ferrara, J.; Correa-Basurto, J.; Espinosa, J.; Garcia, J.; Martinez, F.; Miranda, R. Solvent-free synthesis of arylamides and arylimides, analogues of acetylcholine. *Synth. Commun.* **2005,** 35, 2017-2023.
538. Tawney, P. O. (1950) N-Methylolmaleimide. US patent 2526517 A
539. Furdik, M.; Sutoris, V.; Drabek, J.; Pospisilova, S. Synergists in pyrethrum. III. N-Substituted 4-cyclohexene-1,2-dicarboximides and their 4-chloro derivatives. *Chem. Zvesti* **1959,** 13, 581-7.
540. Sauers, C. K.; Cotter, R. J. (1961) Preparation of Maleimides. US patent 3018290 A
541. Yamamoto, G.; Kobayashi, Y.; Ono, K.; Yano, E.; Minoura, M.; Mazaki, Y. Synthesis and structures of 9-triptycylallene derivatives. *Bull. Chem. Soc. Jpn.* **2006,** 79, 1293-1299.
542. Bartlett, P. D.; Greene, F. D. Triptycene 1-carboxylic acid and related compounds. The decomposition of triptoyl peroxide. *J. Am. Chem. Soc.* **1954,** 76, 1088-96.
543. Nanu, I.; Boboescu, V.; Secosan, E. Esters of 9,10-dihydroanthracene endo-α,β-succinic acid as models for the study of large-molecule plasticizers. *Bul. Stiint. Teh. Inst. Politeh. Timisoara* **1969,** 14, 141-6.
544. Bova, S.; Saponara, S.; Rampa, A.; Gobbi, S.; Cima, L.; Fusi, F.; Sgaragli, G.; Cavalli, M.; de los Rios, C.; Striessnig, J.; Bisi, A. Anthracene Based Compounds as New L-type Ca2+ Channel Blockers: Design, Synthesis, and Full Biological Profile. *J. Med. Chem.* **2009,** 52, 1259-1262.
545. Grossmann, G.; Potrzebowski, M. J.; Olejniczak, S.; Ziolkowska, N. E.; Bujacz, G. D.; Ciesielski, W.; Prezdo, W.; Nazarov, V.; Golovko, V. Structural studies of N-(2'-substituted phenyl)-9,10-dihydro-9,10-ethanoanthracene-11,12-dicarboximides by X-ray diffraction and NMR spectroscopy-proofs for CH/π interactions in liquid and solid phases. *New J. Chem.* **2003,** 27, 1095-1101.
546. Yasmin, L.; Stubbs, K. A.; Raston, C. L. Vortex fluidic promoted Diels-Alder reactions in an aqueous medium. *Tetrahedron Lett.* **2014,** 55, 2246-2248.
547. Alder, K.; Heimbach, K. The diene synthesis. XXXVII. The addition of anions of acrylic acid and butadiene-1-carboxylic acid. *Chem. Ber.* **1953,** 86, 1312-17.
548. Kiriazis, A.; Leikoski, T.; Mutikainen, I.; Yli-Kauhaluoma, J. The Diels-Alder Reaction between Deactivated Dienes and Electron-Deficient Dienophiles on Solid Support: Stereoselective Synthesis of Hexahydro-1,3-dioxoisoindoles. *J. Comb. Chem.* **2004,** 6, 283-285.
549. Goh, Y. W.; White, J. M. Structure Correlation Study of Some Diels-Alder Cycloadducts of Anthracene. *Aust. J. Chem.* **2009,** 62, 419-424.

Appendices
(Compact Disc)

Appendix 1: Biological screen data tables

Appendix 2: X-ray crystallography reports